VERITEC MARINE TECHNOLOGY CONSULTANTS

POSTAL ADDRESS: P.O.BOX 300, 1322 Høvik, NORWAY
TELEPHONE: +47 (02) 12 99 00
TELEX: 76 192 VERIT N

TECHNICAL REPORT

Date 29. Juni 1984			
Report No. 84-3361	Subject Group P2,P3	Department VT/66	Project No. 66 40 17
Title of Report: CNRD 13-2, TENSION PILE STUDY FINAL REPORT		Approved by: for Rune Dahlberg, Senior Principal Engineer	
Client/Sponsor of project: Conoco Norway Inc.		Client/Sponsor ref.: Harry Wahl	
Work carried out by: Kjell Hauge		Reporter's sign.	

Summary

See Excecutive Summary

The total report consists of:

CNRD 13-2 TENSION PILE STUDY
- FINAL REPORT
- APPENDICES A TO E
- APPENDICES F TO L

4 Indexing terms

TENSION PILES
CYCLIC LOADING
SKIN FRICTION
CAPACITY

Distribution statement:

- [x] No distribution without permission from the responsible department
- [ ] Limited distribution within VERITEC.
- [ ] Free distribution.

Date of last rev.	Rev. No.

Number of pages: 114/847

CONOCO NORWAY
RESEARCH AND DEVELOPMENT

CNRD 13-2: TENSION PILE STUDY

FINAL REPORT

LABORATORY MODEL PILE TESTS

THEORETICAL DEVELOPMENT

PREDICTIONS

PREFACE

This report presents the results of the work carried out within the subproject CNRD 13-2, TENSION PILE STUDY. CNRD 13-2 is sponsored by Conoco Norway Inc. and is a part of a larger research program consisting of the following subprojects:

CNRD 13-1: Tension Pile Planning Study

CNRD 13-2: Tension Pile Study

- Laboratory model pile tests, theoretical development and predictions; Responsibility VERITAS

- Field test with 3" diameter segment pile, theoretical development and predictions: Responsibility ERTEC

CNRD 13-3: Tension Pile Large Scale Test

- Perform a large scale field test on a 30" diameter pile, embedded 67 m in a soft clay deposit, Block 58, West Delta Area, Gulf of Mexico

- Conclude and finalize theoretical development

- Work out recommendations for design procedures based on the findings from the overall research program

The three subprojects are closely interconnected and have the common objective of improving the understanding of pile-soil interaction and produce design procedure recommendations for pile foundations for anchoring of Tension Leg Platforms.

Det norske Veritas (VERITAS) acted as main contractor to Conoco Norway Inc. with

The Earth Technology Corporation (ERTEC) as a designated subcontractor. The contract was transferred to A.S Veritec, a subsidiary of VERITAS as of 1. January 1984, with the same obligations to the involved parties as VERITAS had in the past. The name VERITAS will be used throughout this report for work performed by or for VERITAS prior to this date and A.S Veritec after this date. The Norwegian Geotechnical Institute (NGI) and the University of Trondheim (NTH) acted as consultants to VERITAS throughout the project.

The work performed by VERITAS within CNRD 13-2 has mainly consisted of the following:

* Perform laboratory model pile test program
* Theoretical work and improvement of analytical methods
* Prediction of test results and comparison with observed behaviour
* Reporting and overall administration of CNRD 13-2.

The project staff at VERITAS consisted of the following:

* Tore J. Kvalstad, project manager and main responsible for overall administration and technical direction of Veritas' work as well as theoretical work and improvement of analysis methods.
* Kjell Hauge was responsible for the execution of the laboratory part of the project, the data reduction and the production of the project reports, and assisted in the administrative work.
* Gunnar Flaten carried out the work related to sample preparation, soil testing and most of the practical execution of the laboratory investigations.
* Knut Ronold assisted in execution of theoretical analysis and predictions.
* Sergio Matos of Veritas' Technical Services in Houston assisted in in project coordination and information.

The valuable technical support through discussions and comments provided by Ertec's staff, especially Hudson Matlock and Dewaine Bogard, by NGI's Ove Eide, Fritz Nowacki and Kjell Karlsrud and by NTH's Lars Grande is greatly acknowledged.

Special thanks go to Conoco's staff, Ron Gratz, Jack H.C. Chan, Jeff Mueller and Harry Wahl for their administrative and technical support throughout the project.

CONTENT

PREFACE ii

CONTENT iv

EXECUTIVE SUMMARY ix

1. INTRODUCTION 1

1.1 GENERAL 1
1.2 RELATIONSHIP TO CNRD PROGRAM 2
1.3 REFERENCE TO ERTEC'S WORK WITHIN CNRD 13-2 3
1.4 REFERENCE TO WORK BY NGI AND NTH WITHIN CNRD 13-2 3
1.5 PREVIOUS REPORTS BY VERITAS WITHIN CNRD 13-2 4
1.6 FINAL REPORT 5
1.7 FURTHER WORK 5

2. DESCRIPTION OF LABORATORY MODEL PILE TESTS 6
2.1 GENERAL 6
2.2 EQUIPMENT 7
2.2.1 Model Pile Test Chamber 7
2.2.2 Model Pile 7
2.2.3 Loading System 9
2.3 DATA ACQUISITION SYSTEM 9
2.4 PREPARATION OF SOIL SAMPLES 10
2.5 CHARACTERIZATION OF REMOULDED, RECONSOLIDATED SOIL SAMPLES AND COMPARISON WITH UNDISTURBED SAMPLES AND FIELD CONDITIONS 12
2.5.1 General 12
2.5.2 Plasticity Properties 12
2.5.3 Natural Water Content 13
2.5.4 Consolidation Properties 14
2.5.5 Static Stress-Strain and Strength 14
2.5.6 Cyclic Stress-Strain-Porepressure Generation 15
2.5.7 Comparison of Soil Conditions in the Laboratory Tests with the Field Conditions 17

2.6 LABORATORY MODEL PILE TEST PROGRAM 23

2.6.1 Objective of the Different Test Types 23

2.6.2 Summary of Test Program 23

3. MODEL PILE TEST RESULTS 25

3.1 GENERAL 25

3.2 EVALUATION OF CHANGE IN SKIN FRICTION WITH TIME IN THE LABORATORY MODEL PILE TESTS 25

3.3 STATIC CAPACITY 28

3.4 CYCLIC STRESS CONTROLLED TESTS 31

3.5 CYCLIC DISPLACEMENT CONTROLLED TESTS 34

3.6 CREEP AND RELAXATION TESTS 37

4. THEORETICAL WORK 38

4.1 GENERAL 38

4.2 PORE PRESSURE AND NORMAL STRESS GENERATION DURING INSTALLATION 39

4.2.1 Theoretical Estimates of Excess Pore Pressure 39

4.2.2 Comparison with Measured Values 39

4.3 SET-UP (PORE PRESSURE DISSIPATION) 41

4.3.1 Theoretical Initial Distribution of Pore Pressure 41

4.3.2 Consolidation Analysis Method 41

4.3.3 Consolidation Properties 42

4.3.4 Comparison between Predicted and Measured Behaviour 43

4.4 LOAD - DISPLACEMENT (T-Z) RELATIONSHIP 43

4.4.1 Theoretical Single Slice Model 43

4.5 EVALUATION OF PORE PRESSURE GENERATION UNDER CYCLIC LOADING 45

4.5.1 General 45

4.5.2 Analysis Model 46

4.5.3 Finite Element Model 49

4.5.4 Soil Consolidation Parameters 50

4.5.5 Simulation of Cyclic Loading 50

4.5.6 Comparison with Measured Behaviour 51

4.6 DEGRADATION MODELS 52

4.6.1 General 52

4.6.2 The DRIVE 15 Degradation Model 52

4.6.3 Proposal for Extended Degradation Model 53

4.7 EFFECT OF PILE FLEXIBILITY ON DEGRADATION 53
4.7.1 Analysis with DRIVE 15 53
4.7.2 Consequences of Other Degradation Models 54
4.8 PILE CREEP ANALYSIS 55
4.8.1 General 55
4.8.2 T-Z Creep Model 56
4.8.3 Creep Analysis of Elastic Piles 58
4.8.4 Sample Calculations 60
5. REFERENCES 63

LIST OF APPENDICES

APPENDIX A: TEST 4, STRATUM III: DETAILED RESULTS
APPENDIX B: TEST 5, STRATUM II : DETAILED RESULTS
APPENDIX C: TEST 6, STRATUM III: DETAILED RESULTS
APPENDIX D: TEST 7, STRATUM II : DETAILED RESULTS
APPENDIX E: TEST 8, STRATUM III: DETAILED RESULTS
APPENDIX F: TEST 9, STRATUM II : DETAILED RESULTS
APPENDIX G: TEST 10, STRATUM III: DETAILED RESULTS
APPENDIX H: TEST 11, STRATUM II : DETAILED RESULTS
APPENDIX I: TEST 12, STRATUM III: DETAILED RESULTS
APPENDIX J: TEST 13, STRATUM II : DETAILED RESULTS
APPENDIX K: RESULTS OF LABORATORY TESTS FOR COMPARISON OF REMOULDED, RECONSOLIDATED MATERIAL AND UNDISTURBED MATERIAL
APPENDIX L: DESCRIPTION OF COMPUTER PROGRAM **CRAPIL** **CR**eep Analysis of **PIL**es

LIST OF TABLES

Table 2.1 Plasticity Properties for Model Test Clay 13
Table 2.2 Water Content Compariso 13
Table 2.3 Comparison of Triaxial Test Results 17
Table 2.4 Shear Strength Test Correlations 19
Table 2.5 Relationship between Undrained Shear Strengths Measured by Different Test Methods 20
Table 2.6 Shear Strength Comparison with Segment Tests 21

Table 3.1	Summary of Laboratory Model Pile Test Program and Test Results	26
Table 4.1	Comparison Between Predicted and Measured Pressures	40
Table 4.2	Number of Cycles to Liquefaction, N_l	51
Table 4.3	Rayleigh Distribution of Load Amplitudes for Wave Parcels - Example Problem with CRAPIL	61

LIST OF FIGURES

Figure 2.1	Laboratory Model Pile Test Chamber and Model Pile	64
Figure 2.2	Photograph of Model Pile Test Chamber	65
Figure 2.3	Photograph of Model Pile	66
Figure 2.4	Photograph of Model Pile	67
Figure 2.5	Schematic Diagram of Test Set-Up and Signal Flow	68
Figure 2.6	Proposed Shear Strength Profile at West Delta	69
Figure 3.1	Undrained Shear Strength in Clay Samples (free field) Measured after Consolidation and Completion of Test	70
Figure 3.2	Measured Undrained Shear Strength vs. Water Content for Test Samples	71
Figure 3.3	α-Factors vs. Free Field Undrained Shear Strength	72
Figure 3.4	α-Factors vs. Set-Up Time	73
Figure 3.5	Friction Reduction Factor vs. Undrained Shear Strength	74
Figure 3.6	β-Factors vs. Effective Overburden Pressure	75
Figure 3.7	Interface Cyclic Shear Module vs. Undrained Shear Strength	76
Figure 4.1	Theoretical Prediction of Excess Pore Pressure vs. Radial Distance due to Pile Installation	77
Figure 4.2	Predicted and Measured Pore Pressure at Pile Wall vs. Time for Laboratory Tests	78
Figure 4.3	Predicted and Measured Pore Pressure at Pile Wall vs. Time for 3"" Segment Tests	79
Figure 4.4	Theoretical $t-z$-Curves for Laboratory Model Pile Tests	80
Figure 4.5	Theoretical $t-z$-Curves for Segment Tests	81
Figure 4.6	Single Slice Model for Laboratory and Segment Pile	82

Figure 4.7	Theoretical Prediction of Increase in Undrained Shear Strength due to Pile Installation	83
Figure 4.8	Rate of Pore Pressure Generation	84
Figure 4.9	Pore Pressure Generation for Cyclic Triaxial Test. Comparison Between OCEAN2-Predictions and Measured Values	85
Figure 4.10	Number of Cycles to Failure vs. Shear Stress Level	86
Figure 4.11	Theoretical Prediction of Pore Pressure Increase at Pile Wall due to 100 Uniform Load Cycles as a Function of Stress Level and Coefficient of Consolidation	87
Figure 4.12	Skin Friction Degradation Model in DRIVE15	88
Figure 4.13	Effect of DRIVE15 Degradation Model on Test Pile	89
Figure 4.14	Soil Model in CRAPIL, Elastic, Visco-Plastic	90
Figure 4.15	Mobilization of Shear Stress along a Tension Pile with Pretension of 33 perc. of Ultimate Capacity and Cyclic Loads between ± 5 to ± 40 percent of Ultimate Capacity. - DRIVE 15 Analysis	91
Figure 4.16	Degree of Mobilization of Skin Friction	92
Figure 4.17	Axial Pile Top Load Variations	93
Figure 4.18	Shear Stress Mobilization at Pile Station no. 8	94
Figure 4.19	Total Creep Displacement after Application of Total Set of Wave Parcels	95
Figure 4.20	Redistribution of Mobilized Shear from Creep due to Pretension	96
Figure 4.21	Pile Head Displacement vs. no. of Cycles and Safety Factor	97
Figure 4.22	Pile Head Creep and Variation of Shear Stress Distribution. - Parameter Study	98

EXECUTIVE SUMMARY

GENERAL

The objective of this subproject CNRD 13-2 and the connected subprojects CNRD 13-1 and CNRD 13-3 is to improve the understanding of pile-soil interaction resulting from static and cyclic tensile loading as produced by a deepwater Tension Leg Platform (TLP) and to produce design procedure recommendations for pile foundations for anchoring of TLPs.

The overall project plans were developed under subproject CNRD 13-1; Tension Pile Planning Study, and is described in two separate reports by Veritas and Ertec where a research program consisting of a 3-part experimental program combined with theoretical and analytical investigations was presented.

The three-part experimental program consists of:

a) Laboratory model pile tests

b) Field tests with 3" diameter pile segments

c) Field tests with a 30" diameter, 67 m long instrumented pile

The latter part has been authorized under contract CNRD 13-3; Tension Pile Large Scale Test and is well under way at the time of writing with Ertec acting as a designated subcontractor to Veritas and mainly responsible for the technical execution of the large scale test program.

Part b) the field tests with the 3" diameter segment piles was carried out by Ertec acting as a designated subcontractor to Veritas under this CNRD 13-2 contract. Part b) has been completed and reported by Ertec.

This report presents the results of part a) the laboratory model pile test program, which has been the main responsibilty of Veritas under the CNRD 13-2 contract, together with the theoretical development and predictions under the overall CNRD 13 program.

LABORATORY MODEL PILE TESTS

The model pile test equipment was developed by Veritas mainly prior to this project, but during the execution of the test program, a second improved version of the model pile had to be constructed in order to solve problems in connection with pore pressure measurements.

Soil material was delivered from the West Delta Area, Block 58 site and based on the site characterization study performed by Ertec and presented in /4/ the material was divided in three groups, Stratum I, II and III, according to the main stratification identified through the site investigations. The model tests were performed on remoulded and reconsolidated samples and a special laboratory investigation was carried out in order to quantify and describe the effect of remoulding on the soil properties compared with the in-situ undisturbed conditions (see Appendix K).

The laboratory test program was performed during 1982 and the first half of 1983. The time schedule and test program had to be prolonged and modified to a certain extent due to the unexpectedly long consolidation time required for the remoulded materials used in the tests.

Basically the test program consisted of 4 different types of tests:

* Static tests (i.e. monotonically increasing displacement at a low displacement rate) to determine the ultimate capacity and establish a reference value for the other types of tests.
* Static creep and relaxation tests to evaluate long term stress redistribution under static (pretension) loading.
* Load-controlled cyclic tests at various static load levels combined with series of gradually increasing cyclic load levels to determine critical load combinations and to study the effect of cyclic loading below failure on the capacity of a pile. Further two tests were run with random cyclic loading simulating storm loading superimposed on a static (pretension) load.
* Displacement-controlled tests with two-way cyclic loading to evaluate degradation of skin friction caused by severe cyclic displacements. The cyclic displacement was applied in parcels of 100 cycles with gradually increasing amplitude.

The results of the laboratory model pile test program has been interpreted and is presented in this report and the main findings are summarized below:

* **Static Capacity**

The shear displacement relationships for the pile-soil segments were very close to linearly elastic-plastic, with a pronounced peak at point of yield. The initial slip (yield) occured at relative displacement between pile and soil of about 1-2% of the pile diameter (0.25-0.5mm). When relating the ultimate friction to the undrained shear strength of the clay through α-factors, values ranging from 0.45-0.85 resulted. Tests with full set-up on the pile-soil interface indicated α of 0.85. For the effective stress approach, relating the ultimate friction to the effective vertical pressure prior to installation of the pile through the so-called β-factors, resulted in values ranging from 0.1 to 0.25. These factors are directly dependent on the determination of the effective vertical pressure, which for the laboratory tests were associated with some uncertainty.

* **Cyclic Loading Below the Ultimate Capacity**

Cyclic loading below the ultimate capacity did not produce any pore pressure build-up on the pile wall and only minimal changes in the total and (thus) effective pressure. The permanent pile displacement during cycling (cyclic creep) was minimal for stress levels less than 80% of the static capacity. Signs of permanent uplift started at stress levels of 90-100% percent of the ultimate static strength. Failure occured as a sudden pullout of the pile at maximum stress and at load levels generally higher than the previous static capacity. The combination of static bias level and the cyclic component seemed to have minimal effect on the occurence of pile failure, and only minior signs of cyclic displacement of the pile was seen during the tests. The friction displacement curves during cyclic loading below failure were almost ideally elastic with only small signs of hysteresis as the load approached the ultimate static capacity. There were no signs of degradation in the slope of these curves after several hundered cycles.

* **Displacement-Controlled Cyclic Loading (Degradation Tests)**

The two-way cyclic loading (full reversal in the direction of shear on the pile-soil interface caused degradation (reduction) of the maximum and residual mobilized skin friction. The major part of the degradation occured during the first ($\sim$10) cycles after the yield level was reached. The maximum degradation from initial maximum to steady residual friction during large slip was generally between 20 to 30% but could be as drastic as about 40% . The skin friction versus displacement

relationship was almost linearly elastic plastic after the initial degradation, and was very repetitive with no sign of degradation in the slope of the elastic portion of the loading curve. Some gain in the mobilized friction was seen in large deformation cycling due to rate effects, although this increase diminished after the first cycles.

* **Creep and Relaxation**

Static creep and relaxation tests were performed and indicated that no pile creep started before the interface friction reached about 80% of the ultimate static capacity, in fact most of these tests showed measureable pile displacements first when the stress reached about 90% of the static capacity, although these load levels were kept for only about one hour. The relaxation tests indicated almost no loss in interface friction for load levels below about 75% of the ultimate static capacity.

THEORETICAL WORK AND IMPROVEMENT OF ANALYTICAL METHODS

This part of the project work was concentrated on the effects of cyclic loading on the capacity of tension piles and to explain the findings of the experimental test programs.

The following areas have been adressed:

* Evaluation of progressive degradation of skin friction down along a long flexible pile under combined static and cyclic tensile loading.
* Evaluation of cyclic creep and redistribution of shear stress along a flexible pile based on an elasto-plastic and viscous t-z model.
* Evaluation of simultaneous pore pressure generation and dissipation during cyclic loading.

The basic findings of these studies are as follows:

* **Progressive Degradation**

Based on a number of analyses with the computer program DRIVE 15 it was found that degradation of skin friction will be limited to the upper part of a long

flexible pile. This is especially so for a soil deposit with increasing shear strength with depth as is the case of West Delta and deepwater blocks in the Gulf of Mexico and the Norwegian Trench. The conclusion is based on the assumption of a reasonable safety against static pull-out. Only a minor reduction in capacity was found. The West Delta large scale pile test was simulated in the analysis and the results indicated a capacity reduction in the order of a few percent.

* **Cyclic Creep and Redistribution of Skin Friction**

The elasto-plastic and viscous t-z model implemented in the computer program CRAPIL allowed a number of analyses simulating pile creep due to cyclic loading to be carried out. Material parameters were fitted to a limited number of test data from laboratory model pile tests and in-situ segment tests. The results of the analysis showed that no significant creep would develop provided a reasonable safety factor against pull-out was included. The redistribution effect caused by cyclic creep tended to reduce the static (pretension) shear stress in the top part and to increase the shear stress correspondingly further down the pile. The calculated pile head creep displacements were in the range of a few millimeters for a pile similar to the large scale pile tested at West Delta.

* **Pore Pressure Generation and Dissipation Under Cyclic Loading**

Based on the pore pressure generation measured in the cyclic triaxial tests on undisturbed and on remolded reconsolidated samples from the West Delta site, a pore pressure generation model was developed for this material and fitted to a pore pressure generation function already implemented in the FEM-program OCEAN2. A number of computer runs were carried out simulating storm loading on a pile segment. The analyses were simulating the laboratory model pile tests as well as the 3 inch diameter segment tests under a cyclic loading. The pore pressure generation at the pile wall due to cyclic loading was found to be minor for both test types, which corresponds well with the measured behaviour. For tension piles with a total safety factor in the range 1.5 to 2.0 the reduction in skin friction caused by pore pressure generation during storm loading is considered unlikely to be significant.

FURTHER WORK

The findings presented above will have to be compared with and calibrated against the results of the large scale pile test and the theoretical development work performed by Ertec within the total research program before final conclusions and more general recommendations for design procedures for tension piles for TLP foundations can be finally worked out.

Nevertheless, it is felt by the authors that the CNRD 13-2 project has already at this stage contributed significantly to improve the basic understanding of the mechanisms governing pile-soil interaction and the development and degradation of skin friction on piles subjected to combined static and cyclic loading. There is in the authors opininon a good correspondence between the theoretical models and the findings from the tests and this is considered to be very promising for the further development within the CNRD 13-3 project.

1. INTRODUCTION

1.1 GENERAL

The concept of Tension Leg Platforms (TLP) involves design and installation of anchors. Piles/pilegroups are considered to represent a technically and economically feasable type of anchor foundation able to resist the large tensile forces produced by a vertically moored, pretensioned floating platform in the offshore environment. Deepwater blocks in the Gulf of Mexico, in the North Sea, in the Mediterranean as well as in other parts of the world represents potential locations where the TLP concept is considered to be a feasable solution.

The fundamental failure mode of TLP pile foundation is pull-out failure, either as an abrupt large upward displacement under extreme tensile loads or as an upward displacement gradually accumulating under the combination of static and cyclic tensile forces, i.e cyclic creep. Degradation of skin friction due to cyclic displacements caused by cyclic load variations and pile flexibility will have to be carefully evaluated.

The existing methods used in design of piles today do generally not account for these effects and have mainly been developed for prediction of static capacity. The methods are based on empirical relationships between in situ soil strength properties and ultimate skin friction, and the mechanisms involved in cyclic creep and degradation of skin friction are not well understood.

To improve this situation Conoco Norway Inc. authorized Det norske Veritas (Veritas) with The Earth Technology Corporation (Ertec) acting as a designated subcontractor to conduct a study focusing on tension piles for anchoring of TLPs. The objective was to improve the basic understanding of pile-soil interaction and to produce design procedure recommendations for tension piles for TLP anchoring.

1.2 RELATIONSHIP TO CONOCO NORWAY RESEARCH AND DEVELOPMENT (CNRD) PROGRAM

This subproject CNRD 13-2: TENSION PILE STUDY is the second subproject in Conoco Norway Inc.'s Project CNRD 13: FOUNDATIONS. The first subproject CNRD 13-1: TENSION PILE PLANNING STUDY was performed during summer 1981 by Veritas with Ertec acting as a designated subcontractor and with the Norwegian Geotechnical Institute (NGI) and the Geotechnical Division at the Norwegian Institute of Technology (NTH) at the University of Trondheim as consultants.

The results of the planning study formed the basis for this subproject CNRD 13-2 as well as for the third subproject CNRD 13-3: TENSION PILE LARGE SCALE TEST and are described in the two final reports by Veritas and Ertec respectively:

* Veritas Report No. 81-0587: "Tension Pile Planning Study, Subproject CNRD 13-1, Final Report", August 28, 1981.
* Final Techincal Report, Subproject CNRD 13-1, August 28, 1981, Project No. 81-204, Ertec Inc.

These two reports are integral parts of this contract CNRD 13-2 as well as CNRD 13-3 and describe the proposed 3-phase experimental program consisting of:

- 25 mm (1") Diameter Laboratory Model Pile Tests
- 76 mm (3") Diameter Segment Pile Tests in the Field
- 0.76 m (30") Diameter Large Scale Field Test

The laboratory model pile tests and the 3" diameter segment tests were authorized by Conoco under the CNRD 13-2 contract. Veritas has been mainly responsible for the overall administration and management of the CNRD 13-2 project and for the laboratory model pile test program, while Ertec has been responsible for the 3" diameter segment pile test program and the field work in general, including the site investigation. NGI and NTH have acted as technical consultants to Veritas throughout the CNRD 13-2 project.

1.3 REFERENCE TO ERTEC'S WORK WITHIN CNRD 13-2

The details regarding the field work within CNRD 13-2 has been reported by Ertec and only a brief summary will be given in this report. The field work within CNRD 13-2 consisted mainly of the following:

- A site characterization study consisting of a rather comprehensive field and laboratory investigation in order to define all soil properties relevant for pile design and to provide the project with special information in order to allow a better interpretation of the field tests.
- Planning and implementation of the 3" diameter segment pile tests
- Data reduction and analysis of the test result

In parallel to these tasks a part of the planning of the large scale field test with preparation of functional drawings and specifications for the physical test system has been carried out within the CNRD 13-2 contract. This work will be completed and reported under the CNRD 13-3 contract.

Within the CNRD 13-2 project Ertec has issued the following reports:

- Tension Pile Study, CNRD 13-2, Volume I, Site Investigation and Soil Characterization Study at Block 58, West Delta Area, Gulf of Mexico, April, 1982.
- Tension Pile Study, CNRD 13-2, Volume II, Plan for Performing Small-Diameter Pile Segment Tests, August 1982.
- Tension Pile Study, CNRD 13-2, Volume III, Final Report on Small-Diameter Pile Segment Tests, June 1983.

1.4 REFERENCE TO WORK BY NGI AND NTH WITHIN CNRD 13-2

NGI and NTH, acting as technical consultants to Veritas, have worked mainly with reviewing and commenting on reports issued within the study. Further, predictions regarding the 3" diameter segment pile behaviour have been made and additionally NGI and NTH have conducted limited series of independent laboratory investigations

on samples from the West Delta location in order to provide special information for predictions and interpretation based on NGI's and NTH's methods for analysis of pile behaviour under cyclic loading.

The following reports and notes have been issuedby NGI and NTH within the CNRD 13-2 project:

NGI: Contract Report, Det norske Veritas, Block 58, West Delta Area, Gulf of Mexico, Laboratory Report, 81222-2, June 1982.

Contract Report, Det norske Veritas, Block 58, West Delta Area, Gulf of Mexico, Segment Pile Tests, Predictions of Response during Pile Installation and Monotonic Static Axial Loading, 81222-3, September, 1982.

NTH: Conoco Tension Pile, Triaxial and Oedometer Tests on Cyl. No. 71 and 119 from McClelland's Boring 5, 0.82.02-1, NTH, May 1982.

Subproject CNRD 13-2, Tension Pile Study, Technical Note on Prediction of Static Behaviour of 3" Diameter Segment Pile, 0.82.02, Note No. 1, September 1982.

1.5 PREVIOUS REPORTS BY VERITAS WITHIN CNRD 13-2

Under the CNRD 13-2 contract the following reports and technical notes have been issued by Veritas:

Veritas Report No. 82-0302: "Tension Pile Study, Subproject CNRD 13-2, Description of Test Procedures and Equipment for Laboratory Model Pile Test", June 20, 1982.

Veritas Technical Note No. FDIV/23-82-01: "CNRD 13-2 Tension Pile Study, Review of Ertec's Report No. 82-200-1, Site Investigation and Soil Characterization Study at Block 58, West Delta Area, Gulf of Mexico", June 20, 1982.

Veritas Technical Note No. FDIV/23-82-02: "Subproject CNRD 13-2, Tension Pile

Study, Comments to Segment Test Program", July 7, 1982.

Veritas Technical Note No. FDIV/23-82-03: "Subproject CNRD 13-2, Tension Pile Study, Prediction of Small Scale (3") Segment Pile Test Results", July 19, 1982.

Veritas Technical Note No. FDIV/23-82-04: "Subproject CNRD 13-2, Tension Pile Study, Revised Model Pile Test Program", July 28, 1982. July 19, 1982.

1.6 FINAL REPORT

This report is the final report to be issued under the CNRD 13-2 contract. It describes the laboratory model pile test equipment and test program and gives a characterization of the soil material used in these tests in Section 2, see also Appendix K.

In Section 3 the results of the tests are presented and interpreted regarding static capacity, effect of combined static and cyclic loading, degradation of skin friction and cyclic creep. Detailed test results are presented in the Appendices A through J of this report.

The theoretical work has been concentrated on improvement of understanding with respect to pore pressure generation under cyclic loading, effect of local degradation on the overall pile capacity and pile head displacement, as well as cyclic creep. The findings of the study is presented in Section 4. The predictions of the segment tests are commented on and compared with the test results.

1.7 FURTHER WORK

As stated previously the three subprojects CNRD 13-1, 13-2 and 13-3 are integral parts of a comprehensive research program on tension piles for anchoring of TLPs. Veritas is presently continuing this research for Conoco in cooperation with Ertec, NGI and NTH under the third subproject CNRD 13-3: Tension Pile Large Scale Test. The results, conclusions and recommendations presented in this report and in Ertec's final report on CNRD 13-2 should be reevaluated together with the large scale test results and the additional 3" diameter "long-term" segment tests included in the CNRD 13-3 project.

2. DESCRIPTION OF LABORATORY TEST PROGRAM

2.1 GENERAL

A general description of the apparatus and the test procedures were presented in an early phase of the test program in Veritas Report No. 82-0302, "Tension Pile Study, Subproject CNRD 13-2, Description of Test Procedures and Equipment for Laboratory Model Pile Test".

Further details about the individual tests are presented in the detailed test reports (Appendices A through J) regarding special effects and deviations from the standard test procedures.

The basic purpose of the equipment is to allow simulation of a pile segment embedded in the soil at a given depth with boundary conditions as close as possible to the in situ conditions and with the possibility to apply axial loading to the pile.

This has been achieved by insertion of a 25 mm diameter pile segment into a soil sample subjected to vertical and radial stress conditions similar to what was expected to be found in situ at a given depth below mudline. After a certain degree of reconsolidation the pile is subjected to combined static and cyclic loading or to axial displacement variations in order to study pile-soil interaction mechanisms.

In the following a short summary of the equipment and test procedures will be given. Further the results of a study of the material properties of the remoulded, reconsolidated material used in the laboratory model pile test compared with the properties of undisturbed material is commented on with reference to the soil conditions in the field versus the soil conditions in the laboratory model pile tests (see also Appendix K). Finally a summary of the conducted model pile test program is given.

2.2 DESCRIPTION OF MODEL PILE TEST EQUIPMENT

2.2.1 Model Pile Test Chamber

The model pile test chamber with the model pile is shown in Figure 2.1 and a photograph of the model pile chamber in Figure 2.2. It consists of the confining cylinder with top and bottom plates connected by lock bolts and guide cylinders. The top and bottom plate have cylindrical center holes with a floating bearing that can move relative to the top and bottom plates and the pile.

The soil sample is sealed from the radial confining water pressure and the vertical water pressure acting on top and bottom of the soil sample by means of reinforced rubber membranes. This allows independent application of radial and vertical consolidation stresses on the soil sample.

The dimensions of the soil sample is as follows:

Diameter = 20 cm (8")
Height = 35 cm (14")

The top and bottom pressure chambers and the radial confining pressure chamber are connected to the pneumatic pressure system used for triaxial tests in Veritas' Geotechnical Laboratory.

2.2.2 Model Pile

Photographs of the model pile are shown in Figures 2.3 and 2.4. The model pile outside diameter is 25 mm (1") and the total length is about 600 mm. It consists of three separate parts with measurements taken in the middle instrumented part which is centered in the soil sample during pile installation.

The middle section is 250 mm long (10") leaving 50 mm on both ends to the top and bottom of the soil sample in order to avoid boundary effects and achieve uniform stress conditions over the instrumented part.

Shear Force Measurement

Two axial force transducers connect the middle section to the two end parts and allow measurement of the shear force transferred between soil and pile over the middle section which have a total side area of 196 cm^2 (30.4 sq.in.).

Total Normal Stress

In the middle of the center piece a lid of about 15 mm width and with a length of about 100 mm is cut out of the pile wall. The lid fits closely into the pile perimeter and rests on a load cell measuring the total lateral force due to earth pressure acting on the lid. The first pile version was equipped with two commercially available independent miniature load cells under the upper and lower part of the lid. The second version of the model pile is equipped with a strain gauge instrumented load beam on which the lid is resting. The first pile version had silicone seals around the lid, while the second version made use of a thin and very flexible steel membrane welded to the pile in order to prevent pore water to enter into the instrumented section.

Pore Pressure

In the middle of the lid a filter stone has been inserted. The first version made use of an externally mounted pore pressure transducer connected to the filter stone by a saran tube coming up through the center of the pile. The second version made use of a miniature pore pressure transducer monted directly into the pile wall behind the filter stone.

The second version allowed realiable pore water pressure measurements to be taken with a small time lag compared with the first version where the compliance of the pore pressure measurement system obviously introduced a serious time lag effect.

The first version of the model pile was used during tests 1 through 9 while the second version was used during tests 10 through 13 (see also test program).

Axial Displacement

Axial displacement is measured at the top of the load piston by means of a LVDT.

2.2.3 Loading System

The model pile chamber with the inserted pile was placed in the load frame normally used for triaxial test, and the pile head was connected to an electro-hydraulic jack which is mounted on the top of the load frame. The load system is based on closed loop control and allows accurate simulation of any kind of load or displacement time history of relevance for this type of problem.

The control signal was normally generated by a function generator which allowed monotonic or sinusoidal variations to be applied superimposed on a static level. For the storm load test (tests 12 and 13) a time history consisting of a sinusoidal signal with constant period of 10 seconds and random variation of amplitudes had been generated by a microprocessor and recorded on tape. The amplitudes were generated to give a Rayleigh distribution of the double amplitudes, and the order was generated by a random number generator.

2.3 DATA ACQUISITION SYSTEM

The transducer signals from pore water pressure, total normal stress, axial loads and axial displacement were recorded on an 8-channel PCM (Pulse Code Modulation) tape recorder together with time signal and identification signals (to separate recording sequences). Confining pressures in the vertical and lateral direction as well as backpressure were kept constant and read from pressure gauges manually.

Only sequences of the test were recorded on tape. A typical recording sequence was 5 cycles every 20 cycles, i.e. 5 sequences of 5 cycles per 100 cycles.

A 4-channel strip chart recorder monitored pore pressure, normal stress, axial displacement and shear force on the mid section of the pile throughout the tests from installation to extraction of the pile. A x-y plotter was used to follow shear force vs axial load during static and cyclic loading.

A data analysis program was developed to allow a consistent analysis of the recorded signals and preparation of plots. A schematic diagram showing test set-up and signal flow is shown in Figure 2.5. The results are presented in form of the following types of plots:

* skin friction, displacement, pore pressure, normal stress and effective stress vs number of cycles.
* skin friction vs axial displacement
* skin friction vs effective stress
* pore pressure, total pressure and skin friction vs time, for selected cycles

See also the detailed test reults in Appendices A through J.

2.4 PREPARATION OF SOIL SAMPLES

Based on the available soil information from the site investigation the soil profile was divided in three strata over the depth of interest for the large scale pile test, in this report referred to as Stratum I, Stratum II and Stratum III, mainly based on distinct changes in plasticity properties, water content and partly shear strength with depth below mudline. There are no absolutely clear boundaries between the layers but we have found Ertec's definition acceptable.

STRATUM I: 0.0 to 24.4 m

STRATUM II: 24.4 to 48.8 m

STRATUM III: 48.8 to 77.1 m

Stratum III overlays a fine gray sand. For further details we refer to Ertecs's Volume I report under this subproject.

Soil samples were taken during the site investigation carried out by McClelland Engineers in November/December 1981. A large number of cores were packed and transported to Veritas for use in the model pile tests. A summary of the visual classification and simple strength tests performed during opening of the samples is contained in Appendix K. Basically the samples were sorted according to the defined stratification, and within each stratum the samples were mixed to produce a homogenous sample representative for each stratum.

The samples were mixed with an industrial type of mixer and water (with the same salt content and composition as the original pore water fluid) was added to give the sample a consistency allowing a simple building-in in the consolidometer. The remoulded clay was formed into small balls and placed in the consolidometer by

pressing it with the fist and tamping it with the end of a large diameter bar, in a crude attempt to avoid formation of entrapped air pockets. After completion of a pile test the material was again remoulded and water added. This means that the same material was used several times and subjected to repeated remoulding and reconsolidation.

The remoulded material was filled into a specially built consolidometer, 60 cm (24") high and with an inner diameter of 20 cm (8"). The load piston and the bottom plate are equipped with filter stones. Additionally two to three internal horizontal filter plates were used to speed up the unexpectedly slow consolidation process. The internal filter plates were connected to the top and bottom filters through sealed plastic drains at the perifery of the sample to avoid radial drainage.

A pore pressure transducer was mounted at the side wall at approximately mid height of the sample to allow monitoring of the pore pressure dissipation together with recording of axial load and axial compression of the samples.

The final sample preparation procedure was selected on the basis of a series of trial tests which are described in Veritas Report No. 82-0302, "Description of Test Procedures and Equipment". After an acceptable degree of consolidation had been achieved, the sample was transferred to the pile test chamber where the selected axial and radial confining pressures, and in some of the tests a back pressure were applied. The samples were allowed to continue consolidation in the pile test chamber for a number of days before the model pile was inserted.

2.5 CHARACTERIZATION OF REMOULDED SAMPLES AND COMPARISON WITH UNDISTURBED SAMPLES AND FIELD CONDITIONS

2.5.1 General

The remoulded and reconsolidated samples represent a soi0l type different from the in situ soil regarding the grain structure, density, water content, permeability, etc. This may influence the stress-strain behaviour and in particular the response of the material to cyclic loading regarding pore pressure generation and degradation of strength.

To evaluate the differences between the in situ undisturbed conditions and the conditions in the laboratory model pile tests a spesific series of tests were carried out in order to quantify these differences.

Totally thirteen triaxial tests, five pure static tests and eight cyclic tests with post cyclic static loading, were performed on remoulded and undisturbed material from Stratum II and Stratum III. Water content and plasticity properties were determined on a number of samples during the test program.

Seven oedometer tests were carried out on remoulded material in order to allow comparison of compressibility, permeability and coefficients of consolidation. Oedometer samples were taken from the reconsolidated samples for the pile model tests and samples were cut horizontally and vertically to compare the properties in the vertical and radial direction. Detailed results of this investigation are presented in Appendix K.

2.5.2 Plasticity Properties

Several checks of plastic and liquid limits of the material were made. The results have been compared with the results of the site characterization study and are summarized in the table below.

Table 2.1 Plasticity Properties for Model Test Clay

	Remoulded			Undisturbed		
	w_L	w_P	I_P	w_L	w_P	I_P
Stratum II	56-62	18-22	35-42	50-65	20-27	25-37
Stratum III	92	26	64	75-99	30-40	39-63

Based on these results there seems to be no significant effect on the material's plasticity properties due to repeated remoulding and reconsolidation.

2.5.3 Natural Water Content

A comparison of the water contents of undisturbed and remoulded reconsolidated samples after being subjected to equal consolidation stresses in the triaxial test showed a clear difference. The water content of the undisturbed samples was consistently higher than the water content of the remoulded samples as shown below.

Table 2.2 Water Content Comparison

	Consolidation	Remoulded	Undisturbed	Difference
	Stress	w(percent)	w(percent)	percent
Stratum II	300 kPa	27-29	38-41	9-15
Stratum III	500 kPa	35-36	44-48	9-13

2.5.4 Consolidation Properties

Seven compression tests were carried out on remoulded, reconsolidated material. The c_v-values were consistently lower than the results reported on undisturbed material from the previous investigation by the other laboratories involved.

The compression moduli of the two types of material in the stress range above the consolidation stress (i.e in the virgin range beyond 200 to 300 kPa for the remoulded samples) were found to fall in a fairly close range. Tests from all laboratories have been compared and no significant differences can be pointed out.

An interpretation of the permeability, k, based on the measured compression moduli, M and coefficients of consolidation c_v has been based on the expression:

$$k = \frac{c_v \gamma_w}{M}$$

where γ_w = unit weight of water = 10 kN/m^3

This gives k-values for the remoulded material about 3 to 10 times smaller than for the undisturbed material.

Three of the consolidation tests on remoulded material were carried out on samples cut vertically from the big consolidometer, i.e. the compression tests were performed in the radial direction when relating to the model pile tests. A comparison of these results with the results from the horizontally cut samples gave the following differences:

Compression modulus :	no significant differences
Coeff. of consolidation: and permeability	25 to 50 percent higher in the radial direction than in the vertical direction.

2.5.5 Static Stress-Strain and Strength

Seven static triaxial tests were carried out on remoulded, reconsolidated material. Three of these tests were static only, four were cyclic load- controlled tests followed by postcyclic static loading. Six comparable tests were carried out on undisturbed material from strata II and III.

The tests performed on material from Stratum II revealed no significant differences in the behaviour of the remoulded material when compared with the behaviour of the undisturbed material regarding undrained static shear strength, stress-strain behaviour and pore pressure development.

The tests performed on material from Stratum III indicated a 10 to 30 percent lower shear strength for the remoulded, reconsolidated samples. However, the tests giving the lowest shear strengths were found not to be fully consolidated when the static test was started, and this would tend to reduce the differences. Further, when comparing with triaxial and simple shear tests carried out by NGI, NTH, ERTEC and McClelland we find a scatter in the results that covers this range of variation. The conclusion must be that the differences are small.

The drained strength parameters, cohesion and friction angle, seem to fall well inside the range of values indicated by the overall laboratory investigations on undisturbed material.

2.5.6 Cyclic Stress-Strain-Porepressure Generation

A set of comparable cyclic, two-way, CIU tests on remoulded, reconsolidated and on undisturbed material were performed in order to determine possible deviations in material behaviour when subjected to cyclic loading.

The results have been compared regarding:

* pore pressure generation
* development of cyclic shear strain (stiffness reduction)
* degradation in static shear strength

For Stratum II material there seem to be no significant differences between the two types of material neither regarding development of pore pressure, cyclic strain nor strength degradation. The differences are considered to be within the normal range of variations.

For Stratum III it seemed at first to be a clear difference in development of cyclic strain and pore pressure. However, a closer review of the consolidation data revealed that test T13 most probably was not completely consolidated when testing was started. The cyclic stress ratio τ/s_u was misjudged prior to testing and the sample was subjected to cyclic shear stress levels above what was planned for comparison with tests T9 and T10.

When adjusting for this misjudgment the results for Stratum III seems to follow the same trend as in Stratum II, i.e. no significant differences between the two types of material. It must, however, be pointed out that due to the much denser structure of the remoulded material, the coefficient of consolidation is considerably lower than for undisturbed material. This leads to a time lag in the pore pressure measurement. It turned out to be impossible to get reliable pore pressure measurements during cyclic testing of the remoulded material.

Based on our experience with cyclic triaxial tests we are convinced about the very close relationship betwen cyclic shear strain development and effective stress levels. The close correspondance in cyclic shear strain development between the two types of materials indicates clearly that the effective stress development and thus also the pore pressure generation within the samples must be approximately the same.

The reduction in undrained shear strength after cyclic loading was found to be very limited for the undisturbed samples and limited to some 10 percent for the remoulded, reconsolidated samples.

Table 2.3 Comparison of Triaxial Test Results

Sample	Depth	Index Properties					Consolidation			Strength Data					Stratum	Laboratory
-	-	w_i	w_f	w_L	w_p	I_p	σ_{rc}'	σ_{vc}'	OCR	tanφ	a	s_u	$\frac{s_u}{\sigma_{ac}'}$	ε_{af}	-	-
-	m	percent					kPa	kPa	-		kPa	kPa	-	perc.		
5-61	32.4	45.8	33.4				103.4	103.4	1.0	0.43	0.0	34.9	0.34	16.6		ERTEC
6-61	25.0	39.2	32.0				196.5	283.0	1.0	0.58	0.0	88.0	0.31	7.2		ERTEC
5-69	34.9	42.0	30.0	64	27	37	434.0	711.0	1.0	0.53	0.0	193.0	0.27	4.4	II	McClelland
5-71	35.4						136.0	226.0	1.0	0.52	20.0	83.0	0.37	8.8		NTH CON1. pc
5-71	35.4	44.0		65	35	30	125.0	219.0	1.0	0.55	15.0	60.0	0.27	4.4		NTH CN102. pc
5-71	35.4	40.0					98.0	212.0	1.0	0.54	25.0	54.0	0.26	11.4		NTH CN103. pc
5-87	45.9	50.3	40.2				300.0	300.0	1.0	0.53	0.0	97.0	0.32	10.8		VERITAS T5
5-87	45.9	49.2	38.0	79	24	54	300.0	300.0	1.0	0.53	40.0	95.0	0.32	8.9		VERITAS T6.pc
5-87	45.9	49.2	41.4				300.0	300.0	1.0	0.53	40.0	102.0	0.34	10.5		VERITAS T7.pc
Remoulded		28.0	27.7				350.0	350.0	1.0	0.49	0.0	108.0	0.31	10.1		VERITAS T1
Remoulded		27.0	28.6	62	20	42	300.0	300.0	1.0	0.49	30.0	88.0	0.29	10.7		VERITAS T2.pc
Remoulded		27.4	27.5				300.0	300.0	1.0	0.49	10.0	85.0	0.28	10.1		VERITAS T3.pc
Remoulded		28.0	27.0				300.0	300.0	1.0	0.49	0.0	95.0	0.32	6.1		VERITAS T4.pc
6-45	49.2	52.9	41.4				358.6	358.6	1.0	0.47	0.0	105.2	0.29	7.5		ERTEC
6-62	64.3	49.3	43.4				503.3	503.3	1.0	0.46	0.0	133.1	0.26	10.0		ERTEC
6-53	55.0	56.4	43.0				361.3	480.5	1.0	0.46	0.0	127.0	0.26	6.2	III	ERTEC
5-110	57.7	54.0	36.0	89	36	53	765.0	968.0	1.0	0.35	0.0	226.5	0.23	5.5		MCCLELLAND
5-119	62.7	51.0					199.0	371.0	1.0	0.50	20.0	137.0	0.37	10.8		NTH CON10.pc
5-119	62.7			98	40	58	224.0	384.0	1.0	0.49	20.0	138.0	0.36	11.5		NTH CON11.pc
6-64	67.3	58.6	47.6				500.0	500.0	1.0	0.52	0.0	143.0	0.29	10.8		VERITAS T8
6-64	67.3	58.7	45.6	99	28	71	500.0	500.0	1.0	0.52	15.0	141.0	0.28	8.7		VERITAS T9.pc
6-64	67.3	53.7	44.0				500.0	500.0	1.0	0.52	15.0	144.0	0.29	8.7		VERITAS T10.pc
Remoulded		40.4	36.5				<500	<500	1.0	0.39	0.0	107.0	>0.21	9.2		VERITAS T11
Remoulded		40.6	34.9	92	26	66	500.0	500.0	1.0	0.37	0.0	134.0	0.27	8.4		VERITAS T12
Remoulded		40.1	36.2				<500	<500	1.0	0.35	0.0	104.0	>0.21	8.8		VERITAS T13.pc

2.5.7 Comparison of Soil Conditions in the Laboratory Tests with the Field Conditions

General

The stress-strain and strenght properties of a clay surrounding a pile are heavily dependent on the effective consolidation stresses, but also on the mineral type and grain structure of the soil.

The initial effective stress conditions depend on the total overburden pressure due to the weight of the soil, the coefficient of lateral earth pressure at rest, K_0, and the ambient pore water pressure (which may exceed the hydrostatic water pressure as in the case of the West Delta area). The effective stress conditions at the pile surface or at a failure surface a small distance out from the pile will depend on the initial conditions in the surrounding soil, the stress changes caused by pile installation and the consolidation (set-up) time. It may further be influenced by a static pretension force acting at the pile head and also by eventual residual stresses after pile driving.

The soil strength will thus change from the free field towards the pile surface as a function of time after pile installation. In order to compare the results of the laboratory model pile tests and the 3" diameter field segment tests the effective stress situation close to the pile and in the free field will have to be evaluated for both types of tests. However, as pile design is very often based on total stress methods like the α - method, the free field undrained shear strength before pile installation is an equally interesting parameter to compare.

Undrained Shear Strength

The undrained shear strength s_u of a soil is to a considerable degree dependent on the sampling and test method applied. Sample disturbance can be considerable, especially for gassy soils. Field tests like the cone penetration test (CPT) and the remote vane test (RVT) avoid the sample disturbance effects caused by stress reduction and gas expansion, however, pushing a vane or cone into the soil may cause a certain degree of disturbance also for these test methods.

Triaxial compression tests normally give higher values of undrained shear strength than simple shear tests which again normally exceeds triaxial extension tests.

Any relationship between measured skin friction and undrained shear strength should therefore be connected to a special test method like the unconfined compression test (UCT) or the miniature vane test (MVT) as specified by API in their "Recommended Practice for Planning, Designing, and Constructing Fixed Offshore Platforms".

The reference test methods applied by Veritas in the model pile tests were the UCT and the pocket penetrometer test (PPT). The latter test is a very simple and rapid method to check the undrained shear strength and to determine variations of strength

locally in a soil sample. Further the fall cone test (FCT) was used for rapid strength determination when the samples with undisturbed samples were opended and classified visually before remoulding and mixing and to some extent the FCT was used also on remoulded reconsolidated samples.

Based on their soil characterization study Ertec proposed a design shear strength profile as shown in Figure 2.6. The strength profile is based on a variety of different strength tests. RVT, MVT, CPT, and unconfined, undrained compression tests (UU) plus, the in our opinion somewhat uncertain and operator dependent, torvane tests (TVT), which have been adjusted by a set of adjustment factors.

The extremely detailed soil investigation carried out within this research project contains a considerable amount of strenght determinations with the various methods. This makes a statistical treatment of data possible in order to determine correlations between the different strength tests. Only strenght determinations on the same samples or on neighbour samples have been used in this study which gave the following correlations:

Table 2.4 Shear Strength Test Correlations

	Number of samples n	Average ratio $\bar{x}$	Standard deviation s	Comments
Ratio between MVT and UU strength	18	0.93	0.29	
Ratio between MVT and TVT strength	16	1.46	0.69	
Ratio between MVT and RVT strength	2	0.71	0.13	(down to 220 ft)
Ratio between UCT and UU strength	6	0.71	0.10	(down to 220 ft)
Ratio between PPT and UCT strength	33	0.98	0.09	
Ratio between PPT and TVT strength	3	1.18	0.07	
Ratio between PPT and FCT strength	20	0.65	-	
Ratio between PPT and CIU strength	13	0.66	0.14	

This allows a cross correlation to be developed between the eight different test methods applied in the combined field and laboratory test program. Although including some uncertainty it is felt that the table below could be a valuabel tool when comparing the laboratory and the field tests as well when correlations between undrained shear strength and skin friction are to be evaluated with recommendations for design procedures in mind.

Table 2.5 Relationship Between Undrained Shear Strengths Measured by Different Methods (ie. $\frac{s_{u,pp}}{s_{u,rv}} = 0.53$)

	Ratio between test method in horizontal row and test method in vertical column							
	UCT	PPT	RVT	MVT	TVT	FCT	UU	CIU
UCT	1.00	1.02	0.54	0.77	1.13	0.66	0.71	0.67
PPT	0.98	1.00	0.53	0.75	1.18	0.65	0.70	0.66
RVT	1.85	1.89	1.00	1.41	2.10	1.23	1.31	1.25
MVT	1.31	1.34	0.71	1.00	1.46	0.87	0.93	0.89
TVT	0.88	0.85	0.48	0.68	1.00	0.58	0.62	0.59
FCT	1.51	1.54	0.81	1.15	1.72	1.00	1.07	1.02
UU	1.41	1.44	0.76	1.08	1.61	0.93	1.00	0.95
CIU	1.48	1.52	0.80	1.12	1.69	0.98	1.05	1.00

For a comparison of the segment tests and the laboratory model pile tests the actual undrained shear strength at the test depths should be reevaluated. Using the correlation factors in the table above the average values of shear strength measurement with the different test methods have been scaled to UCT and CIU strengths for the three test depths of 17.7m (58 ft), 45.1 m (148 ft) and 63.4 m (208 ft) using strength measurements in the vicinity of the test depth. This gave the following results:

Table 2.6 Shear Strength Comparison with Segment Tests

Test	Stratum	UCT-strength		CIU-strength		Ertec's reference	Veritas model pile
depth	No.	range	average	range	average	shear strength	tests, range of S_u
m	-	kPa	kPa	kPa	kPa	kPa	kPa(UCT)
17.7	I	13 to 16	14	19 to 23	21	18	-
45.1	II	26 to 38	30	38 to 55	44	34	30 to 60
63.4	III	45 to 63	57	65 to 93	80	62	60 to 100

This indicates that the laboratory model pile tests have been performed at levels of undrained shear strength comparable to the segment pile tests in Stratum II and III.

Effective Stress Conditions

The consolidation stresses selected for the model pile tests were as follows:

	σ_{vc}'	σ_{rc}'	K_0
Stratum II	300	210	0.7
Stratum III	500	350	0.7

These vertical consolidation stresses were applied in the large consolidometer where the samples were prepared. However, due to considerable side friction the consolidation stress dropped towards the bottom of the sample and the low coefficient of consolidation led to consolidation times considerably longer than what was expected prior to testing.

The lower 35 cm of the samples were always used for the pile tests and transferred to the pile chamber where the above described consolidation stresses were applied. As the sample obviously was not consolidated to the planned stress level in the

	σ_{vc}'	σ_{rc}'	K_0
Stratum II	300	210	0.7
Stratum III	500	350	0.7

These vertical consolidation stresses were applied in the large consolidometer where the samples were prepared. However, due to considerable side friction the consolidation stress dropped towards the bottom of the sample and the low coefficient of consolidation led to consolidation times considerably longer than what was expected prior to testing.

The lower 35 cm of the samples were always used for the pile tests and transferred to the pile chamber where the above described consolidation stresses were applied. As the sample obviously was not consolidated to the planned stress level in the consolidometer, the application of the consolidation stresses in the pile chamber will lead to a pore pressure increase.

The evaluation of all tests indicates that the first 4 tests (Test 4 to test 7) may have had limited drainage possiblities in the pile chamber. The excess pore pressure caused by the change in consolidation stresses may have equaled out over the sample but not dissipated and has thus been present as an ambient pressure during pile installation and testing.

In the rest of the tests the drainage system was changed and it is believed that the outer boundary of the sample was completely drained during pile insertion and testing as originally planned. The effective stress conditions in the samples may thus have varied to some extent from test to test. This is further commented on in Section 3.

2.6 LABORATORY MODEL PILE TEST PROGRAM

2.6.1 Objective of the Different Test Types

The test set-up was designed to allow all the different phases of the life of a pile to be followed, and the following observations were planned to be made at the different stages of testing:

* Installation:

  development of pore water pressure and normal stress, skin friction during insertion

* Set-up:

  changes in pore-water pressure and normal stress during consolidation

* Static loading:

  load-displacement behaviour (t-z) curves, axial capacity as a reference for cyclic load tests

* Cyclic load controlled tests:

  cyclic creep effects, changes in t-z curves due to cyclic loading, generation of pore pressure and changes in normal stress

* Cyclic displacement contolled tests:

  degradation of skin friction and stiffness, generation of pore pressure and changes in total stress

* Static creep and relaxation tests:

  Observation of creep and relaxation effects under static load/displacement

2.6.2 Summary of Test Program

Totally 13 tests were carried out. The three first tests were pretests to test and adjust the equipment and the test procedures. The reporting will thus be limited to the 10 last tests starting with Test 4 and ending with Test 13.

As outlined previously the tests were performed on material from Stratum II and III. The excessively long consolidation time required made a reduction of the number of test samples necessary as described in Veritas' Technical Note No. FDIV/23-82-04: "Subproject CNRD 13-2, Tension Pile Study, Revised Model Pile Test Program". All tests on material from Stratum I were dropped from the test program.

Within each test a large number of different load combinations were applied to the pile in order to bring forward as much information as possible. A typical test comprised normally of a static load test to failure followed by a load controlled test where parcels of gradually increasing cyclic load were superimposed on a static (pretension) level. After failure in this one-way type of loading test, a displacement controlled test was performed with parcels of gradually increasing axial pile displacement. Creep and relaxation were studied in some tests. A summary of the test program is presented in table 3.1.

3. MODEL PILE TEST RESULTS

3.1 GENERAL

A total of 13 clay samples were prepared in the oedometer and subsequently transferred to the pile model chamber for pile model tests. These tests were numbered consecutively as Test 1 through Test 13, where odd numbers refer to clay from Stratum II and even numbers from Stratum III. As mentioned earlier, the first three tests were used for calibration and adjustment of the test procedures and no results are therefore reported. Appendix A through J contain the detailed results from Test 4 through Test 13, giving five tests from each of the two lower strata.

Table 3.1 contains a summary of the results from the pile model tests and an overview of the different types of tests performed. The table gives the essential information starting with the preparation of the clay sample in the consolidometer through installation of the pile and the testing phase. Prior to the loading of the pile, a time for set-up was allowed. This time varied for each test, and was a result of several factors.

Initially it was the intention that testing was to start after the excess pore pressure at the pile surface from installation, had dissipated. But due to poor drainage conditions, very low permeability of the remoulded, reconsolidated clay, and extremely slow pore pressure response of the pore pressure system on the pile wall, the time for full dissipation was never reached. Start-up of tests were therefore determined by a seemingly steady-state of the pore pressure and in some cases due to practicality in the laboratory test program.

3.2 EVALUATION OF CHANGE IN SKIN FRICTION WITH TIME IN THE LABORATORY MODEL PILE TESTS

Remoulded samples were consolidated in the consolidometer with 300 kPa and 500 kPa vertical stress for Stratum II and III respectively. Based on measurements of pore pressure dissipation and axial compression as a function of time it can bee concluded that the tests were consolidated to 90% or more (average degree of consolidation).

TEST NO.	STRATUM	CONSOLI-DOMETER			RECONSOLIDAT. IN PILE CHAMB				INSTALLAT. OF PILE				SET-UP			STATIC TEST PRIOR TO CYCLIC LOAD								CYCLIC STRESS CONTROLLED TESTING	CYCLIC DISPLACEMENT CONTROLLED TESTING	SPECIAL TESTS	BUILDING OUT				COMM-ENTS
		σ_v	$s_{u,PP}$	NO. DAYS	σ_{vc}	σ_{rc}	u_b	NO. DAYS	τ_s	u	σ_n	σ_v' (res.)	u_s	$\sigma_{n,f}$	NO. DAYS	τ_{ult}	τ_{res}	$\sigma_{n,ult}$	u_{ult}	σ_{max}	σ_{res}	τ_{max}	δ (deg.)	$\tau_{stat} \pm \tau_{cycl}, \tau_{cyc2}, \ldots$ (kPa) τ_{stat}/τ_{ult}, $\tau_{max,cyc}/\tau_{ult}$ No. OF PARCELS AND CYCLES	$\delta_{cycl} = \pm \ldots\ldots\ldots$ (mm) $\tau_{res,min}/\tau_{max}$, % DEGR. No. OF PARCELS		$s_{u,av}$ (pp)	$s_{u,av}$ (UC)	$s_{u,piles}$ (PP)	No. DAYS Test	
4	III	500	59	17	700	550	200	1	10	49 (3d)	500	250	470	600	3	28.5 32.5	475 610	0.48 0.54	135 0.13					$\tau = 6.5 \pm 5, 10, 15, 20, \ldots\ldots 45$ 20% , 1.59 8 Parcels + 8 cycl = 808	$\delta = \pm 0.1, 0.2, 0.4, 0.6, 0.8, 1, 2$ 30/50 , 28% 7 Parcels of 100 cycles	–	62	65	75	9	–
5	II	300	50	14	600	510	300	6	19	335 (1d)	565	210	445	625	11	30 33	445 610	0.6 0.66	11.3 0.16					$\tau = 14.5 \pm 3, 6, 9, \ldots\ldots 24$ 44% , 1.17 7 Parcels + 37 cycl =737	$\delta = \pm 0.1, 0.2, 0.4, 0.6, 0.8, 1, 2$ 26/34 , 24% 7 Parcels of 100 cycles	RELAXATION TEST (init/τ_{ult} = 1.0 after 16 hrs =.5 ult	55	46	65	1	–
6	III	500	65	21	700	550	200	3	25	215 (1d)	435	230	390	640	11	37 39	395 640	0.51 0.54	9.1 0.14					$\tau = 21.5 \pm 9.5, 14, 15, 8, 16.5$ 55% , 0.97 3 Parcels + 8 cycl = 308	$\delta = \pm 0.2, 0.4, 0.6, 0.8, 1., 2.$ 33/42 , 21% 6 Parcels of 100 cycles	–	77	76	83	4	Cyclic displ. ran prior to cycl load
7	II	300	30	16	600	510	300	2	1.5	310	565	160	470	550	6	16 19	470 545	0.4 0.48	14.2 0.11					$\tau = 6 \pm 1.5, 3.5, 5.5, \ldots 13.5$ 52% , 1.01 6 Parcels + 1 cycl = 601	$\delta = \pm 0.1, 0.2, 0.4, 0.6, 0.8, 1., 2.$ 15.5/21, 27% 7 Parcels of 100 cycles	–	40	37	44	1.5	Poor drainage
8	III	500	65	19	500	350	0	2	27	155 (4d)	365	327	75	445	14	56 60	75 420	0.66 0.71	9.8 0.18					$\tau = 3 \pm 6, 12, 18, 24, 27, 30, 33$ 58% , 1.14 6 Parcels + 6 cycl = 606	$\delta = \pm 0.1, 0.2, 0.4, 0.6, 0.8, 1., 2.$ 49/62 , 21% 7 Parcels of 100 cycles	–	90	95	102	4.5	No bad pressure Good drainage
9	II	300	50	26	300	210	0	18	–	15	150	290	70	195	9	23 27	70 195	0.38 0.45	12.2 0.11					$\tau = 19 \pm 2, 4, 6, 8, 10$ 70% , 1.07 4 Parcels + 97 cycl = 497	$\delta = \pm 1.0$, 250 cycles 34/52 , 27% 4 Parcels ; 24 hrs inbetw.	Creep Test: τ_{cr}/τ_{ult} .5,.6,.7,.8,.85,.9,.95 Relaxation: τ_i/τ_{ult} .37,.6,.8, .85, .95, 1.0	60	67	76	10	Special Cyclic displ. test
10	III	500	80	22	500	350	0	53	30	245	380	423	125	315	2	37 46	1.5 305	0.34 0.42	14.3 0.11					$\tau = 30 \pm 5, 7.5, 10, \ldots 20$ 65% , 1.09 6 Parcels + 23 cycl = 623	$\delta = \pm 0.25, 0.4, 1.0, 2.0$ 32/45 , 28% 4 Parcels of 100 cycles	Creep Test: τ_{cr}/τ_{ult} .6,.7, .8, .9, .95, 1., 1.05 Relaxation: τ_i/τ_{ult} 0.7,1.0	110	110	118	7	NEW MODEL PILE
11	II	300	55	55	300	210	0	6	78	260 (1d)	150	340	250	170	325	15	32 41	175 375	0.53 0.7	11.6 0.17				$\tau = 14 \pm 7, 14, 20$ 40% , 0.8 3 Parcels + 21 cycl = 221	$\delta = \pm 1.0$ 27/40 , 38% 1 Parcel of 75 cycles	–	60	55	72	4	Reduced Cycl. displ. test
12	III	500	40	21	500	350	0	20	25	85	325	167	99	420	30	32 35	295 410	0.8 0.87	16.9 0.21					Random Cyclic Load Control: $\tau_r = \tau_{stat} \pm \tau_{cycl}$ 4 Parcels of 1250 + 397 cycl	Random test no. 1 2 3 4 5 τ_{sta}/τ_{ult} .33 .5 .5 .6 .7 τ_{cym}/τ_{ult} .33 .4 .5 .5 .5	–	40	37	44	14	Random cyclic loading
13	II	300	60	61	300	210	0	21	–	220	280	300	75	275	28	55 70	350 250	0.65 0.87	35 0.23					Random Cyclic Load Control $\tau_r = \tau_{stat} \pm \tau_{cycl}$ 3 Parcels Of 1250 + 233 cycl	Random test no. 1 2 3 4 τ_{sta}/τ_{ult} .5 .5 .6 .7 τ_{cym}/τ_{ult} .4 .5 .5 .5	Static Tests with confining pressure reduction	85	90	95	14	Random cyclic loading

Table 3.1: Summary of Model Pile Test Program and Test Results

However, the height of the samples introduce considerable skin friction along the wall of the consolidometer, leading to a gradually decreasing vertical stress with depth below the load piston. This effect could clearly be seen from the pocket penetrometer determination of undrained shear strength on the sides of the samples before installation in the pile test chamber.

As the lower part of the samples from the consolidometer were always used for the model pile tests, it is obvious that the samples were subjected to higher consolidation stresses in the model pile test chamber than in the consolidometer. This must have generated an additional pore pressure generation which gradually dissipated through radial drainage towards the filter strips on the outer periphery of the samples in the pile test chamber.

Based on the c_v - values measured in oedometer tests we conclude that the c_v - values most probably lies in the range 0.1 to 0.2 $m^2/year$ for the remoulded reconsolidated material in the relevant stress range.

The effective consolidation stress acting on the sample in the consolidometer tests can be estimated from undrained shear strength relationships described in Chapter 2.5.

The excess pore pressure due to application of σ_{Vc} and σ_{Rc} of 300 kPa and 210 kPa for Stratum II and 500 kPa and 350 kPa for Stratum III respectively, can be estimated to be approximately equal to the difference in the vertical stress.

The excess pore pressure caused by pile insertion, and later on additional pore pressure caused by static and cyclic loading, has to be superimposed on the excess pore pressure caused by the stress change from consolidometer to the pile chamber described above. This mainly affects the soil close to the pile wall and decreases rapidly with increasing distance. We consider the effects to be negligible close to the periphery of the samples and have assumed that the conditions here correspond more or less to the free field conditions far away from a full size pile.

The dissipation of this excess pore water pressure can be estimated with radial consolidation theory (Scott,1963).

$$t = r^2/c_v T$$

To achieve an average degree of consolidation of more than 90% the T factor is estimated to be about 0.3 to 0.5, giving consolidation times of:

$$t \sim 3 \text{ to } 5 \text{ days}$$

Except for tests 4,6,7 and 8 more than 5 days were allowed for consolidation in the pile chamber before the pile was installed.

In Figure 3.1 is shown the measured shear strength in the clay samples (average "free-field") taken after consolidation in the consolidometer and after completion of the pile test. A quite consistent picture is here revealed of the undrained shear strengths in the reported tests. The low shear strength for Test 12 is explained by the poor consolidation for this sample as explained in Appendix I. Figure 3.2 also enlightens this picture by showing the measured undrained shear strengths versus the water content at the end of the tests. The water content for Stratum II (PI=26%) clay was around 30% and for Stratum III clay (PI=55%) around 40% . Both strata showed clear trends of increasing shear strength with decreasing water content.

3.3 STATIC CAPACITY

After pile installation and the following set-up period, the testing phase always started with a static test. In addition to the information of the static strength, these tests were performed in order to have a reference for the cyclic tests and to calibrate and check the stability of the frictional measurement system.

The static test comprised of pulling the pile up with a constant speed of extraction. The deformation rate was set to 1 mm per hour in the first tests and for the later tests increased to 10 mm per hour. This increase showed no sign of increase in friction due to rate effects.

As the pile was displaced, the friction increased up to a peak point, which generally was around 1 to 2% of the pile diameter (ie. 0.25 to 0.5 mm). After this yield (ultimate) friction point, the mobilized friction reduced, as the pile continued to move up, but quite quickly reached a stable residual value. At a total upward pile displacement

of about 3 mm the direction of the pile movement was reversed keeping the speed constant. This caused reduction of the friction at about the same slope as the initial loading phase, and then the direction of the interface shear was reversed and again reached a maximum in the compression side. As the pile still moved down the residual compression was reached and the test was stopped as the pile reached the original position. Usually this cycle was repeated once in order to check the repeatability. The results of these tests can be seen in Figure 5 of all the Appendix A through J.

The maximum friction obtained for the different tests varied quite significantly, depending on the consolidation time and the strata tested, and thereby on the shear strength of the clay.

For the total stress approach the ultimate friction is related to the undrained shear strength by the α-factor, and in Figure 3.3 the resulting α-factors are plotted versus the interpreted free-field shear strength at time of testing. Values ranging from 0.45 to 0.85 resulted for the computed α-factors and with a seemingly inconsistent scatter. The factors recommended by API for this type of clay is drawn up for comparison. As recommended by the API, the model pile test results also indicates lower α-factors for higher shear strengths.

As mentioned in the previous section the permeability of the remolded clay was extremely low, implying very long times for excess pore pressures to dissipate. It would therefore seem natural that tests with shorter set-up times would give lower friction values, and α- factors, since the time for full dissipation of pore pressure and healing of soil structure in the remolded zone generated by the pile installation had not yet been finalized. The plot in Figure 3.4 indicate such effects, where the α-factors are plotted versus the set-up time. For the model pile in the remolded clay (c_v of about 0.1 $m^2/year$) the time for full dissipation is about 20 days, which from the plot in Figure 3.4 indicates an α- factor of about 0.8 at full set-up. This conclusion then implies that most tests were performed before full set-up (consolidation) had taken place. It must here be kept in mind that in the above determination of α-factors a significant degree of judgement is also inherent in the determination of the undrained shear strength. A change in this will directly change the value of the α-factor.

Another interesting aspect of the results is seen when plotting the ratio of the ultimate and the residual friction (reduction factor) versus the undrained shear strength, as done in Figure 3.5 . This ratio is consistently larger for Stratum II clay than Stratum III,

which might be a result of the difference in plasticity between the two layers. Also, the ratio seemed to increase with increasing shear strength, as indicated by the straight line fits.

In the effective stress approach, where the ultimate friction is related to the effective vertical pressure, σ'_{vo}, prior to pile installation by the β-factor, the estimation of the σ'_{vo} is very crucial for the outcome of the results. For the laboratory model pile tests this estimation was made on the basis of results from the consolidation and triaxial tests on the remoulded material and the mentioned relationships between the shear strengths measured by pocket penetrometer and CU-tests. The results of computing the β-values for the static tests are shown in Figure 3.6, where it can be seen that values in the range from 0.1 to about 0.25 were found. Again, there do not seem to be any consistent relationship in these results with regard to trends for the two strata.

Measurements of the total and pore pressures on the pile wall during the tests were made for all the pile model tests. The response of the pore pressure for the first tests (Test 4 through 9) was, however, very slow so no radical changes in the pressures on the pile wall were seen during failure nor for changes in the direction of shear etc.

From readings of the available pressures at failure the effective pressures were calculated, and the interface friction angles, δ, determined. The results are listed in Table 3.1, which show quite small values, in the range from about 9 to 17 degrees. For Test 13 the computed interface friction angle showed 35 degrees, and is most likely the result of very long times for consolidation before the static test.

3.4 CYCLIC STRESS CONTROLLED TESTS

A total of eight regular cyclic stress controlled tests with increasing levels of cyclic stress superimposed on a static bias level were performed. In addition, random cyclic stress controlled tests were performed for Test 12 and 13.

The regular cyclic stress (load) controlled test comprised of applying a static uplift load on the model pile, expressed as a percentage of the static ultimate capacity. Superimposed on this static stress (load), parcels of 100 cycles of 10 seconds period and with constant stress amplitude were applied. The mobilized interface friction was therefore controlled to cycle about the static bias level. The cyclic stress amplitude was increased in subsequent parcels until the pile suddenly failed. This failure was characterized as an excessive deformation at the peak load during one cycle.

During the cyclic testing, measurements were made of the pile deformation and of the total and pore pressures acting on the pile wall due to the application of the cyclic skin friction.

In the random cyclic stress controlled test the cyclic amplitude varied randomly for each cycle, with a Rayleigh distribution over 1250 cycles. The maximum amplitude for one parcel of 1250 cycles was chosen, and then increased for subsequent parcels until failure occured. The maximum cyclic amlitude was chosen not to exceed 50% of the static ultimate capacity and in order to increase the actual stress on the pile for consecutive parcels the static bias level was increased.

Common for all (but one) cyclic stress controlled tests were that failure occured as a sudden pullout without almost no warning, such as increase in the pore pressure on the pile wall or large increase in permanent (mean) or cyclic pile deformation. When the maximum stress on the pile interface incresed to about the level of the static capacity some hysteresis in the friction versus displacement relationship could be seen, and minimal signs of permanent pile movement resulted. At failure, however, the pile suddenly was pulled up at point of maximum friction. This maxumum friction was generally larger than the previous static capacity, but after failure the mobilized friction seemed to degrade. In some cases the loss in friction was comparable to the residual friction in the static test, although this was hard to verify since the cyclic tests were stopped after failure, and also that due to the fact that pile friction was controlled in a cyclic varying fashion the actual residual level was hard to determine.

As can be seen from Table 3.1 the static level was kept constant within each test, and varied from 20% to 70% of the ultimate static capacity in Test 4 through 11. For the tests with a static bias below 50% of static capacity the interface friction changed direction (tension to compression) during the last parcels since the maximum cyclic capacity generally was higher than the static. The fact that a change in direction of shear on the interface did take place, might have influenced the cyclic capacity such that failure occured earlier (after less number of cycles) than if the tests had been performed such that the interface friction always had been in one direction (ie. tension). There were, however, no unique indications that such an effect was present.

As can be seen from the curves of skin friction versus pile displacement for the stress controlled tests in the Apendices, the behaviour is almost linearly elastic with only very small signs of hysteresis, almost up to point of failure. An interface shear module can be computed by taking the mobilized friction at failure and divide by the pile displacement normalized by the pile diameter. Figure 3.7 shows the computed moduli versus the undrained shear strength for the different tests. Values in the range from 4000 to 8000 kPa resulted, and with a tendency for clay from Stratum II to have a higher module than Stratum III at the same undrained shear strength.

One test differed drastically from the other tests with regard to development of pile displacement. In Test 6 the cyclic stress controlled tests were performed after the the two-way cyclic deformation controlled "degradation" tests, and the pile started to move upwards and permanent deformations resulted in the second parcel, with a maximum stress of about 0.9 of the static capacity. The increase in permanent deformation did not produce large uncontrollable uplift of the pile, but a small finite deformation for each cycle. The deformation rate seemed quite constant, until the next parcel where the stress level was increased. It seemed like the previous degradation tests had the impact on the interface such that the creep level was reduced.

The cyclic load program performed here did not allow for an investigation into the number of cycles to failure for certain stress levels. Each stress level (parcel) was kept for 100 cycles and then increased until failure occured within a parcel. The pile displacement was monitored during the cycling which gave information of the cyclic and average (mean) pile movement due to the applied stress on the pile-soil interface. As mentioned earlier, the failure of the pile generally happened suddenly with very few signs of change in the parameters measured. For most of the tests, however, one could see signs of increasing permanent displacement as the maximum stress during one cycle

reached the previous static capacity. When calculating the ratio of the maximum cyclic side friction to the ultimate static capacity for Test 5 through 10, at the time when signs of permanent pile displacement occured, vales ranging from 0.92 to 1.07 results, and for Test 4 and 11 values of 1.43 and 0.8 respectively. The tests performed indicated that the actual maximum stress during cycling controlled the behaviour of the pile and that the combination of the static and cyclic components did not have any serious influence on the pile behaviour within the number of cycles tested.

The measurements of total and pore pressure on the pile wall during tests indicated that the cyclic stress controlled testing did not produce any pore pressure build-up along the pile wall. The pore pressure measurement system used for Tests 4 through 9 was too slow in the response time in order to give reliable information, but the results from the tests with the new model pile were similar to the previous in this respect and indicated that the cyclic testing was not able to introduce enough shear stress into the soil mass in order to produce a pore pressure build-up. Theoretical modelling and calculations also supports this theory.

At the time of failure the pore pressure was in many cases seen to decrease, when at the same time the total pressure measurements showed increase. From an effective stress point of view, this behaviour seems quite strange, since there is reason to beleave that failure was caused by loss of mobilized friction due to a reduction in the effective pressure. From the measurements at the pile wall the opposite phenomenon seems to result as the effective pressure on the pile wall increased.

For more details on each test, reference should be made to the results in the Appendices A through J. The mentioned behaviour was quite general, however, and the measurements do not give a basis for traditional effective stress considerations with regard to mobilized skin friction during cyclic loading. The measurements of total and pore pressure on the field segment tests also gave similar conclusions.

In the random cyclic tests the findings and indications from the regular stress controlled tests were again present. No permanent or cyclic creep were seen in the first parcels where the maximum stress was below the ultimate static capacity. Even when the maximum stress was set to about the static capacity and 10% higher, no signs of permanent deformation or pressure build-up resulted. It must here be kept in mind that only one cycle of the 1250 cycles in one parcel had the maximum stress due to the Rayleigh distribution, which again implies that only a few cycles actually produced stresses above the static capacity. Both random tests produced failure with the same

stress combination, with the maximum stress of 1.2 times the ultimate static capacity. Common for both tests were that the pile failed at a stress lower than what had previously been produced in earlier cycles. The deformation was pronounced, but not larger than that the test could continue without interuption for several cycles. In this phase it was observed that the pile failed (large permanent deformation) at stress levels smaller than that of the initial failure. This level was again comparable to the residual level of the static tests.

As for the regular stress controlled tests the failure during the random tests gave an increase in the total pressure and a reduction in the pore pressure.

3.5 CYCLIC DISPLACEMENT CONTROLLED TESTS

After the cyclic stress controlled tests the pile was brought back to the original position and a time was allowed for reconsolidation. This time varied from a couple of hours to several days for the different tests.

The two-way displacement controlled tests consisted of parcels of 100 cycles of 10 seconds period with a prescribed cyclic deformation amplitude applied to the pile. This amplitude was kept constant throughout one parcel and increased for subsequent parcels. Generally the deformation amplitude for the first parcel was such that the mobilized friction was below the ultimate cyclic capacity, and for subsequent parcels the deformation amplitude was increased so that the ultimate capacity was reached and for the last parcels a residual friction level during large plastic slip developed.

These deformation controlled cyclic tests were often referred to as degradation tests since the pile was pulled (and pushed) beyond the elastic range and through a plastic range for numerous cycles in both tension and compression, which resulted in a reduction in the maximum mobilized friction and also in the residual level.

As can be seen in Table 3.1 the cyclic amplitudes for the consecutive parcels were generally 0.1, 0.2, 0.4, 0.6, 0.8, 1.0 and 2.0 mm. The ultimate friction was generally not reached in the first parcel with only 0.1 mm as maximum displacement. The friction versus displacement curves for these parcels were almost purely linearly elastic and repetitive. For the consecutive parcels the pile was displaced beyond the socalled

quake, or the pile displacement at ultimate friction. As the pile was pulled beyond this point the mobilized friction reduced towards a residual value, which was reached when the pile was pulled (pushed) far enough. As it reached the maximum displacement the direction of movement was reversed, causing a reduction in the mobilized friction similar to a static test.

The friction versus displacement curves for the cyclic displacement controlled tests were similar to the results from the static tests. For the second cycle the ultimate friction would be less than the virgin cycle to failure and the residual level also reduced with number of cycles. Most of the degradation of maximum mobilized interface friction occured in the first cycles in the parcel with deformations beyond the yield point.

When the deformation amplitude was increased the mobilized friction in first cycle would generally be higher than the peak friction in the last cycle in previous parcel. This might be a result of the increased load rate, since the period was kept constant at 10 seconds, or also that inbetween parcels a time of about ten minutes were spent to readjust the loading equipment. This time wold give a limited time for set-up effects to develop and may thus partly explain this regain in capacity. The previous level was generally reached after just a few cycles and a tendency to even continued degradation was sometimes seen.

In Table 3.1 the minimum residual level and the highest maximum peak are listed for all the displacement controlled tests, and the degradation is calculated as the difference between these two. For most of the tests the degradation was from 20% to 30 %. For one test, however, the maximum degradation was measured to 38% .

The pressure respons for the displacement controlled tests were more pronounced than for the stress controlled tests, most likely due to the two-way movement of the pile causing full reversal of the pile-soil interface friction. For the tests with the old model pile the pore pressure response was quite slow, but after some parcels (about 200 cycles) with failure and plastic slip the pore pressure is seen to increase. During the last parcels with large two-way displacements the pore pressure decreased again.

With the new model pile the pore pressure response was improved and indicated a quite rapid increase in the pore pressure after the initial cycles through failure. This increase in the pore pressure is accompanied by a slight increase in the total pressure also, resulting in almost no change in effective pressure. The development of the average total pressure was generally unpredictable and was therefore seen to increase slightly for some tests and decrease for others.

The cyclic behaviour of the pressures on the pile wall seemed quite consistent in that the total pressure generally increased as the pile was pulled up (tension) and decreased as the pile movement was reversed to compression. The total pressure generally had the maximum at maximum skin friction and minimum at peak skin friction in compression. (See for instance Figure A-14 in the Appendix C for Test 6). The magnitude of the cyclic total pressure also seemed to increase with increased pile displacement amplitude and was around one third of the peak skin friction of the same cycle.

The pore pressure, however, generally did not show any cyclic change for the old model pile. For the new pile some cyclic variation was seen in Test 10 (W310SC), although with seemingly no general trend. In Test 11 (W211SC) the pore pressure changes were fairly consistent from cycle to cycle with a tendency to have twice the frequency as the total pressure and skin friction. The peaks occured at times of peak skin friction (tension and compression) and lowest values at times of pile movement reversal.

The monitoring of the pressures on the pile wall might aid in the mechanistic explanation of the mobilization of interface friction in a qualitative way, but through the many tests performed within this program it has not been possible to relate pressure development to reduction in mobilized skin friction due to cyclic pile motion. In fact the skin friction sometimes reduced with increasing effective horizontal pressure measured at the pile wall. It must here be kept in mind that the pressures are measured at the pile wall, whereas the actual failure and critical zone might be located a small distance from the pile wall, where the pressures might show a drastically different behaviour. Attempts were made to check if a zone of clay material stuck to the pile wall after the pile was extracted from the pile chamber. Unfortunately this was impossible since the equipment was such that eventual material on the pile wall would be scraped off during the pulling process. Such a formation of a socalled "soil-cake" around the pile was seen for most of the small scale field segment tests.

3.6 CREEP AND RELAXATION TESTS

As can be seen in Table 3.1 several creep and relaxation tests were performed during the test program. A creep test was performed as a stress controlled test where the side friction on the pile was held constant (some percentage of ultimate capacity) while the pile displacement was monitored with time. In the relaxation test the pile displacement was controlled and the pile was pulled to a displacement and then held constant when the side friction reached a prescribed level (a percentage of the ultimate capacity) and the side friction was monitored with time.

For the creep tests almost no pile creep (after application of load) was seen before the side friction applied to the pile reached about 90% of the ultimate capacity. The pile displacement was in these cases monitored for about one hour. Increasing the side friction beyond this level resulted in quite fast developing pile displacements (abrupt pullout).

The relaxation tests indicated similar behaviour in that the side friction was able to more or less maintain at the initial level (pile was restrained from movement) when this initial level was below about 75-80% of the ultimate static capacity. When the pile was pulled to failure and then restrained for movement the side friction dropped quite drastically within the first minutes but seemed to stabilize around 70% of the ultimate level, even after 24 hours.

4. THEORETICAL WORK

4.1 GENERAL

In this section the results of the theoretical work performed at Veritas under the CNRD 13-2 project is presented. The work has been directed mainly towards the following items:

* Evaluation of pore pressure dissipation (set-up) in connection with pile installation in clayey soils in the field and in the laboratory tests

* Axial load-displacement relationships (t-z curves)

* Effect of pile flexibility on strength degradation

* Pore pressure generation around piles under cyclic loading and corresponding strength degradation

* Cyclic creep of piles under combined static and cyclic loading

In addition a few comments will be given to other factors influencing the deformation behaviour and capacity of tension piles, and to a limited extent comparisons between the 3" diameter segment tests and the laboratory model pile tests will be given. To some extent the results have been extrapolated to large piles, with special reference to the field test with the 30" diameter pile at West Delta Platform A.

4.2 PORE PRESSURE AND NORMAL STRESS GENERATION DURING INSTALLATION

4.2.1 Theoretical Estimates of Excess Pore Pressure

The best reference known to the authors on this item is the work by Randolph, Carter and Wroth (1979) based on cavity expansion theory and a modified Cam-clay model. For full displacement piles the following estimates of pore pressure and total normal stress is given:

$$\frac{\sigma_n}{s_u} = 5 \text{ to } 6$$

$$\frac{u}{s_u} = 3 \text{ to } 4$$

For pipe piles (non-plugged) the values of pore pressure and total normal stress will be lower dependent on the degree of cavity expansion caused by the pile wall thickness and the shape of the cutting shoe. The thickness of the cutting shoe of the 3" diameter segment pile indicates that at least a 20 to 30 % expansion relative to diameter of the cutting shoe could be expected which gives the following lower bound values for pore pressure and total stress generation due to pile installation:

$$\frac{\sigma_n}{s_u} = 4.5 \text{ to } 5$$

$$\frac{u}{s_u} = 2.5 \text{ to } 3$$

4.2.2 Comparison with Measured Values

The results of the laboratory model pile tests and the results of the 3" diameter segment pile tests have been compared with the above estimates for pore pressure and normal stress development due to pile installation. The results are summarized below.

Table 4.1 Theoretical vs. Measured Pressures on Pile Wall

TEST NO.	OPEN (O)	SHEAR	THEORY		MEASURED	
	CLOSED (F)	STRENGTH	(RANDOLPH et al.)		(BEST EST.)	
		s_u	u	σ_n	u	σ_n
		kPa	kPa	kPa	kPa	kPa
TEST 4	F	59	180-235	295-360	250	260
TEST 5	F	50	150-200	250-300	150	350
TEST 6	F	65	195-260	325-390	250	270
TEST 7	F	30	90-120	150-180	150	300
TEST 8	F	65	195-260	325-390	200	~50?
TEST 9	F	50	150-200	250-300	unrel.	
TEST 10	F	80	240-320	400-480	190	reinst.
TEST 11	F	55	165-220	275-330	200	50
TEST 12	F	40	120-160	200-240	330	280
TEST 13	F	60	180-240	300-360	120	80
DEPTH1/H1	F	18	55-75	90-110	110	?
DEPTH1/H2	F	18	55-75	90-110	91	?
DEPTH1/H3	F	18	55-75	90-110	105	?
DEPTH2/H1	O	27	67-81	120-135	115	86
DEPTH2/H2	F	27	81-108	135-162	197	?
DEPTH2/H3	O	27	67-81	120-135	67	?
DEPTH3/H3	O	34	85-102	153-170	165	163
DEPTH4/H1	O	45	112-135	202-225	290	295
DEPTH4/H2	O	45	112-135	202-225	115	?
DEPTH4/H3	O	45	112-135	202-225	320	?

The values listed in this table for measured total pressure increase are based on estimates of the horizontal pressures in the field prior to pile installation, which might be quite unreliable for both the laboratory and field tests.

This preliminary comparison indicates quite a scatter and discrepancy between the measured and predicted values for pore pressure and total normal pressure due to pile installation corresponding to the above described theory. The pore pressures, however, for the laboratory tests corresponds fairly well. For the segment tests the measured pore pressures are generally higher than the ones predicted. Only three values were found for the total pressures after installation from the segment test report.

4.3 SET-UP (PORE PRESSURE DISSIPATION)

4.3.1 Theoretical Initial Distribution of Pore Pressure

The initial distribution of excess pore pressure with radial distance from the pile surface has been assumed according to Randolph, Carter and Wroth (1979) as shown in Figure 4.1. For the laboratory model pile tests it has been assumed that the pore pressure approaches zero at the boundary of the sample, i.e. at a distance $r/r_o = 8$ . .

4.3.2 Consolidation Analysis Method

The analysis of set-up was performed with the finite element program OCEAN 2 (Rahman, 1976). The program allows linear and nonlinear consolidation analysis of axisymmetric problems with a given initial pore pressure distribution. However, all analyses were performed assuming constant coefficients of consolidation and isotropic permeability.

Due to the height to radius ratio of the models involved it was found acceptable to simplify the geometry to a radial single slice. The effect of top and bottom plate drainage in the laboratory model pile tests was investigated with a full model, however, the results indicated only minor differences over the instrumented section of the model pile, and all further analyses were thus performed with single slice models.

4.3.3 Consolidation Properties

The site characterization study and the comparative investigation of the material properties of the remoulded, reconsolidated material used in the laboratory model pile tests showed very significant differences in coefficients of consolidation. Based on Ertec's compression tests on samples from the three different strata the coefficient of consolidation could be expected to lie in the follwing ranges for the approximate stress conditions at the different test depths:

Stratum I	:	6 to 7 $m^2/year$
Stratum II	:	3 to 5 $m^2/year$
Stratum III	:	2 to 3 $m^2/year$

However, the compression tests carried out by NGI, NTH and McClelland indicated values considerably below Ertec's values. In fact their c_v values are approximately 1/3 to 1/5 of Ertec's values. The reason for this consistent difference is not understood.

Summarizing the results of the three other laboratories we get the following:

Stratum I	:	1.0 to 2.0 $m^2/year$
Stratum II	:	0.8 to 1.5 $m^2/year$
Stratum III	:	0.5 to 0.8 $m^2/year$

The remoulded, reconsolidated material used in the laboratory model pile tests showed considerably smaller values. For the stress ranges in question the following values were found most representative based on compression tests:

Stratum II	:	0.06 to 0.25 $m^2/year$
Stratum III	:	0.06 to 0.13 $m^2/year$

4.3.4 Comparison between Predicted and Measured Behaviour

In Figures 4.2 and 4.3 the results of the OCEAN2 analyses are presented for the laboratory model pile tests and the 3" pile segment tests respectively. For the laboratory tests pore pressure dissipation curves for three different c_v-values are presented. On the same plot the measured pore pressure dissipation for Test 12 and 13 are included.

Figure 4.3 also includes pore pressure dissipation curves for three different c_v-values and in addition two ranges for the theoretical location of "free draining boundary". Also on this plot the measured results from the segment tests are included. The weighted average of the measured pore pressure for the three test holes at three test depths were used for the measured results.

This comparison between the predicted and measured pore pressure dissipation clearly shows that the remoulded material used for the laboratory tests has much lower coefficient of consolidation than in the field. It also indicates that full dissipation was never reached for the laboratory tests,although the determination of initial pore pressure in the clay prior to model pile installation is somewhat uncertain.

4.4 LOAD - DISPLACEMENT (T-Z) RELATIONSHIP

4.4.1 Theoretical Single Slice Model

A theoretical prediction of the model pile behaviour as well as the segment pile behaviour under axial loading was performed and presented in Veritas Technical Note No. FDIV/23-82-03. The model is based on the assumption that the material follows a hyperbolic stress-strain relationship. The shear stress decreases from the value $\tau(r_o)$ at the pile surface to a value of $\tau(r)$ at a radial distance r from the center of the pile according to the following expression:

$$\tau(r) = \tau(r_o)\frac{r_o}{r}$$

where r_o = pile radius

The hyperbolic model gives the following relationship between the shear stress, τ, and the shear strain, γ :

$$\tau = \frac{\gamma}{\frac{1}{G_i} + \frac{\gamma}{\tau_{ult}}}$$

where G_i = initial shear modulus
τ_{ult} = shear strength

The following relationship can be shown to exist between the secant shear modulus and the the degree of shear stress mobilization, (i.e. $\frac{\tau}{\tau_{ult}}$) :

$$G_{sec} = G_i(1 - \frac{\tau}{\tau_{ult}})$$

The axial displacement δv of a section of a single slice with thickness δr subjected to shear stress τ will be:

$$\delta v = \frac{\tau}{G_{sec}}\delta r$$

By inserting the above expressions for $\tau(r)$ and $G_{sec}(tau)$ into the latter expression and integrating from $r = r_o$ to a certain distance R from the pile center, the following expression is derived:

$$v = \frac{\tau(r_o)r_o}{G_i}\ [\ \ln(\frac{R}{r_o} - \frac{\tau(r_o)}{\tau_{ult}}) - \ln(1 - \frac{\tau(r_o)}{\tau_{ult}})\ ]$$

Based on G_i - moduli extrapolated from the triaxial and simple shear test results from the laboratory investigations, which tended to lie in the range 80 to 180 times the undrained shear strength for the undisturbed material and in the range 180 to 225 times the undrained shear strength for the remoulded reconsolidated material, and by assuming an outer boundary for the single slice model at 8 r_o for the model pile and 20 r_o for the segment pile the shear stress versus axial displacement curves shown in Figures 4.4 and 4.5 could be derived for the two devices respectively. By further assuming α - values in the range 0.5 to 0.6 at the pile - soil interface the shaded ranges could be taken as a best estimate of normalized load-displacement behaviour under static loading. Thus the best estimate of failure displacement is in the order of .5 to 1.0 percent of the pile diameter for G_i/s_u values in the range 100 to 200.

The t-z curves measured in the laboratory model pile tests and the field segment tests fall reasonably well into this range.

Under cyclic loading the t-z curves tend to be more linear. This is especially so for displacement controlled tests where the skin friction degrades and the shear stress - displacement relationship approaches a parallelogram, but also load controlled tests with one way loading below failure show a close to linear behaviour with very little tendencies to hysteresis.

For all practical purposes an ideal elasto-plastic shear stress - displacement relationship seems to be a reasonable approximation.

4.5 EVALUATION OF PORE PRESSURE GENERATION UNDER CYCLIC LOADING

4.5.1 General

Cyclic loading of soils will generally lead to a gradual volume reduction if drainage is allowed to take place. Dependent on the permeability of the soil and the drainage conditions as well as the frequency and intensity of the cyclic shear stress variations a gradual pore pressure increase could be expected. This phenomenon can in the extreme case lead to a total loss of strength as the effective stresses in the soil will

decrease with increasing pore pressure. The extreme situation where the pore pressure equals the effective stress is called liquefaction, a well known situation in connection with earthquakes and loose sandy soils. It is also known as "failure in cyclic loading" in connection with offshore gravity platforms and has been demonstrated through sentrifuge testing as well as medium scale model tests.

For piles it could be expected that a similar phenomenon could take place. However, neither the laboratory model test nor the field segment tests carried out within this project showed any significant increase in pore pressure during the various cyclic load tests.

At the end of the pile test program a series of two-way triaxial tests were run on the remoulded material used in the pile test program as well as a comparative series on undisturbed material from stratum II and III.

The two-way triaxial tests on the remoulded material revealed that the pore pressure generation was slower in the remoulded West-Delta clay than what has been found for Drammen clay (an extensively investigated material in this connection) and the cyclic strength is thus better for the WD-clay. The results of the cyclic tests are presented in Appendix K.

4.5.2 Analysis Model

For piles the shear stress level decreases with increasing distance from the pile. In a single slice model as shown in Figure 4.6 the shear stress decreases according to the following expression.

$$\tau(r) = \tau_o \frac{r_o}{r}$$

where $\tau(r)$ = shear stress at distance v from pile center

τ_o = shear stress at pile wall

r_o = radius of pile

r = distance from pile center

If the clay strength is constant in the soil mass the shear stress ratio can be expressed as

$$\frac{\tau(r)}{s_u} = \frac{\tau_o}{s_u} \frac{r_o}{r}$$

However, driven and push in piles will normally experience set-up effects which tend to increase the shear strength of the soil in the surrounding of the pile. Based on the work of Randolph, Carter and Wroth (1979) the increase in undrained shear strength could be as illustrated in Figure 4.7.

For the fully consolidated situation the undrained shear strength can be expressed approximately as:

$$s_u(r) = s_{uo} + \Delta s_{uo} \frac{r_o}{r}$$

where s_{uo} = undrained shear strength prior to pile installation

Δs_{uo} = increase in shear strength at pile surface after set-up

This leads to the following expression for stress level:

$$\frac{\tau(r)}{s_u(r)} = \frac{\tau_o}{(s_{uo} + \Delta s_{uo}\ r_o/r)} \left(\frac{r_o}{r}\right)$$

Based on the above expression for stress level and the test results from the two-way cyclic triaxial tests on the WD-clay a pore pressure generation model can be established.

The computer program OCEAN2 (Rahman, 1976) which is an axial symmetric finite element program for analysis of combined pore pressure generation and dissipation is available at VERITAS. The program contains a pore pressure generation model developed by Martin (1975) expressing the pore pressure generation as:

$$u_g = \sigma_{vo}' \left[\frac{1}{2} + \frac{1}{\pi}\sin^{-1}(2C^{\frac{1}{\theta}} - 1)\right]$$

where:

u_g = generated pore pressure

σ_{vo}' = initial mean normal effective stress for trixial test or the initial vertical effective stress for simple shear conditions.

C = N/N_l

N = Applied number of cycles

N_l = number of cycles required to develop $u_g = \sigma_{vo}'$ (i.e. initial liquefaction in sand)

θ = an empirical constant

The expression is shown graphically in a normalized form in Figure 4.8.

Comparing with the results of the two-way triaxial tests on WD clay (see Appendix K) it is seen that the pressure generation curves are of similar shape, but only 50 to 60% of the consolidation stress is generated as pore pressure before the samples undergo excessive cyclic deformations.

The pore pressure generation curves from the triaxial tests were replotted into the OCEAN2 pore pressure generation model. A value of θ = 1,0 was chosen as a best fit curve and "the number of cycles to liquefaction", N_l was adjusted to give a reasonable correspondence between the test data and the model curve.

The results are shown in Figure 4.9, where selected points from the triaxial tests were plotted vs the relative number of cycles and show an acceptable correspondence for all tests for θ values in the range 1.0 to 1.5.

The evaluated "number of cycles for liquefaction" has been plotted vs the cyclic shear stress level τ / s_u in Figure 4.10.

A curve fit has been made giving

$$\log N_l \approx 7.6 \left(1 - \frac{\tau}{1.05\, s_u}\right)$$

or

$$N_l \approx 10^{7.6\left(1 - \frac{\tau}{1.05\, s_u}\right)}$$

Combination of the above expression with the expression for stress level gives the following relationship between the cyclic stress level in the soil mass and the number of cycles to generate 100% pore pressure.

$$N_l(r) = 10^{7.6\left(1 - 0.95 \frac{r_o}{r} \frac{\tau_o}{\left(s_{uo} + \Delta s_{uo} \frac{r_o}{r}\right)}\right)}$$

4.5.3 Finite Element Model

The laboratory model pile test has been evaluated with the derived pore pressure generation model. The test was modelled by a single slice consisting of 11 elements from the pile surface to an outer boundary set at 8 times the pile radius. The nodal points were placed at relative distances r / r_o as follows:

NP No.	1	2	3	4	5	6	7	8	9	10	11	12
r / r_o	1.00	1.05	1.10	1.20	1.40	1.70	2.10	2.60	3.4	4.5	6.0	8.0
NP No.	13	14	15	16	17	18	19	20	21	22	23	24

The laboratory model pile test was simulated as drained at the outer boundary (i.e. nodal points 12 and 24).

4.5.4 Soil Consolidation Parameters

The soil parameters involved in the analysis in addition to the pore pressure generation model are:

k_r = the radial permeability
m_v = the radial compressibility of the soil
γ_w = the unit weight of water

These parameters are combined to give the radial coefficient of consolidation c_{vr}

$$c_{vr} = \frac{k_r}{m_v \cdot \gamma w}$$

c_v has been determined by Ertec, McClelland, NGI and NTH for undisturbed material and by VERITAS for the remoulded and reconsolidated material as commented on previously.

For the undisturbed material c_v-values in the range 0.5 to 3 m^2/year have been reported while the remoulded and reconsolidated material gave c_v values in the range 0.06 to 0.25 m^2/year.

4.5.5 Simulation of Cyclic Loading

Two-way cyclic loading was performed in the laboratory pile tests. The number of cycles was restricted. The computer runs simulates a series of 100 cycles which is considered sufficient to see any significant effects of pore pressure generation.

The cyclic shear stress levels were varied within reasonable limits and the effect of shear strength increase close to the pile due to set-up was evaluated by analysing two cases:

a) uniform shear strength s_{uo} with stress ratios
τ/s_{uo} = 0.4,0.6,0.7

b) $s_{uo}(r) = s_{uo} + \Delta s_{uo} \frac{r_o}{r}$
with Δs_{uo} being 0.6 s_{uo} and τ/s_{uo} = 0.8,1.0,1.2

For these cases the following "number of cycles to liquefaction", N_l, were evaluated and introduced in the FEM analysis.

Table 4.2 Number of cycles to liquefaction, N_l

Node no.	1	2	3	4	5	6	7	8	9	10	11	12
r_o/r	1.00	0.952	0.909	0.833	0.714	0.588	0.476	0.385	0.284	0.222	0.167	0.125
a) τ/s_{uo}												
0.4	51522	70896	94364	> 100000	...	...	...	...	...	...	...	...
0.6	1853	2992	4594	9805	32133	> 100000	...	...	...	...	...	...
0.7	67	126	223	614	2992	15985	70896	> 100000	...	...	...	...
b) τ/s_{uo}												
0.8	9772	12597	15943	24658	51619	> 100000	...	...	...	...	...	...
1.0	1223	1680	2255	3890	9795	28960	84480	> 100000	...	...	...	...
1.2	153	224	319	614	1859	6826	24667	77678	> 100000	...	...	...

The results of the analysis for the 1" diameter laboratory model pile are shown in Figure 4.11 as pore pressure ratio generated by 100 uniform cycles versus cyclic stress level, and shows that the generation of pore pressure is mainly a function of the cyclic shear stress level.

For the 1" diameter laboratory pile consolidation effects may have a certain influence on the accumulation of pore pressure, which may also be so for the 3" diameter segment test. However, for large diameter piles like the 30" test pile at West Delta and prototype piles with diameters in the range 60" to 120" the analysis indicates that the consolidation effects during a single storm will be insignificant for piles in clay.

With maximum cyclic stress levels below ± 0.25 (i.e. $\tau_c/s_{uo} < \pm 0.25$ at the pile surface) the predicted pore pressure generation will be insignificant. This stress level corresponds fairly well with the design criteria for tension piles and only a limited number of cycles will approach or exceed this stress level.

4.5.6 Comparison With Measured Behaviour

The results from the laboratory model pile tests and the 3" diameter segment tests at West Delta seem to confirm the theoretical predictions. Only minor pore pressure generation was observed during cyclic loading of these pile segments. The reason is believed to be the relatively moderate α-factors resulting in low cyclic stress levels being imposed on the soil elements adjacent to the pile.

4.6 DEGRADATION MODELS

4.6.1 General

Cyclic loading beyond failure leeds to degradation of the skin friction. Based on the results of the laboratory model pile tests as well as the 3" diameter segment tests it was concluded that for two-way cyclic loading degradation of the peak ultimate capacity was in the order of 25 to 40 %, and that most of the degradation takes place during the first 10 to 20 cycles.

However, tests with one-way cyclic loading showed degradation after failure as well. The shear stress level where excessive displacement initiated reduced gradually towards the residual static skin friction and some tests approached the fully degraded skin friction as determined from displacement controlled testing. This could clearly be seen from the random cyclic stress controlled tests with the laboratory model pile.

It has further been noted that one-way static and cyclic loading beyond failure leads to a change in shear-stress - displacement behaviour compared with the two-way tests. In the laboratory model pile tests a peak friction was always observed under two-way cyclic loading, even after severe degradation of the peak strength. Under one-way cyclic loading beyond failure and in static tests starting from a tensile stress without previous loading to failure in compression the peak was not observed. The explanation for this behaviour could be that peak friction is connected to full shear stress reversal and reorientation of the clay mineral plates at the failure surface.

4.6.2 The DRIVE 15 Degradation Model

The degradation model included in DRIVE 15 (a program developed by Ertec) requires full two-way reversals of the direction of slip to start degradation. A degradation factor λ is applied to the ultimate plastic skin friction in the following way:

$$f_{n+1} = (1 - \lambda) * (f_n - f_{min}) + f_{\min}$$

where $f_1 = f_{ult}$ = ultimate (peak) skin friction

f_{n+1} = degraded skin friction after n cycles of of full slip reversals

$f_{\min}$ = fully degraded skin friction

Figure 4.12 shows how the model works for a case with 30 percent degradation and various λ values.

4.6.3 Proposal for Extended Degradation Model

The general experience from laboratory model tests and the 3" diameter segment tests is that also one-way loading beyond failure will lead to degradation of skin friction.

It is believed that the DRIVE 15 degradation model could easily be modified to cover this effect.

4.7 EFFECT OF PILE FLEXIBILITY ON DEGRADATION

4.7.1 Analysis with DRIVE 15

A few runs were carried out with the program DRIVE 15 with a two-way degradation model as described in Section 4.6 in order to evaluate the effect of degradation on a flexible pile.

The pile was modelled with 20 elements as a 67 m long pile, outer diameter 30" and a wall thickness of 0.5". The skin friction was assumed close to the values recommended by Ertec according to API. (Ertec's Volume I report, Plate 31, using an α-value of 1.0). Degradation values were chosen as follows:

$$f_{\min} = 70\% \ of \ f_1 \ , \ \lambda = 30\%$$

The loading program consisted of 10 cycles stepping from zero load to 1/3 of the ultimate capacity, Q_{ult}, then to 2/3 of Q_{ult} which gives a total safety factor of 1.5, back to 1/3, to zero, to 1/3, to 2/3, to 1/3 and so on for 10 cycles. The results showed that degradation of skin friction only took place in the upper 10 to 15 m of the pile under loading conditions as described.

The effect of the local degradation of skin friction in the upper part was small seen in relation to the total capacity of the pile. Only 3 to 5% reduction took place during the first cycle as shown in Figure 4.13.

4.7.2 Consequences of Other Degradation Models and Boundary Conditions

As the degradation problem was found to be very limited using the DRIVE 15 two-way degradation model it was decided not to go further with investigations in that direction. It is, however, obvious that a one way degradation model may have stronger influence on the reduction of total capacity.

The pile length and the relative axial deformation required to achieve failure will certainly affect the degree of degradation and so will the load level for (or safety factor) and the distribution of load amplitudes. Also the distribution of skin friction with depth may have a significant influenc, and capacity degradation must be expected to be more severe in case of a uniform shear strength with depth.

For normally consolidated deposits it is, however, not expected that degradation of skin friction will introduce serious capacity reductions. Most of the pile capacity will be located in the lower half of the pile where the degree of mobilization of skin friction is low.

4.8 PILE CREEP ANALYSIS

4.8.1 General

One of the major concerns in tension pile design is the possibility of cyclic and static creep under combined static and cyclic loading. One of the objectives of the laboratory model pile test programme was to investigate the response of a pile element subjcted to various combinations of static and cyclic loads and possibly quantify creep effects.

As outlined in Section 3 static creep does not seem to represent a major problem. The static longterm pretension from a TLP is expected to cause average mobilization of skin friction of less than 30%. This is based on the assumption that a total safety factor of 1.5 or more is applied to the maximum load and that the environmental component of the axial load is of the same order of magnitude as the pretension force. At static load levels of this magnitude no tendency of creep deformations were observed.

Small cyclic creep displacements were observed in all tests with one-way loading. For most of the tests, however, cyclic creep displacements developed before failure were small and a gradual accumulation of axial displacements started to develop first at relatively high stress levels.

An elastic pile in a soil where the undrained shear strength increases considerably with depth (as in the case of the West Delta area and all areas with normally consolidated clay deposits) will mobilize high static and cyclic shear stresses at the pile-soil interface down to a considerable depth.

The model pile tests indicates clearly that a stress redistribution will have to take place as the top part of the pile starts to creep.

In order to study the effects of cyclic creep on a long elastic pile, an elasto-viscoplastic t-z model was developed implemented in the computer program CRAPIL, **CR**eep Analysis of **PIL**es. (See Appendix L).

Parametres involved in the soil model can be derived from laboratory model pile test or segment pile tests in the field.

4.8.2 T-Z Creep Model

The elastic, visco-plastic soil model shown in Figure 4.14 was considered relevant for simulation of creep between a pile element and the soil for a pile subjected to tensile cyclic loading.

The model consists of the standard spring element (spring constant K) and friction element (capacity R_1) in series required for simulation of ideal elasto-plastic behaviour. Coupled in series with these elements is a creep element consisting of a friction element (capacity $R_2 < R_1$) and a dashpot (damping constant C) coupled in parallel. When subjected to a time varying axial force P(t) the model will undergo a displacement $\delta(t)$.

The model's behaviour can be described as follows (see Figure 4.14):

When subjected to loads lower than R_2 the dashpot will not undergo any displacements and the model will displace elastically due to the spring K. For loads exceeding R_2, an additional time dependent creep displacement will start to develop in the dashpot. When the load reaches the value R_1 the system will slide. These three load stages can be described in the following way:

First load stage: $P(t) \leqslant R_2$

$$\delta = \frac{P(t)}{K} \tag{4.8.2.1}$$

Second load stage: $R_2 \leqslant P(t) \leqslant R_1$

At this load stage the spring and damper are acting in series, so:

$$\delta = \frac{P(t)}{K} + \delta_{damper}$$

Here δ_{damper} can be found considering the damper C and the slider R_2 coupled in parallel, so:

$$C\,\dot{\delta}_{damper} + R_2 = P(t)$$

$$\delta_{damper} = \frac{1}{C}\int_{t_1}^{t_2} P(t)dt - \frac{R2}{C}(t_2 - t_1)$$

then

$$\delta = \frac{P(t)}{K} + \frac{1}{C}\int_{t_1}^{t_2} P(t)dt - \frac{R2}{C}\ (t_2 - t_1) \qquad (4.8.2.2)$$

Practically this can be interpreted as the sum of an elastic and a creep displacement. The latter is the time integral of the force exceeding R_2 divided by the damping constant.

Third load stage: $P(t) \geqslant R_1$

The system will slide for loads greater than R_1 .

The proposed creep model is illustrated with the following example:

Wave forces represent the dominating environmental load on a TLP structure. In a storm the occurrence of individual waves is random with small and large waves interspersed. For practical reasons, however, the cyclic wave loads have been sorted in blocks (or parcels) with constant amplitude and the blocks arranged in order of increasing amplitude.

The wave parcels and the number of waves contained in the different parcels are selected to fit closely to a Rayleigh distribution of amplitudes. This is an acceptable method provided the response spectrum is narrow banded and there is a quasi-linear relationship between the wave heights and the tether loads of a TLP.

A 67 m long, 30" diameter pipe pile with wall thickness 1/2" was analyzed with the DRIVE15 computer program. The skin friction was selected according to Ertec's recommended distribution in their report on the site characerization. The pile was loaded with a cyclic tensile load beginning with a pretension load of 33% of the pile's capacity and then varying the load amplitude in a series of steps between ±5% to ±40% of the pile's capacity. The shear stress mobilization along the pile due to the different loads is shown in Figure 4.15.

Figure 4.16 shows the degree of mobilization of skin friction for these load variations caused by axial load variations as shown in Figure 4.17. The stress situation at pile station number 8 was selected for evaluation with the outlined creep model (see Figure 4.18).

The following parameters were selected for the creep model:

R_1 = 171 kN
R_2 = 70% of R_1
Static load level = 52% of R_1
K = R_1 / (0.01 D_{pil}) = 224.4 kN/cm
C = 10.000 kNs/cm

The value of the damping constant C was estimated very roughly from laboratory test results.

N = 1800 cycles
Storm duration = 6 hours
Wave period = 12 seconds

The pile load is represented by a static pretension force on which a sine variation of the wave force is superimposed.

$$P(t) = F_{pret} + F_o \sin\omega t \qquad (4.8.2.4)$$

The first two wave parcels shown in Figure 4.15 do not exceed R_2 and will not introduce creep. Figure 4.19 shows the total creep displacement after application of the total set of wave parcels.

4.8.3 Creep Analysis of Elastic Piles

The creep displacements calculated for a single pile element will not develop for a pile element being part of an elastic pile. As soon as creep is introduced in one pile element a redistribution of forces to the other pile elements will start.

This effect could be modelled in a time step analysis, stepping with fractions of the wave period through a complete storm. Keeping in mind the relatively long storm duration and thus the large number of cycles this approach would be extreemely time consuming.

Instead the following approach has been made:

* Sort the storm introduced load variations of the pile head load into wave parcels as outlined previously.

* Sort the storm introduced load variations of the pile head load into wave parcels as outlined previously.

* Calculate the distribution of shear stress down along the pile for the maximum load, the minimum load and the pretension load starting with the first cycle in the firts wave parcel.

* Assume a sine variation of the cyclic shear stress between the maximum value and the minimum value. If the maximum value exceeds the creep level (corresponding to R_2) and/or the minimum value goes below the creep level on the negative (compression) side, calculate the resulting time integral of the stress exceeding the creep level and the corresponding creep displacement caused by one cycle.

* Assume the pile to be fixed. The creep displacement caused by one cycle will now introduce a reduction in shear stress as the elastic spring will relax. In order to speed up the analysis process more than one cycle will have to be considered at a time. The number of cycles ΔN that can be accounted for in one step must be connected to the amount of stress reduction that can be tolerated without changing the overall force distribution significantly.

* In CRAPIL the tolerance is related to the ultimate capacity (R_1) by assuming a percentage, P (say 10%), as acceptable. The element showing the largest relative stress reduction is found and the allowable number of cycles per step ΔN is calculated as

$$\Delta N = \frac{P\ R_1}{\Delta F}$$

* For this ΔN the shear stress reduction is calculated for all elements with creep and a reduced spring stiffness is evaluated:

$$K_n = \frac{F - \Delta F}{\delta}$$

and the pretension load is again applied to the pile head leading to a new stress distribution with an increased pile displacement approximately simulating the creep due to ΔN cycles.

* Upon this new redistributed stress situation the maximum, the minimum and the pretension load are applied again with original spring stiffnesses. Again the corresponding creep displacements due to one cycle is calculated and a new ΔN determined.

* The procedure is continued in this way until the sum of ΔN's equals the number of cycles in the first wave parcel. Then the load level is increased corresponding to the second parcel and the procedure is again continued until all cycles and all the wave parcels have been treated.

4.8.4 Sample Calculations

A number of CRAPIL runs have been made in order to illustrate the effect of pile creep and to some extent evaluate the possible effects of pile creep on distribution of shear stress and pile head displacement.

It must be stated here that the two parameters (constants) C and R_2 controlling the creep rate and the creep limit are difficult to determine and may be a too simplified representation of the creep mechanism. Nevertheless, a comparison with the data from the segment tests and the laboratory model pile tests have been made, showing that at least an approximate representation of the measured performance is possible.

The pile head loads were selected in order to simulate a 6 hour storm with a Rayleigh distribution of the load amplitudes being assumed.The waves were sorted in 8 parcels with increasing amplitude as can be seen from Table 4.3.

The extreme cyclic load amplitude (in parcel 8) was always set equal to the pretension load. Thus the extreme load variation was set to minimum zero axial load to maximum twice the pretension load level. The pretension axial load was varied in order to simulate the effect of safety factor variations. Cases were run with safety factors of 1.2, 1.3, 1.5 and 2.0. (See Table 4.3).

LOAD DATA:
****

LOAD CARD NO.	NO. OF CYCLES IN PARCEL	PRETENSION OR STATIC FORCE	MAX. LOAD IN WAVE PARCEL	MIN. LOAD IN WAVE PARCEL	WAVE PERIOD
1	1110	0.1200E+01	0.1470E+01	0.9300E+00	12.00
2	500	0.1200E+01	0.1720E+01	0.6800E+00	12.00
3	100	0.1200E+01	0.1900E+01	0.5000E+00	12.00
4	50	0.1200E+01	0.2000E+01	0.4000E+00	12.00
5	20	0.1200E+01	0.2090E+01	0.3100E+00	12.00
6	12	0.1200E+01	0.2160E+01	0.2400E+00	12.00
7	6	0.1200E+01	0.2250E+01	0.1500E+00	12.00
8	2	0.1200E+01	0.2370E+01	0.3200E-01	12.00

Load data for case with safety factor 2.0

LOAD DATA:
****

LOAD CARD NO.	NO. OF CYCLES IN PARCEL	PRETENSION OR STATIC FORCE	MAX. LOAD IN WAVE PARCEL	MIN. LOAD IN WAVE PARCEL	WAVE PERIOD
1	1110	0.1600E+01	0.1960E+01	0.1240E+01	12.00
2	500	0.1600E+01	0.2290E+01	0.9100E+00	12.00
3	100	0.1600E+01	0.2530E+01	0.6700E+00	12.00
4	50	0.1600E+01	0.2660E+01	0.5400E+00	12.00
5	20	0.1600E+01	0.2780E+01	0.4200E+00	12.00
6	12	0.1600E+01	0.2880E+01	0.3200E+00	12.00
7	6	0.1600E+01	0.3010E+01	0.1900E+00	12.00
8	2	0.1600E+01	0.3160E+01	0.4000E-01	12.00

Load data for case with safety factor 1.5

LOAD DATA:
****

LOAD CARD NO.	NO. OF CYCLES IN PARCEL	PRETENSION OR STATIC FORCE	MAX. LOAD IN WAVE PARCEL	MIN. LOAD IN WAVE PARCEL	WAVE PERIOD
1	1110	0.1850E+01	0.2260E+01	0.1440E+01	12.00
2	500	0.1850E+01	0.2650E+01	0.1050E+01	12.00
3	100	0.1850E+01	0.2920E+01	0.7700E+00	12.00
4	50	0.1850E+01	0.3070E+01	0.6200E+00	12.00
5	20	0.1850E+01	0.3210E+01	0.4800E+00	12.00
6	12	0.1850E+01	0.3330E+01	0.3700E+00	12.00
7	6	0.1850E+01	0.3470E+01	0.2200E+00	12.00
8	2	0.1850E+01	0.3640E+01	0.5000E-01	12.00

Load data for case with safety factor 1.3

LOAD DATA:
****

LOAD CARD NO.	NO. OF CYCLES IN PARCEL	PRETENSION OR STATIC FORCE	MAX. LOAD IN WAVE PARCEL	MIN. LOAD IN WAVE PARCEL	WAVE PERIOD
1	0	0.2000E+01	0.0000E+00	0.0000E+00	0.00
2	1110	0.2000E+01	0.2440E+01	0.1560E+01	12.00
3	500	0.2000E+01	0.2870E+01	0.1130E+01	12.00
4	100	0.2000E+01	0.3170E+01	0.8300E+00	12.00
5	50	0.2000E+01	0.3330E+01	0.6700E+00	12.00
6	20	0.2000E+01	0.3480E+01	0.5200E+00	12.00
7	12	0.2000E+01	0.3600E+01	0.4000E+00	12.00
8	6	0.2000E+01	0.3760E+01	0.2400E+00	12.00
9	2	0.2000E+01	0.3950E+01	0.5000E-01	12.00

Load data for case with safety factor 1.2

Table 4.3: Rayleigh Distribution of Load Amplitudes for Wave Parcels - Example Problem with CRAPIL

The pile used in the analysis was the same 30" diameter pile of 67 m length and with a wall thickness of 1/2". The skin friction was assumed as in previous calculation with DRIVE 15. The ultimate capacity of the pile was for these assumptions calculated to 4.8 MN.

Figure 4.20 shows the results of cyclic creep on the redistribution of mobilized shear stress due to pretension along the pile. Figure 4.20.a shows the shear stress distribution prior to cyclic loading, while Figure 4.20.b shows the distribution of skin friction at the end of the simulated 6 hour storm. A cleasr redistribution can be seen, leading to reduced shear stresses under pretension load in the upper part. The effect of the safety factor variations can be seen as well.

Figure 4.21 shows the pile head displacements as a function of number of cycles and safety factor. The cyclic creep tends to introduce a gradual vertical pile head creep which is seen to be significantly affected by the safety factor level.

The described analyses were all run with a dashpot constant C = 1.000 MNs/m, a creep ratio, R_2/R_1 of 0.7 and a quake of 1% of the pile diameter. As the selection of these parameters, and especially the former two, is connected with considerable uncertainty the case with a safety factor of 1.2 was selected for a few parametric variations. The dashpot constant was reduced by a factor 10 in one run and the creep ratio was varied. The results of these parameter changes are shown in Figure 4.22, showing development of axial pile head creep in Figure 4.22.a and the variation of shear stress distribution in Figure 4.22.b.

As mentioned above the selection of the parameters for the elastic, visco-plastic creep model is connected with much uncertainty. Nevertheless, the parametric evaluation indicates that creep displacements of the pile head will be small as long as the safety level is adequate. Still a considerable redistribution of shear stresses in the top part can be expected to result from storm loading.

The dashpot constant, C, is dependent on the pile element size, the α- factor and certainly other parameters. The backcalculation of C is dependent on the choice of the creep ratio as well. Basically C can be evaluated from segment tests with load control. It should be noted that C will depend also on the load period.

5. REFERENCES

API, Amercan Petroleum Institute, 'Recommended Practice for Planning , Designing and Constructing Fixed Offshore Platforms.' 12th Edition, 1981.

DnV, DET NORSKE VERITAS, 'Tension Pile Study - Comments to the Segment Test Program.' Technical Note FDIV/23-82-02.

ERTEC INC., 'Site Investigation and Doil Characteriztion Study at Block 58 West Delta Area Gulf of Mexico.' Report no. 82-200-1, 1982, for Conoco Norway Inc.

HOLMQUIST, D. and MATLOCK, H. (1976), 'Resistance - Displacement Relationship for Axially Loaded Piles in Soft Clay.' OTC paper 2474, Houston, Texas 1976.

KVALSTAD, T.J. and DAHLBERG, R. (1980), 'Cyclic Behaviour of Clays as Measured in Laboratory.' Proc. of the Interntl. Symposium on Soil under Cyclic and Transient Loading. Swansea, 7-11 January 1980.

MARTIN, P.P. (1975), 'Non-Linear Methods for Dynamic Analysis of Ground Response.' Ph.D. Thesis, University of California, Berkeley.

MATLOCK,H. and FOO, S.H.C. (1979), 'Axial Analysis of Piles using a Hysteretic and Degrading Soil Model.' Proc. Conference on Numerical Methods in Offshore Piling. I.C.E., London. pp. 99-106.

RAHMAN, M.S. (1977), 'Analyses for Wave-Induced Liquefaction in Relation to Offshore Construction.' Ph.D. Thesis, University of California, Berkeley.

RANDOLPH, M.F., CARTER, J.P. and WROTH, C.P. (1979), 'Driven Piles in Clay - the Effects of Installation and Subsequent Consolidation.' Geoteqnique 29, No.4, 361-393.

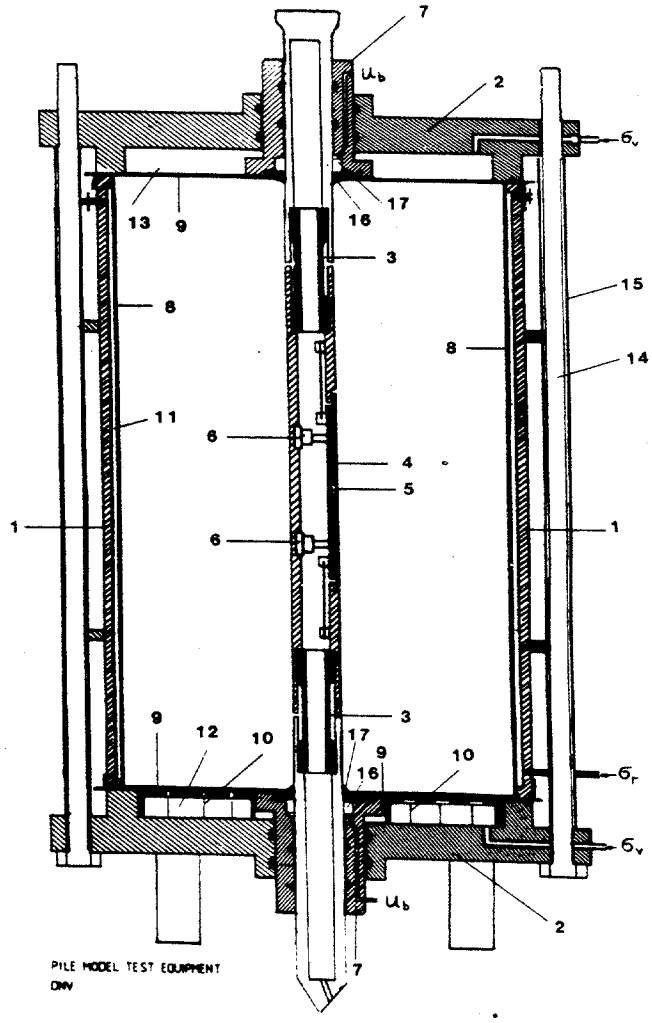

1 - Confining Cylinder
2 - Top and Bottom Plate (Identical)
3 - Axial Load Transdusers for skin friction measurement
4 - Total Pressure Cell
5 - Porous Stone Filter
6 - Load Cells for total pressure measurement
7 - Top and Bottom Center Bearing sealed with rubber "o-rings"
8 - Axially Reinforced Rubber Membrane for application of radial confining pressure
9 - Circular Rubber Membranes for application of vertical confining pressure
10 - Perforated Base Plate
11 - Radial Pressure Chamber
12 - Bottom Pressure Chamber
13 - Top Pressure Chamber
14 - Lock Bolt
15 - Guide Cylinder
16 - Back Pressure Chamber
17 - Hard Rubber Seal

CNRD 13-2 TENSION PILE STUDY		Proj.No.
Pile Model Test Chamber with Model Pile		Scale 1:4
DET NORSKE VERITAS Geotechnical Laboratory	Drawn by Approved	Date Fig.No. 2.1

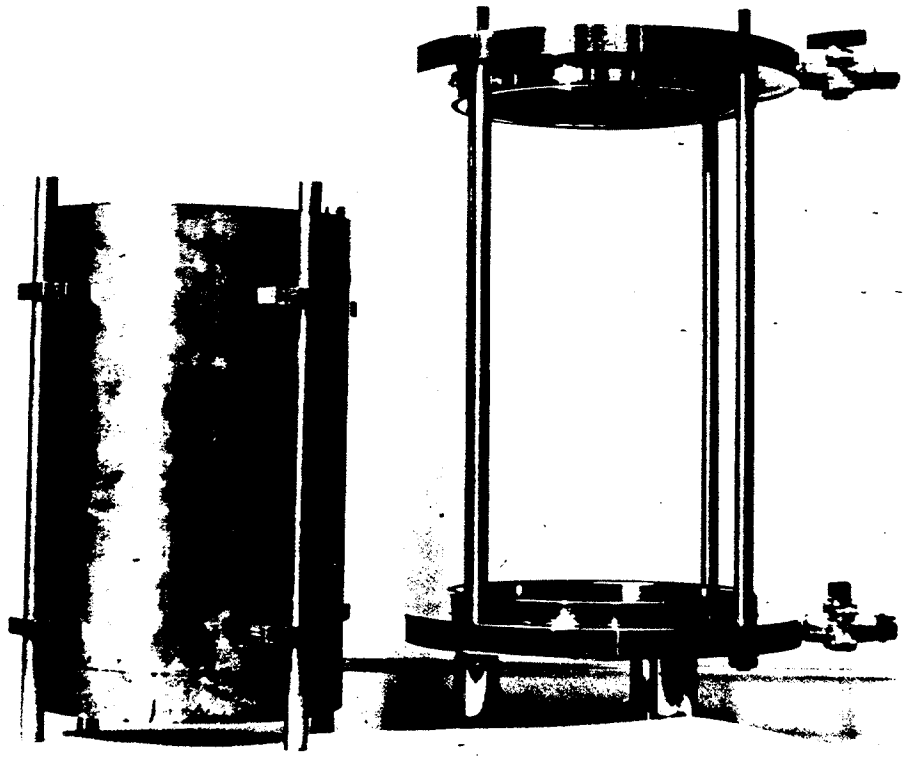

CNRD 13-2 TENSION PILE STUDY LABORATORY MODEL PILE TESTS		
Model Pile Test Equipment, Pressure Chamber		Scale
DET NORSKE VERITAS Geotechnical Laboratory	Drawn by	Date
	Approved	Fig. No. 2.2

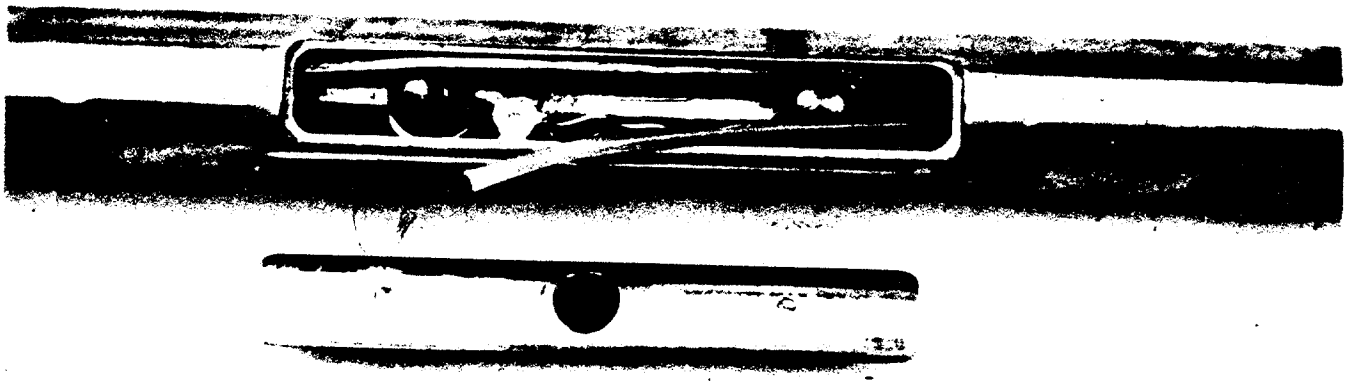

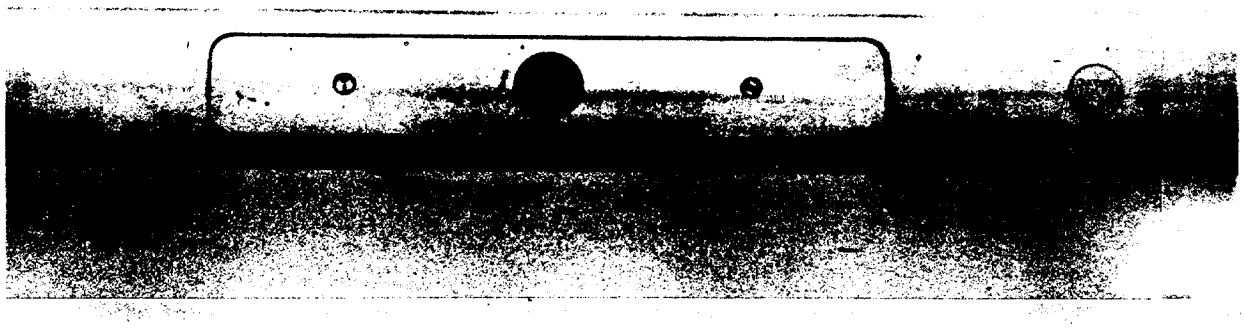

Model pile test equipment: Close view of total normal stress transducer

CNRD 13-2 TENSION PILE STUDY LABORATORY MODEL PILE TESTS

		Scale
DET NORSKE VERITAS Geotechnical Laboratory	Drawn by	Date
	Approved	Fig.No. 2.3

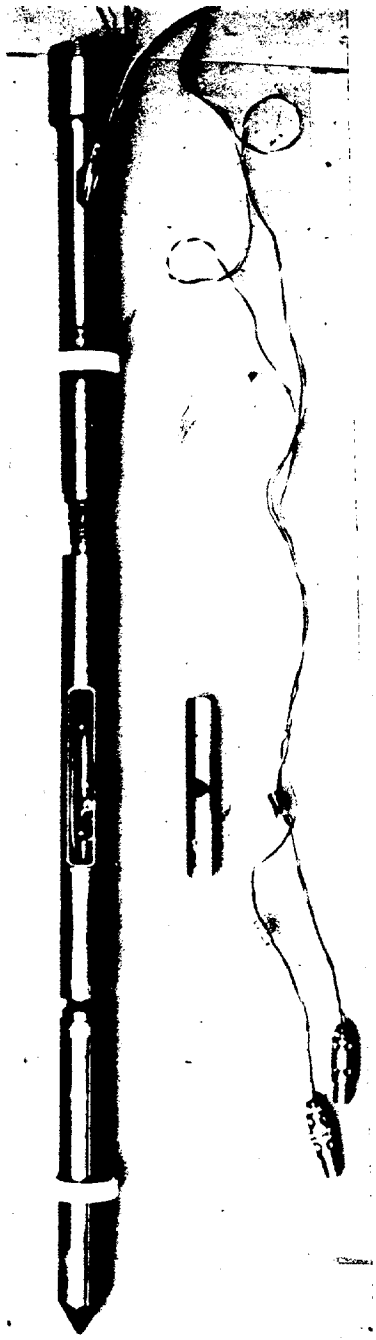

Model pile

CNRD 13-2 TENSION PILE STUDY LABORATORY MODEL PILE TESTS

		Scale
DET NORSKE VERITAS Geotechnical Laboratory	Drawn by	Date
	Approved	Fig. No. 2.4

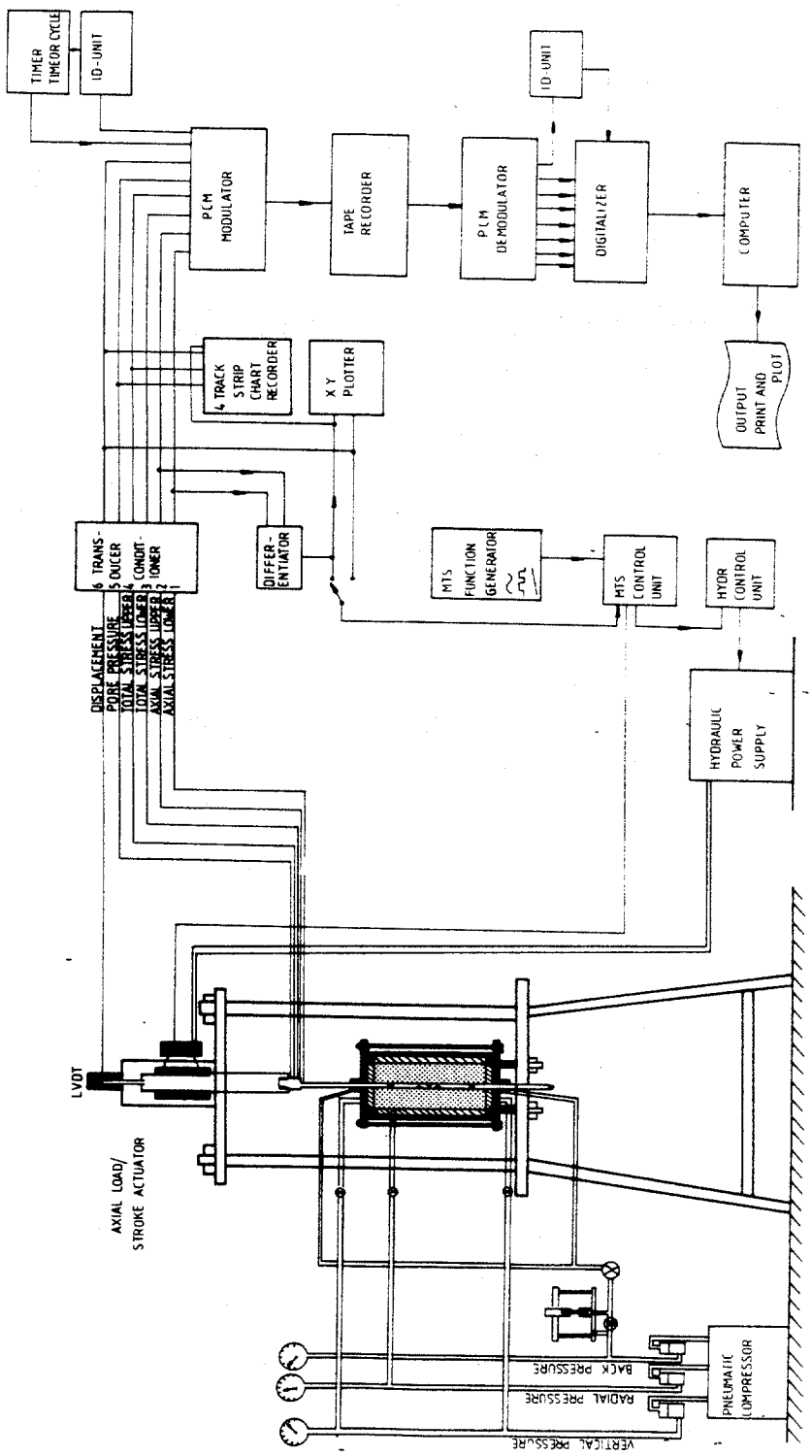

CNRD 13-2 TENSION PILE STUDY	Proj.No.
Test Set-up with indication if Instrumentation and data aquisition system	
DET NORSKE VERITAS Geotechnical Laboratory	Drawn by Approved
	Fig.No. 2.5

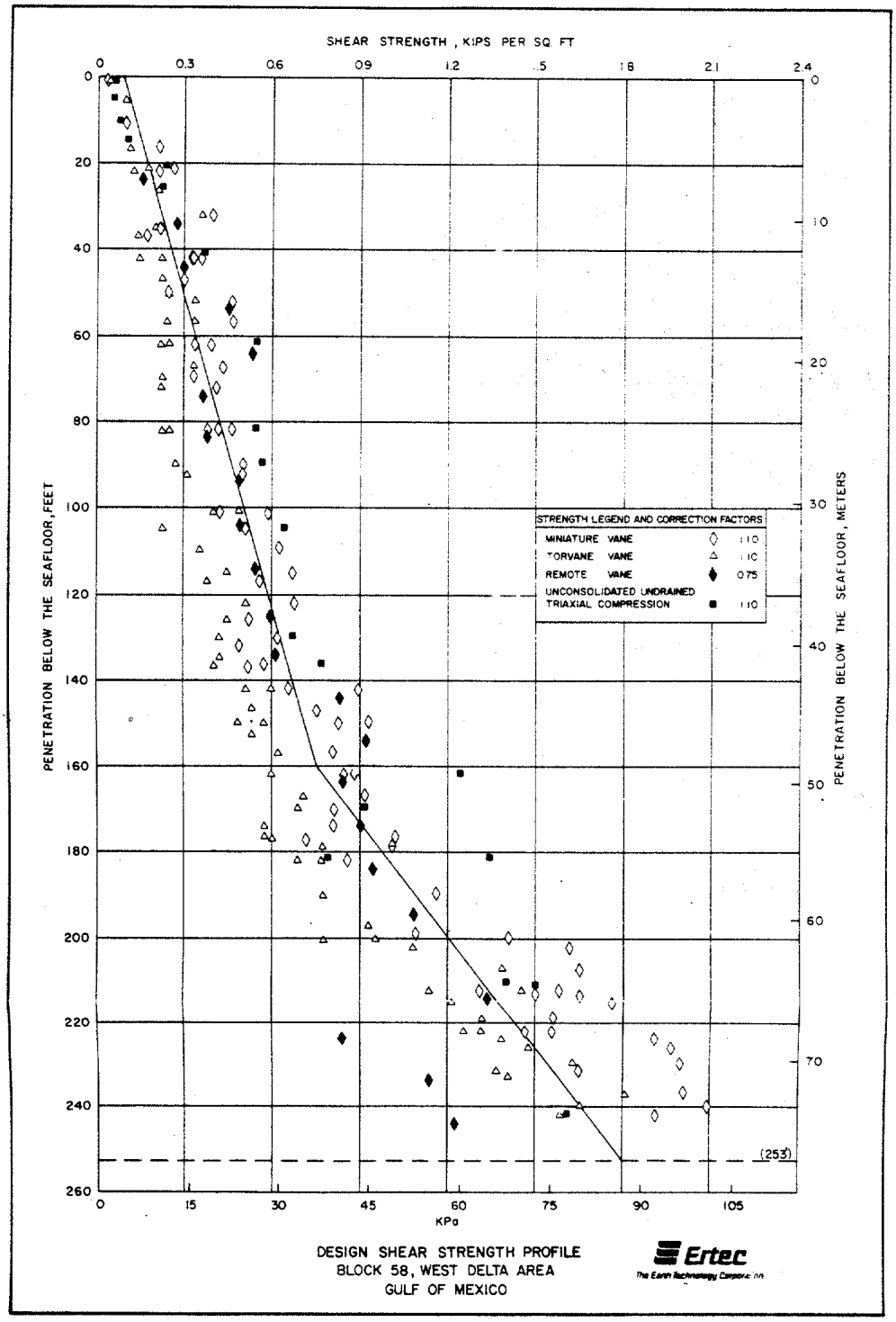

DESIGN SHEAR STRENGTH PROFILE
BLOCK 58, WEST DELTA AREA
GULF OF MEXICO

CNRD 13-2 TENSION PILE STUDY LABORATORY MODEL PILE TESTS

Proposed Shear Strength Profile at West Delta Blk.58A		Scale
DET NORSKE VERITAS Geotechnical Laboratory	Drawn by	Date
	Approved	Fig. No. 2.6

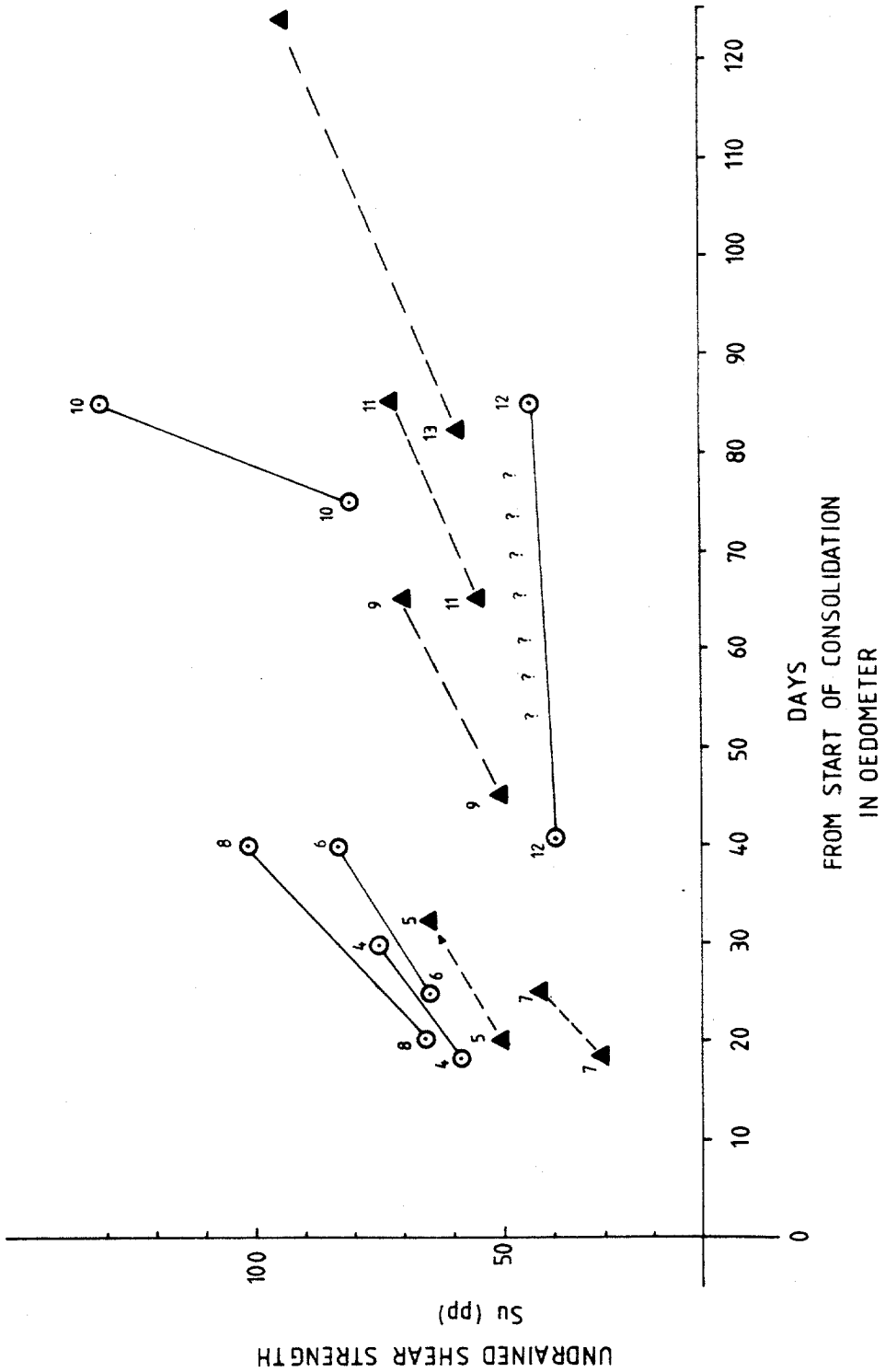

CNRD 13-2 TENSION PILE STUDY LABORATORY MODEL PILE TESTS

		Scale
DET NORSKE VERITAS Geotechnical Laboratory	Drawn by	Date
	Approved	Fig. No. 3.1

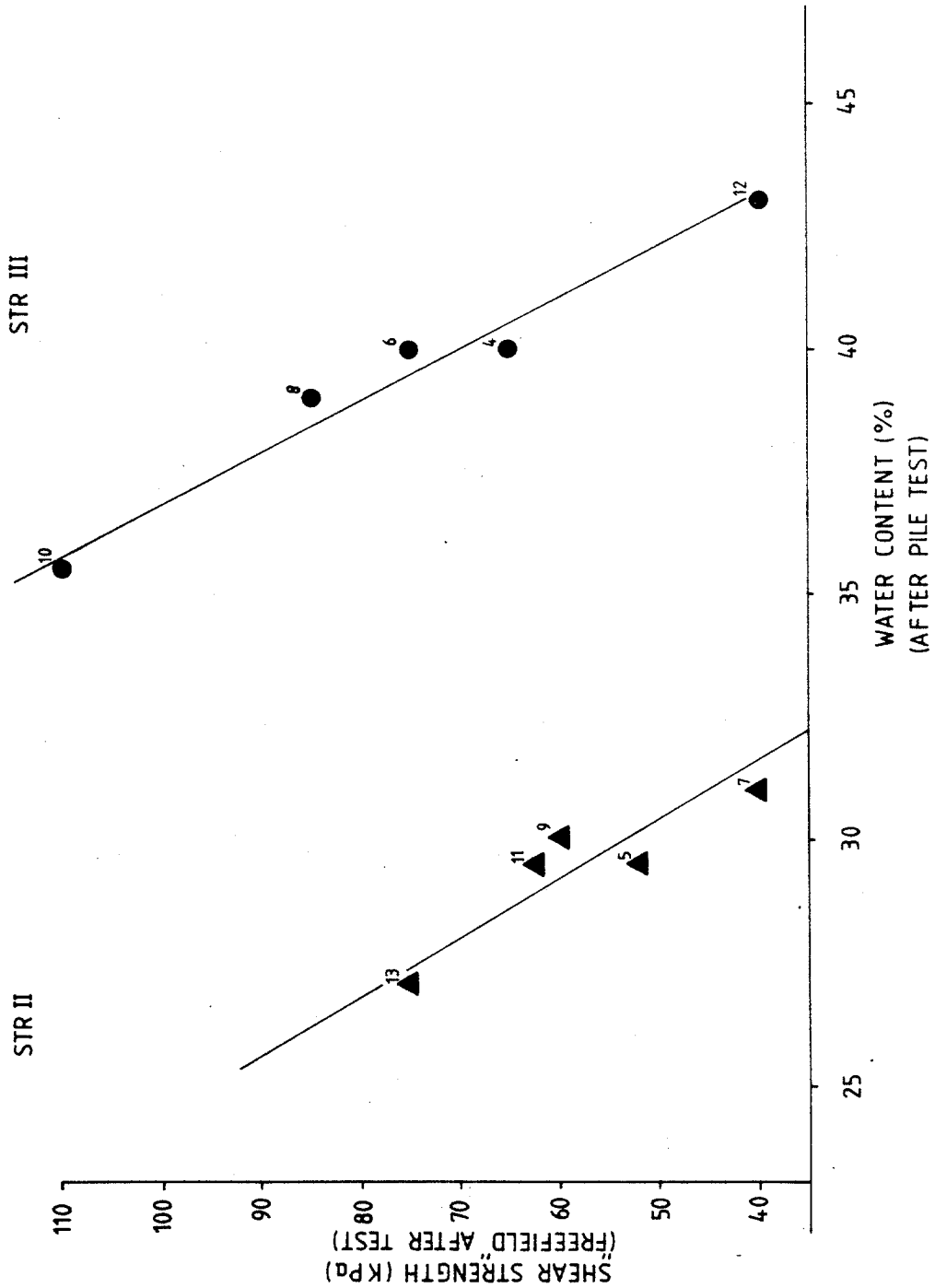

CNRD 13-2 TENSION PILE STUDY LABORATORY MODEL PILE TESTS

		Scale
DET NORSKE VERITAS Geotechnical Laboratory	Drawn by	Date
	Approved	Fig. No. 3.2

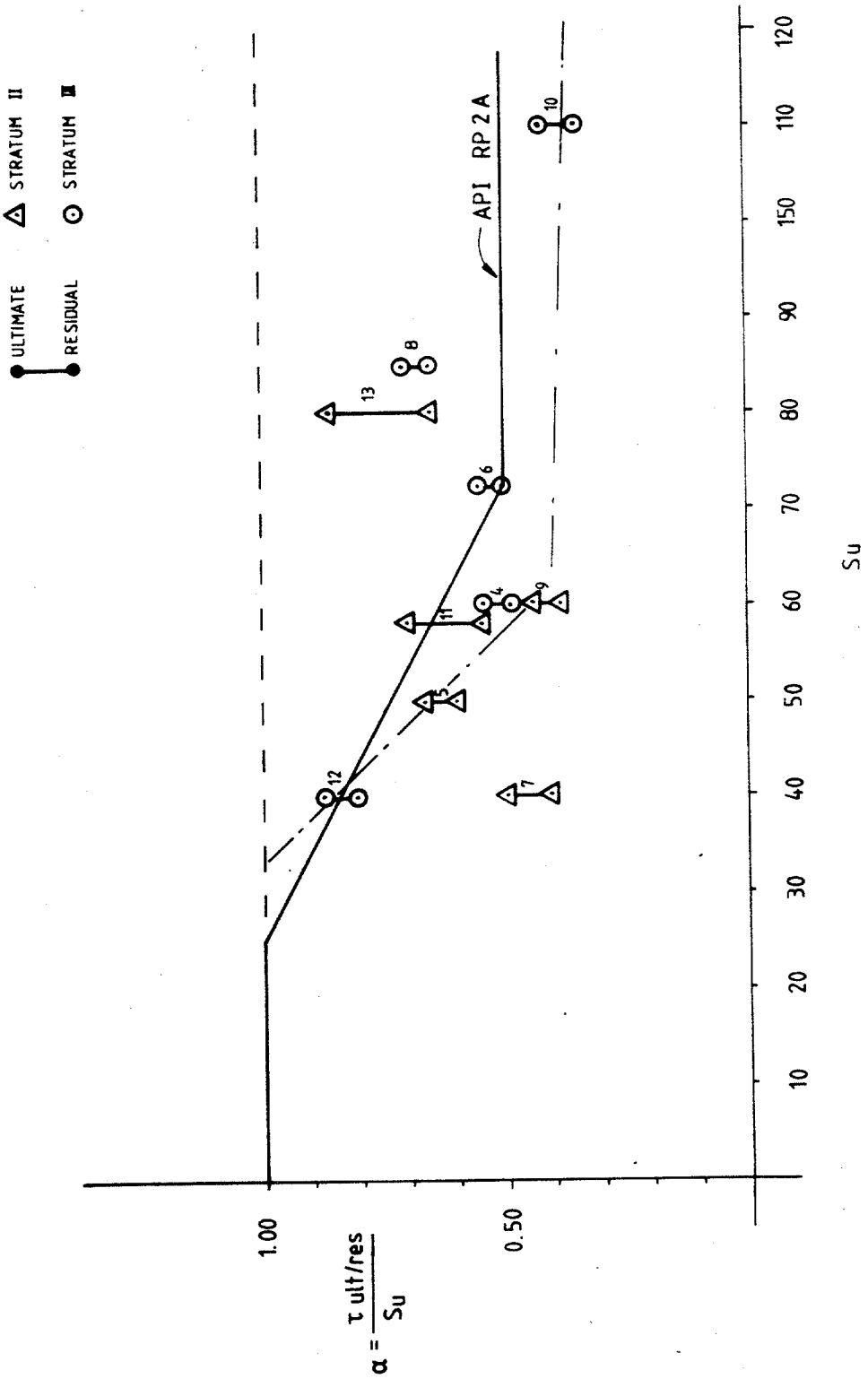

CNRD 13-2 TENSION PILE STUDY LABORATORY MODEL PILE TESTS

		Scale
DET NORSKE VERITAS Geotechnical Laboratory	Drawn by	Date
	Approved	Fig. No. 3.3

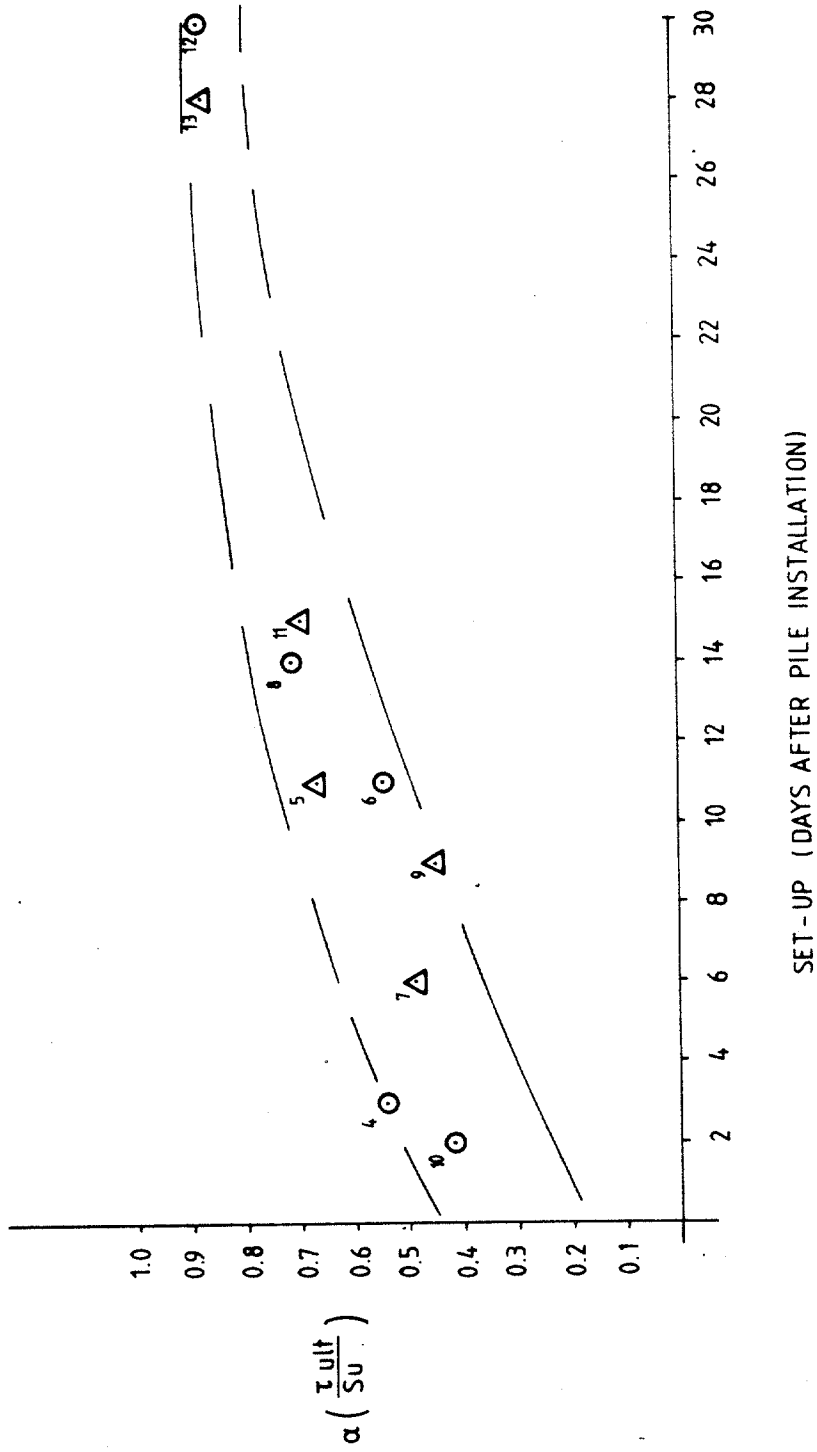

CNRD 13-2 TENSION PILE STUDY LABORATORY MODEL PILE TESTS

		Scale
DET NORSKE VERITAS Geotechnical Laboratory	Drawn by	Date
	Approved	Fig. No. 3.4

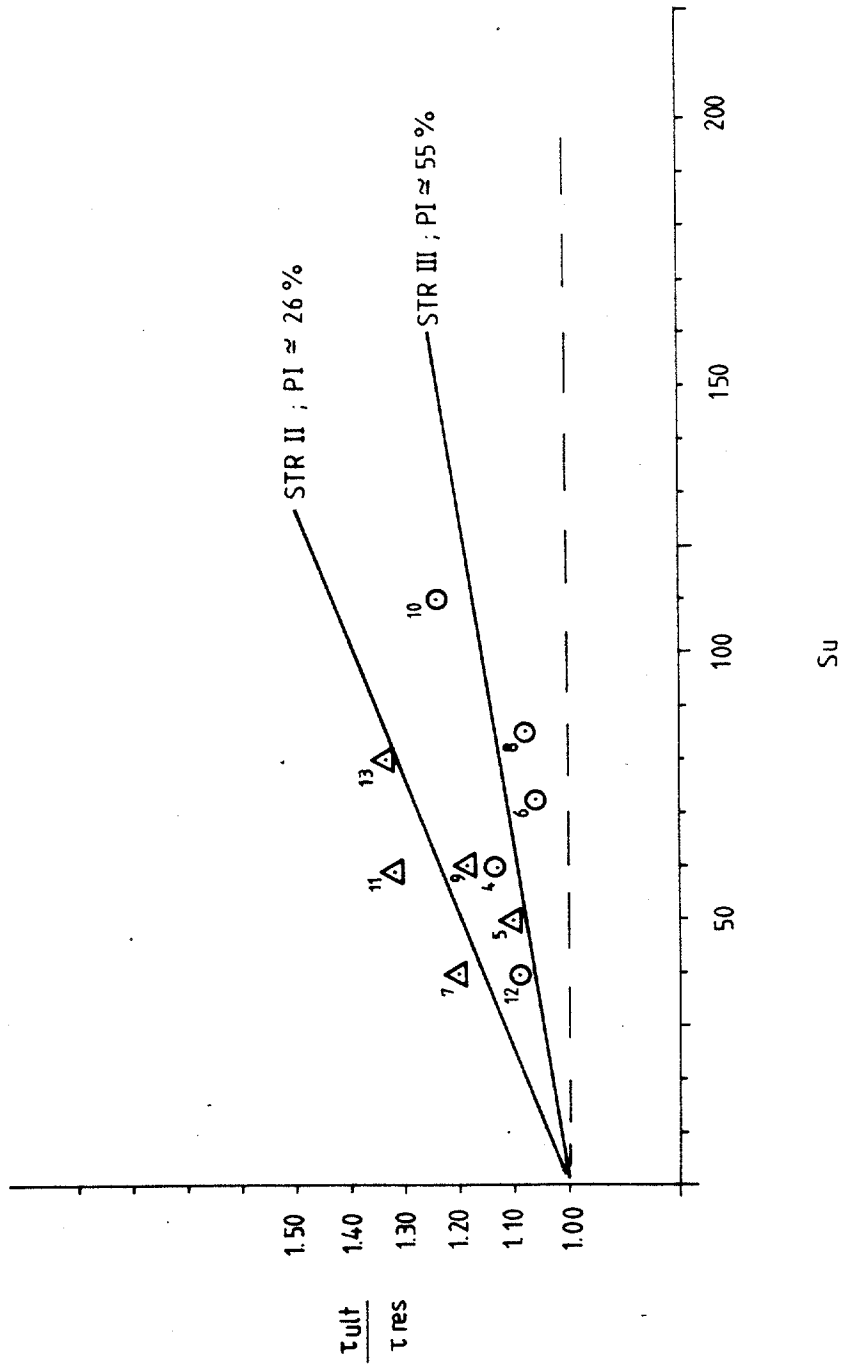

CNRD 13-2 TENSION PILE STUDY LABORATORY MODEL PILE TESTS

		Scale
DET NORSKE VERITAS Geotechnical Laboratory	Drawn by	Date
	Approved	Fig. No. 3.5

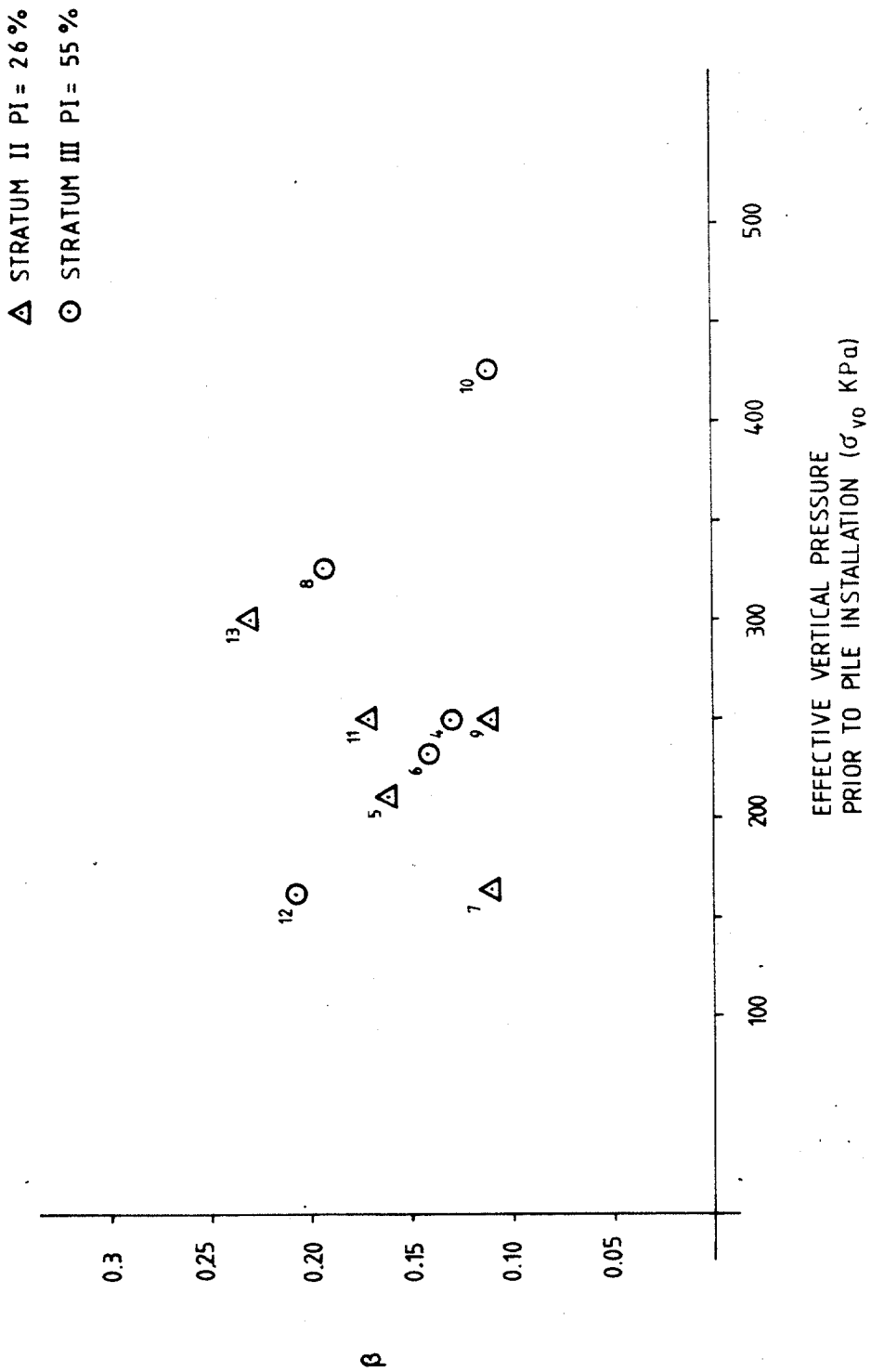

CNRD 13-2 TENSION PILE STUDY LABORATORY MODEL PILE TESTS

		Scale
DET NORSKE VERITAS Geotechnical Laboratory	Drawn by	Date
	Approved	Fig. No. 3.6

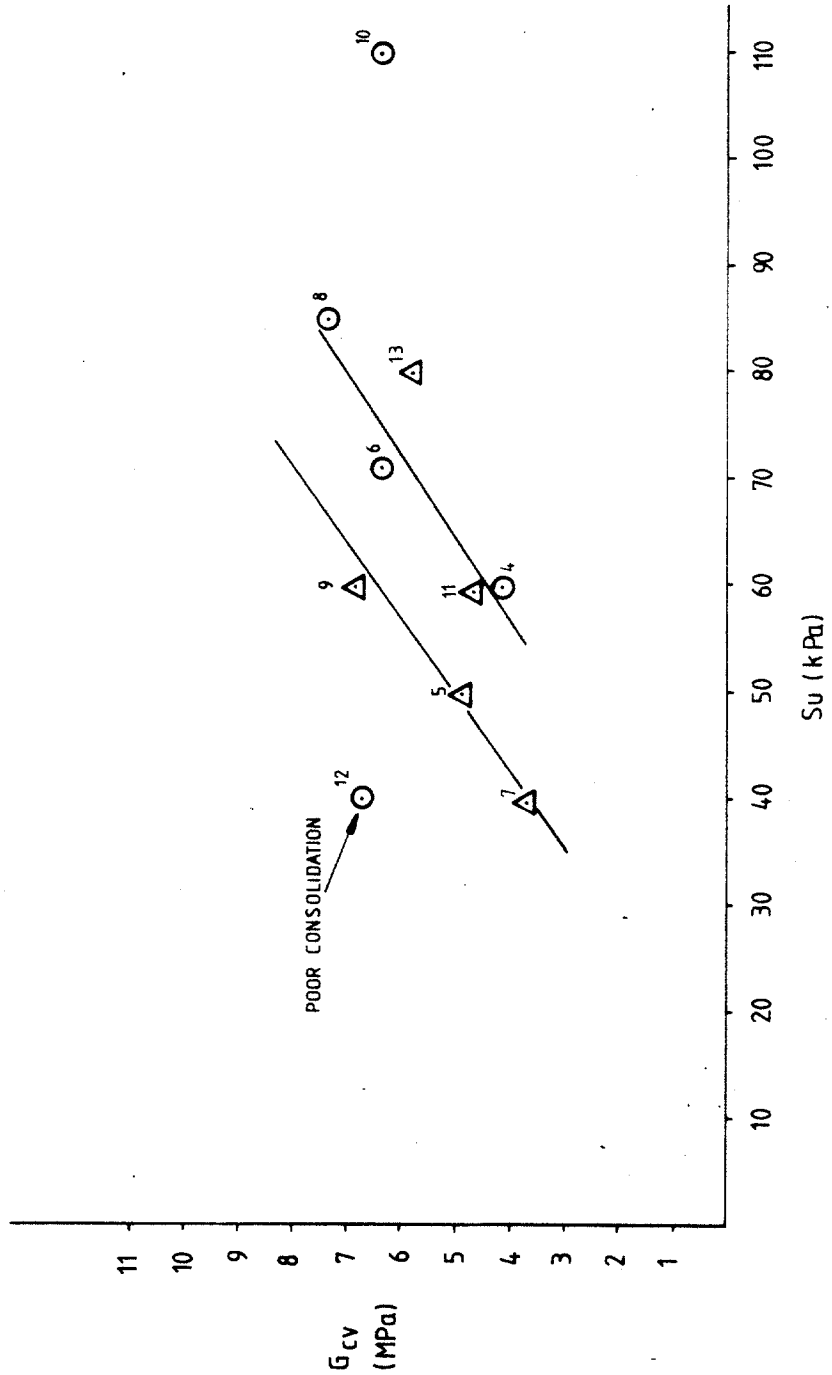

CNRD 13-2 TENSION PILE STUDY LABORATORY MODEL PILE TESTS

		Scale
DET NORSKE VERITAS Geotechnical Laboratory	Drawn by	Date
	Approved	Fig. No. 3.7

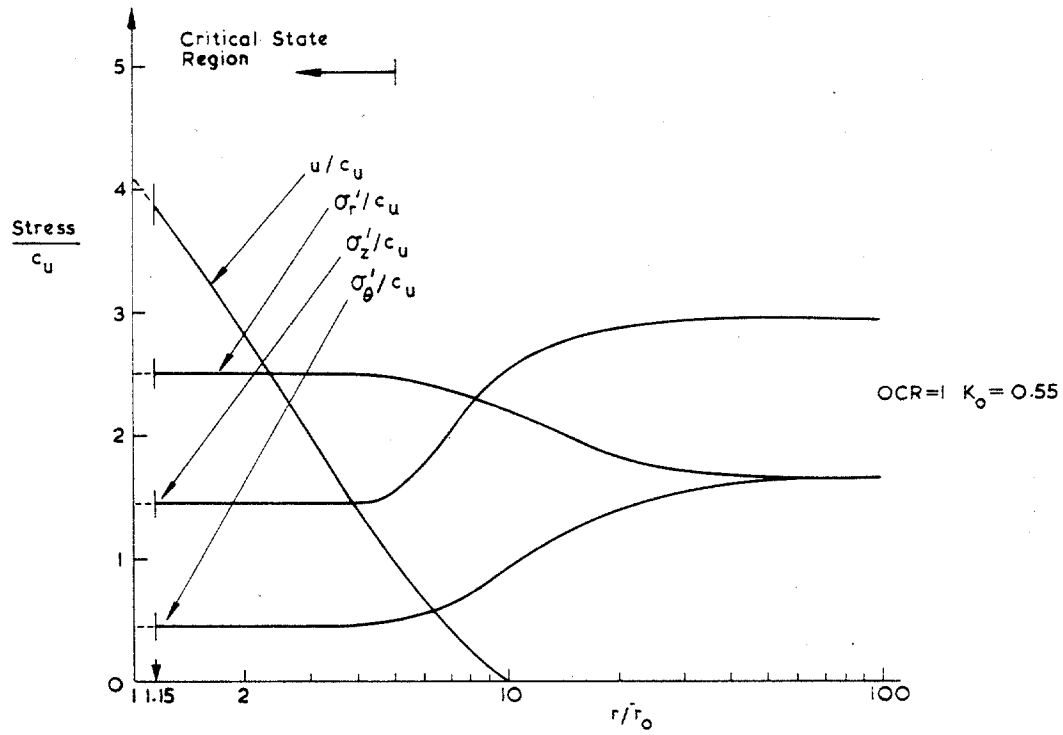

Stress distributions in the soil around the pile immediately after driving, OCR = 1

(From Randolph et al. (1979))

CNRD 13-2 TENSION PILE STUDY LABORATORY MODEL PILE TESTS		
		Scale
DET NORSKE VERITAS Geotechnical Laboratory	Drawn by	Date
	Approved	Fig.No. 4.1

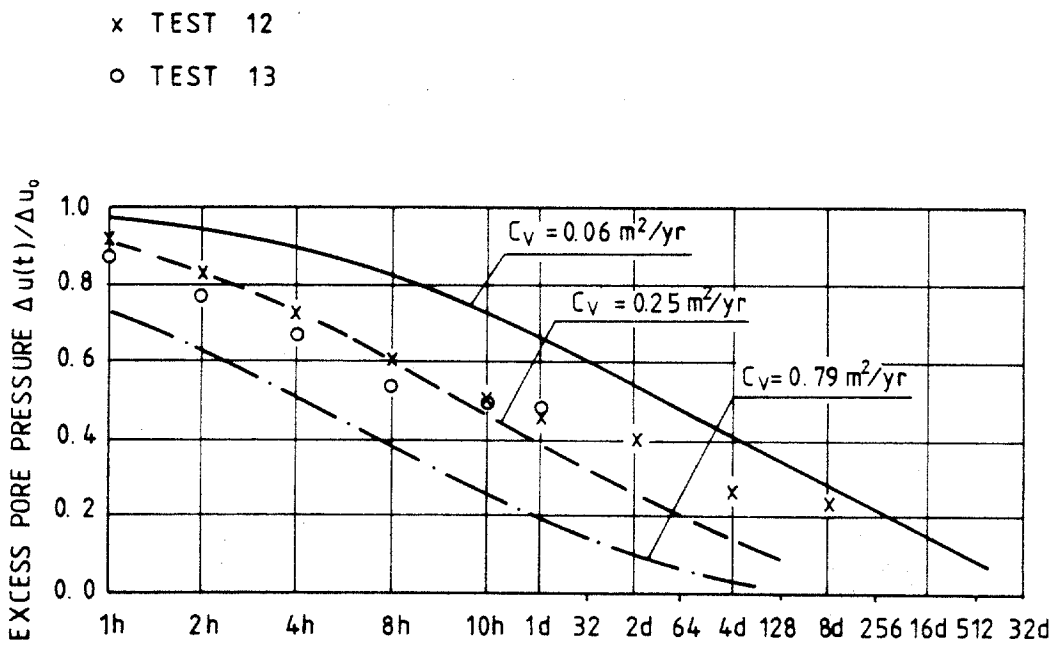

Dissipation of Excess Pore Pressure at Pile Surface vs. Time After Pile Installation of Laboratory Model Pile

CNRD 13-2 TENSION PILE STUDY LABORATORY MODEL PILE TESTS 231004		
		Scale
DET NORSKE VERITAS Geotechnical Laboratory	Drawn by	Date
	Approved	Fig. No. 4.2

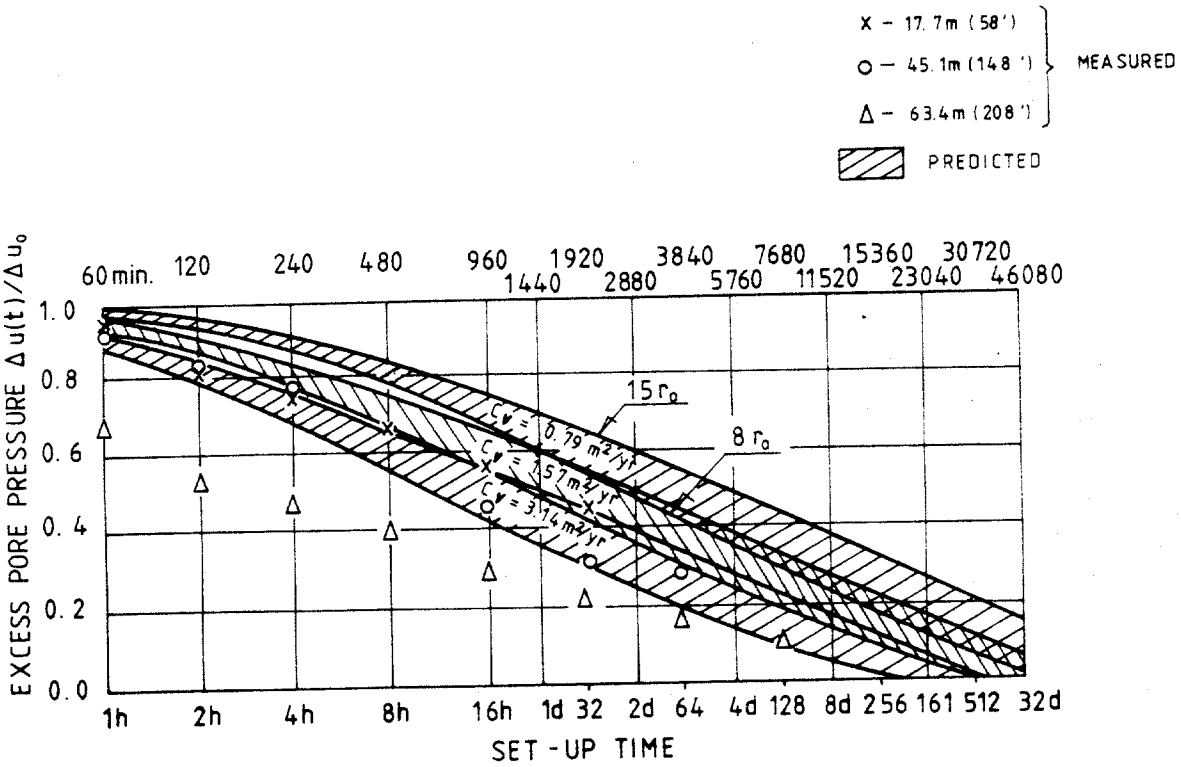

Dissipation of Excess Pore Pressure at Pile Wall vs. Time after Installation for 3" Segment Test

CNRD 13-2 TENSION PILE STUDY LABORATORY MODEL PILE TESTS

		Scale
DET NORSKE VERITAS Geotechnical Laboratory	Drawn by	Date
	Approved	Fig. No. 4.3

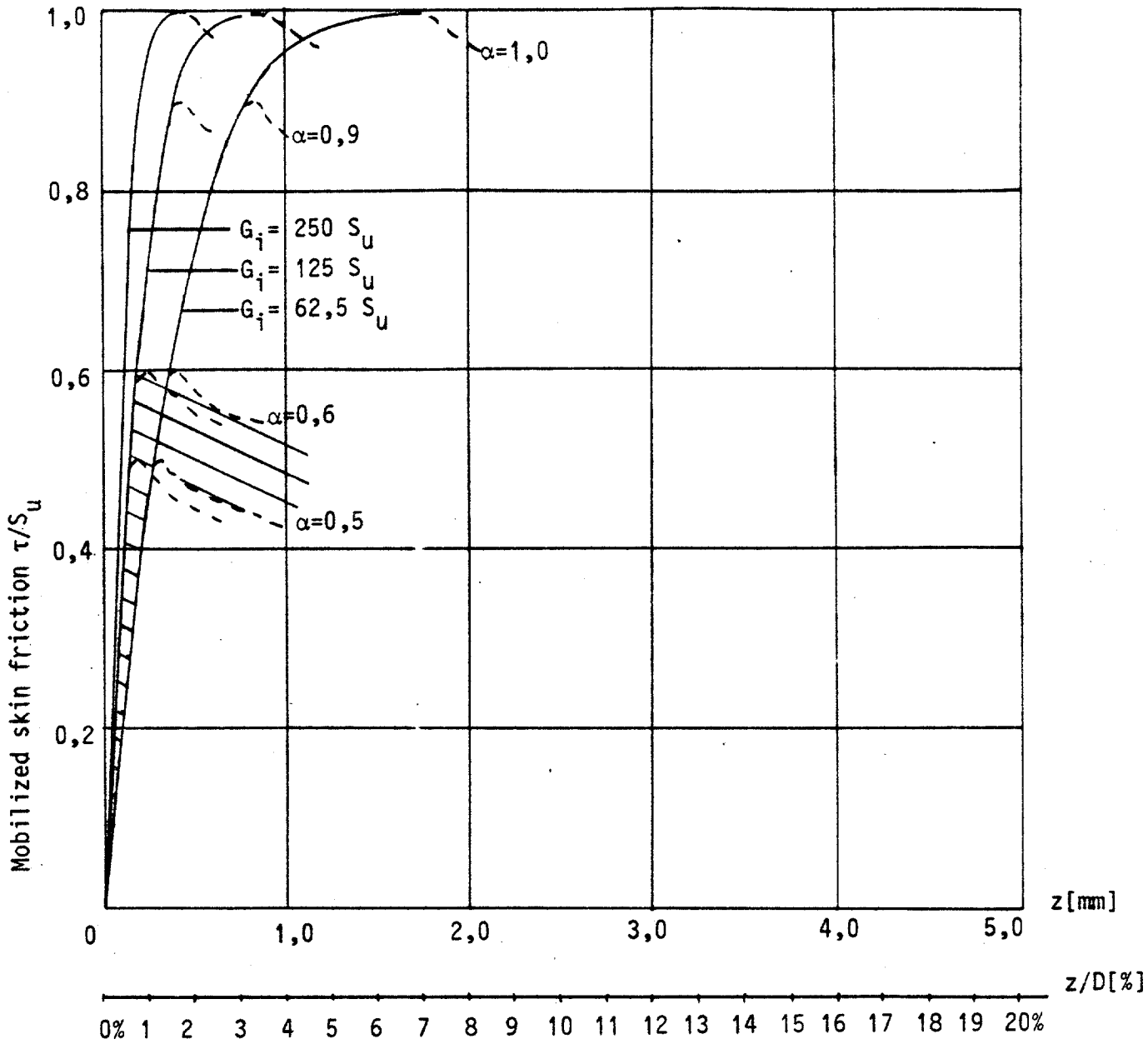

Normalized τ-z curves predicted for laboratory model pile.

CNRD 13-2 TENSION PILE STUDY LABORATORY MODEL PILE TESTS

		Scale
DET NORSKE VERITAS Geotechnical Laboratory	Drawn by	Date
	Approved	Fig.No. 4.4

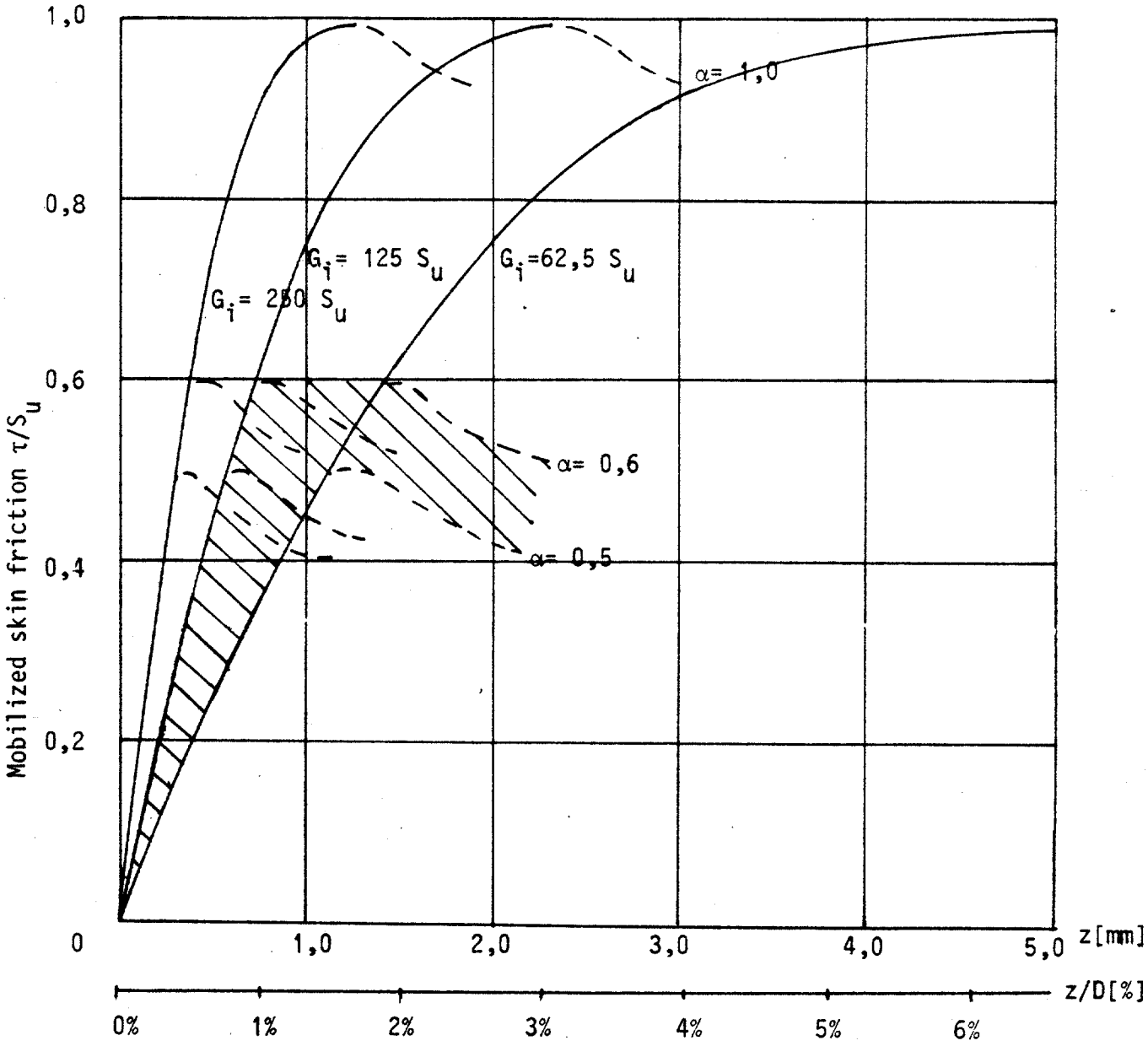

Normalized τ-z curves predicted for segment tests.

CNRD 13-2 TENSION PILE STUDY LABORATORY MODEL PILE TESTS		
		Scale
DET NORSKE VERITAS Geotechnical Laboratory	Drawn by	Date
	Approved	Fig. No. 4.5

Single Slice Model for
Laboratory Model Pile

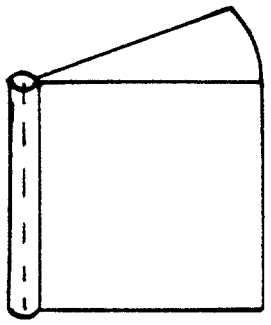

r_o R

r_o=1,25cm R/r_o=8

R =10cm

Single Slice Model for
Segment Pile

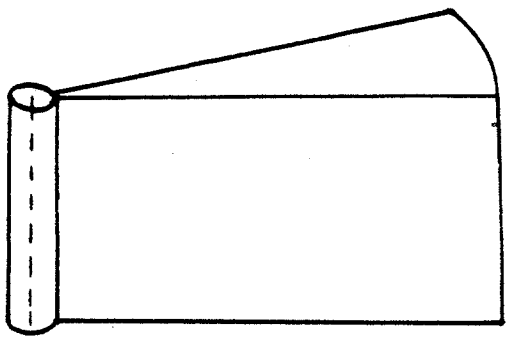

r_o R

r_o=1,5" R/r_o=20

R =30"

CNRD 13-2 TENSION PILE STUDY LABORATORY MODEL PILE TESTS

		Scale
DET NORSKE VERITAS Geotechnical Laboratory	Drawn by	Date
	Approved	Fig. No. 4.6

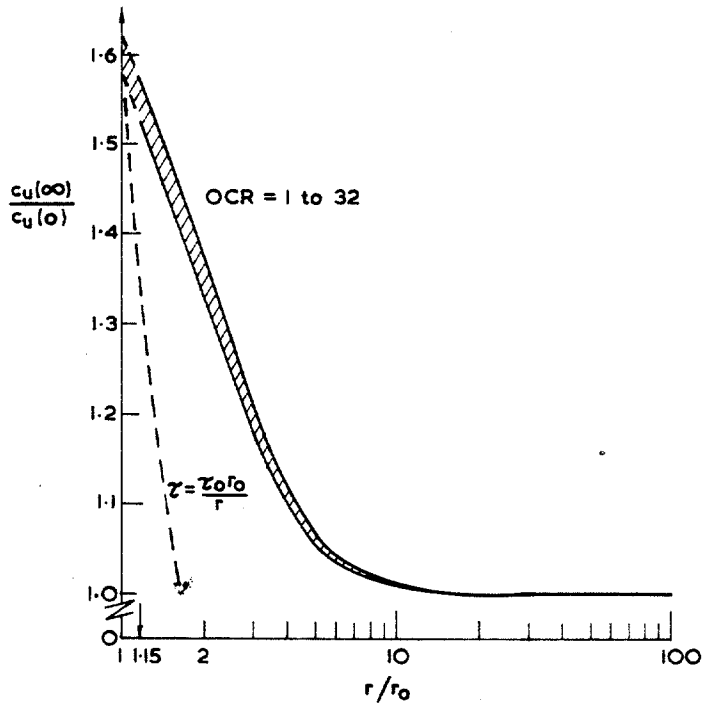

Distribution of soil strength with radius and comparison with possible shear stress distribution

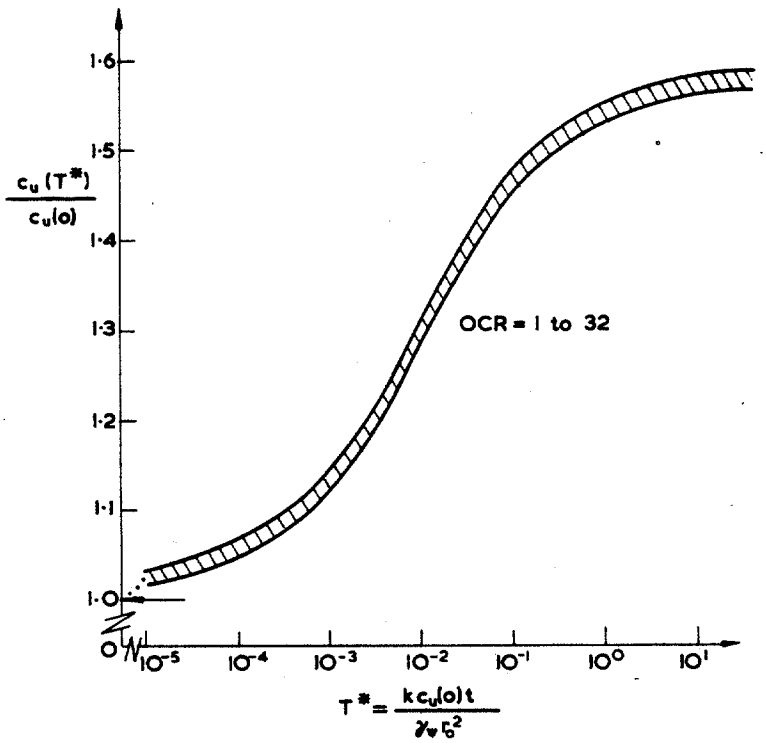

Variation with time of undrained shear strength of soil at $r = 1{\cdot}15\, r_0$

(From Randolph et al. (1979))

CNRD 13-2 TENSION PILE STUDY LABORATORY MODEL PILE TESTS

		Scale
DET NORSKE VERITAS Geotechnical Laboratory	Drawn by	Date
	Approved	Fig. No. 4.7

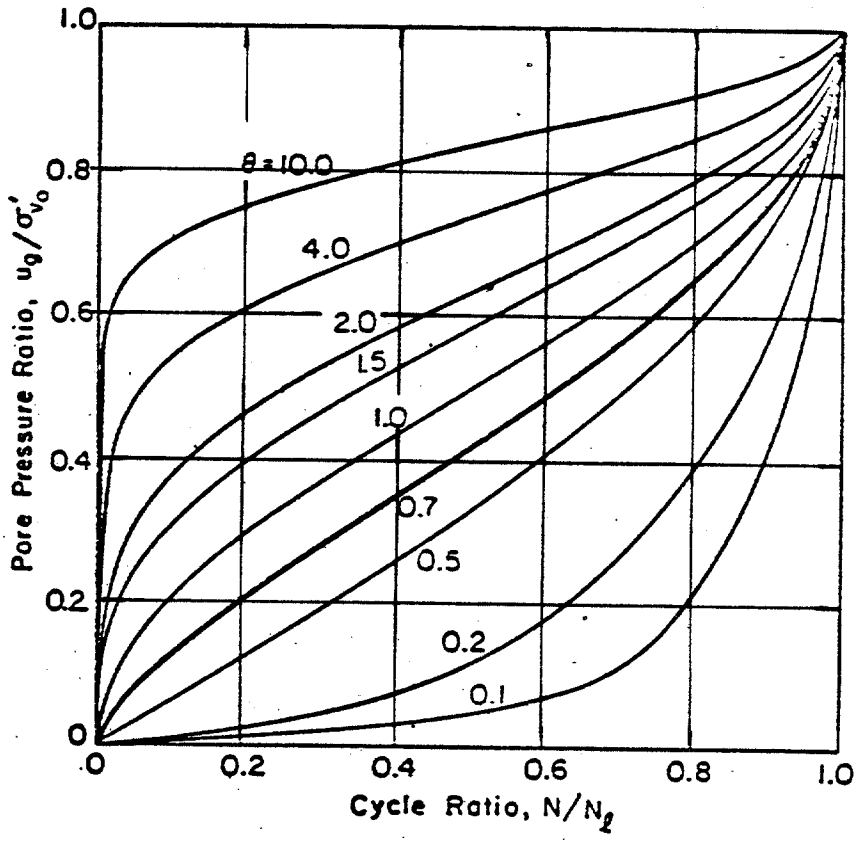

RATE OF PORE PRESSURE GENERATION

(From Rahman 1976)

CNRD 13-2 TENSION PILE STUDY LABORATORY MODEL PILE TESTS		
		Scale
DET NORSKE VERITAS Geotechnical Laboratory	Drawn by	Date
	Approved	Fig. No. 4.8

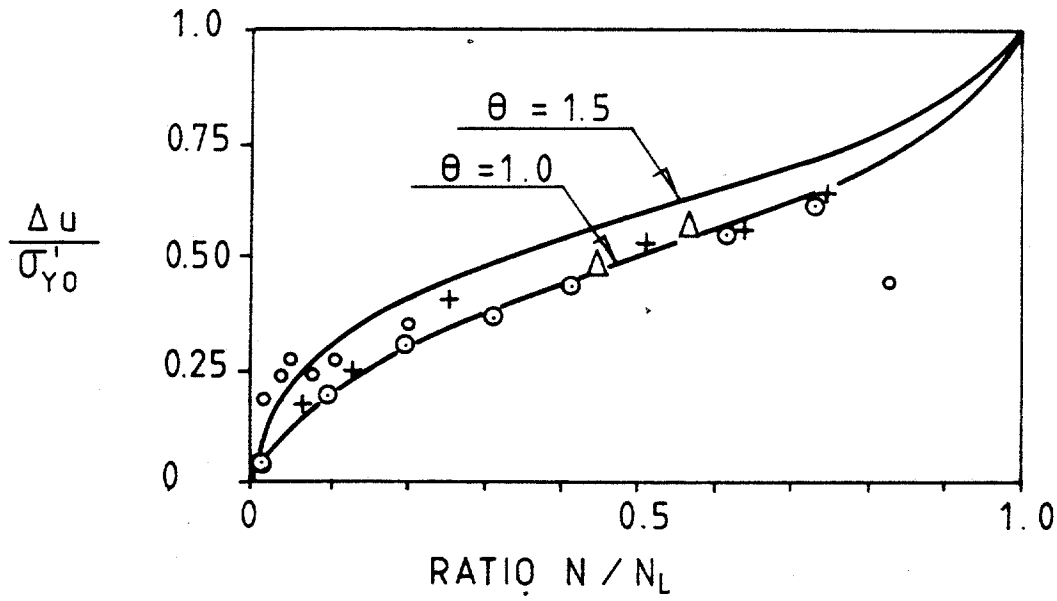

N - ACTUAL NUMBER OF CYCLES

N_L - NUMBER OF CYCLES TO FAILURE (ie. $\Delta u = \sigma'_{vo}$)

Pore Pressure Generation for Cyclic Triaxial Test. Comparison Between OCEAN2 Predictions and measured values.

CNRD 13-2 TENSION PILE STUDY LABORATORY MODEL PILE TESTS		
		Scale
DET NORSKE VERITAS Geotechnical Laboratory	Drawn by	Date
	Approved	Fig. No. 4.9

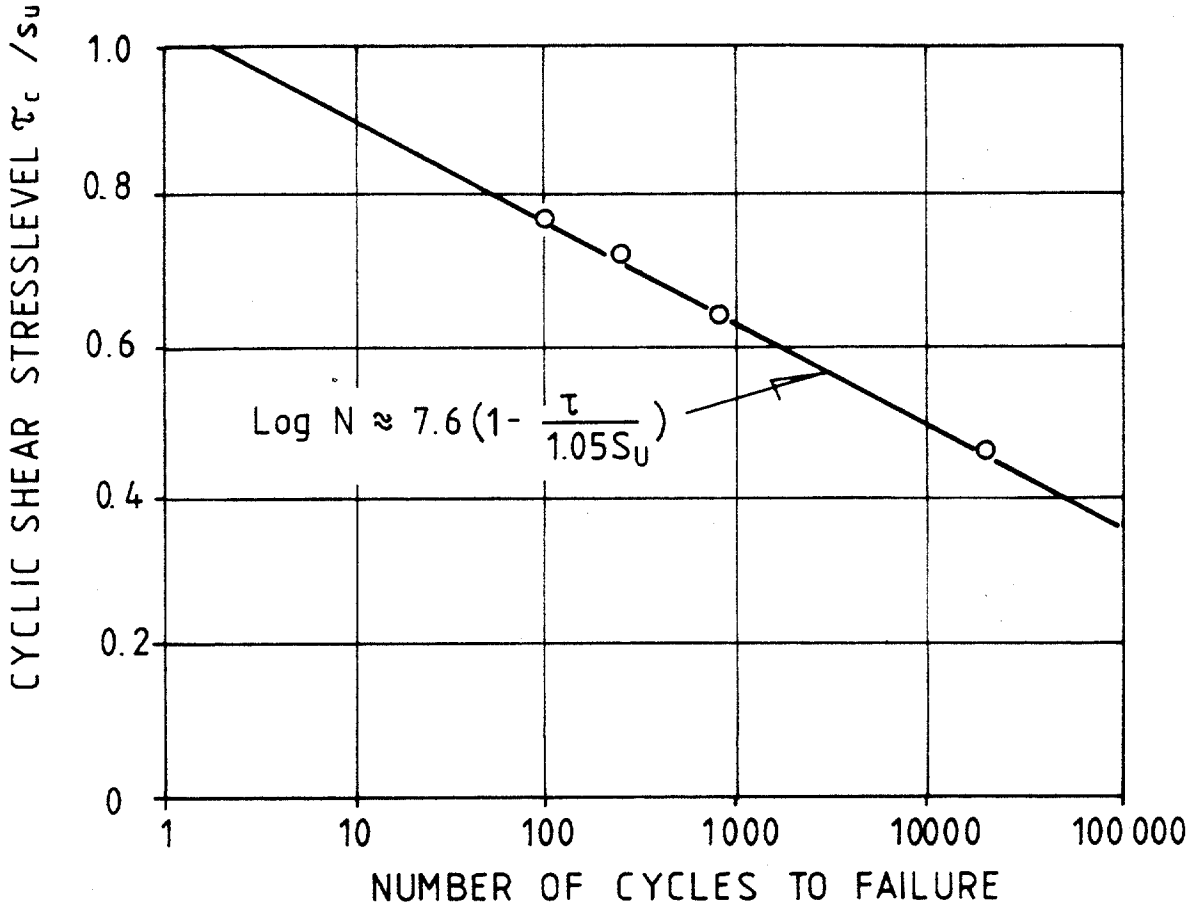

Number of Cycles to Failure vs. Shear Stress Level

CNRD 13-2 TENSION PILE STUDY LABORATORY MODEL PILE TESTS		
		Scale
DET NORSKE VERITAS Geotechnical Laboratory	Drawn by	Date
	Approved	Fig. No. 4.10

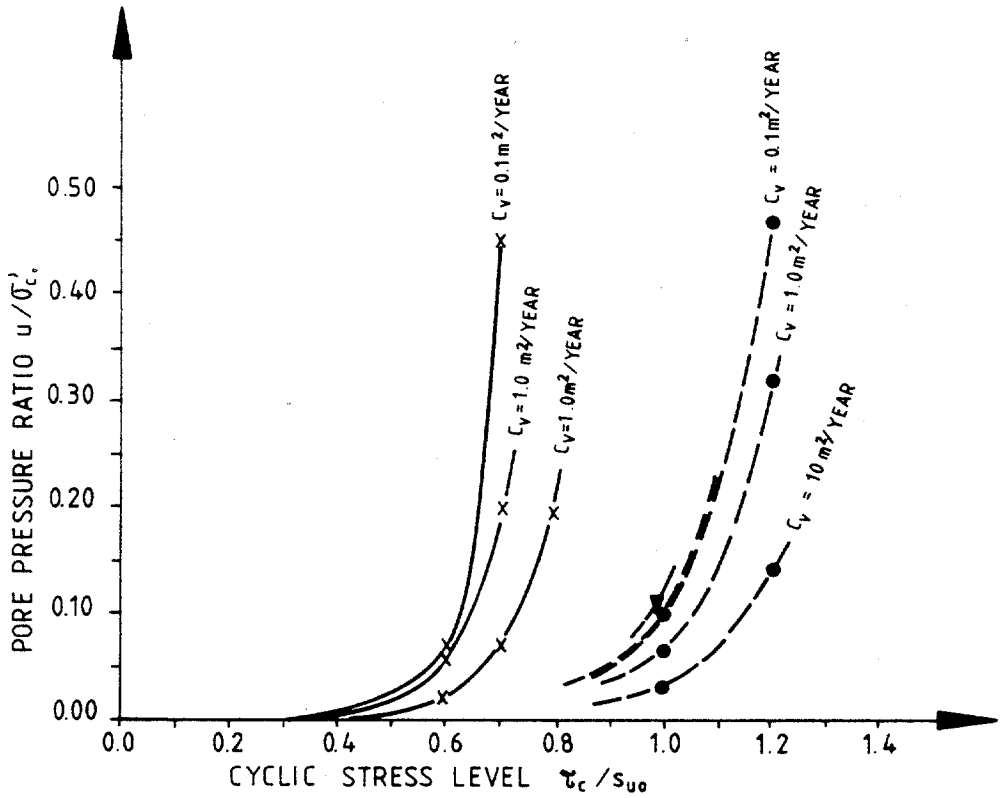

Uniform Shear Strength $s_u(r) = s_{uo}$

Non-Uniform Shear Strength $s_u(r) = s_{uo} + \Delta s_{uo} \cdot \frac{r}{r}$

due to set-up Effects, with $\Delta s_{uo}/s_{uo} = 0.6$

▽ Spot Check with Large Diameter Pile

Theoretical Prediction of Pore Pressure Increase at Pile Wall due to 100 Uniform Cycles as a Function of Stress Level and Coefficient of Consolidation. Pile Diameter D=25mm .

CNRD 13-2 TENSION PILE STUDY LABORATORY MODEL PILE TESTS 231004		
		Scale
DET NORSKE VERITAS Geotechnical Laboratory	Drawn by	Date
	Approved	Fig. No. 4.11

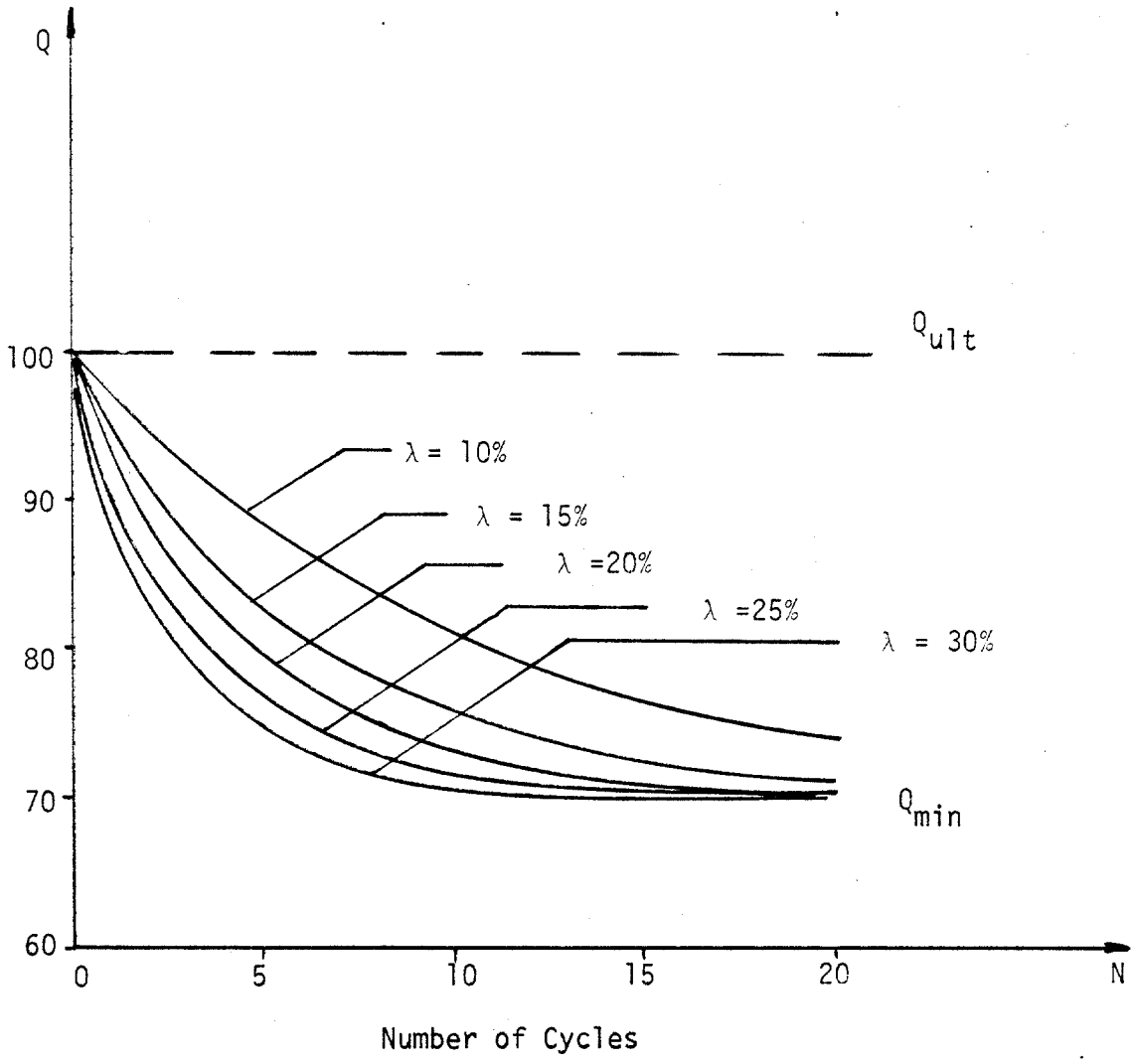

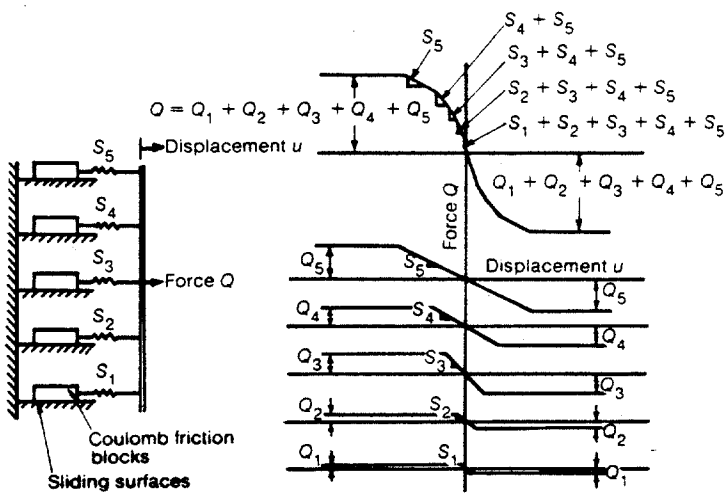

Sub-element model used in DRIVE 7

(From Matlock et al. (1979))

CNRD 13-2 TENSION PILE STUDY LABORATORY MODEL PILE TESTS		
		Scale
DET NORSKE VERITAS Geotechnical Laboratory	Drawn by	Date
	Approved	Fig. No. 4.12

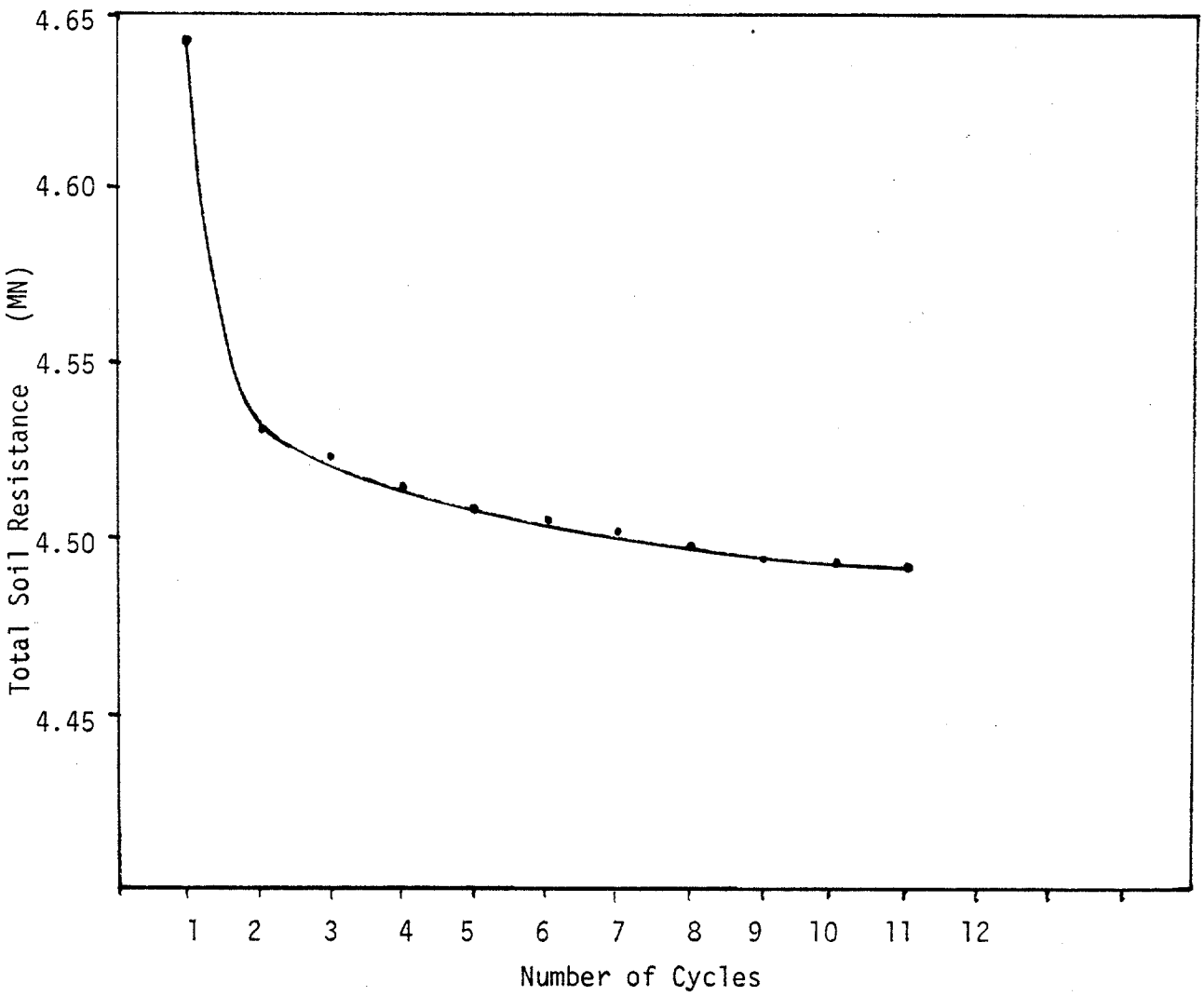

Effect of DRIVE 15 Degradation Model

CNRD 13-2 TENSION PILE STUDY LABORATORY MODEL PILE TESTS

		Scale
DET NORSKE VERITAS Geotechnical Laboratory	Drawn by	Date
	Approved	Fig. No. 4.13

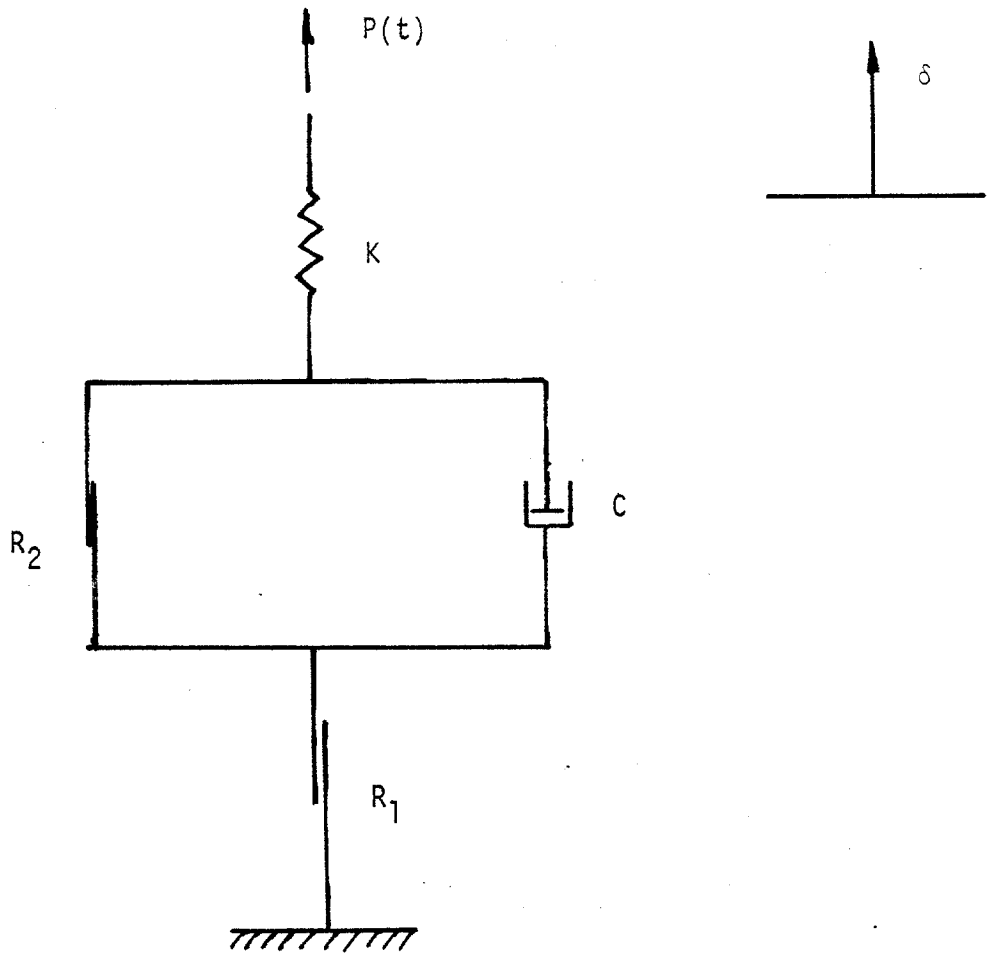

P(t) = Exciting Force Varying with Time
K = Linear or Non-Linear Spring Constant
R_2 = Sliding Resistance After Certain Applied Load
C = Damping Coefficient
R_1 = Sliding Resistance After the Ultimate Load Capacity is Reached. ($R_1 > R_2$)

CNRD 13-2 TENSION PILE STUDY LABORATORY MODEL PILE TESTS

Soil Model in CRAPIL, Elastic, Visco-Plastic

DET NORSKE VERITAS Geotechnical Laboratory	Drawn by	Scale
	Approved	Date
		Fig. No. 4.14

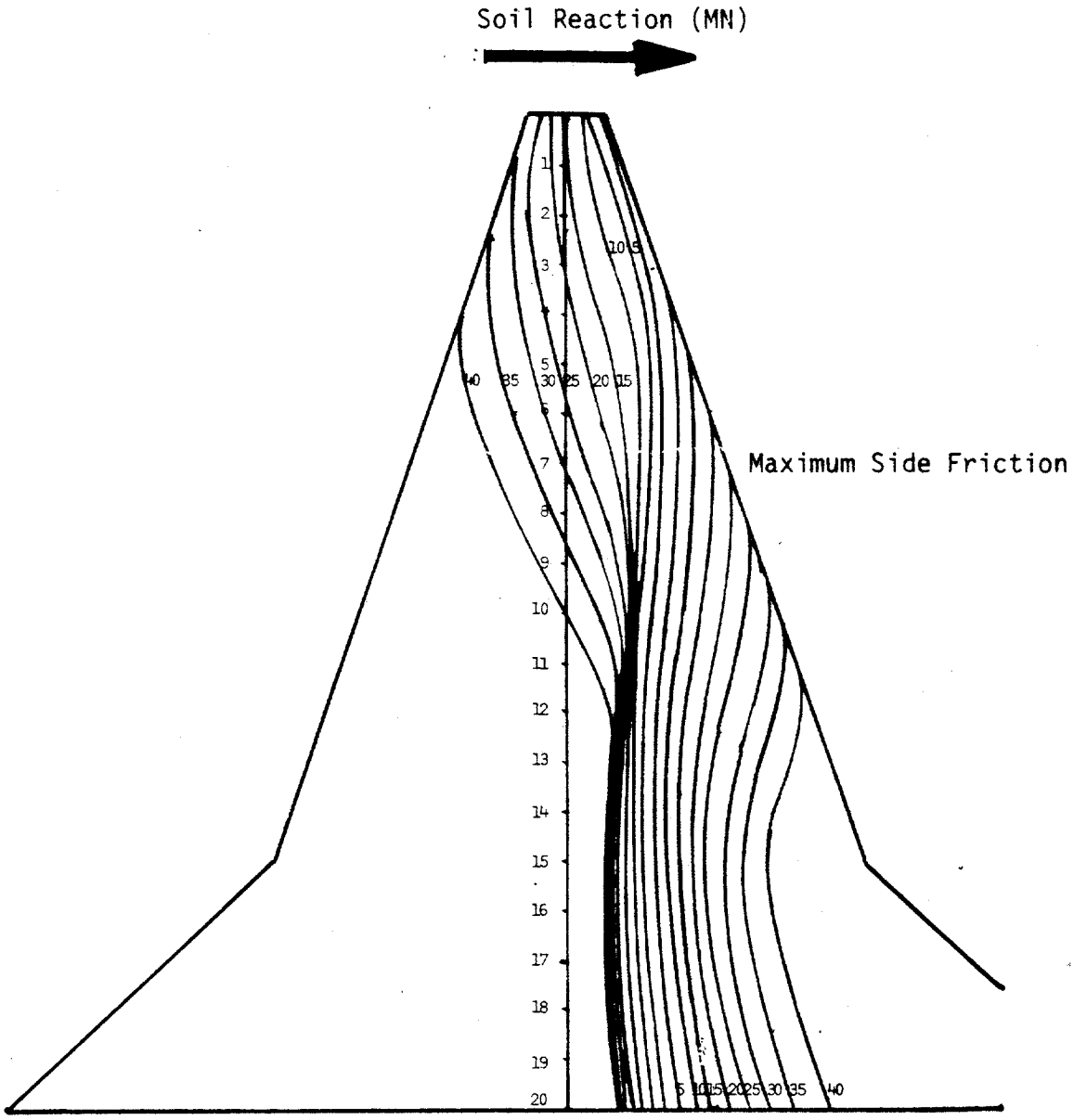

Mobilization of Shear Stress along a Pile with Pretension of 33% of the Ultimate Capacity and Varying Cyclic Loads Between ∓5% to ∓40% of the Ultimate Capacity. $d_f/D=1\%$. DRIVE15 Analysis.

CNRD 13-2 TENSION PILE STUDY LABORATORY MODEL PILE TESTS

		Scale
DET NORSKE VERITAS Geotechnical Laboratory	Drawn by	Date
	Approved	Fig.No. 4.15

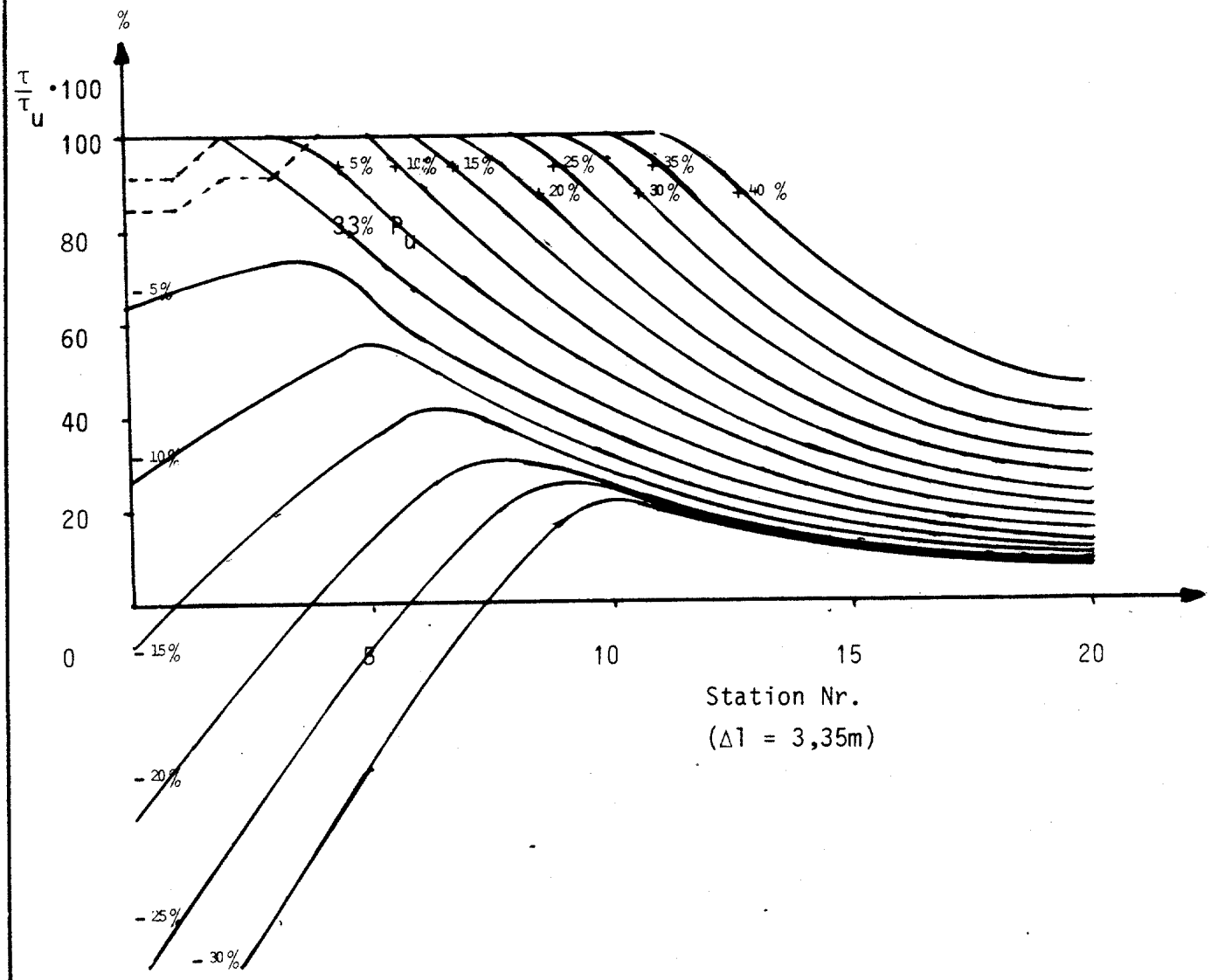

Mobilization of the shear stress along the pile under tensile cyclic loads.

δ_f/D = 1%

CNRD 13-2 TENSION PILE STUDY LABORATORY MODEL PILE TESTS		
		Scale
DET NORSKE VERITAS Geotechnical Laboratory	Drawn by	Date
	Approved	Fig.No. 4.16

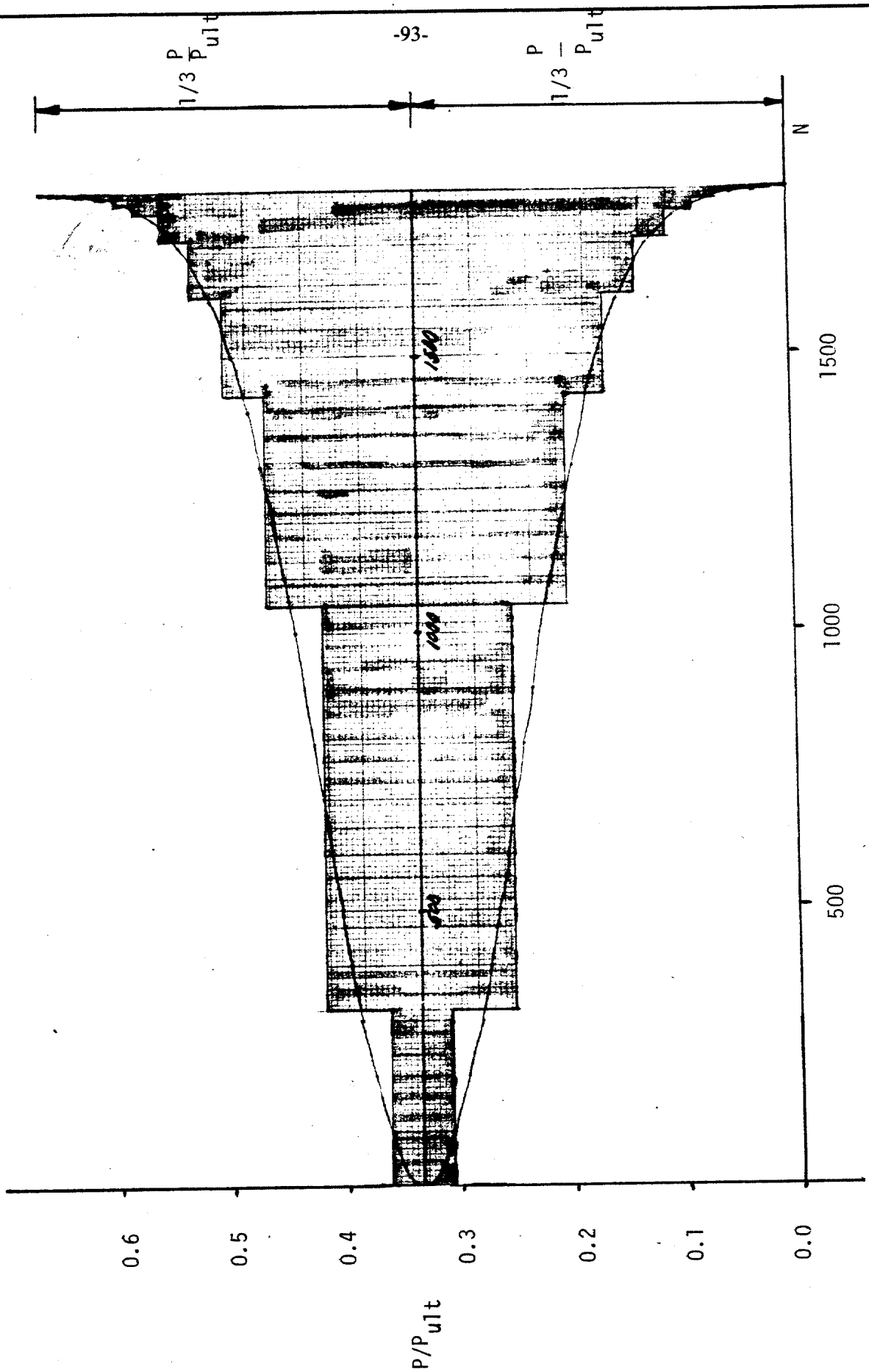

CNRD 13-2 TENSION PILE STUDY LABORATORY MODEL PILE TESTS

Axial Pile Top Variations, Simulation of 6 Hour Storm

Scale

DET NORSKE VERITAS
Geotechnical Laboratory

Drawn by

Date

Approved

Fig. No. 4.17

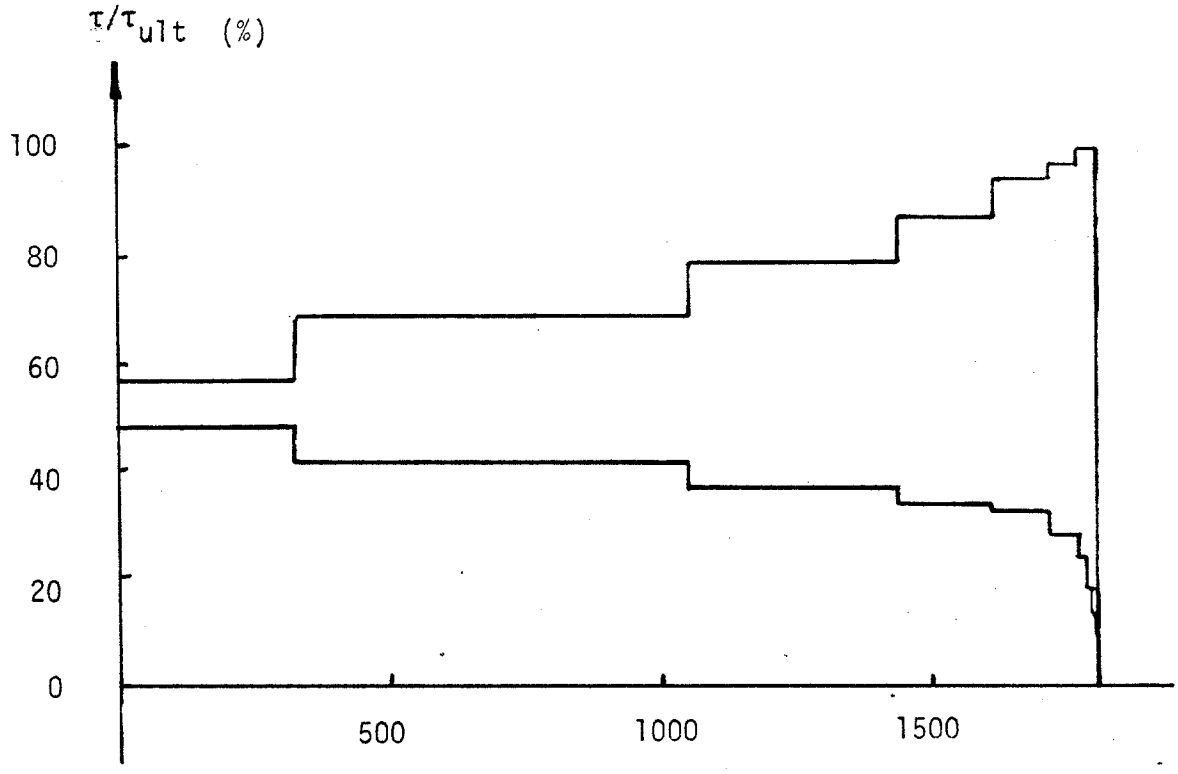

Shear Stress Mobilizations at Pile Station Number 8

CNRD 13-2 TENSION PILE STUDY LABORATORY MODEL PILE TESTS

		Scale
DET NORSKE VERITAS Geotechnical Laboratory	Drawn by	Date
	Approved	Fig. No. 4.18

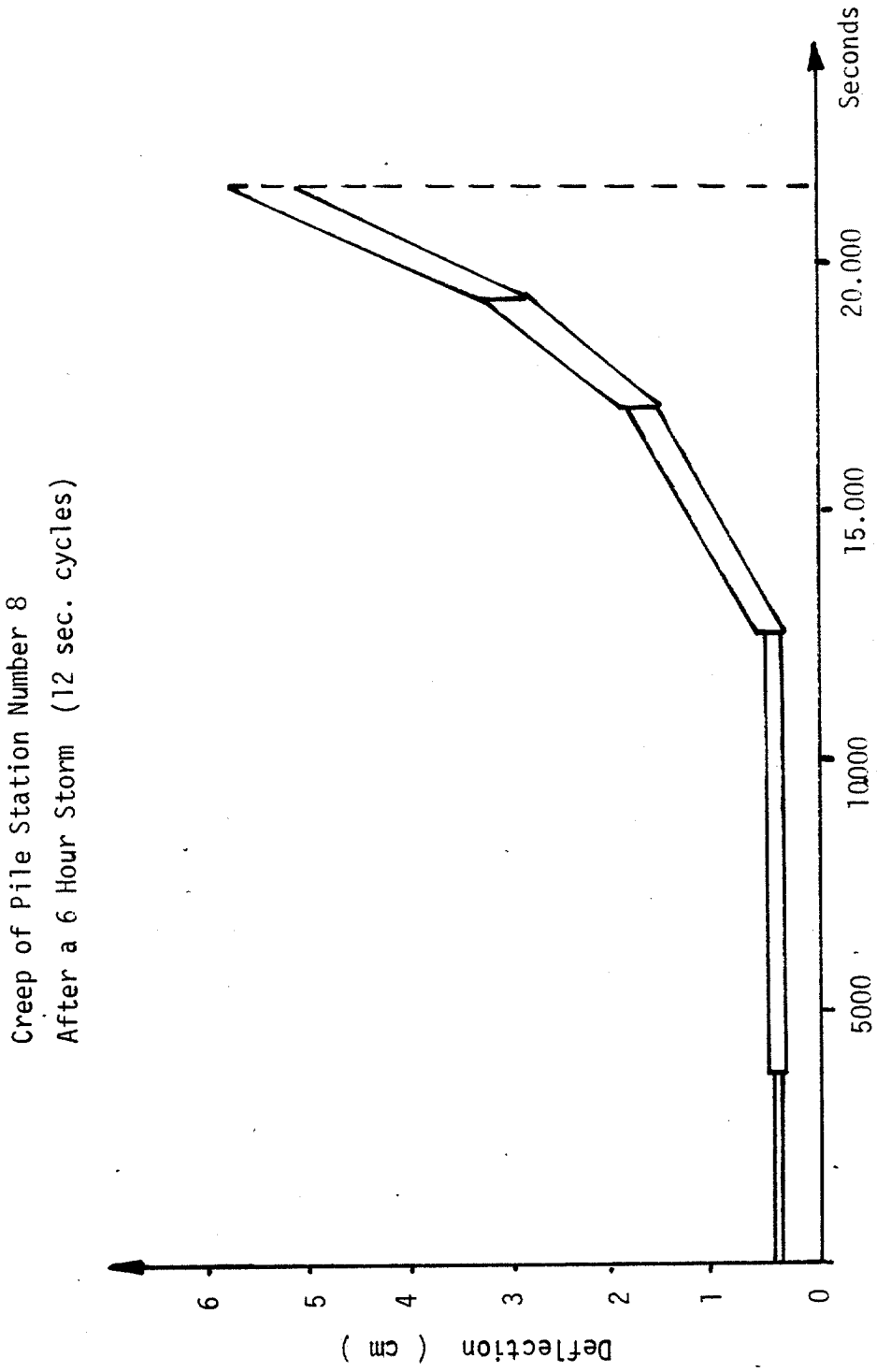

CNRD 13-2 TENSION PILE STUDY LABORATORY MODEL PILE TESTS

		Scale
DET NORSKE VERITAS Geotechnical Laboratory	Drawn by	Date
	Approved	Fig.No. 4.19

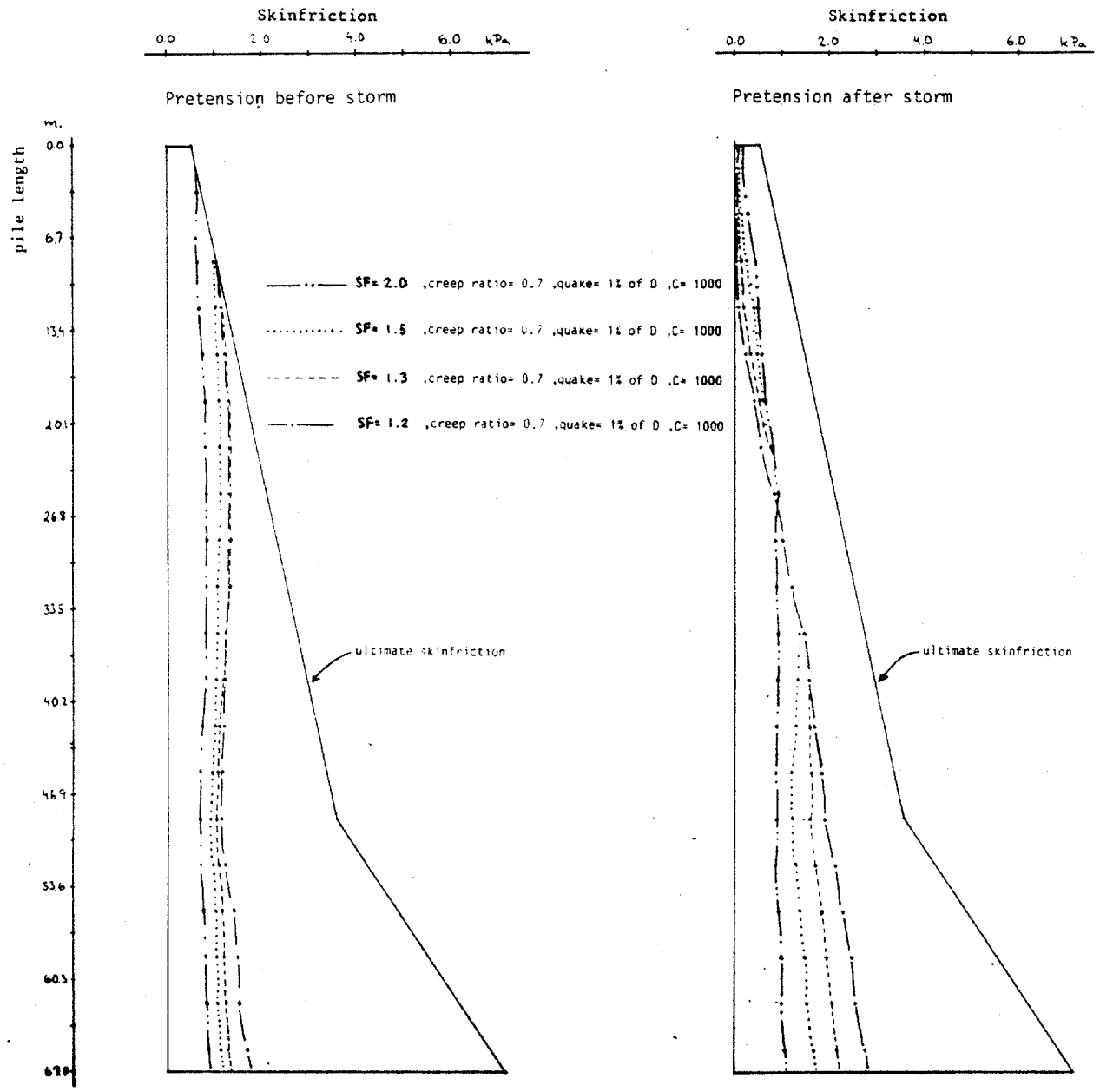

(a) (b)

Redistribution of Mobilized Shear Stress from Creep due to Pretension

CNRD 13-2 TENSION PILE STUDY LABORATORY MODEL PILE TESTS

		Scale
DET NORSKE VERITAS Geotechnical Laboratory	Drawn by	Date
	Approved	Fig. No. 4.20

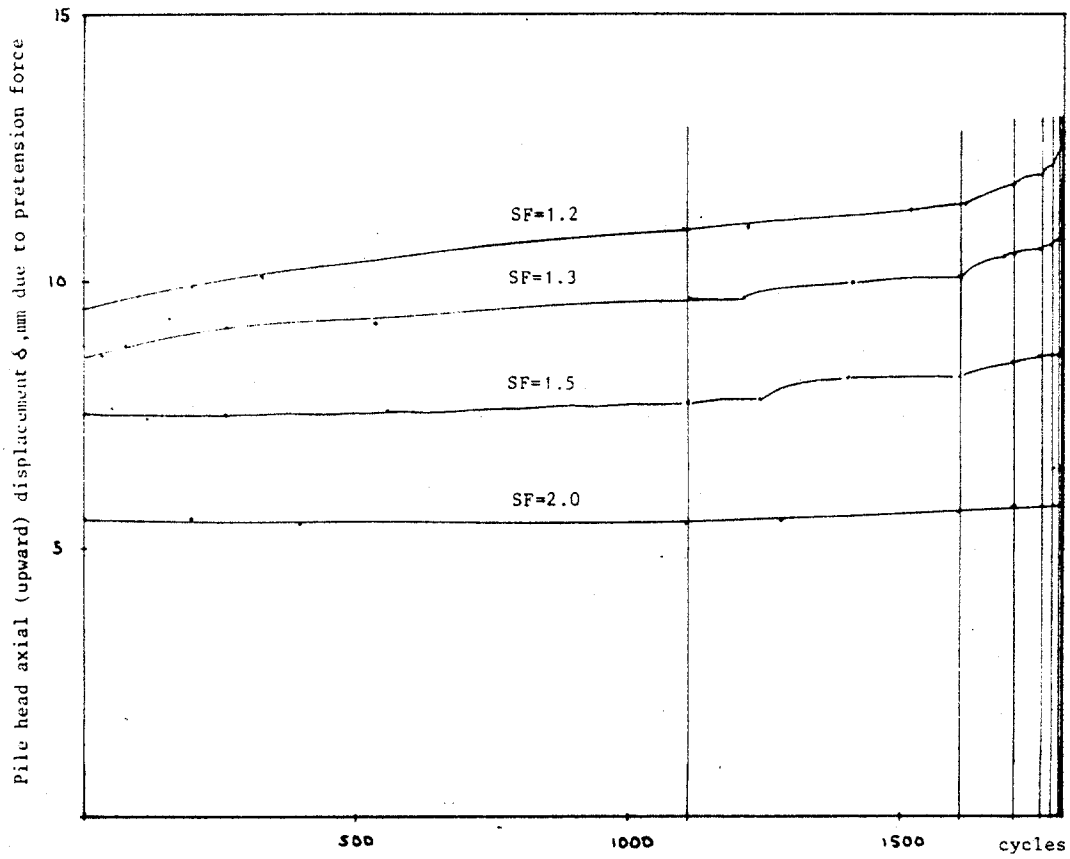

SF= 1.2 ,creep ratio= 0.7 ,quake=1% of D ,C= 1000

SF= 1.3 ,creep ratio= 0.7 ,quake=1% of D ,C= 1000

SF= 1.5 ,creep ratio= 0.7 ,quake=1% of D ,C= 1000

SF= 2.0 ,creep ratio= 0.7 ,quake=1% of D ,C= 1000

Pile Head Displacement vs. Number of Cycles and Safety Factor

CNRD 13-2 TENSION PILE STUDY LABORATORY MODEL PILE TESTS

		Scale
DET NORSKE VERITAS Geotechnical Laboratory	Drawn by	Date
	Approved	Fig. No. 4.21

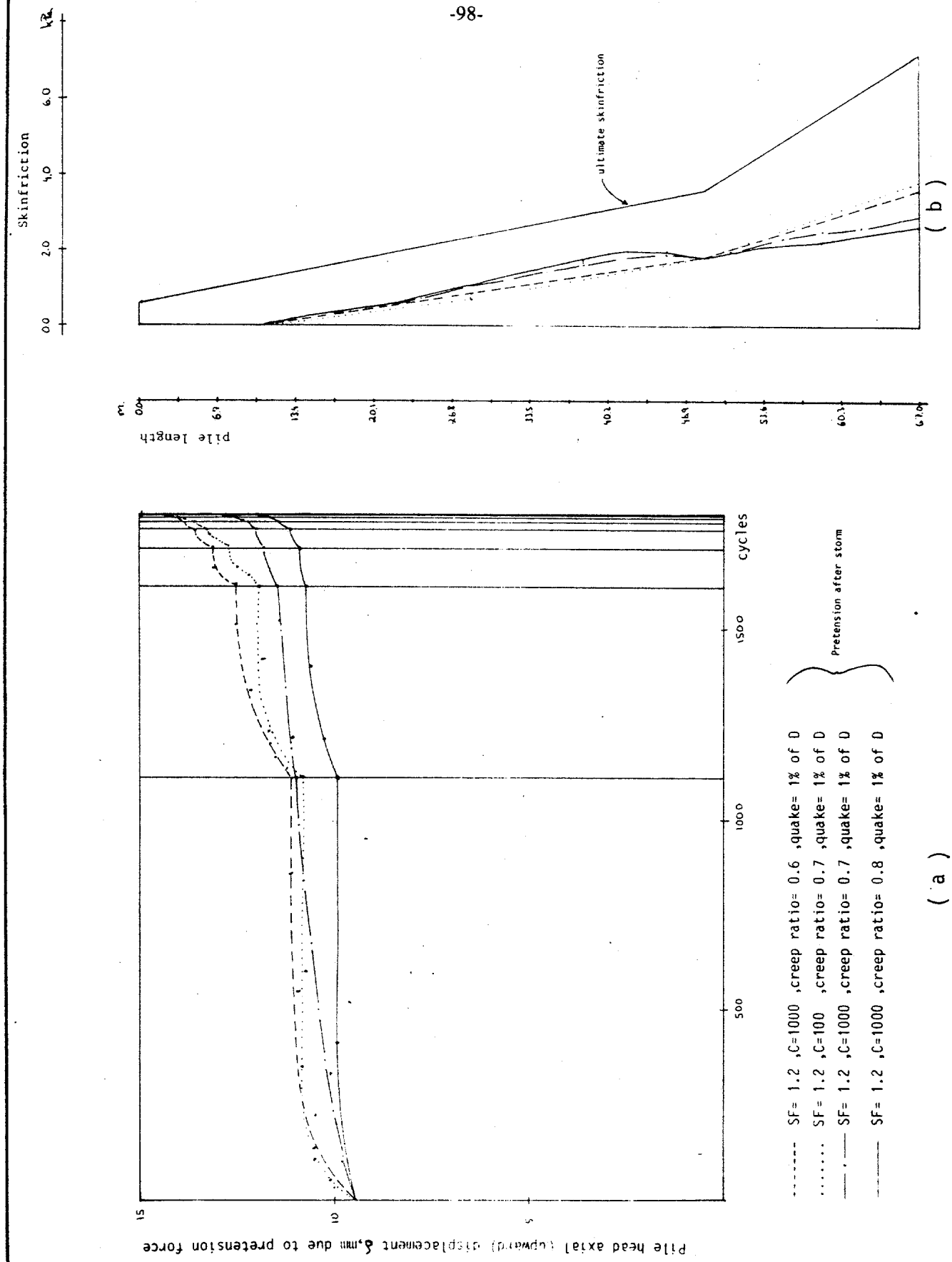

Pile Head Creep and Variation of Shear Stress Distribution. Parameter Study

CNRD 13-2 TENSION PILE STUDY LABORATORY MODEL PILE TESTS

		Scale
DET NORSKE VERITAS Geotechnical Laboratory	Drawn by	Date
	Approved	Fig. No. 4.22

VERITEC MARINE TECHNOLOGY CONSULTANTS

POSTAL ADDRESS: P.O.BOX 300, 1322 Høvik, NORWAY
TELEPHONE: + 47 (02) 12 99 00
TELEX: 76 192 VERIT N

TECHNICAL REPORT

Date 29. Juni 1984			
Report No. 84-3361	Subject Group P2,P3	Department VT/66	Project No. 66 40 17
Title of Report CNRD 13-2, TENSION PILE STUDY APPENDICES A TO E OF FINAL REPORT		Approved by Rune Dahlberg Senior Principal Engineer	
Client/Sponsor of project Conoco Norway Inc.		Client/Sponsor ref. Harry Wahl	
Work carried out by Kjell Hauge		Reporter's sign.	

Summary

This report contains the Appendices A through E of the Final Report, CNRD 13-2 TENSION PILE STUDY.

See the Excecutive Summary of the Final Report for summary.

The total report consists of:

CNRD 13-2 TENSION PILE STUDY
- FINAL REPORT
- APPENDICES A TO E
- APPENDICES F TO L

4 Indexing terms

TENSION PILES
CYCLIC LOADING
SKIN FRICTION
CAPACITY

Date of last rev.	Rev. No.

Distribution statement:

- [x] No distribution without permission from the responsible department
- [ ] Limited distribution within VERITEC.
- [ ] Free distribution.

Number of pages 406/847

CONOCO NORWAY
RESEARCH AND DEVELOPMENT

CNRD 13-2: TENSION PILE STUDY

FINAL REPORT

APPENDICES A TO E

CONTENT

FINAL REPORT

PREFACE ii

CONTENT iv

EXECUTIVE SUMMARY ix

1. INTRODUCTION 1

1.1 GENERAL 1
1.2 RELATIONSHIP TO CNRD PROGRAM 2
1.3 REFERENCE TO ERTEC'S WORK WITHIN CNRD 13-2 3
1.4 REFERENCE TO WORK BY NGI AND NTH WITHIN CNRD 13-2 3
1.5 PREVIOUS REPORTS BY VERITAS WITHIN CNRD 13-2 4
1.6 FINAL REPORT 5
1.7 FURTHER WORK 5

2. DESCRIPTION OF LABORATORY MODEL PILE TESTS 6

2.1 GENERAL 6
2.2 EQUIPMENT 7
2.2.1 Model Pile Test Chamber 7
2.2.2 Model Pile 7
2.2.3 Loading System 9
2.3 DATA ACQUISITION SYSTEM 9
2.4 PREPARATION OF SOIL SAMPLES 10
2.5 CHARACTERIZATION OF REMOULDED, RECONSOLIDATED SOIL SAMPLES AND COMPARISON WITH UNDISTURBED SAMPLES AND FIELD CONDITIONS 12
2.5.1 General 12
2.5.2 Plasticity Properties 12
2.5.3 Natural Water Content 13
2.5.4 Consolidation Properties 14
2.5.5 Static Stress-Strain and Strength 14
2.5.6 Cyclic Stress-Strain-Porepressure Generation 15
2.5.7 Comparison of Soil Conditions in the Laboratory Tests with the Field Conditions 17

2.6 LABORATORY MODEL PILE TEST PROGRAM 23
2.6.1 Objective of the Different Test Types 23
2.6.2 Summary of Test Program 23

3. MODEL PILE TEST RESULTS 25
3.1 GENERAL 25
3.2 EVALUATION OF CHANGE IN SKIN FRICTION WITH TIME IN THE LABORATORY MODEL PILE TESTS 25
3.3 STATIC CAPACITY 28
3.4 CYCLIC STRESS CONTROLLED TESTS 31
3.5 CYCLIC DISPLACEMENT CONTROLLED TESTS 34
3.6 CREEP AND RELAXATION TESTS 37

4. THEORETICAL WORK 38
4.1 GENERAL 38
4.2 PORE PRESSURE AND NORMAL STRESS GENERATION DURING INSTALLATION 39
4.2.1 Theoretical Estimates of Excess Pore Pressure 39
4.2.2 Comparison with Measured Values 39
4.3 SET-UP (PORE PRESSURE DISSIPATION) 41
4.3.1 Theoretical Initial Distribution of Pore Pressure 41
4.3.2 Consolidation Analysis Method 41
4.3.3 Consolidation Properties 42
4.3.4 Comparison between Predicted and Measured Behaviour 43
4.4 LOAD - DISPLACEMENT (T-Z) RELATIONSHIP 43
4.4.1 Theoretical Single Slice Model 43
4.5 EVALUATION OF PORE PRESSURE GENERATION UNDER CYCLIC LOADING 45
4.5.1 General 45
4.5.2 Analysis Model 46
4.5.3 Finite Element Model 49
4.5.4 Soil Consolidation Parameters 50
4.5.5 Simulation of Cyclic Loading 50
4.5.6 Comparison with Measured Behaviour 51
4.6 DEGRADATION MODELS 52
4.6.1 General 52
4.6.2 The DRIVE 15 Degradation Model 52
4.6.3 Proposal for Extended Degradation Model 53

4.7 EFFECT OF PILE FLEXIBILITY ON DEGRADATION 53
4.7.1 Analysis with DRIVE 15 53
4.7.2 Consequences of Other Degradation Models 54
4.8 PILE CREEP ANALYSIS 55
4.8.1 General 55
4.8.2 T-Z Creep Model 56
4.8.3 Creep Analysis of Elastic Piles 58
4.8.4 Sample Calculations 60
5. REFERENCES 63

LIST OF APPENDICES

APPENDIX A: TEST 4, STRATUM III: DETAILED RESULTS
APPENDIX B: TEST 5, STRATUM II : DETAILED RESULTS
APPENDIX C: TEST 6, STRATUM III: DETAILED RESULTS
APPENDIX D: TEST 7, STRATUM II : DETAILED RESULTS
APPENDIX E: TEST 8, STRATUM III: DETAILED RESULTS
APPENDIX F: TEST 9, STRATUM II : DETAILED RESULTS
APPENDIX G: TEST 10, STRATUM III: DETAILED RESULTS
APPENDIX H: TEST 11, STRATUM II : DETAILED RESULTS
APPENDIX I: TEST 12, STRATUM III: DETAILED RESULTS
APPENDIX J: TEST 13, STRATUM II : DETAILED RESULTS
APPENDIX K: RESULTS OF LABORATORY TESTS FOR COMPARISON OF REMOULDED, RECONSOLIDATED MATERIAL AND UNDISTURBED MATERIAL
APPENDIX L: DESCRIPTION OF COMPUTER PROGRAM **CRAPIL** **CR**eep Analysis of **PIL**es

LIST OF TABLES

Table 2.1 Plasticity Properties for Model Test Clay 13
Table 2.2 Water Content Compariso 13
Table 2.3 Comparison of Triaxial Test Results 17
Table 2.4 Shear Strength Test Correlations 19
Table 2.5 Relationship between Undrained Shear Strengths Measured by Different Test Methods 20
Table 2.6 Shear Strength Comparison with Segment Tests 21

Table 3.1	Summary of Laboratory Model Pile Test Program and Test Results	26
Table 4.1	Comparison Between Predicted and Measured Pressures	40
Table 4.2	Number of Cycles to Liquefaction, N_l	51
Table 4.3	Rayleigh Distribution of Load Amplitudes for Wave Parcels - Example Problem with CRAPIL	61

LIST OF FIGURES

Figure 2.1	Laboratory Model Pile Test Chamber and Model Pile	64
Figure 2.2	Photograph of Model Pile Test Chamber	65
Figure 2.3	Photograph of Model Pile	66
Figure 2.4	Photograph of Model Pile	67
Figure 2.5	Schematic Diagram of Test Set-Up and Signal Flow	68
Figure 2.6	Proposed Shear Strength Profile at West Delta	69
Figure 3.1	Undrained Shear Strength in Clay Samples (free field) Measured after Consolidation and Completion of Test	70
Figure 3.2	Measured Undrained Shear Strength vs. Water Content for Test Samples	71
Figure 3.3	α-Factors vs. Free Field Undrained Shear Strength	72
Figure 3.4	α-Factors vs. Set-Up Time	73
Figure 3.5	Friction Reduction Factor vs. Undrained Shear Strength	74
Figure 3.6	β-Factors vs. Effective Overburden Pressure	75
Figure 3.7	Interface Cyclic Shear Module vs. Undrained Shear Strength	76
Figure 4.1	Theoretical Prediction of Excess Pore Pressure vs. Radial Distance due to Pile Installation	77
Figure 4.2	Predicted and Measured Pore Pressure at Pile Wall vs. Time for Laboratory Tests	78
Figure 4.3	Predicted and Measured Pore Pressure at Pile Wall vs. Time for 3"" Segment Tests	79
Figure 4.4	Theoretical $t-z$-Curves for Laboratory Model Pile Tests	80
Figure 4.5	Theoretical $t-z$-Curves for Segment Tests	81
Figure 4.6	Single Slice Model for Laboratory and Segment Pile	82

Figure 4.7	Theoretical Prediction of Increase in Undrained Shear Strength due to Pile Installation	83
Figure 4.8	Rate of Pore Pressure Generation	84
Figure 4.9	Pore Pressure Generation for Cyclic Triaxial Test. Comparison Between OCEAN2-Predictions and Measured Values	85
Figure 4.10	Number of Cycles to Failure vs. Shear Stress Level	86
Figure 4.11	Theoretical Prediction of Pore Pressure Increase at Pile Wall due to 100 Uniform Load Cycles as a Function of Stress Level and Coefficient of Consolidation	87
Figure 4.12	Skin Friction Degradation Model in DRIVE15	88
Figure 4.13	Effect of DRIVE15 Degradation Model on Test Pile	89
Figure 4.14	Soil Model in CRAPIL, Elastic, Visco-Plastic	90
Figure 4.15	Mobilization of Shear Stress along a Tension Pile with Pretension of 33 perc. of Ultimate Capacity and Cyclic Loads between ± 5 to ± 40 percent of Ultimate Capacity. - DRIVE 15 Analysis	91
Figure 4.16	Degree of Mobilization of Skin Friction	92
Figure 4.17	Axial Pile Top Load Variations	93
Figure 4.18	Shear Stress Mobilization at Pile Station no. 8	94
Figure 4.19	Total Creep Displacement after Application of Total Set of Wave Parcels	95
Figure 4.20	Redistribution of Mobilized Shear from Creep due to Pretension	96
Figure 4.21	Pile Head Displacement vs. no. of Cycles and Safety Factor	97
Figure 4.22	Pile Head Creep and Variation of Shear Stress Distribution. - Parameter Study	98

APPENDIX A

DETAILED RESULTS FROM **TEST 4, STRATUM III** MODEL PILE TESTS

CONTENTS

Summary	A3
Test 4, Stratum III	A4
Consolidation	A4
Pile Instatllation and Set-Up	A4
Static Test 1	A5
Cyclic Tests	A6
Stress Controlled Tests (WD34LC)	A6
Displacement Controlled Tests (WD34SC)	A7
Static Test 2	A8
Strength Tests	A9

LIST OF FIGURES

Figure 1	Sample Properties
Figure 2	Consolidation Diagram
Figure 3	Pocket Penetrometer Tests After Consolidation
Figure 4	Pressures at Pile Wall after Installation
Figure 5	Static Test 1
Figure 6	Skin Friction vs no. of Cycles, WD34LC
Figure 7	Deflection vs no. of Cycles, WD34LC
Figure 8	Total Normal Pressure vs no. of Cycles, WD34LC
Figure 9	Pore Pressure vs no. of Cycles, WD34LC
Figure 10	Eff. Normal Pressure vs no. of Cycles, WD34LC
Figure 11	Deflection vs no. of Cycles, WD34SC
Figure 12	Skin Friction vs no. of Cycles, WD34SC

Figure 13 Total Normal Pressure vs no. of Cycles, WD34SC
Figure 14 Pore Pressure vs no. of Cycles, WD34SC
Figure 15 Eff. Normal Pressure vs no. of Cycles, WD34SC
Figure 16 Static Test 2
Figure 17 Pocket Penetrometer Tests after Pile Test
Figure 18 Water Content and Shear Strength
Figure 19 Unconfined Compression Tests

Appendix AA
Plotted Results from WD34LC
Figures AA-1 through AA-9
Skin Friction vs Deflection, Selected Cycles
Figures AA-10 through AA-18
Skin Friction vs Eff. Normal Pressure, Selected Cycl.
Figures AA-19 through AA-36
Skin Friction, Pore and Total Pressure, Selected Cycles

Appendix AB
Plotted Results from WD34SC
Figures AB-1 through AB-7
Skin Friction vs Deflection, Selected Cycles
Figures AB-8 through AB-14
Skin Friction vs Eff. Normal Pressure, Selected Cycl.
Figures AB-15 through AB-26
Skin Friction, Pore and Total Pressure, Selected Cycles

SUMMARY

This report contains the results of the laboratory model pile tests designated TEST 4, STRATUM III, in the project CNRD 13-2, TENSION PILE STUDY, for Conoco Norway Inc.

The clay sample was consolidated for 17 days under 500 KPa applied pressure. A considerable amount of excess pore pressure, 225 KPa, was still present. One day of consolidation of the clay in pile chamber was allowed before pile installation was started. A substantial amount of pore pressure from consolidation was present. After three days of set-up the pore pressure was still present. Testing was then started.

Static test gave peak friction 32,5 KPa with residual value of 28.5 KPa. Undrained shear strength was interpreted to 60 KPa, which gives an alpha (α) value of 0.54 and o.48 for peak and residual respectively. Estimating the effective vertical soil pressure to 250 KPa the resulting beta (β) factor becomes 0.13.

After seven more days of set-up cyclic tests were performed, starting with stress controlled cyclic tests with static tension bias. The tension bias was 6.5 KPa, (20% of previous static capacity) and parcels of 100 cycles with specified cyclic stress amplitude was then applied. In the ninth parcel with cyclic stress amplitude of 45 KPa the pile failed after 14 cycles.

Subsequently a displacement controlled test was performed. A maximum friction of 50 KPa was obtained, which reduced with number of cycles setling at 40 KPa after about 40 cycles. A static test two days later gave similar values for friction, with a peak of 48 KPa and residual value during large slip of 40 KPa.

TEST 4, STRATUM III

CONSOLIDATION

The sample was prepared from cylinder numbers S-1, S-100, S-102, S-104, S-108, S-113, S-117, S-127, S-135, all from Stratum III.

After remoulding, the clay was filled into the consolidometer and a vertical consolidation pressure of 500 KPa applied on top. The sample was divided horizontally into four layers with intermediate filters to provide better vertical drainage conditions.

As can be seen from Figure 2 the pore pressure at middle height had dropped to 45% of the consolidation stress after 11 days. At this time the consolidation was stopped and sample transferred to the pile chamber. Shear strength was measured by use of a pocket penetrometer at the top and along the side of the sample. The shear strength, s_u, along the side is considered most reliable and has an average of about 50 KPa. The higher values of about 105 KPa on top is considered as a top crust. A substantial degree of underconsolidation is present in the sample shown by the ratio of s_u/σ_{ve} (Shear strength versus applied vertical consolidation stress) of about 0.12. The excess pore pressure thus has a significant influence on the strength of the soil.

Upon extrusion of the sample from the consolidometer a substantial degree of side friction is experienced. This friction is measured as a force in the piston pushing the sample, and converting this to side friction by dividing by the circumferential area of the sample a value of 23 KPa is obtained. This relatively high value will tend to reduce the consolidation stress in the lower parts of the consolidometer.

PILE INSTALLATION AND SET-UP

After extrusion from the consolidometer the sample was mounted in the pile chamber and left to reconsolidate for one day under a vertical pressure of 500 KPa and a radial pressure of 350 KPa, (K = 0.7) . A back pressure of 200 KPa was applied to the sample to help speed up the pore pressure response. The pile was inserted using a hydraulic jack. The tip resistance measured by the lower axial pile transducer, showed a gradual increase as did the side friction, which reached a maximum value of

approximately 8 to 10 KPa. Total normal pressure directly after installation was measured to 600 KPa.

Pore pressure response was unsatisfactory and only reflected the back pressure directly after installation, as seen in Figure 4. After two days of consolidation with constant confining and back pressures the pore pressure gradually increased to a maximum of 495 KPa reducing to 475 KPa after three additional days, the total pressure reading being constant at 600 KPa.

The sample obviously has a considerable amount of excess pore water pressure after installation of the pile. It was uncertain if this was due to the low permeability of the clay, insufficient drainage conditions of the pile chamber or also due to a slow response of the pore pressure measurement equipment at the pile surface. It was decided that time for full dissipation of the excess pressure would be too long and therefore to proceede with load testing of the model pile.

STATIC TEST I

A displacement controlled static test with deformation rate 1 mm per hour was conducted, as shown in Figure 5. The pile was pulled 5 mm in tension and pushed down to original position causing failure in compression, and the cycle repeated once.

As can be seen in Figure 5 the displacement to cause failure was about 0.5 mm corresponding to 2% of the pile diameter. The shaft friction reached a maximum of 32.5 KPa with a residual value of 28.5 KPa.

Based on the pocket penetrometer test of the clay after consolidation, the undrained shear strength can be estimated to be about 60 KPa. This gives an alpha (α) value (f_{max}/S_u) of 0.54 for total stress analysis.

For the effective stress approach where the side friction is estimated from the value of effective vertical soil pressure (σ'_{vo}) prior to pile installation ($f = \beta \cdot \sigma'_{vo}$) , the corresponding beta factor (β) is dependent on the value of σ'_{vo}. The pore pressure in the sample at time of transfer to the pile chamber was 221 KPa. After pile installation the pore pressure at the pile wall was measured to 490 KPa including a back pressure of 210 KPa, giving an actual pore pressure of 280 KPa.

The pore pressure in the sample should be somewhere inbetween these two values. With an applied total vertical pressure of 500 KPa the effective vertical pressure in the sample then is estimated to be σ'_{vo} = 500 - 250 = 250 KPa, resulting in the beta factor of ($\beta = f/\sigma'_{vo}$) 0.13.

Based on the soil characterization from West Delta a relationship between undrained shear stre0ngth and effective vertical stress was suggested to

$$s_u = (0.23 \pm 0.05) \cdot \sigma'_{vo}$$

with undrained shear strength measured by direct shear tests. With a s_u of 60 KPa (although measured by UCT or pocket penetrometer) this corresponds to an effective overburden pressure between 214 and 333 KPa.

From the total normal, σ_n, and pore pressure, u , readings at maximum side friction, fmax, the interface friction angle, δ , can be calculated

$$f_{max} = \sigma'_n \cdot \tan\delta$$

For f_{max}= 32.5 KPa, σ_n = 610 KPa and u = 475 KPa this gives an interface friction angle δ = 13.5 degrees.

CYCLIC TESTS

The sample, with the pile in original zero position, was now left to consolidate for a period of seven days before cyclic loading of the pile started. Total pressure on the pile wall had increased to 665 KPa and the pore pressure showed 412 KPa..

Stress Controlled Tests (WD34LC)

A stress controlled test comprised of applying a prescribed static tensile (uplift) stress on the pile and then parcels of 100 cycles with 10 seconds period and prescribed cyclic stress amplitude. The stress amplitude was then increased in the following parcels until failure (excessive uplift) occured in tension.

For this test the static tensile stress level was 6.5 KPa, about 20% of the previous static capacity. In the first parcel the cyclic level was 5 KPa and for the following parcels

the cyclic level was incremented by 5 KPa as seen in Figure 6 which shows skin friction (envelope of max. and min.) versus number of cycles. In the following four figures the resulting deformations and pressures due to the applied skin friction, are plotted versus cycle numbers.

As can be seen from the skin friction versus deformation curves in Appendix A the response is linearly elastic for the first 5 parcels.The maximum stress level in the 5th parcel was about 31 KPa. In the next parcel a small hysteresis in the friction deformation curve is developed whereas no significant sign of pull-out is seen. Increasing the cyclic friction further yields a larger hysteresis in the response and a distinct, although small, uplift of the pile results. Finally in the last parcel with an applied cyclic friction of 45 KPa a distinct cyclic deformation of the pile is seen with an abrupt pull-out after 14 cycles. The maximum friction reached was about 52 KPa.

Referring to the plot of deformation versus cycle numbers a downward movement of the pile versus cycles is seen. The reason for this is unknown and quite unlikely since the pile is subjected to a constant uplift. Since this is a stress controlled test an explanation can be a drift in the two load sensors and thereby seemingly pressing the pile down in order to maintain the prescribed voltage.

Displacement Controlled Tests (WD34SC)

The pile was brought back to original position and left for a set-up time of four hours before displacement (stroke) controlled tests were performed. One parcel here consisted of 100 cycles with 10 seconds period in two-way cyclic loading from the zero position of the pile.

A total of seven consecutive parcels were performed with increasing displacement amplitude, starting with 0.1 mm in the first parcel and with 0.2, 0.4, 0.65, 0.8 and 1.0 mm in the following parcels. The last parcel was a large displacement two-way cyclic test with an amplitude of 2 mm.

The applied pile displacement versus cycle numbers are shown in Figure 11 with the resulting skin friction, total pressure, pore pressure and effective pressure versus cycle number shown in Figures 12, 13, 14 and 15 respectively. More detailed plots of selected cycles are shown in Appendix B.

and in the subsequent cycle a pronounced peak of 48 KPa occured before settling at a residual value of 40 KPa during large slip, which then indicates no regain in strength after the stroke controlled tests 48 hours earlier.

STRENGTH TESTS

The pile was then pulled out of the pile chamber and the sample built out. Pocket penetrometer tests were then performed on the side of the sample with results shown in Figure 17. Three standard triaxial samples were then prepared from the centre of the sample and unconfined compression tests (UCT) were performed. The results are shown in Figure 19.

In Figure 18 are shown the water content and interpreted undrained shear strength of the clay specimen versus the distance from the pile center after completion of the pile test. An increase in shear strength is seen close to the pile wall, with a tendency of the water content to be lowest close to the pile wall.

As can be seen from the resulting skin friction in Figure 12 the pile had a residual compression from the previous downward movement to zero position after failure in the stress controlled test. During the first parcel (100 cycles) the mean stress was about 6 KPa.

In the second parcel with cyclic deformation of 0.2 mm it seems to yield a maximum stress in compression at -45 KPa with a residual value of about -40 KPa whereas the maximum tension was quite steady at about 30 KPa. The third parcel with cyclic deformation 0.4 mm yields failure in both tension and compression with a maximum in first cycle of about 50 KPa. After about 40 cycles a steady residual friction of 40 KPa was established, which yields 20% degradiation from ultimate cyclic capacity.

In the subsequent parcels the peak friction was somewhat lower since only about 10 minutes delay was allowed inbetween parcels, while the residual friction was steady at 40 KPa.

The pore pressure showed no cyclic variation during testing which is most likely due to a slow response of the pore pressure measurement system. A steady rise in pore pressure of 10 KPa from 420 KPa, is seen over the first six parcels whereas a small drop, 5 KPa is registered in the large deformation parcel.

Total normal pressure showed a cyclic response proportional to the cyclic deformation level, with the average pressure almost constant at about 620 KPa throughout the parcels. The resulting effective normal pressure, shown in Figure 15, thus shows a slow drop with increasing cyclic deformation with an apparent increase during the last large deformation parcel.

STATIC TEST II

The pile was then left for two days to reconsolidate which made the pore pressure go back to the original value before cyclic testing, about 420 KPa. Total normal pressure stayed constant at about 620 KPa.

A static test was now performed with deformation rate 10 mm per hour (increased with a factor of 10 from first test). Two cycles were made, and as can be seen from Figure 16 no peak value occured in the first tension failure. In compression, however,

TABLE 1.

SAMPLE PROPERTIES TEST 4, STRATUM III

SAMPLE PREPARATION		CONSOLIDATION			END OF PILE TEST
INITIAL WATER CONTENT	INITIAL HEIGHT	AXIAL DEFORMATION	AXIAL STRAIN	WATER CONTENT	WATER CONTENT
w_i (%)	H_o (cm)	ΔH (cm)	ε (%)	w_e (%)	w_{ep} (%)
	54.09	6.87	12.7	40.17 42.20	A - 40.47 B - 40.04 C - 38.14

CONFINING PRESSURE		
AXIAL	KPa	700
RADIAL	KPa	550
BACK PRESSURE	KPa	200
SAMPLE CONSOLIDATION		
IN OEDOMETER	Days	17
IN PILE CHAMBER	Days	1
INTERPRETED SHEAR STRENGTH		
END OF CONSOLIDATION	KPa	59
END OF PILE TEST	KPa	62

Fig. 1

CONSOLIDATION DIAGRAM									Test No. 4 Stratum III		Start date 26.4.82	
H_i 54.09 cm		H_e 47.22 cm		$\Delta\varepsilon_v$ 12.7 %							σ_c 500 kPa	
Time h	21	69	90	142	159	186	212	236	255	326	351
Δh cm	1.43	5.02	5.24	5.68	5.81	5.97	6.1	6.22	6.31	6.63	6.71
u kPa	70.3	318	308	289	282	274	268	262	258	236	232
	375	400									
	6.79	6.87									
	226	222									

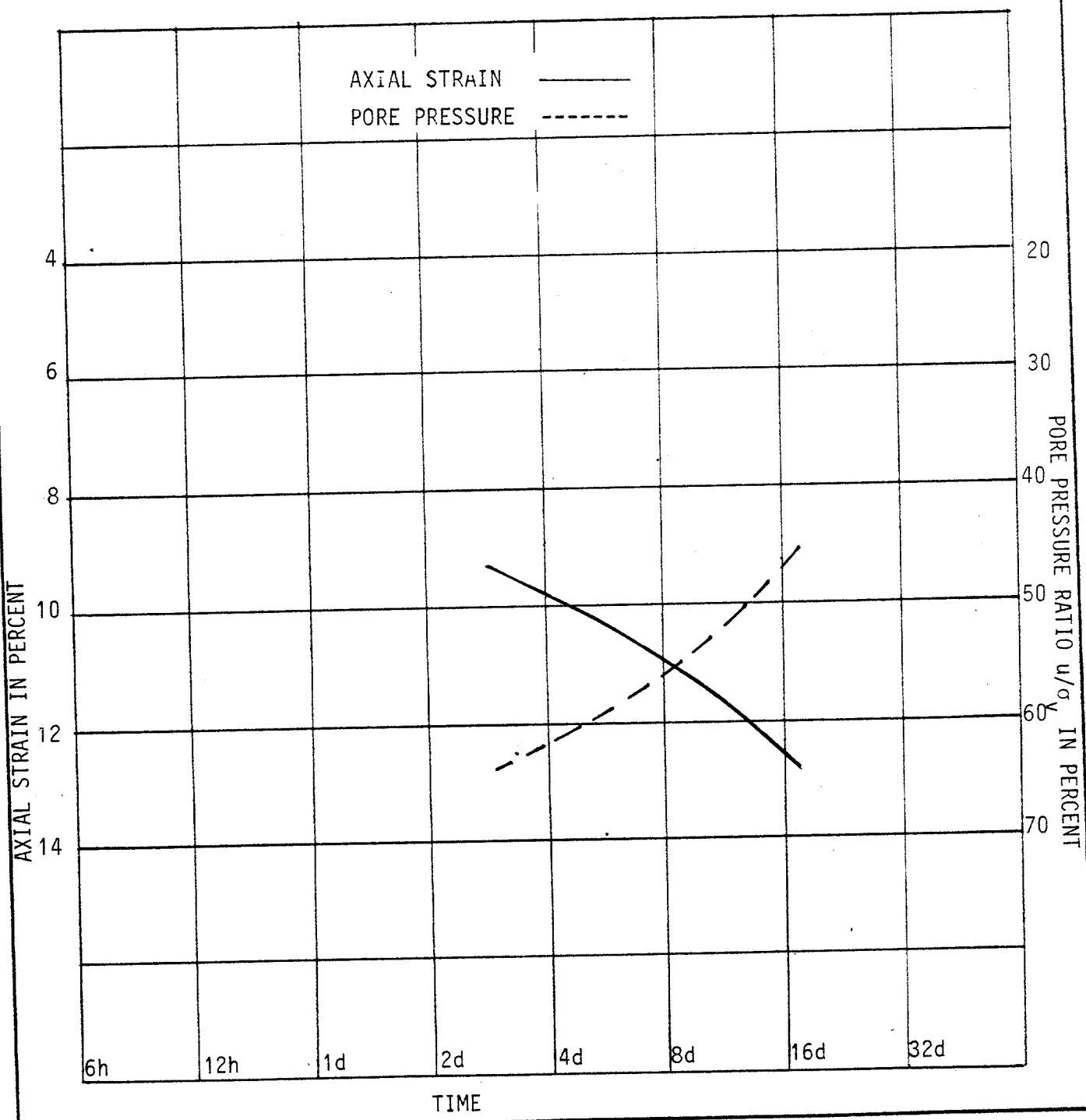

CNRD 13-2 TENSION PILE STUDY LABORATORY MODEL PILE TESTS

		Scale
DET NORSKE VERITAS Geotechnical Laboratory	Drawn by	Date
	Approved	Fig. No. 2

TEST 4, STRATUM III

SHEAR STRENGTH AFTER CONSOLIDATION (KPa)

FROM POCKET PENETROMETER TESTS

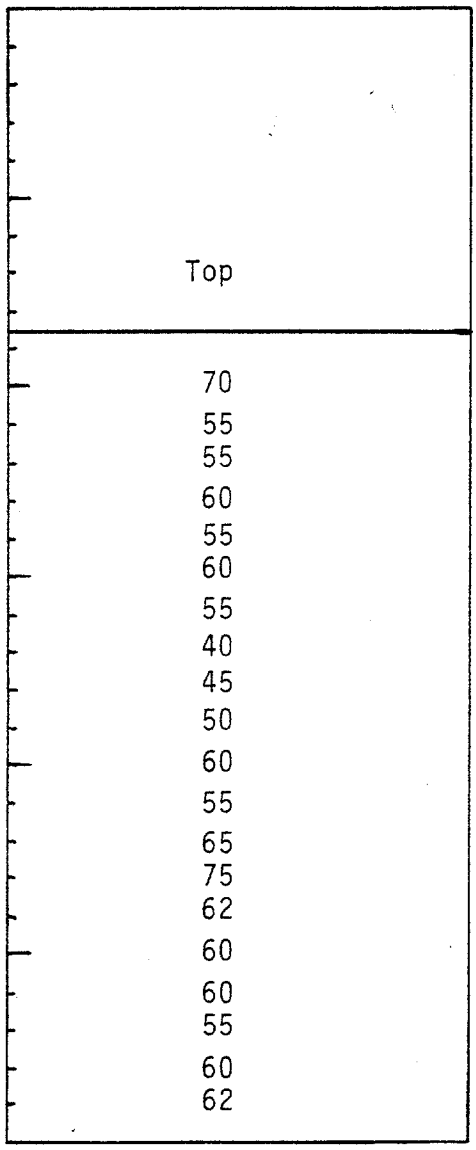

Scale: 1:4

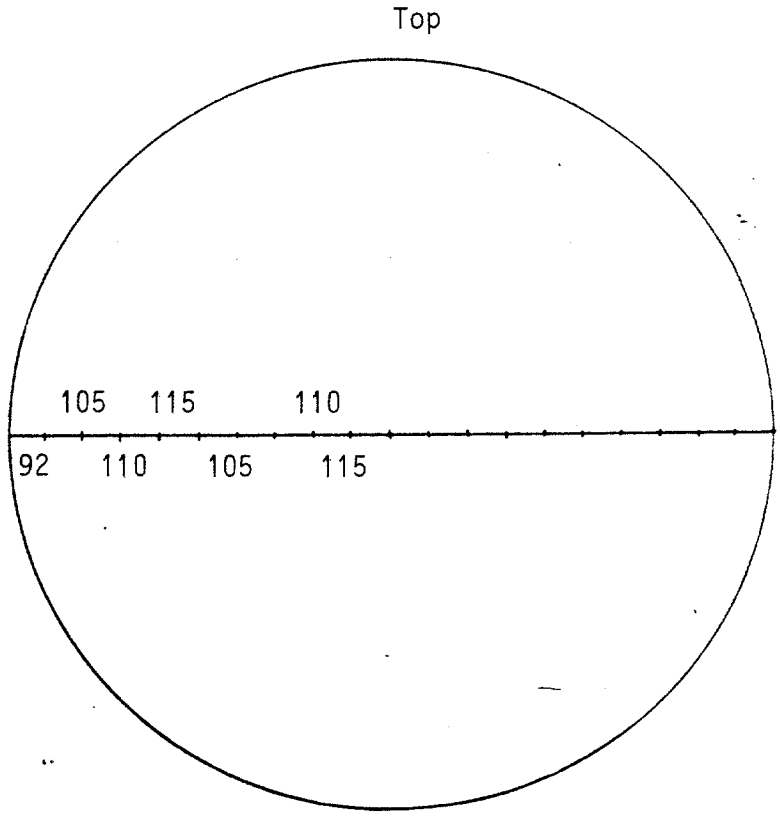

Scale: 1:2

CNRD 13-2 TENSION PILE STUDY LABORATORY MODEL PILE TESTS

		Scale
DET NORSKE VERITAS Geotechnical Laboratory	Drawn by	Date
	Approved	Fig. No. 3

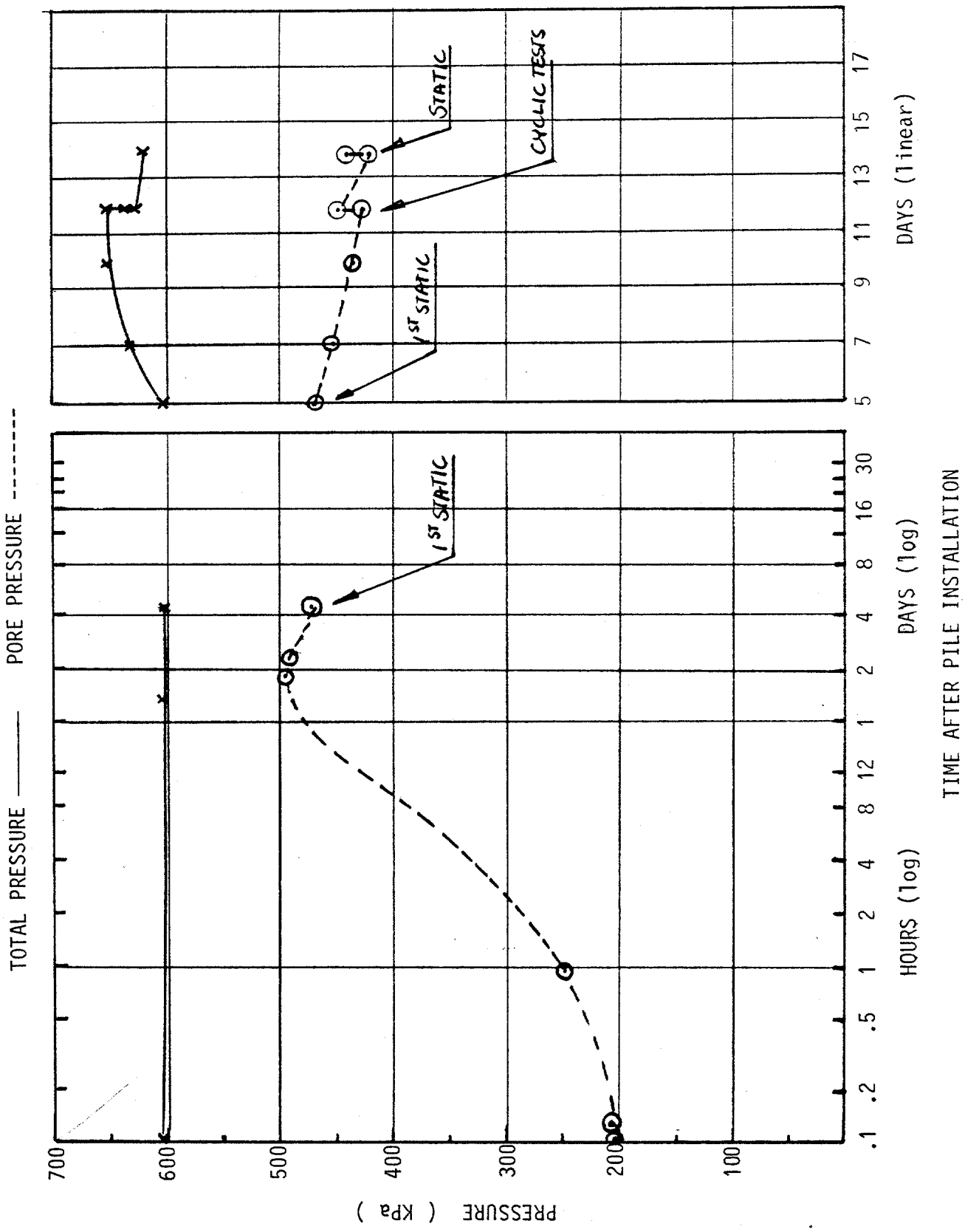

CNRD 13-2 TENSION PILE STUDY LABORATORY MODEL PILE TESTS

TEST 4, STRATUM III. Pressures at pile wall after insallation

DET NORSKE VERITAS Geotechnical Laboratory	Drawn by	Scale
	Approved	Date
		Fig. No. 4

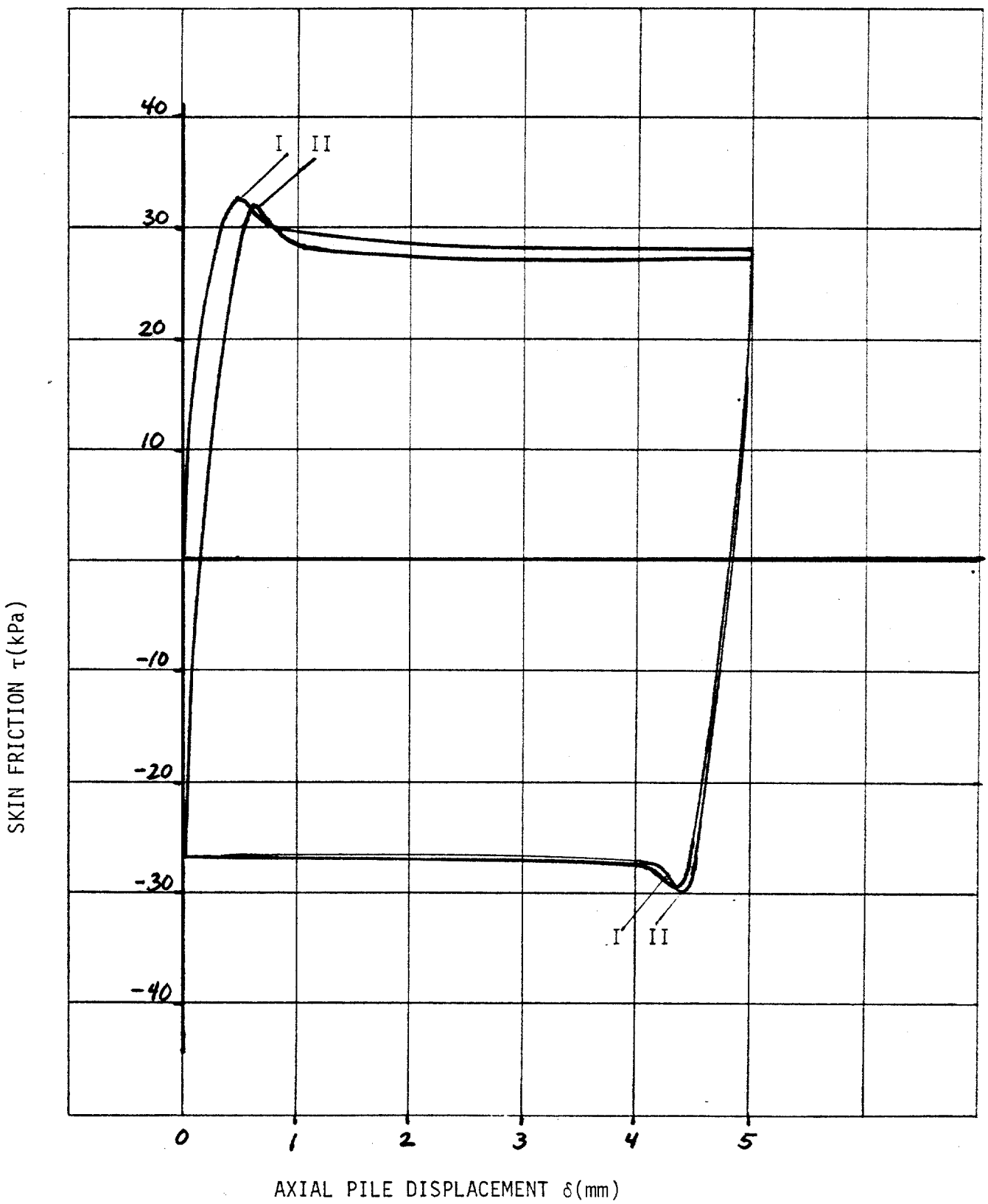

CNRD 13-2 TENSION PILE STUDY LABORATORY MODEL PILE TESTS

TEST 4, STRATUM III. STATIC TEST 1

DET NORSKE VERITAS Geotechnical Laboratory	Drawn by	Scale
	Approved	Date
		Fig. No. 5

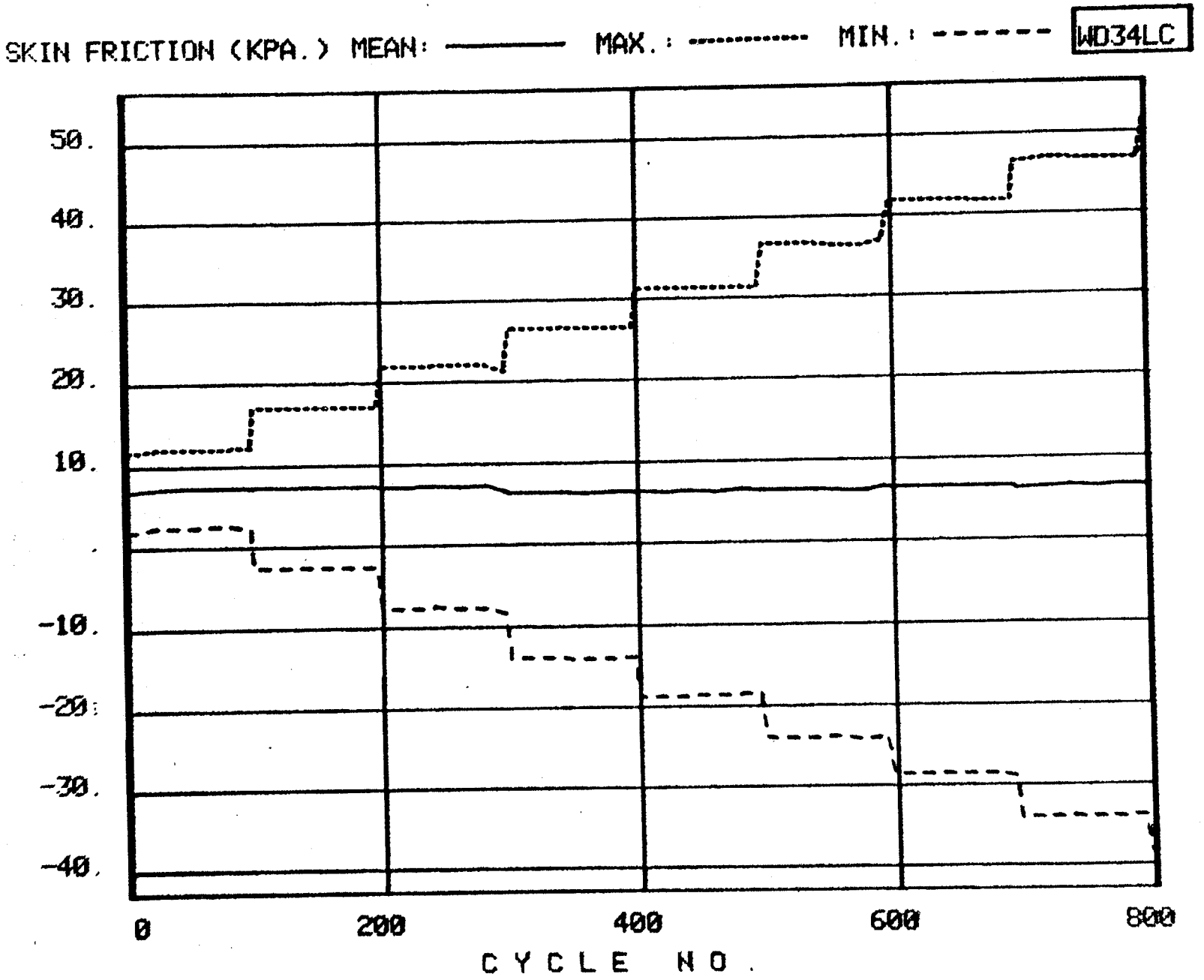
SKIN FRICTION (KPA.) MEAN: ——— MAX.: ····· MIN.: - - - - - -
WD34LC
50.
40.
30.
20.
10.
-10.
-20.
-30.
-40.
0
200
400
600
800
CYCLE NO.

Fig.6

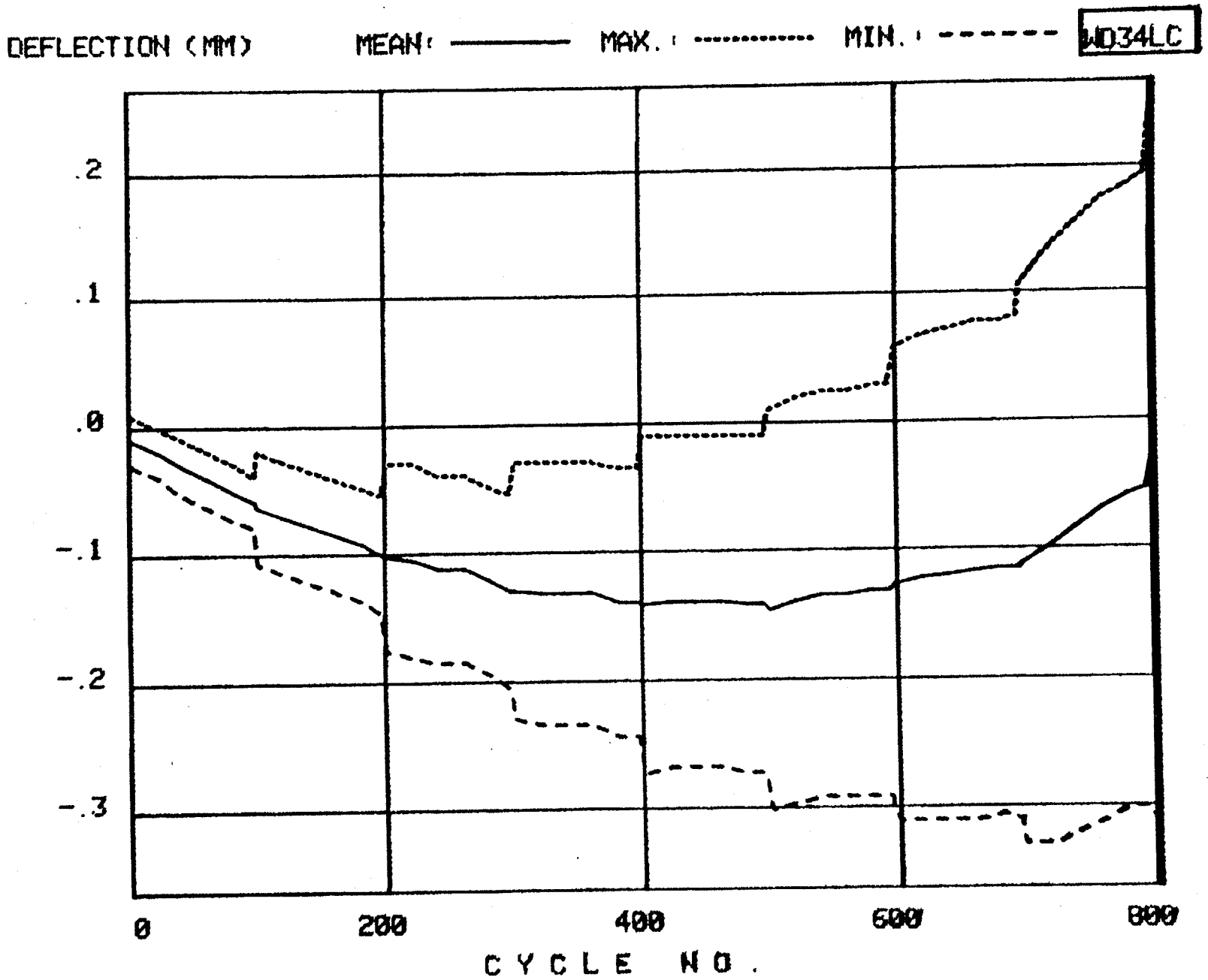
DEFLECTION (MM)
MEAN:
MAX.:
MIN.:
WD34LC
.2
.1
.0
-.1
-.2
-.3
0
200
400
600
800
CYCLE NO.

Fig.7

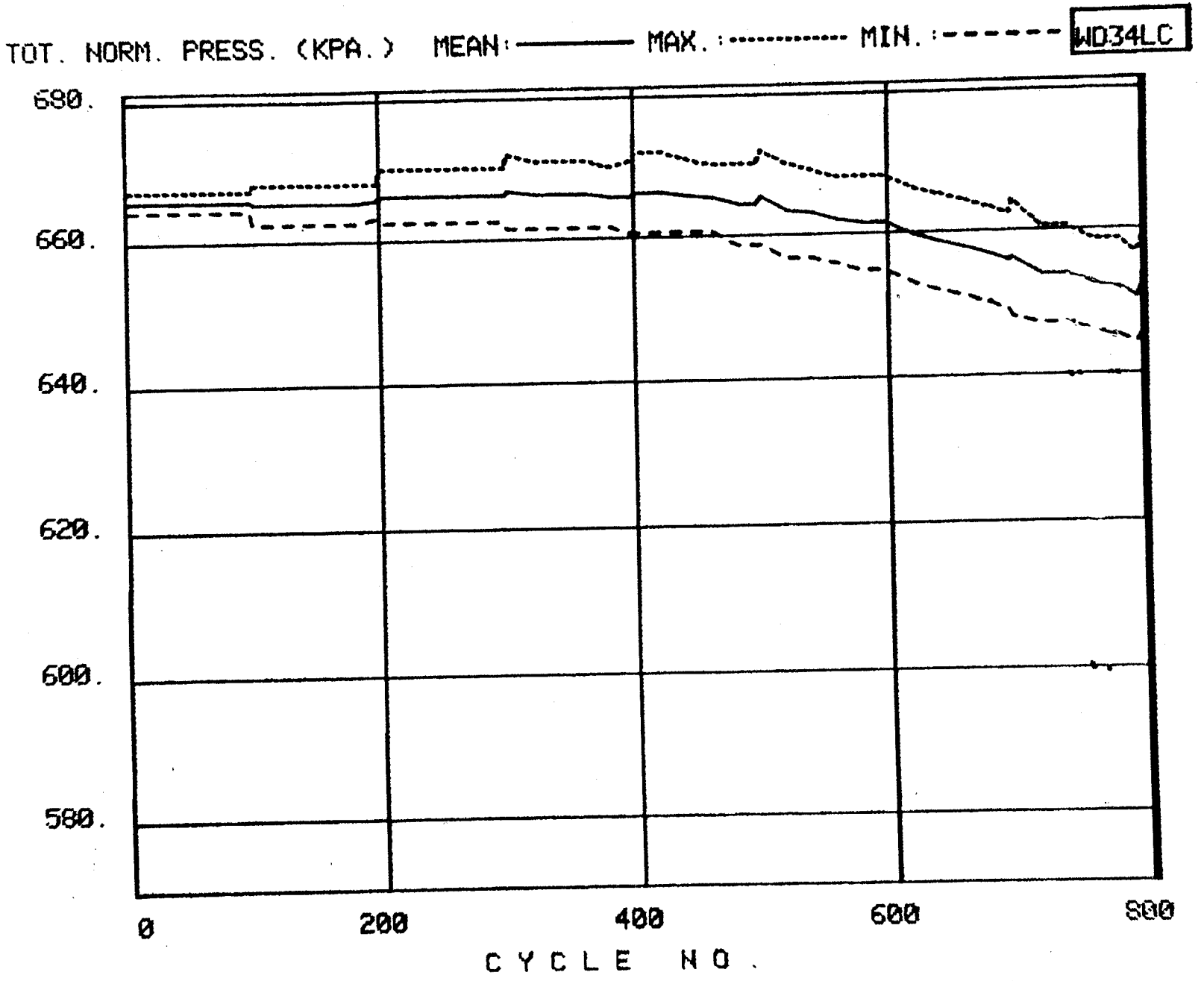
TOT. NORM. PRESS. (KPA.) MEAN: MAX.: MIN.:
WD34LC
680.
660.
640.
620.
600.
580.
0
200
400
600
800
CYCLE NO.

Fig.8

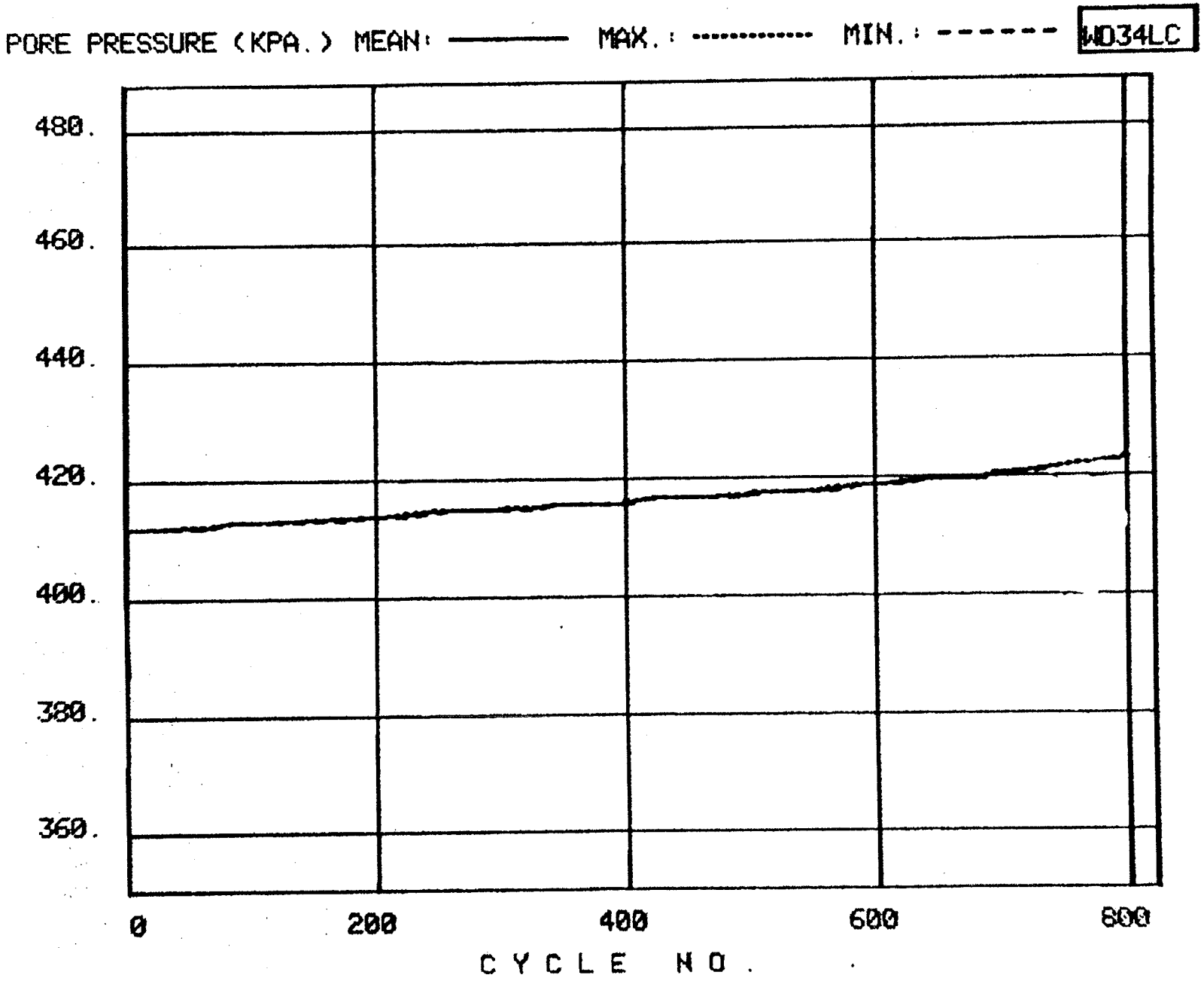
PORE PRESSURE (KPA.) MEAN: MAX.: MIN.:
WD34LC
480.
460.
440.
420.
400.
380.
360.
0
200
400
600
800
CYCLE NO.

Fig.9

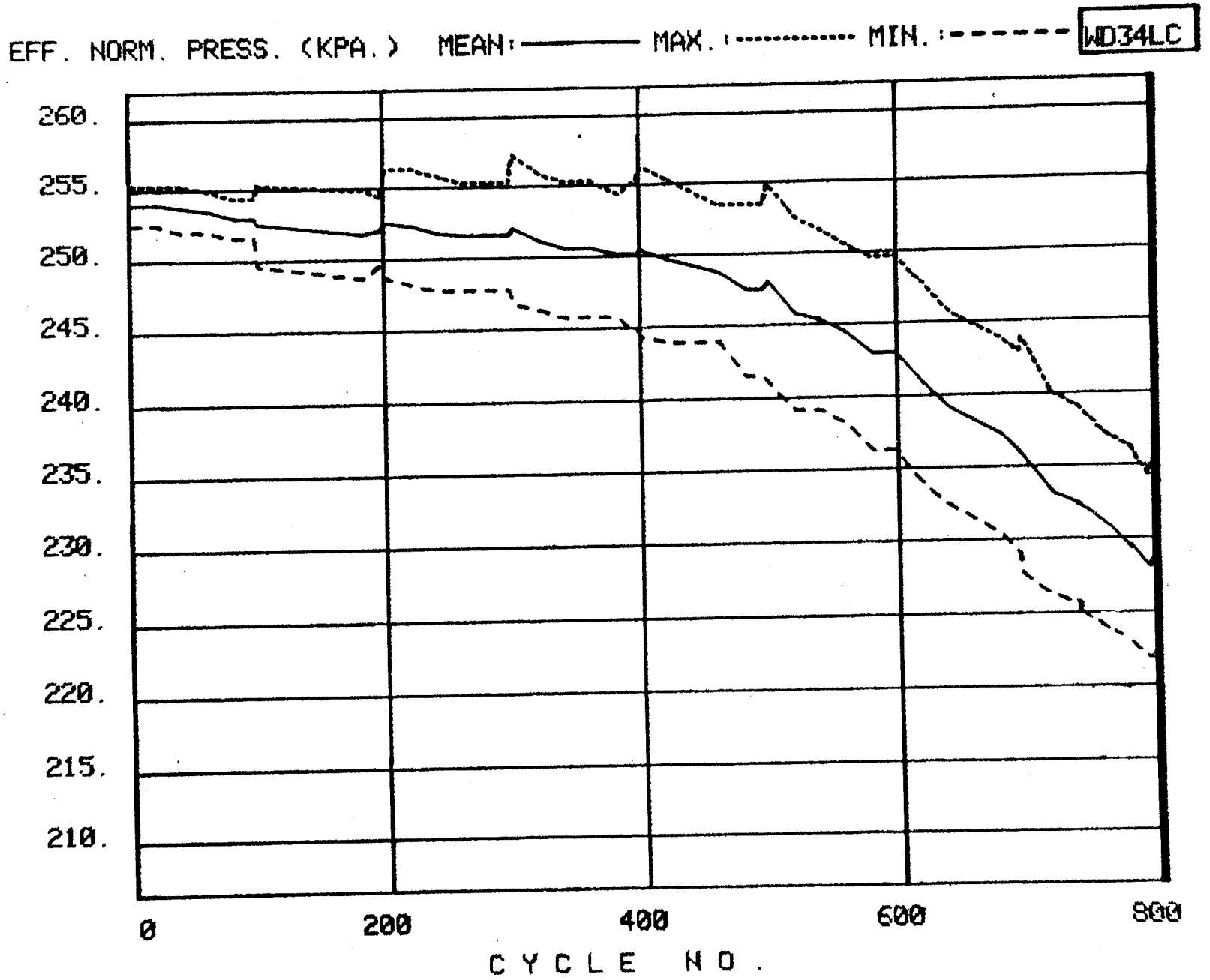
EFF. NORM. PRESS. (KPA.)
MEAN:
MAX.:
MIN.:
WD34LC
260.
255.
250.
245.
240.
235.
230.
225.
220.
215.
210.
0
200
400
600
800
CYCLE NO.

Fig.10

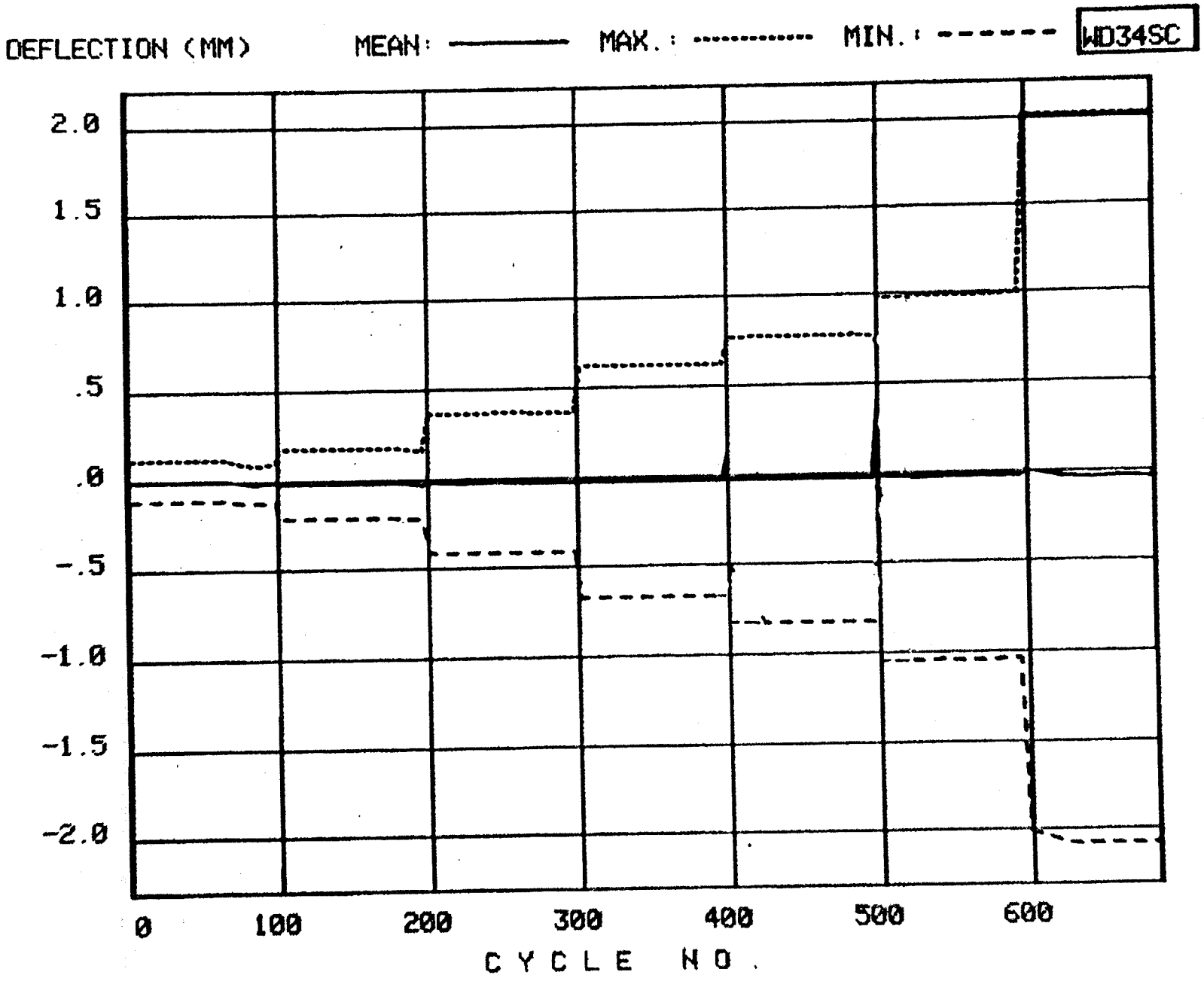
DEFLECTION (MM)
MEAN:
MAX.:
MIN.:
WD34SC
2.0
1.5
1.0
.5
.0
-.5
-1.0
-1.5
-2.0
0
100
200
300
400
500
600
CYCLE NO.

Fig.11

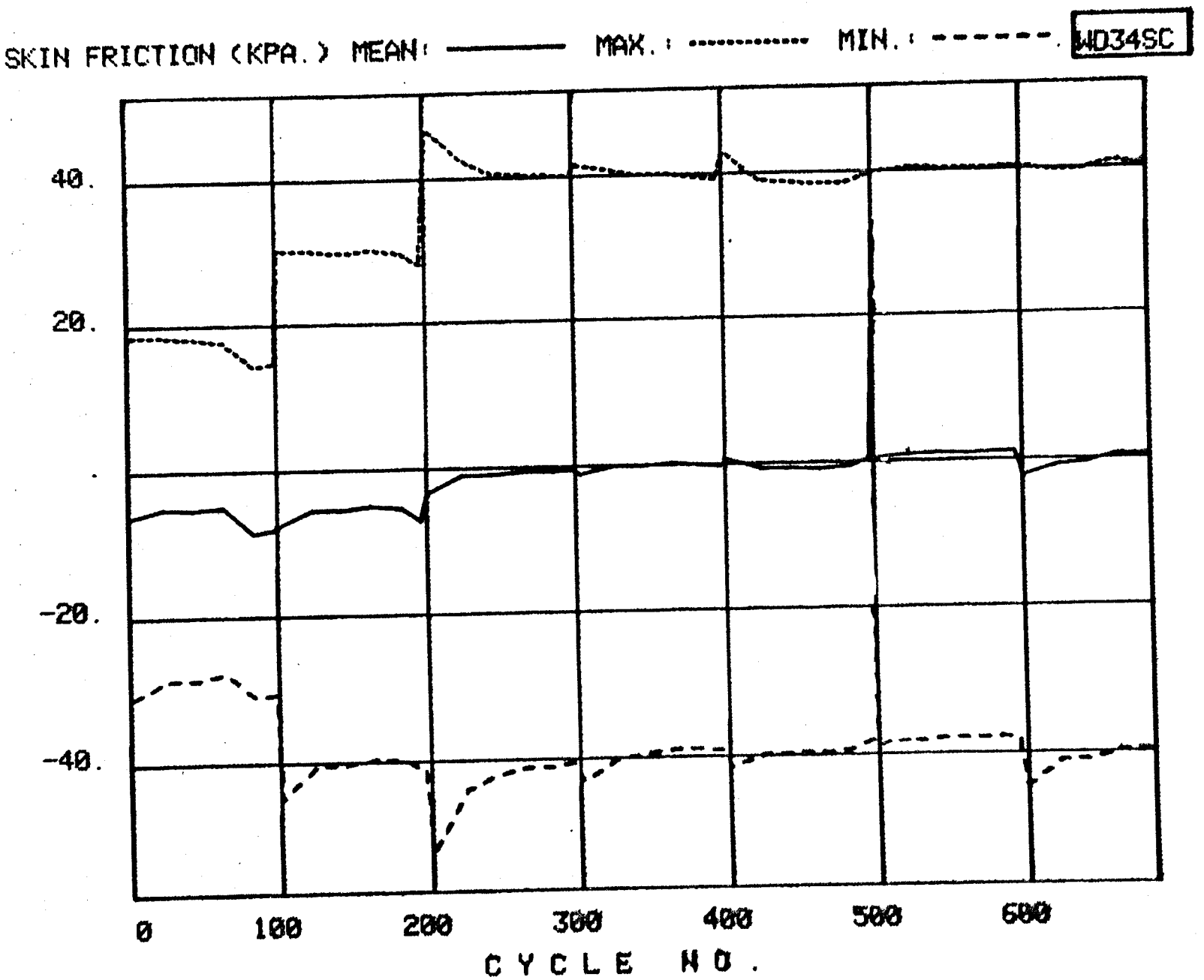
SKIN FRICTION (KPA.) MEAN: MAX.: MIN.:
WD34SC
40.
20.
-20.
-40.
0
100
200
300
400
500
600
CYCLE NO.

Fig.12

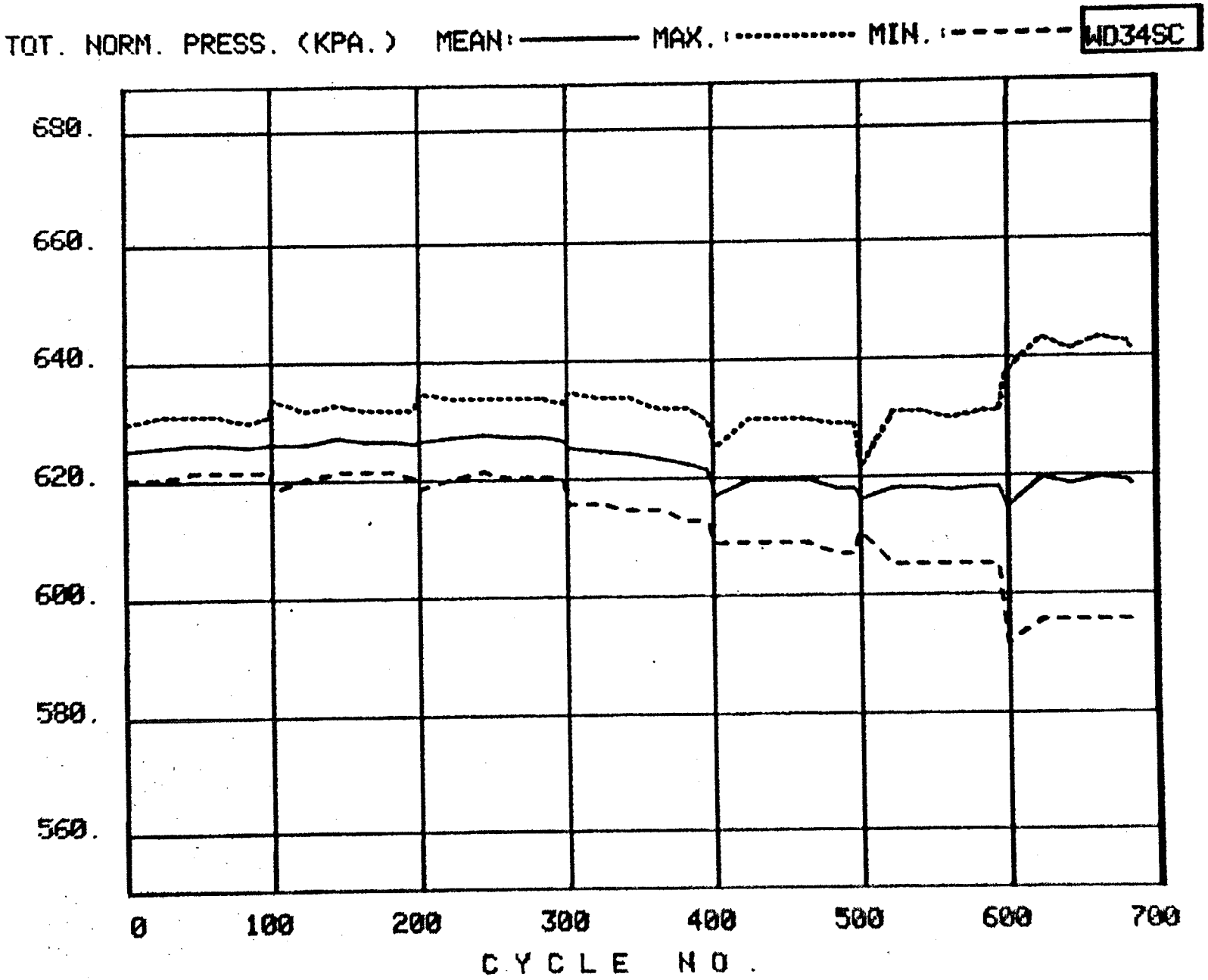
TOT. NORM. PRESS. (KPA.) MEAN: MAX.: MIN.:
WD34SC
680.
660.
640.
620.
600.
580.
560.
0
100
200
300
400
500
600
700
CYCLE NO.

Fig.13

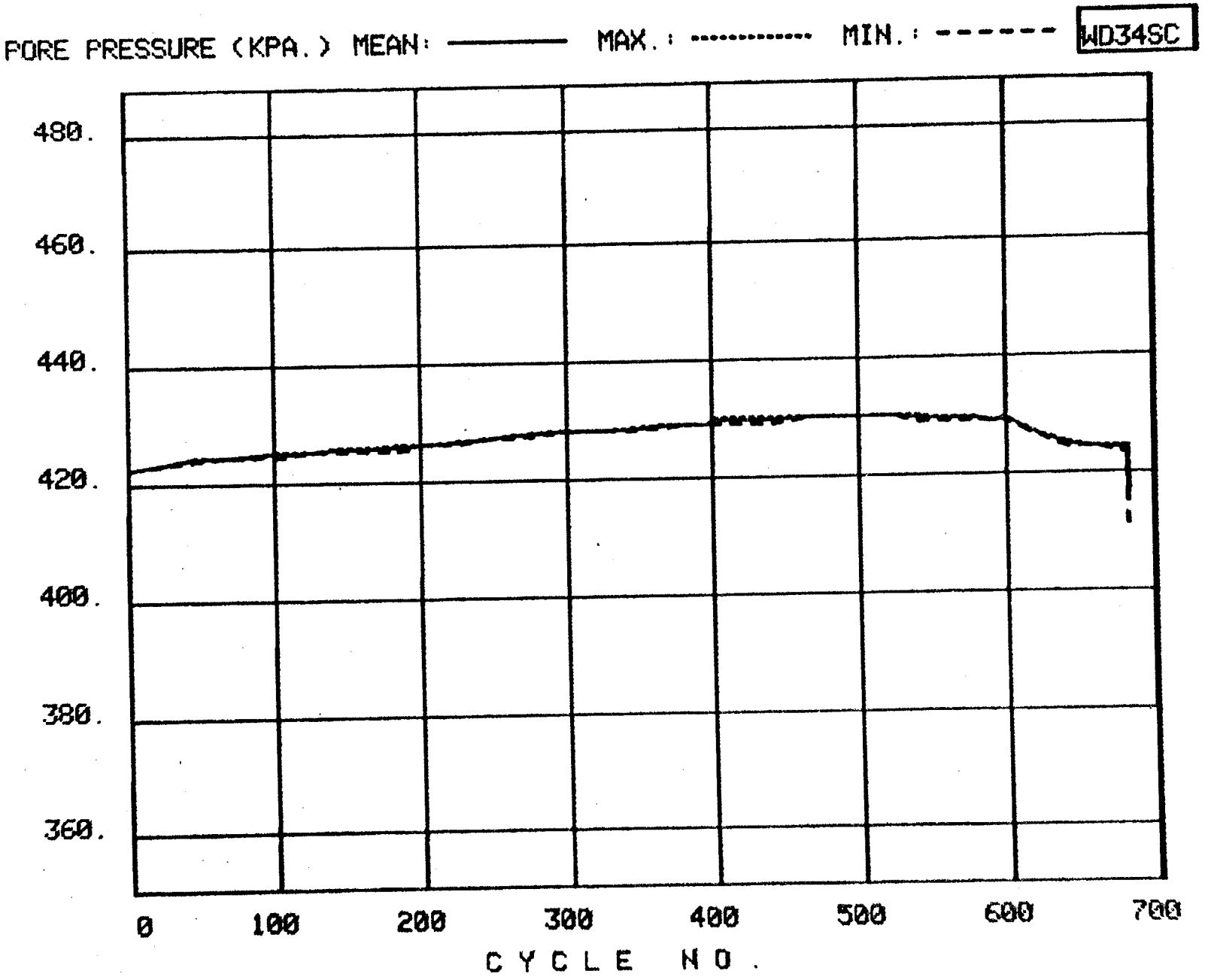
PORE PRESSURE (KPA.) MEAN: MAX.: MIN.:
WD34SC
480.
460.
440.
420.
400.
380.
360.
0
100
200
300
400
500
600
700
CYCLE NO.

Fig.14

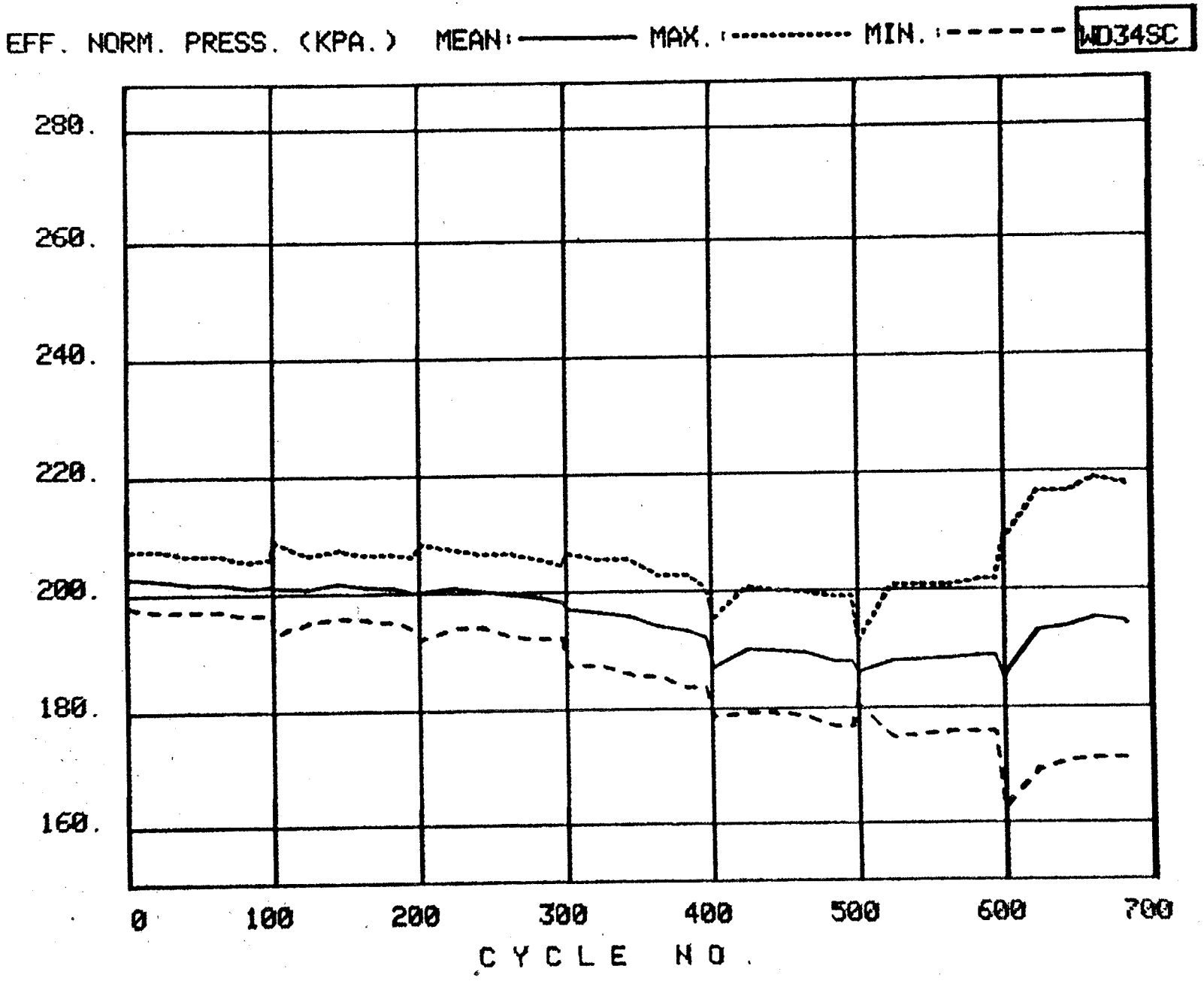
EFF. NORM. PRESS. (KPA.)
MEAN:
MAX.:
MIN.:
WD34SC
280.
260.
240.
220.
200.
180.
160.
0
100
200
300
400
500
600
700
CYCLE NO.

Fig.15

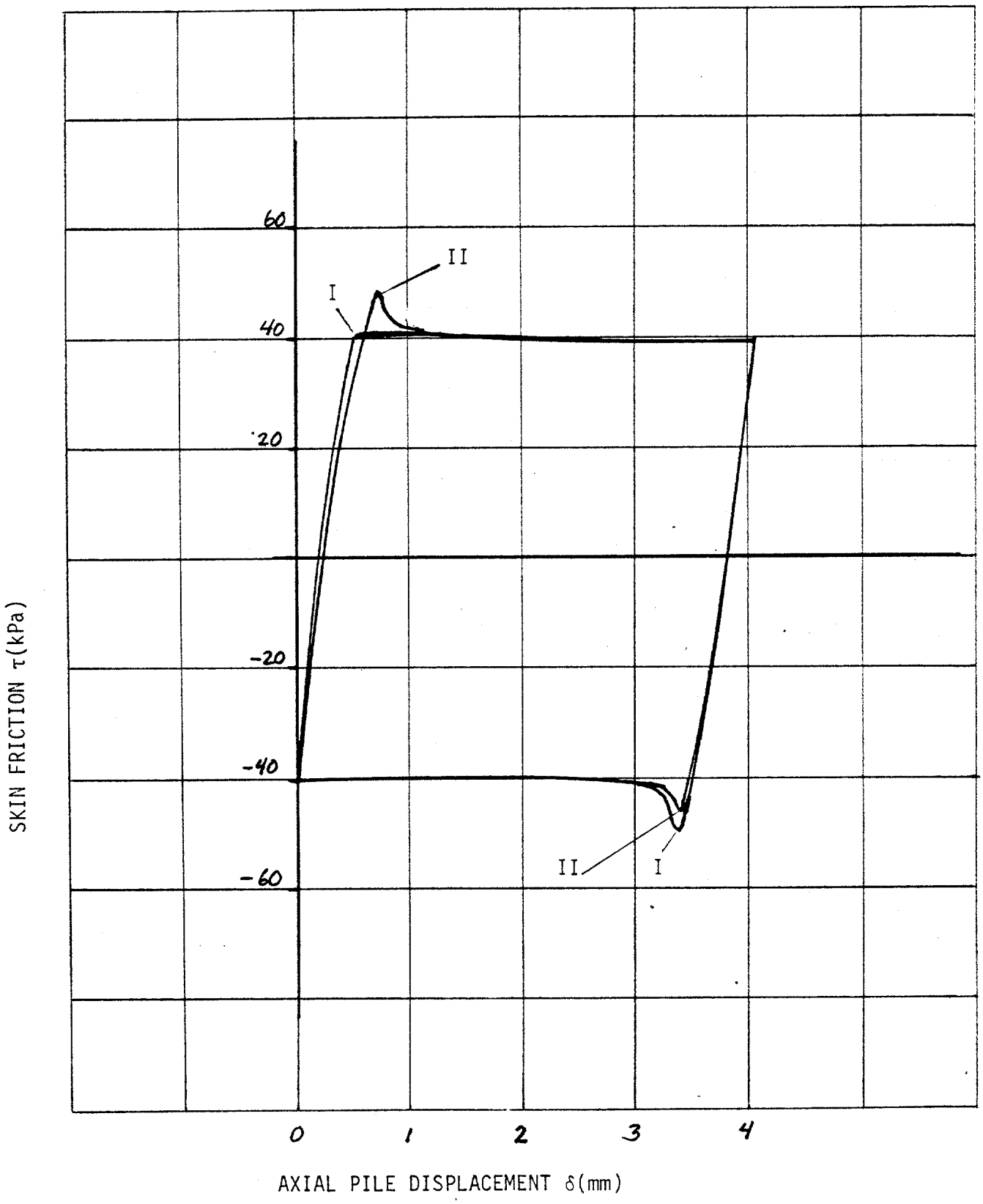

CNRD 13-2 TENSION PILE STUDY LABORATORY MODEL PILE TESTS

TEST 4, STRATUM III . STATIC TEST 2

DET NORSKE VERITAS Geotechnical Laboratory	Drawn by	Scale
	Approved	Date
		Fig. No. 16

TEST 4, STRATUM III

SHEAR STRENGTH AFTER PILE TEST (KPa)

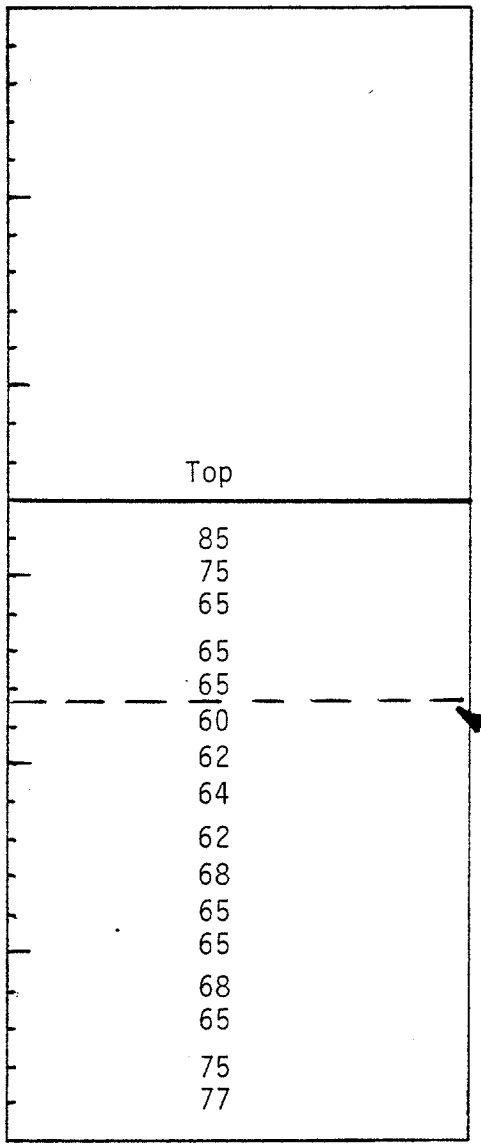

Scale: 1:4

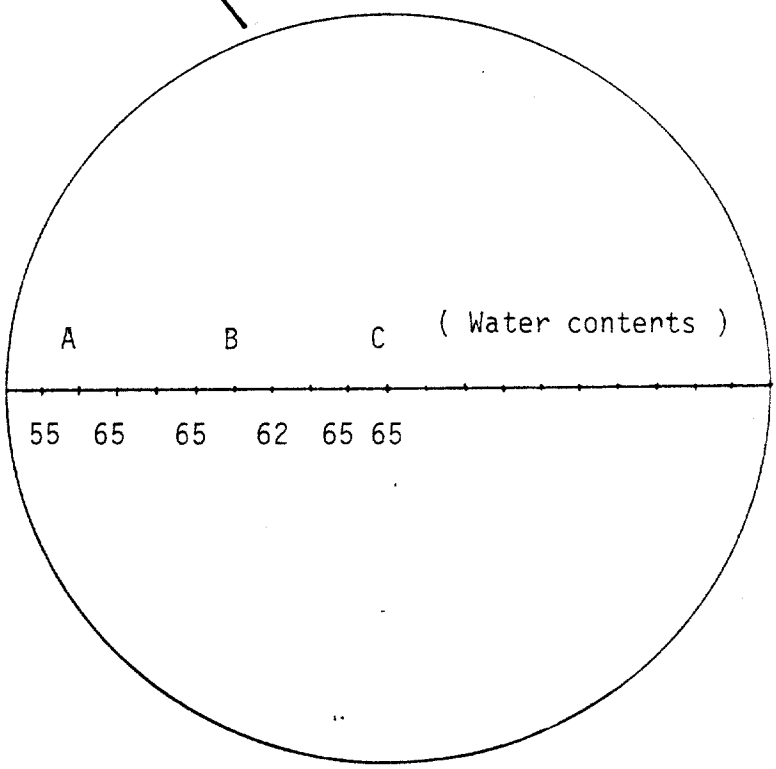

Scale: 1:2

CNRD 13-2 TENSION PILE STUDY LABORATORY MODEL PILE TESTS

TEST 4, STRATUM III, Pocket penetrometer tests after pile test

DET NORSKE VERITAS Geotechnical Laboratory	Drawn by	Scale
	Approved	Date
		Fig. No. 17

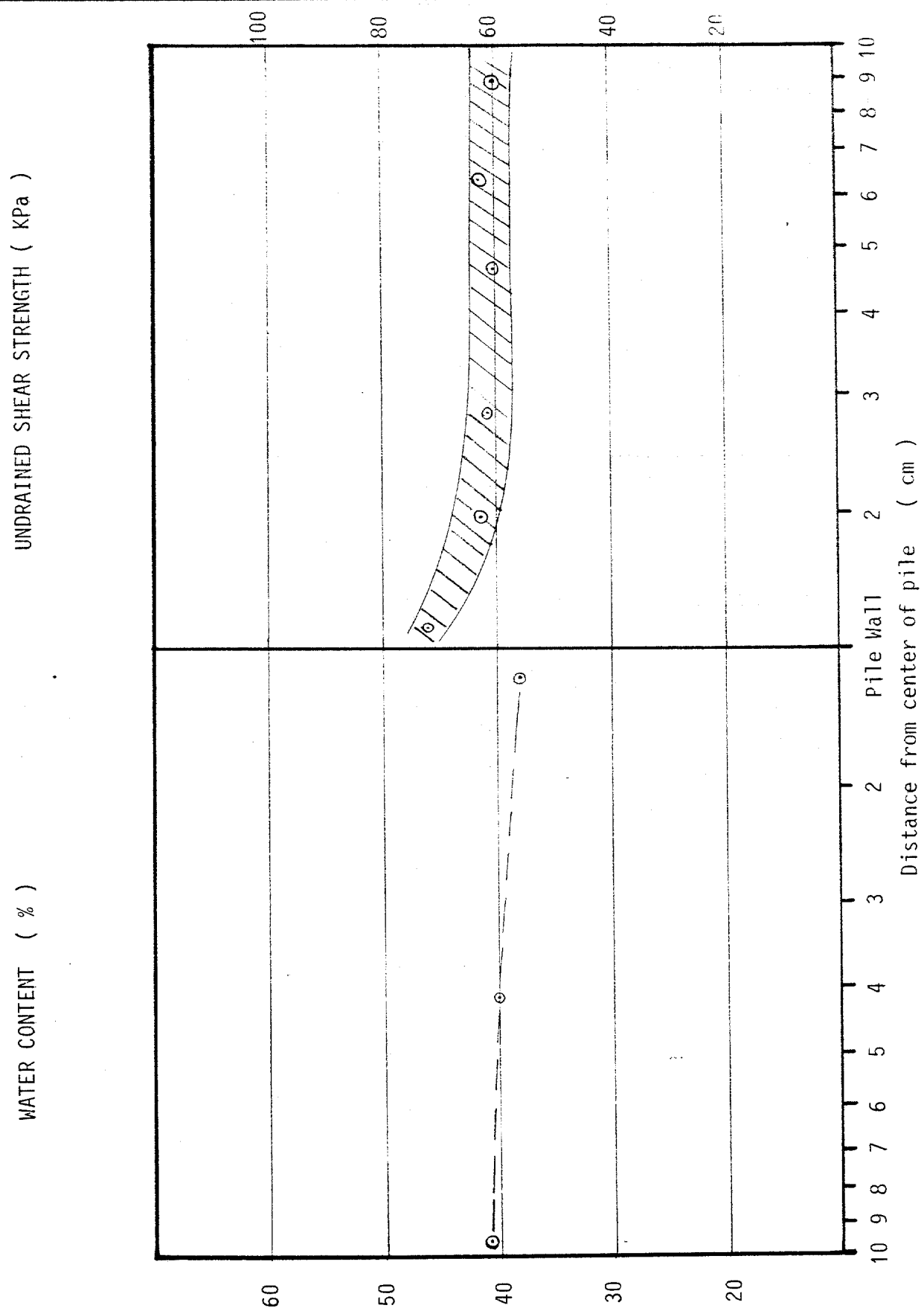

CNRD 13-2 TENSION PILE STUDY LABORATORY MODEL PILE TESTS

TEST 4,STRATUM III, Water content and shear strength after test

DET NORSKE VERITAS Geotechnical Laboratory	Drawn by	Scale
	Approved	Date
		Fig. No. 18

TEST 4, STRATUM III

UNCONFINED COMPRESSION TEST ON MATERIAL AFTER PILE TEST

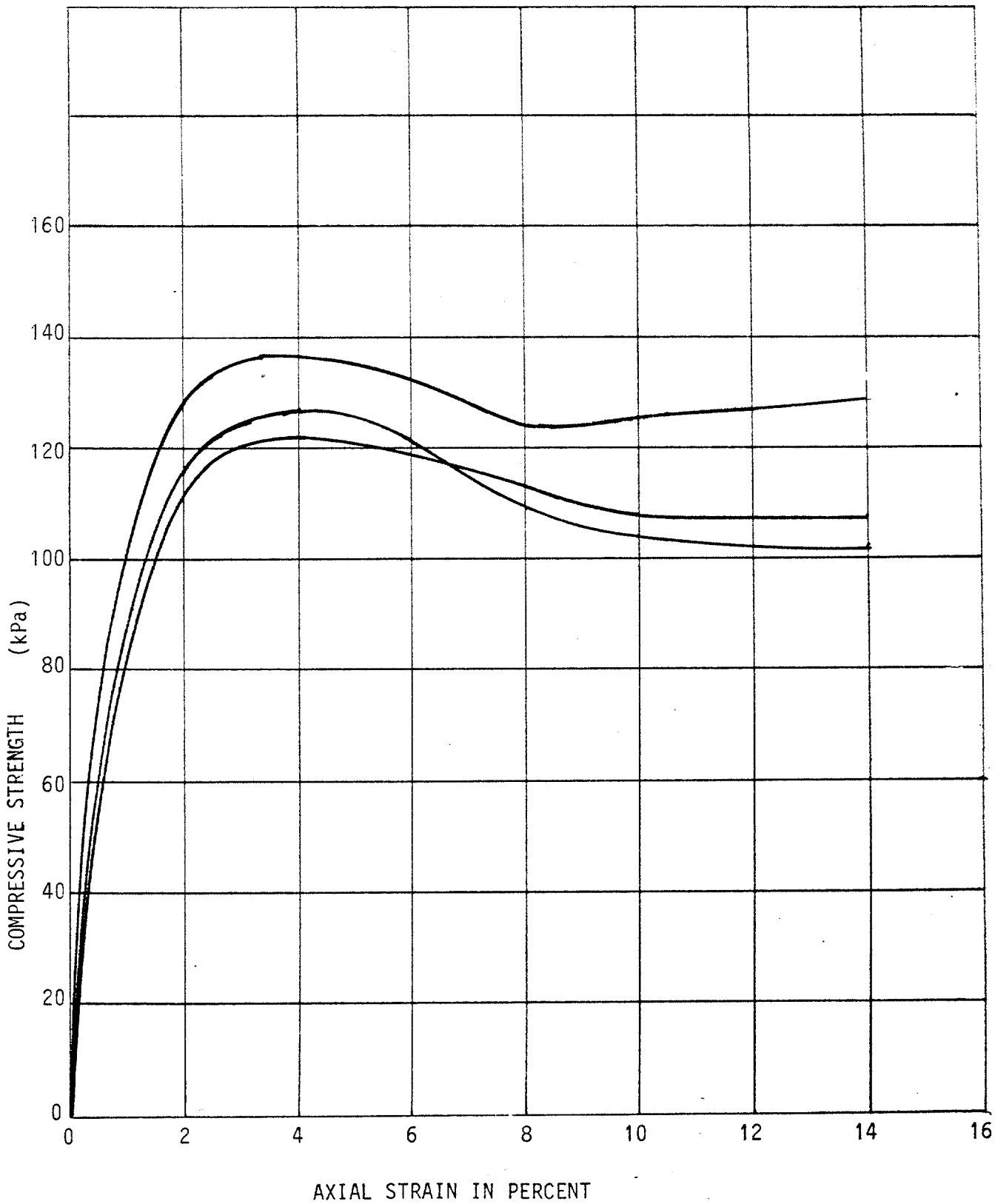

CNRD 13-2 TENSION PILE STUDY LABORATORY MODEL PILE TESTS

TEST 4, STRATUM III, Unconfined compr. test after pile test

Scale

DET NORSKE VERITAS
Geotechnical Laboratory

Drawn by Ivar Engesæt

Approved

Date

Fig. No. 19

Appendix AA

Plotted Results from WD34LC

Figures AA-1 through AA-9

Skin Friction vs Deflection, Selected Cycles

Figures AA-10 through AA-18

Skin Friction vs Eff. Normal Pressure, Selected Cycl.

Figures AA-19 through AA-36

Skin Friction, Pore and Total Pressure, Selected Cycles

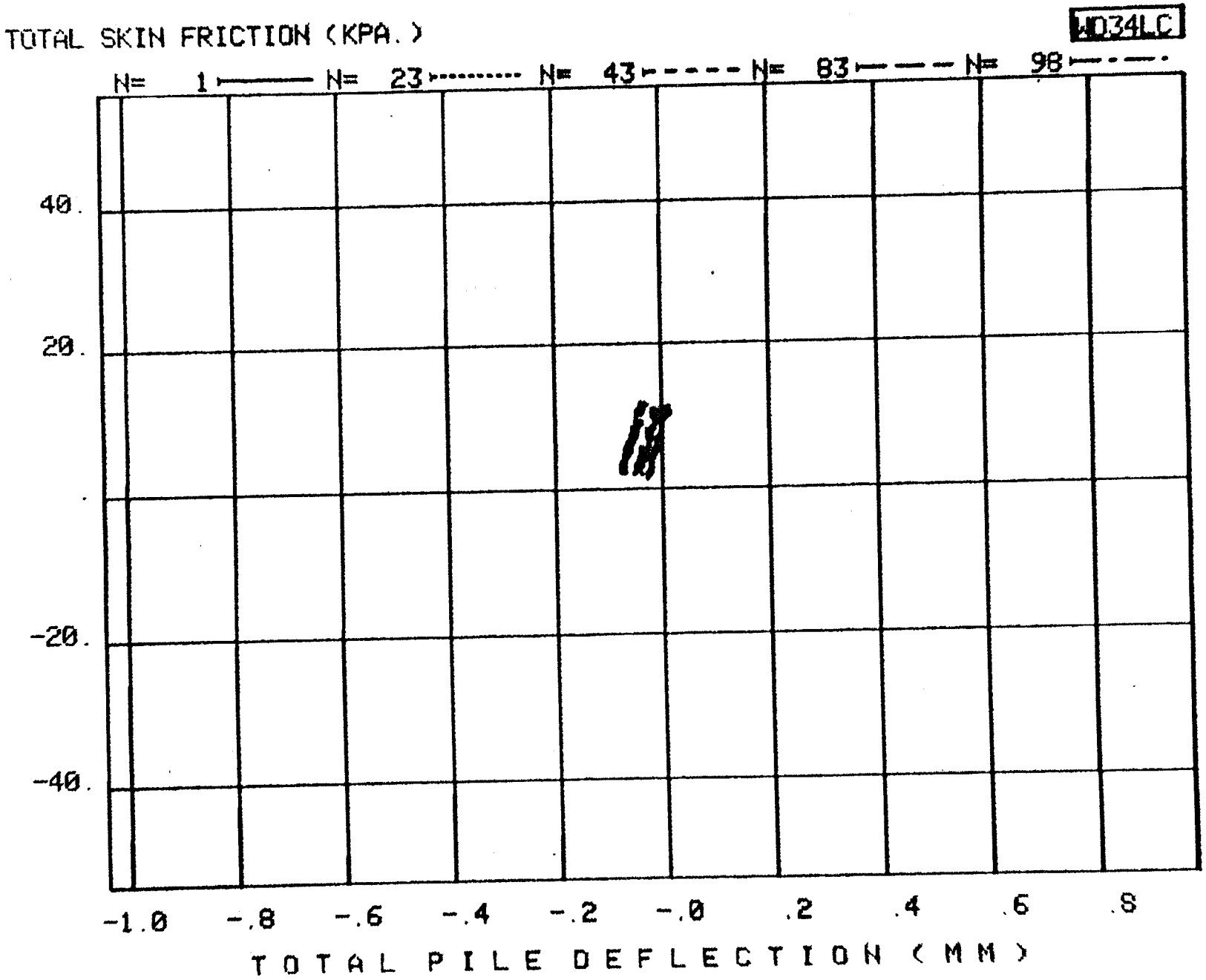
TOTAL SKIN FRICTION (KPA.)
WD34LC
N= 1
N= 23
N= 43
N= 83
N= 98
40.
20.
-20.
-40.
-1.0
-.8
-.6
-.4
-.2
-.0
.2
.4
.6
.8
TOTAL PILE DEFLECTION (MM)

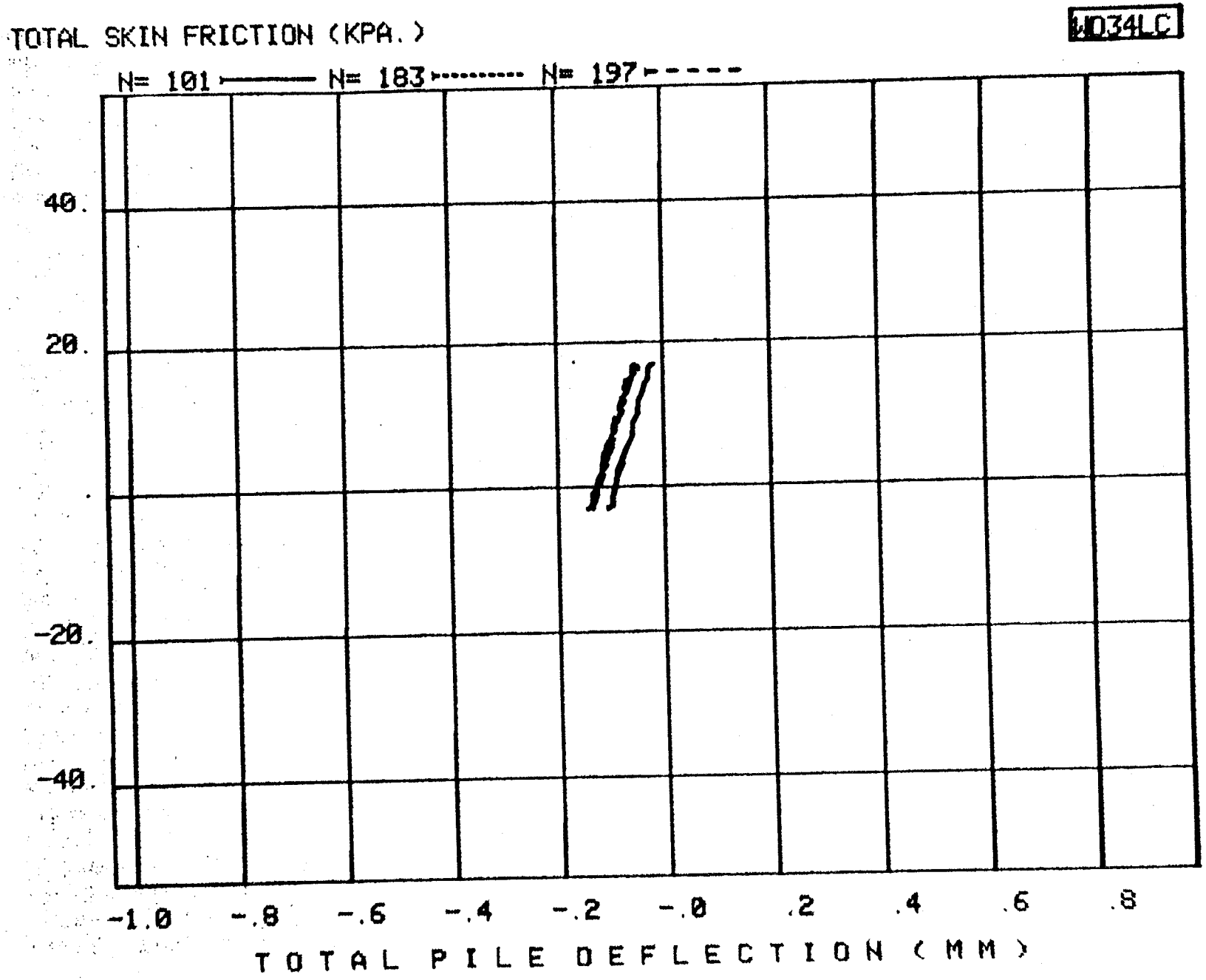
TOTAL SKIN FRICTION (KPA.)
WD34LC
N= 101
N= 183
N= 197
40.
20.
-20.
-40.
-1.0
-.8
-.6
-.4
-.2
-.0
.2
.4
.6
.8
TOTAL PILE DEFLECTION (MM)

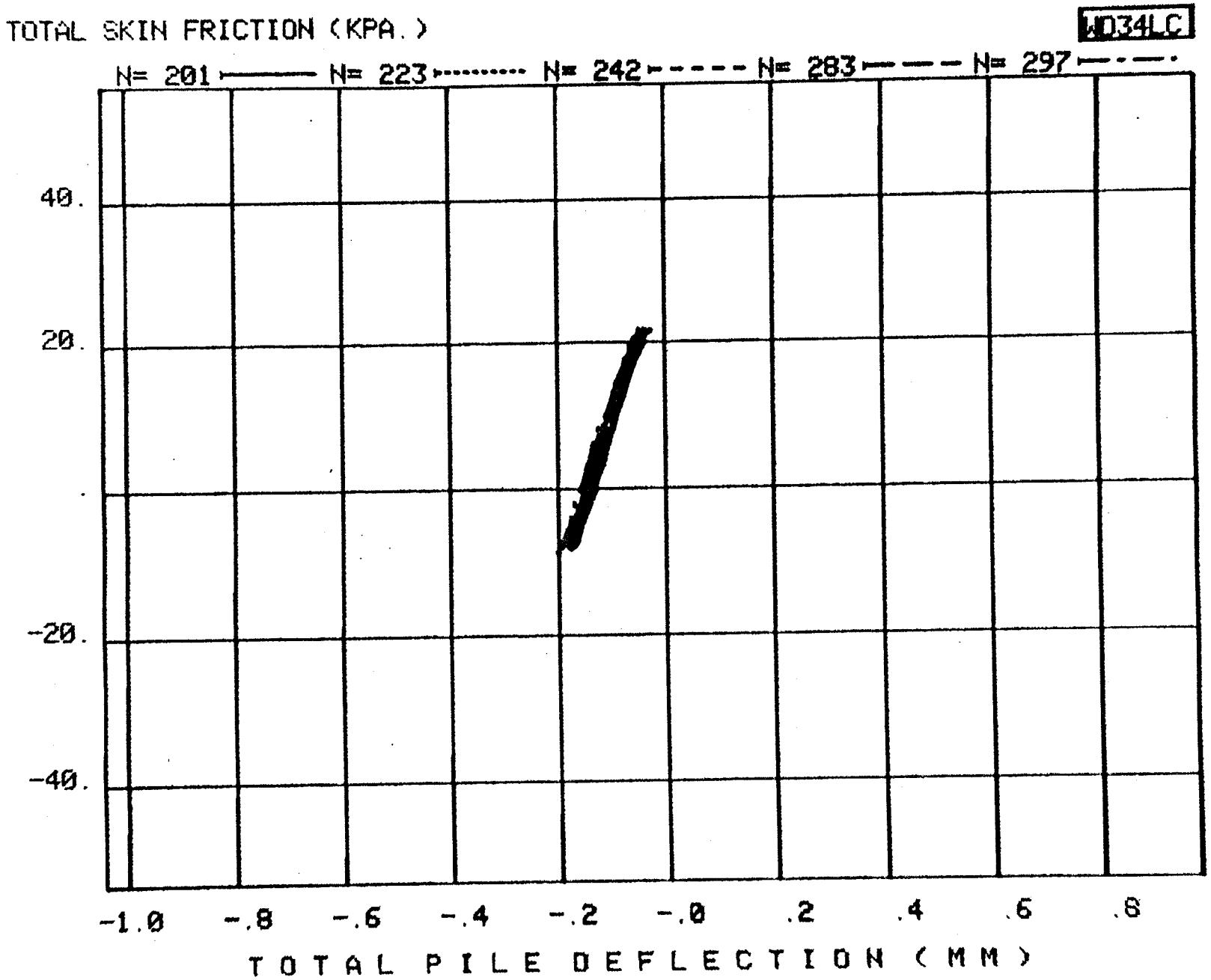
TOTAL SKIN FRICTION (KPA.)
W034LC
N= 201
N= 223
N= 242
N= 283
N= 297
40.
20.
-20.
-40.
-1.0
-.8
-.6
-.4
-.2
-.0
.2
.4
.6
.8
TOTAL PILE DEFLECTION (MM)

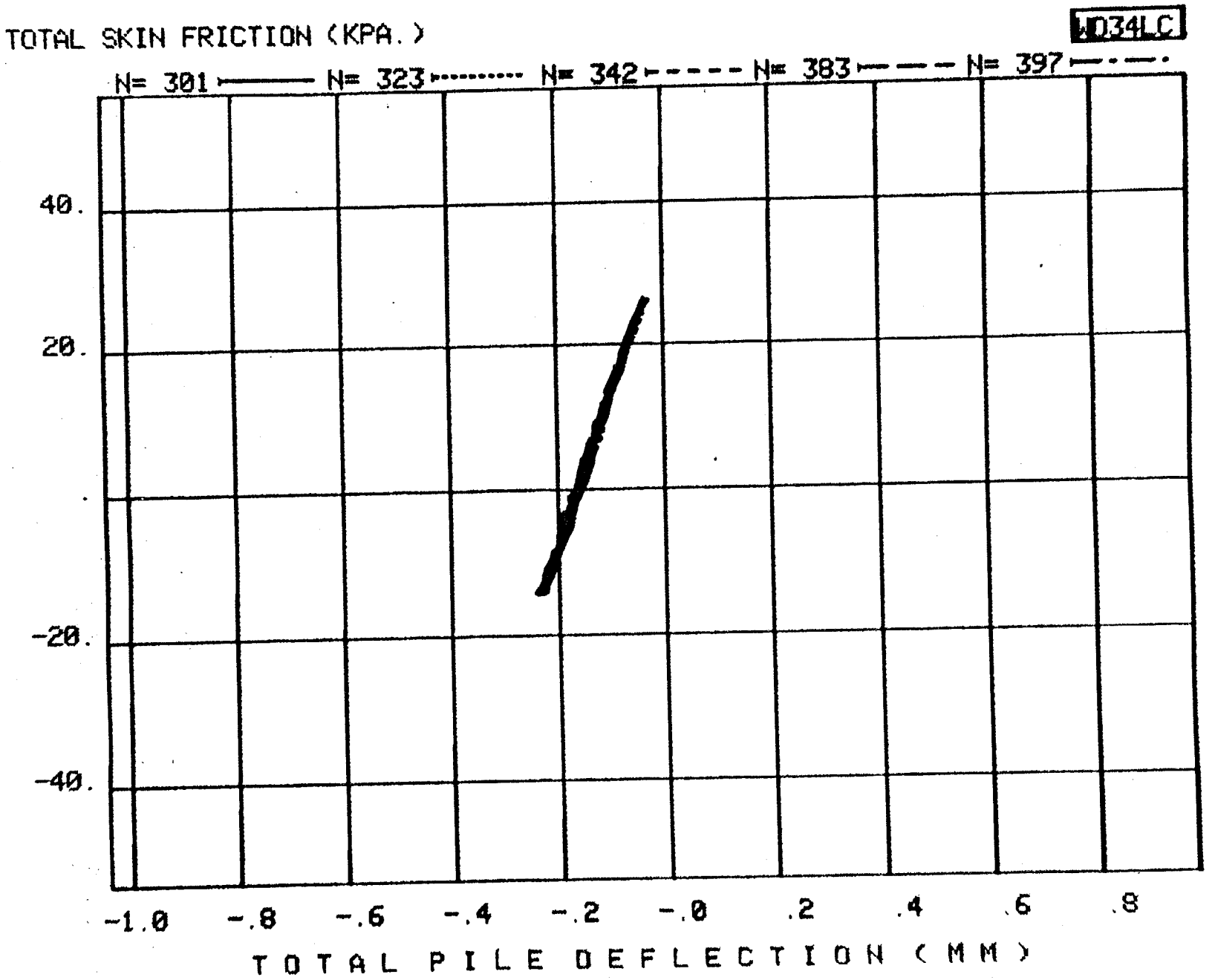
TOTAL SKIN FRICTION (KPA.)
WD34LC
N= 301
N= 323
N= 342
N= 383
N= 397
40.
20.
-20.
-40.
-1.0
-.8
-.6
-.4
-.2
-.0
.2
.4
.6
.8
TOTAL PILE DEFLECTION (MM)

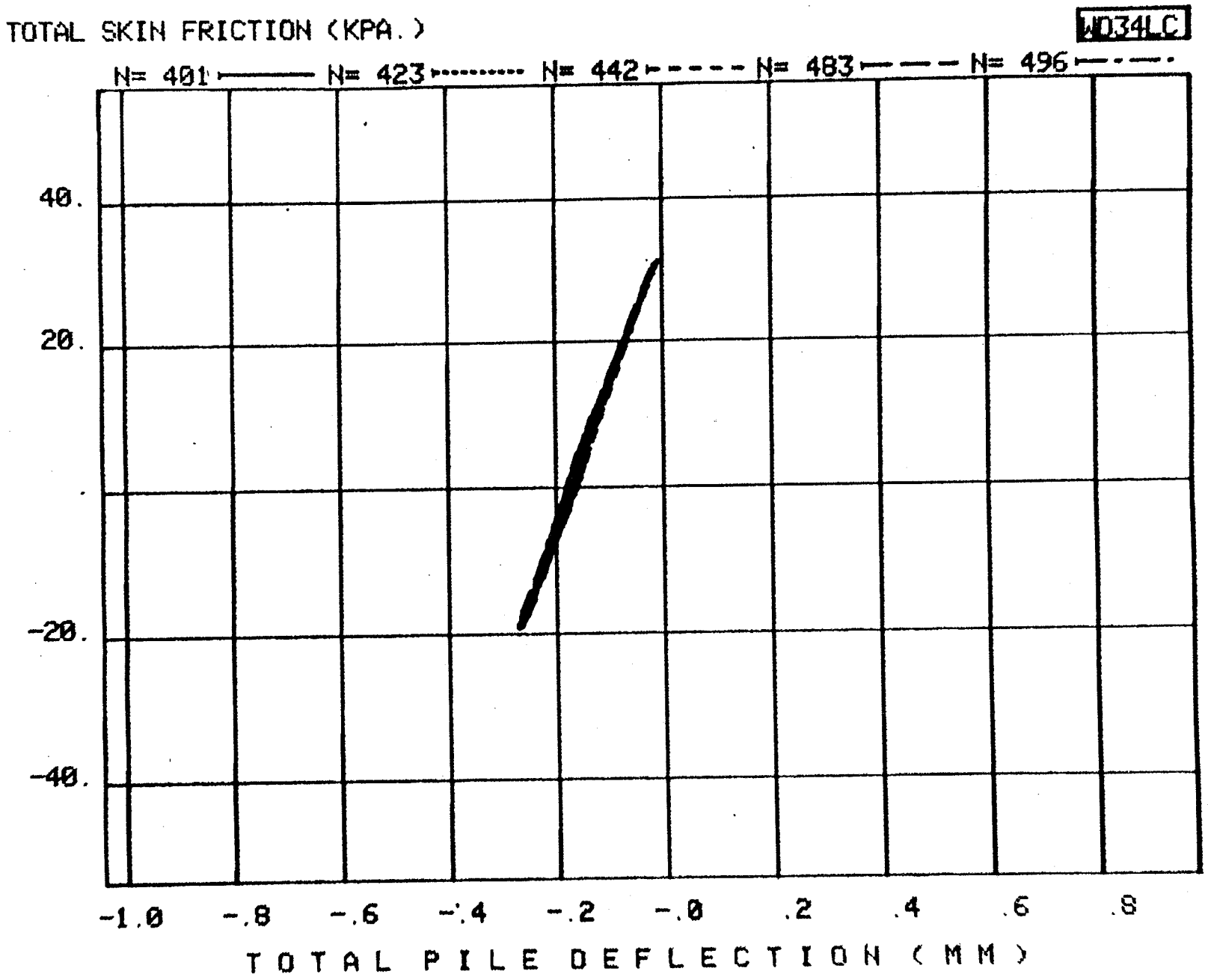
TOTAL SKIN FRICTION (KPA.)
WD34LC
N= 401
N= 423
N= 442
N= 483
N= 496
40.
20.
-20.
-40.
-1.0
-.8
-.6
-.4
-.2
-.0
.2
.4
.6
.8
TOTAL PILE DEFLECTION (MM)

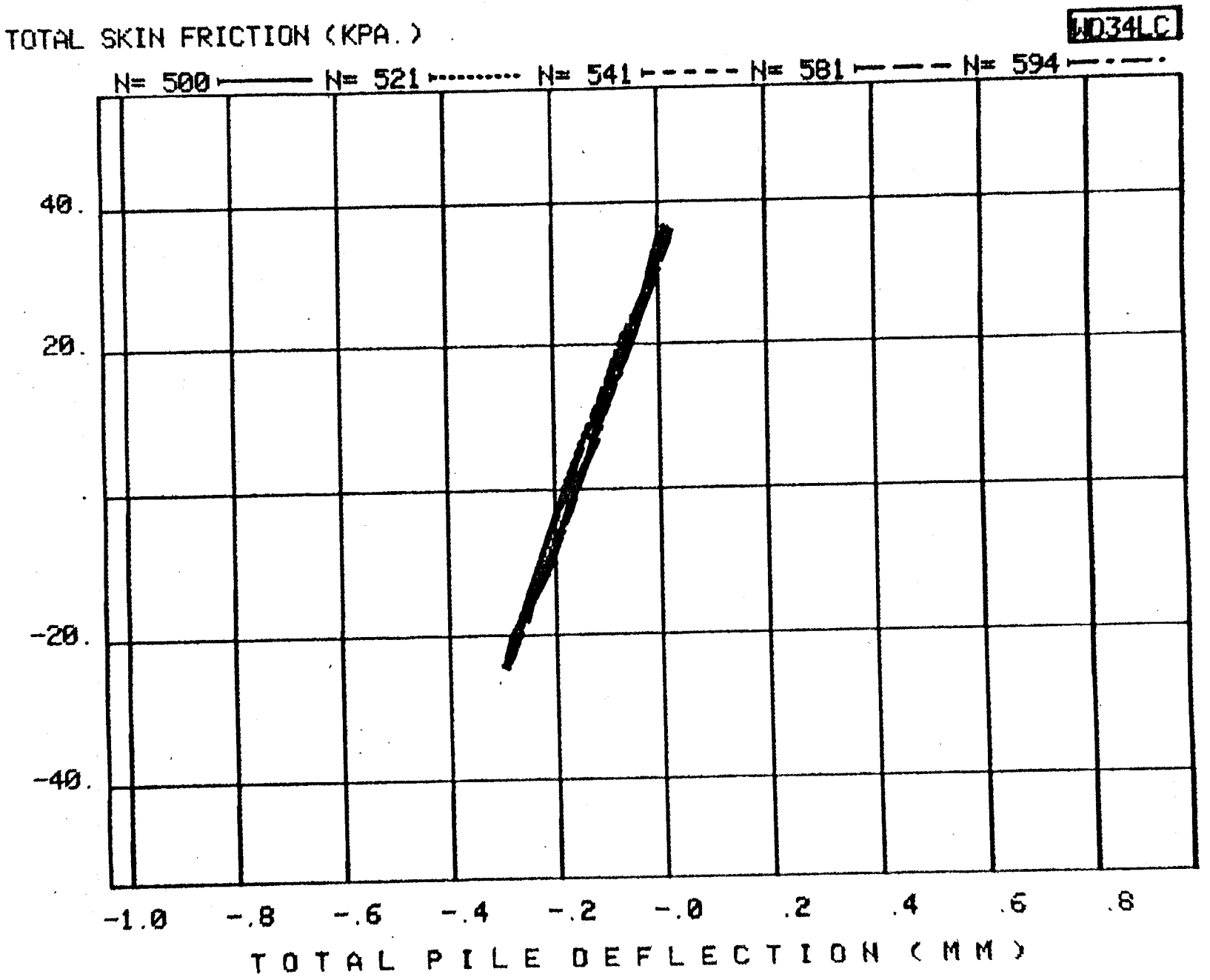
TOTAL SKIN FRICTION (KPA.)
WD34LC
N= 500
N= 521
N= 541
N= 581
N= 594
40.
20.
-20.
-40.
-1.0
-.8
-.6
-.4
-.2
-.0
.2
.4
.6
.8
TOTAL PILE DEFLECTION (MM)

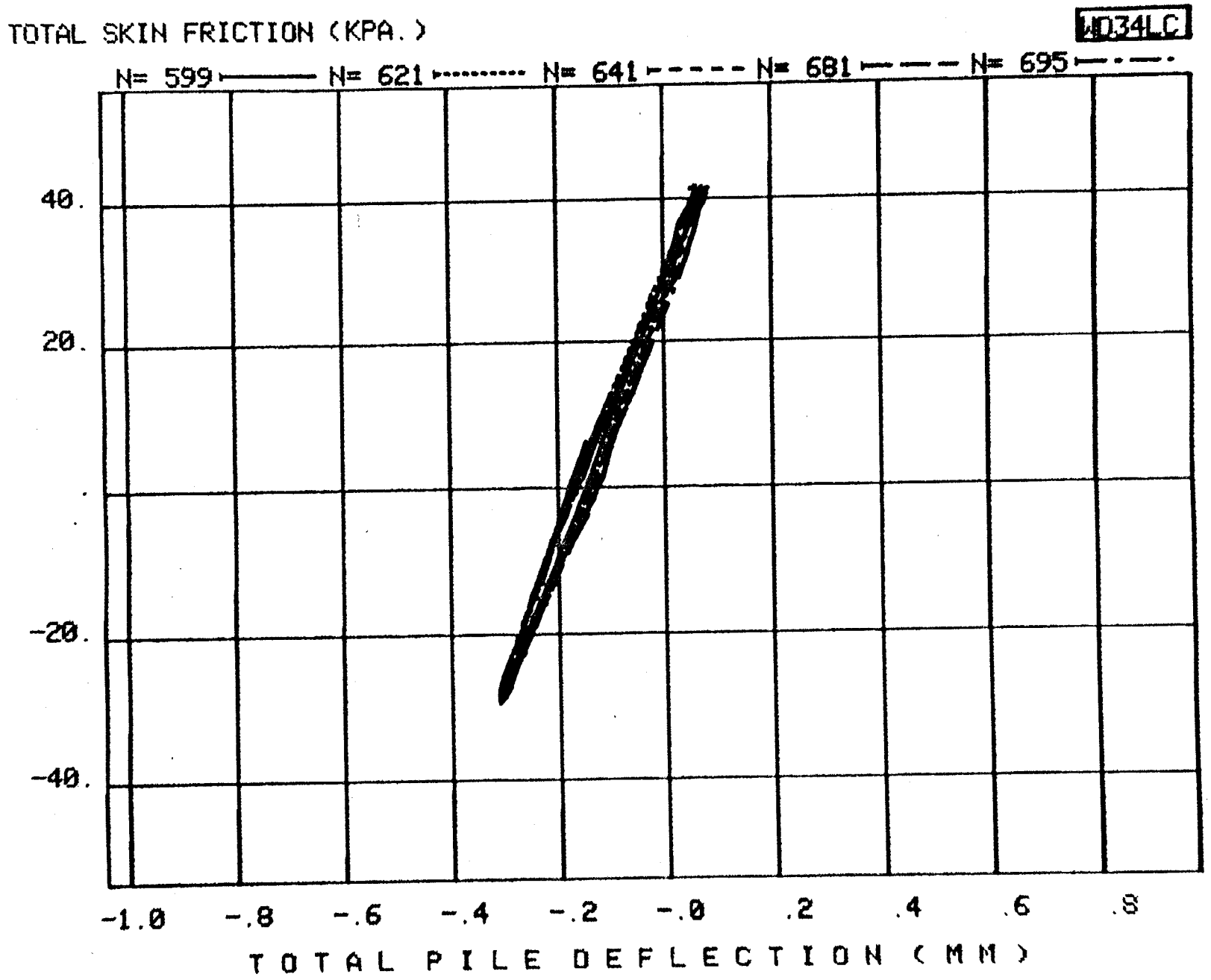
TOTAL SKIN FRICTION (KPA.)
WD34LC
N= 599
N= 621
N= 641
N= 681
N= 695
40.
20.
-20.
-40.
-1.0
-.8
-.6
-.4
-.2
-.0
.2
.4
.6
.8
TOTAL PILE DEFLECTION (MM)

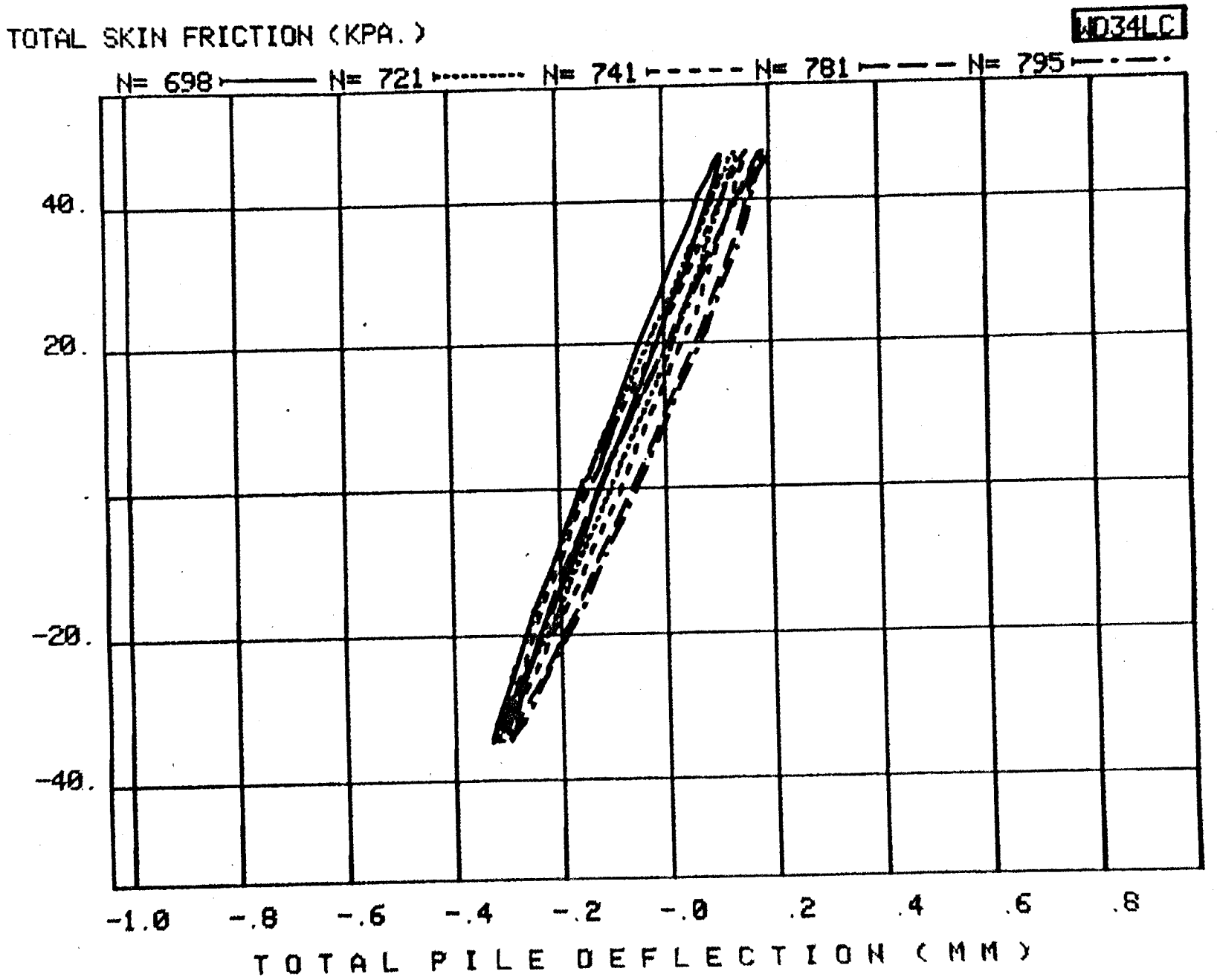
WD34LC
TOTAL SKIN FRICTION (KPA.)
N= 698
N= 721
N= 741
N= 781
N= 795
40.
20.
-20.
-40.
-1.0
-.8
-.6
-.4
-.2
-.0
.2
.4
.6
.8
TOTAL PILE DEFLECTION (MM)

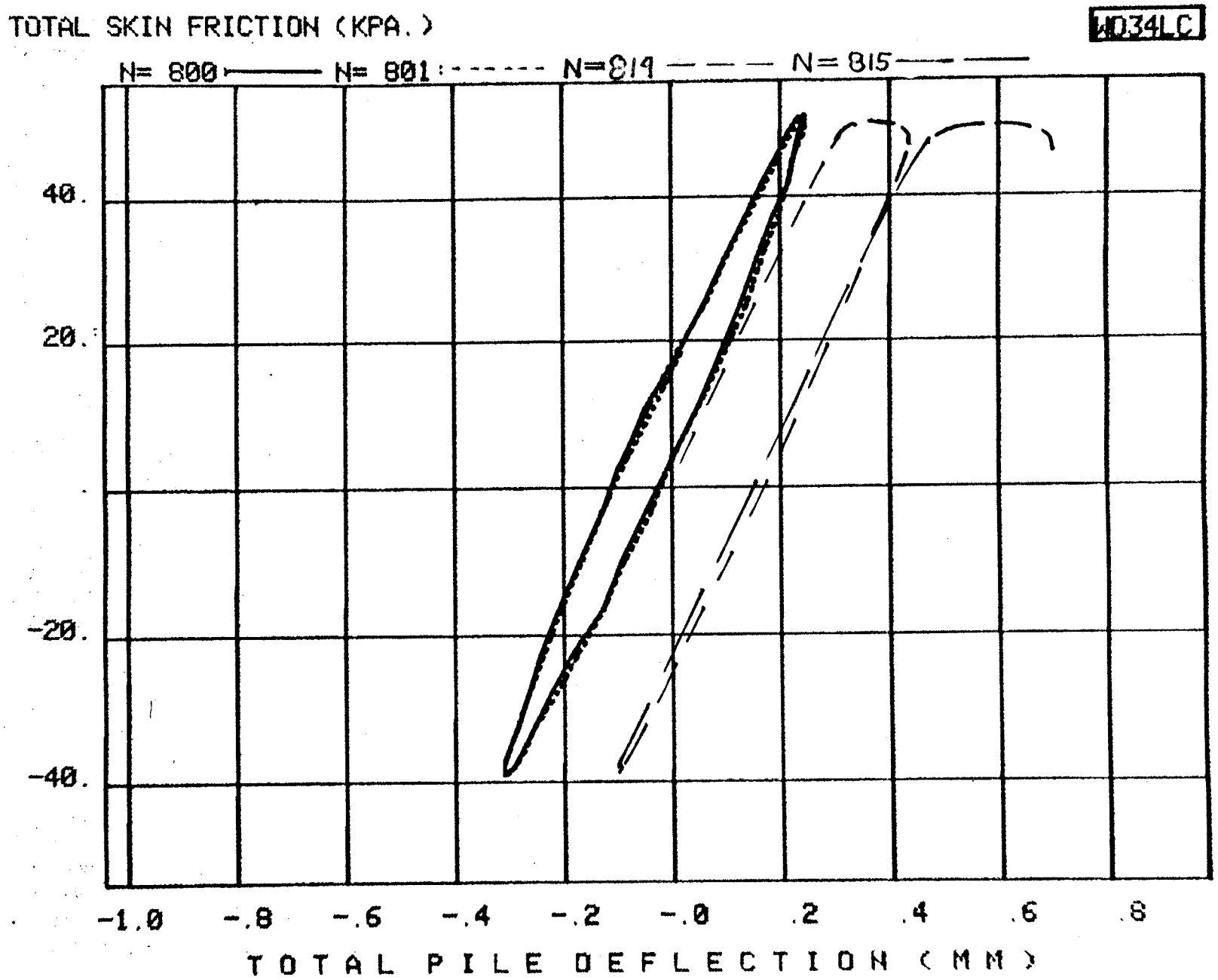
TOTAL SKIN FRICTION (KPA.)
W034LC
N= 800
N= 801
N=814
N= 815
40.
20.
-20.
-40.
-1.0
-.8
-.6
-.4
-.2
-.0
.2
.4
.6
.8
TOTAL PILE DEFLECTION (MM)

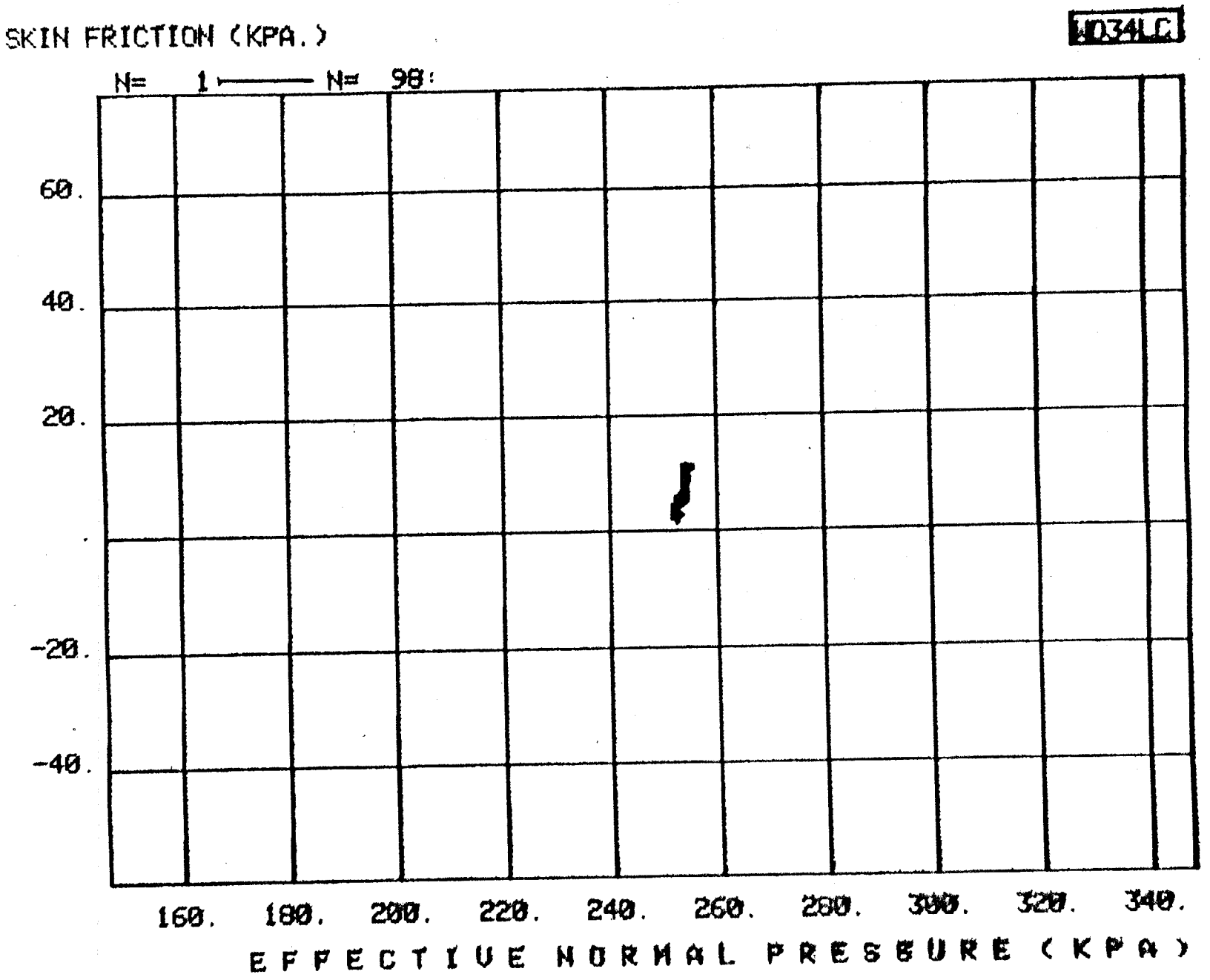
SKIN FRICTION (KPA.)
W034LC
N= 1 ——— N= 98
60.
40.
20.
-20.
-40.
160. 180. 200. 220. 240. 260. 280. 300. 320. 340.
EFFECTIVE NORMAL PRESSURE (KPA)

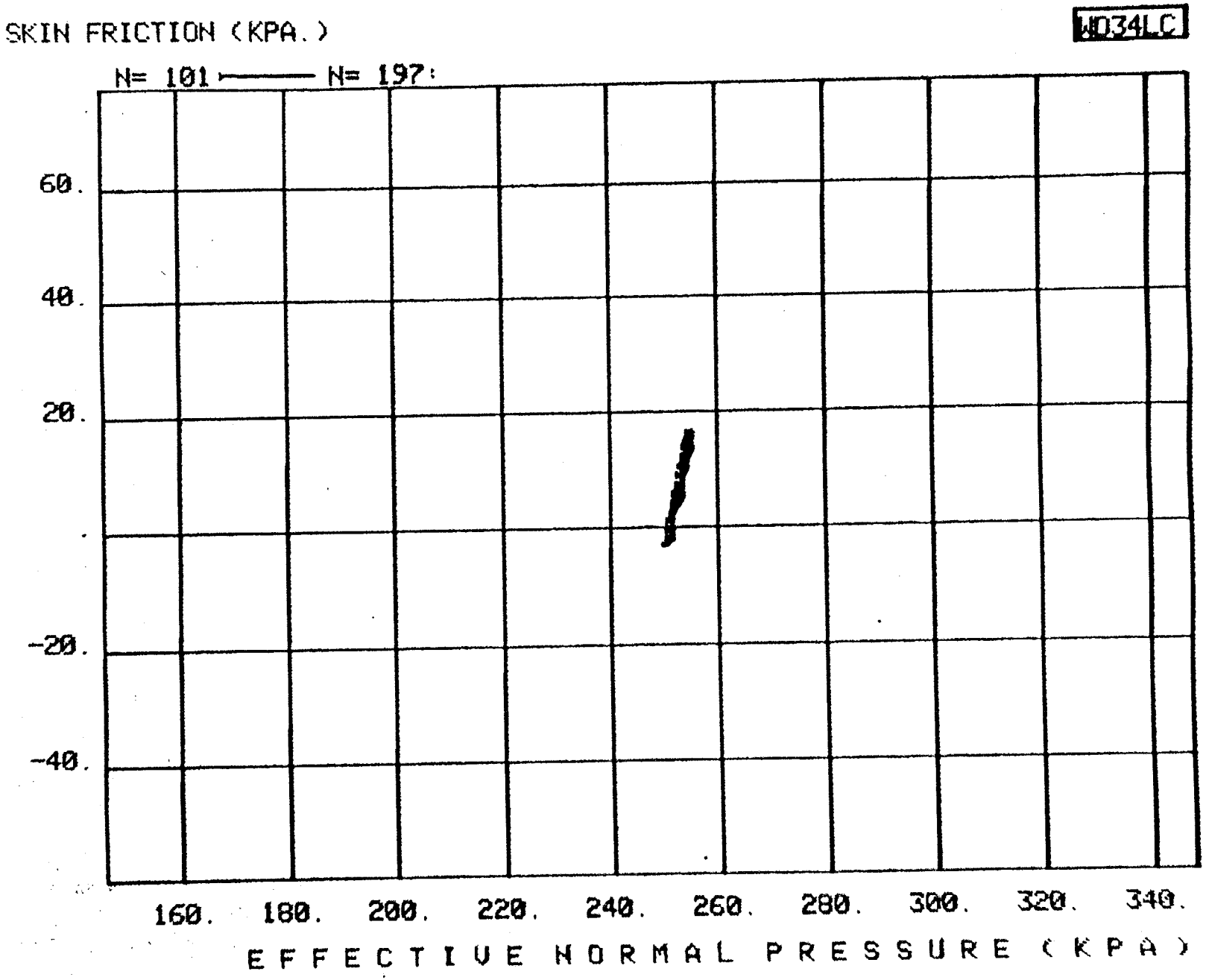
SKIN FRICTION (KPA.)
W034LC
N= 101 ——— N= 197:
60.
40.
20.
-20.
-40.
160. 180. 200. 220. 240. 260. 280. 300. 320. 340.
EFFECTIVE NORMAL PRESSURE (KPA)

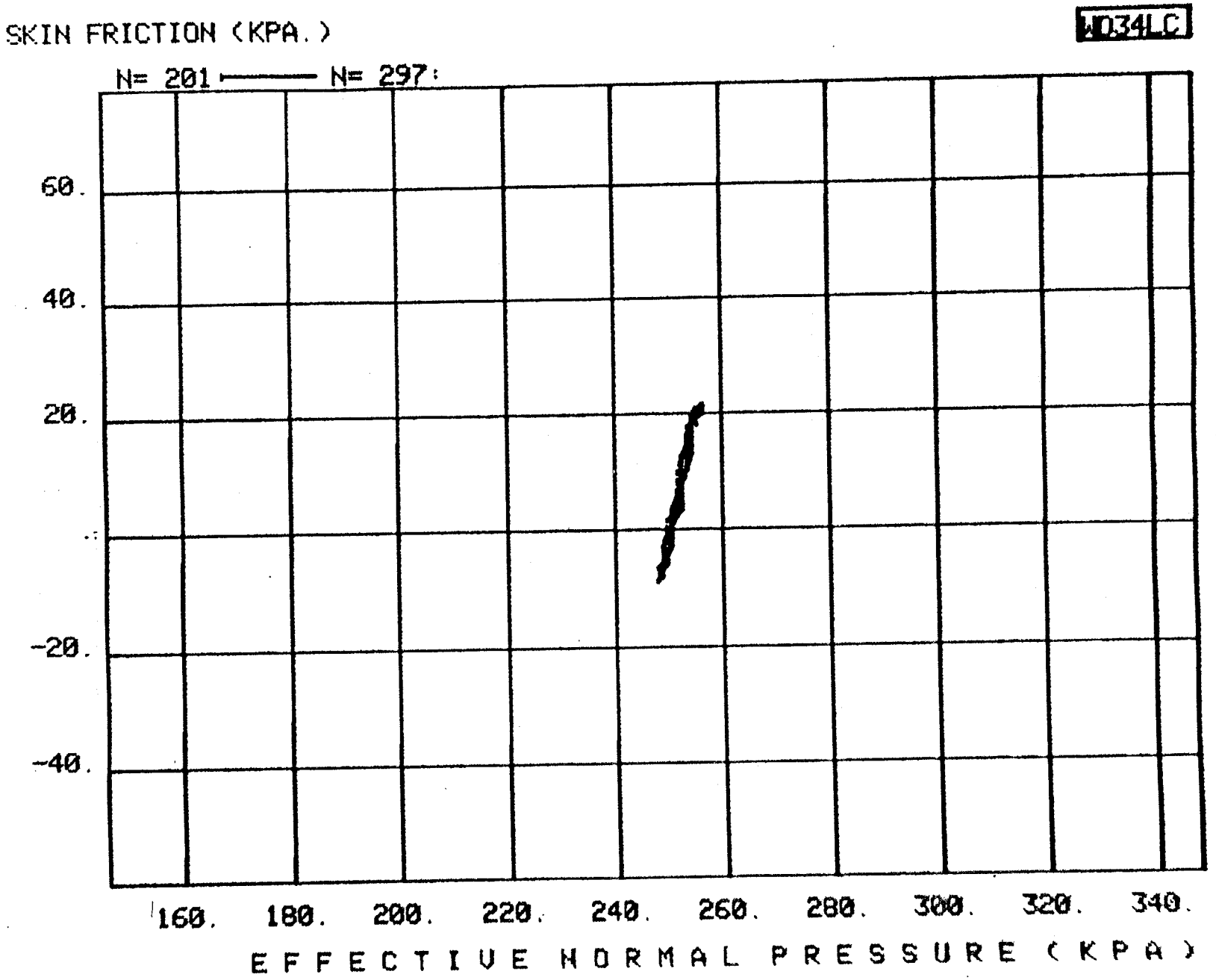
SKIN FRICTION (KPA.)
W034LC
N= 201
N= 297
60.
40.
20.
-20.
-40.
160.
180.
200.
220.
240.
260.
280.
300.
320.
340.
EFFECTIVE NORMAL PRESSURE (KPA)

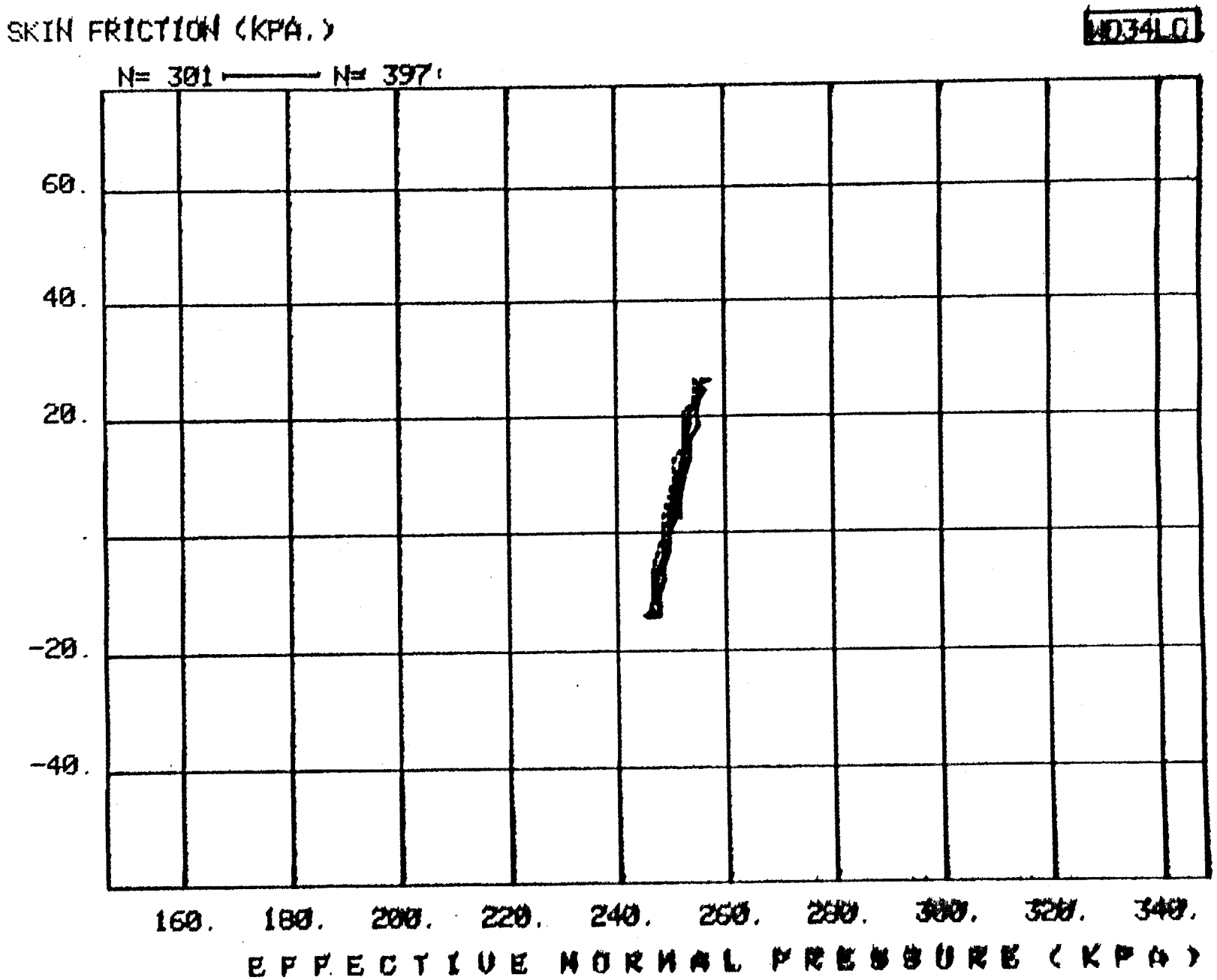
SKIN FRICTION (KPA.)
WD34LO
N= 301 N= 397
60.
40.
20.
-20.
-40.
160. 180. 200. 220. 240. 260. 280. 300. 320. 340.
EFFECTIVE NORMAL PRESSURE (KPA)

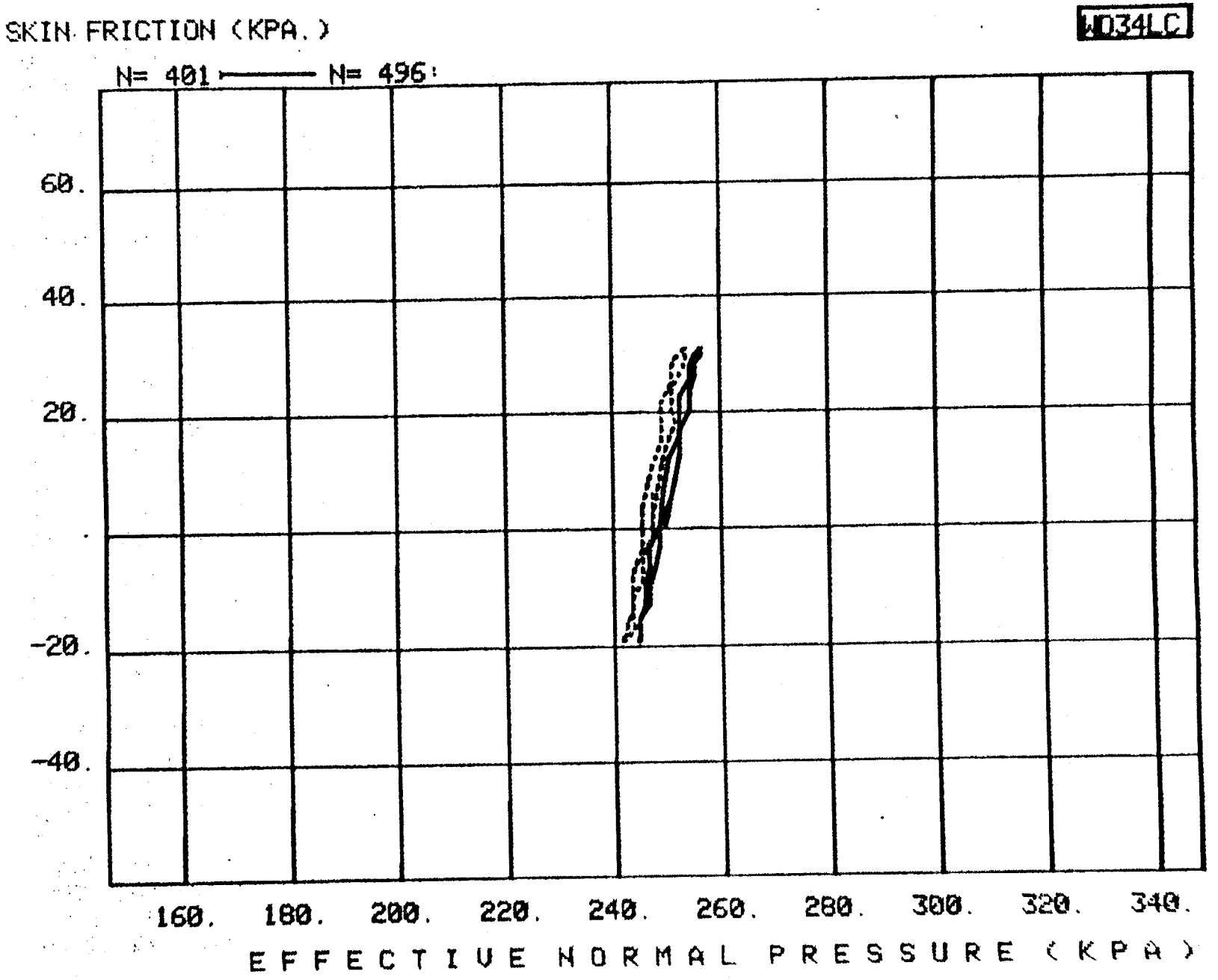
SKIN FRICTION (KPA.)
W034LC
N= 401 ——— N= 496
60.
40.
20.
-20.
-40.
160.
180.
200.
220.
240.
260.
280.
300.
320.
340.
EFFECTIVE NORMAL PRESSURE (KPA)

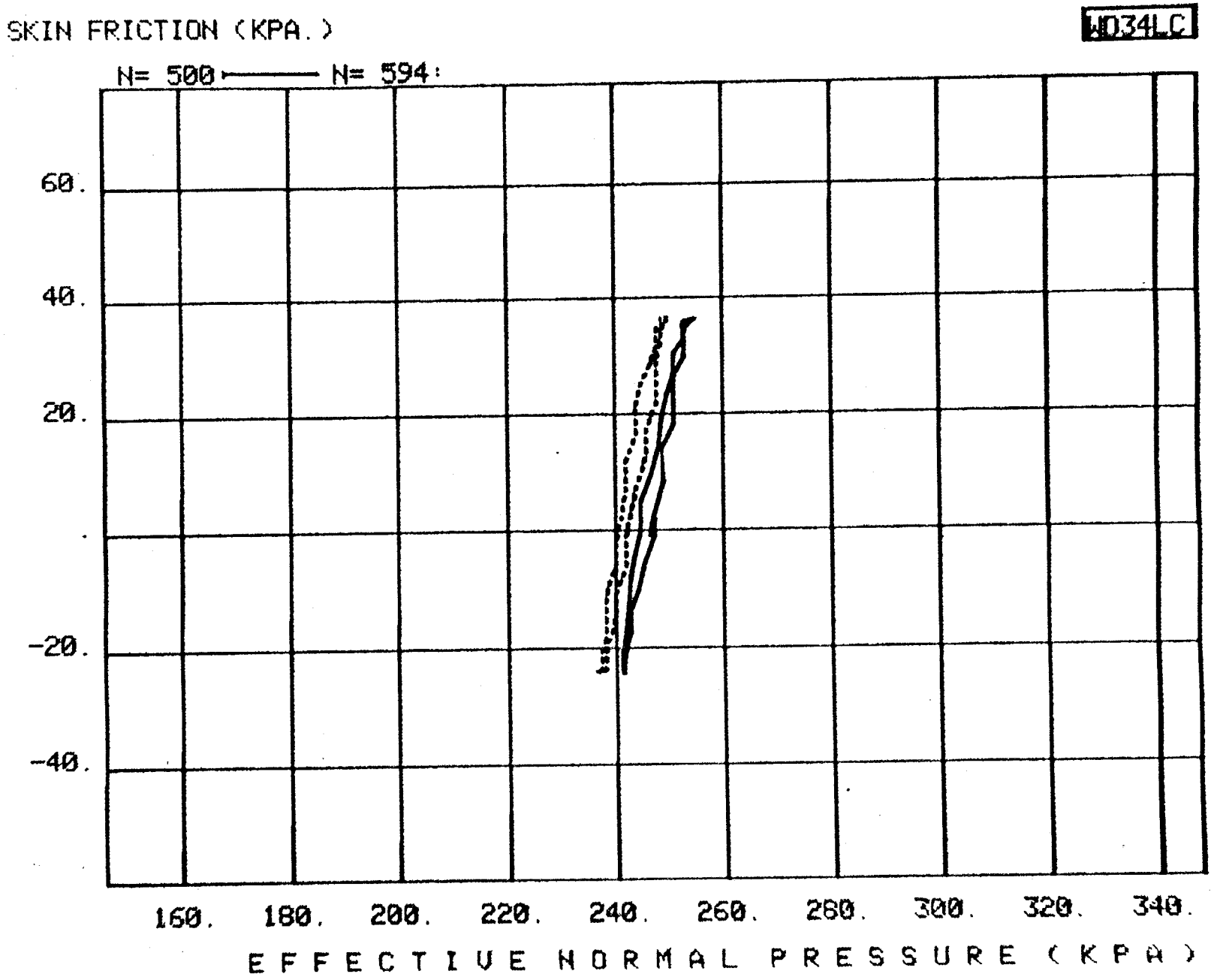
SKIN FRICTION (KPA.)
W034LC
N= 500 N= 594
60.
40.
20.
-20.
-40.
160. 180. 200. 220. 240. 260. 280. 300. 320. 340.
EFFECTIVE NORMAL PRESSURE (KPA)

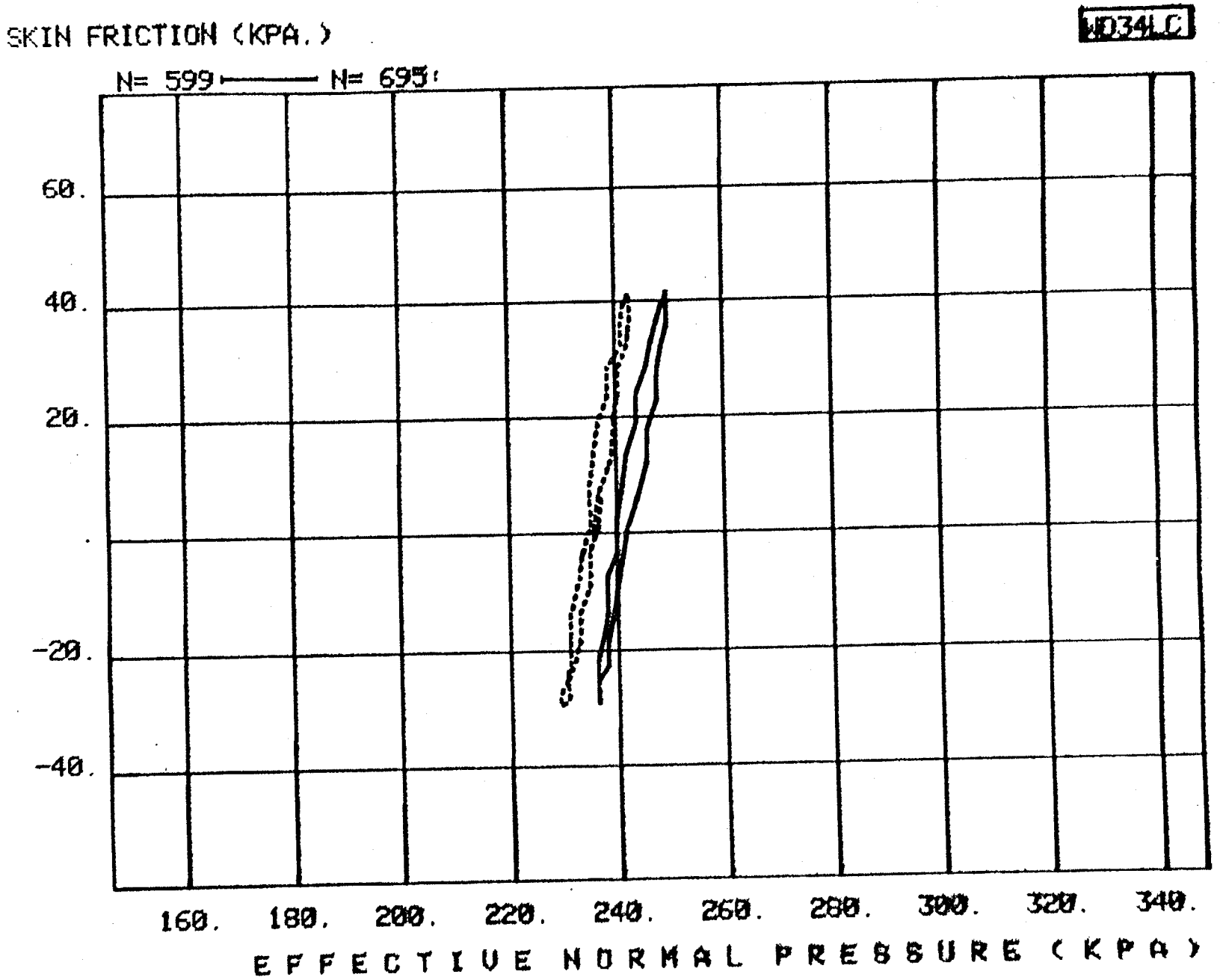
SKIN FRICTION (KPA.)
WD34LC
N= 599
N= 695
60.
40.
20.
-20.
-40.
160.
180.
200.
220.
240.
260.
280.
300.
320.
340.
EFFECTIVE NORMAL PRESSURE (KPA)

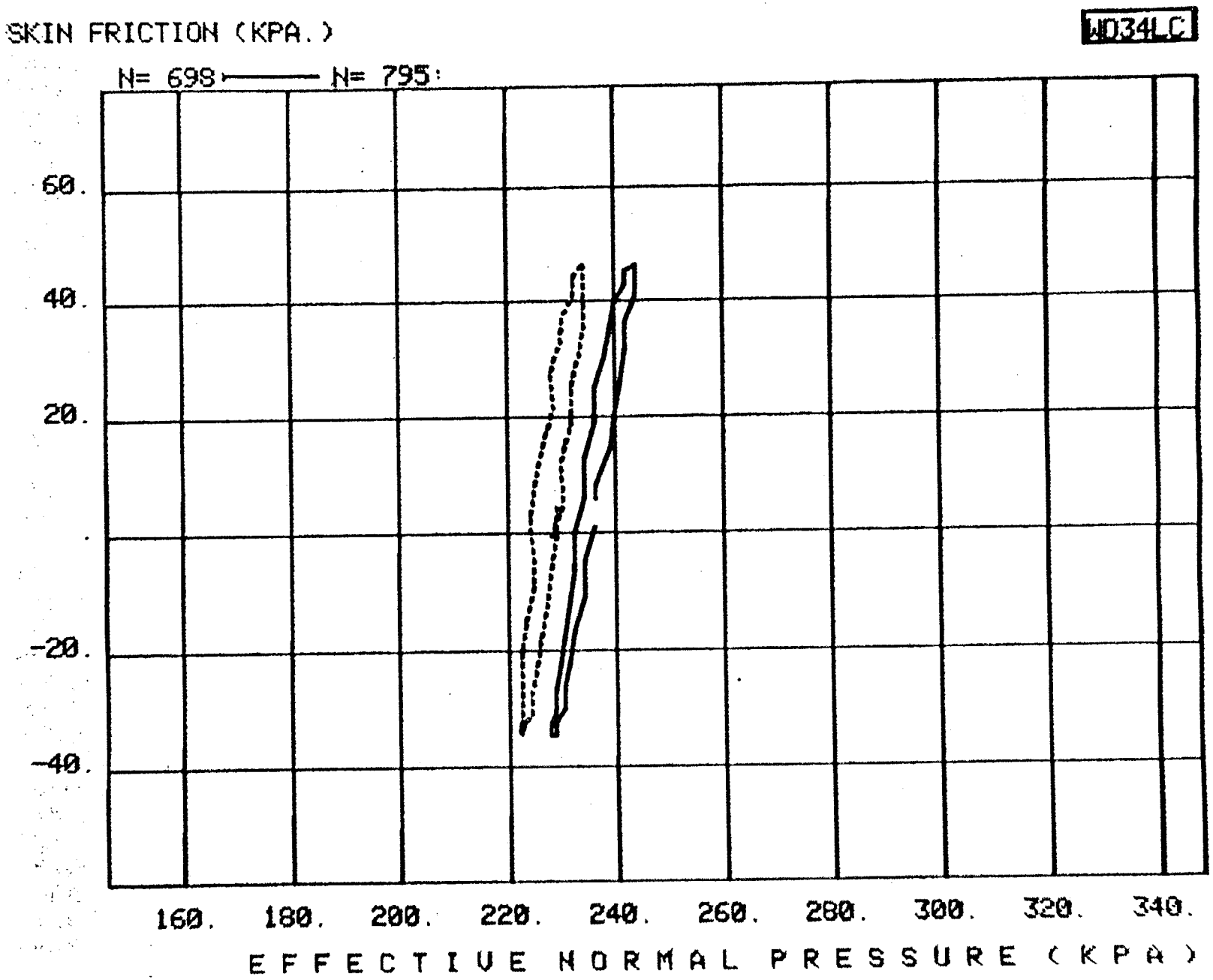
SKIN FRICTION (KPA.)
W034LC
N= 698
N= 795
60.
40.
20.
-20.
-40.
160.
180.
200.
220.
240.
260.
280.
300.
320.
340.
EFFECTIVE NORMAL PRESSURE (KPA)

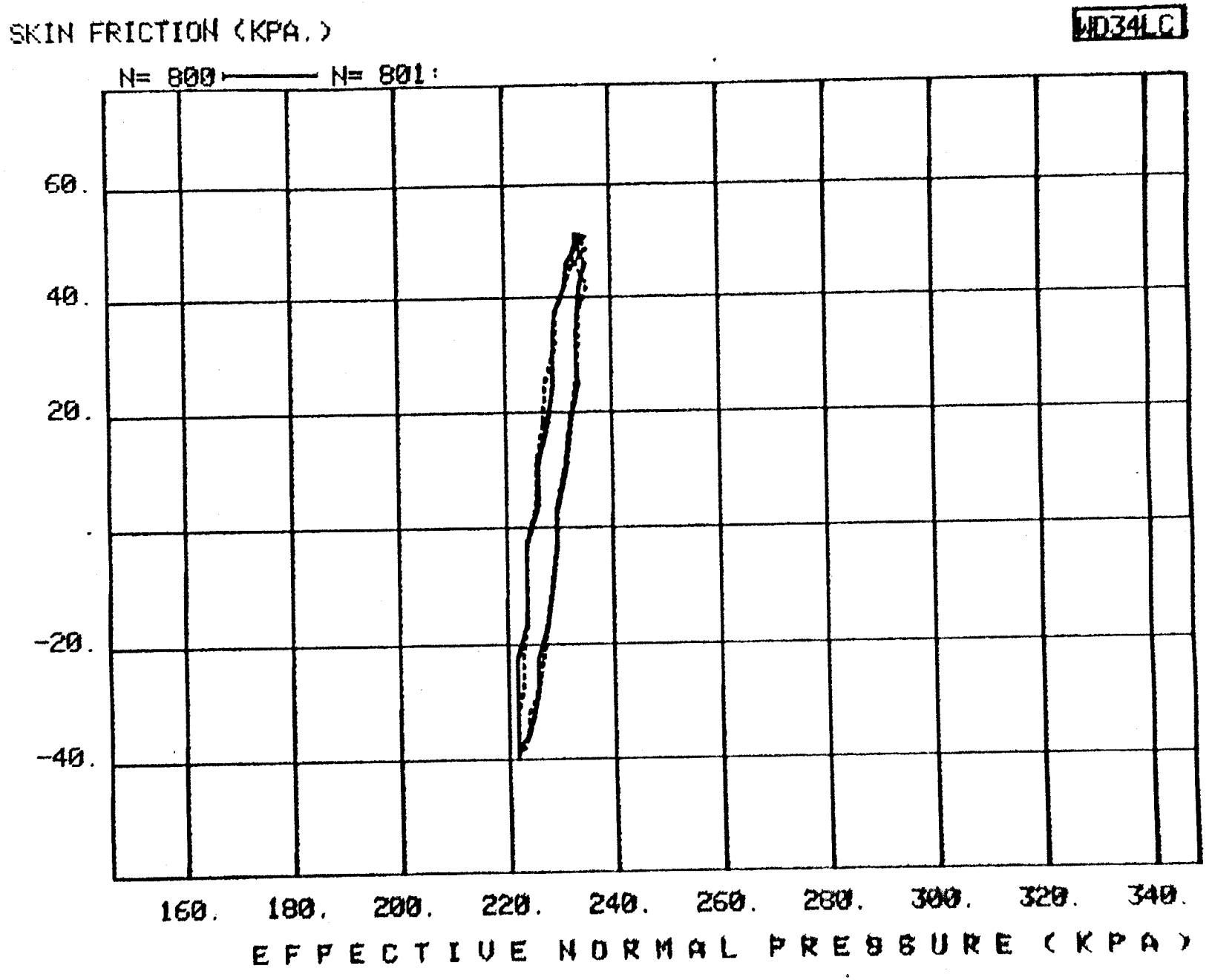
SKIN FRICTION (KPA.)
WD34LC
N= 800 N= 801:
60.
40.
20.
-20.
-40.
160.
180.
200.
220.
240.
260.
280.
300.
320.
340.
EFFECTIVE NORMAL PRESSURE (KPA)

As can be seen from the resulting skin friction in Figure 12 the pile had a residual compression from the previous downward movement to zero position after failure in the stress controlled test. During the first parcel (100 cycles) the mean stress was about 6 KPa.

In the second parcel with cyclic deformation of 0.2 mm it seems to yield a maximum stress in compression at -45 KPa with a residual value of about -40 KPa whereas the maximum tension was quite steady at about 30 KPa. The third parcel with cyclic deformation 0.4 mm yields failure in both tension and compression with a maximum in first cycle of about 50 KPa. After about 40 cycles a steady residual friction of 40 KPa was established, which yields 20% degradiation from ultimate cyclic capacity.

In the subsequent parcels the peak friction was somewhat lower since only about 10 minutes delay was allowed inbetween parcels, while the residual friction was steady at 40 KPa.

The pore pressure showed no cyclic variation during testing which is most likely due to a slow response of the pore pressure measurement system. A steady rise in pore pressure of 10 KPa from 420 KPa, is seen over the first six parcels whereas a small drop, 5 KPa is registered in the large deformation parcel.

Total normal pressure showed a cyclic response proportional to the cyclic deformation level, with the average pressure almost constant at about 620 KPa throughout the parcels. The resulting effective normal pressure, shown in Figure 15, thus shows a slow drop with increasing cyclic deformation with an apparent increase during the last large deformation parcel.

STATIC TEST II

The pile was then left for two days to reconsolidate which made the pore pressure go back to the original value before cyclic testing, about 420 KPa. Total normal pressure stayed constant at about 620 KPa.

A static test was now performed with deformation rate 10 mm per hour (increased with a factor of 10 from first test). Two cycles were made, and as can be seen from Figure 16 no peak value occured in the first tension failure. In compression, however,

RESPONSE ON CYCLIC LOADING (KPA.) CYCLE NO. 1 WD34LC

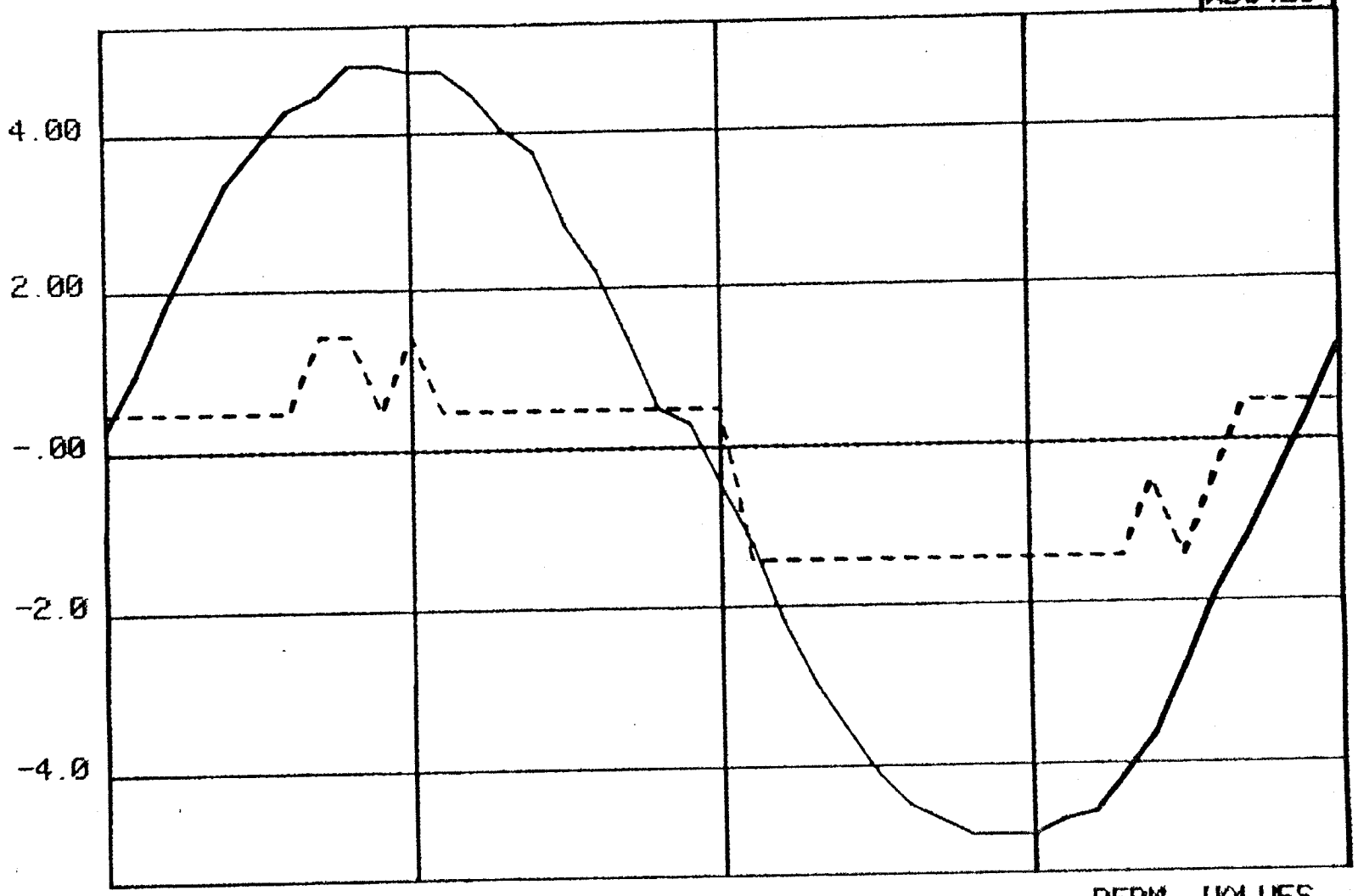

LEGEND:

SKIN FRICTION
PORE PRESSURE
TOTAL NORMAL PRESSURE

PERM. VALUES

6.51 KPA.
411.9 KPA.
665.9 KPA.

RESPONSE ON CYCLIC LOADING (KPA.) · CYCLE NO. 98

WD34LC

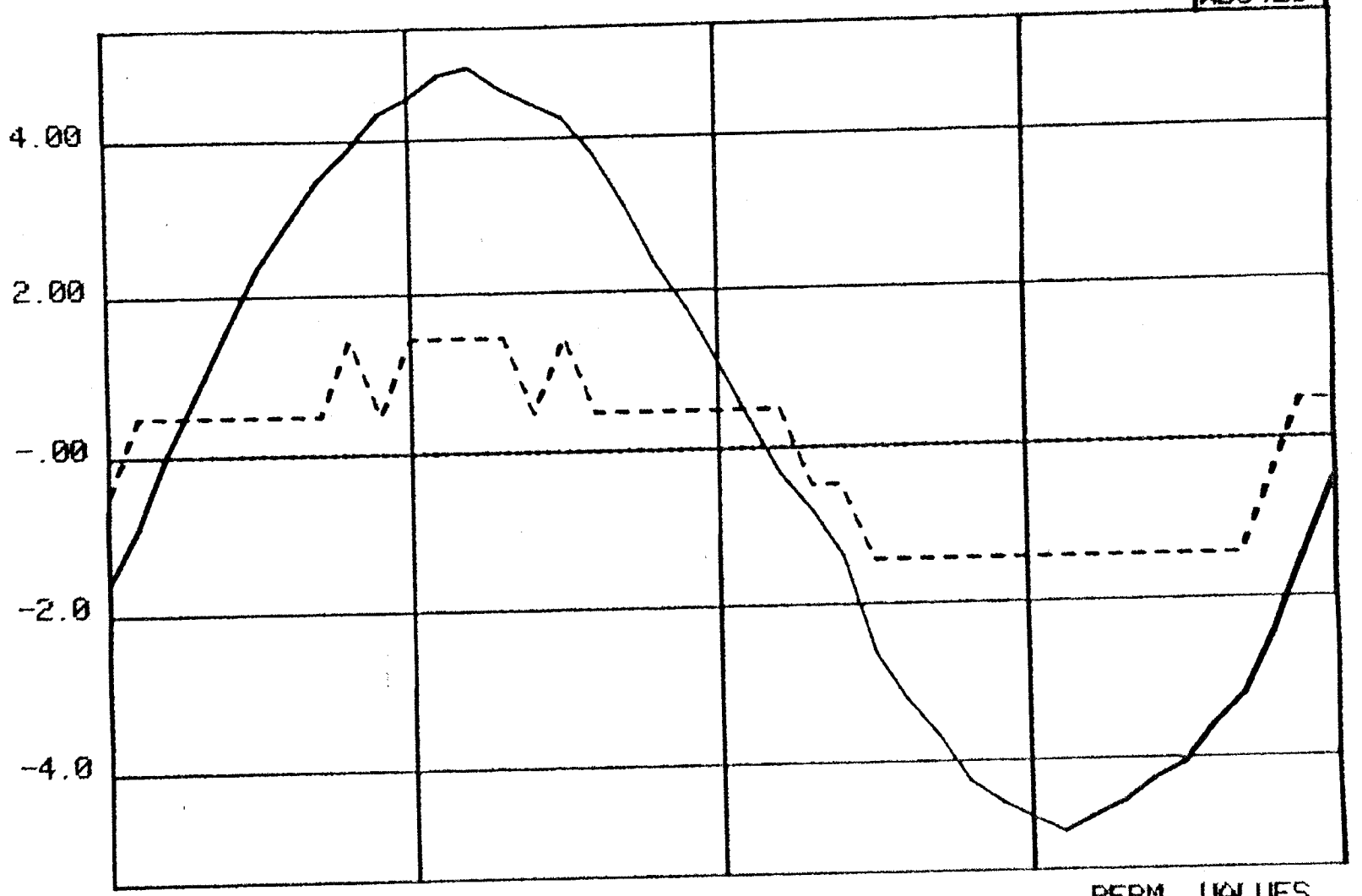

LEGEND:

SKIN FRICTION

PORE PRESSURE

TOTAL NORMAL PRESSURE

PERM. VALUES

6.94 KPA.

412.9 KPA.

665.9 KPA.

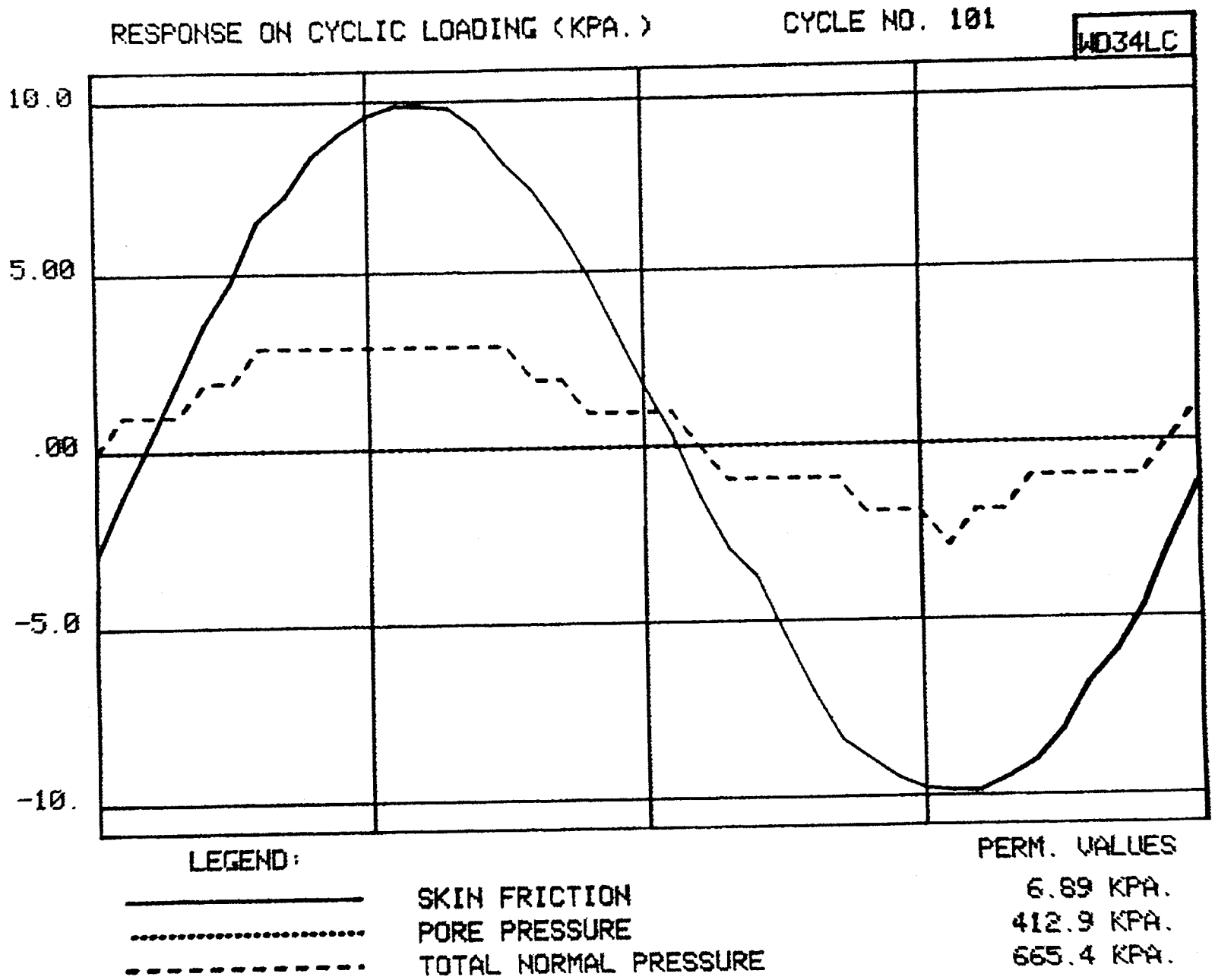
RESPONSE ON CYCLIC LOADING (KPA.)
CYCLE NO. 101
WD34LC
10.0
5.00
.00
-5.0
-10.
LEGEND:
SKIN FRICTION
PORE PRESSURE
TOTAL NORMAL PRESSURE
PERM. VALUES
6.89 KPA.
412.9 KPA.
665.4 KPA.

RESPONSE ON CYCLIC LOADING (KPA.)

CYCLE NO. 197

WD34LC

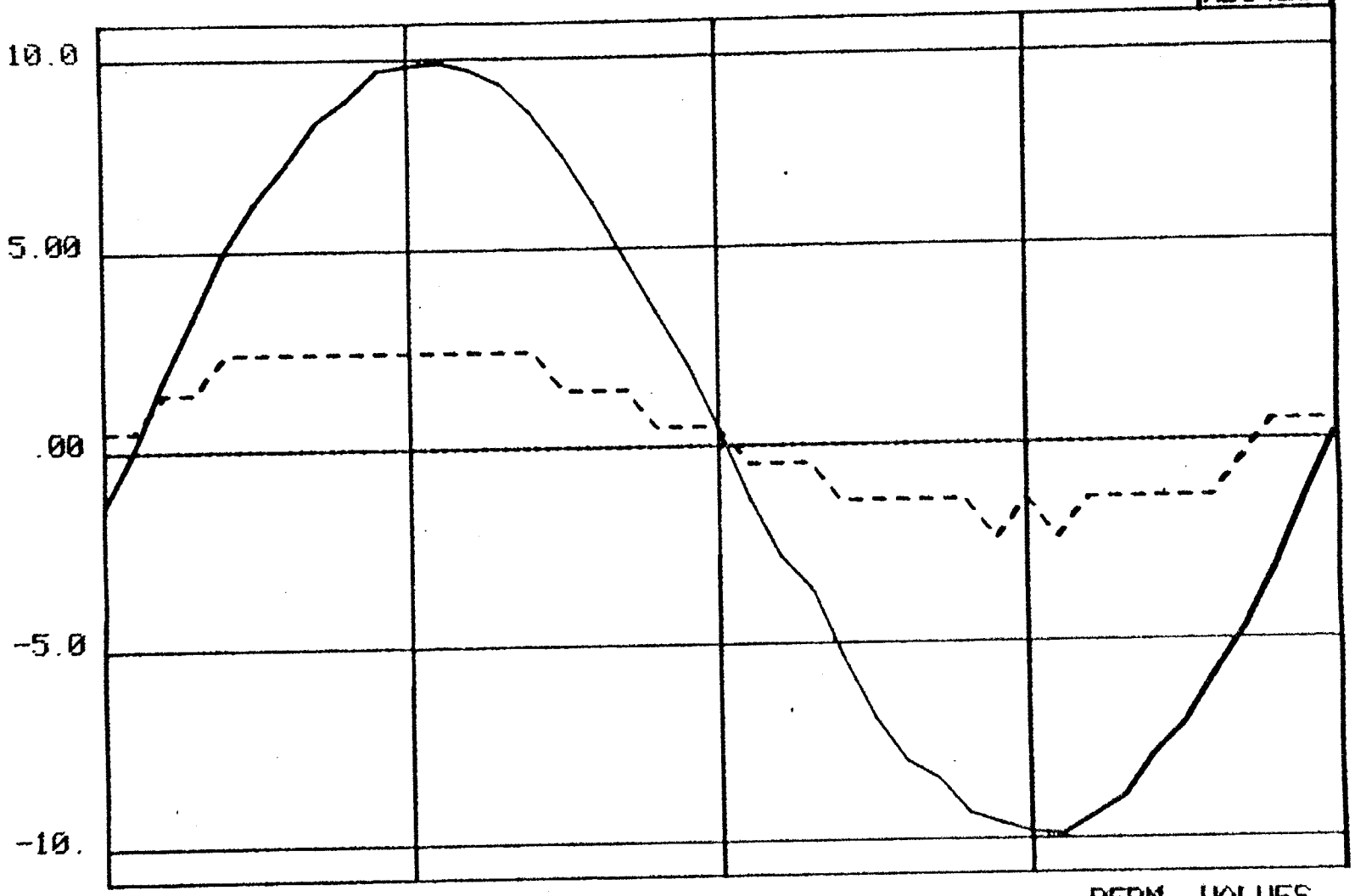

LEGEND:

		PERM. VALUES
———	SKIN FRICTION	6.85 KPA.
·····	PORE PRESSURE	413.9 KPA.
- - - -	TOTAL NORMAL PRESSURE	665.9 KPA.

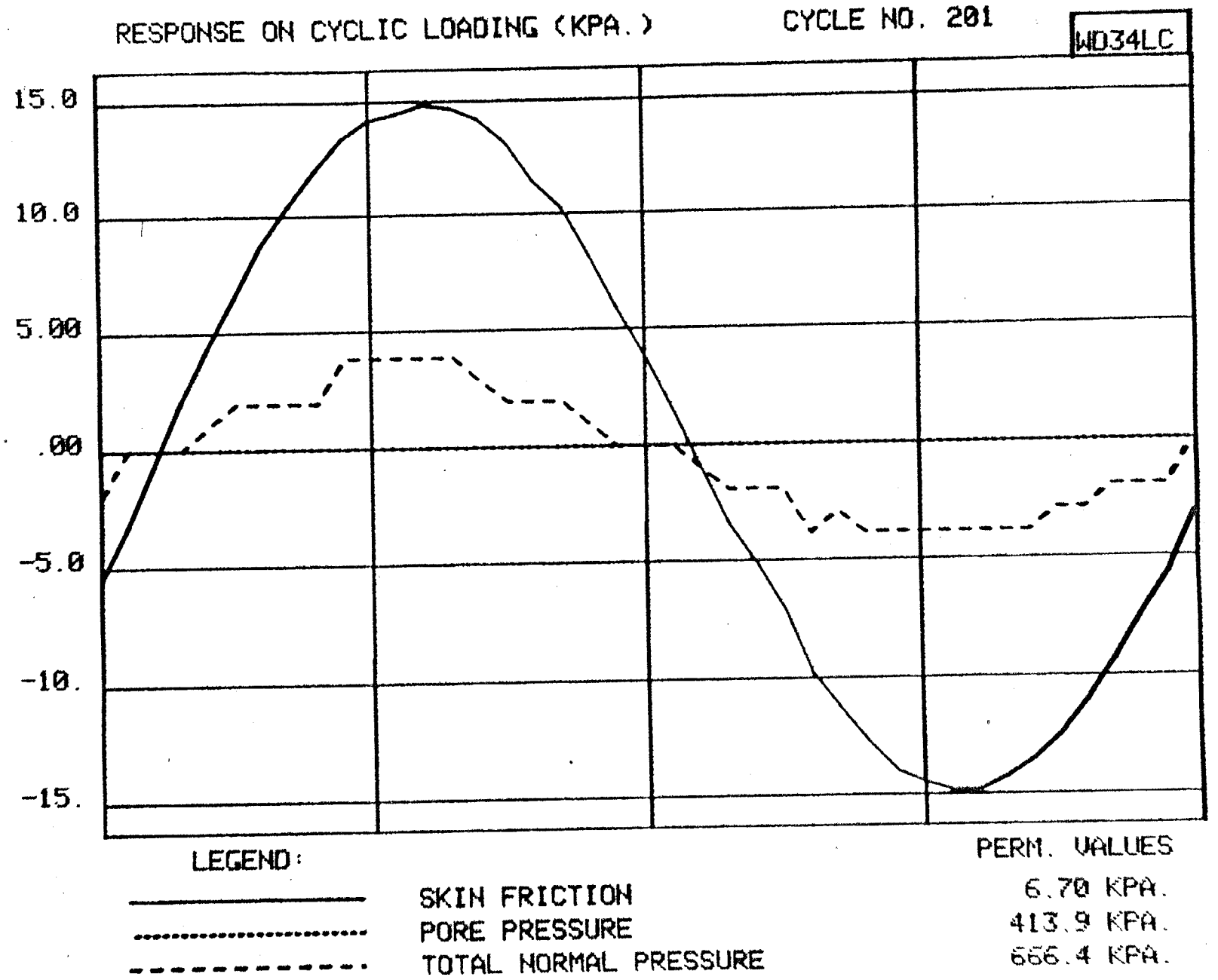
RESPONSE ON CYCLIC LOADING (KPA.)
CYCLE NO. 201
WD34LC
15.0
10.0
5.00
.00
-5.0
-10.
-15.
LEGEND:
SKIN FRICTION
PORE PRESSURE
TOTAL NORMAL PRESSURE
PERM. VALUES
6.70 KPA.
413.9 KPA.
656.4 KPA.

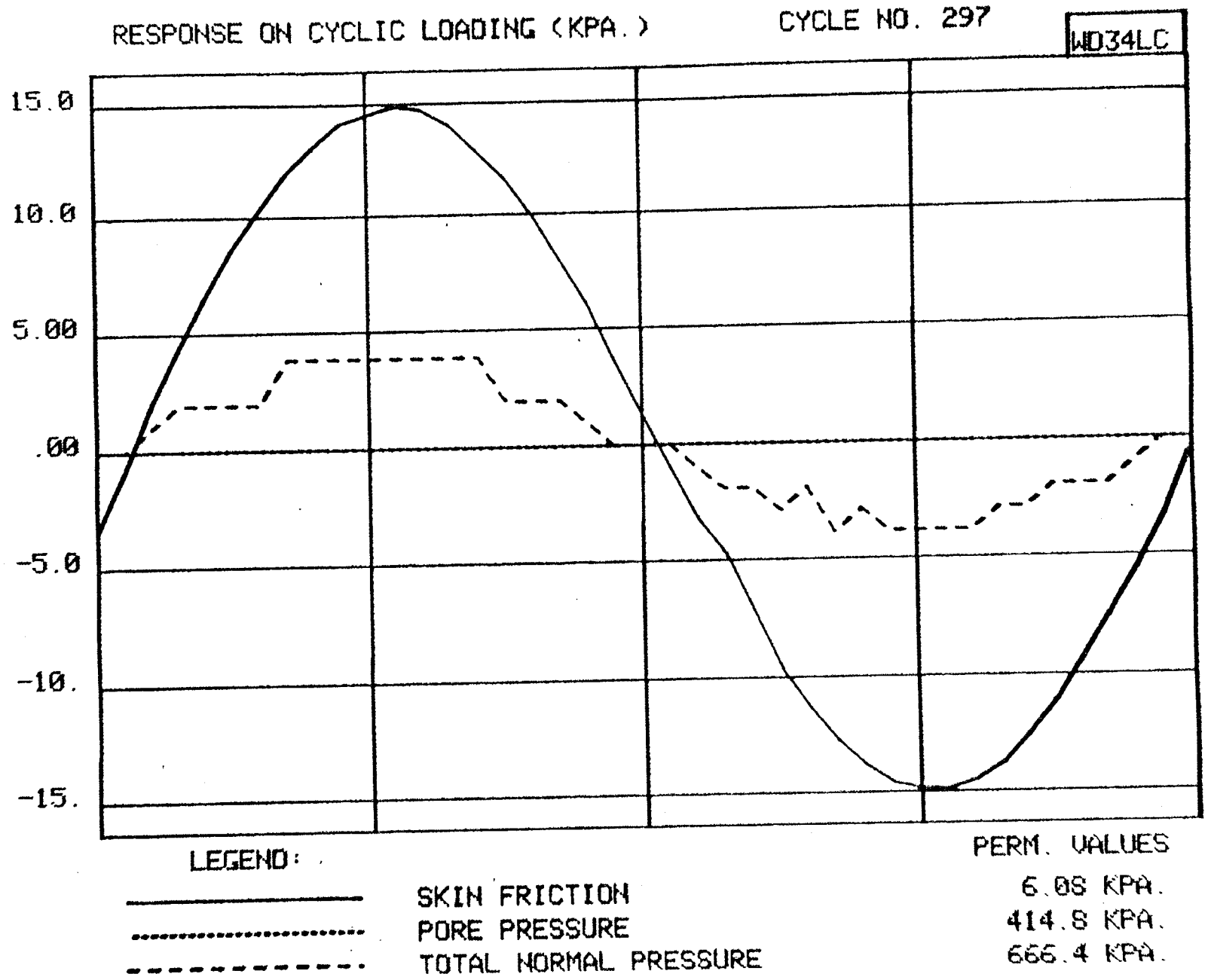
RESPONSE ON CYCLIC LOADING (KPA.)
CYCLE NO. 297
WD34LC
15.0
10.0
5.00
.00
-5.0
-10.
-15.
LEGEND:
SKIN FRICTION
PORE PRESSURE
TOTAL NORMAL PRESSURE
PERM. VALUES
6.08 KPA.
414.8 KPA.
666.4 KPA.

RESPONSE ON CYCLIC LOADING (KPA.) CYCLE NO. 301 WD34LC

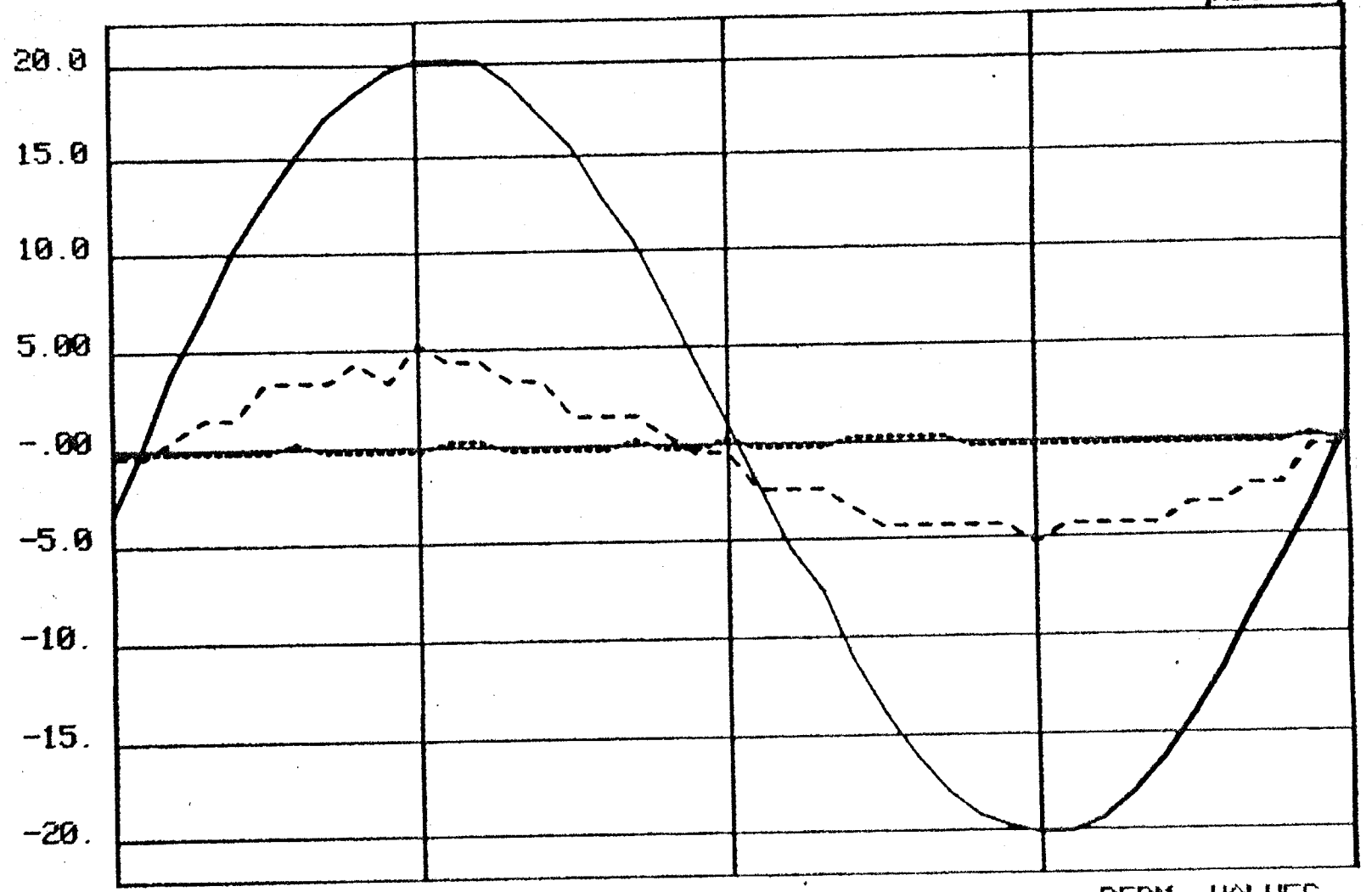

LEGEND:

		PERM. VALUES
———	SKIN FRICTION	5.94 KPA.
·····	PORE PRESSURE	415.1 KPA.
- - - -	TOTAL NORMAL PRESSURE	666.9 KPA.

RESPONSE ON CYCLIC LOADING (KPA.)

CYCLE NO. 397

WD34LC

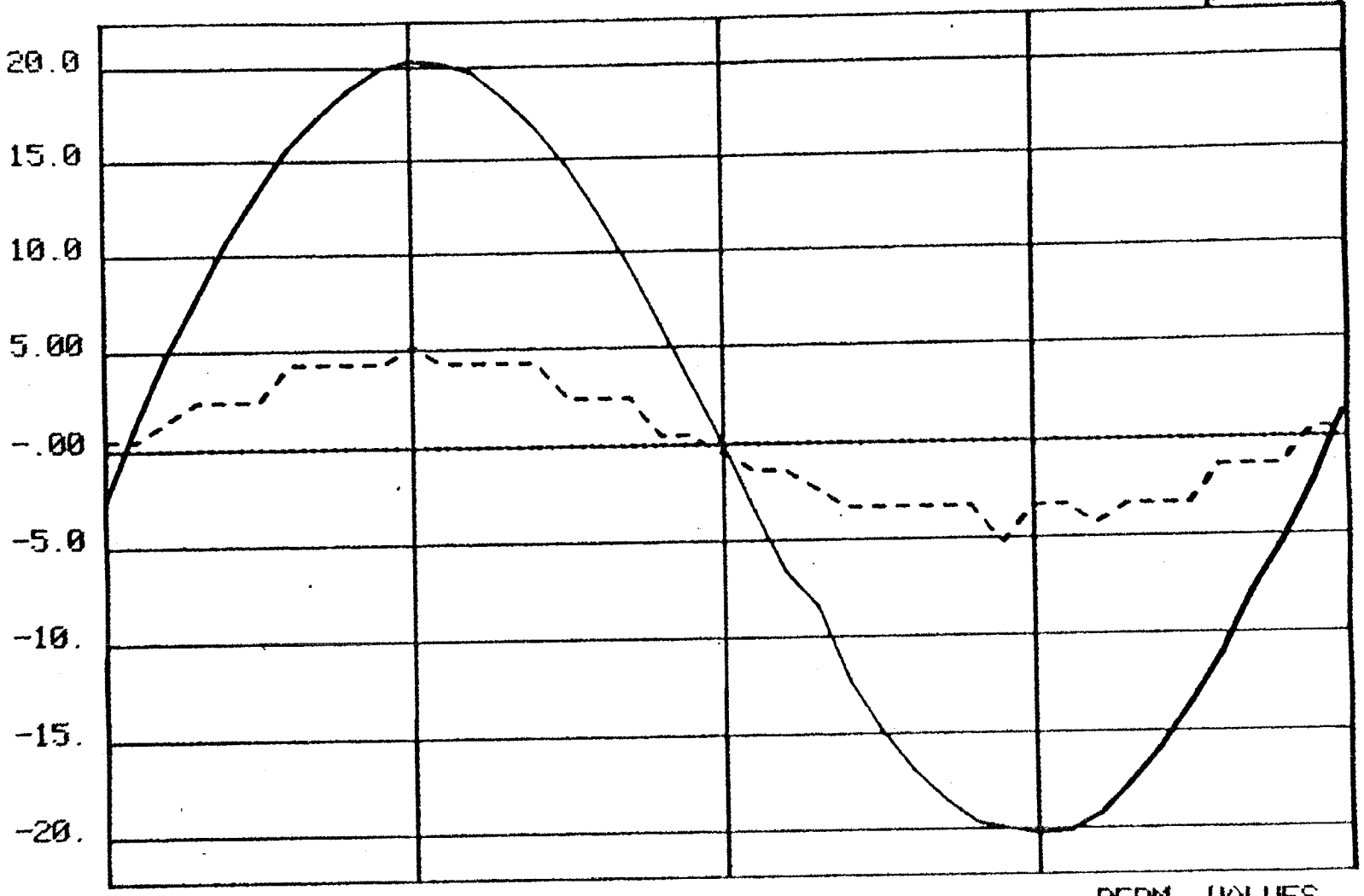

LEGEND:

		PERM. VALUES
———	SKIN FRICTION	5.98 KPA.
·····	PORE PRESSURE	415.8 KPA.
- - - -	TOTAL NORMAL PRESSURE	665.9 KPA.

RESPONSE ON CYCLIC LOADING (KPA.) CYCLE NO. 401 WD34LC

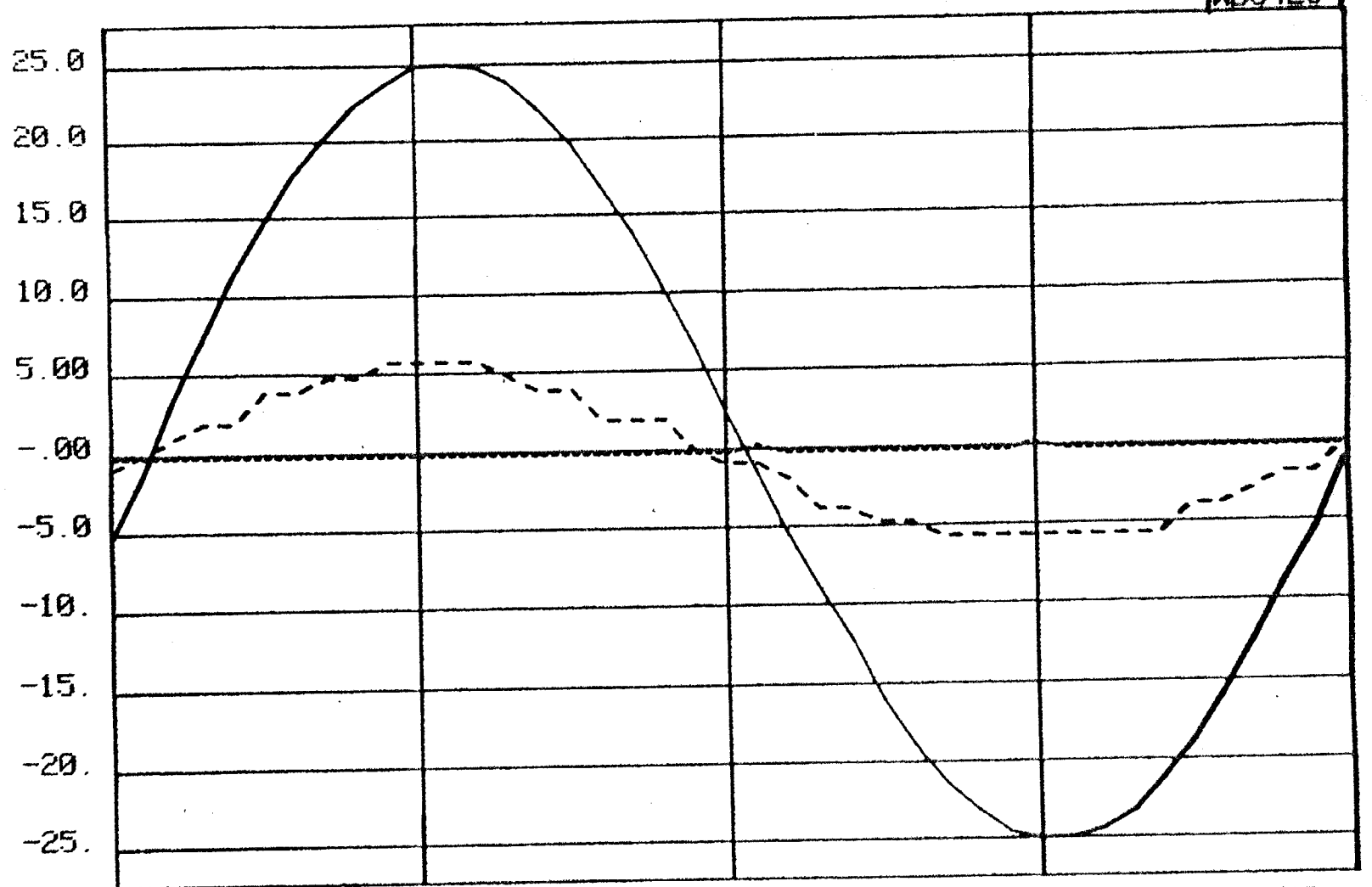

LEGEND:

SKIN FRICTION
PORE PRESSURE
TOTAL NORMAL PRESSURE

PERM. VALUES

5.94 KPA.
416.0 KPA.
666.4 KPA.

RESPONSE ON CYCLIC LOADING (KPA.)

CYCLE NO. 496

WD34LC

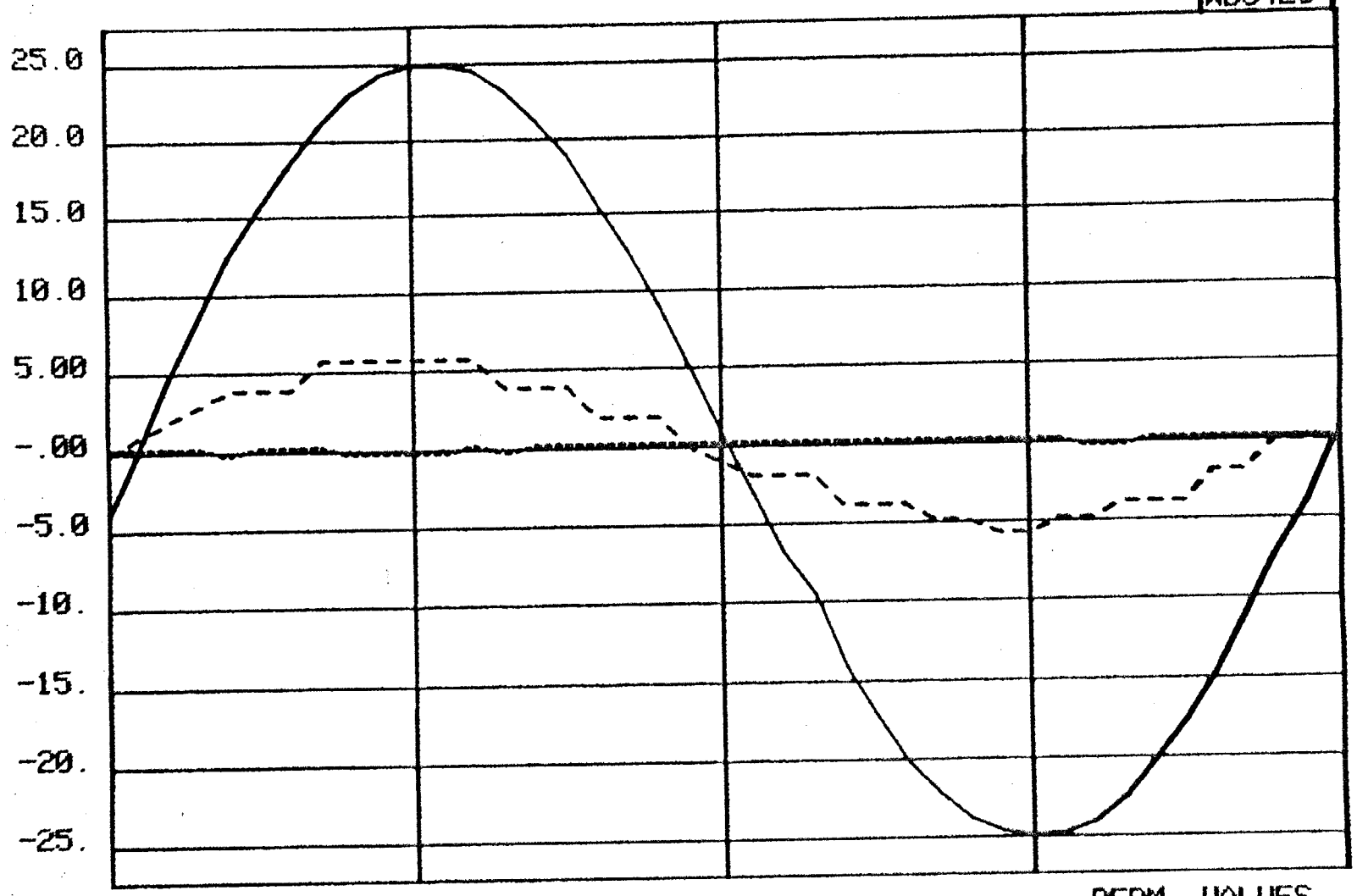

LEGEND:

SKIN FRICTION

PORE PRESSURE

TOTAL NORMAL PRESSURE

PERM. VALUES

5.98 KPA.

417.0 KPA.

664.5 KPA.

RESPONSE ON CYCLIC LOADING (KPA.) CYCLE NO. 500 WD34LC

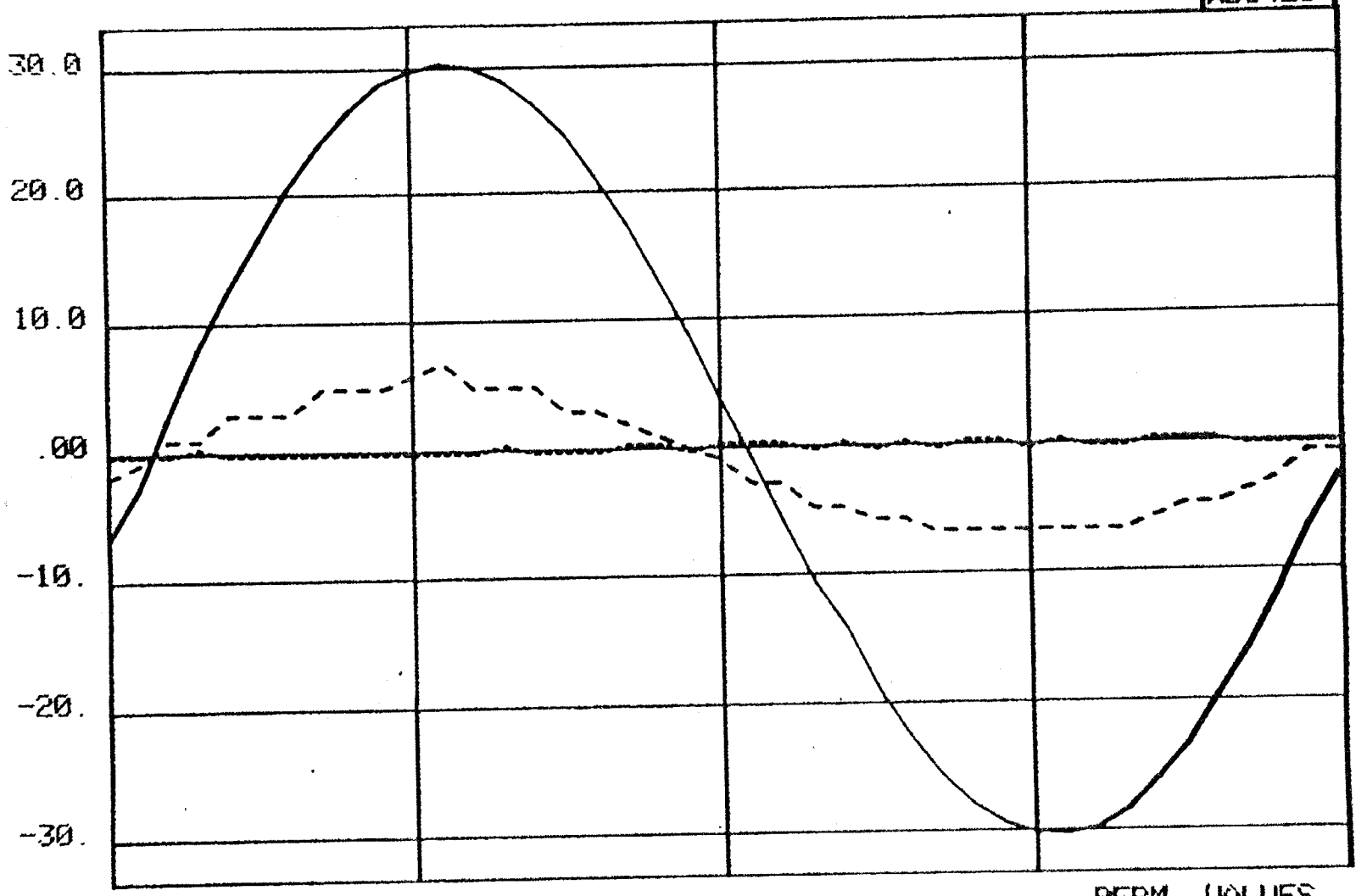

LEGEND:

SKIN FRICTION
PORE PRESSURE
TOTAL NORMAL PRESSURE

PERM. VALUES

5.98 KPA.
417.5 KPA.
665.4 KPA.

RESPONSE ON CYCLIC LOADING (KPA.)

CYCLE NO. 594

WD34LC

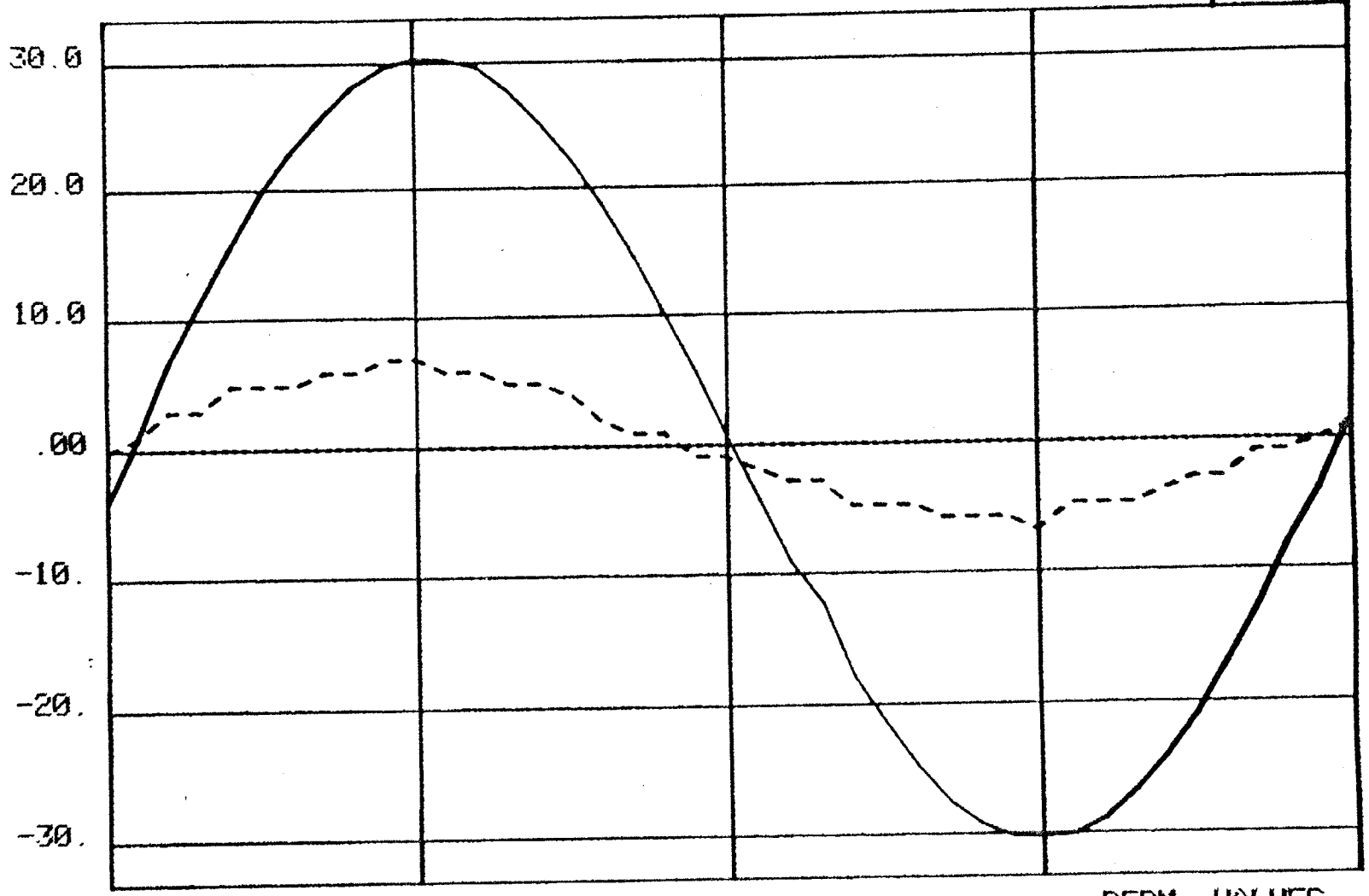

LEGEND:

		PERM. VALUES
————————	SKIN FRICTION	6.27 KPA.
.....	PORE PRESSURE	418.6 KPA.
- - - - - - - - - -	TOTAL NORMAL PRESSURE	661.6 KPA.

RESPONSE ON CYCLIC LOADING (KPA.) CYCLE NO. 599 WD34LC

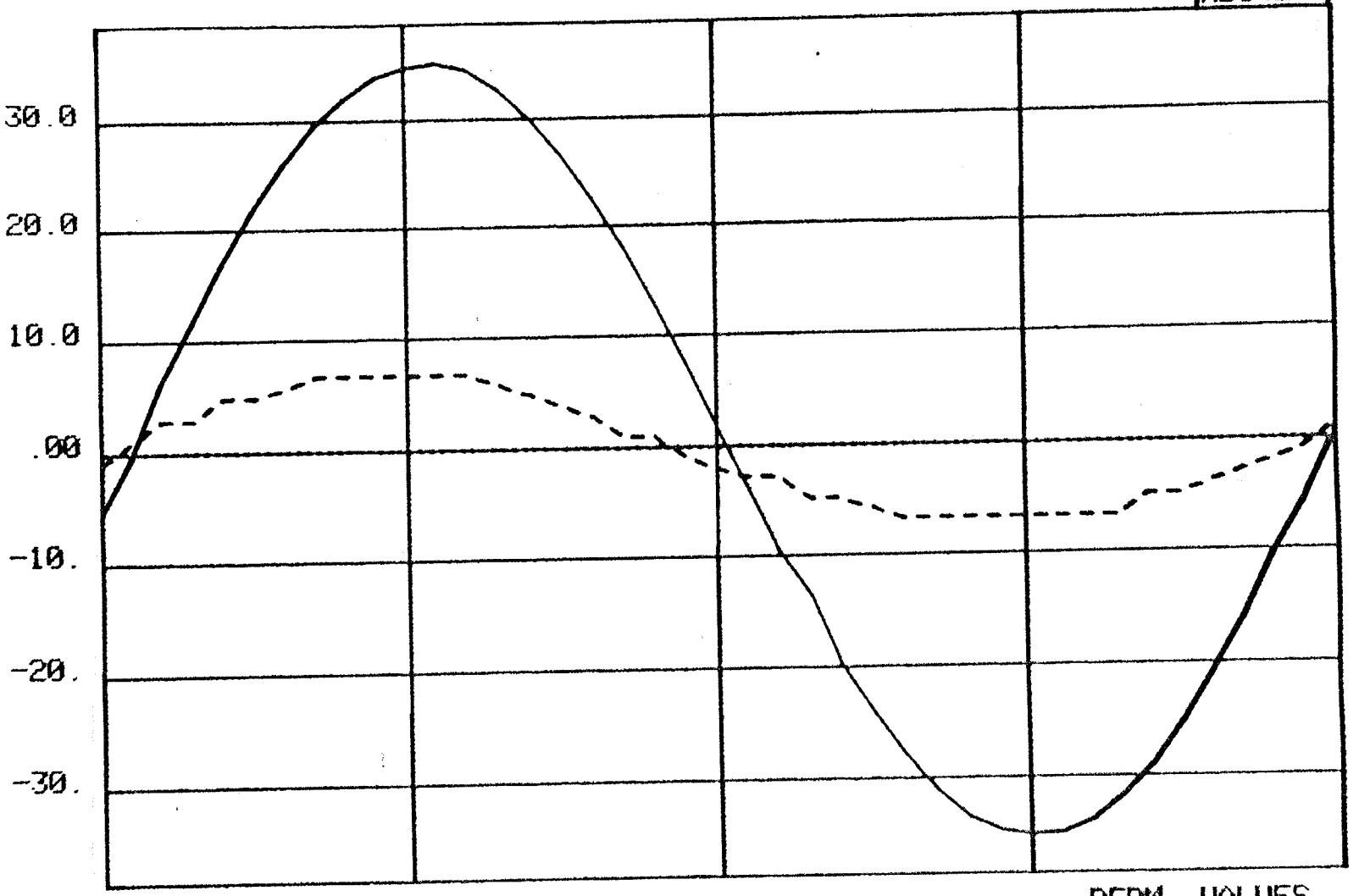

LEGEND:

		PERM. VALUES
————	SKIN FRICTION	6.22 KPA.
.....	PORE PRESSURE	418.6 KPA.
- - - - - -	TOTAL NORMAL PRESSURE	661.6 KPA.

RESPONSE ON CYCLIC LOADING (KPA.)

CYCLE NO. 695

WD34LC

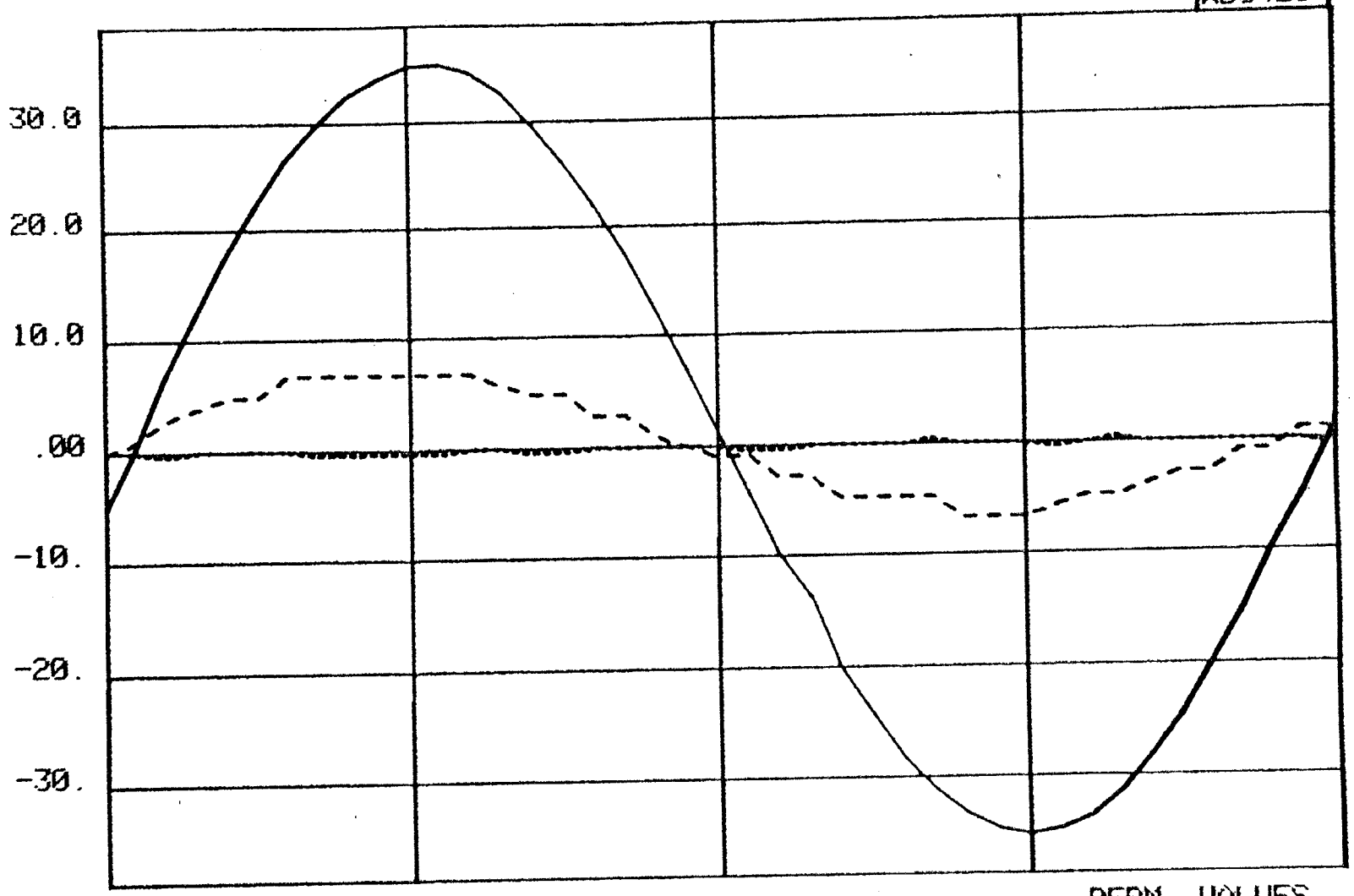

LEGEND:

SKIN FRICTION

PORE PRESSURE

TOTAL NORMAL PRESSURE

PERM. VALUES

6.08 KPA.

420.1 KPA.

655.9 KPA.

RESPONSE ON CYCLIC LOADING (KPA.) CYCLE NO. 698 WD34LC

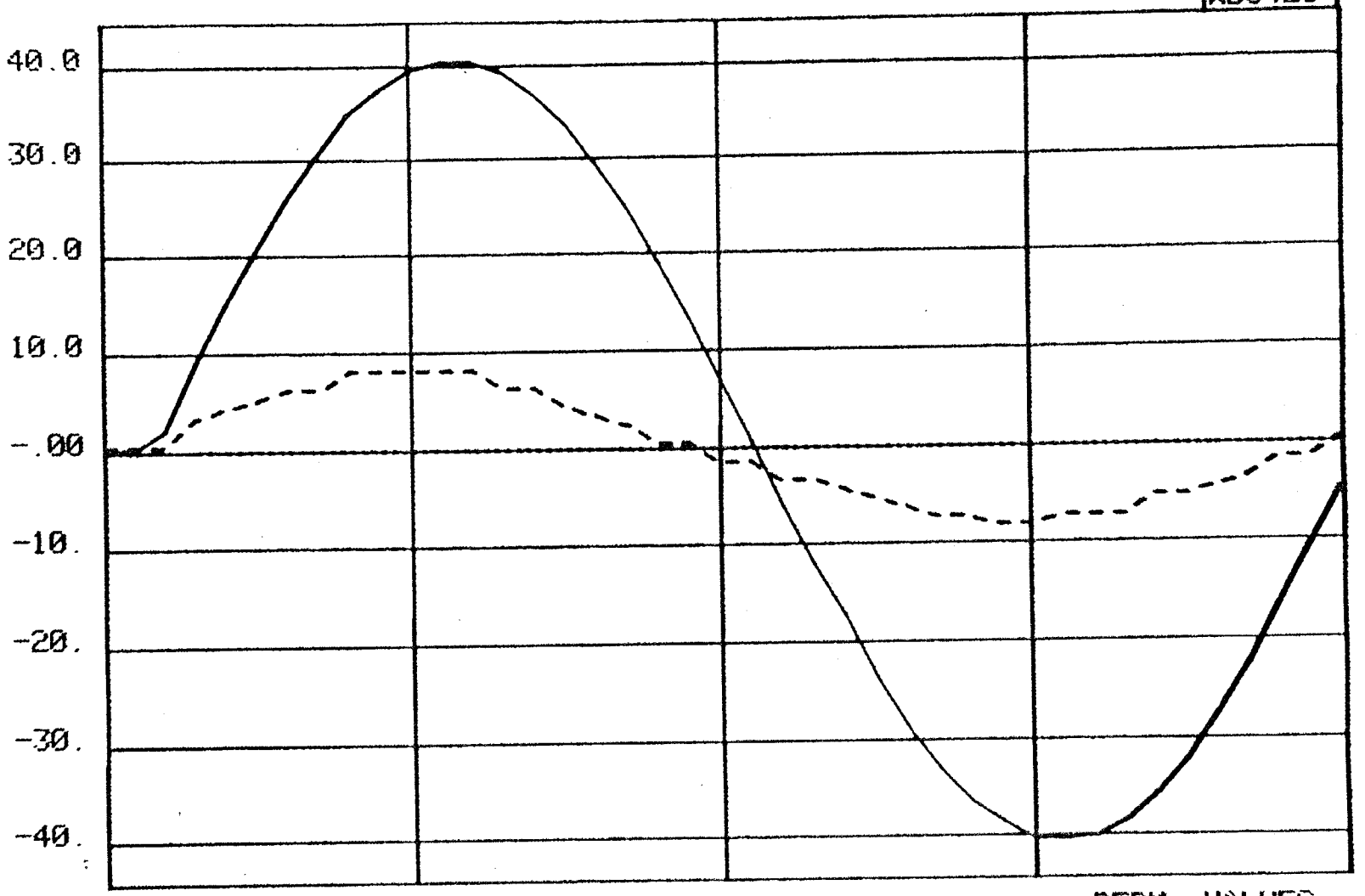

LEGEND:

		PERM. VALUES
————	SKIN FRICTION	5.84 KPA.
.....	PORE PRESSURE	420.6 KPA.
- - - - -	TOTAL NORMAL PRESSURE	656.3 KPA.

RESPONSE ON CYCLIC LOADING (KPA.)

CYCLE NO. 795

W034LC

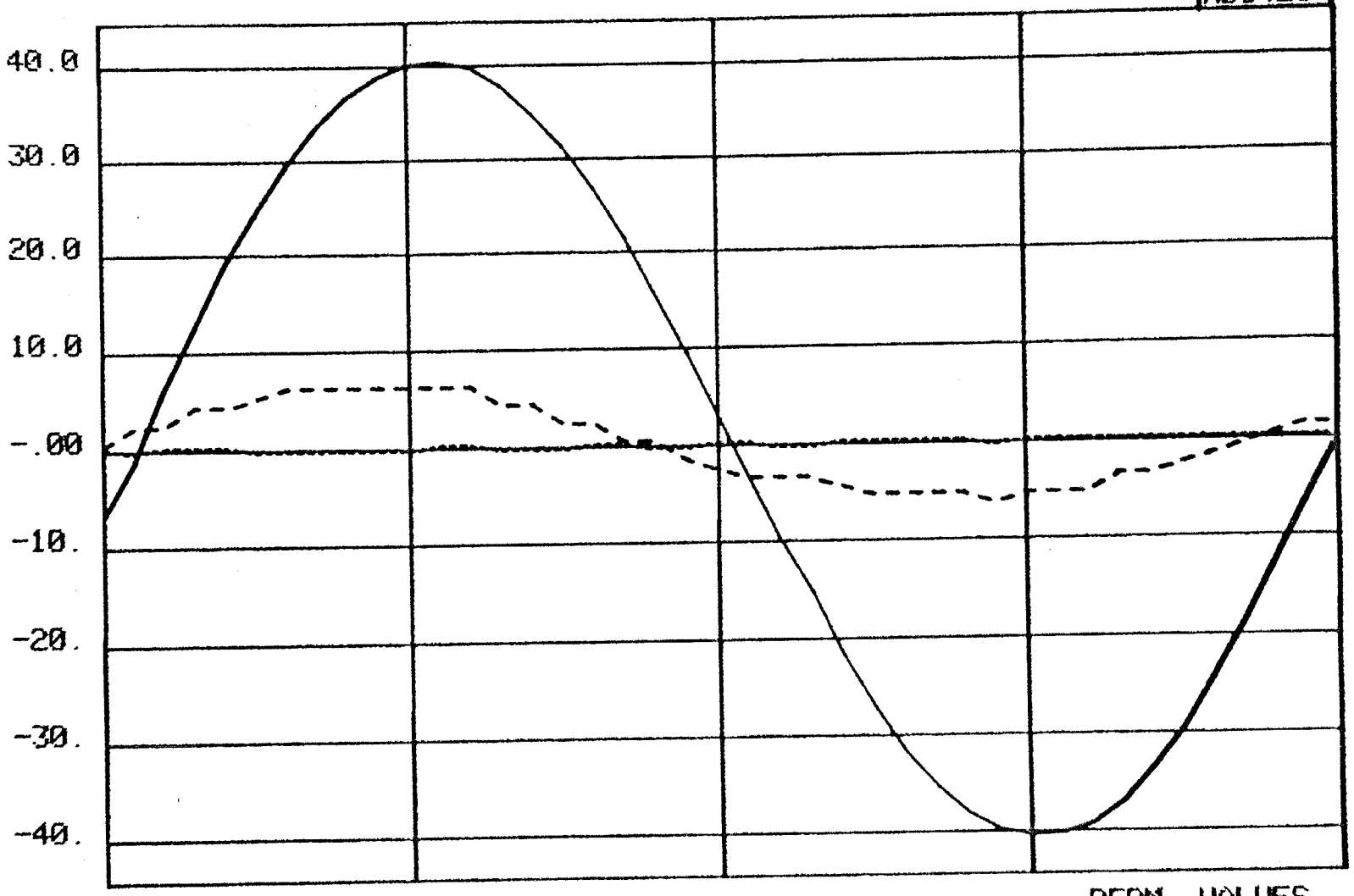

LEGEND:

SKIN FRICTION

PORE PRESSURE

TOTAL NORMAL PRESSURE

PERM. VALUES

6.08 KPA.

422.7 KPA.

650.6 KPA.

RESPONSE ON CYCLIC LOADING (KPA.) CYCLE NO. 800 WD34LC

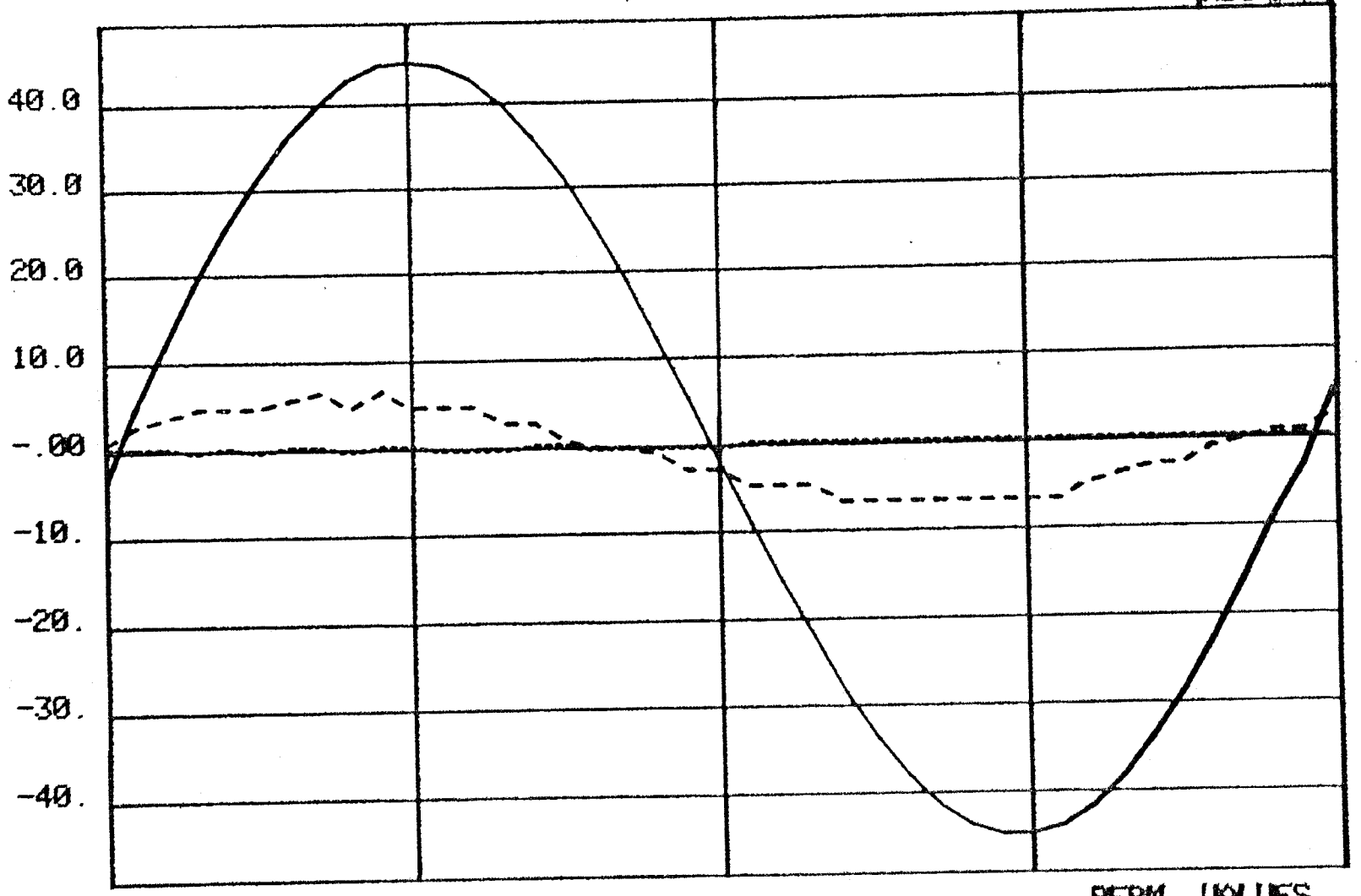

LEGEND:

		PERM. VALUES
————	SKIN FRICTION	5.98 KPA.
·····	PORE PRESSURE	423.2 KPA.
- - - -	TOTAL NORMAL PRESSURE	682.0 KPA.

RESPONSE ON CYCLIC LOADING (KPA.) CYCLE NO. 801 WD34LC

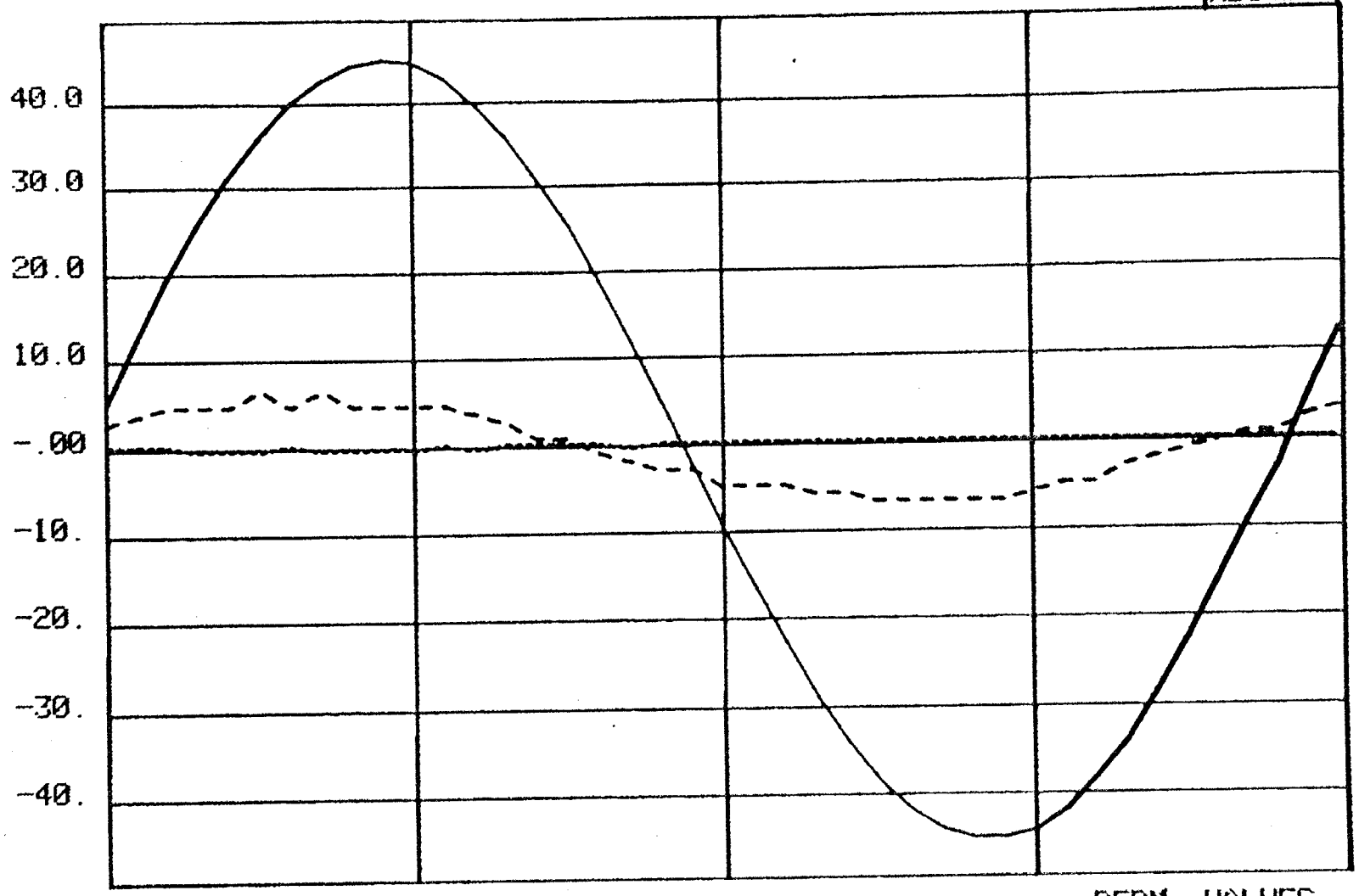

LEGEND:

		PERM. VALUES
———	SKIN FRICTION	6.13 KPA.
·····	PORE PRESSURE	423.2 KPA.
- - - -	TOTAL NORMAL PRESSURE	652.0 KPA.

Appendix AB

Plotted Results from WD34SC

Figures AB-1 through AB-7

Skin Friction vs Deflection, Selected Cycles

Figures AB-8 through AB-14

Skin Friction vs Eff. Normal Pressure, Selected Cycl.

Figures AB-15 through AB-26

Skin Friction, Pore and Total Pressure, Selected Cycles

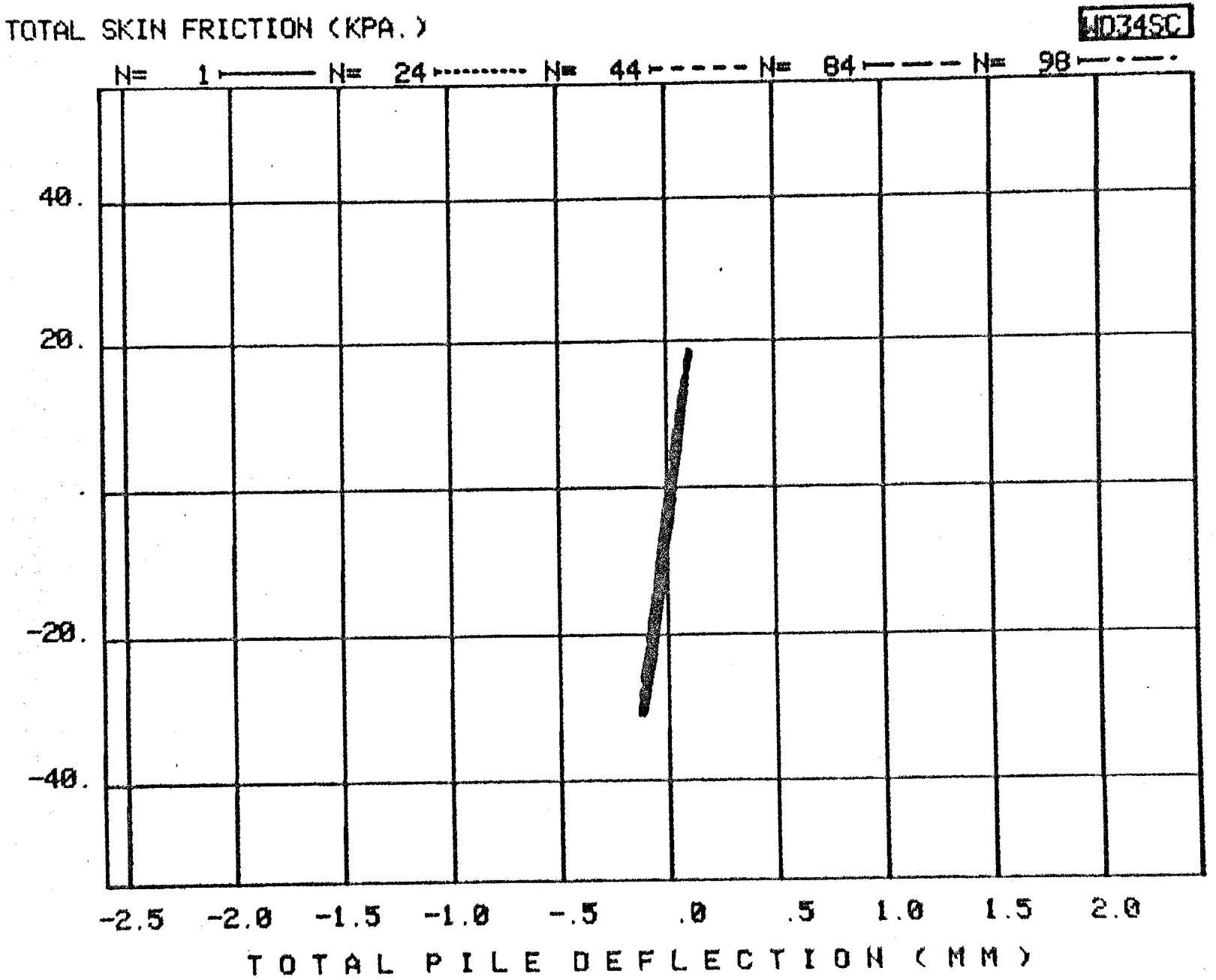
TOTAL SKIN FRICTION (KPA.)
WD34SC
N= 1
N= 24
N= 44
N= 84
N= 98
40.
20.
-20.
-40.
-2.5
-2.0
-1.5
-1.0
-.5
.0
.5
1.0
1.5
2.0
TOTAL PILE DEFLECTION (MM)

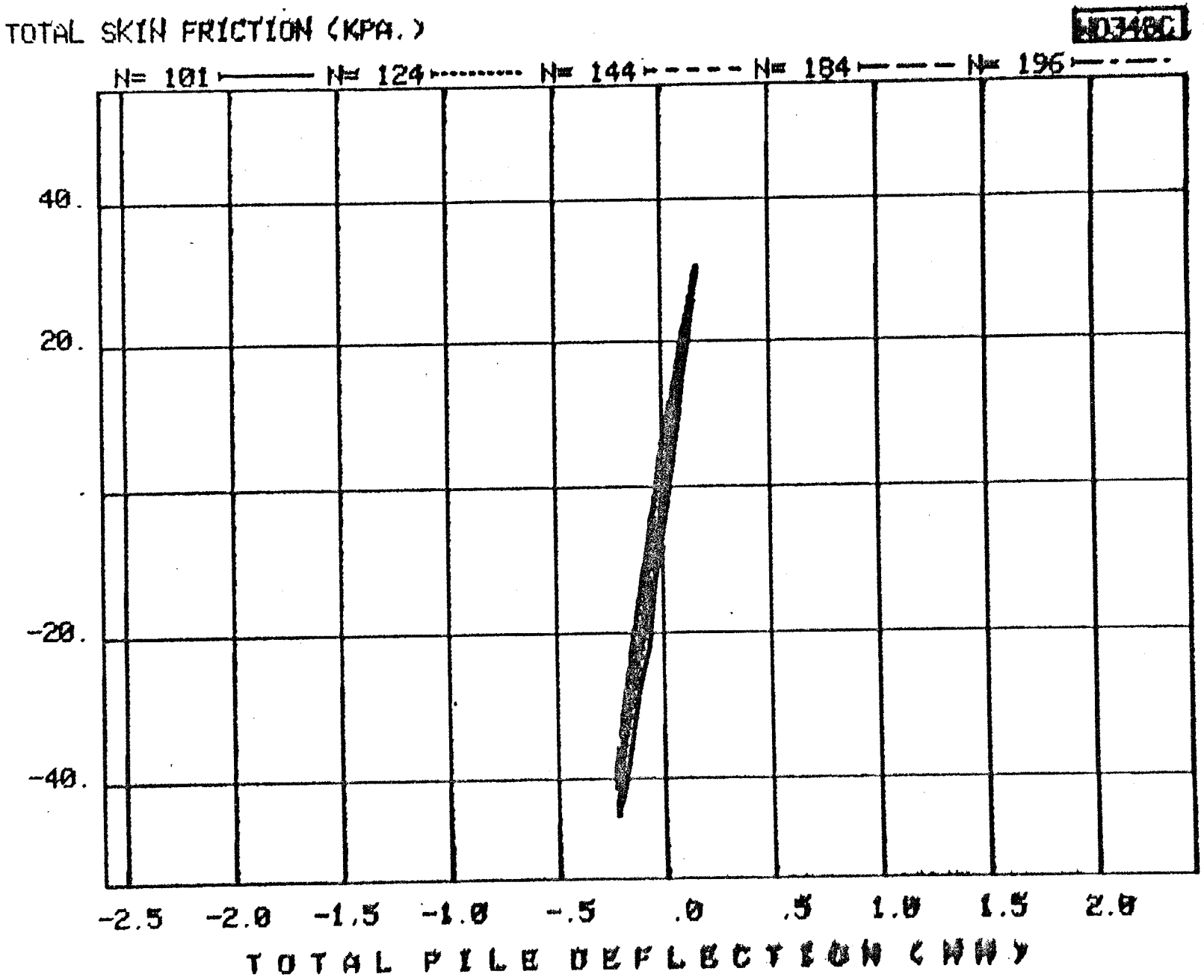
TOTAL SKIN FRICTION (KPA.)
N= 101
N= 124
N= 144
N= 184
N= 196
40.
20.
-20.
-40.
-2.5
-2.0
-1.5
-1.0
-.5
.0
.5
1.0
1.5
2.0
TOTAL PILE DEFLECTION (MM)

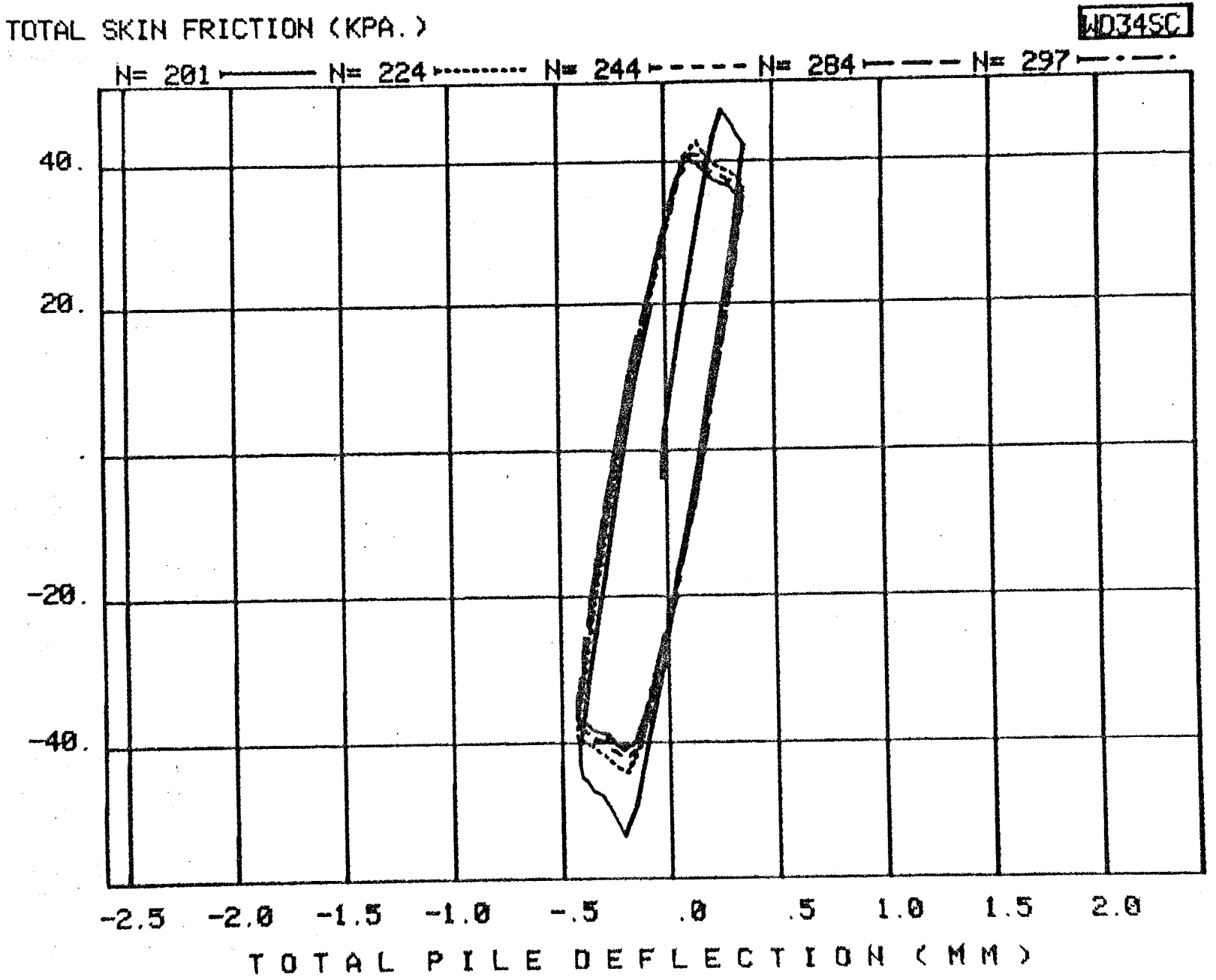
TOTAL SKIN FRICTION (KPA.)
WD34SC
N= 201
N= 224
N= 244
N= 284
N= 297
40.
20.
-20.
-40.
-2.5
-2.0
-1.5
-1.0
-.5
.0
.5
1.0
1.5
2.0
TOTAL PILE DEFLECTION (MM)

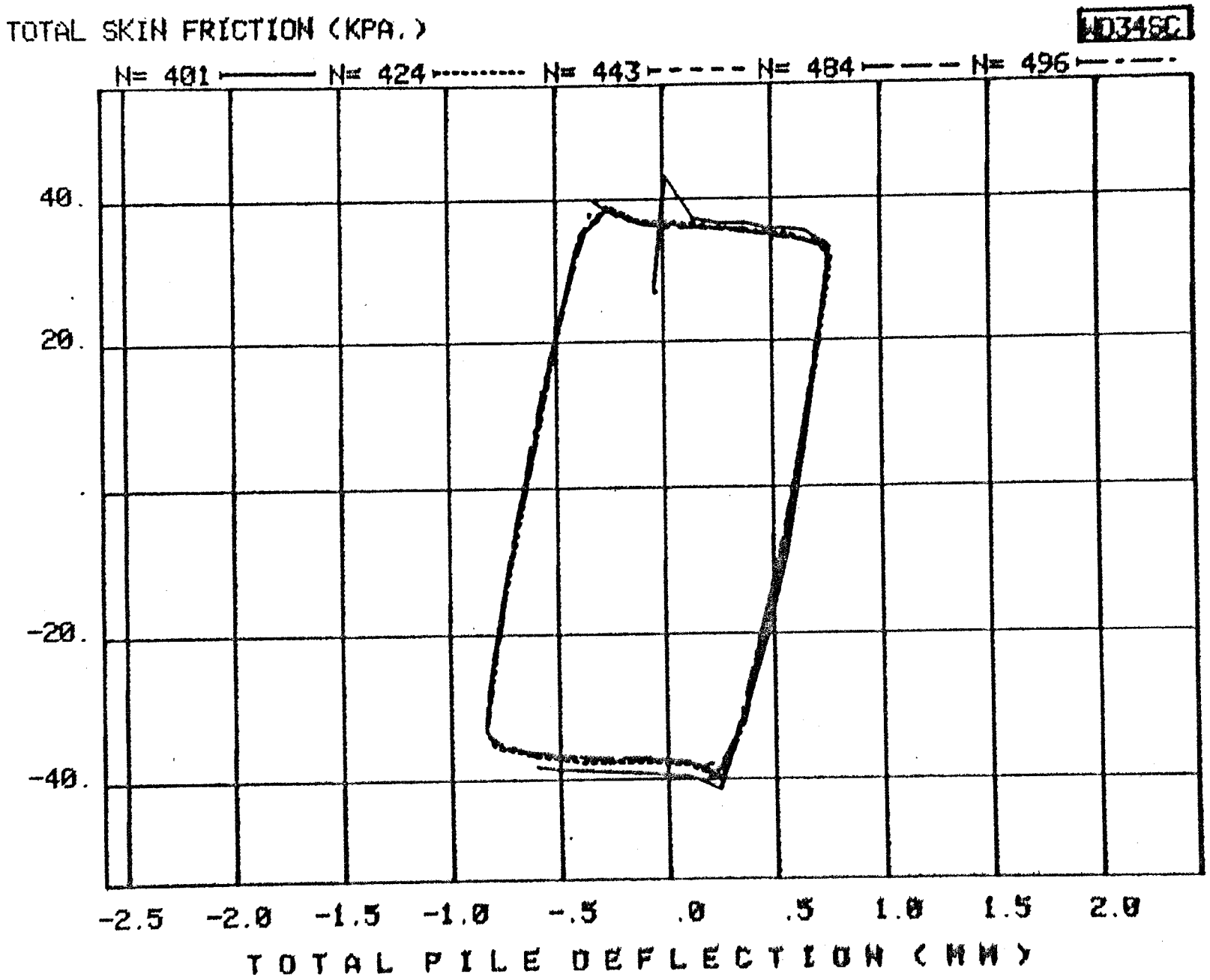
TOTAL SKIN FRICTION (KPA.)
WD34SC
N= 401
N= 424
N= 443
N= 484
N= 496
40.
20.
-20.
-40.
-2.5
-2.0
-1.5
-1.0
-.5
.0
.5
1.0
1.5
2.0
TOTAL PILE DEFLECTION (MM)

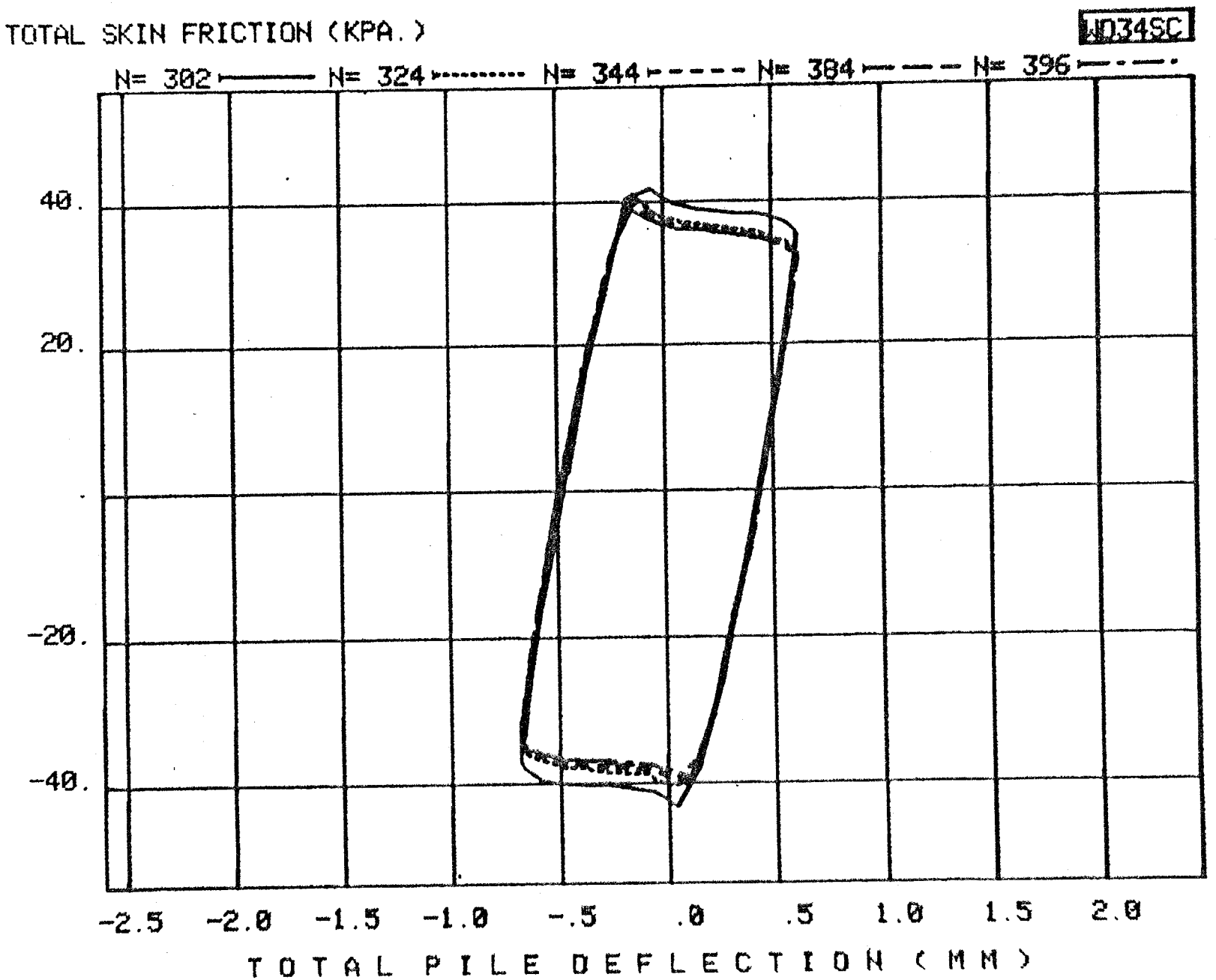
TOTAL SKIN FRICTION (KPA.)
WD34SC
N= 302
N= 324
N= 344
N= 384
N= 396
40.
20.
-20.
-40.
-2.5
-2.0
-1.5
-1.0
-.5
.0
.5
1.0
1.5
2.0
TOTAL PILE DEFLECTION (MM)

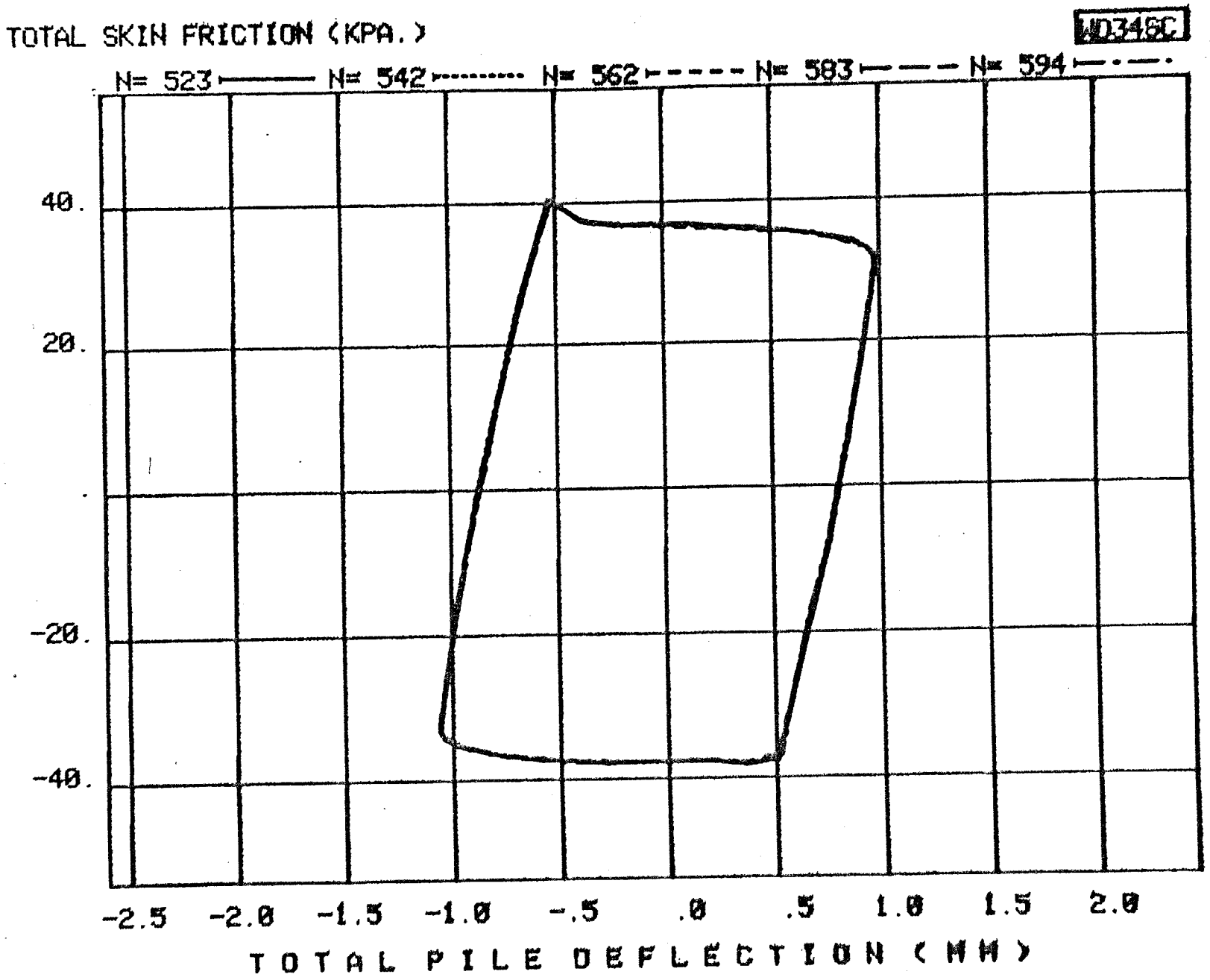
TOTAL SKIN FRICTION (KPA.)
WD348C
N= 523
N= 542
N= 562
N= 583
N= 594
40.
20.
-20.
-40.
-2.5
-2.0
-1.5
-1.0
-.5
.0
.5
1.0
1.5
2.0
TOTAL PILE DEFLECTION (MM)

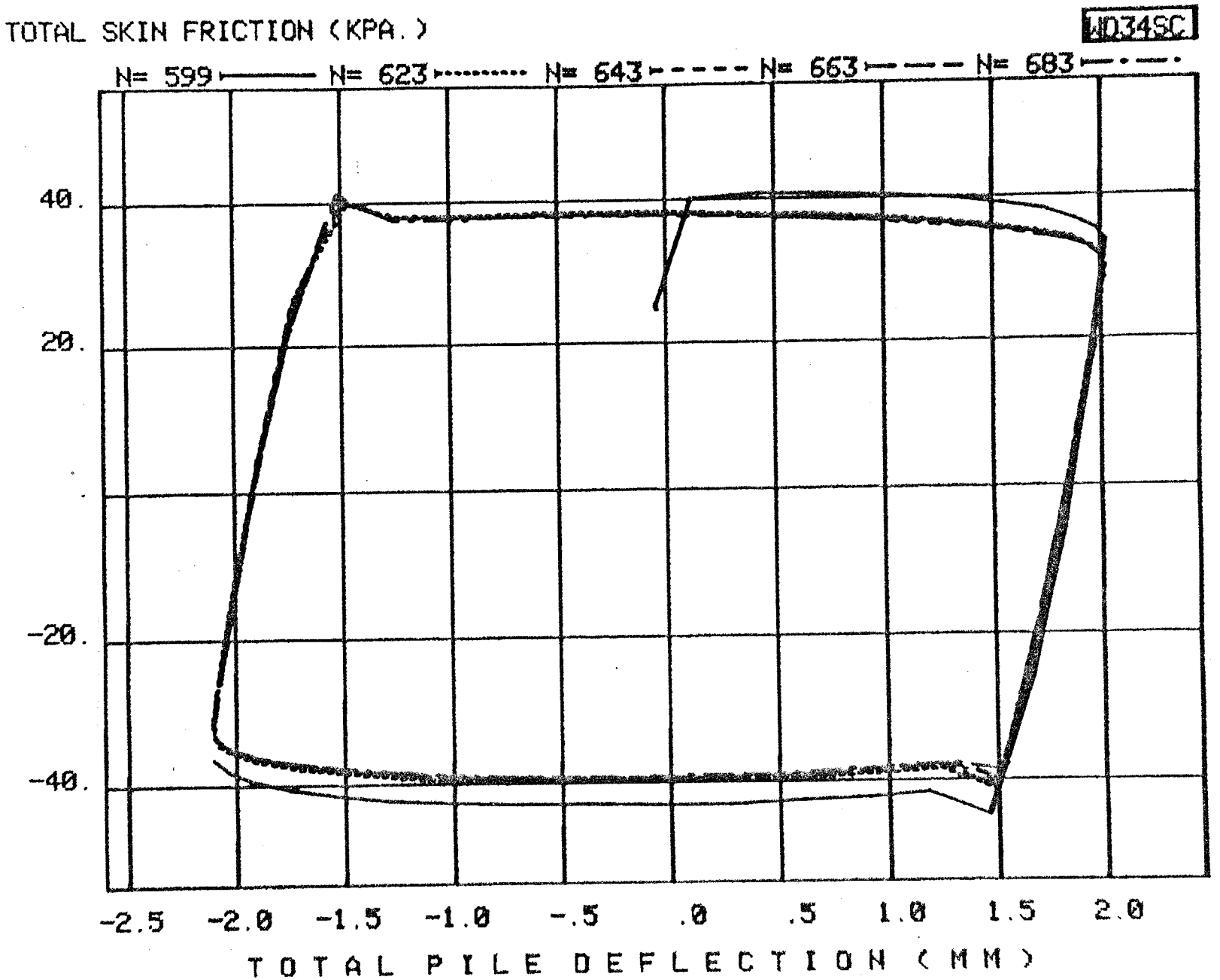
TOTAL SKIN FRICTION (KPA.)
WD34SC
N= 599
N= 623
N= 643
N= 663
N= 683
40.
20.
-20.
-40.
-2.5
-2.0
-1.5
-1.0
-.5
.0
.5
1.0
1.5
2.0
TOTAL PILE DEFLECTION (MM)

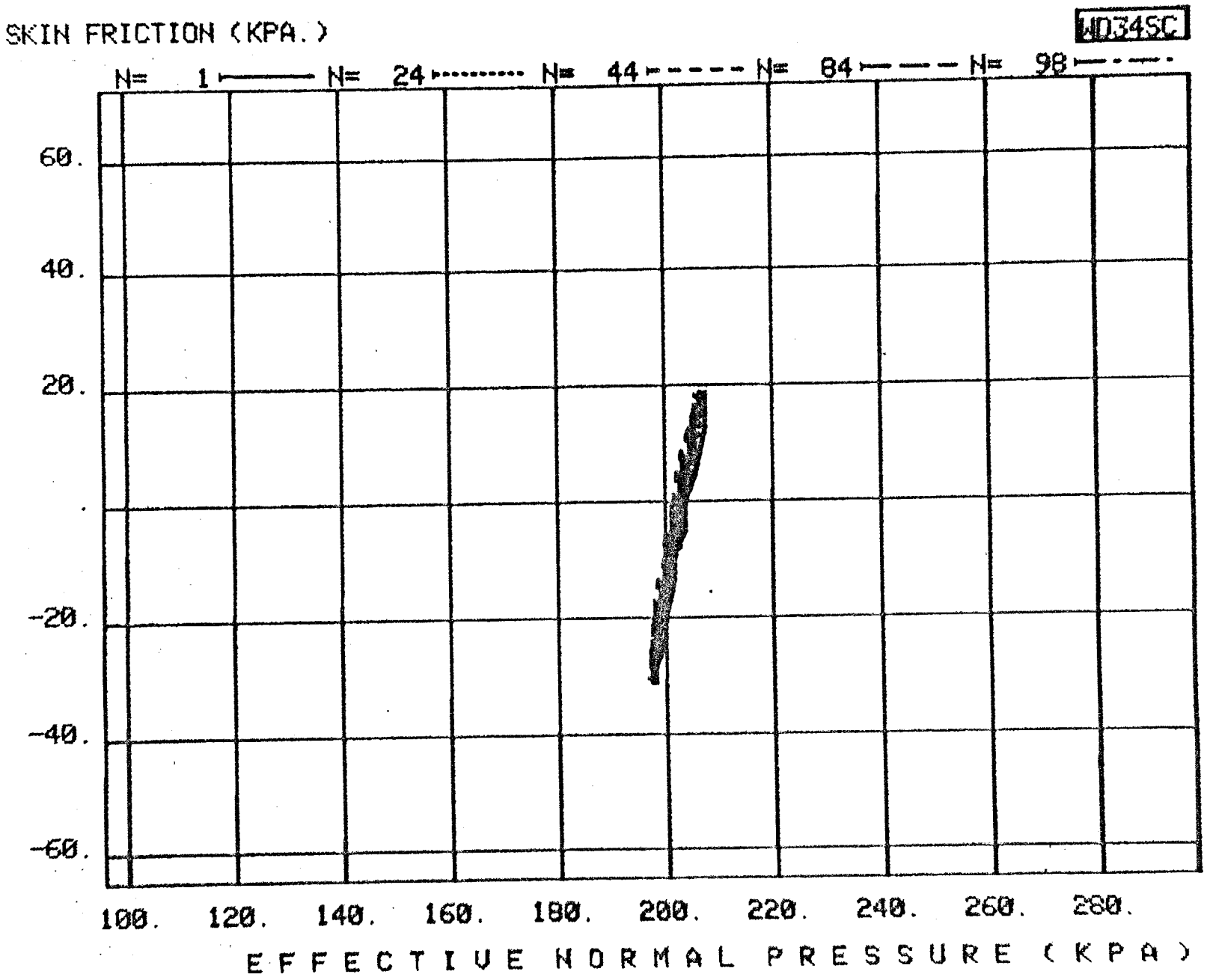
SKIN FRICTION (KPA.)
WD34SC
N= 1
N= 24
N= 44
N= 84
N= 98
60.
40.
20.
-20.
-40.
-60.
100.
120.
140.
160.
180.
200.
220.
240.
260.
280.
EFFECTIVE NORMAL PRESSURE (KPA)

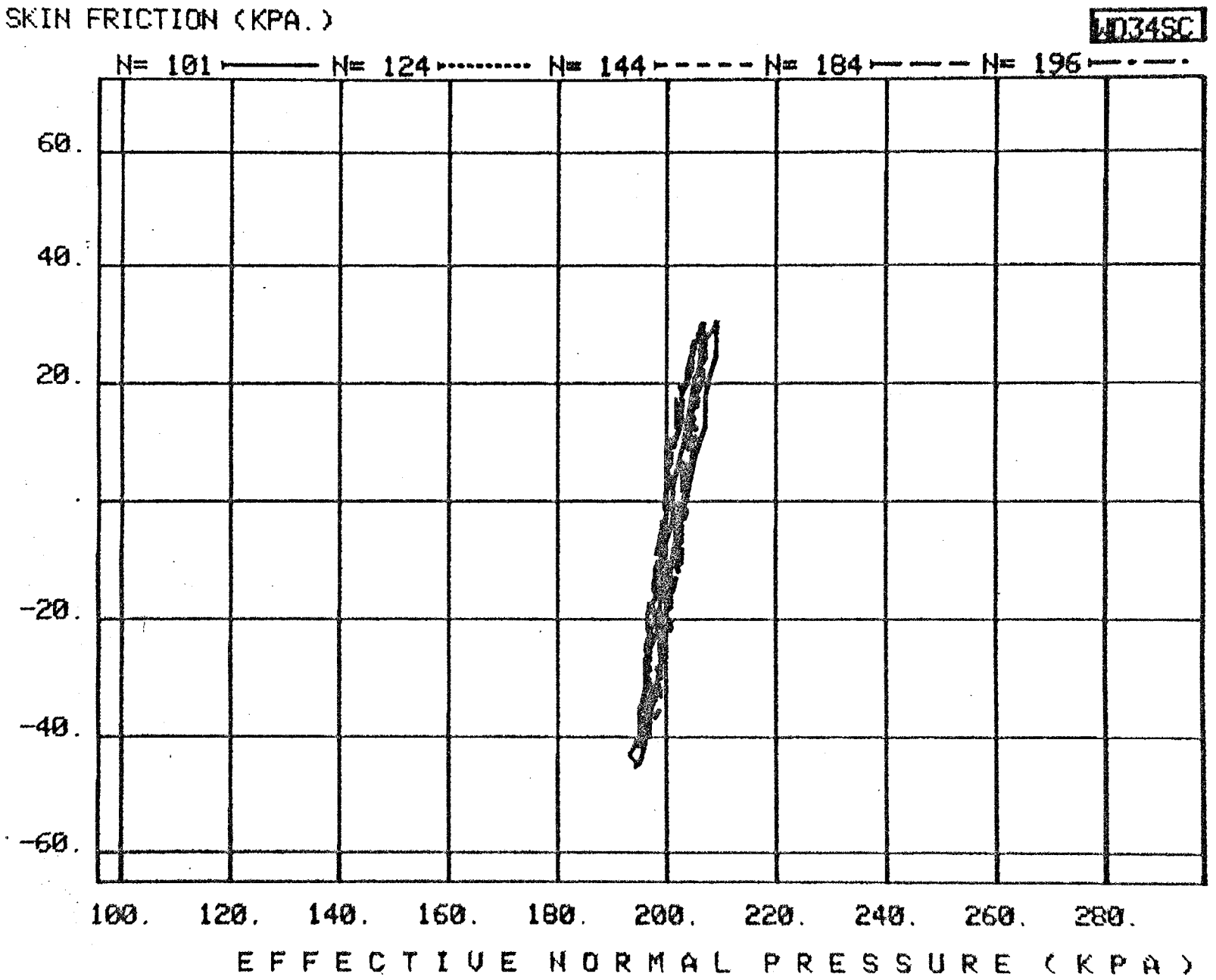
SKIN FRICTION (KPA.)
WD34SC
N= 101
N= 124
N= 144
N= 184
N= 196
60.
40.
20.
-20.
-40.
-60.
100.
120.
140.
160.
180.
200.
220.
240.
260.
280.
EFFECTIVE NORMAL PRESSURE (KPA)

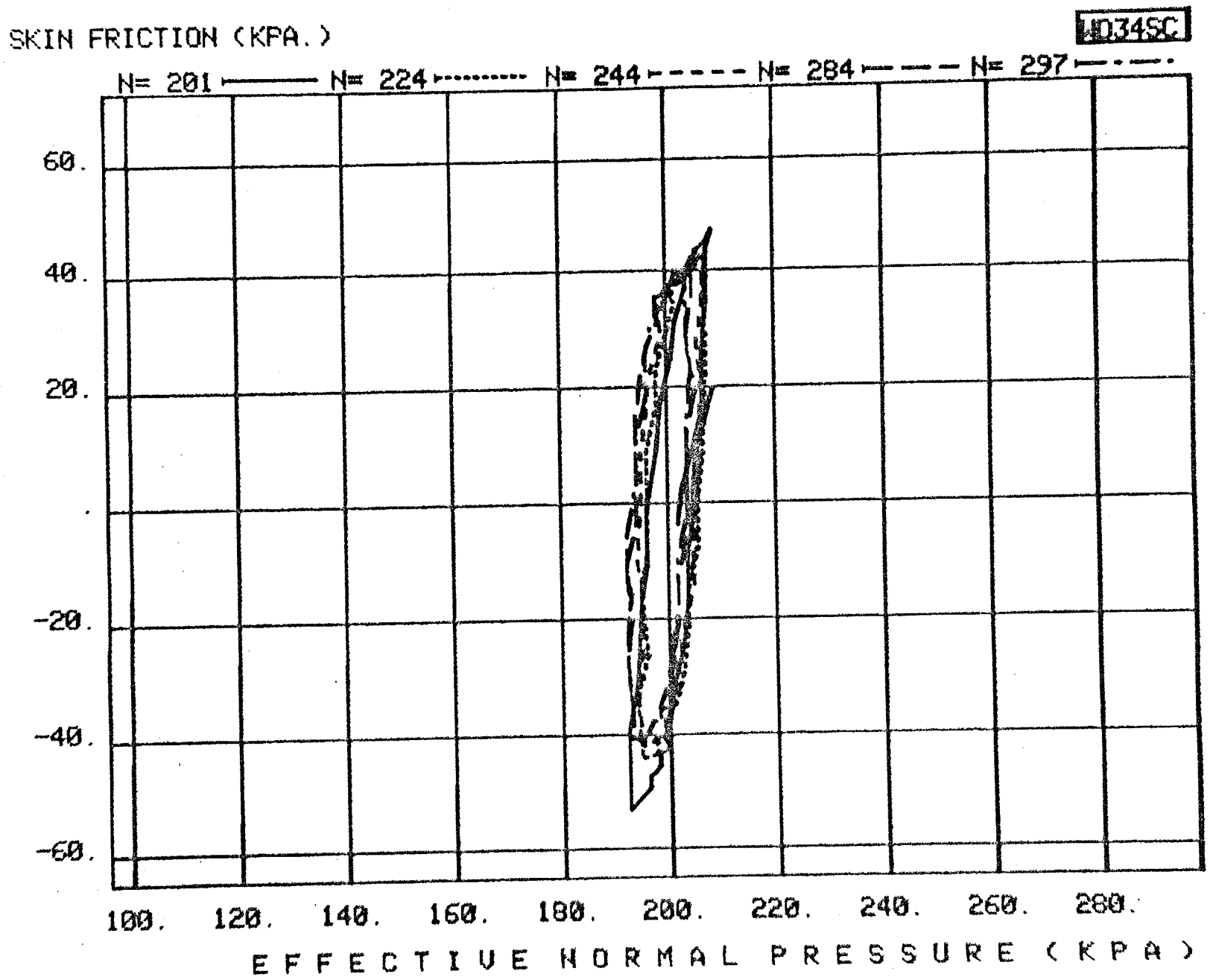
SKIN FRICTION (KPA.)
WD34SC
N= 201
N= 224
N= 244
N= 284
N= 297
60.
40.
20.
-20.
-40.
-60.
100.
120.
140.
160.
180.
200.
220.
240.
260.
280.
EFFECTIVE NORMAL PRESSURE (KPA)

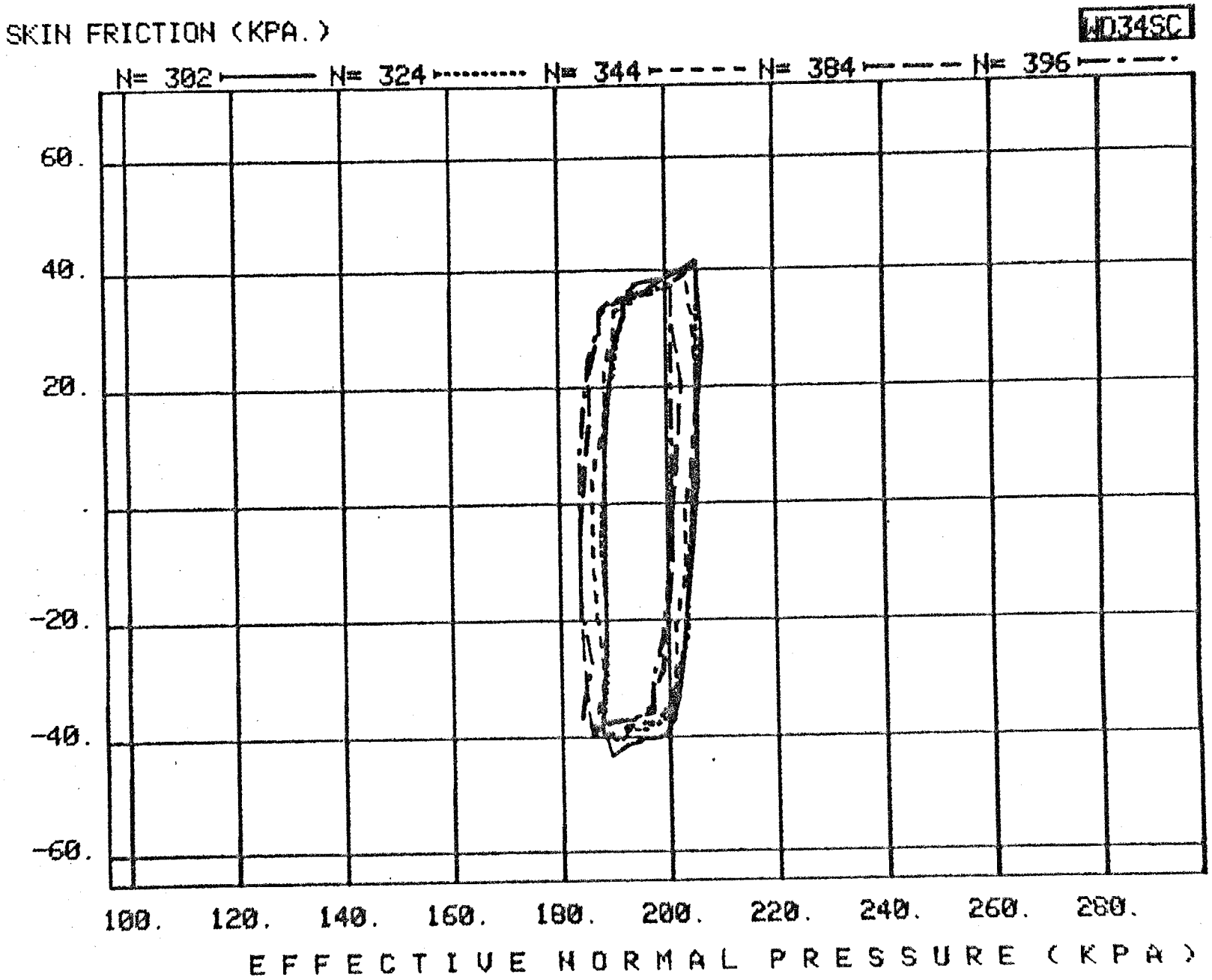
SKIN FRICTION (KPA.)
WD34SC
N= 302
N= 324
N= 344
N= 384
N= 396
60.
40.
20.
-20.
-40.
-60.
100.
120.
140.
160.
180.
200.
220.
240.
260.
280.
EFFECTIVE NORMAL PRESSURE (KPA)

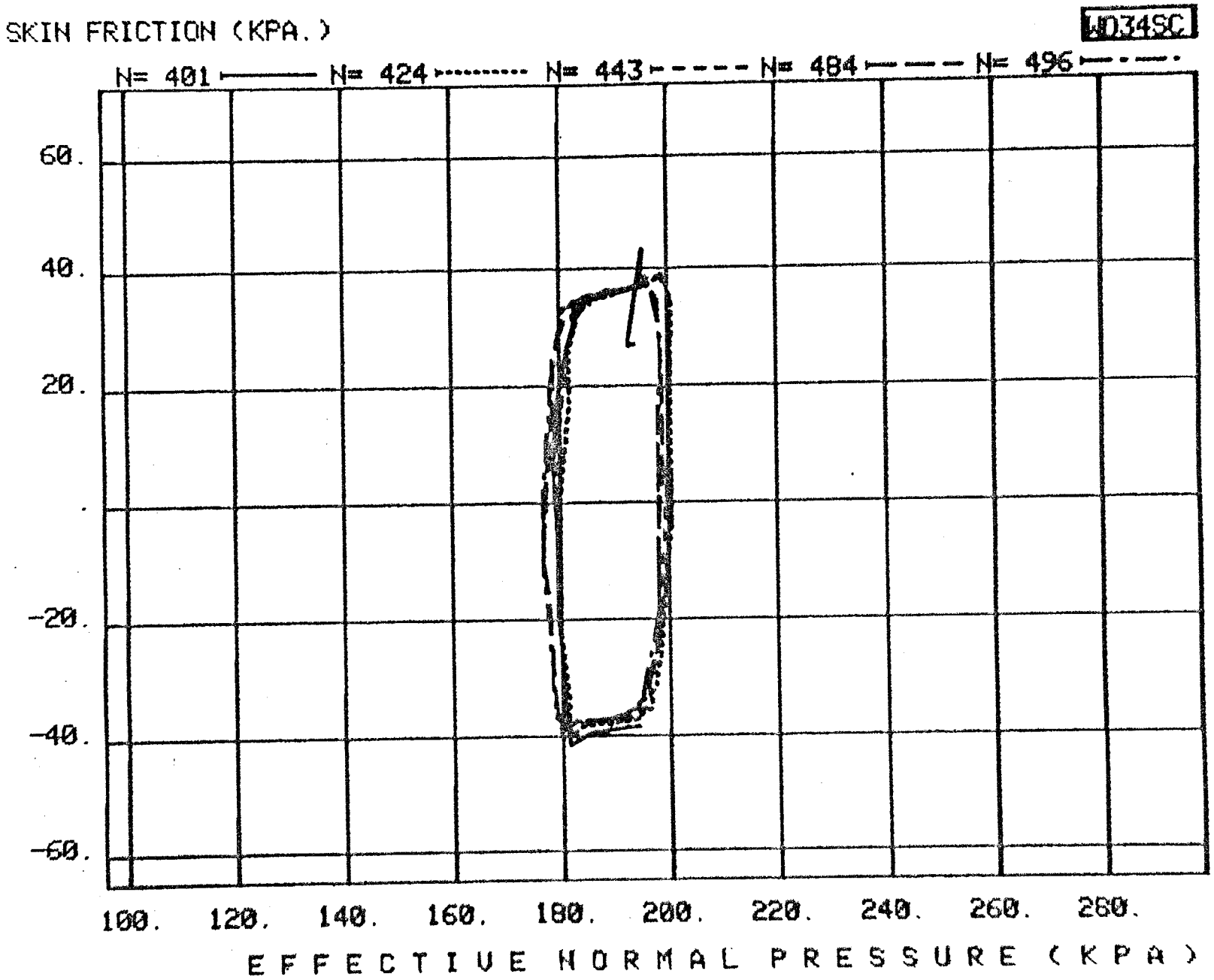
SKIN FRICTION (KPA.)
W034SC
N= 401
N= 424
N= 443
N= 484
N= 496
60.
40.
20.
-20.
-40.
-60.
100.
120.
140.
160.
180.
200.
220.
240.
260.
280.
EFFECTIVE NORMAL PRESSURE (KPA)

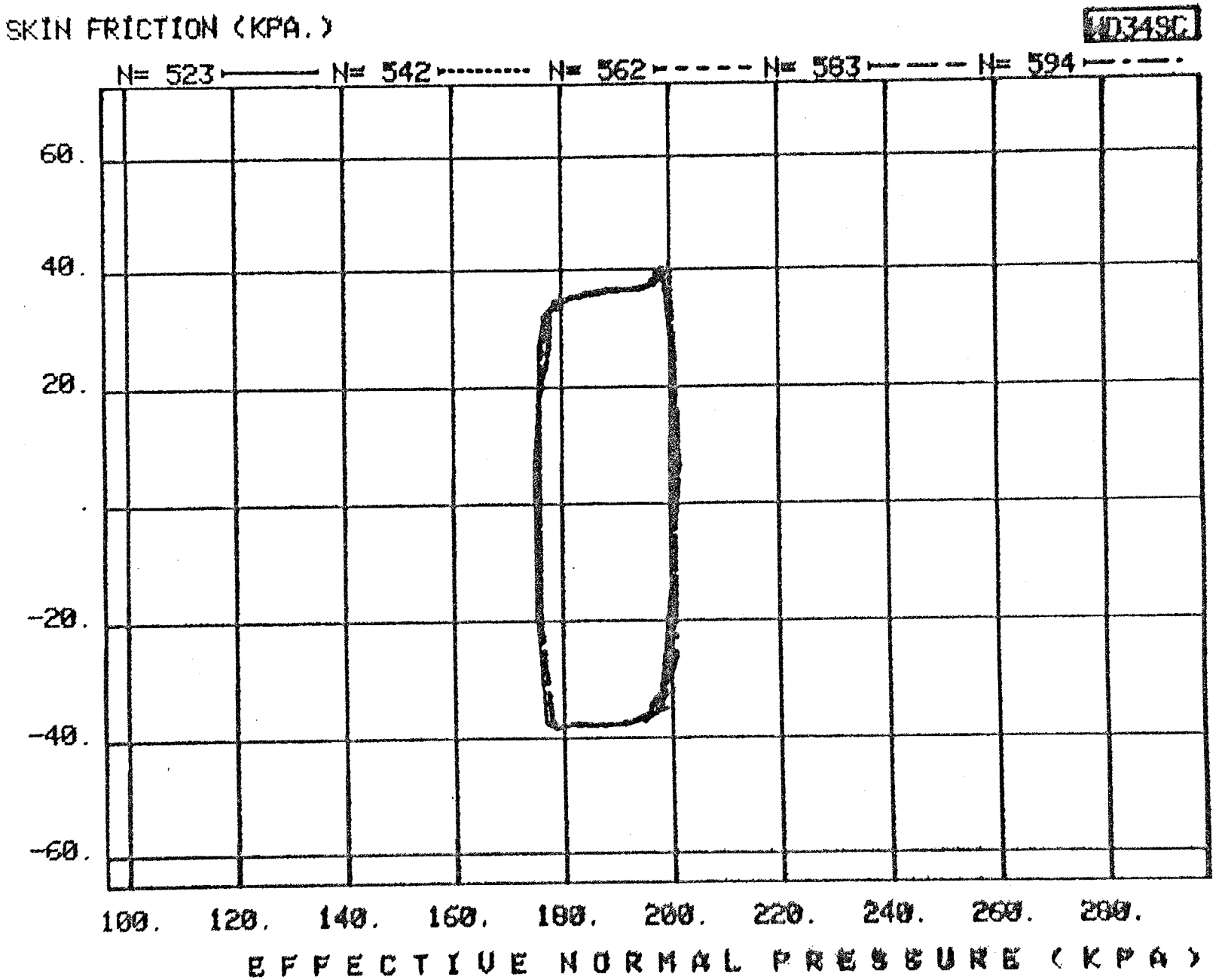
SKIN FRICTION (KPA.)
WD348C
N= 523
N= 542
N= 562
N= 583
N= 594
60.
40.
20.
-20.
-40.
-60.
100.
120.
140.
160.
180.
200.
220.
240.
260.
280.
EFFECTIVE NORMAL PRESSURE (KPA)

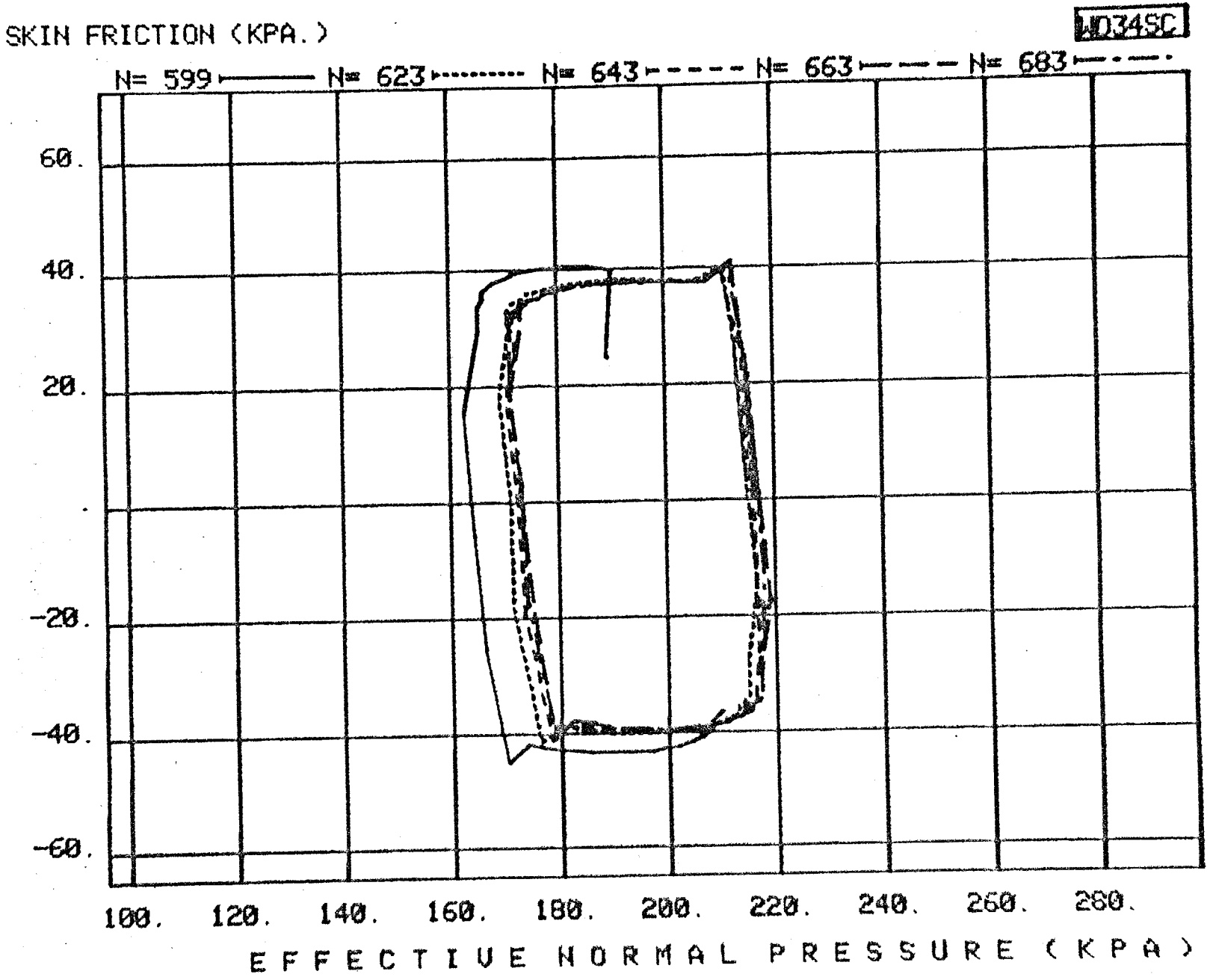
WD34SC
SKIN FRICTION (KPA.)
N= 599
N= 623
N= 643
N= 663
N= 683
60.
40.
20.
-20.
-40.
-60.
100.
120.
140.
160.
180.
200.
220.
240.
260.
280.
EFFECTIVE NORMAL PRESSURE (KPA)

RESPONSE ON CYCLIC LOADING (KPA.) CYCLE NO. 1

WD34SC

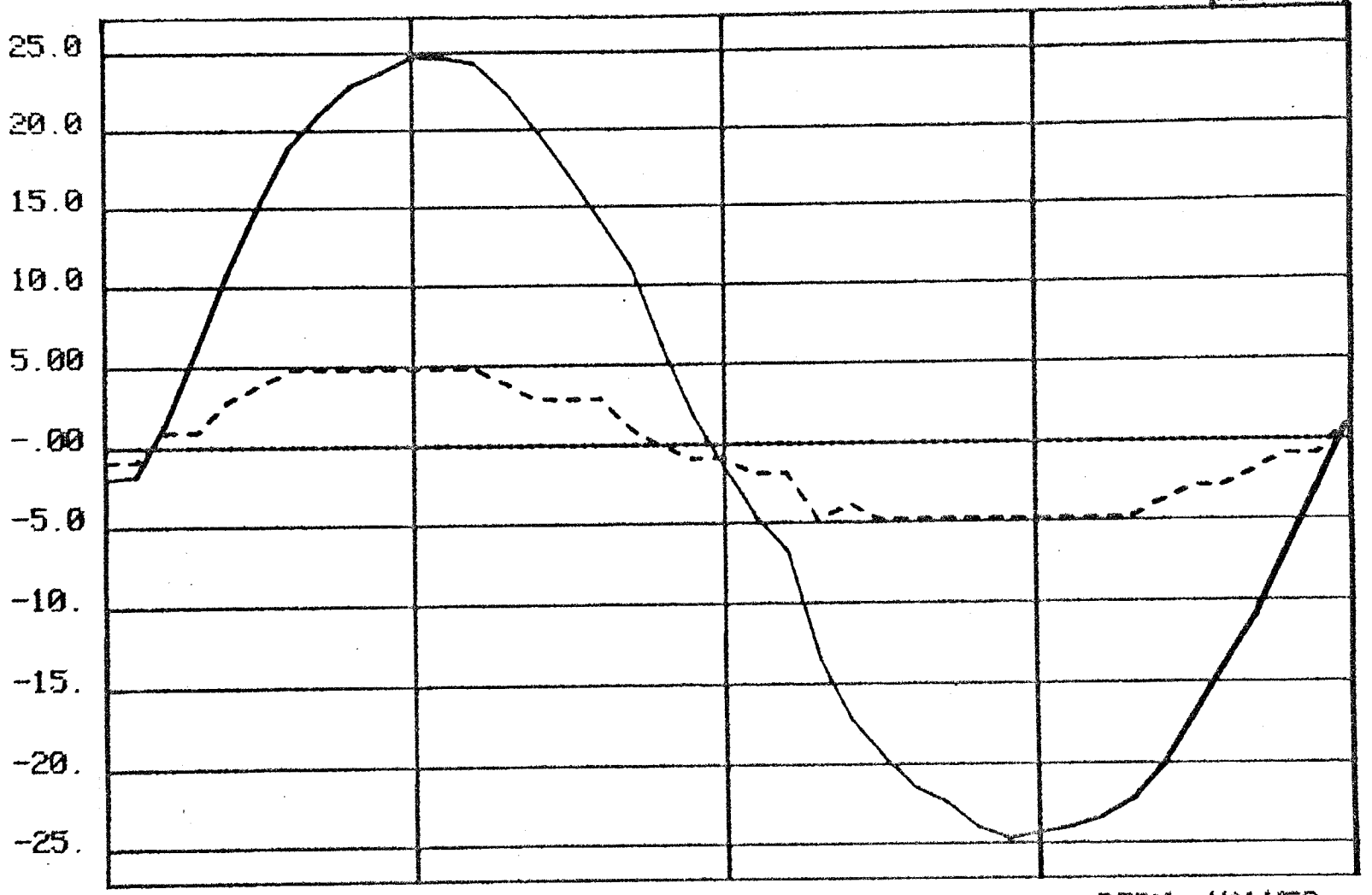

LEGEND:

		PERM. VALUES
———	SKIN FRICTION	-6.18 KPA.
·····	PORE PRESSURE	422.5 KPA.
- - - -	TOTAL NORMAL PRESSURE	625.2 KPA.

RESPONSE ON CYCLIC LOADING (KPA.) CYCLE NO. 98 WD34SC

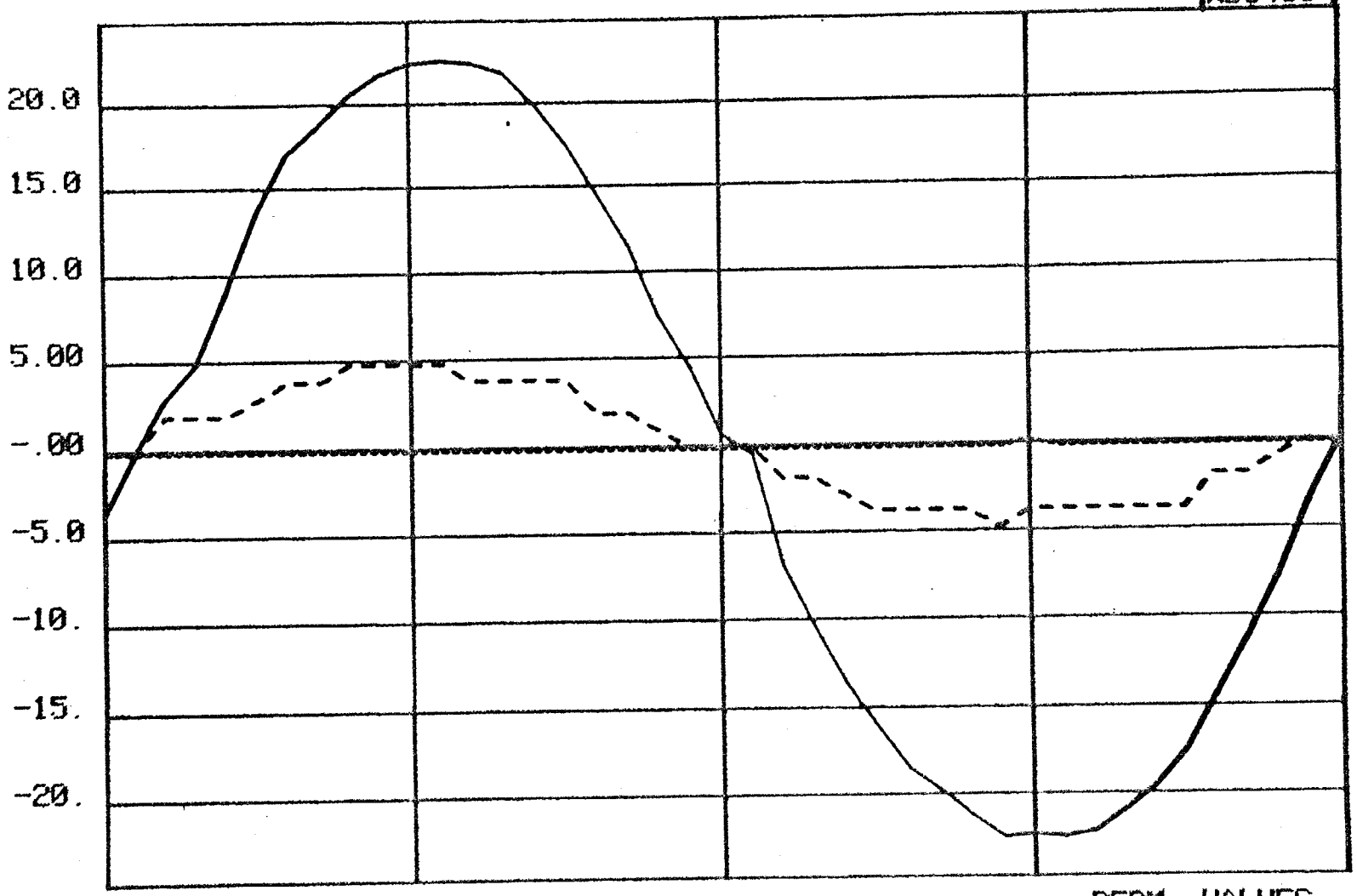

LEGEND:

		PERM. VALUES
————	SKIN FRICTION	-7.91 KPA.
·····	PORE PRESSURE	425.1 KPA.
- - - -	TOTAL NORMAL PRESSURE	626.2 KPA.

RESPONSE ON CYCLIC LOADING (KPA.) CYCLE NO. 201 WD34SC

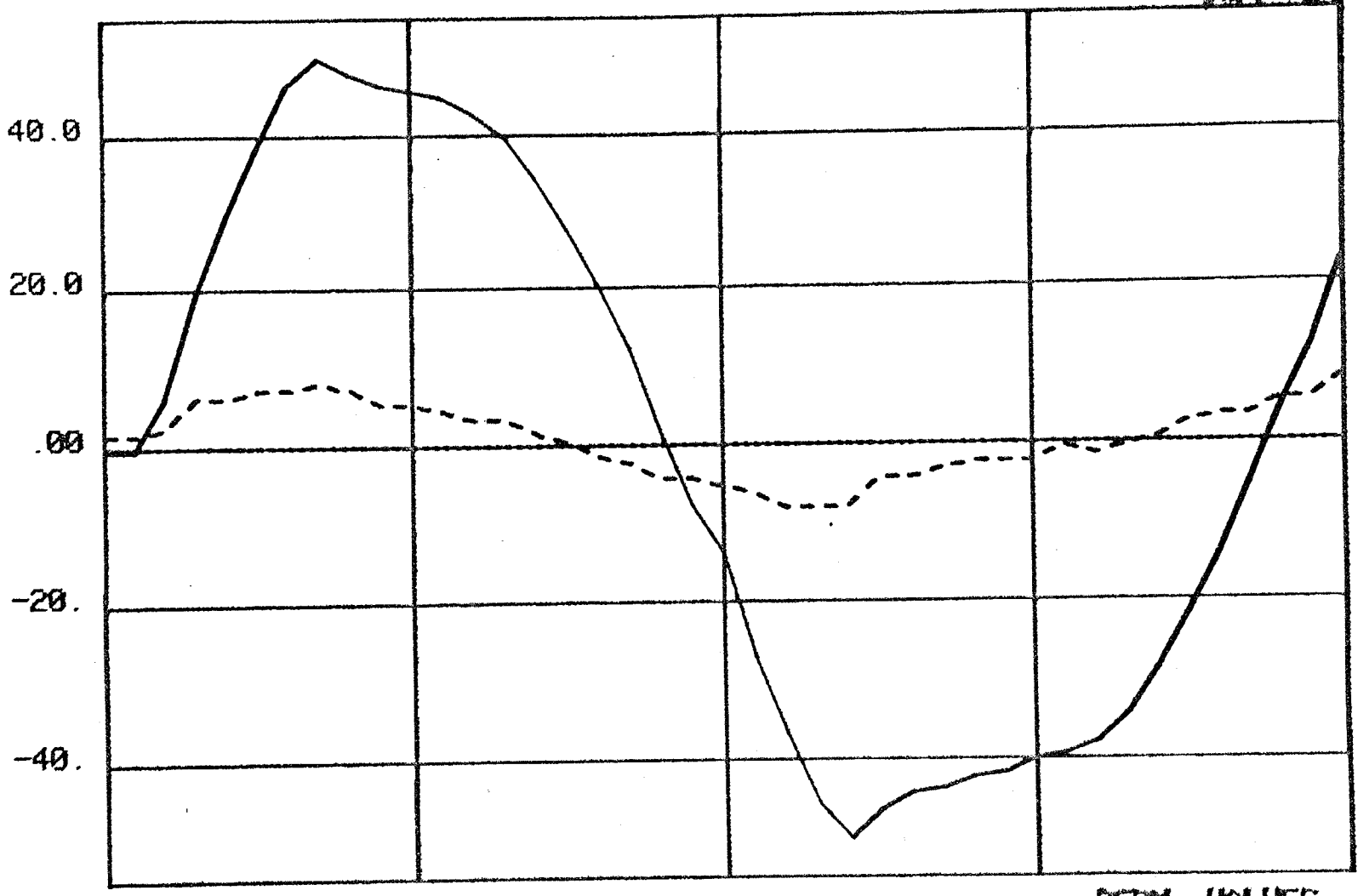

LEGEND:

		PERM. VALUES
———	SKIN FRICTION	-2.93 KPA.
.....	PORE PRESSURE	426.3 KPA.
- - - - -	TOTAL NORMAL PRESSURE	626.6 KPA.

RESPONSE ON CYCLIC LOADING (KPA.)

CYCLE NO. 297

WD34SC

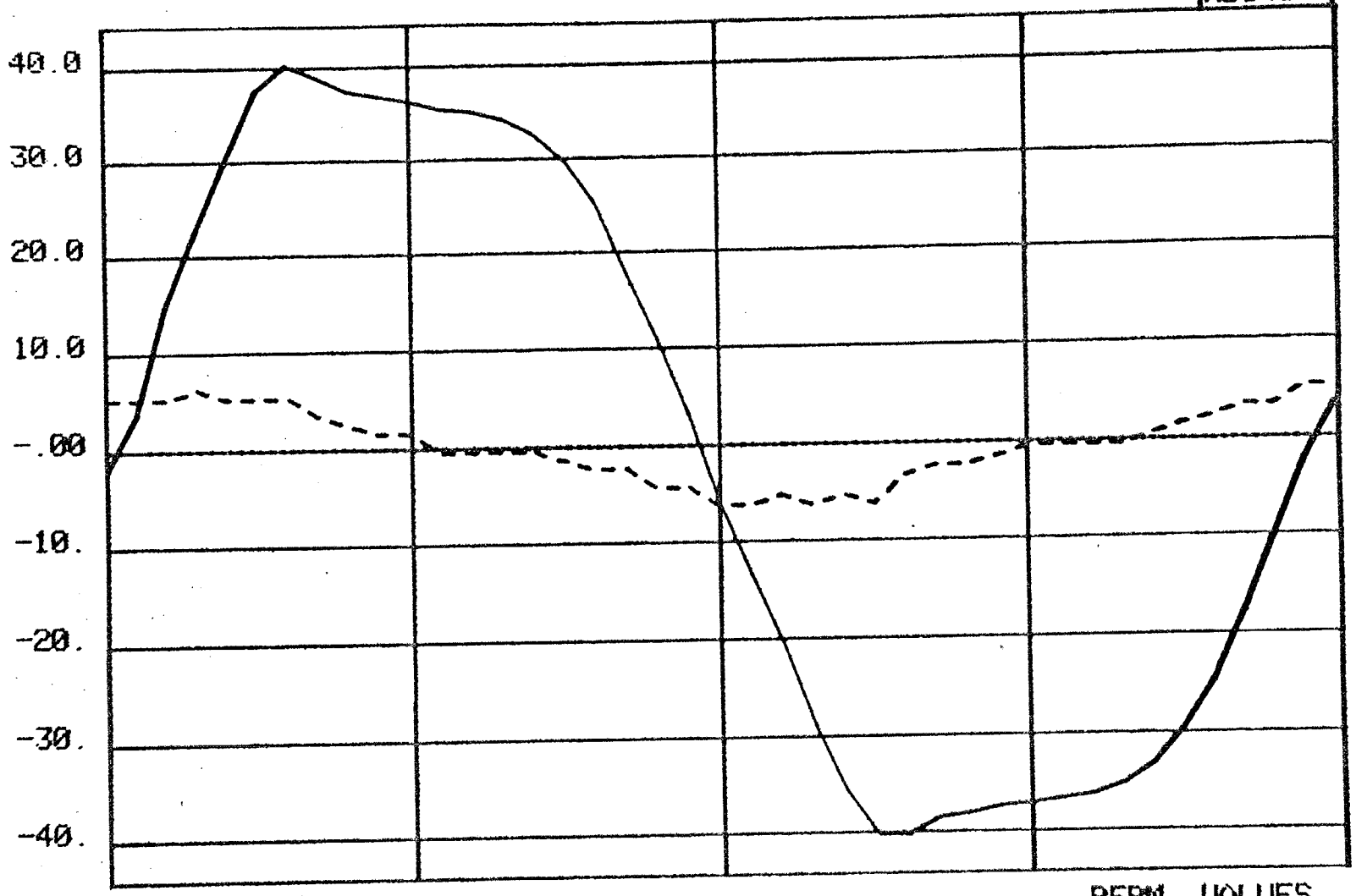

LEGEND:

SKIN FRICTION

PORE PRESSURE

TOTAL NORMAL PRESSURE

PERM. VALUES

-.15 KPA.

428.2 KPA.

626.6 KPA.

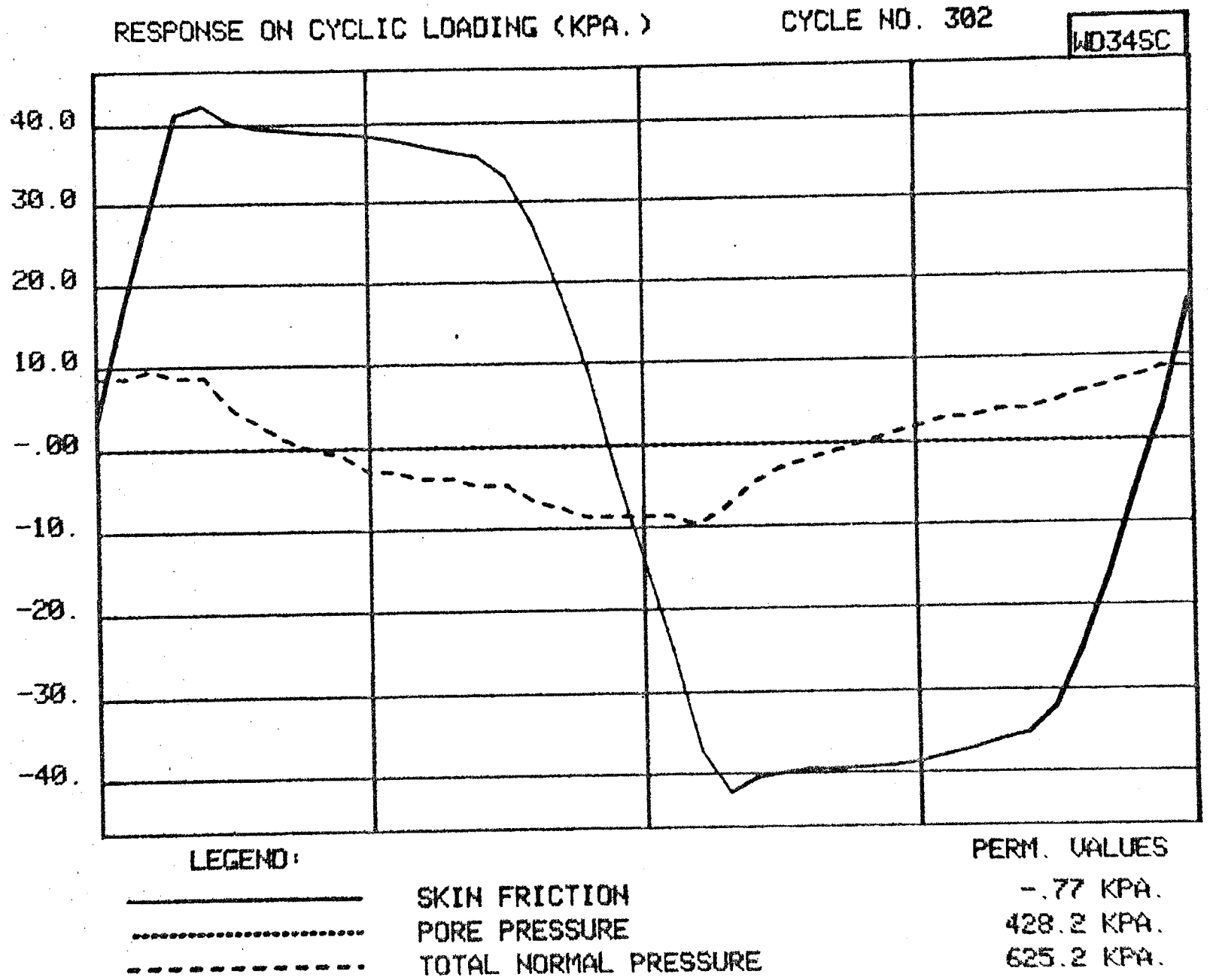
RESPONSE ON CYCLIC LOADING (KPA.)
CYCLE NO. 302
WD345C
40.0
30.0
20.0
10.0
-.00
-10.
-20.
-30.
-40.
LEGEND:
SKIN FRICTION
PORE PRESSURE
TOTAL NORMAL PRESSURE
PERM. VALUES
-.77 KPA.
428.2 KPA.
625.2 KPA.

RESPONSE ON CYCLIC LOADING (KPA.)

CYCLE NO. 396

WD345C

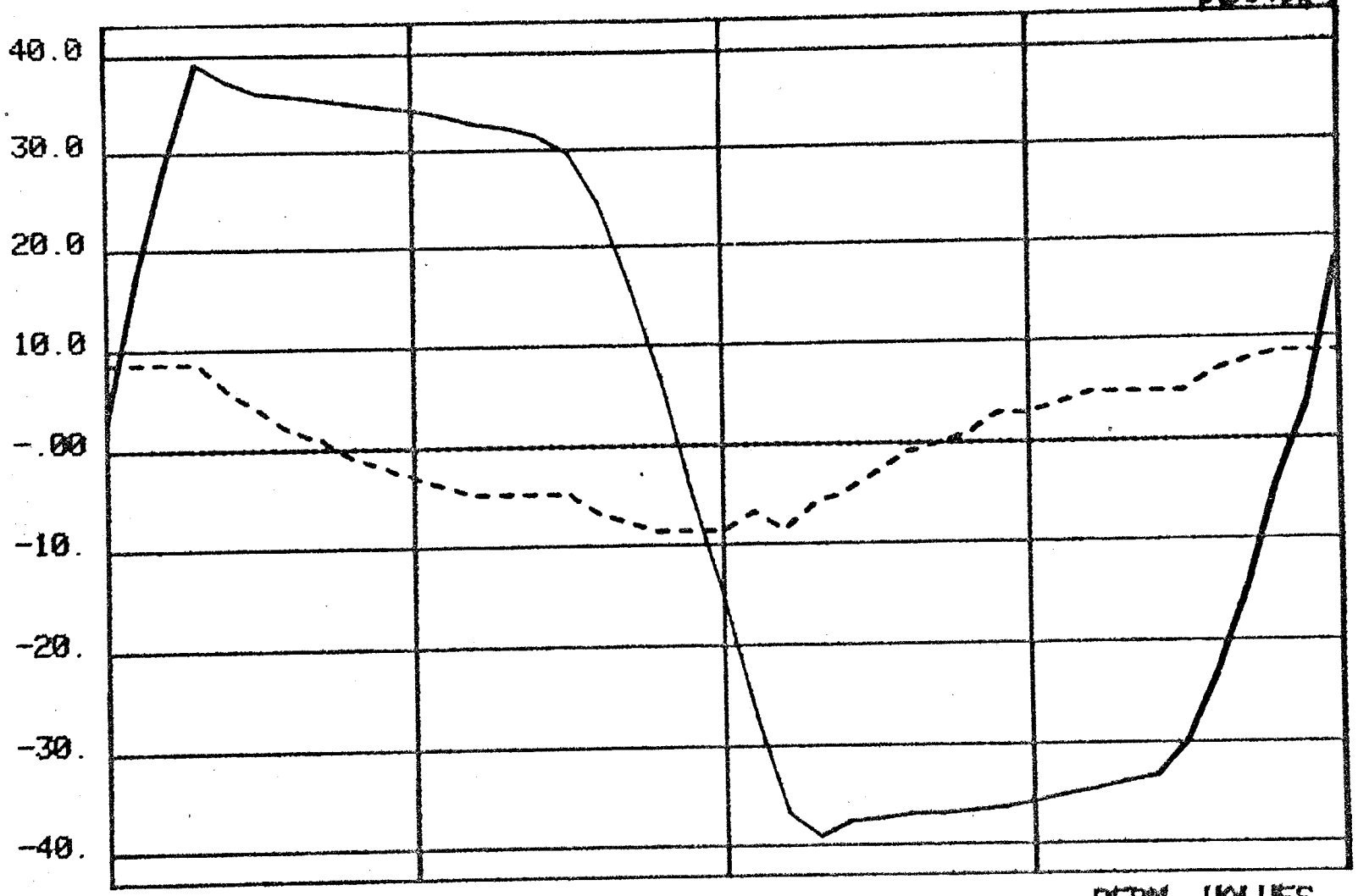

LEGEND:

SKIN FRICTION

PORE PRESSURE

TOTAL NORMAL PRESSURE

PERM. VALUES

.14 KPA.

429.2 KPA.

621.4 KPA.

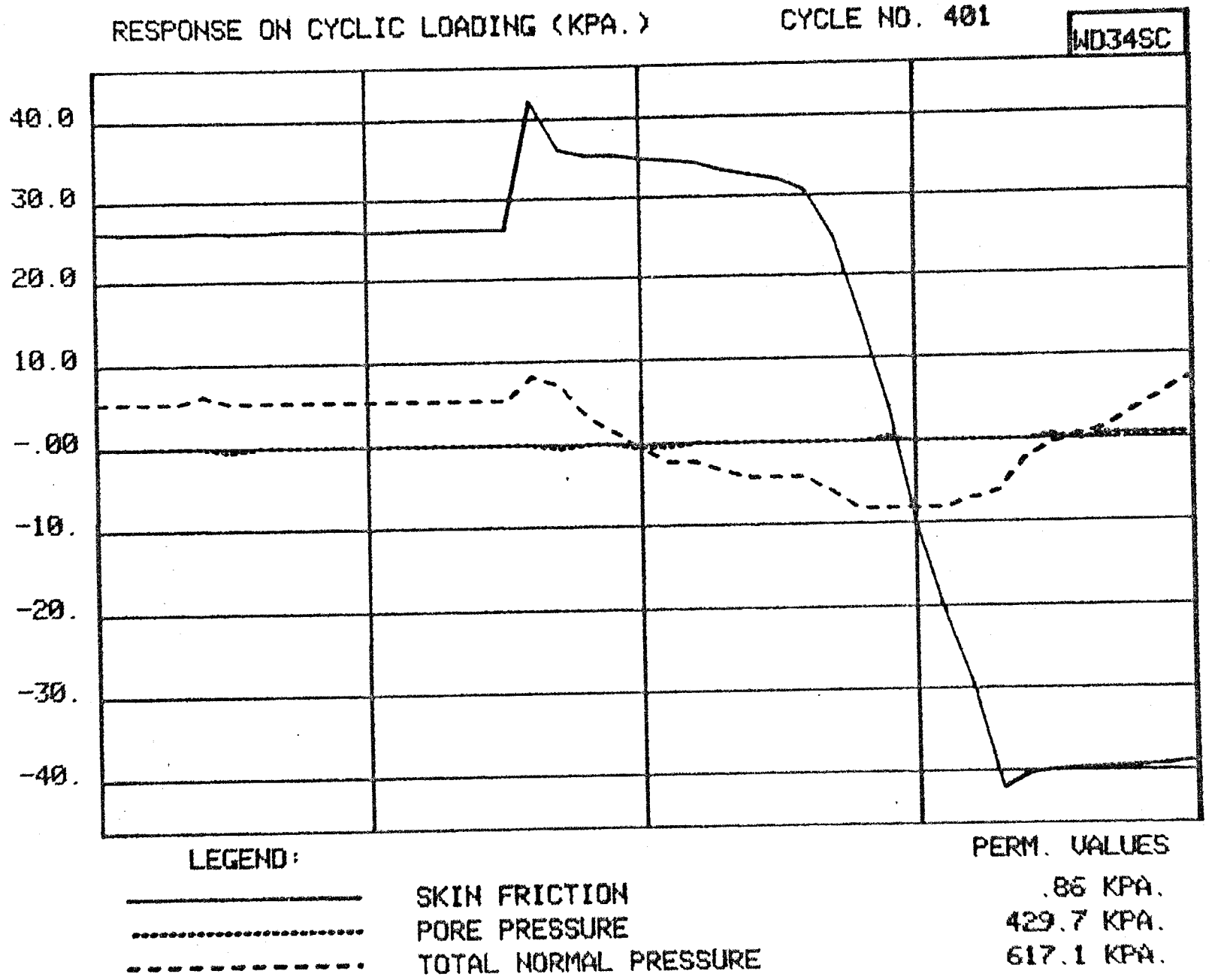
RESPONSE ON CYCLIC LOADING (KPA.)
CYCLE NO. 401
WD34SC
40.0
30.0
20.0
10.0
-.00
-10.
-20.
-30.
-40.
LEGEND:
SKIN FRICTION
PORE PRESSURE
TOTAL NORMAL PRESSURE
PERM. VALUES
.86 KPA.
429.7 KPA.
617.1 KPA.

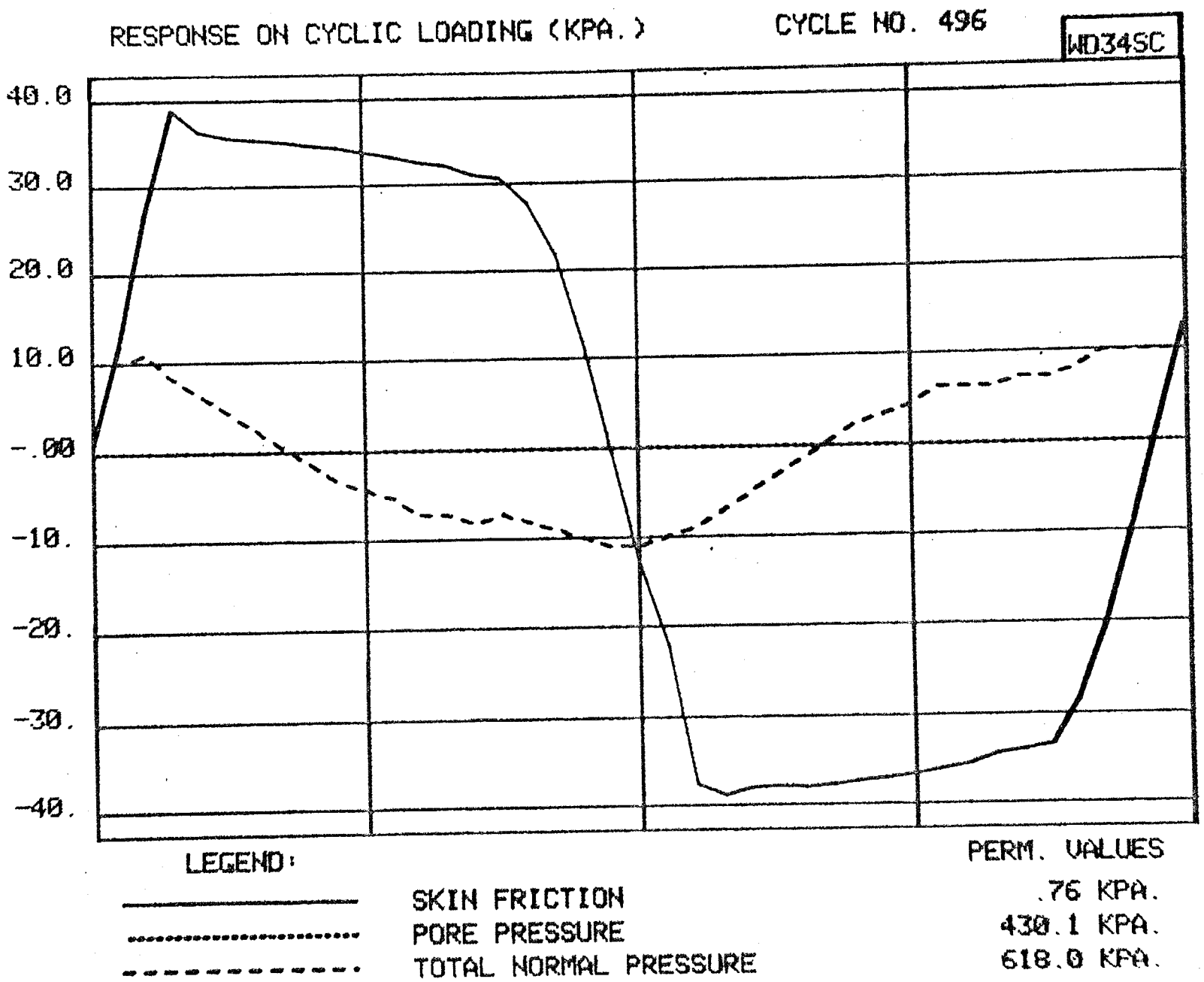
RESPONSE ON CYCLIC LOADING (KPA.)
CYCLE NO. 496
WD34SC
40.0
30.0
20.0
10.0
-.00
-10.
-20.
-30.
-40.
LEGEND:
SKIN FRICTION
PORE PRESSURE
TOTAL NORMAL PRESSURE
PERM. VALUES
.76 KPA.
430.1 KPA.
618.0 KPA.

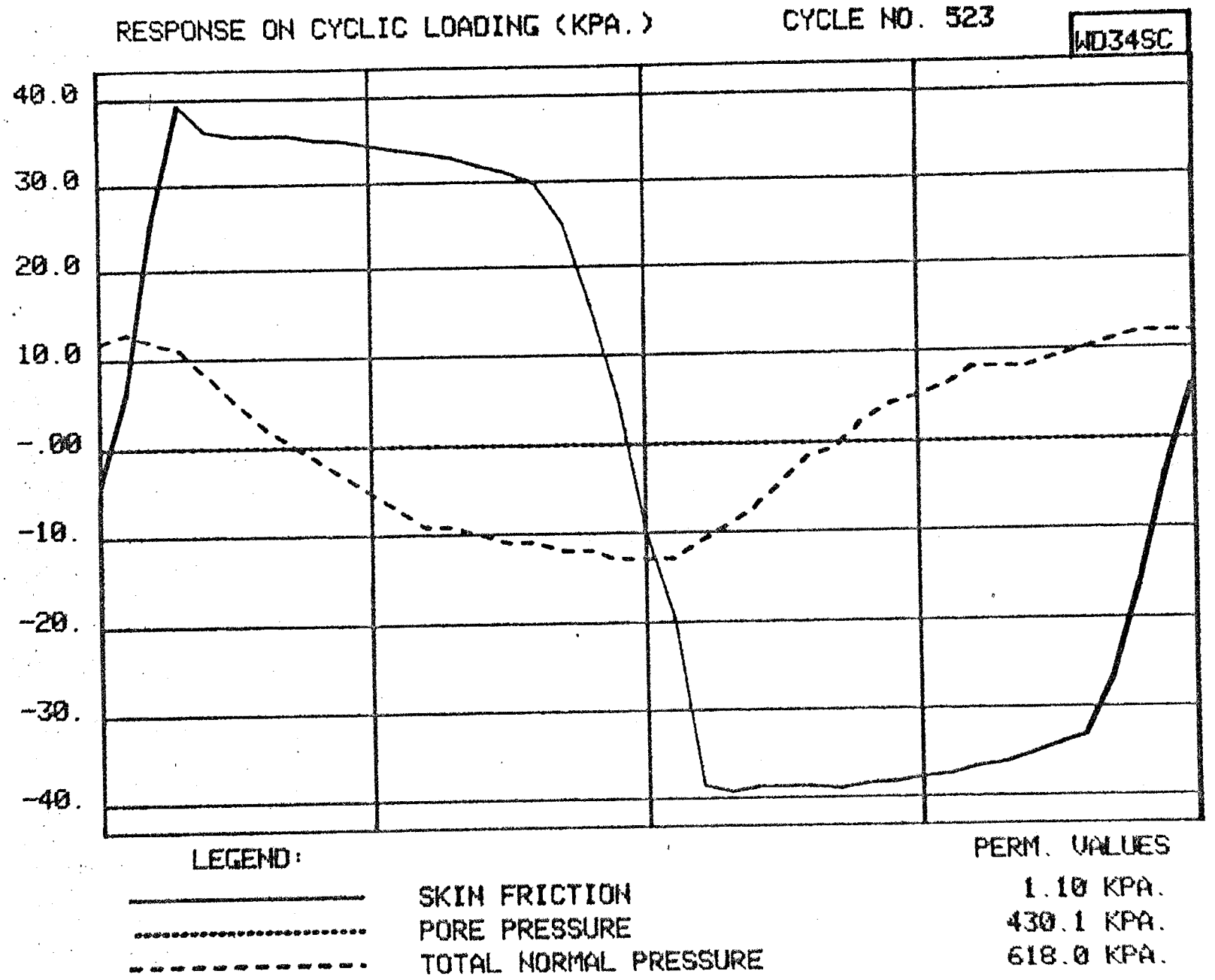
RESPONSE ON CYCLIC LOADING (KPA.)
CYCLE NO. 523
WD34SC
40.0
30.0
20.0
10.0
-.00
-10.
-20.
-30.
-40.
LEGEND:
SKIN FRICTION
PORE PRESSURE
TOTAL NORMAL PRESSURE
PERM. VALUES
1.10 KPA.
430.1 KPA.
618.0 KPA.

RESPONSE ON CYCLIC LOADING (KPA.)

CYCLE NO. 594

WD34SC

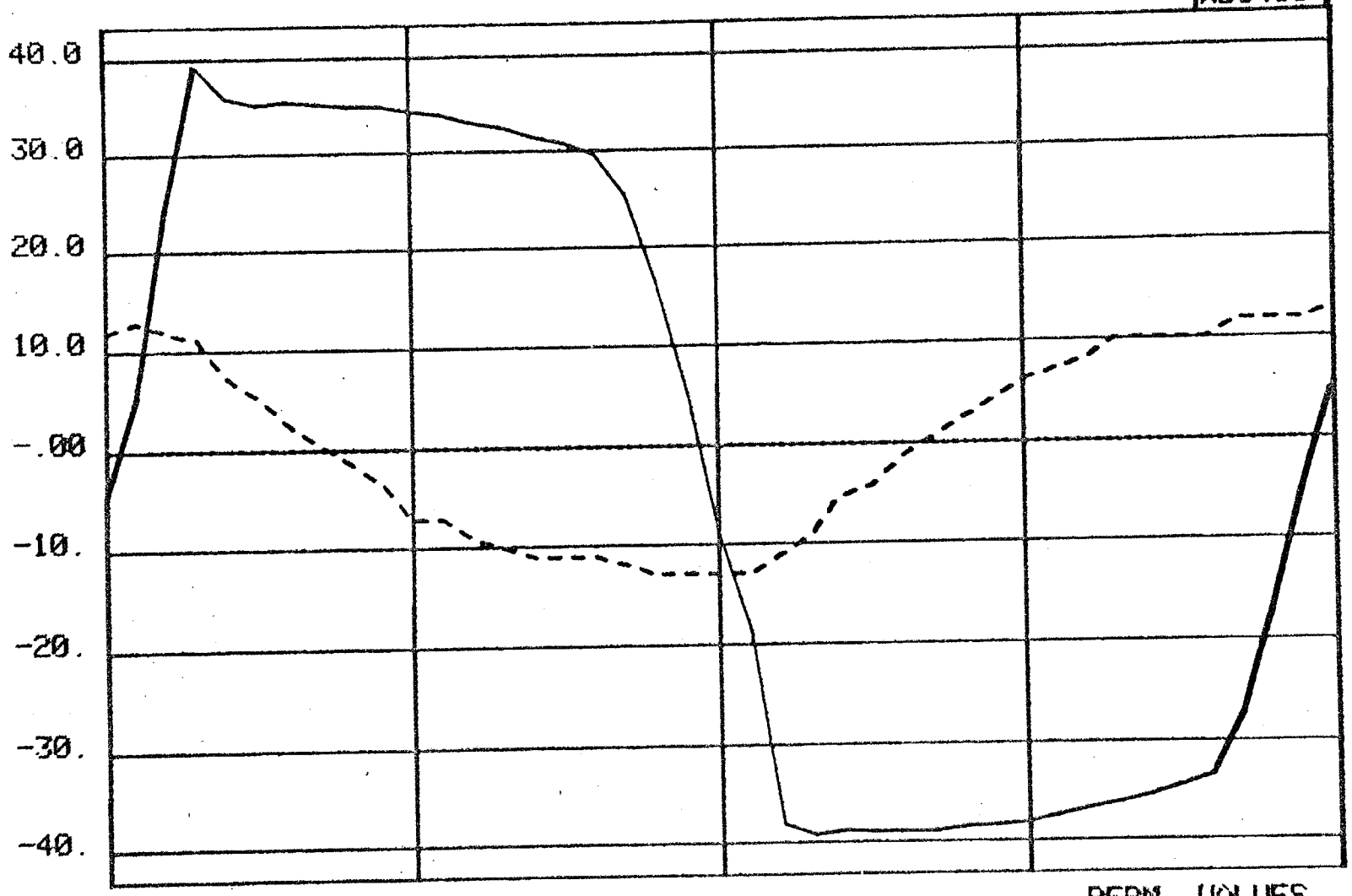

LEGEND:

		PERM. VALUES
———	SKIN FRICTION	1.24 KPA.
·····	PORE PRESSURE	429.2 KPA.
- - - -	TOTAL NORMAL PRESSURE	618.0 KPA.

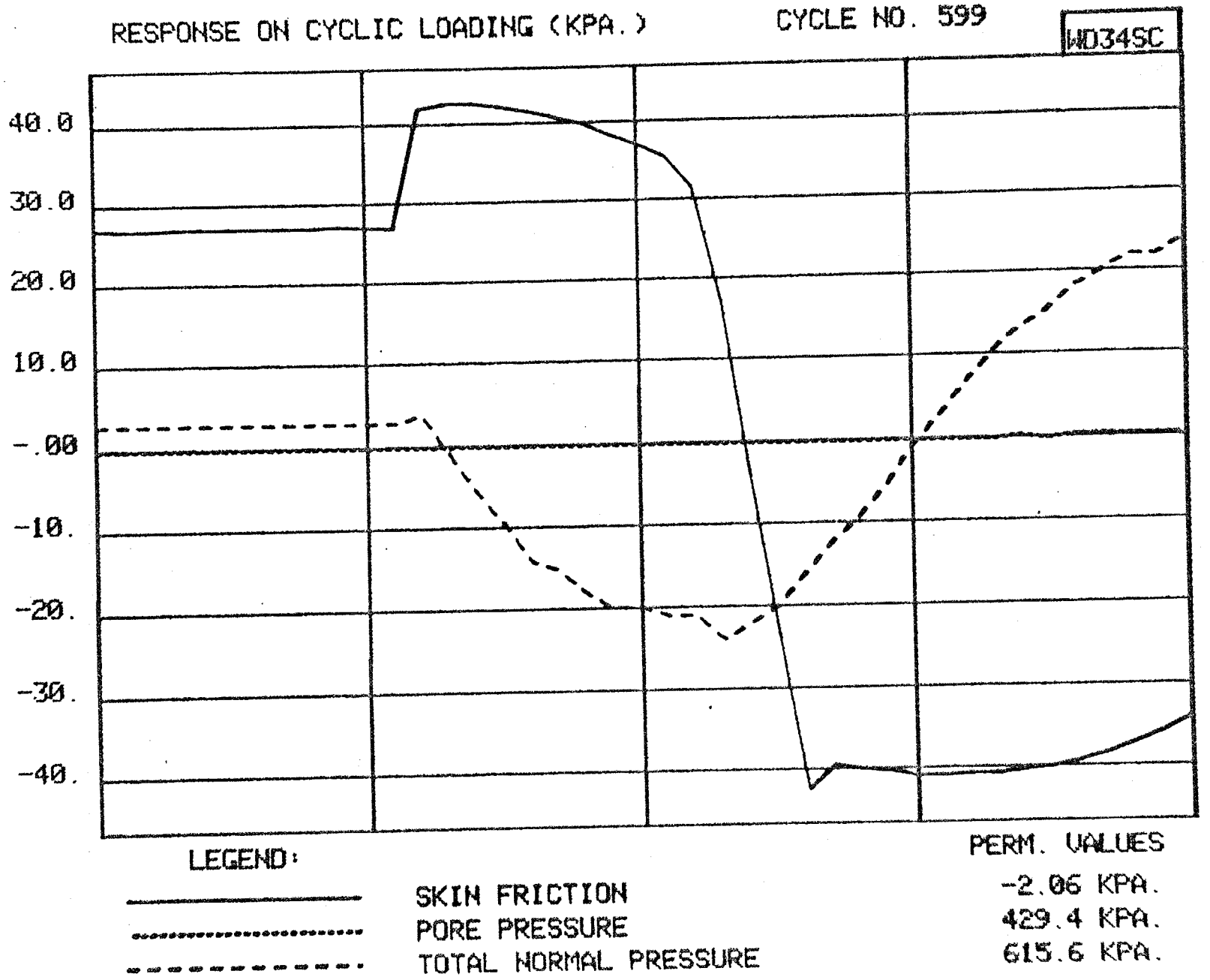
RESPONSE ON CYCLIC LOADING (KPA.)
CYCLE NO. 599
WD34SC
40.0
30.0
20.0
10.0
-.00
-10.
-20.
-30.
-40.
LEGEND:
SKIN FRICTION
PORE PRESSURE
TOTAL NORMAL PRESSURE
PERM. VALUES
-2.06 KPA.
429.4 KPA.
615.6 KPA.

RESPONSE ON CYCLIC LOADING (KPA.) CYCLE NO. 683

WD34SC

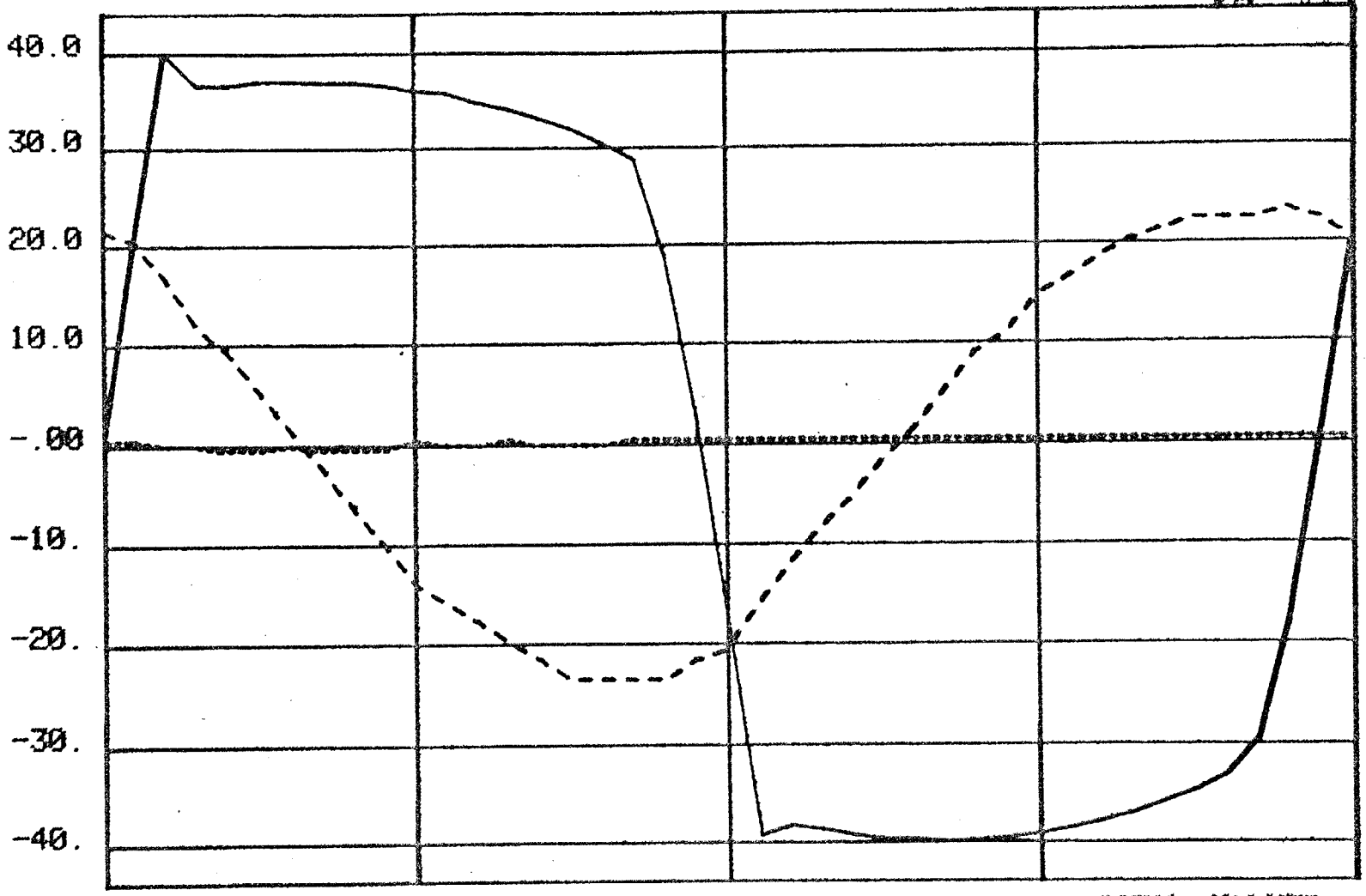

LEGEND:

		PERM. VALUES
———	SKIN FRICTION	.67 KPA.
·····	PORE PRESSURE	423.9 KPA.
- - - -	TOTAL NORMAL PRESSURE	619.0 KPA.

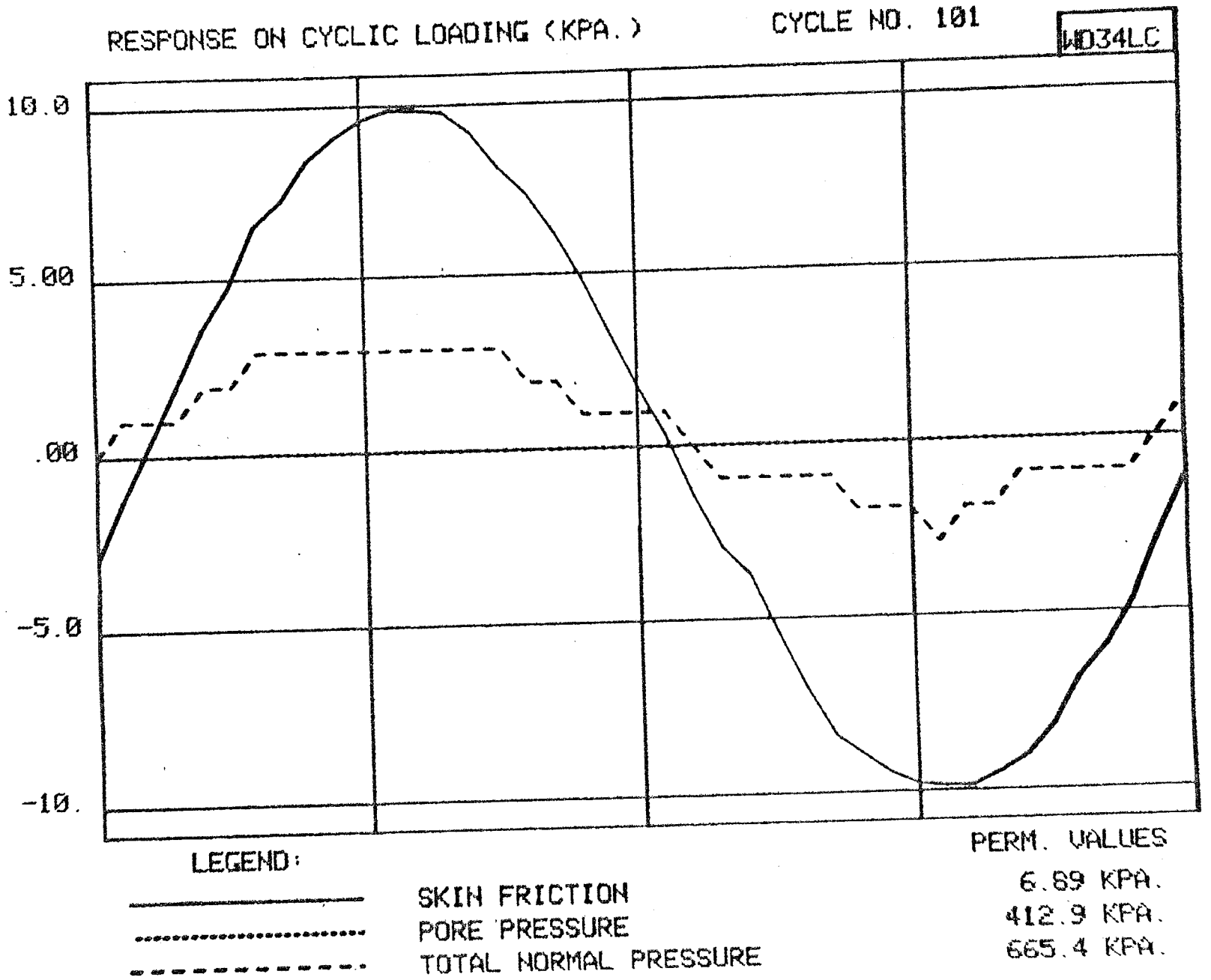
RESPONSE ON CYCLIC LOADING (KPA.)
CYCLE NO. 101
WD34LC
10.0
5.00
.00
-5.0
-10.
LEGEND:
SKIN FRICTION
PORE PRESSURE
TOTAL NORMAL PRESSURE
PERM. VALUES
6.89 KPA.
412.9 KPA.
665.4 KPA.

APPENDIX B

DETAILED RESULTS FROM **TEST 5, STRATUM II** MODEL PILE TESTS

CONTENTS

Summary	B3
Test 5, Stratum II	B4
Consolidation	B4
Pile Instatllation and Set-Up	B4
Static Test	B5
Relaxation Test	B5
Cyclic Tests	B6
Stress Controlled Tests (WD25LC)	B6
Displacement Controlled Tests (WD254SC)	B7
Strength Tests	B8

LIST OF FIGURES

Figure 1 Sample Properties
Figure 2 Consolidation Diagram
Figure 3 Pocket Penetrometer Tests After Consolidation
Figure 4 Pressures at Pile Wall after Installation
Figure 5 Static Test
Figure 6 Relaxation Test
Figure 7 Skin Friction vs no. of Cycles, WD25LC
Figure 8 Deflection vs no. of Cycles, WD25LC
Figure 9 Total Normal Pressure vs no. of Cycles, WD25LC
Figure 10 Pore Pressure vs no. of Cycles, WD25LC
Figure 11 Eff. Normal Pressure vs no. of Cycles, WD25LC
Figure 12 Deflection vs no. of Cycles, WD25SC

Figure 13 Skin Friction vs no. of Cycles, WD25SC
Figure 14 Pore Pressure vs no. of Cycles, WD25SC
Figure 15 Total Normal Pressure vs no. of Cycles, WD25SC
Figure 16 Eff. Normal Pressure vs no. of Cycles, WD25SC
Figure 17 Pocket Penetrometer Tests after Pile Test
Figure 18 Unconfined Compression Tests
Figure 19 Water Content and Shear Strength

Appendix BA
Plotted Results from WD25LC
Figures BA-1 through BA-9
Skin Friction vs Deflection, Selected Cycles
Figures BA-10 through BA-13
Skin Friction vs Eff. Normal Pressure, Selected Cycl.
Figures BA-14 through BA-29
Skin Friction, Pore and Total Pressure, Selected Cycles

Appendix BB
Plotted Results from WD25SC
Figures BB-1 through BB-7
Skin Friction vs Deflection, Selected Cycles
Figures BB-8 through BB-11
Skin Friction vs Eff. Normal Pressure, Selected Cycl.
Figures BB-12 through B-25
Skin Friction, Pore and Total Pressure, Selected Cycles

SUMMARY

This report contains the results of the laboratory model pile tests designated TEST 5, STRATUM II, in the project CNRD 13-2, TENSION PILE STUDY, for Conoco Norway Inc.

The clay sample was consolidated for 14 days under 300 kPa applied vertical pressure. Pore pressure in the sample was about 10% of the applied pressure. After 6 days of consolidation in the pile chamber the pile was installed. After 11 days of consolidation (set-up) the excess pore pressure was still about 150 kPa. Testing was then started.

Static test gave peak friction of 33 kPa with residual value of 30 kPa. Undrained shear strength was interpreted to 50 kPa, giving alpha value (α) of 0.66 and 0.6 for peak and residual respectively. Estimating the effective vertical pressure to 210 kPa results in a beta factor (β) of 0.16 and 0.14 for peak and residual respectively.

A relaxation test from peak friction resulted in a friction loss from 32 kPa down to 16 kPa in 16 hours.

Cyclic tests were performed immediately following the relaxation test. Stress controlled tests with static tension bias of 14.5 kPa (44% of previous max.friction) with parcels of 100 cycles with specified cyclic stress amplitude increasing for consecutive parcels resulted in failure (abrupt pull-out of pile) in eighth parcel. The cyclic stress level was 24 kPa giving a maximum friction of about 38 kPa.

Subsequently a displacement controlled test with two-way cyclic loading was performed. Seven parcels of 100 cycles with increasing cyclic displacements were made. Maximum friction obtained was 34 kPa which reduced to 30 kPa in subsequent parcels. The residual friction during large slip was 26 kPa.

TEST 5, STRATUM II

CONSOLIDATION

The sample was prepared from cylinder numbers S-50, S-55, S-57, S-59, S-20, S-73, S-32, S-78, S-80 and S-82, all from Stratum II, from the site investigation performed by McClelland Engineers in November 1981.

After remoulding the clay was filled into the consolidometer with a vertical pressure of 300 kPa applied on top. The sample was divided into four layers in the consolidometer with intermediate filters to provide better vertical drainage conditions.

As seen in Figure 2 the pore pressure at middle height had dropped to 10% of the consolidation stress after 14 days of consolidation. At this time the sample was transferred to the pile chamber. Pocket penetrometer tests on the side of the sample and at the top of the sample when trimmed in the pile chamber were performed, with results shown in Figure 3. The shear strength, s_u, showed an average of about 50 kPa.

PILE INSTALLATION AND SET-UP

After extrusion from the consolidometer and pocket penetrometer tests the sample was mounted in the pile chamber and left to reconsolidate for six days under a vertical pressure of 300 kPa and radial pressure of 210 kPa, (K = 0.7). In addition a back pressure of 300 kPa was applied to help speed up the pore pressure response.

During insertion of the pile the side friction showed a maximum of about 19 kPa. Total normal pressure showed 565 kPa and the pore pressure only showed 335 kPa directly after installation as shown in Figure 4. After one day of set up the total pressure was unchanged whereas the pore pressure had increased to a maximum of 465 kPa. Ten additional days of consolidation made the pore pressure drop down again to 445 kPa and the total pressure showed 625 kPa. At this time it was decided to start with the loading program, even though the excess pore pressure was about 150 kPa (above the back pressure).

STATIC TEST

A displacement controlled static test with deformation rate 1 mm per hour was now conducted, as shown in Figure 5. The pile was pulled in tension through failure and large slip and then pushed down to original position causing failure and large slip (residual friction) in compression.

The displacement to cause failure, as shown in Figure 5, was about 0.3 mm corresponding to 1.2% of the pile diameter. A maximum friction of 33 kPa was achieved, with a residual value of 30 kPa. This results in an (α) value of 0.66 and 0.6 for peak and residual respectively, with an interpreted shear strength of 50 kPa.

For the effective stress approach where the side friction, f, is estimated from the effective vertical soil pressure ,σ'_{vo}, prior to pile installation ($f = \beta \cdot \sigma'_{vo}$ the corresponding beta factor (β) is dependent on σ'_{vo}.

From the soil characterization of samples from the West Delta site a relationship between undrained shear strength and effective vertical stress for Stratum II is suggested to:

$$s_u = 0.24 \cdot \sigma'_{vo}$$

With an undrained shear strength of 50 kPa the effective vertical pressure is estimated to 210 kPa. This gives a beta factor (β) of 0.16 and 0.14 for maximum and residual friction respectively.

The total pressure at failure (maximum friction) was about 610 kPa and the pore pressure showed 445 kPa, resulting in a horizontal effective pressure of 165 kPa. The interface friction angle (δ) can then be estimated from

$$f_{max} = \sigma'_n \cdot \tan \delta$$

giving δ = 11.3 degrees.

RELAXATION TEST

After the pile was brought back to the original zero position in the static test the pile was again loaded in tension up to the point of failure. At this time the deformation

was held constant and the mobilized friction and pressures at the pile wall was monitored for a period of 16 hours. The friction versus time is shown in Figure 5 in both linear and log scale showing a quite fast drop during the first hour. After 16 hours the side friction had dropped to about 16 kPa which is a reduction of 50% from the peak friction. The pore pressure on the pile wall was constant throughout the test and the total pressure only showed a slight decrease.

No relaxation tests were performed with the initial friction lower than the peak friction for this sample.

CYCLIC TESTS

After the relaxation test the pile was brought back to original position. It was decided to proceed with cyclic testing of the pile with no further time allowed for consolidation.

Stress Controlled Tests (WD25LC)

A stress controlled test comprised of applying a prescribed static tensile (uplift) stress on the pile, superimposed with parcels of 100 cycles with 10 seconds period and prescribed cyclic stress amplitude. The stress amplitude was then increased in the following parcels until failure (excessive uplift) occured in tension

For this test the static tensile stress level was about 14.5 kPa, corresponding to 44% of the previous maximum static capacity. In the first parcel the cyclic level was about 3 kPa and for the following parcels the cyclic level was incremented by 3 kPa as seen in Figure 7, showing skin friction (envelope of max. and min.) versus number of cycles. In the following four figures the resulting deformations and pressures due to the applied skin friction are plotted versus cycle numbers. In Appendix A selected cycle numbers are plotted as friction versus deflection, friction versus effective pressure and friction, pore pressure and total pressure variation during one cycle.

As can be seen from the friction versus deformation curves in figures A-1 through A-9 in Appendix A, the response is linearly elastic for at least the five first parcels. In parcel six (cycle numbers 501 etc) a small hysteresis is being developed and the

deformation is seen to slightly increase. Increasing the cyclic stress to 21 kPa (giving maximum applied friction of about 35 kPa), the hysteresis is seen to increase and the pile is very slowly pulled up for each cycle. This is shown in a blown up scale in Figure A-8, where it is seen that the pile does not experience an abrupt pull-out but is capable of mobilizing the prescribed friction. In the last parcel, however, with a prescribed cyclic stress of 24 kPa (max. friction of 38 kPa) the hysteresis is significant for the two first cycles and the pile is pulled up for each cycle to mobilize the prescribed friction. Finally in cycle 735 an abrupt pullout is seen.

From the pressure diagrams in Figures 9 and 10 it is seen that the pressures at the pile wall stays fairly constant throughout the tests with only minor cyclic variations in total normal pressure, increasing with cyclic stress level to a maximum variation of about 4 kPa during the last parcel. The pore pressure shows a slight decrease during the first four parcels of about 10 kPa resulting in a slight increase in effective pressure stabilizing at about 140 kPa as seen in Figure 11.

Displacement Controlled Tests (WD25SC)

After failure in the stress controlled test the pile was brought back to original position and left to reconsolidate for a period of one hour before displacement (stroke) controlled tests were performed.

One parcel here consisted of one hundred cycles with 10 seconds period in two-way cyclic loading from the zero position of the pile.

A total of seven consecutive parcels were performed with increasing displacement amplitude, starting with 0.1 mm in the first parcel and with 0.2, 0.4, 0.6, 0.8, 1.0 and 2.0 mm in the following parcels.

The applied displacement versus cycles numbers are shown in Figure 12 with the resulting skin friction, pore pressure, total pressure and effective pressure versus cycle numbers shown in Figures 13, 14, 15 and 16 respectively. More detailed plots of selected cycles are shown in Appendix B.

As can be seen from the resulting skin friction in Figure 13 the two way cycling of 0.1 mm amplitude does not cause failure of the pile which is also seen in Figure B-1

showing a linear response in the friction-displacement curves. Increasing the displacement amplitude to 0.2 mm yields a maximum friction in the first cycles of about 32 kPa which during subsequent cycles reduces to about 30 kPa. This can also be seen in Figure B-2 which also shows the pile does not reach plastic slip down to full residual value in friction.

In the subsequent parcel with displacement amplitude of 0.4 mm a maximum friction in the first cycle of 34 kPa is measured. In the following cycles the maximum friction reduces to 30 kPa with a residual value during large slip of 26 kPa.

Increasing the displacement amplitude in the following parcels leads to a further degradation of the maximum peak friction, whereas the residual friction during large slip seems to stabilize at about 25 kPa as seen in Figures B-4 through B-7. The general form of the friction-deformation curve is seen to form the well known elastic-plastic paralellogram shape.

In the Figures B-8 through B-11 are shown effective normal pressure versus friction on the pile wall for selected cycles. From Figure B-9 showing cycle 202 which is in the beginning of the yield period a max friction of 34 kPa and effective pressure of 120 kPa is measured. This gives an interface friction angle of about 14.2 degrees.

STRENGTH TESTS

After last parcel in stroke controlled cyclic tests the pile was pulled out of the pile chamber and the sample built out. Pocket penetrometer tests were performed on the side of the sample with results shown in Figure 17.

Three standard triaxial test samples were then prepared from the centre of the sample and unconfined compression tests (UCT) were performed. The results are shown in Figure 18.

In Figure 19 are shown the water content and interpreted undrained shear strength of the clay specimen versus the distance from the pile center after completion of the pile test.

TABLE 1.

SAMPLE PROPERTIES TEST 5, STRATUM II

SAMPLE PREPARATION		CONSOLIDATION			END OF PILE TEST
INITIAL WATER CONTENT	INITIAL HEIGHT	AXIAL DEFORMATION	AXIAL STRAIN	WATER CONTENT	WATER CONTENT
w_i (%)	H_o (cm)	ΔH (cm)	ε (%)	w_e (%)	w_{ep} (%)
	51.2	4.36	8.52	A 29.07 B 29.18 C 29.09	A 29.61 B 29.30 C 28.36

CONFINING PRESSURE		
AXIAL	KPa	600
RADIAL	KPa	510
BACK PRESSURE	KPa	300
SAMPLE CONSOLIDATION		
IN OEDOMETER	Days	14
IN PILE CHAMBER	Days	6
INTERPRETED SHEAR STRENGTH		
END OF CONSOLIDATION	KPa	50
END OF PILE TEST	KPa	55

Fig.1

CONSOLIDATION DIAGRAM

Test No. 5
Stratum II

Start date

σ_c 300 kPa

H_i 51.2 cm H_e 46.8 cm $\Delta\varepsilon_v$ 8.52 %

Time h	46	94	115	132	170	235	259	283	307	331	332
Δh cm	2.41	3.22	3.44	3.62	3.89	4.17	4.23	4.27	4.32	4.36	4.36
u kPa	17.04	131.8	115.3	102.0	78.6	50.1	43.0	38.1	34.9	30.7	30.2

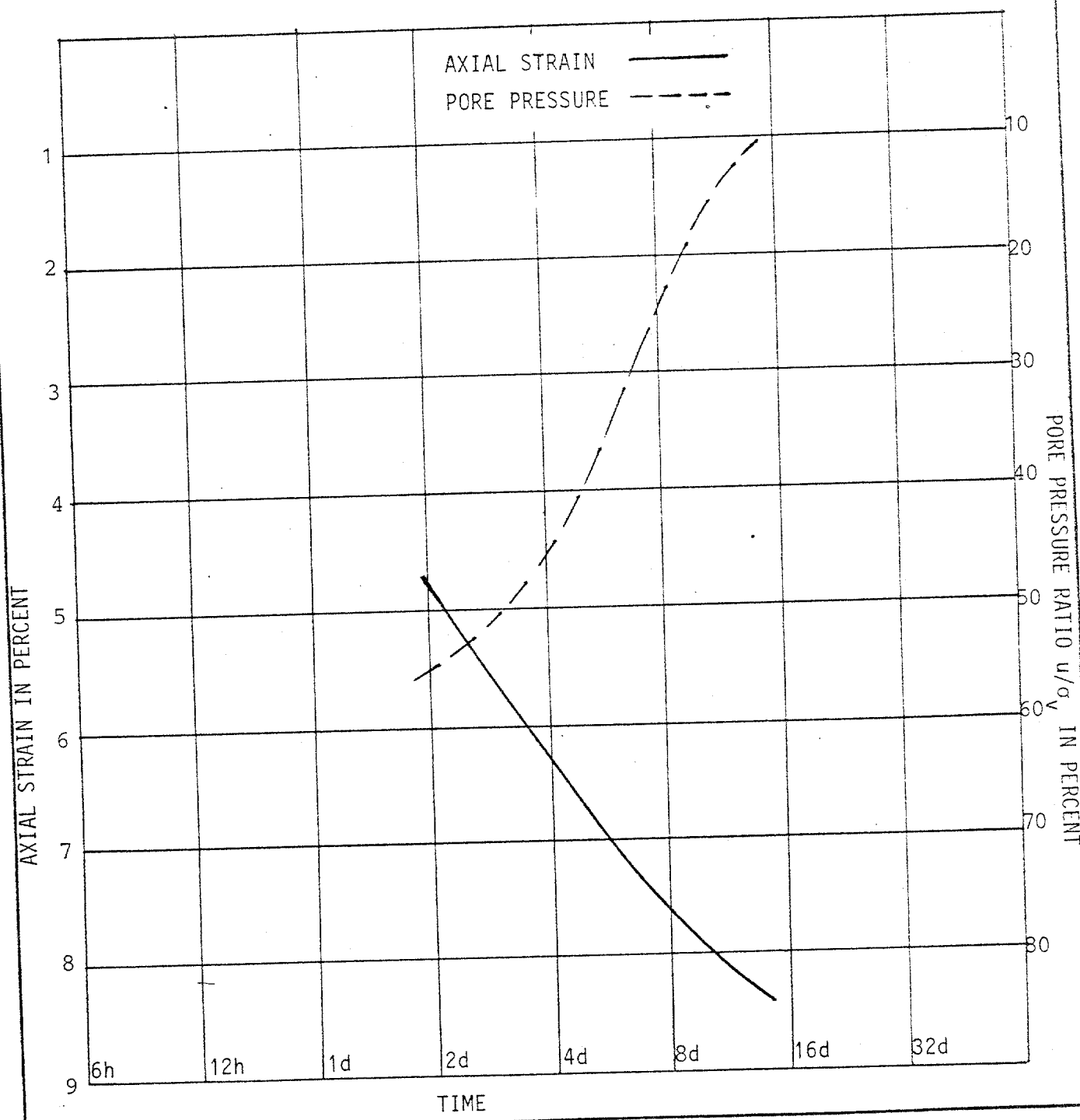

CNRD 13-2 TENSION PILE STUDY LABORATORY MODEL PILE TESTS

DET NORSKE VERITAS
Geotechnical Laboratory

Scale

Drawn by

Date

Approved

Fig. No. 2

TEST 5, STRATUM II

SHEAR STRENGTH (KPa) FROM POCKET PENETROMETER TESTS AFTER CONSOLIDATION

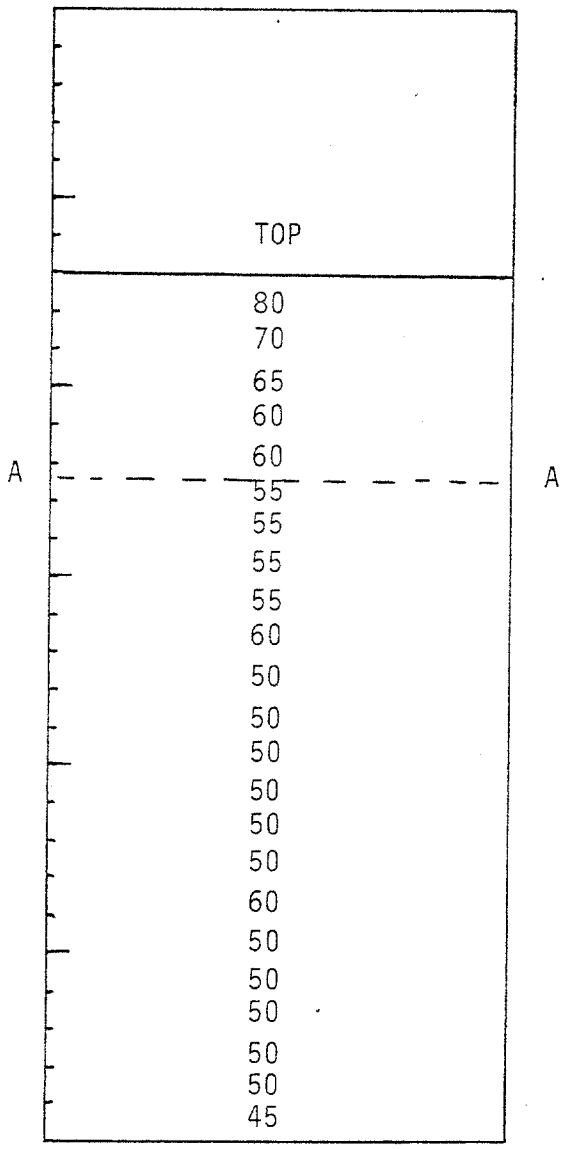

Scale: 1:4

LEVEL A-A

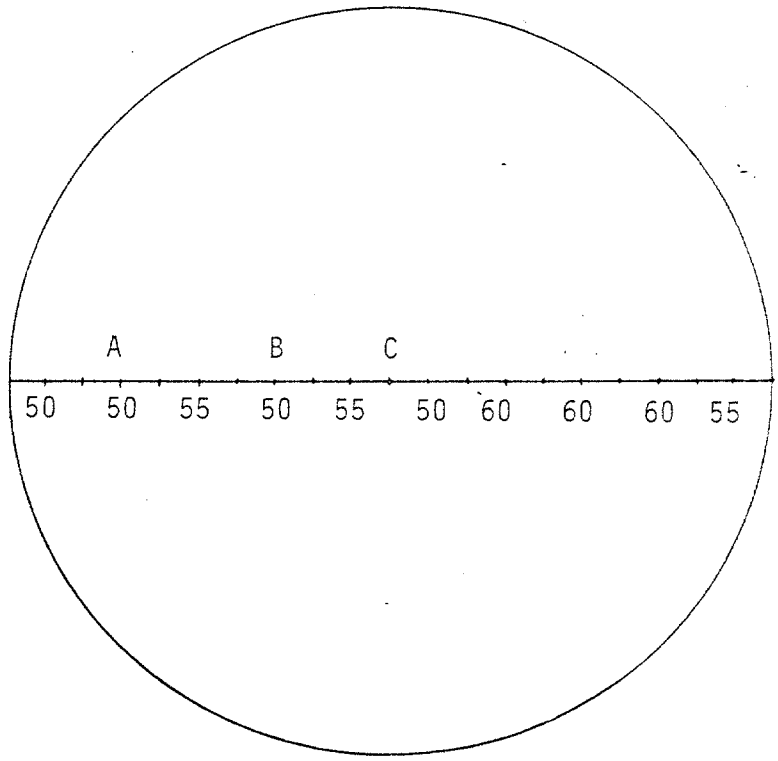

Scale: 1:2

CNRD 13-2 TENSION PILE STUDY LABORATORY MODEL PILE TESTS

		Scale
DET NORSKE VERITAS Geotechnical Laboratory	Drawn by	Date
	Approved	Fig. No. 3

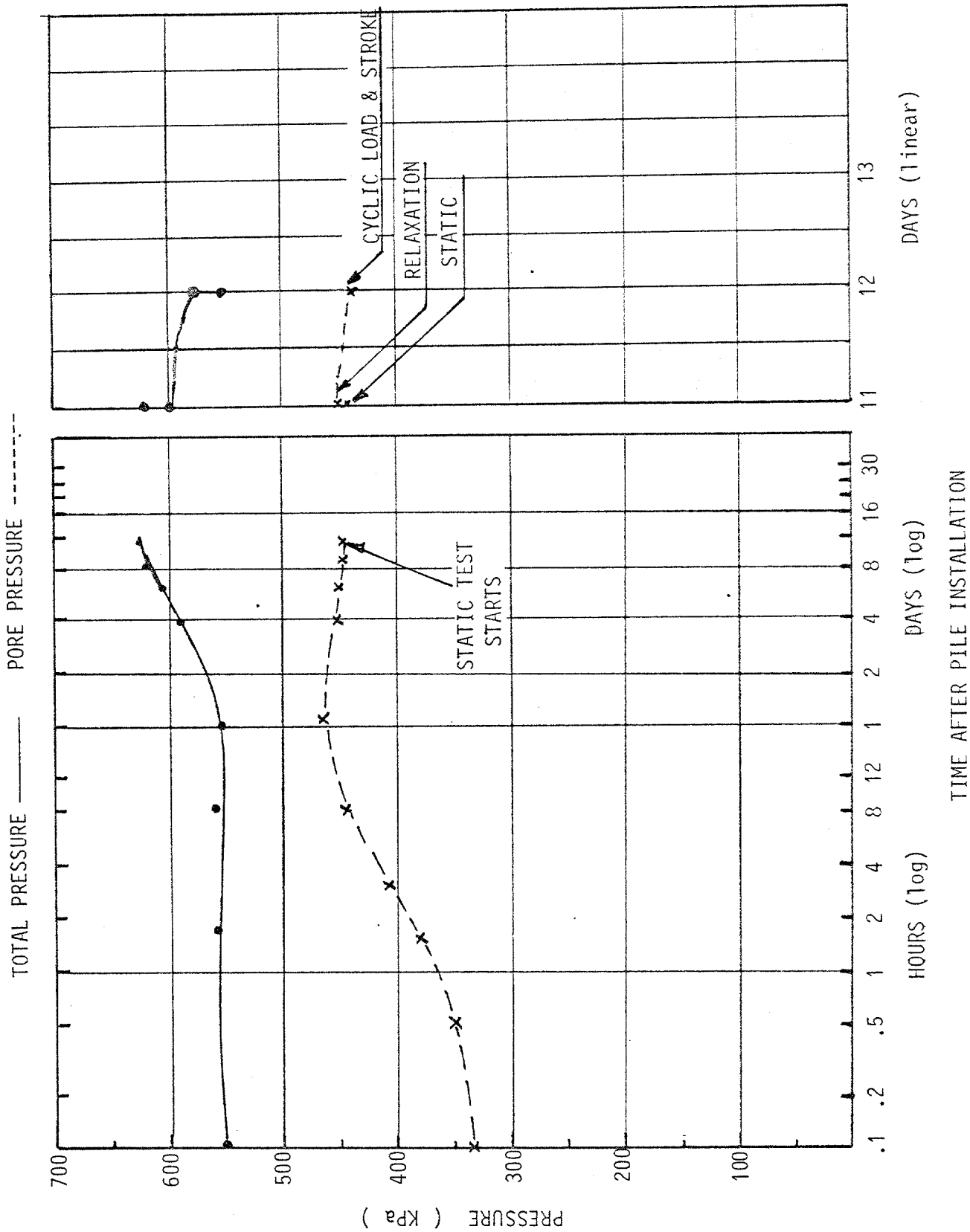

CNRD 13-2 TENSION PILE STUDY LABORATORY MODEL PILE TESTS

TEST 5, STRATUM II. Pressures at pile wall after installation

DET NORSKE VERITAS Geotechnical Laboratory	Drawn by	Scale
	Approved	Date
		Fig. No. 4

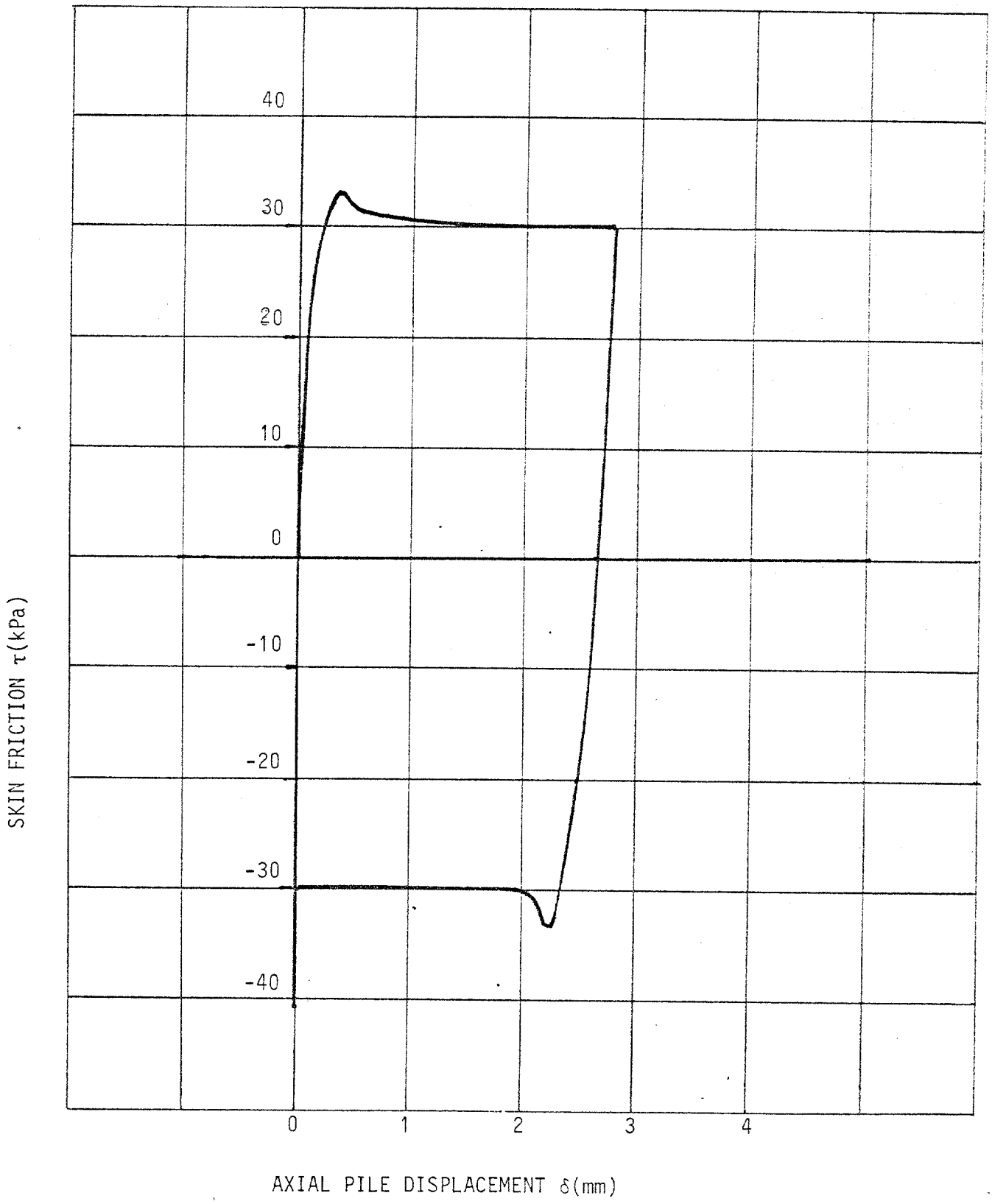

CNRD 13-2 TENSION PILE STUDY LABORATORY MODEL PILE TESTS

TEST 5, STRATUM II STATIC TEST

DET NORSKE VERITAS Geotechnical Laboratory	Drawn by	Scale
	Approved	Date
		Fig. No. 5

TEST 4, STRATUM II

RELAXATION TEST

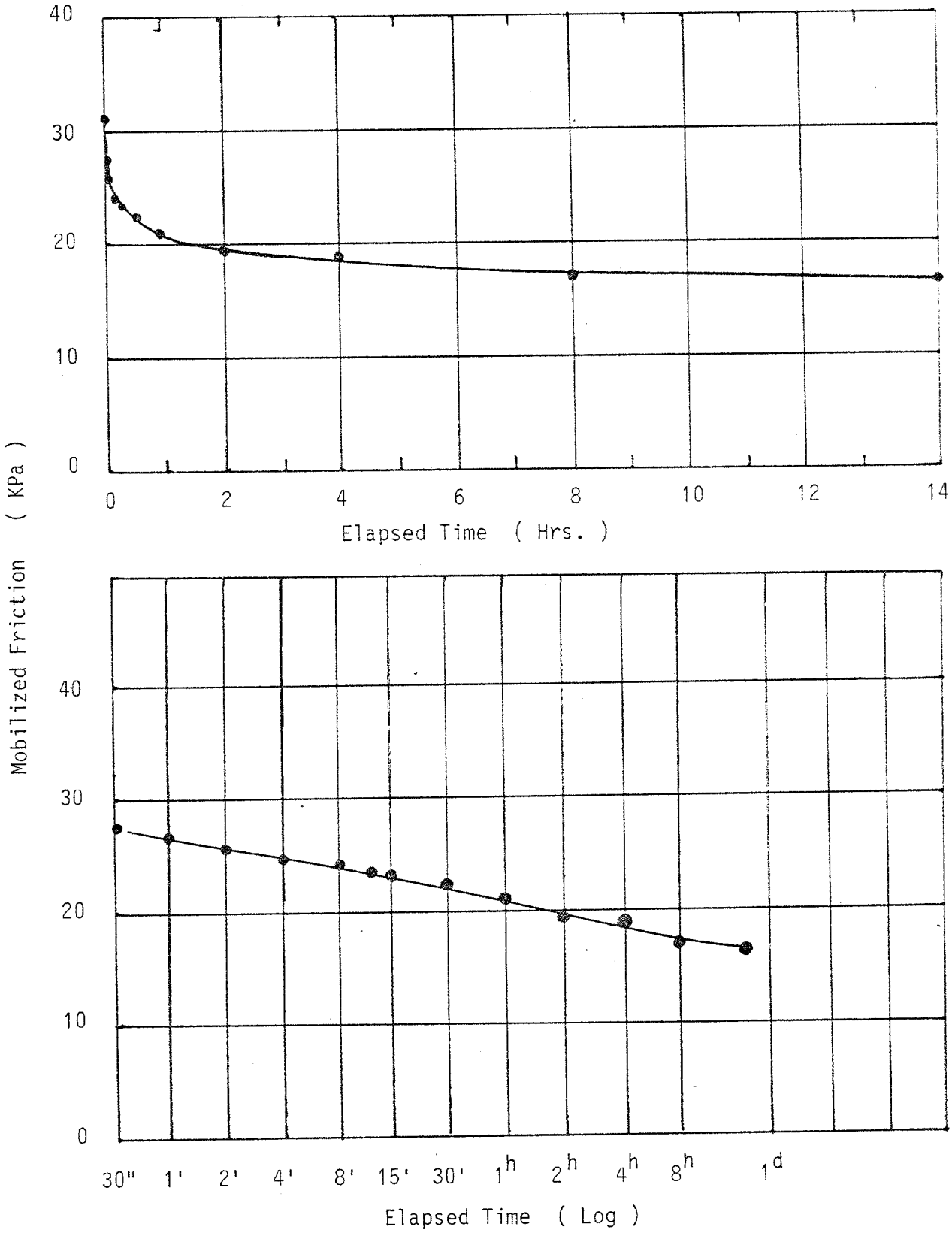

CNRD 13-2 TENSION PILE STUDY LABORATORY MODEL PILE TESTS

TEST 4, STRATUM II Relaxation Test		Scale
DET NORSKE VERITAS Geotechnical Laboratory	Drawn by	Date
	Approved	Fig. No. 6

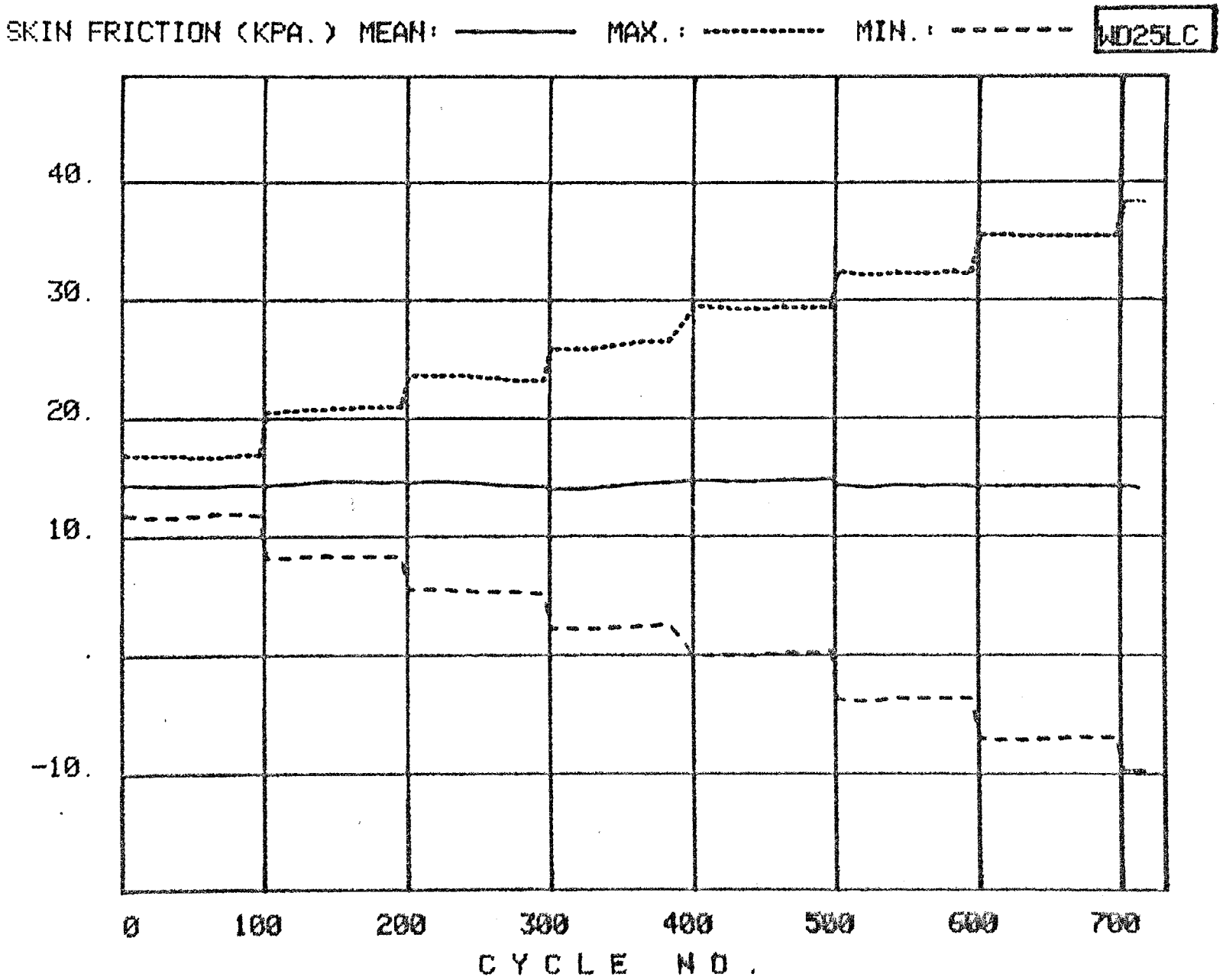
SKIN FRICTION (KPA.) MEAN: MAX.: MIN.:
WD25LC
40.
30.
20.
10.
-10.
0
100
200
300
400
500
600
700
CYCLE NO.

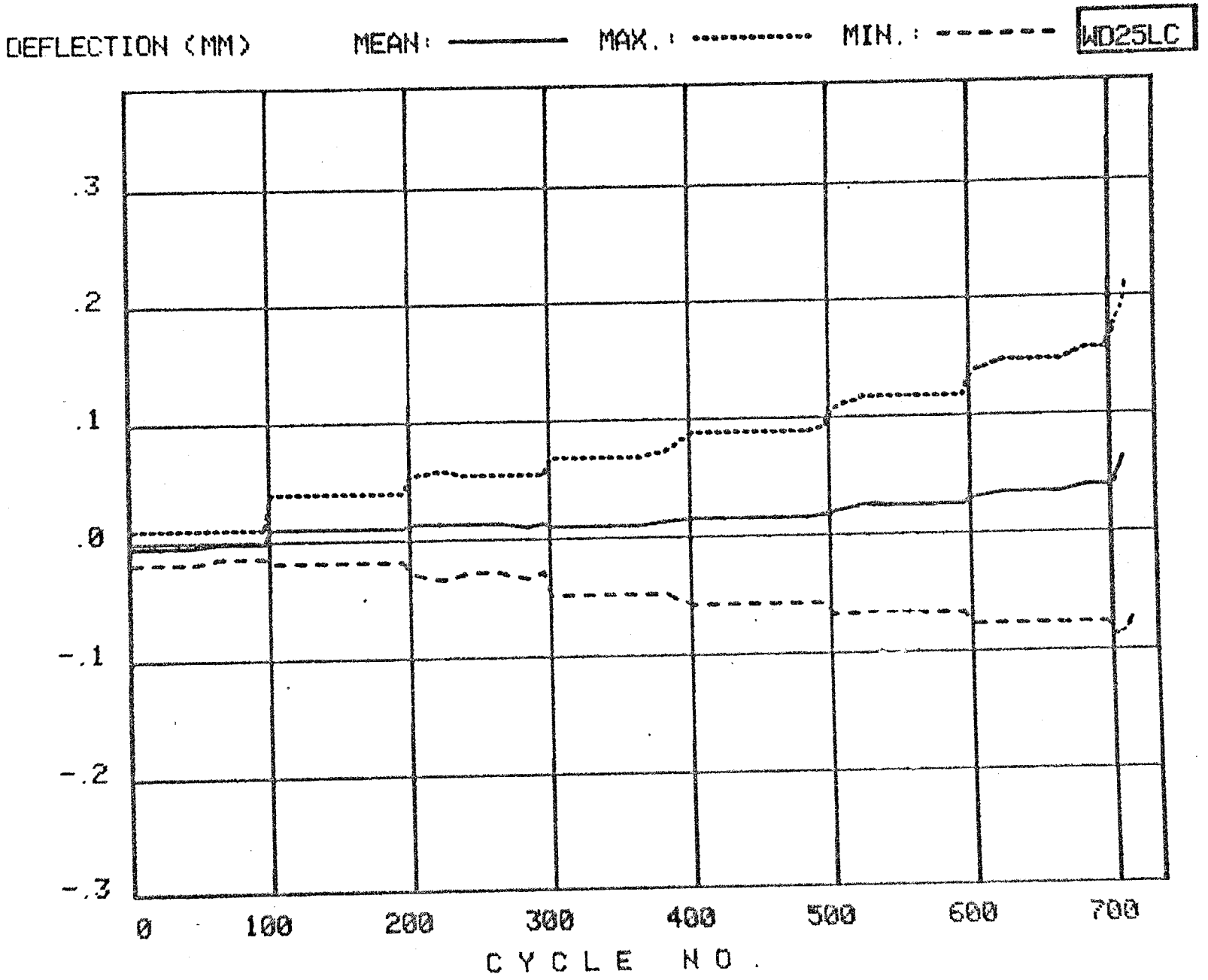
DEFLECTION (MM)
MEAN:
MAX.:
MIN.:
WD25LC
.3
.2
.1
.0
-.1
-.2
-.3
0
100
200
300
400
500
600
700
CYCLE NO.

Fig-8

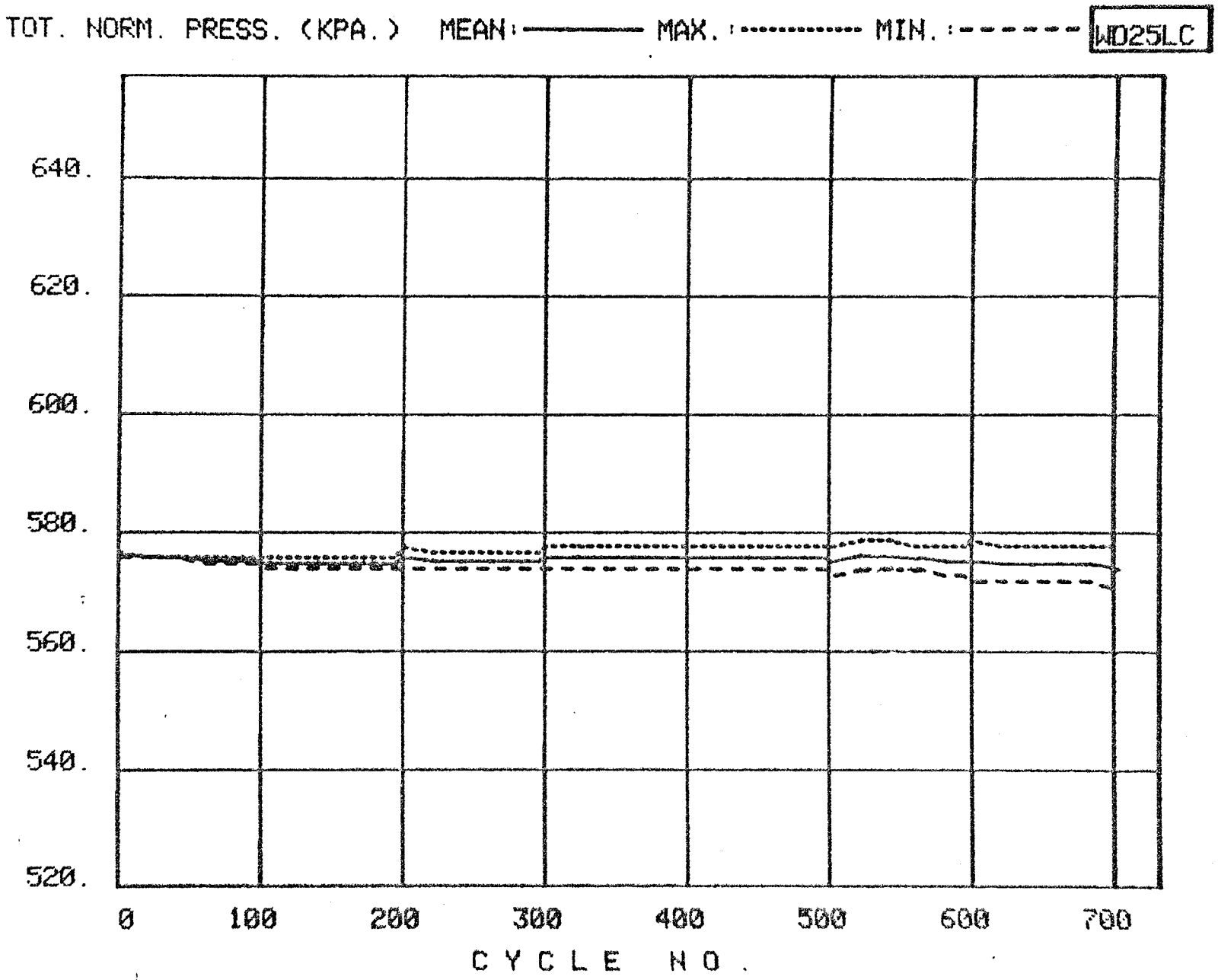
TOT. NORM. PRESS. (KPA.)
MEAN:
MAX.:
MIN.:
WD25LC
640.
620.
600.
580.
560.
540.
520.
0
100
200
300
400
500
600
700
CYCLE NO.

Fig-9

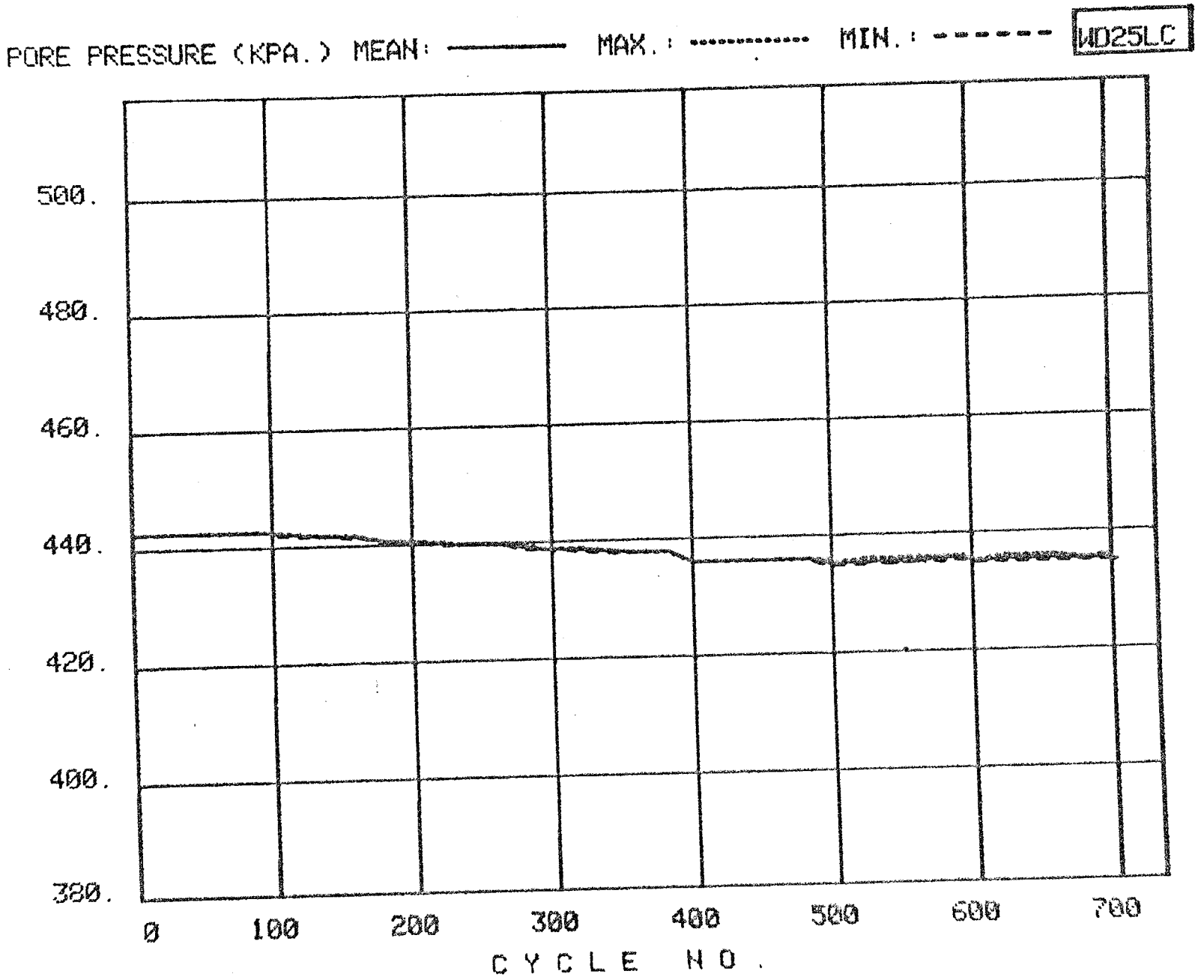
PORE PRESSURE (KPA.) MEAN: MAX.: MIN.:
WD25LC
500.
480.
460.
440.
420.
400.
380.
0
100
200
300
400
500
600
700
CYCLE NO.

Fig-10

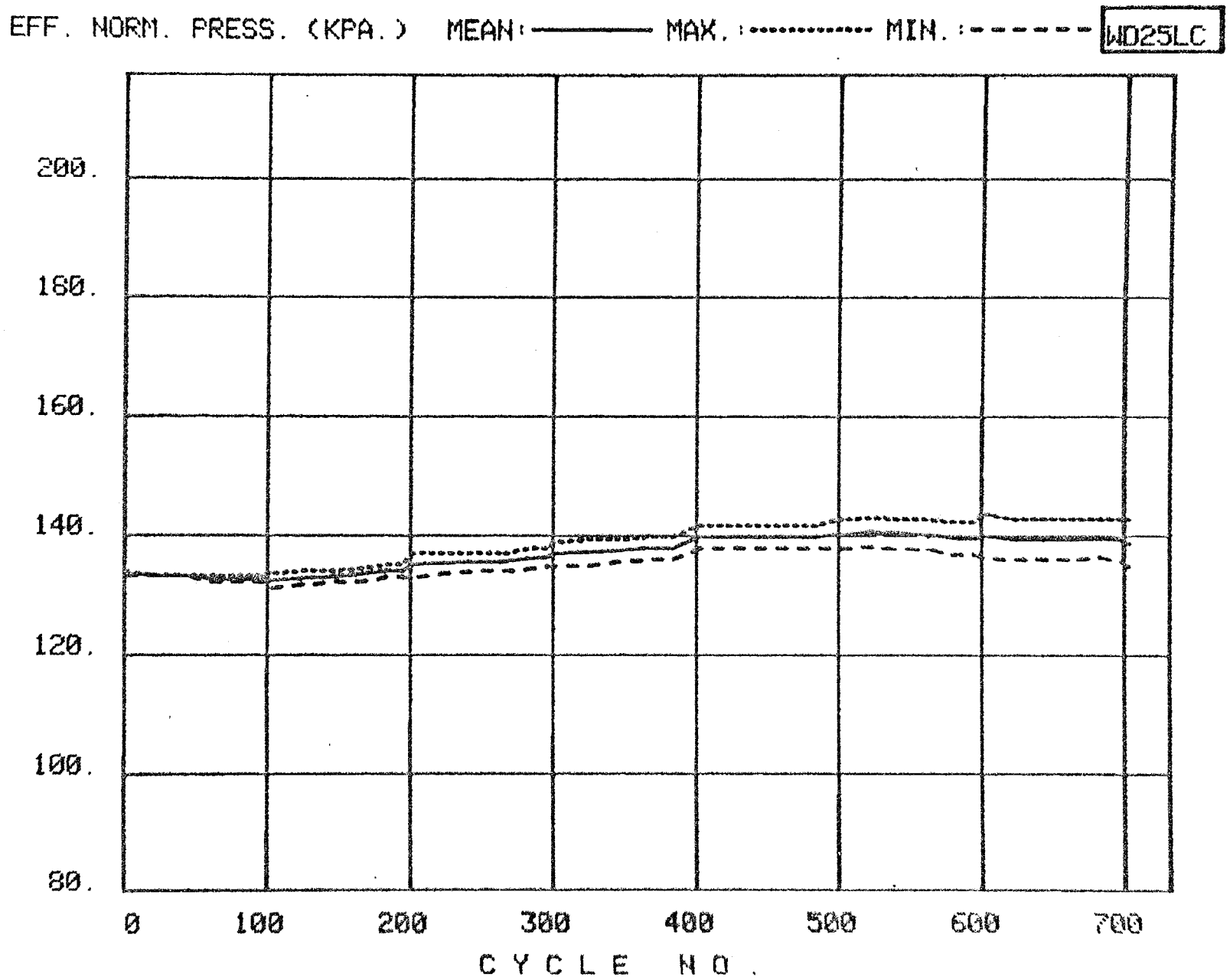
EFF. NORM. PRESS. (KPA.)
MEAN:
MAX.:
MIN.:
WD25LC
200.
180.
160.
140.
120.
100.
80.
0
100
200
300
400
500
600
700
CYCLE NO.

Fig-11

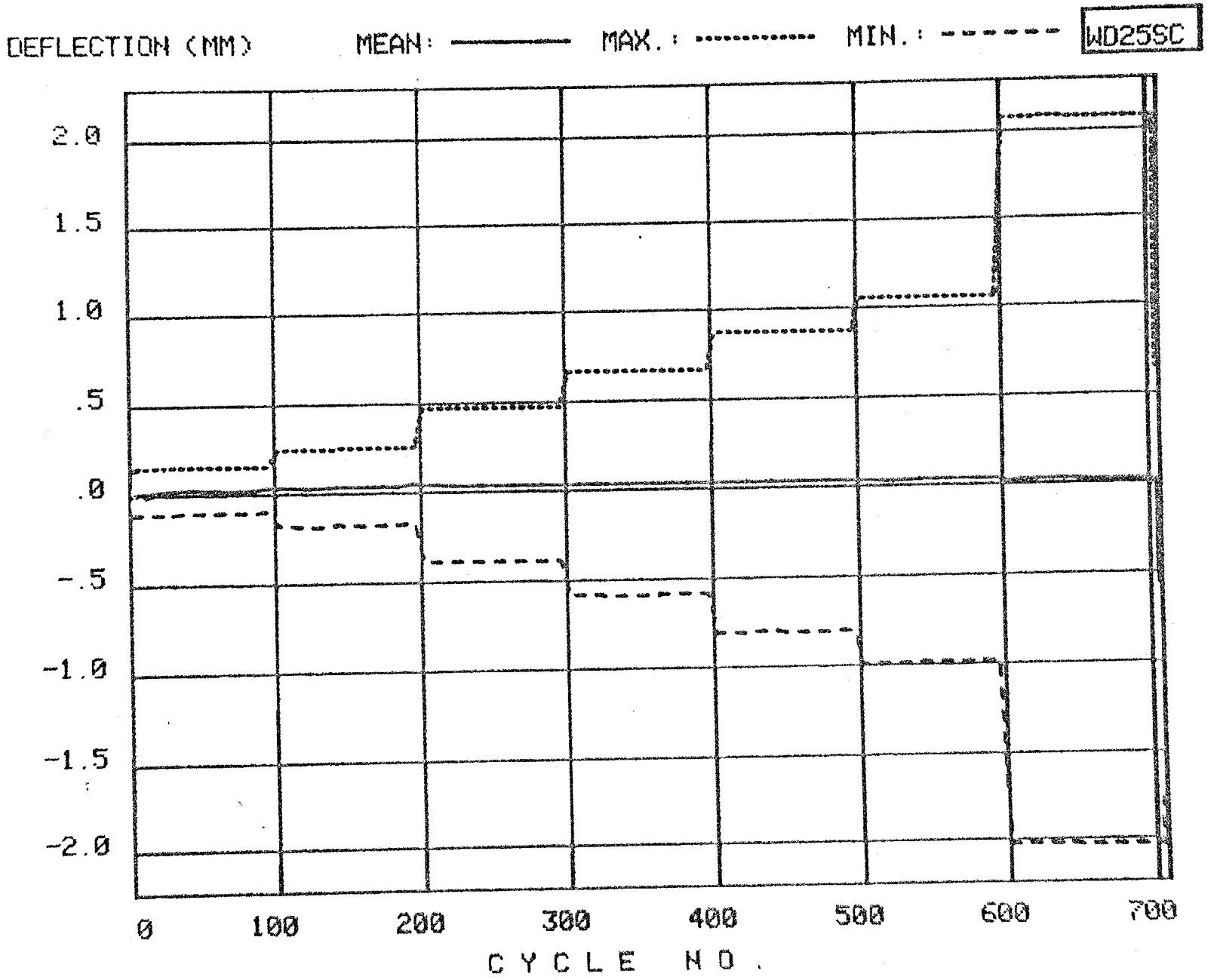
DEFLECTION (MM)
MEAN:
MAX.:
MIN.:
WD25SC
2.0
1.5
1.0
.5
.0
-.5
-1.0
-1.5
-2.0
0
100
200
300
400
500
600
700
CYCLE NO.

Fig-12

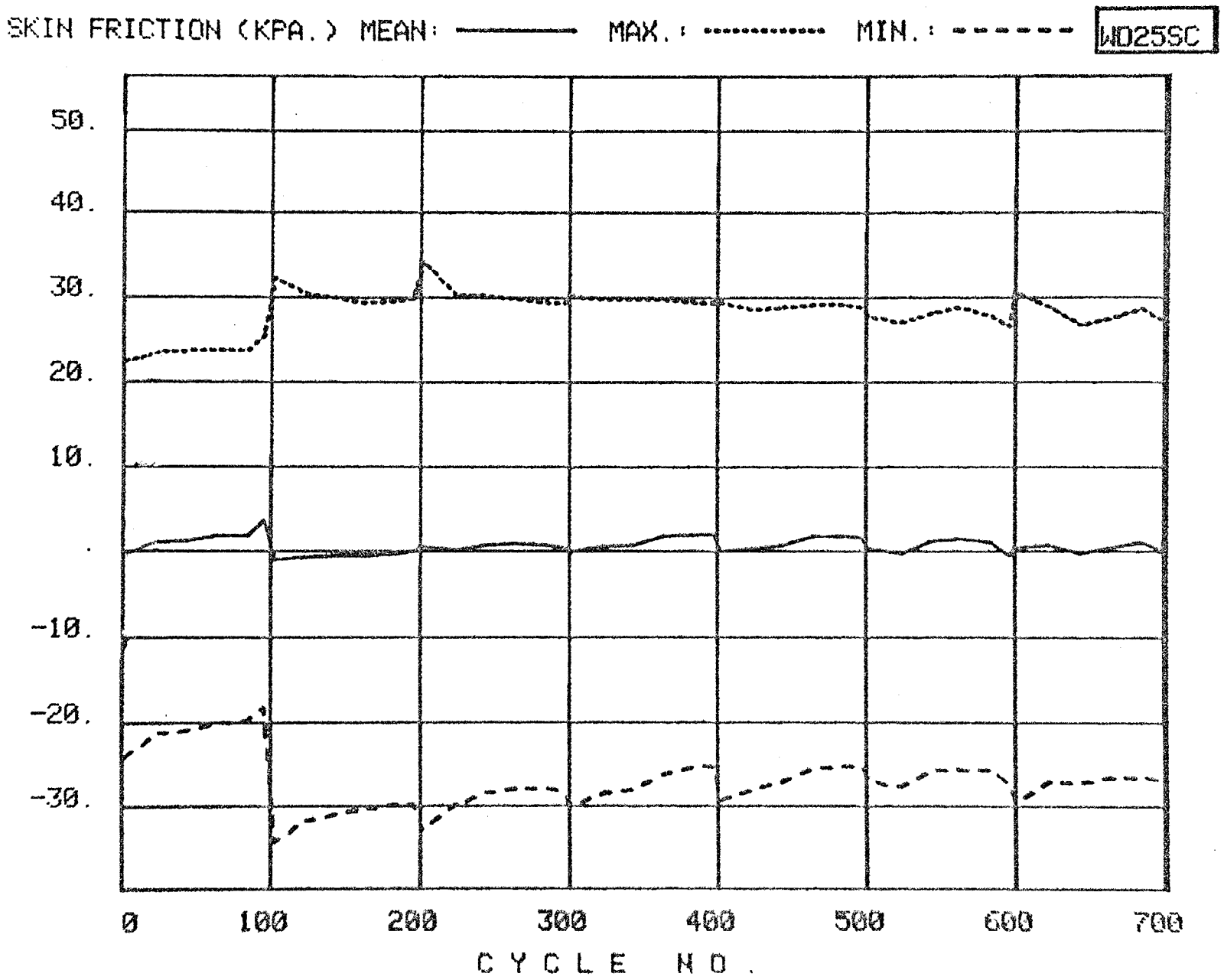
SKIN FRICTION (KPA.) MEAN: MAX.: MIN.:
WD25SC
50.
40.
30.
20.
10.
-10.
-20.
-30.
0
100
200
300
400
500
600
700
CYCLE NO.

Fig-13

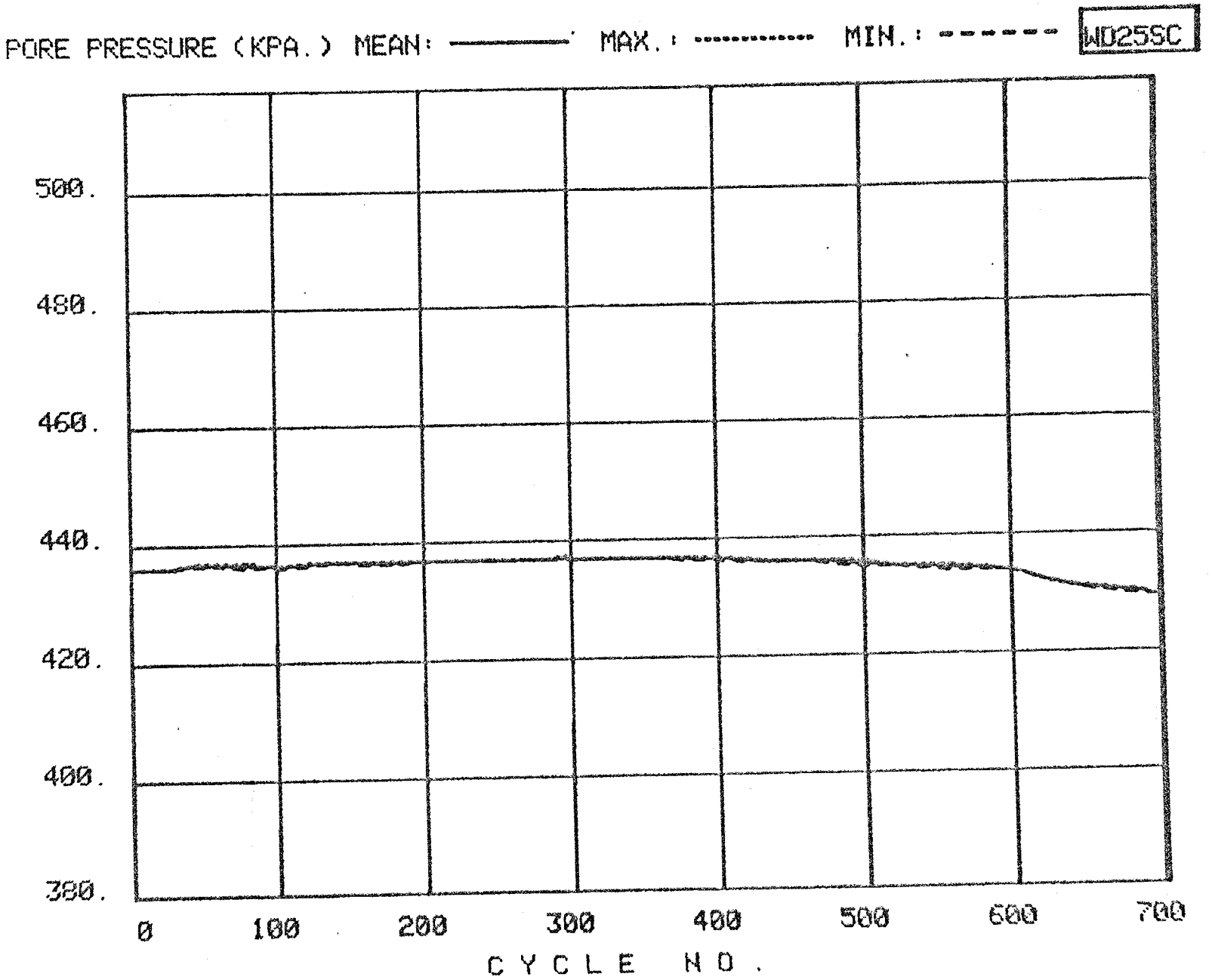
PORE PRESSURE (KPA.) MEAN: ——— MAX.: ····· MIN.: - - - - - -
WD25SC
500.
480.
460.
440.
420.
400.
380.
0
100
200
300
400
500
600
700
CYCLE NO.

Fig. 14

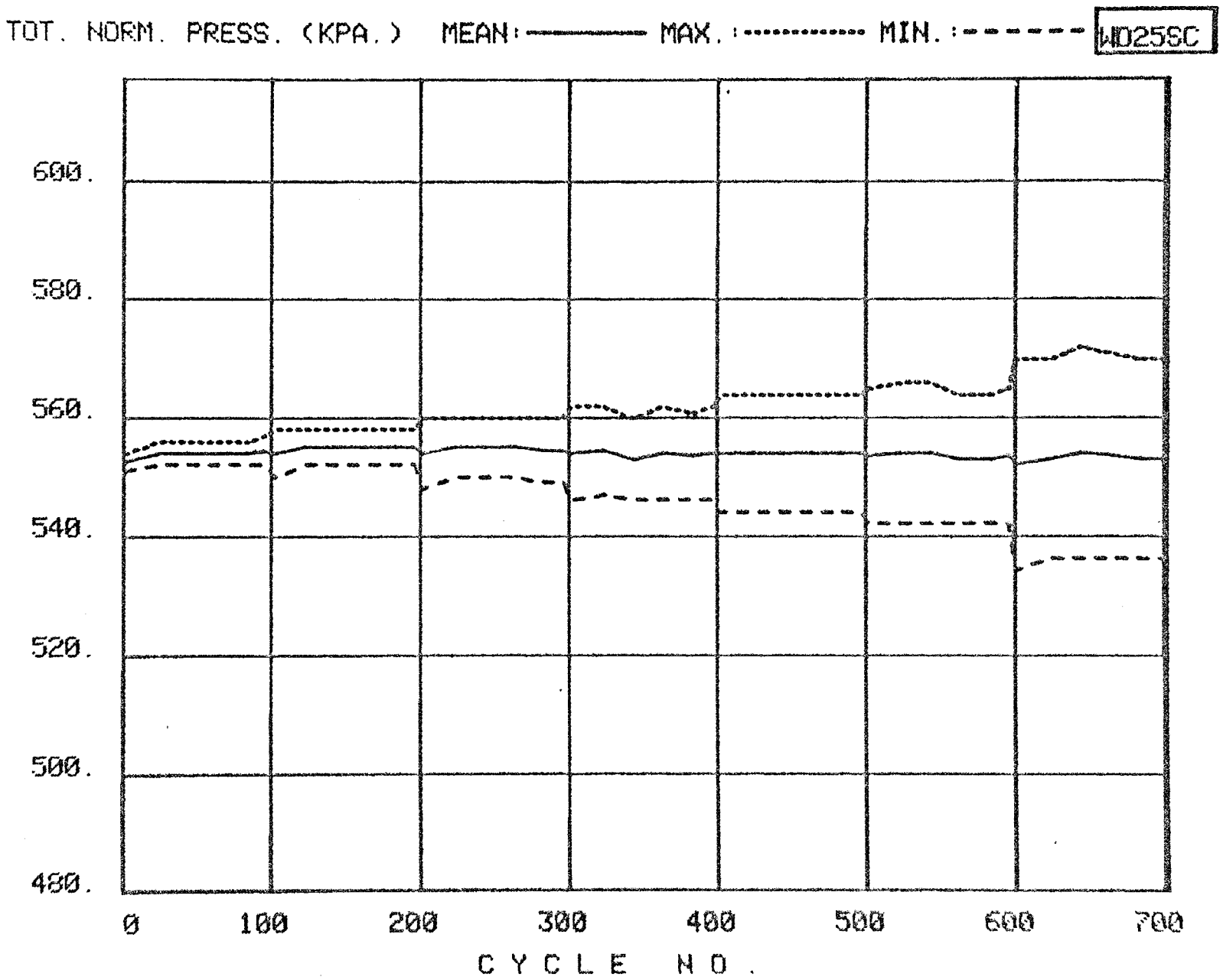
TOT. NORM. PRESS. (KPA.) MEAN: MAX.: MIN.:
WD25SC
600.
580.
560.
540.
520.
500.
480.
0
100
200
300
400
500
600
700
CYCLE NO.

Fig-15

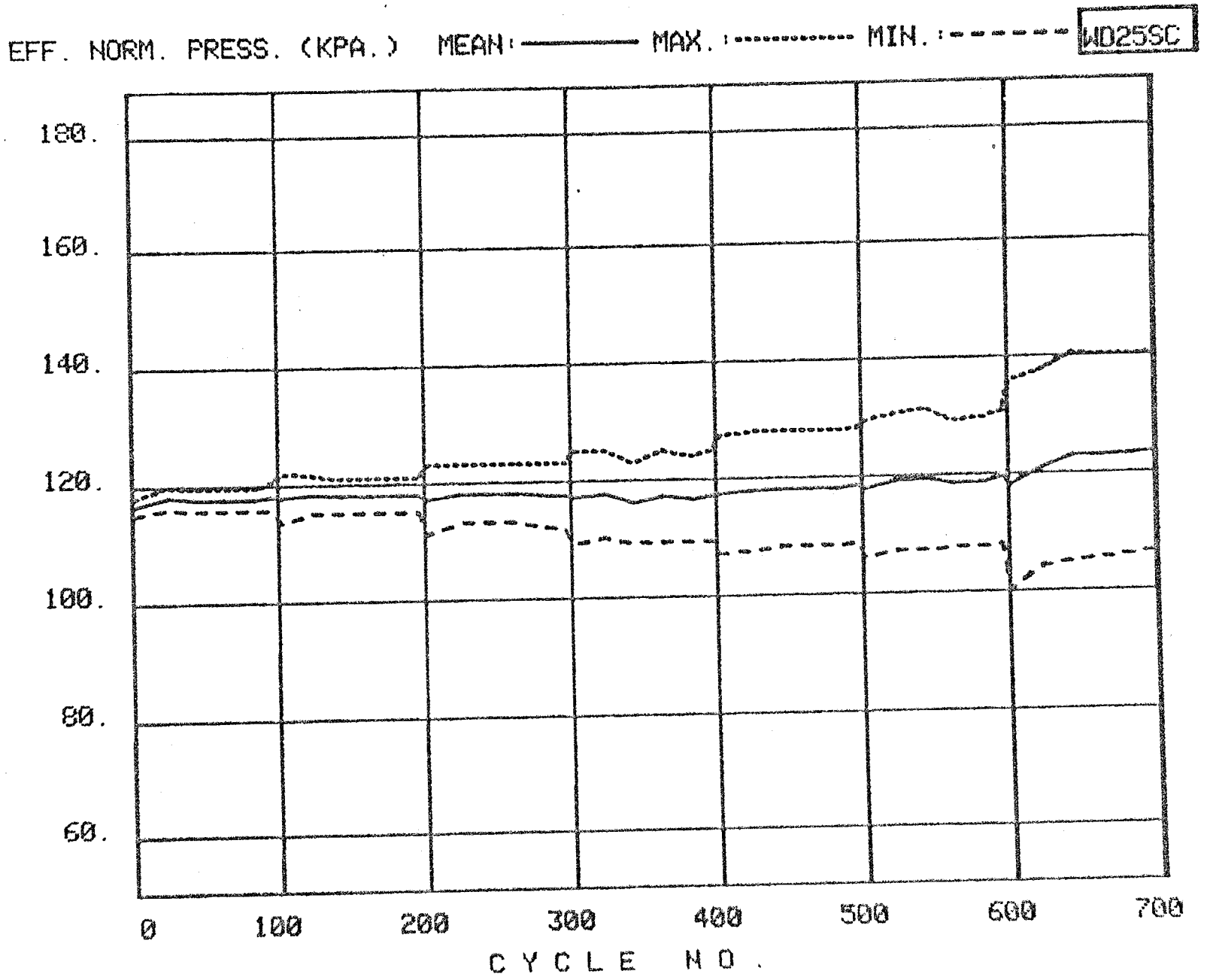
EFF. NORM. PRESS. (KPA.)
MEAN:
MAX.:
MIN.:
WD25SC
180.
160.
140.
120.
100.
80.
60.
0
100
200
300
400
500
600
700
CYCLE NO.

Fig-16

TEST 5, STRATUM II

SHEAR STRENGTH FROM POCKET PENETROMETER
AFTER PILE TEST (KPa)

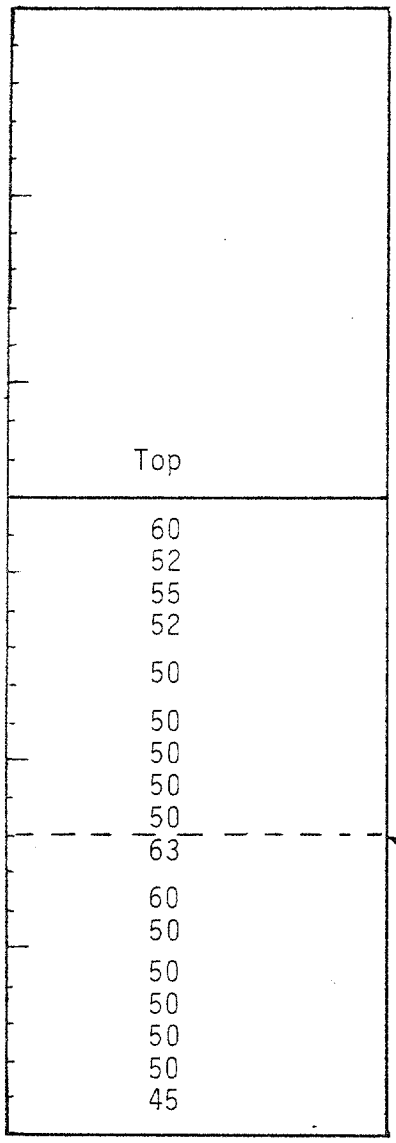

Scale 1:4

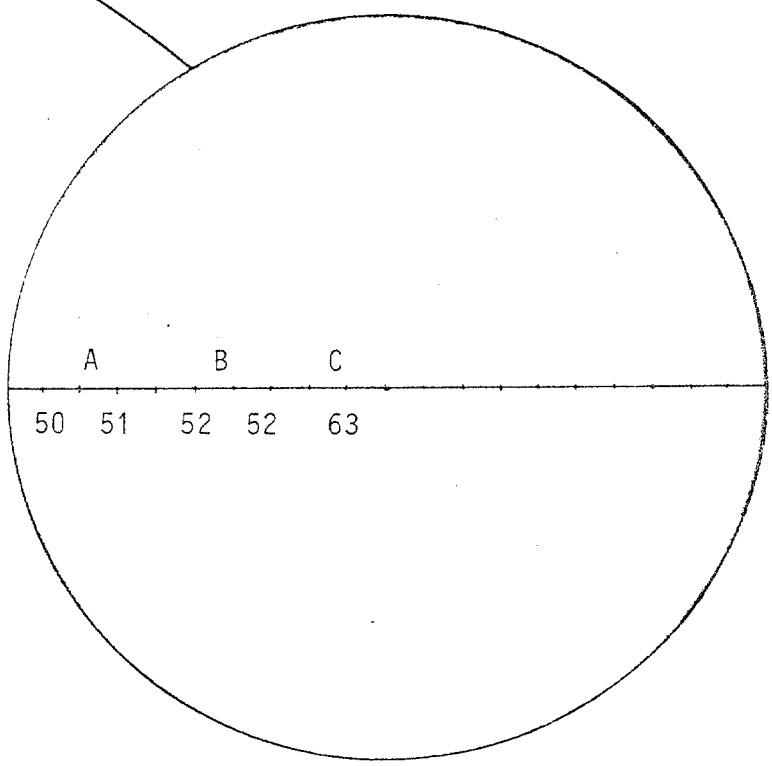

Scale: 1:2

CNRD 13-2 TENSION PILE STUDY LABORATORY MODEL PILE TESTS

TEST 5, STRATUM II, Pocket penetrometer tests after pile test		Scale
DET NORSKE VERITAS Geotechnical Laboratory	Drawn by	Date
	Approved	Fig.No. 17

TEST 5, STRATUM II

UNCONFINED COMPRESSION TEST ON MATERIAL AFTER PILE TEST

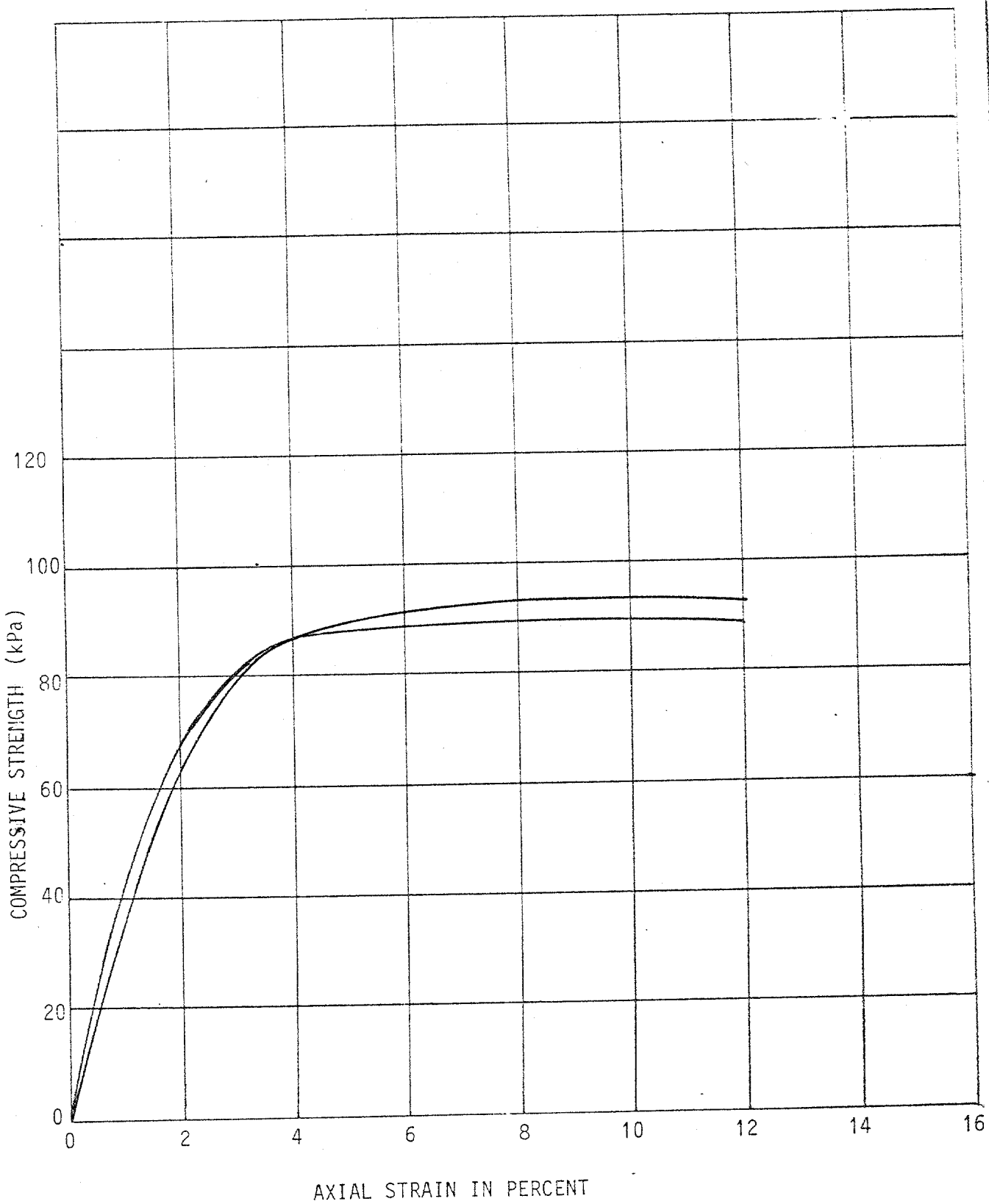

CNRD 13-2 TENSION PILE STUDY LABORATORY MODEL PILE TESTS		
TEST 5, STRATUM II, Unconfined compr. test after pile test		Scale
DET NORSKE VERITAS Geotechnical Laboratory	Drawn by	Date
	Approved	Fig. No. 18

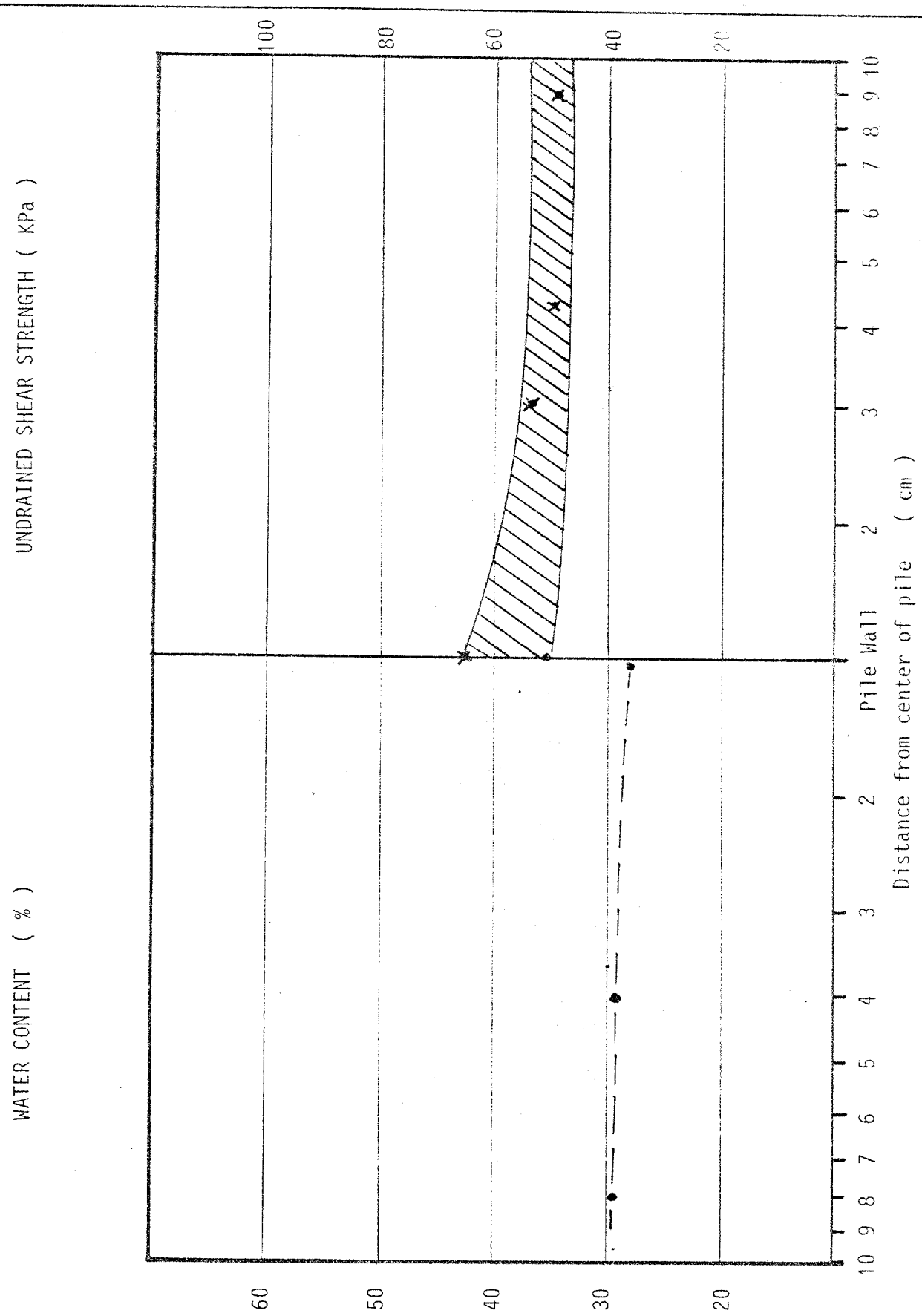

CNRD 13-2 TENSION PILE STUDY LABORATORY MODEL PILE TESTS

TEST 5, STRATUM II, Water content and shear strength after test

DET NORSKE VERITAS Geotechnical Laboratory	Drawn by	Scale
	Approved	Date
		Fig. No. 19

Appendix BA

Plotted Results from WD25LC

Figures BA-1 through BA-9

Skin Friction vs Deflection, Selected Cycles

Figures BA-10 through BA-13

Skin Friction vs Eff. Normal Pressure, Selected Cycl.

Figures BA-14 through BA-29

Skin Friction, Pore and Total Pressure, Selected Cycles

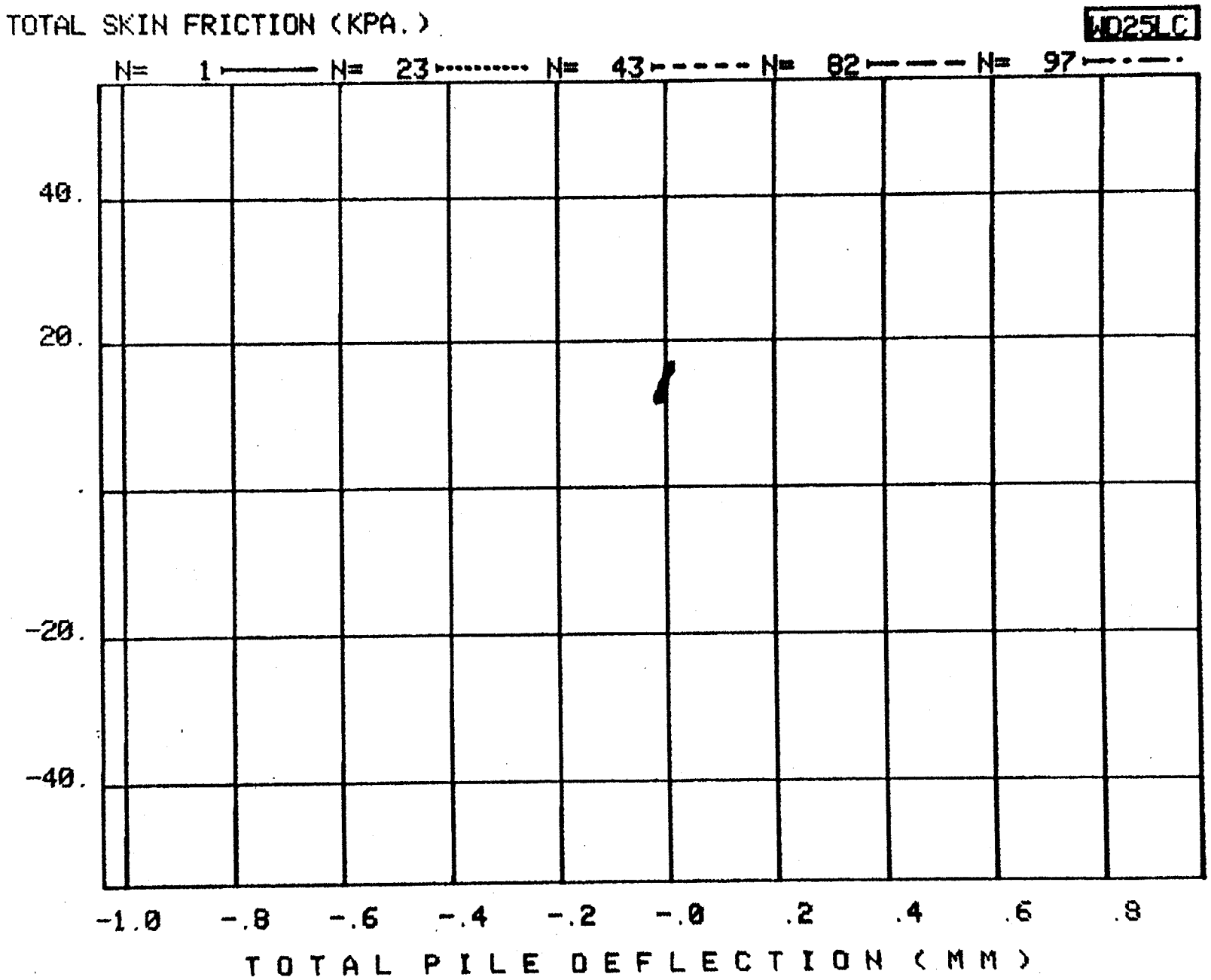
TOTAL SKIN FRICTION (KPA.)
WD25LC
N= 1
N= 23
N= 43
N= 82
N= 97
40.
20.
-20.
-40.
-1.0
-.8
-.6
-.4
-.2
-.0
.2
.4
.6
.8
TOTAL PILE DEFLECTION (MM)

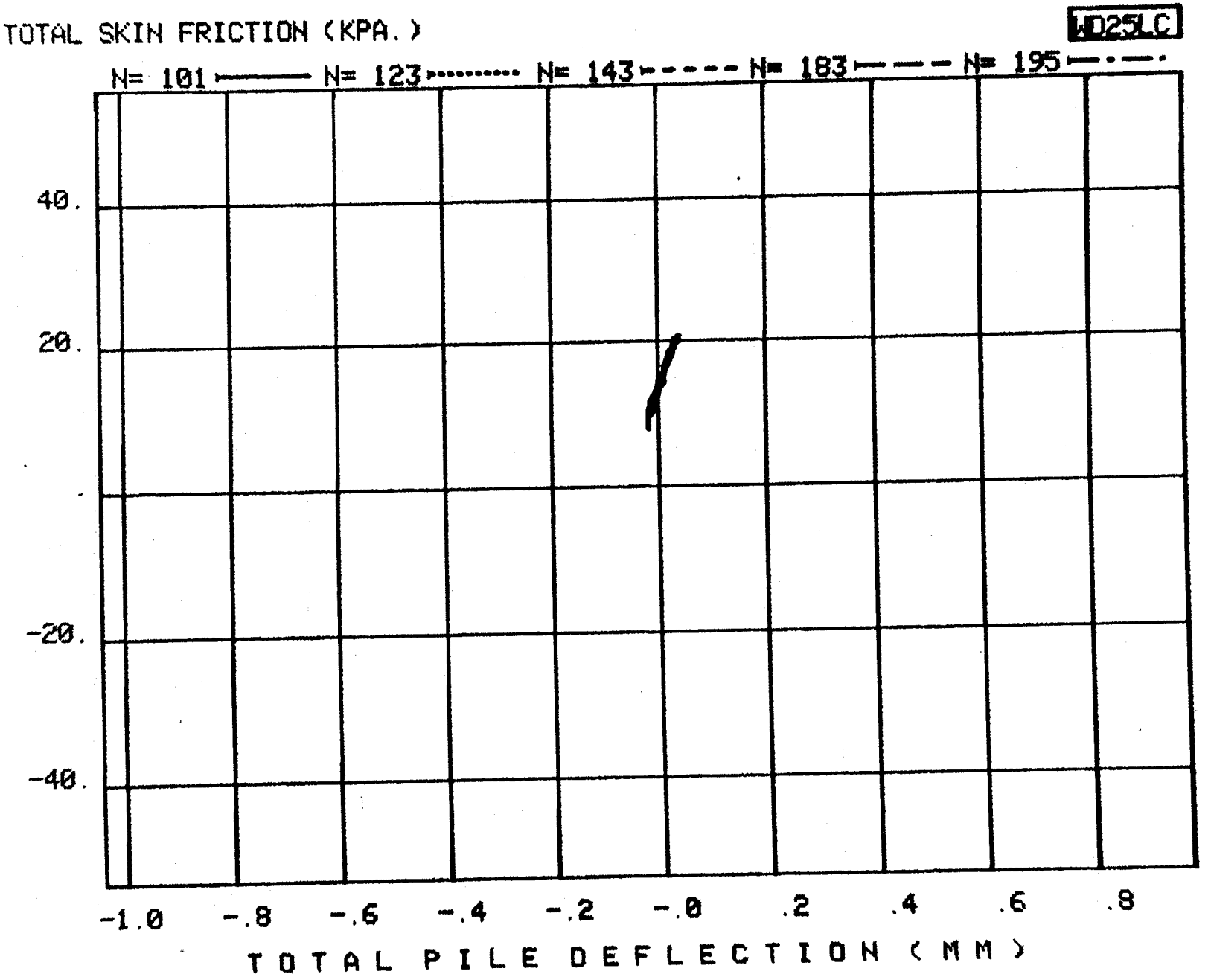
TOTAL SKIN FRICTION (KPA.)
WD25LC
N= 101
N= 123
N= 143
N= 183
N= 195
40.
20.
-20.
-40.
-1.0
-.8
-.6
-.4
-.2
-.0
.2
.4
.6
.8
TOTAL PILE DEFLECTION (MM)

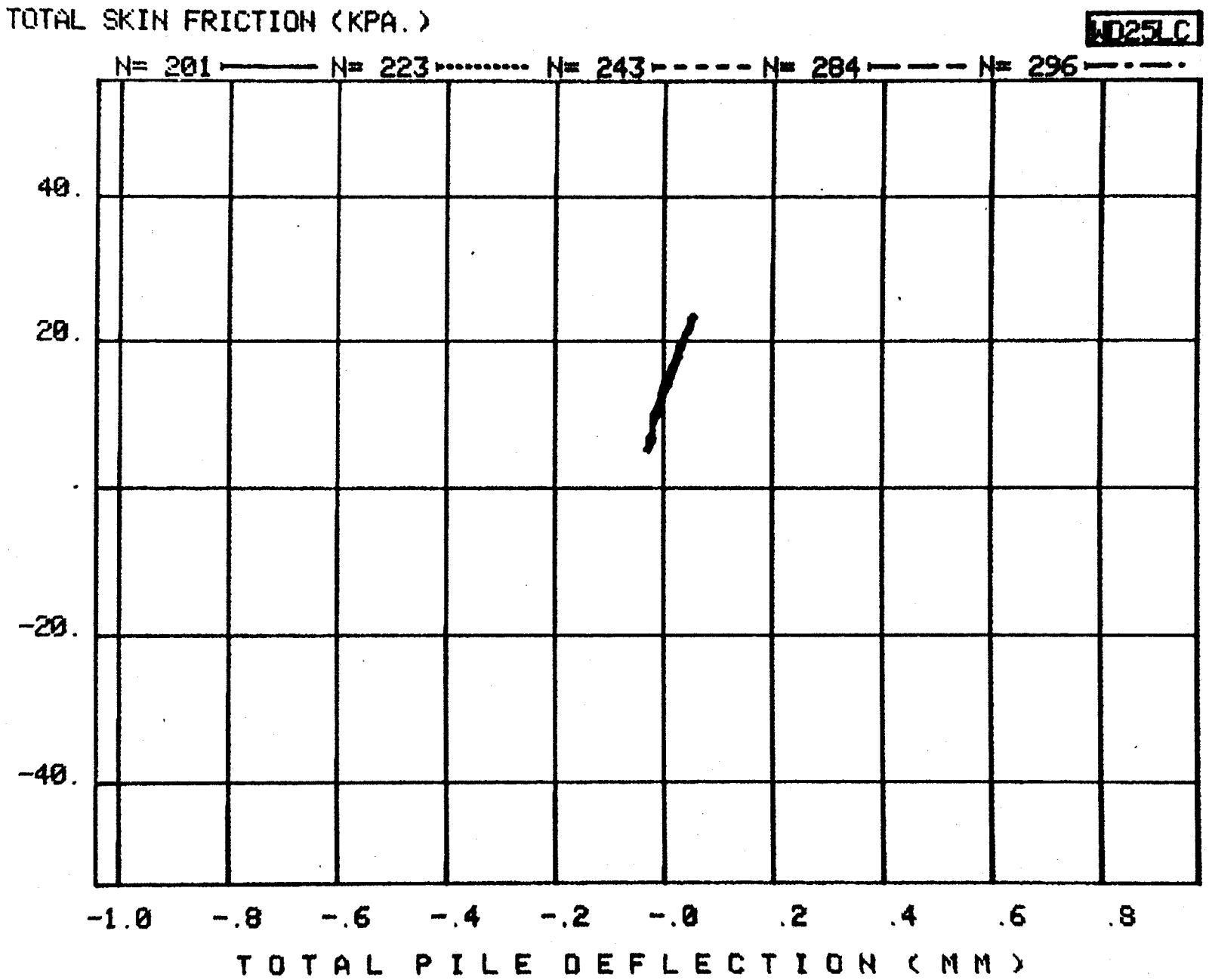
TOTAL SKIN FRICTION (KPA.)
WD25LC
N= 201
N= 223
N= 243
N= 284
N= 296
40.
20.
-20.
-40.
-1.0
-.8
-.6
-.4
-.2
-.0
.2
.4
.6
.8
TOTAL PILE DEFLECTION (MM)

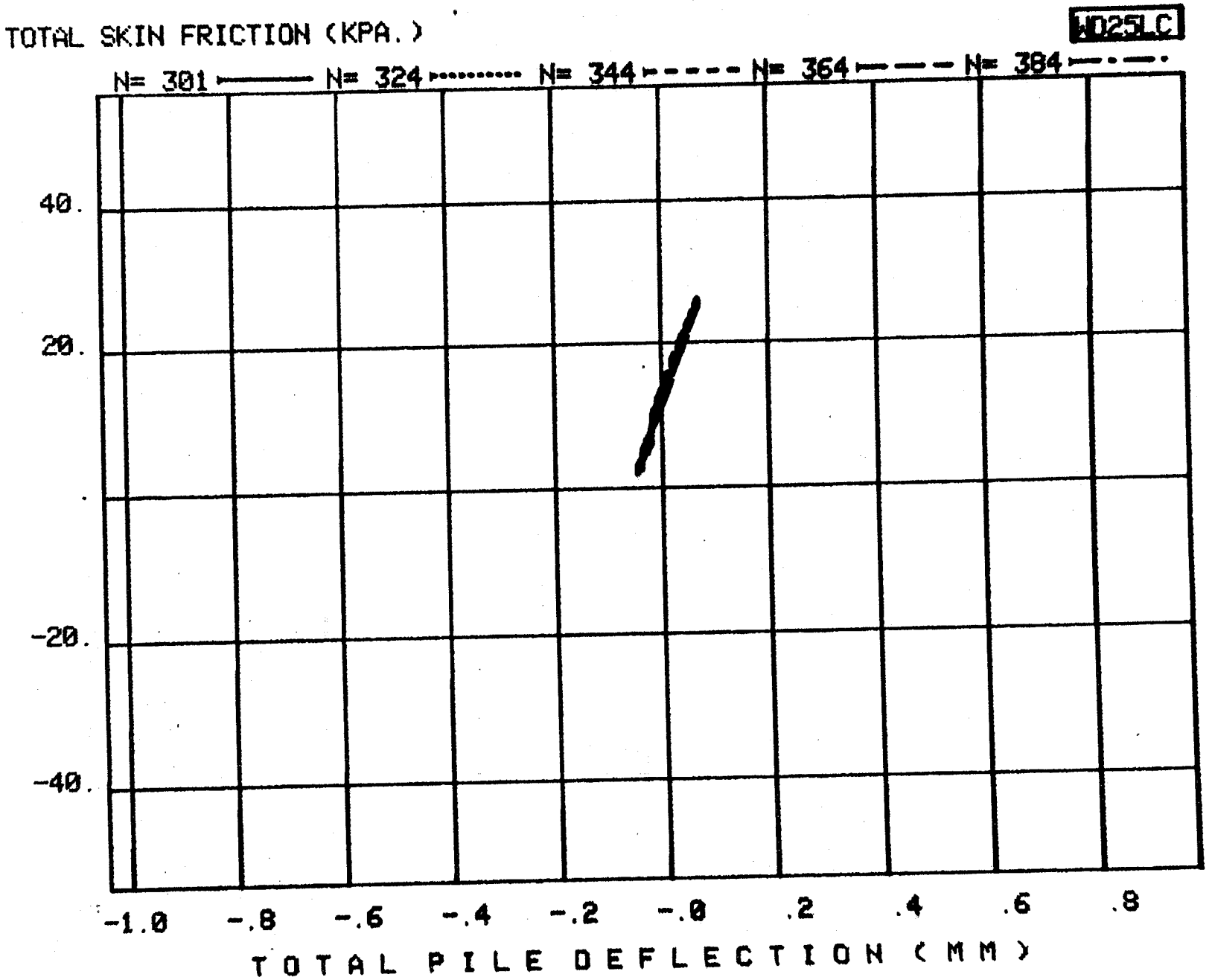
TOTAL SKIN FRICTION (KPA.)
W025LC
N= 301
N= 324
N= 344
N= 364
N= 384
40.
20.
-20.
-40.
-1.0
-.8
-.6
-.4
-.2
-.0
.2
.4
.6
.8
TOTAL PILE DEFLECTION (MM)

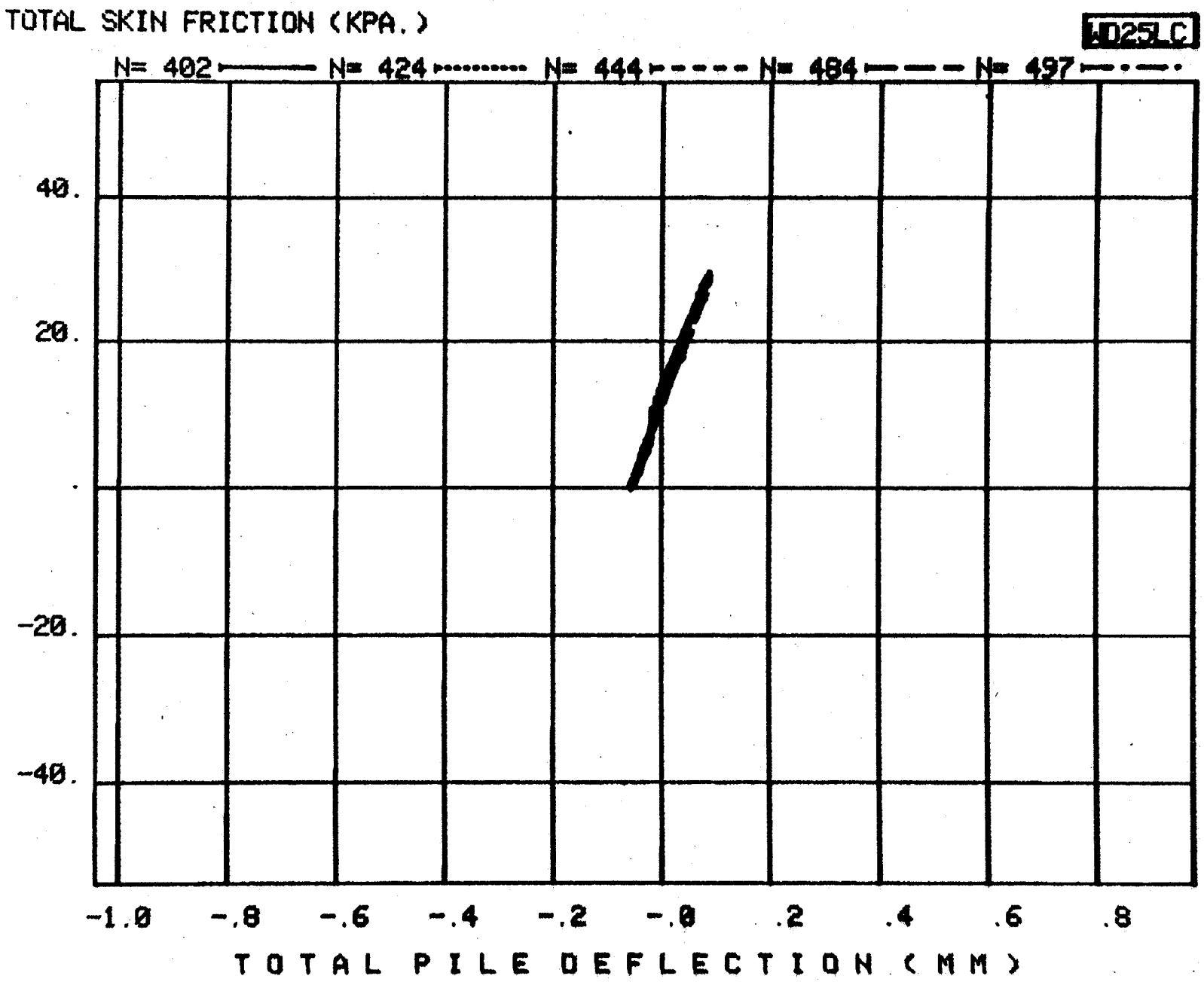
TOTAL SKIN FRICTION (KPA.)
WD25LC
N= 402
N= 424
N= 444
N= 484
N= 497
40.
20.
-20.
-40.
-1.0
-.8
-.6
-.4
-.2
-.0
.2
.4
.6
.8
TOTAL PILE DEFLECTION (MM)

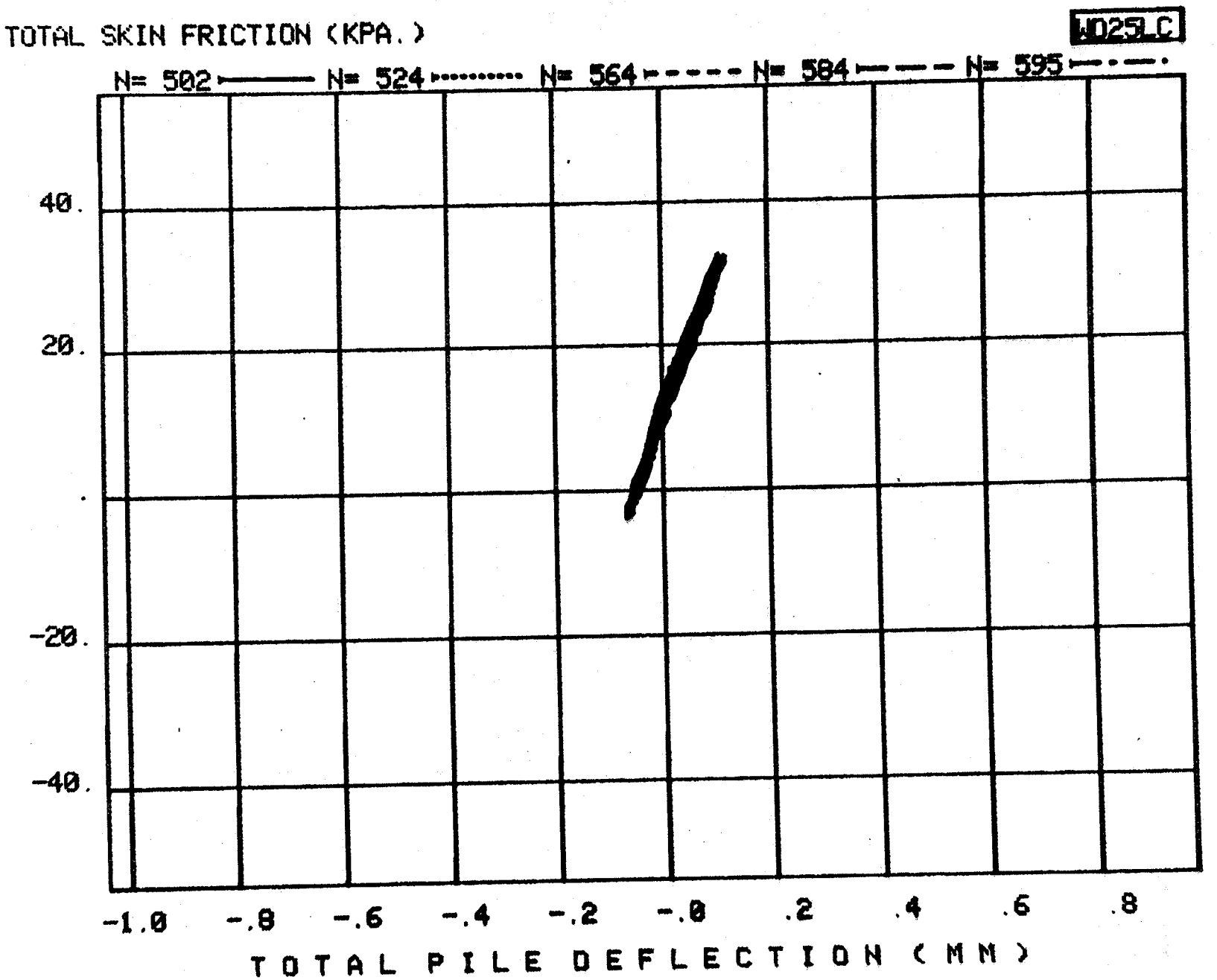
TOTAL SKIN FRICTION (KPA.)
W025LC
N= 502
N= 524
N= 564
N= 584
N= 595
40.
20.
-20.
-40.
-1.0
-.8
-.6
-.4
-.2
-.0
.2
.4
.6
.8
TOTAL PILE DEFLECTION (MM)

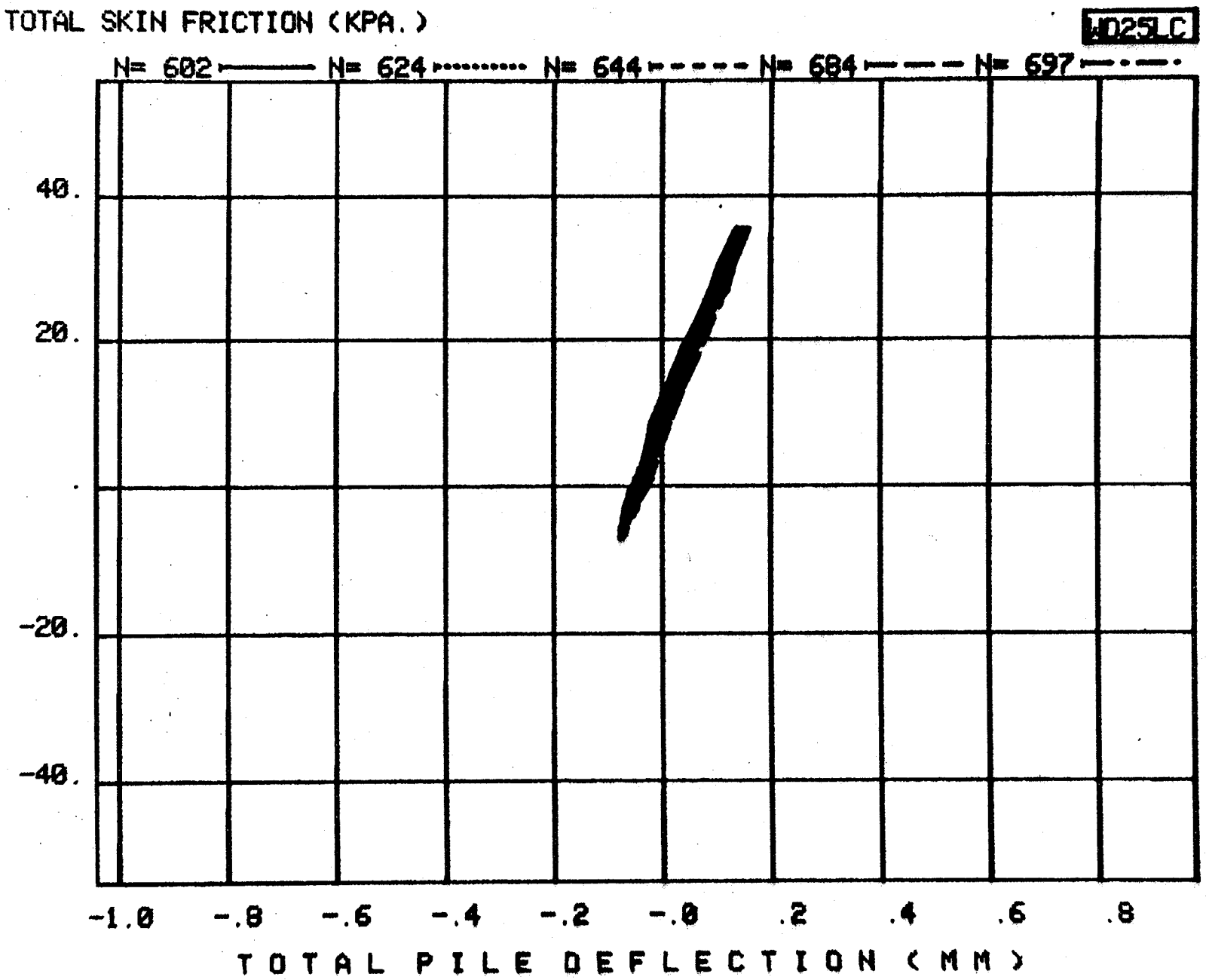
TOTAL SKIN FRICTION (KPA.)
WD25LC
N= 602
N= 624
N= 644
N= 684
N= 697
40.
20.
-20.
-40.
-1.0
-.8
-.6
-.4
-.2
-.0
.2
.4
.6
.8
TOTAL PILE DEFLECTION (MM)

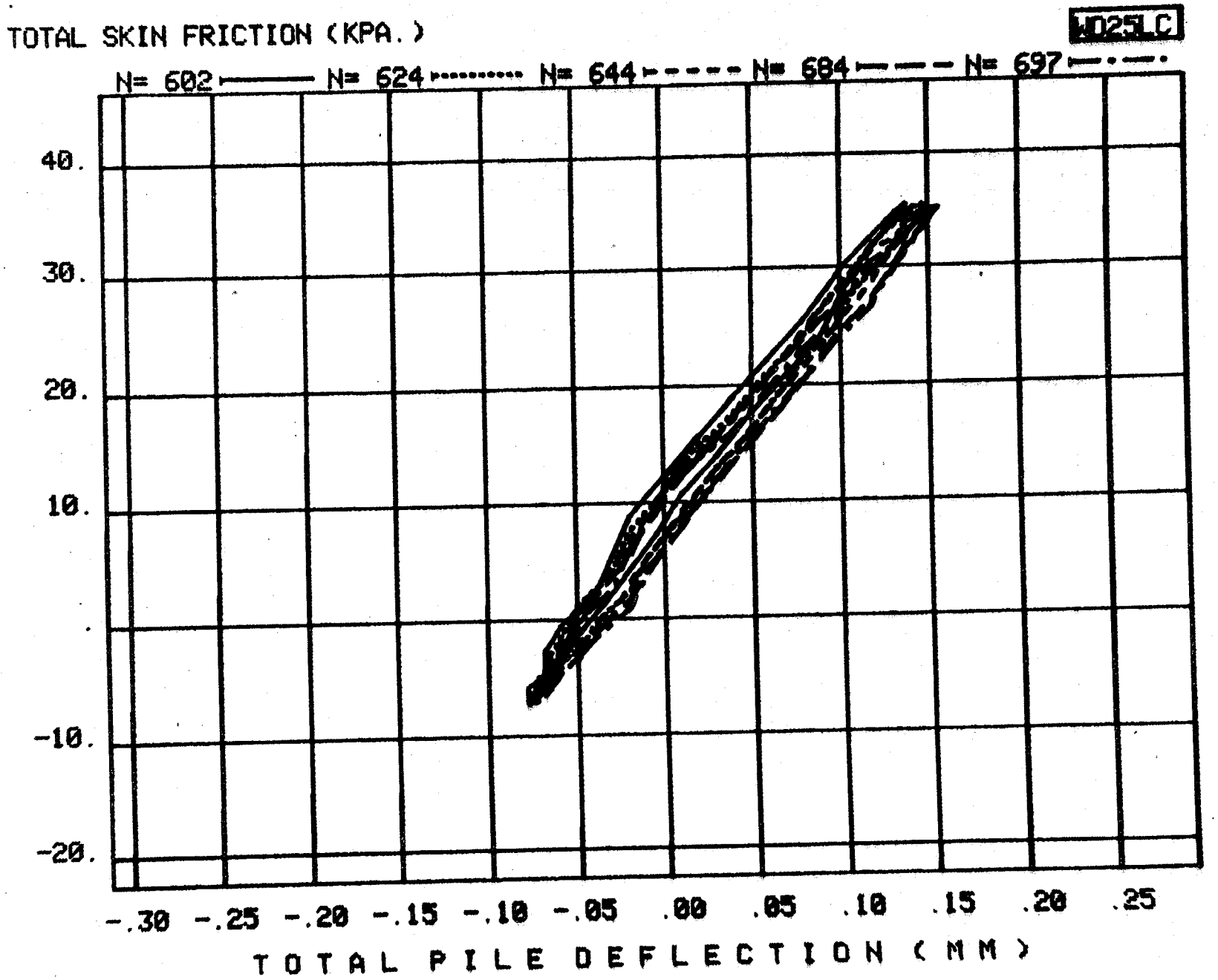
TOTAL SKIN FRICTION (KPA.)
W025LC
N= 602
N= 624
N= 644
N= 684
N= 697
40.
30.
20.
10.
-10.
-20.
-.30
-.25
-.20
-.15
-.10
-.05
.00
.05
.10
.15
.20
.25
TOTAL PILE DEFLECTION (MM)

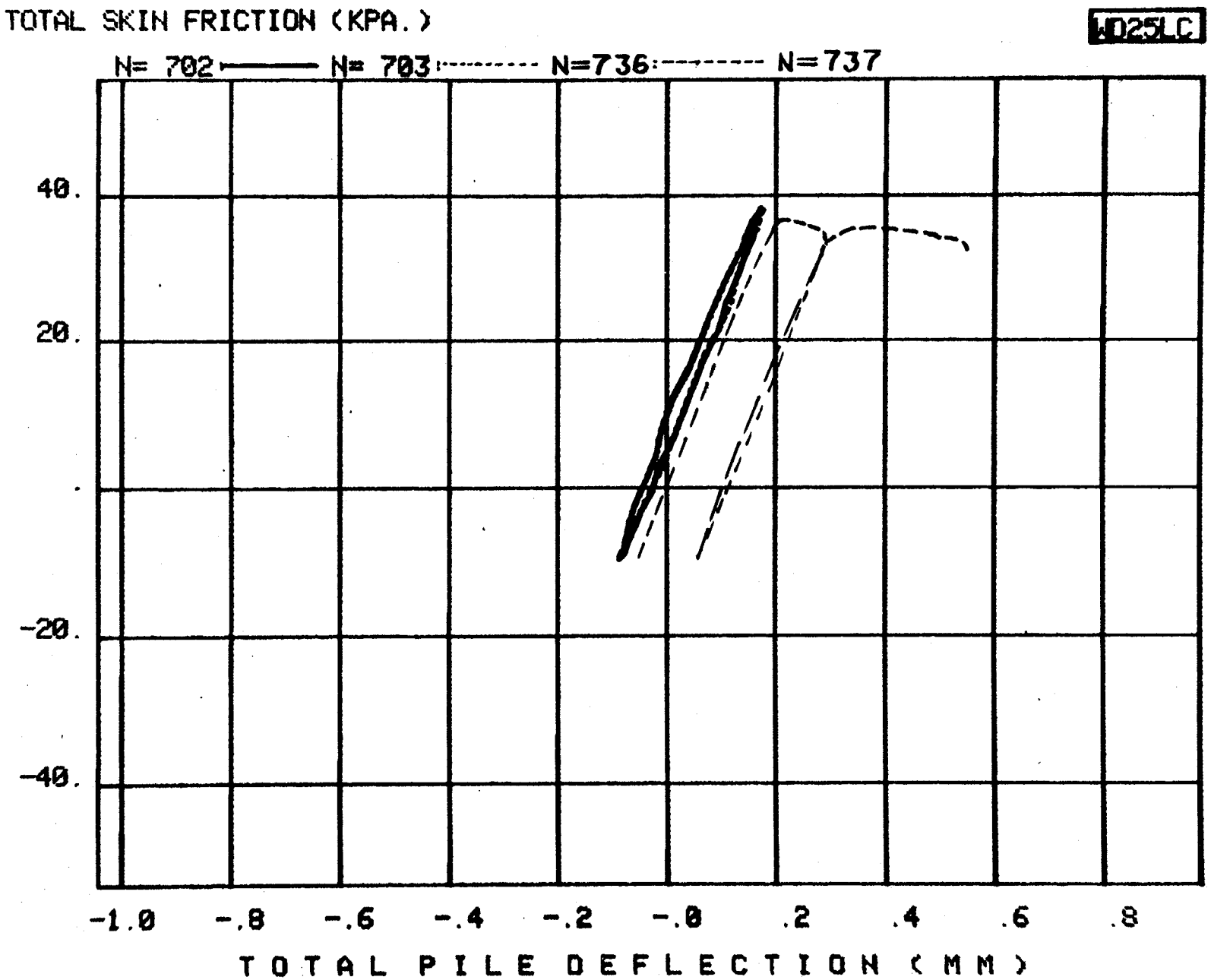
TOTAL SKIN FRICTION (KPA.)
WD25LC
N= 702
N= 703
N=736
N=737
40.
20.
-20.
-40.
-1.0
-.8
-.6
-.4
-.2
-.0
.2
.4
.6
.8
TOTAL PILE DEFLECTION (MM)

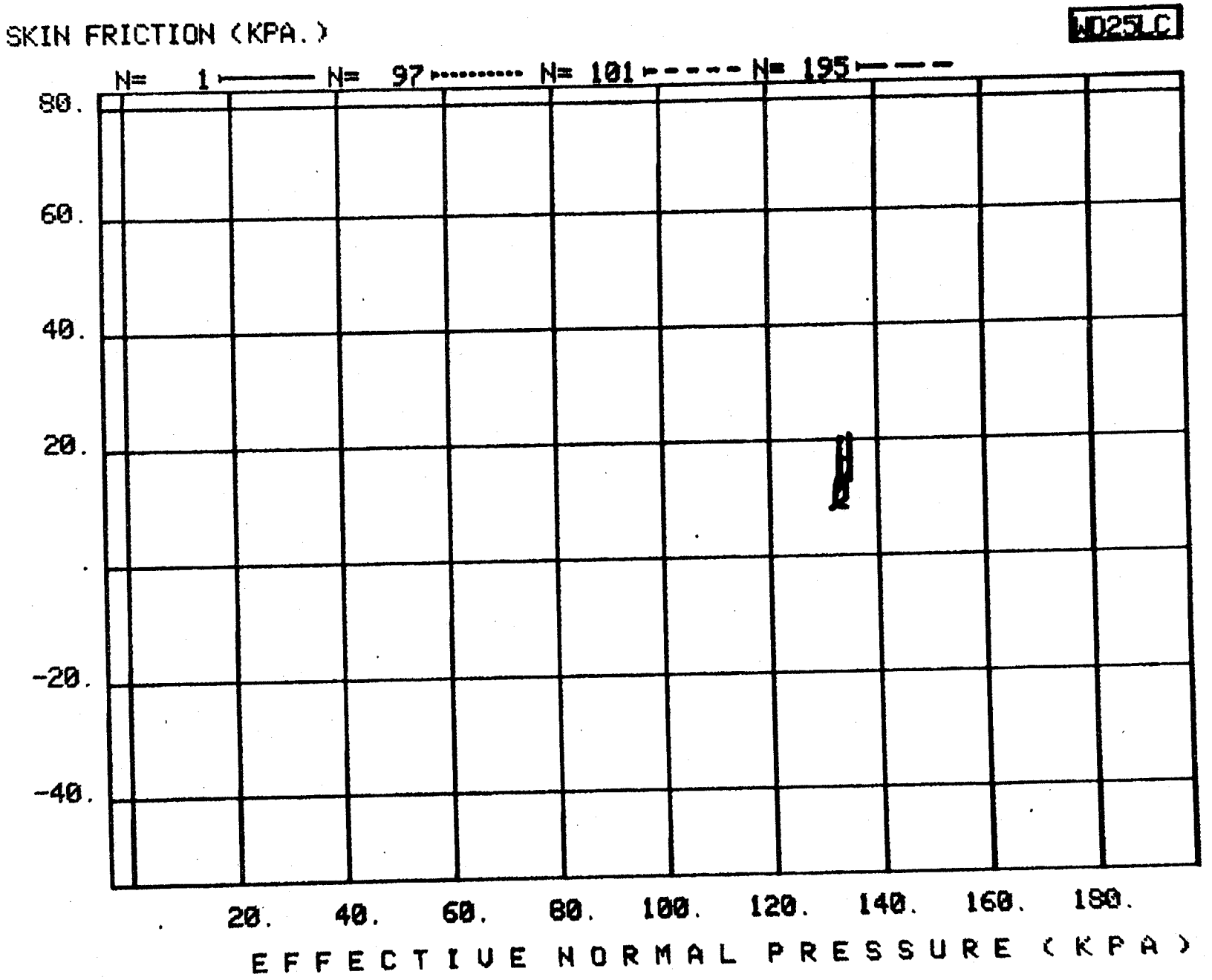
SKIN FRICTION (KPA.)
W025LC
N= 1
N= 97
N= 101
N= 195
80.
60.
40.
20.
-20.
-40.
20.
40.
60.
80.
100.
120.
140.
160.
180.
EFFECTIVE NORMAL PRESSURE (KPA)

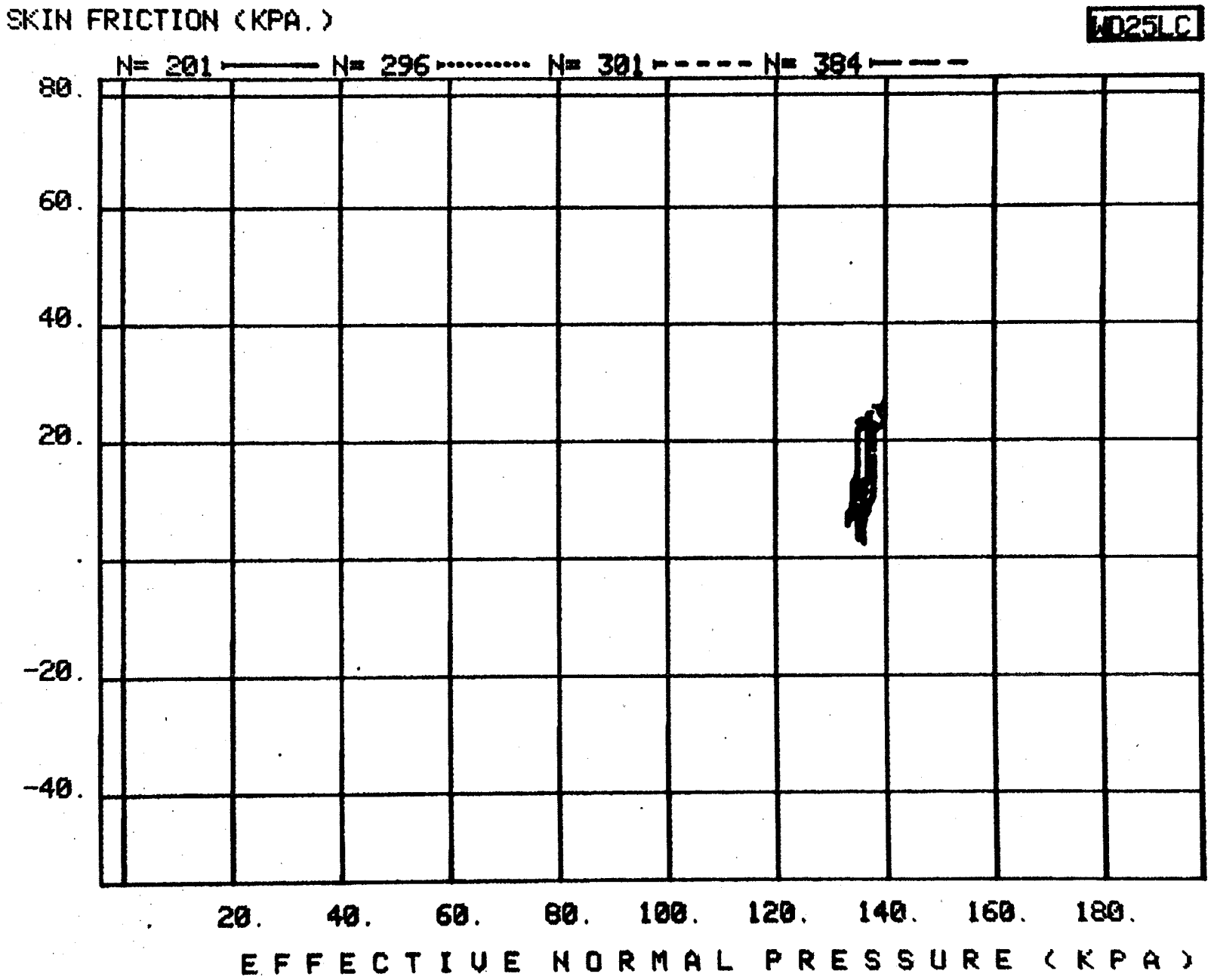
SKIN FRICTION (KPA.)
WD25LC
N= 201
N= 296
N= 301
N= 384
80.
60.
40.
20.
-20.
-40.
20.
40.
60.
80.
100.
120.
140.
160.
180.
EFFECTIVE NORMAL PRESSURE (KPA)

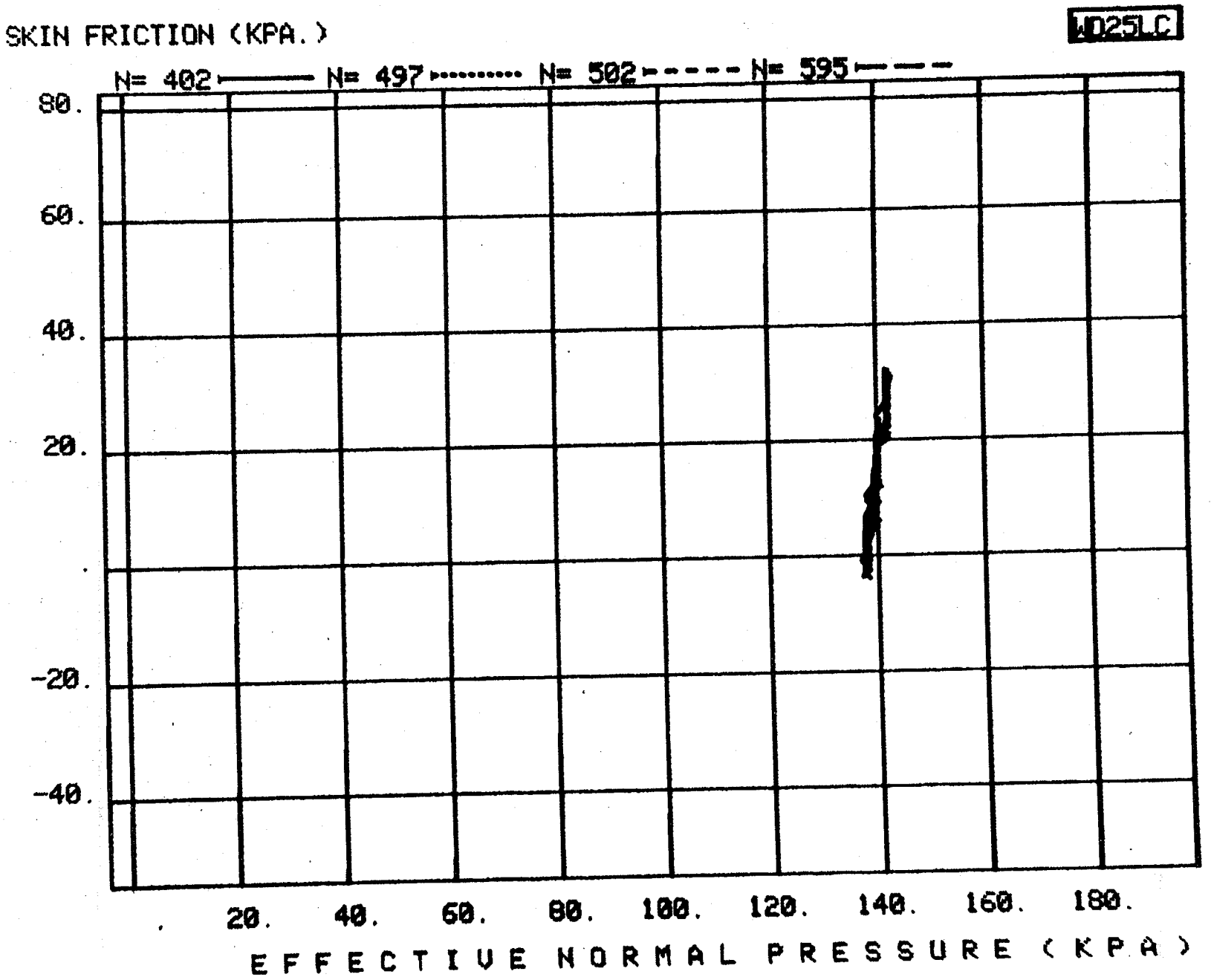
SKIN FRICTION (KPA.)
WD25LC
N= 402
N= 497
N= 502
N= 595
80.
60.
40.
20.
-20.
-40.
20.
40.
60.
80.
100.
120.
140.
160.
180.
EFFECTIVE NORMAL PRESSURE (KPA)

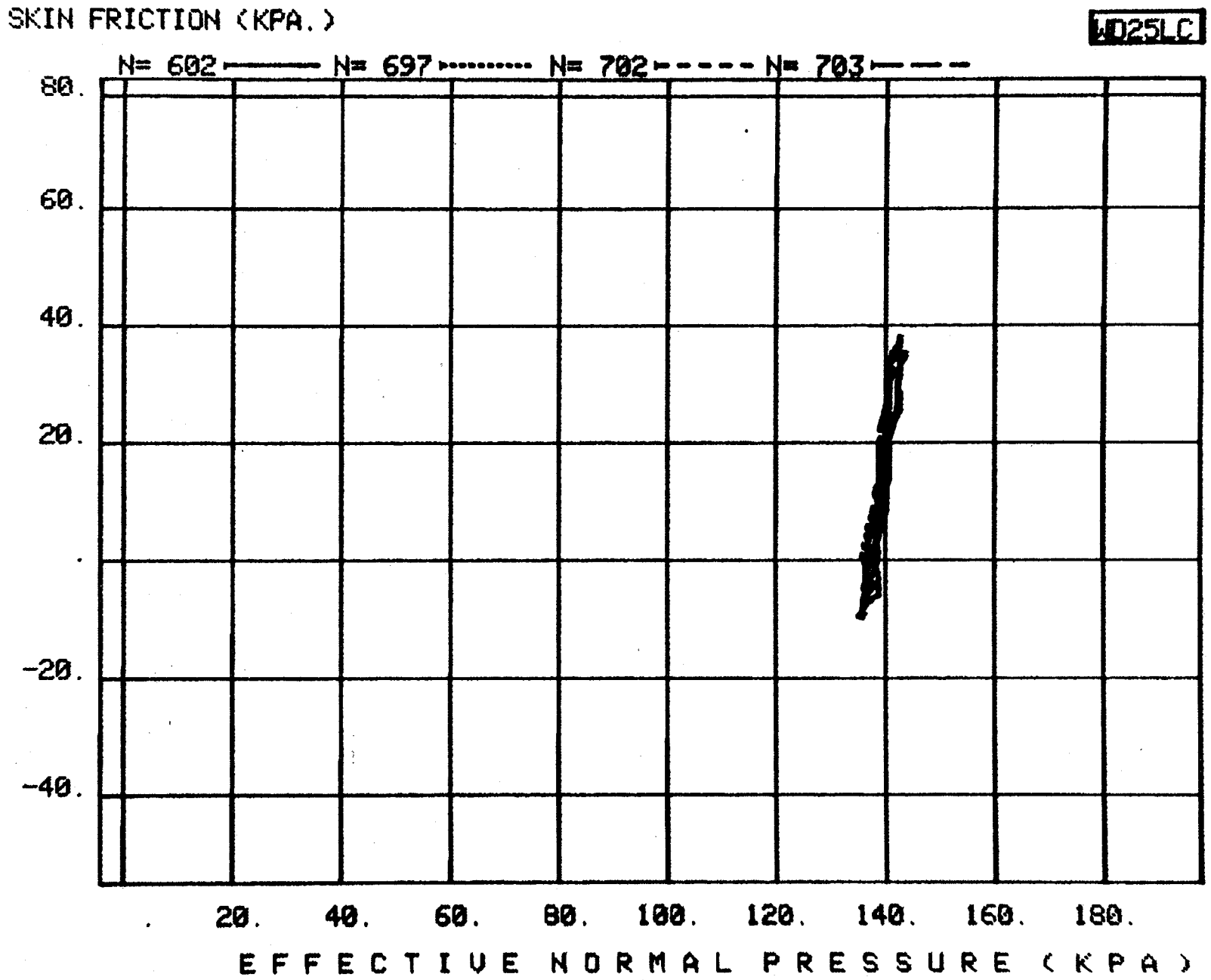
SKIN FRICTION (KPA.)
WD25LC
N= 602
N= 697
N= 702
N= 703
80.
60.
40.
20.
-20.
-40.
20.
40.
60.
80.
100.
120.
140.
160.
180.
EFFECTIVE NORMAL PRESSURE (KPA)

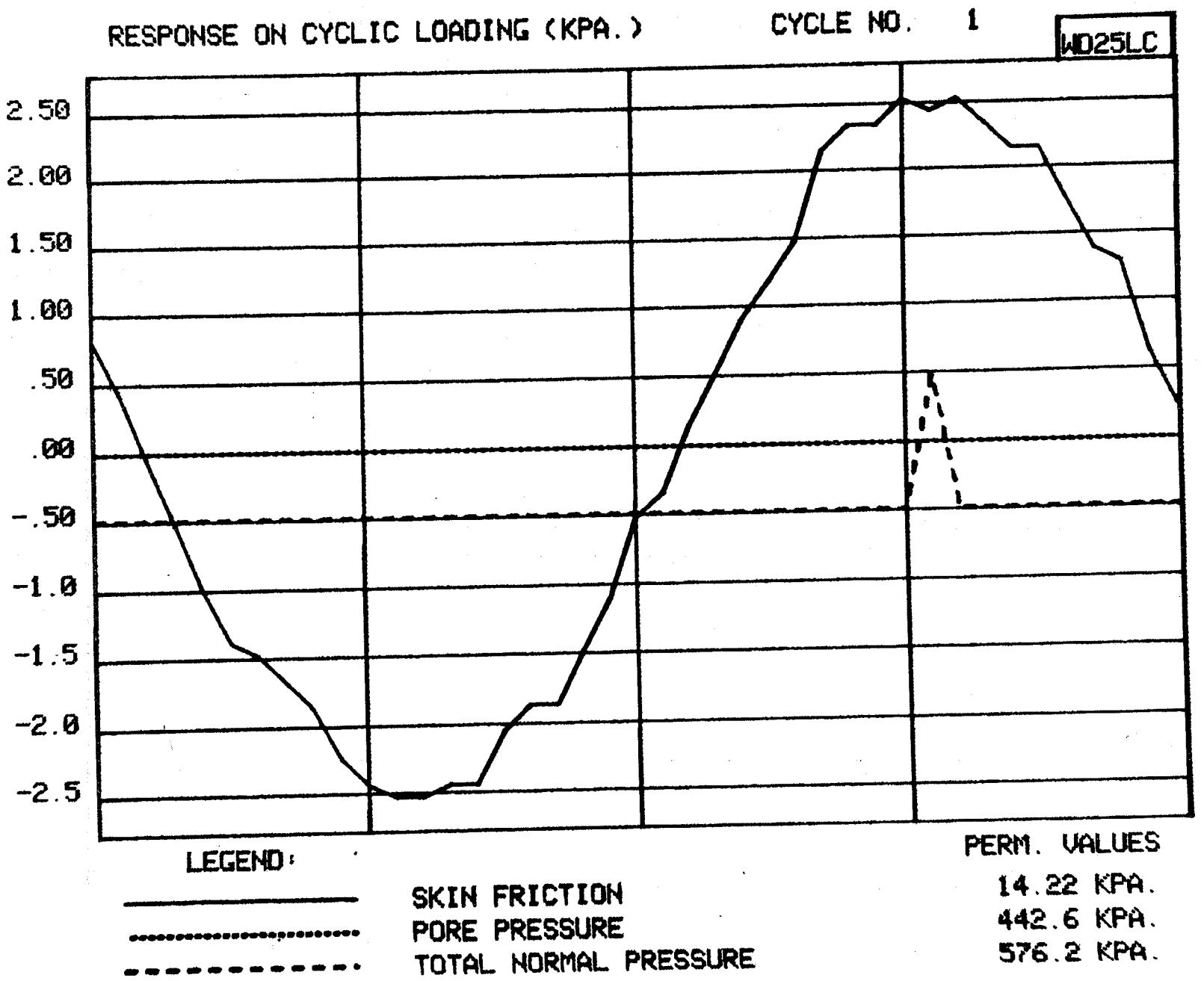
RESPONSE ON CYCLIC LOADING (KPA.)
CYCLE NO. 1
WD25LC
2.50
2.00
1.50
1.00
.50
.00
-.50
-1.0
-1.5
-2.0
-2.5
LEGEND:
SKIN FRICTION
PORE PRESSURE
TOTAL NORMAL PRESSURE
PERM. VALUES
14.22 KPA.
442.6 KPA.
576.2 KPA.

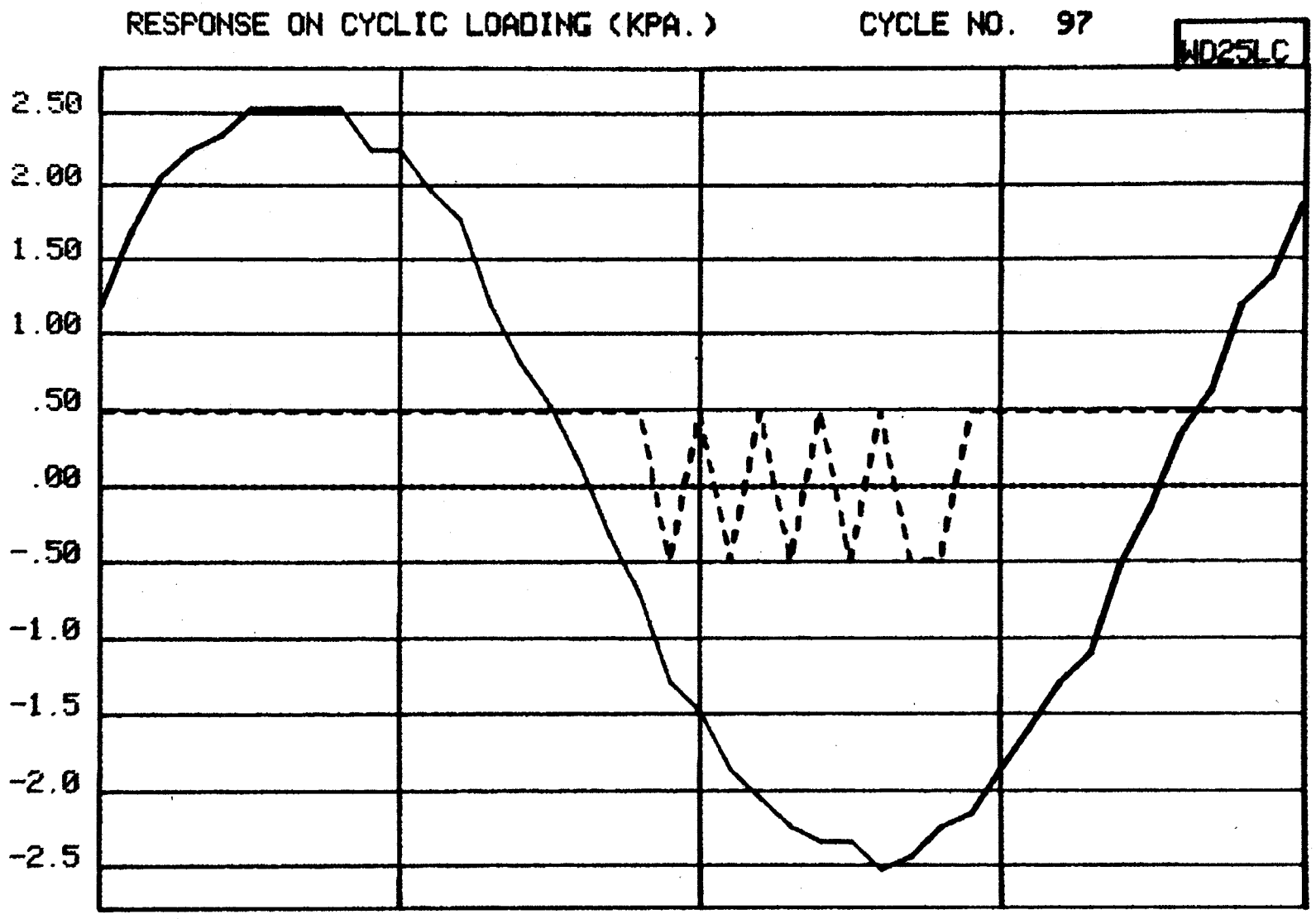

LEGEND:		PERM. VALUES
———	SKIN FRICTION	14.22 KPA.
·····	PORE PRESSURE	442.6 KPA.
- - - -	TOTAL NORMAL PRESSURE	575.2 KPA.

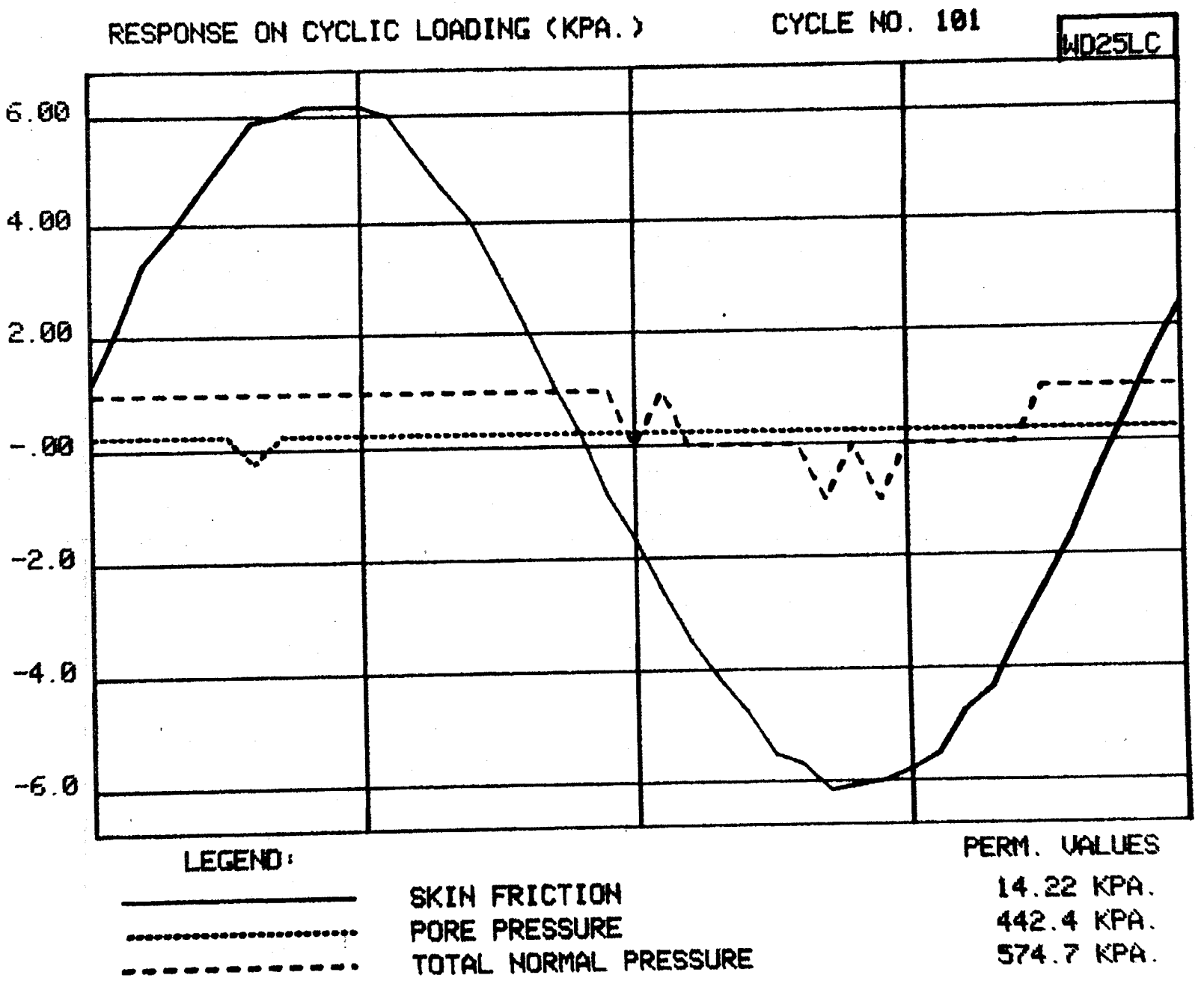
RESPONSE ON CYCLIC LOADING (KPA.)
CYCLE NO. 101
WD25LC
6.00
4.00
2.00
-.00
-2.0
-4.0
-6.0
LEGEND:
SKIN FRICTION
PORE PRESSURE
TOTAL NORMAL PRESSURE
PERM. VALUES
14.22 KPA.
442.4 KPA.
574.7 KPA.

RESPONSE ON CYCLIC LOADING (KPA.) CYCLE NO. 195

WD25LC

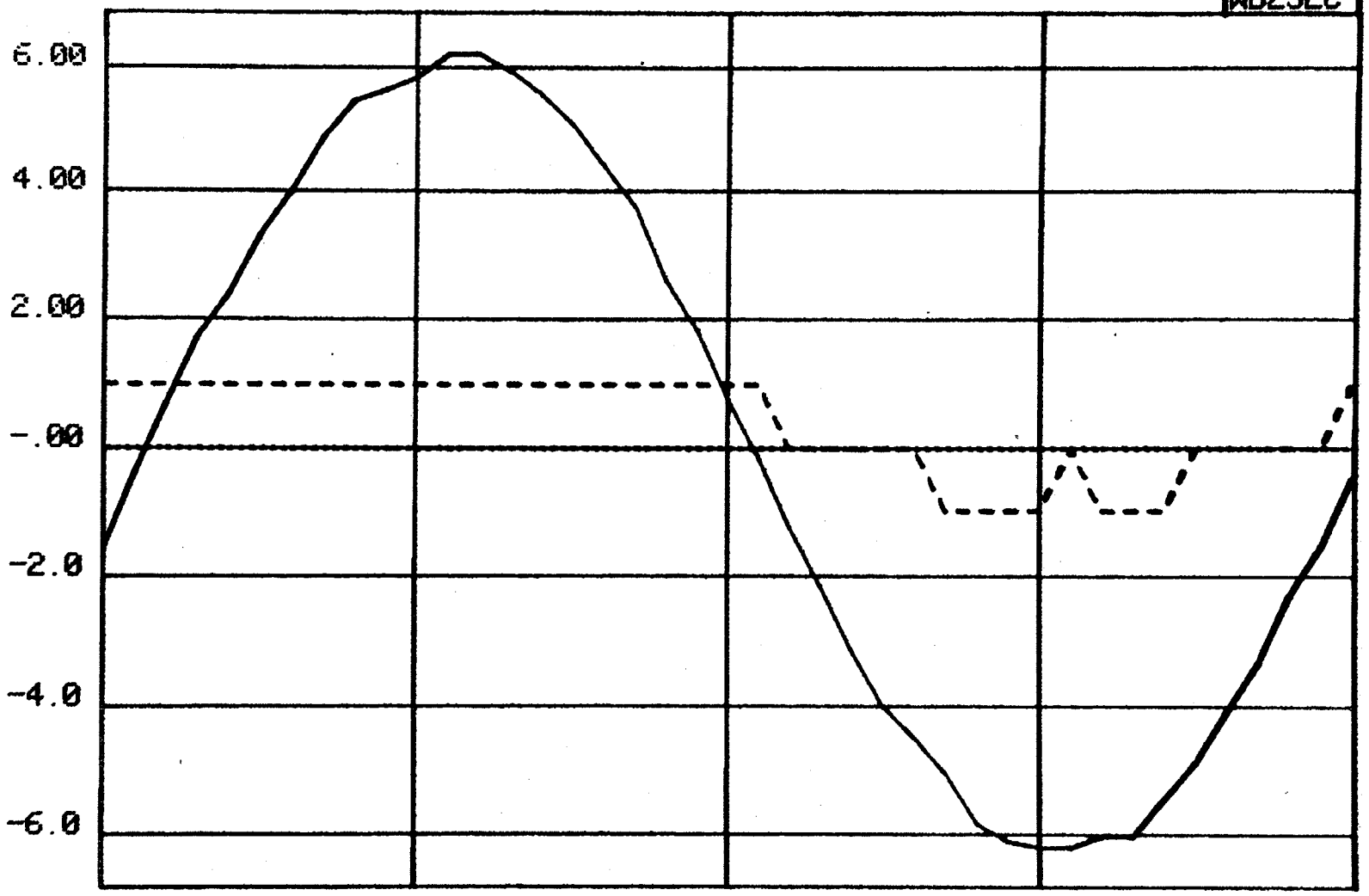

LEGEND:

		PERM. VALUES
———	SKIN FRICTION	14.56 KPA.
·····	PORE PRESSURE	440.7 KPA.
- - - -	TOTAL NORMAL PRESSURE	574.7 KPA.

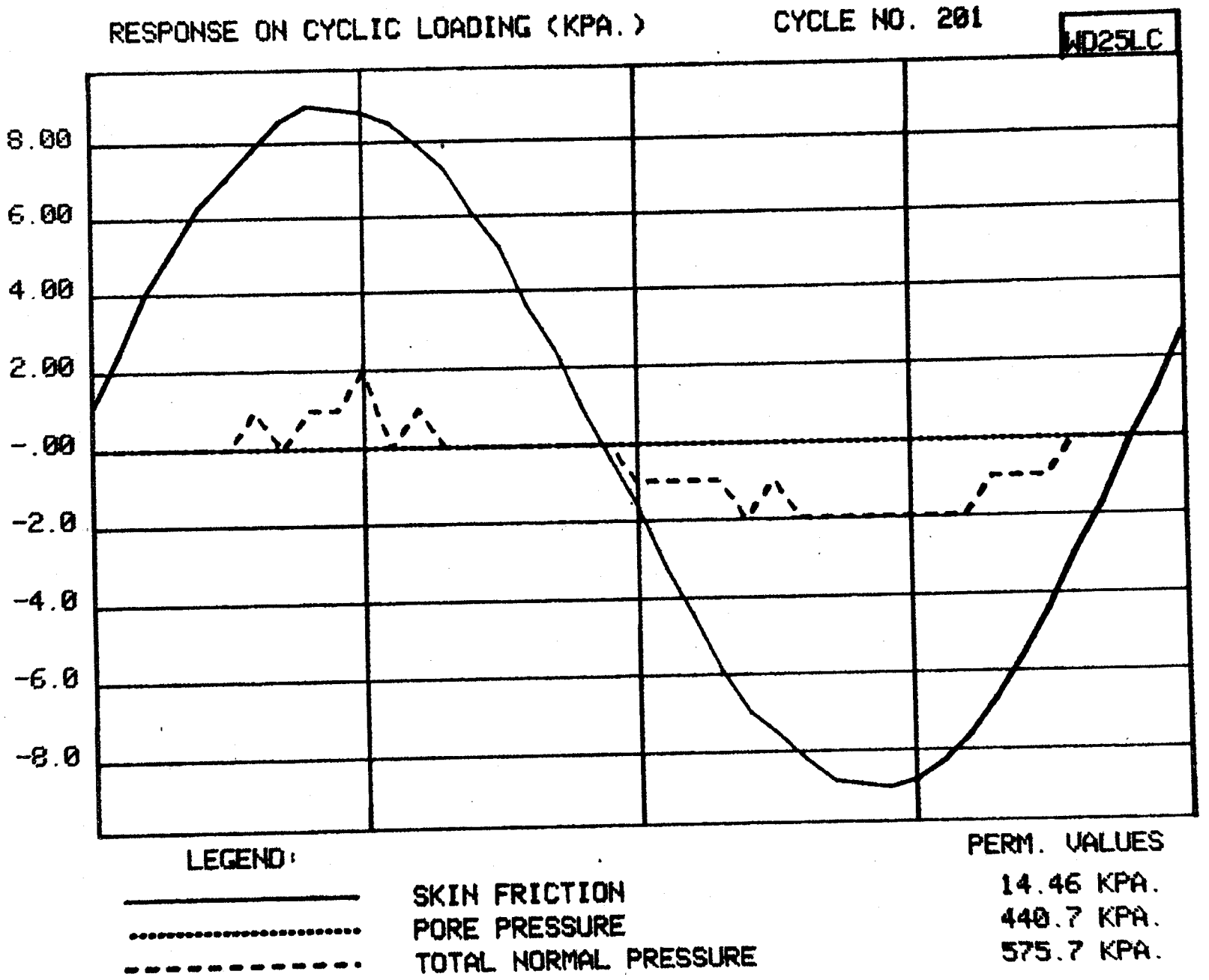
RESPONSE ON CYCLIC LOADING (KPA.)
CYCLE NO. 201
WD25LC
8.00
6.00
4.00
2.00
-.00
-2.0
-4.0
-6.0
-8.0
LEGEND:
SKIN FRICTION
PORE PRESSURE
TOTAL NORMAL PRESSURE
PERM. VALUES
14.46 KPA.
440.7 KPA.
575.7 KPA.

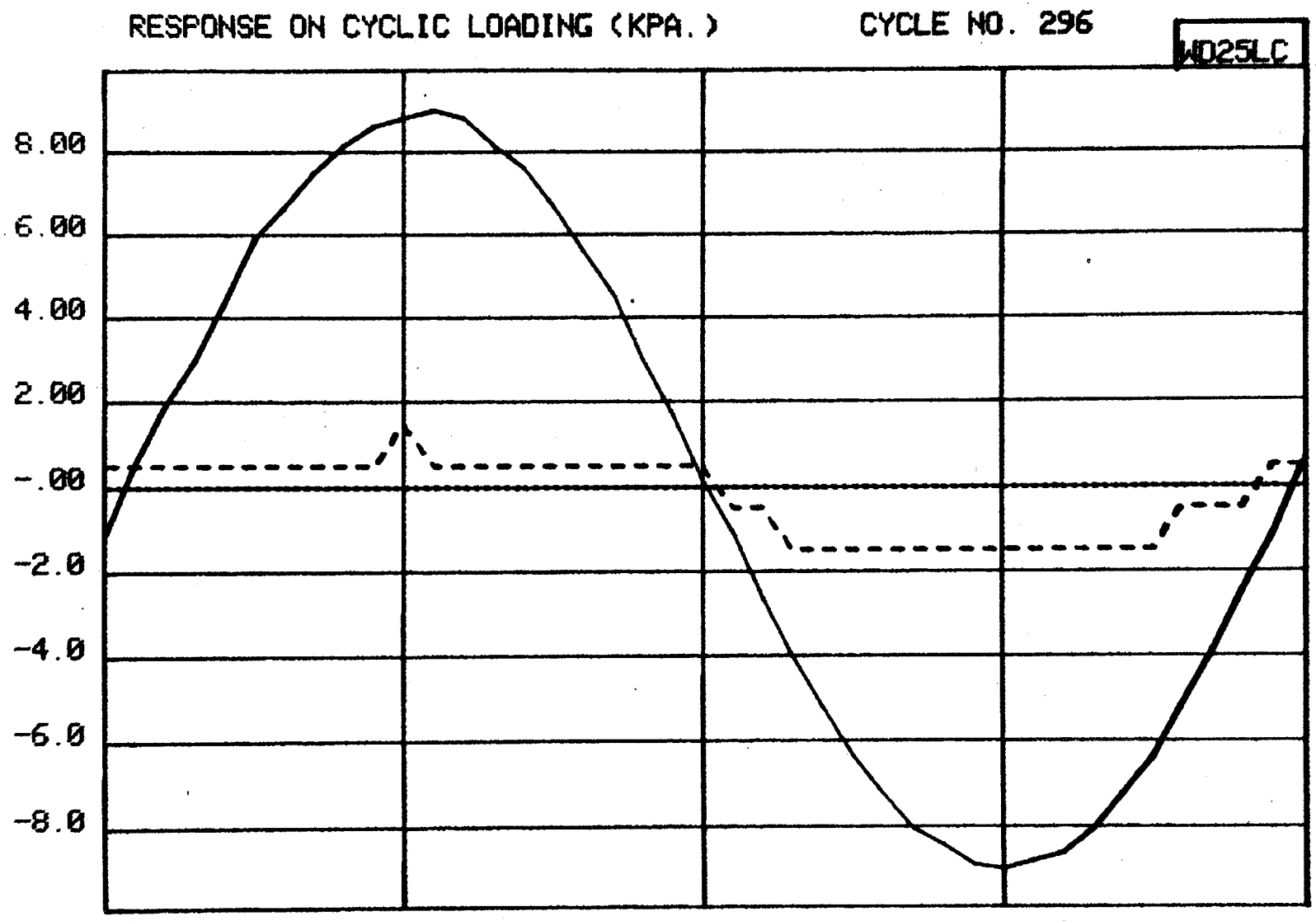

LEGEND:

		PERM. VALUES
———	SKIN FRICTION	14.13 KPA.
·····	PORE PRESSURE	438.8 KPA.
- - - -	TOTAL NORMAL PRESSURE	575.2 KPA.

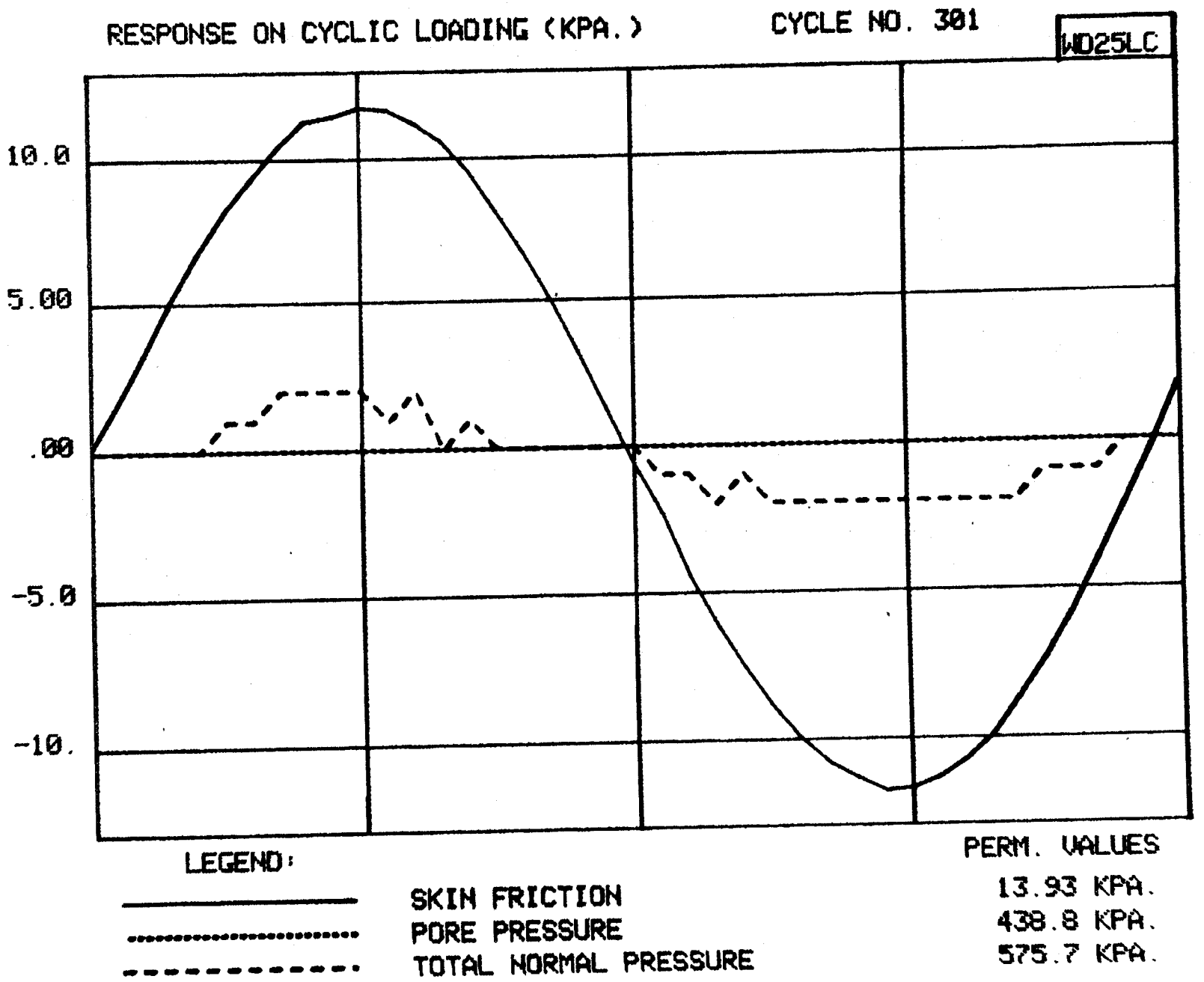
RESPONSE ON CYCLIC LOADING (KPA.)
CYCLE NO. 301
WD25LC
10.0
5.00
.00
-5.0
-10.
LEGEND:
SKIN FRICTION
PORE PRESSURE
TOTAL NORMAL PRESSURE
PERM. VALUES
13.93 KPA.
438.8 KPA.
575.7 KPA.

RESPONSE ON CYCLIC LOADING (KPA.) CYCLE NO. 384

WD25LC

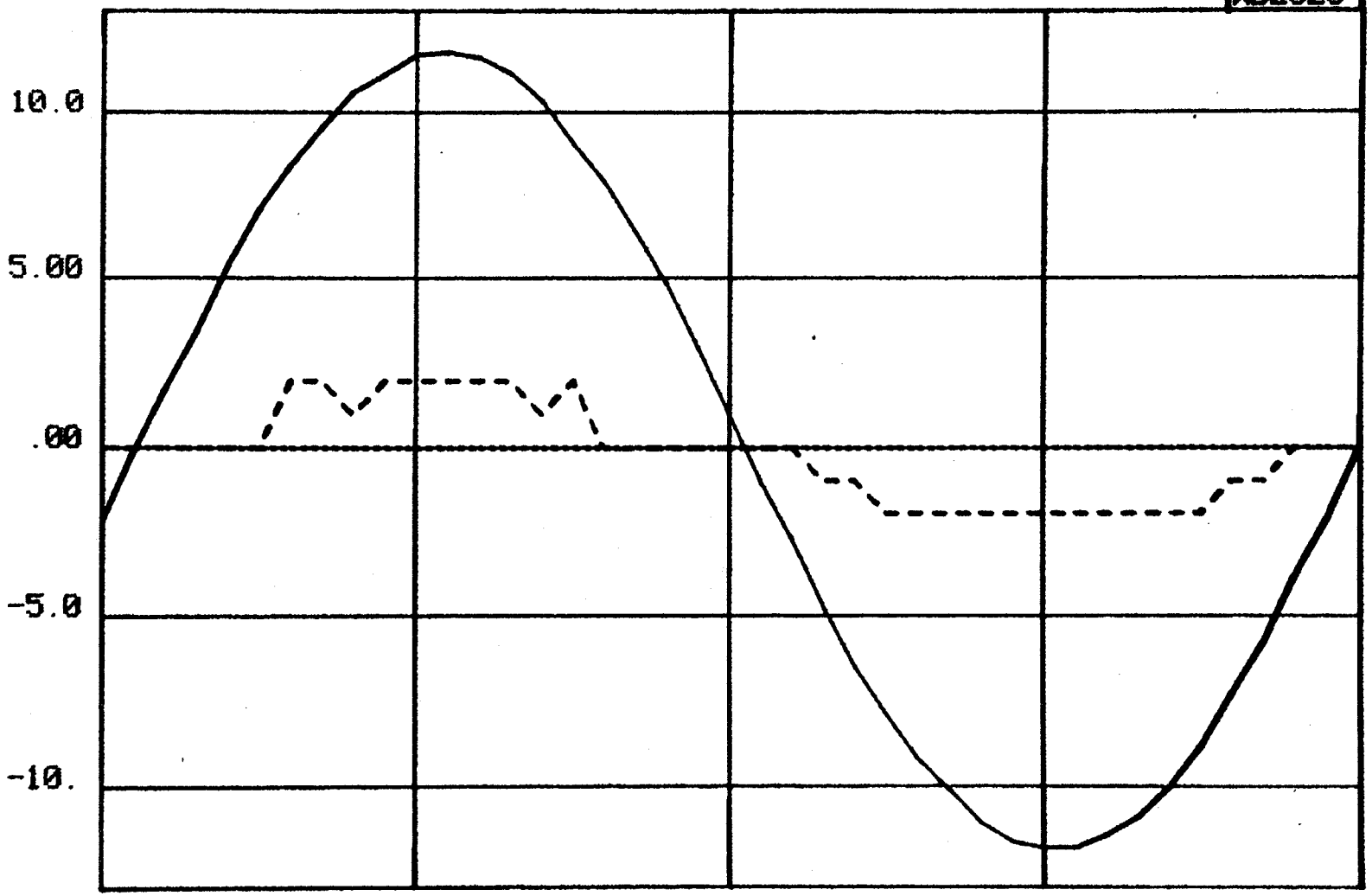

LEGEND:

		PERM. VALUES
————	SKIN FRICTION	14.46 KPA.
·····	PORE PRESSURE	437.8 KPA.
- - - - -	TOTAL NORMAL PRESSURE	575.7 KPA.

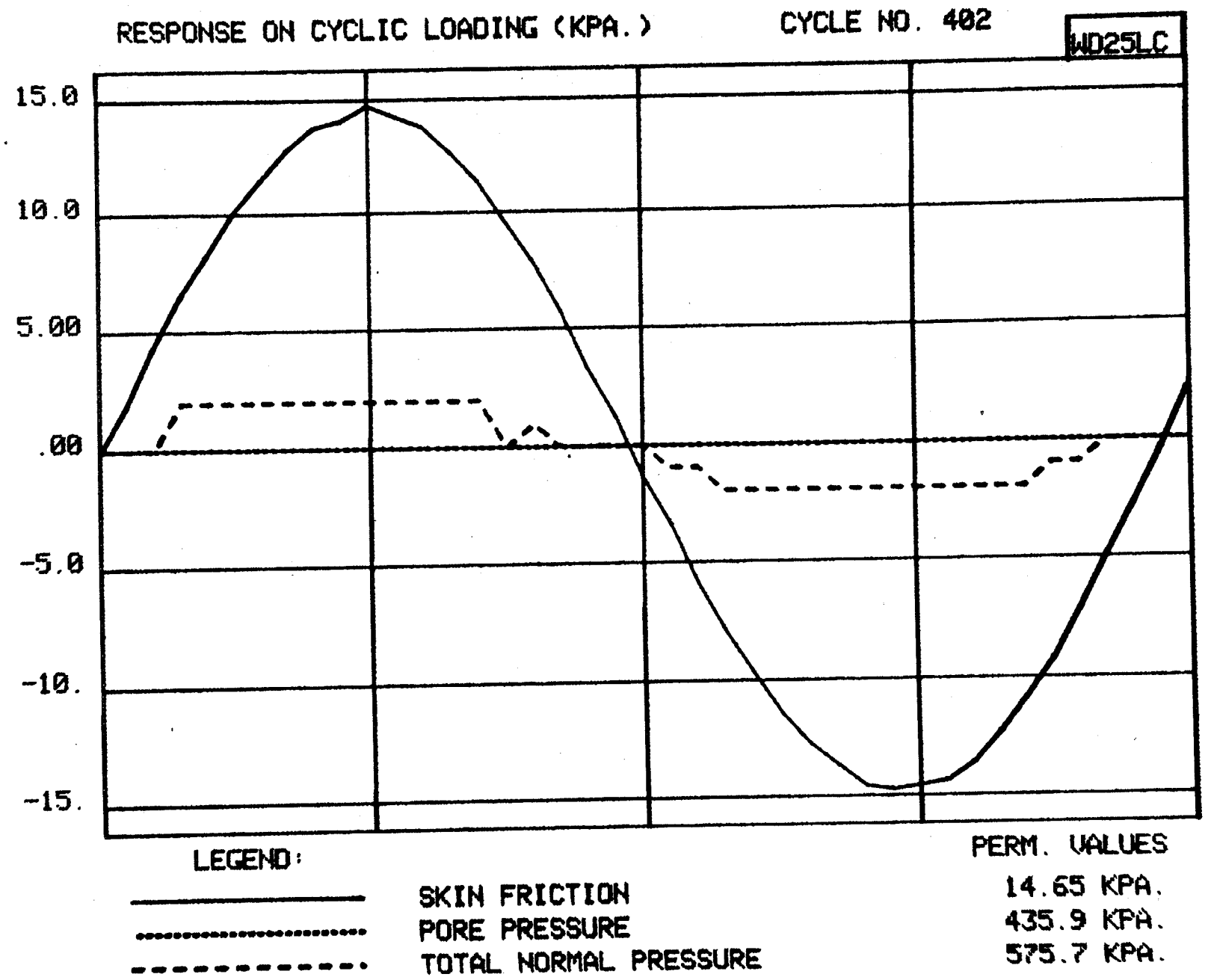
RESPONSE ON CYCLIC LOADING (KPA.)
CYCLE NO. 402
WD25LC
15.0
10.0
5.00
.00
-5.0
-10.
-15.
LEGEND:
SKIN FRICTION
PORE PRESSURE
TOTAL NORMAL PRESSURE
PERM. VALUES
14.65 KPA.
435.9 KPA.
575.7 KPA.

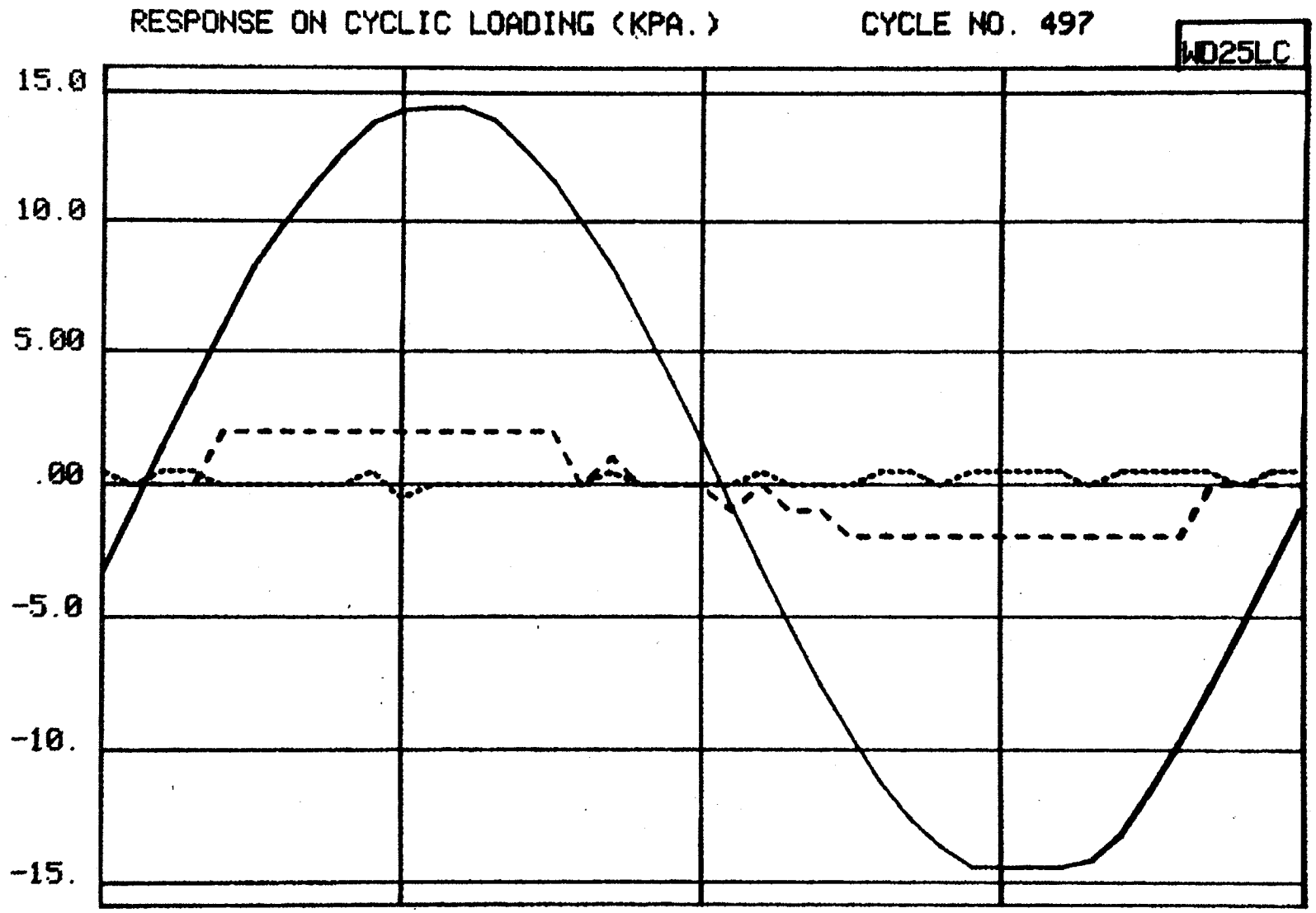

LEGEND:

		PERM. VALUES
———	SKIN FRICTION	14.75 KPA.
·····	PORE PRESSURE	435.4 KPA.
- - - -	TOTAL NORMAL PRESSURE	575.7 KPA.

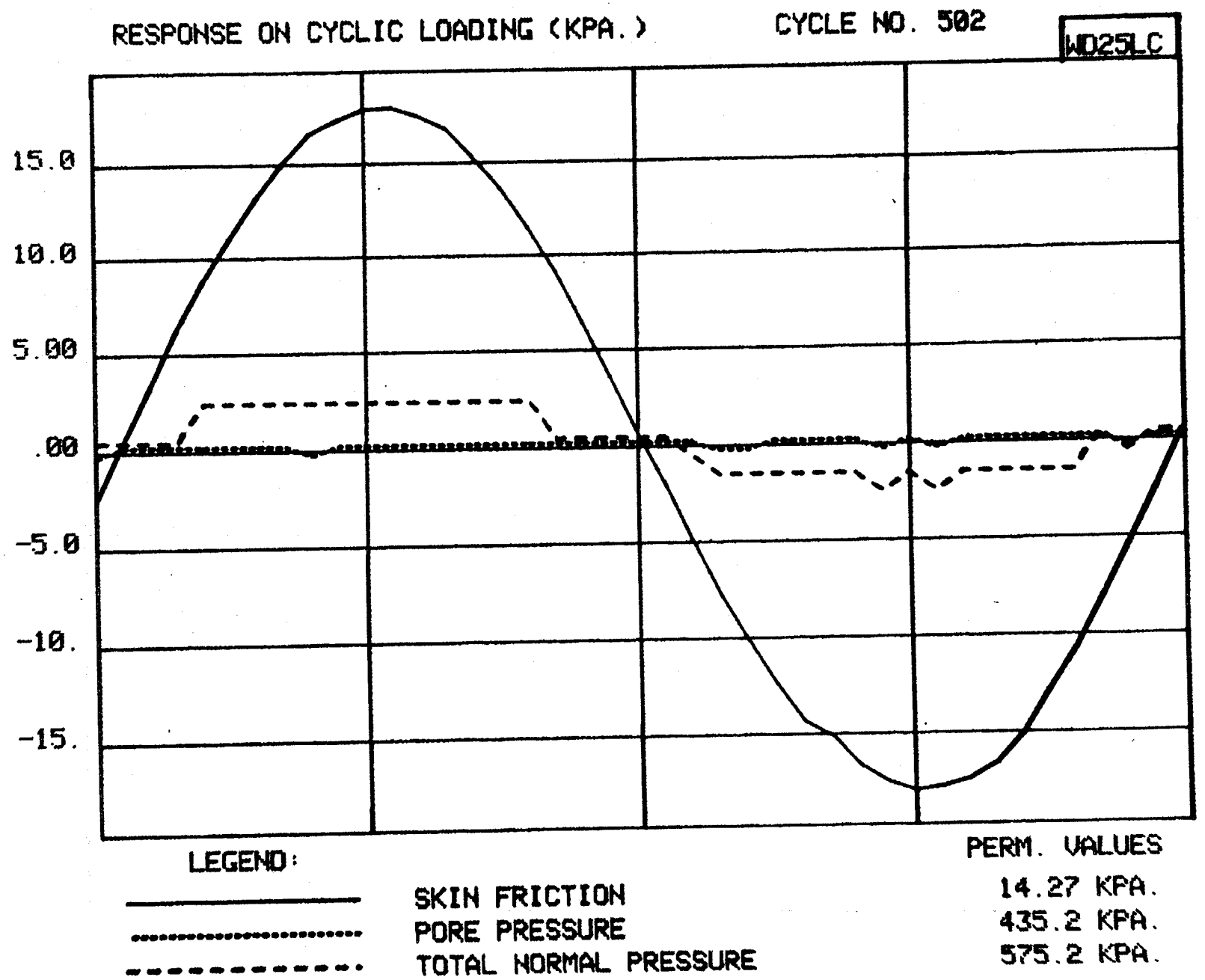
RESPONSE ON CYCLIC LOADING (KPA.)
CYCLE NO. 502
WD25LC
15.0
10.0
5.00
.00
-5.0
-10.
-15.
LEGEND:
SKIN FRICTION
PORE PRESSURE
TOTAL NORMAL PRESSURE
PERM. VALUES
14.27 KPA.
435.2 KPA.
575.2 KPA.

RESPONSE ON CYCLIC LOADING (KPA.) CYCLE NO. 595

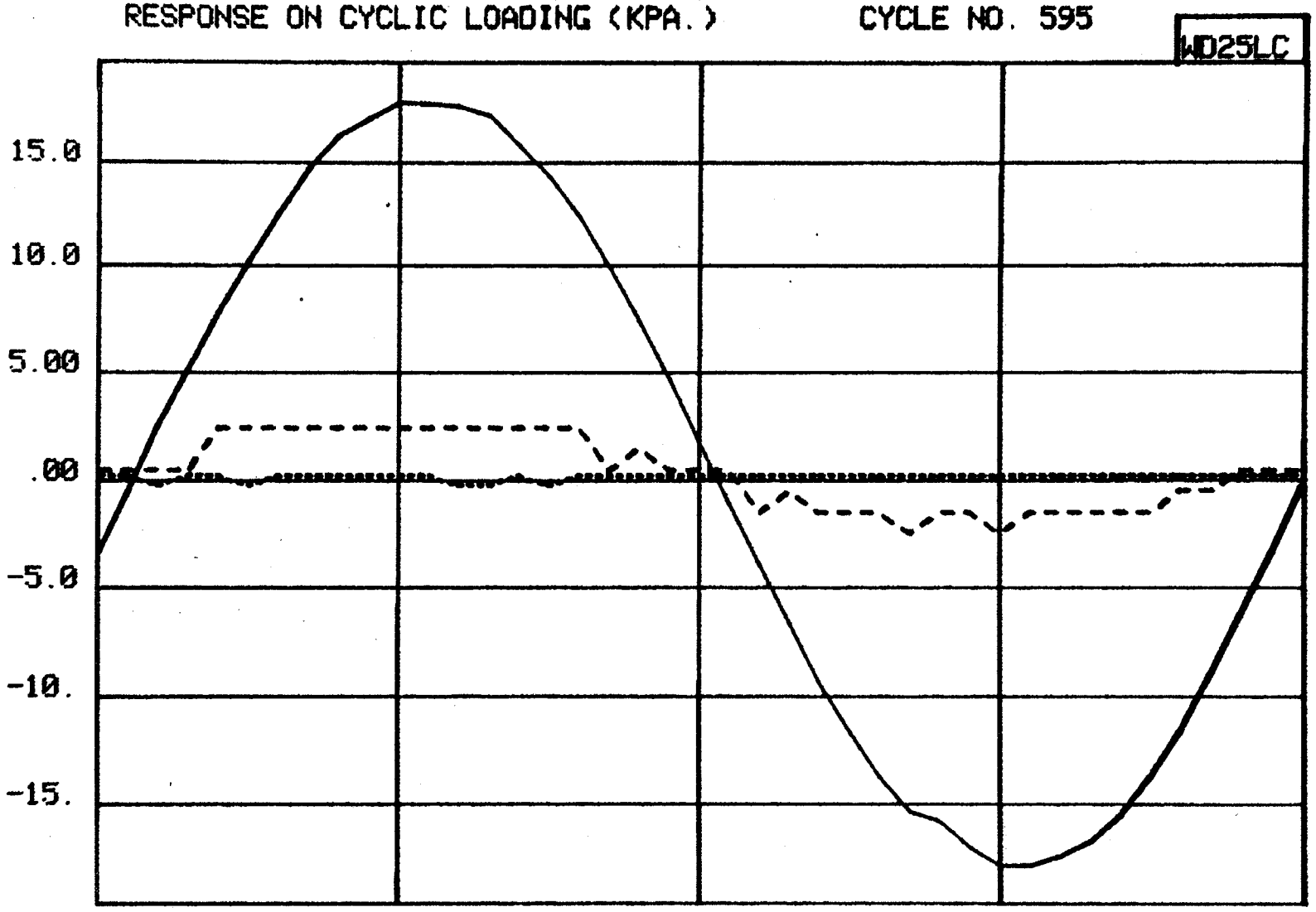

LEGEND:		PERM. VALUES
———	SKIN FRICTION	14.17 KPA.
·····	PORE PRESSURE	435.7 KPA.
- - - -	TOTAL NORMAL PRESSURE	575.2 KPA.

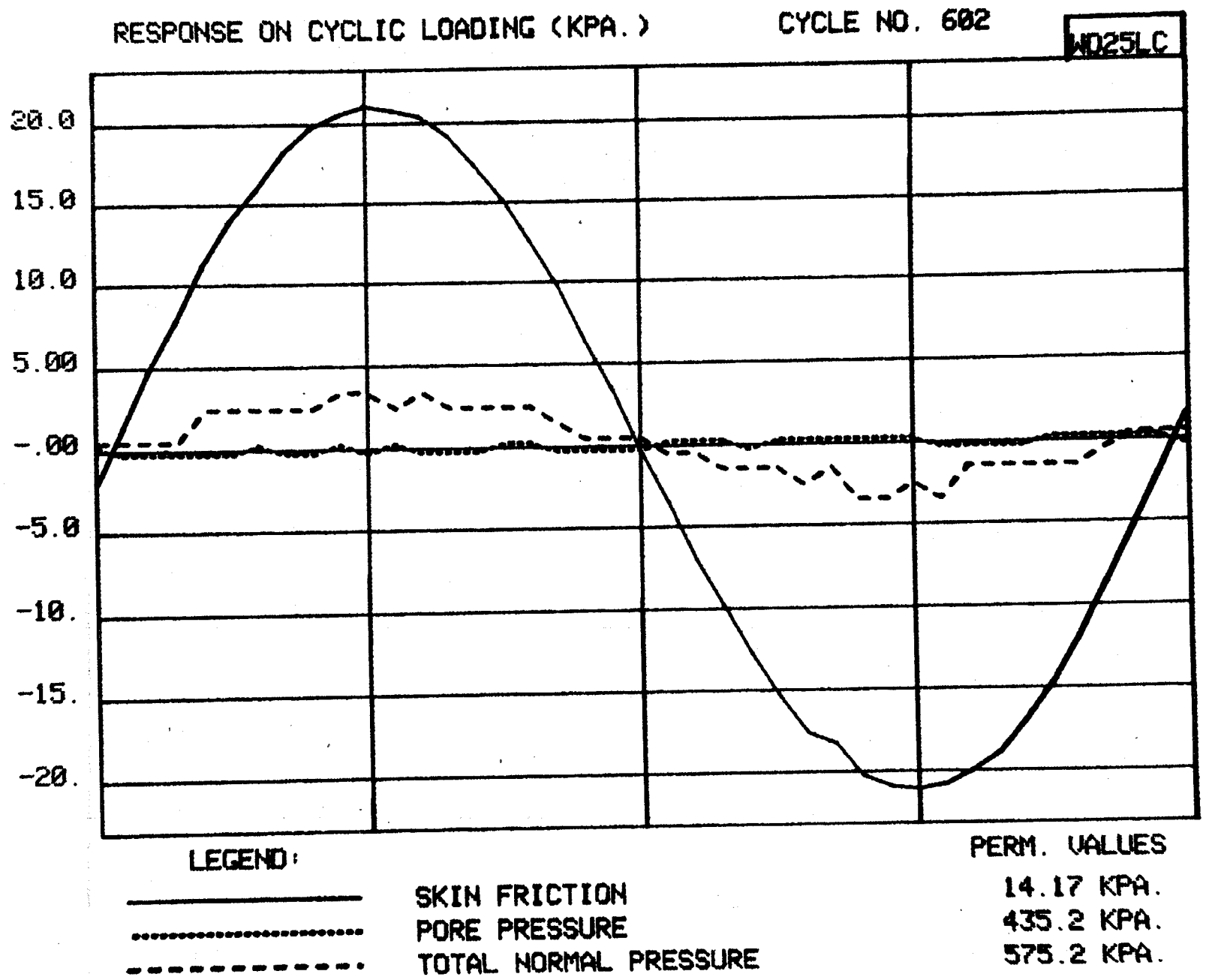
RESPONSE ON CYCLIC LOADING (KPA.)
CYCLE NO. 602
WD25LC
20.0
15.0
10.0
5.00
-.00
-5.0
-10.
-15.
-20.
LEGEND:
SKIN FRICTION
PORE PRESSURE
TOTAL NORMAL PRESSURE
PERM. VALUES
14.17 KPA.
435.2 KPA.
575.2 KPA.

RESPONSE ON CYCLIC LOADING (KPA.) CYCLE NO. 697

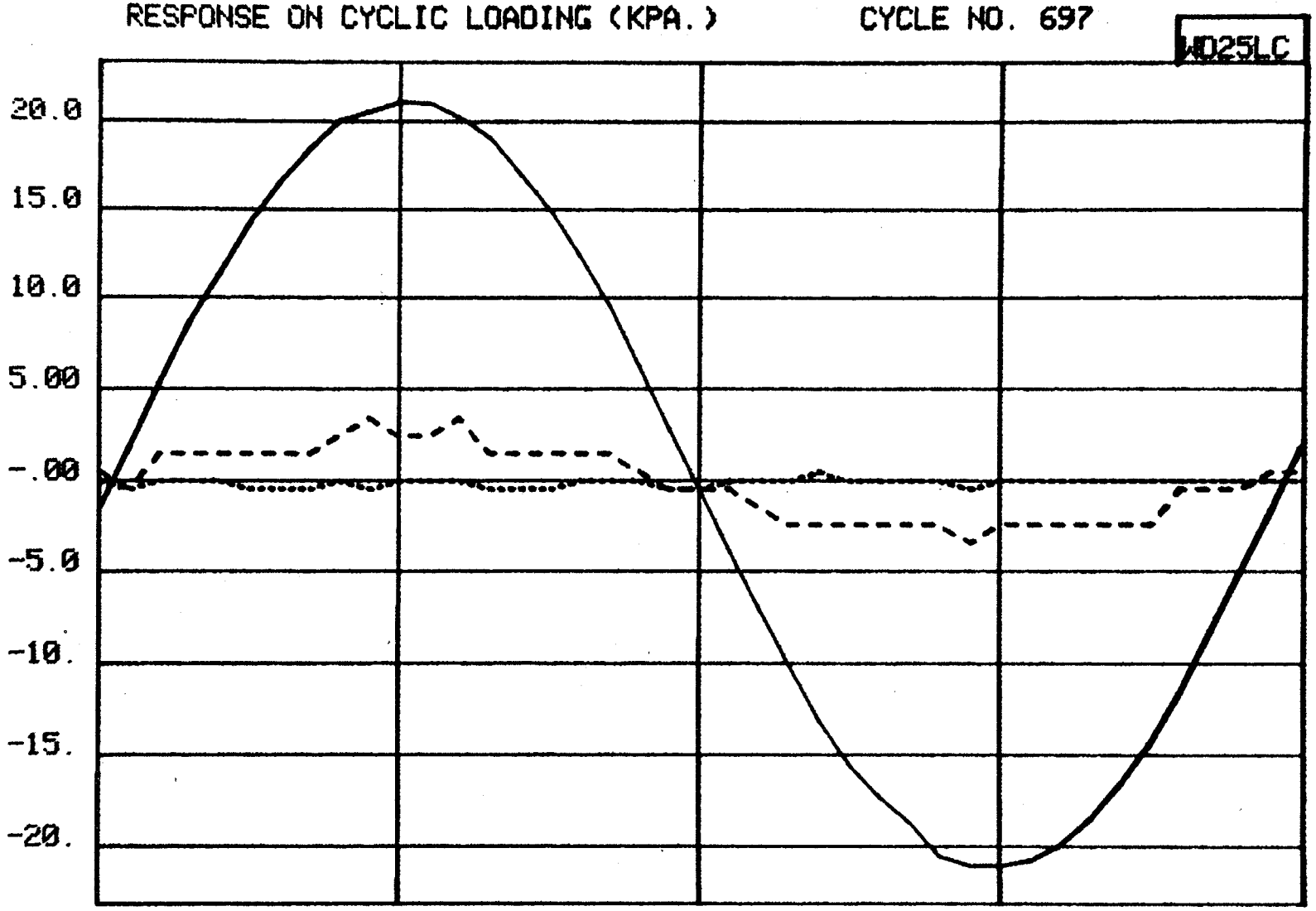

LEGEND:		PERM. VALUES
———	SKIN FRICTION	14.17 KPA.
·····	PORE PRESSURE	435.4 KPA.
- - - -	TOTAL NORMAL PRESSURE	574.2 KPA.

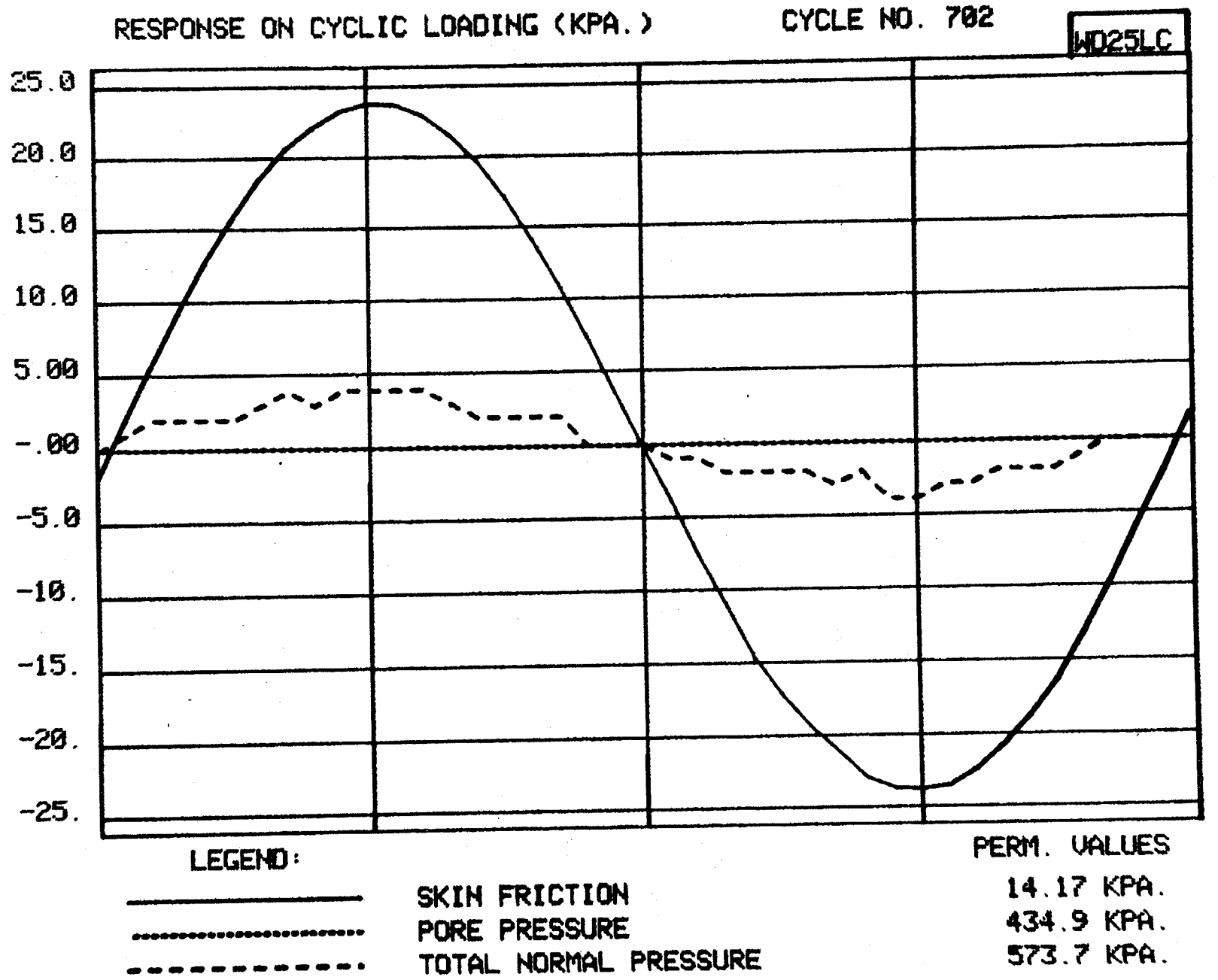
RESPONSE ON CYCLIC LOADING (KPA.)
CYCLE NO. 702
WD25LC
25.0
20.0
15.0
10.0
5.00
-.00
-5.0
-10.
-15.
-20.
-25.
LEGEND:
SKIN FRICTION
PORE PRESSURE
TOTAL NORMAL PRESSURE
PERM. VALUES
14.17 KPA.
434.9 KPA.
573.7 KPA.

RESPONSE ON CYCLIC LOADING (KPA.) CYCLE NO. 703

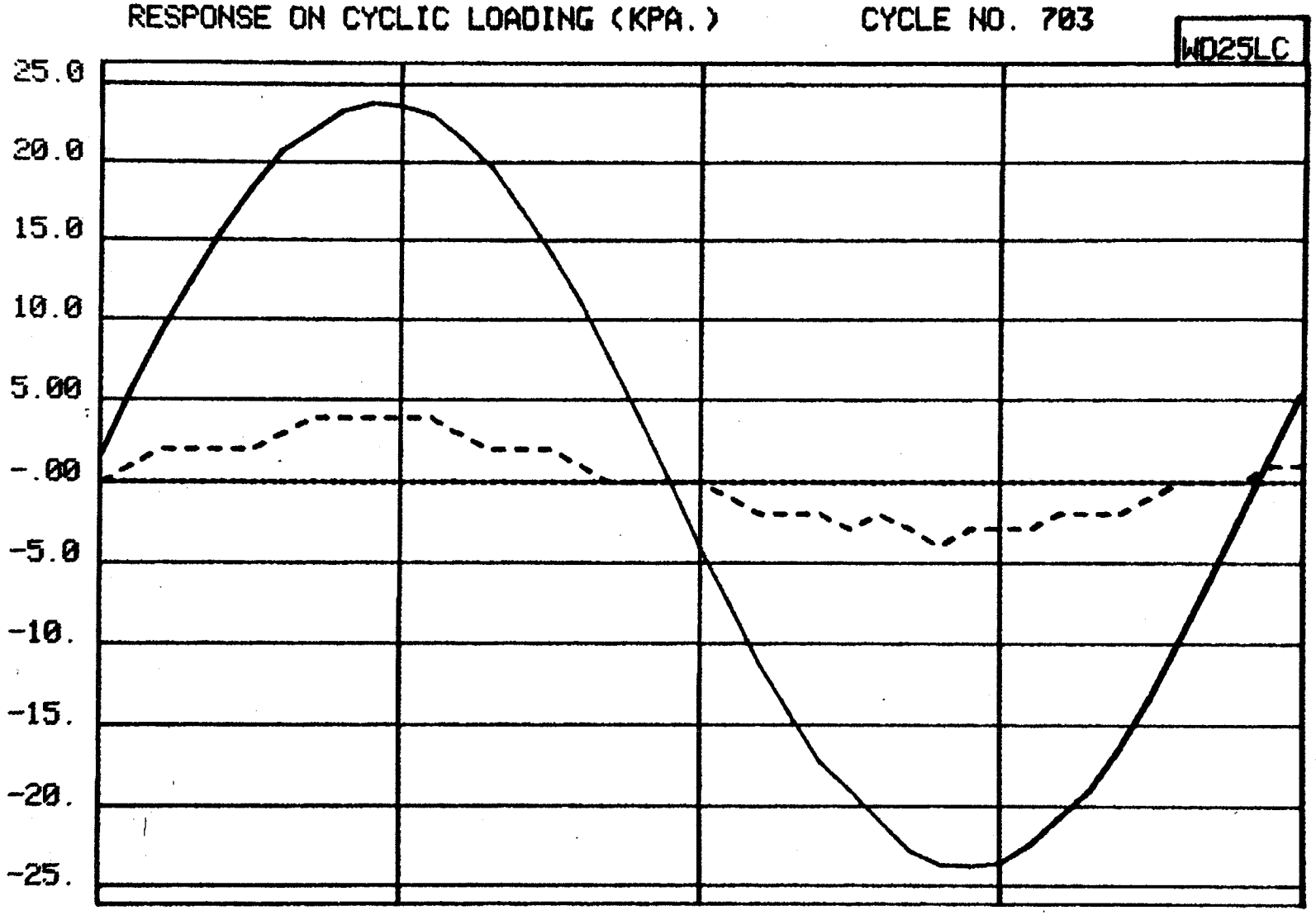

LEGEND:		PERM. VALUES
———	SKIN FRICTION	14.17 KPA.
·····	PORE PRESSURE	434.9 KPA.
- - - -	TOTAL NORMAL PRESSURE	573.7 KPA.

Appendix BB

Plotted Results from WD25SC

Figures BB-1 through BB-7

Skin Friction vs Deflection, Selected Cycles

Figures BB-8 through BB-11

Skin Friction vs Eff. Normal Pressure, Selected Cycl.

Figures BB-12 through B-25

Skin Friction, Pore and Total Pressure, Selected Cycles

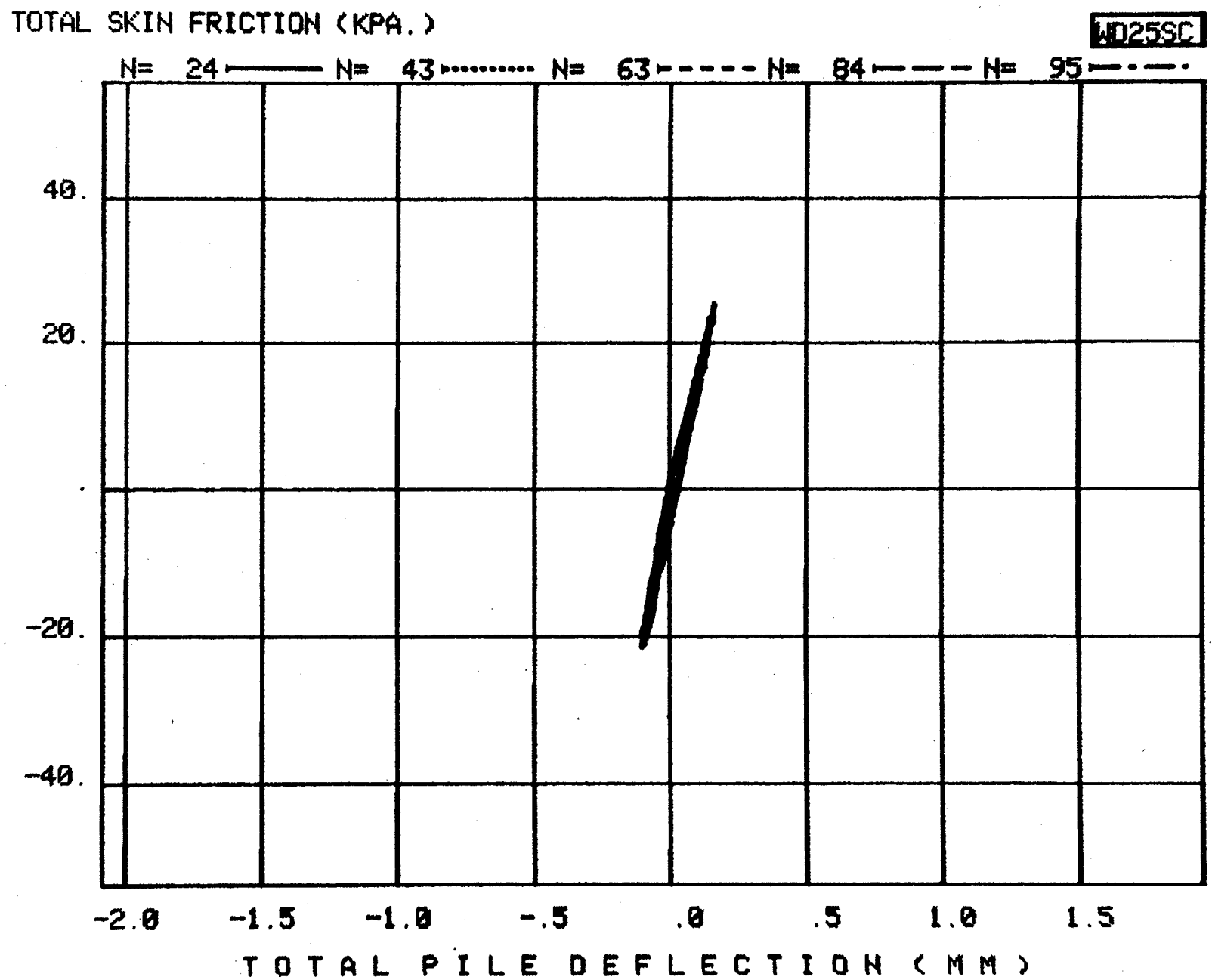
TOTAL SKIN FRICTION (KPA.)
WD25SC
N= 24
N= 43
N= 63
N= 84
N= 95
40.
20.
-20.
-40.
-2.0
-1.5
-1.0
-.5
.0
.5
1.0
1.5
TOTAL PILE DEFLECTION (MM)

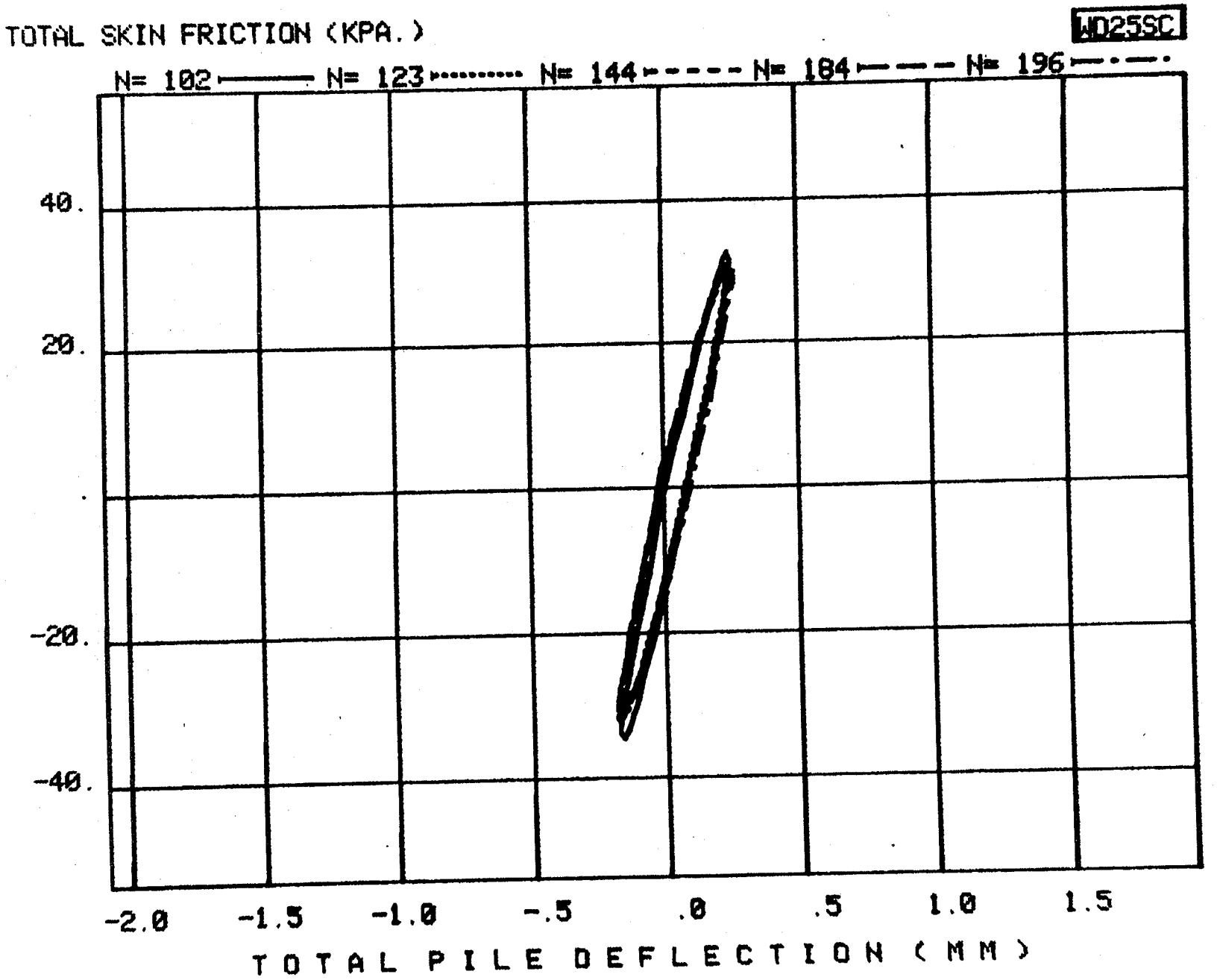
WD25SC
TOTAL SKIN FRICTION (KPA.)
N= 102
N= 123
N= 144
N= 184
N= 196
40.
20.
-20.
-40.
-2.0
-1.5
-1.0
-.5
.0
.5
1.0
1.5
TOTAL PILE DEFLECTION (MM)

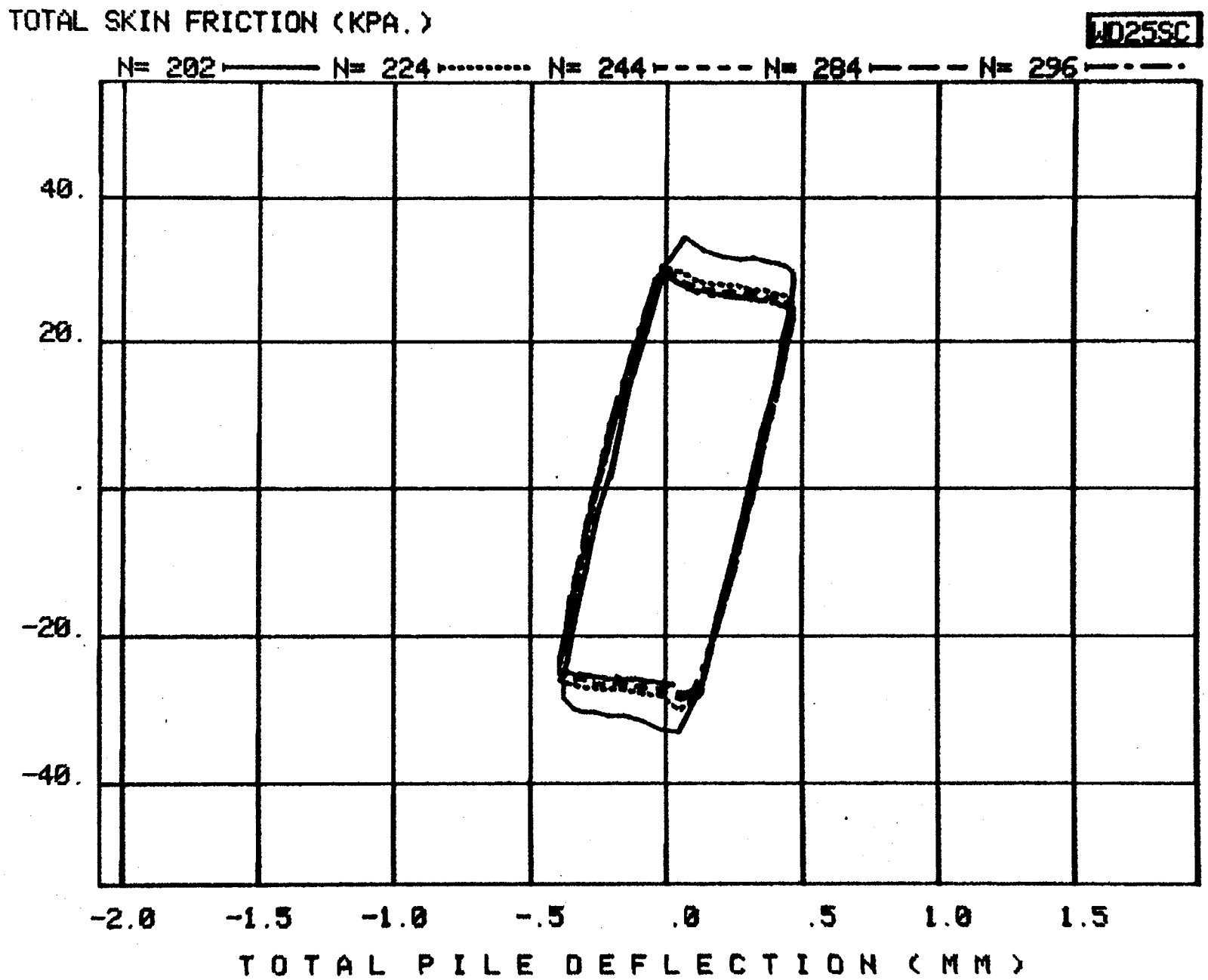
TOTAL SKIN FRICTION (KPA.)
WD25SC
N= 202
N= 224
N= 244
N= 284
N= 296
40.
20.
-20.
-40.
-2.0
-1.5
-1.0
-.5
.0
.5
1.0
1.5
TOTAL PILE DEFLECTION (MM)

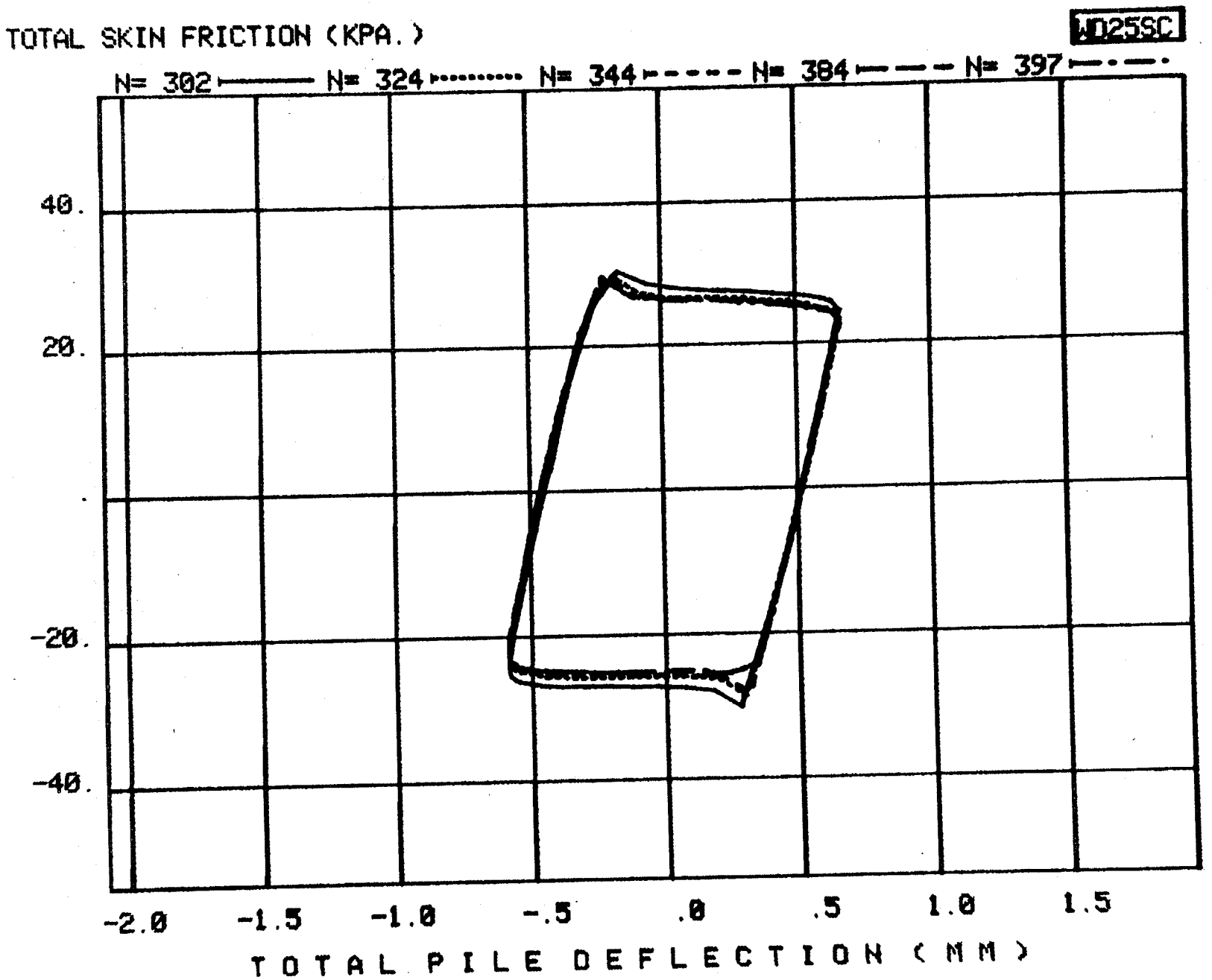
TOTAL SKIN FRICTION (KPA.)
WD25SC
N= 302
N= 324
N= 344
N= 384
N= 397
40.
20.
-20.
-40.
-2.0
-1.5
-1.0
-.5
.0
.5
1.0
1.5
TOTAL PILE DEFLECTION (MM)

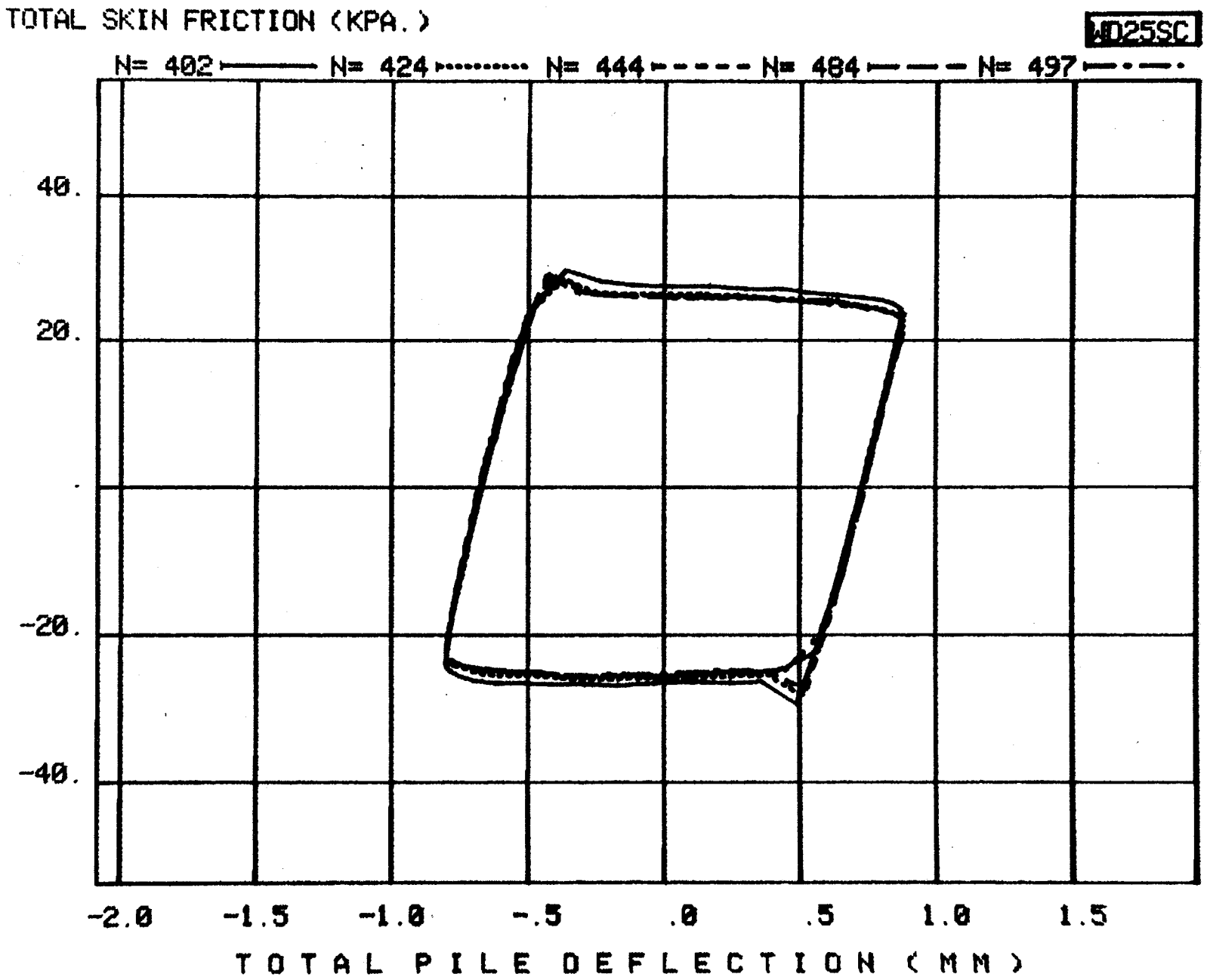
TOTAL SKIN FRICTION (KPA.)
WD25SC
N= 402
N= 424
N= 444
N= 484
N= 497
40.
20.
-20.
-40.
-2.0
-1.5
-1.0
-.5
.0
.5
1.0
1.5
TOTAL PILE DEFLECTION (MM)

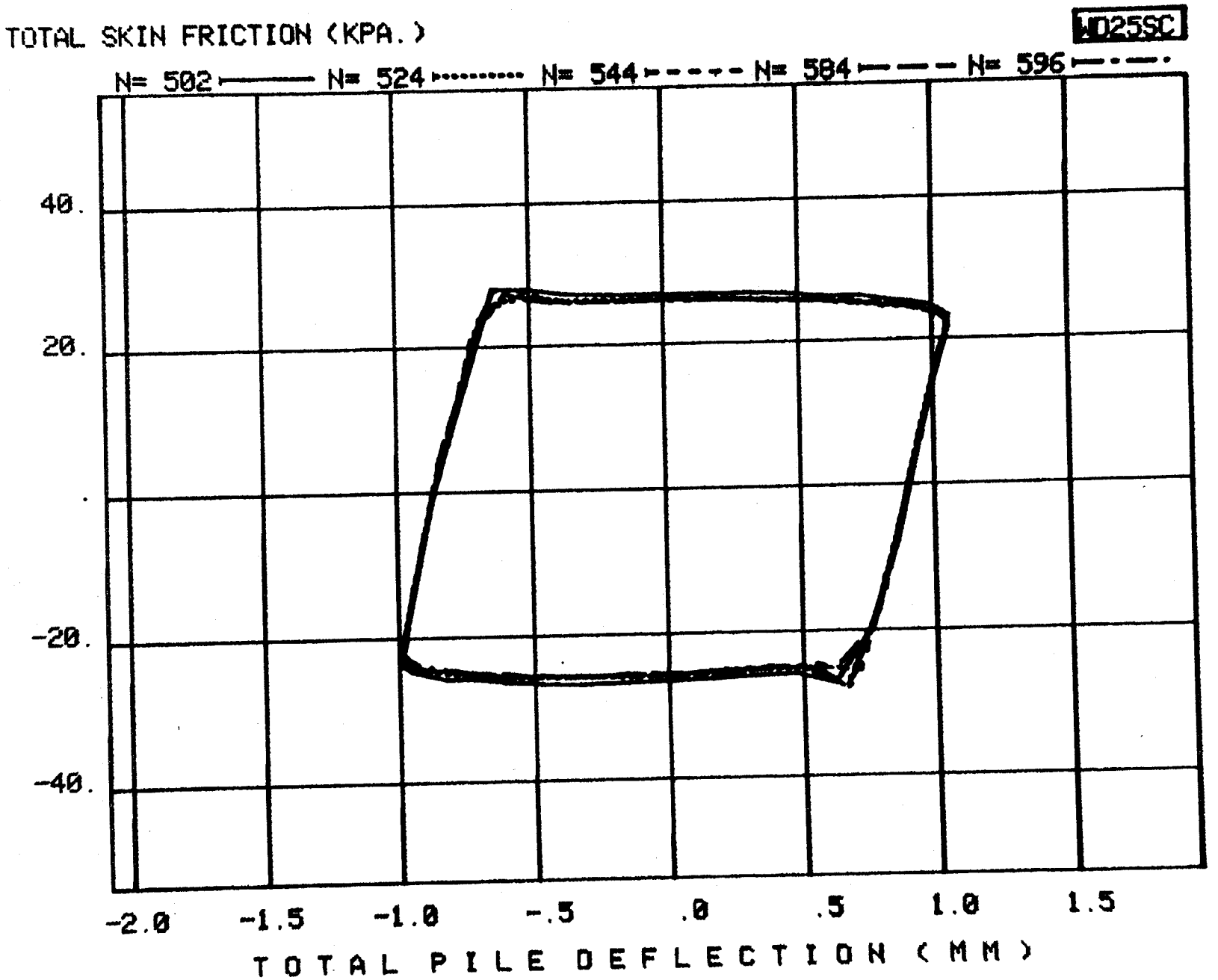
TOTAL SKIN FRICTION (KPA.)
WD25SC
N= 502
N= 524
N= 544
N= 584
N= 596
40.
20.
-20.
-40.
-2.0
-1.5
-1.0
-.5
.0
.5
1.0
1.5
TOTAL PILE DEFLECTION (MM)

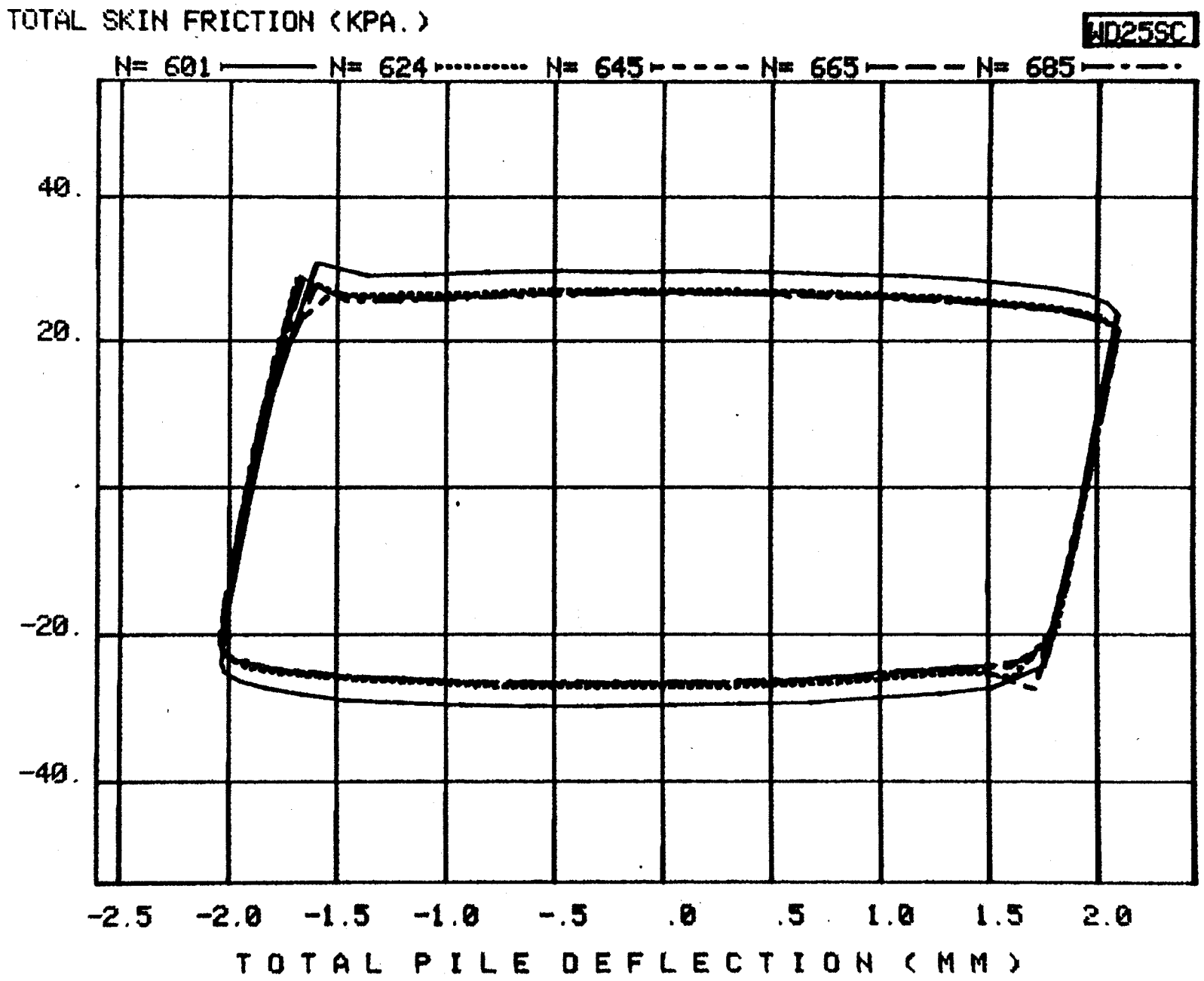
TOTAL SKIN FRICTION (KPA.)
WD25SC
N= 601
N= 624
N= 645
N= 665
N= 685
40.
20.
-20.
-40.
-2.5
-2.0
-1.5
-1.0
-.5
.0
.5
1.0
1.5
2.0
TOTAL PILE DEFLECTION (MM)

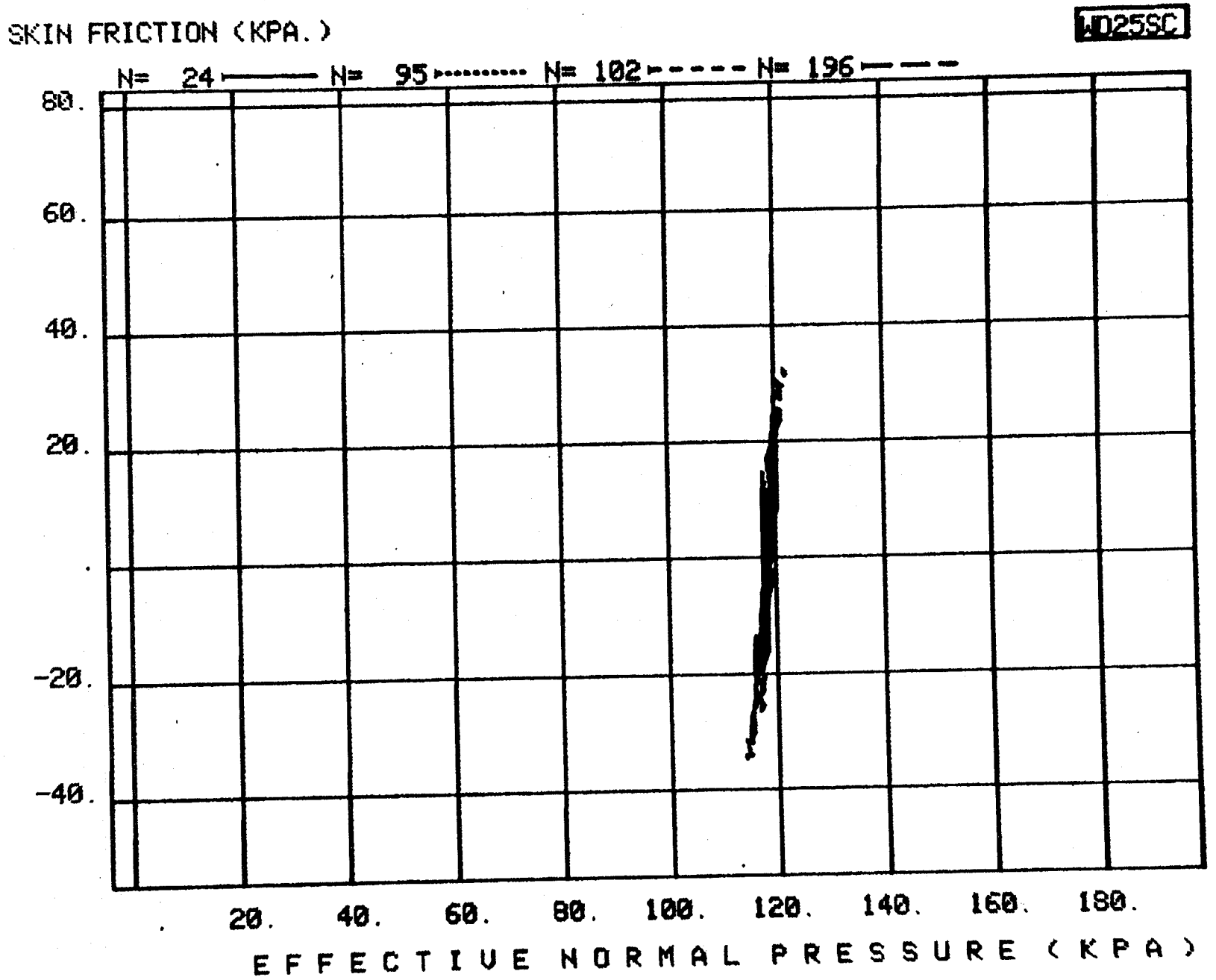
WD25SC
SKIN FRICTION (KPA.)
N= 24
N= 95
N= 102
N= 196
80.
60.
40.
20.
-20.
-40.
20.
40.
60.
80.
100.
120.
140.
160.
180.
EFFECTIVE NORMAL PRESSURE (KPA)

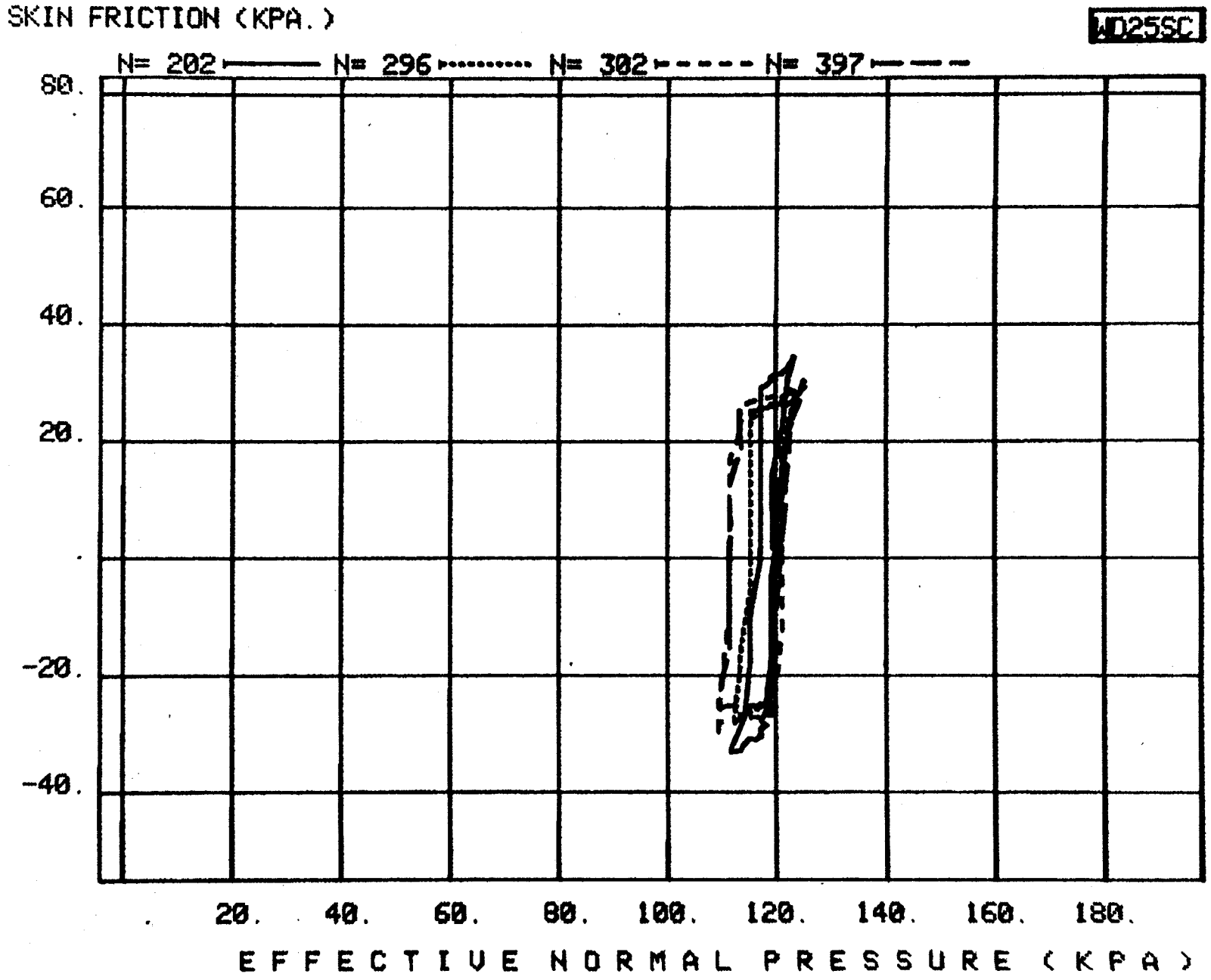
SKIN FRICTION (KPA.)
WD25SC
N= 202
N= 296
N= 302
N= 397
80.
60.
40.
20.
-20.
-40.
20.
40.
60.
80.
100.
120.
140.
160.
180.
EFFECTIVE NORMAL PRESSURE (KPA)

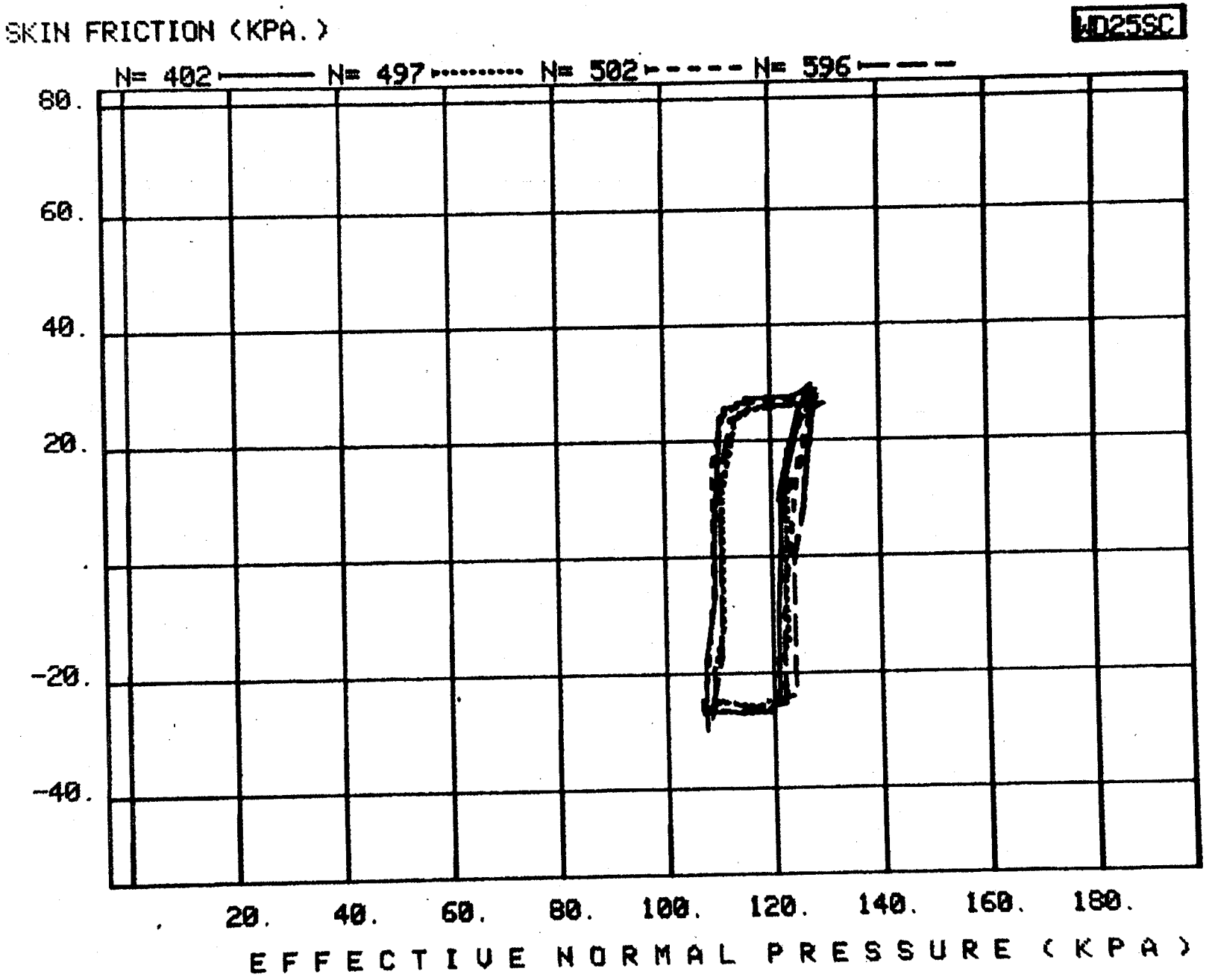
SKIN FRICTION (KPA.)
WD25SC
N= 402
N= 497
N= 502
N= 596
80.
60.
40.
20.
-20.
-40.
20.
40.
60.
80.
100.
120.
140.
160.
180.
EFFECTIVE NORMAL PRESSURE (KPA)

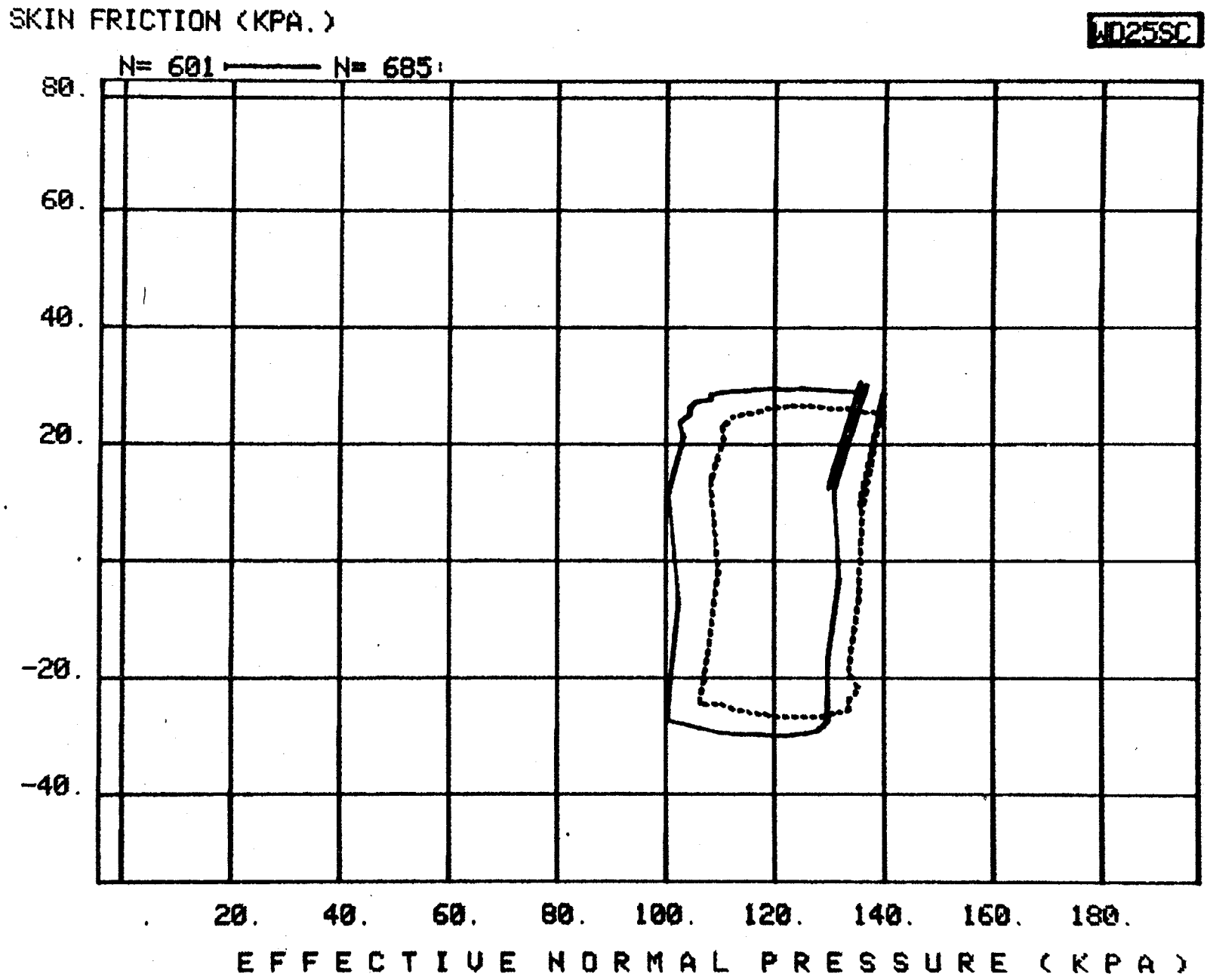
SKIN FRICTION (KPA.)
WD25SC
N= 601
N= 685
80.
60.
40.
20.
-20.
-40.
20.
40.
60.
80.
100.
120.
140.
160.
180.
EFFECTIVE NORMAL PRESSURE (KPA)

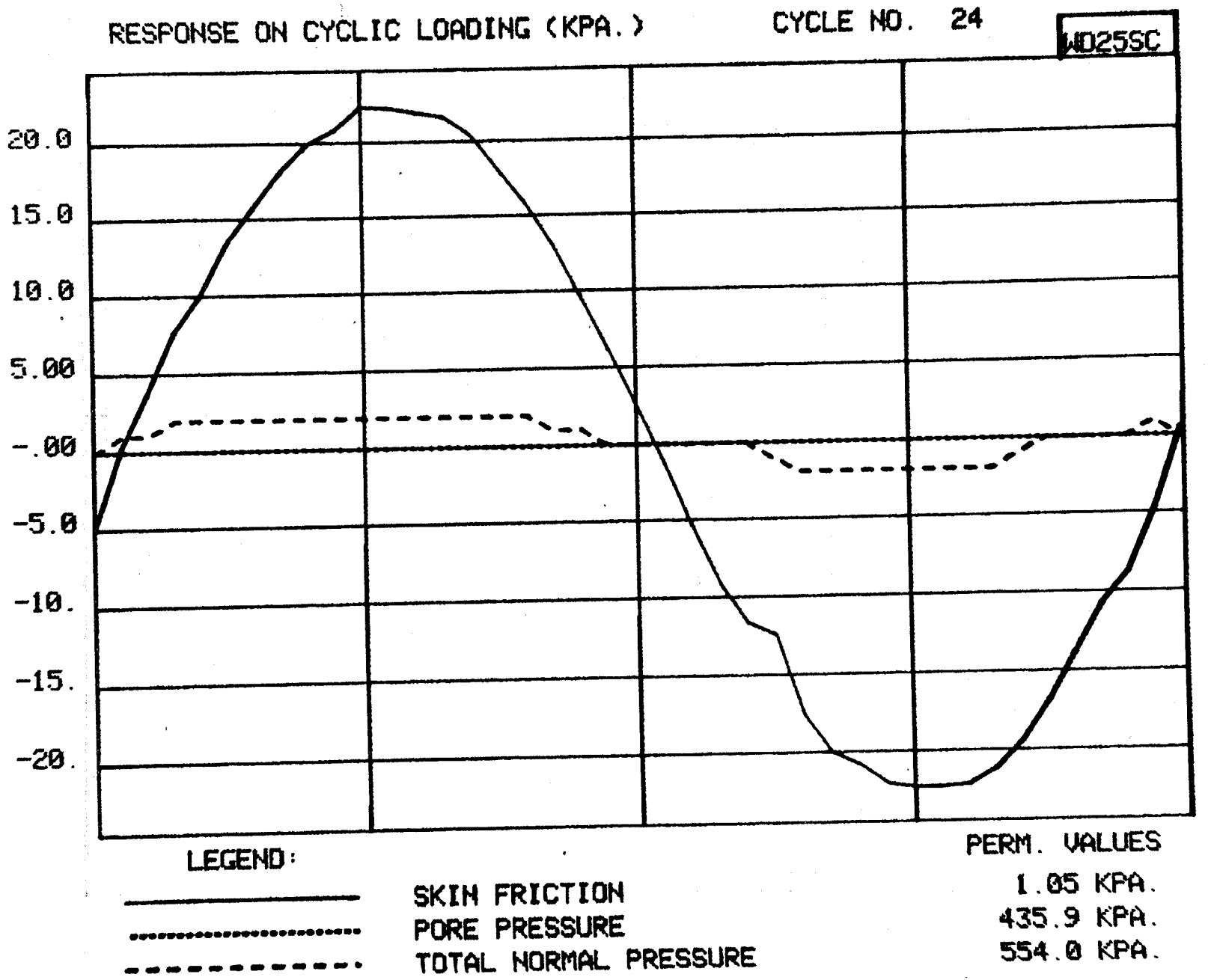
RESPONSE ON CYCLIC LOADING (KPA.)
CYCLE NO. 24
WD25SC
20.0
15.0
10.0
5.00
-.00
-5.0
-10.
-15.
-20.
LEGEND:
SKIN FRICTION
PORE PRESSURE
TOTAL NORMAL PRESSURE
PERM. VALUES
1.05 KPA.
435.9 KPA.
554.0 KPA.

RESPONSE ON CYCLIC LOADING (KPA.) CYCLE NO. 95

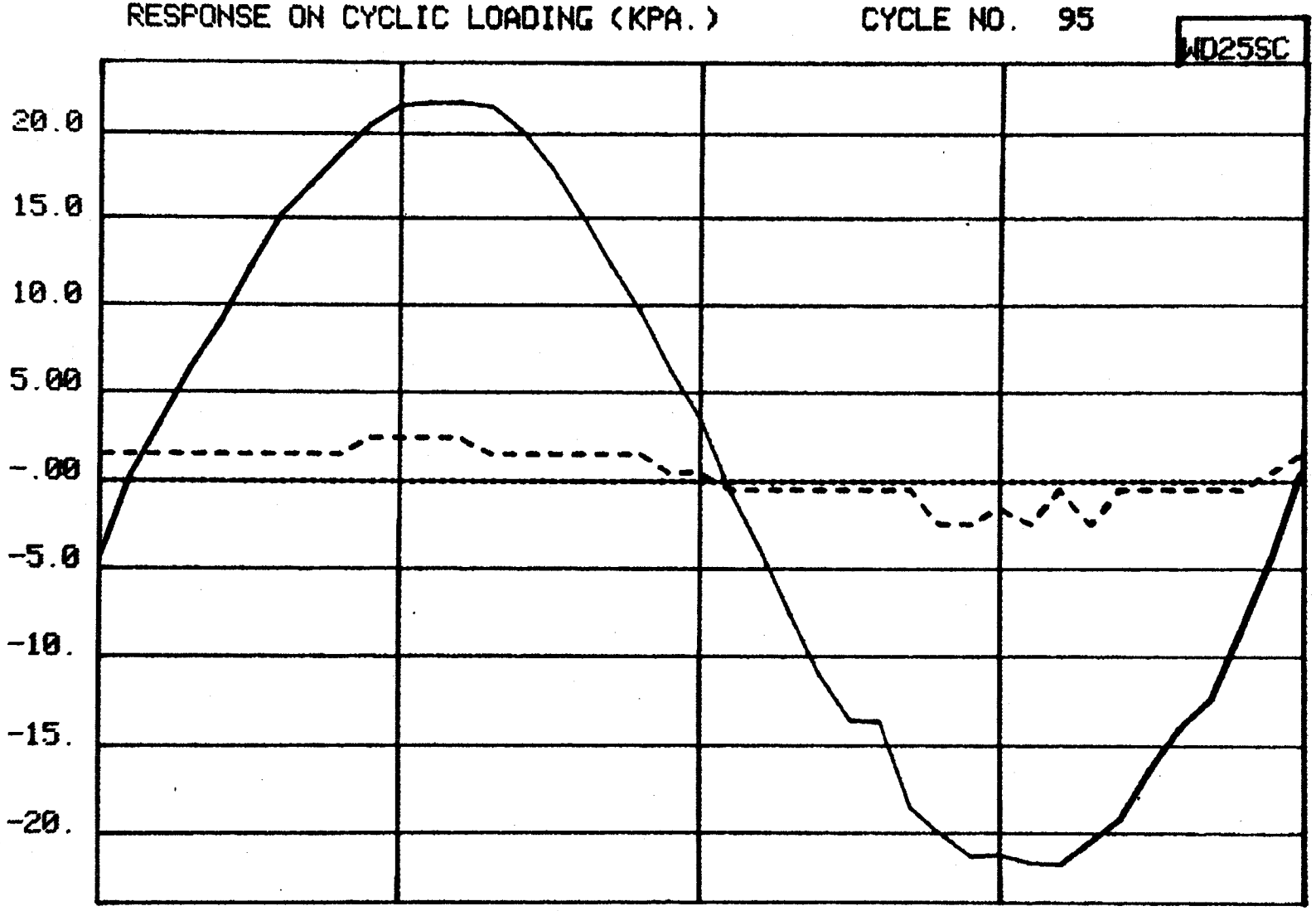

LEGEND:

		PERM. VALUES
———	SKIN FRICTION	3.59 KPA.
·····	PORE PRESSURE	436.4 KPA.
- - - -	TOTAL NORMAL PRESSURE	554.5 KPA.

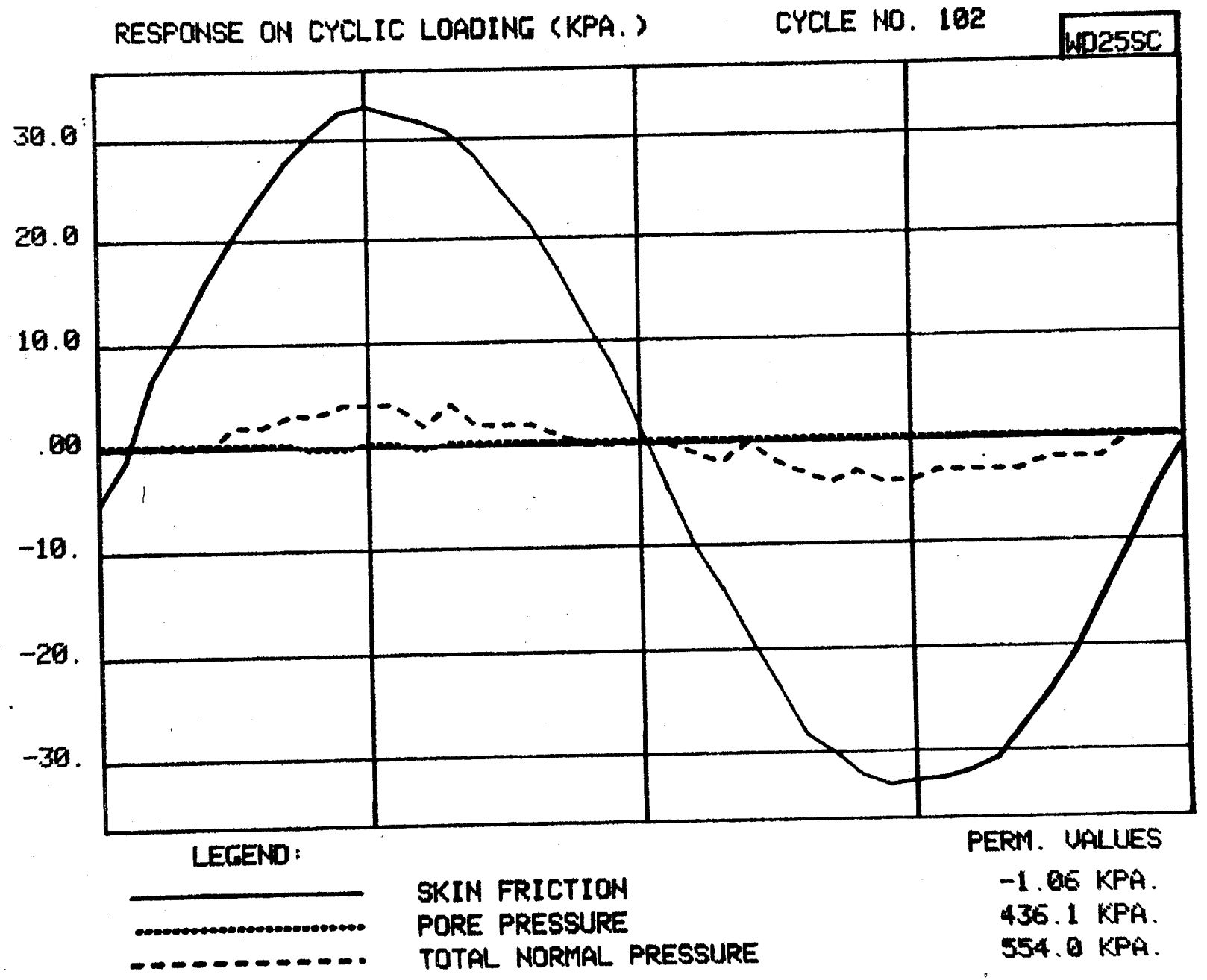
RESPONSE ON CYCLIC LOADING (KPA.)
CYCLE NO. 102
WD25SC
30.0
20.0
10.0
.00
-10.
-20.
-30.
LEGEND:
SKIN FRICTION
PORE PRESSURE
TOTAL NORMAL PRESSURE
PERM. VALUES
-1.06 KPA.
436.1 KPA.
554.0 KPA.

RESPONSE ON CYCLIC LOADING (KPA.) CYCLE NO. 196

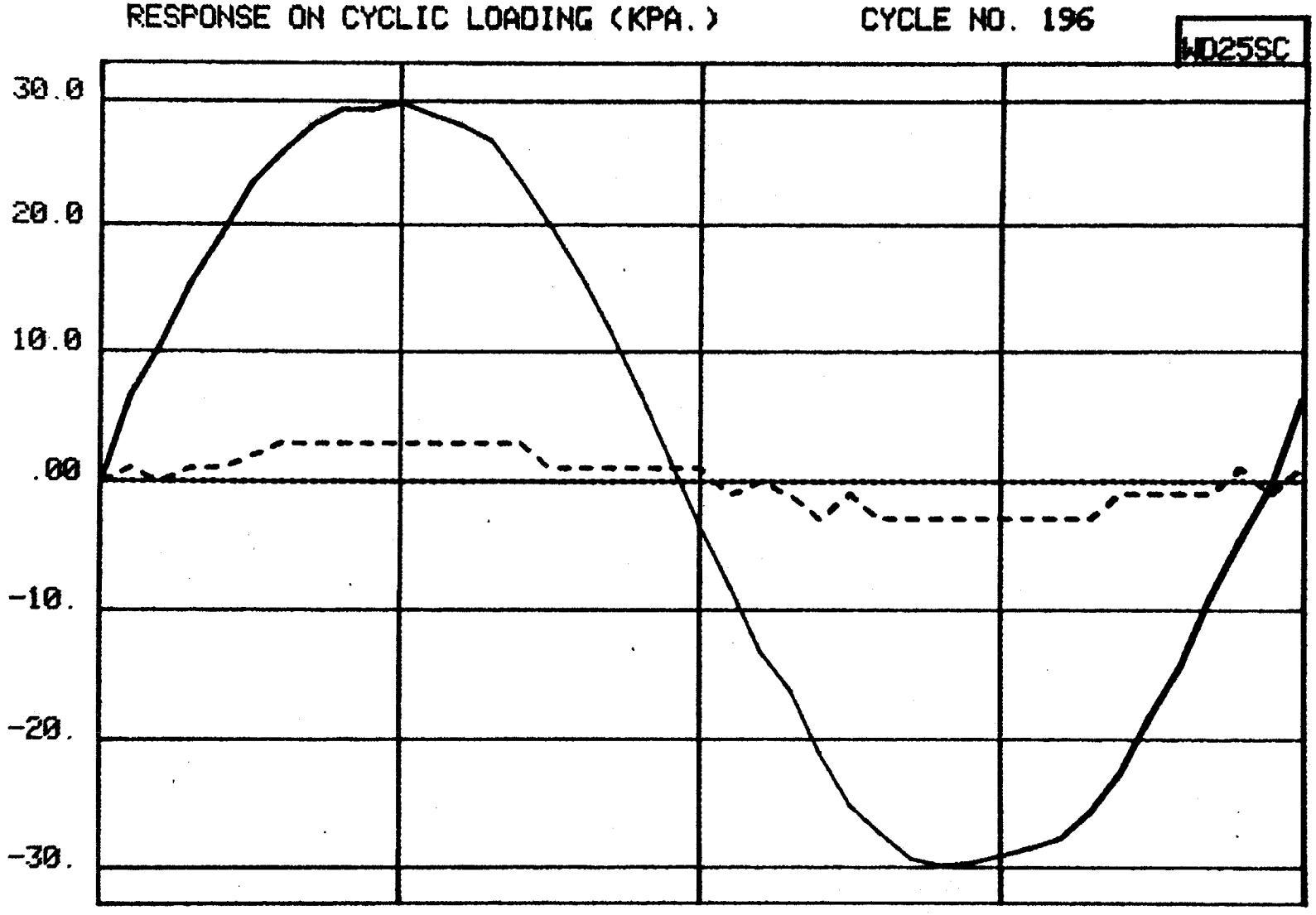

LEGEND:		PERM. VALUES
————————	SKIN FRICTION	.04 KPA.
·····	PORE PRESSURE	436.9 KPA.
- - - - - - - - - -	TOTAL NORMAL PRESSURE	555.0 KPA.

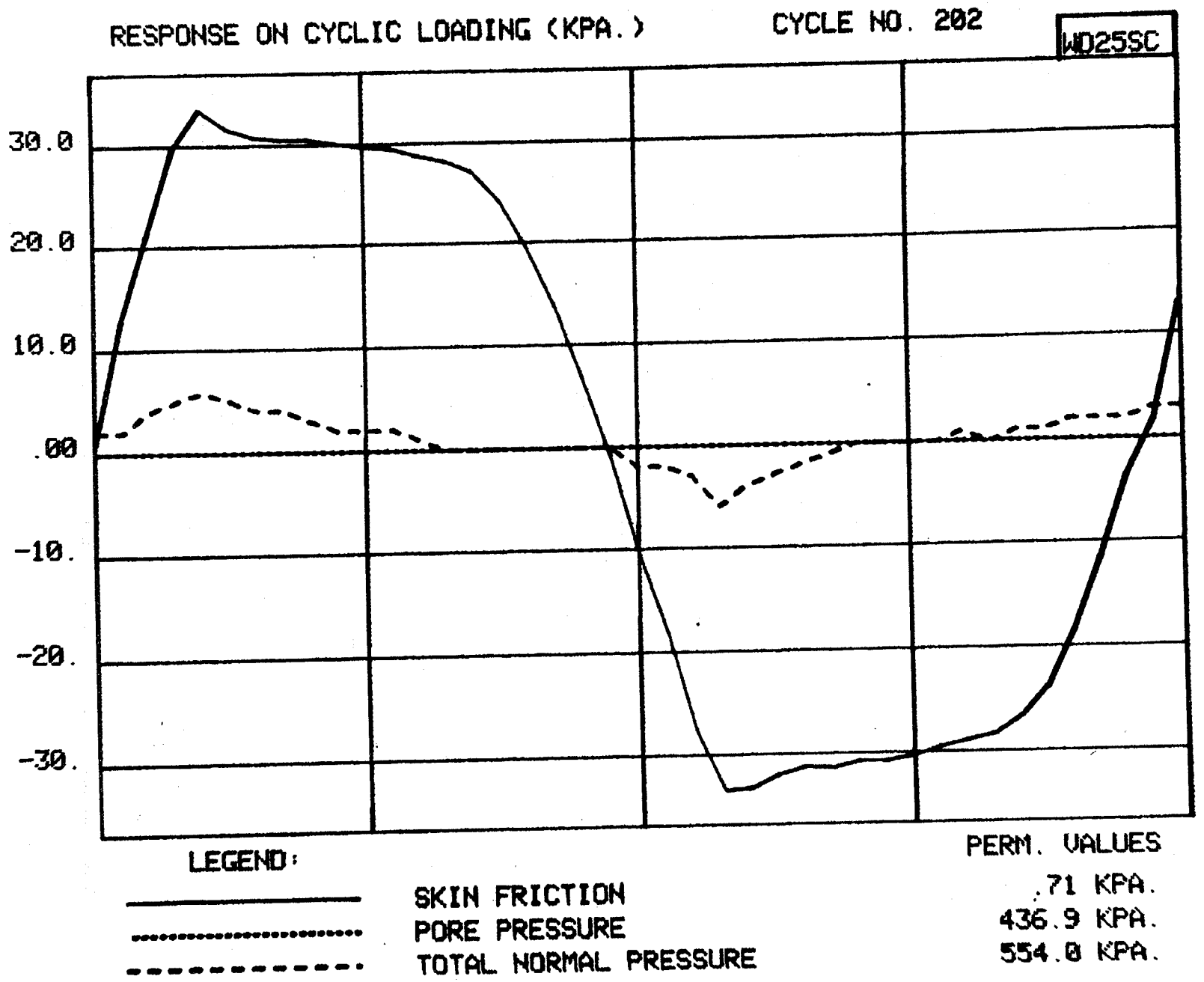
RESPONSE ON CYCLIC LOADING (KPA.)
CYCLE NO. 202
WD25SC
30.0
20.0
10.0
.00
-10.
-20.
-30.
LEGEND:
SKIN FRICTION
PORE PRESSURE
TOTAL NORMAL PRESSURE
PERM. VALUES
.71 KPA.
436.9 KPA.
554.0 KPA.

RESPONSE ON CYCLIC LOADING (KPA.) CYCLE NO. 296

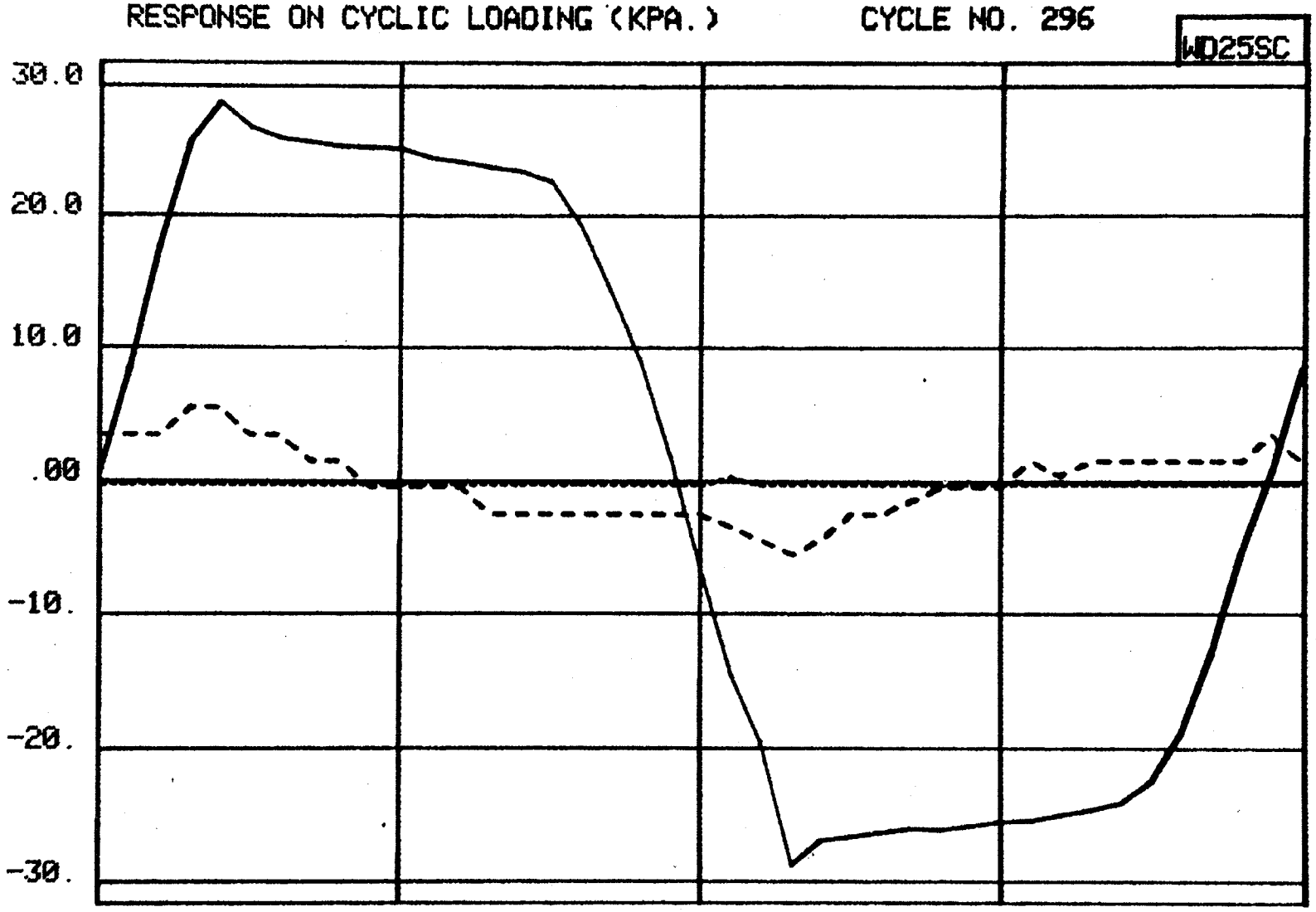

LEGEND:		PERM. VALUES
———	SKIN FRICTION	.52 KPA.
·····	PORE PRESSURE	437.1 KPA.
- - - -	TOTAL NORMAL PRESSURE	554.5 KPA.

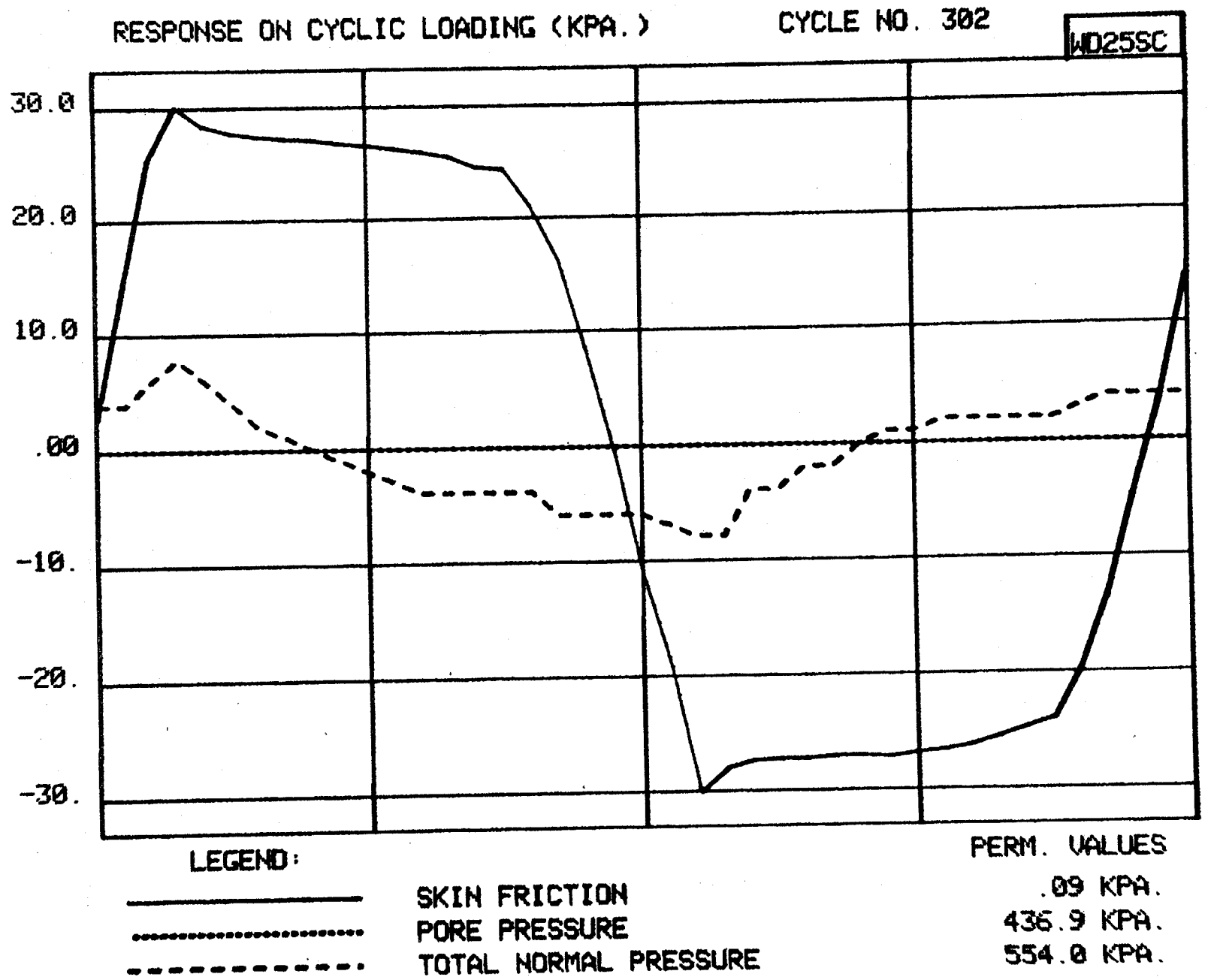
RESPONSE ON CYCLIC LOADING (KPA.)
CYCLE NO. 302
WD25SC
30.0
20.0
10.0
.00
-10.
-20.
-30.
LEGEND:
SKIN FRICTION
PORE PRESSURE
TOTAL NORMAL PRESSURE
PERM. VALUES
.09 KPA.
436.9 KPA.
554.0 KPA.

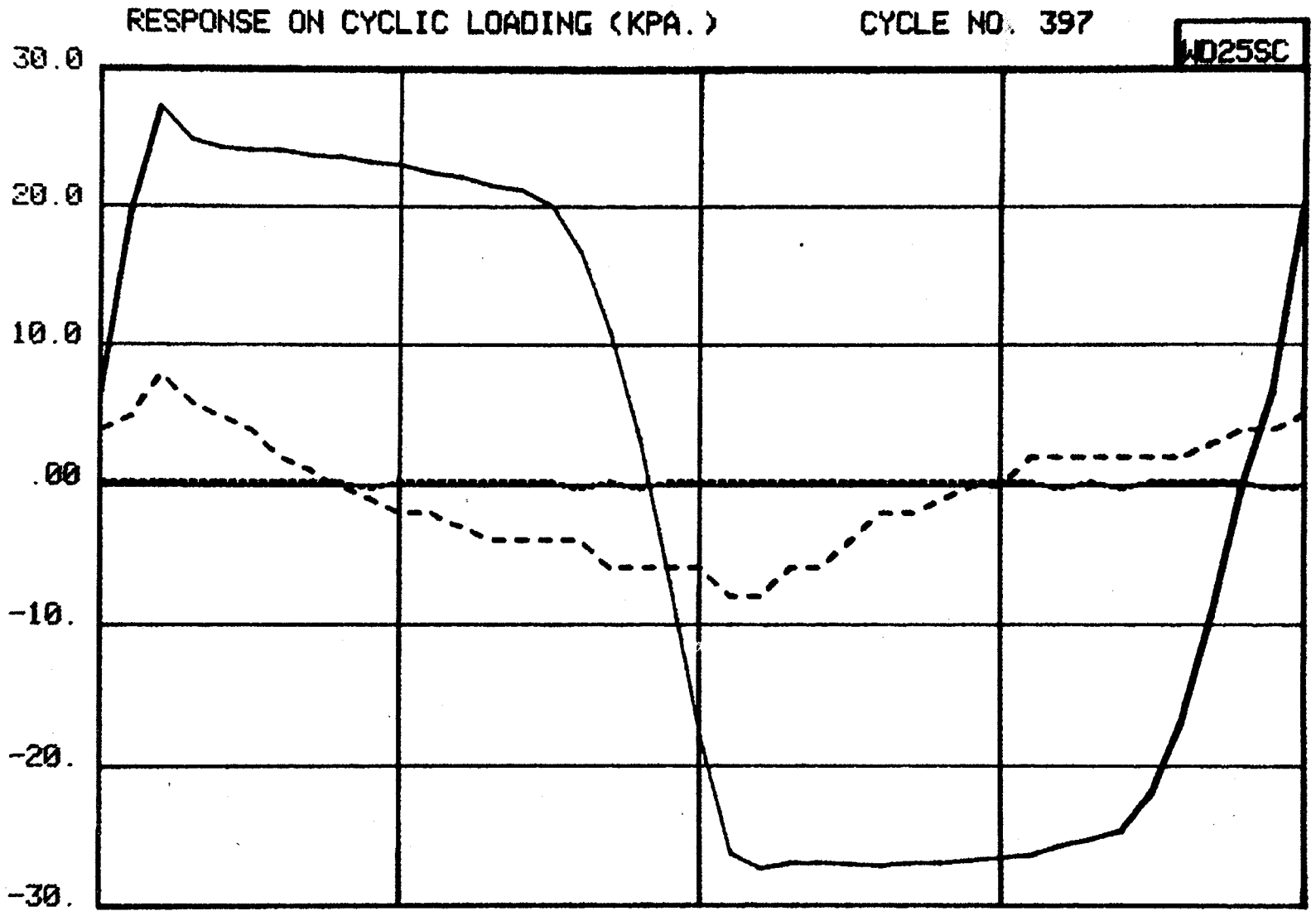

LEGEND:		PERM. VALUES
———	SKIN FRICTION	2.01 KPA.
·····	PORE PRESSURE	436.6 KPA.
- - - -	TOTAL NORMAL PRESSURE	554.0 KPA.

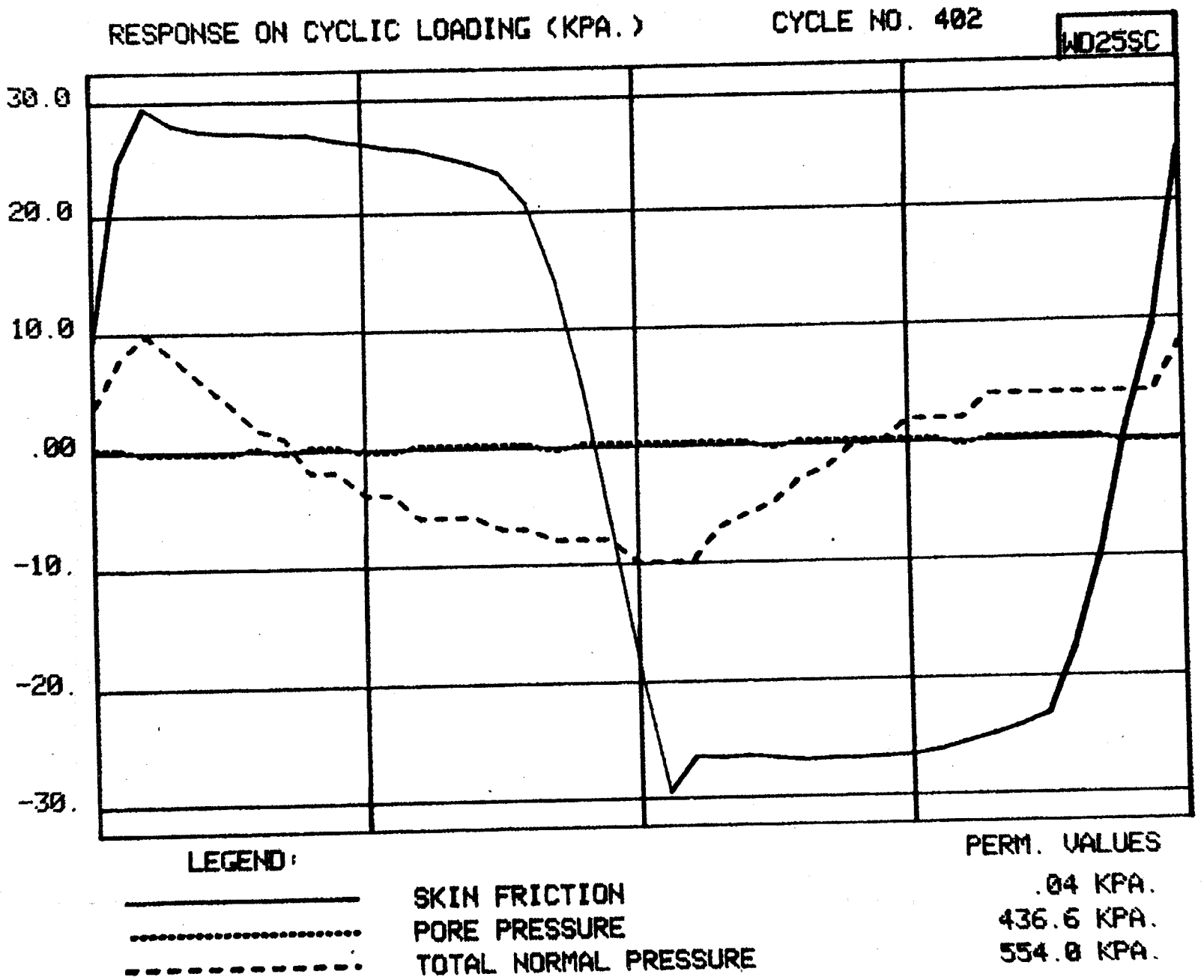
RESPONSE ON CYCLIC LOADING (KPA.)
CYCLE NO. 402
WD25SC
30.0
20.0
10.0
.00
-10.
-20.
-30.
LEGEND:
SKIN FRICTION
PORE PRESSURE
TOTAL NORMAL PRESSURE
PERM. VALUES
.04 KPA.
436.6 KPA.
554.0 KPA.

RESPONSE ON CYCLIC LOADING (KPA.) CYCLE NO. 497

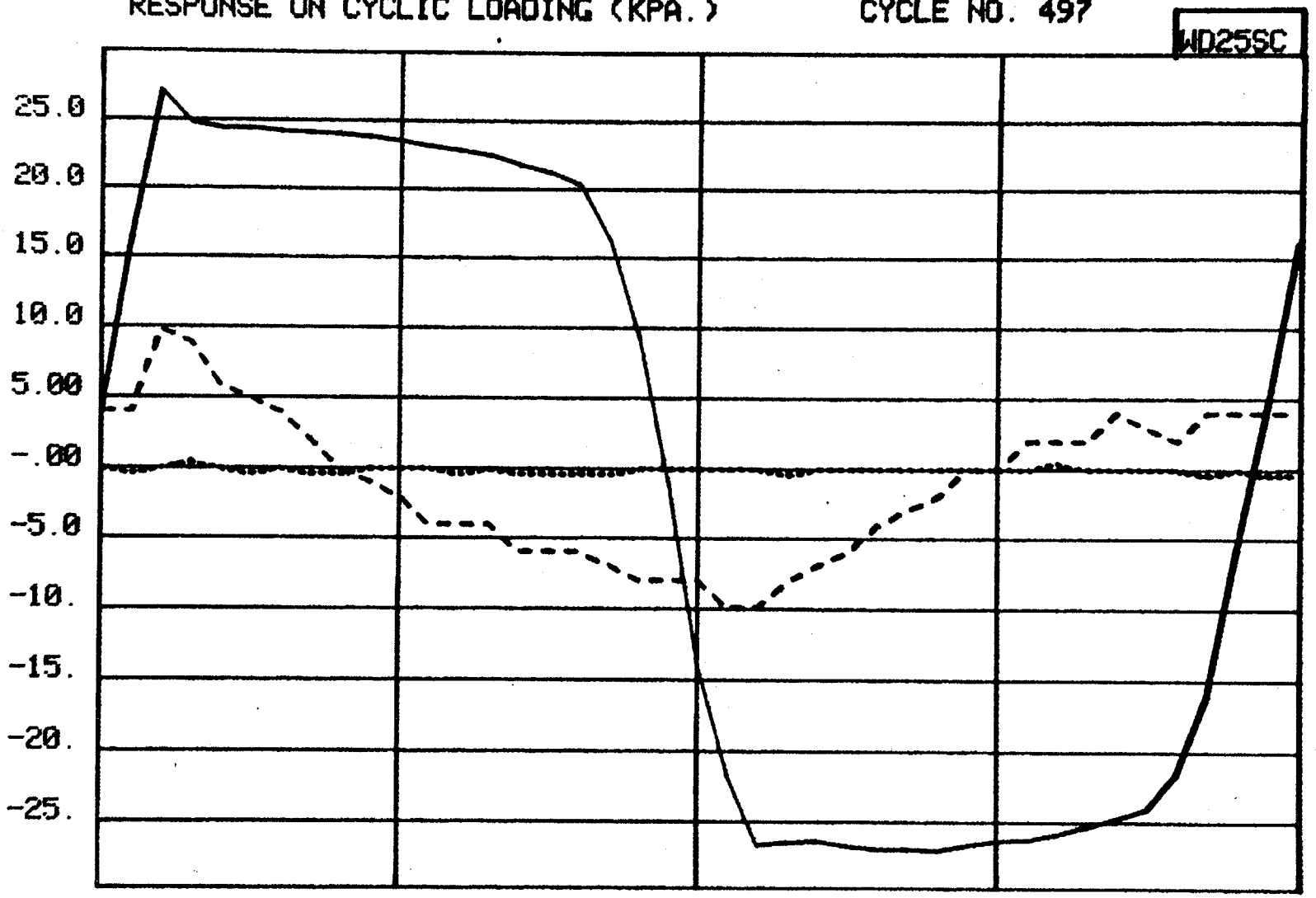

LEGEND:

		PERM. VALUES
———	SKIN FRICTION	1.72 KPA.
·····	PORE PRESSURE	435.4 KPA.
- - - -	TOTAL NORMAL PRESSURE	554.0 KPA.

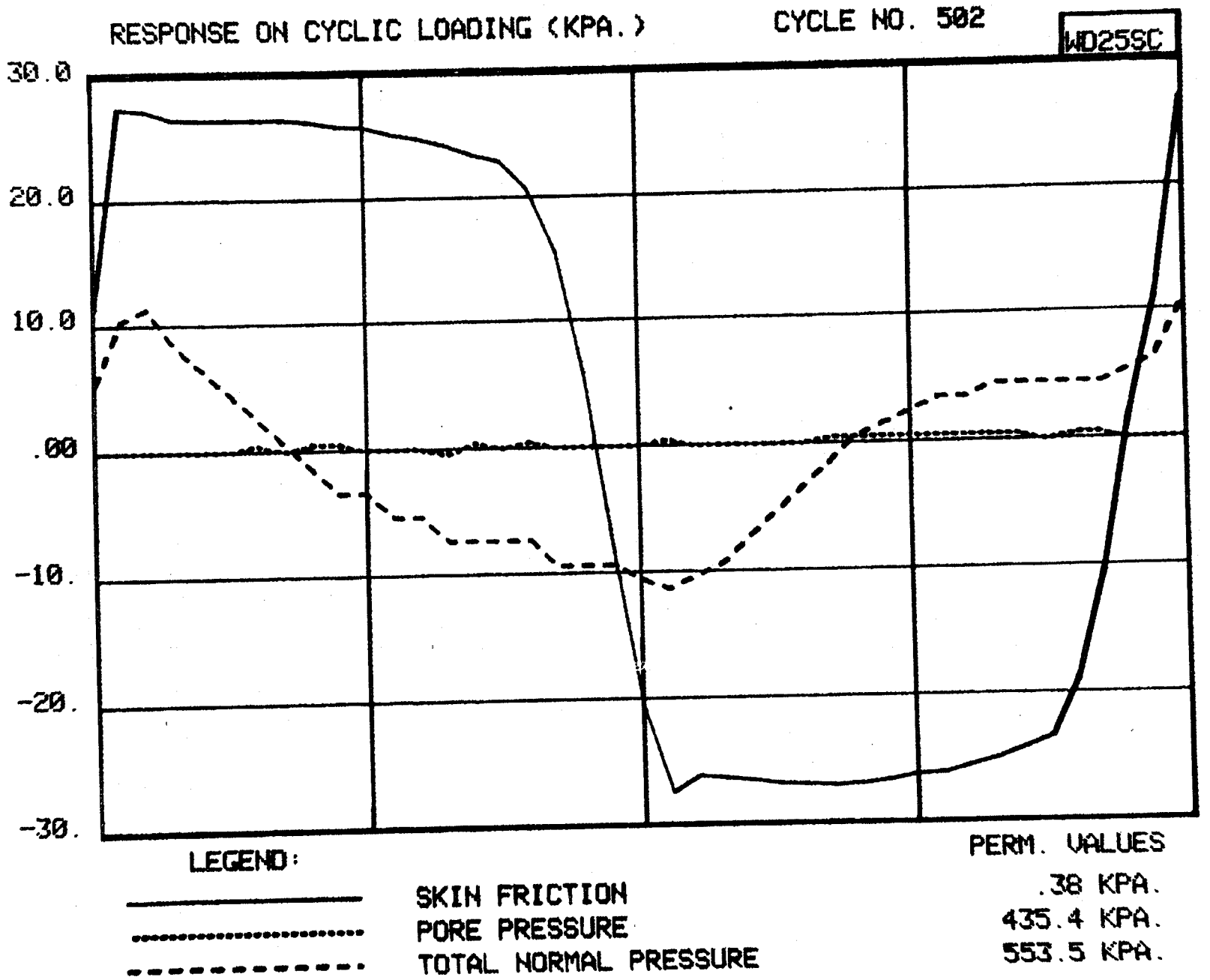
RESPONSE ON CYCLIC LOADING (KPA.)
CYCLE NO. 502
WD25SC
30.0
20.0
10.0
.00
-10.
-20.
-30.
LEGEND:
SKIN FRICTION
PORE PRESSURE
TOTAL NORMAL PRESSURE
PERM. VALUES
.38 KPA.
435.4 KPA.
553.5 KPA.

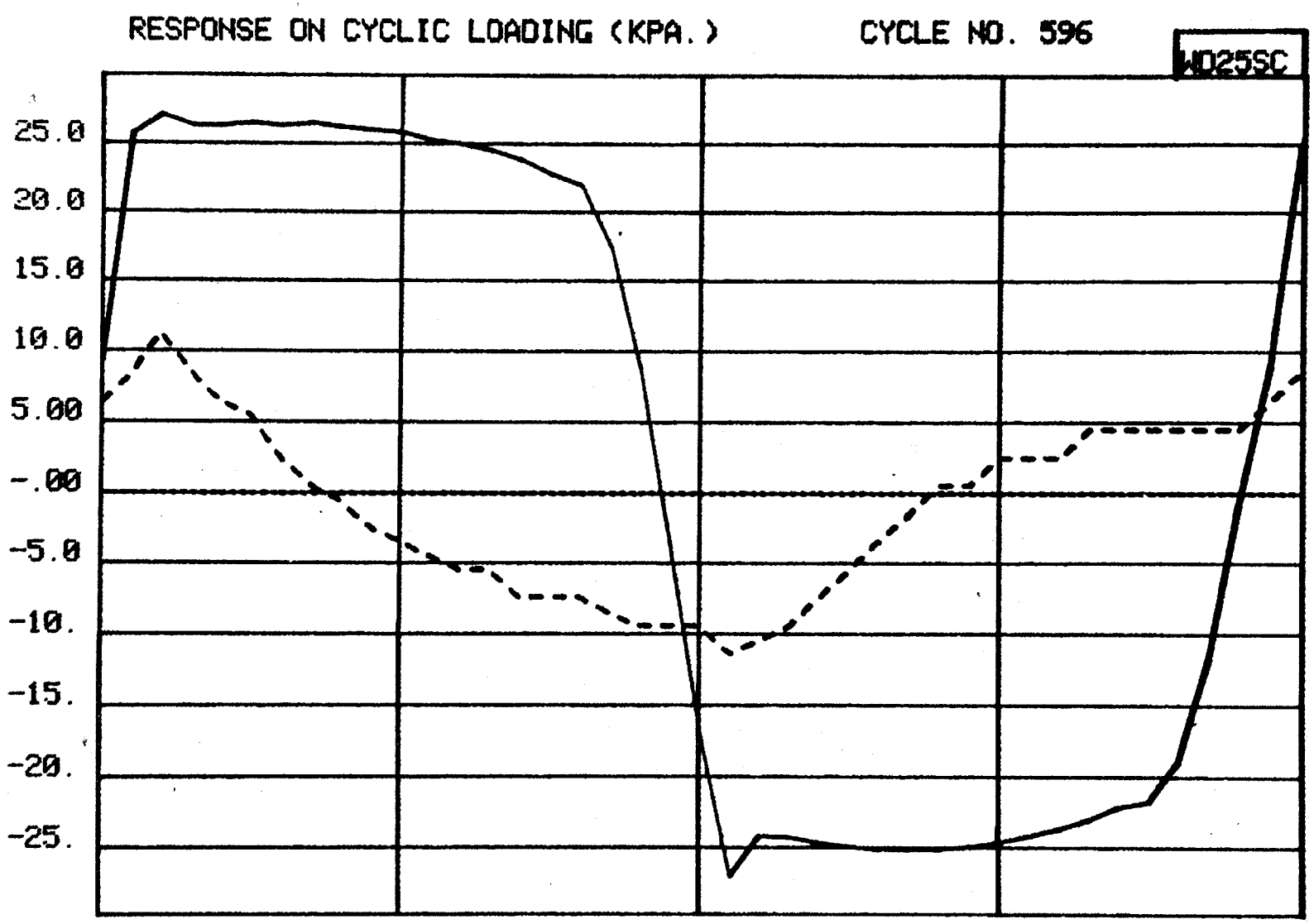

LEGEND:		PERM. VALUES
———	SKIN FRICTION	-.39 KPA.
·····	PORE PRESSURE	434.0 KPA.
- - - -	TOTAL NORMAL PRESSURE	553.5 KPA.

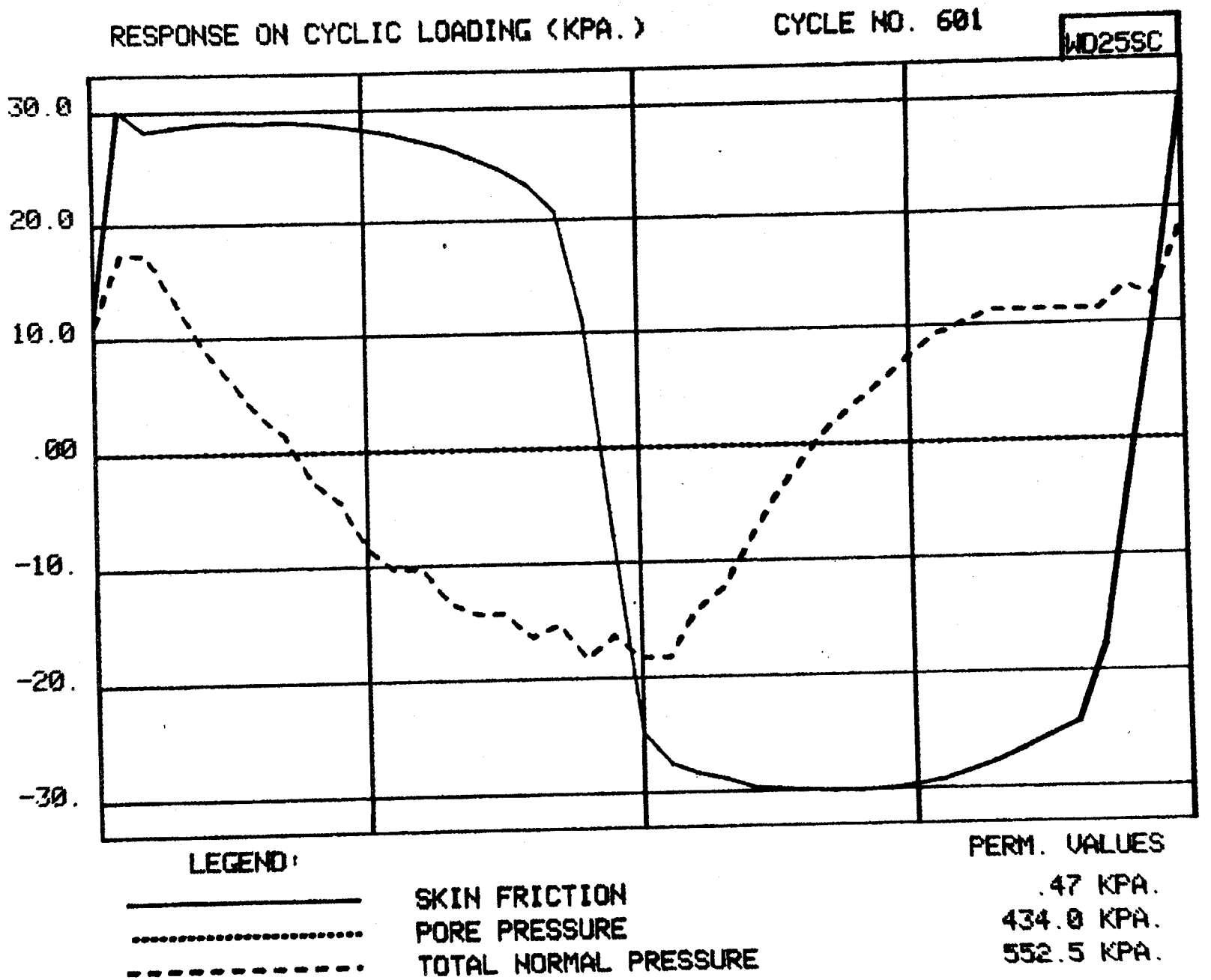
RESPONSE ON CYCLIC LOADING (KPA.)
CYCLE NO. 601
WD25SC
30.0
20.0
10.0
.00
-10.
-20.
-30.
LEGEND:
SKIN FRICTION
PORE PRESSURE
TOTAL NORMAL PRESSURE
PERM. VALUES
.47 KPA.
434.0 KPA.
552.5 KPA.

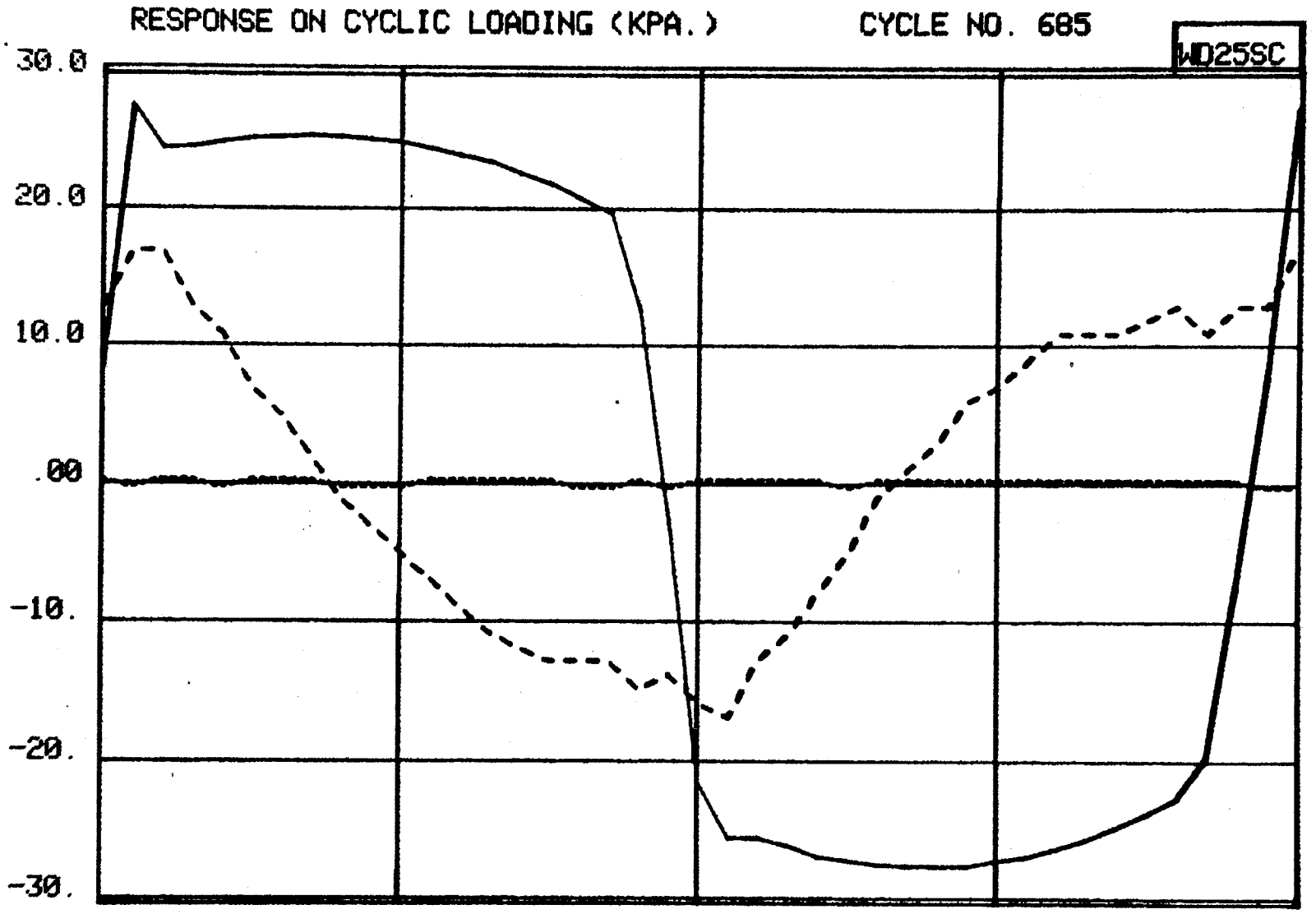

LEGEND:

		PERM. VALUES
———	SKIN FRICTION	1.10 KPA.
·····	PORE PRESSURE	429.9 KPA.
- - - -	TOTAL NORMAL PRESSURE	553.0 KPA.

APPENDIX C

DETAILED RESULTS FROM **TEST 6, STRATUM III** MODEL PILE TESTS

CONTENTS

Summary	C3
Test 6, Stratum III	C4
Consolidation	C4
Pile Instatllation and Set-Up	B4
Static Test	C4
Cyclic Tests	C5
Stress Controlled Tests (WD36LC)	C6
Displacement Controlled Tests (WD36SC)	C7
Strength Tests	C8

LIST OF FIGURES

Figure 1	Sample Properties
Figure 2	Consolidation Diagram
Figure 3	Pocket Penetrometer Tests After Consolidation
Figure 4	Pressures at Pile Wall after Installation
Figure 5	Static Test
Figure 6	Deflection vs no. of Cycles, WD36SC
Figure 7	Skin Friction vs no. of Cycles, WD36SC
Figure 8	Pore Pressure vs no. of Cycles, WD36SC
Figure 9	Total Normal Pressure vs no. of Cycles, WD36SC
Figure 10	Eff. Normal Pressure vs no. of Cycles, WD36SC
Figure 11	Skin Friction vs no. of Cycles, WD36LC
Figure 12	Deflection vs no. of Cycles, WD36LC
Figure 13	Total Normal Pressure vs no. of Cycles, WD36LC

Figure 14 Pore Pressure vs no. of Cycles, WD36LC
Figure 15 Eff. Normal Pressure vs no. of Cycles, WD36LC
Figure 16 Pocket Penetrometer Tests after Pile Test
Figure 17 Unconfined Compression Tests
Figure 18 Water Content and Shear Strength

Appendix CA
Plotted Results from WD36SC
Figures CA-1 through CA-6
Skin Friction vs Deflection, Selected Cycles
Figures CA-7 through CA-9
Skin Friction vs Eff. Normal Pressure, Selected Cycl.
Figures CA-10 through CA-20
Skin Friction, Pore and Total Pressure, Selected Cycles

Appendix CB
Plotted Results from WD36SC
Figures CB-1 through CB-4
Skin Friction vs Deflection, Selected Cycles
Figures CB-5 through CB-8
Skin Friction vs Eff. Normal Pressure, Selected Cycl.
Figures CB-9 through CB-16
Skin Friction, Pore and Total Pressure, Selected Cycles

SUMMARY

This report contains the results of the laboratory model pile tests designated TEST 6, STRATUM III, in the project CNRD 13-2, Tension Pile Study, for Conoco Norway Inc.

The clay sample was consolidated for 21 days under 500 kPa applied vertical pressure. Pore pressure in the sample was about 10% of the applied pressure at this time. After three days of consolidation in the pile chamber the pile was installed.

After 11 days of consolidation (set-up) the excess pore pressure was still about 190 kPa. Testing was then started.

Static test gave peak friction of 39 kPa with residual value of 37 kPa. Undrained shear strength was interpreted to 72 kPa, giving alpha value (α) of 0.54 and 0.51 for peak and residual respectively. Estimating the effective vertical pressure to 230 kPa results in a beta factor (β) of 0.14 for peak friction.

After three days of further set-up cyclic testing was started. Due to malfunctioning of the loading system the displacement controlled tests were performed first, with two-way cyclic loading. Six parcels of 100 cycles with increasing cyclic displacements were performed. Maximum friction obtained was 42 kPa which reduced to 38 kPa in subsequent parcels. The residual friction during large slip was 33 kPa.

Giving 20 hrs for reconsolidation a cyclic stress controlled test was performed. Tension bias was 21.5 kPa (55% of previous static peak friction) with parcels of 100 cycles with specified cyclic stress amplitude superimposed. Due to the previous degradation tests excessive deformation of the pile was experienced during the second and third parcel. The maximum cyclic stress level was 16.5 kPa giving a maximum friction of 38 kPa.

TEST 6, STRATUM III

CONSOLIDATION

The sample was prepared from the same material as used in Test 4. Water was added during the remoulding process to a water content of about 51%. Horizontal filters were placed in the oedometer to provide better vertical drainage.

A vertical pressure of 500 kPa was applied on top. As seen in Figure 2 the pore pressure at middle height had dropped down to about 10% of the consolidation stress after 21 days. At this time the sample was transferred to the pile chamber. Pocket penetrometer tests were performed on the side of the sample at the top of the sample when trimmed in the pile chamber (Level A-A) as shown in Figure 3. The shear strength , s_u, showed an average of about 65 kPa.

PILE INSTALLATION AND SET-UP

After pocket penetrometer tests the sample was mounted in the pile chamber and left to reconsolidate for 3 days under a vertical pressure of 500 kPa and radial pressure of 350 kPa (K = 0.7). In addition a back pressure of 200 kPa was applied in an attempt to help speed up the pore pressure response.

During insertion of the pile the side friction showed a maximum of about 25 kPa. Total normal pressure showed 635 kPa and the pore pressure only showed 220 kPa directly after installation as shown in Figure 4. After about one day of set-up the total pressure was constant at 635 kPa whereas the pore pressure had reached a maximum of 445 kPa. Ten additional days of consolidation made the pore pressure drop down to 390 kPa and total pressure went up to 640 kPa. At this time it was decided to start with the loading program, even though the excess pore pressure was 190 kPa (above back pressure).

STATIC TEST

A displacement controlled static test with deformation rate 1 mm per hour was now

conducted, as shown in Figure 5. The pile was pulled in tension through failure and large slip and then pushed down to original position causing failure and large slip (residual friction) in compression.

The displacement to cause failure, as shown in Figure 5, as about 0.25mm or 1% of the pile diameter. A maximum friction of 39 kPa was achieved with a residual value of 37 kPa. The shear strength at end consolidation was measured to 65 kPa, but as shown later the shear strength after pile test when sample was built out of pile chamber was measured to about 77 kPa. Since the strength obviously increased during consolidation in the pile chamber, the shear strength during testing is estimated to lie in between these two values. The shear strength chosen for this test is $s_u = 72 kPa$. This results in an alpha (α) value of 0.54 and 0.51 for peak and residual respectively.

For the effective stress approach, estimating σ'_{vo} from the relationship

$$S_u = 0.26 \cdot \sigma'_{vo}$$

which gives σ'_{vo} = 230 kPa, the beta value (β) becomes 0.17 for maximum friction. This using s_u = 72 kPa.

Total pressure at failure was about 640 kPa and the pore pressure showed 395 kPa, resulting in a horizontal effective pressure of 245 kPa. The interface friction angle (δ) can then be estimated from

$$f_{max} = \sigma'_n \cdot \tan\delta$$

giving δ = 9.1 degrees.

CYCLIC TESTS

After the static test the pile was brought back to zero position and left to reconsolidate for three days. The plan was to start with cyclic stress controlled tests at this time but malfunctioning of the loading system with resulting shock movements of the pile made this impossible. These movements made the total pressure and pore pressure on the pile wall drop with about 50 kPa and 30 kPa respectively. It was therefore decided to run the displacement controlled test first.

Displacement Controlled Tests (WD36SC)

A displacement controlled test comprised of applying parcels of 100 cycles with 10 seconds period in two-way cyclic loading from the zero position of the pile. A total of six consecutive parcels were performed with increasing displacement amplitude, starting with 0.2mm in the first parcel and with 0.4, o.6, 0.8, 1.0 and 2.0mm in the following parcels.

The applied displacement versus cycle numbers are shown in Figure 6 with the resulting skin friction, total pressure, pore pressure and effective pressure versus cycle numbers are shown in Figures 7, 8, 9 and 10 respectively. More detailed plots of selected cycles are shown in the Appendix A.

As seen from the resulting skin friction in Figure 7 and in Figure A1 the two way cycling of 0.2mm amplitude did not cause failure of the pile, although some hysteresis is present in the friction versus displacement. Increasing the amplitude to 0.4mm yields a maximum friction of 42 kPa in the first cycle, reducing to 38 kPa after five cycles and stabilizing at 36 kPa as a maximum after about 20 cycles. The residual value during large slip was quite steady at 33 kPa after 20 cycles as seen in Figure A-2.

In the following parcels the peak friction never reached the previous maximum but was quite consistent at about 38 kPa with a residual value during large slip of about 33 kPa. This gives a degradation in strength from maximum peak (42 kPa) of about 21%.

As can be seen in Figures A-3, A-4, A-5 and A-6 the general form of the friction-deformation curve has the form of a parallelogram.

From the pressure diagrams in Figures 8,9 and 10 the pore pressure is seen to show no cyclic variation and only slightly increasing during the application of parcels. The average total pressure decreases slihtly and has a cyclic variation of about 10 kPa in first parcel increasing with increasing stroke amplitude to about 27 kPa in the last parcel. As a result of this the effective pressure resembles the total pressure with the average pressure decreasing from 227 kPa in first parcel to about 210 in the last.

In Figures A-7 through A-9 are shown effective normal pressure versus friction on the pile wall for selected cycles. From Figure A-7 showing cycle 100 which is the

maximum yield friction of 42 kPa, effective pressure is measured to 223 kPa. This gives an interface friction angle of about 10,7 degrees.

Stress Controlled Tests (WD36LC)

After the displacement controlled test the pile was left to reconsolidate for one day (20 hrs.) before stress controlled tests were performed.

A stress controlled test comprised of applying a prescribed static tensile (uplift) stress on the pile, superimposed with parcels of 100 cycles with 10 seconds period and prescribed cyclic stress amplitude. The stress amplitude was then increased in the following parcels until failure (excessive uplift) occured in tension.

For this test the static tensile stress level was 21.5 kPa, corresponding to 55% of the previous maximum static capacity. In the first parcel the cyclic level was about 9.5 kPa and for the following parcels the cyclic level was incremented to 14 kPa, 15.8 kPa and 16.5 kPa in the final parcel as shown in Figure 11, showing skin friction (envelope of max. and min.) versus number of cycles. In the following four figures the resulting deformations, and pressures due to the applied skin friction are plotted versus cycle numbers. In Appendix B selected cycle numbers are plotted as friction versus deflection, friction versus effective pressure and friction, pore pressure and total pressure variation during the cycle.

As seen in Figure 11 a total of four parcels were performed. Already in the first parcel an upward movement of the pile is experienced as depicted in Figure B-1. In the second parcel with cyclic stress level of 14 kPa (giving maximum stress of 35.5 kPa) the pile is significantly moving upwards for each cycle even though the stress level is below the previous static capacity. This fact is most likely due to the cyclic stroke controlled test (degradation) performed the day before where the degraded maximum friction during slip was 33 kPa. Referring to Figure 12 it is seen that the deformation rate is larger in the beginning at the parcel whereas is seems to stabilize more after about 50 cycles.

Increasing the cyclic stress still further to 15.8 kPa in third parcel it is seen that the pile is forced up very drastically for each cycle (in the order of 0.04mm per cycle) with seemingly no tendency to stabilize. Finally in the last parcel with applied cyclic

stress of 16.5 kPa the pile is pulled up beyond the control point of the testing system.

The pressure diagrams in Figures 13, 14 and 15 show quite steady average total pressure in the first parcel with a cyclic variation of about 3 kPa. In the second parcel the cyclic variation increases to about 5 kPa with a reduction in the average pressure to 570 kPa. In the third parcel the average pressure declines quite distinctly down to 542 kPa with the same cyclic level as in second parcel and finally in the last parcel the decline is more pronounced and ends at 520 kPa after about 20 cycles duration at which time the test was stopped. The pore pressure showed no cyclic response and had only a small increase from 357 to 361 kPa from start to end of the test. The effective pressure thus shows a mirror image of the total pressure starting at an average of 211 in the first parcel and ending at 160 kPa after the test.

This stress controlled test showed different behaviour than the previous tests in that the upward deformation of the pile started almost immediately in the first parcel. This is most likely due to the displacement controlled test being performed before the stress controlled test which had fully degraded the soil from its peak friction value, and with insufficient time to reconsolidate. In addition the static tensile bias was as high as 55% of the previous static capacity which also might give reason for the excessive deformation during testing.

The maximum obtained side friction was 38 kPa although this was after an excessive uplift with the effective lateral pressure at this time measured to about 187 kPa resulting in an internal friction angle of about 11.4 degrees.

STRENGTH TESTS

After the stress controlled cyclic tests the pile was pulled out of the pile chamber and the sample built out. Pocket penetrometer tests were performed on the side of the sample with results shown in Figure 16.

Three standard triaxial test samples were then prepared from the center of the sample and unconfined compression tests (UCT) were performed, with results shown in Figure 17.

In Figure 18 are shown the water content and interpreted undrained shear strength of

the clay specimen versus the distance from the pile center after completion of the pile test.

TABLE 1.

SAMPLE PROPERTIES TEST 6, STRATUM III

SAMPLE PREPARATION		CONSOLIDATION			END OF PILE TEST
INITIAL WATER CONTENT	INITIAL HEIGHT	AXIAL DEFORMATION	AXIAL STRAIN	WATER CONTENT	WATER CONTENT
w_i (%)	H_o (cm)	ΔH (cm)	ε (%)	w_e (%)	w_{ep} (%)
51.06	51.4	6.5	12.65	A 40.2	A 40.17 B 40.16 C 39.29 D 38.16

CONFINING PRESSURE		
AXIAL	KPa	700
RADIAL	KPa	550
BACK PRESSURE	KPa	200
SAMPLE CONSOLIDATION		
IN OEDOMETER	Days	21
IN PILE CHAMBER	Days	3
INTERPRETED SHEAR STRENGTH		
END OF CONSOLIDATION	KPa	65
END OF PILE TEST	KPa	77

Fig. 1

CONSOLIDATION DIAGRAM								Test No. 6 Stratum III		Start date 28/5/82	
H_i 51.4 cm		H_e 44.9 cm		$\Delta\varepsilon_v$ 12.65%						σ_c 500 kPa	
Time h	70	94	104	142	166	191	233	257	282	302	326
Δh cm	3.5	4.3	4.6	5.0	5.4	5.5	5.9	6.1	6.2	6.3	6.3
u kPa	300	268	262	204	171.6	124.6	123.8	107.8	96.4	85.8	78.9
350	374	396	420	468	492						
6.4	6.5	6.5	6.5	6.6	6.6						
69.9	62.0	59.3	58.5	53.3	49.4						

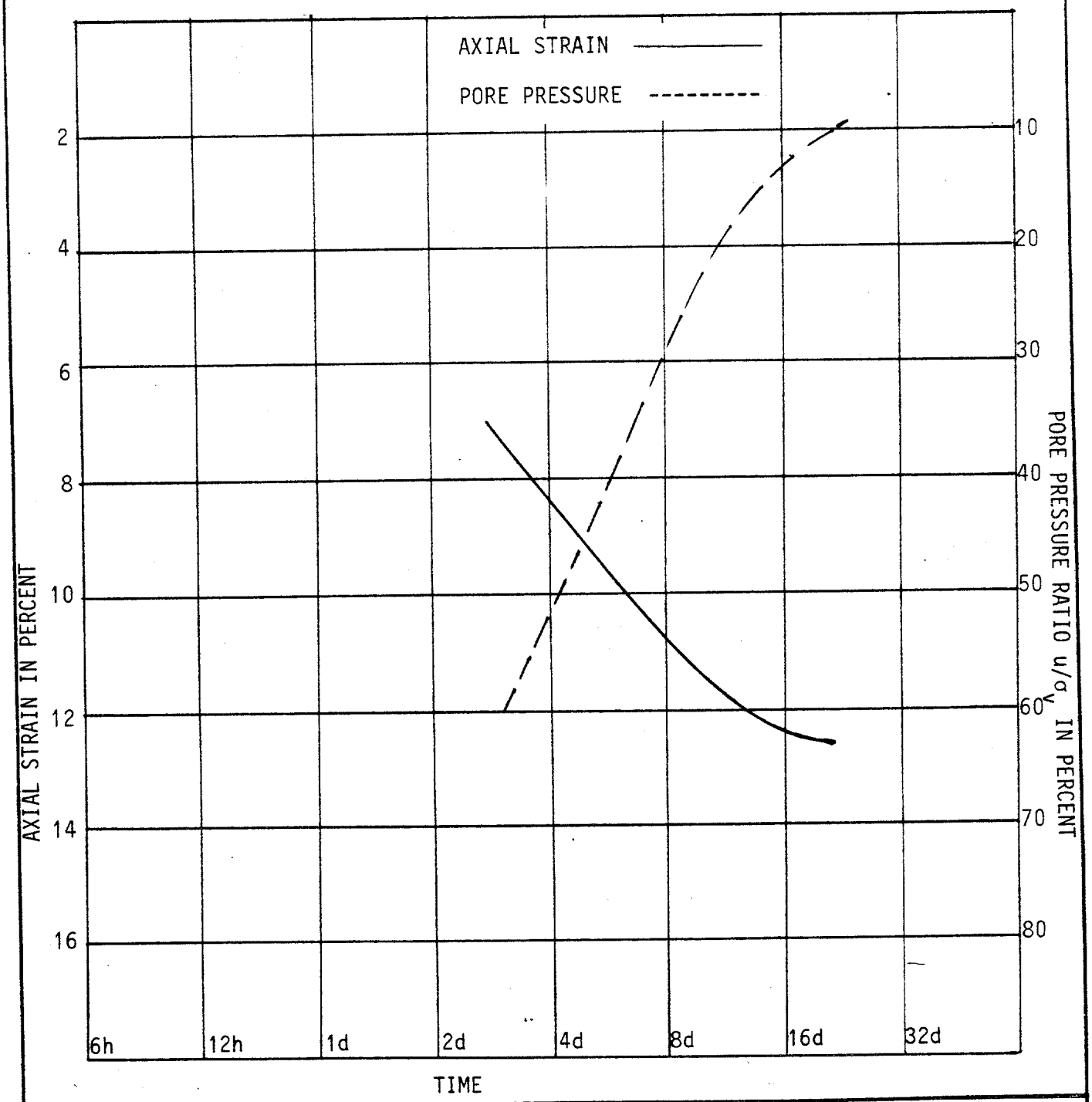

CNRD 13-2 TENSION PILE STUDY LABORATORY MODEL PILE TESTS

TEST 6, STRATUM III, Cosolidation diagrams for clay sample

DET NORSKE VERITAS
Geotechnical Laboratory

Drawn by | Date | Approved | Fig. No. 2

TEST 6, STRATUM III

SHEAR STRENGTH (KPa) FROM POCKET PENETROMETER TESTS AFTER CONSOLIDATION

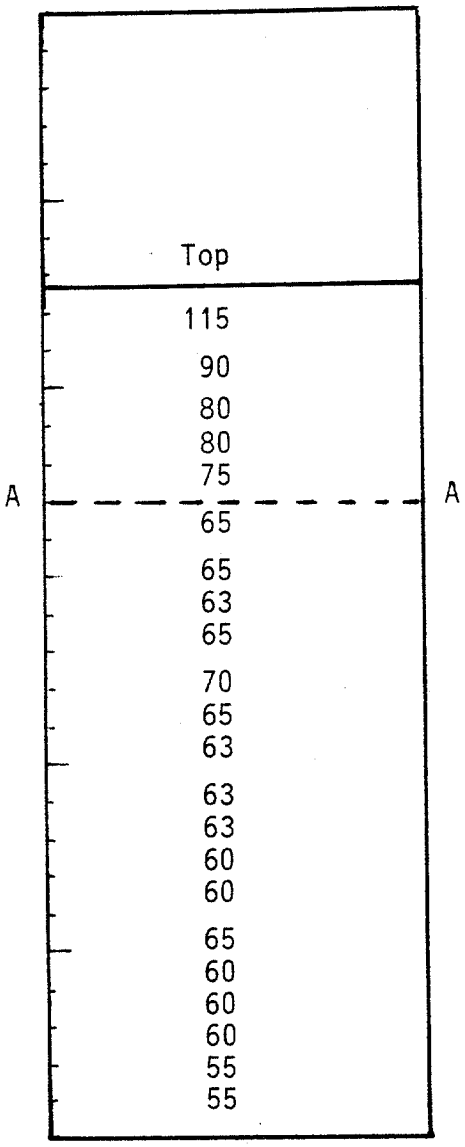

Scale 1:4

Level A-A

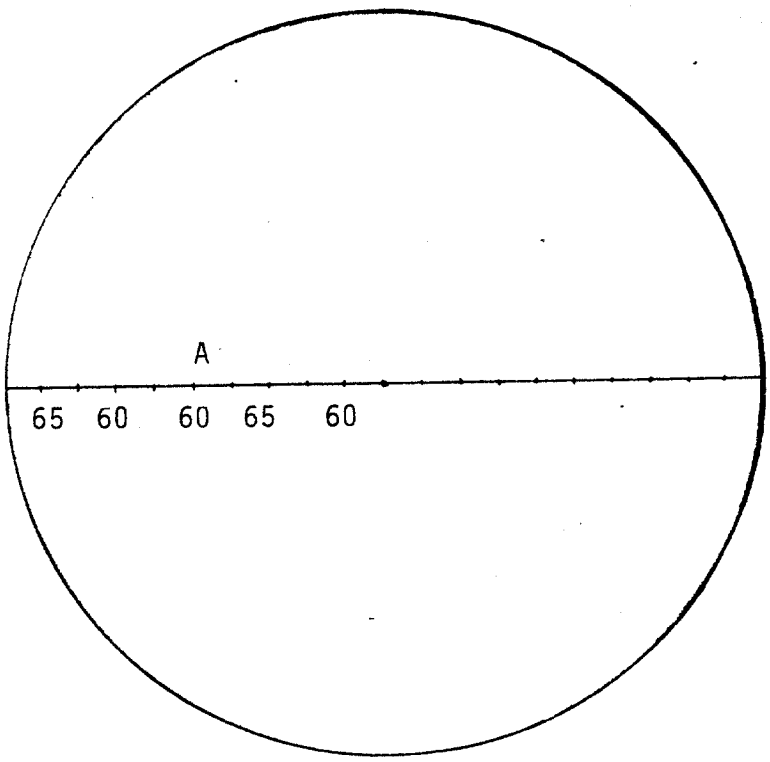

Scale: 1:2

CNRD 13-2 TENSION PILE STUDY LABORATORY MODEL PILE TESTS

TEST 6, STRATUM III, Pocket penetrometer tests		Scale
DET NORSKE VERITAS Geotechnical Laboratory	Drawn by	Date
	Approved	Fig. No. 3

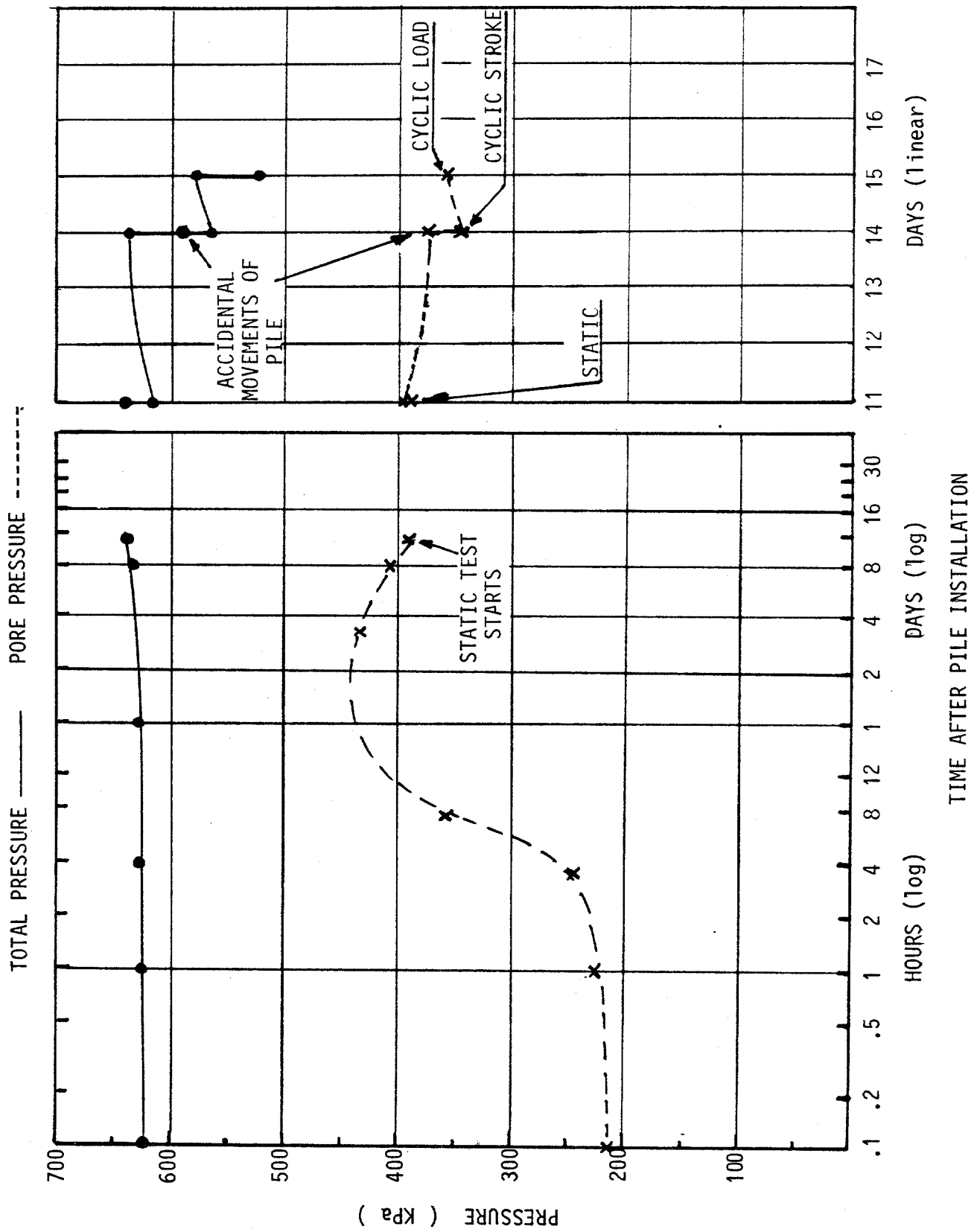

CNRD 13-2 TENSION PILE STUDY LABORATORY MODEL PILE TESTS

TEST 6, STRATUM III, Pressures at pile wall after installation

DET NORSKE VERITAS Geotechnical Laboratory	Drawn by	Scale
	Approved	Date
		Fig. No. 4

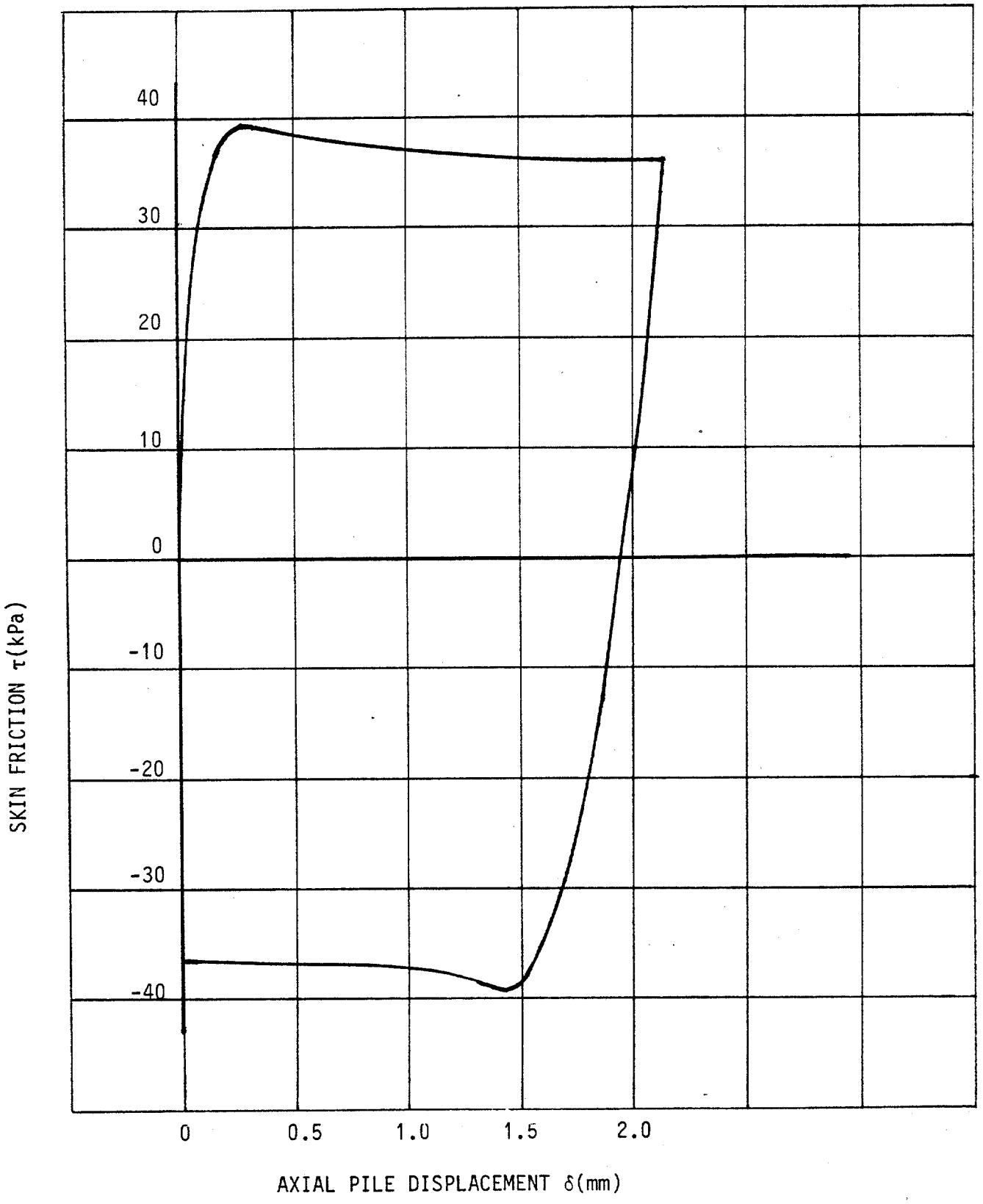

CNRD 13-2 TENSION PILE STUDY LABORATORY MODEL PILE TESTS

TEST 6, STRATUM III, STATIC TEST

DET NORSKE VERITAS Geotechnical Laboratory	Drawn by	Scale
	Approved	Date
		Fig. No. 5

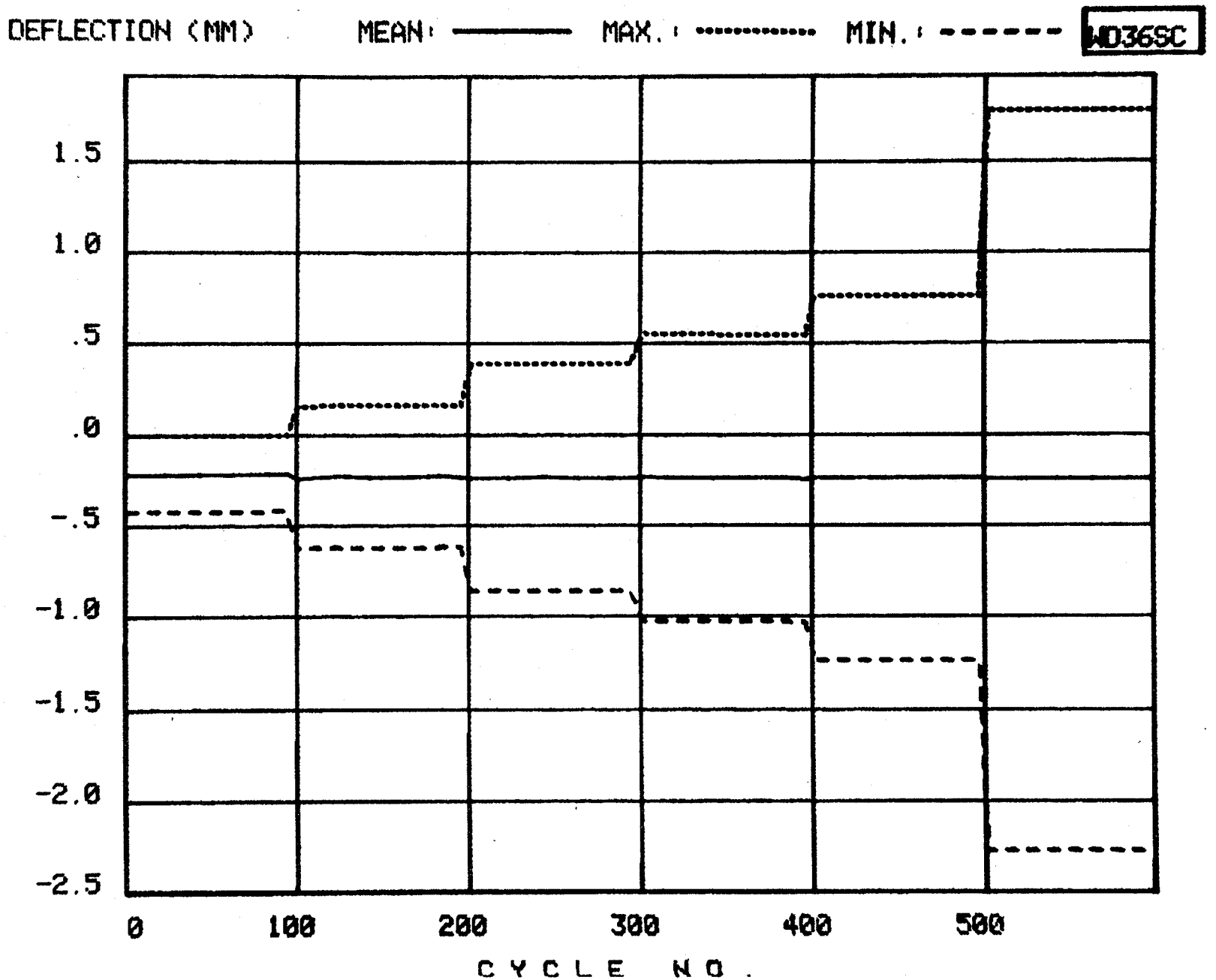
DEFLECTION (MM)
MEAN:
MAX.:
MIN.:
WD36SC
1.5
1.0
.5
.0
-.5
-1.0
-1.5
-2.0
-2.5
0
100
200
300
400
500
CYCLE NO.

Fig. 6

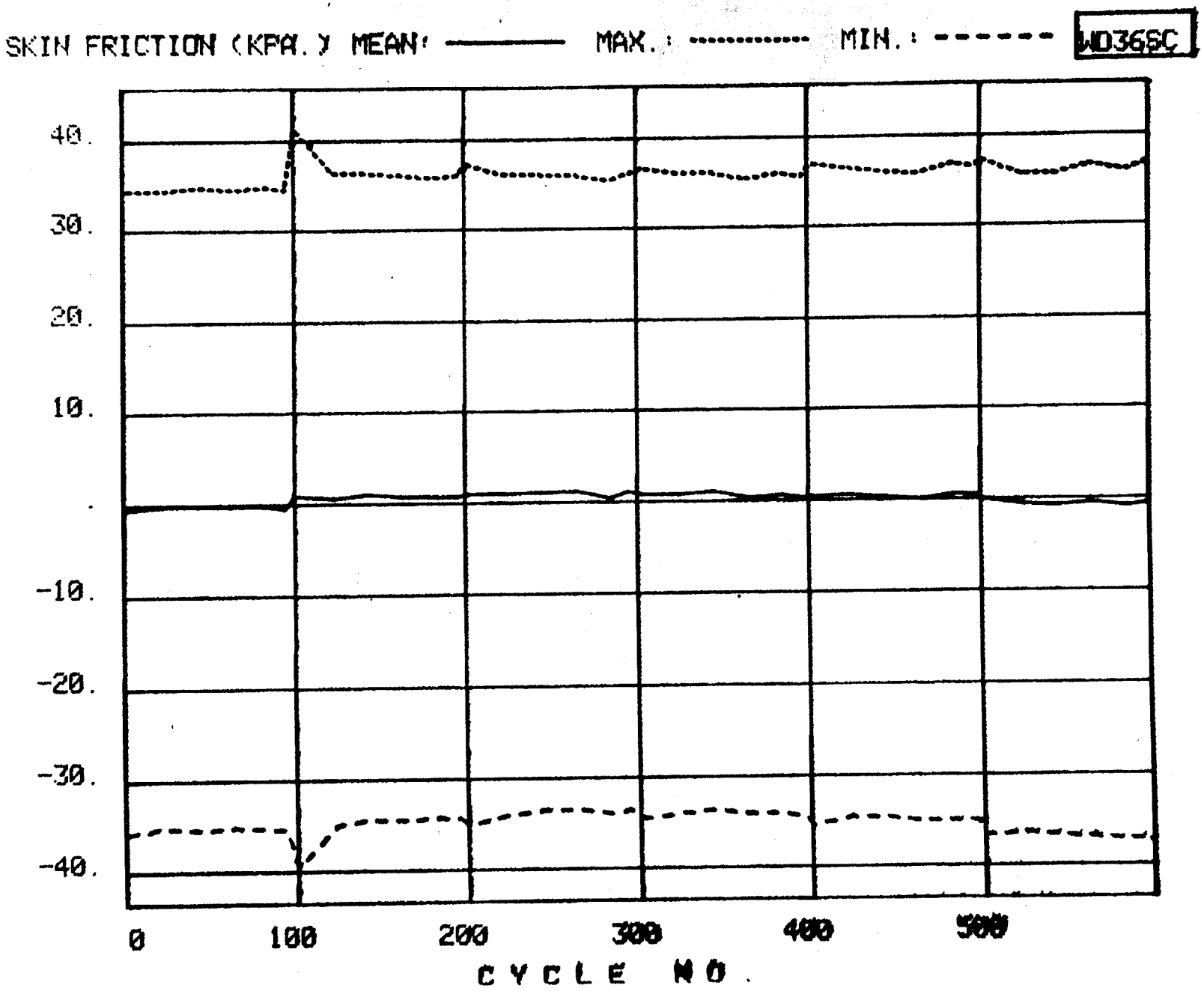
SKIN FRICTION (KPA.) MEAN: MAX.: MIN.:
WD36SC
40.
30.
20.
10.
-10.
-20.
-30.
-40.
0
100
200
300
400
500
CYCLE NO.

Fig. 7

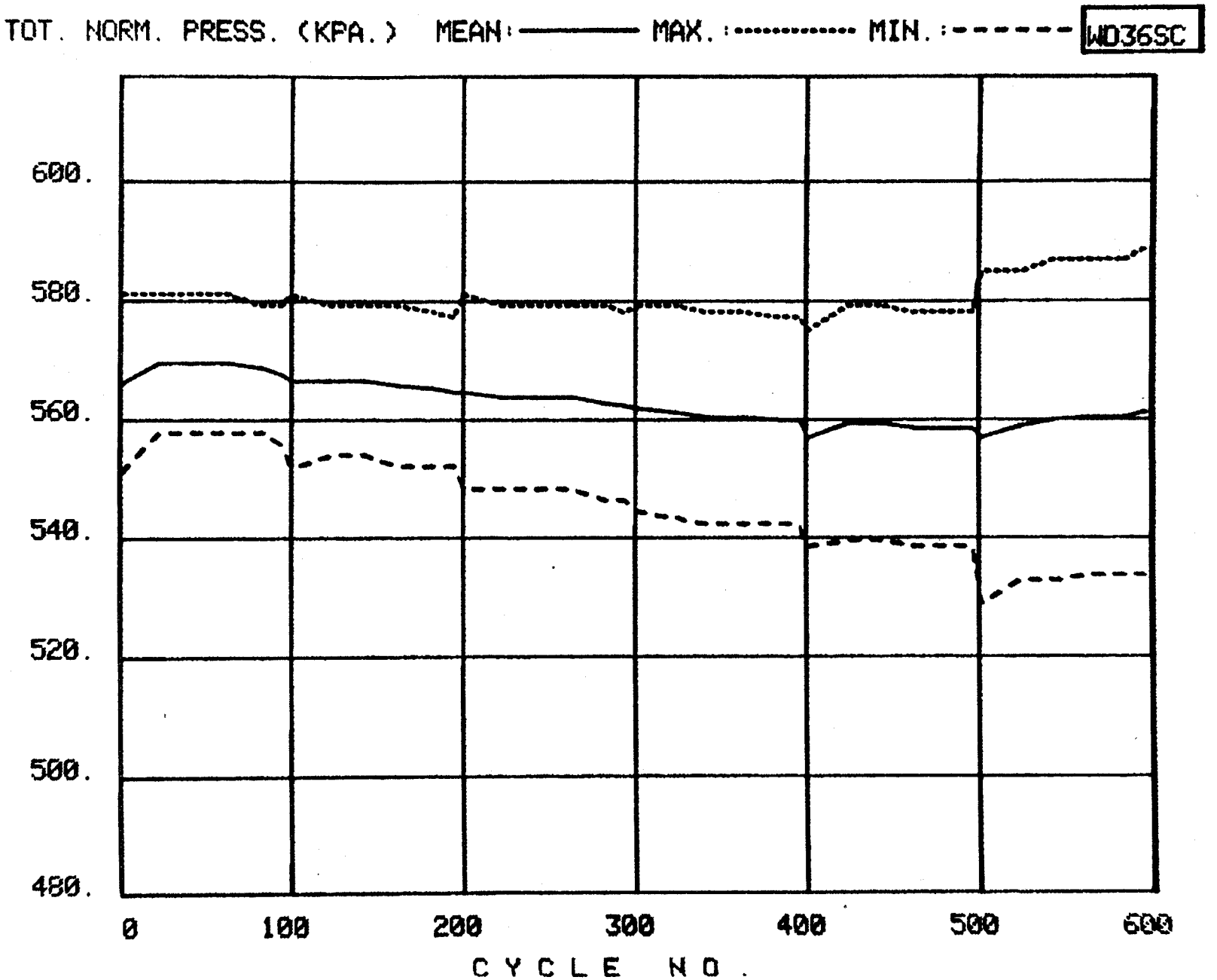
TOT. NORM. PRESS. (KPA.) MEAN: MAX.: MIN.:
WD36SC
600.
580.
560.
540.
520.
500.
480.
0
100
200
300
400
500
600
CYCLE NO.

Fig. 8

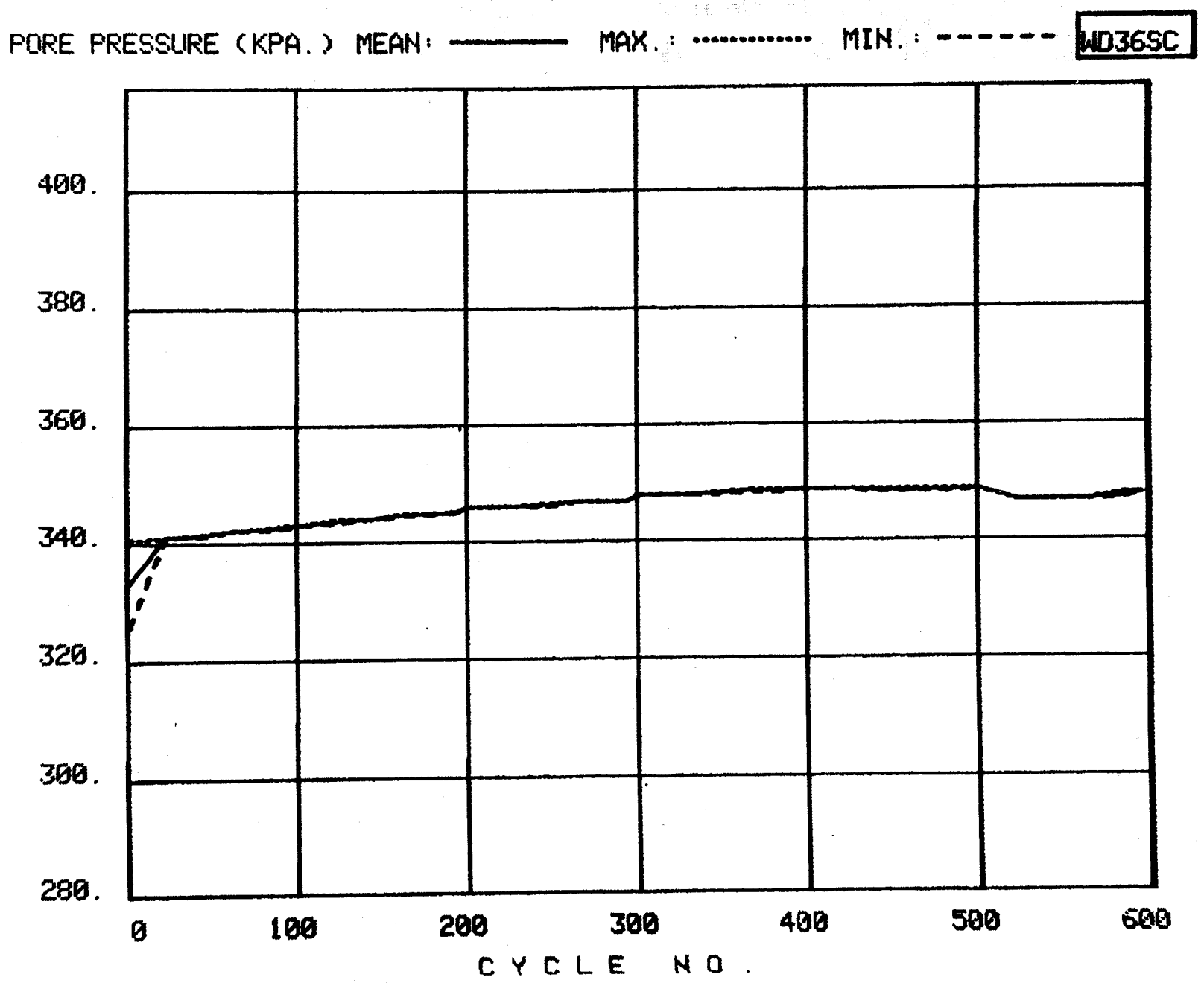
PORE PRESSURE (KPA.) MEAN: MAX.: MIN.:
WD36SC
400.
380.
360.
340.
320.
300.
280.
0
100
200
300
400
500
600
CYCLE NO.

Fig. 9

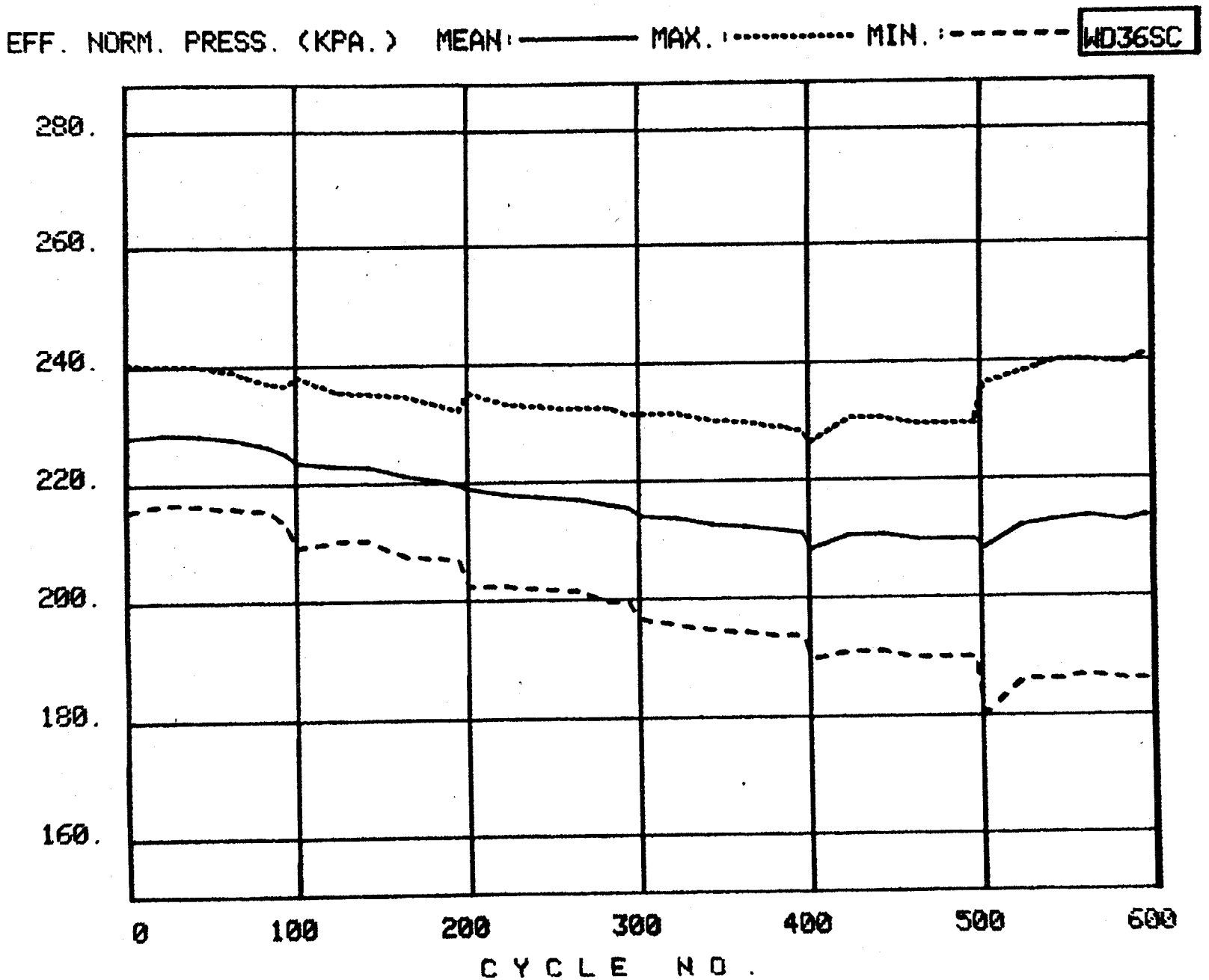
EFF. NORM. PRESS. (KPA.)
MEAN:
MAX.:
MIN.:
WD36SC
280.
260.
240.
220.
200.
180.
160.
0
100
200
300
400
500
600
CYCLE NO.

Fig.10

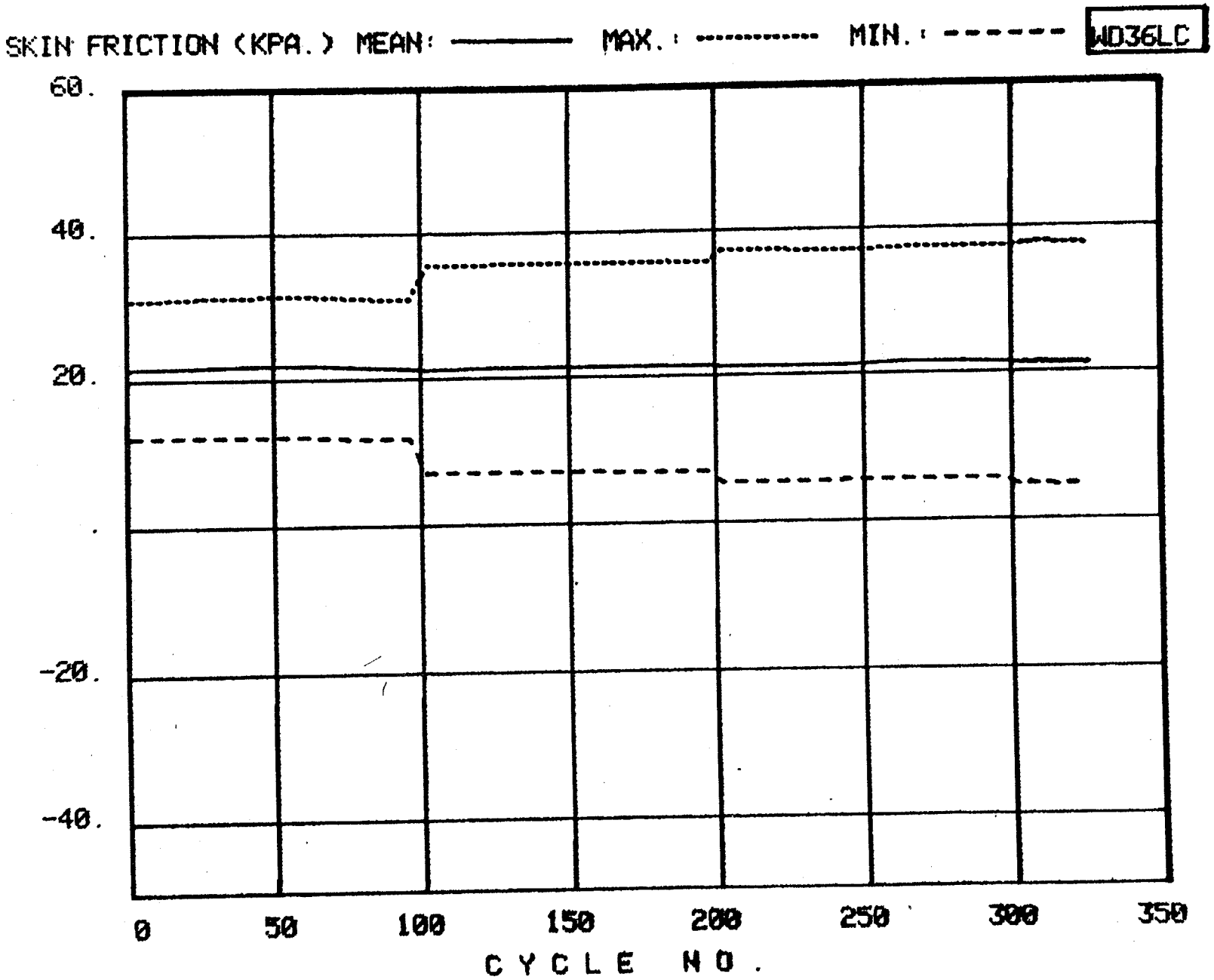
SKIN FRICTION (KPA.) MEAN: MAX.: MIN.:
WD36LC
60.
40.
20.
-20.
-40.
0
50
100
150
200
250
300
350
CYCLE NO.

Fig.11

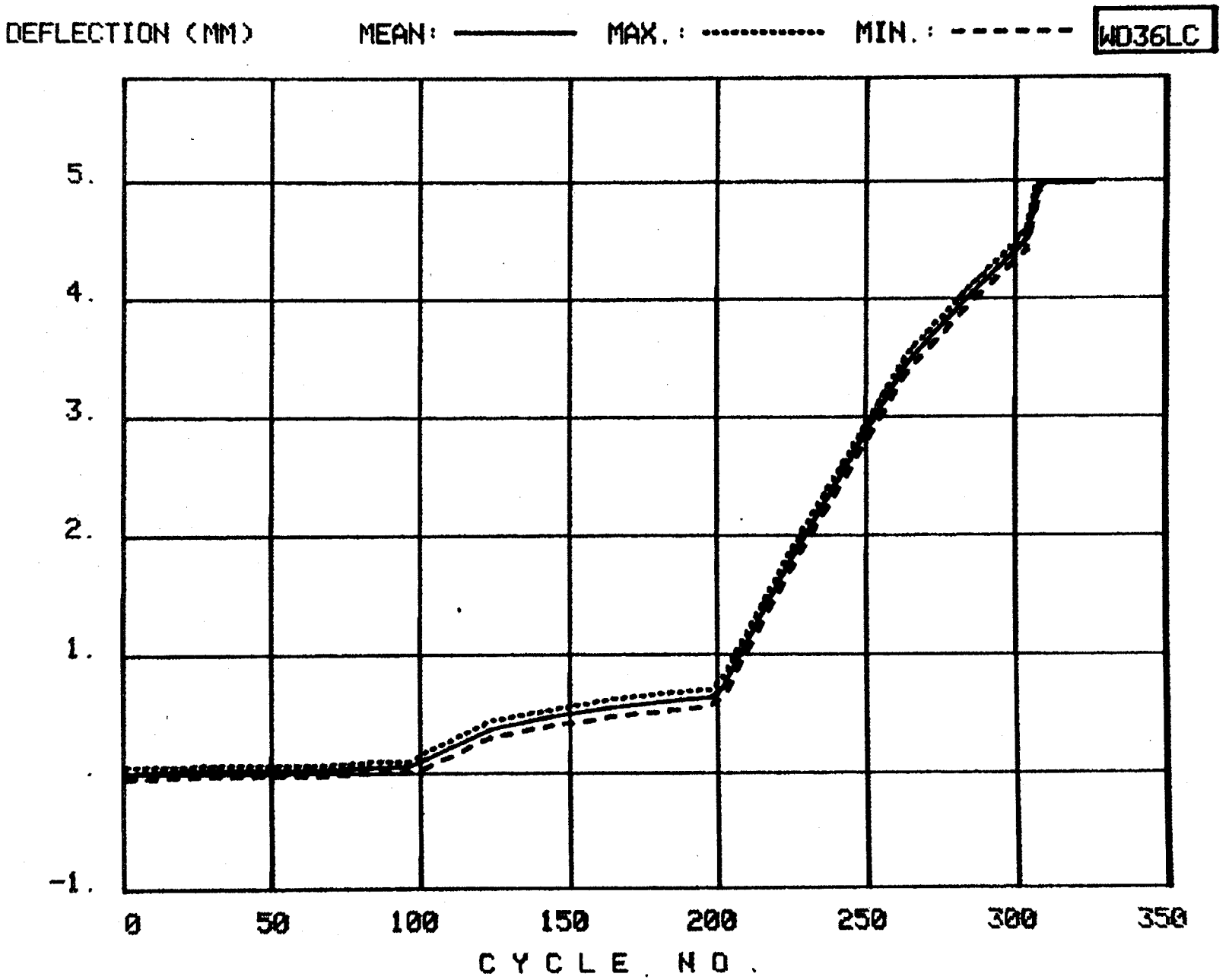
DEFLECTION (MM)
MEAN:
MAX.:
MIN.:
WD36LC
5.
4.
3.
2.
1.
.
-1.
0
50
100
150
200
250
300
350
CYCLE NO.

Fig.12

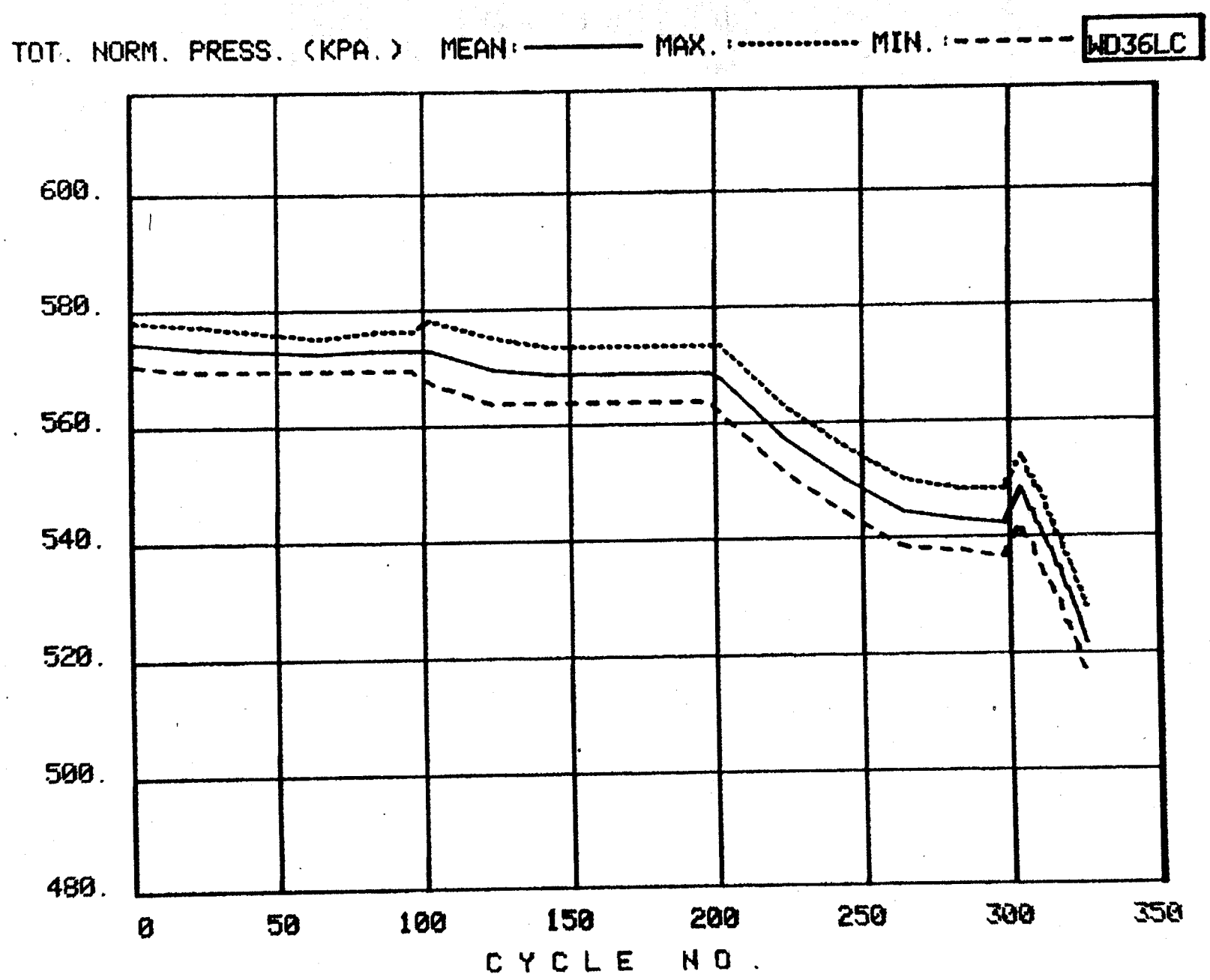
TOT. NORM. PRESS. (KPA.) MEAN: MAX.: MIN.:
WD36LC
600.
580.
560.
540.
520.
500.
480.
0
50
100
150
200
250
300
350
CYCLE NO.

Fig.13

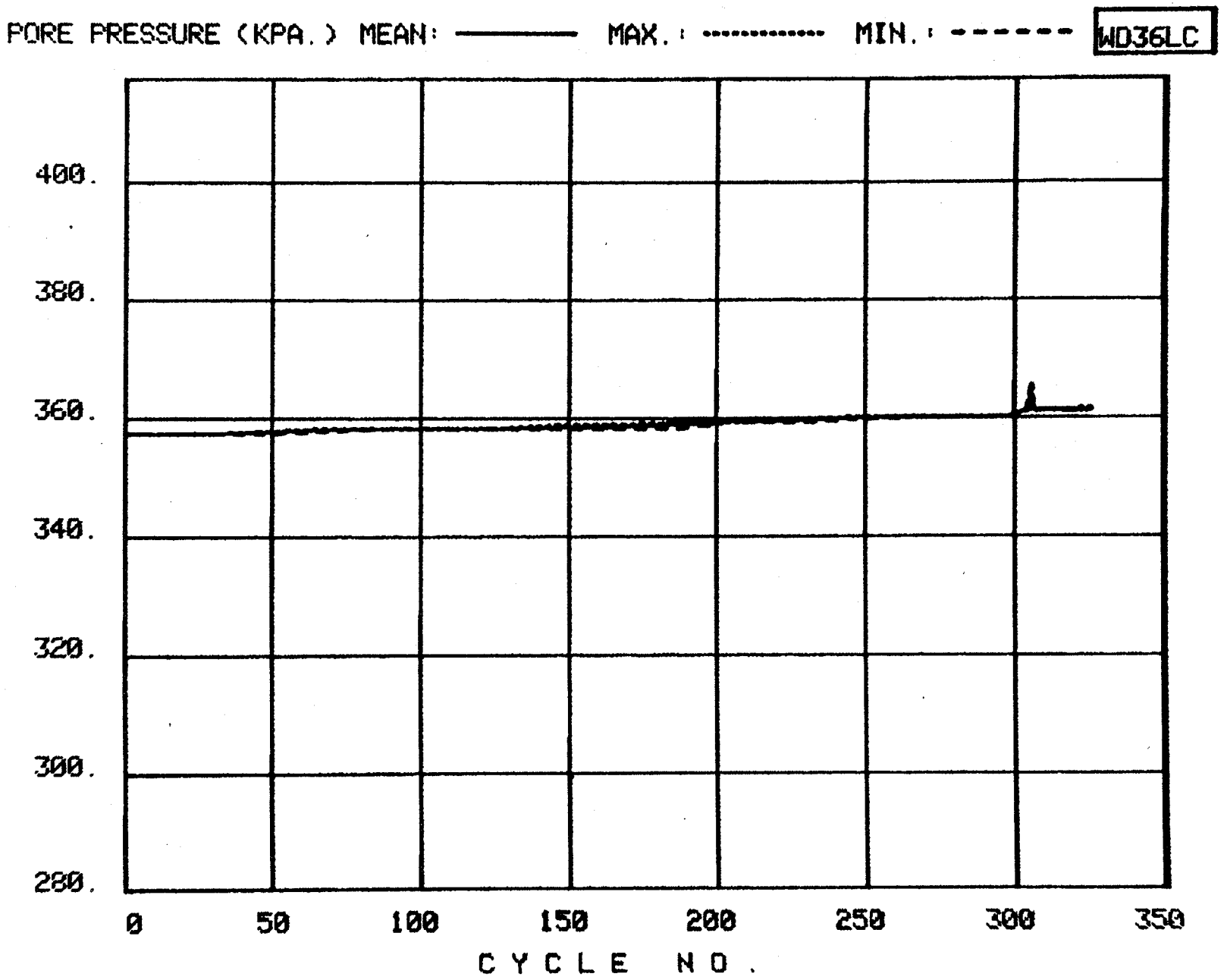
PORE PRESSURE (KPA.) MEAN: MAX.: MIN.:
WD36LC
400.
380.
360.
340.
320.
300.
280.
0
50
100
150
200
250
300
350
CYCLE NO.

Fig.14

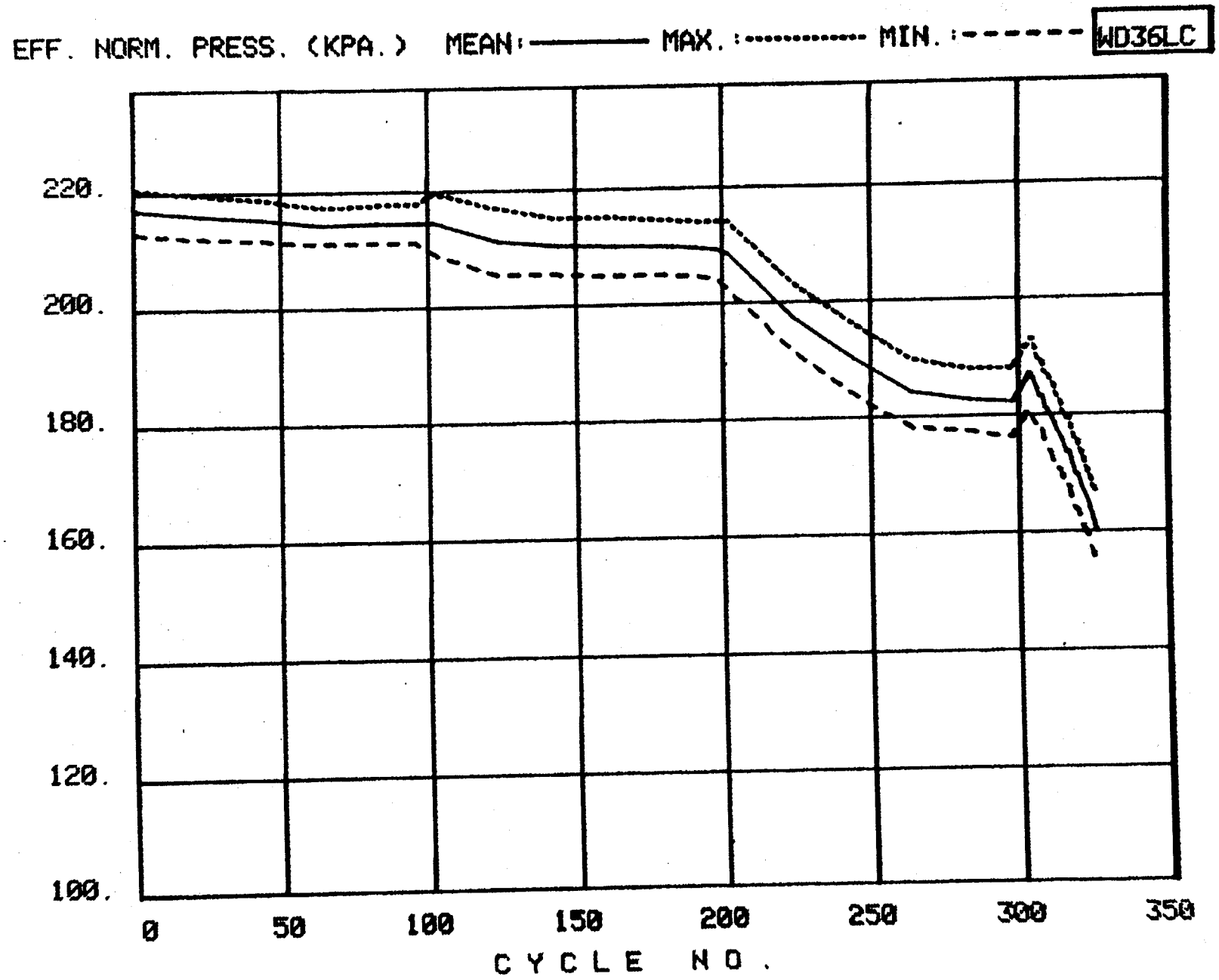
EFF. NORM. PRESS. (KPA.)
MEAN:
MAX.:
MIN.:
WD36LC
220.
200.
180.
160.
140.
120.
100.
0
50
100
150
200
250
300
350
CYCLE NO.

Fig.15

TEST 6, STRATUM III

SHEAR STRNGTH (KPa) FROM POCKET PENETROMETER TESTS AFTER PILE TEST

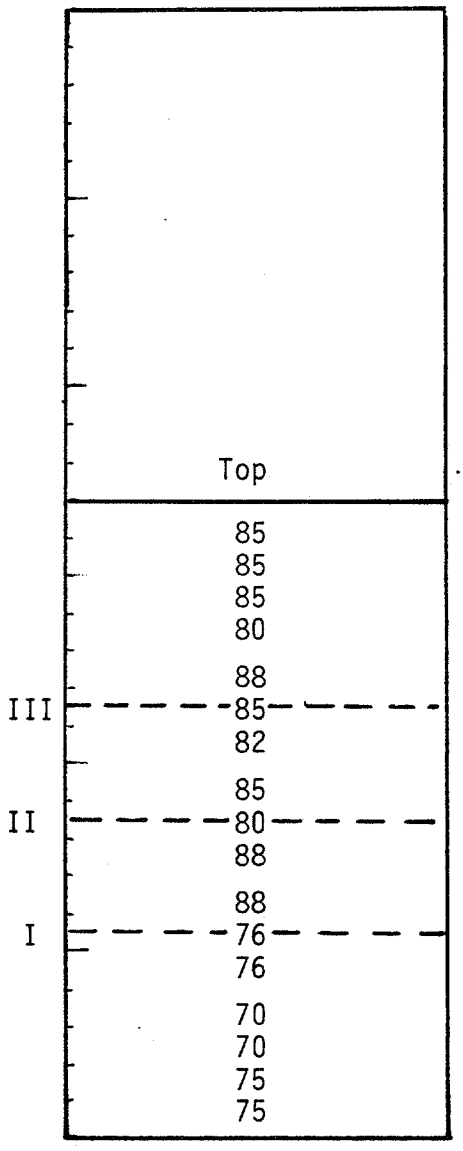

Scale 1:4

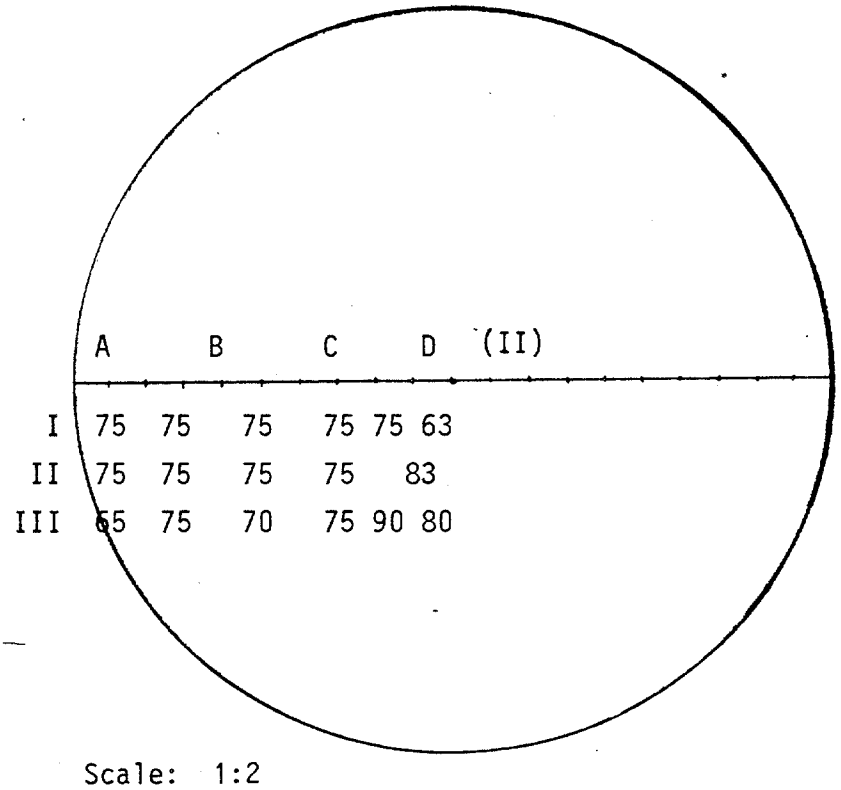

Scale: 1:2

CNRD 13-2 TENSION PILE STUDY LABORATORY MODEL PILE TESTS

TEST 6, STRATUM III, Pocket penetrometer tests after pile test

DET NORSKE VERITAS
Geotechnical Laboratory

Scale	
Drawn by	Date
Approved	Fig. No. 16

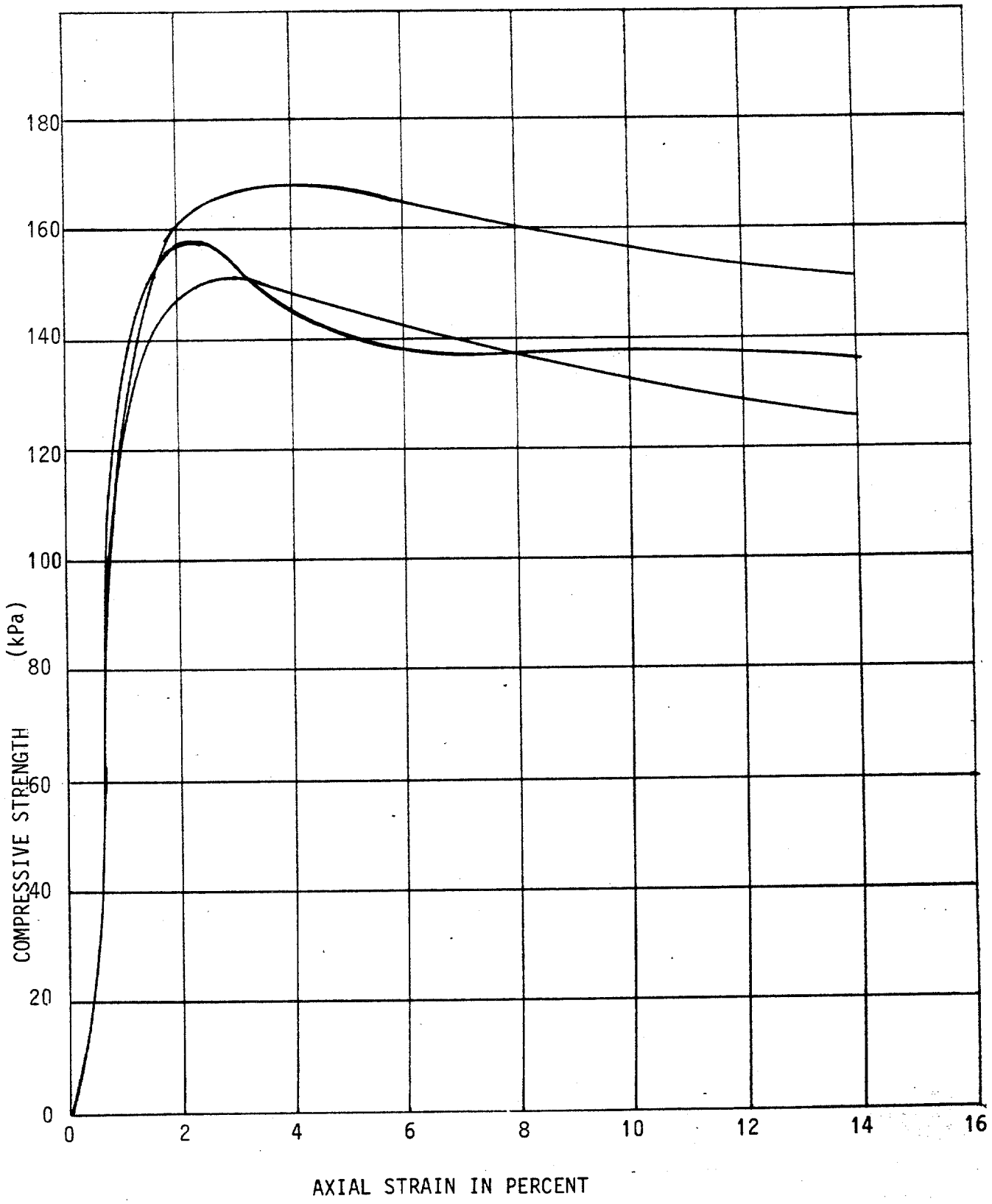

CNRD 13-2 TENSION PILE STUDY LABORATORY MODEL PILE TESTS

TEST 6, STRATUM III, Unconfined compression tests after pile test

Scale

DET NORSKE VERITAS
Geotechnical Laboratory

Drawn by Ivar Engeset

Approved

Date

Fig. No. 17

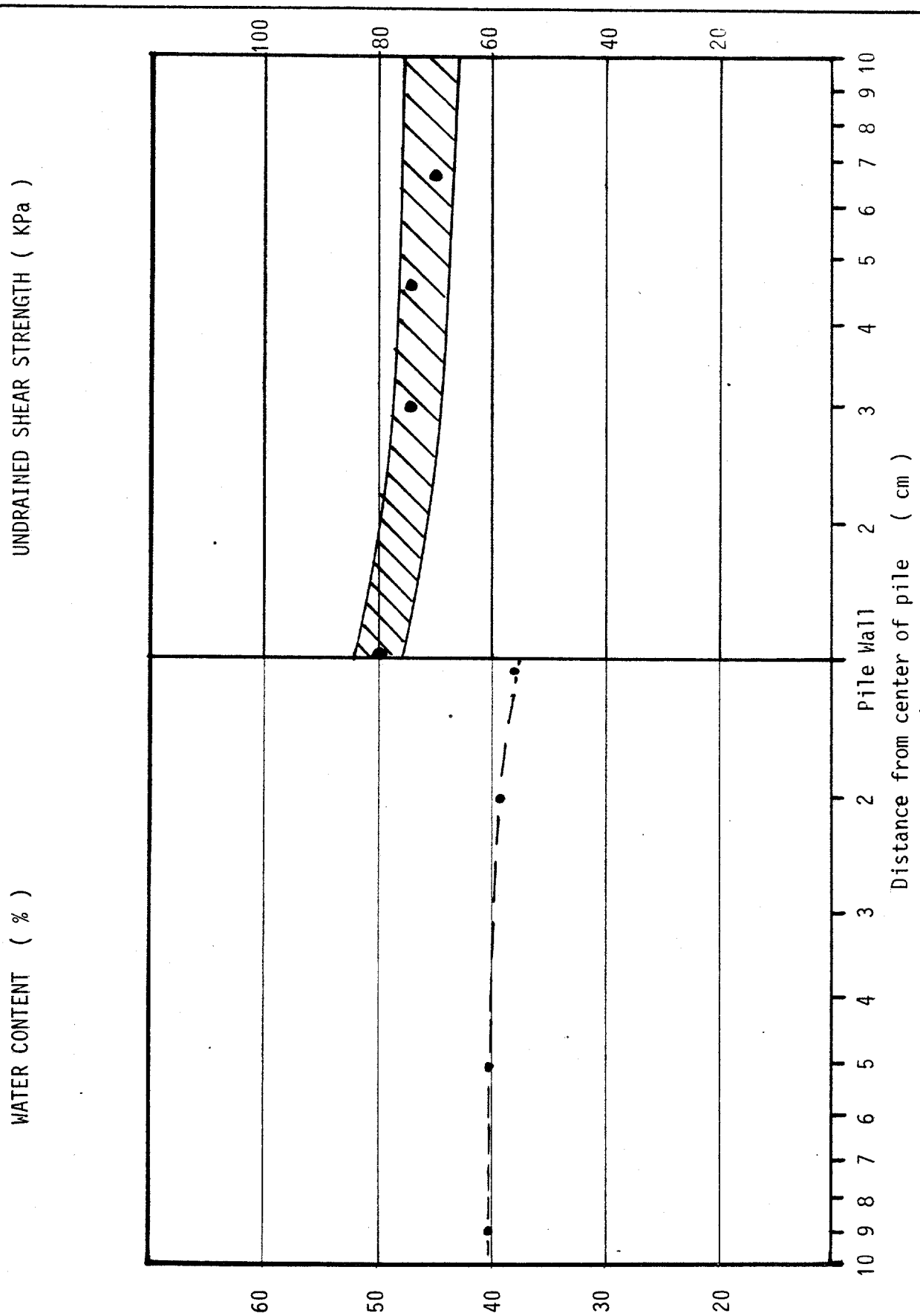

CNRD 13-2 TENSION PILE STUDY LABORATORY MODEL PILE TESTS

TEST 6, STRATUM III, Water content and shear strength after test

DET NORSKE VERITAS Geotechnical Laboratory	Drawn by	Scale
	Approved	Date
		Fig. No. 18

Appendix CA

Plotted Results from WD36SC

Figures CA-1 through CA-6

Skin Friction vs Deflection, Selected Cycles

Figures CA-7 through CA-9

Skin Friction vs Eff. Normal Pressure, Selected Cycl.

Figures CA-10 through CA-20

Skin Friction, Pore and Total Pressure, Selected Cycles

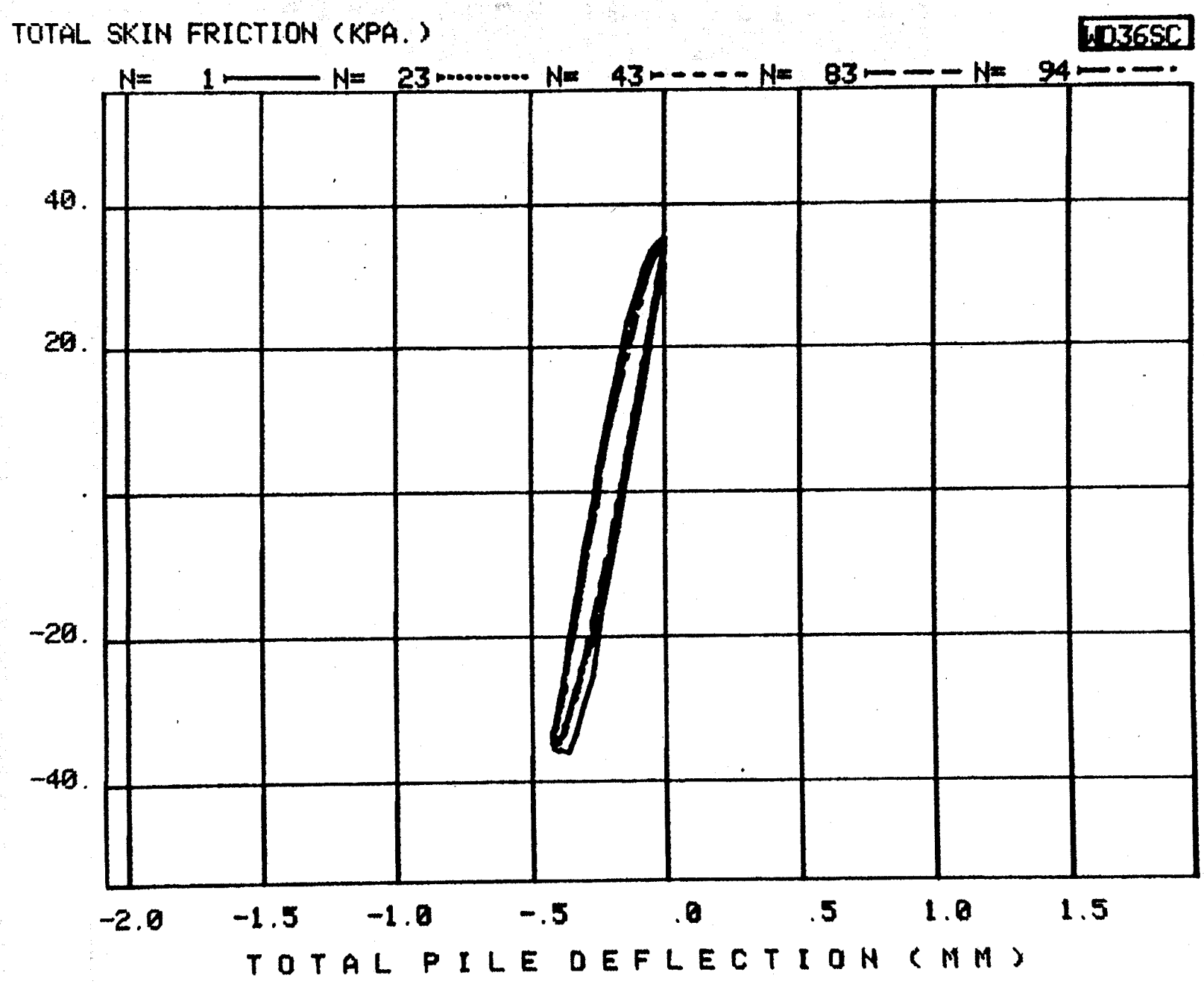
TOTAL SKIN FRICTION (KPA.)
WD36SC
N= 1
N= 23
N= 43
N= 83
N= 94
40.
20.
-20.
-40.
-2.0
-1.5
-1.0
-.5
.0
.5
1.0
1.5
TOTAL PILE DEFLECTION (MM)

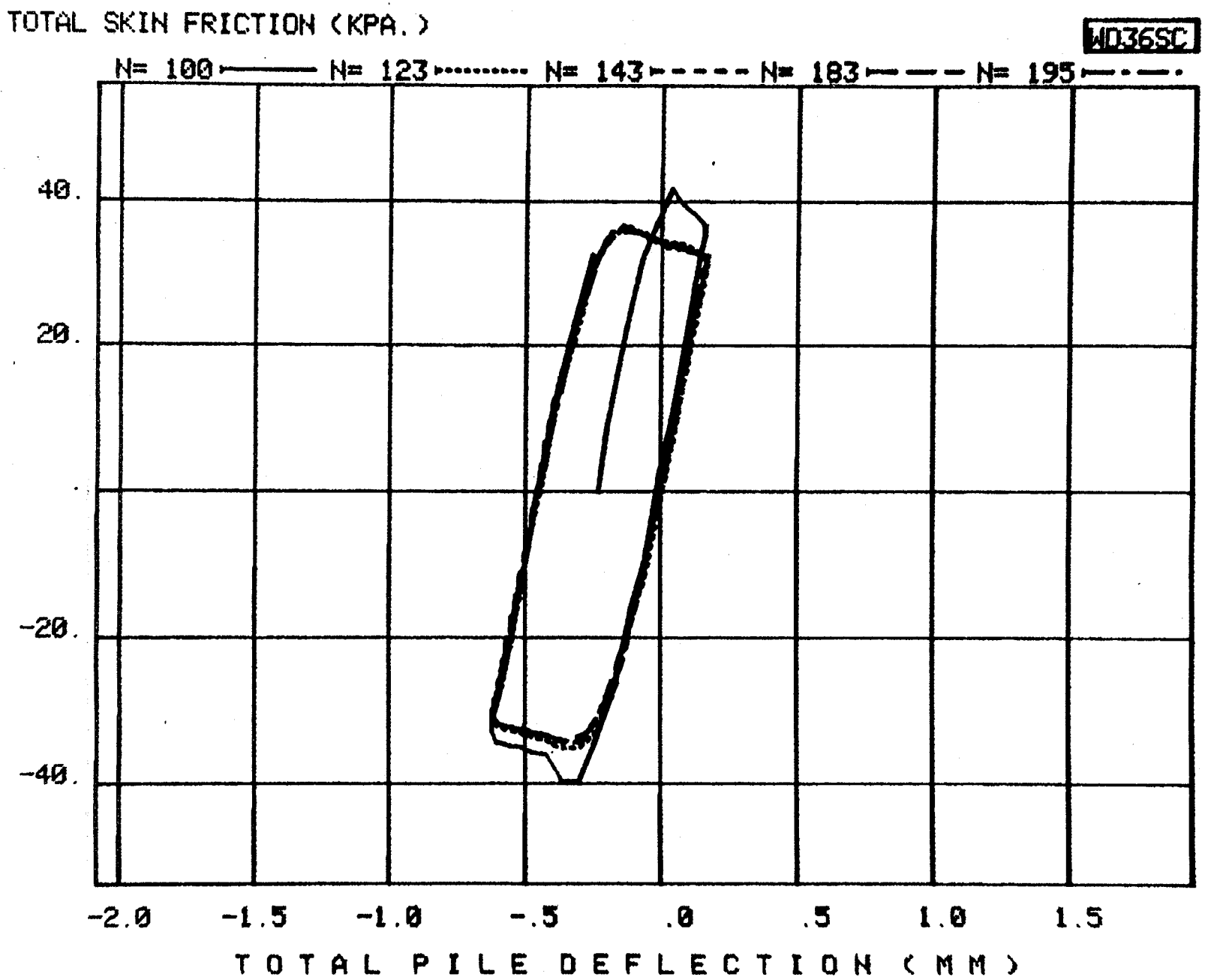
TOTAL SKIN FRICTION (KPA.)
WD36SC
N= 100
N= 123
N= 143
N= 183
N= 195
40.
20.
-20.
-40.
-2.0
-1.5
-1.0
-.5
.0
.5
1.0
1.5
TOTAL PILE DEFLECTION (MM)

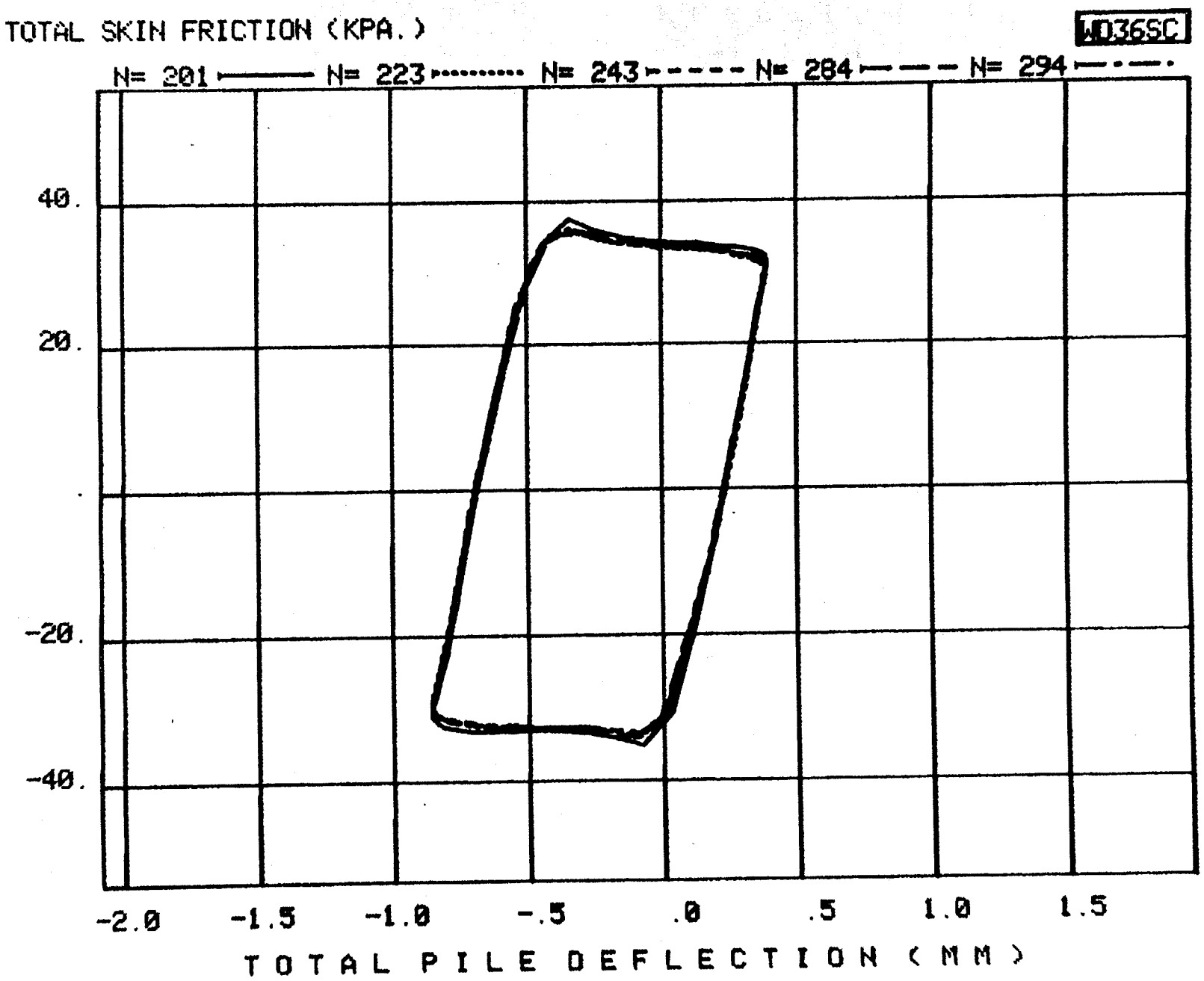
TOTAL SKIN FRICTION (KPA.)
WD36SC
N= 201
N= 223
N= 243
N= 284
N= 294
40.
20.
-20.
-40.
-2.0
-1.5
-1.0
-.5
.0
.5
1.0
1.5
TOTAL PILE DEFLECTION (MM)

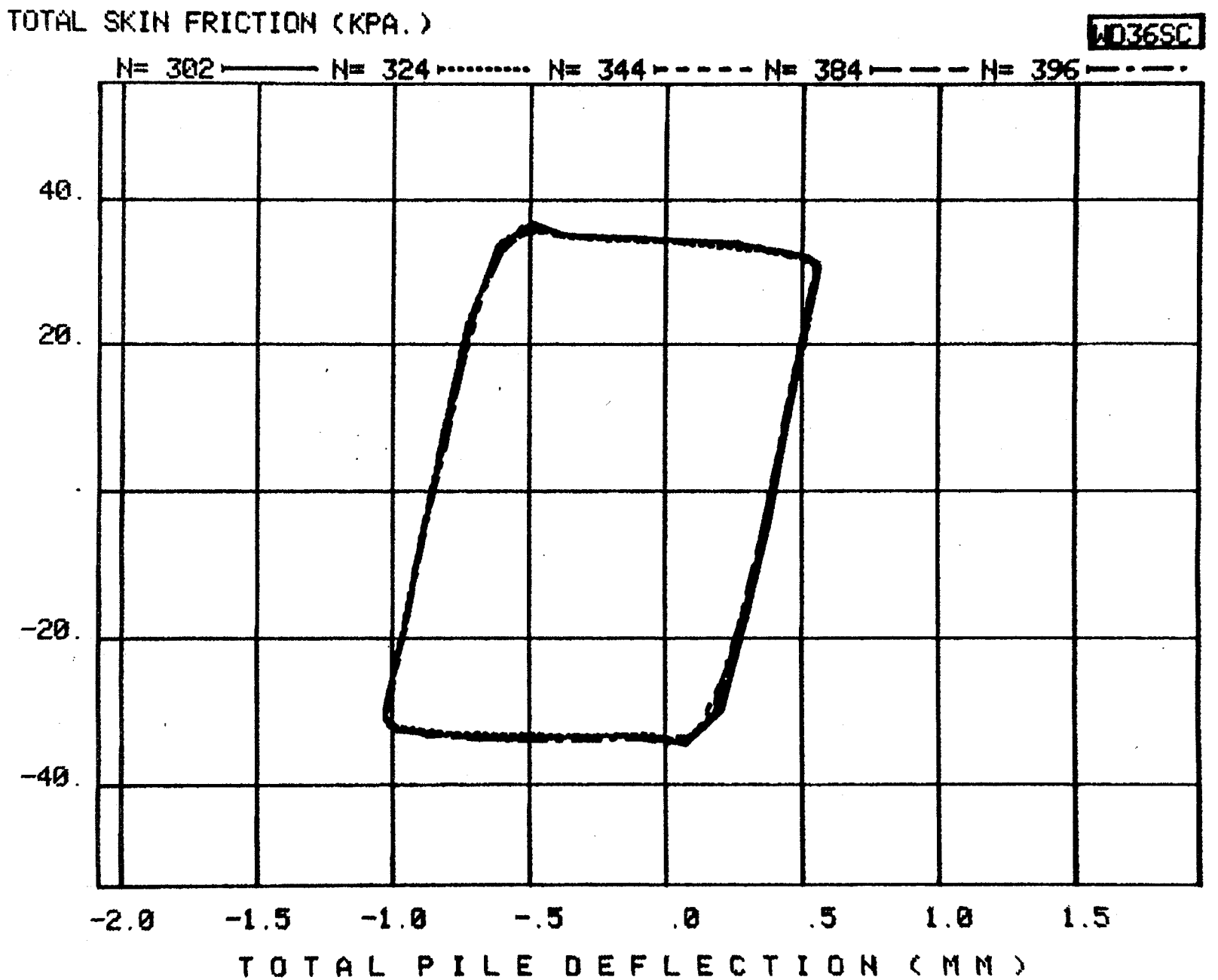
TOTAL SKIN FRICTION (KPA.)
W036SC
N= 302
N= 324
N= 344
N= 384
N= 396
40.
20.
-20.
-40.
-2.0
-1.5
-1.0
-.5
.0
.5
1.0
1.5
TOTAL PILE DEFLECTION (MM)

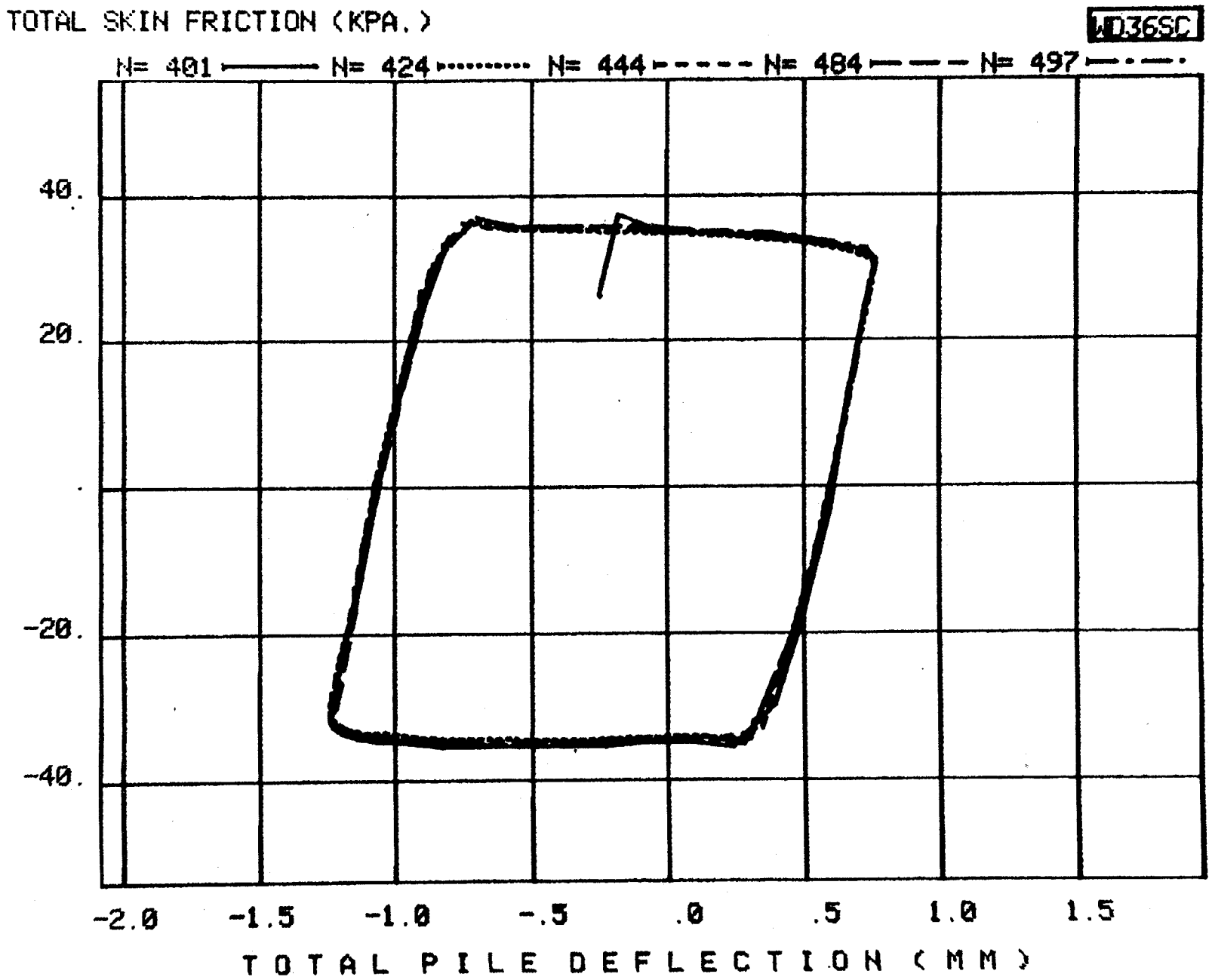
TOTAL SKIN FRICTION (KPA.)
WD36SC
N= 401
N= 424
N= 444
N= 484
N= 497
40.
20.
-20.
-40.
-2.0
-1.5
-1.0
-.5
.0
.5
1.0
1.5
TOTAL PILE DEFLECTION (MM)

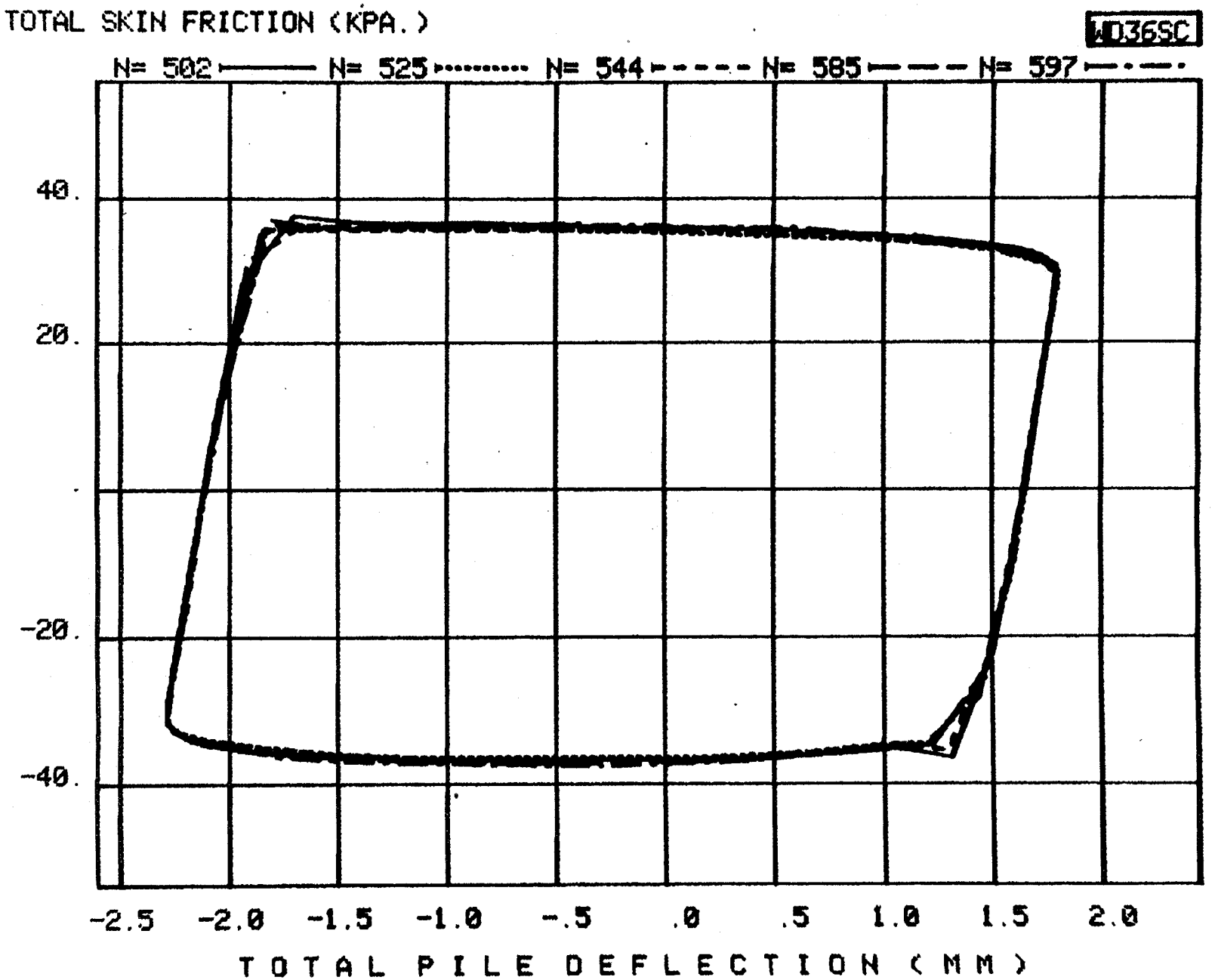
TOTAL SKIN FRICTION (KPA.)
WD36SC
N= 502
N= 525
N= 544
N= 585
N= 597
40.
20.
-20.
-40.
-2.5
-2.0
-1.5
-1.0
-.5
.0
.5
1.0
1.5
2.0
TOTAL PILE DEFLECTION (MM)

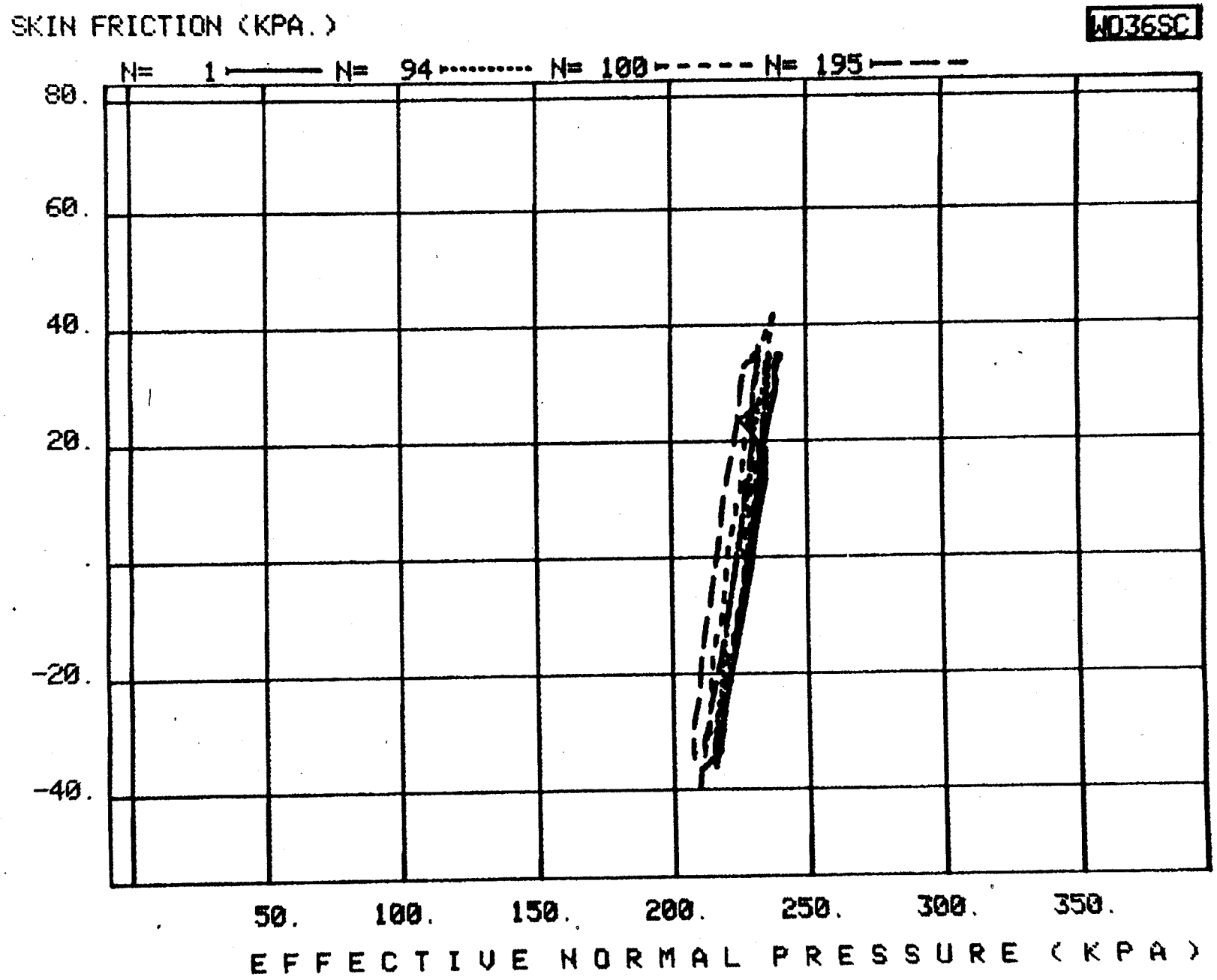
SKIN FRICTION (KPA.)
W036SC
N= 1
N= 94
N= 100
N= 195
80.
60.
40.
20.
-20.
-40.
50.
100.
150.
200.
250.
300.
350.
EFFECTIVE NORMAL PRESSURE (KPA)

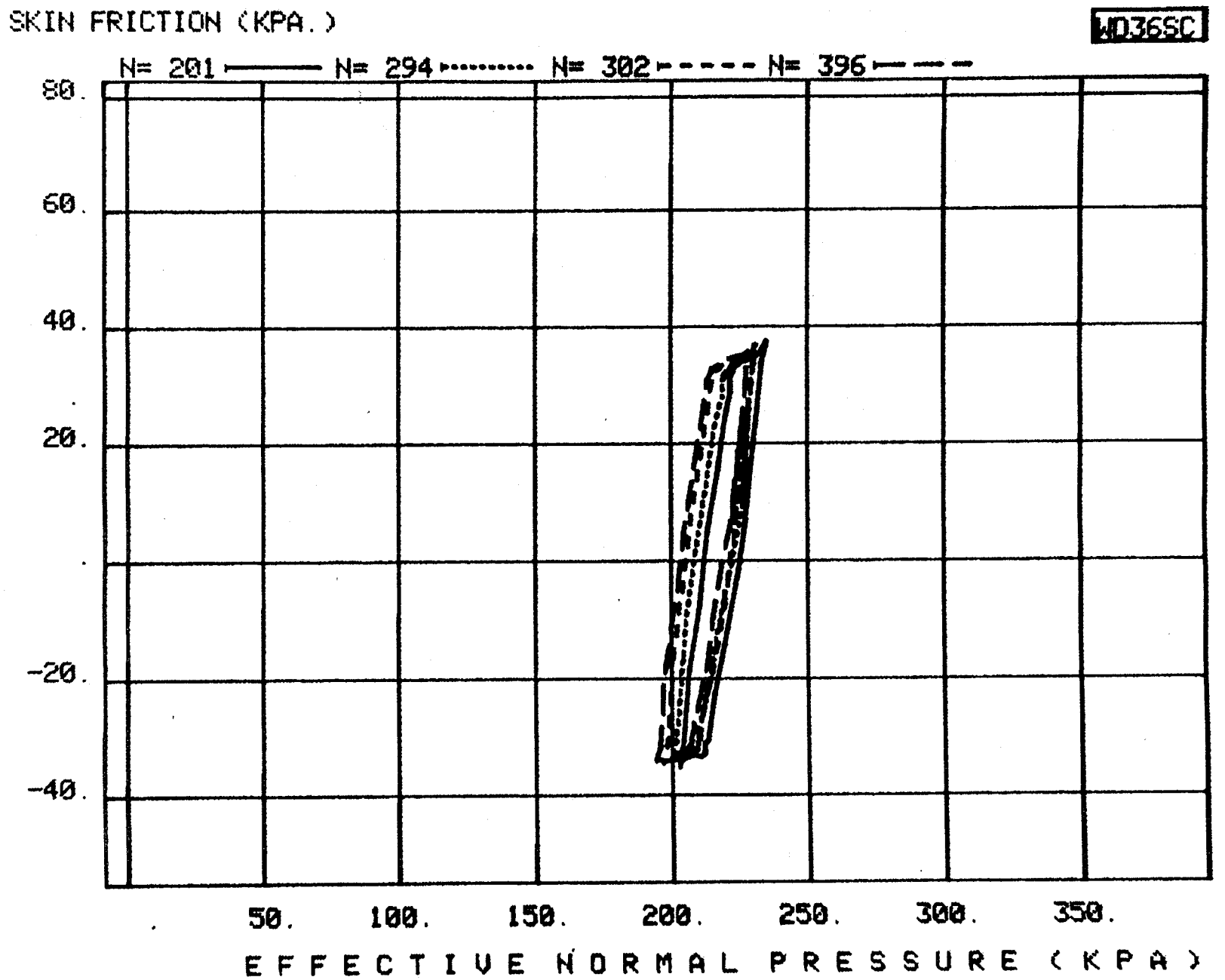
SKIN FRICTION (KPA.)
WD36SC
N= 201
N= 294
N= 302
N= 396
80.
60.
40.
20.
-20.
-40.
50.
100.
150.
200.
250.
300.
350.
EFFECTIVE NORMAL PRESSURE (KPA)

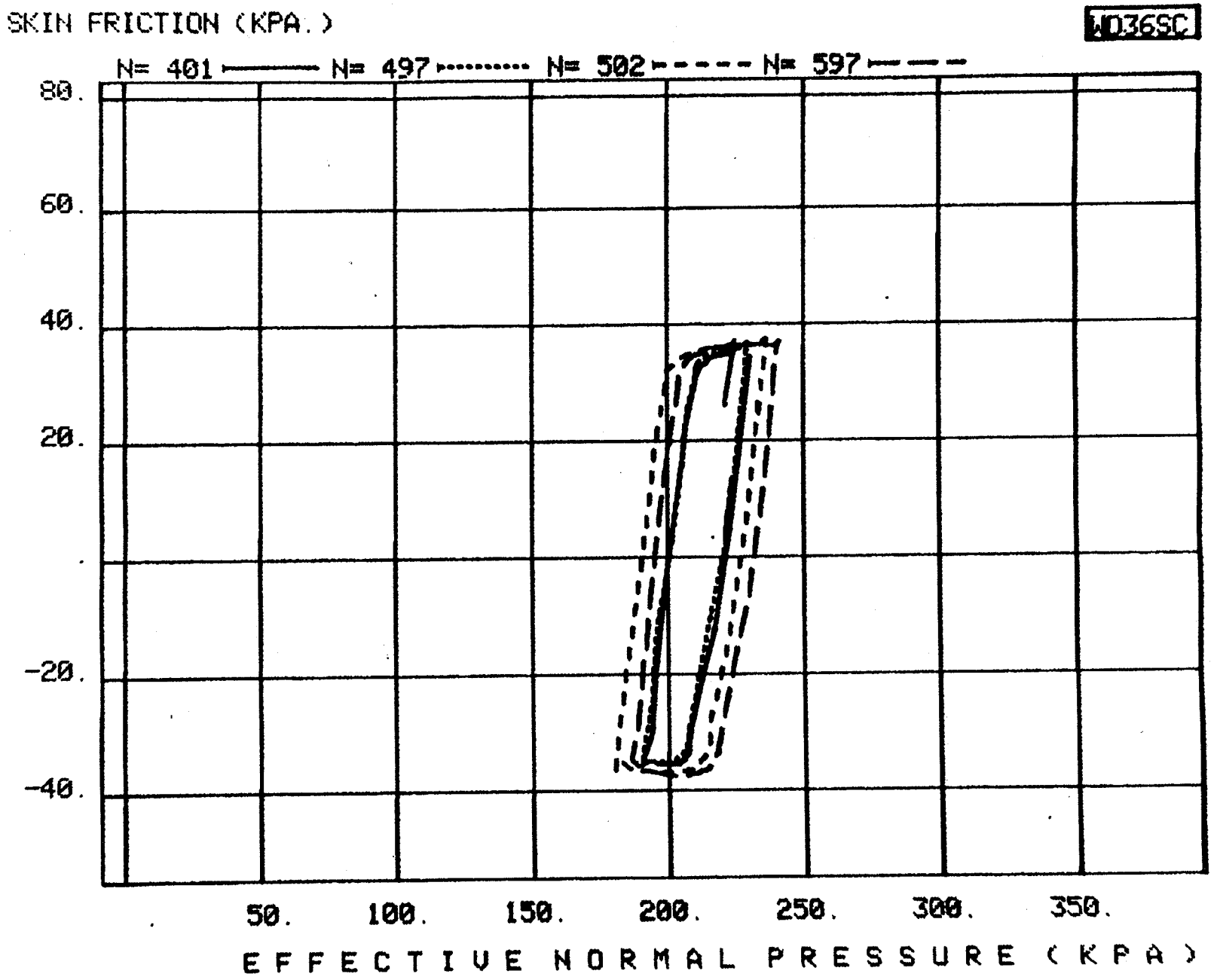
SKIN FRICTION (KPA.)
W036SC
N= 401
N= 497
N= 502
N= 597
80.
60.
40.
20.
-20.
-40.
50.
100.
150.
200.
250.
300.
350.
EFFECTIVE NORMAL PRESSURE (KPA)

RESPONSE ON CYCLIC LOADING (KPA.) CYCLE NO. 1

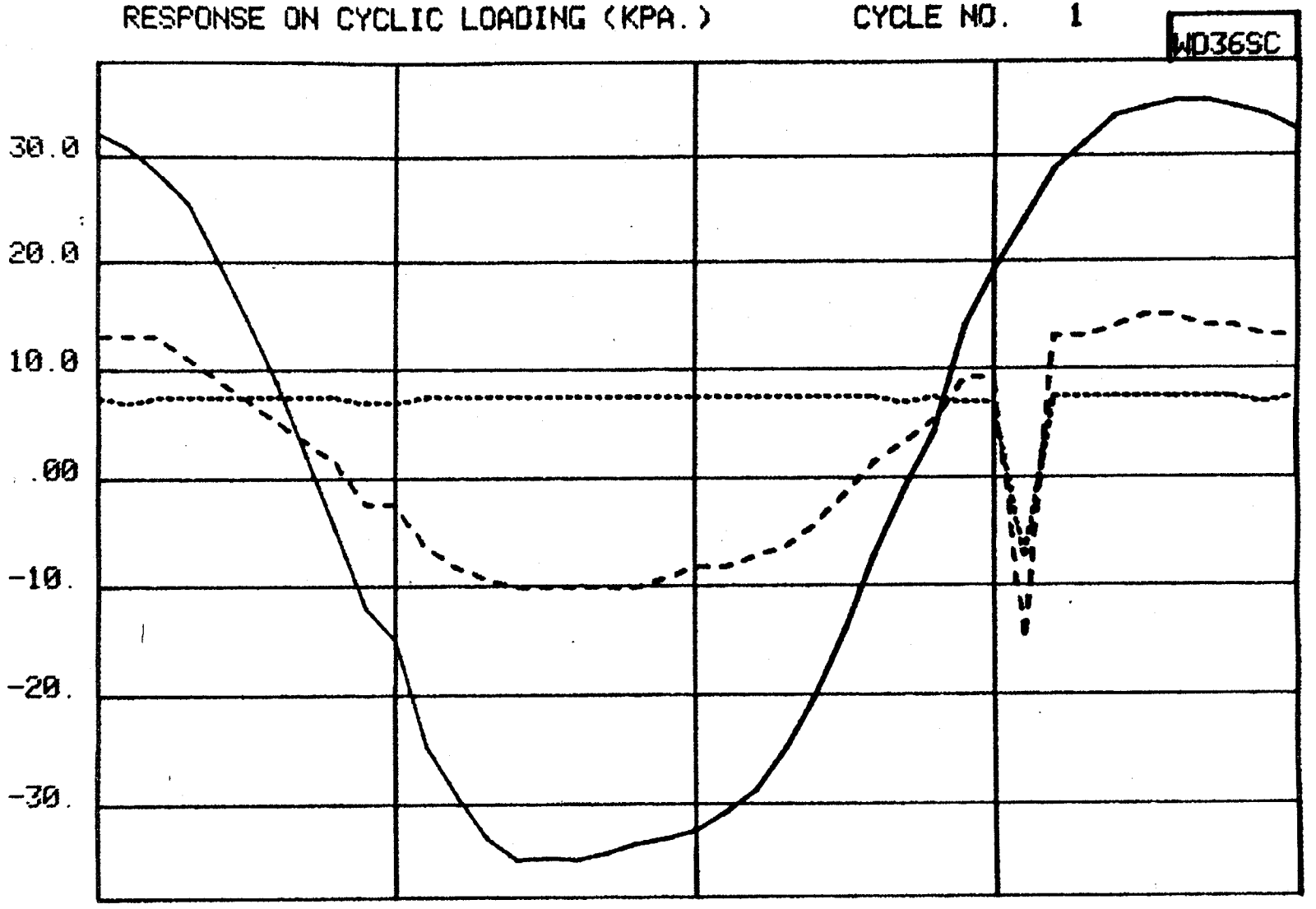

LEGEND:

		PERM. VALUES
———	SKIN FRICTION	-.57 KPA.
·····	PORE PRESSURE	333.1 KPA.
- - - -	TOTAL NORMAL PRESSURE	566.1 KPA.

RESPONSE ON CYCLIC LOADING (KPA.) CYCLE NO. 94

WD36SC

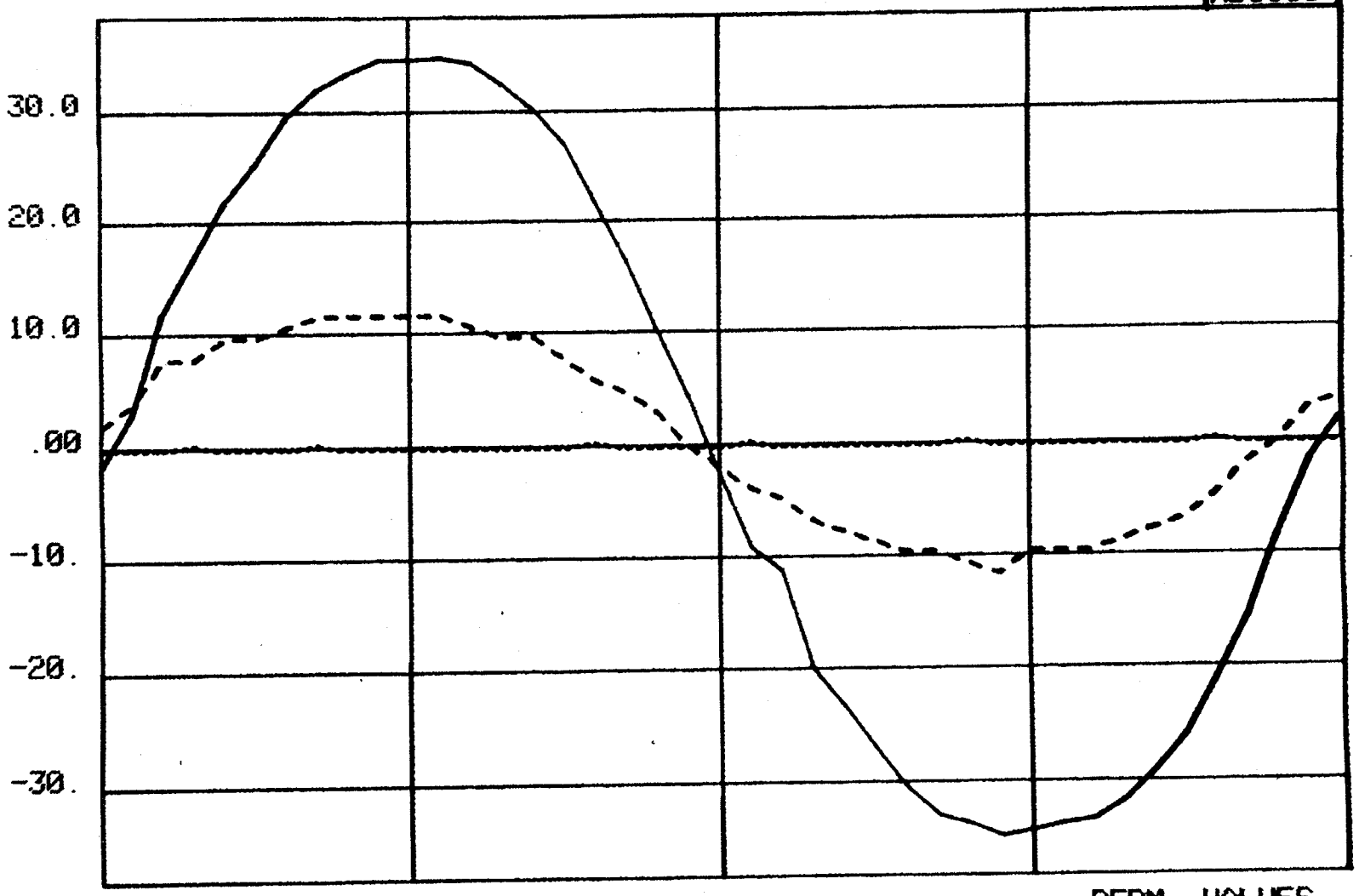

LEGEND:

SKIN FRICTION
PORE PRESSURE
TOTAL NORMAL PRESSURE

PERM. VALUES

-.38 KPA.
342.7 KPA.
567.6 KPA.

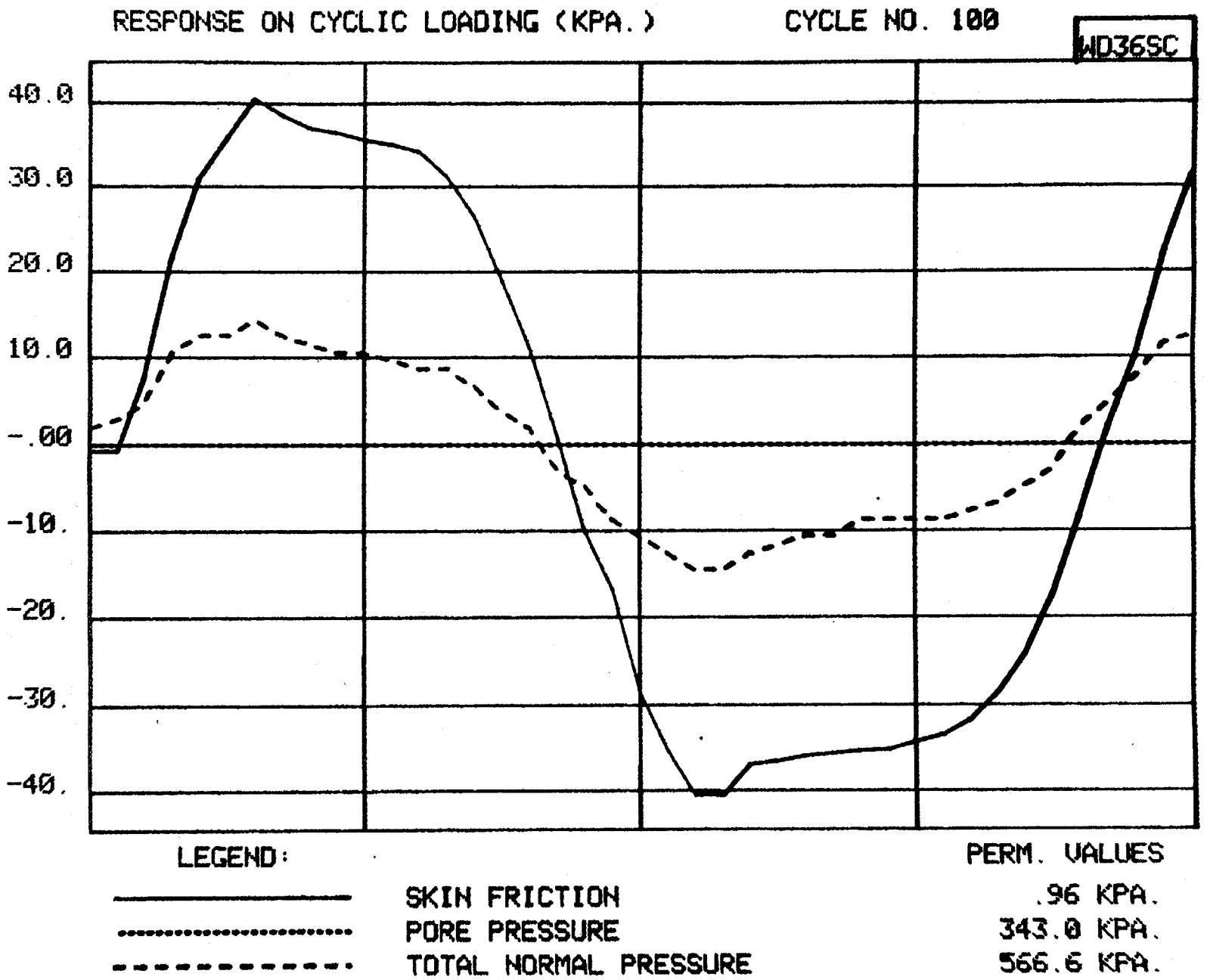
RESPONSE ON CYCLIC LOADING (KPA.)
CYCLE NO. 100
WD36SC
40.0
30.0
20.0
10.0
-.00
-10.
-20.
-30.
-40.
LEGEND:
SKIN FRICTION
PORE PRESSURE
TOTAL NORMAL PRESSURE
PERM. VALUES
.96 KPA.
343.0 KPA.
566.6 KPA.

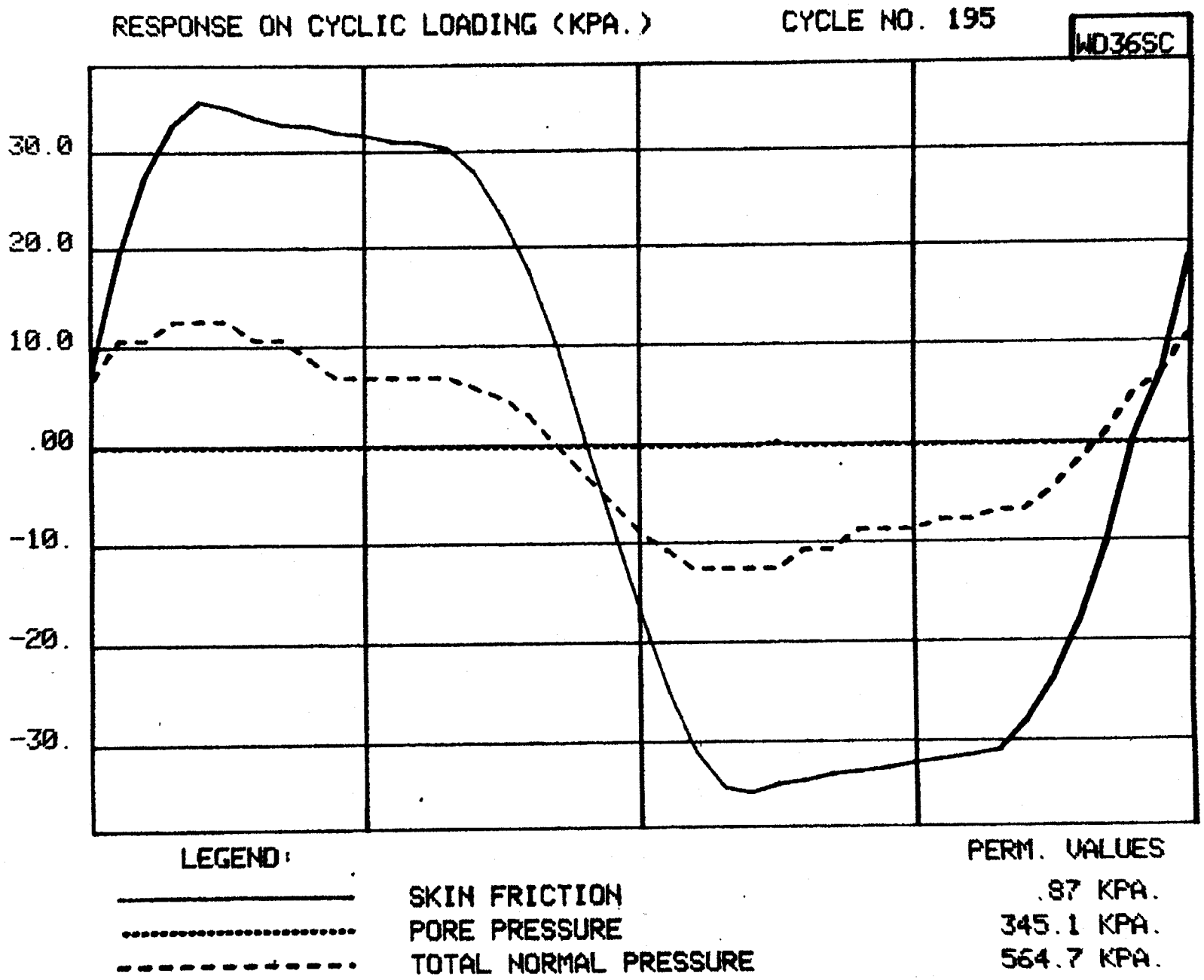
RESPONSE ON CYCLIC LOADING (KPA.)
CYCLE NO. 195
WD36SC
30.0
20.0
10.0
.00
-10.
-20.
-30.
LEGEND:
SKIN FRICTION
PORE PRESSURE
TOTAL NORMAL PRESSURE
PERM. VALUES
.87 KPA.
345.1 KPA.
564.7 KPA.

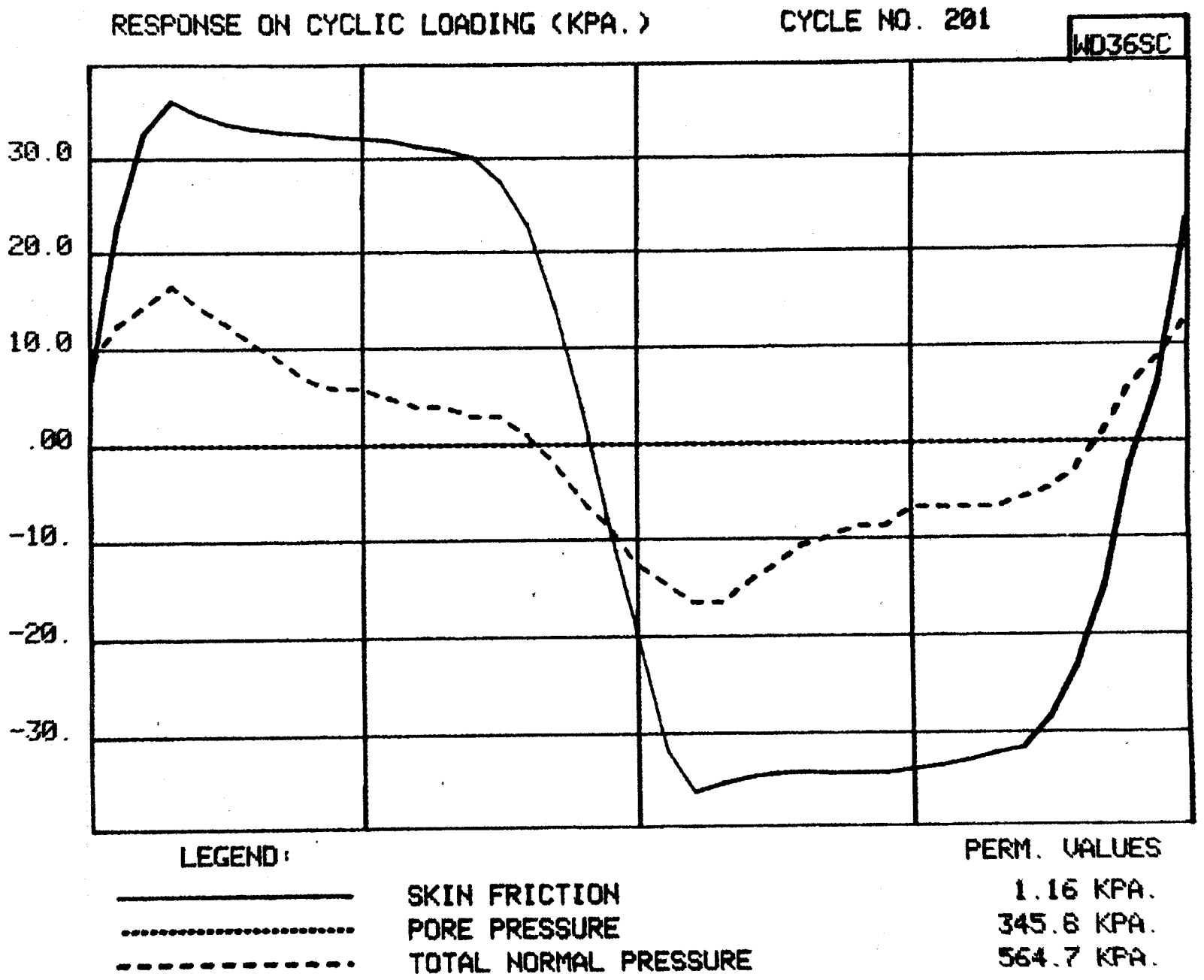
RESPONSE ON CYCLIC LOADING (KPA.)
CYCLE NO. 201
WD36SC
30.0
20.0
10.0
.00
-10.
-20.
-30.
LEGEND:
SKIN FRICTION
PORE PRESSURE
TOTAL NORMAL PRESSURE
PERM. VALUES
1.16 KPA.
345.6 KPA.
564.7 KPA.

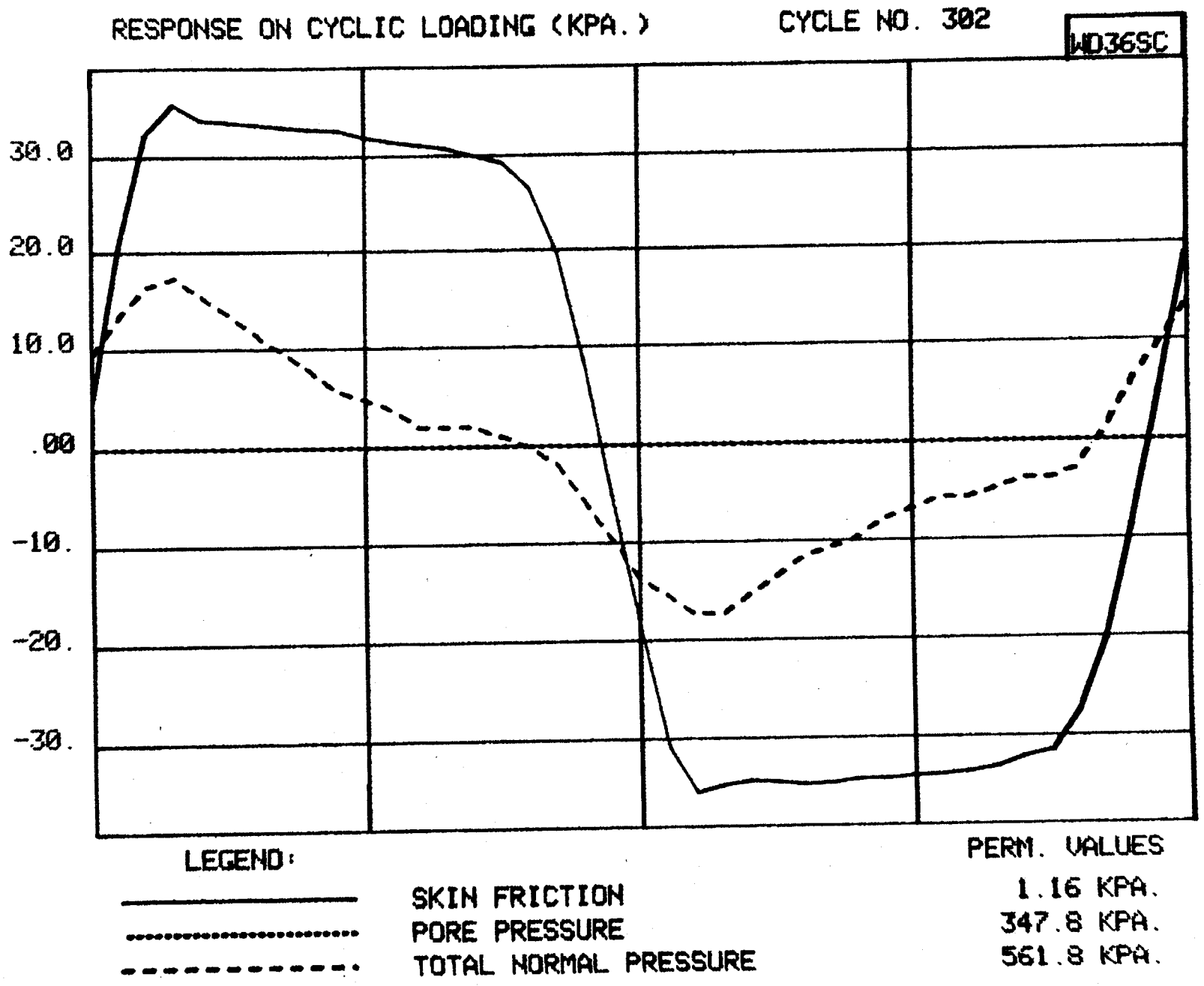
RESPONSE ON CYCLIC LOADING (KPA.)
CYCLE NO. 302
WD36SC
30.0
20.0
10.0
.00
-10.
-20.
-30.
LEGEND:
SKIN FRICTION
PORE PRESSURE
TOTAL NORMAL PRESSURE
PERM. VALUES
1.16 KPA.
347.8 KPA.
561.8 KPA.

RESPONSE ON CYCLIC LOADING (KPA.) CYCLE NO. 396

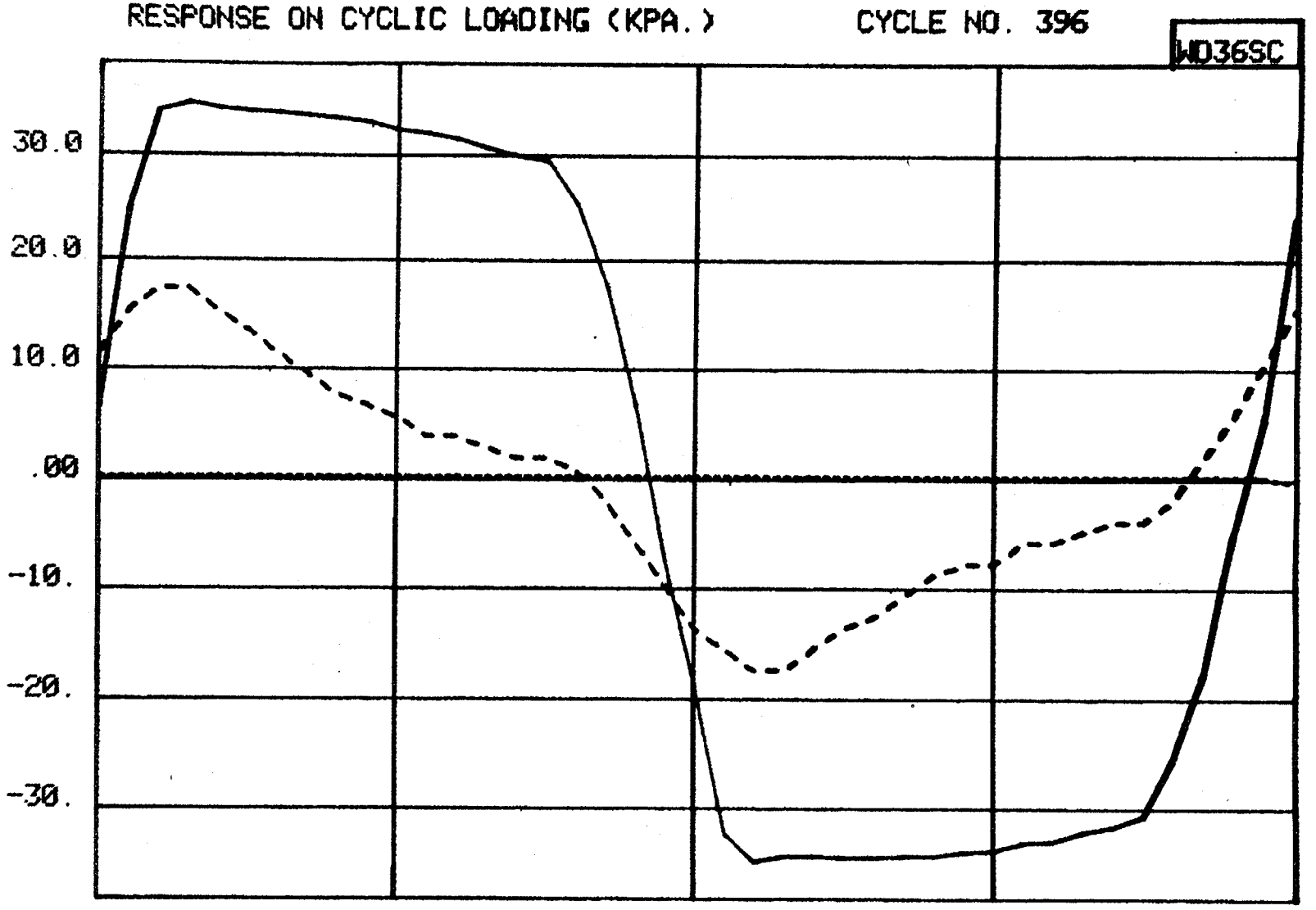

LEGEND:

		PERM. VALUES
———	SKIN FRICTION	.68 KPA.
·····	PORE PRESSURE	348.5 KPA.
- - - -	TOTAL NORMAL PRESSURE	559.8 KPA.

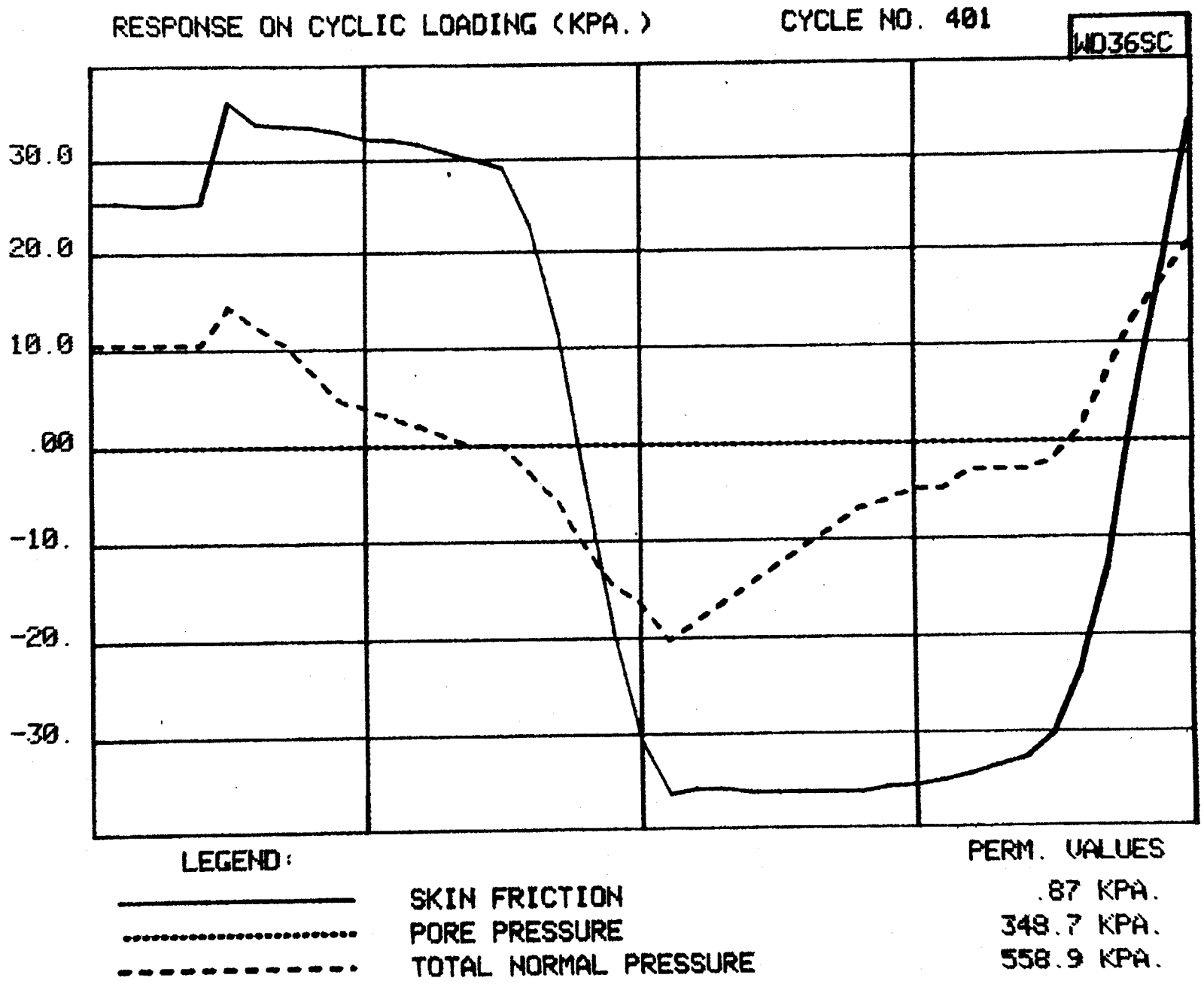
RESPONSE ON CYCLIC LOADING (KPA.)
CYCLE NO. 401
WD36SC
30.0
20.0
10.0
.00
-10.
-20.
-30.
LEGEND:
SKIN FRICTION
PORE PRESSURE
TOTAL NORMAL PRESSURE
PERM. VALUES
.87 KPA.
348.7 KPA.
558.9 KPA.

RESPONSE ON CYCLIC LOADING (KPA.) CYCLE NO. 497

WD36SC

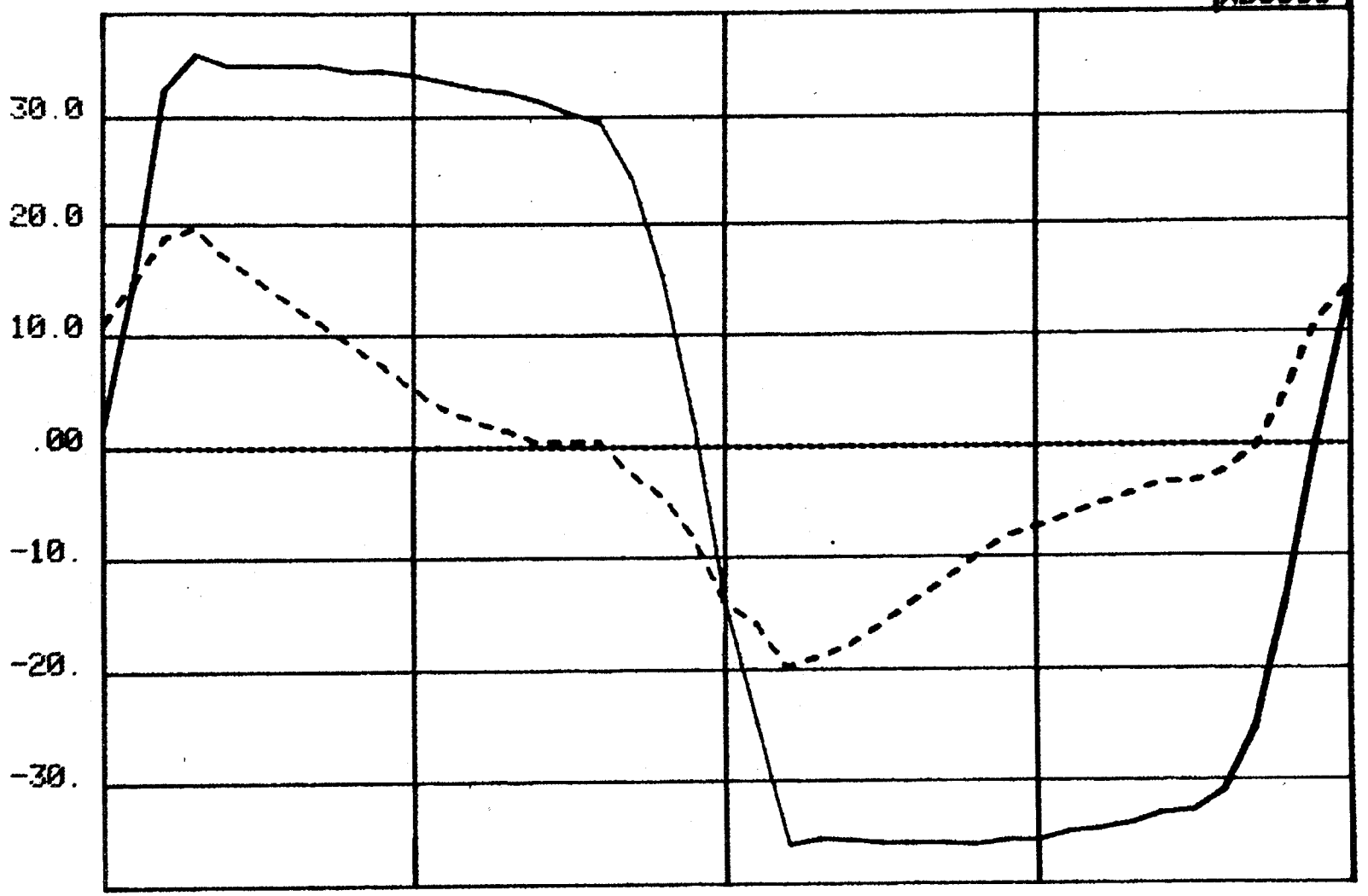

LEGEND:

		PERM. VALUES
————	SKIN FRICTION	.82 KPA.
·····	PORE PRESSURE	348.7 KPA.
- - - -	TOTAL NORMAL PRESSURE	558.4 KPA.

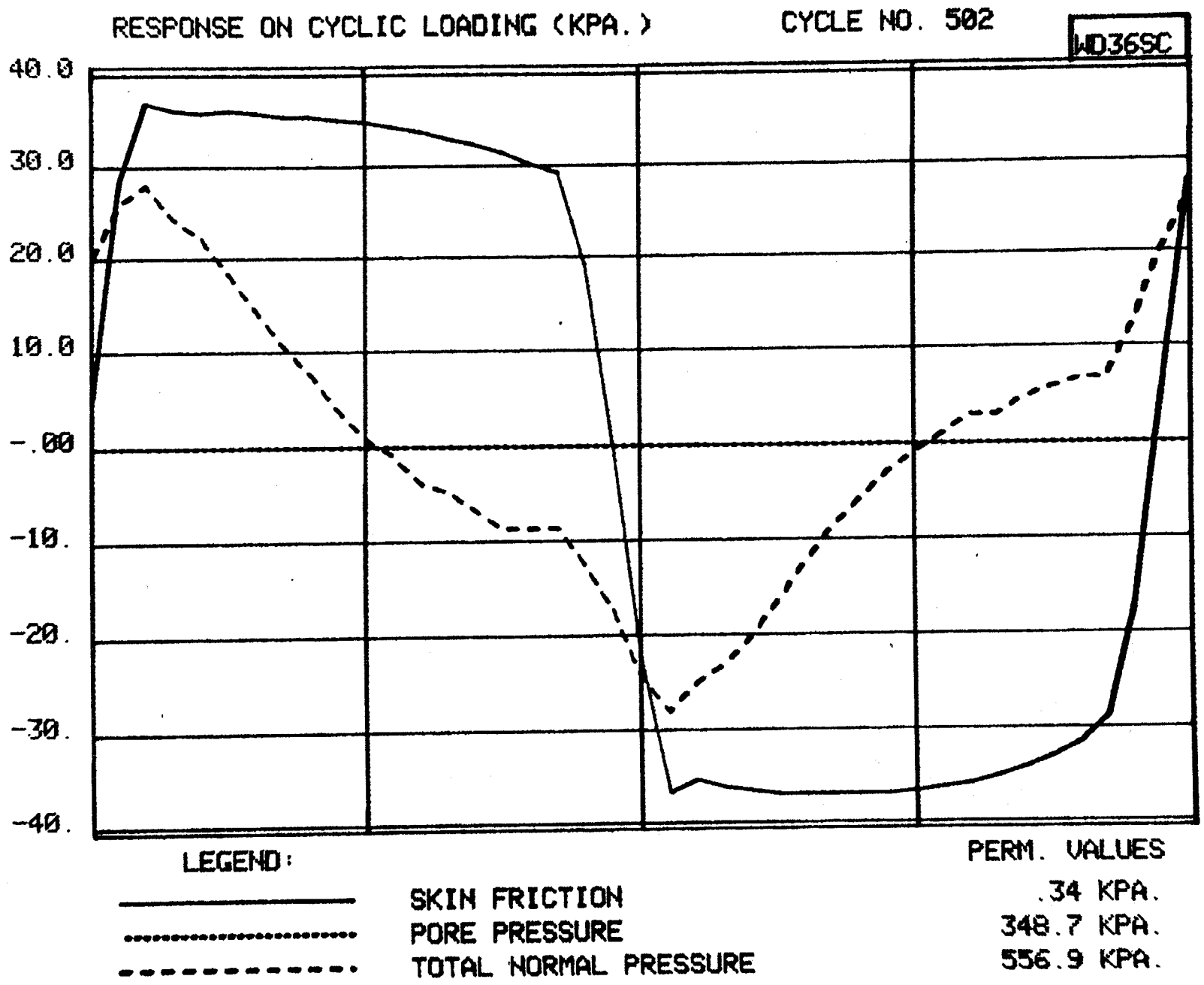
RESPONSE ON CYCLIC LOADING (KPA.)
CYCLE NO. 502
WD36SC
40.0
30.0
20.0
10.0
-.00
-10.
-20.
-30.
-40.
LEGEND:
SKIN FRICTION
PORE PRESSURE
TOTAL NORMAL PRESSURE
PERM. VALUES
.34 KPA.
348.7 KPA.
556.9 KPA.

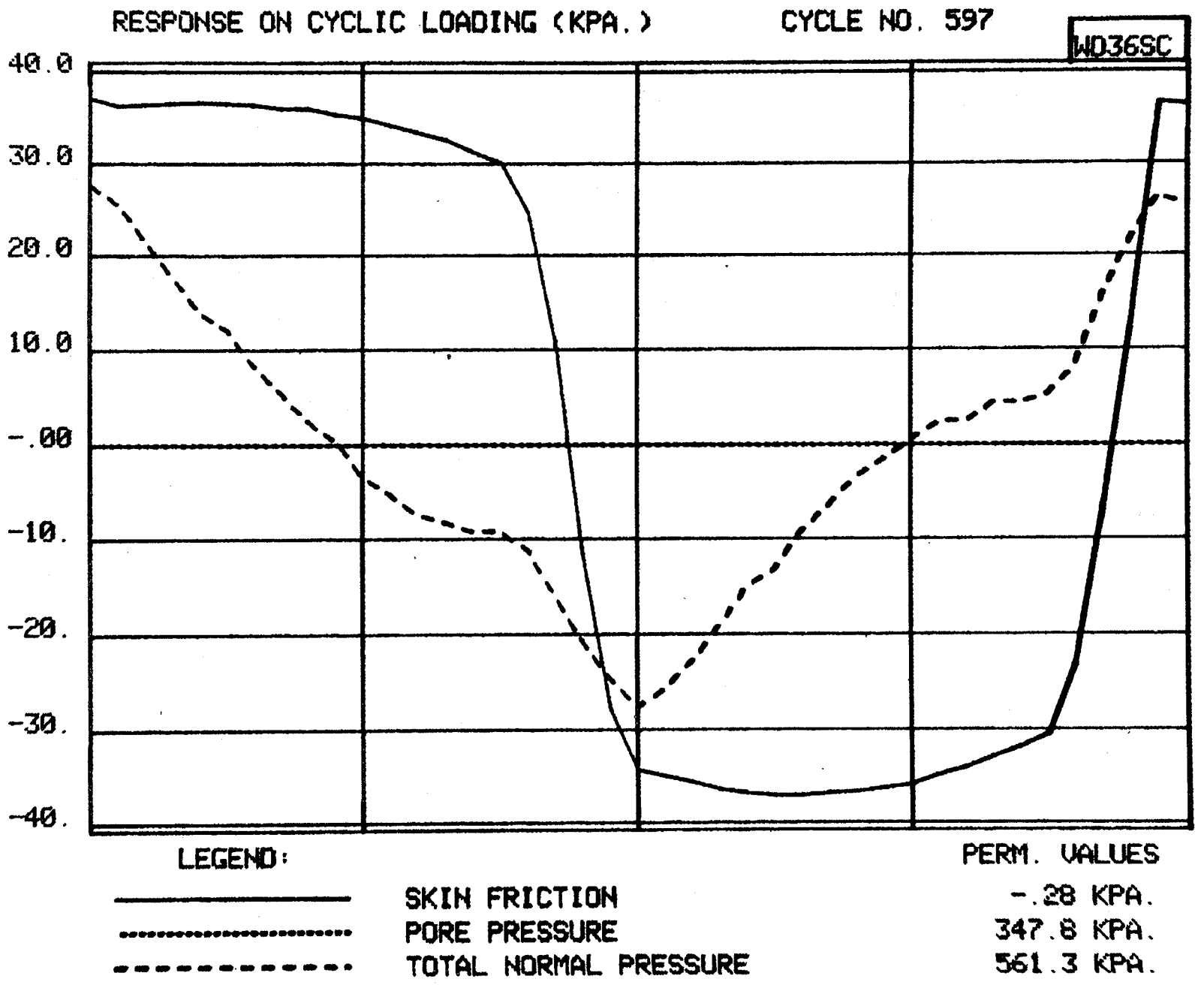
RESPONSE ON CYCLIC LOADING (KPA.)
CYCLE NO. 597
W036SC
40.0
30.0
20.0
10.0
-.00
-10.
-20.
-30.
-40.
LEGEND:
SKIN FRICTION
PORE PRESSURE
TOTAL NORMAL PRESSURE
PERM. VALUES
-.28 KPA.
347.8 KPA.
561.3 KPA.

Appendix CB

Plotted Results from WD36SC

Figures CB-1 through CB-4

Skin Friction vs Deflection, Selected Cycles

Figures CB-5 through CB-8

Skin Friction vs Eff. Normal Pressure, Selected Cycl.

Figures CB-9 through CB-16

Skin Friction, Pore and Total Pressure, Selected Cycles

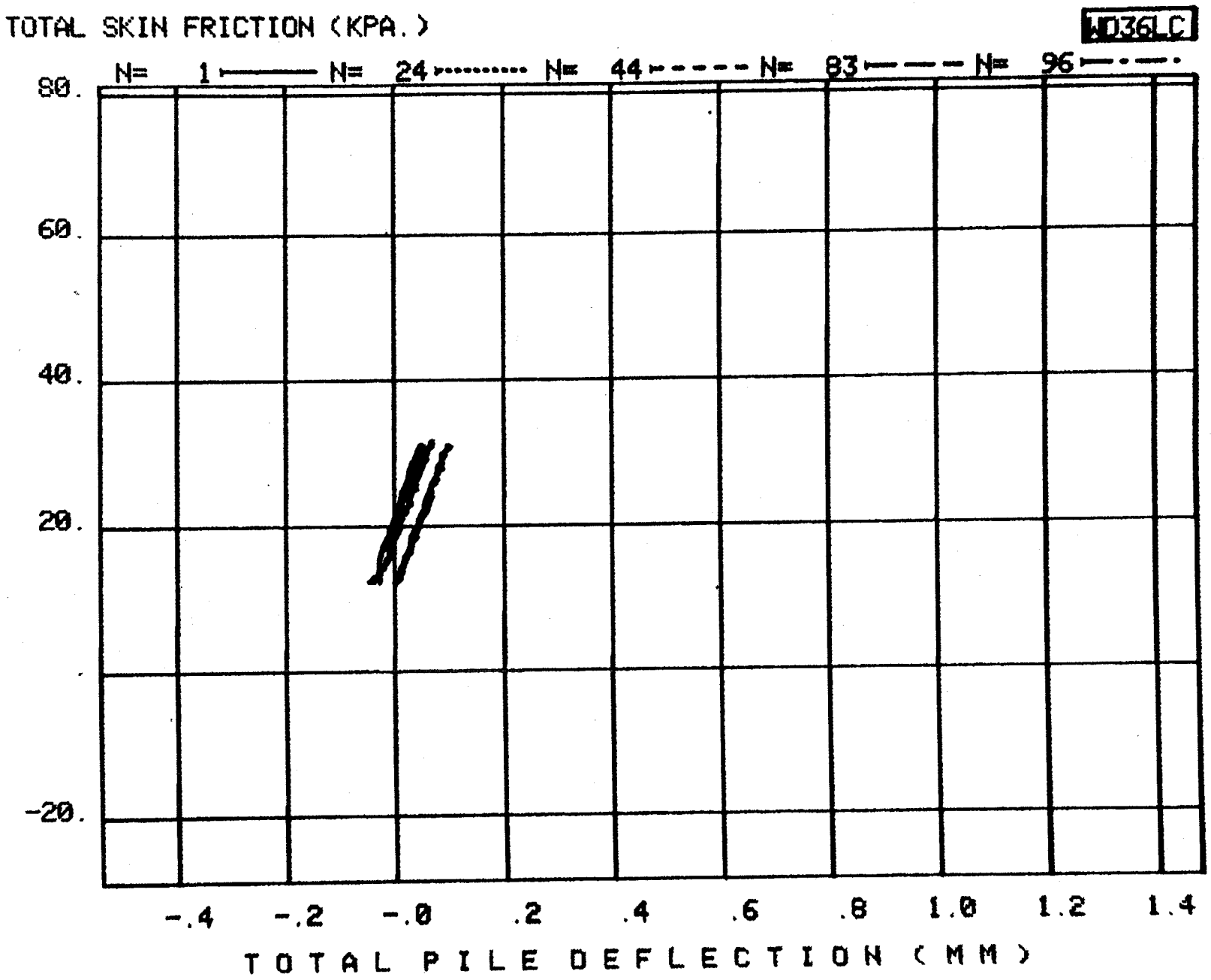
TOTAL SKIN FRICTION (KPA.)
WD36LC
N= 1
N= 24
N= 44
N= 83
N= 96
80.
60.
40.
20.
-20.
-.4
-.2
-.0
.2
.4
.6
.8
1.0
1.2
1.4
TOTAL PILE DEFLECTION (MM)

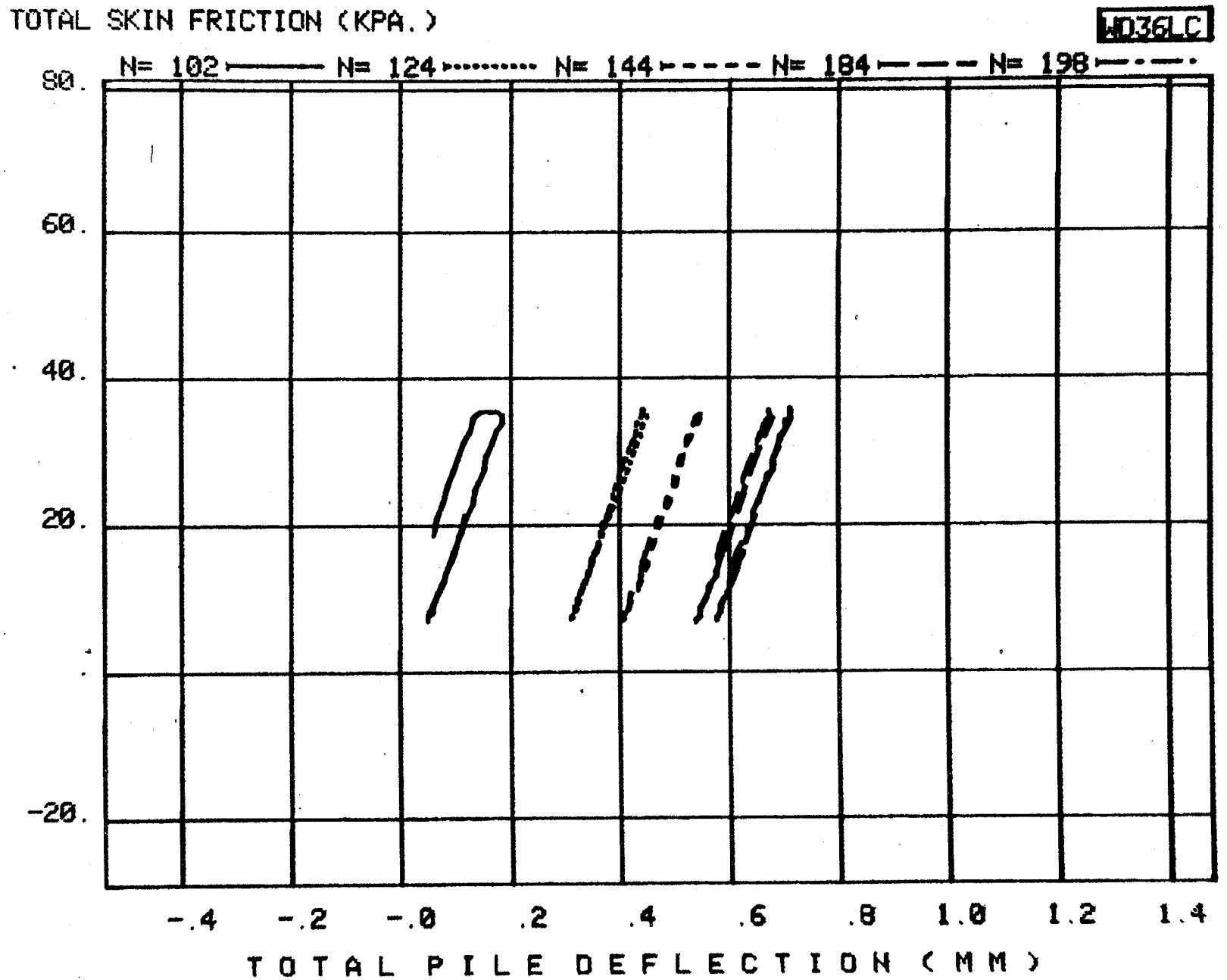
TOTAL SKIN FRICTION (KPA.)
WD36LC
N= 102
N= 124
N= 144
N= 184
N= 198
80.
60.
40.
20.
-20.
-.4
-.2
-.0
.2
.4
.6
.8
1.0
1.2
1.4
TOTAL PILE DEFLECTION (MM)

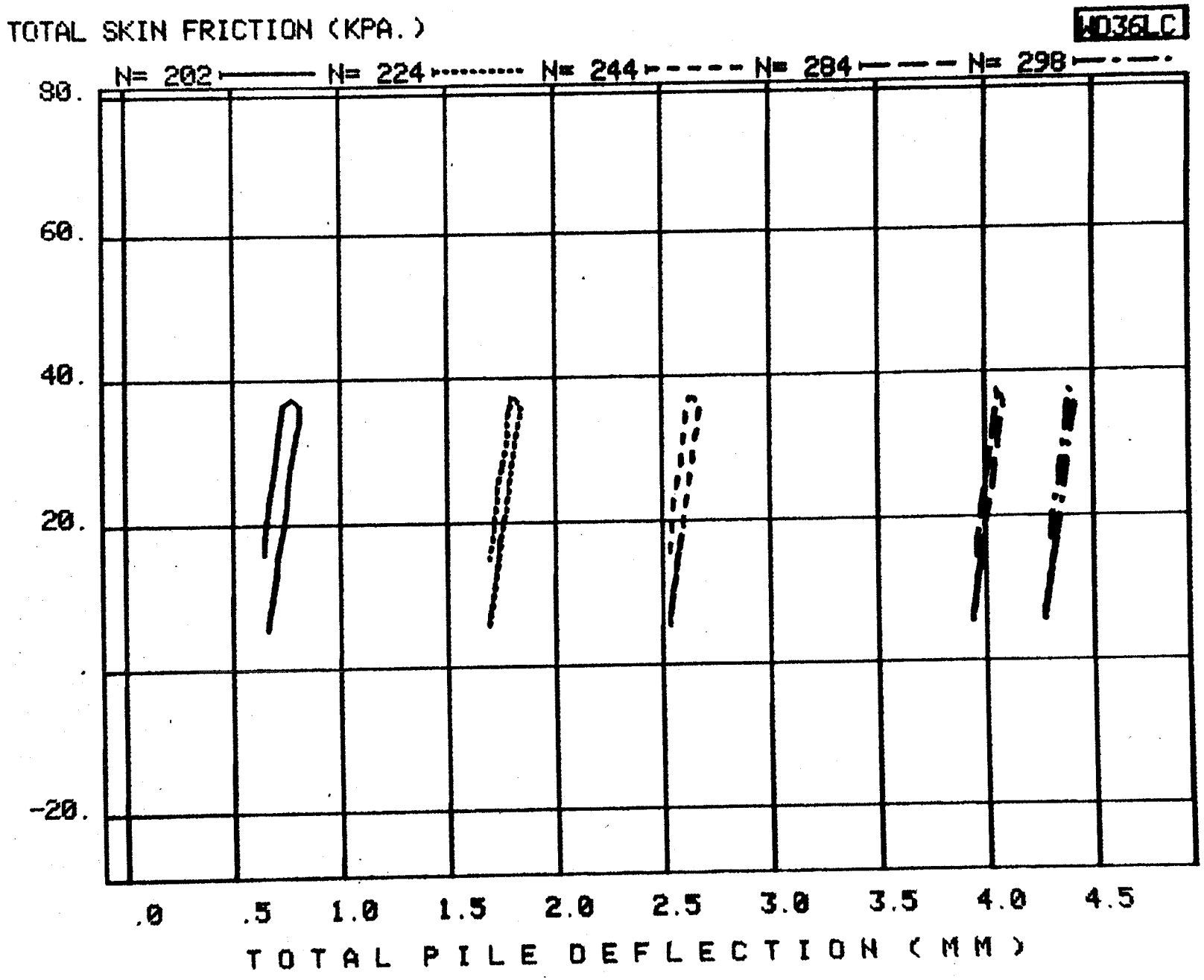
TOTAL SKIN FRICTION (KPA.)
WD36LC
N= 202
N= 224
N= 244
N= 284
N= 298
80.
60.
40.
20.
-20.
.0
.5
1.0
1.5
2.0
2.5
3.0
3.5
4.0
4.5
TOTAL PILE DEFLECTION (MM)

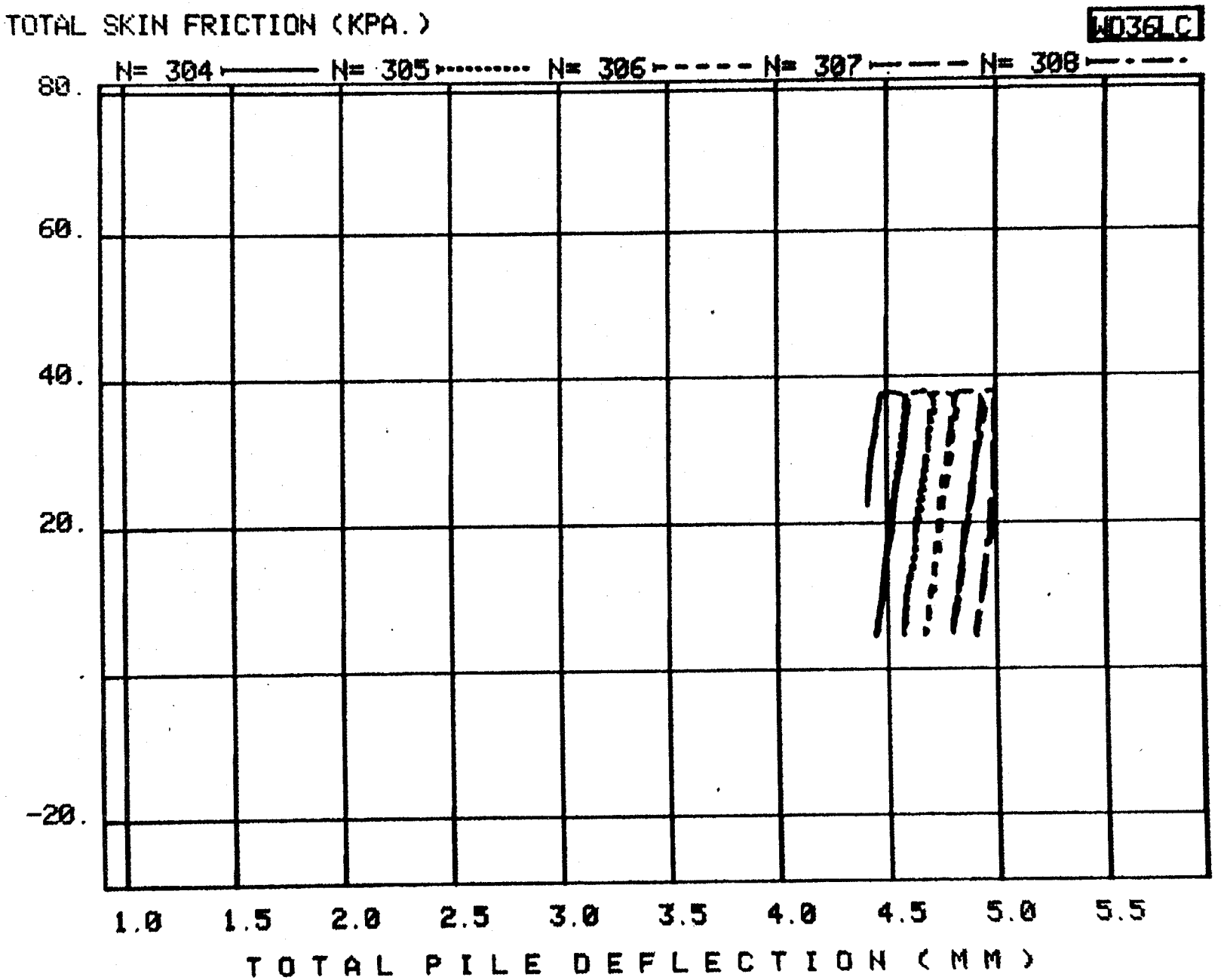
TOTAL SKIN FRICTION (KPA.)
WD36LC
N= 304
N= 305
N= 306
N= 307
N= 308
80.
60.
40.
20.
-20.
1.0
1.5
2.0
2.5
3.0
3.5
4.0
4.5
5.0
5.5
TOTAL PILE DEFLECTION (MM)

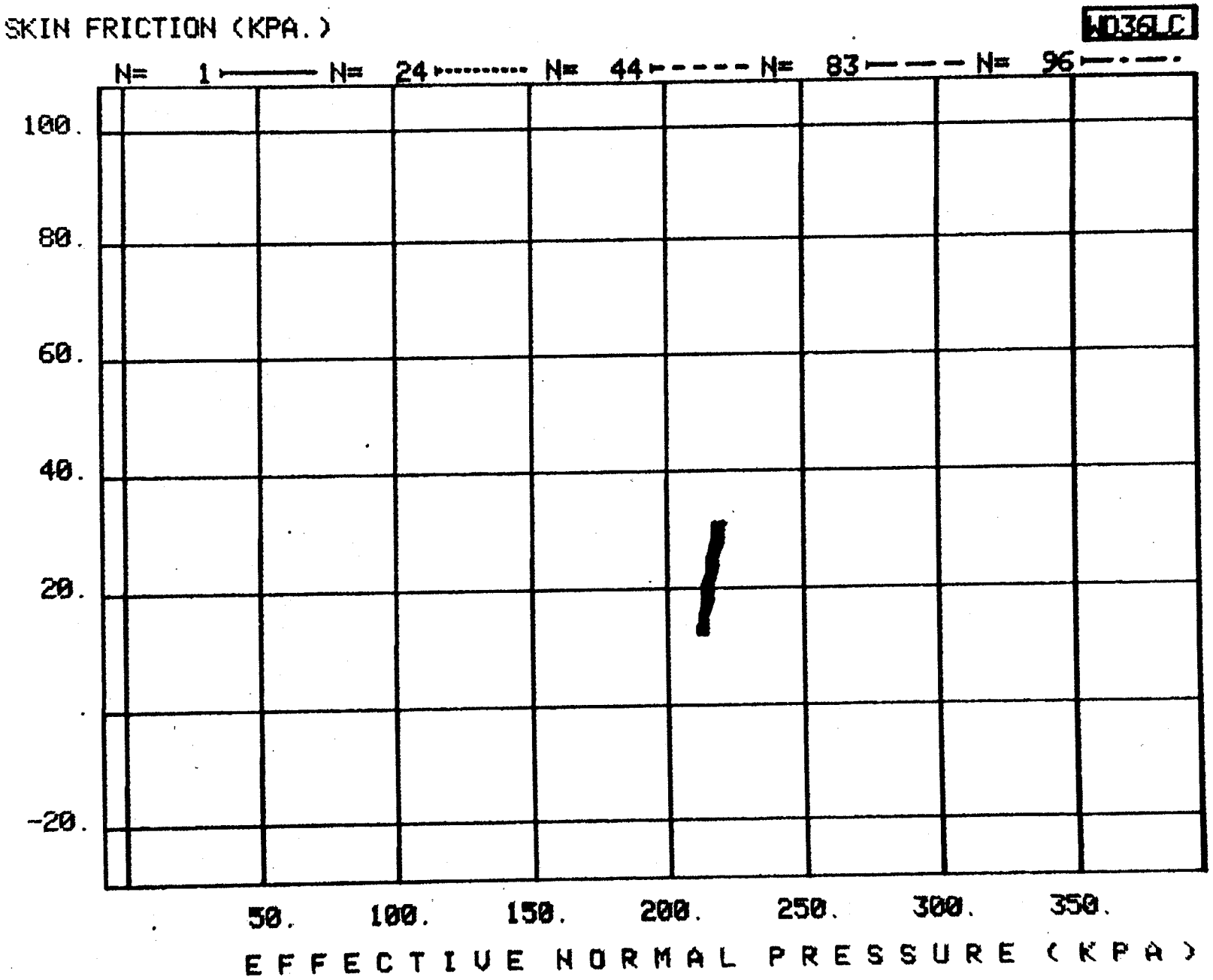
SKIN FRICTION (KPA.)
W036.C
N= 1
N= 24
N= 44
N= 83
N= 96
100.
80.
60.
40.
20.
-20.
50.
100.
150.
200.
250.
300.
350.
EFFECTIVE NORMAL PRESSURE (KPA)

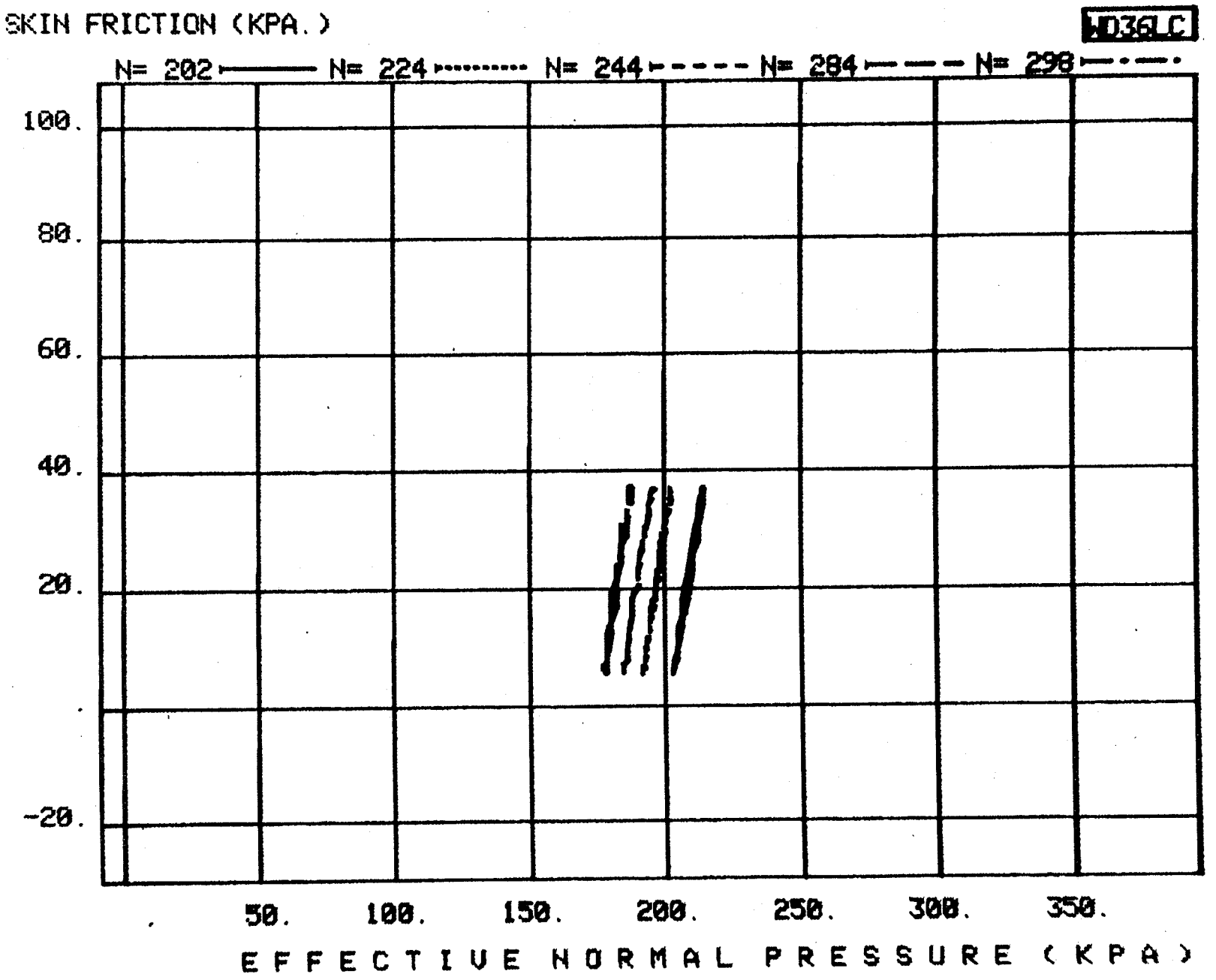
SKIN FRICTION (KPA.)
WD36LC
N= 202
N= 224
N= 244
N= 284
N= 298
100.
80.
60.
40.
20.
-20.
50.
100.
150.
200.
250.
300.
350.
EFFECTIVE NORMAL PRESSURE (KPA)

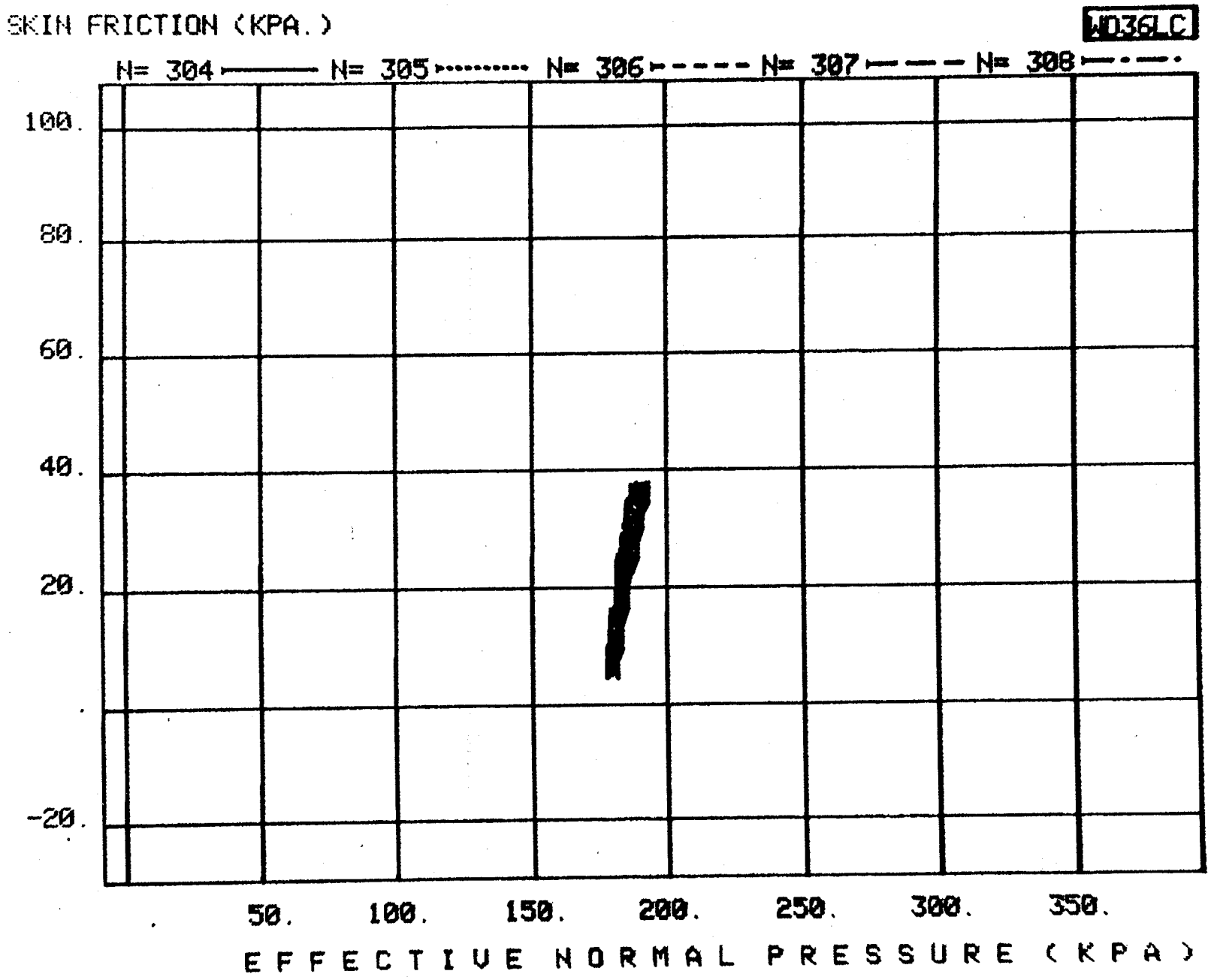
SKIN FRICTION (KPA.)
WD36LC
N= 304
N= 305
N= 306
N= 307
N= 308
100.
80.
60.
40.
20.
-20.
50.
100.
150.
200.
250.
300.
350.
EFFECTIVE NORMAL PRESSURE (KPA)

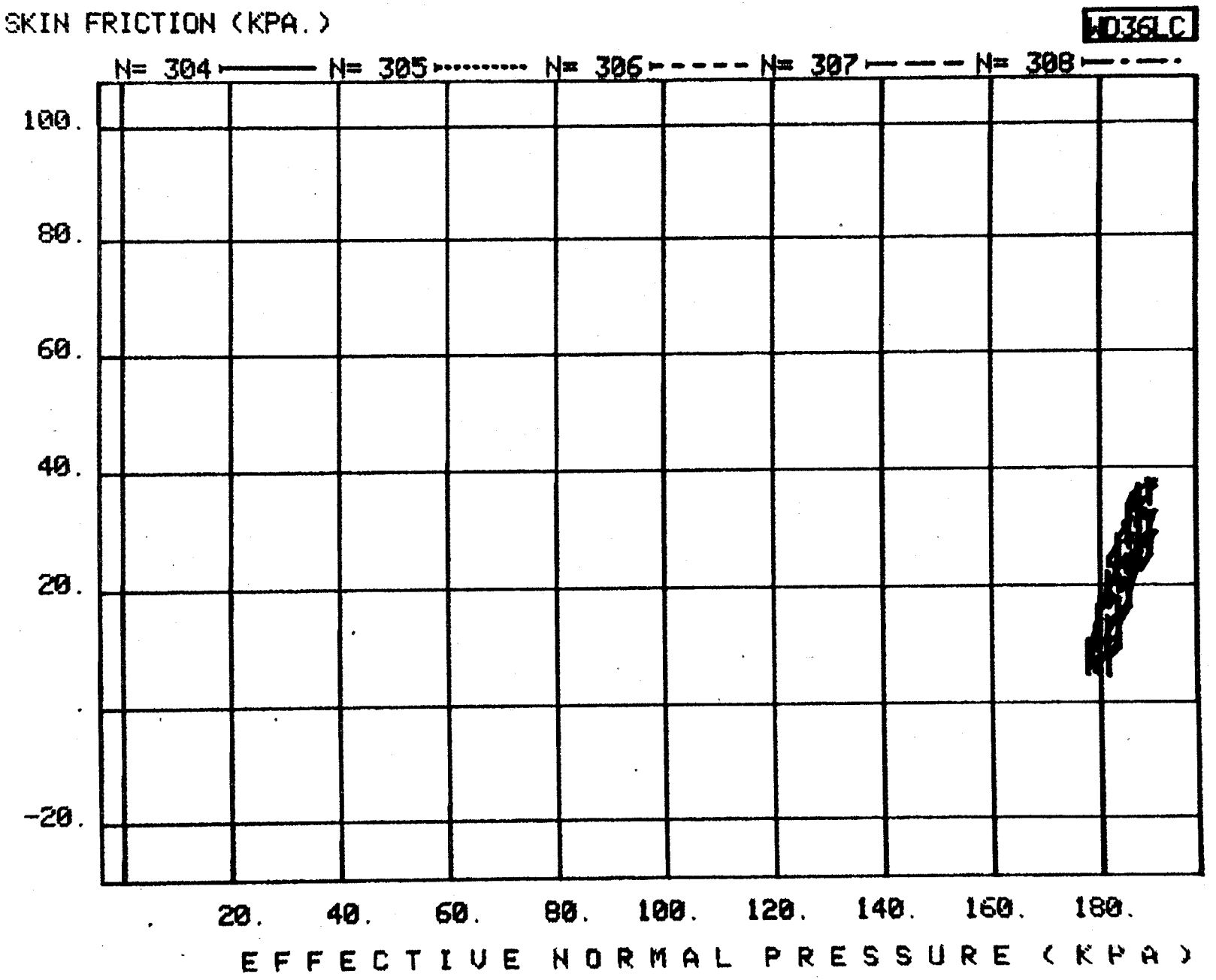
SKIN FRICTION (KPA.)
WD36LC
N= 304
N= 305
N= 306
N= 307
N= 308
100.
80.
60.
40.
20.
-20.
20.
40.
60.
80.
100.
120.
140.
160.
180.
EFFECTIVE NORMAL PRESSURE (KPA)

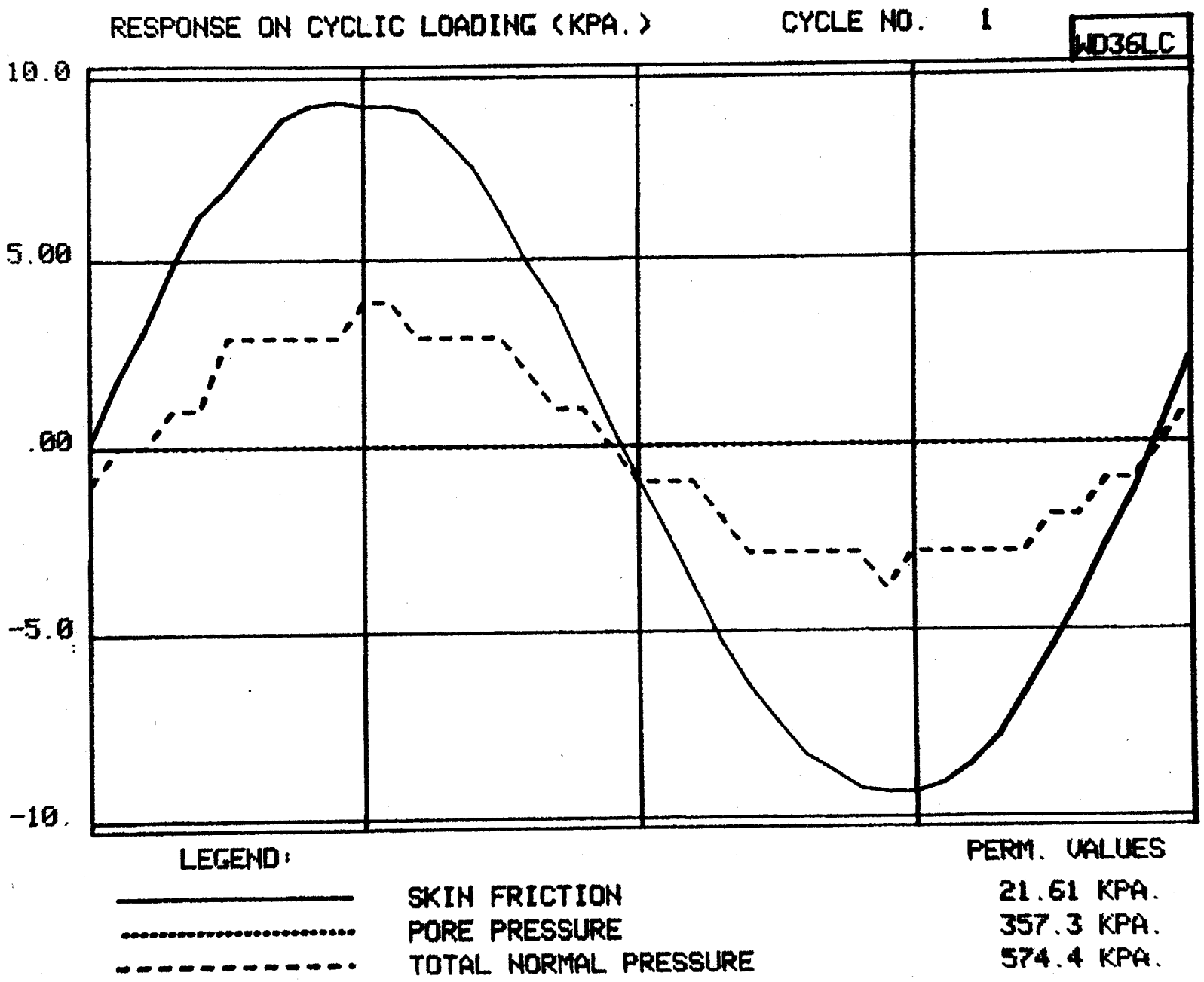
RESPONSE ON CYCLIC LOADING (KPA.)
CYCLE NO. 1
WD36LC
10.0
5.00
.00
-5.0
-10.
LEGEND:
SKIN FRICTION
PORE PRESSURE
TOTAL NORMAL PRESSURE
PERM. VALUES
21.61 KPA.
357.3 KPA.
574.4 KPA.

RESPONSE ON CYCLIC LOADING (KPA.) CYCLE NO. 96

WD36LC

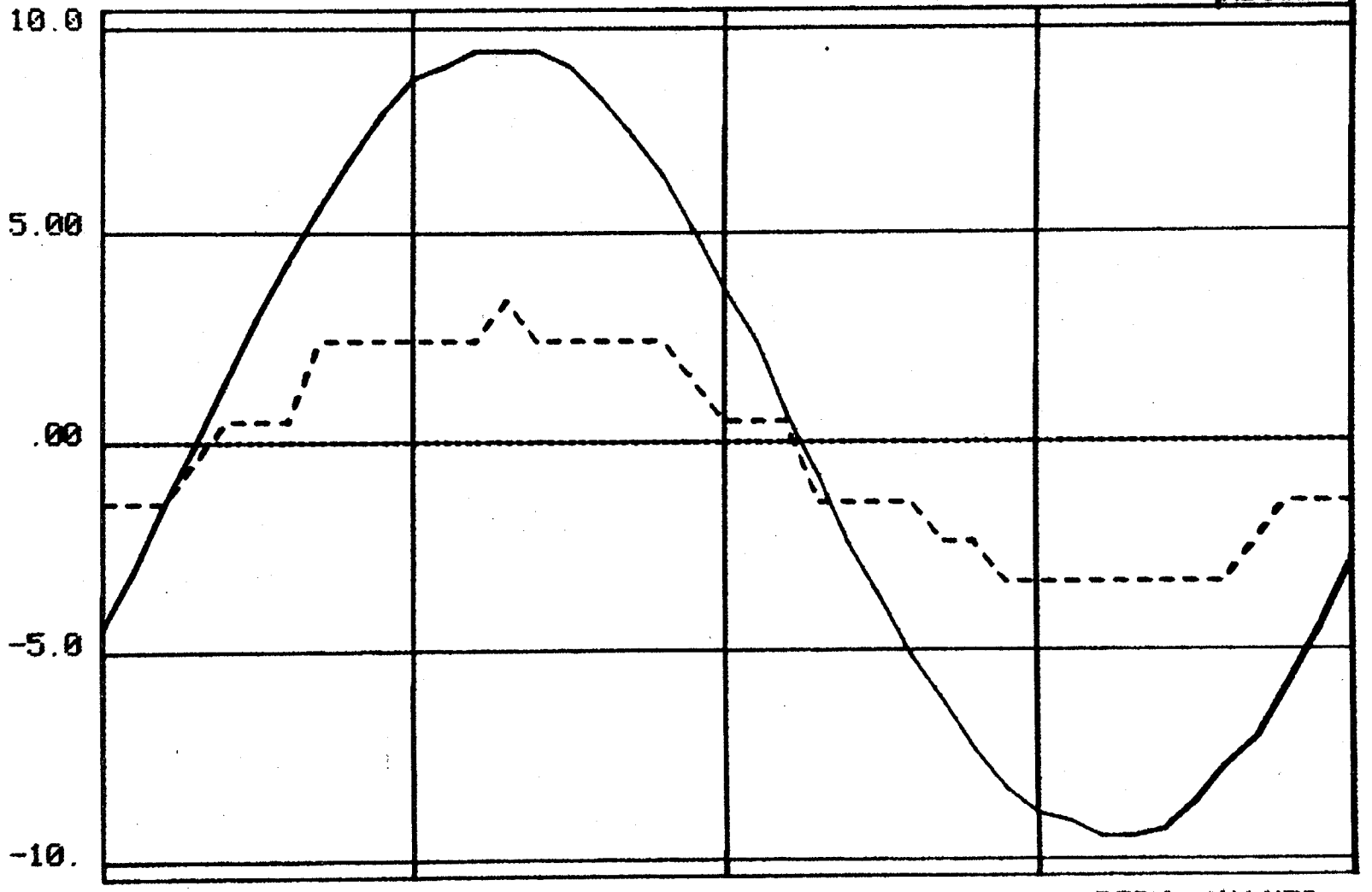

LEGEND:

		PERM. VALUES
———	SKIN FRICTION	21.37 KPA.
·····	PORE PRESSURE	358.3 KPA.
- - - -	TOTAL NORMAL PRESSURE	572.9 KPA.

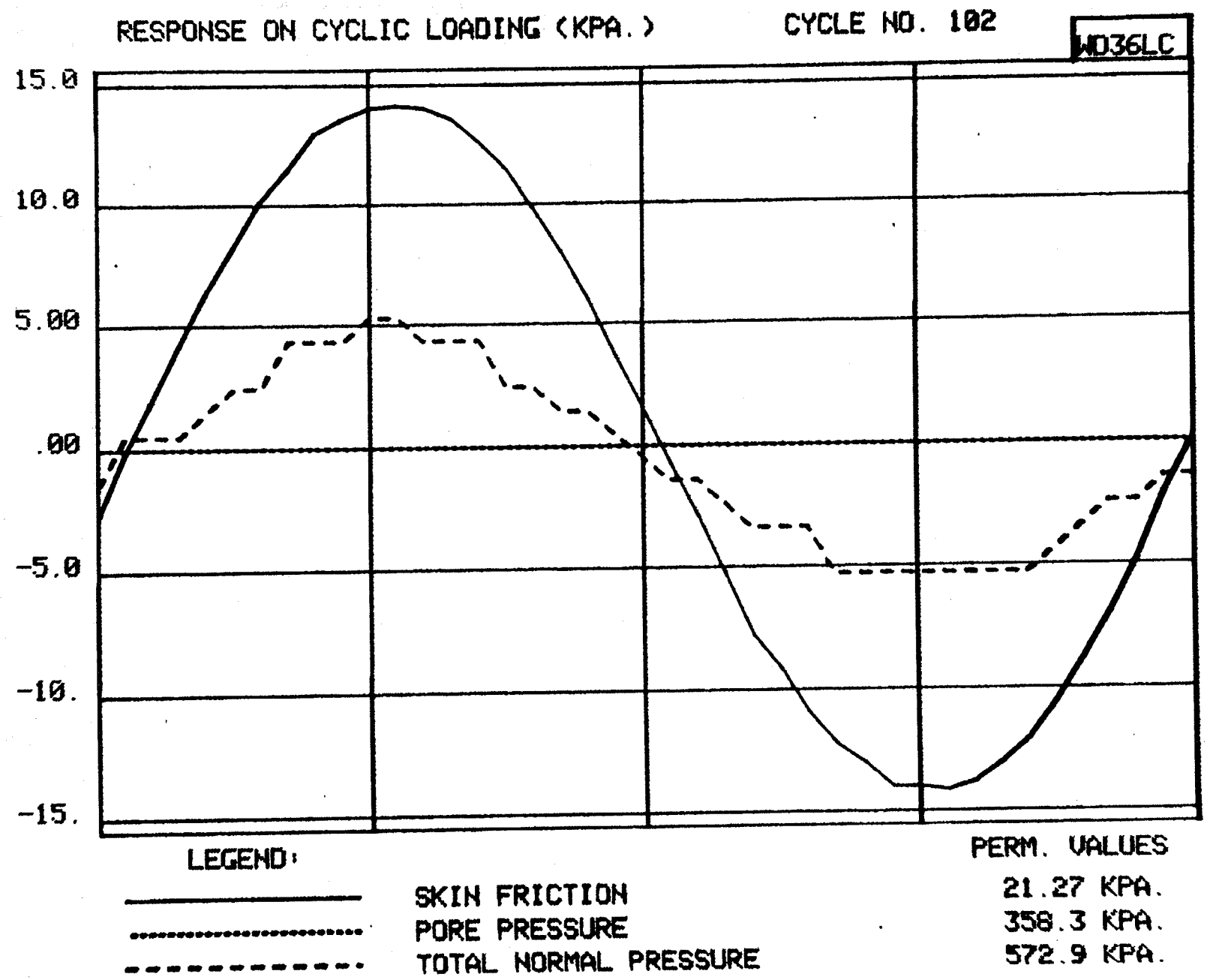
RESPONSE ON CYCLIC LOADING (KPA.)
CYCLE NO. 102
WD36LC
15.0
10.0
5.00
.00
-5.0
-10.
-15.
LEGEND:
SKIN FRICTION
PORE PRESSURE
TOTAL NORMAL PRESSURE
PERM. VALUES
21.27 KPA.
358.3 KPA.
572.9 KPA.

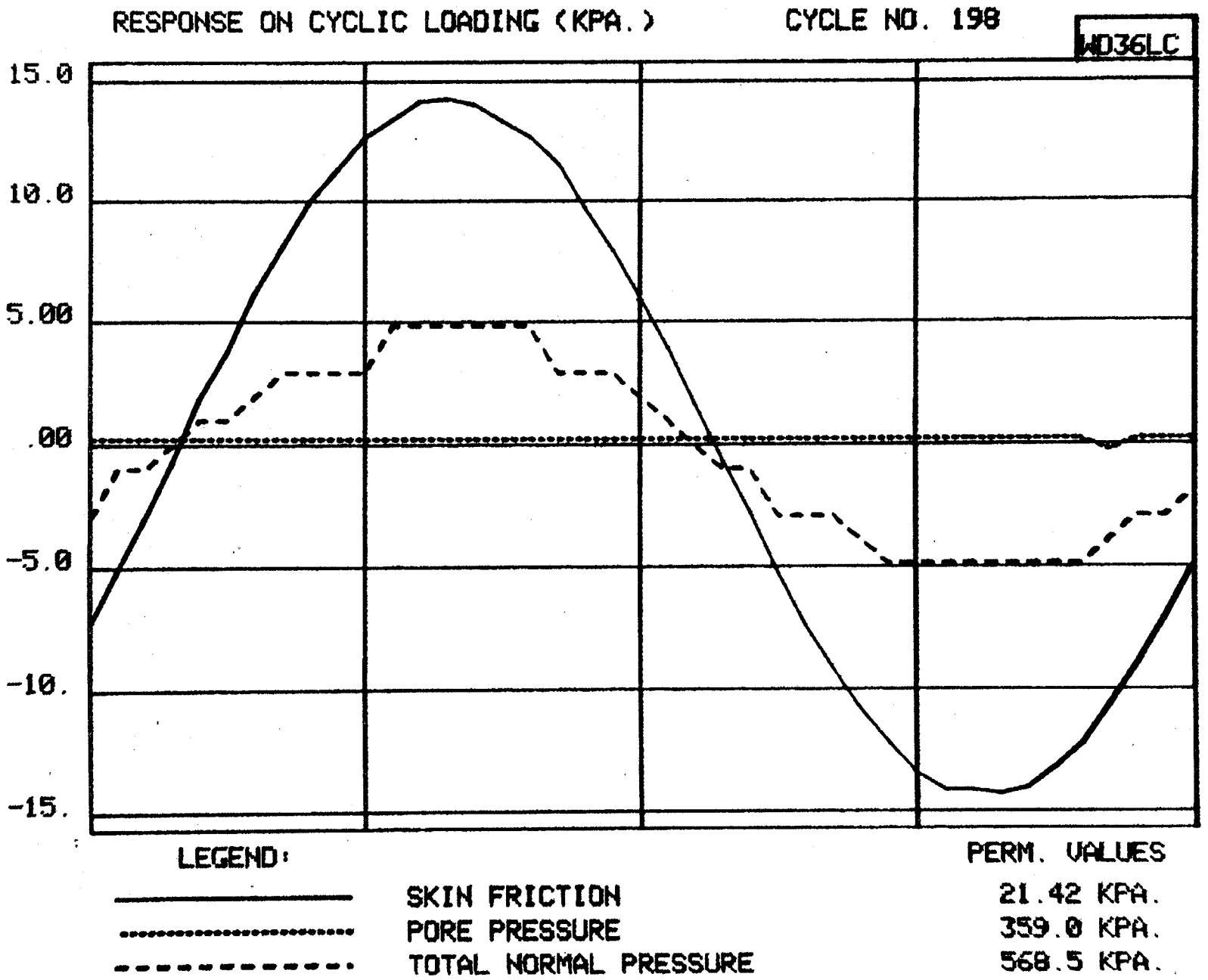
RESPONSE ON CYCLIC LOADING (KPA.)
CYCLE NO. 198
WD36LC
15.0
10.0
5.00
.00
-5.0
-10.
-15.
LEGEND:
SKIN FRICTION
PORE PRESSURE
TOTAL NORMAL PRESSURE
PERM. VALUES
21.42 KPA.
359.0 KPA.
568.5 KPA.

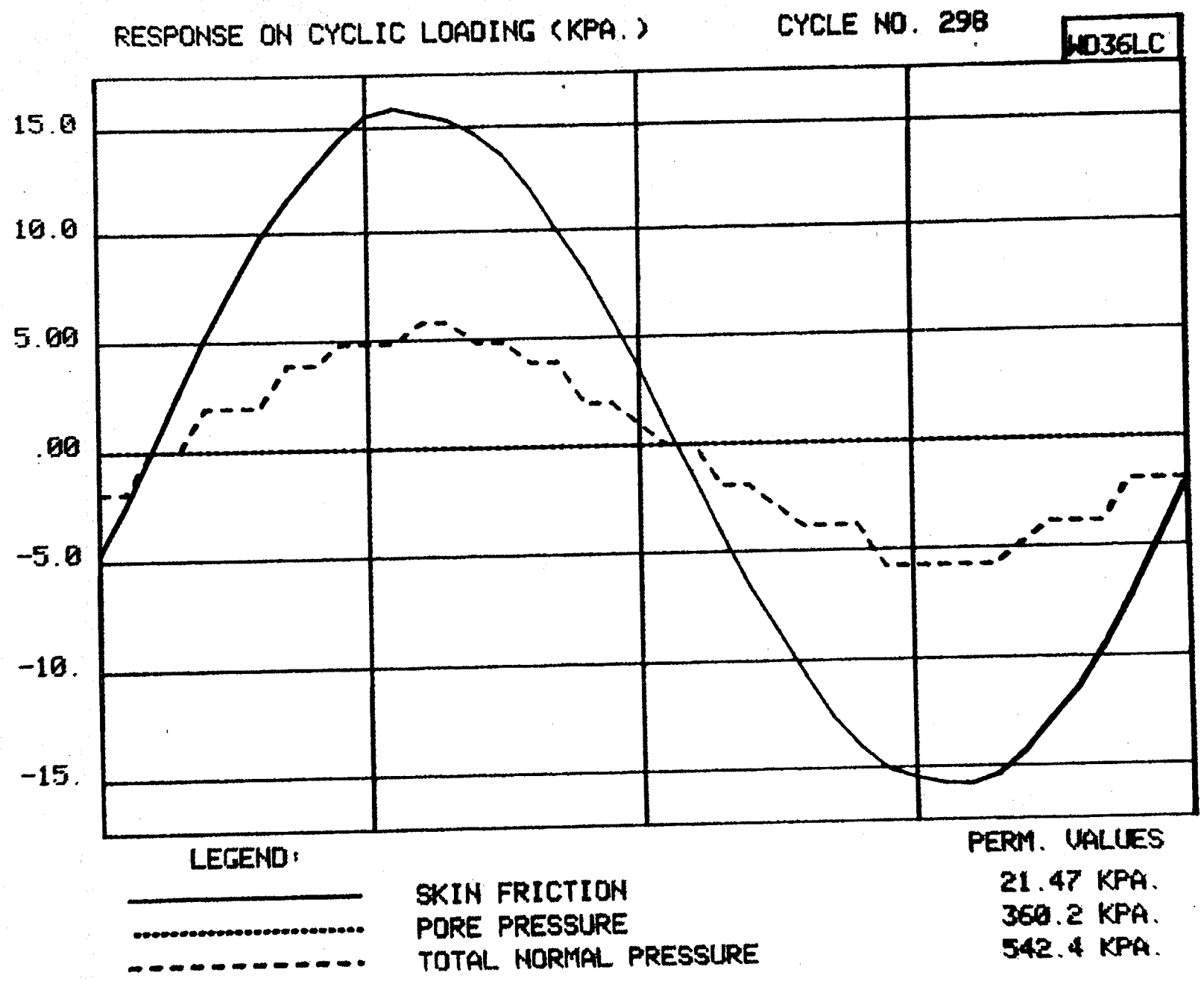
RESPONSE ON CYCLIC LOADING (KPA.)
CYCLE NO. 298
WD36LC
15.0
10.0
5.00
.00
-5.0
-10.
-15.
LEGEND:
SKIN FRICTION
PORE PRESSURE
TOTAL NORMAL PRESSURE
PERM. VALUES
21.47 KPA.
360.2 KPA.
542.4 KPA.

RESPONSE ON CYCLIC LOADING (KPA.) CYCLE NO. 304

WD36LC

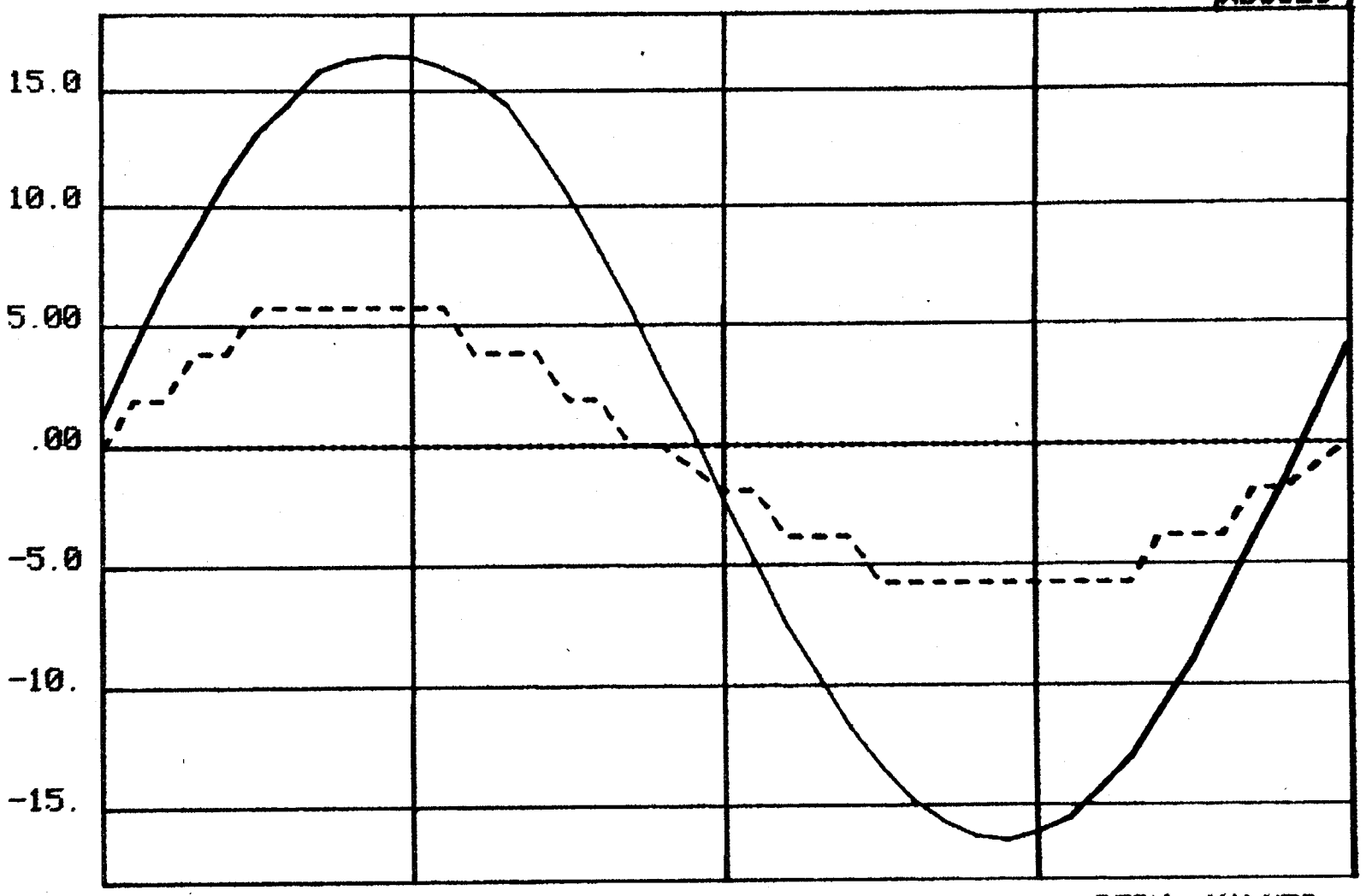

LEGEND:

		PERM. VALUES
———	SKIN FRICTION	21.18 KPA.
·····	PORE PRESSURE	361.2 KPA.
- - - -	TOTAL NORMAL PRESSURE	548.2 KPA.

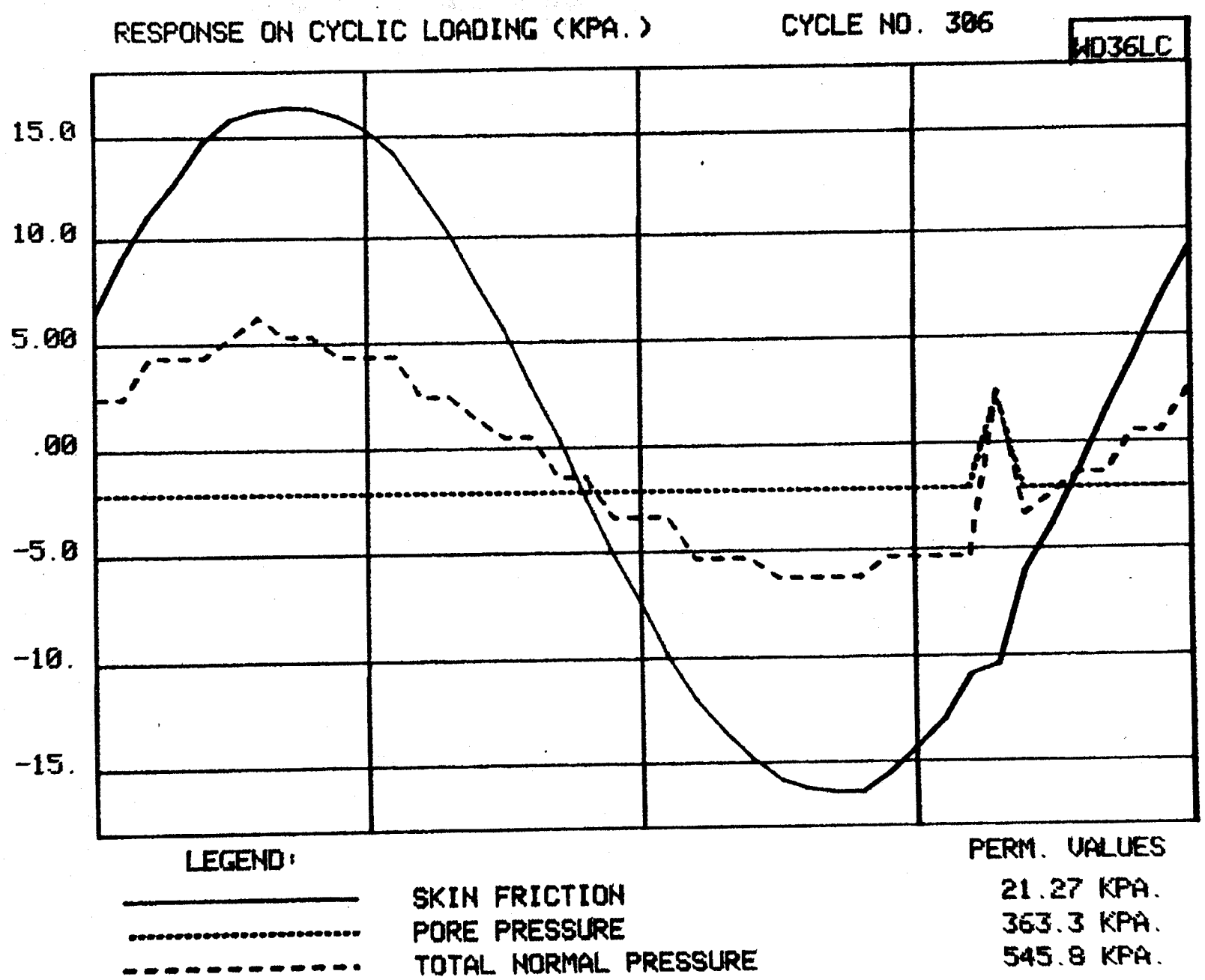
RESPONSE ON CYCLIC LOADING (KPA.)
CYCLE NO. 306
WD36LC
15.0
10.0
5.00
.00
-5.0
-10.
-15.
LEGEND:
SKIN FRICTION
PORE PRESSURE
TOTAL NORMAL PRESSURE
PERM. VALUES
21.27 KPA.
363.3 KPA.
545.8 KPA.

RESPONSE ON CYCLIC LOADING (KPA.) CYCLE NO. 308

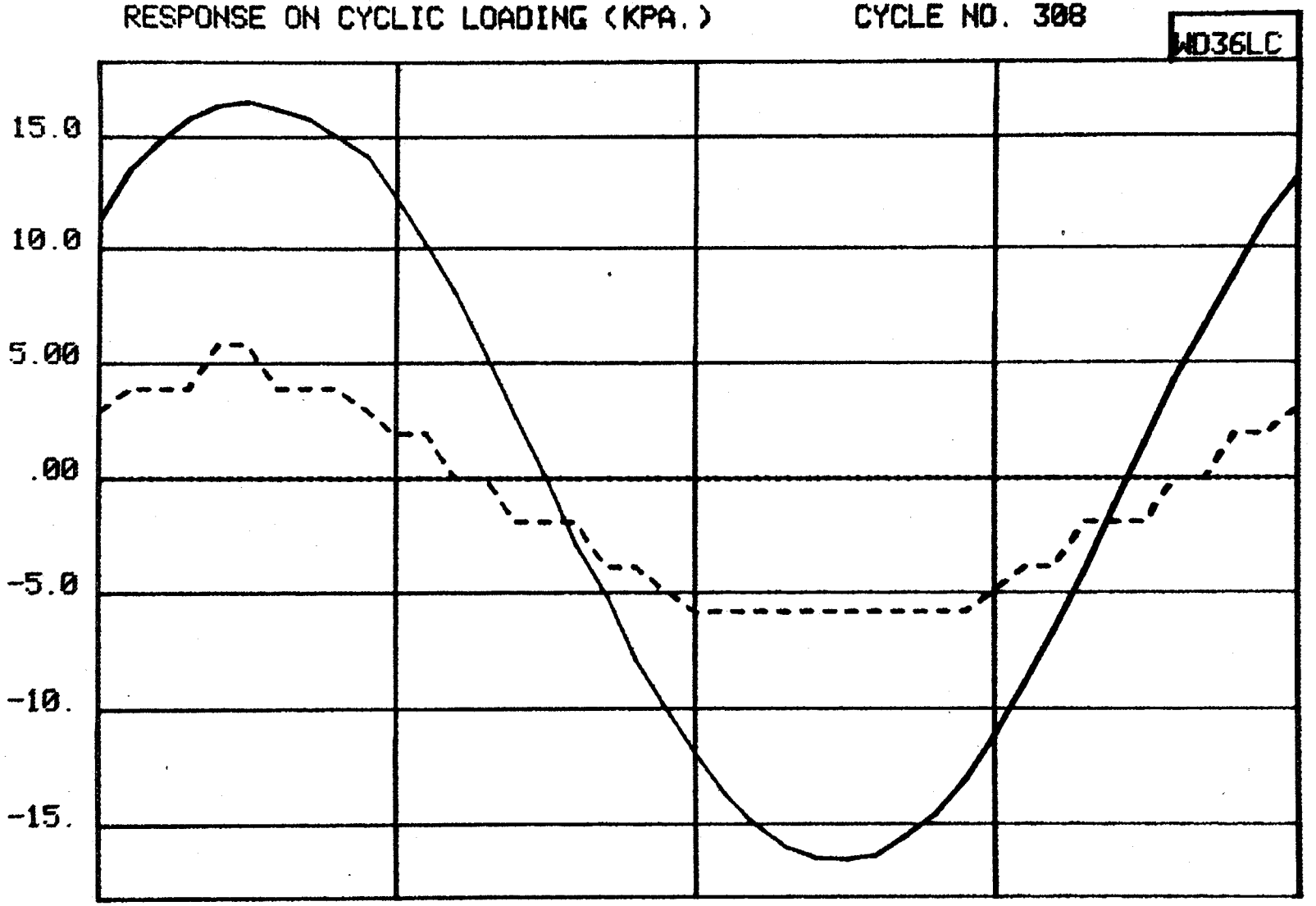

LEGEND:		PERM. VALUES
———	SKIN FRICTION	21.32 KPA.
·····	PORE PRESSURE	361.2 KPA.
- - - -	TOTAL NORMAL PRESSURE	544.4 KPA.

APPENDIX D

DETAILED RESULTS FROM **TEST 7, STRATUM II** MODEL PILE TESTS

CONTENTS

Summary	D3
Test 7, Stratum II	D4
Consolidation	D4
Pile Instatllation and Set-Up	D4
Static Test	D4
Cyclic Tests	D5
Stress Controlled Tests (WD27LC)	D5
Displacement Controlled Tests (WD27SC)	D6
Strength Tests	D7

LIST OF FIGURES

Figure 1	Sample Properties
Figure 2	Consolidation Diagram
Figure 3	Pocket Penetrometer Tests After Consolidation
Figure 4	Pressures at Pile Wall after Installation
Figure 5	Static Test
Figure 6	Skin Friction vs no. of Cycles, WD27LC
Figure 7	Deflection vs no. of Cycles, WD27LC
Figure 8	Total Normal Pressure vs no. of Cycles, WD27LC
Figure 9	Pore Pressure vs no. of Cycles, WD27LC
Figure 10	Eff. Normal Pressure vs no. of Cycles, WD27LC
Figure 11	Deflection vs no. of Cycles, WD27SC
Figure 12	Skin Friction vs no. of Cycles, WD27SC
Figure 13	Pore Pressure vs no. of Cycles, WD27SC

Figure 14 Total Normal Pressure vs no. of Cycles, WD27SC
Figure 15 Eff. Normal Pressure vs no. of Cycles, WD27SC
Figure 16 Pocket Penetrometer Tests after Pile Test
Figure 17 Unconfined Compression Tests
Figure 18 Water Content and Shear Strength

Appendix DA
Plotted Results from WD27LC
Figures DA-1 through DA-8
Skin Friction vs Deflection, Selected Cycles
Figures DA-9 through DA-12
Skin Friction vs Eff. Normal Pressure, Selected Cycl.
Figures DA-13 through DA-27
Skin Friction, Pore and Total Pressure, Selected Cycles

Appendix DB
Plotted Results from WD27SC
Figures DB-1 through DB-7
Skin Friction vs Deflection, Selected Cycles
Figures DB-8 through DB-11
Skin Friction vs Eff. Normal Pressure, Selected Cycl.
Figures DB-12 through DB-24
Skin Friction, Pore and Total Pressure, Selected Cycles

SUMMARY

This report contains the results of the laboratory model pile tests designated TEST 7, STRATUM II, in the project CNRD 13-2, TENSION PILE STUDY, for Conoco Norway Inc.

The clay sample was consolidated for 16 days under 300 kPa applied vertical pressure. Pore pressure in the sample was about 15 % of the applied pressure. After two days of consolidation in the pile chamber the pile was installed. After 6 days of set-up the excess pore pressure was still about 170 kPa. Testing was then started.

Static test gave peak friction of 19 kPa with residual value of 16 kPa. Undrained shear strength was interpreted to 40 kPa, giving alpha value of 0.48 and 0.4 for peak and residual respectively. Estimating the effective vertical pressure to 167 kPa results in a beta factor of 0.11.

Cyclic tests were started 8 hrs following the static test starting with stress controlled tests with static tension bias of 6 kPa (32% of previous max. friction) with parcels of 100 cycles with specified cyclic stress amplitude increasing for consecutive parcels resulted in failure (abrupt pull-out of pile) in seventh parcel. The maximum friction at failure was measured to 19.2 kPa.

After 14 hrs of set-up a displacement controlled test with two-way cyclic loading was performed. Seven parcels of 100 cycles with increasing cyclic displacements were made. Maximum friction obtained was 21.3 kPa which reduced to 17 kPa in subsequent parcels. The residual friction during large slip was 15.5 kPa which gives a reduction of strength of 27 % .

TEST 7, STRATUM II

CONSOLIDATION

The sample was prepared from the same material as used in Test 5. Water was added during the remoulding process to a water content of about 39% . Horizontal filters were placed in the oedometer to provide better vertical drainage.

A vertical pressure of 300 kPa was applied on top. As seen in Figure 2 the pore pressure at middle height had dropped down to about 15% of the consolidation stress after 16 days. At this time the sample was transferred to the pile chamber. Pocket penetrometer tests were performed on the side of the sample and on the top when trimmed in the pile chamber (level I-I) as shown in Figure 3. The shear strength, s_u, showed an average of about 30 kPa.

PILE INSTALLATION AND SET-UP

After pocket penetrometer tests the sample was mounted in the pile chamber and left to reconsolidate for two days under a vertical pressure of 300 kPa and radial pressure of 210 kPa (K=0.7). In addition a back pressure of 300 kPa was applied in an attempt to help speed up the pore pressure response.

During insertion of the pile the side friction showed a maximum of about 12 kPa. Total normal pressure showed 565 kPa and the pore pressure only showed 310 kPa, reflecting the back pressure directly after pile installation. After about two days of set-up the total pressure had slightly reduced to 550 kPa whereas the pore pressure had reached a maximum of 470 kPa. Four additional days of consolidation (set-up) made the total and pore pressure drop only slightly. At this time it was decided to start with the loading program, even though the excess pore pressure was 170 kPa (above back pressure).

STATIC TEST

A displacement controlled static test with deformation rate 1 mm per hour was now

conducted, as shown in Figure 5. The pile was pulled in tension through failure and large slip and then pushed down to original position causing failure in compression and large slip (residual friction).

The displacement to cause failure, as shown in Figure 5, was about 0.2 mm or 0.8% of the pile diameter. A maximum friction of 19 kPa was achieved with a residual friction of 16 kPa. The shear strength of the clay was estimated to 40 kPa at time of testing, which results in an alpha (α) value of 0.48 and 0.4 for peak and residual friction respectively.

For the effective stress approach, estimating σ'_{vo} from the relationship

$$s_u = 0.24 \cdot \sigma'_{vo}$$

which gives $\sigma'_{vo} =$ 167 kPa, the beta value (β) becomes 0.11 for maximum friction.

Total pressure on the pile wall at time of failure was about 545 kPa and the pore pressure showed 470 kPa, resulting in a horizontal effective pressure of 75 kPa. The interface friction angle (δ) can then be estimated to 14.2 degrees.

CYCLIC TESTS

After the static test the pile was brought back to original position and left to reconsolidate for 8 hours, at which time cyclic stress controlled tests were started.

Stress Controlled Tests (WD27LC)

A stress controlled test comprised of applying a prescribed static tensile (uplift) stress on the pile, superimposed with parcels of 100 cycles with 10 seconds period and prescribed cyclic stress amplitude. The stress amplitude was the increased in the following parcels until failure (excessive uplift) occured in tension.

For this test the static tensile stress (bias) level was about 6 kPa, corresponding to 32% of the previous static capacity.

In the first parcel the the cyclic level was about 1.5 kPa and for the following parcels

the cyclic stress level was incremented by 2 kPa as can be seen in Figure 6, showing skin friction (envelope of max. and min.) versus cycle numbers. In the following four figures the resulting deformations and pressures due to the applied skin friction are plotted versus cycle numbers. In Appendix A selected cycle numbers are plotted as friction versus deflection, friction versus effective pressure and friction, pore pressure and total pressure variation during one cycle.

As seen in Figure 6 a total of seven parcels were performed. The first two parcels do not produce any significant deformation of the pile as shown in Figure 7 and in Figures A-1 and A-2. Starting the third parcel the average deformation is to have "jumped" up a small amount and the cyclic deformation is increased. The friction deformation behaviour is, however, linear with only minimal signs of hysteresis. Increasing the cyclic level in parcels four and five results in larger cyclic deformations and some more pronounced hysteresis, but with the average deformation fairly constant, as depicted in Figure 7 and A-4 and A-5. In the sixth parcel with a cyclic level of 11.5 kPa (maximum friction of 17.5 kPa) the pile is slowly pulled up indicated by the increasing average deformation. Finally in parcel seven with prescribed cyclic stress level of 13.5 kPa the pile fails already in the first cycle at a fiction of 19.2 kPa as can be seen in Figures A-7 and A-8 where the pile is pulled up excessively in an attempt to produce the prescribed cyclic friction.

From the pressure diagrams in Figures 8,9 and 10 it is seen that the average pressures during the cyclic testing stays fairly constant. The total normal pressure is seen to drop drastically at the time of failure as does the effective pressure which is a mirror image of the total pressure since the pore pressure showed no cyclic variation and stayed constant throughout the test. The effective pressure at time of failure was about 60 kPa giving an interface friction angle of 17.7 degrees. This can also be seen in the "effective stress " plots in Figures A-9 through A-12.

Displacement (stroke) Controlled Tests (WD27SC)

After failure in the stress controlled tests the pile was brought back to original position and left to reconsolidate for a period of 14 hours before cyclic displacement controlled test was performed.

One parcel here consisted of 100 cycles with 10 seconds period in two way cyclic

loading from the zero position of the pile. A total of seven consecutive parcels were performed with increasing displacement amplitude, starting with 0.1 mm in the first parcel and with 0.2, 0.4, 0.6, 0.8, 1.0 and 2.0 mm in the following parcels.

The applied displacement versus cycle numbers are shown in Figure 11 with the resulting skin friction , total pressure, pore pressure and effective pressure versus cycle numbers shown in Figures 12,13,14 and 15 respectively. More detailed plots of selected cycles are shown in Appendix B.

In the first parcel with cyclic displacement of 0.1 mm the pile is not brought to failure as seen in Figure 12 and the response is linearly elastic as shown in Figure B-1 showing only a small hysteresis in the friction-displacement relationship. In the second parcel, however, failure is reached at 21.3 kPa in the first cycle which reduces to 20 kPa after about five cycles and down to 17 after 100 cycles. The friction during large slip (residual) was 20 kPa in the first cycle and reduced to 16 kPa after 100 cycles. In the following parcels with increasing cyclic displacements the peak friction in the first cycle stabilized at about 17.5 kPa stabilizing at about 16 kPa after 100 cycles. The residual friction during large slip was about 15.5 kPa as can be seen in Figures B-3 through B-6. In the last parcel with cyclic displacement of 2.0 mm the peak friction in the first cycle was 19 kPa which reduced down to the previous level of 17.5 kPa after about 10 cycles with the same value of residual strength during large slip of 15.5 kPa.

The degradation of strength from maximum peak friction to residual friction during large slip was then 27%.

The pressures at the pile wall stayed fairly constant during the test with no cyclic variation seen in the pore pressure which showed a tendency to decrease slightly (10 kPa) for the large cyclic deformation. The total pressure, Figure 13, showed cyclic variation increasing with the deformation, with a cyclic amplitude of 12 kPa in the last parcel. In Figures B-8 through B-11 are shown skin friction versus effective pressure, and from these it is seen that in cycle 101 with the peak friction of 21.3 kPa the effective pressure shows 70 kPa giving an interface friction angle of 16.9 degrees.

STRENGTH TESTS

After the last parcel in stroke controlled cyclic tests the pile was pulled out of the pile

chamber and the sample built out. Pocket penetrometer tests were performed on the side of the sample and in two horizontal layers as shown in Figure 16.

Three standard triaxial test samples were then prepared from the center of the clay specimen and unconfined compression tests (UCT) were performed with the results shown in Figure 17.

In Figure 18 are shown the water content and interpreted undrained shear strength of the clay sample versus the distance from the center after completion of the pile test. The water content showed about 30% with a slight tendency to reduce towards the center.

TABLE 1.

SAMPLE PROPERTIES TEST 7, STRATUM II

SAMPLE PREPARATION		CONSOLIDATION			END OF PILE TEST
INITIAL WATER CONTENT	INITIAL HEIGHT	AXIAL DEFORMATION	AXIAL STRAIN	WATER CONTENT	WATER CONTENT
w_i (%)	H_o (cm)	ΔH (cm)	ε (%)	w_e (%)	w_{ep} (%)
39.-	50.85	6.58	12.94	A 36.26 B - C 34.85	A 30.84 B 31.18 C 30.34

CONFINING PRESSURE		
AXIAL	KPa	600
RADIAL	KPa	510
BACK PRESSURE	KPa	300
SAMPLE CONSOLIDATION		
IN OEDOMETER	Days	16
IN PILE CHAMBER	Days	2
INTERPRETED SHEAR STRENGTH		
END OF CONSOLIDATION	KPa	30
END OF PILE TEST	KPa	40

Fig. 1

CONSOLIDATION DIAGRAM								Test No. 7 Stratum II		Start date	
H_i 50.85 cm		H_e 44.27 cm		$\Delta\varepsilon_v$ 12.94 %						σ_c 300 kPa	
Time h	12	18	42	48	66	72	89	162	186	210	234
Δh cm	0.83	1.46	2.88	3.29	4.19	4.38	4.74	5.61	5.77	5.89	6.00
u kPa		6.7	81.8	113.1	178.6	179.5	168.8	120.0	108.0	98.1	82.0
	258	330	354	378							
	6.07	6.24	6.27	6.58							
	77	51	49	45							

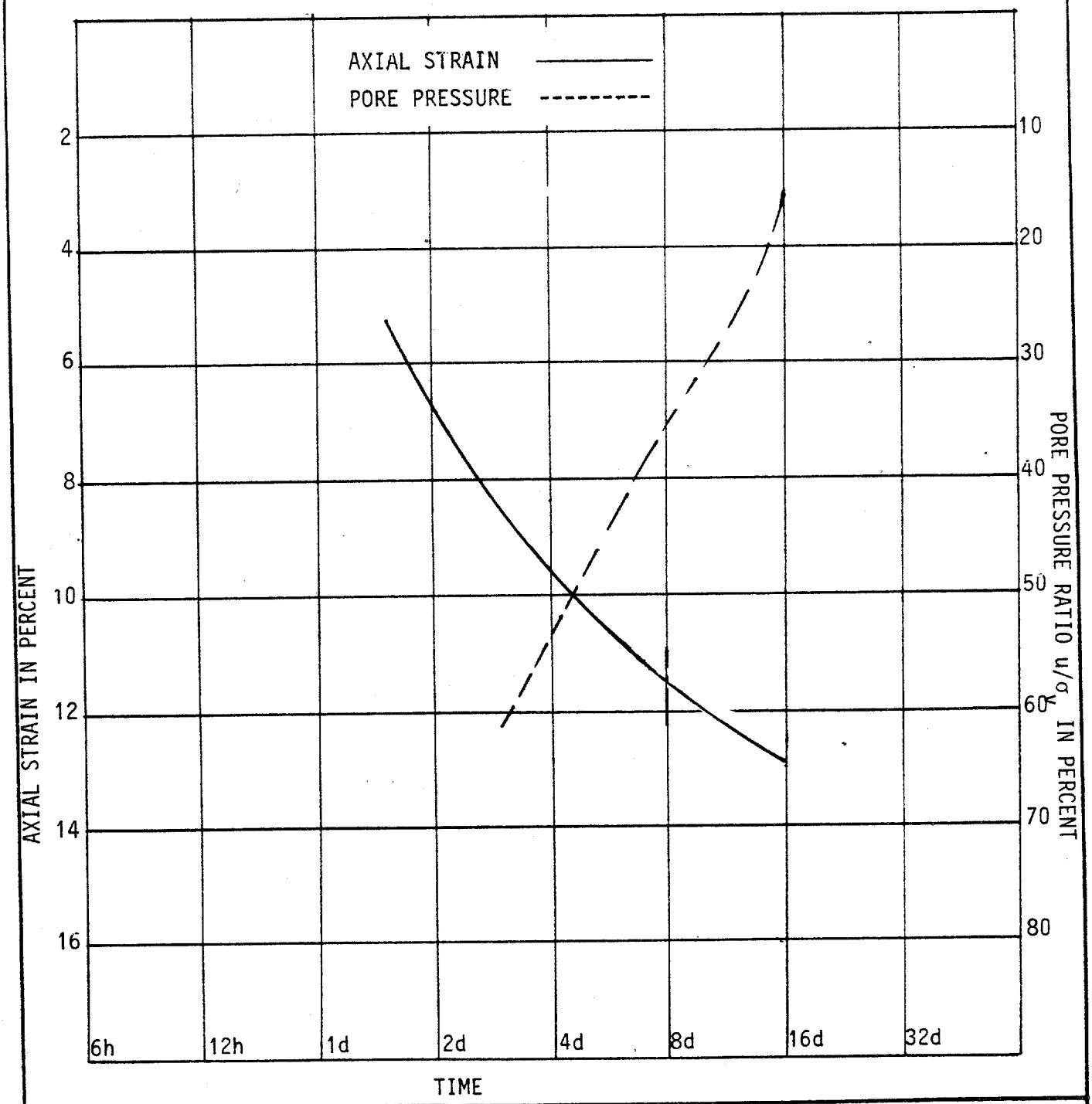

CNRD 13-2 TENSION PILE STUDY LABORATORY MODEL PILE TESTS

TEST 7, STRATUM II, Consolidation Diagram

DET NORSKE VERITAS
Geotechnical Laboratory

Scale

Drawn by

Date

Approved

Fig. No. 2

TEST 7, STRATUM II

SHEAR STRENGTH (kPa) FROM POCKET PENETROMETER TESTS AFTER CONSOLIDATION

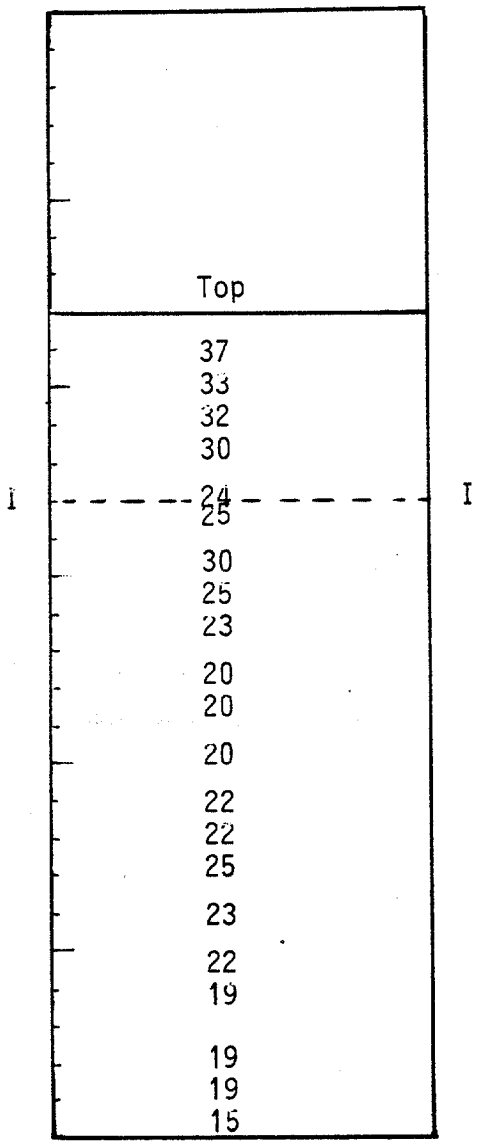

Scale 1:4

LEVEL I-I

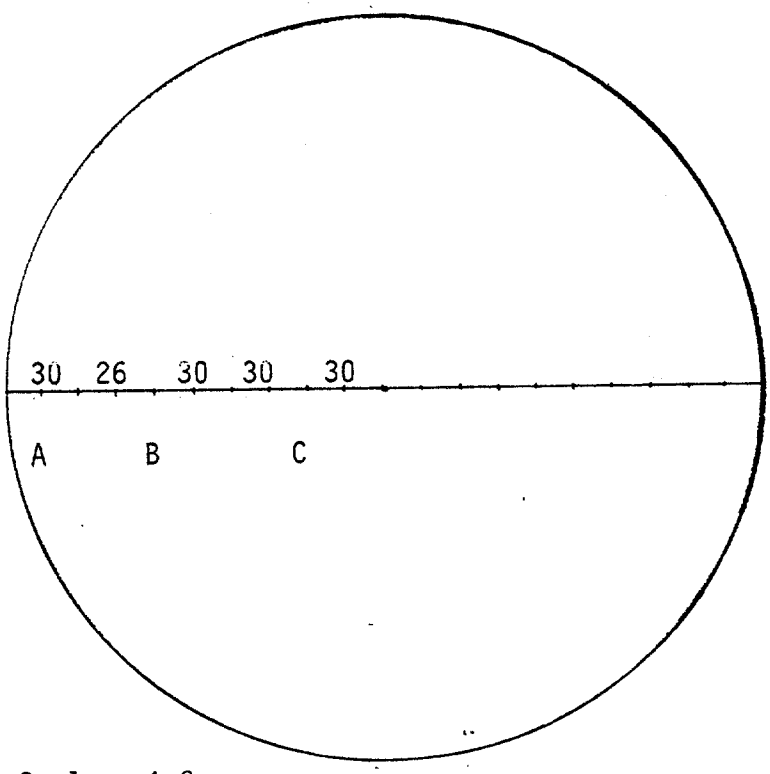

Scale: 1:2

CNRD 13-2 TENSION PILE STUDY LABORATORY MODEL PILE TESTS

		Scale
DET NORSKE VERITAS Geotechnical Laboratory	Drawn by	Date
	Approved	Fig. No. 3

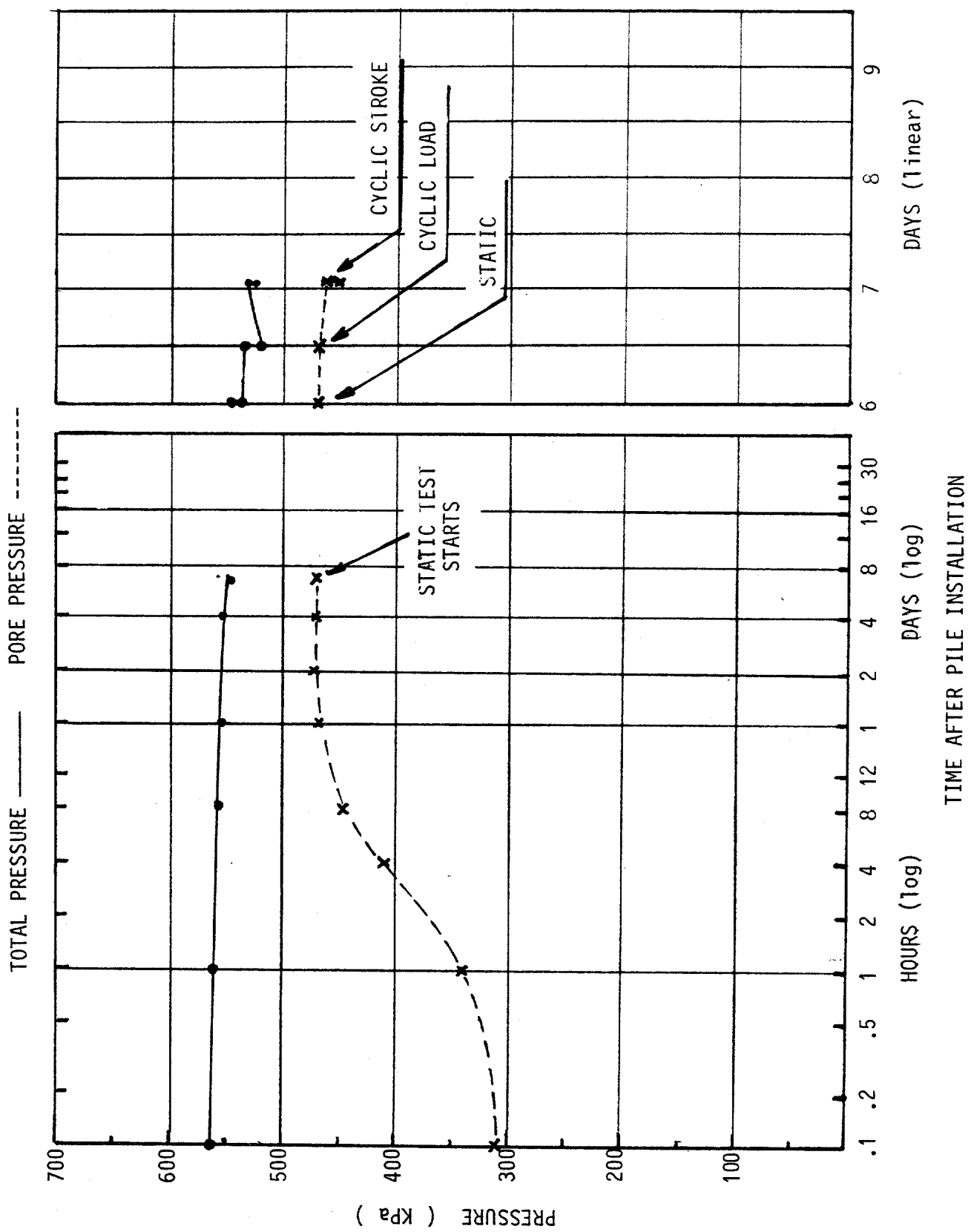

CNRD 13-2 TENSION PILE STUDY LABORATORY MODEL PILE TESTS

TEST/7, STRATUM II ‹Pressure at pile wall after installation

DET NORSKE VERITAS Geotechnical Laboratory	Drawn by	Scale
	Approved	Date
		Fig. No. 4

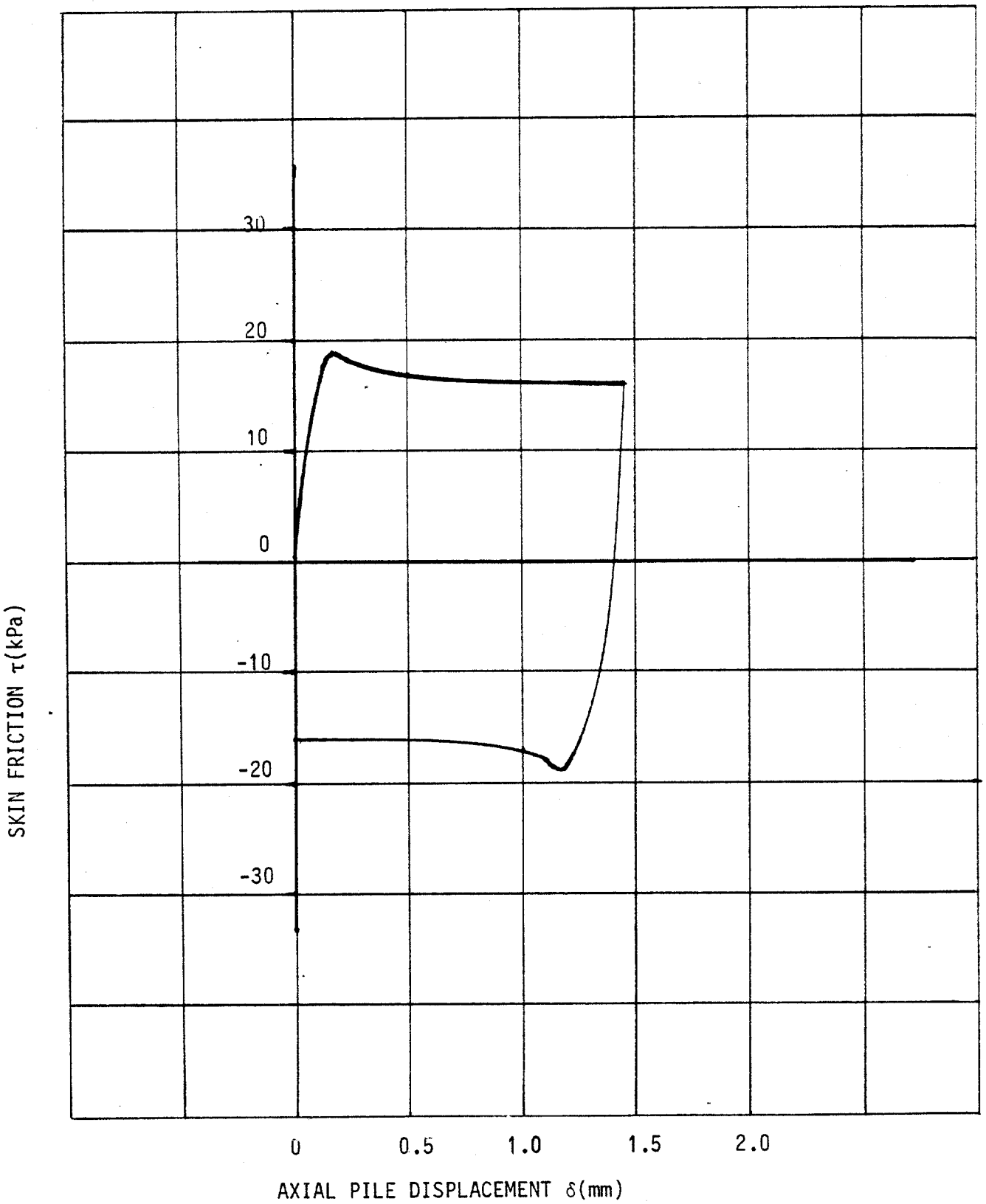

CNRD 13-2 TENSION PILE STUDY LABORATORY MODEL PILE TESTS

TEST 7, STRATUM II STATIC TEST		Scale
DET NORSKE VERITAS Geotechnical Laboratory	Drawn by	Date
	Approved	Fig. No. 5

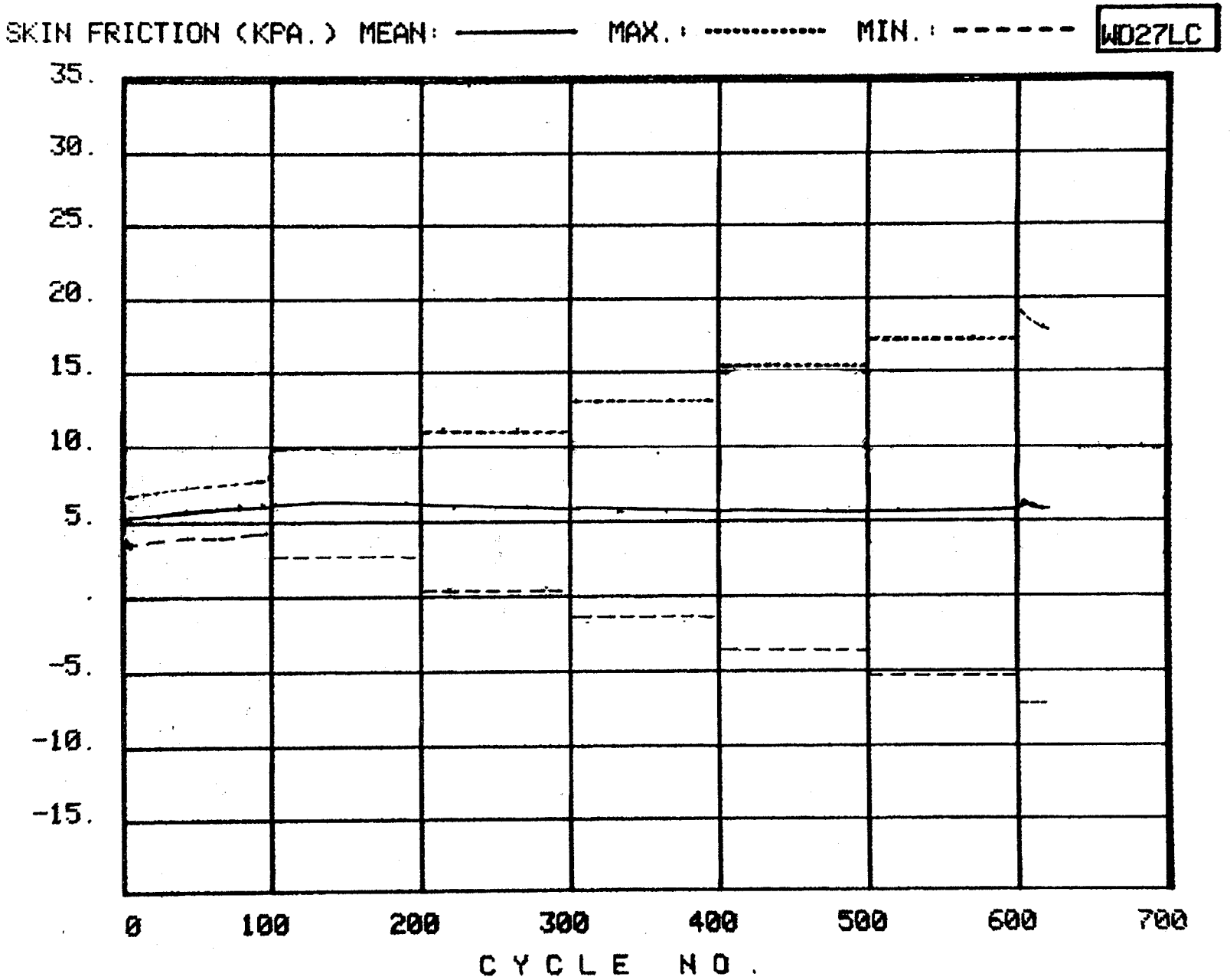
SKIN FRICTION (KPA.) MEAN: MAX.: MIN.:
WD27LC
35.
30.
25.
20.
15.
10.
5.
-5.
-10.
-15.
0
100
200
300
400
500
600
700
CYCLE NO.

Fig.6

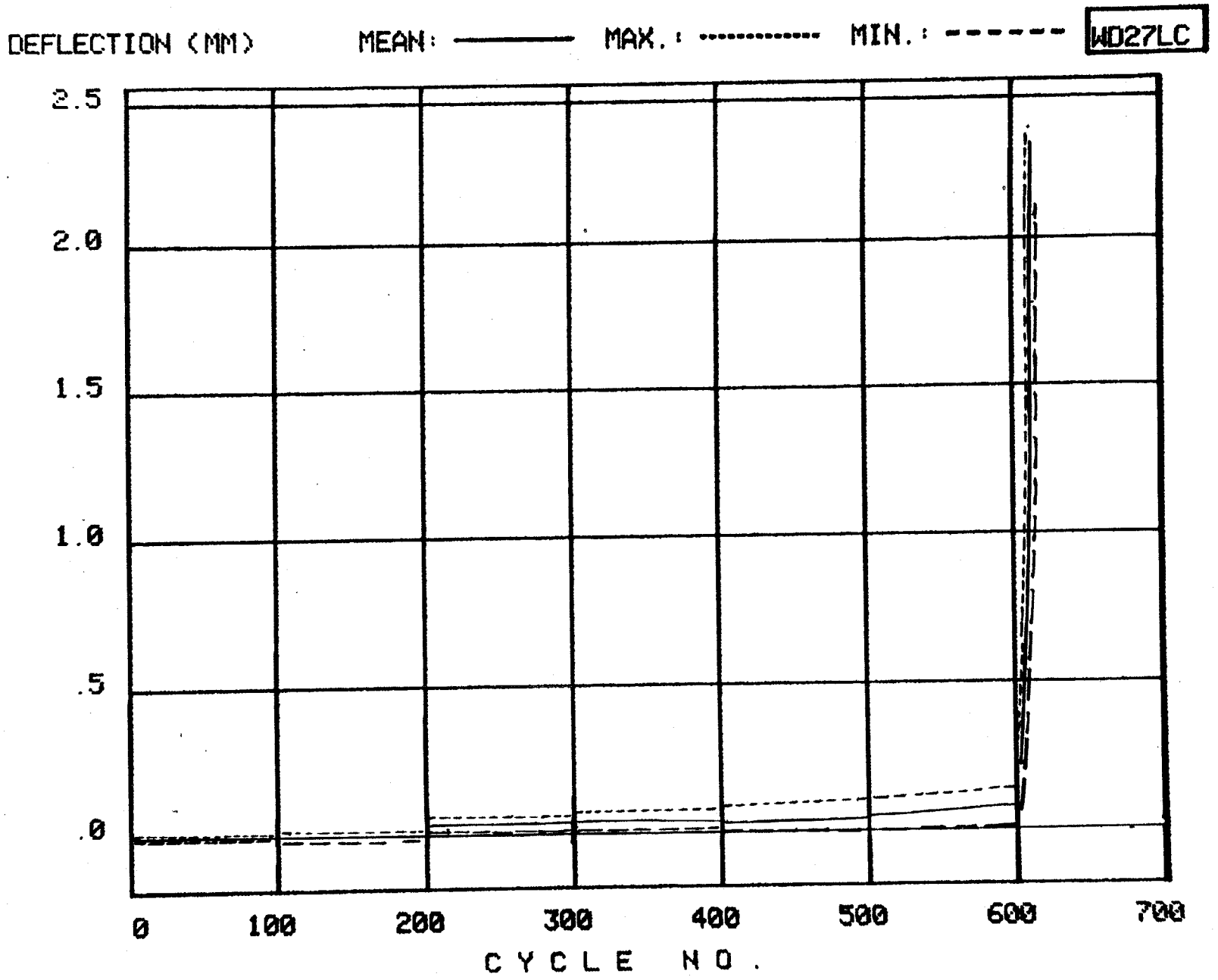
DEFLECTION (MM)
MEAN:
MAX.:
MIN.:
WD27LC
2.5
2.0
1.5
1.0
.5
.0
0
100
200
300
400
500
600
700
CYCLE NO.

Fig.7

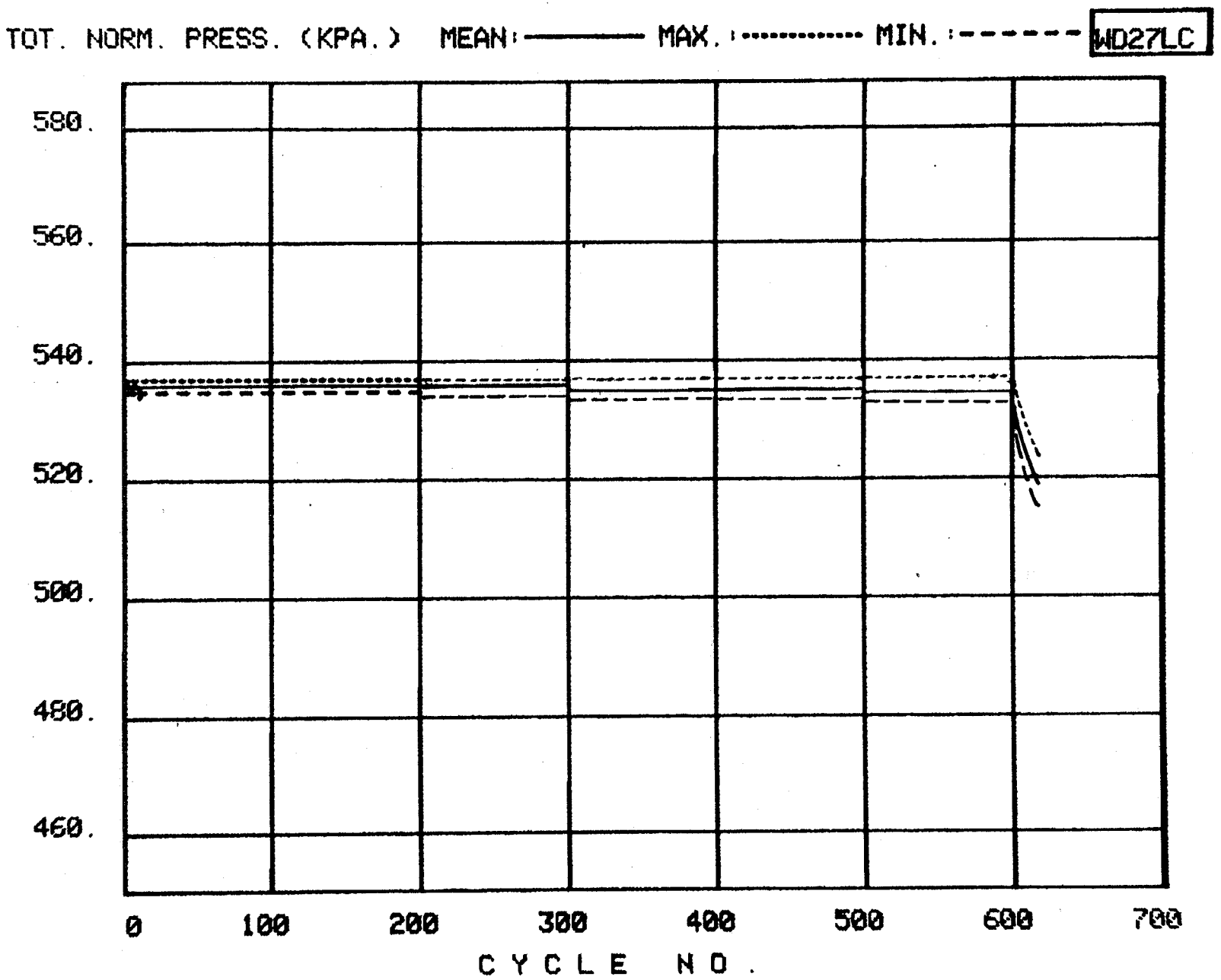
TOT. NORM. PRESS. (KPA.)
MEAN:
MAX.:
MIN.:
WD27LC
580.
560.
540.
520.
500.
480.
460.
0
100
200
300
400
500
600
700
CYCLE NO.

Fig. 8

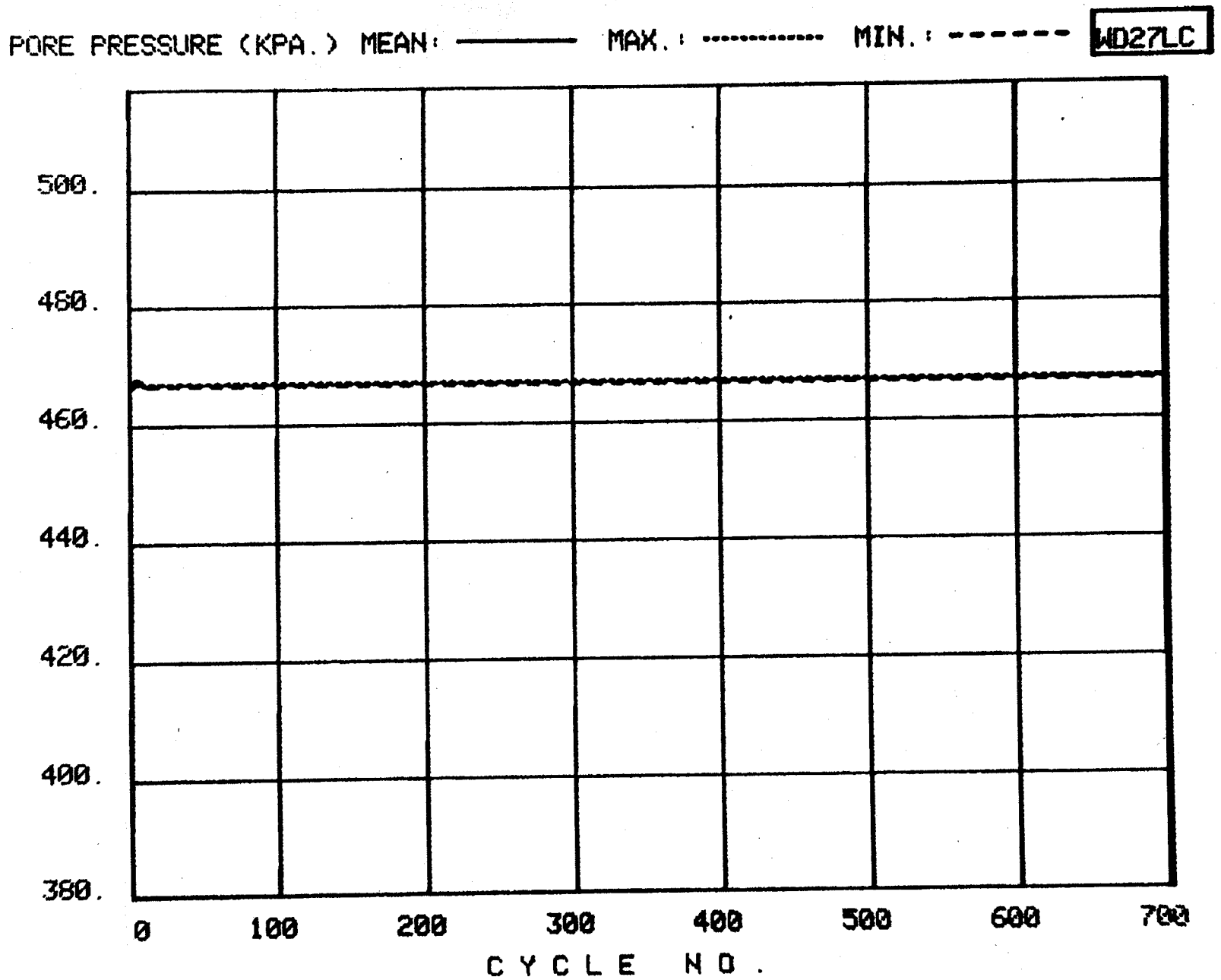
PORE PRESSURE (KPA.) MEAN: MAX.: MIN.:
WD27LC
500.
480.
460.
440.
420.
400.
380.
0
100
200
300
400
500
600
700
CYCLE NO.

Fig.9

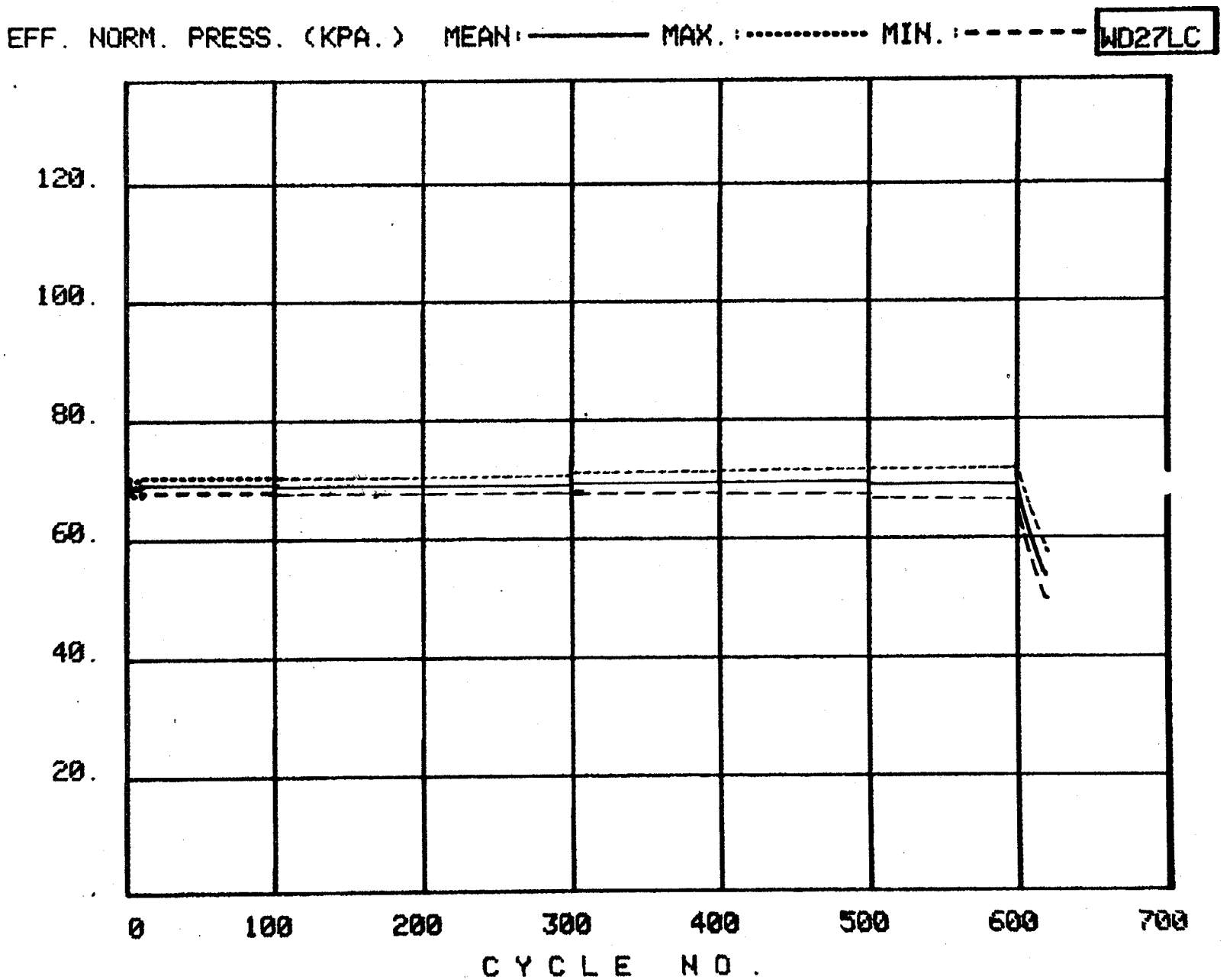
EFF. NORM. PRESS. (KPA.)
MEAN:
MAX.:
MIN.:
WD27LC
120.
100.
80.
60.
40.
20.
0
100
200
300
400
500
600
700
CYCLE NO.

Fig.10

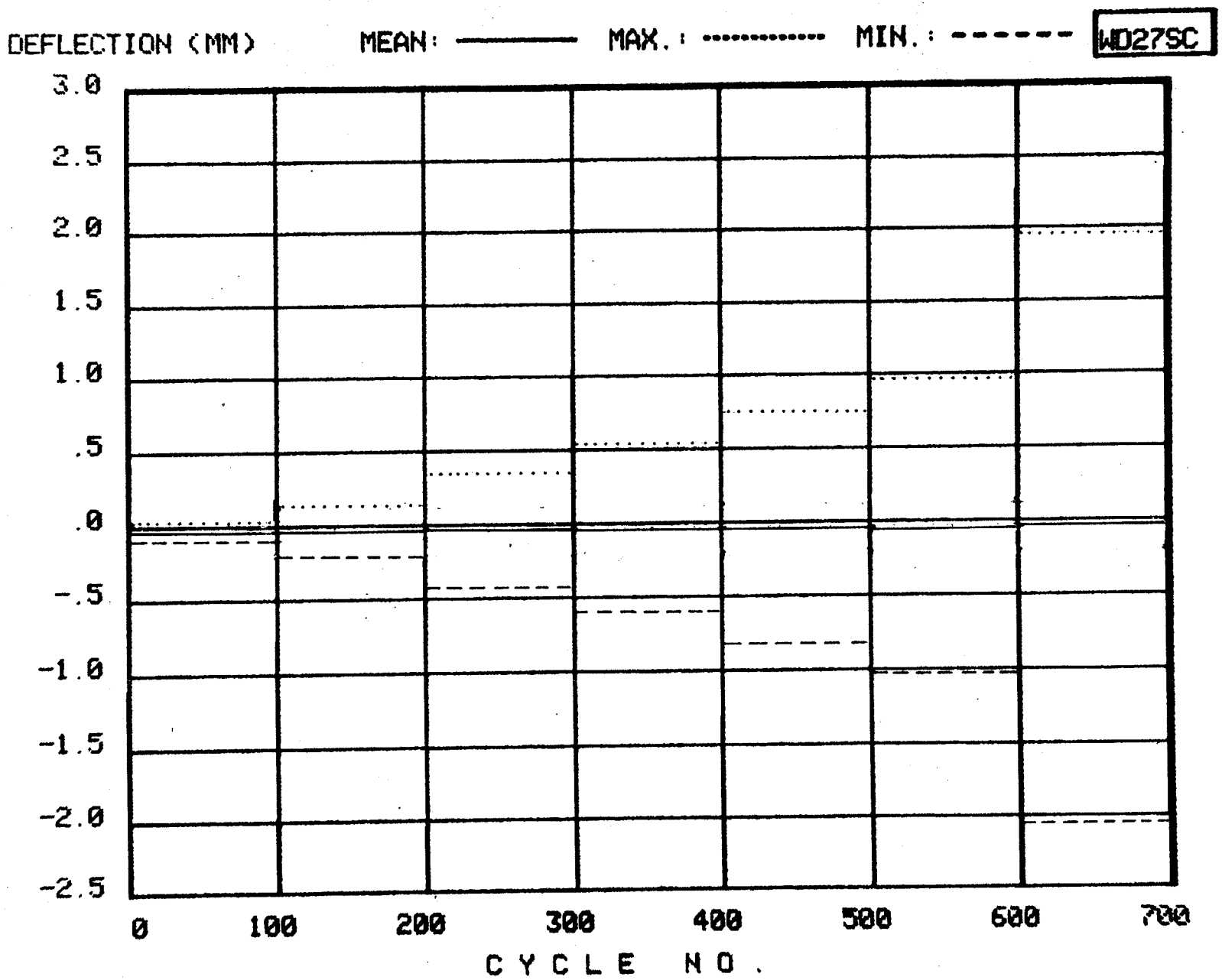
DEFLECTION (MM)
MEAN:
MAX.:
MIN.:
WD27SC
3.0
2.5
2.0
1.5
1.0
.5
.0
-.5
-1.0
-1.5
-2.0
-2.5
0
100
200
300
400
500
600
700
CYCLE NO.

Fig.11

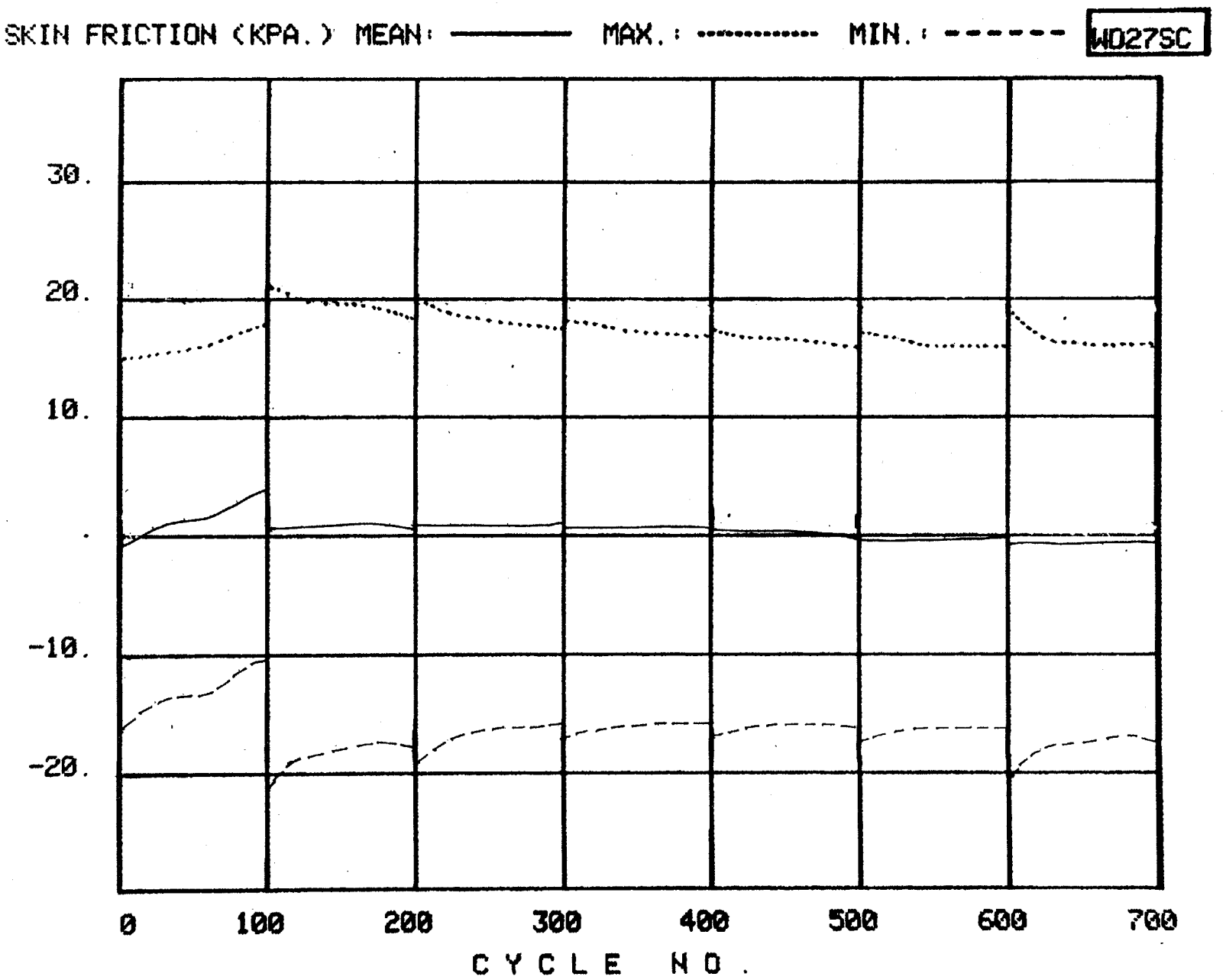
SKIN FRICTION (KPA.) MEAN: MAX.: MIN.:
WD27SC
30.
20.
10.
.
-10.
-20.
0
100
200
300
400
500
600
700
CYCLE NO.

Fig.12

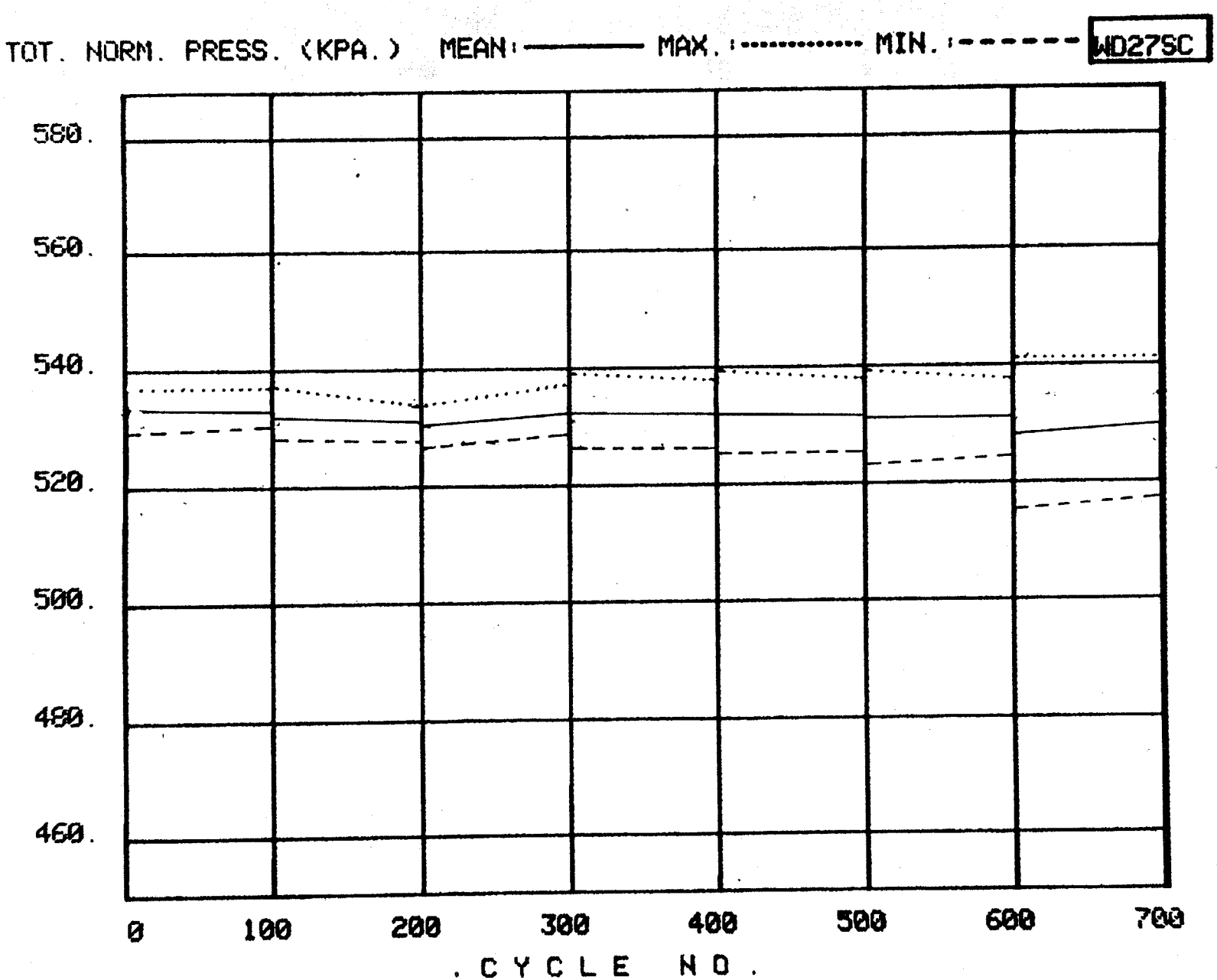
TOT. NORM. PRESS. (KPA.)
MEAN:
MAX.:
MIN.:
WD27SC
580.
560.
540.
520.
500.
480.
460.
0
100
200
300
400
500
600
700
. C Y C L E N O .

Fig.13

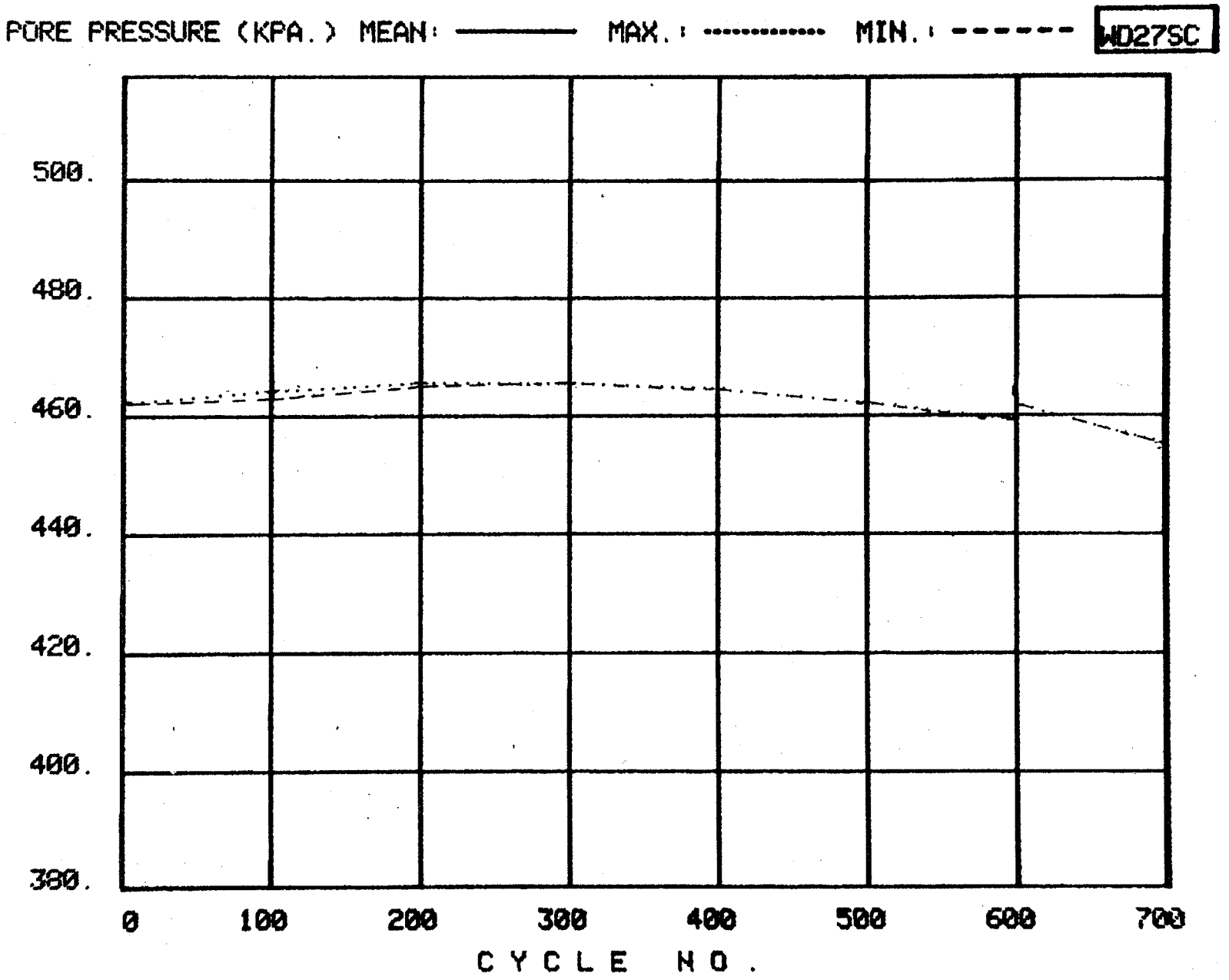
PORE PRESSURE (KPA.) MEAN: MAX.: MIN.:
WD27SC
500.
480.
460.
440.
420.
400.
380.
0
100
200
300
400
500
600
700
CYCLE NO.

Fig.14

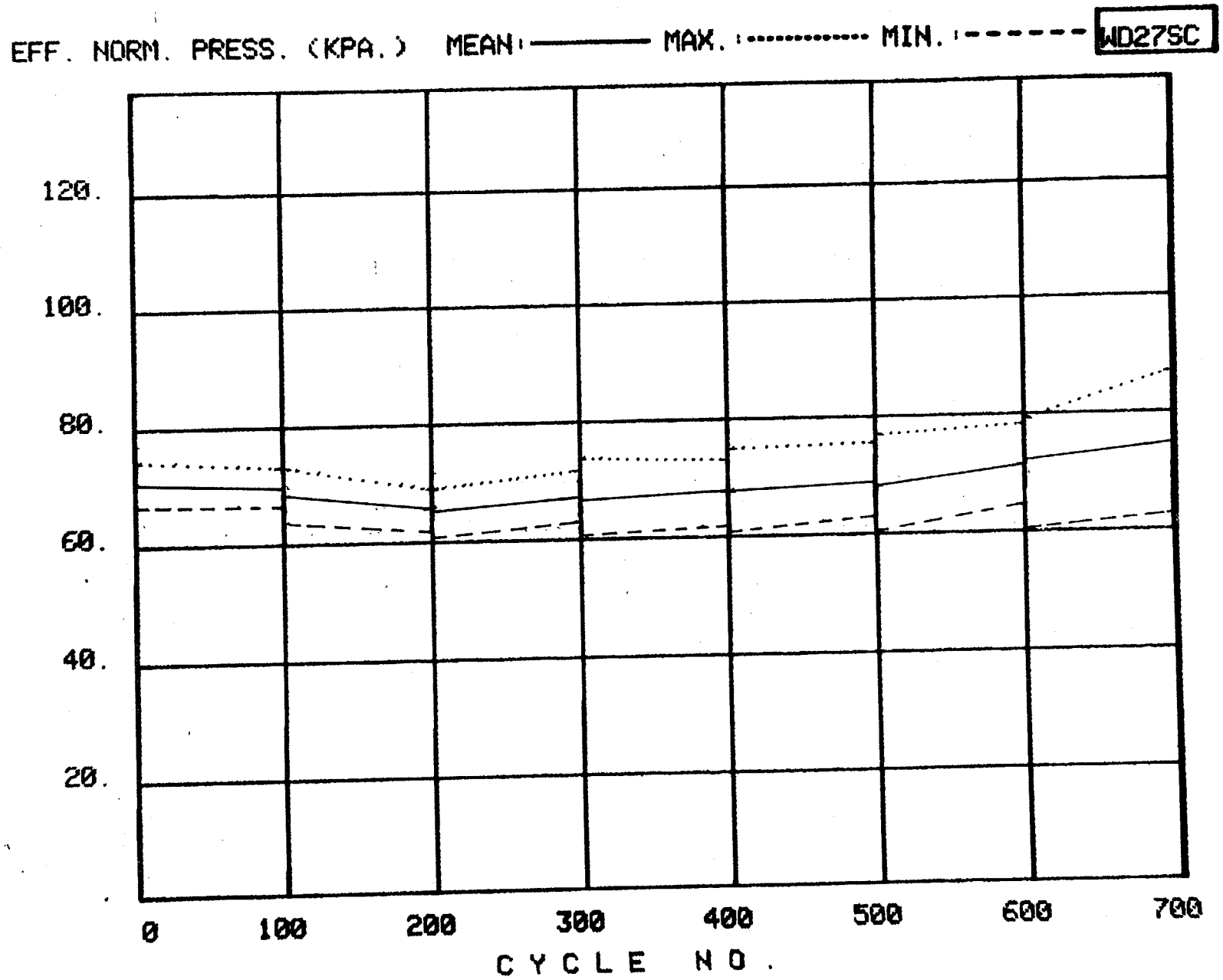
EFF. NORM. PRESS. (KPA.)
MEAN
MAX.
MIN.
WD27SC
120.
100.
80.
60.
40.
20.
0
100
200
300
400
500
600
700
CYCLE NO.

Fig.15

TEST 7, STRATUM II

SHEAR STRENGTH FROM POCKET PENETROMETER
AFTER PILE TEST (kPa)

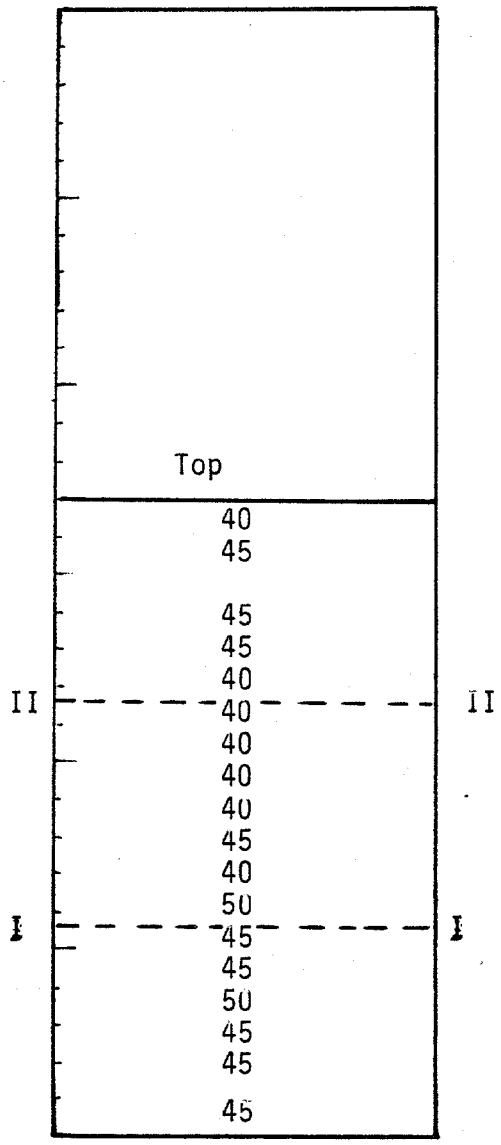

Scale 1:4

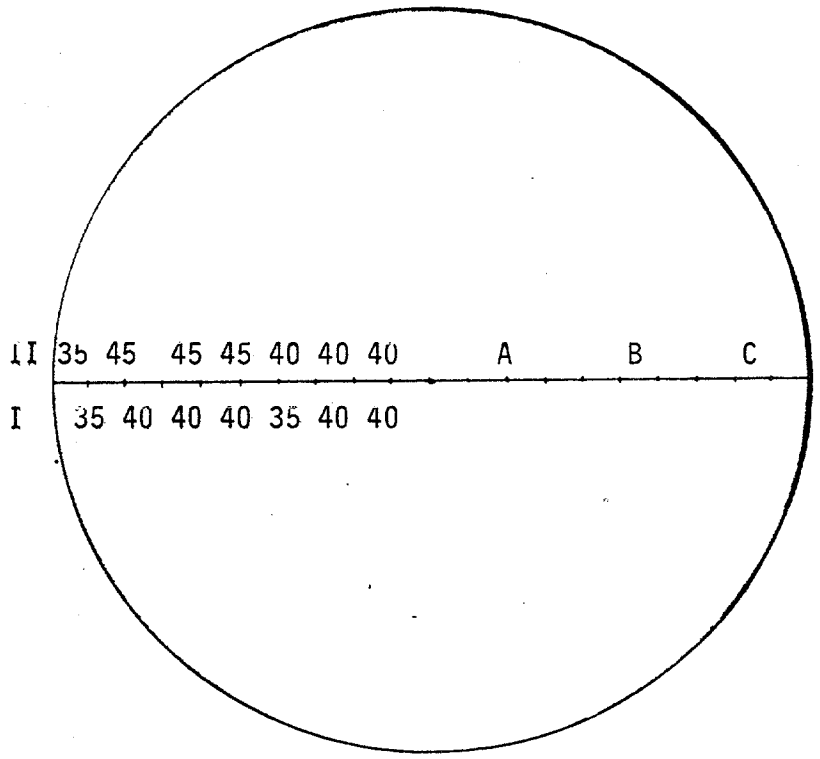

Scale: 1:2

CNRD 13-2 TENSION PILE STUDY LABORATORY MODEL PILE TESTS

TEST 7, STRATUM II, Pocket penetrometer tests after pile test

DET NORSKE VERITAS Geotechnical Laboratory	Drawn by	Scale
	Approved	Date
		Fig. No. 16

TEST 7, STRATUM II

UNCONFINED COMPRESSION TESTS AFTER PILE TEST

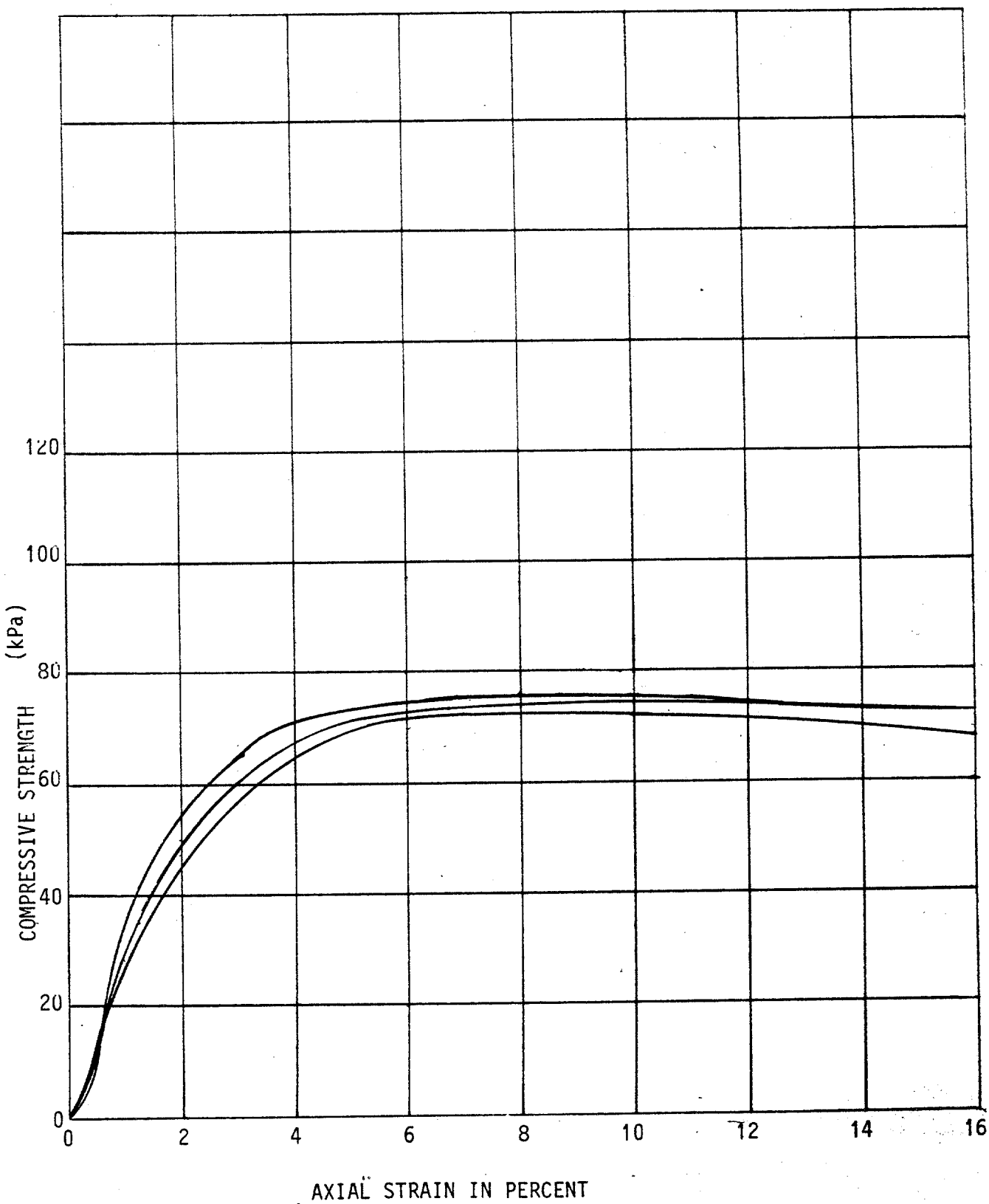

CNRD 13-2 TENSION PILE STUDY LABORATORY MODEL PILE TESTS

TEST 7 - STRATUM II, Unconfined Compr. tests

DET NORSKE VERITAS
Geotechnical Laboratory

Drawn by

Approved

Scale

Date

Fig. No. 17

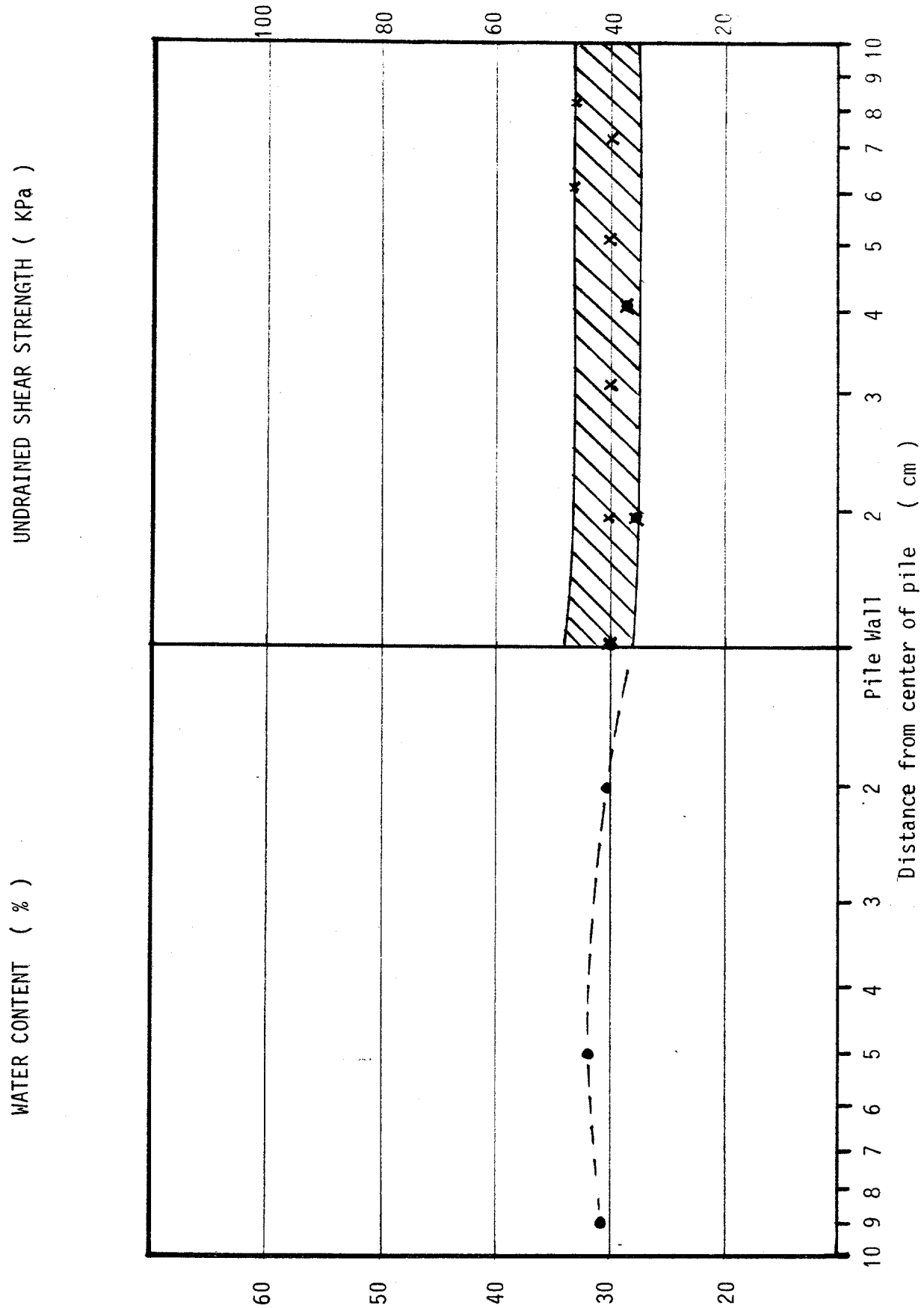

CNRD 13-2 TENSION PILE STUDY LABORATORY MODEL PILE TESTS

TEST 7, STRATUM II, Water content and shear strength after test

DET NORSKE VERITAS Geotechnical Laboratory	Drawn by	Scale
	Approved	Date
		Fig. No. 18

Appendix DA

Plotted Results from WD27LC

Figures DA-1 through DA-8

Skin Friction vs Deflection, Selected Cycles

Figures DA-9 through DA-12

Skin Friction vs Eff. Normal Pressure, Selected Cycl.

Figures DA-13 through DA-27

Skin Friction, Pore and Total Pressure, Selected Cycles

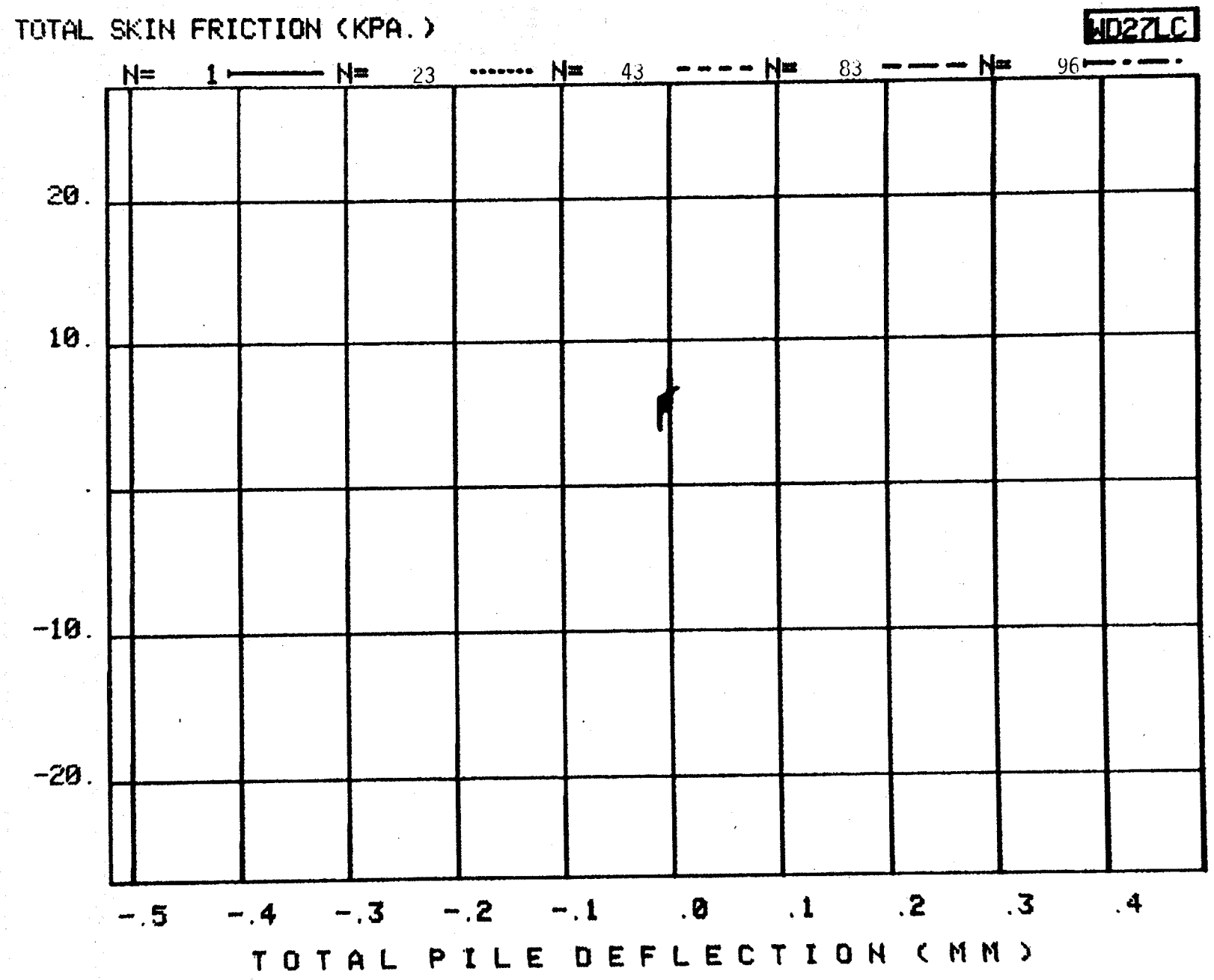
TOTAL SKIN FRICTION (KPA.)
WD27LC
N= 1
N= 23
N= 43
N= 83
N= 96
20.
10.
-10.
-20.
-.5
-.4
-.3
-.2
-.1
.0
.1
.2
.3
.4
TOTAL PILE DEFLECTION (MM)

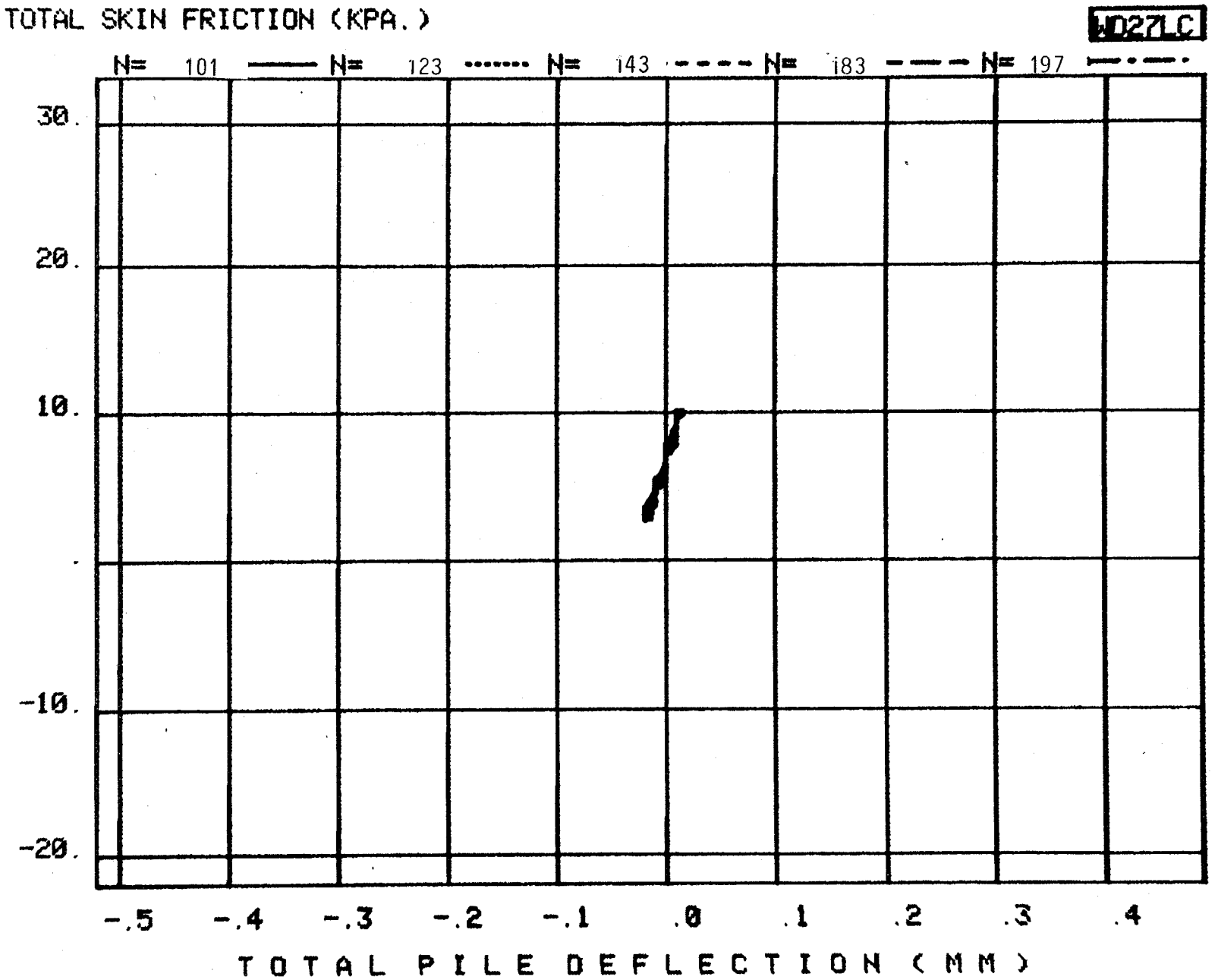
TOTAL SKIN FRICTION (KPA.)
WD27LC
N= 101
N= 123
N= 143
N= 183
N= 197
30.
20.
10.
-10.
-20.
-.5
-.4
-.3
-.2
-.1
.0
.1
.2
.3
.4
TOTAL PILE DEFLECTION (MM)

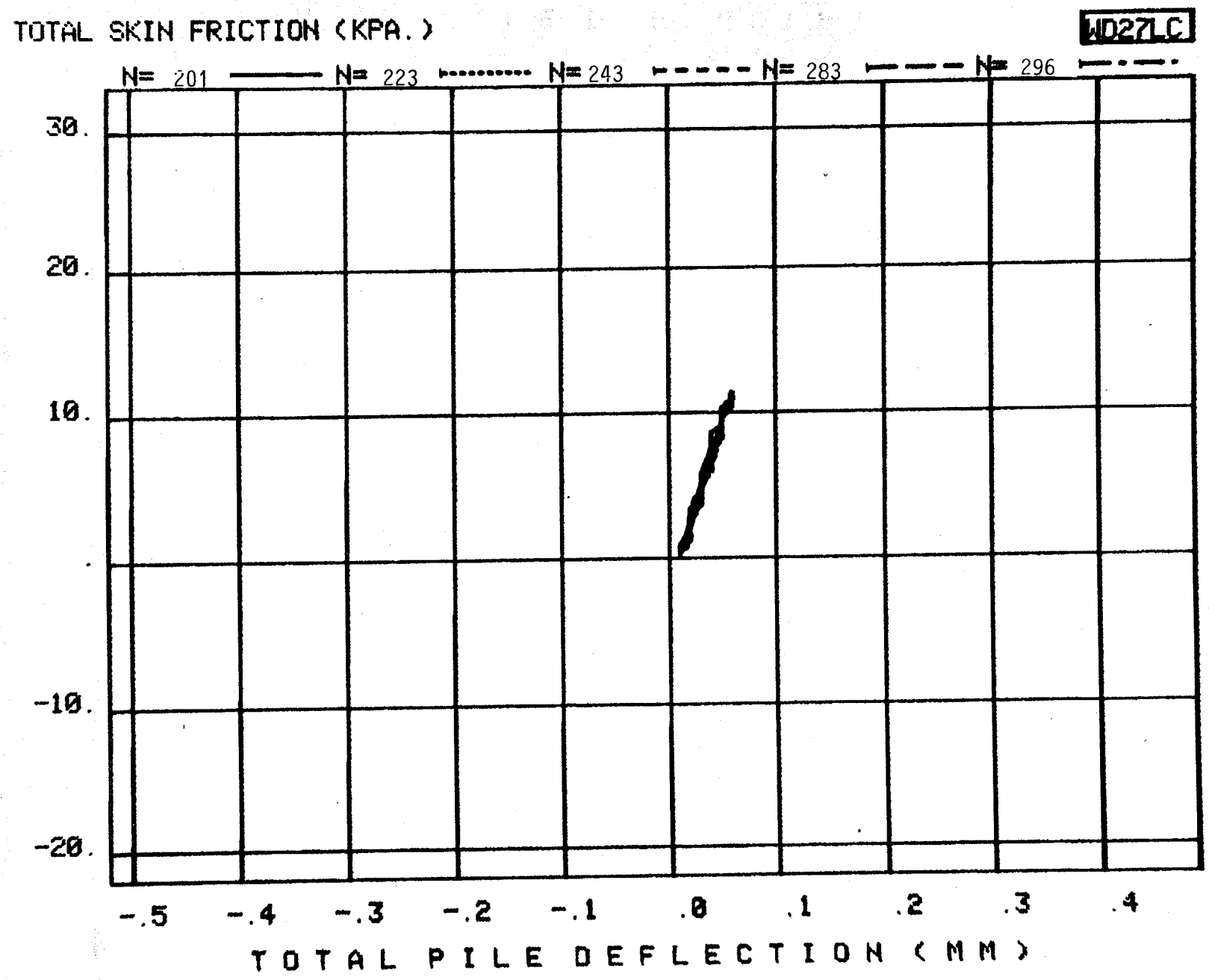
TOTAL SKIN FRICTION (KPA.)
WD27LC
N= 201
N= 223
N= 243
N= 283
N= 296
30.
20.
10.
-10.
-20.
-.5
-.4
-.3
-.2
-.1
.0
.1
.2
.3
.4
TOTAL PILE DEFLECTION (MM)

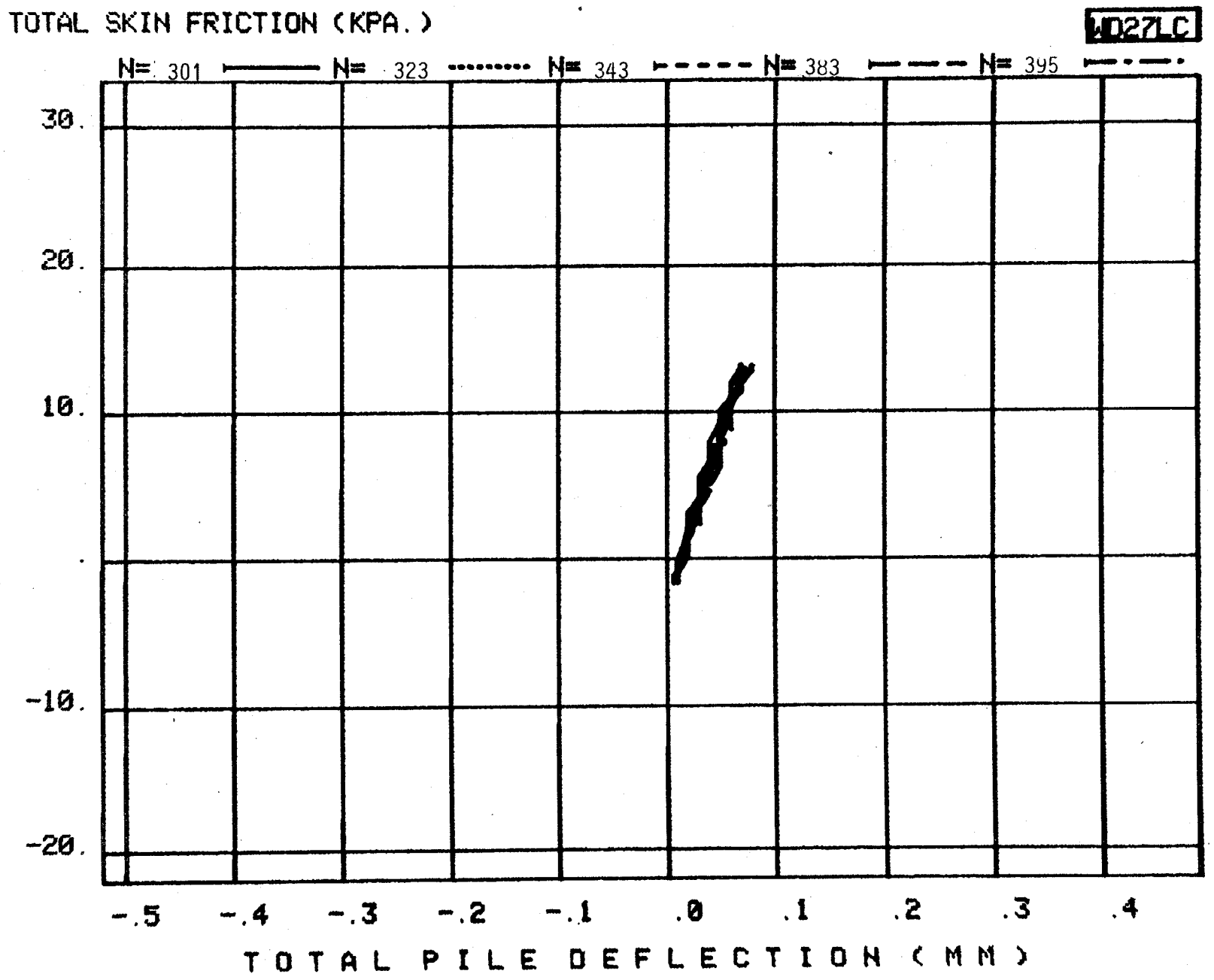
TOTAL SKIN FRICTION (KPA.)
WD27LC
N= 301
N= 323
N= 343
N= 383
N= 395
30.
20.
10.
-10.
-20.
-.5
-.4
-.3
-.2
-.1
.0
.1
.2
.3
.4
TOTAL PILE DEFLECTION (MM)

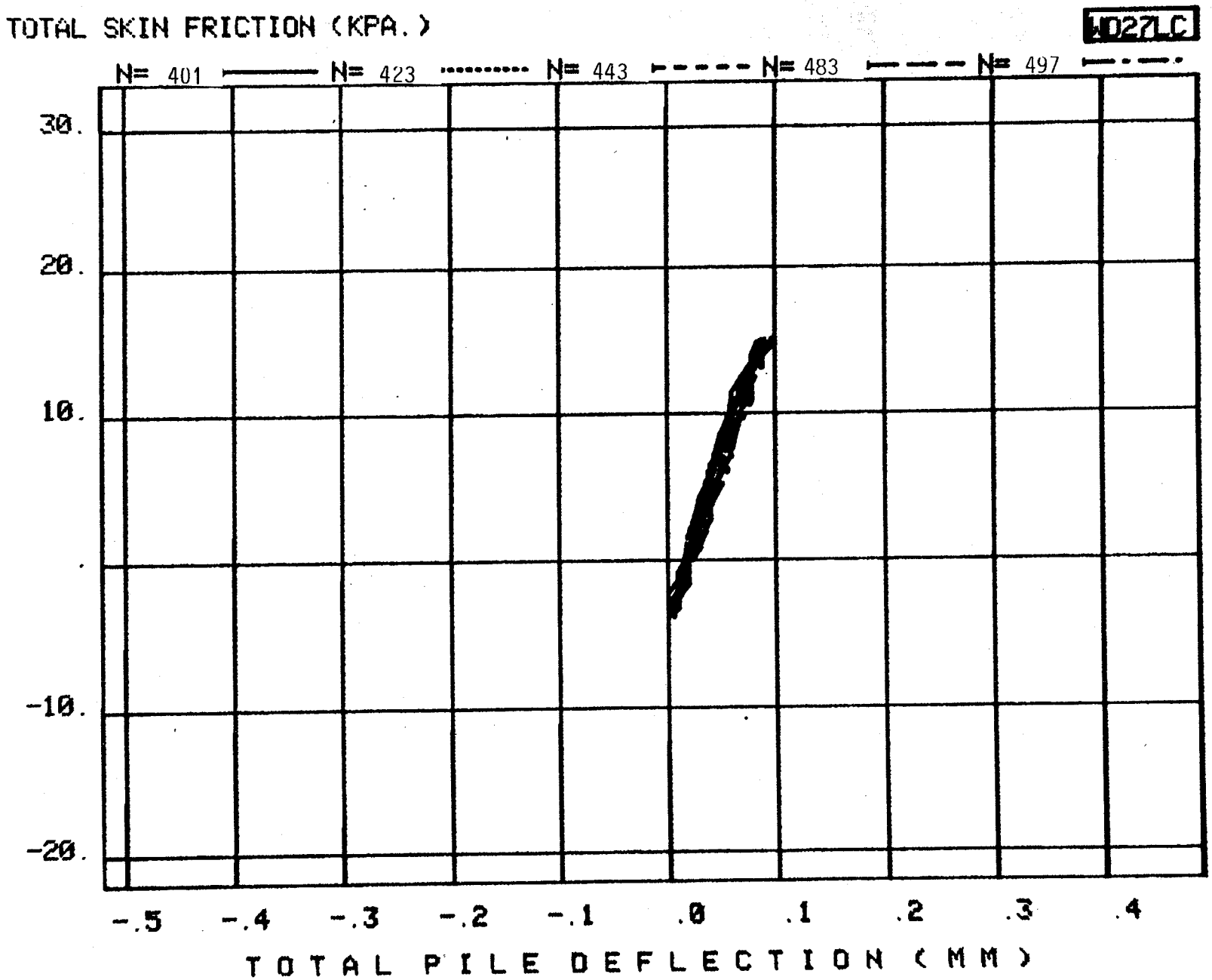
TOTAL SKIN FRICTION (KPA.)
WD27LC
N= 401
N= 423
N= 443
N= 483
N= 497
30.
20.
10.
-10.
-20.
-.5
-.4
-.3
-.2
-.1
.0
.1
.2
.3
.4
TOTAL PILE DEFLECTION (MM)

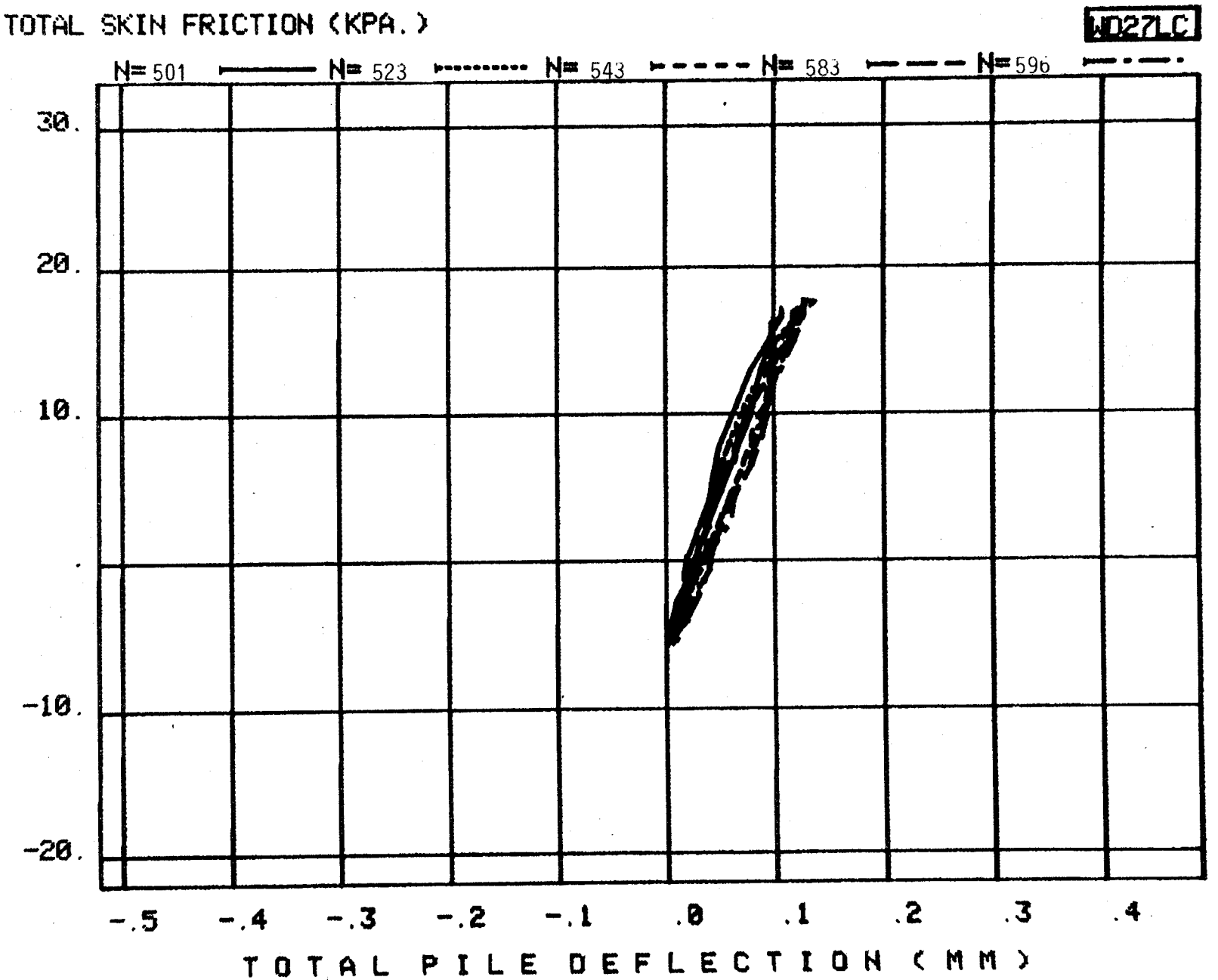
TOTAL SKIN FRICTION (KPA.)
WD27LC
N= 501
N= 523
N= 543
N= 583
N= 596
30.
20.
10.
-10.
-20.
-.5
-.4
-.3
-.2
-.1
.0
.1
.2
.3
.4
TOTAL PILE DEFLECTION (MM)

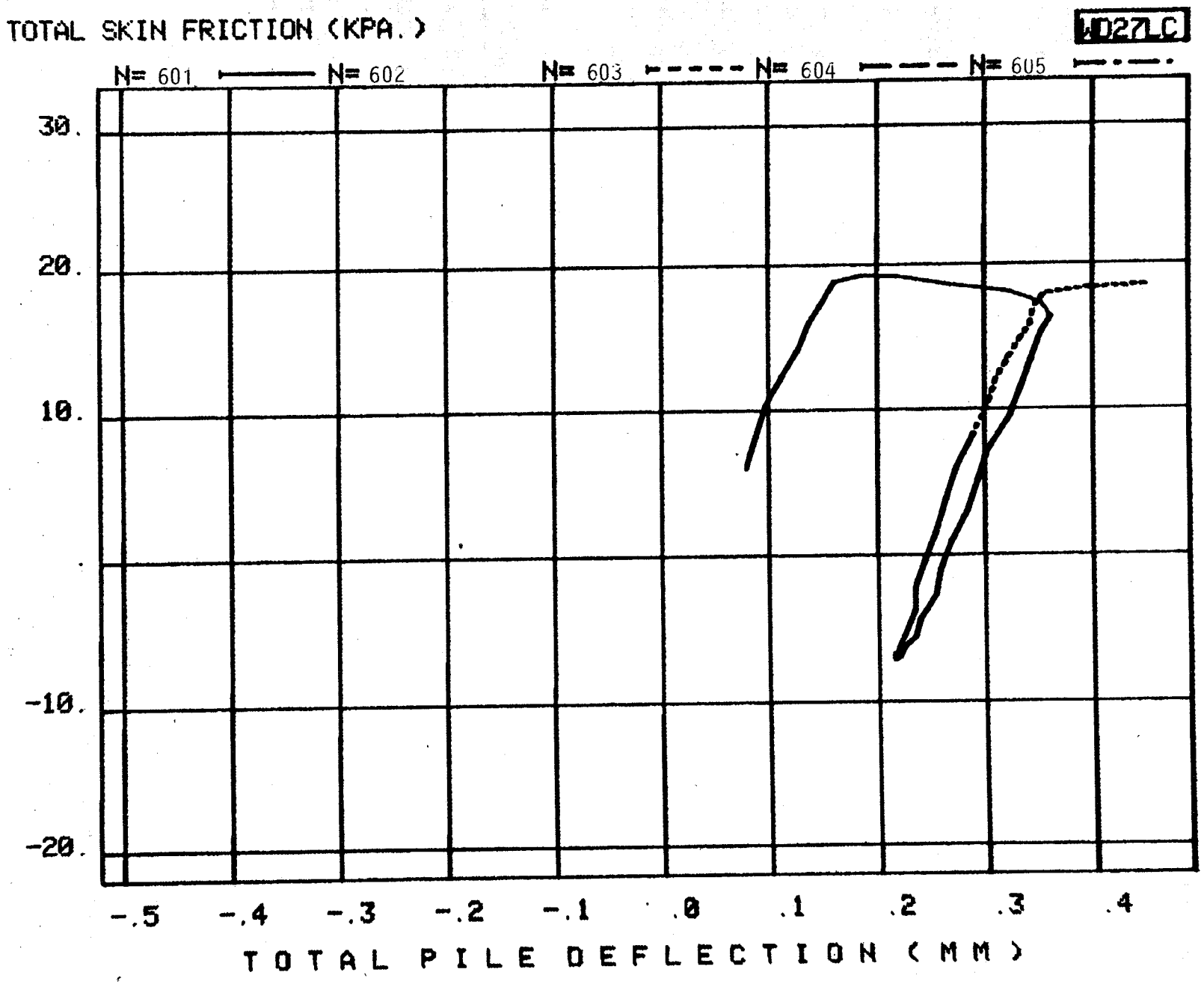
TOTAL SKIN FRICTION (KPA.)
WD27LC
N= 601
N= 602
N= 603
N= 604
N= 605
30.
20.
10.
-10.
-20.
-.5
-.4
-.3
-.2
-.1
.0
.1
.2
.3
.4
TOTAL PILE DEFLECTION (MM)

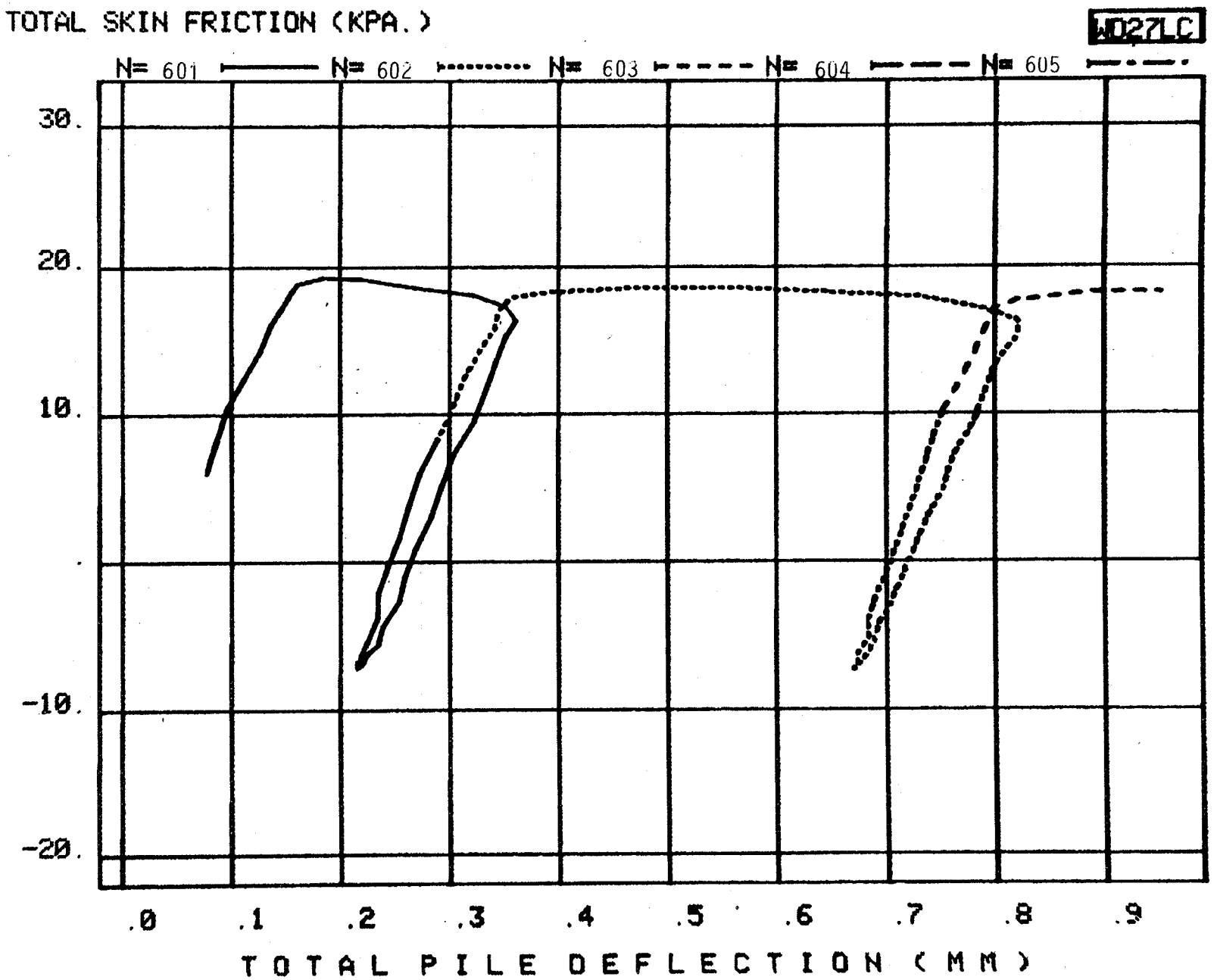
TOTAL SKIN FRICTION (KPA.)
WD27LC
N= 601
N= 602
N= 603
N= 604
N= 605
30.
20.
10.
-10.
-20.
.0
.1
.2
.3
.4
.5
.6
.7
.8
.9
TOTAL PILE DEFLECTION (MM)

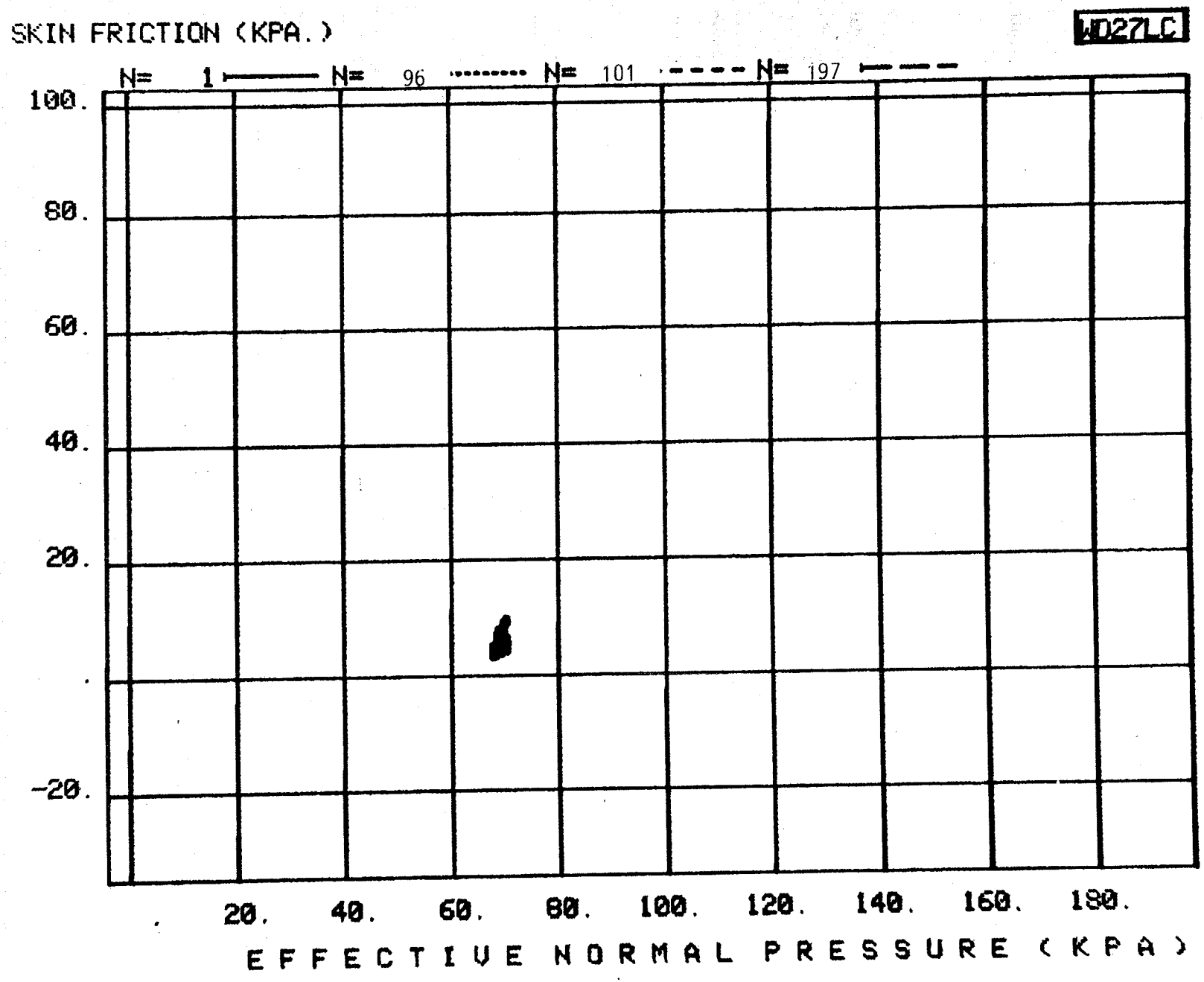
SKIN FRICTION (KPA.)
WD27LC
N= 1
N= 96
N= 101
N= 197
100.
80.
60.
40.
20.
-20.
20.
40.
60.
80.
100.
120.
140.
160.
180.
EFFECTIVE NORMAL PRESSURE (KPA)

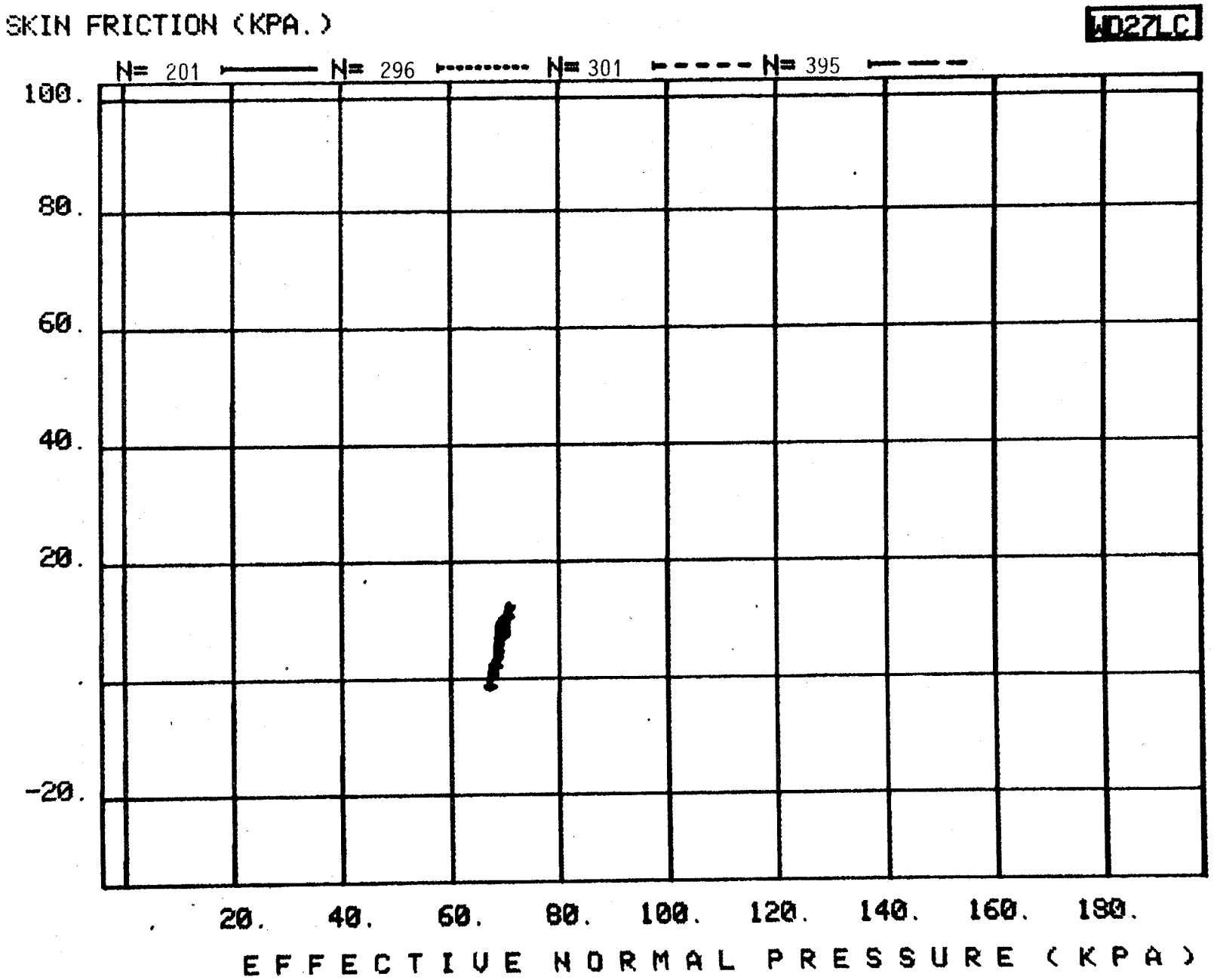
SKIN FRICTION (KPA.)
WD27LC
N= 201
N= 296
N= 301
N= 395
100.
80.
60.
40.
20.
-20.
20.
40.
60.
80.
100.
120.
140.
160.
180.
EFFECTIVE NORMAL PRESSURE (KPA)

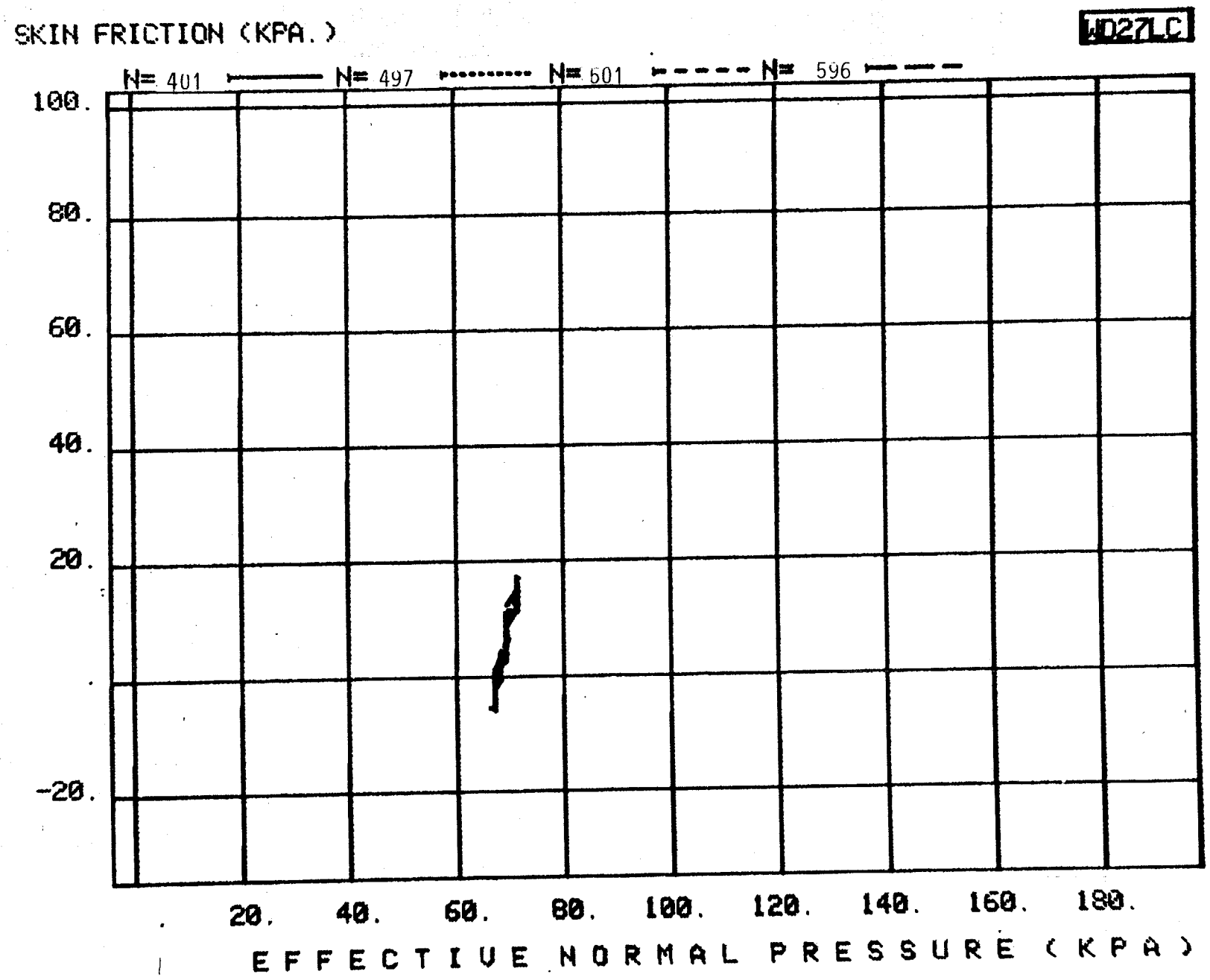
SKIN FRICTION (KPA.)
WD27LC
N= 401
N= 497
N= 601
N= 596
100.
80.
60.
40.
20.
-20.
20.
40.
60.
80.
100.
120.
140.
160.
180.
EFFECTIVE NORMAL PRESSURE (KPA)

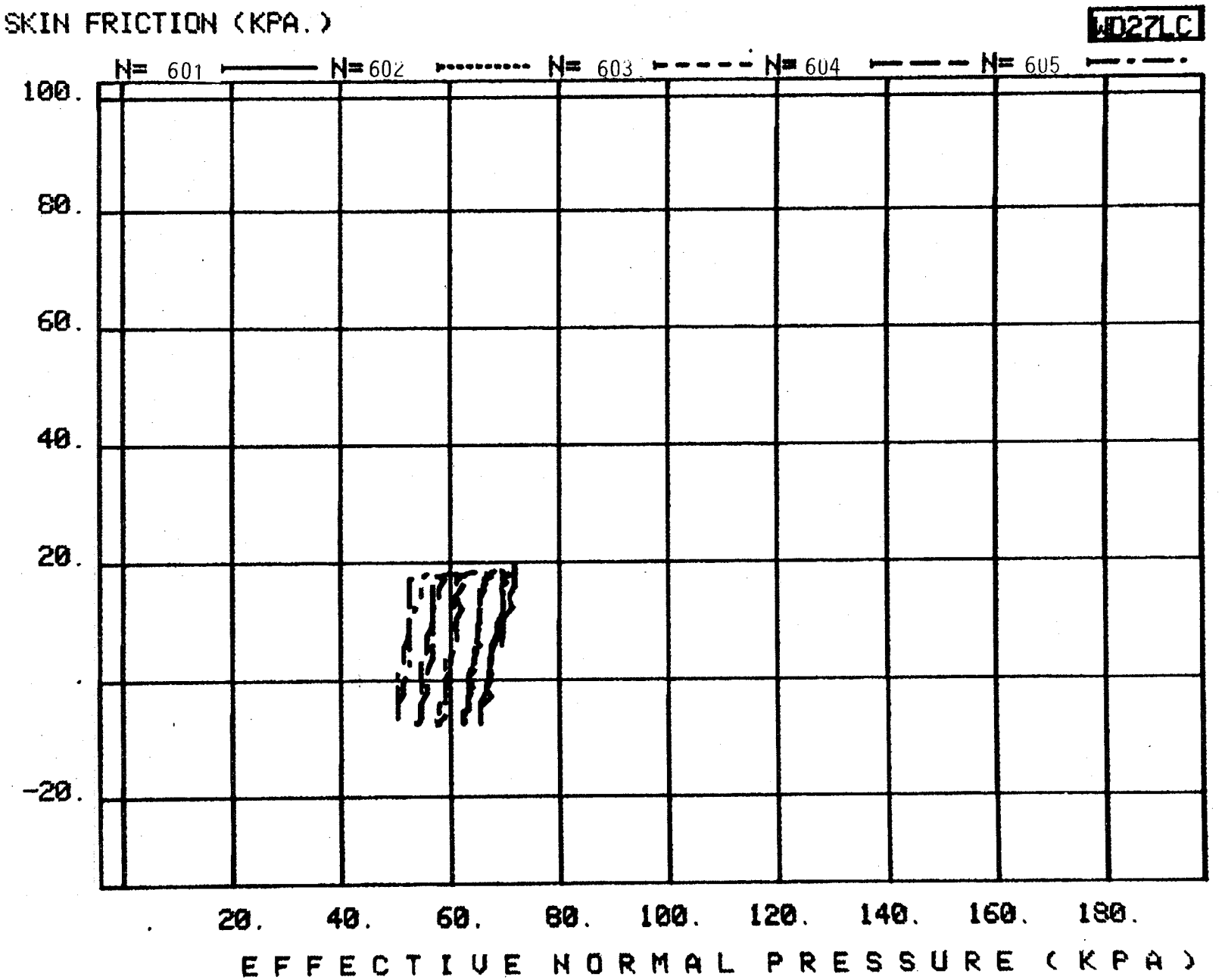
SKIN FRICTION (KPA.)
WD27LC
N= 601
N= 602
N= 603
N= 604
N= 605
100.
80.
60.
40.
20.
-20.
20.
40.
60.
80.
100.
120.
140.
160.
180.
EFFECTIVE NORMAL PRESSURE (KPA)

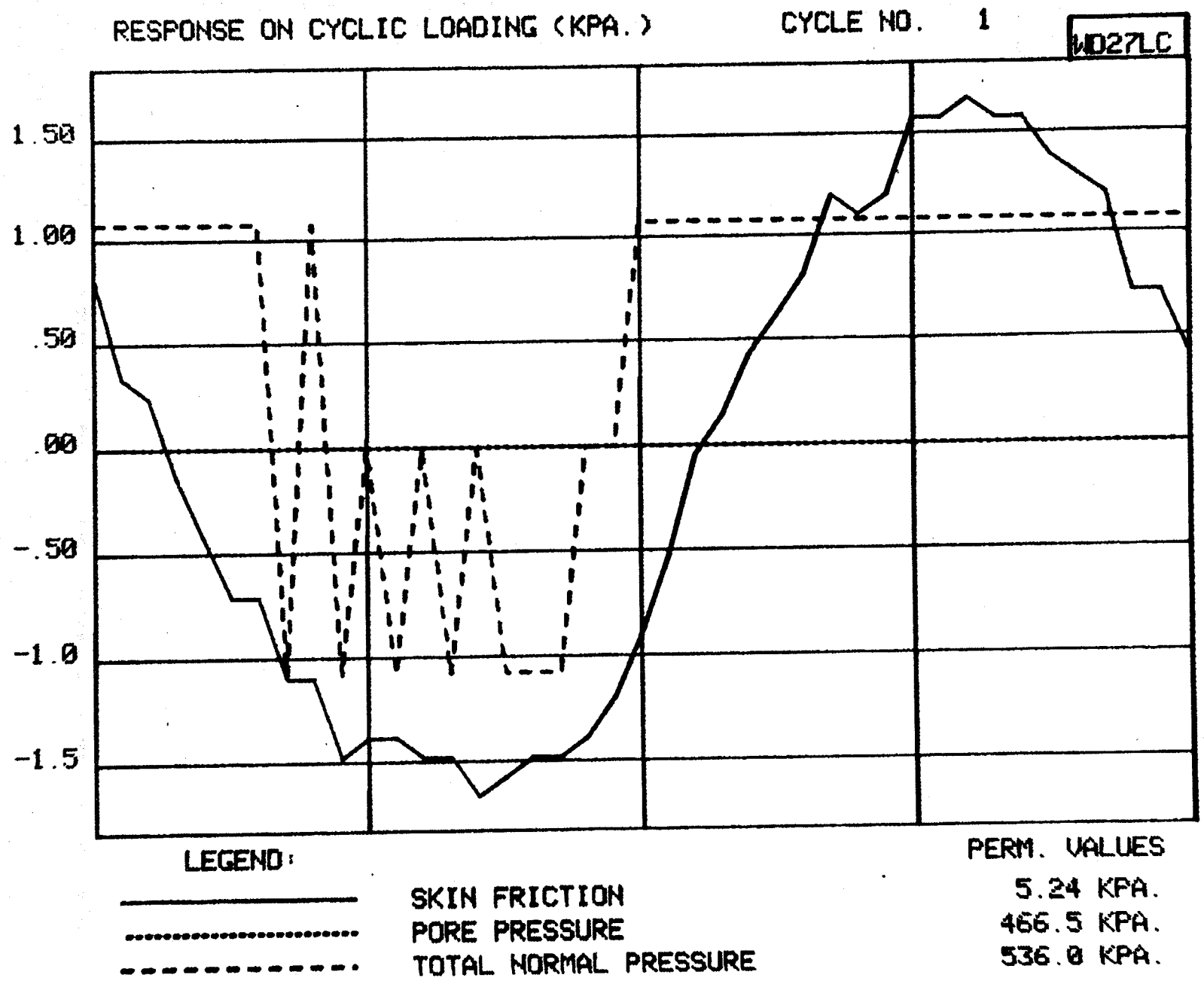
RESPONSE ON CYCLIC LOADING (KPA.)
CYCLE NO. 1
WD27LC
1.50
1.00
.50
.00
-.50
-1.0
-1.5
LEGEND:
SKIN FRICTION
PORE PRESSURE
TOTAL NORMAL PRESSURE
PERM. VALUES
5.24 KPA.
466.5 KPA.
536.0 KPA.

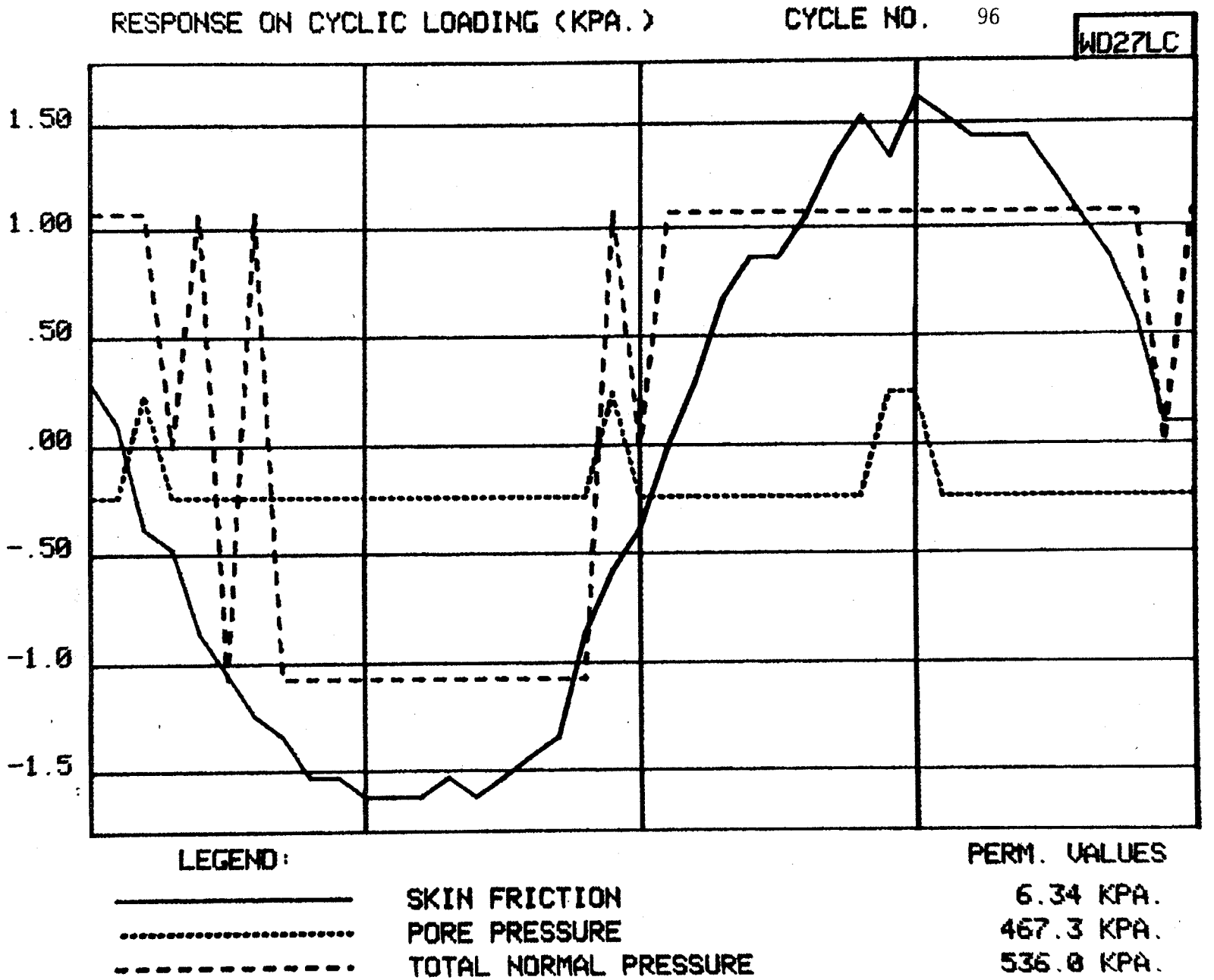
RESPONSE ON CYCLIC LOADING (KPA.)
CYCLE NO. 96
WD27LC
1.50
1.00
.50
.00
-.50
-1.0
-1.5
LEGEND:
SKIN FRICTION
PORE PRESSURE
TOTAL NORMAL PRESSURE
PERM. VALUES
6.34 KPA.
467.3 KPA.
536.0 KPA.

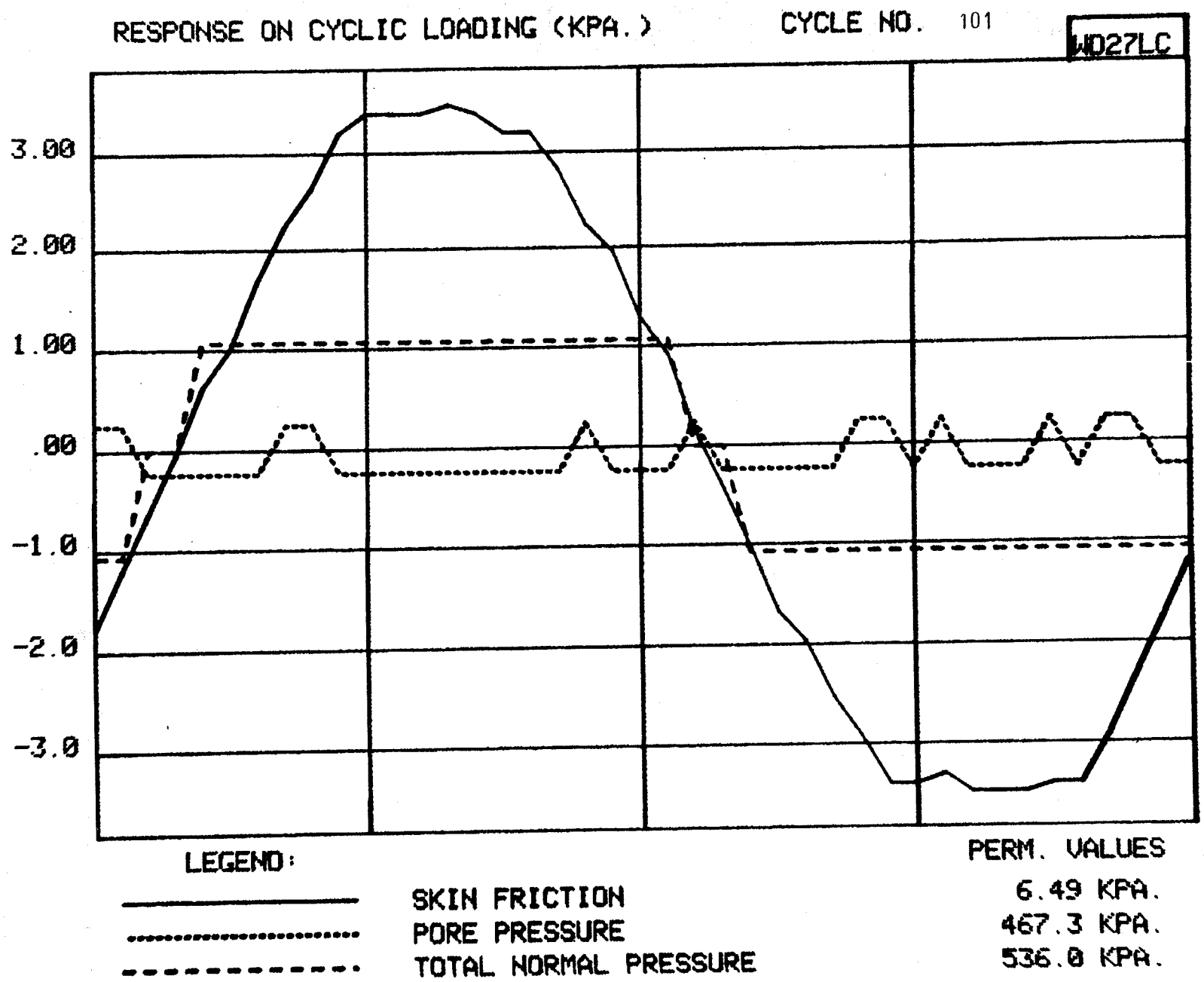
RESPONSE ON CYCLIC LOADING (KPA.)
CYCLE NO. 101
WD27LC
3.00
2.00
1.00
.00
-1.0
-2.0
-3.0
LEGEND:
SKIN FRICTION
PORE PRESSURE
TOTAL NORMAL PRESSURE
PERM. VALUES
6.49 KPA.
467.3 KPA.
536.0 KPA.

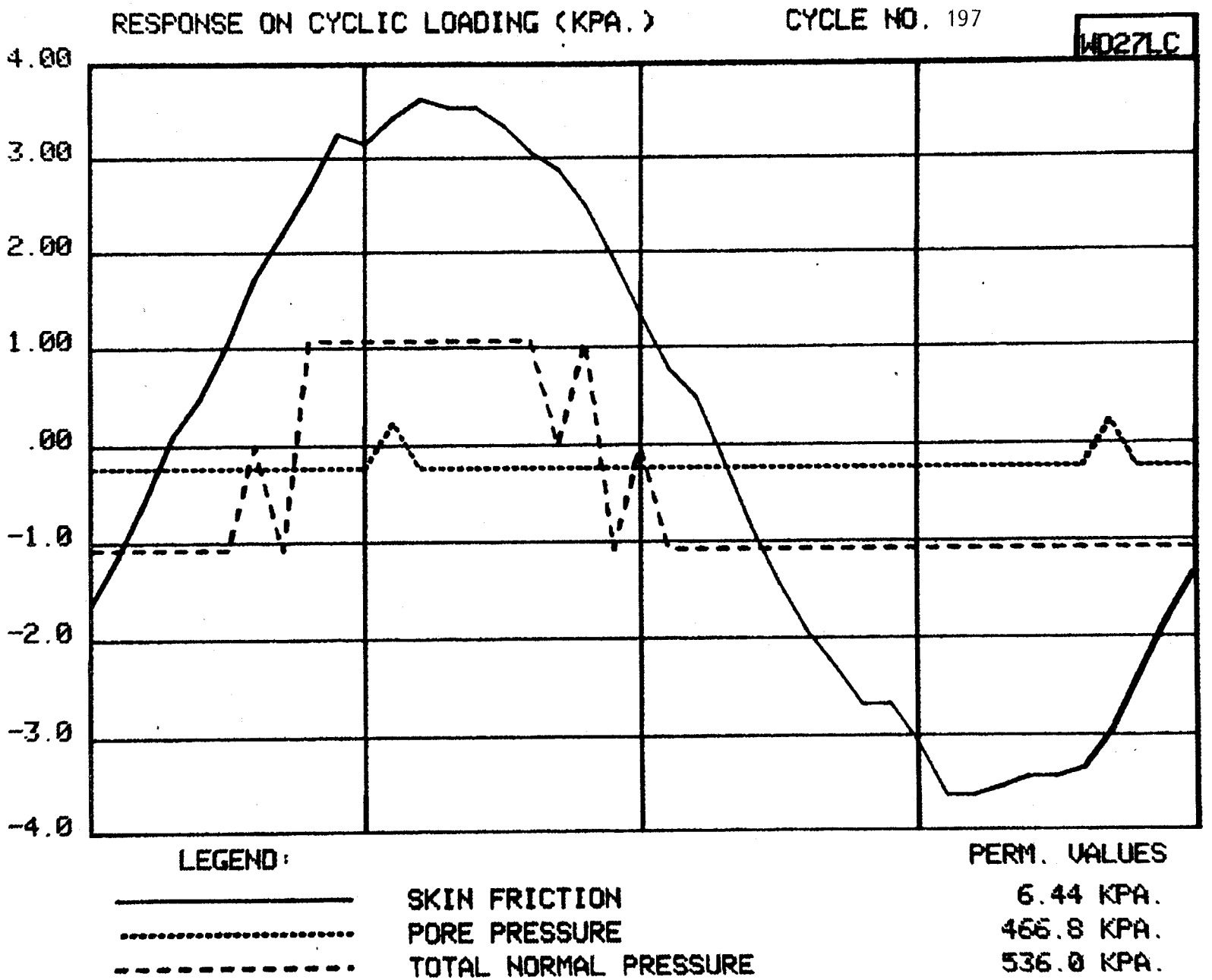
RESPONSE ON CYCLIC LOADING (KPA.)
CYCLE NO. 197
WD27LC
4.00
3.00
2.00
1.00
.00
-1.0
-2.0
-3.0
-4.0
LEGEND:
SKIN FRICTION
PORE PRESSURE
TOTAL NORMAL PRESSURE
PERM. VALUES
6.44 KPA.
466.8 KPA.
536.0 KPA.

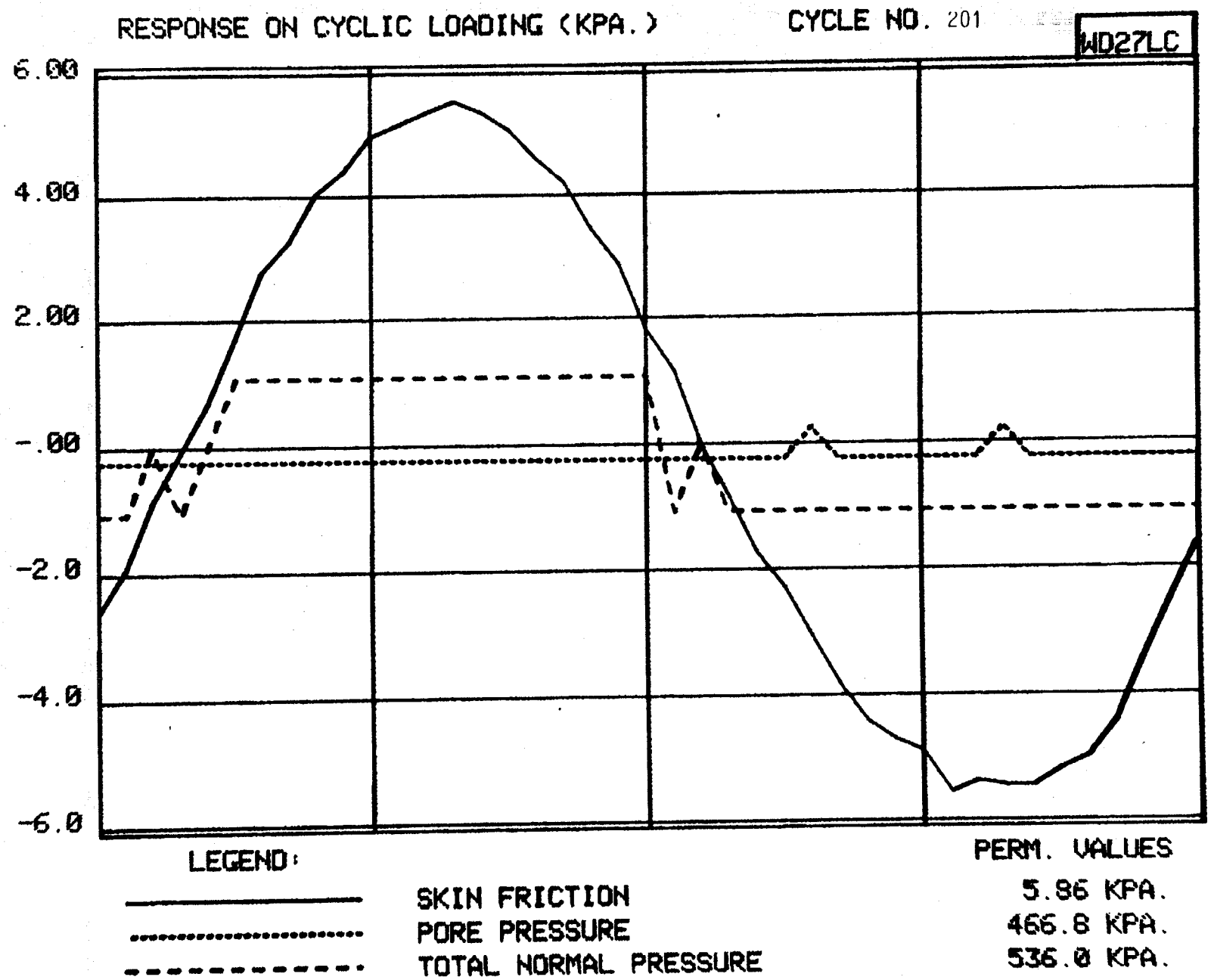
RESPONSE ON CYCLIC LOADING (KPA.)
CYCLE NO. 201
WD27LC
6.00
4.00
2.00
-.00
-2.0
-4.0
-6.0
LEGEND:
SKIN FRICTION
PORE PRESSURE
TOTAL NORMAL PRESSURE
PERM. VALUES
5.86 KPA.
466.8 KPA.
536.0 KPA.

RESPONSE ON CYCLIC LOADING (KPA.) CYCLE NO. 296

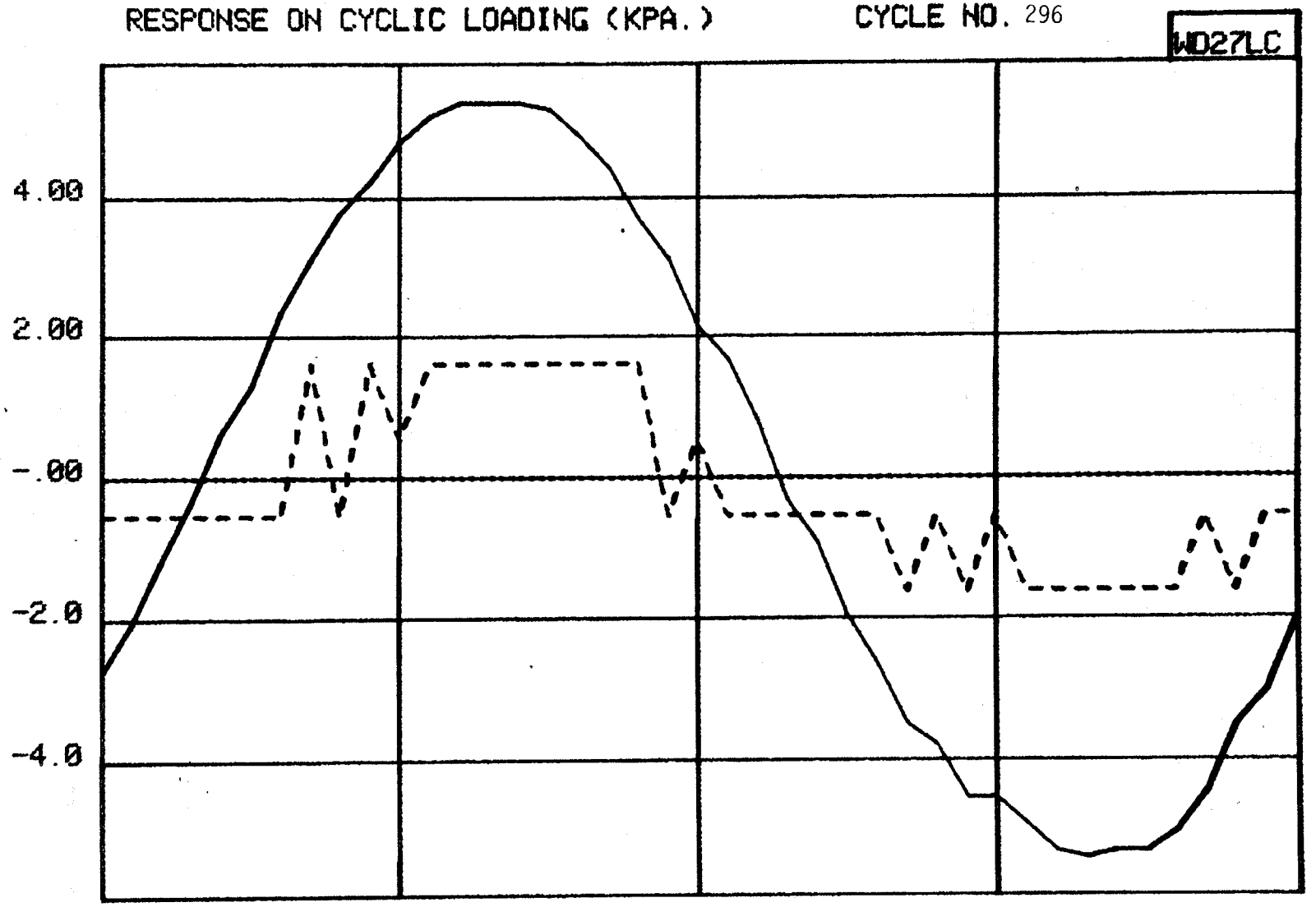

LEGEND:

		PERM. VALUES
———	SKIN FRICTION	5.82 KPA.
·····	PORE PRESSURE	466.5 KPA.
- - - -	TOTAL NORMAL PRESSURE	535.4 KPA.

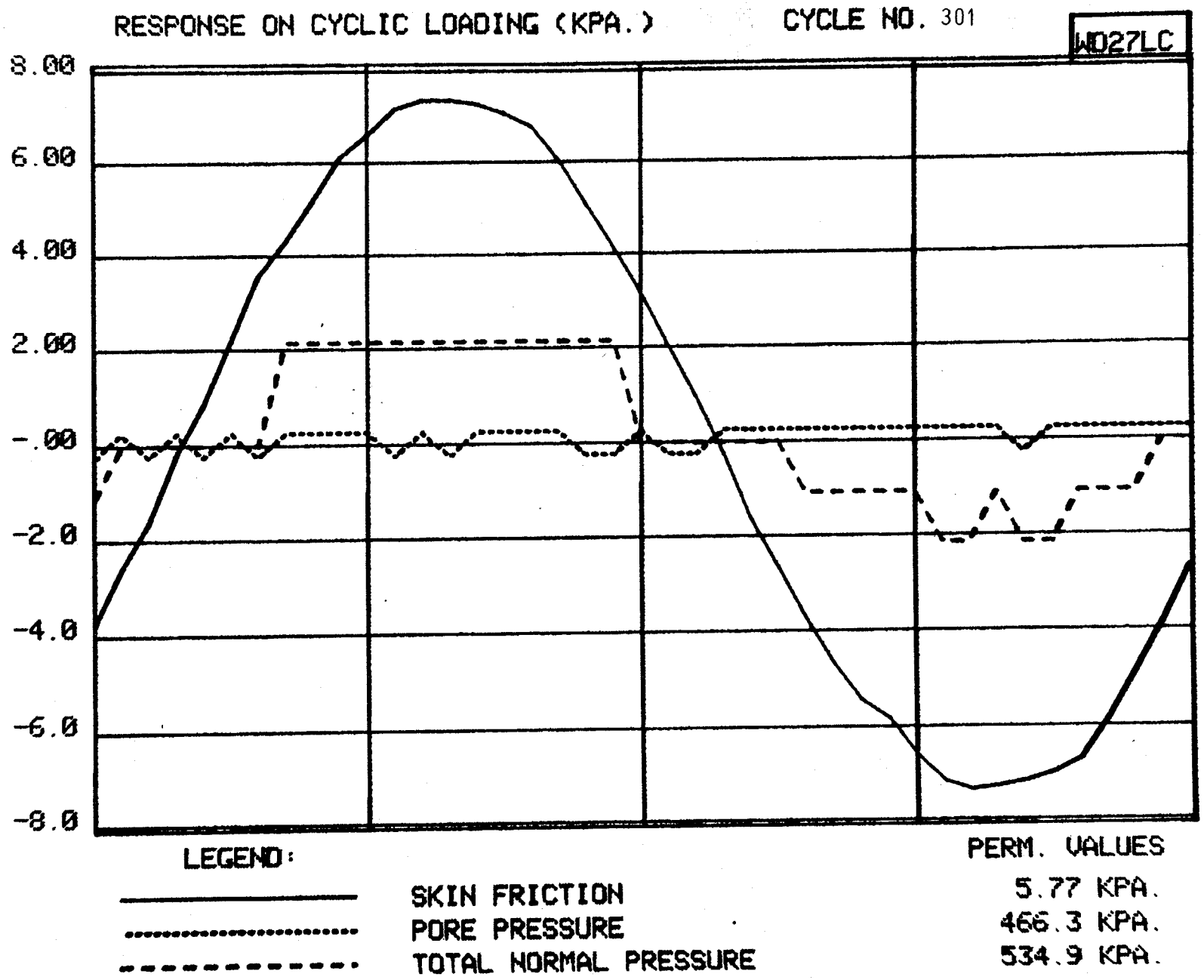
RESPONSE ON CYCLIC LOADING (KPA.)
CYCLE NO. 301
WD27LC
8.00
6.00
4.00
2.00
-.00
-2.0
-4.0
-6.0
-8.0
LEGEND:
SKIN FRICTION
PORE PRESSURE
TOTAL NORMAL PRESSURE
PERM. VALUES
5.77 KPA.
466.3 KPA.
534.9 KPA.

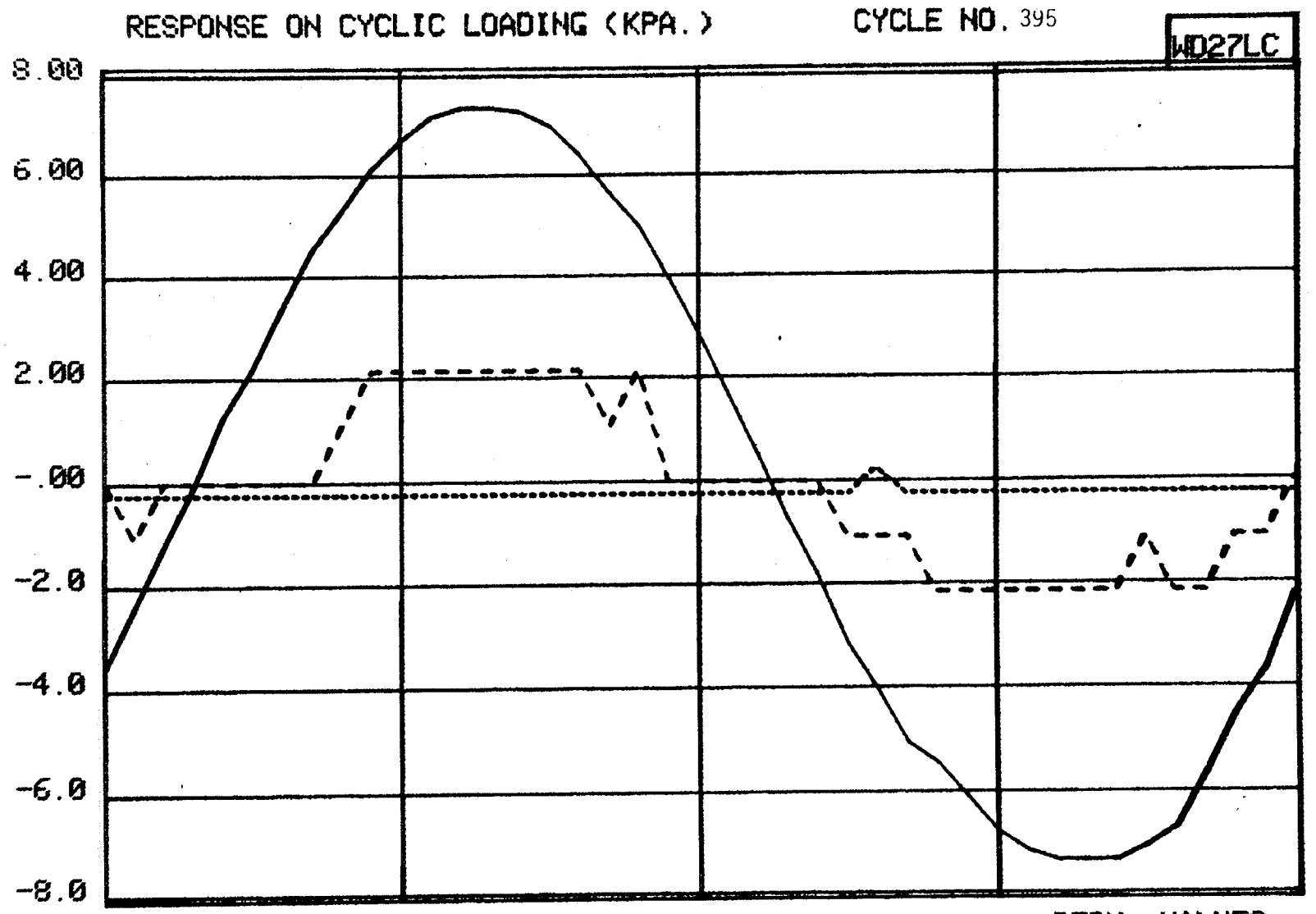

LEGEND:

		PERM. VALUES
———	SKIN FRICTION	5.77 KPA.
·····	PORE PRESSURE	465.8 KPA.
- - - -	TOTAL NORMAL PRESSURE	534.9 KPA.

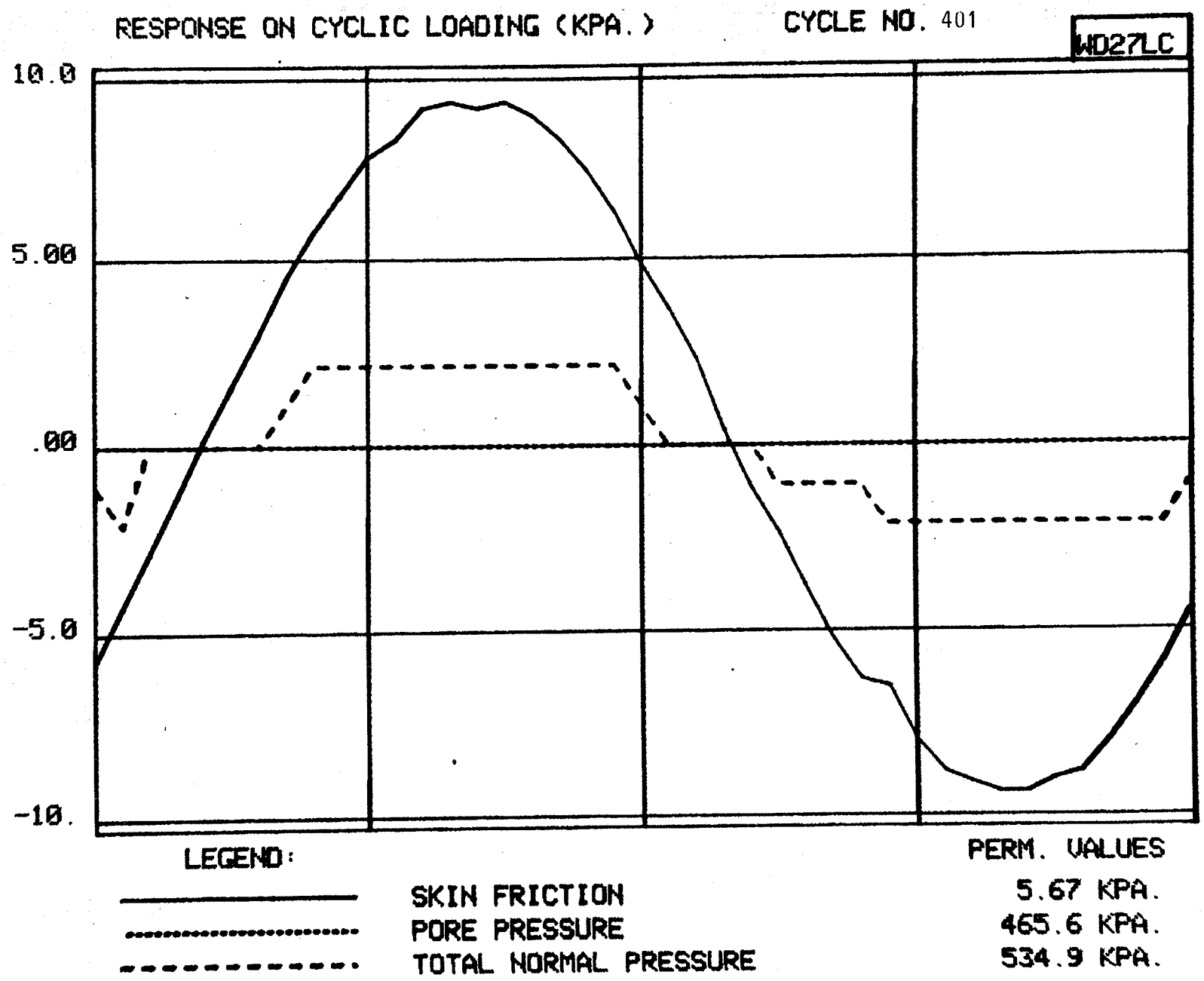
RESPONSE ON CYCLIC LOADING (KPA.)
CYCLE NO. 401
WD27LC
10.0
5.00
.00
-5.0
-10.
LEGEND:
SKIN FRICTION
PORE PRESSURE
TOTAL NORMAL PRESSURE
PERM. VALUES
5.67 KPA.
465.6 KPA.
534.9 KPA.

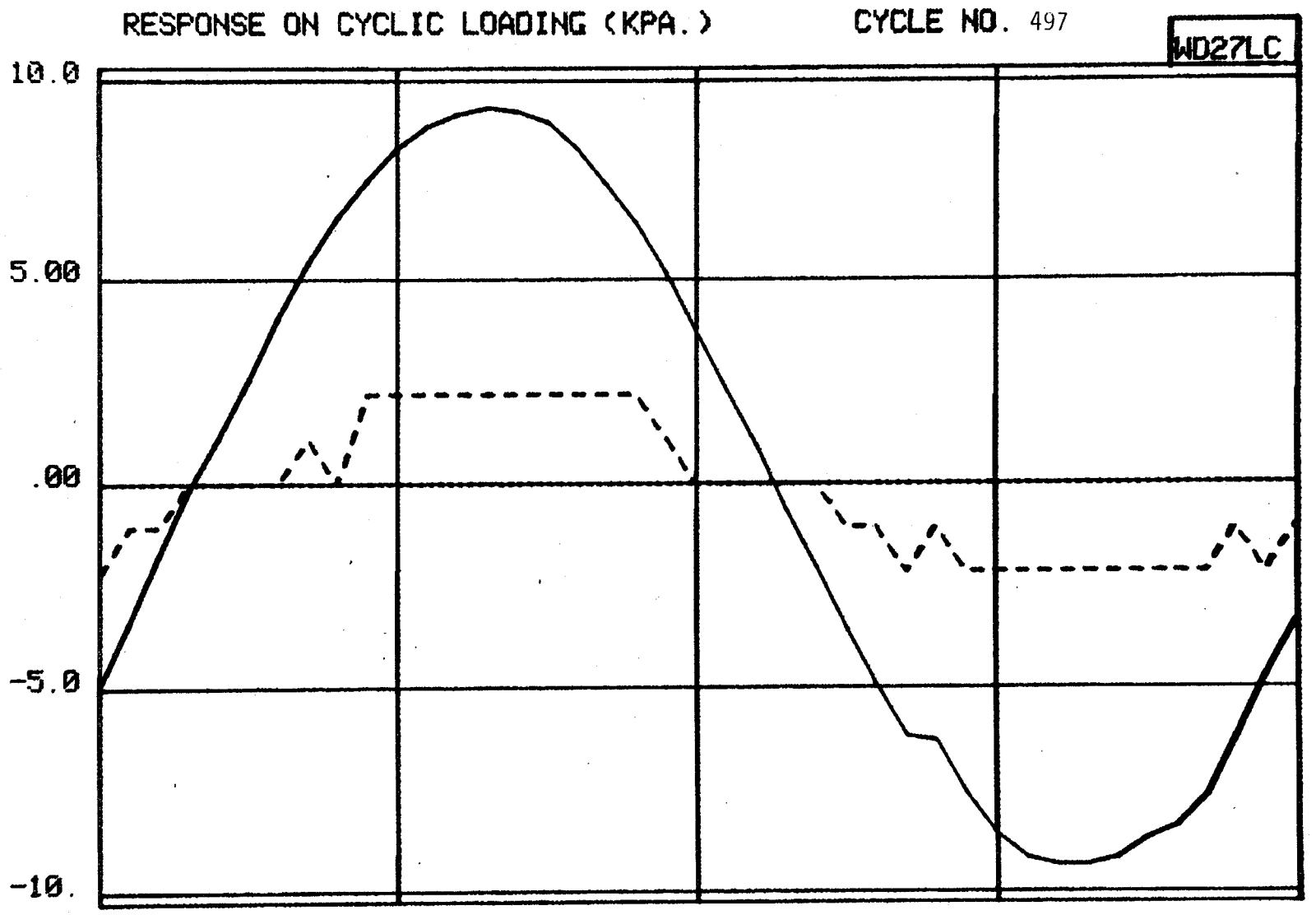
RESPONSE ON CYCLIC LOADING (KPA.)
CYCLE NO. 497
WD27LC
10.0
5.00
.00
-5.0
-10.
LEGEND:
SKIN FRICTION
PORE PRESSURE
TOTAL NORMAL PRESSURE
PERM. VALUES
5.82 KPA.
465.6 KPA.
534.9 KPA.

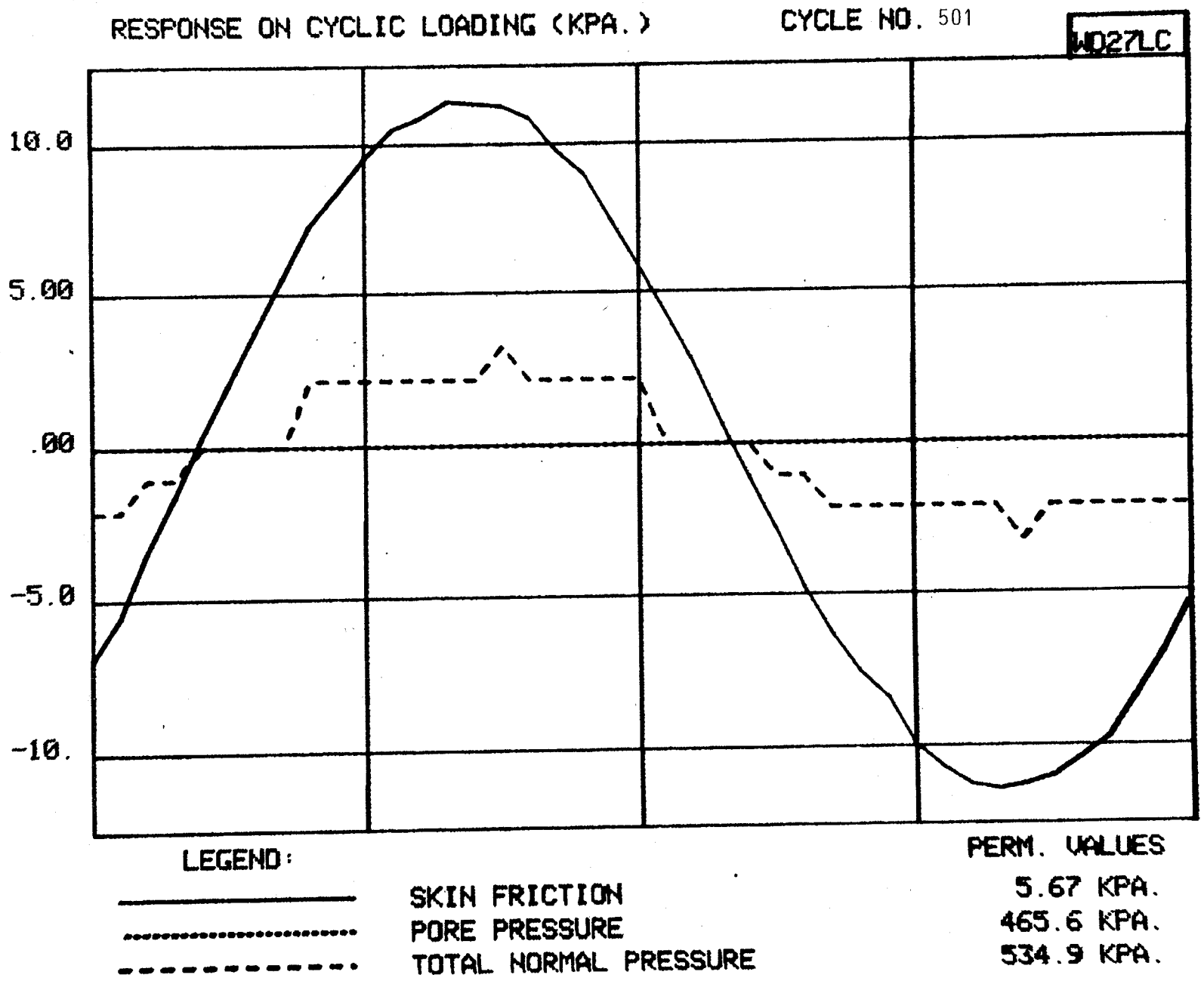
RESPONSE ON CYCLIC LOADING (KPA.)
CYCLE NO. 501
WD27LC
10.0
5.00
.00
-5.0
-10.
LEGEND:
SKIN FRICTION
PORE PRESSURE
TOTAL NORMAL PRESSURE
PERM. VALUES
5.67 KPA.
465.6 KPA.
534.9 KPA.

RESPONSE ON CYCLIC LOADING (KPA.) CYCLE NO. 596

WD27LC

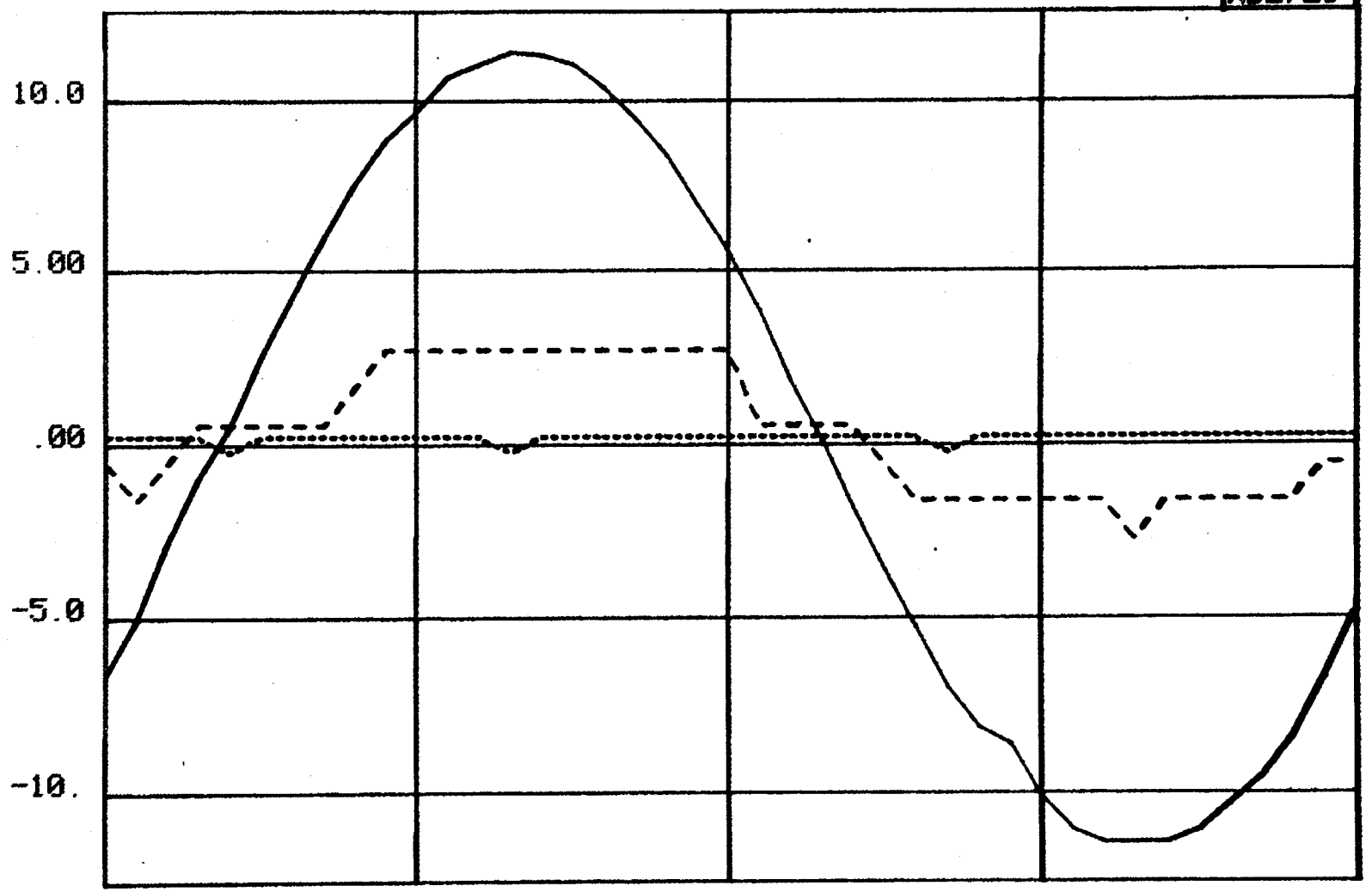

LEGEND:

		PERM. VALUES
———	SKIN FRICTION	6.25 KPA.
·····	PORE PRESSURE	465.4 KPA.
- - - -	TOTAL NORMAL PRESSURE	534.3 KPA.

RESPONSE ON CYCLIC LOADING (KPA.) CYCLE NO. 601

WD27LC

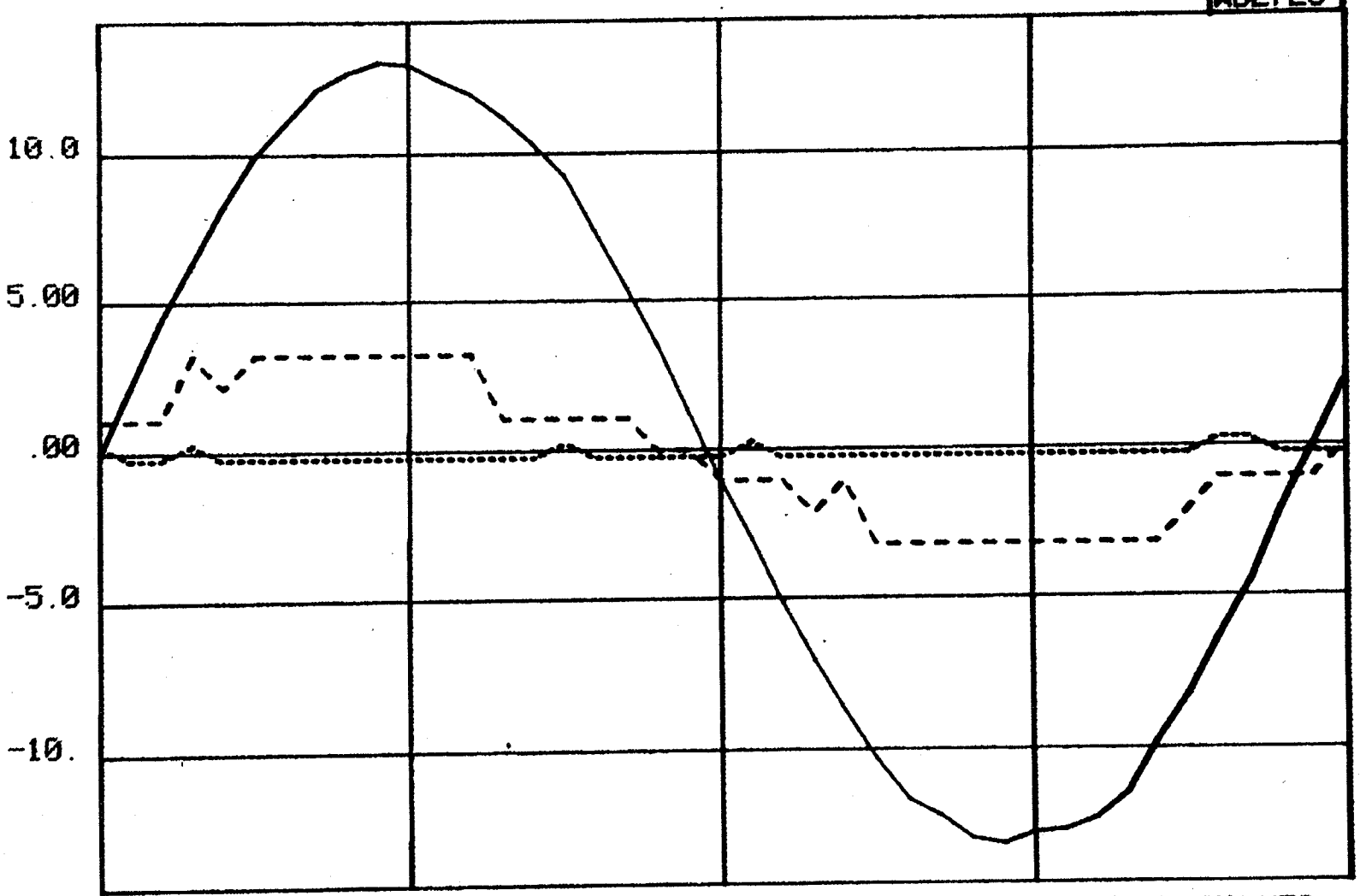

LEGEND:

		PERM. VALUES
———	SKIN FRICTION	6.05 KPA.
·····	PORE PRESSURE	465.4 KPA.
- - - -	TOTAL NORMAL PRESSURE	533.8 KPA.

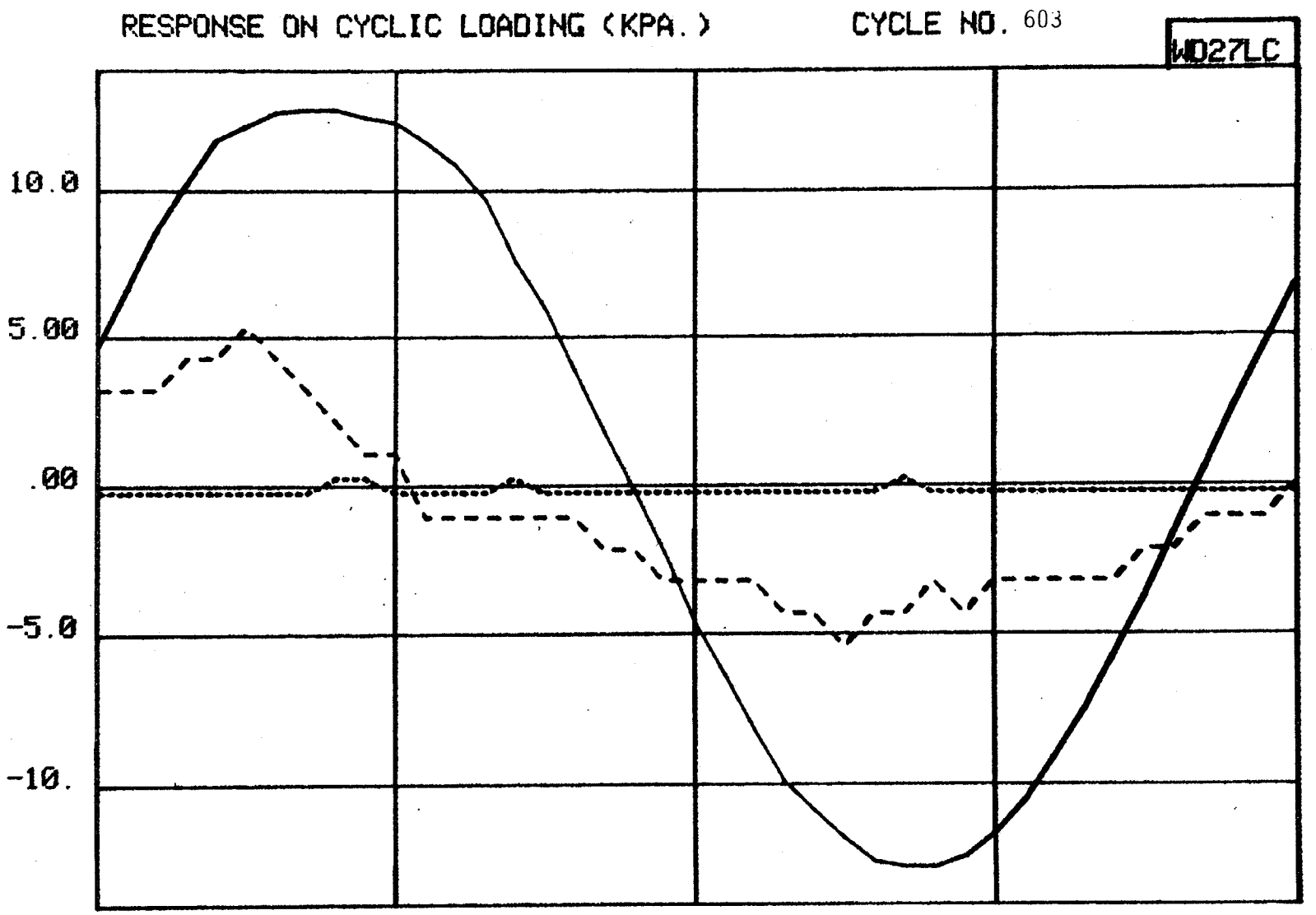

LEGEND:

		PERM. VALUES
———	SKIN FRICTION	5.48 KPA.
·····	PORE PRESSURE	465.4 KPA.
- - - -	TOTAL NORMAL PRESSURE	527.3 KPA.

RESPONSE ON CYCLIC LOADING (KPA.) CYCLE NO. 605

WD27LC

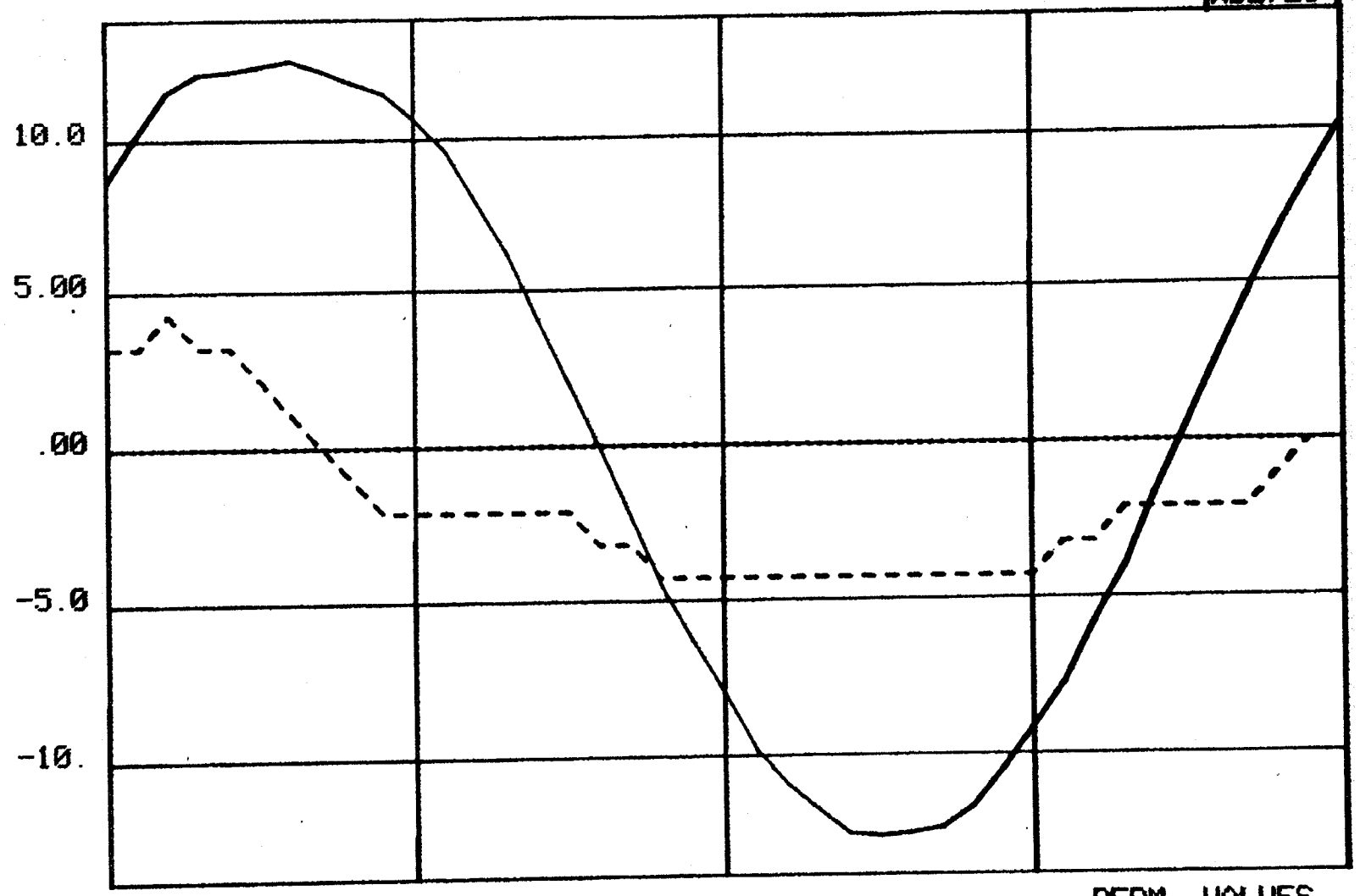

LEGEND:

SKIN FRICTION
PORE PRESSURE
TOTAL NORMAL PRESSURE

PERM. VALUES

5.43 KPA.
465.1 KPA.
519.8 KPA.

Appendix DB

Plotted Results from WD27SC

Figures DB-1 through DB-7

Skin Friction vs Deflection, Selected Cycles

Figures DB-8 through DB-11

Skin Friction vs Eff. Normal Pressure, Selected Cycl.

Figures DB-12 through DB-24

Skin Friction, Pore and Total Pressure, Selected Cycles

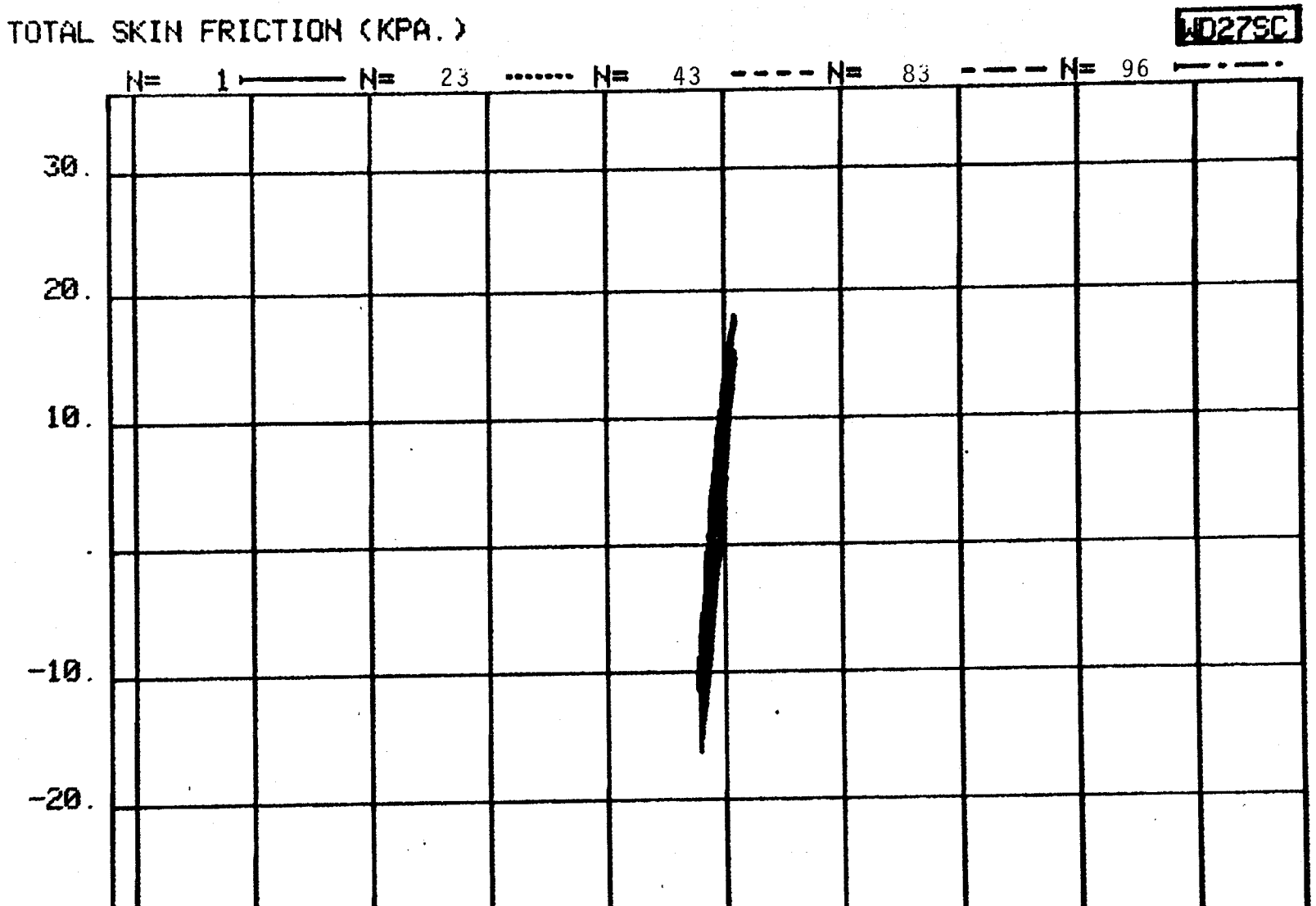
TOTAL SKIN FRICTION (KPA.)
WD27SC
N= 1
N= 23
N= 43
N= 83
N= 96
30.
20.
10.
-10.
-20.
-30.
-2.5
-2.0
-1.5
-1.0
-.5
.0
.5
1.0
1.5
2.0
TOTAL PILE DEFLECTION (MM)

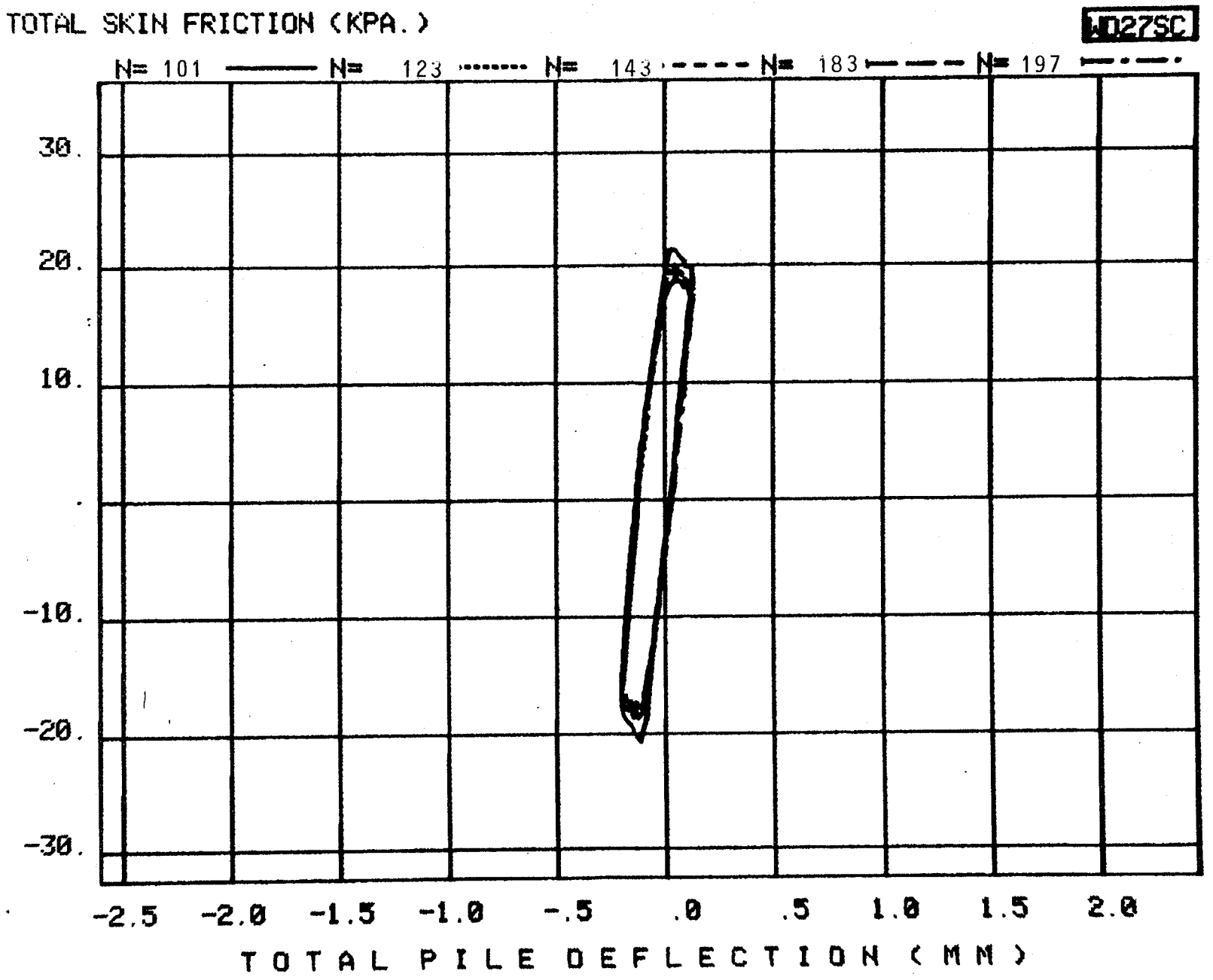
TOTAL SKIN FRICTION (KPA.)
WD27SC
N= 101
N= 123
N= 143
N= 183
N= 197
30.
20.
10.
-10.
-20.
-30.
-2.5
-2.0
-1.5
-1.0
-.5
.0
.5
1.0
1.5
2.0
TOTAL PILE DEFLECTION (MM)

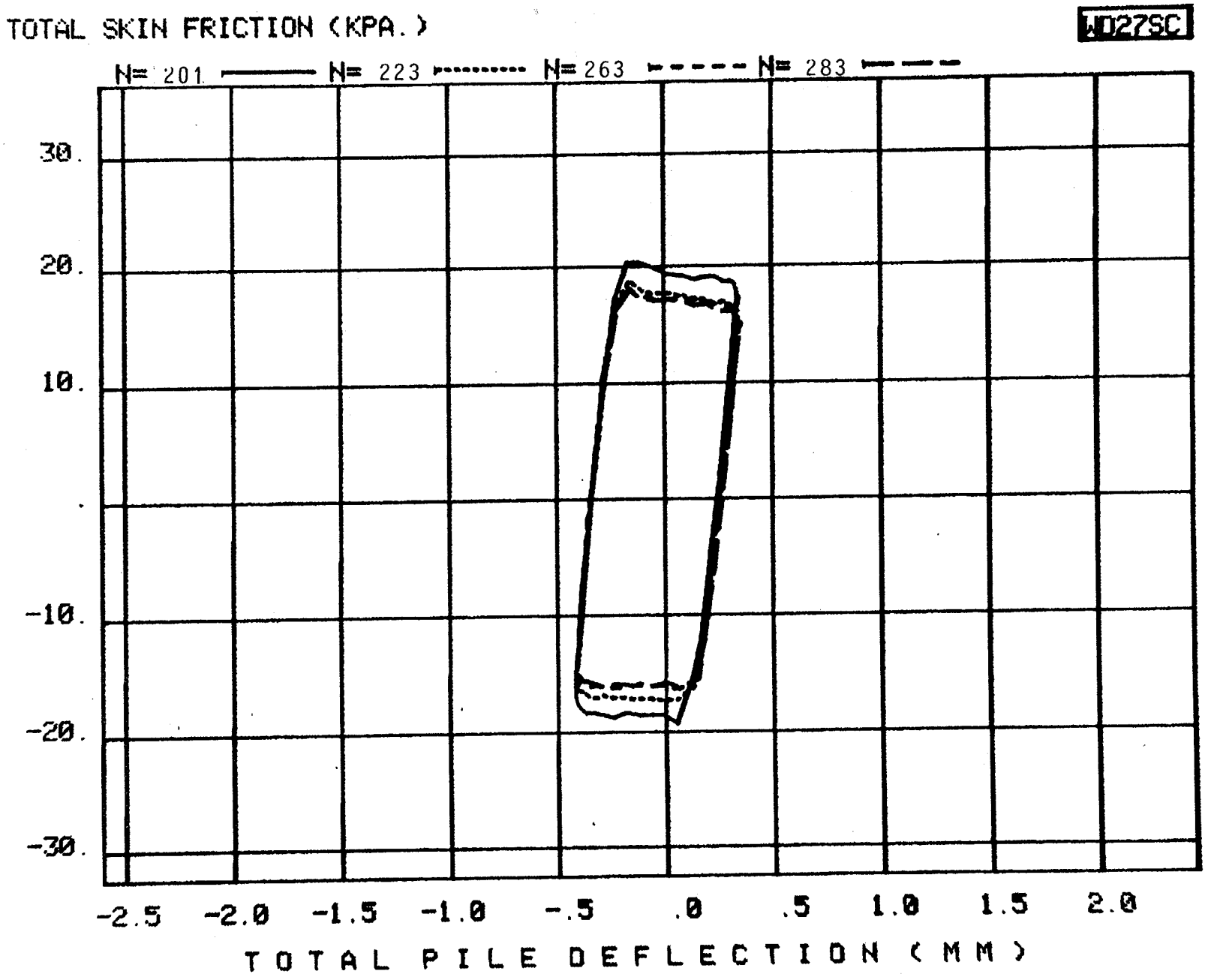
TOTAL SKIN FRICTION (KPA.)
WD27SC
N= 201
N= 223
N= 263
N= 283
30.
20.
10.
-10.
-20.
-30.
-2.5
-2.0
-1.5
-1.0
-.5
.0
.5
1.0
1.5
2.0
TOTAL PILE DEFLECTION (MM)

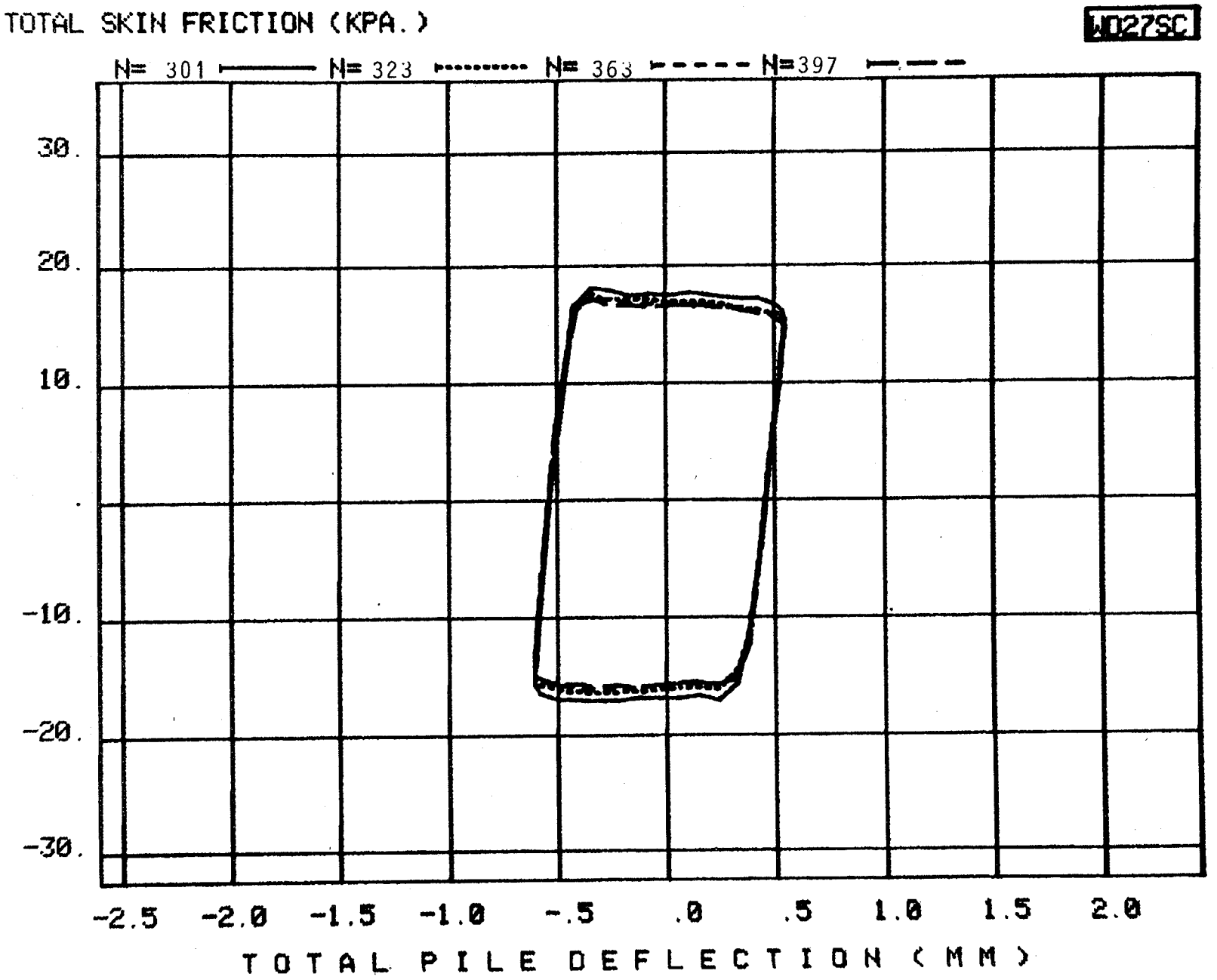
TOTAL SKIN FRICTION (KPA.)
WD27SC
N= 301
N= 323
N= 363
N=397
30.
20.
10.
-10.
-20.
-30.
-2.5
-2.0
-1.5
-1.0
-.5
.0
.5
1.0
1.5
2.0
TOTAL PILE DEFLECTION (MM)

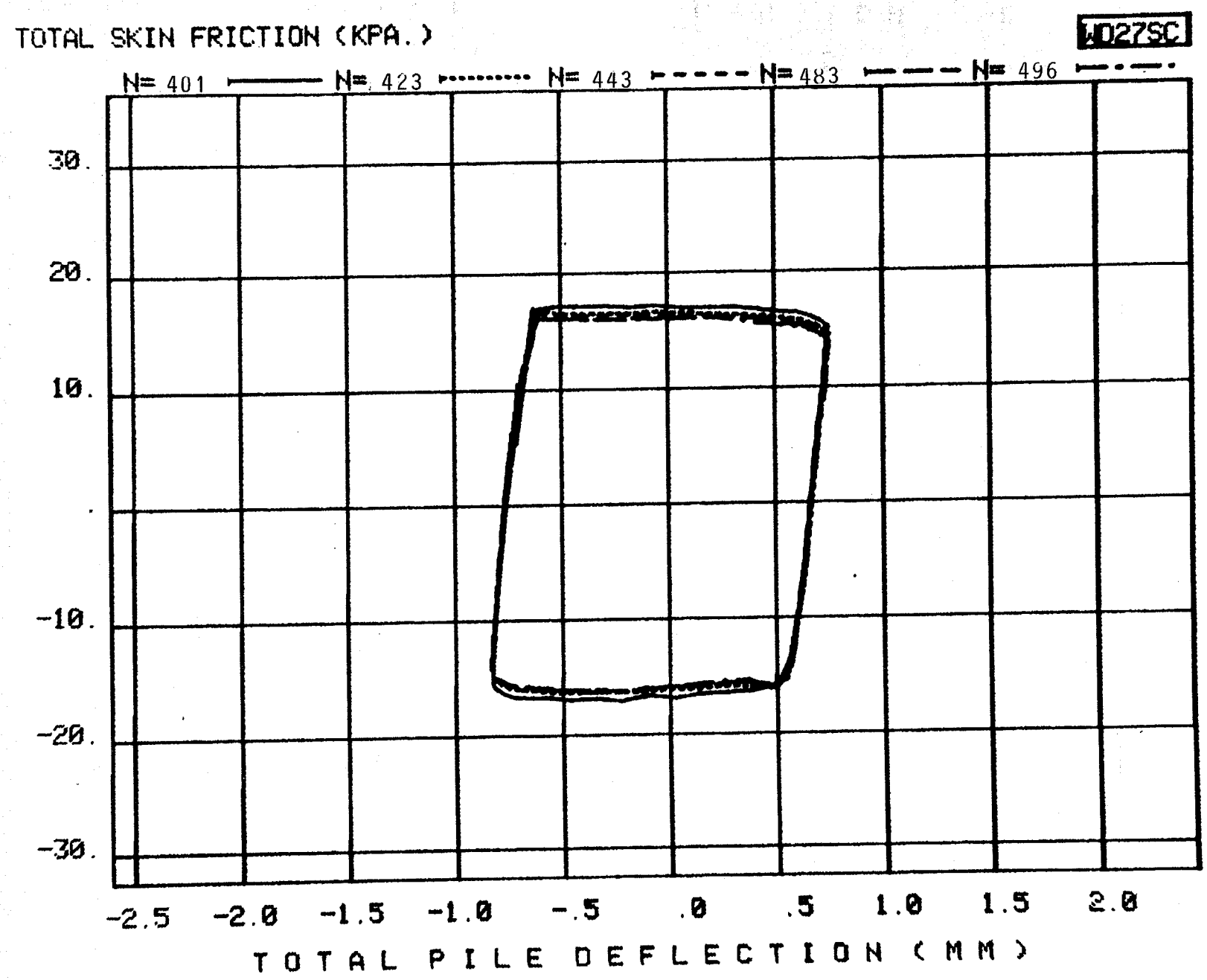
TOTAL SKIN FRICTION (KPA.)
WD27SC
N= 401
N= 423
N= 443
N= 483
N= 496
30.
20.
10.
-10.
-20.
-30.
-2.5
-2.0
-1.5
-1.0
-.5
.0
.5
1.0
1.5
2.0
TOTAL PILE DEFLECTION (MM)

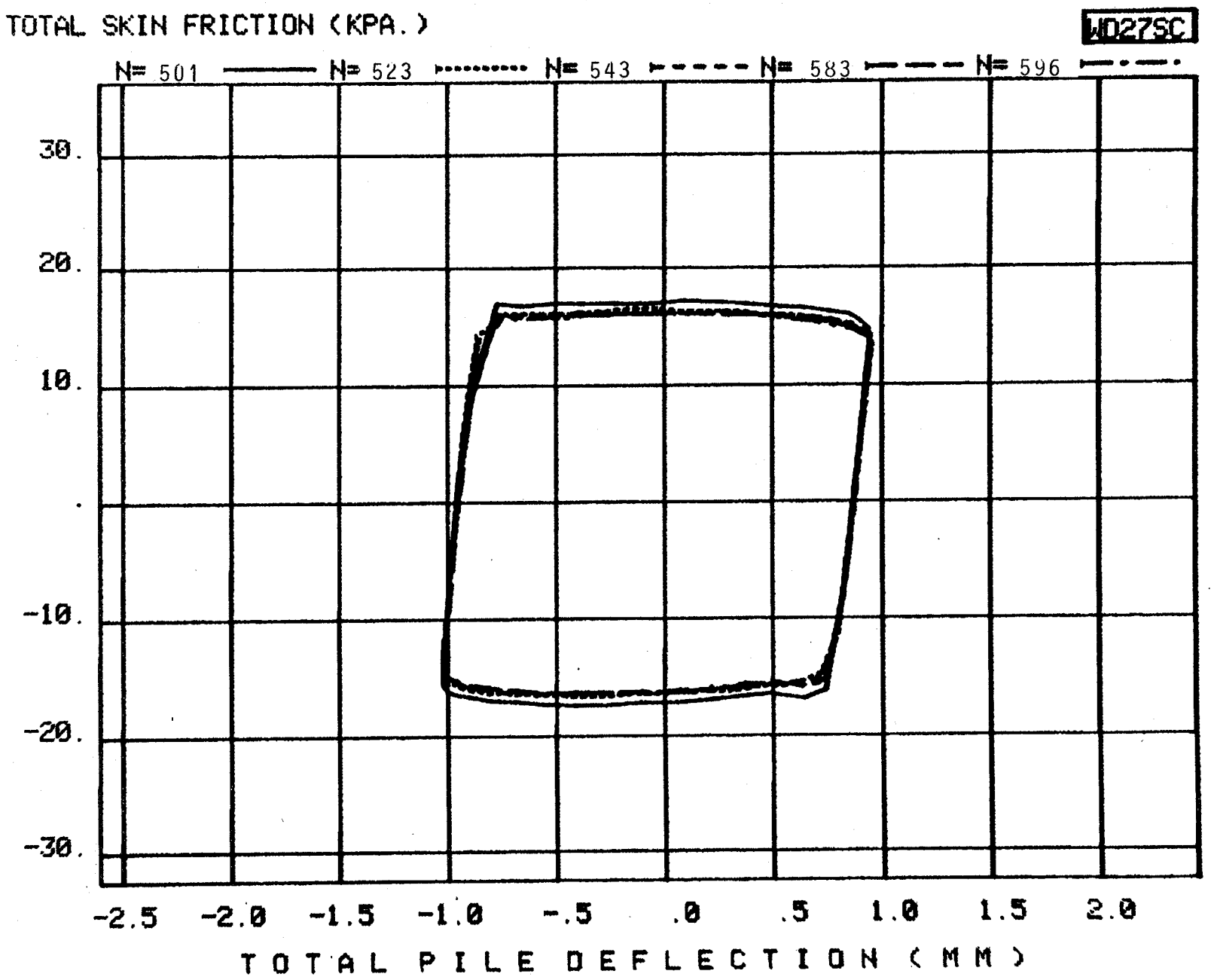
TOTAL SKIN FRICTION (KPA.)
WD27SC
N= 501
N= 523
N= 543
N= 583
N= 596
30.
20.
10.
-10.
-20.
-30.
-2.5
-2.0
-1.5
-1.0
-.5
.0
.5
1.0
1.5
2.0
TOTAL PILE DEFLECTION (MM)

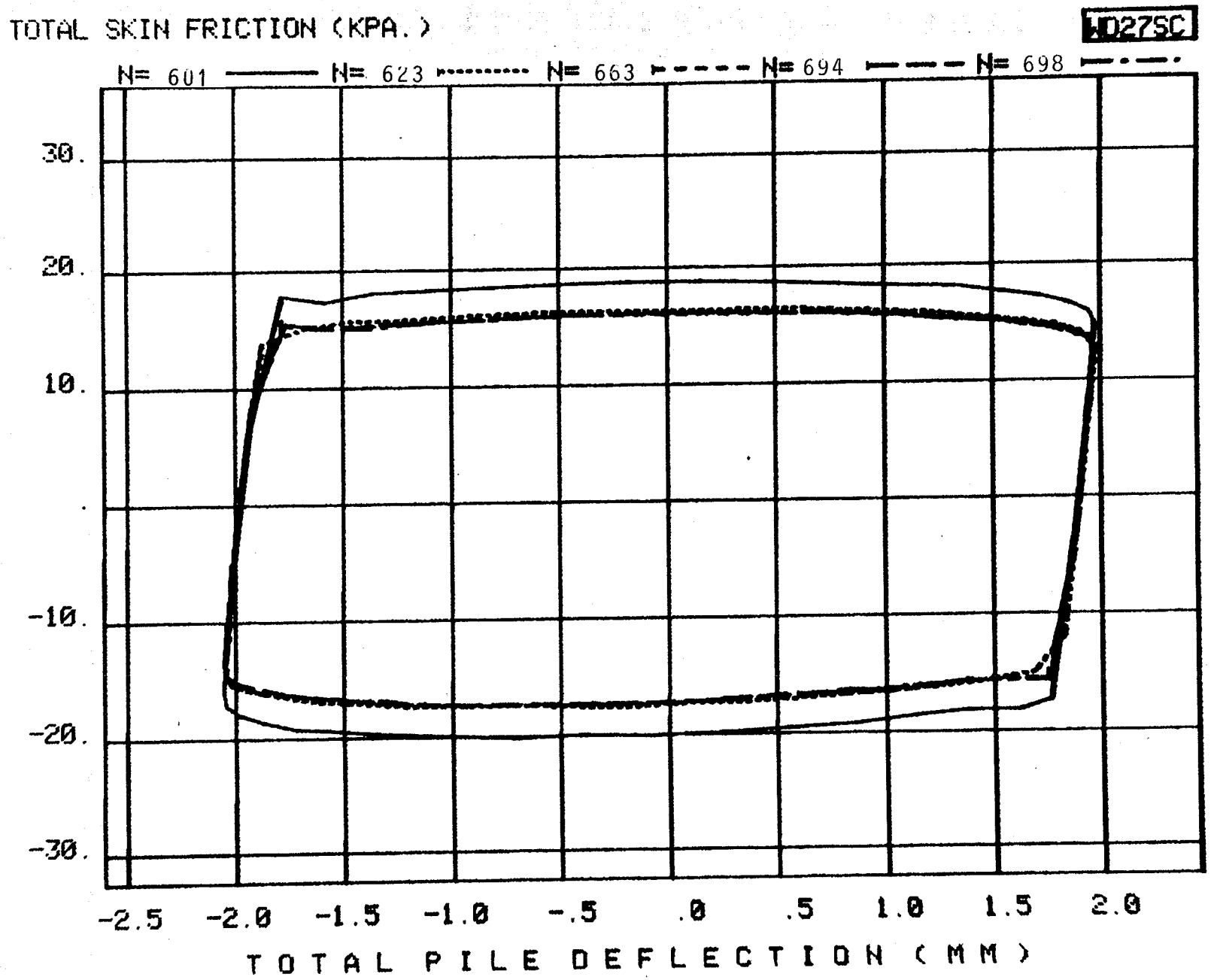
TOTAL SKIN FRICTION (KPA.)
WD27SC
N= 601
N= 623
N= 663
N= 694
N= 698
30.
20.
10.
-10.
-20.
-30.
-2.5
-2.0
-1.5
-1.0
-.5
.0
.5
1.0
1.5
2.0
TOTAL PILE DEFLECTION (MM)

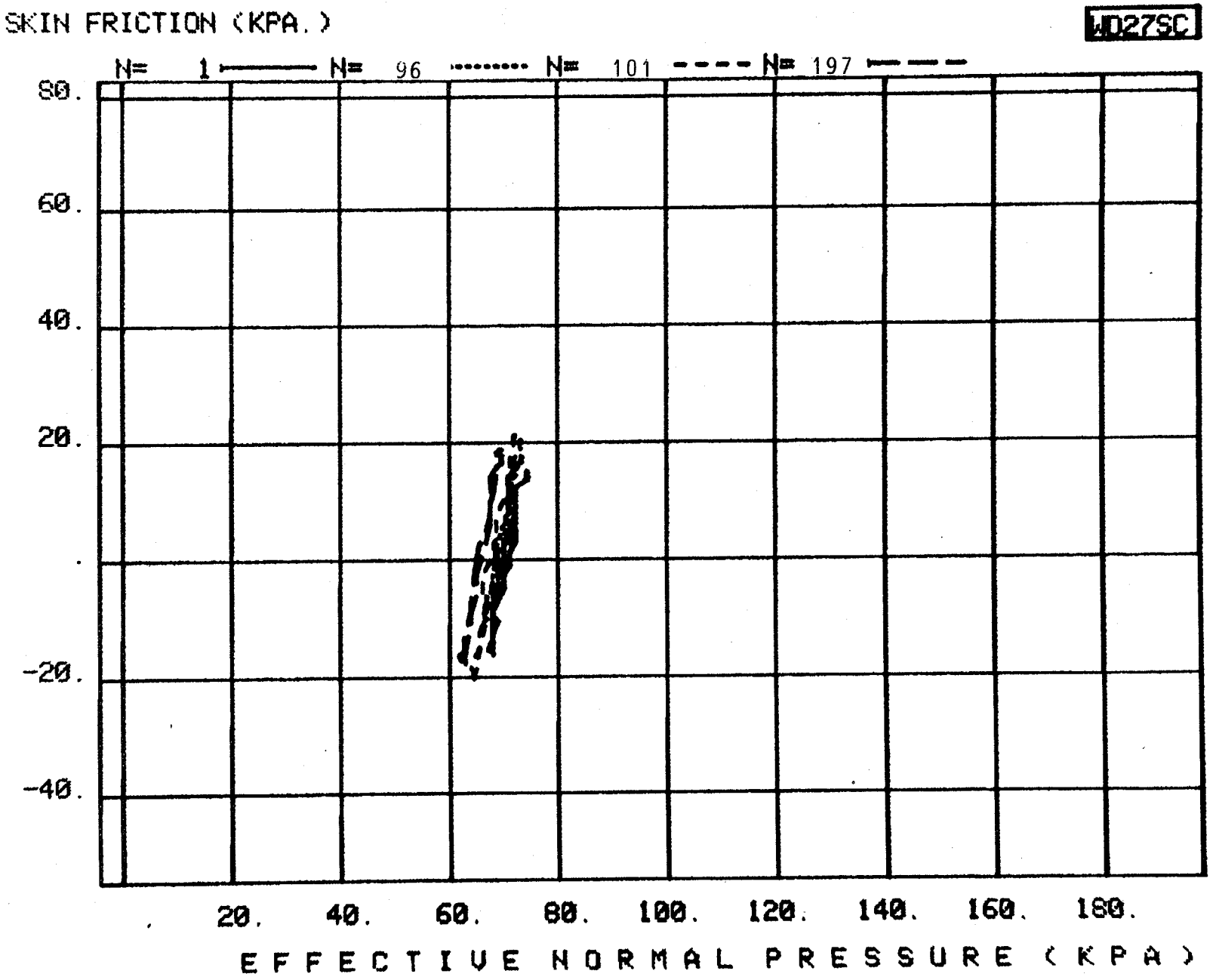
SKIN FRICTION (KPA.)
WD27SC
N= 1
N= 96
N= 101
N= 197
80.
60.
40.
20.
-20.
-40.
20.
40.
60.
80.
100.
120.
140.
160.
180.
EFFECTIVE NORMAL PRESSURE (KPA)

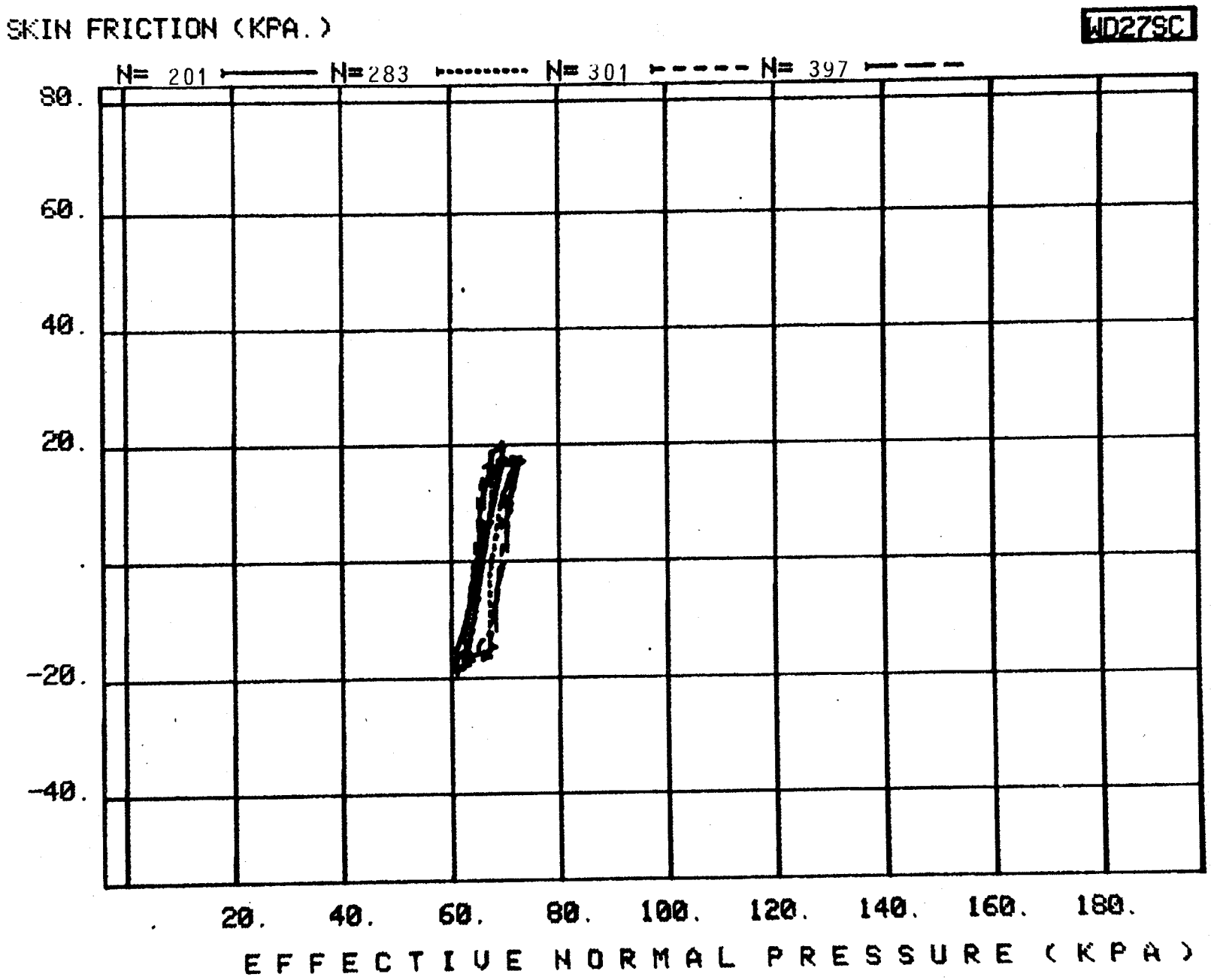
SKIN FRICTION (KPA.)
WD27SC
N= 201
N=283
N= 301
N= 397
80.
60.
40.
20.
-20.
-40.
20.
40.
60.
80.
100.
120.
140.
160.
180.
EFFECTIVE NORMAL PRESSURE (KPA)

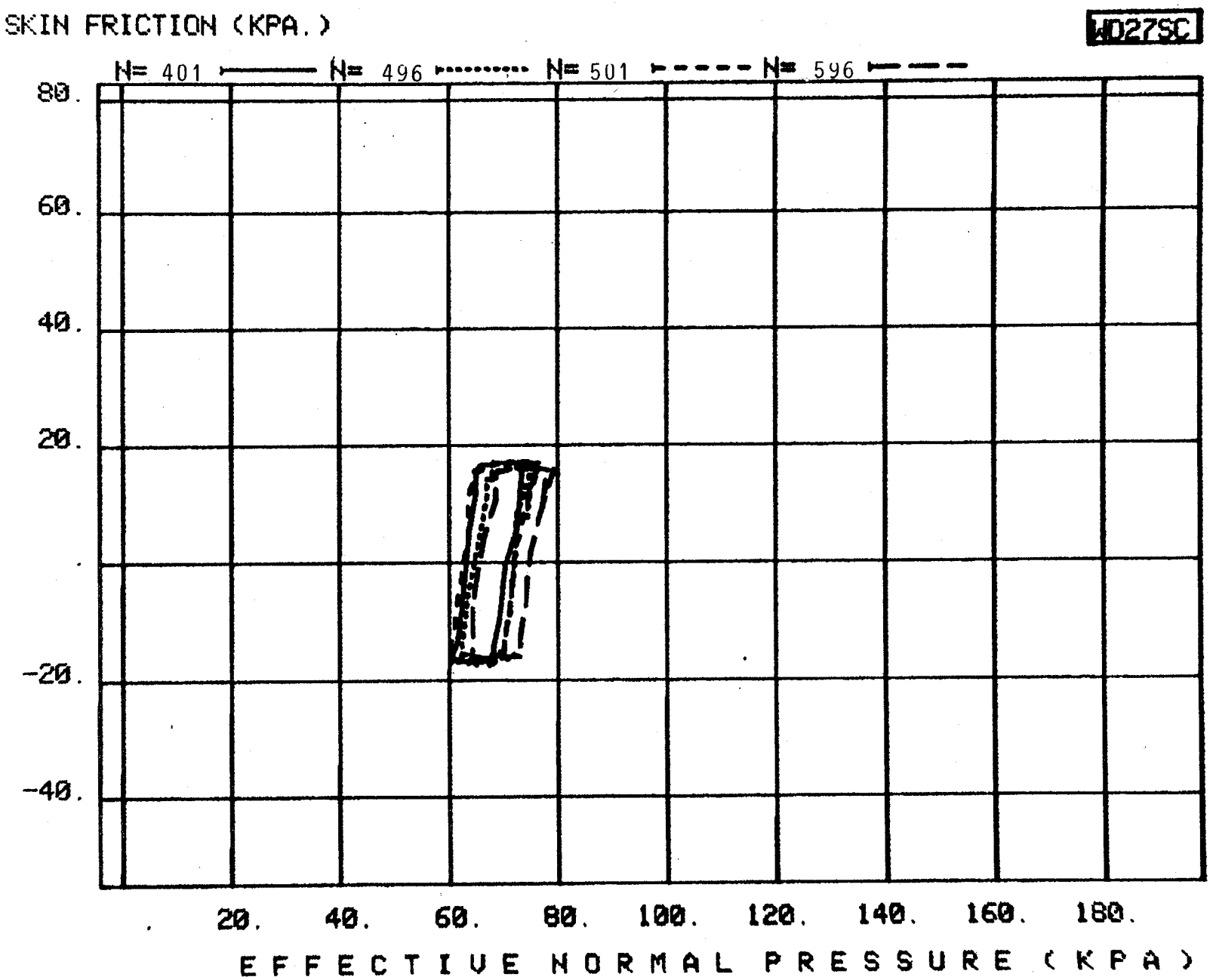
SKIN FRICTION (KPA.)
WD27SC
N= 401
N= 496
N= 501
N= 596
80.
60.
40.
20.
-20.
-40.
20.
40.
60.
80.
100.
120.
140.
160.
180.
EFFECTIVE NORMAL PRESSURE (KPA)

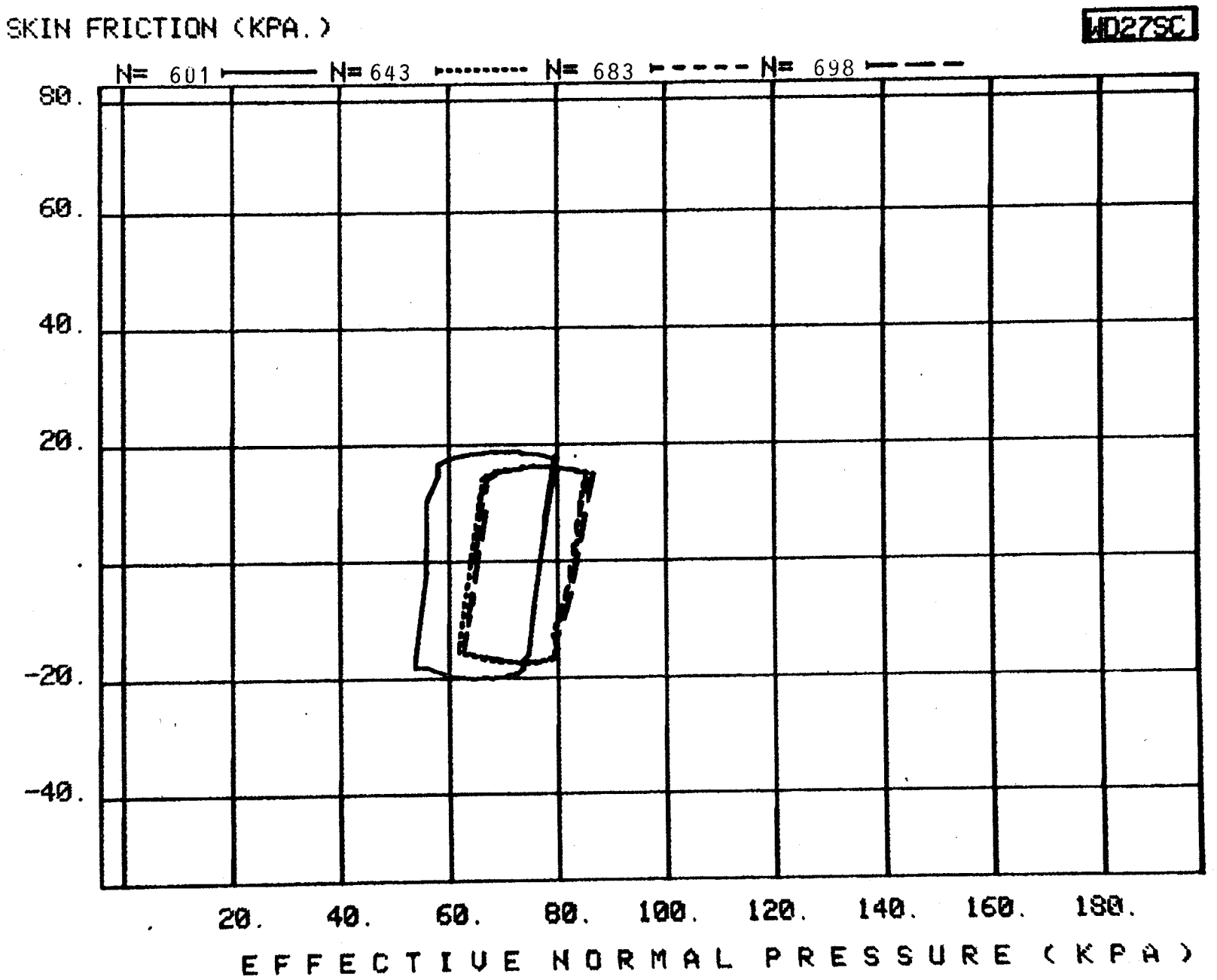
SKIN FRICTION (KPA.)
WD27SC
N= 601
N= 643
N= 683
N= 698
80.
60.
40.
20.
-20.
-40.
20.
40.
60.
80.
100.
120.
140.
160.
180.
EFFECTIVE NORMAL PRESSURE (KPA)

RESPONSE ON CYCLIC LOADING (KPA.) CYCLE NO. 1

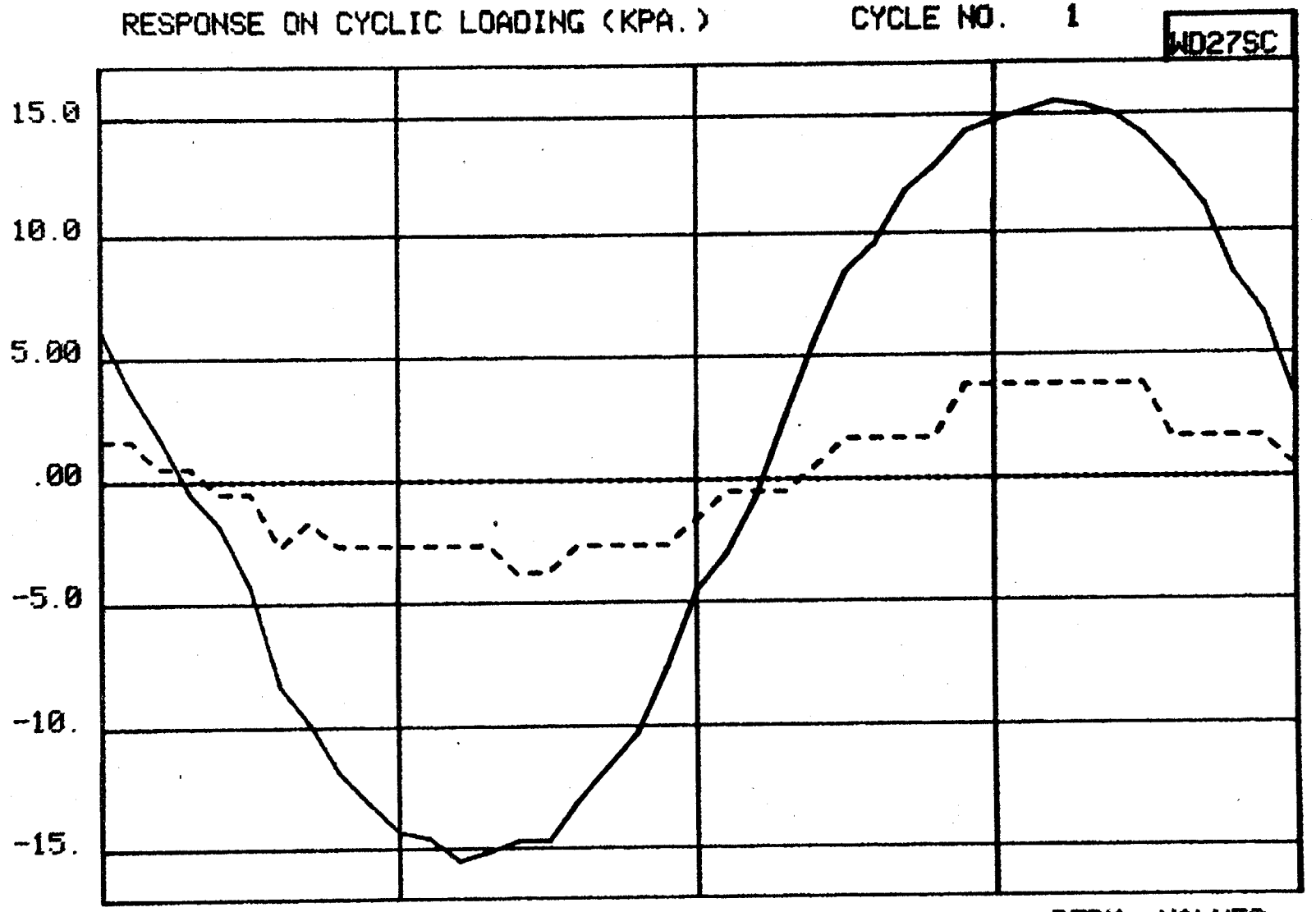

LEGEND:

		PERM. VALUES
————	SKIN FRICTION	-.54 KPA.
·····	PORE PRESSURE	462.7 KPA.
- - - -	TOTAL NORMAL PRESSURE	533.3 KPA.

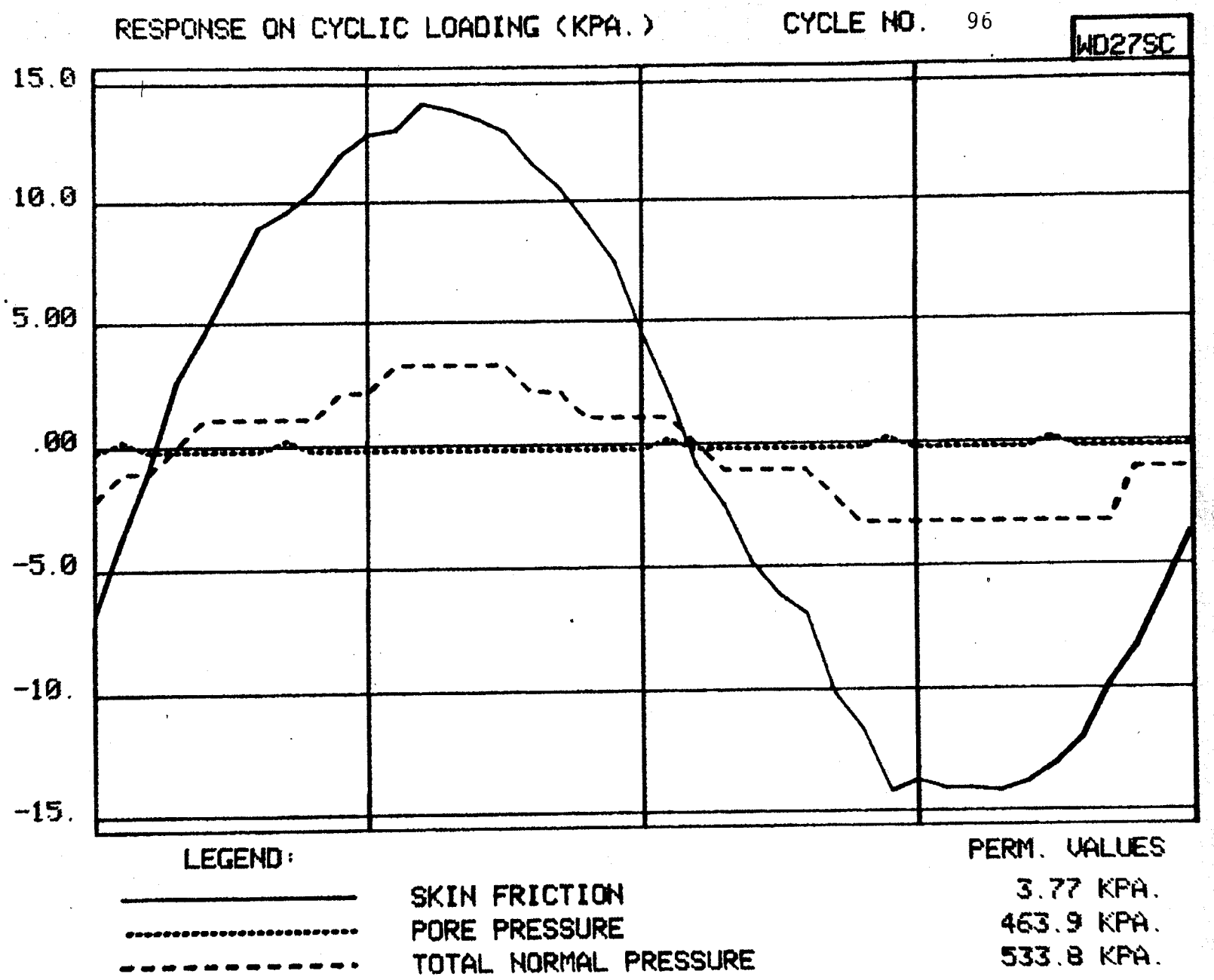
RESPONSE ON CYCLIC LOADING (KPA.)
CYCLE NO. 96
WD27SC
15.0
10.0
5.00
.00
-5.0
-10.
-15.
LEGEND:
SKIN FRICTION
PORE PRESSURE
TOTAL NORMAL PRESSURE
PERM. VALUES
3.77 KPA.
463.9 KPA.
533.8 KPA.

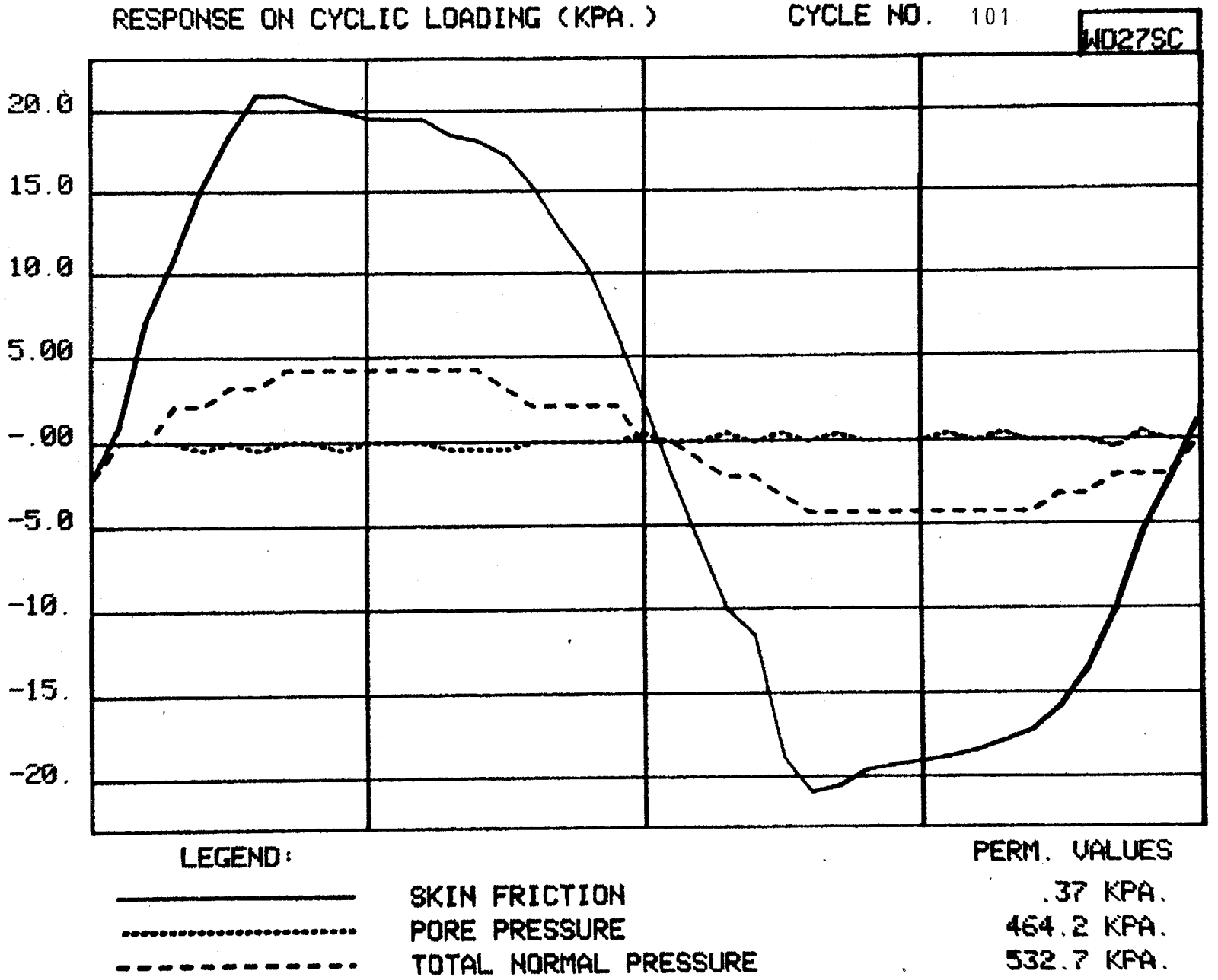
RESPONSE ON CYCLIC LOADING (KPA.)
CYCLE NO. 101
WD27SC
20.0
15.0
10.0
5.00
-.00
-5.0
-10.
-15.
-20.
LEGEND:
SKIN FRICTION
PORE PRESSURE
TOTAL NORMAL PRESSURE
PERM. VALUES
.37 KPA.
464.2 KPA.
532.7 KPA.

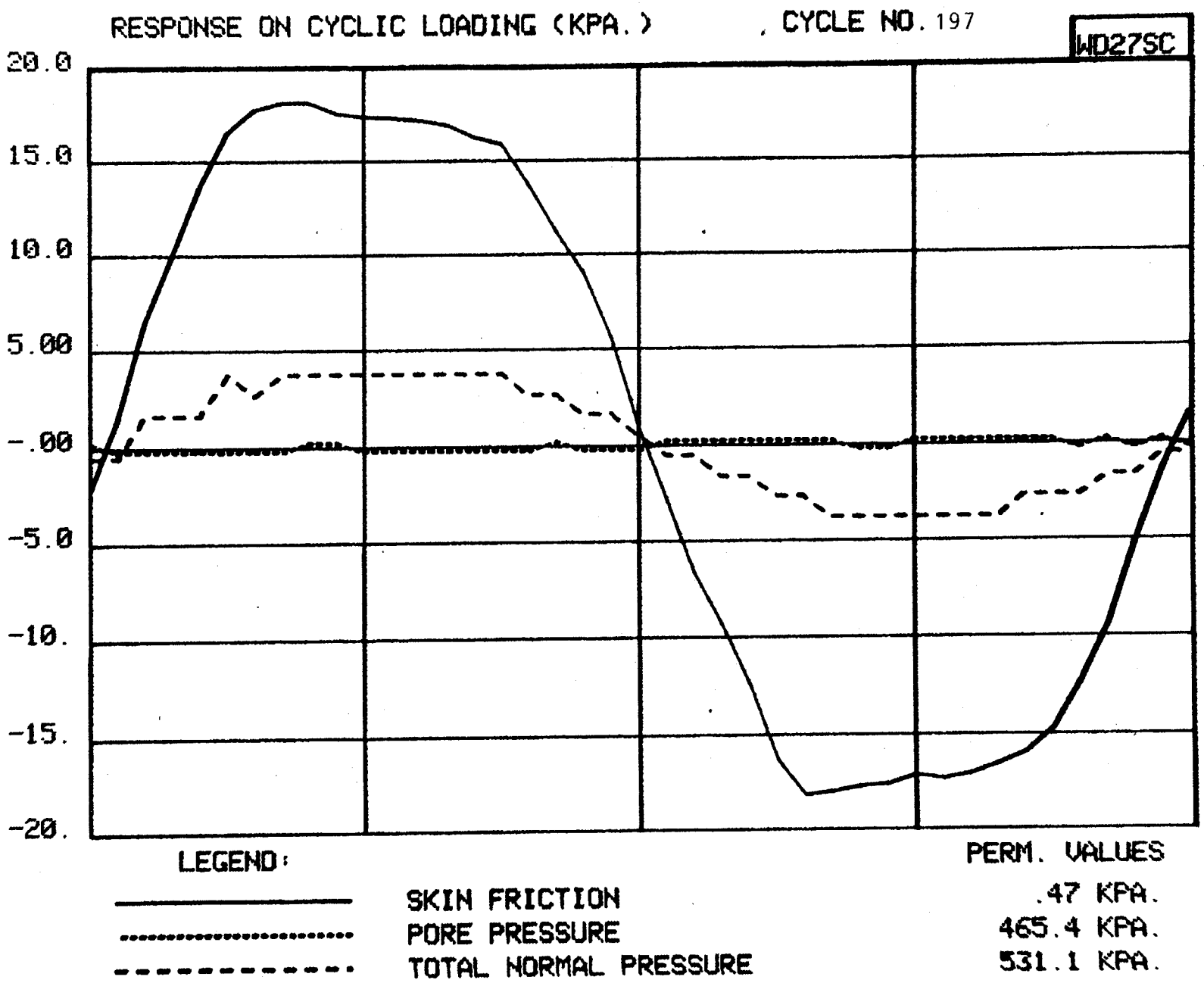
RESPONSE ON CYCLIC LOADING (KPA.)
, CYCLE NO. 197
WD27SC
20.0
15.0
10.0
5.00
-.00
-5.0
-10.
-15.
-20.
LEGEND:
SKIN FRICTION
PORE PRESSURE
TOTAL NORMAL PRESSURE
PERM. VALUES
.47 KPA.
465.4 KPA.
531.1 KPA.

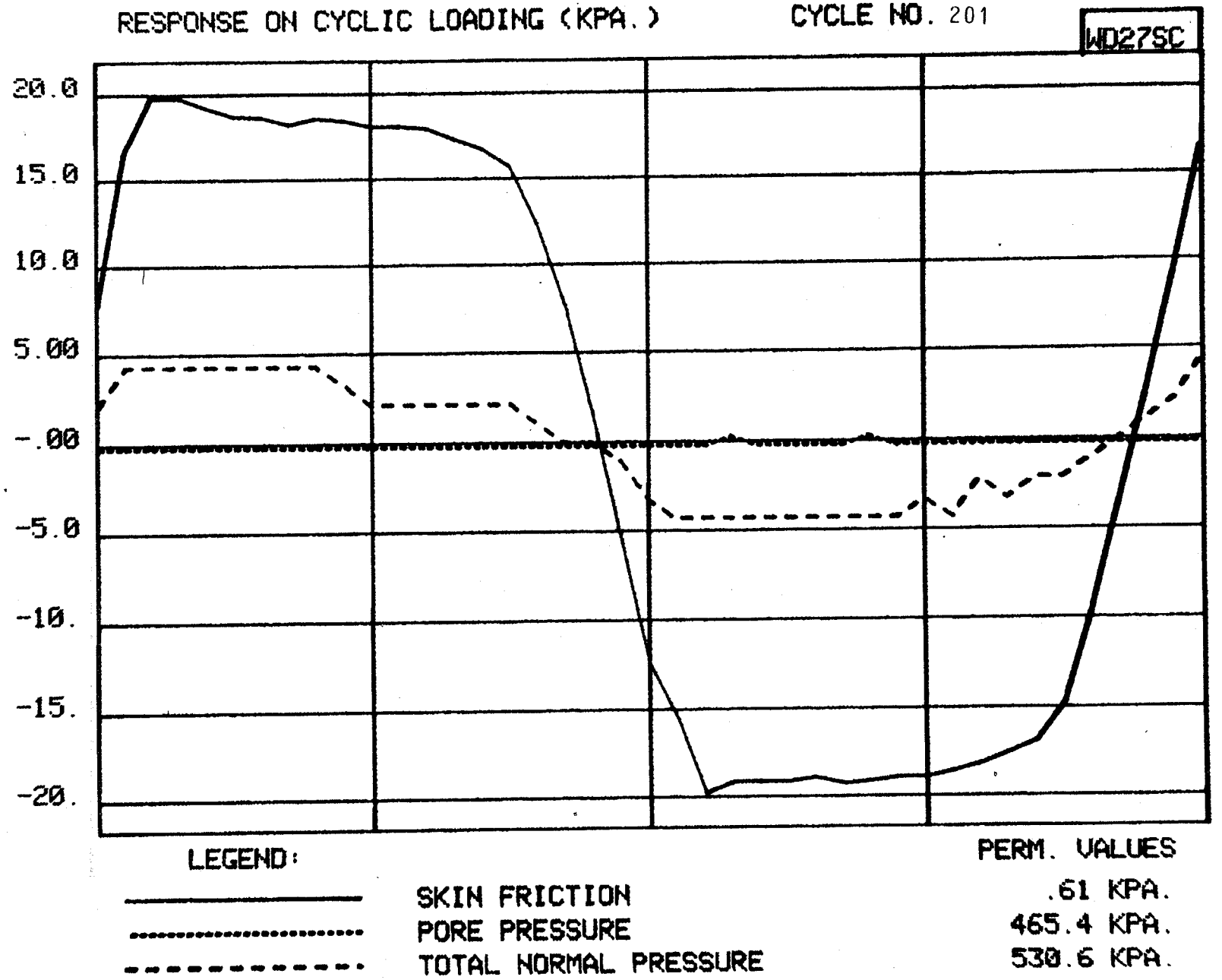
RESPONSE ON CYCLIC LOADING (KPA.)
CYCLE NO. 201
WD27SC
20.0
15.0
10.0
5.00
-.00
-5.0
-10.
-15.
-20.
LEGEND:
SKIN FRICTION
PORE PRESSURE
TOTAL NORMAL PRESSURE
PERM. VALUES
.61 KPA.
465.4 KPA.
530.6 KPA.

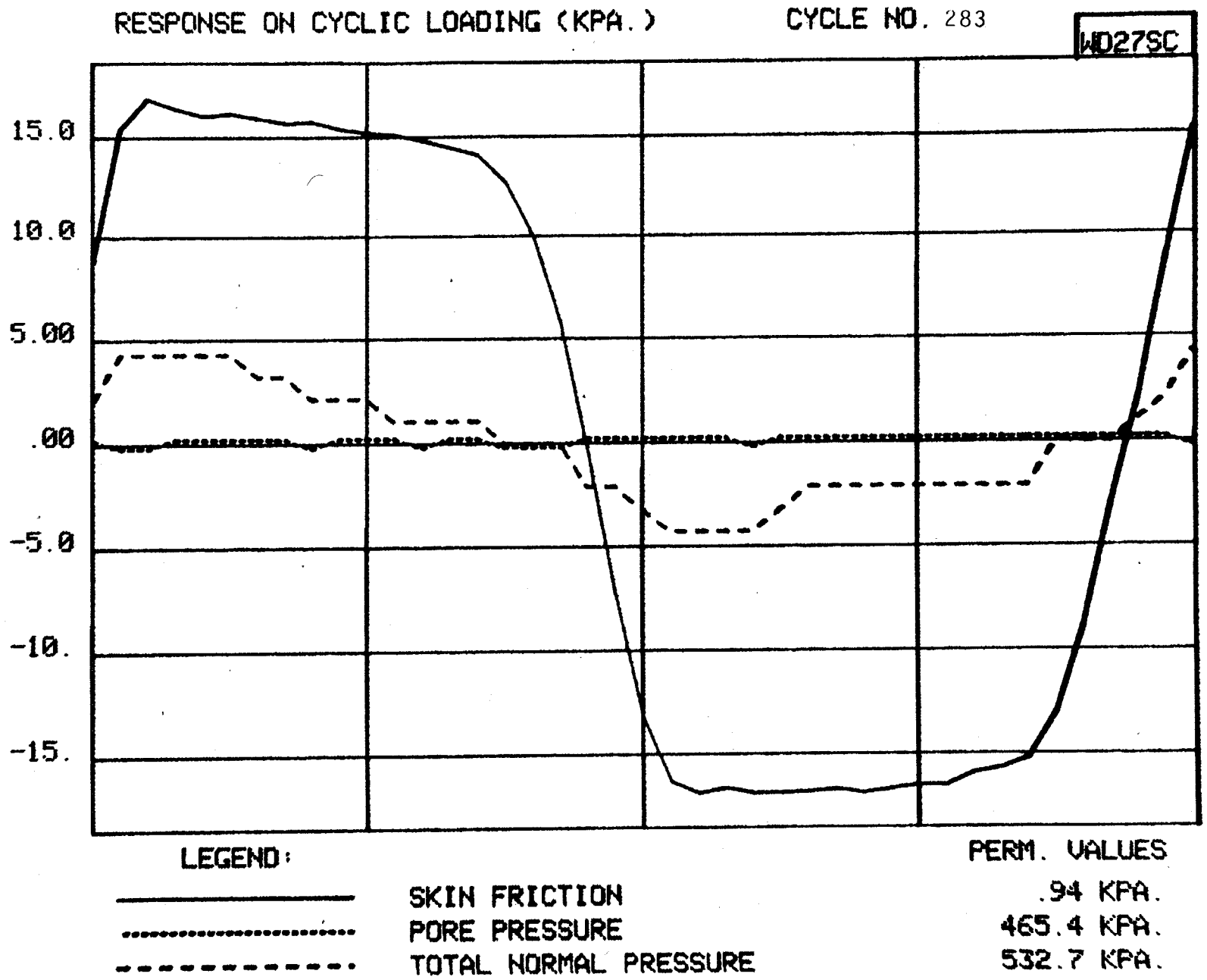
RESPONSE ON CYCLIC LOADING (KPA.)
CYCLE NO. 283
WD27SC
15.0
10.0
5.00
.00
-5.0
-10.
-15.
LEGEND:
SKIN FRICTION
PORE PRESSURE
TOTAL NORMAL PRESSURE
PERM. VALUES
.94 KPA.
465.4 KPA.
532.7 KPA.

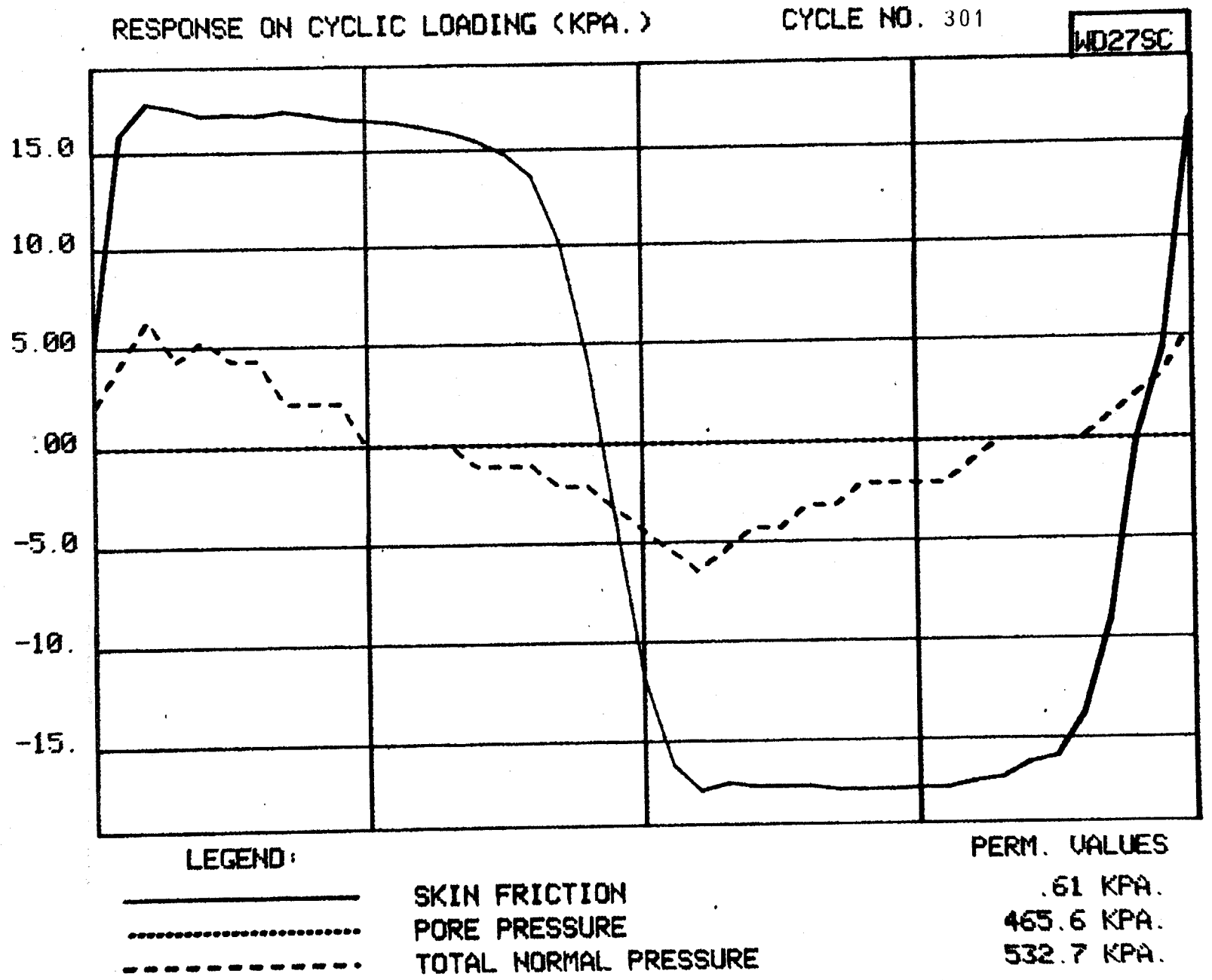
RESPONSE ON CYCLIC LOADING (KPA.)
CYCLE NO. 301
WD27SC
15.0
10.0
5.00
.00
-5.0
-10.
-15.
LEGEND:
SKIN FRICTION
PORE PRESSURE
TOTAL NORMAL PRESSURE
PERM. VALUES
.61 KPA.
465.6 KPA.
532.7 KPA.

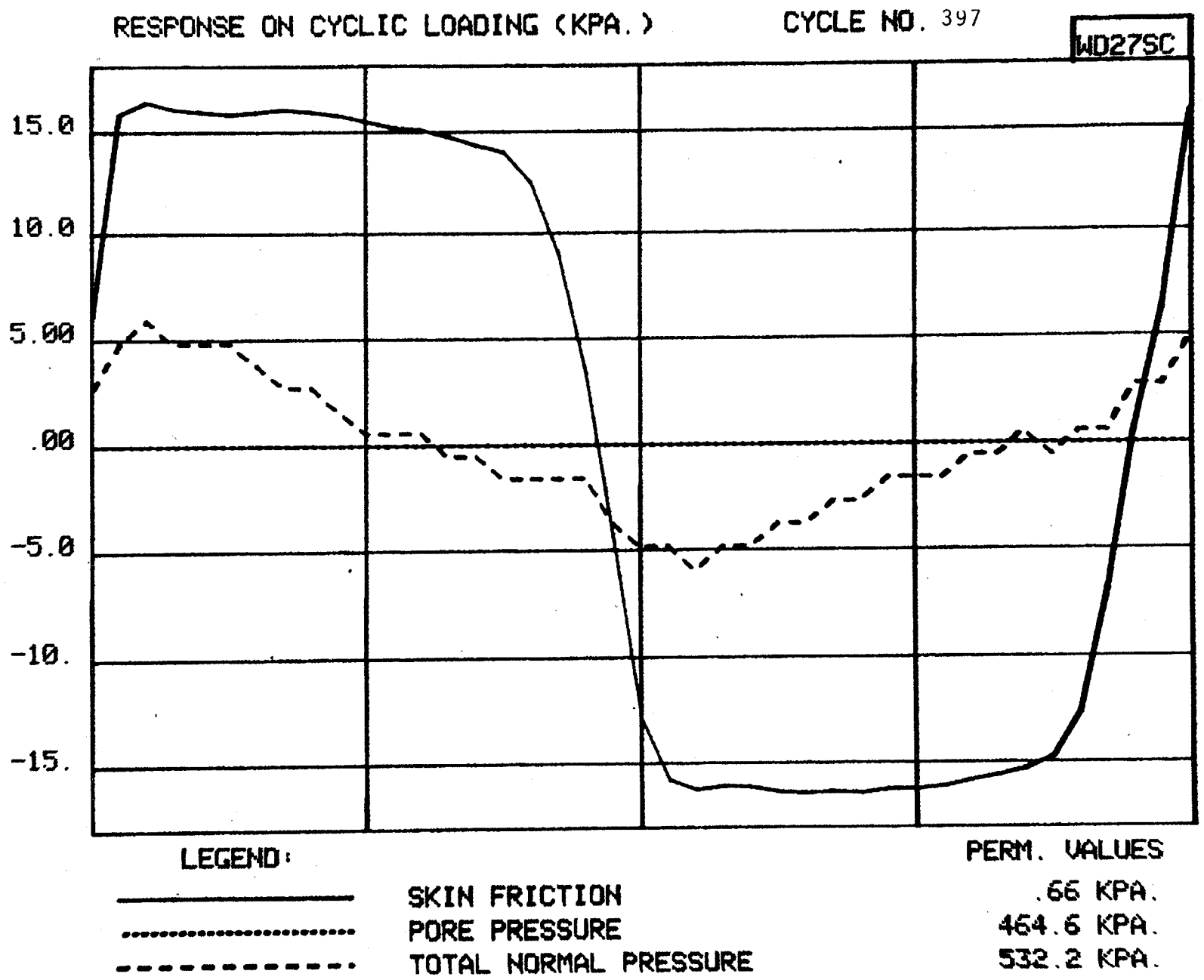
RESPONSE ON CYCLIC LOADING (KPA.)
CYCLE NO. 397
WD27SC
15.0
10.0
5.00
.00
-5.0
-10.
-15.
LEGEND:
SKIN FRICTION
PORE PRESSURE
TOTAL NORMAL PRESSURE
PERM. VALUES
.66 KPA.
464.6 KPA.
532.2 KPA.

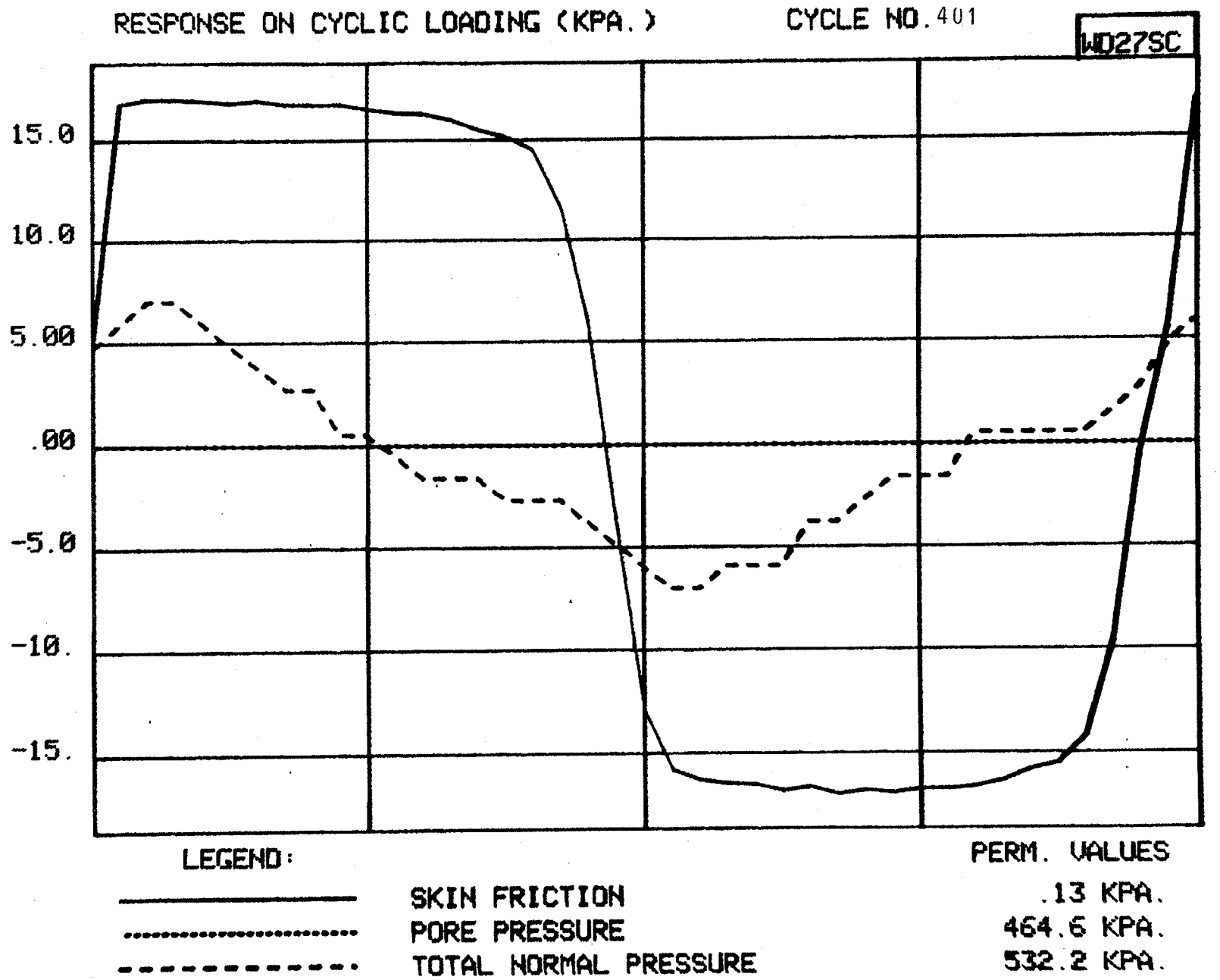
RESPONSE ON CYCLIC LOADING (KPA.)
CYCLE NO.401
WD27SC
15.0
10.0
5.00
.00
-5.0
-10.
-15.
LEGEND:
SKIN FRICTION
PORE PRESSURE
TOTAL NORMAL PRESSURE
PERM. VALUES
.13 KPA.
464.6 KPA.
532.2 KPA.

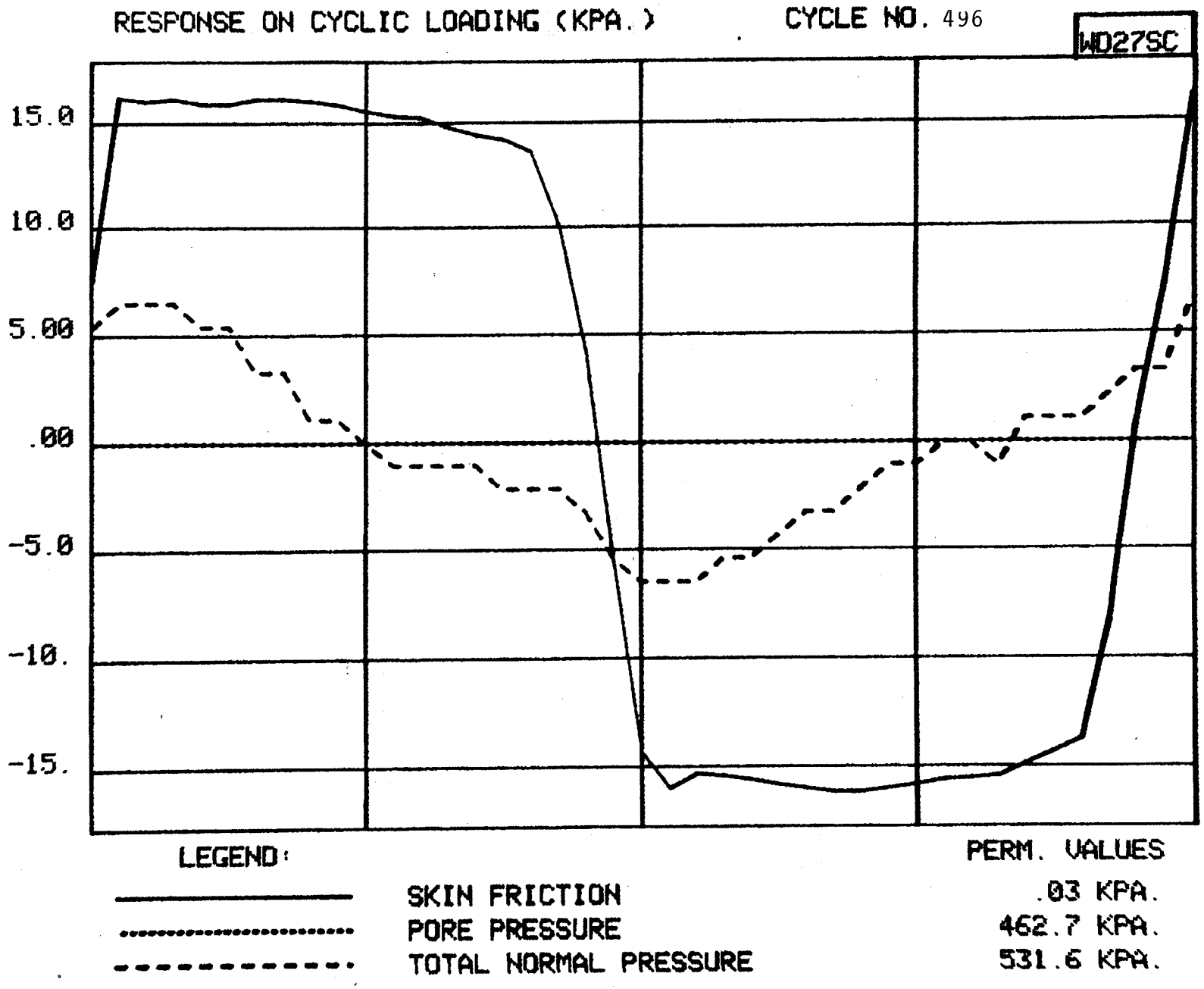
RESPONSE ON CYCLIC LOADING (KPA.)
CYCLE NO. 496
WD27SC
15.0
10.0
5.00
.00
-5.0
-10.
-15.
LEGEND:
SKIN FRICTION
PORE PRESSURE
TOTAL NORMAL PRESSURE
PERM. VALUES
.03 KPA.
462.7 KPA.
531.6 KPA.

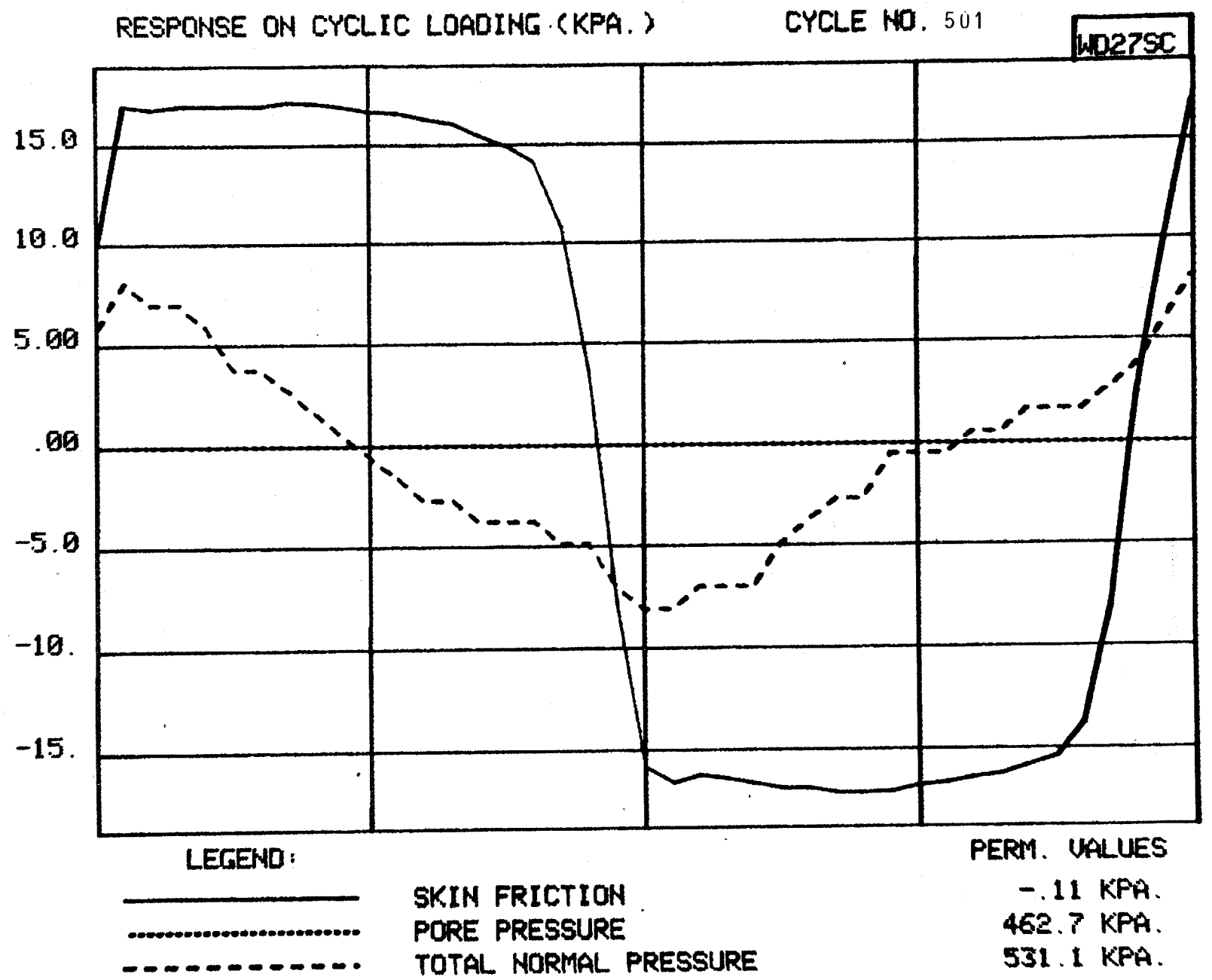
RESPONSE ON CYCLIC LOADING (KPA.)
CYCLE NO. 501
WD27SC
15.0
10.0
5.00
.00
-5.0
-10.
-15.
LEGEND:
SKIN FRICTION
PORE PRESSURE
TOTAL NORMAL PRESSURE
PERM. VALUES
-.11 KPA.
462.7 KPA.
531.1 KPA.

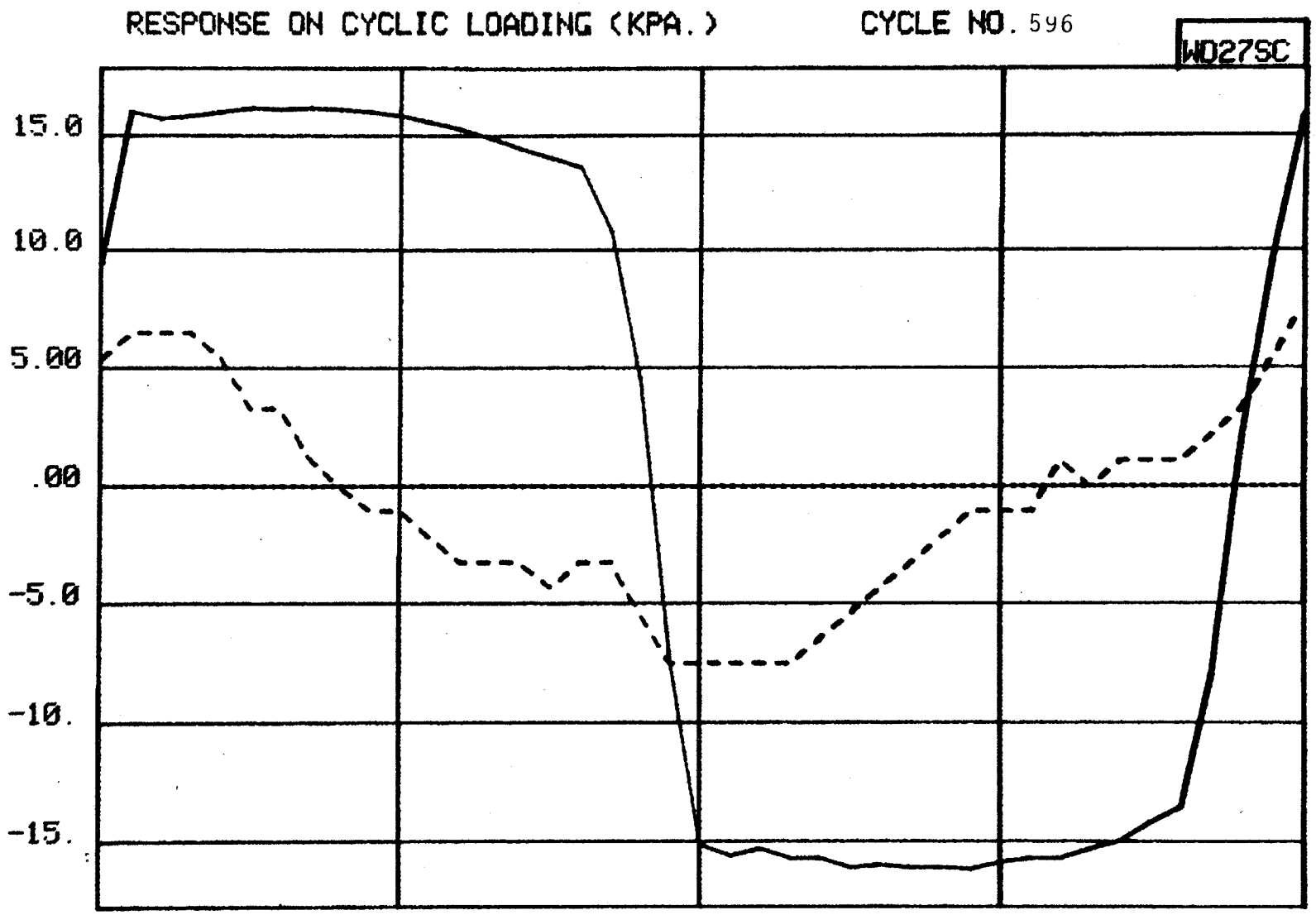

LEGEND:

		PERM. VALUES
———	SKIN FRICTION	-.06 KPA.
·····	PORE PRESSURE	459.8 KPA.
- - - -	TOTAL NORMAL PRESSURE	531.6 KPA.

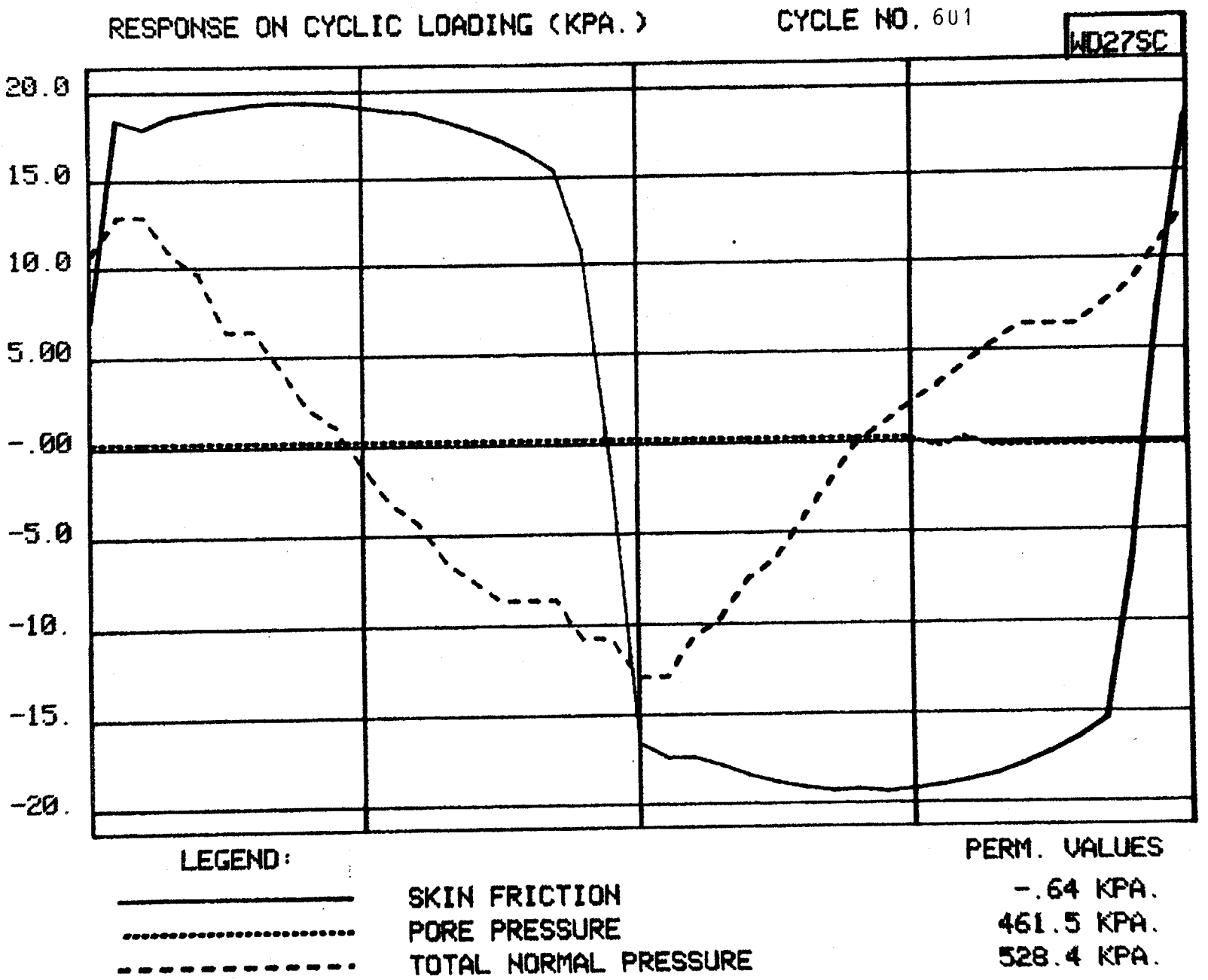
RESPONSE ON CYCLIC LOADING (KPA.)
CYCLE NO. 601
WD27SC
20.0
15.0
10.0
5.00
-.00
-5.0
-10.
-15.
-20.
LEGEND:
SKIN FRICTION
PORE PRESSURE
TOTAL NORMAL PRESSURE
PERM. VALUES
-.64 KPA.
461.5 KPA.
528.4 KPA.

APPENDIX E

DETAILED RESULTS FROM **TEST 8, STRATUM III** MODEL PILE TESTS

CONTENTS

Summary	E3
Test 8, Stratum III	E4
Consolidation	E4
Pile Instatllation and Set-Up	E4
Static Test	E5
Cyclic Tests	E5
Stress Controlled Tests (WD38LC)	E5
Displacement Controlled Tests (WD38SC)	E7
Strength Tests	E8

LIST OF FIGURES

Figure 1	Sample Properties
Figure 2	Consolidation Diagram
Figure 3	Pocket Penetrometer Tests After Consolidation
Figure 4	Pressures at Pile Wall after Installation
Figure 5	Static Test 1
Figure 6	Static Test 2
Figure 7	Skin Friction vs no. of Cycles, WD38LC
Figure 8	Deflection vs no. of Cycles, WD38LC
Figure 9	Total Normal Pressure vs no. of Cycles, WD38LC
Figure 10	Pore Pressure vs no. of Cycles, WD38LC
Figure 11	Eff. Normal Pressure vs no. of Cycles, WD38LC
Figure 12	Deflection vs no. of Cycles, WD38SC
Figure 13	Skin Friction vs no. of Cycles, WD38SC

Figure 14 Pore Pressure vs no. of Cycles, WD38SC
Figure 15 Total Normal Pressure vs no. of Cycles, WD38SC
Figure 16 Eff. Normal Pressure vs no. of Cycles, WD38SC
Figure 17 Pocket Penetrometer Tests after Pile Test
Figure 18 Unconfined Compression Tests
Figure 19 Water Content and Shear Strength

Appendix EA
Plotted Results from WD38LC
Figures EA-1 through EA-9
Skin Friction vs Deflection, Selected Cycles
Figures EA-10 through EA-13
Skin Friction vs Eff. Normal Pressure, Selected Cycl.
Figures EA-14 through EA-28
Skin Friction, Pore and Total Pressure, Selected Cycles

Appendix EB
Plotted Results from WD38SC
Figures EB-1 through EB-7
Skin Friction vs Deflection, Selected Cycles
Figures EB-8 through EB-11
Skin Friction vs Eff. Normal Pressure, Selected Cycl.
Figures EB-12 through EB-24
Skin Friction, Pore and Total Pressure, Selected Cycles

SUMMARY

This report contains the results of the laboratory model pile tests designated TEST 8, STRATUM III, in the project CNRD 13-2, TENSION PILE STUDY, for Conoco Norway Inc.

The clay sample was consolidated for 19 days under 500 kPa applied vertical pressure. Pore pressure in the sample was about 39 % of the applied pressure. After two days of consolidation in the pile chamber the pile was installed. After 14 days of set-up the excess pore pressure was about 75 kPa. Testing was then started.

Static test gave peak friction of 60 kPa with residual value of 56 kPa. Undrained shear strength was interpreted to 85 kPa, giving alpha value of 0.71 and 0.66 for peak and residual respectively. Estimating the effective vertical pressure to 327 kPa results in a beta factor of 0.18 . A new static test 24 hours later showed almost identical results.

Cyclic tests were started 3 days following the last static test starting with stress controlled tests with static tension bias of 35 kPa (58% of previous max. friction) with parcels of 100 cycles with specified cyclic stress amplitude increasing for consecutive parcels resulted in failure (abrupt pull-out of pile) in sixth cycle of seventh parcel. The maximum friction at failure was measured to 68.5 kPa.

After 10 hrs of set-up a displacement controlled test with two-way cyclic loading was performed. Seven parcels of 100 cycles with increasing cyclic displacement amplitudes were made. Maximum friction obtained was 62 kPa which reduced to 56 kPa in subsequent parcels. The residual friction during large slip was 49 kPa which gives a reduction of strength of 21 % .

TEST 8, STRATUM III

CONSOLIDATION

The sample was prepared from the same material as used in Test 4. Water was added during the remoulding process to a water content of about 54% . Horizontal filters were placed in the oedometer to provide better vertical drainage.

A vertical pressure of 500 kPa was applied on top. As seen in Figure 2 the pore pressure at middle height had dropped down to about 39% of the consolidation stress after 19 days. At this time the sample was transferred to the pile chamber. Pocket penetrometer tests were performed on the side of the sample and on the top when trimmed in the pile chamber (level I-I) as shown in Figure 3. The shear strength, s_u, showed an average of about 65 kPa.

PILE INSTALLATION AND SET-UP

After pocket penetrometer tests the sample was mounted in the pile chamber and left to reconsolidate for two days under a vertical pressure of 500 kPa and radial pressure of 350 kPa (K=0.7). Due to the slow pore pressure response and the slow pore pressure dissipation in the previous tests, which was thougth to be due to poor drainage conditions, vertical filter strips were placed around the periphery of the soil specimen and led out in free air between the confining cyclinder and the top and bottom plate of the pile chamber. This in turn made it impossible to apply any back pressure to the soil specimen. During the two days of consolidation in the pile chamber good drainage was proved by formation of salt on the filter strips sticking out, which came from the expelled water from the marine clay.

During insertion of the pile the side friction showed a maximum of about 27 kPa. Total normal pressure showed 365 kPa and the pore pressure only showed 25 kPa directly after pile installation. After about four days of set-up the pore pressure showed a maximum of 165. kPa whereas the total pressure showed a maximum of 450 kPa after eight days as shown in Figure 4. After 14 days of set-up the pore pressure was down at 75 kPa and the total pressure showed 445 kPa. At this time it was decided to start with the loading program.

STATIC TEST

A displacement controlled static test with deformation rate 1 mm per hour was now conducted, as shown in Figure 5. The pile was pulled in tension through failure and large slip and then pushed down to original position causing failure in compression and large slip (residual friction).

The displacement to cause failure, as shown in Figure 5, was about 0.4 mm or 1.6% of the pile diameter. A maximum friction of 60 kPa was achieved with a residual friction of 56 kPa. The shear strength of the clay at time of testing was estimated to 85 kPa which results in an alpha (α) value of 0.71 and 0.66 for peak and residual friction respectively.

For the effective stress approach, estimating σ'_{vo} from the relationship

$$s_u = 0.26 \cdot \sigma'_{vo}$$

which gives $\sigma'_{vo} =$ 327 kPa, the beta value (β) becomes 0.18 for maximum friction.

Total pressure on the pile wall at time of failure was about 420 kPa and the pore pressure showed 75 kPa, resulting in a horizontal effective pressure of 345 kPa. The interface friction angle (δ) can then be estimated to 9.8 degrees.

CYCLIC TESTS

After this static test the pile was brought back to original position and left to reconsolidate for one day. During this time a fault was detected, and fixed, in the load controlling equipment. In order to check the performance a new static test was conducted at this time, as shown in Figure 6. The maximum friction had slightly increased to 62 kPa and the total pressure reduced slightly with about 20 kPa. The pile was now left to reconsolidate for three days before a stress controlled test was started. At this time the total pressure had increased to 400 kPa and the pore pressure reduced to 60 kPa.

Stress Controlled Tests (WD38LC)

A stress controlled test comprised of applying a prescribed static tensile (uplift) stress

on the pile, superimposed with parcels of 100 cycles with 10 seconds period and prescribed cyclic stress amplitude. The stress amplitude was then increased in the following parcels until failure (excessive uplift) occured in tension.

For this test the static tensile stress (bias) level was about 35 kPa, corresponding to 58% of the previous static capacity.

In the first parcel the cyclic level was about 6.0 kPa and for the following three parcels the cyclic stress level was incremented by 6 kPa as can be seen in Figure 7, showing skin friction (envelope of max. and min.) versus cycle numbers. In the last three parcels the cyclic level was incremented by 3 kPa until failure occured after six cycles in the seventh parcel. In Figures 8,9,10 and 11 the resulting deformations and pressures due to the applied skin friction are plotted versus cycle numbers. In Appendix A selected cycle numbers are plotted as friction versus deflection, friction versus effective pressure and friction, pore pressure and total pressure variation during one cycle.

As seen in Figure 7 a total of seven parcels were performed. The first parcel does not produce any significant deformation of the pile as shown in Figure 8 and in Figure A-1. In the second parcel the average deformation is to show a downward movement which was caused by transients in the loading system during the first parcel. The friction deformation behaviour in second and third parcel, as shown in Figures A-2 and A-3 is linear with only minimal signs of hysteresis. Increasing the cyclic level in parcels four and five results in larger cyclic deformations and some more pronounced hysteresis, and permanent upward deformation is also seen by the increasing average deformation, depicted in Figure 8 and A-4 and A-5. In the sixth parcel with a cyclic level of 30 kPa (maximum friction of 65.5 kPa) the pile is slowly pulled up indicated by the increasing average deformation as seen in Figure A-6. Finally in parcel seven with prescribed cyclic stress level of 33 kPa the pile fails in the sixth cycle at a friction of 68.5 kPa as seen in Figures A-7 and A-8 where the pile is suddenly pulled up excessively in an attempt to produce the prescribed cyclic friction. In Figure A-9 is a summary plot of selected cycles from the different parcels indicating the amount of deformation from start up to point of failure.

From the pressure diagrams in Figures 9,10 and 11 it is seen that the average pressures during the cyclic testing stays fairly constant. The total normal pressure is seen to drop during the sixth parcel and at the time of failure as does the effective pressure

which is a mirror image of the total pressure since the pore pressure showed no cyclic variation and stayed constant throughout the test. The effective pressure at time of failure was about 337 kPa and reducing to 285 kPa during the failure cycle, giving an interface angle of 13.5 degrees at time of failure. This can also be seen in the "effective stress " plots in Figures A-10 through A-13.

Displacement (stroke) Controlled Tests (WD38SC)

After failure in the stress controlled tests the pile was brought back to original position and left to reconsolidate for a period of 10 hours before cyclic displacement controlled tests were performed.

One parcel here consisted of 100 cycles with 10 seconds period in two way cyclic loading from the zero position of the pile. A total of seven consecutive parcels were performed with increasing displacement amplitude, starting with 0.1 mm in the first parcel and with 0.2, 0.4, 0.6, 0.8, 1.0 and 2.0 mm in the following parcels.

The applied displacement versus cycle numbers are shown in Figure 12 with the resulting skin friction , total pressure, pore pressure and effective pressure versus cycle numbers shown in Figures 13,14,15 and 16 respectively. More detailed plots of selected cycles are shown in Appendix B.

In the two first parcels with cyclic displacement of 0.1 and 0.2mm the pile is not brought to failure as seen in Figure 13 and the response is linearly elastic as shown in Figure B-1 and B-2, showing only a small hysteresis in the friction-displacement relationship. In the third parcel, however, failure is reached at 62 kPa in the first cycle which reduces to 56 kPa after about five cycles. The friction during large slip (residual) was 52 kPa in the first cycle and reduced to 49 kPa after 100 cycles. In the following parcels with increasing cyclic displacements the peak friction in the first cycle stabilized at about 60 kPa and at about 55 kPa after 100 cycles. The residual friction during large slip was about 50 kPa as can be seen in Figures B-3 through B-6. In the last parcel with cyclic displacement of 2.0 mm the peak friction in the first cycle was 59 kPa which reduced down to the previous level of 55 kPa after about 10 cycles with a slightly higher value of residual strength during large slip of 52 kPa, most likely due to the increased strain rate. (The cycle period is held constant at 10 seconds.)

The degradation of strength from maximum peak friction to residual friction during large slip was then 21 % .

The pore pressure at the pile wall stayed constant at 60 kPa during the test with no cyclic variation. The total pressure, Figure 14, showed cyclic variation increasing with the deformation, with a cyclic amplitude of 44 kPa in the last parcel. In Figures B-8 through B-11 are shown skin friction versus effective pressure, and from these it is seen that in cycle 202 with the peak friction of 62 kPa the effective pressure shows 304 kPa giving an interface friction angle of 11.5 degrees.

STRENGTH TESTS

After the last parcel in stroke controlled cyclic tests the pile was pulled out of the pile chamber and the sample built out. Pocket penetrometer tests were performed on the side of the sample and in two horizontal layers with results shown in Figure 17.

Three standard triaxial test samples were then prepared from the center of the clay specimen and unconfined compression tests (UCT) were performed with the results shown in Figure 18.

In Figure 19 are shown the water content and interpreted undrained shear strength of the clay sample versus the distance from the center after completion of the pile test. The water content showed about 39 % with a slight tendency to decrease towards the center.

TABLE 1.

SAMPLE PROPERTIES, TEST 8, STRATUM III

SAMPLE PREPARATION		CONSOLIDATION			END OF PILE TEST	
INITIAL WATER CONTENT	INITIAL HEIGHT	AXIAL DEFORMATION	AXIAL STRAIN	WATER CONTENT	WATER CONTENT	
w_i (%)	H_o (cm)	ΔH (cm)	ε (%)	w_e (%)	w_{ep} (%)	
55.92 53.90	53.92	8.78	16.28	A 39.39 B 39.29 C 39.57	A-37.78 B-39.35 C-38.89	D-37.43 E-39.73 F-38.62

CONFINING PRESSURE		
AXIAL	KPa	500
RADIAL	KPa	350
BACK PRESSURE	KPa	0
SAMPLE CONSOLIDATION		
IN OEDOMETER	Days	19
IN PILE CHAMBER	Days	2
INTERPRETED SHEAR STRENGTH		
END OF CONSOLIDATION	KPa	65
END OF PILE TEST	KPa	90

Fig. 1

CONSOLIDATION DIAGRAM								Test No. 8 Stratum III		Start date	
H_i 53.92 cm		H_e 45.14 cm		$\Delta\varepsilon_v$ 16.28 %						σ_c 500 kPa	
Time h	18	89	113	138	162	186	259	282	306	329	355
Δh cm	1.09	5.28	6.14	6.72	7-07	7.38	7.99	8.13	8.26	8.37	8.47
u kPa	22.4	346.1	328.1	312.1	300.1	286.1	252	243	234	229	218
	425	449	453								
	8.71	8.77	8.78								
	199	195	194								

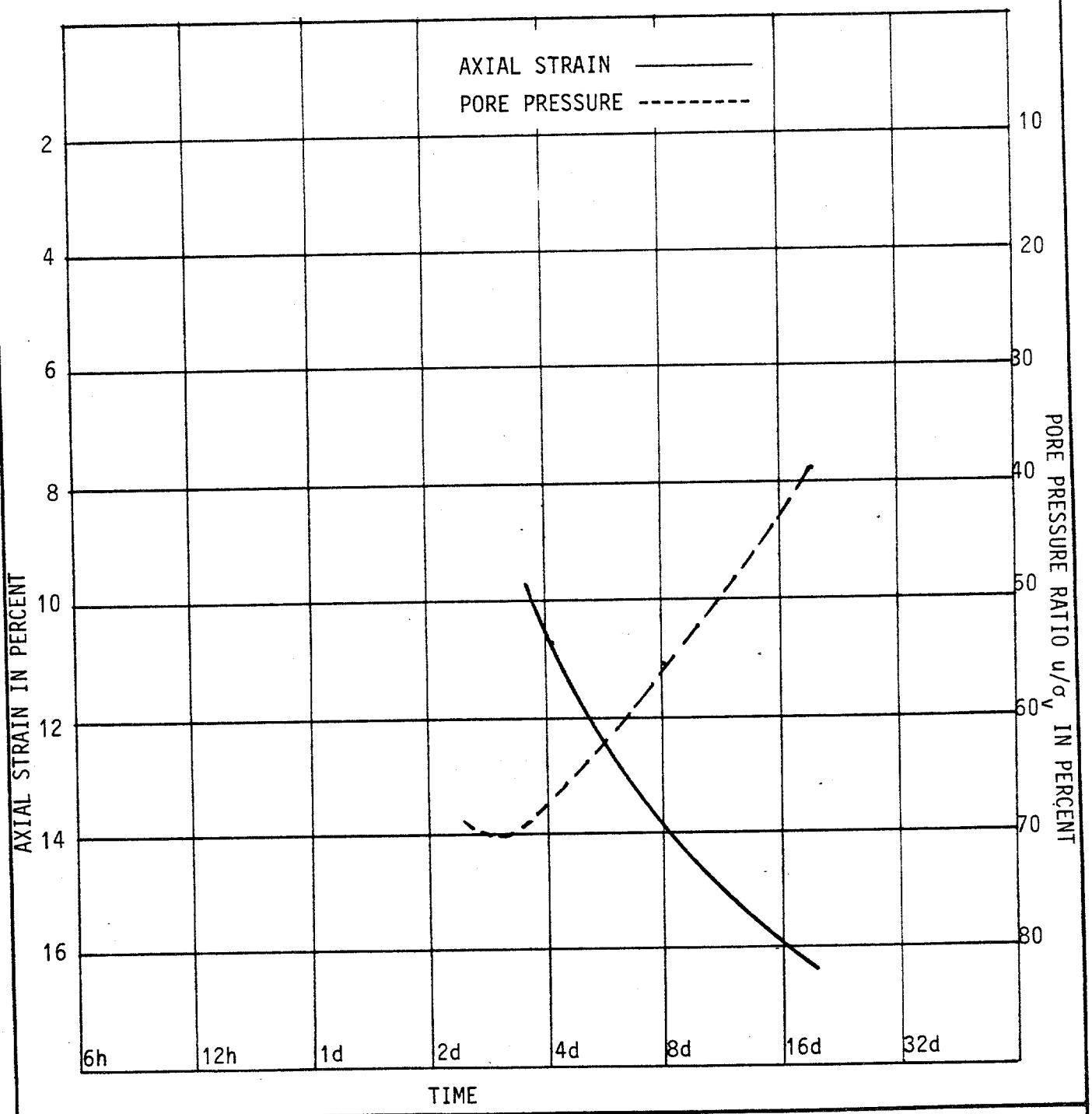

CNRD 13-2 TENSION PILE STUDY LABORATORY MODEL PILE TESTS

TEST 8 , STRATUM III, Consolidation Diagram

Scale

DET NORSKE VERITAS
Geotechnical Laboratory

Drawn by

Date

Approved

Fig. No. 2

TEST 8, STRATUM III

SHEAR STRENGTH (kPa) FROM POCKET PENETROMETER TESTS AFTER CONSOLIDATION

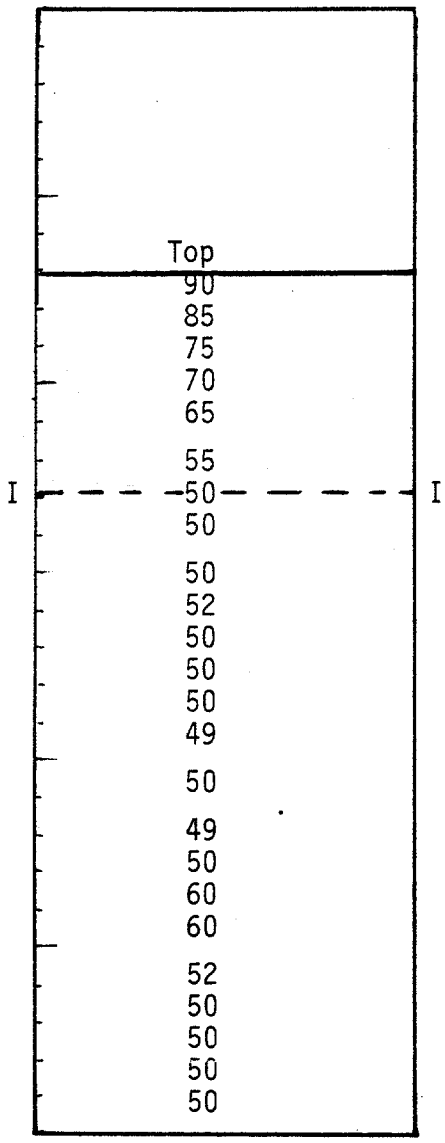

Scale 1:4

Level I - I

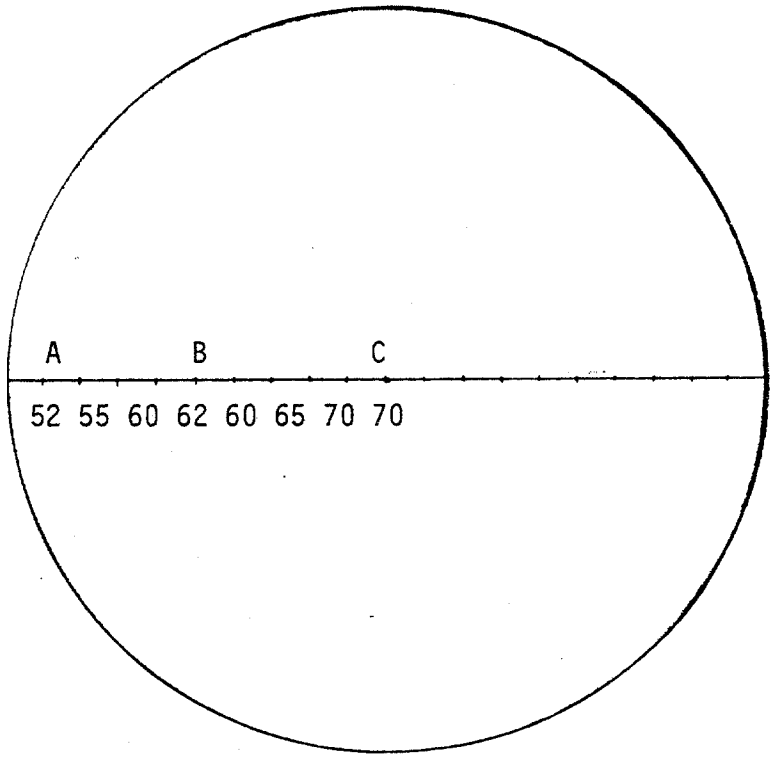

Scale: 1:2

CNRD 13-2 TENSION PILE STUDY LABORATORY MODEL PILE TESTS

		Scale
DET NORSKE VERITAS Geotechnical Laboratory	Drawn by	Date
	Approved	Fig. No. 3

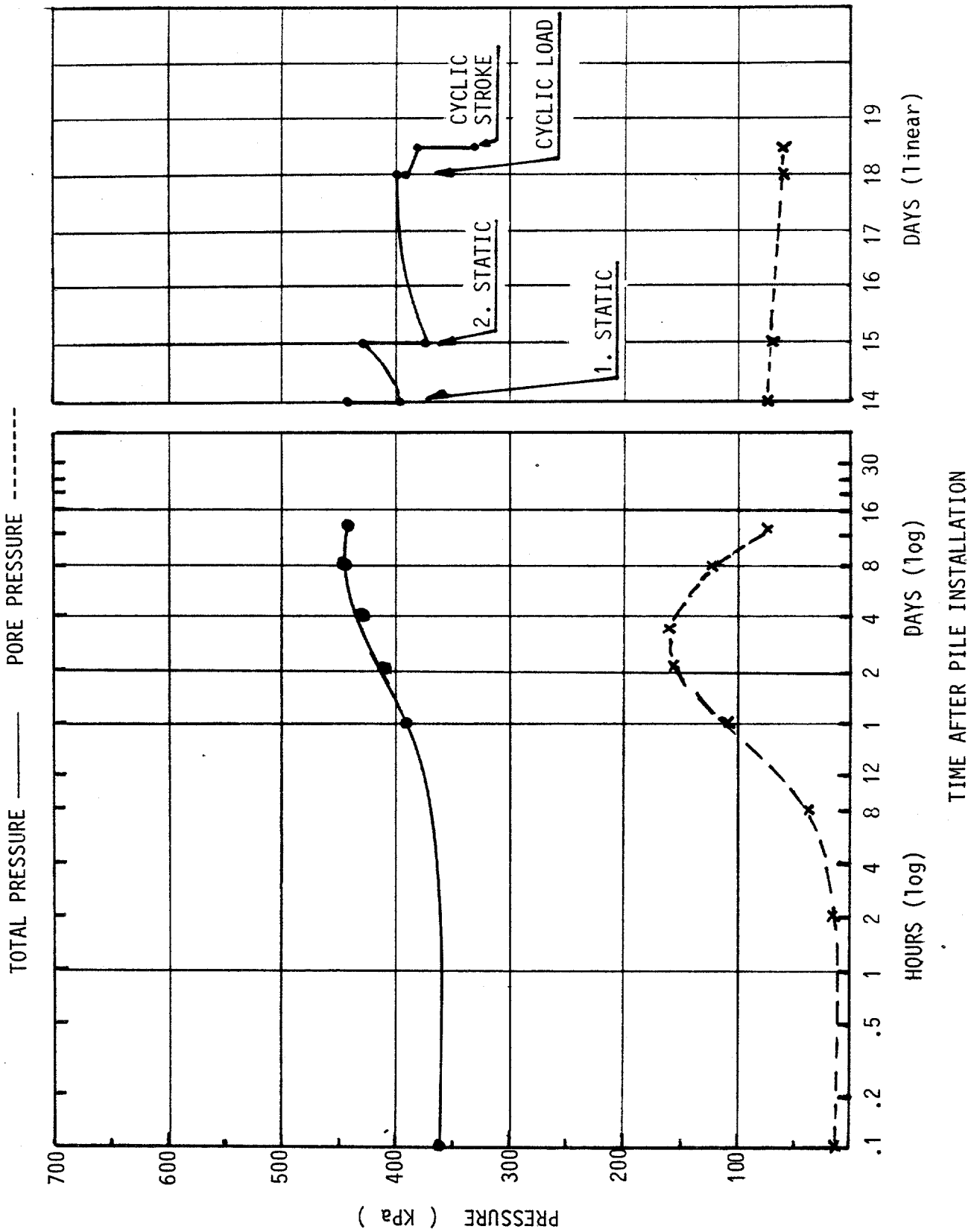

CNRD 13-2 TENSION PILE STUDY LABORATORY MODEL PILE TESTS

TEST 8, STRATUM III, Pressure at pile wall after installation

DET NORSKE VERITAS Geotechnical Laboratory	Drawn by	Scale
	Approved	Date
		Fig. No. 4

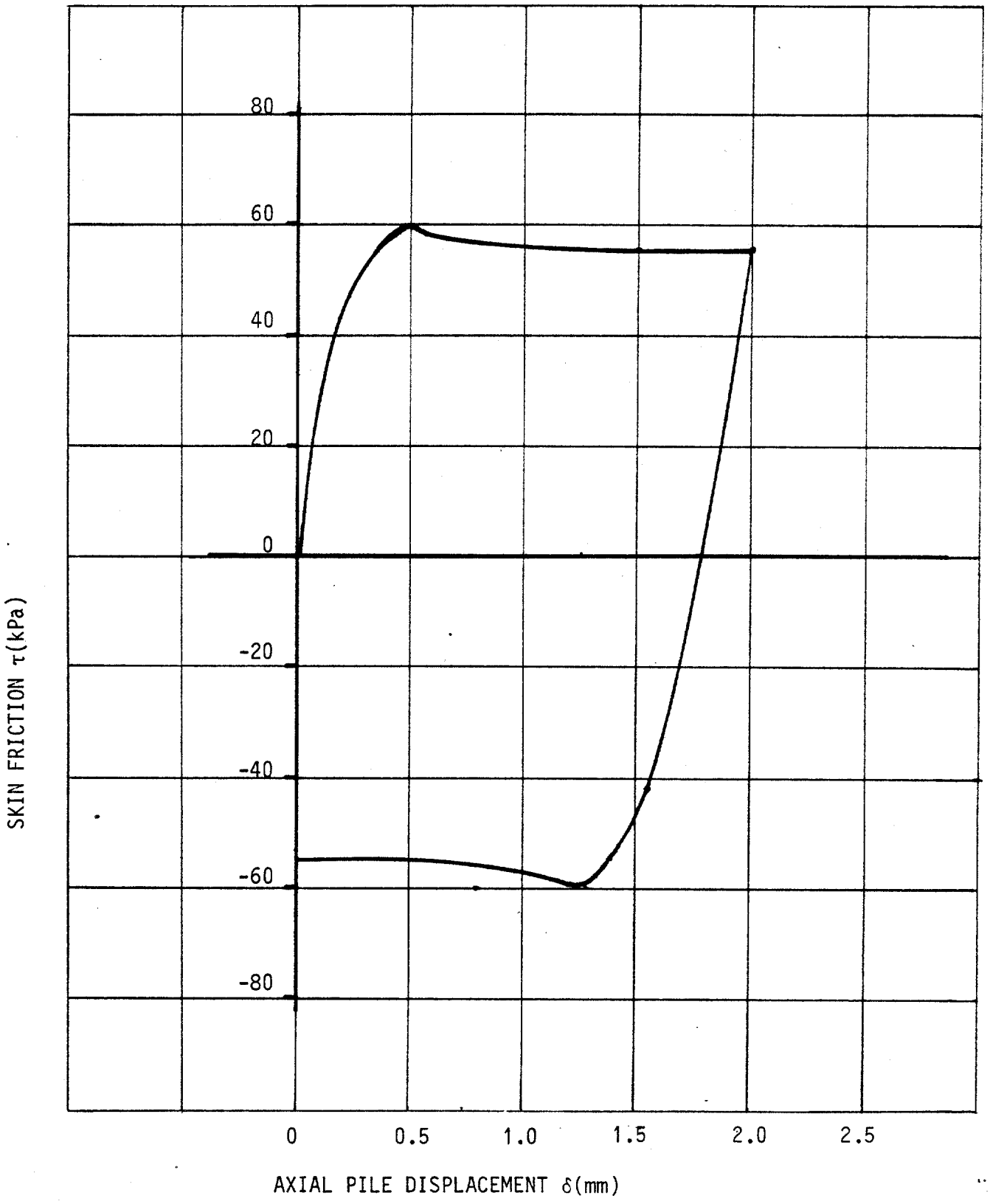

CNRD 13-2 TENSION PILE STUDY LABORATORY MODEL PILE TESTS

TEST 8, STRATUM III, STATIC TEST 1

DET NORSKE VERITAS Geotechnical Laboratory	Drawn by	Scale
	Approved	Date
		Fig. No. 5

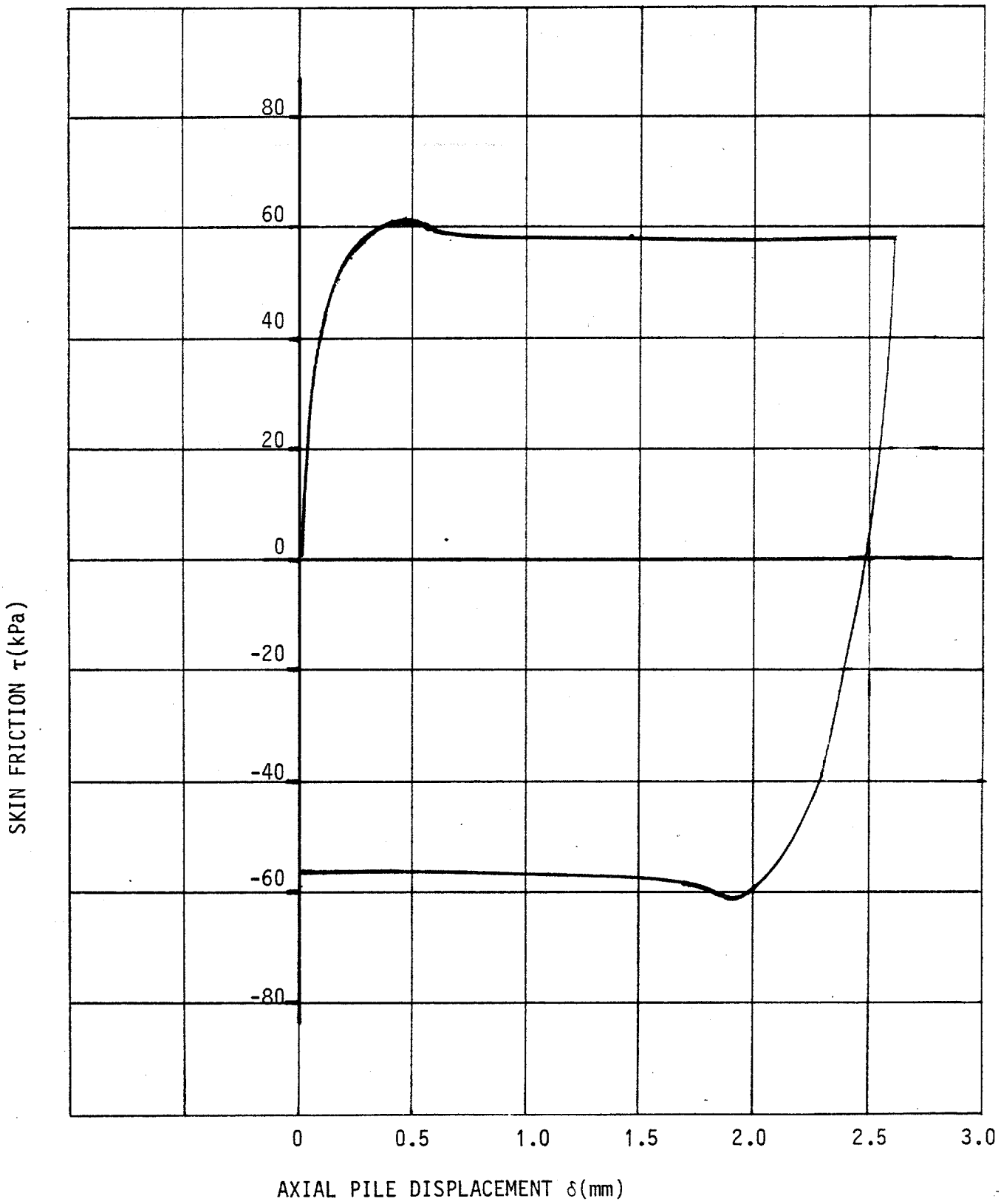

CNRD 13-2 TENSION PILE STUDY LABORATORY MODEL PILE TESTS

TEST 8, STRATUM III, STATIC TEST 2

DET NORSKE VERITAS Geotechnical Laboratory	Drawn by	Scale
	Approved	Date
		Fig. No. 6

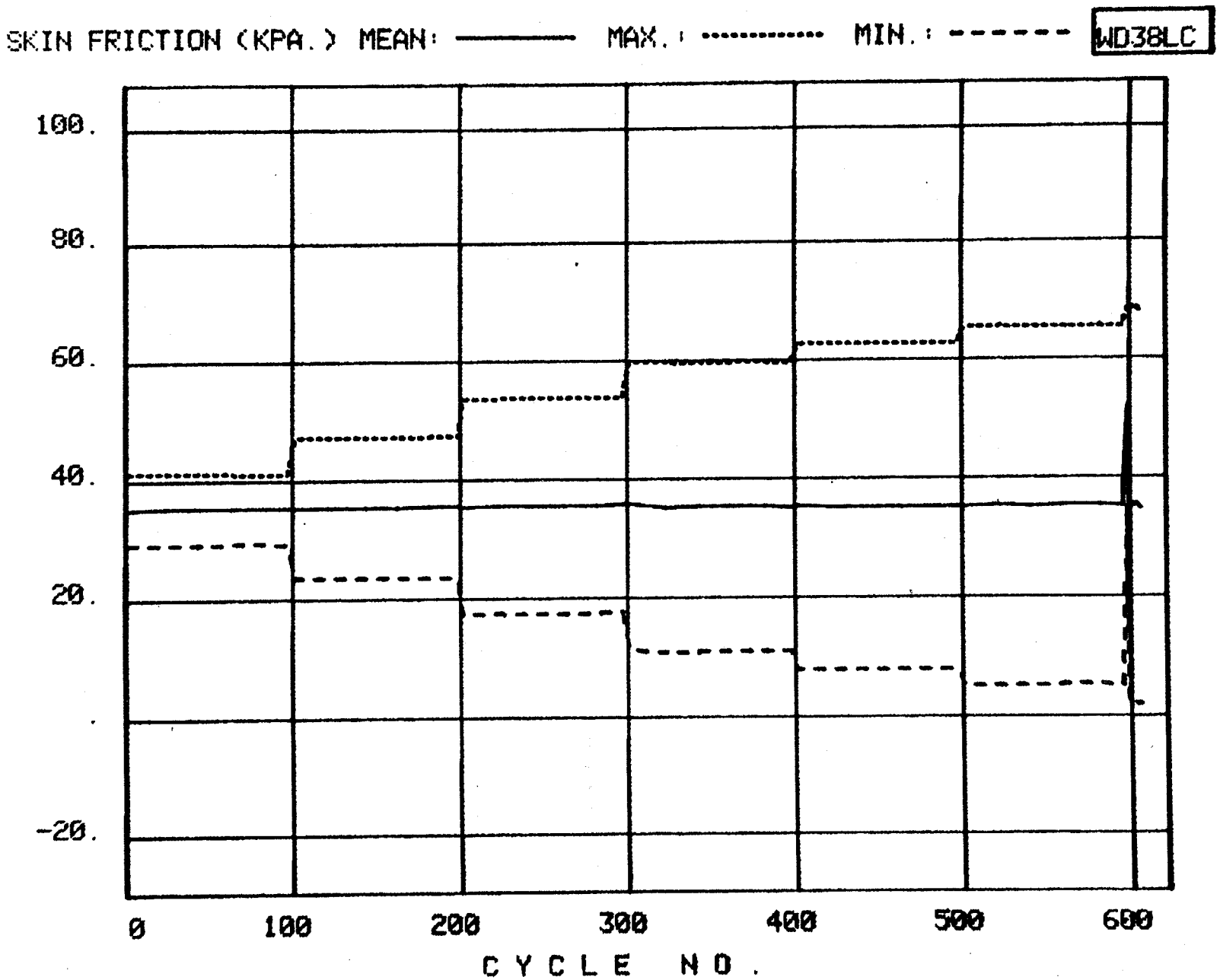
SKIN FRICTION (KPA.) MEAN: MAX.: MIN.:
WD38LC
100.
80.
60.
40.
20.
-20.
0
100
200
300
400
500
600
CYCLE NO.

Fig.7

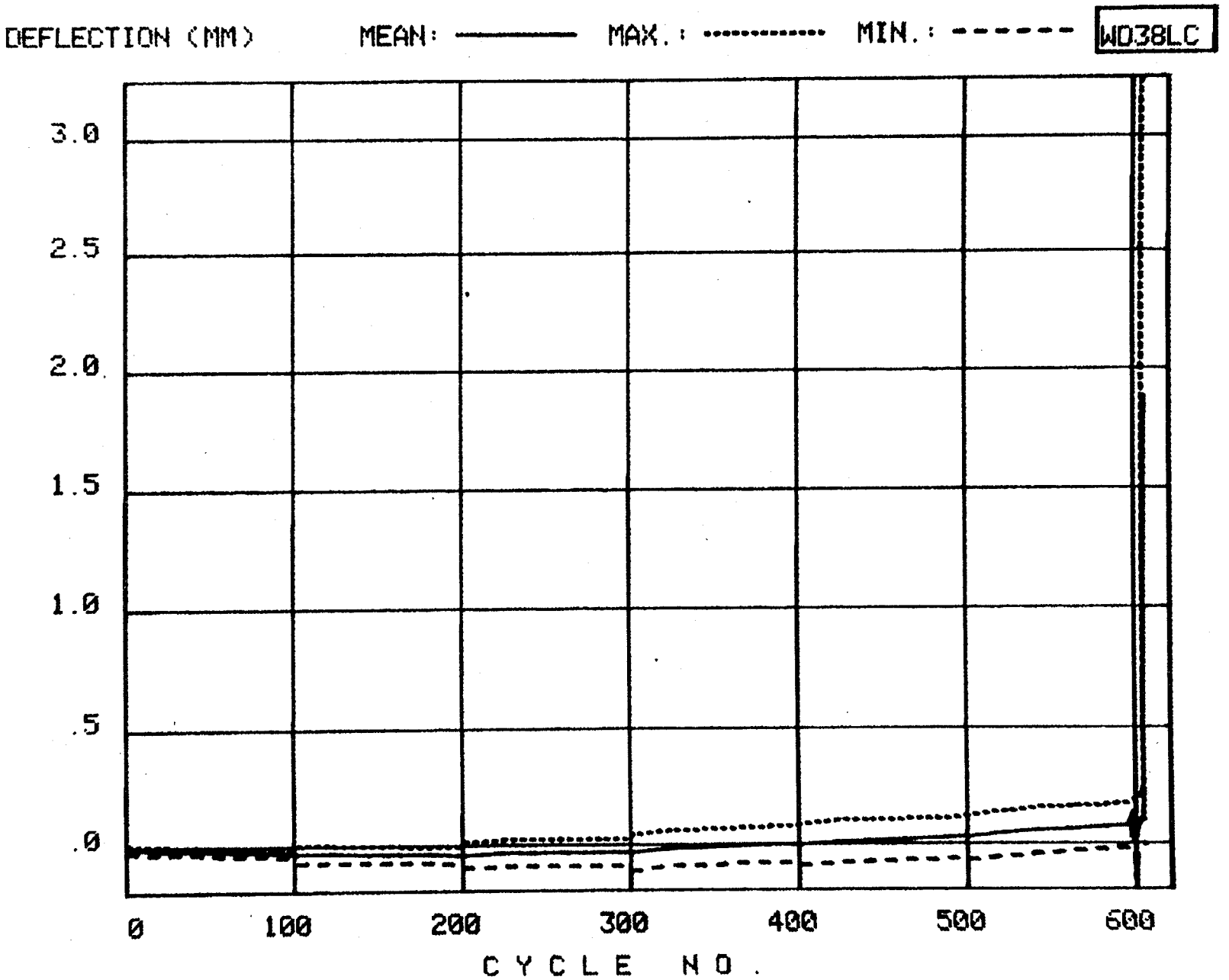
DEFLECTION (MM)
MEAN:
MAX.:
MIN.:
WD38LC
3.0
2.5
2.0
1.5
1.0
.5
.0
0
100
200
300
400
500
600
CYCLE NO.

Fig.8

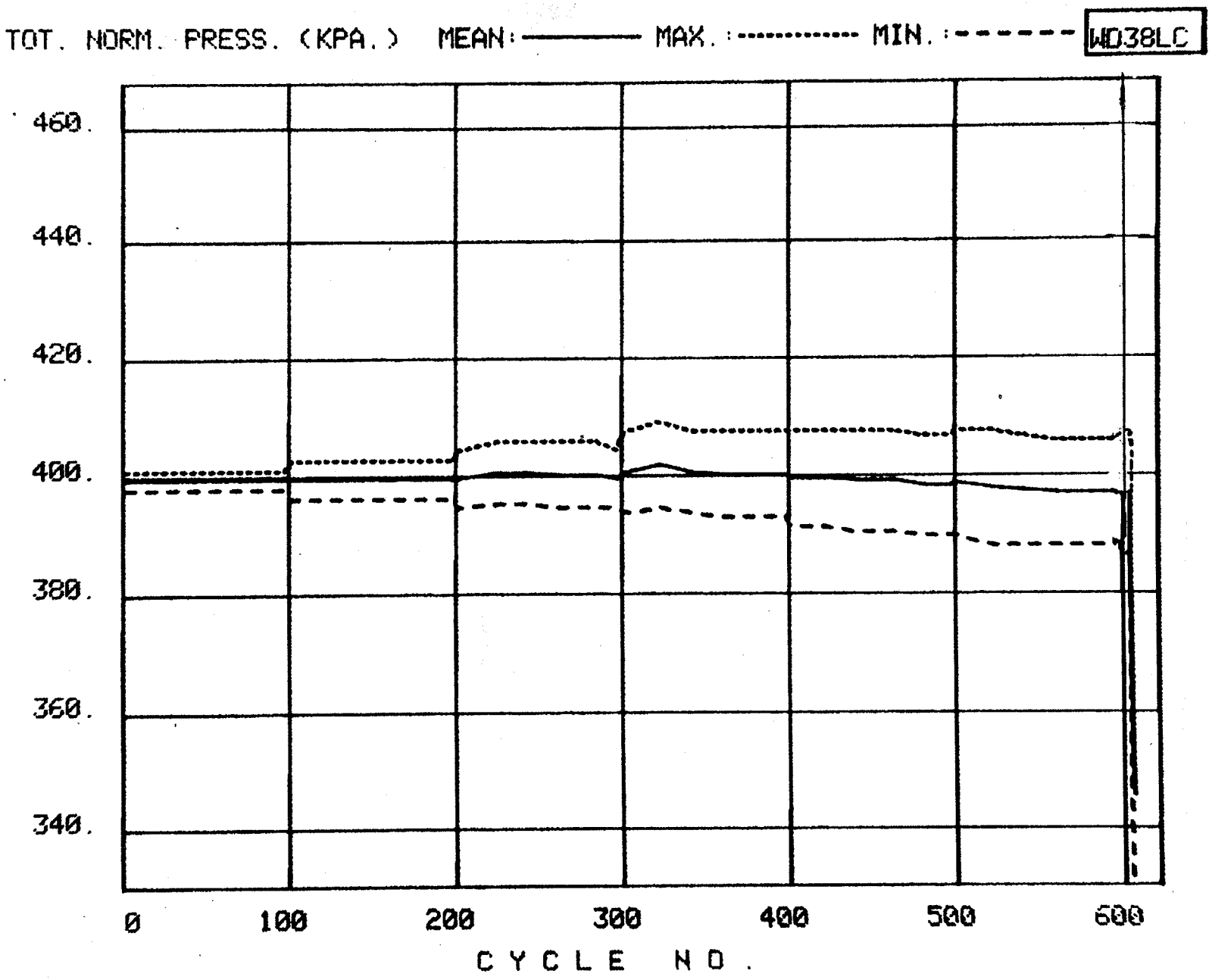
TOT. NORM. PRESS. (KPA.)
MEAN:
MAX.:
MIN.:
WD38LC
460.
440.
420.
400.
380.
360.
340.
0
100
200
300
400
500
600
CYCLE NO.

Fig.9

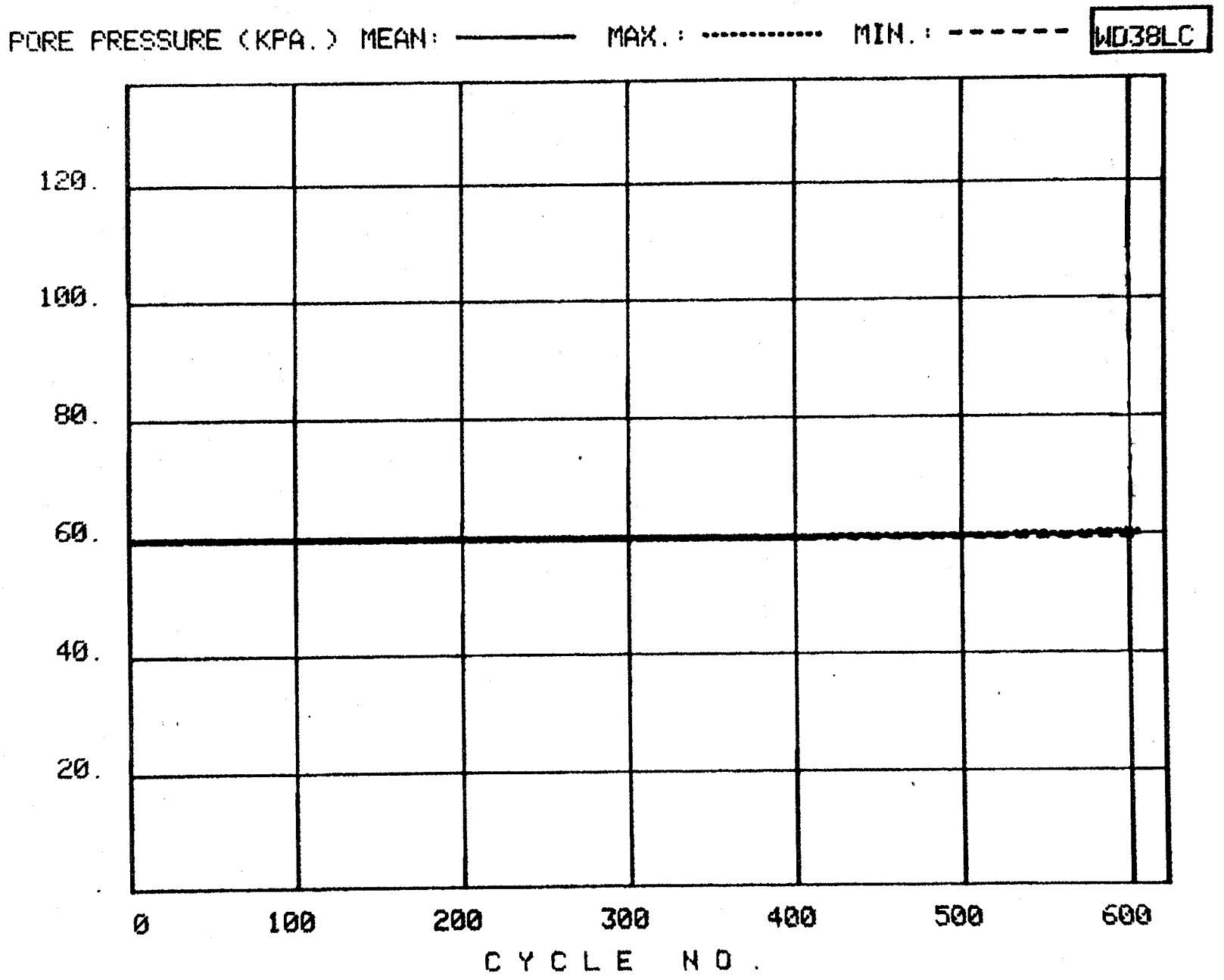
PORE PRESSURE (KPA.) MEAN: MAX.: MIN.:
WD38LC
120.
100.
80.
60.
40.
20.
0
100
200
300
400
500
600
CYCLE NO.

Fig.10

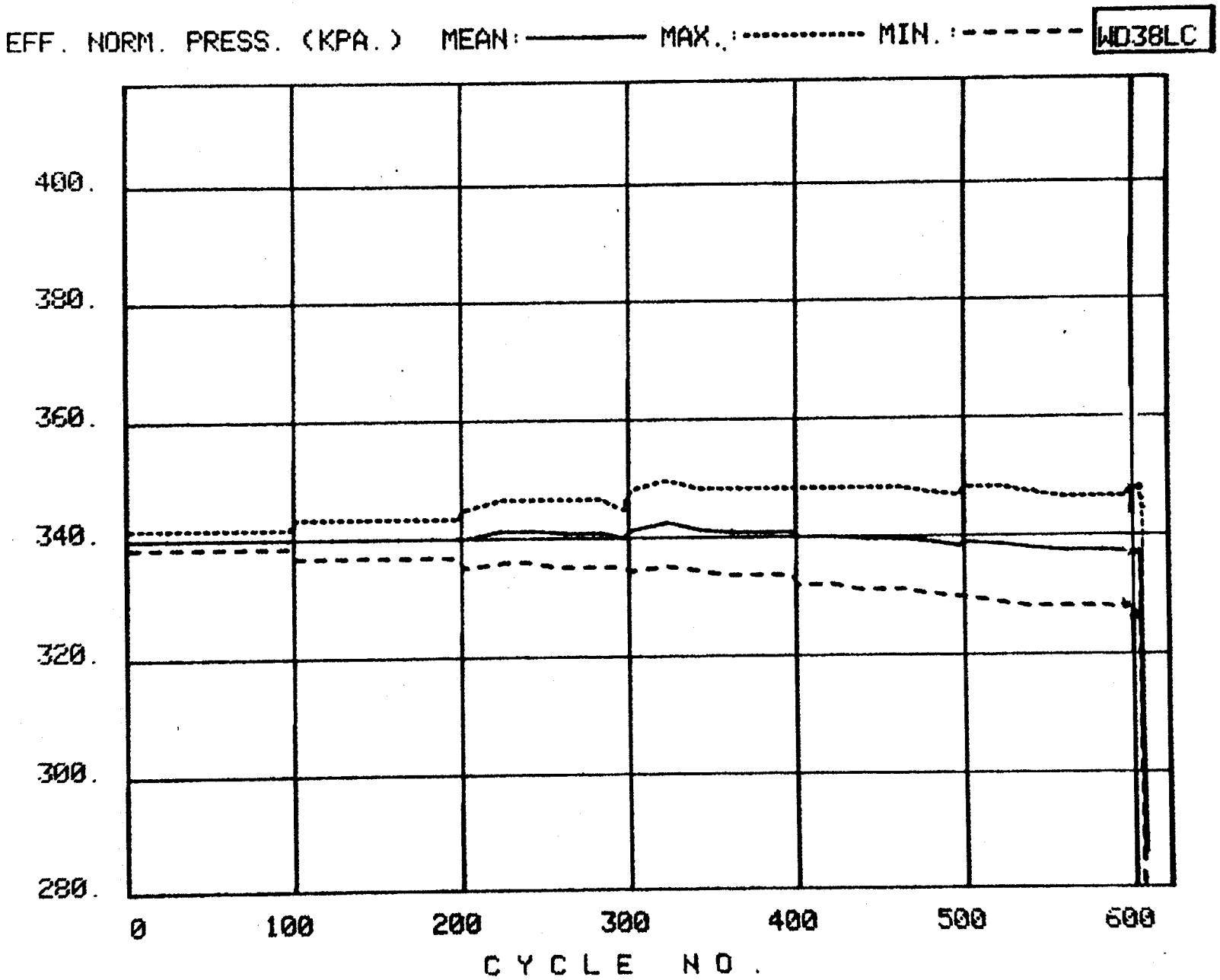
EFF. NORM. PRESS. (KPA.)
MEAN:
MAX.:
MIN.:
WD38LC
400.
380.
360.
340.
320.
300.
280.
0
100
200
300
400
500
600
CYCLE NO.

Fig.11

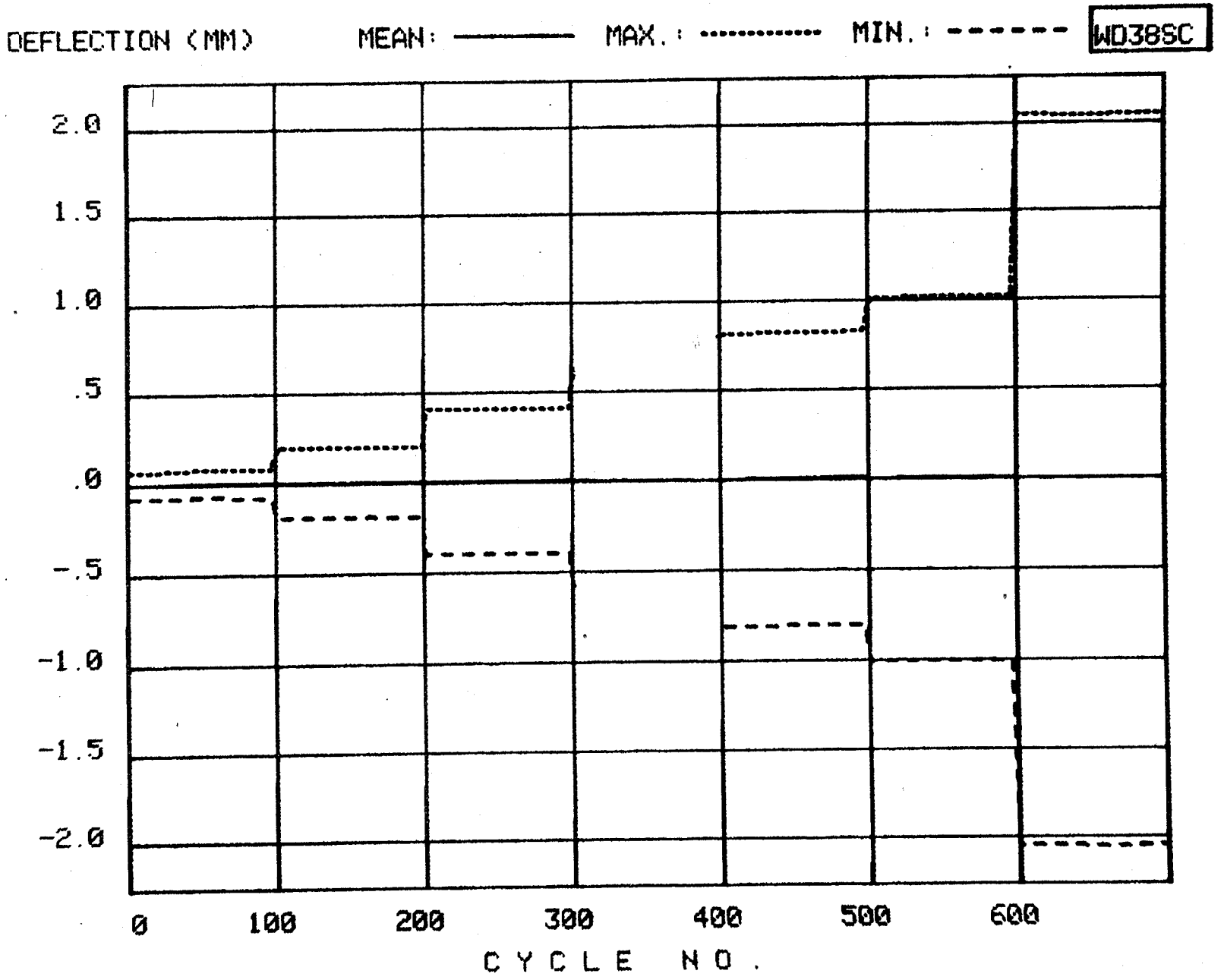
DEFLECTION (MM)
MEAN:
MAX.:
MIN.:
WD38SC
2.0
1.5
1.0
.5
.0
-.5
-1.0
-1.5
-2.0
0
100
200
300
400
500
600
CYCLE NO.

Fig. 12

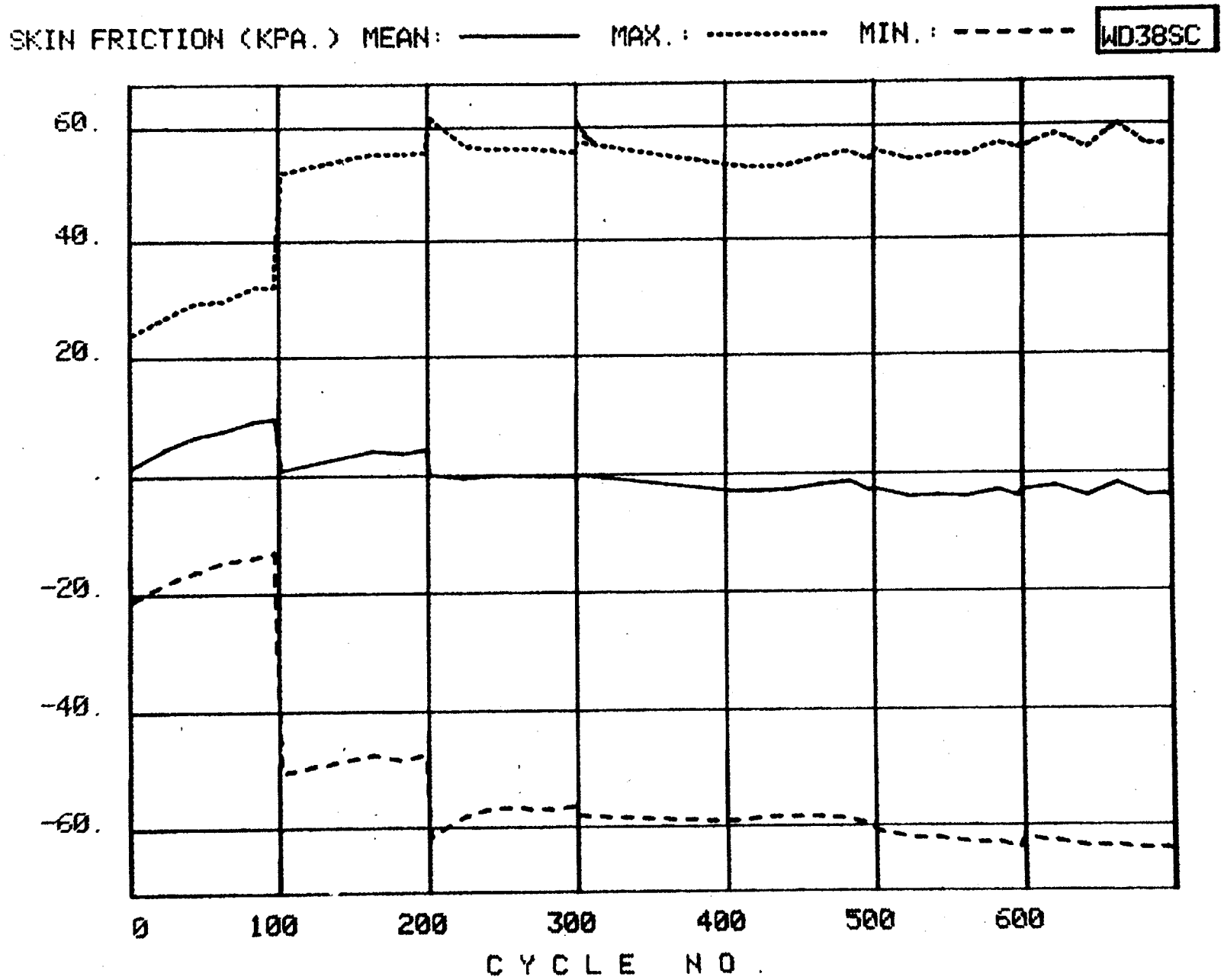
SKIN FRICTION (KPA.) MEAN: MAX.: MIN.:
WD38SC
60.
40.
20.
-20.
-40.
-60.
0
100
200
300
400
500
600
CYCLE NO.

Fig.13

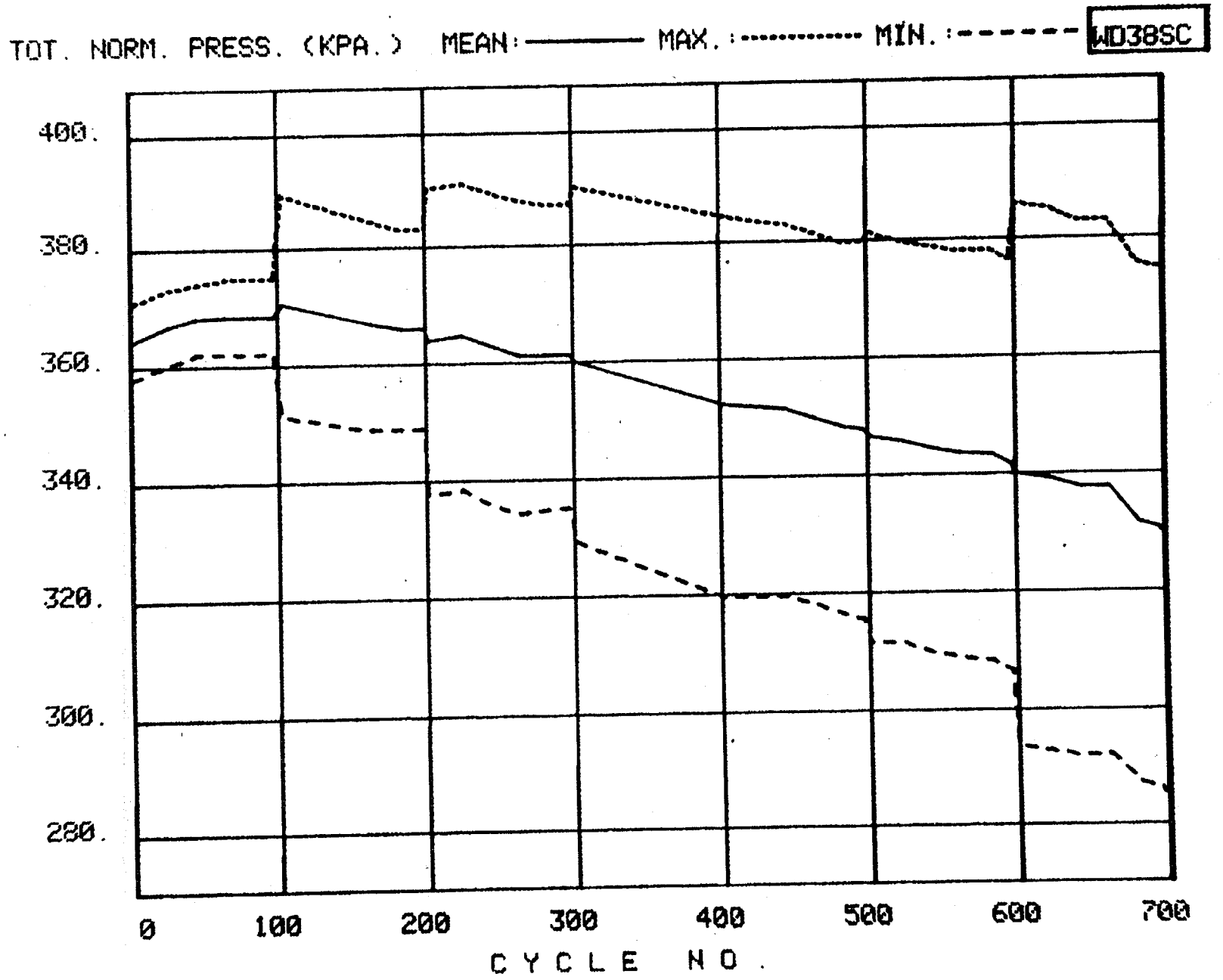
TOT. NORM. PRESS. (KPA.)
MEAN:
MAX.:
MIN.:
WD38SC
400.
380.
360.
340.
320.
300.
280.
0
100
200
300
400
500
600
700
CYCLE NO.

Fig.14

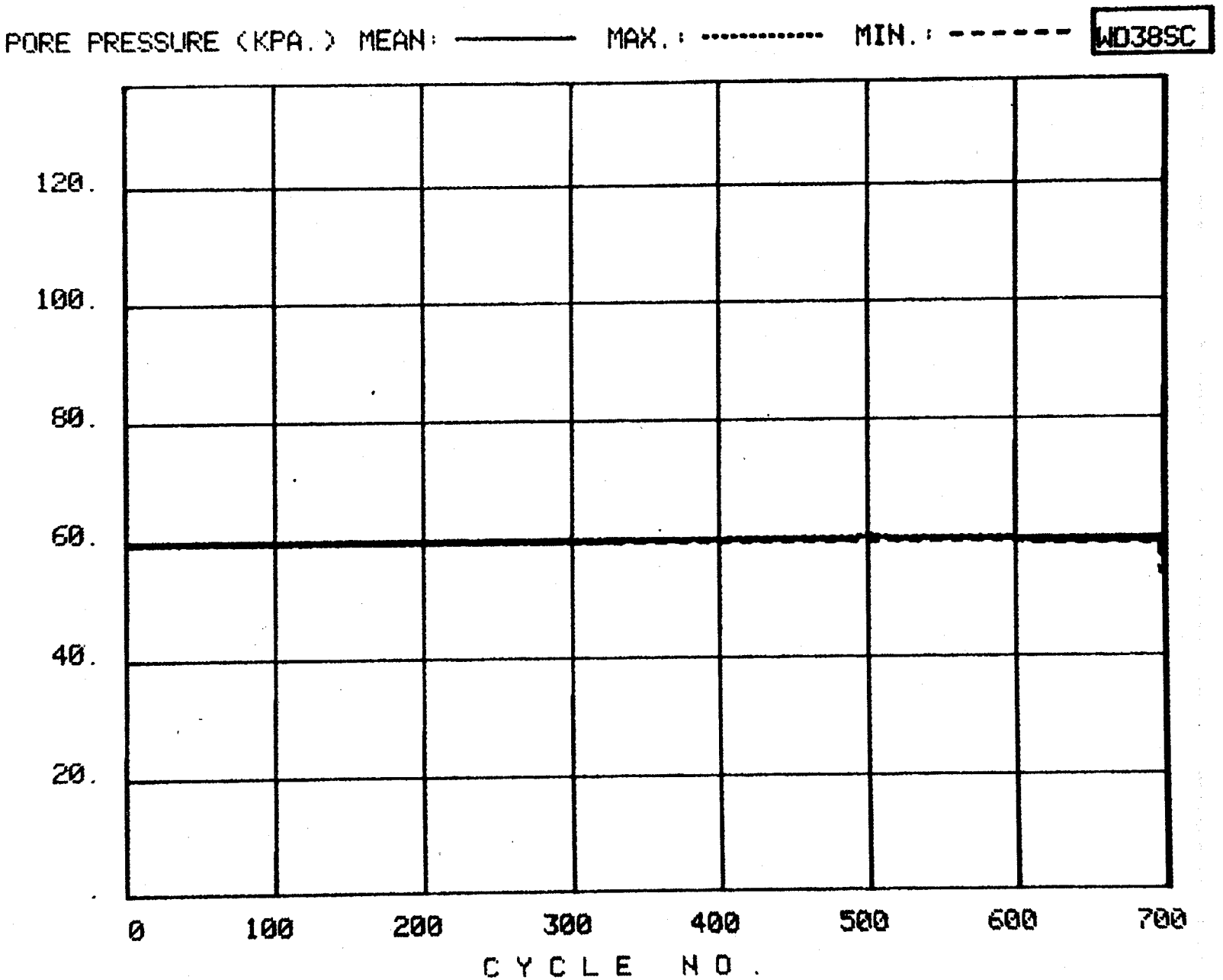
PORE PRESSURE (KPA.) MEAN: ——— MAX.: ····· MIN.: - - - - - -
WD38SC
120.
100.
80.
60.
40.
20.
0
100
200
300
400
500
600
700
CYCLE NO.

Fig.15

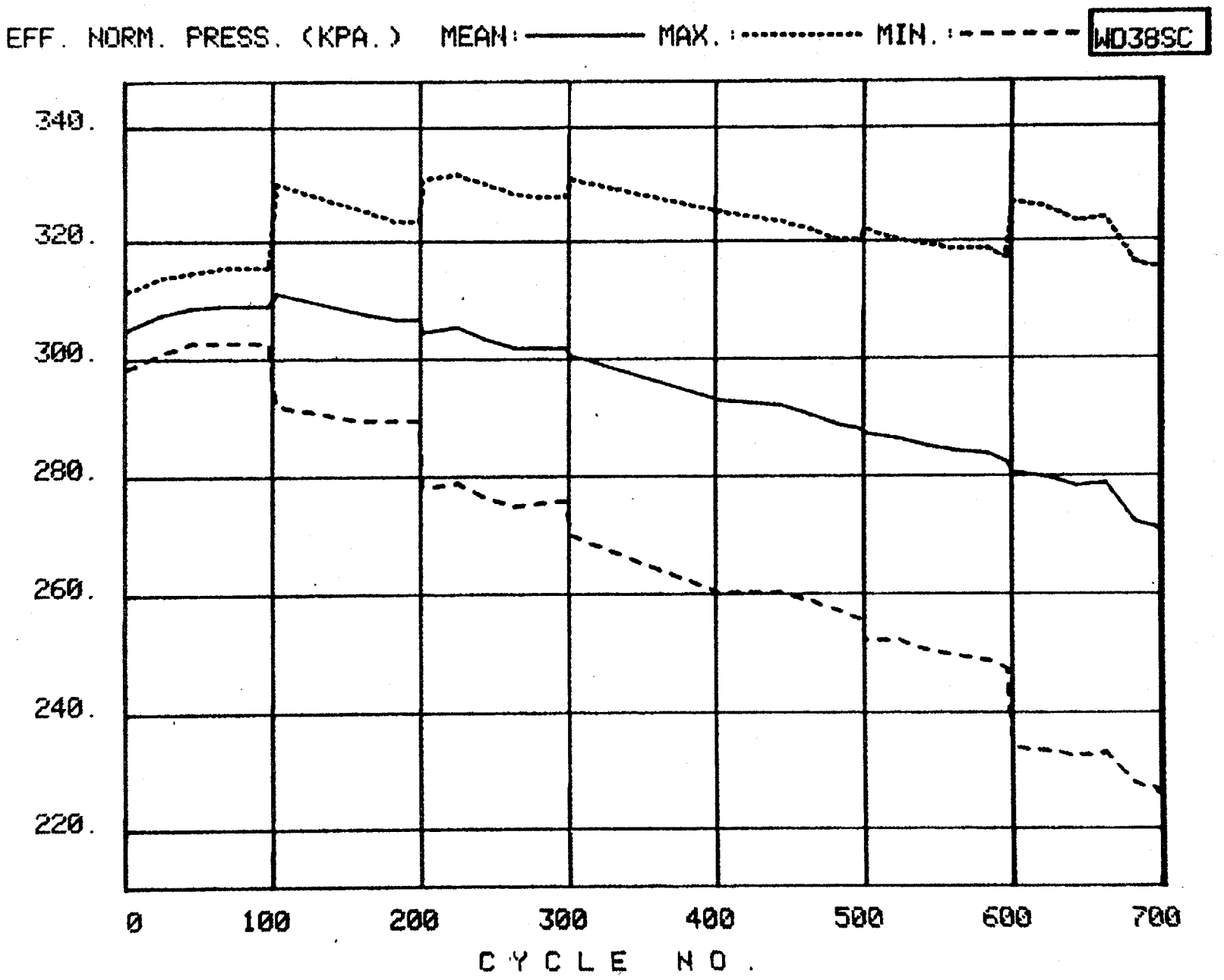
EFF. NORM. PRESS. (KPA.)
MEAN:
MAX.:
MIN.:
WD38SC
340.
320.
300.
280.
260.
240.
220.
0
100
200
300
400
500
600
700
CYCLE NO.

Fig.16

TEST 8, STRATUM III

SHEAR STRENGTH (kPa) FROM POCKET PENETROMETER AFTER PILE TEST

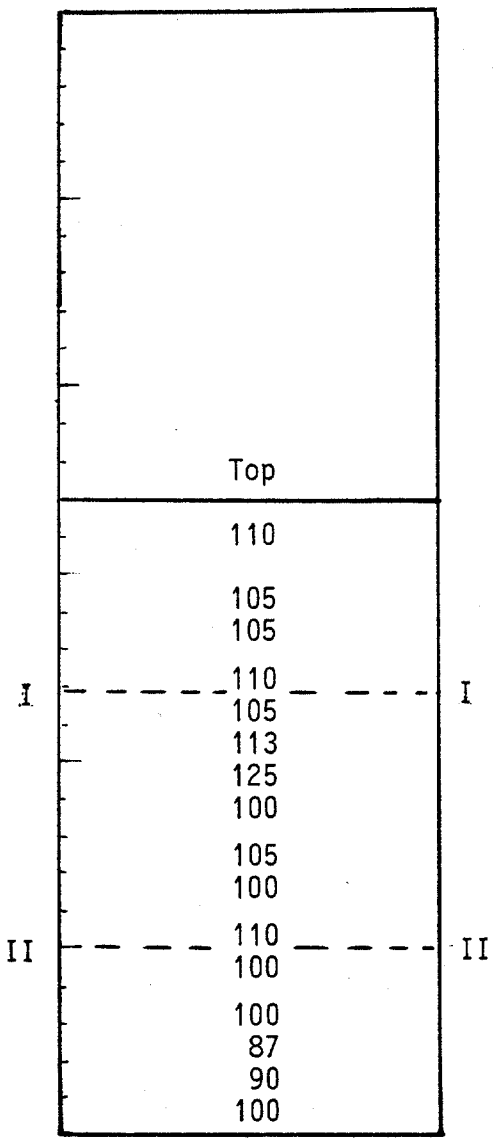

Scale 1:4

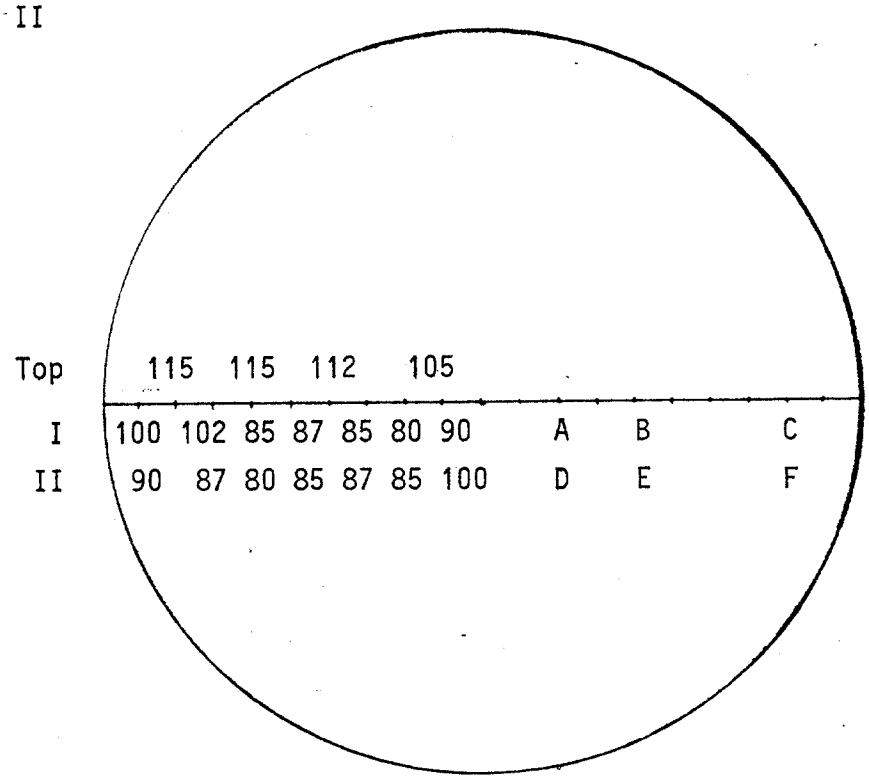

Scale: 1:2

CNRD 13-2 TENSION PILE STUDY LABORATORY MODEL PILE TESTS 231004		
TEST 8 , STRATUM III, Pocket penetrometer tests after pile test		Scale
DET NORSKE VERITAS Geotechnical Laboratory	Drawn by	Date
	Approved	Fig. No. 17

UNCONFINED COMPRESSION TESTS

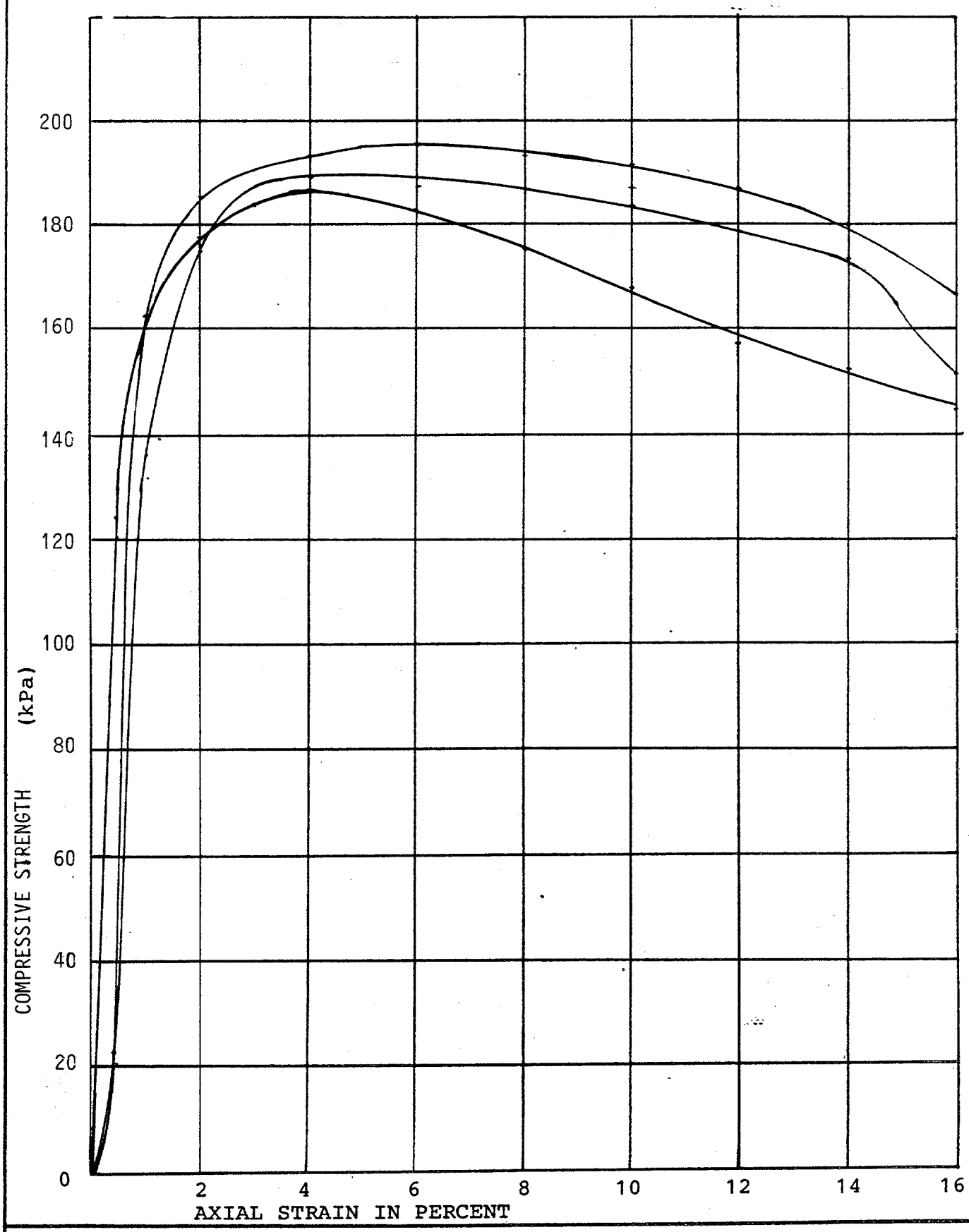

CNRD 13-2 TENSION PILE STUDY LABORATORY MODEL PILE TESTS

TEST 8, STRATUM III, Unconfined compression tests after pile test

DET NORSKE VERITAS Geotechnical Laboratory	Drawn by Terje Engesæt	Scale
	Approved	Date
		Fig. No. 18

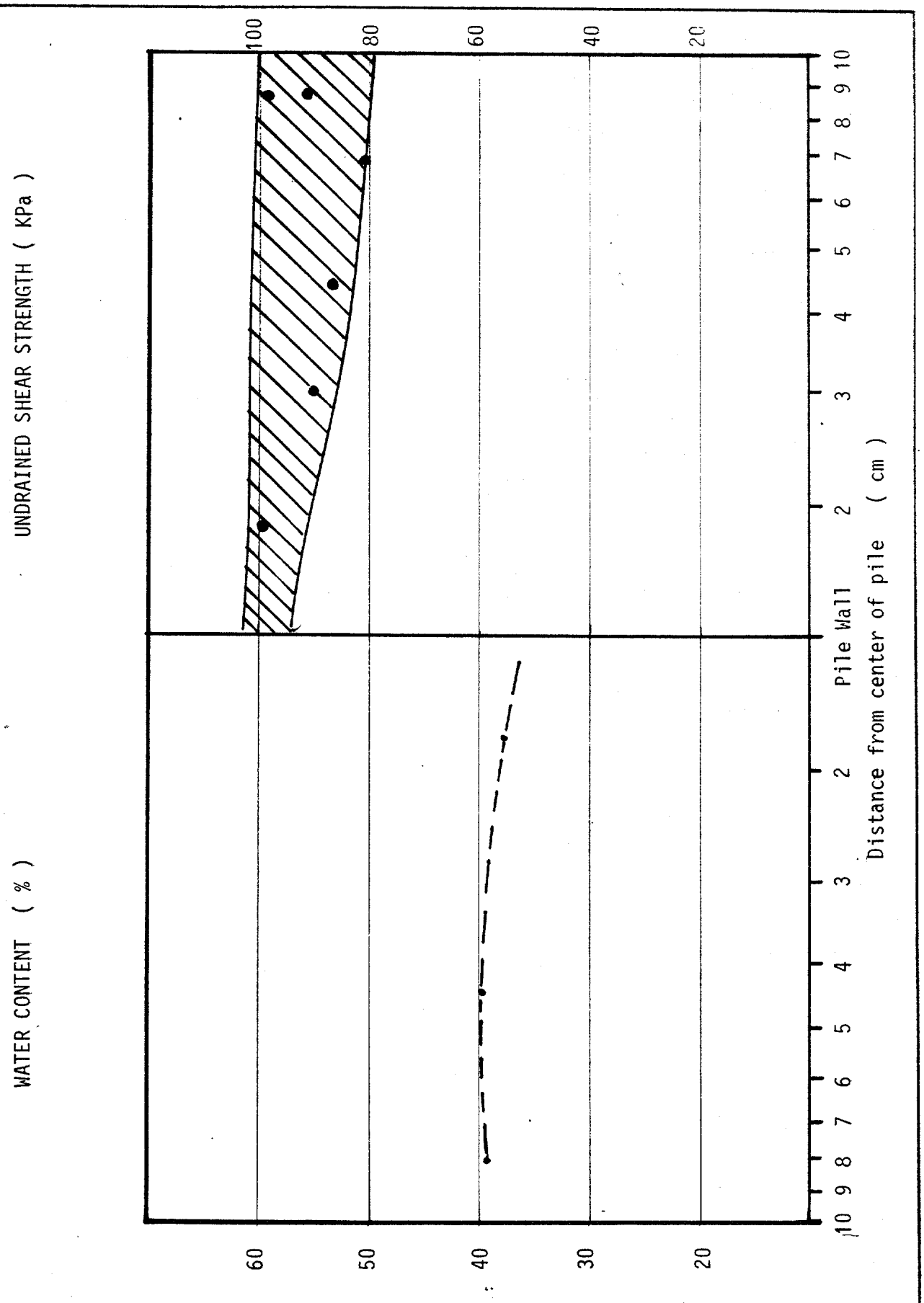

CNRD 13-2 TENSION PILE STUDY LABORATORY MODEL PILE TESTS

TEST 8, STRATUM III, Water content and shear strength after test

DET NORSKE VERITAS Geotechnical Laboratory	Drawn by	Scale
	Approved	Date
		Fig. No. 19

Appendix EA

Plotted Results from WD38LC

Figures EA-1 through EA-9

Skin Friction vs Deflection, Selected Cycles

Figures EA-10 through EA-13

Skin Friction vs Eff. Normal Pressure, Selected Cycl.

Figures EA-14 through EA-28

Skin Friction, Pore and Total Pressure, Selected Cycles

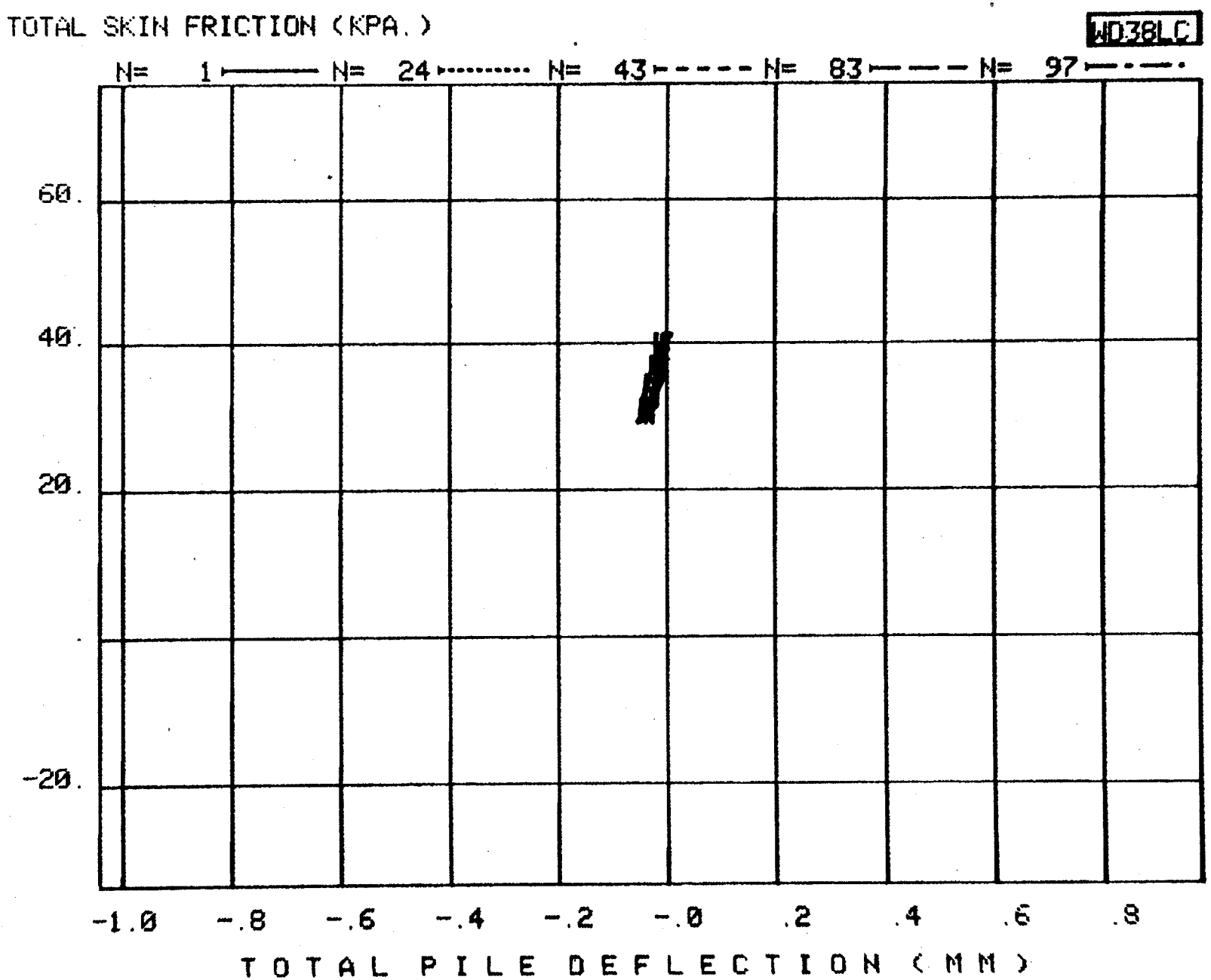
TOTAL SKIN FRICTION (KPA.)
WD38LC
N= 1
N= 24
N= 43
N= 83
N= 97
60.
40.
20.
-20.
-1.0
-.8
-.6
-.4
-.2
-.0
.2
.4
.6
.8
TOTAL PILE DEFLECTION (MM)

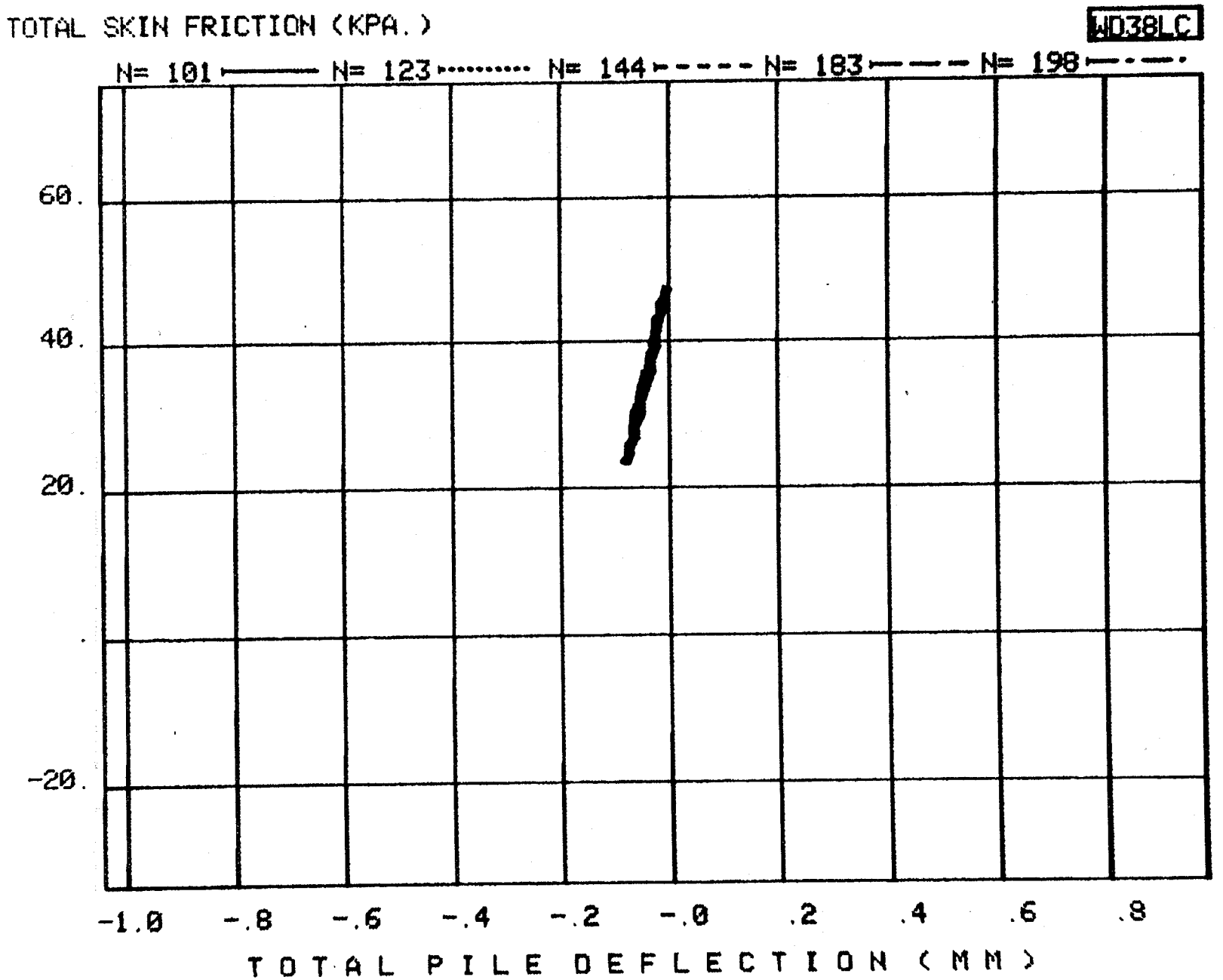
TOTAL SKIN FRICTION (KPA.)
WD38LC
N= 101
N= 123
N= 144
N= 183
N= 198
60.
40.
20.
-20.
-1.0
-.8
-.6
-.4
-.2
-.0
.2
.4
.6
.8
TOTAL PILE DEFLECTION (MM)

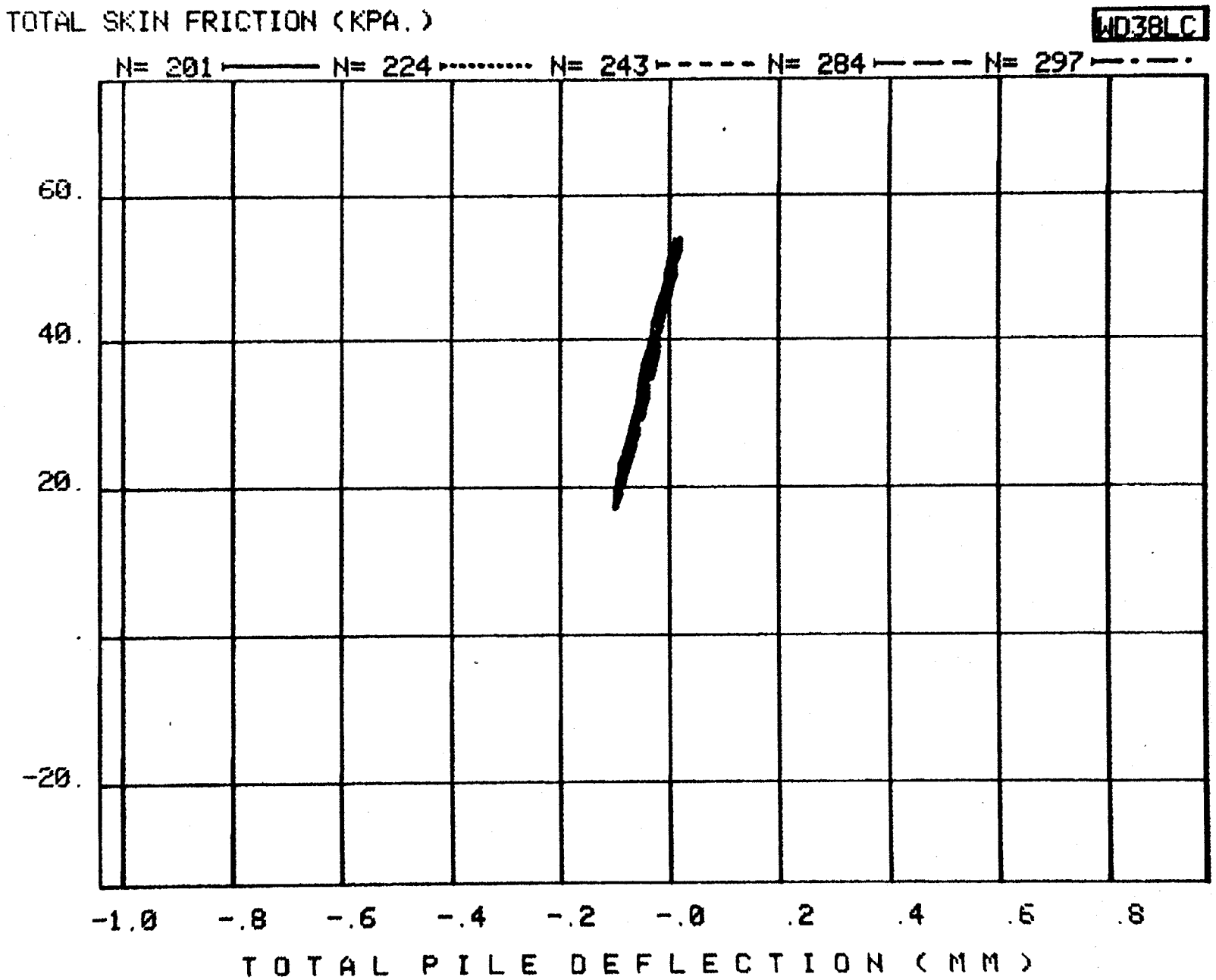
TOTAL SKIN FRICTION (KPA.)
WD38LC
N= 201
N= 224
N= 243
N= 284
N= 297
60.
40.
20.
-20.
-1.0
-.8
-.6
-.4
-.2
-.0
.2
.4
.6
.8
TOTAL PILE DEFLECTION (MM)

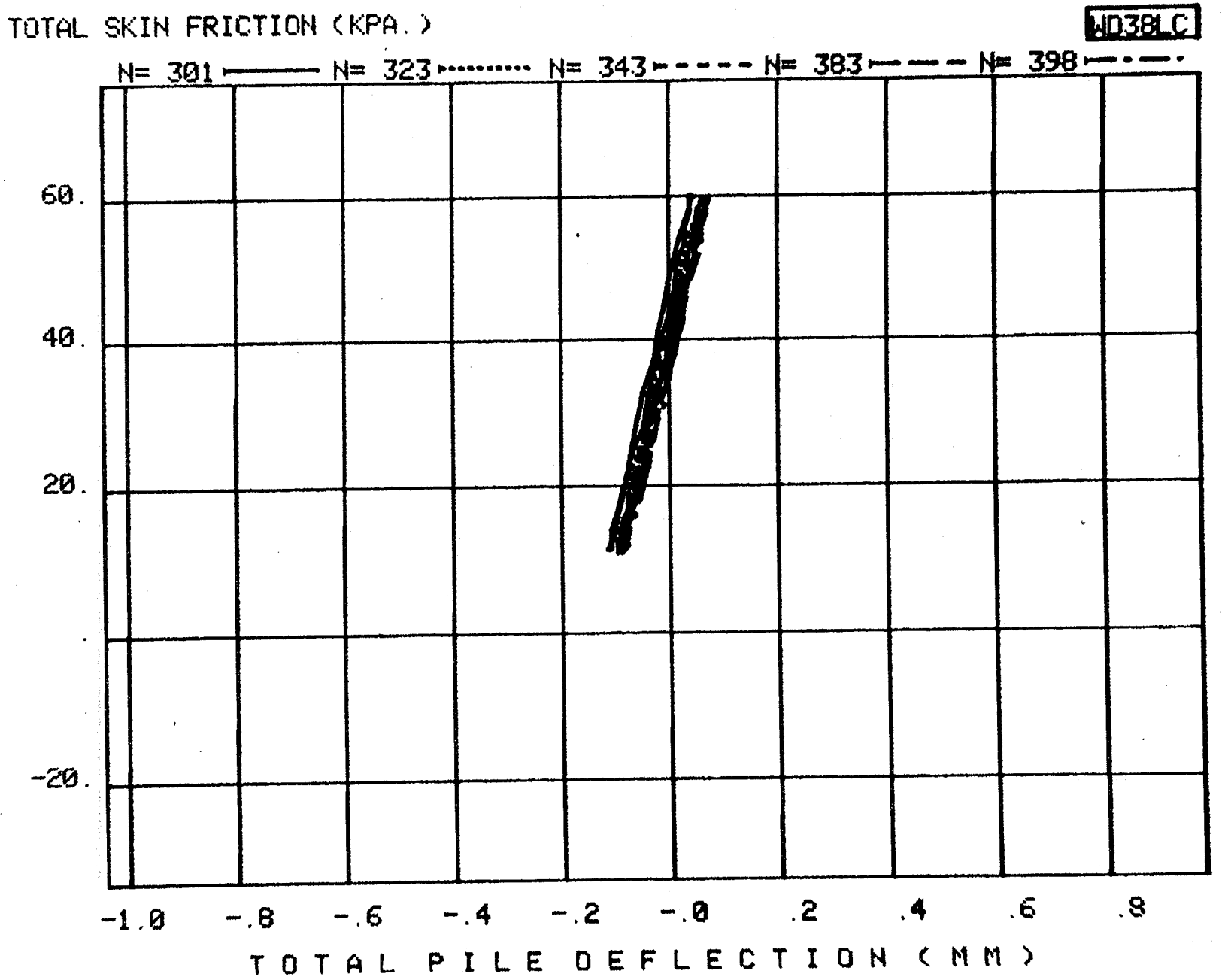
TOTAL SKIN FRICTION (KPA.)
WD38LC
N= 301
N= 323
N= 343
N= 383
N= 398
60.
40.
20.
-20.
-1.0
-.8
-.6
-.4
-.2
-.0
.2
.4
.6
.8
TOTAL PILE DEFLECTION (MM)

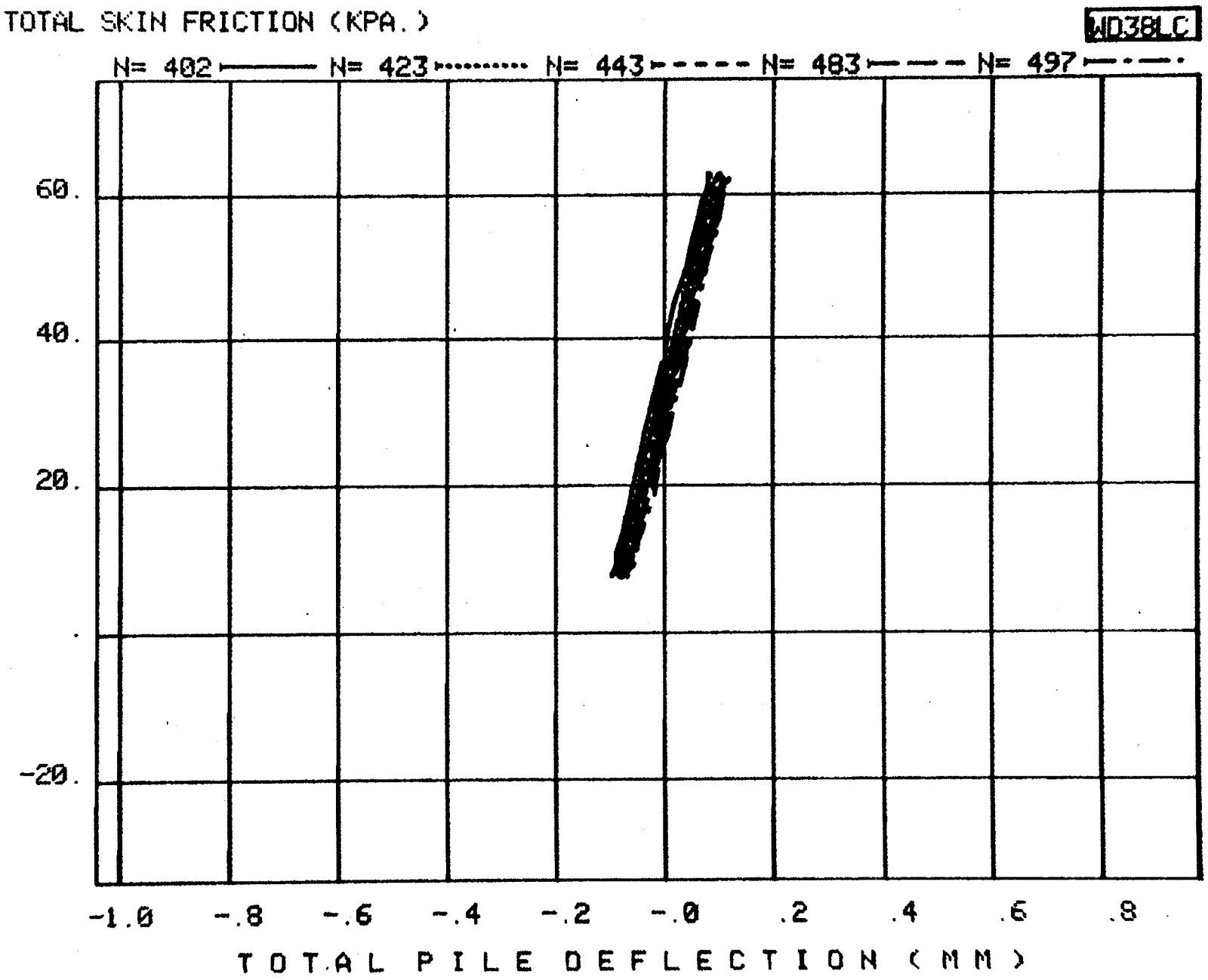
TOTAL SKIN FRICTION (KPA.)
WD38LC
N= 402
N= 423
N= 443
N= 483
N= 497
60.
40.
20.
-20.
-1.0
-.8
-.6
-.4
-.2
-.0
.2
.4
.6
.8
TOTAL PILE DEFLECTION (MM)

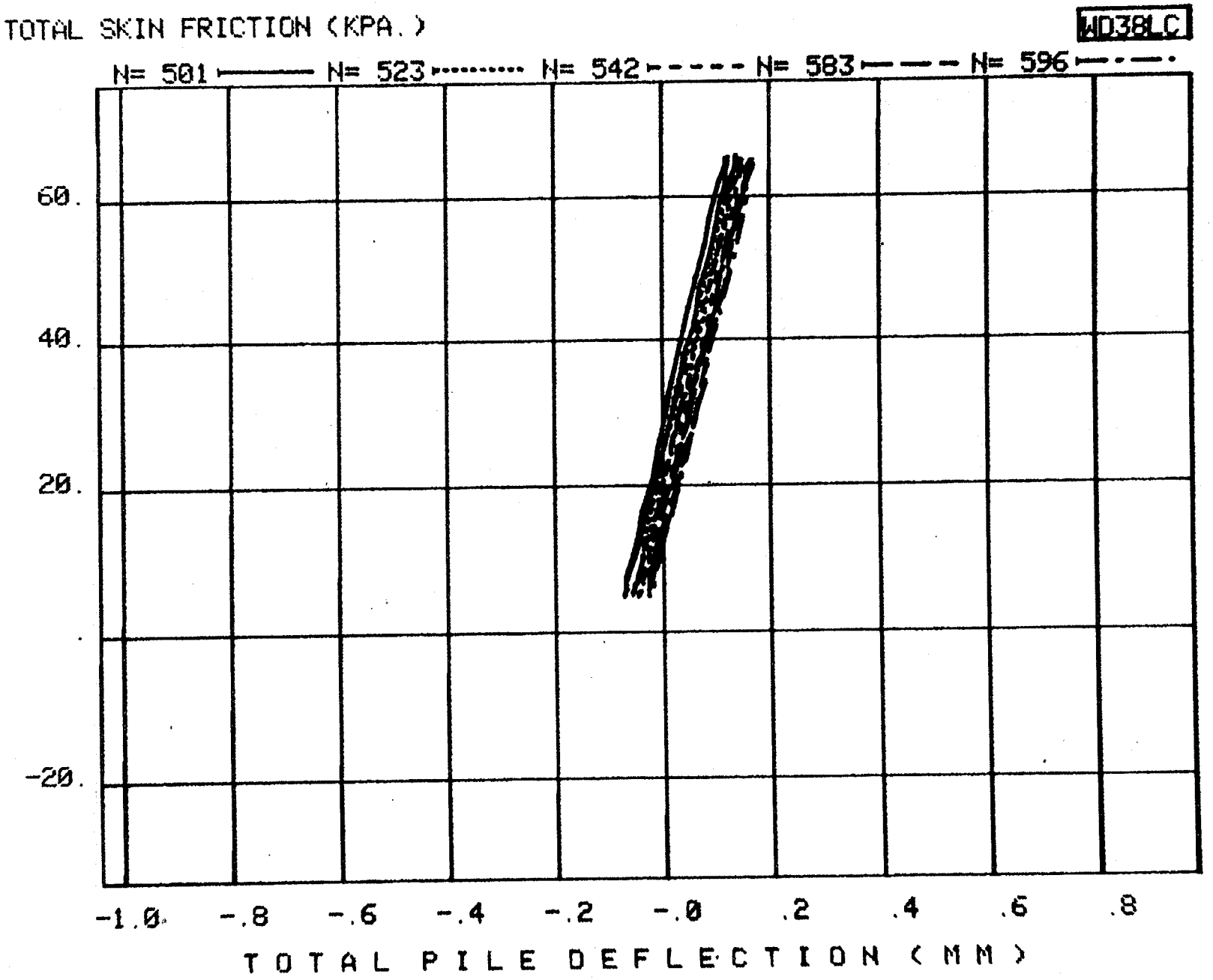
TOTAL SKIN FRICTION (KPA.)
WD38LC
N= 501
N= 523
N= 542
N= 583
N= 596
60.
40.
20.
-20.
-1.0
-.8
-.6
-.4
-.2
-.0
.2
.4
.6
.8
TOTAL PILE DEFLECTION (MM)

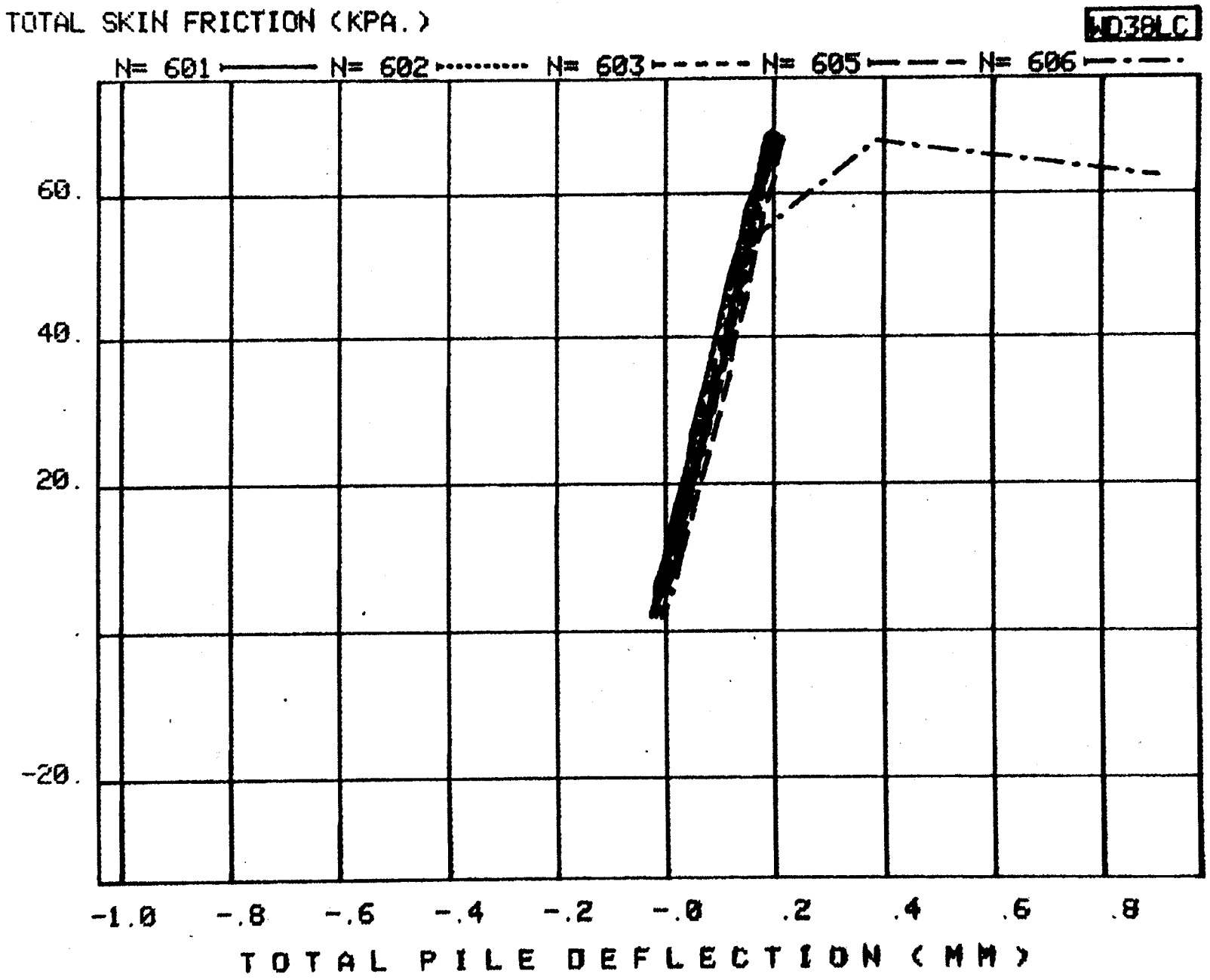
TOTAL SKIN FRICTION (KPA.)
WD38LC
N= 601
N= 602
N= 603
N= 605
N= 606
60.
40.
20.
-20.
-1.0
-.8
-.6
-.4
-.2
-.0
.2
.4
.6
.8
TOTAL PILE DEFLECTION (MM)

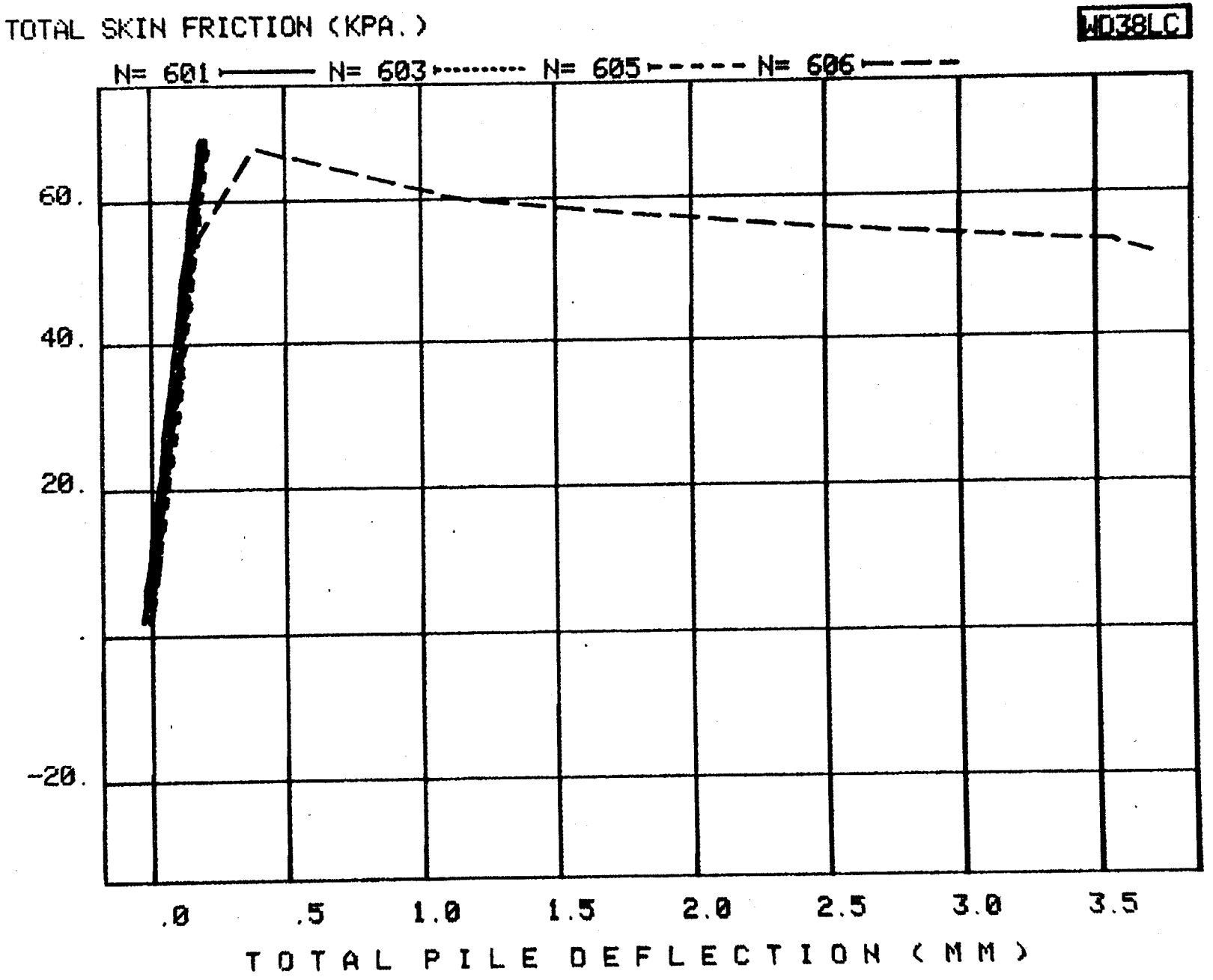
TOTAL SKIN FRICTION (KPA.)
WD38LC
N= 601
N= 603
N= 605
N= 606
60.
40.
20.
-20.
.0
.5
1.0
1.5
2.0
2.5
3.0
3.5
TOTAL PILE DEFLECTION (MM)

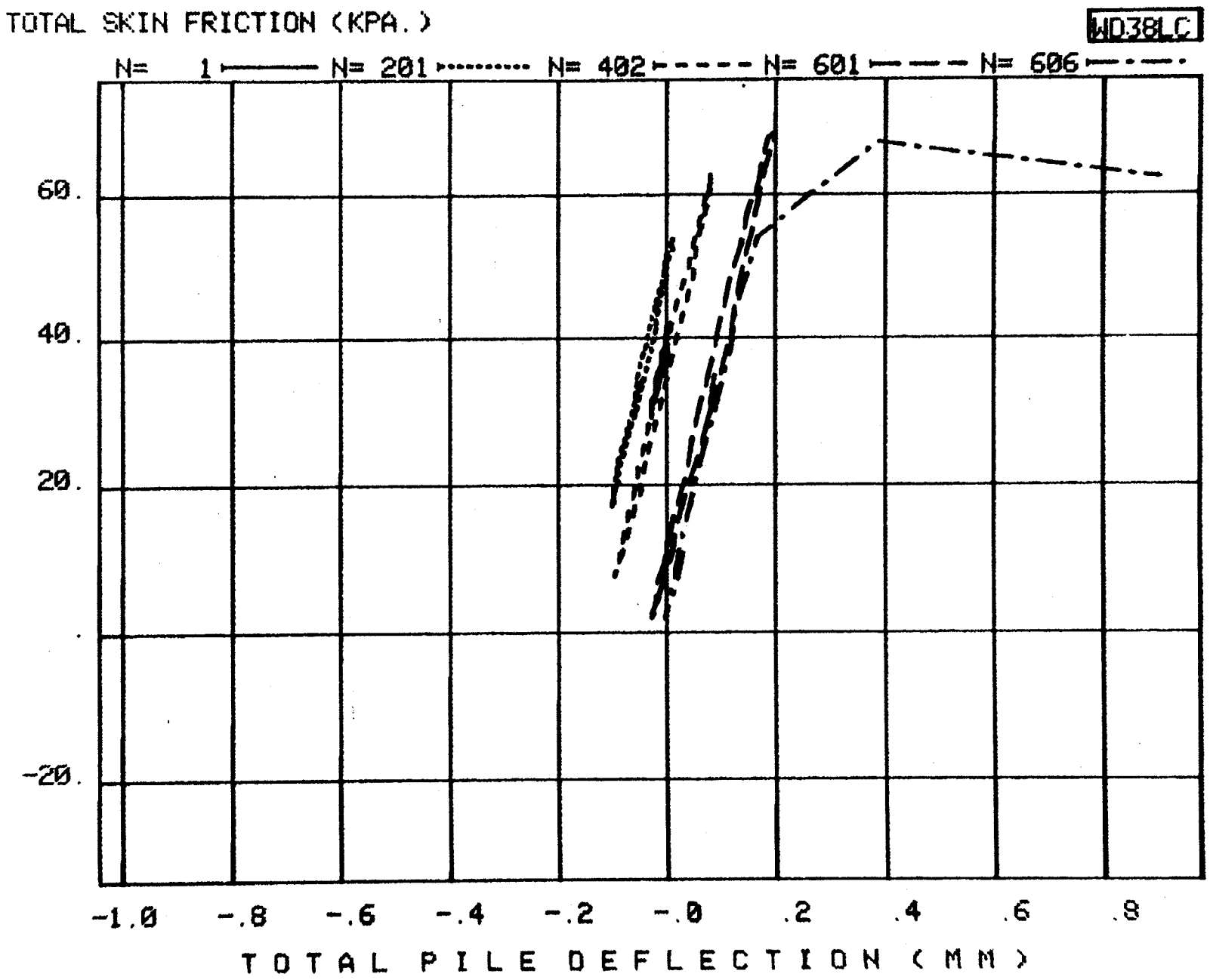
TOTAL SKIN FRICTION (KPA.)
WD38LC
N= 1
N= 201
N= 402
N= 601
N= 606
60.
40.
20.
-20.
-1.0
-.8
-.6
-.4
-.2
-.0
.2
.4
.6
.8
TOTAL PILE DEFLECTION (MM)

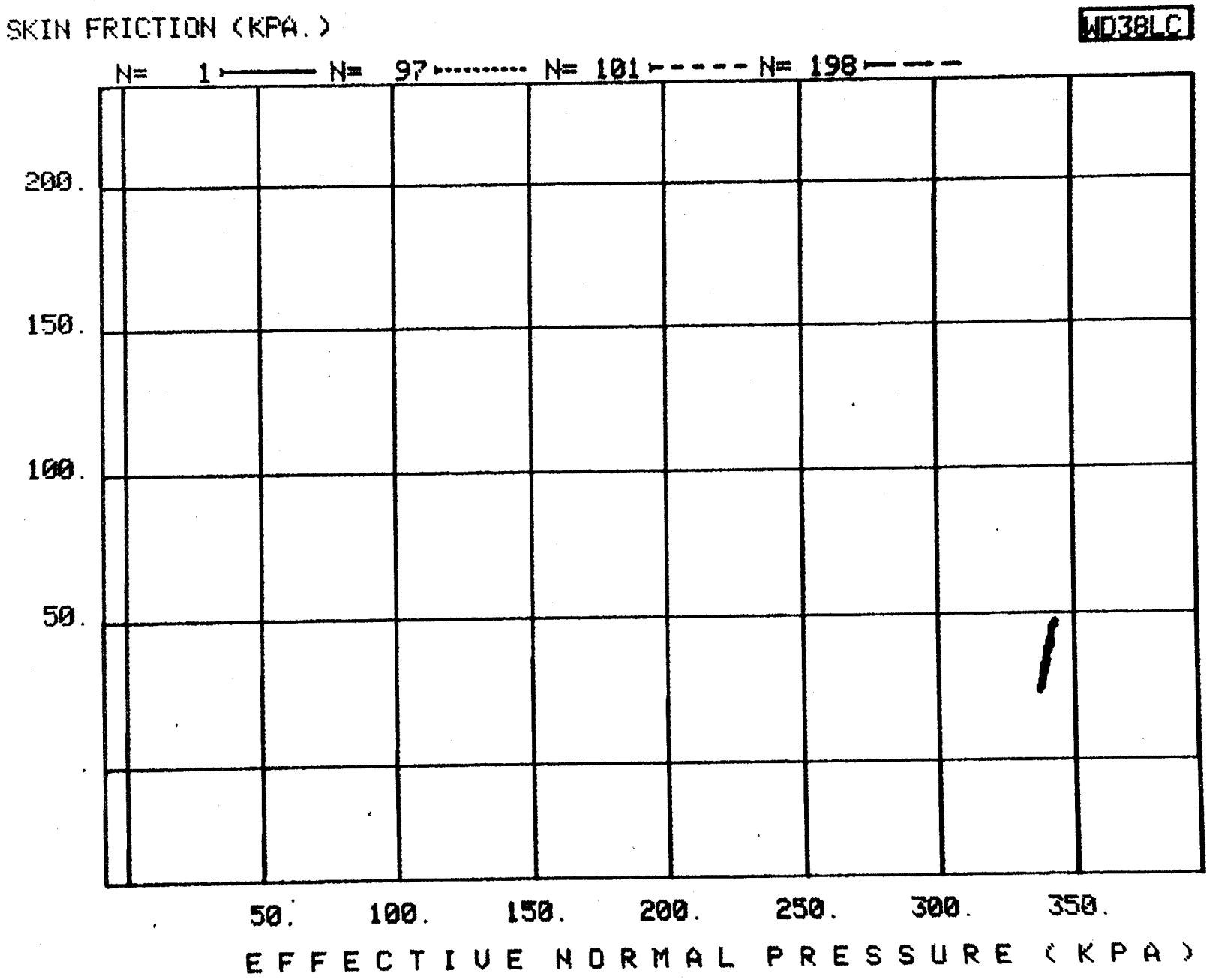
SKIN FRICTION (KPA.)
WD38LC
N= 1
N= 97
N= 101
N= 198
200.
150.
100.
50.
50.
100.
150.
200.
250.
300.
350.
EFFECTIVE NORMAL PRESSURE (KPA)

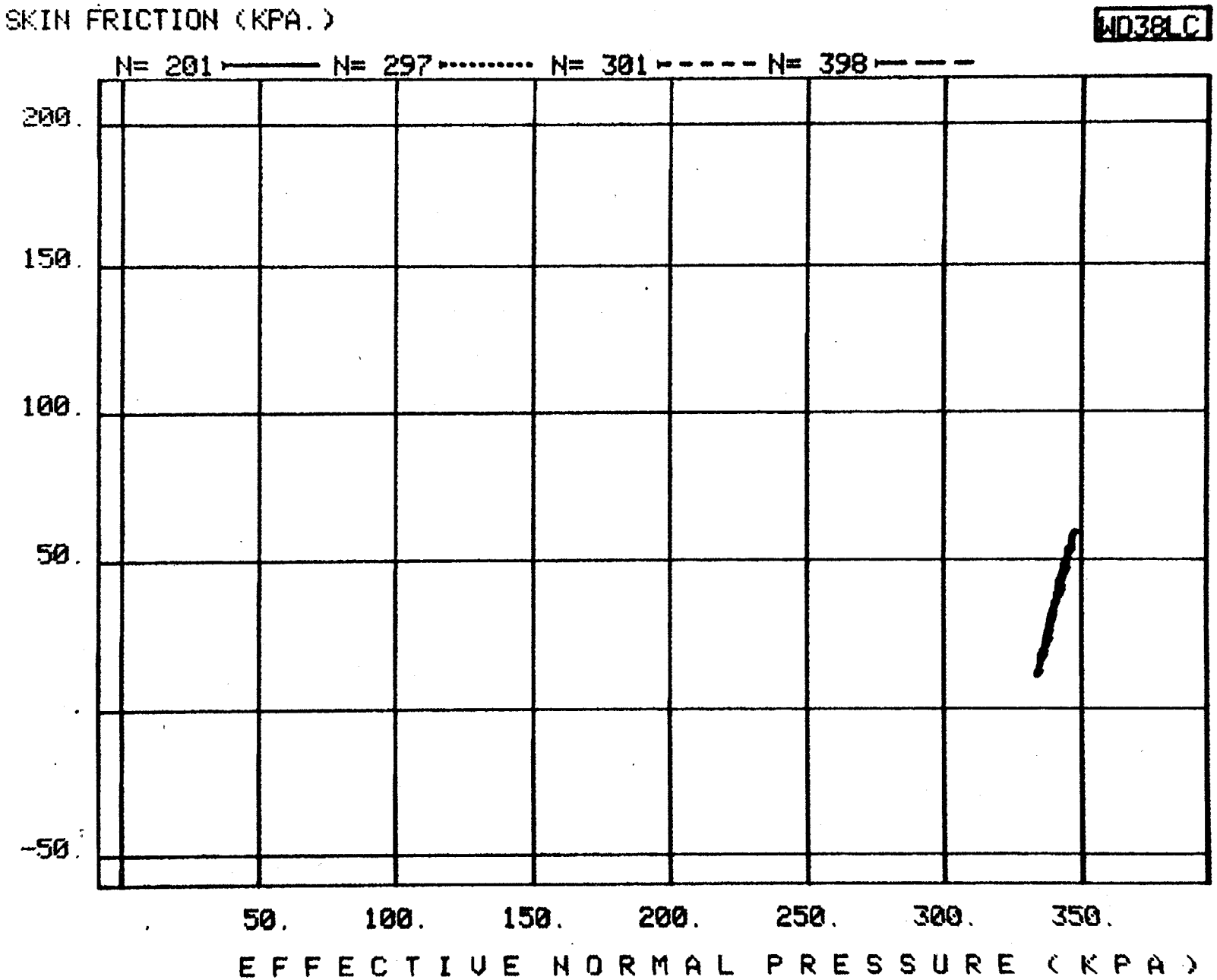
SKIN FRICTION (KPA.)
WD38LC
N= 201
N= 297
N= 301
N= 398
200.
150.
100.
50.
-50.
50.
100.
150.
200.
250.
300.
350.
EFFECTIVE NORMAL PRESSURE (KPA)

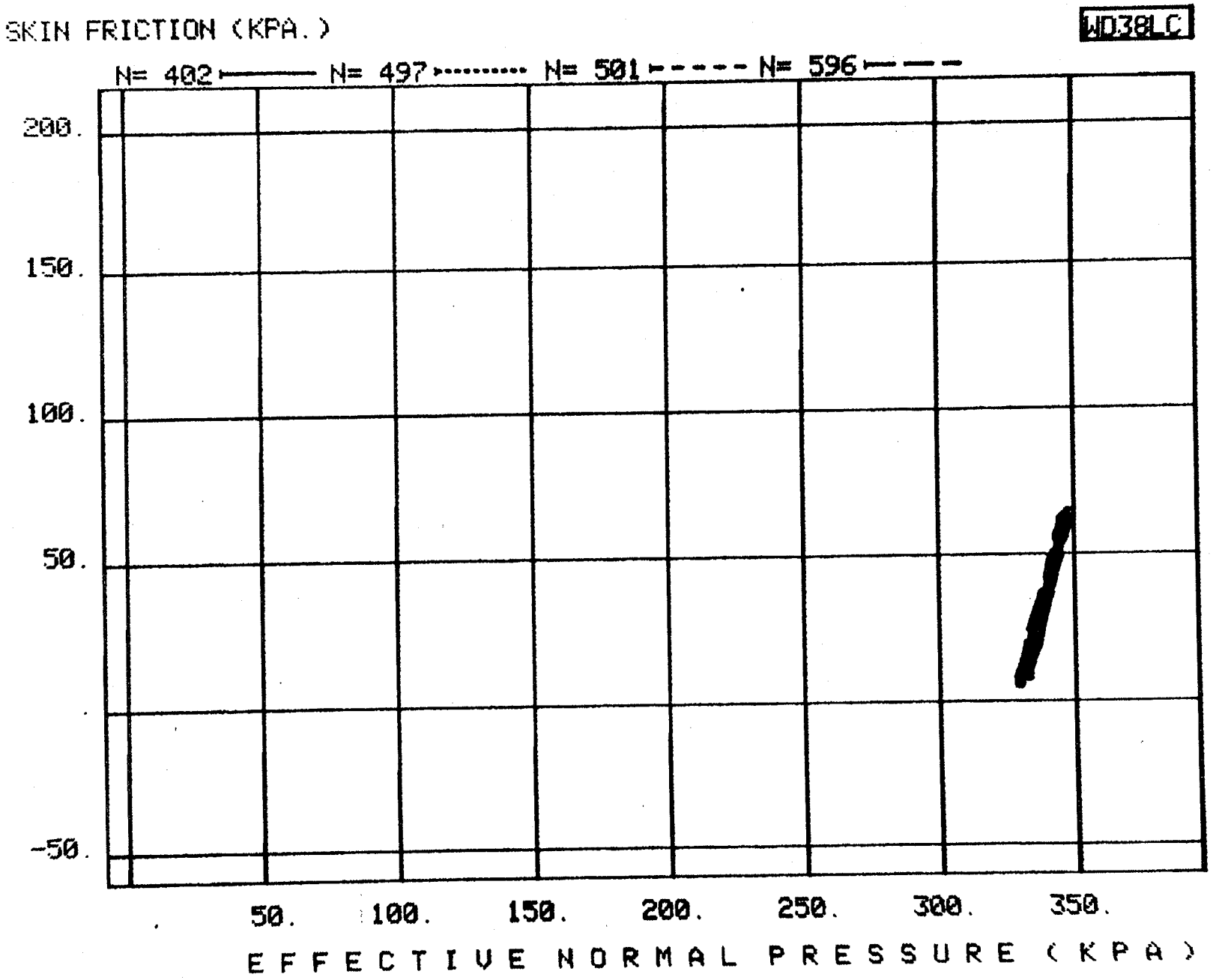
SKIN FRICTION (KPA.)
WD38LC
N= 402
N= 497
N= 501
N= 596
200.
150.
100.
50.
-50.
50.
100.
150.
200.
250.
300.
350.
EFFECTIVE NORMAL PRESSURE (KPA)

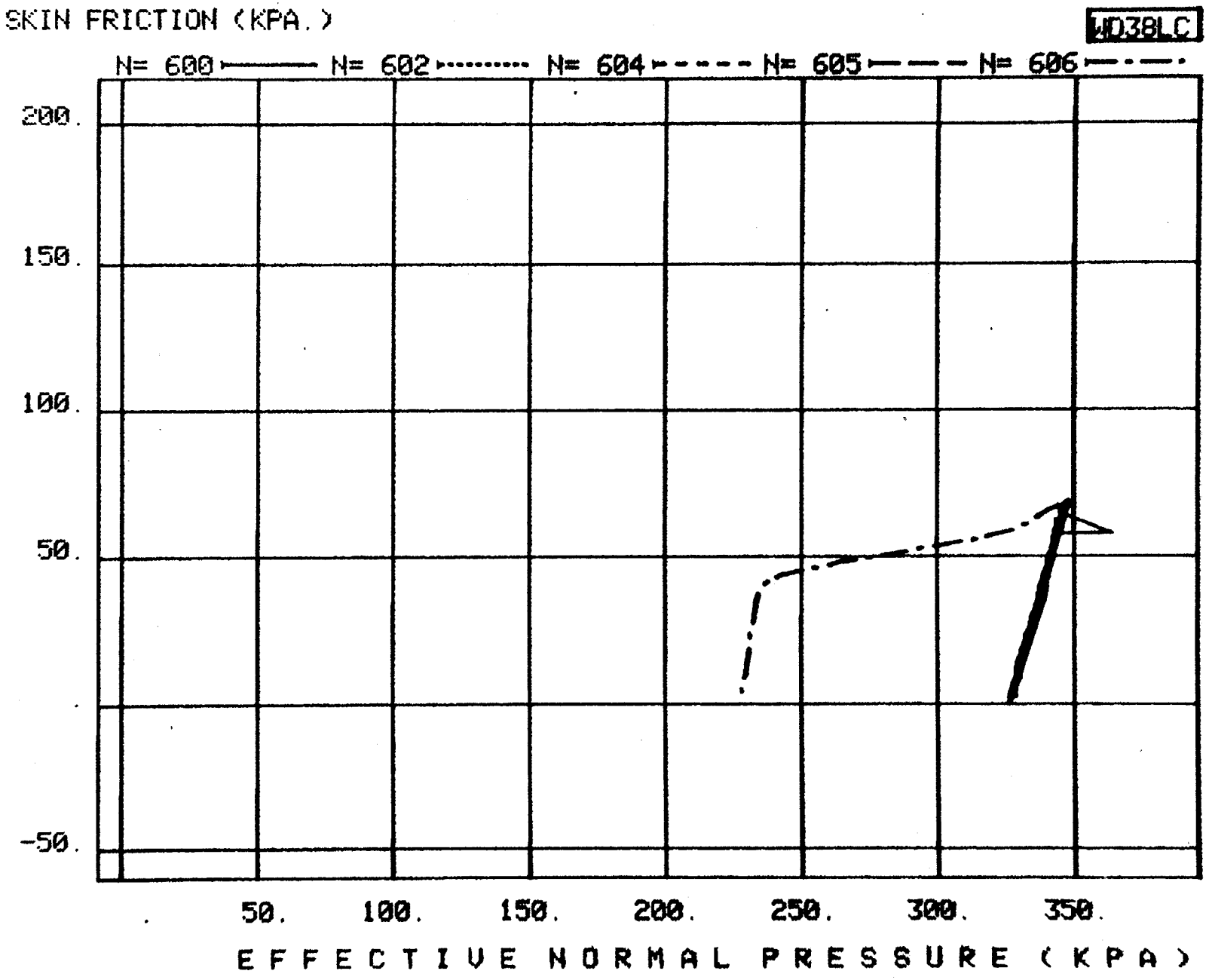
SKIN FRICTION (KPA.)
WD38LC
N= 600
N= 602
N= 604
N= 605
N= 606
200.
150.
100.
50.
-50.
50.
100.
150.
200.
250.
300.
350.
EFFECTIVE NORMAL PRESSURE (KPA)

RESPONSE ON CYCLIC LOADING (KPA.) CYCLE NO. 1 WD38LC

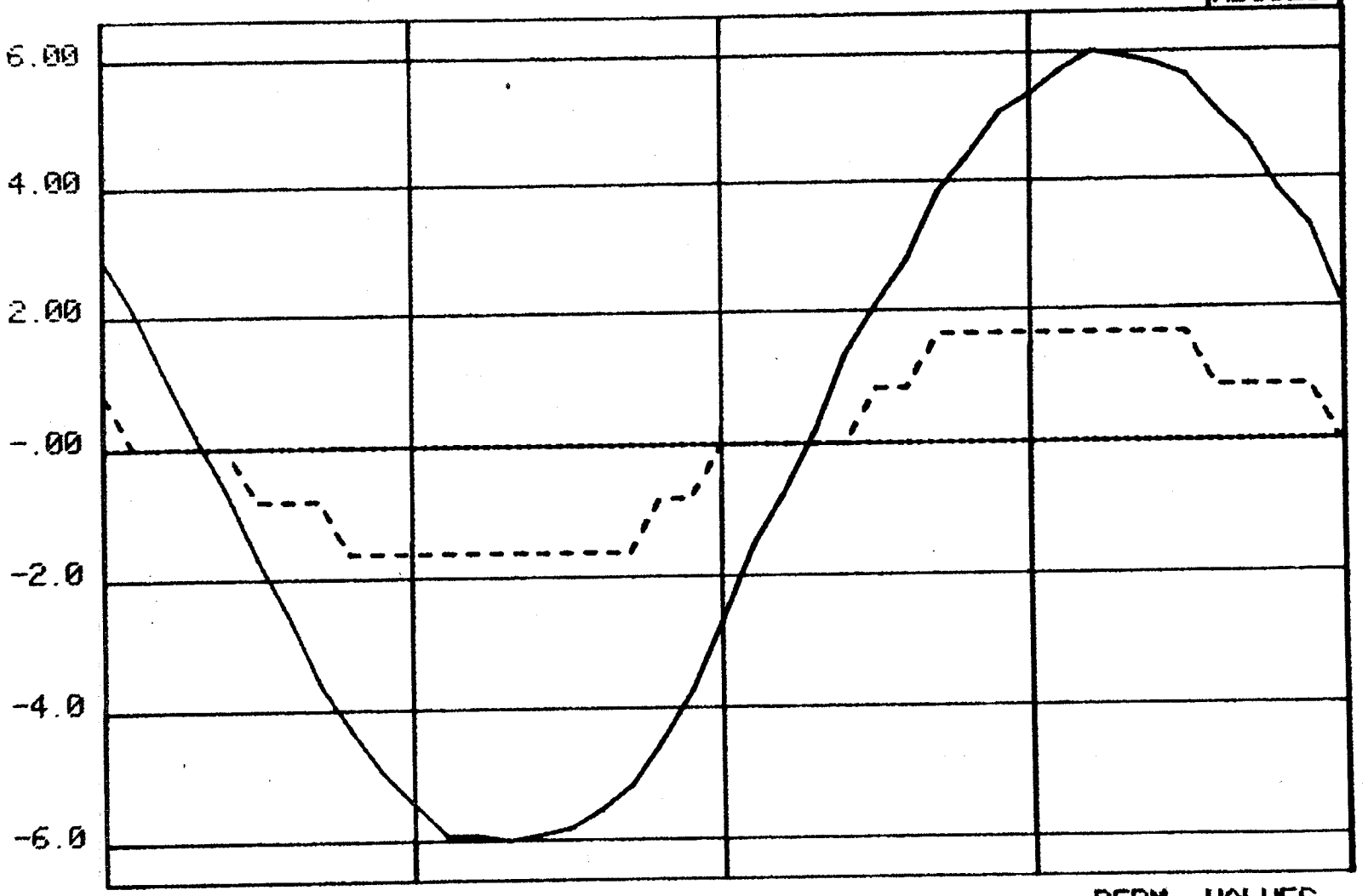

LEGEND:

		PERM. VALUES
———	SKIN FRICTION	35.18 KPA.
·····	PORE PRESSURE	59.40 KPA.
- - - -	TOTAL NORMAL PRESSURE	399.5 KPA.

RESPONSE ON CYCLIC LOADING (KPA.) CYCLE NO. 97

WD38LC

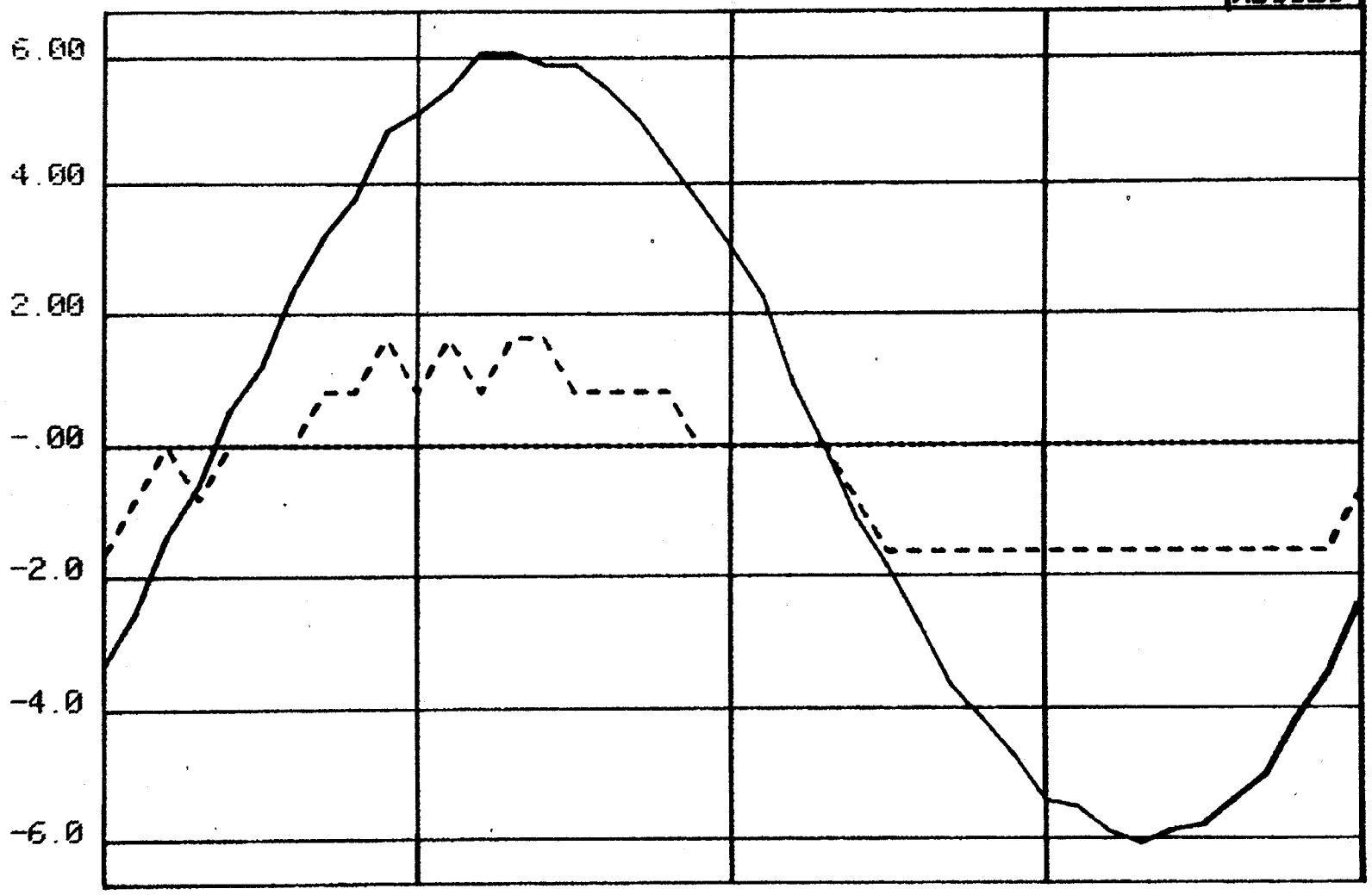

LEGEND:

		PERM. VALUES
———	SKIN FRICTION	35.23 KPA.
·····	PORE PRESSURE	59.40 KPA.
- - - -	TOTAL NORMAL PRESSURE	399.5 KPA.

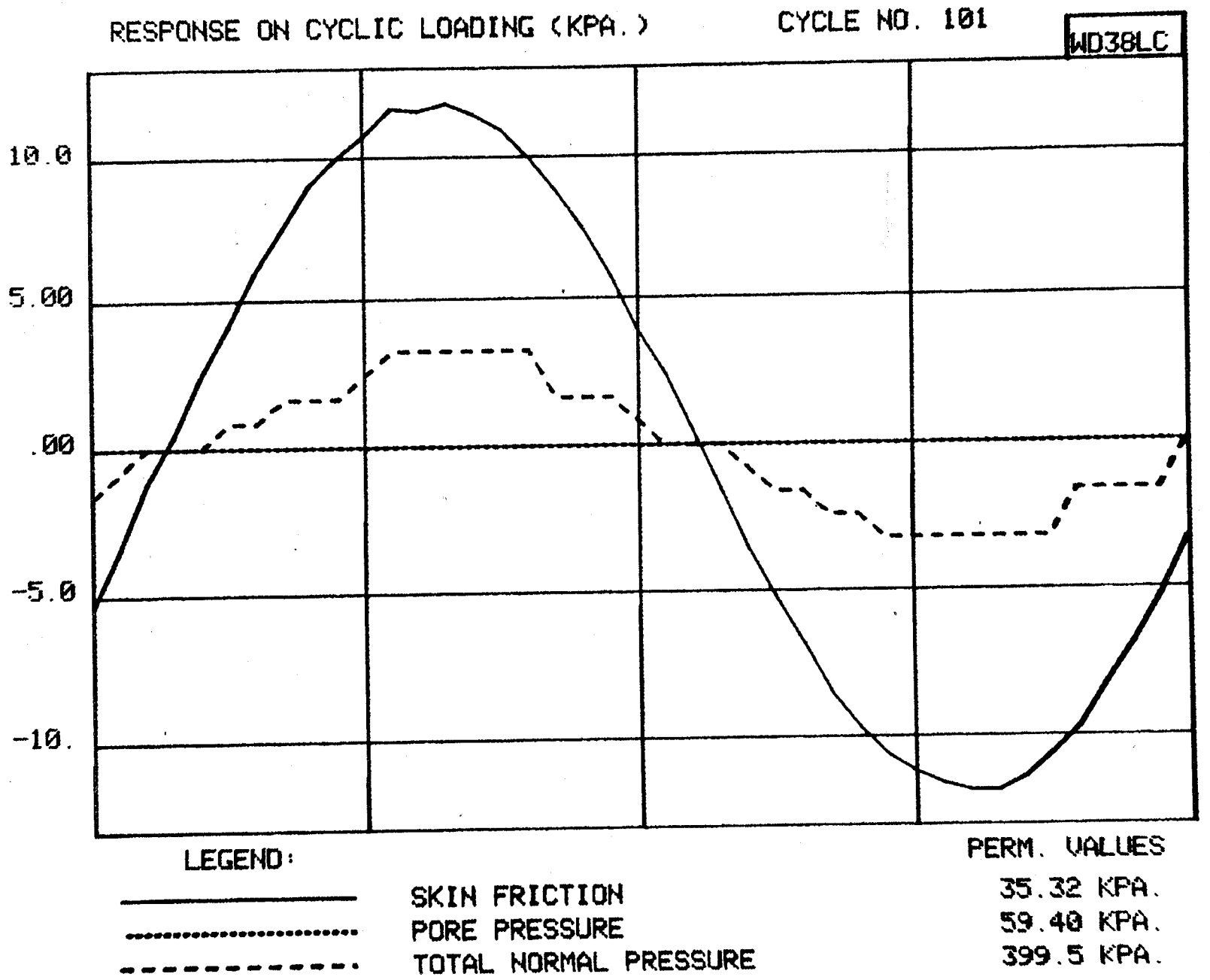
RESPONSE ON CYCLIC LOADING (KPA.)
CYCLE NO. 101
WD38LC
10.0
5.00
.00
-5.0
-10.
LEGEND:
SKIN FRICTION
PORE PRESSURE
TOTAL NORMAL PRESSURE
PERM. VALUES
35.32 KPA.
59.40 KPA.
399.5 KPA.

RESPONSE ON CYCLIC LOADING (KPA.) CYCLE NO. 198

WD38LC

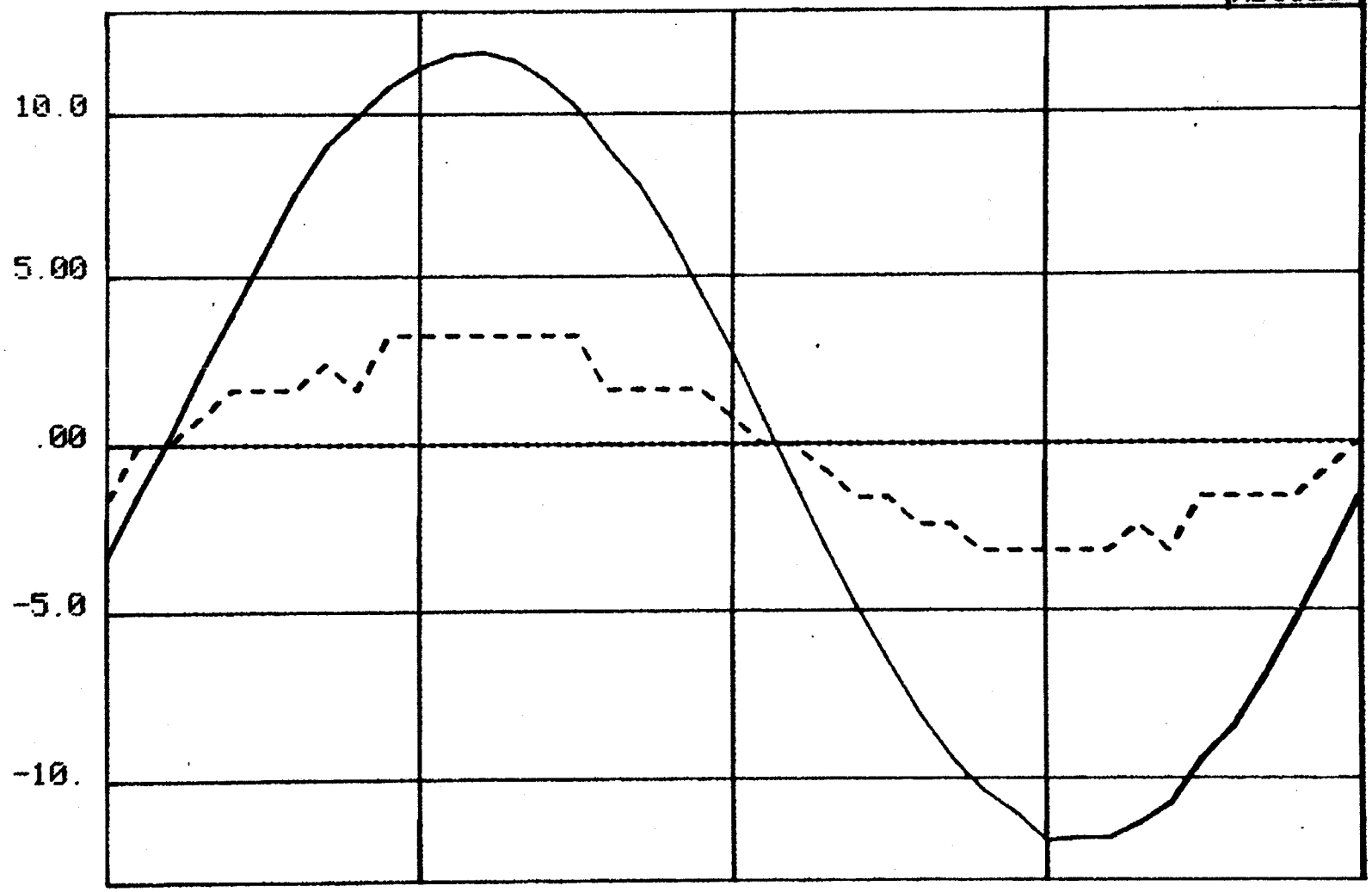

LEGEND:

		PERM. VALUES
———	SKIN FRICTION	35.42 KPA.
·····	PORE PRESSURE	59.40 KPA.
- - - -	TOTAL NORMAL PRESSURE	399.5 KPA.

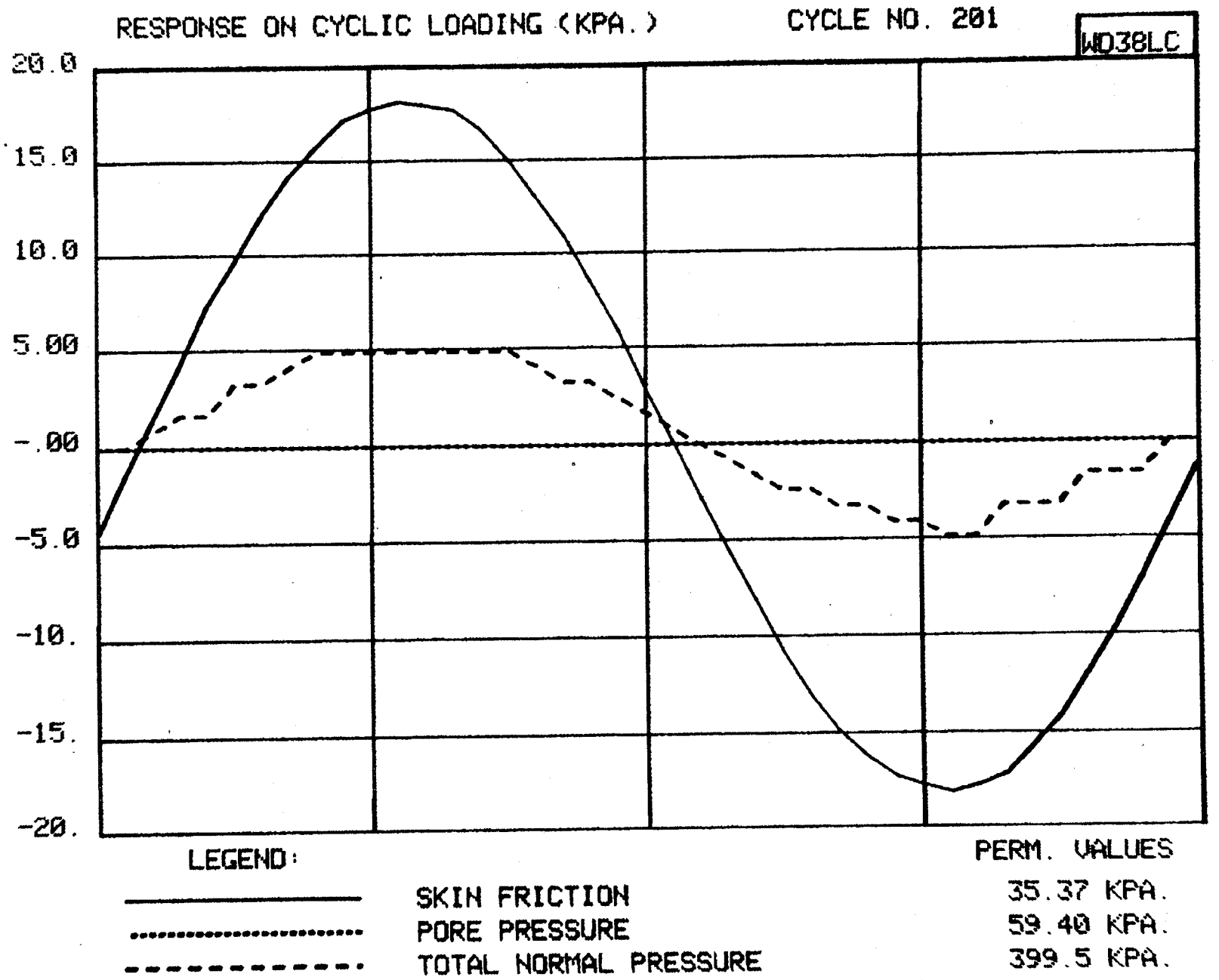
RESPONSE ON CYCLIC LOADING (KPA.)
CYCLE NO. 201
WD38LC
20.0
15.0
10.0
5.00
-.00
-5.0
-10.
-15.
-20.
LEGEND:
SKIN FRICTION
PORE PRESSURE
TOTAL NORMAL PRESSURE
PERM. VALUES
35.37 KPA.
59.40 KPA.
399.5 KPA.

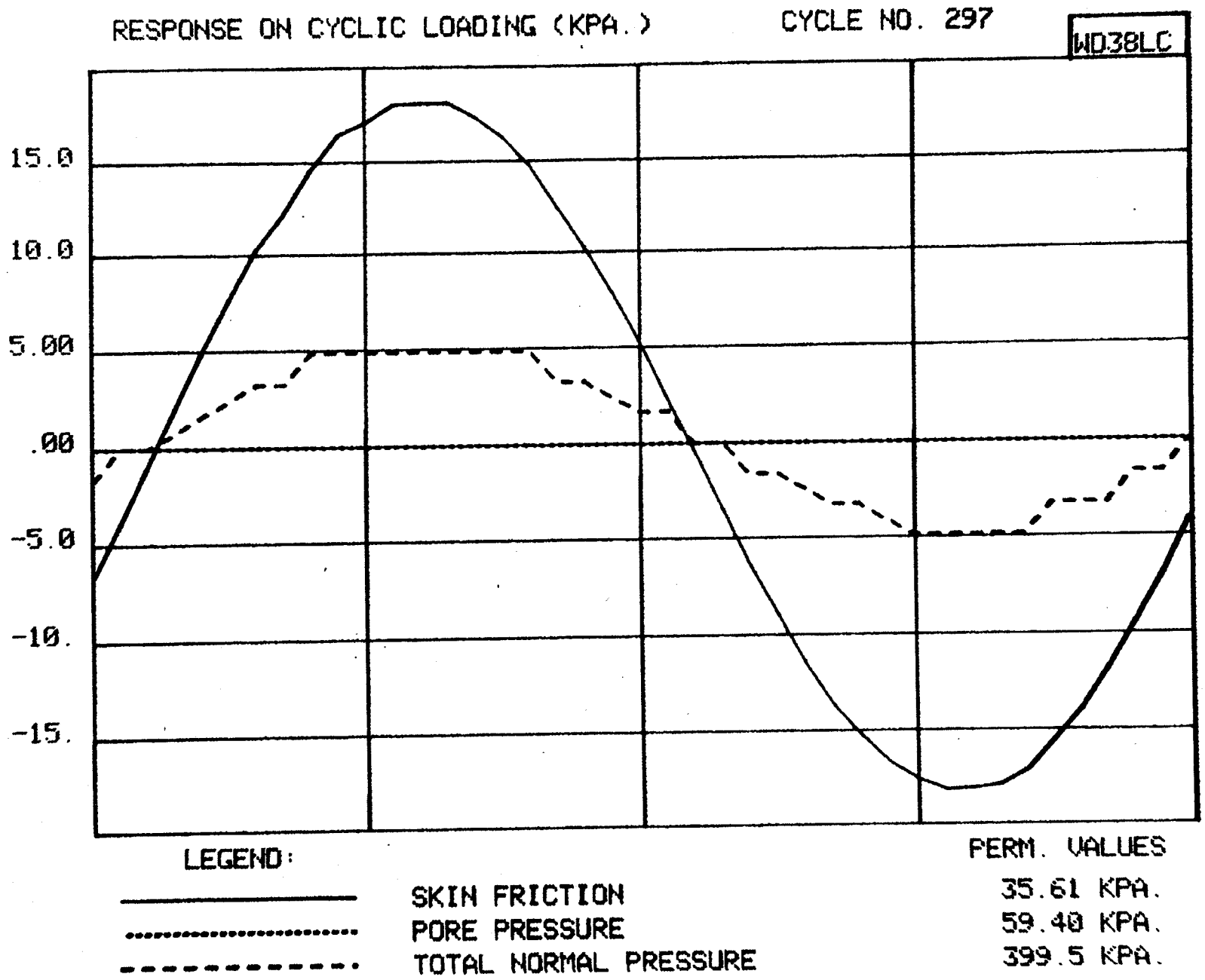
RESPONSE ON CYCLIC LOADING (KPA.)
CYCLE NO. 297
WD38LC
15.0
10.0
5.00
.00
-5.0
-10.
-15.
LEGEND:
SKIN FRICTION
PORE PRESSURE
TOTAL NORMAL PRESSURE
PERM. VALUES
35.61 KPA.
59.40 KPA.
399.5 KPA.

RESPONSE ON CYCLIC LOADING (KPA.) CYCLE NO. 301

WD38LC

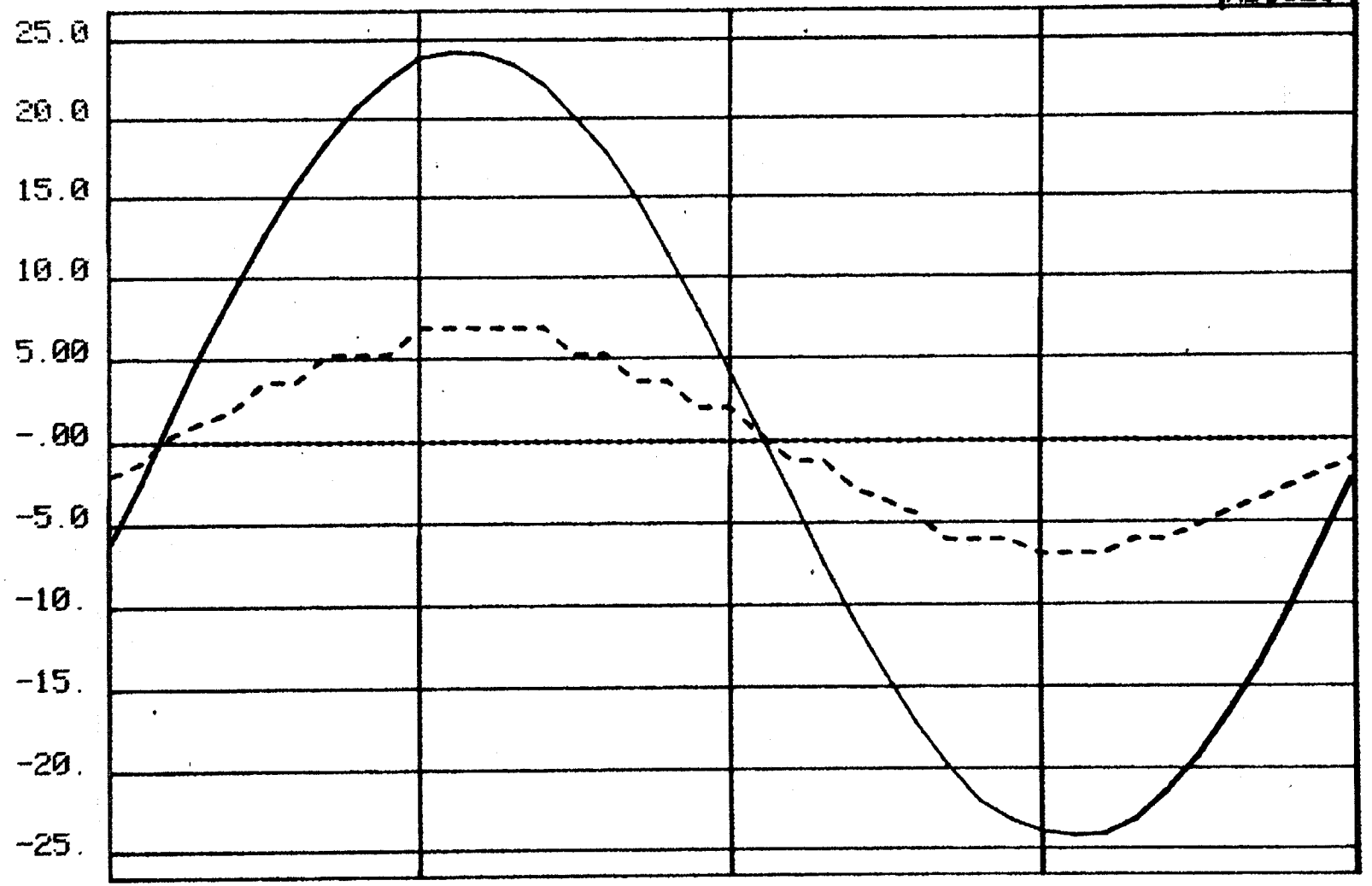

LEGEND:

		PERM. VALUES
———	SKIN FRICTION	35.61 KPA.
·····	PORE PRESSURE	59.40 KPA.
- - - -	TOTAL NORMAL PRESSURE	400.7 KPA.

RESPONSE ON CYCLIC LOADING (KPA.) CYCLE NO. 398 WD38LC

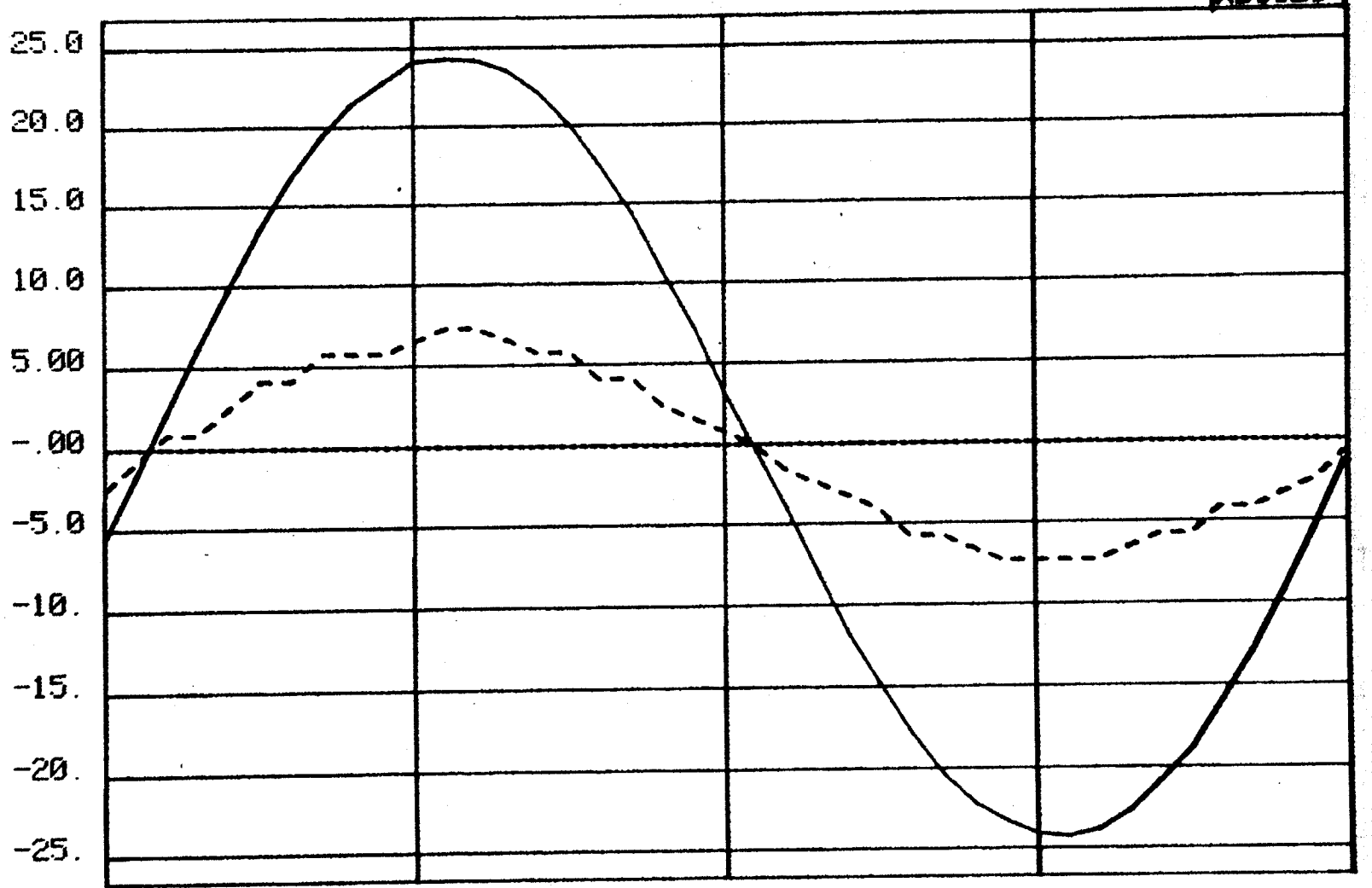

LEGEND:

		PERM. VALUES
———	SKIN FRICTION	35.18 KPA.
.....	PORE PRESSURE	59.40 KPA.
- - - -	TOTAL NORMAL PRESSURE	400.3 KPA.

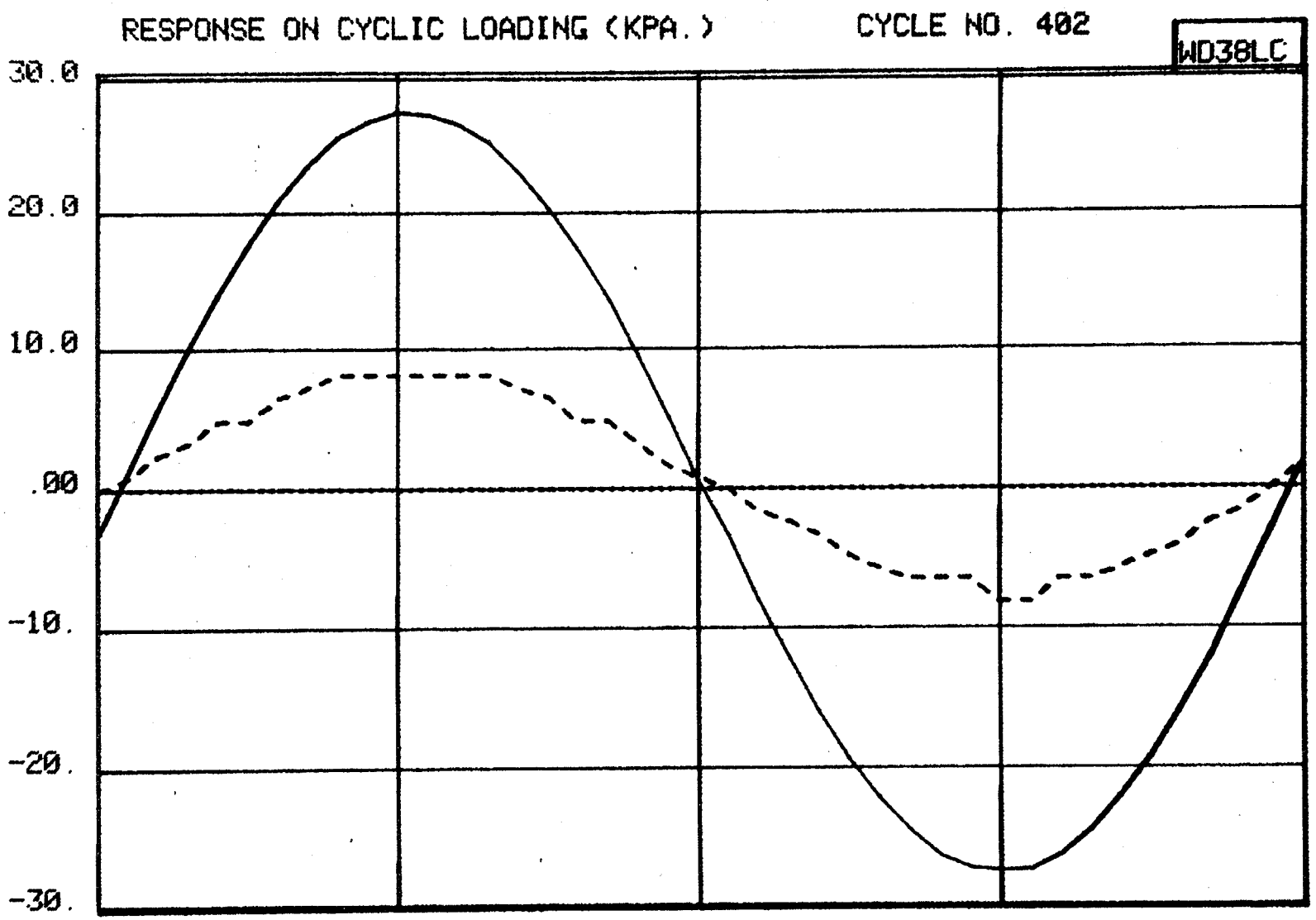

LEGEND:

		PERM. VALUES
———	SKIN FRICTION	35.23 KPA.
·····	PORE PRESSURE	59.40 KPA.
- - - -	TOTAL NORMAL PRESSURE	399.5 KPA.

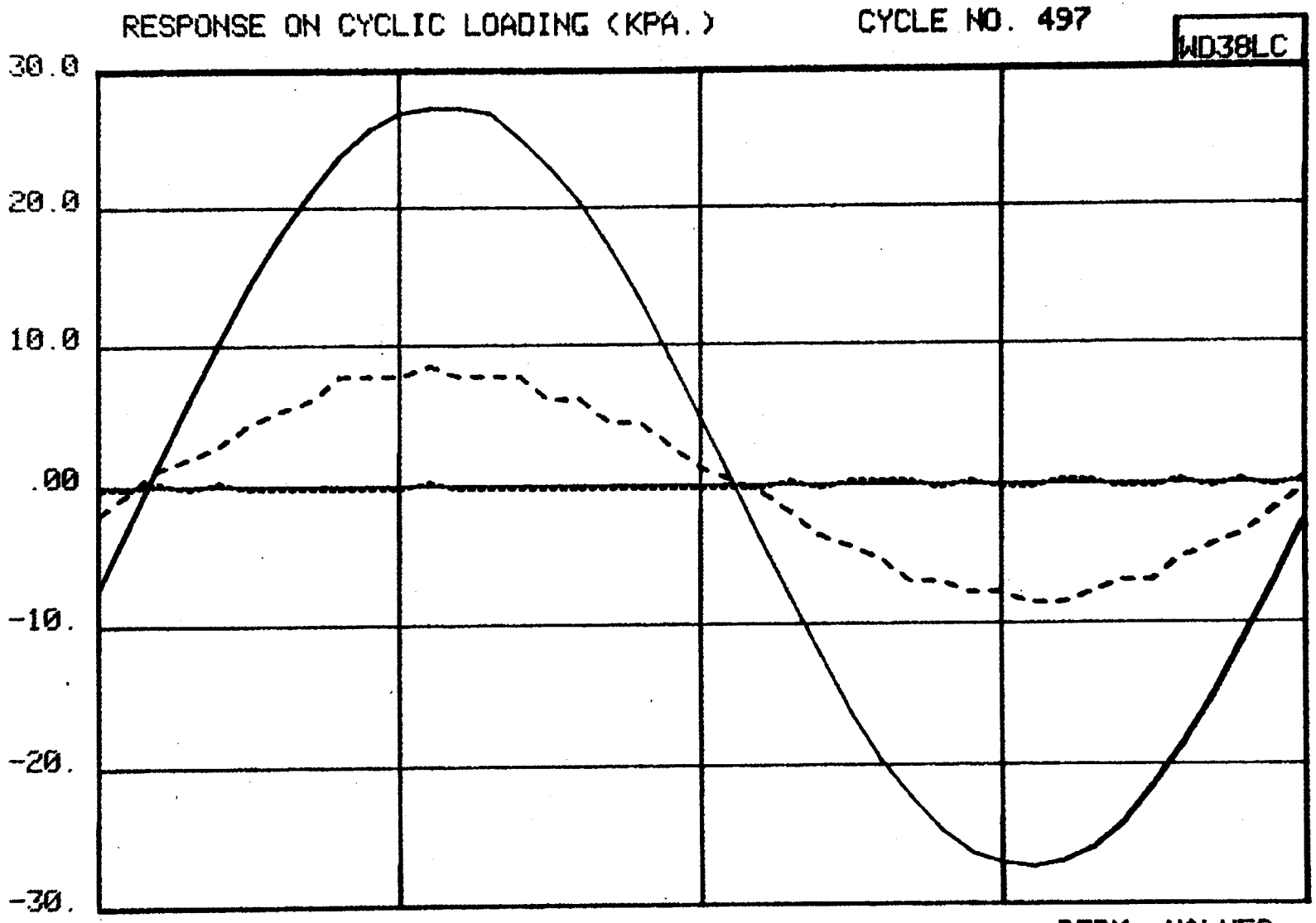

LEGEND:

		PERM. VALUES
———	SKIN FRICTION	35.13 KPA.
·····	PORE PRESSURE	59.64 KPA.
- - - -	TOTAL NORMAL PRESSURE	398.2 KPA.

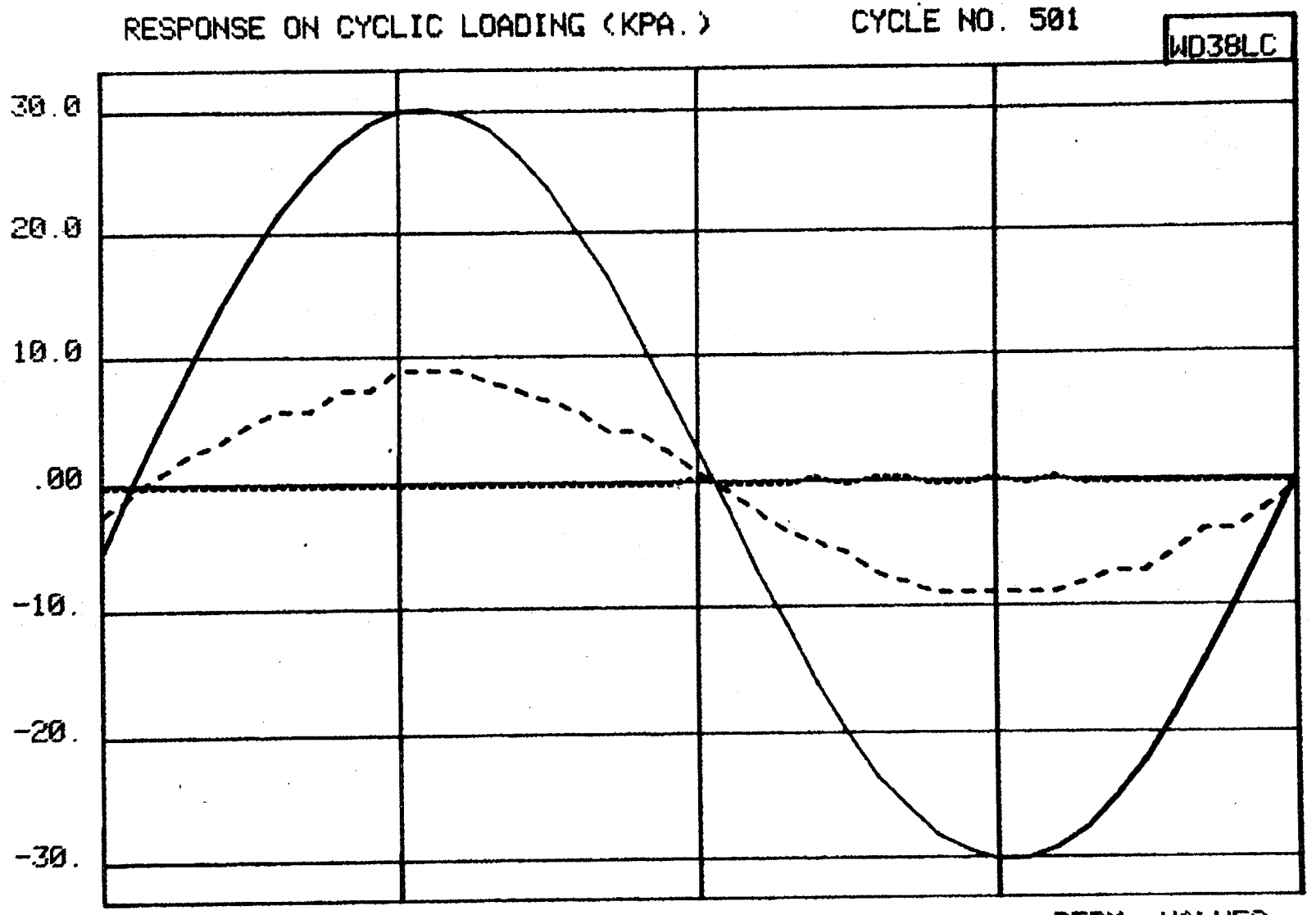

LEGEND:

		PERM. VALUES
———	SKIN FRICTION	35.13 KPA.
·····	PORE PRESSURE	59.64 KPA.
- - - -	TOTAL NORMAL PRESSURE	398.6 KPA.

RESPONSE ON CYCLIC LOADING (KPA.) CYCLE NO. 596

WD38LC

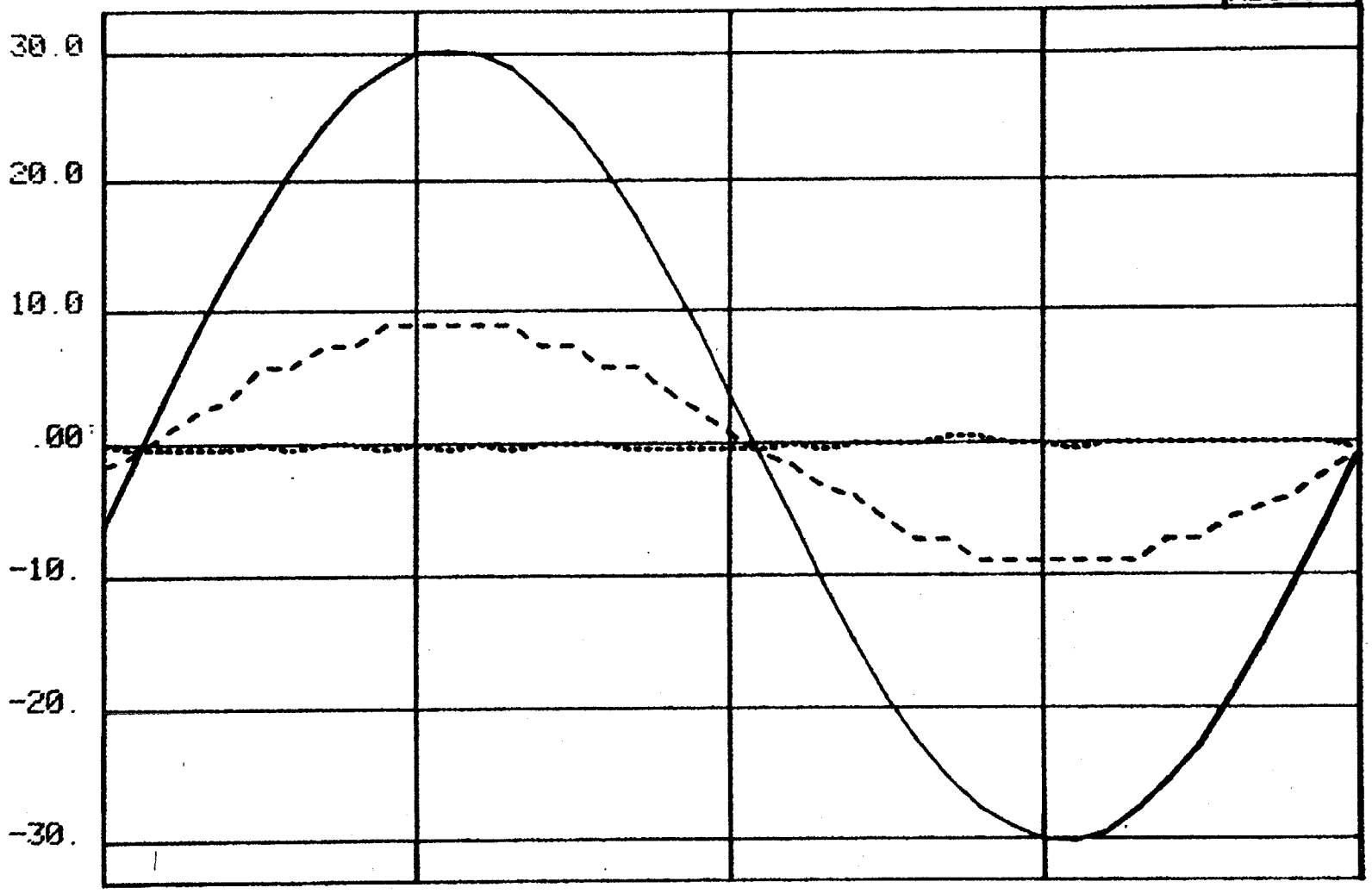

LEGEND:

		PERM. VALUES
———	SKIN FRICTION	35.18 KPA.
·····	PORE PRESSURE	59.88 KPA.
- - - -	TOTAL NORMAL PRESSURE	397.0 KPA.

RESPONSE ON CYCLIC LOADING (KPA.) CYCLE NO. 601

WD38LC

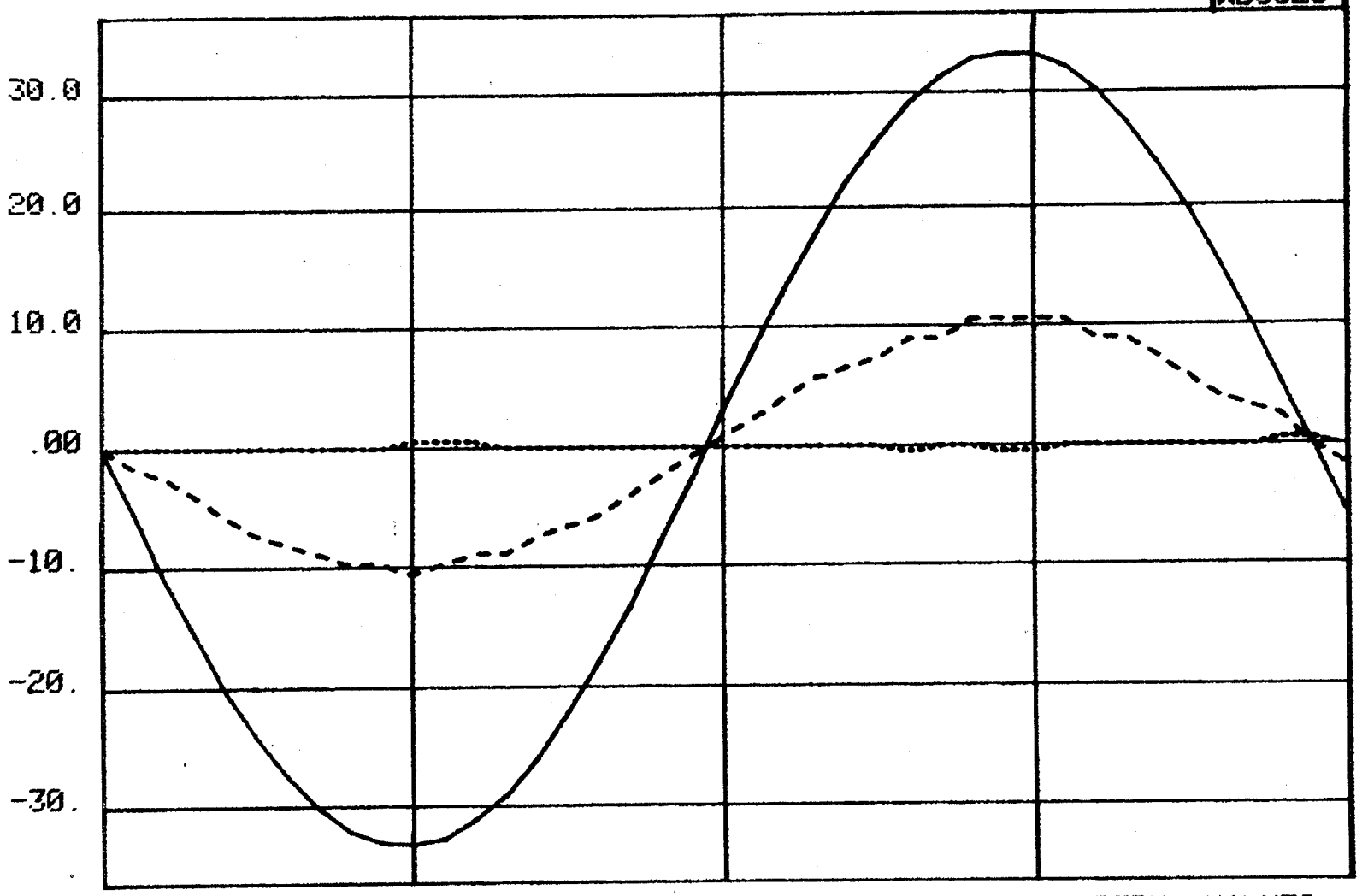

LEGEND:

		PERM. VALUES
———	SKIN FRICTION	35.23 KPA.
·····	PORE PRESSURE	59.88 KPA.
- - - -	TOTAL NORMAL PRESSURE	397.0 KPA.

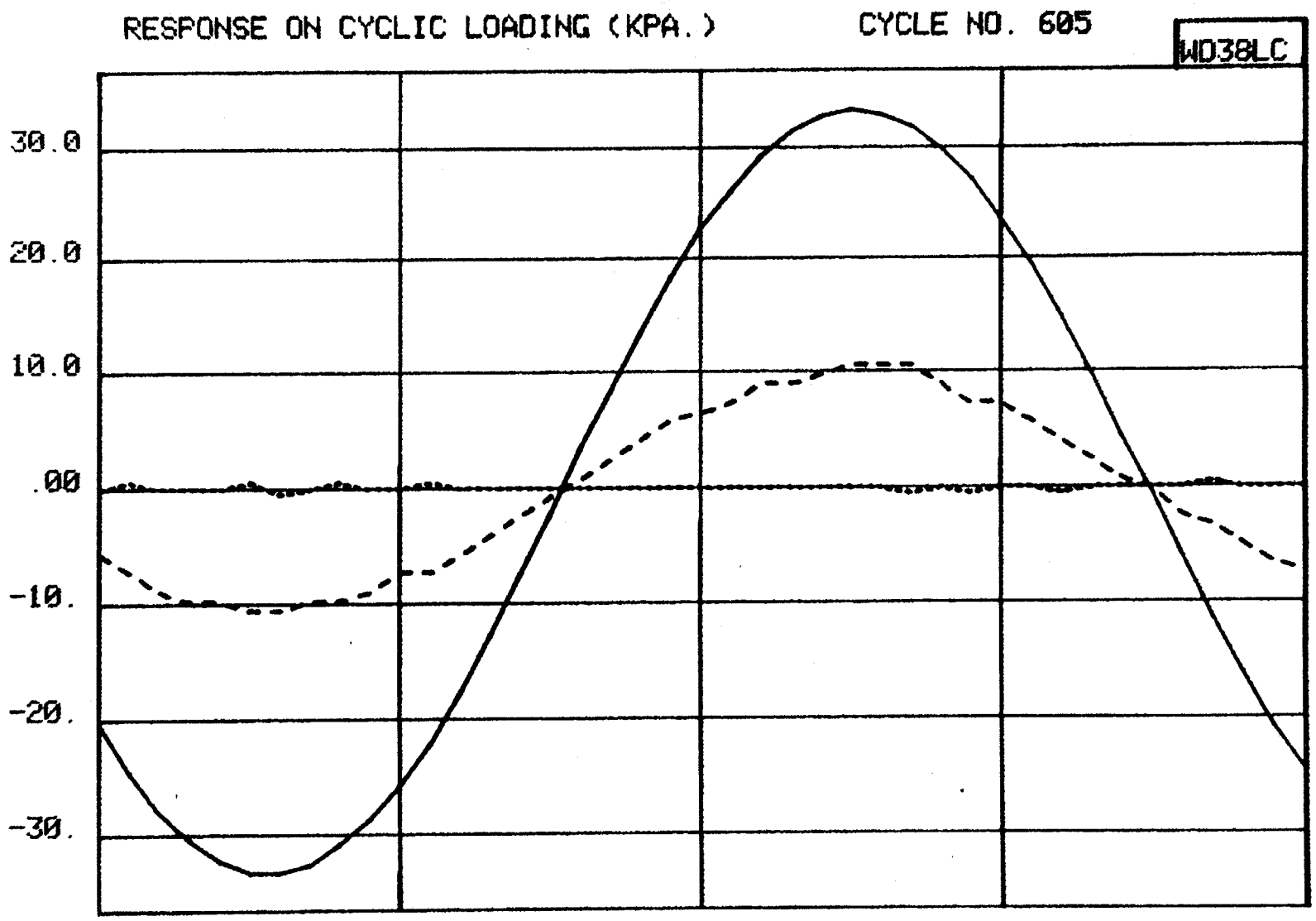

LEGEND:

		PERM. VALUES
———	SKIN FRICTION	35.27 KPA.
·····	PORE PRESSURE	59.88 KPA.
- - - -	TOTAL NORMAL PRESSURE	397.0 KPA.

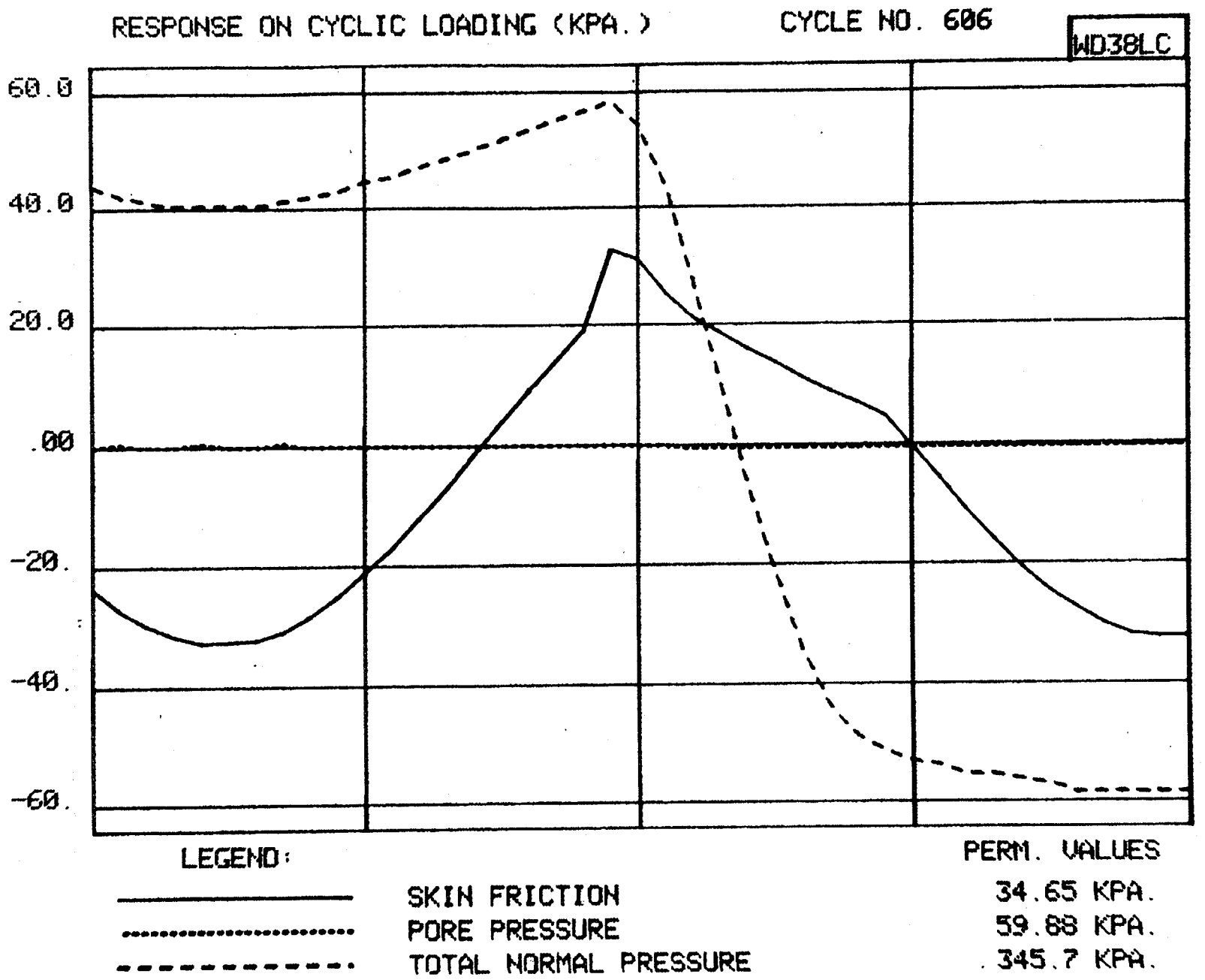
RESPONSE ON CYCLIC LOADING (KPA.)
CYCLE NO. 606
WD38LC
60.0
40.0
20.0
.00
-20.
-40.
-60.
LEGEND:
SKIN FRICTION
PORE PRESSURE
TOTAL NORMAL PRESSURE
PERM. VALUES
34.65 KPA.
59.88 KPA.
345.7 KPA.

Appendix EB

Plotted Results from WD38SC

Figures EB-1 through EB-7

Skin Friction vs Deflection, Selected Cycles

Figures EB-8 through EB-11

Skin Friction vs Eff. Normal Pressure, Selected Cycl.

Figures EB-12 through EB-24

Skin Friction, Pore and Total Pressure, Selected Cycles

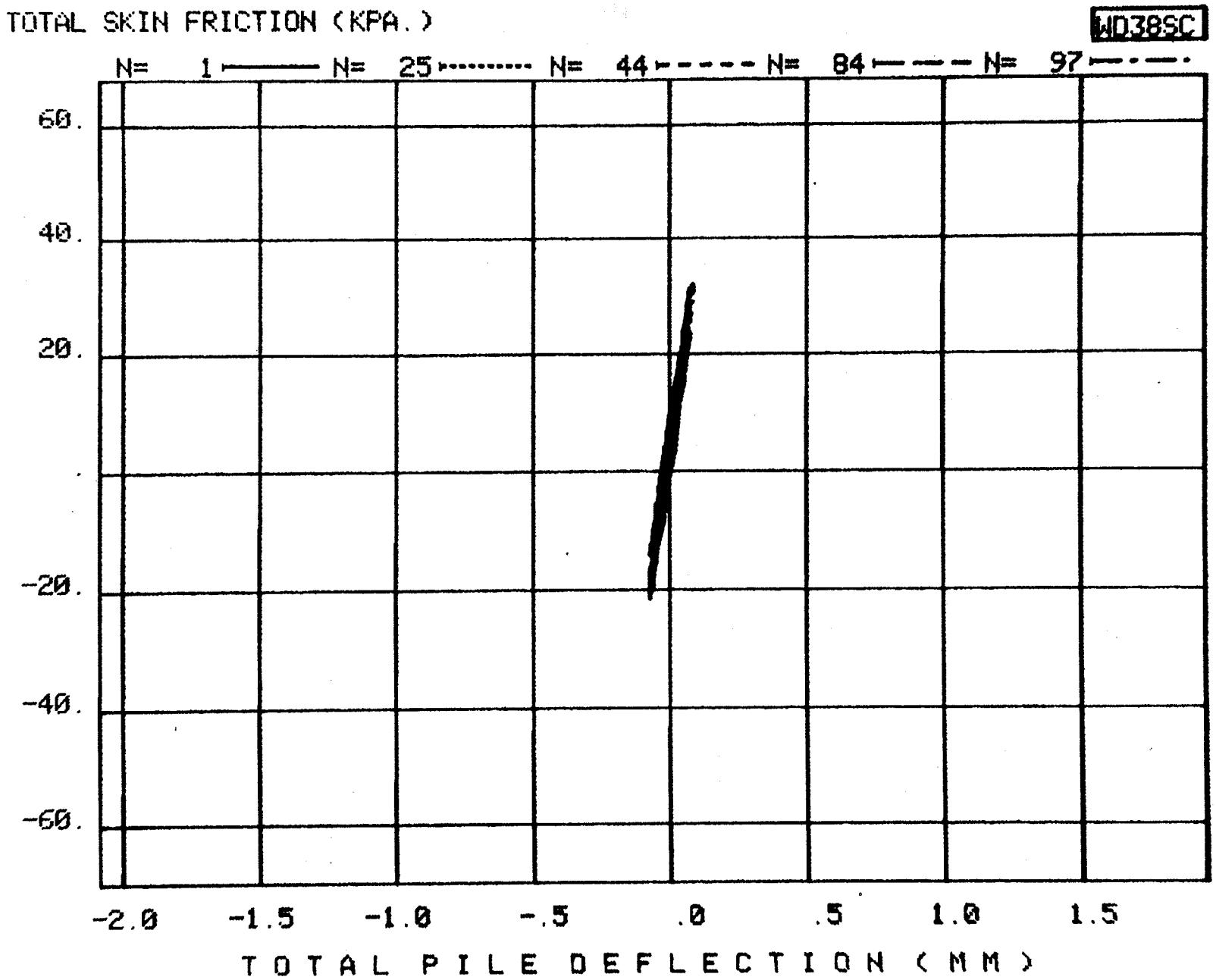
TOTAL SKIN FRICTION (KPA.)
WD38SC
N= 1
N= 25
N= 44
N= 84
N= 97
60.
40.
20.
-20.
-40.
-60.
-2.0
-1.5
-1.0
-.5
.0
.5
1.0
1.5
TOTAL PILE DEFLECTION (MM)

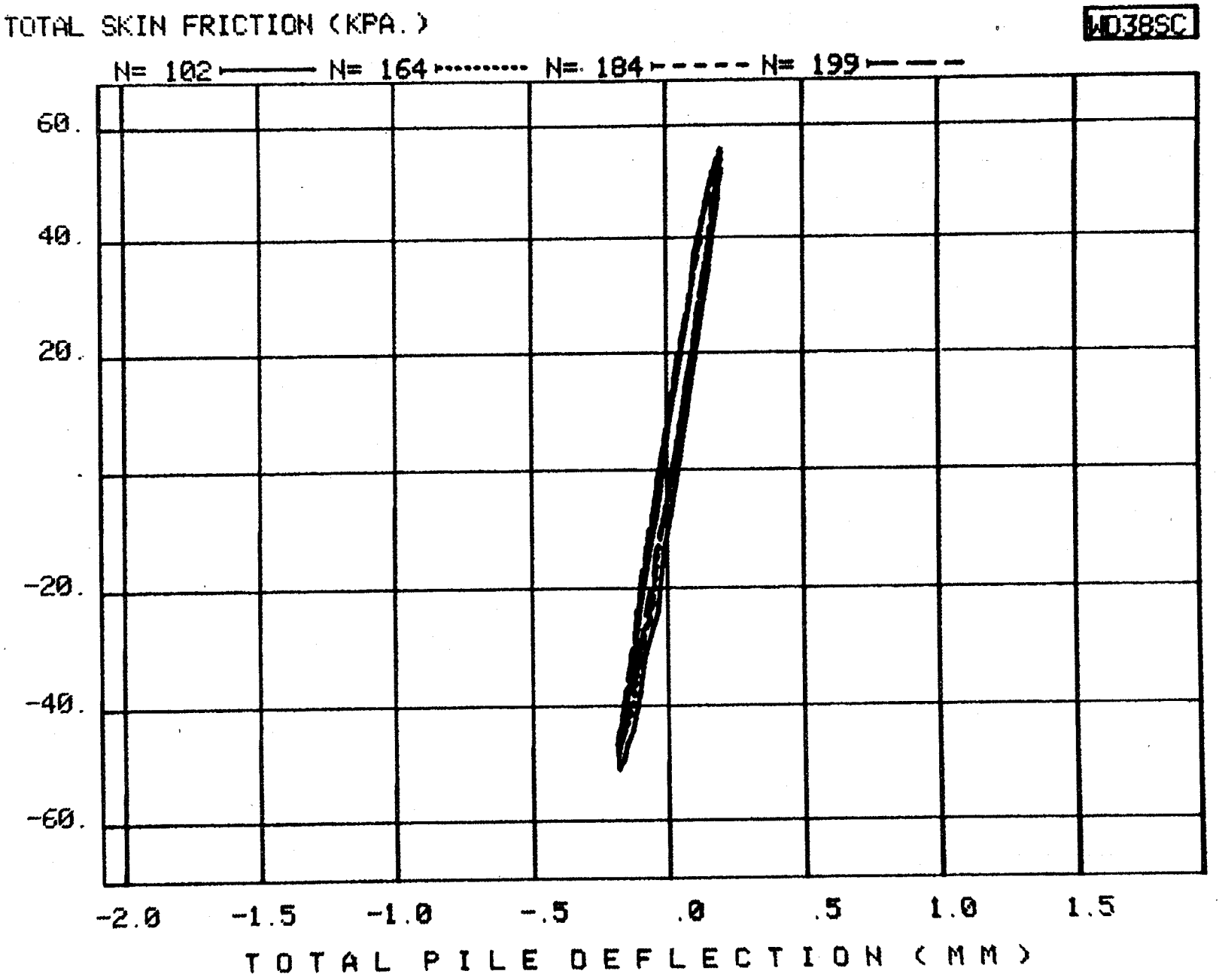
TOTAL SKIN FRICTION (KPA.)
WD38SC
N= 102
N= 164
N= 184
N= 199
60.
40.
20.
-20.
-40.
-60.
-2.0
-1.5
-1.0
-.5
.0
.5
1.0
1.5
TOTAL PILE DEFLECTION (MM)

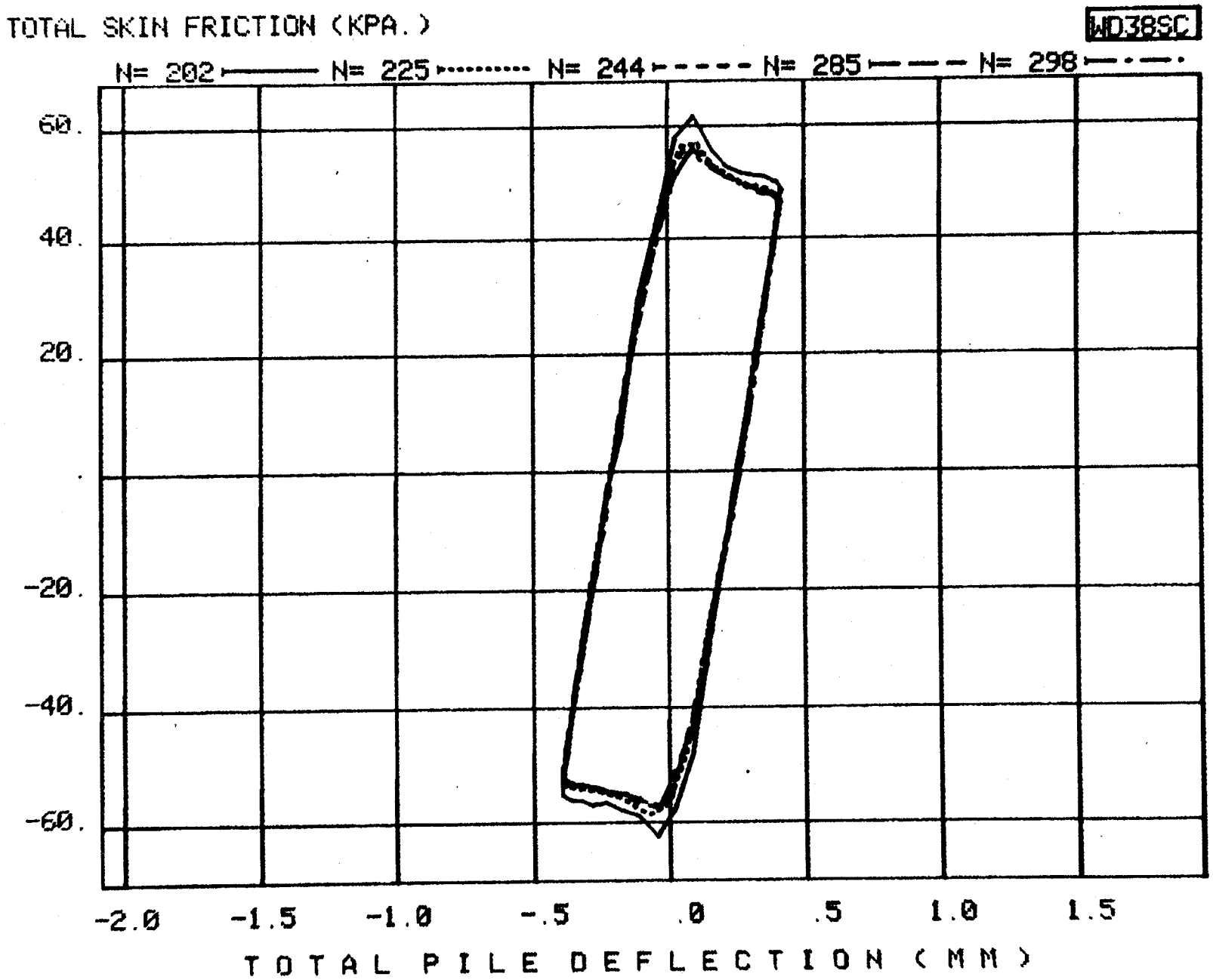
TOTAL SKIN FRICTION (KPA.)
WD38SC
N= 202
N= 225
N= 244
N= 285
N= 298
60.
40.
20.
-20.
-40.
-60.
-2.0
-1.5
-1.0
-.5
.0
.5
1.0
1.5
TOTAL PILE DEFLECTION (MM)

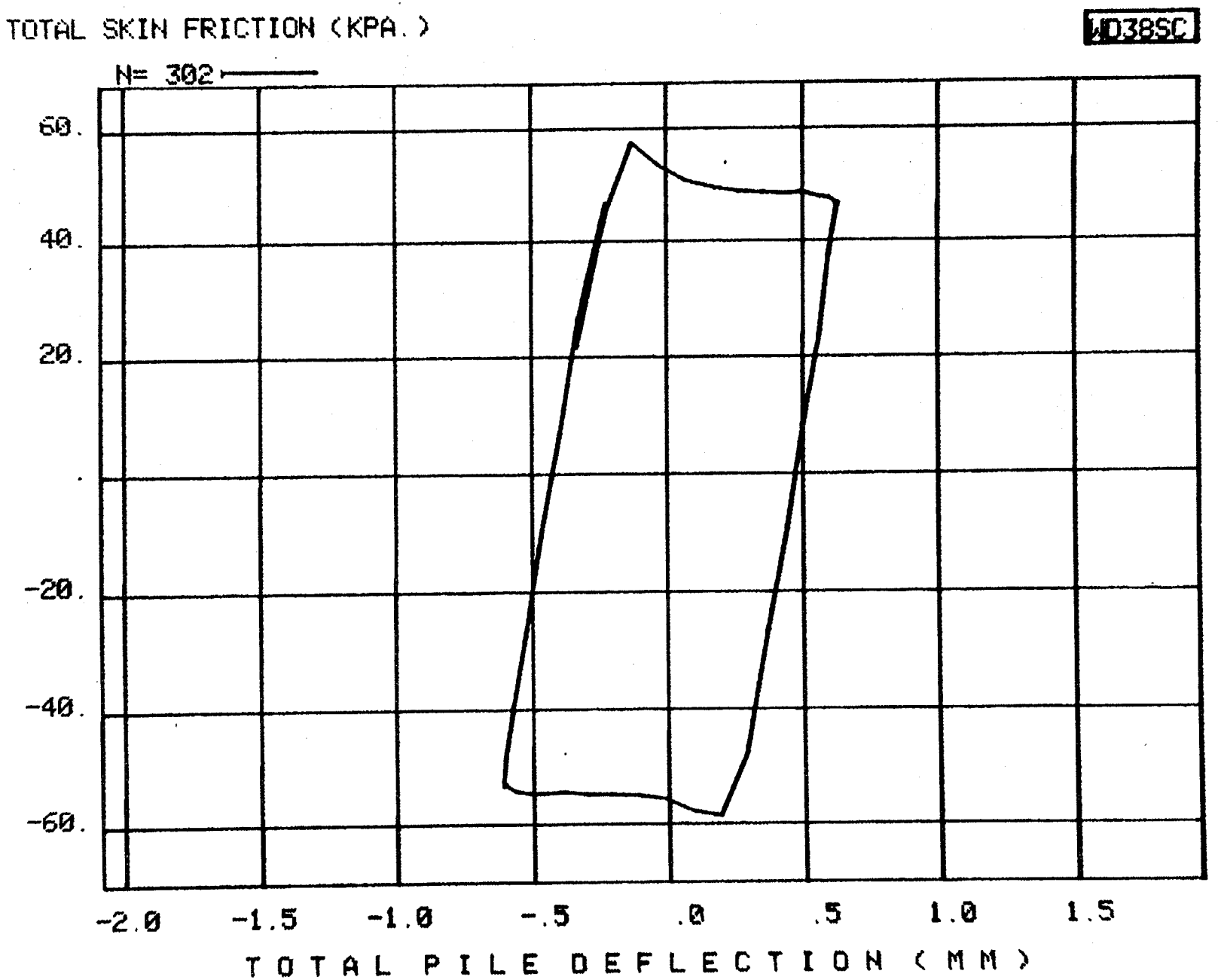
TOTAL SKIN FRICTION (KPA.)
WD38SC
N= 302
60.
40.
20.
-20.
-40.
-60.
-2.0
-1.5
-1.0
-.5
.0
.5
1.0
1.5
TOTAL PILE DEFLECTION (MM)

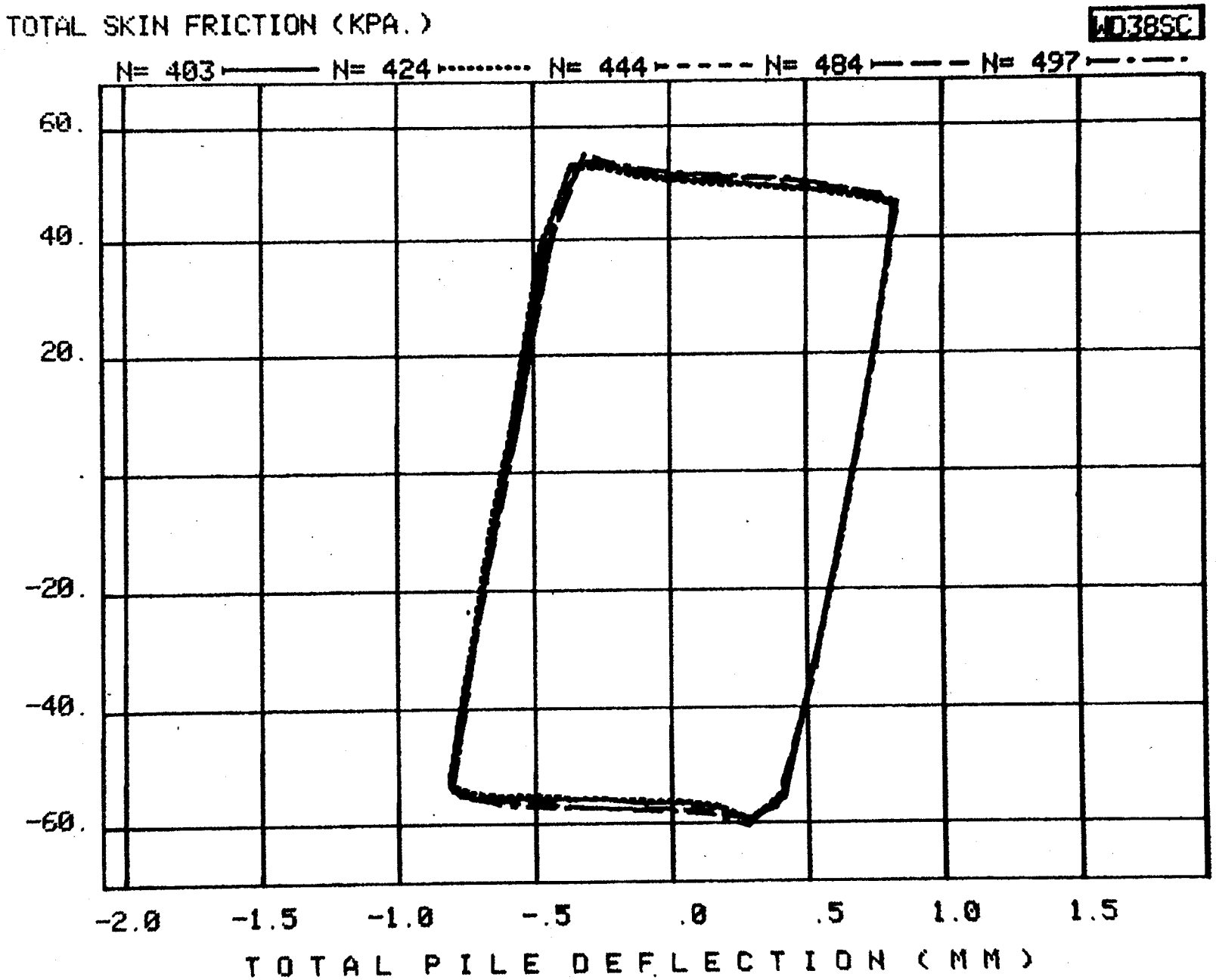
TOTAL SKIN FRICTION (KPA.)
WD38SC
N= 403
N= 424
N= 444
N= 484
N= 497
60.
40.
20.
-20.
-40.
-60.
-2.0
-1.5
-1.0
-.5
.0
.5
1.0
1.5
TOTAL PILE DEFLECTION (MM)

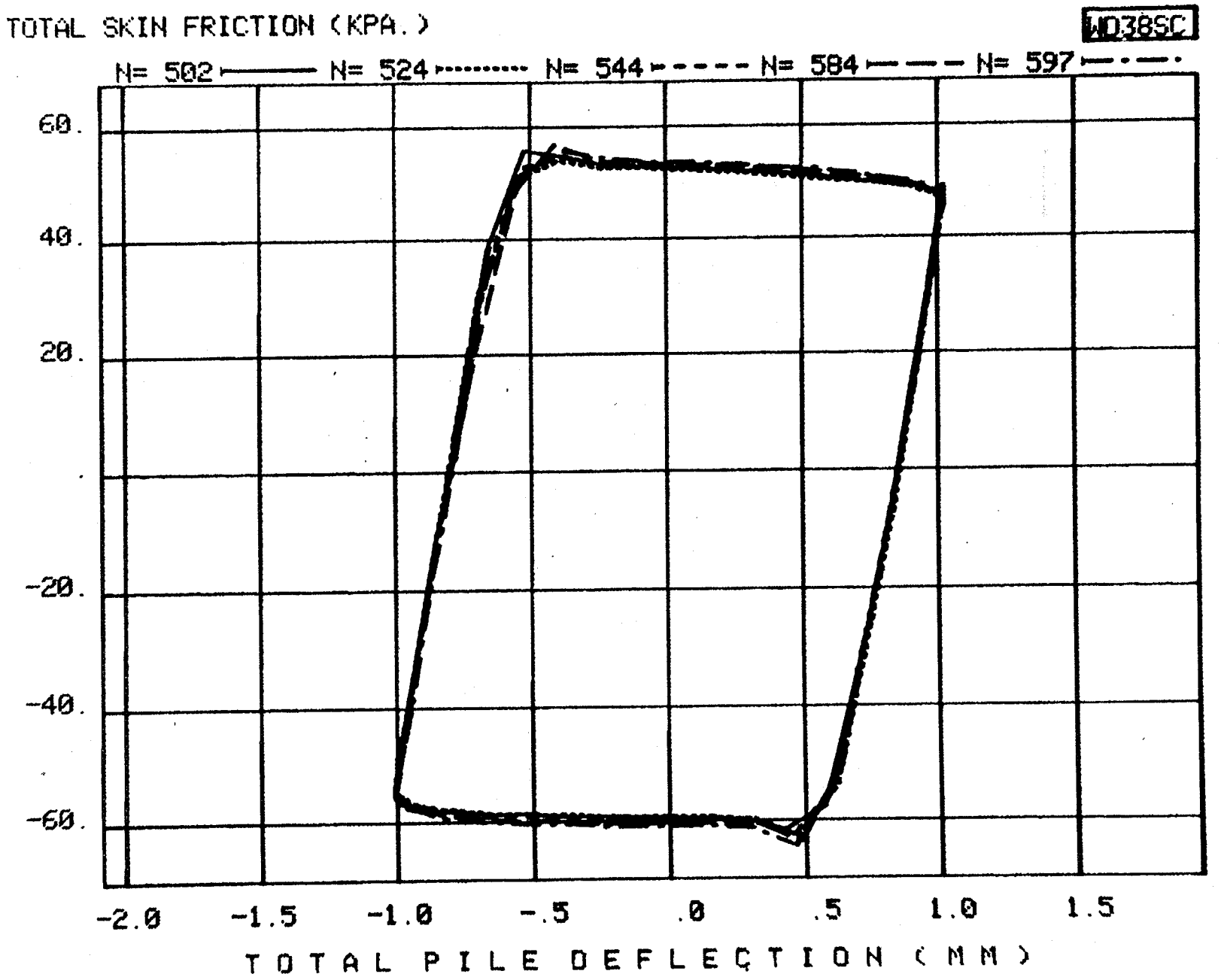
TOTAL SKIN FRICTION (KPA.)
WD38SC
N= 502
N= 524
N= 544
N= 584
N= 597
60.
40.
20.
-20.
-40.
-60.
-2.0
-1.5
-1.0
-.5
.0
.5
1.0
1.5
TOTAL PILE DEFLECTION (MM)

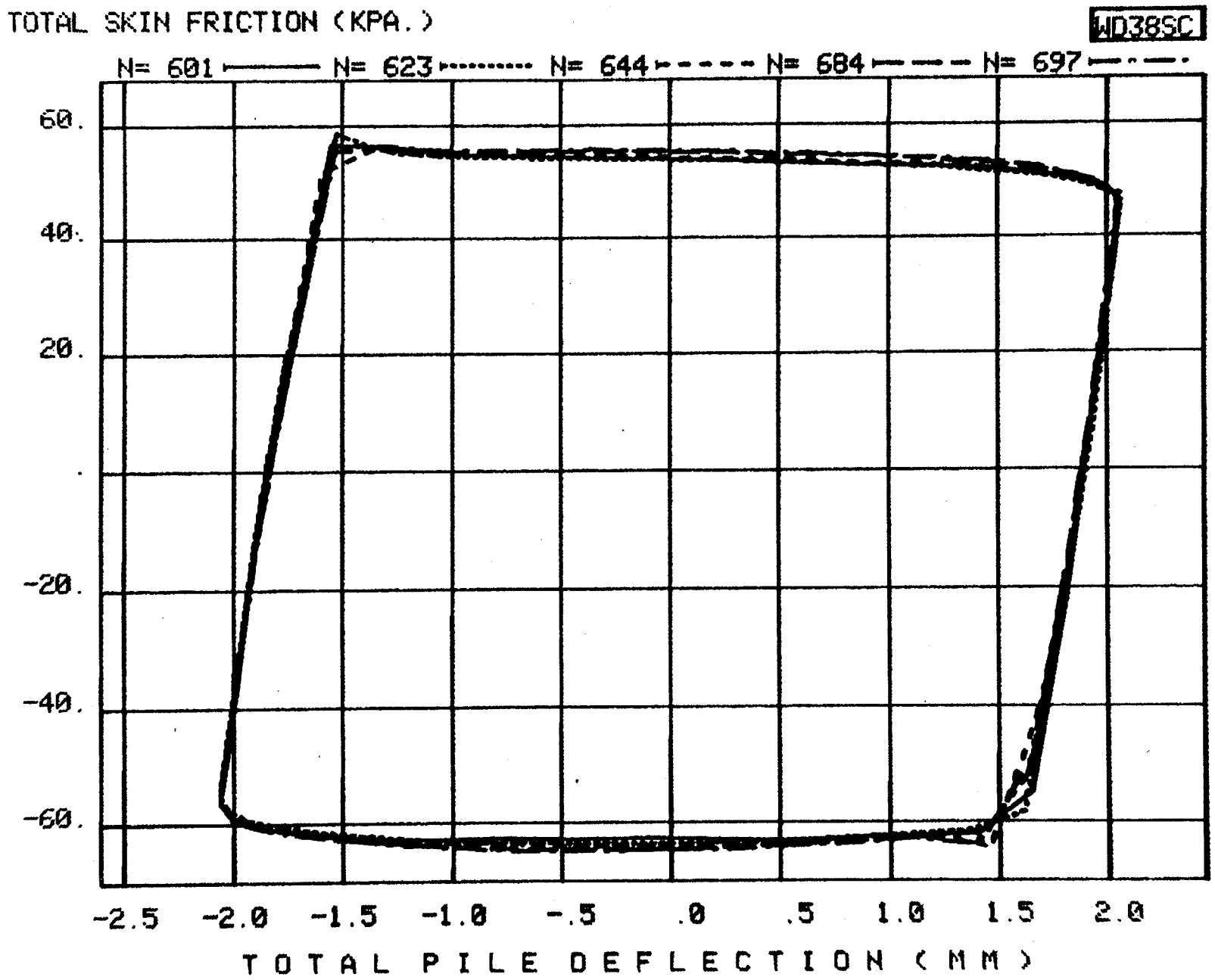
TOTAL SKIN FRICTION (KPA.)
WD38SC
N= 601
N= 623
N= 644
N= 684
N= 697
60.
40.
20.
-20.
-40.
-60.
-2.5
-2.0
-1.5
-1.0
-.5
.0
.5
1.0
1.5
2.0
TOTAL PILE DEFLECTION (MM)

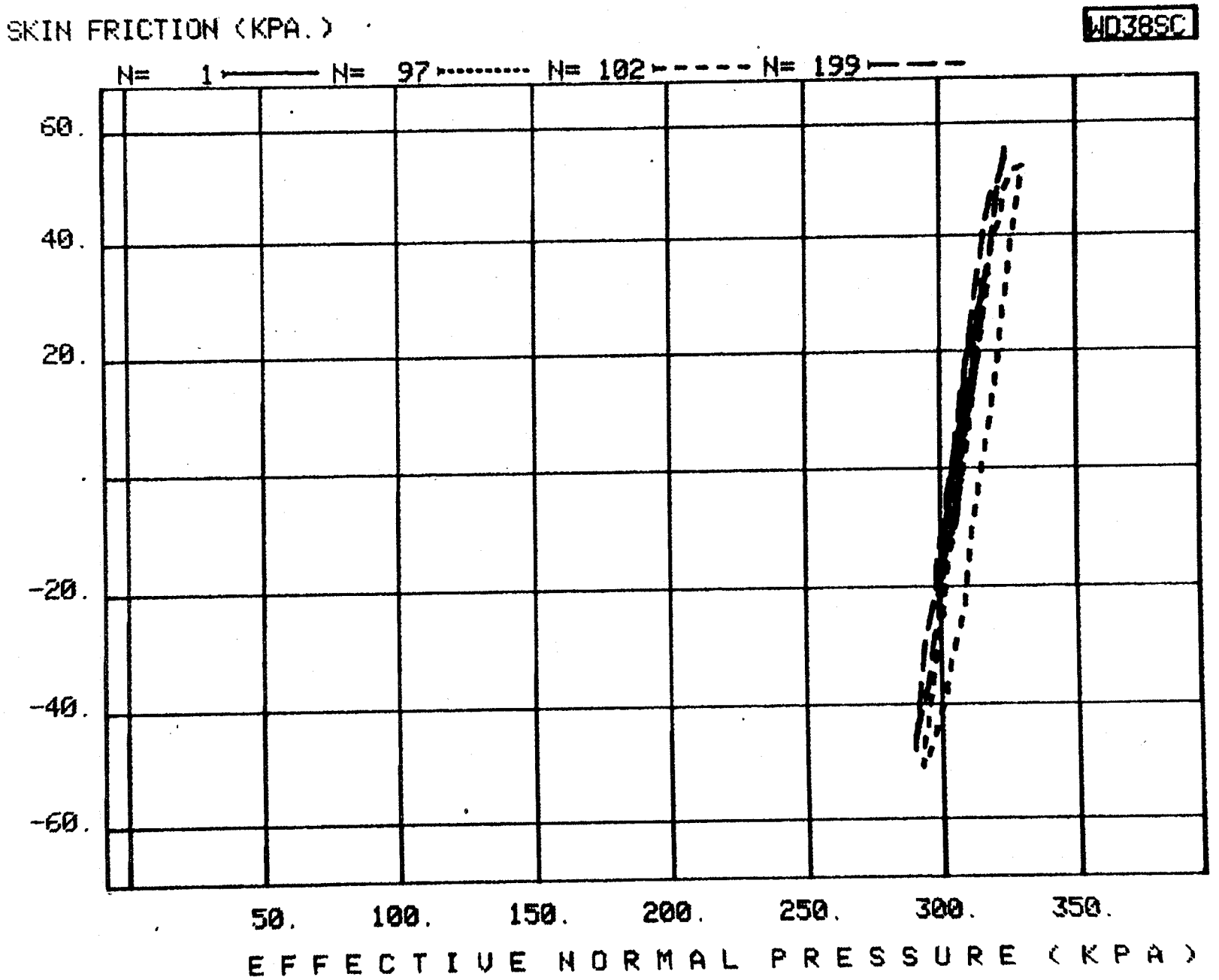
SKIN FRICTION (KPA.)
WD38SC
N= 1
N= 97
N= 102
N= 199
60.
40.
20.
-20.
-40.
-60.
50.
100.
150.
200.
250.
300.
350.
EFFECTIVE NORMAL PRESSURE (KPA)

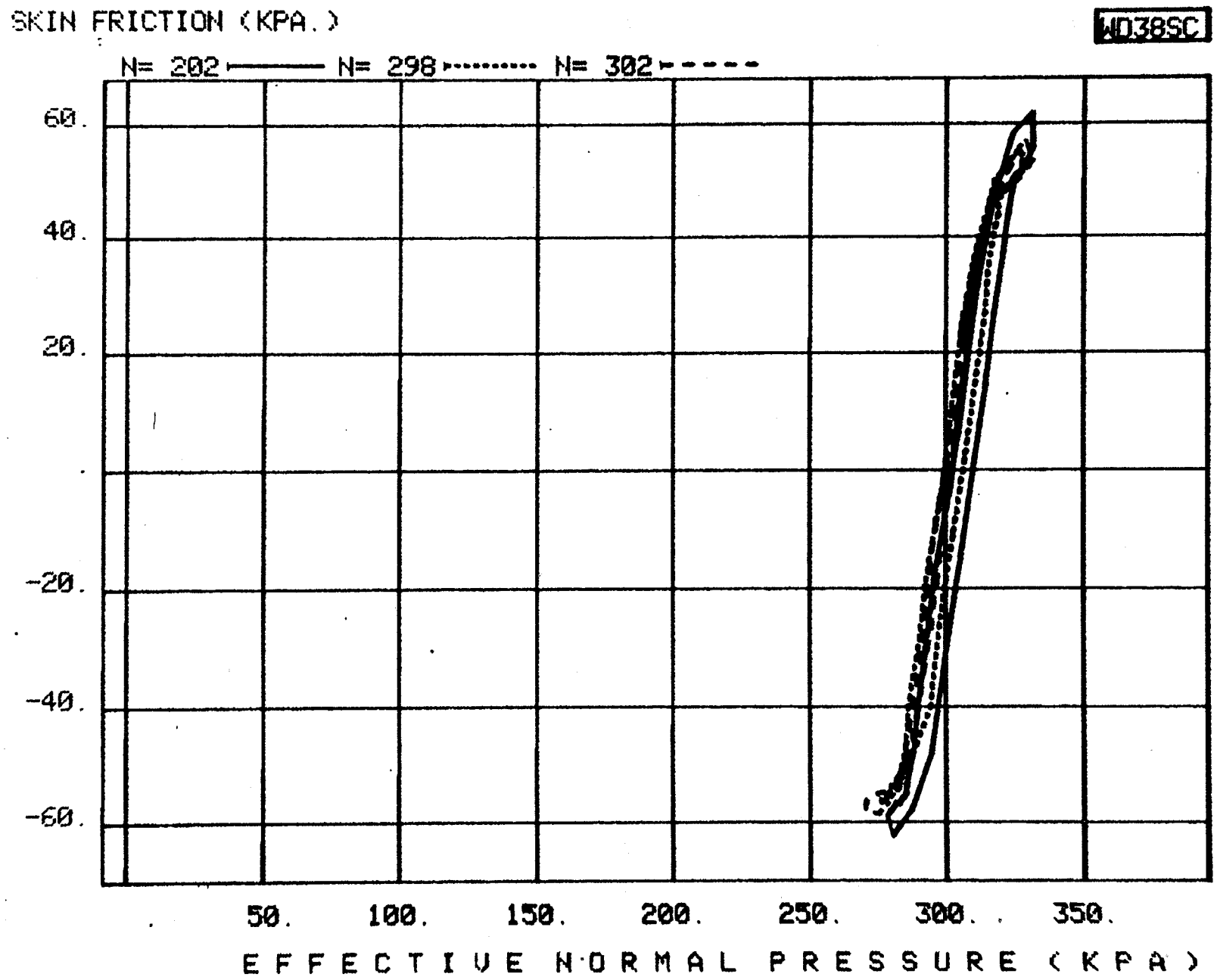
SKIN FRICTION (KPA.)
WD38SC
N= 202
N= 298
N= 302
60.
40.
20.
-20.
-40.
-60.
50.
100.
150.
200.
250.
300.
350.
EFFECTIVE NORMAL PRESSURE (KPA)

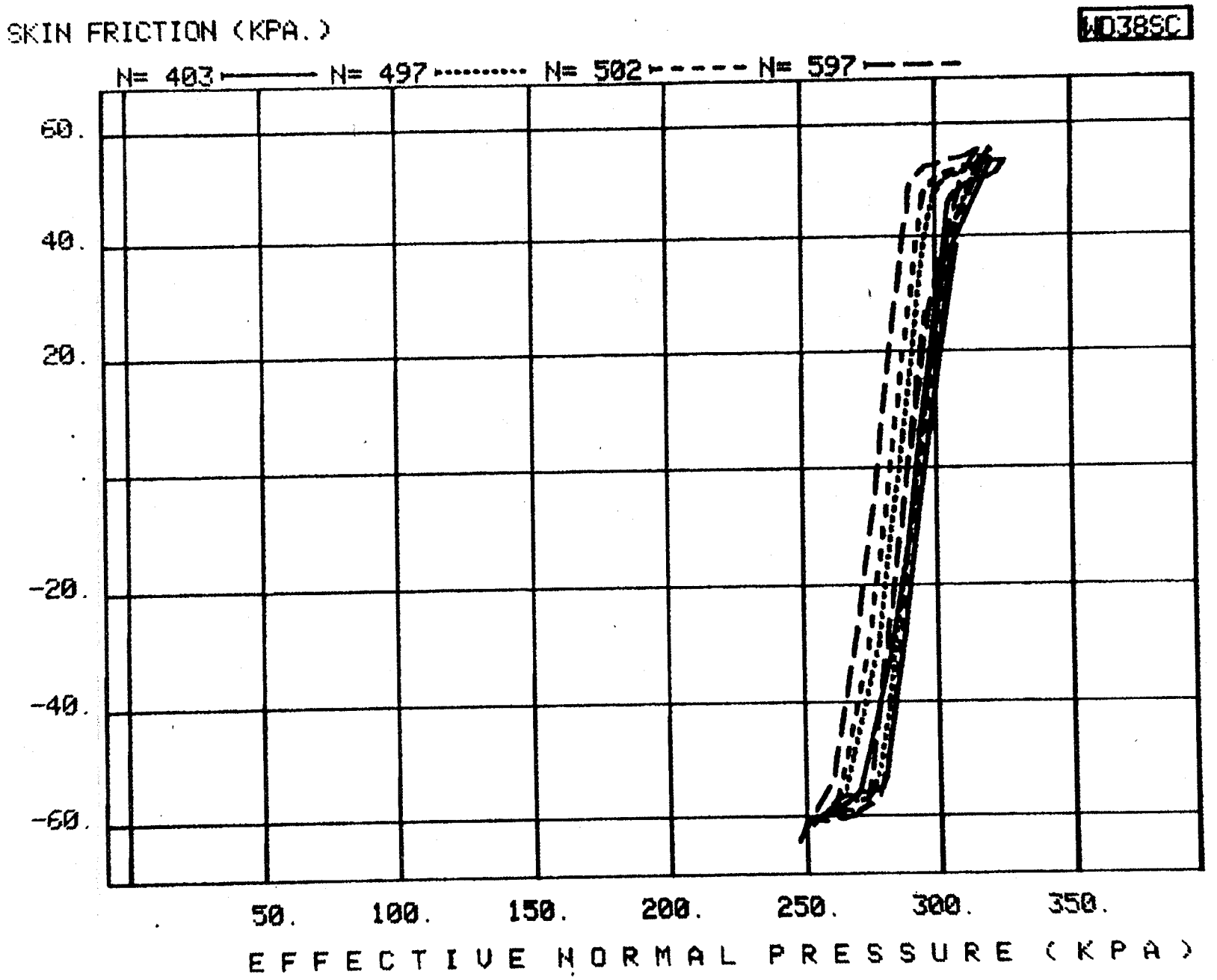
SKIN FRICTION (KPA.)
WD38SC
N= 403
N= 497
N= 502
N= 597
60.
40.
20.
-20.
-40.
-60.
50.
100.
150.
200.
250.
300.
350.
EFFECTIVE NORMAL PRESSURE (KPA)

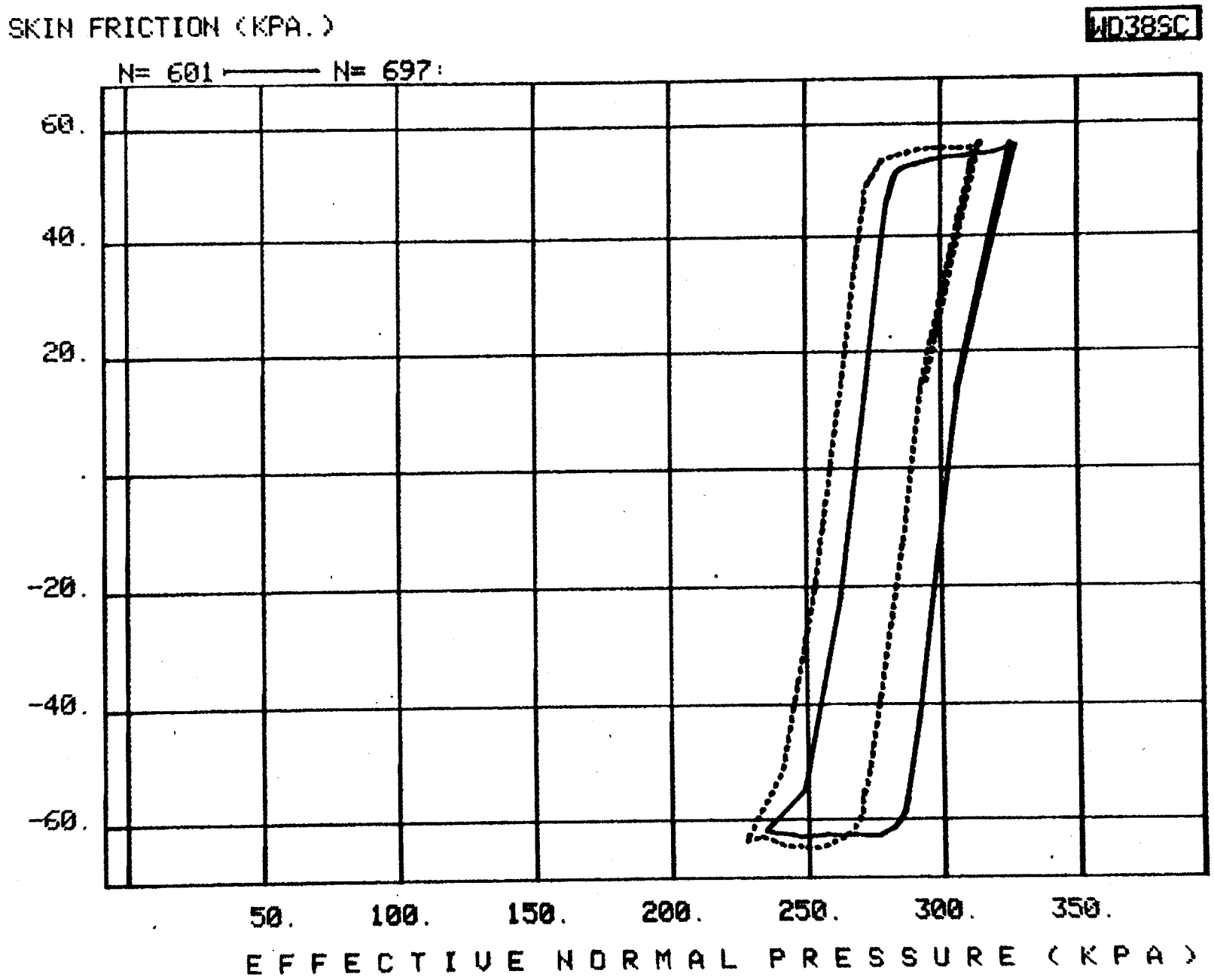
SKIN FRICTION (KPA.)
WD38SC
N= 601 ——— N= 697:
60.
40.
20.
-20.
-40.
-60.
50.
100.
150.
200.
250.
300.
350.
EFFECTIVE NORMAL PRESSURE (KPA)

RESPONSE ON CYCLIC LOADING (KPA.) CYCLE NO. 1

WD38SC

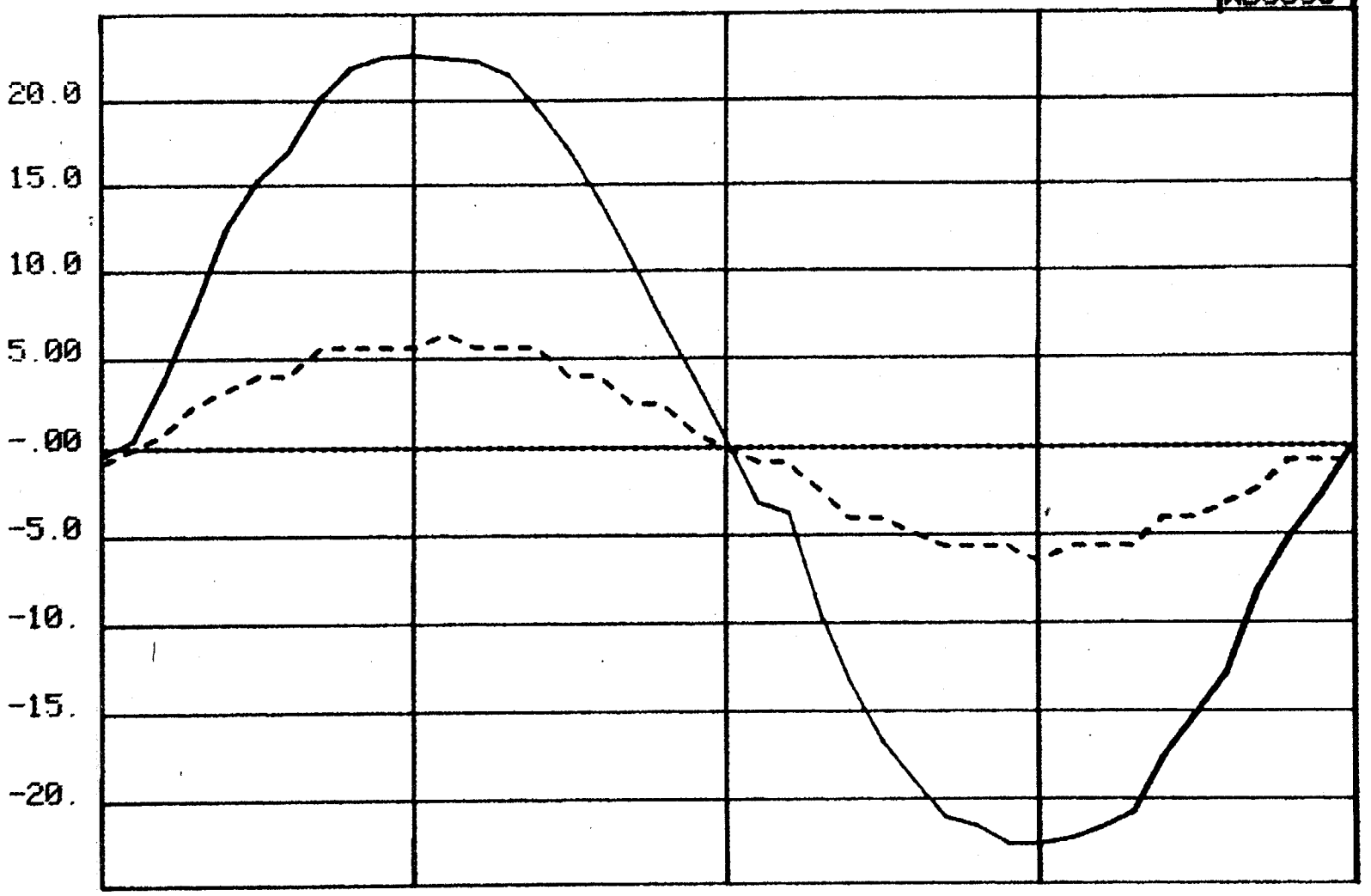

LEGEND:

		PERM. VALUES
———	SKIN FRICTION	1.17 KPA.
·····	PORE PRESSURE	59.40 KPA.
- - - -	TOTAL NORMAL PRESSURE	364.4 KPA.

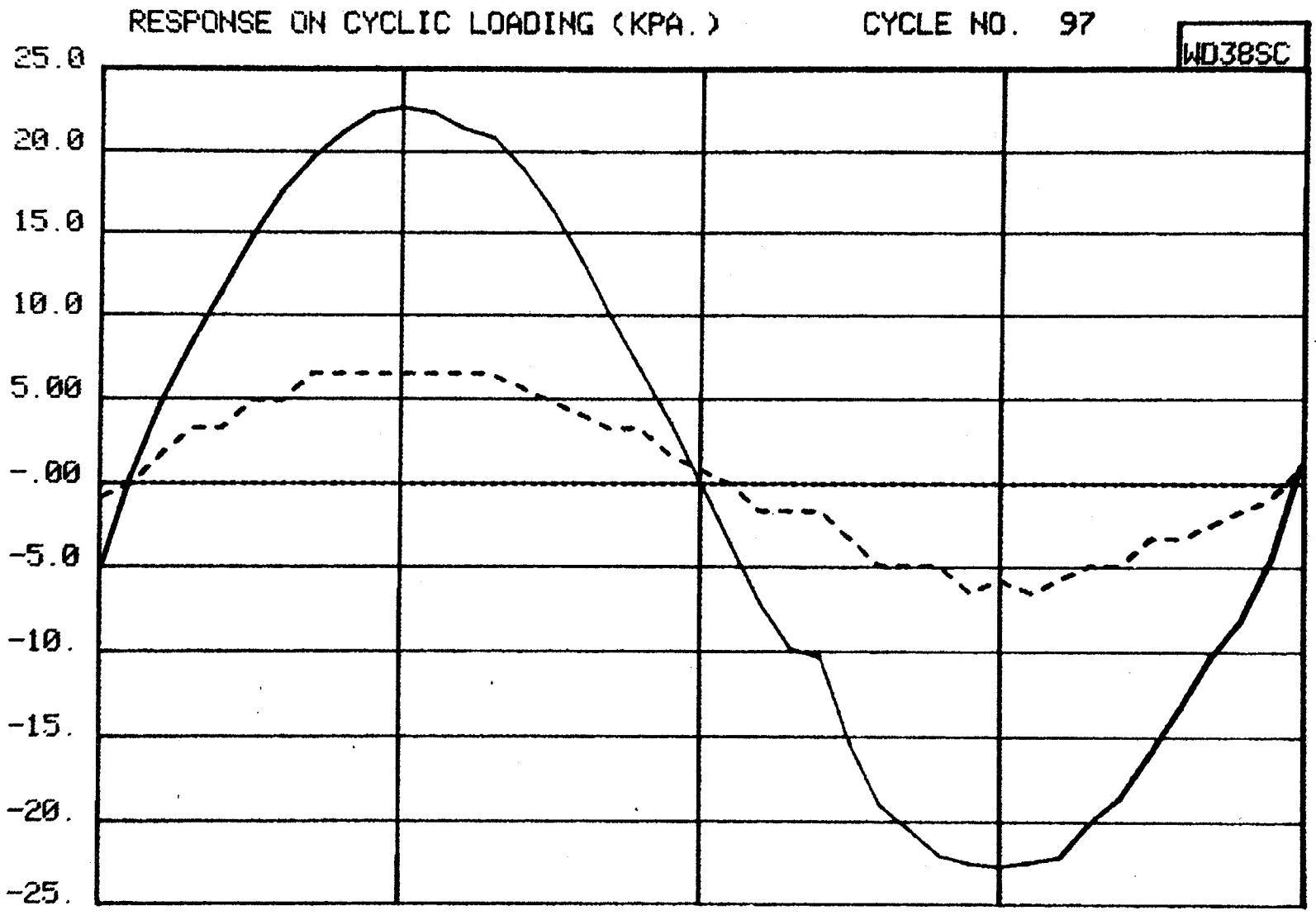

LEGEND:

		PERM. VALUES
———	SKIN FRICTION	9.36 KPA.
·····	PORE PRESSURE	59.40 KPA.
- - - -	TOTAL NORMAL PRESSURE	368.5 KPA.

RESPONSE ON CYCLIC LOADING (KPA.) CYCLE NO. 102 WD38SC

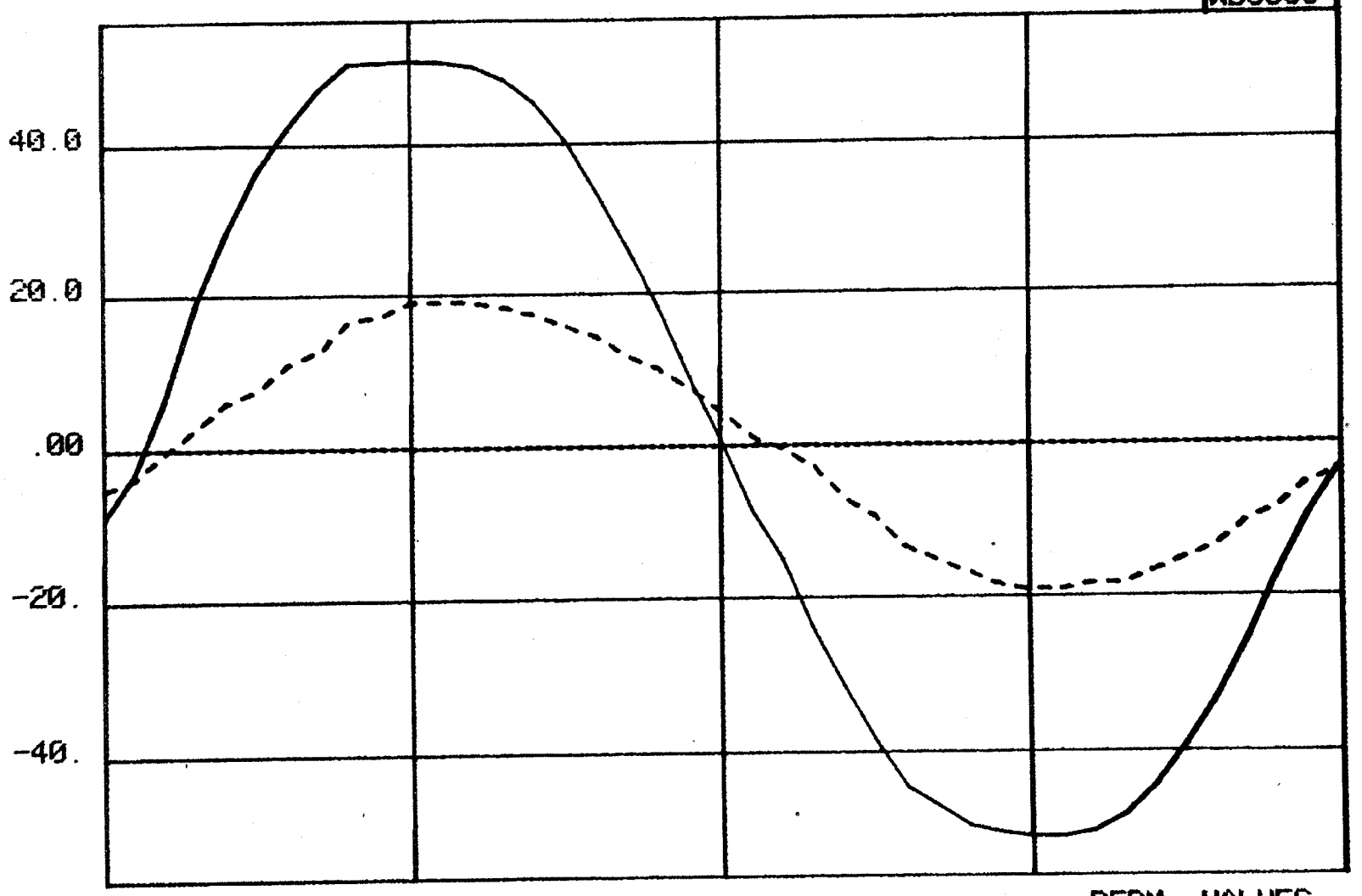

LEGEND:

		PERM. VALUES
———	SKIN FRICTION	.59 KPA.
·····	PORE PRESSURE	59.40 KPA.
- - - -	TOTAL NORMAL PRESSURE	370.5 KPA.

RESPONSE ON CYCLIC LOADING (KPA.) CYCLE NO. 199

WD38SC

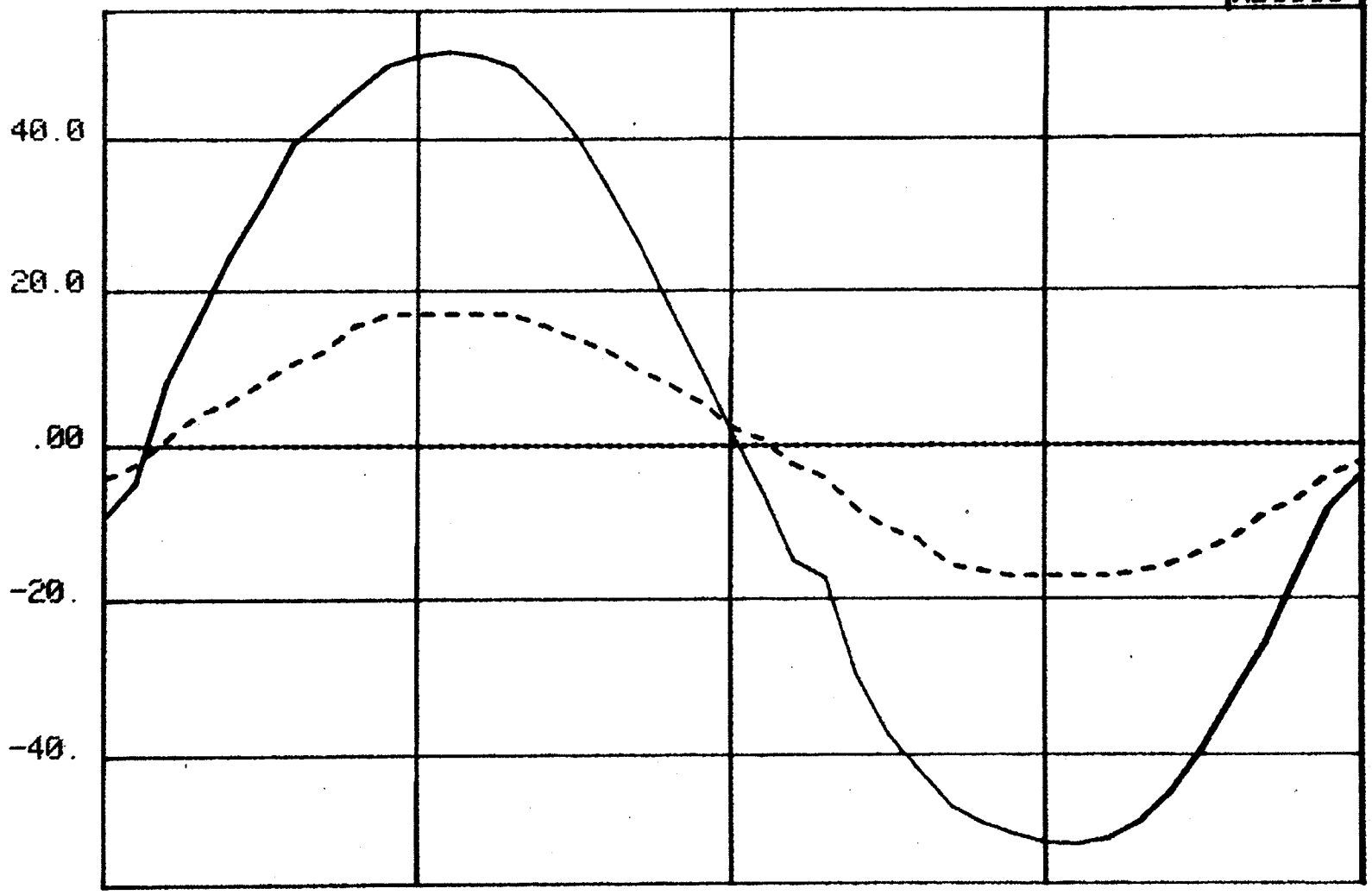

LEGEND:

		PERM. VALUES
———	SKIN FRICTION	3.95 KPA.
·····	PORE PRESSURE	59.40 KPA.
- - - -	TOTAL NORMAL PRESSURE	366.1 KPA.

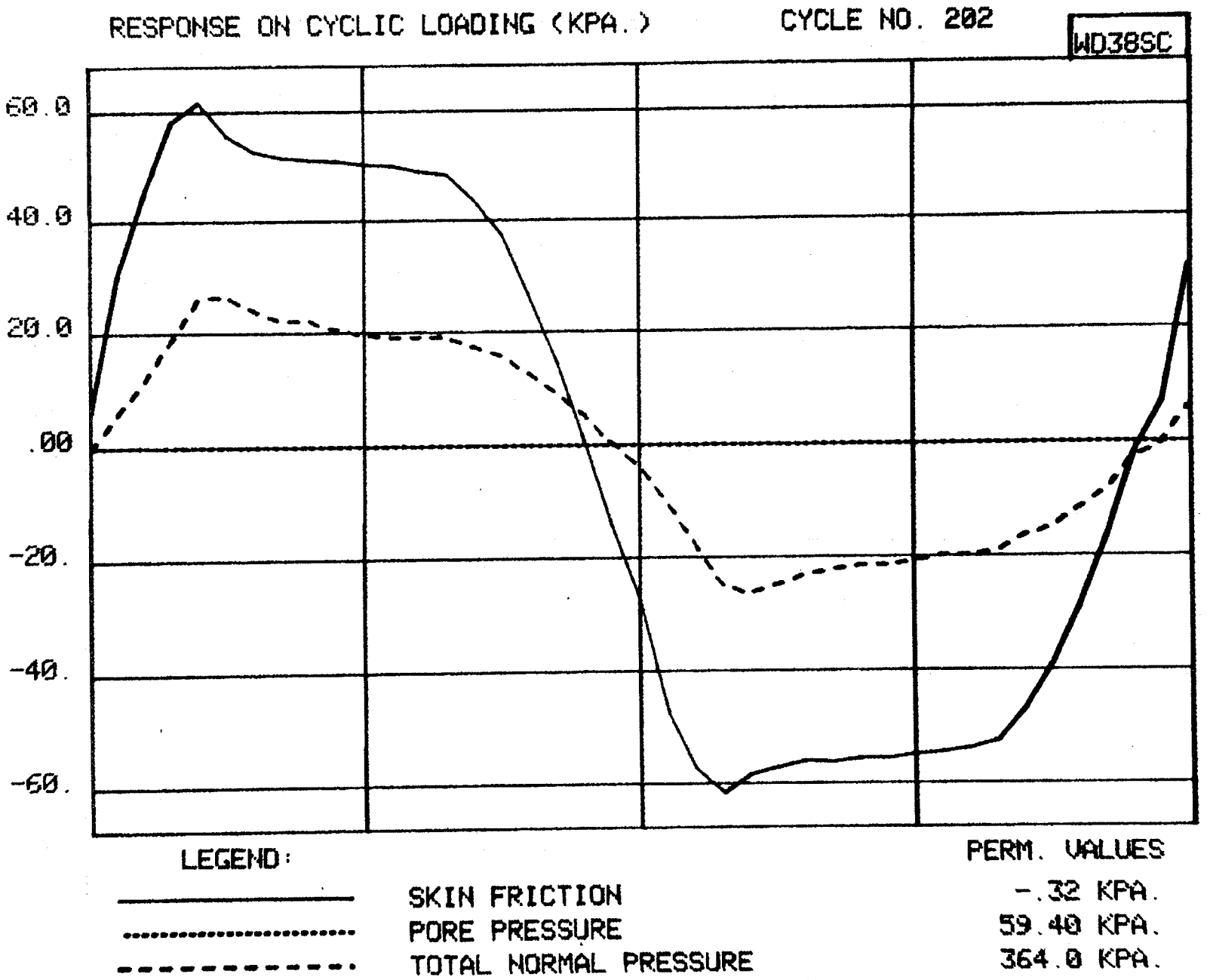
RESPONSE ON CYCLIC LOADING (KPA.)
CYCLE NO. 202
WD38SC
60.0
40.0
20.0
.00
-20.
-40.
-60.
LEGEND:
SKIN FRICTION
PORE PRESSURE
TOTAL NORMAL PRESSURE
PERM. VALUES
-.32 KPA.
59.40 KPA.
364.0 KPA.

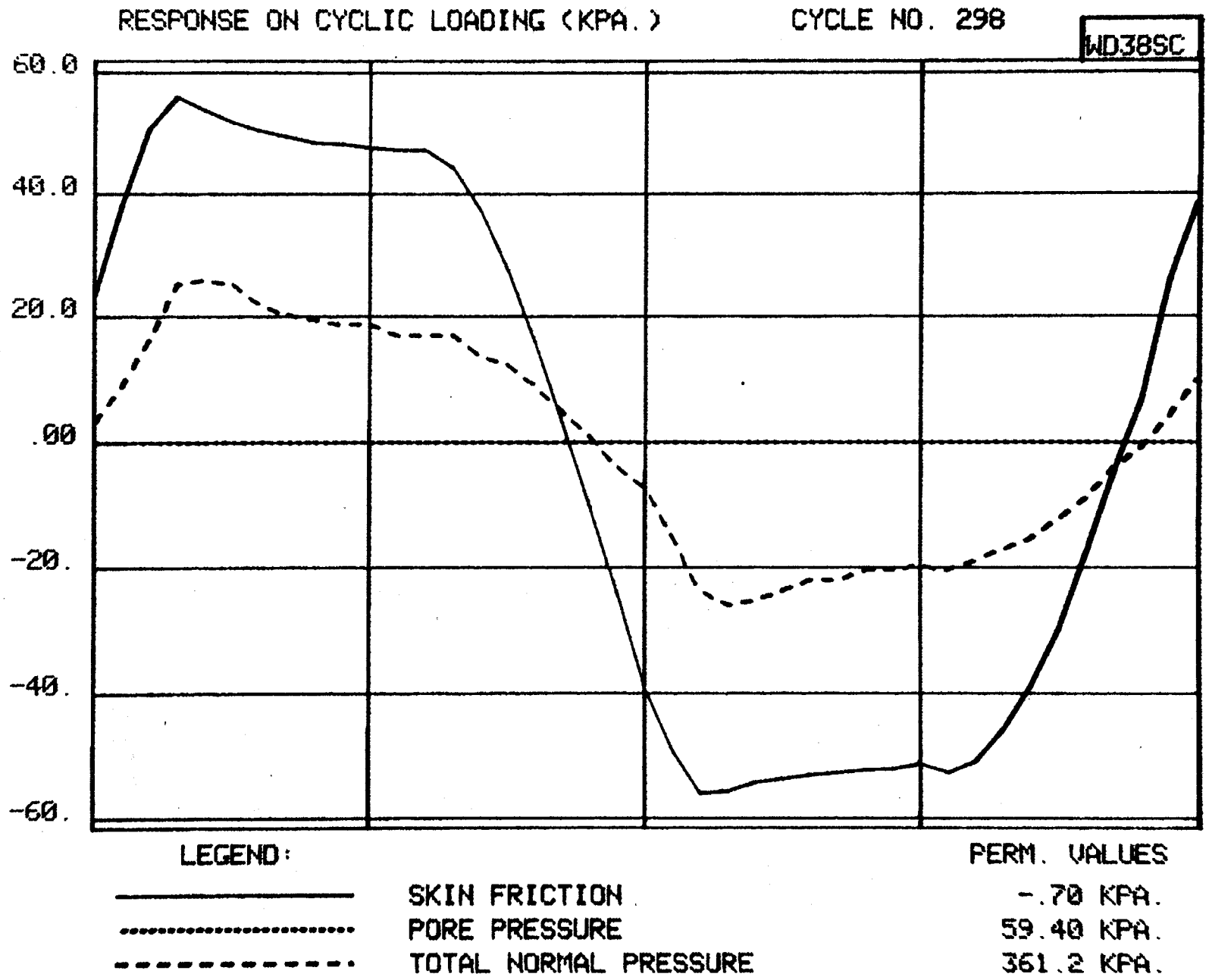
RESPONSE ON CYCLIC LOADING (KPA.)
CYCLE NO. 298
WD38SC
60.0
40.0
20.0
.00
-20.
-40.
-60.
LEGEND:
PERM. VALUES
SKIN FRICTION
-.70 KPA.
PORE PRESSURE
59.40 KPA.
TOTAL NORMAL PRESSURE
361.2 KPA.

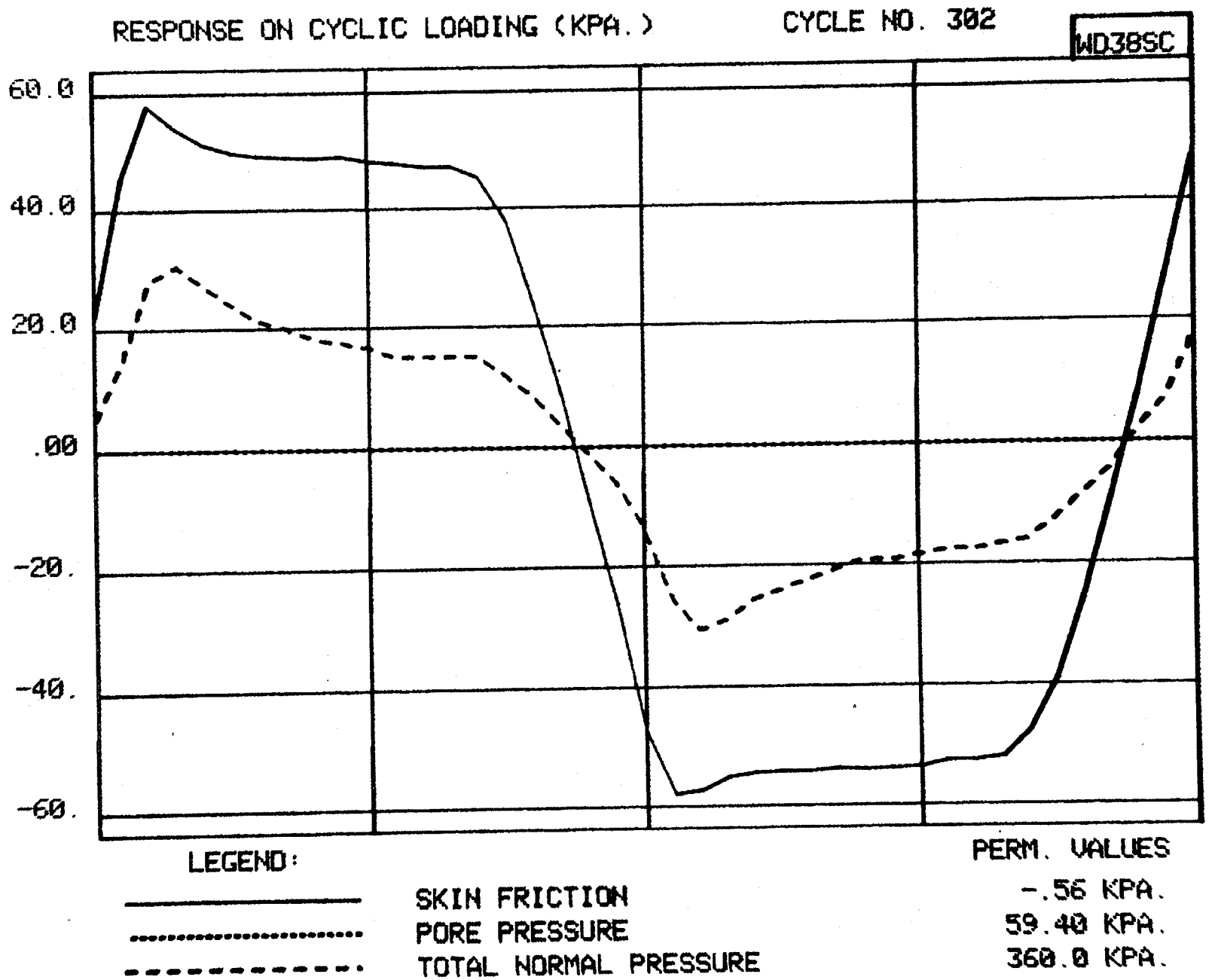
RESPONSE ON CYCLIC LOADING (KPA.)
CYCLE NO. 302
WD38SC
60.0
40.0
20.0
.00
-20.
-40.
-60.
LEGEND:
SKIN FRICTION
PORE PRESSURE
TOTAL NORMAL PRESSURE
PERM. VALUES
-.56 KPA.
59.40 KPA.
360.0 KPA.

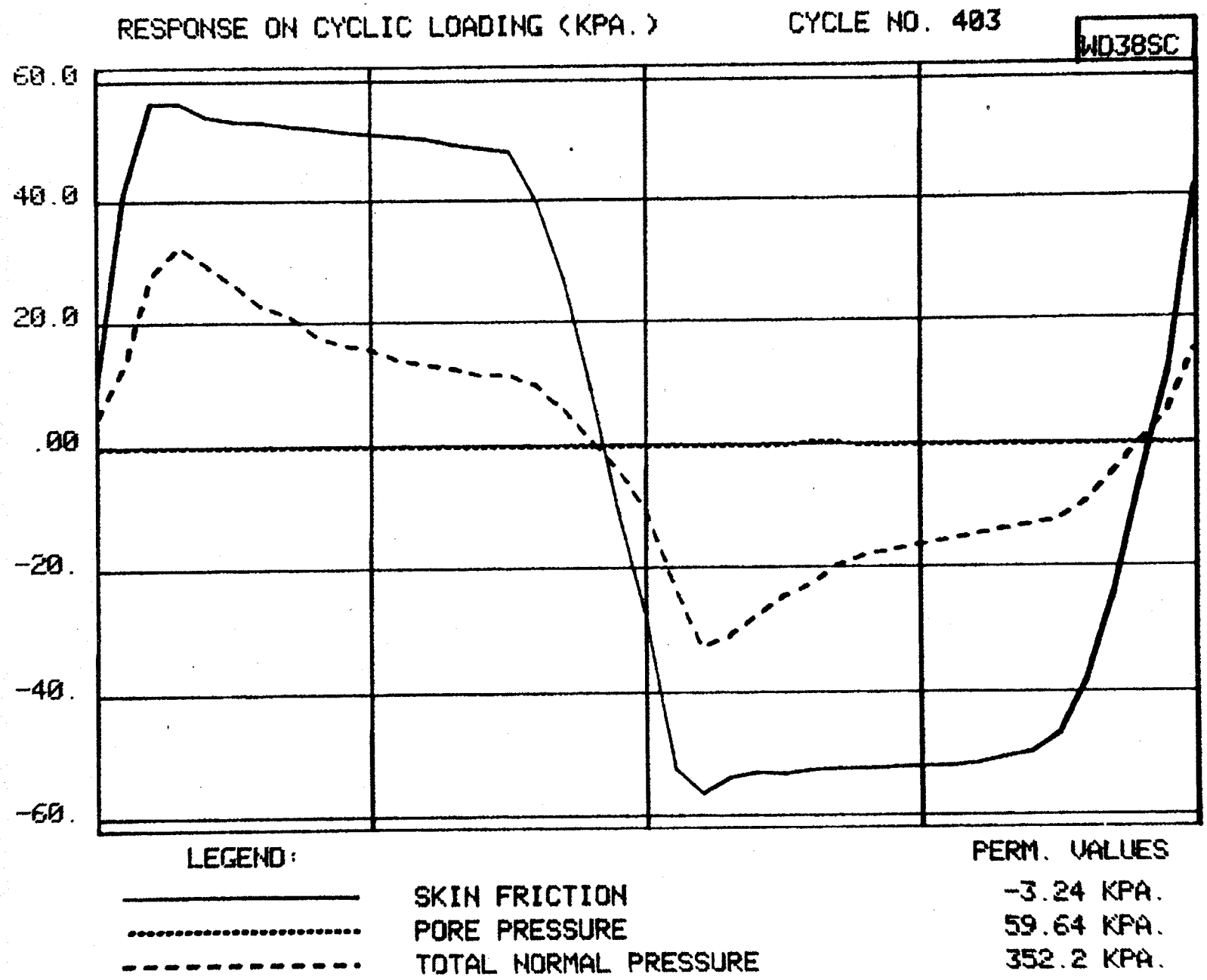
RESPONSE ON CYCLIC LOADING (KPA.)
CYCLE NO. 403
WD38SC
60.0
40.0
20.0
.00
-20.
-40.
-60.
LEGEND:
SKIN FRICTION
PORE PRESSURE
TOTAL NORMAL PRESSURE
PERM. VALUES
-3.24 KPA.
59.64 KPA.
352.2 KPA.

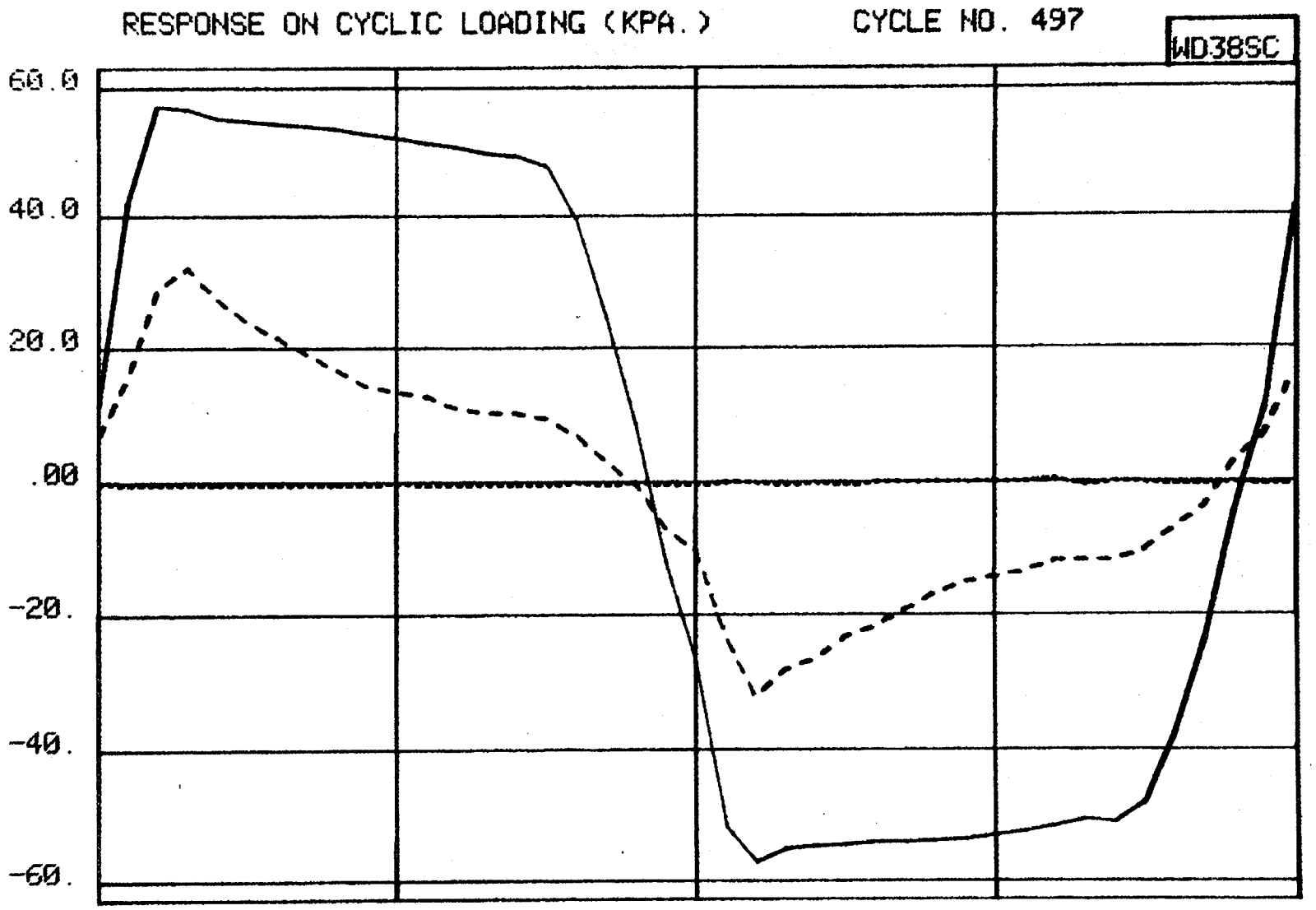

LEGEND:

		PERM. VALUES
———	SKIN FRICTION	-3.24 KPA.
·····	PORE PRESSURE	59.88 KPA.
- - - -	TOTAL NORMAL PRESSURE	347.7 KPA.

RESPONSE ON CYCLIC LOADING (KPA.) CYCLE NO. 502

WD38SC

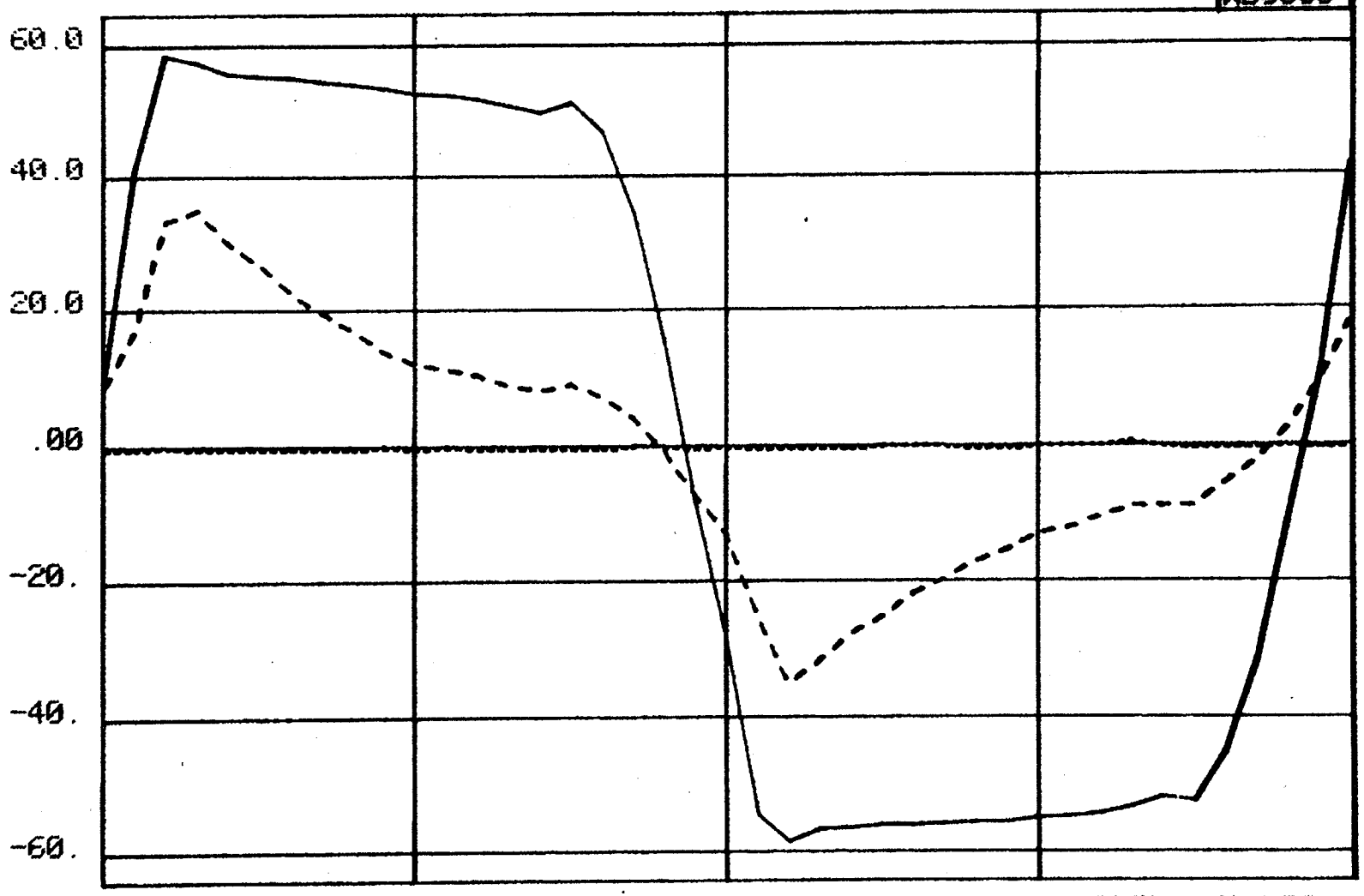

LEGEND:

		PERM. VALUES
———	SKIN FRICTION	-3.00 KPA.
·····	PORE PRESSURE	59.88 KPA.
- - - -	TOTAL NORMAL PRESSURE	346.5 KPA.

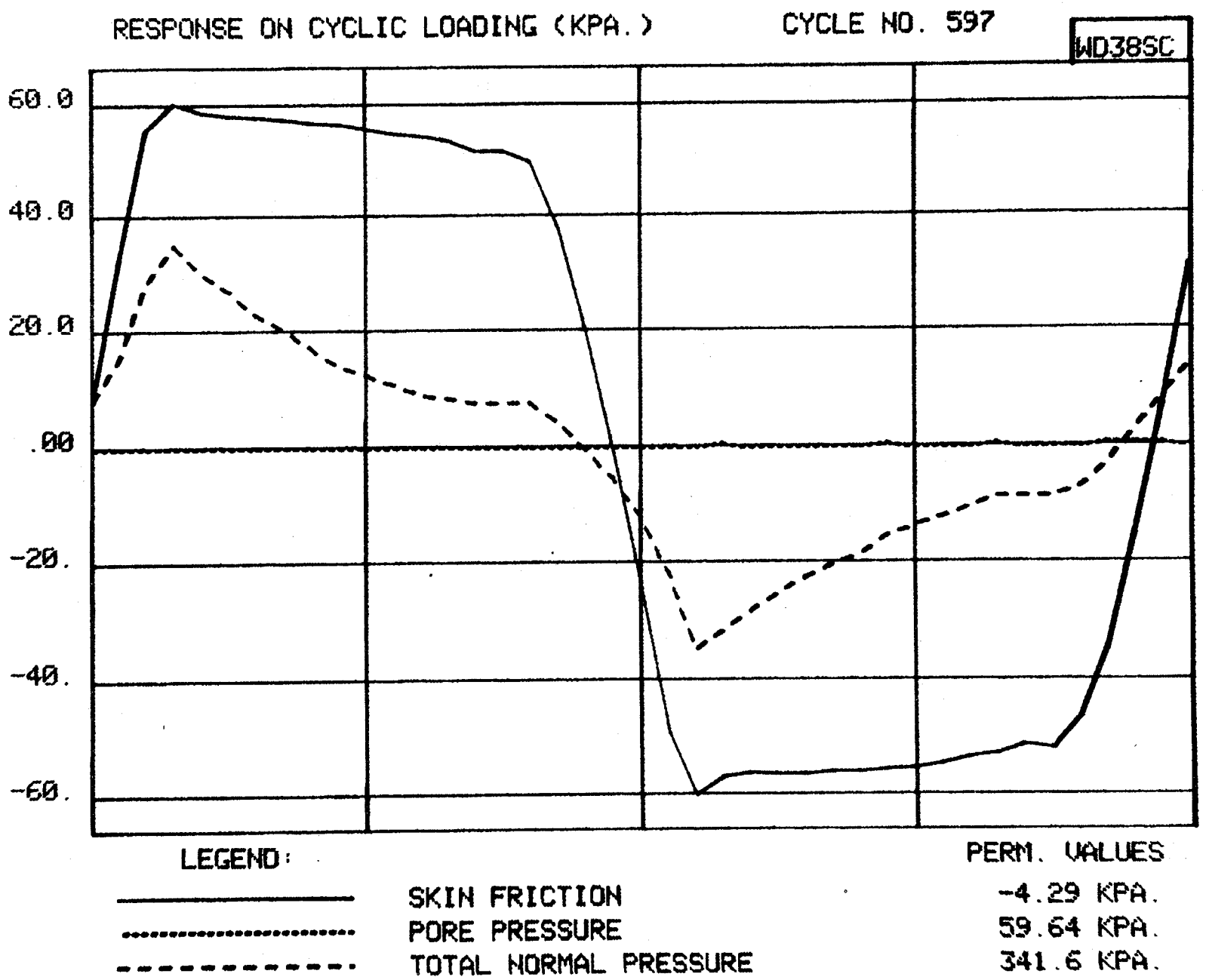
RESPONSE ON CYCLIC LOADING (KPA.)
CYCLE NO. 597
WD38SC
60.0
40.0
20.0
.00
-20.
-40.
-60.
LEGEND:
SKIN FRICTION
PORE PRESSURE
TOTAL NORMAL PRESSURE
PERM. VALUES
-4.29 KPA.
59.64 KPA.
341.6 KPA.

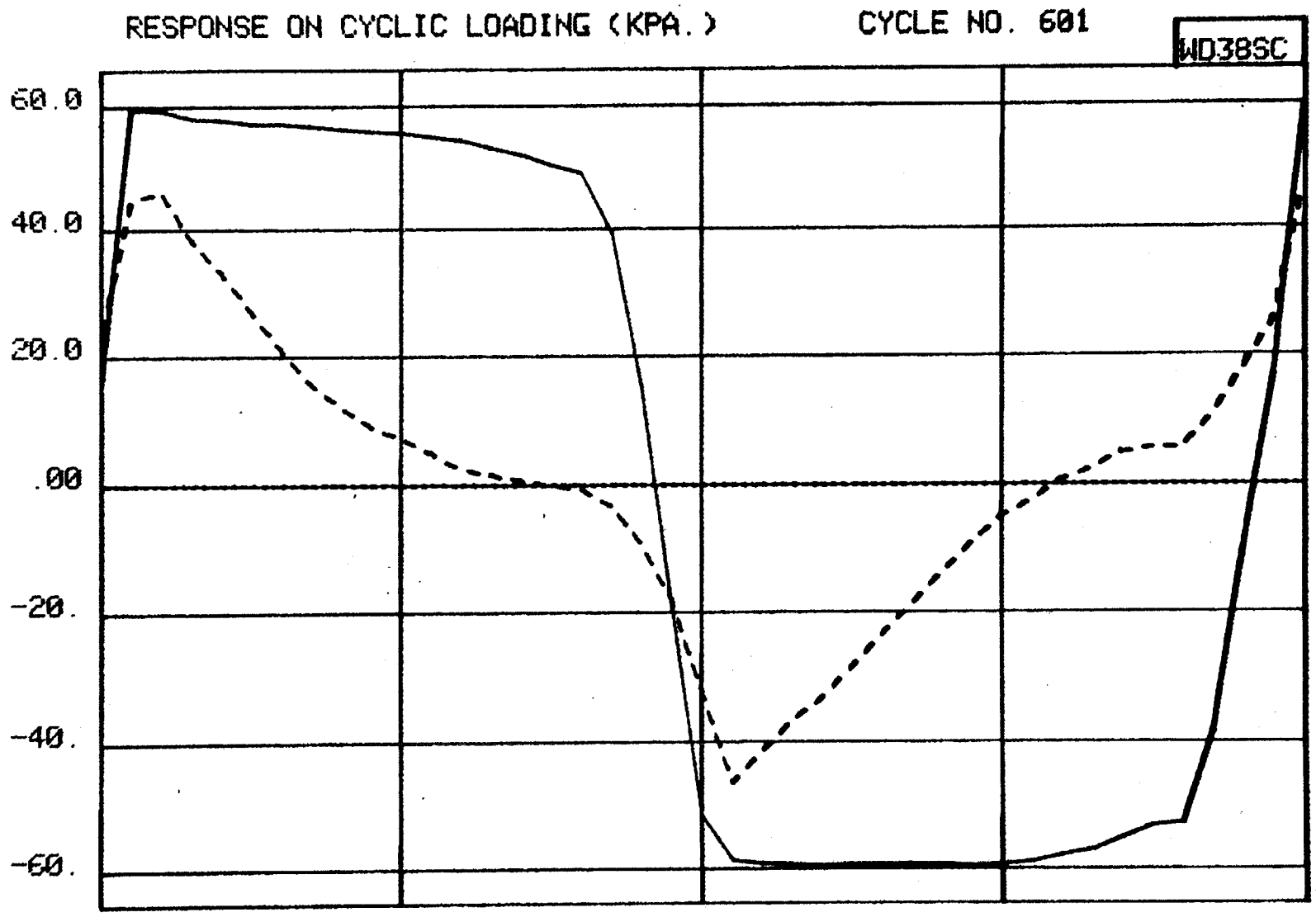

LEGEND:

		PERM. VALUES
———	SKIN FRICTION	-3.33 KPA.
·····	PORE PRESSURE	59.40 KPA.
- - - -	TOTAL NORMAL PRESSURE	340.0 KPA.

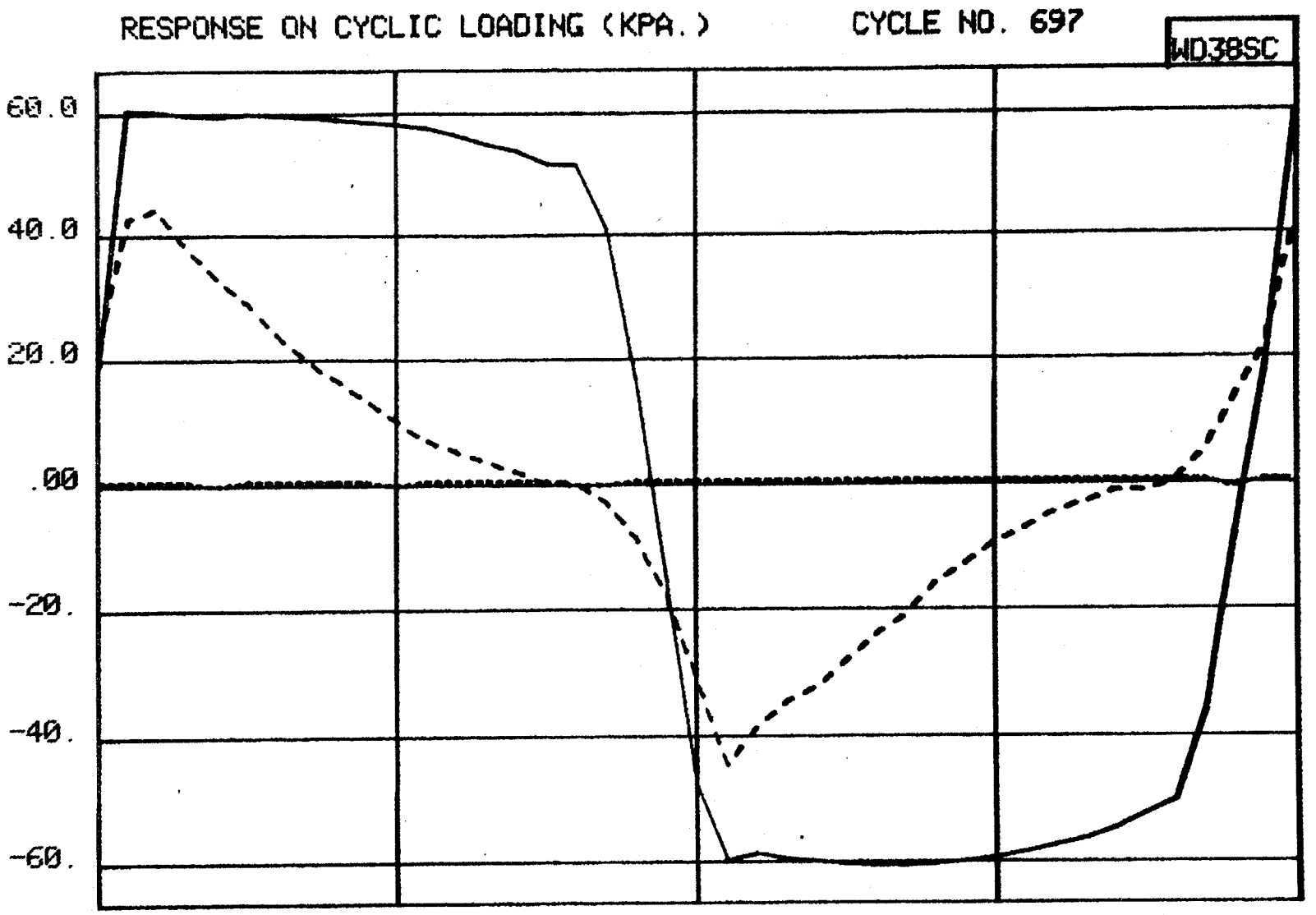

LEGEND:

		PERM. VALUES
———	SKIN FRICTION	-4.20 KPA.
·····	PORE PRESSURE	58.92 KPA.
- - - -	TOTAL NORMAL PRESSURE	330.6 KPA.

VERITEC MARINE TECHNOLOGY CONSULTANTS

POSTAL ADDRESS: P.O.BOX 300, 1322 Høvik, NORWAY

TELEPHONE: + 47 (02) 12 99 00
TELEX: 76 192 VERIT N

TECHNICAL REPORT

Date 29. Juni 1984			
Report No. 84-3361	Subject Group P2,P3	Department VT/66	Project No. 66 40 17
Title of Report CNRD 13-2, TENSION PILE STUDY APPENDICES F TO L OF FINAL REPORT		Approved by for Rune Dahlberg Senior Principal Engineer	
Client/Sponsor of project Conoco Norway Inc.		Client/Sponsor ref. Harry Wahl	
Work carried out by Kjell Hauge		Reporter's sign.	

Summary

This report contains the Appendices F through L of the Final Report, CNRD 13-2 TENSION PILE STUDY.

See the Excecutive Summary of the Final Report for summary.

The total report consists of:

CNRD 13-2 TENSION PILE STUDY
- FINAL REPORT
- APPENDICES A TO E
- APPENDICES F TO L

4 Indexing terms

TENSION PILES
CYCLIC LOADING
SKIN FRICTION
CAPACITY

Distribution statement:

- [x] No distribution without permission from the responsible department
- [ ] Limited distribution within VERITEC.
- [ ] Free distribution.

Date of last rev.	Rev. No.

Number of pages 327/847

CONOCO NORWAY

RESEARCH AND DEVELOPMENT

CNRD 13-2: TENSION PILE STUDY

FINAL REPORT

APPENDICES F TO L

CONTENT

FINAL REPORT

PREFACE ii

CONTENT iv

EXECUTIVE SUMMARY ix

1. INTRODUCTION 1

1.1 GENERAL 1
1.2 RELATIONSHIP TO CNRD PROGRAM 2
1.3 REFERENCE TO ERTEC'S WORK WITHIN CNRD 13-2 3
1.4 REFERENCE TO WORK BY NGI AND NTH WITHIN CNRD 13-2 3
1.5 PREVIOUS REPORTS BY VERITAS WITHIN CNRD 13-2 4
1.6 FINAL REPORT 5
1.7 FURTHER WORK 5

2. DESCRIPTION OF LABORATORY MODEL PILE TESTS 6

2.1 GENERAL 6
2.2 EQUIPMENT 7
2.2.1 Model Pile Test Chamber 7
2.2.2 Model Pile 7
2.2.3 Loading System 9
2.3 DATA ACQUISITION SYSTEM 9
2.4 PREPARATION OF SOIL SAMPLES 10
2.5 CHARACTERIZATION OF REMOULDED, RECONSOLIDATED SOIL SAMPLES AND COMPARISON WITH UNDISTURBED SAMPLES AND FIELD CONDITIONS 12
2.5.1 General 12
2.5.2 Plasticity Properties 12
2.5.3 Natural Water Content 13
2.5.4 Consolidation Properties 14
2.5.5 Static Stress-Strain and Strength 14
2.5.6 Cyclic Stress-Strain-Porepressure Generation 15
2.5.7 Comparison of Soil Conditions in the Laboratory Tests with the Field Conditions 17

2.6 LABORATORY MODEL PILE TEST PROGRAM 23
2.6.1 Objective of the Different Test Types 23
2.6.2 Summary of Test Program 23

3. MODEL PILE TEST RESULTS 25
3.1 GENERAL 25
3.2 EVALUATION OF CHANGE IN SKIN FRICTION WITH TIME IN THE LABORATORY MODEL PILE TESTS 25
3.3 STATIC CAPACITY 28
3.4 CYCLIC STRESS CONTROLLED TESTS 31
3.5 CYCLIC DISPLACEMENT CONTROLLED TESTS 34
3.6 CREEP AND RELAXATION TESTS 37

4. THEORETICAL WORK 38
4.1 GENERAL 38
4.2 PORE PRESSURE AND NORMAL STRESS GENERATION DURING INSTALLATION 39
4.2.1 Theoretical Estimates of Excess Pore Pressure 39
4.2.2 Comparison with Measured Values 39
4.3 SET-UP (PORE PRESSURE DISSIPATION) 41
4.3.1 Theoretical Initial Distribution of Pore Pressure 41
4.3.2 Consolidation Analysis Method 41
4.3.3 Consolidation Properties 42
4.3.4 Comparison between Predicted and Measured Behaviour 43
4.4 LOAD - DISPLACEMENT (T-Z) RELATIONSHIP 43
4.4.1 Theoretical Single Slice Model 43
4.5 EVALUATION OF PORE PRESSURE GENERATION UNDER CYCLIC LOADING 45
4.5.1 General 45
4.5.2 Analysis Model 46
4.5.3 Finite Element Model 49
4.5.4 Soil Consolidation Parameters 50
4.5.5 Simulation of Cyclic Loading 50
4.5.6 Comparison with Measured Behaviour 51
4.6 DEGRADATION MODELS 52
4.6.1 General 52
4.6.2 The DRIVE 15 Degradation Model 52
4.6.3 Proposal for Extended Degradation Model 53

4.7 EFFECT OF PILE FLEXIBILITY ON DEGRADATION 53
4.7.1 Analysis with DRIVE 15 53
4.7.2 Consequences of Other Degradation Models 54
4.8 PILE CREEP ANALYSIS 55
4.8.1 General 55
4.8.2 T-Z Creep Model 56
4.8.3 Creep Analysis of Elastic Piles 58
4.8.4 Sample Calculations 60
5. REFERENCES 63

LIST OF APPENDICES

APPENDIX A: TEST 4, STRATUM III: DETAILED RESULTS
APPENDIX B: TEST 5, STRATUM II : DETAILED RESULTS
APPENDIX C: TEST 6, STRATUM III: DETAILED RESULTS
APPENDIX D: TEST 7, STRATUM II : DETAILED RESULTS
APPENDIX E: TEST 8, STRATUM III: DETAILED RESULTS
APPENDIX F: TEST 9, STRATUM II : DETAILED RESULTS
APPENDIX G: TEST 10, STRATUM III: DETAILED RESULTS
APPENDIX H: TEST 11, STRATUM II : DETAILED RESULTS
APPENDIX I: TEST 12, STRATUM III: DETAILED RESULTS
APPENDIX J: TEST 13, STRATUM II : DETAILED RESULTS
APPENDIX K: RESULTS OF LABORATORY TESTS FOR COMPARISON OF REMOULDED, RECONSOLIDATED MATERIAL AND UNDISTURBED MATERIAL
APPENDIX L: DESCRIPTION OF COMPUTER PROGRAM **CRAPIL** **CR**eep Analysis of **PIL**es

LIST OF TABLES

Table 2.1 Plasticity Properties for Model Test Clay 13
Table 2.2 Water Content Compariso 13
Table 2.3 Comparison of Triaxial Test Results 17
Table 2.4 Shear Strength Test Correlations 19
Table 2.5 Relationship between Undrained Shear Strengths Measured by Different Test Methods 20
Table 2.6 Shear Strength Comparison with Segment Tests 21

Table 3.1	Summary of Laboratory Model Pile Test Program and Test Results	26
Table 4.1	Comparison Between Predicted and Measured Pressures	40
Table 4.2	Number of Cycles to Liquefaction, N_l	51
Table 4.3	Rayleigh Distribution of Load Amplitudes for Wave Parcels - Example Problem with CRAPIL	61

LIST OF FIGURES

Figure 2.1	Laboratory Model Pile Test Chamber and Model Pile	64
Figure 2.2	Photograph of Model Pile Test Chamber	65
Figure 2.3	Photograph of Model Pile	66
Figure 2.4	Photograph of Model Pile	67
Figure 2.5	Schematic Diagram of Test Set-Up and Signal Flow	68
Figure 2.6	Proposed Shear Strength Profile at West Delta	69
Figure 3.1	Undrained Shear Strength in Clay Samples (free field) Measured after Consolidation and Completion of Test	70
Figure 3.2	Measured Undrained Shear Strength vs. Water Content for Test Samples	71
Figure 3.3	α-Factors vs. Free Field Undrained Shear Strength	72
Figure 3.4	α-Factors vs. Set-Up Time	73
Figure 3.5	Friction Reduction Factor vs. Undrained Shear Strength	74
Figure 3.6	β-Factors vs. Effective Overburden Pressure	75
Figure 3.7	Interface Cyclic Shear Module vs. Undrained Shear Strength	76
Figure 4.1	Theoretical Prediction of Excess Pore Pressure vs. Radial Distance due to Pile Installation	77
Figure 4.2	Predicted and Measured Pore Pressure at Pile Wall vs. Time for Laboratory Tests	78
Figure 4.3	Predicted and Measured Pore Pressure at Pile Wall vs. Time for 3"" Segment Tests	79
Figure 4.4	Theoretical $t-z$-Curves for Laboratory Model Pile Tests	80
Figure 4.5	Theoretical $t-z$-Curves for Segment Tests	81
Figure 4.6	Single Slice Model for Laboratory and Segment Pile	82

Figure 4.7	Theoretical Prediction of Increase in Undrained Shear Strength due to Pile Installation	83
Figure 4.8	Rate of Pore Pressure Generation	84
Figure 4.9	Pore Pressure Generation for Cyclic Triaxial Test. Comparison Between OCEAN2-Predictions and Measured Values	85
Figure 4.10	Number of Cycles to Failure vs. Shear Stress Level	86
Figure 4.11	Theoretical Prediction of Pore Pressure Increase at Pile Wall due to 100 Uniform Load Cycles as a Function of Stress Level and Coefficient of Consolidation	87
Figure 4.12	Skin Friction Degradation Model in DRIVE15	88
Figure 4.13	Effect of DRIVE15 Degradation Model on Test Pile	89
Figure 4.14	Soil Model in CRAPIL, Elastic, Visco-Plastic	90
Figure 4.15	Mobilization of Shear Stress along a Tension Pile with Pretension of 33 perc. of Ultimate Capacity and Cyclic Loads between ± 5 to ± 40 percent of Ultimate Capacity. - DRIVE 15 Analysis	91
Figure 4.16	Degree of Mobilization of Skin Friction	92
Figure 4.17	Axial Pile Top Load Variations	93
Figure 4.18	Shear Stress Mobilization at Pile Station no. 8	94
Figure 4.19	Total Creep Displacement after Application of Total Set of Wave Parcels	95
Figure 4.20	Redistribution of Mobilized Shear from Creep due to Pretension	96
Figure 4.21	Pile Head Displacement vs. no. of Cycles and Safety Factor	97
Figure 4.22	Pile Head Creep and Variation of Shear Stress Distribution. - Parameter Study	98

APPENDIX F

DETAILED RESULTS FROM **TEST 9, STRATUM II** MODEL PILE TESTS

CONTENTS

Summary	F3
Test 9, Stratum II	F4
Consolidation	F4
Pile Instatllation and Set-Up	F4
Static Test	F5
Creep Test	F5
Cyclic Tests	F6
Stress Controlled Tests (WD29LC)	F6
Relaxation Tests	F7
Cyclic Stroke Controlled Tests	F8
Strength Tests	F10

LIST OF FIGURES

Figure 1	Sample Properties
Figure 2	Consolidation Diagram
Figure 3	Pocket Penetrometer Tests After Consolidation
Figure 4	Pressures at Pile Wall after Installation
Figure 5	Static Test 1
Figure 6	Creep Tests
Figure 7	Skin Friction vs no. of Cycles, WD29LC
Figure 8	Deflection vs no. of Cycles, WD29LC
Figure 9	Total Normal Pressure vs no. of Cycles, WD29LC
Figure 10	Pore Pressure vs no. of Cycles, WD29LC
Figure 11	Eff. Normal Pressure vs no. of Cycles, WD29LC

Figure 12 Static Test 2
Figure 13 Relaxation Tests
Figure 14 Cyclic Stroke Controlled Test 1
Figure 15 Static Test 3
Figure 16 Cyclic Stroke Controlled Test 2
Figure 17 Static Test 4
Figure 18 Cyclic Stroke Controlled Test 3
Figure 19 Static Test 5
Figure 20 Cyclic Stroke Controlled Test 4
Figure 21 Pocket Penetrometer Tests after Pile Test
Figure 22 Unconfined Compression Tests
Figure 23 Water Content and Shear Strength

Appendix FA
Plotted Results from WD29LC
Figures FA-1 through FA-5
Skin Friction vs Deflection, Selected Cycles
Figures FA-6 through FA-8
Skin Friction vs Eff. Normal Pressure, Selected Cycl.
Figures FA-9 through FA-18
Skin Friction, Pore and Total Pressure, Selected Cycles

SUMMARY

This report contains the results of the laboratory model pile tests designated TEST 9, STRATUM II, in the project CNRD 13-2, TENSION PILE STUDY, for Conoco Norway Inc.

The clay sample was consolidated for 26 days under 300 kPa applied vertical pressure. Pore pressure in the sample was about 24 % of the applied pressure. After 18 days of consolidation in the pile chamber the pile was installed. After 9 days of set-up the excess pore pressure was about 75 kPa. Testing was then started.

Static test gave peak friction of 27 kPa with residual value of 23 kPa. Undrained shear strength was interpreted to 60 kPa, giving alpha value of 0.45 and 0.38 for peak and residual respectively. Estimating the effective vertical pressure to 250 kPa results in a beta factor of 0.11 . A creep test was then performed indicating minimal creep for stress levels below about 85 % of the static capacity.

Cyclic stress controlled tests which were started two days following the creep test with static tension bias of 19 kPa (70% of previous max. friction) and parcels of 100 cycles with specified cyclic stress amplitude increasing for consecutive parcels resulted in failure (abrupt pull-out of pile) in 97 th cycle of fifth parcel. The maximum friction at failure was measured to 29 kPa.

After one day of set-up a new static test with subsequent relaxation tests were performed. Again, similar to the creep test no serious relaxation occured for initial stress levels below about 75 % of the static capacity.

Upon 24 hours additional consolidation a series of cyclic stroke controlled tests with 250 cycles in two-way loading with 10 seconds period were performed. Inbetween the parcels a period of 24 hours was allowed in order to investigate the ability to regain strength after degradation. The tests showed that the time allowed for healing was sufficient to regain the strength and the maximum friction obtained in first cycle was about 33 kPa with a degraded residual value after 250 cycles of about 24 kPa. This gives a degradation of about 27 %.

TEST 9, STRATUM II

CONSOLIDATION

The sample was prepared from the same material as used in Test 5. Water was added during the remoulding process to a water content of about 39.5% . Horizontal filters were placed in the oedometer to provide better vertical drainage.

A vertical pressure of 300 kPa was applied on top. As seen in Figure 2 the pore pressure at middle height had dropped down to about 24% of the consolidation stress after 26 days.The pore pressure reached a minimum after about 12 days of 18 % of the consolidation stress, but during continued consolidation the pore pressure increased as seen in Figure 2. At this time the sample was transferred to the pile chamber. Pocket penetrometer tests were performed on the side of the sample and on the top when trimmed in the pile chamber (level I-I) as shown in Figure 3. The shear strength, s_u, showed an average of about 50 kPa.

PILE INSTALLATION AND SET-UP

After pocket penetrometer tests the sample was mounted in the pile chamber and left to reconsolidate for 18 days under a vertical pressure of 300 kPa and radial pressure of 210 kPa (K=0.7). As in Test 8 no back pressure was applied and vertical filter strips were placed on the outside perimeter of the clay sample with direct drainage on top and bottom of the pile chamber. Again good drainage was proved by formation of salt on the filter strips sticking out, which came from the expelled water from the marine clay.

During insertion of the pile the total normal pressure showed abot 150 kPa and the pore pressure only showed about 15 kPa directly after pile installation. After about four days of set-up the pore pressure showed a maximum of 75 kPa whereas the total pressure showed a maximum of 195 kPa after 9 days as shown in Figure 4. After 9 days of set-up the pore pressure showed 70 kPa. At this time it was decided to start with the loading program.

STATIC TEST

A displacement controlled static test with deformation rate 10 mm per hour was now conducted, as shown in Figure 5. The pile was pulled in tension through failure and large slip and then pushed down to original position causing failure in compression and large slip (residual friction).

The displacement to cause failure, as shown in Figure 5, was about 0.2 mm or 0.8% of the pile diameter. A maximum friction of 27 kPa was achieved with a residual friction of 23 kPa. The shear strength of the clay at time of testing was estimated to 60 kPa which results in an alpha (α) value of 0.45 and 0.38 for peak and residual friction respectively.

For the effective stress approach, estimating σ'_{vo} from the relationship

$$s_u = 0.24 \cdot \sigma'_{vo}$$

which gives $\sigma'_{vo} =$ 250 kPa, the beta value (β) becomes 0.11 for maximum friction.

Total pressure on the pile wall at time of failure was about 195 kPa and the pore pressure showed 70 kPa, resulting in a horizontal effective pressure of 125 kPa. The interface friction angle (δ) can then be estimated to 12.2 degrees.

CREEP TEST

The pile was left to rest for a period of eight hours before a series of creep tests were performed, as shown in Figure 6. The tests were performed as stress controlled tests where a prescribed tensile stress was applied to the pile and the displacement was then monitored for a period of 16 minutes, keeping the applied stress constant. As can be seen in Figure 6, no creep deformation was seen for the five first stress levels of 50,60,70,80, and 85% of the peak (ultimate) friction measured in the static test. Increasing the stress level to 90% of the static strength results in a creep deformation of about 0.03 mm after 16 minutes. Finally at 95% of static strength the pile is seen to come up (failure) after about four minutes with a steadily increasing deformation before the abrupt pull-out.

It must here be noted that some creep might have occured during the first load levels,

but the amount of deformation encountered was close to the accuracy of the resolution of the measurement system used. In addition some degree of variation in the stress level applied was seen due to disturbance of the signals from the load sensors in the pile. Also, it might be argued about the length of time (16 min.) for load application in order to give information of the critical load level with respect to creep deformation. However, the tests show that the applied stress on the pile must be very high (in the order of 80 to 90 %) with respect to the static strength in order to produce any significant creep deformation within the time span tested.

CYCLIC TESTS

After the creep test the pile was brought back to original position and left to reconsolidate for two days before a stress controlled test was started. At this time the total pressure had increased to 230 kPa and the pore pressure was 70 kPa.

Stress Controlled Tests (WD29LC)

A stress controlled test comprised of applying a prescribed static tensile (uplift) stress on the pile, superimposed with parcels of 100 cycles with 10 seconds period and prescribed cyclic stress amplitude. The stress amplitude was then increased in the following parcels until failure (excessive uplift) occured in tension.

For this test the static tensile stress (bias) level was about 19 kPa, corresponding to 70% of the previous static capacity. In the first parcel the cyclic level was about 2.0 kPa and for the following four parcels the cyclic stress level was incremented by 2 kPa as can be seen in Figure 7, showing skin friction (envelope of max. and min.) versus cycle numbers. In Figures 8,9,10 and 11 the resulting deformations and pressures due to the applied skin friction are plotted versus cycle numbers. In Appendix A selected cycle numbers are plotted as friction versus deflection, friction versus effective pressure and friction, pore pressure and total pressure variation during one cycle.

As seen in Figure 7 a total of five parcels were performed. The first parcel does not produce any significant deformation of the pile as shown in Figure 8 and in Figure A-1. In the second parcel the average deformation shows a downward movement which was due to problems keeping the static bias constant with the accuracy of the friction

measurement system. A small drift in the friction control causing a decrease in the static bias will therefore result in a downward movement of the pile from the original start position.

The friction deformation behaviour in second and third parcel, as shown in Figures A-2 and A-3 is linear with only minimal signs of hysteresis. Increasing the cyclic level in parcel four results in larger cyclic deformations and some hysteresis. In the fifth parcel with a cyclic level of 10 kPa (maximum friction of 29 kPa) the pile is very slowly pulled up indicated by the slightly increasing average deformation as seen in Figure 8. This is also depicted in Figure A-5 where the friction- deformation curve is slowly moving to the right. Finally after 97 cycles the pile suddenly fails, by a sudden pull-out showed in Figure 8 and Figure A-5. The maximum friction was 29 kPa.

From the pressure diagrams in Figures 9,10 and 11 it is seen that the average pressures during the cyclic testing stays fairly constant. The total normal pressure is seen to show cyclic variation increasing with increasing deformation. The pore pressure measurements do not show any cyclic variation until the last parcel and stayed constant at about 70 kPa until failure occured. At point of failure the total pressure is seen to drop and the pore pressure increase, resulting in a decrease of the effective horizontal pressure on the pile wall. This is also depicted in the "effective Stress" plots in Figures A-6 through A-8, Where the internal friction angle at point of failure can be measured to 12.5 degrees.

RELAXATION TESTS

After failure in the stress controlled cyclic test the pile was brought back to original position and left to reconsolidate for a period of 24 hours. The total and pore pressures were unchanged from the values after the cyclic test and showed 180 kPa and 65 kPa respectively. At this time a new static test was performed, Figure 12, to have a reference level for the performance of a series of relaxation tests. The static test showed a peak friction of 28 kPa with a residual value during large slip of 25 kPa.

The relaxation tests were performed as stroke controlled tests, where the pile was pulled in tension to a prescribed friction level (a percentage of the peak friction in static test), and the deformation was then held constant while monitoring the friction for a period of 14 minutes. The results of this are shown in Figure 13. Here it is seen

that loss of friction within the time span tested first started in step 3 with initial friction corresponding to 76% of the static capacity. Increasing the friction in the next step to 86% of the capacity, resulted in a friction loss of about 1.5 kPa or 5% of the capacity after 14 minutes. In step 5 with 93% of the capacity as initial load the friction loss almost doubled, but seemed to approach the friction level as in step 4. In step 6 with initial load on the pile equal to the static capacity the friction loss was similar to step 5, but still with a tendency to drop after 14 minutes. Finally in step 7 the pile was pulled slightly beyond point of peak friction and then stopped. The friction loss was now much more severe and was down at the level of step 4 after 14 minutes.

Common for all the relaxation tests performed here is that the major loss in friction occured within the almost immediate time after load application, or at the time when deformation ceased. It is not possible from these tests to define a friction level to which the fiction will approach, but the tests indicate that the loss of friction is minimal, within the time span tested, when the friction level is below about 75% of the static capacity.

CYCLIC STROKE CONTROLLED TESTS

The pile was now brought back to original position and left to reconsolidate for a new period of 24 hours. During the relaxation tests the total pressure decreased slightly, but was now back at 180 kPa with the pore pressure reduced to 60 kPa.

A set of stroke controlled cyclic tests were now to be performed, with a period of 24 hours between the tests in an attempt to investigate the ability to regain strength after degradation in two-way cyclic loading of the pile. One cyclic stroke controlled test consisted of 250 cycles with deformation amplitude of about 1 mm in two-way cyclic loading with a cycle period of 10 seconds.

The results of the first test is shown in Figure 14, which shows a peak friction in the first cycle of 30 kPa with a residual value during large slip of 21 kPa. During subsequent cycles the peak friction stabilized at about 23 kPa with residual of 20 kPa. It is here interesting to note that the lowest friction occured in the tenth cycle, and that during subsequent cycles the mobilized friction appeared to regain strength. The average total pressures on the pile wall increased slightly during the test, to 195 kPa whereas the pore pressure stayed fairly constant at 60 kPa. The maximum loss of

strength from peak in first cycle to residual in tenth cycle is then about 10 kPa or 33%.

After a period of 24 hours a static test was performed before a new parcel of 250 cycles in two-way stroke control was started. The results of the static test is shown in Figure 15, which was performed as an extraction with constant speed of 10 mm per hour from the original position of the pile. After failure and large plastic slip the pile was pushed down to original position, causing failure in compression and residual value during large slip. This cycle was then repeated. It is interesting to note that failure in the first cycle not showed the distinct peak, but showed a direct elastic plastic behaviour, whereas the well-known peak occurs upon reversal of the load. It appears that the peak occurs when the pile-soil interface is subjected to a complete reversal in interface load direction.

In a cyclic test a complete cycle starts with upward movement of the pile from the original position to the prescribed positive amplitude,at which point the pile is pushed down passed the original position down to the prescribed negative amplitude and then back up to the original position. Therefore, after a cyclic stroke controlled test the pile is left in the original position with a residual tension, which will reduce with time left alone (relaxation). When a static test then is performed with initial tensile load the friction is mobilized with no reversal of particle alignement, which apparently does not produce a peak in the friction curve.

The static test gave a peak friction of 29 kPa with a residual value during large slip of about 25 kPa. The cyclic stroke controlled test 2, shown in Figure 16, gives a maximum friction of 31 kPa in the first cycle with a residual value of 24 kPa. In subsequent cycles the peak friction is reduced to a minimum after about ten cycles of 25 kPa with a residual of 23 kPa. After 250 cycles the peak friction is about 26 kPa and the residual 23 kPa. The maximum degradation from first peak to lowest residual is thus 8 kPa or 26%. The test shows that friction had regained the strength from the degradation the day before and that actually the strength had increased. This fact is most probably due to set-up effects and continued consolidation of the clay sample in the pile chamber. During the test the total normal pressure on the pile wall increased slightly from about 200 kPa to 210 kPa, with the pore pressure reducing to 50 kPa after the test.

Another 24 hours was now given for regain of strength before a new static test with

subsequent cyclic loading was performed. The pore pressure was now back at 60 kPa and the total pressure stayed at 210 kPa. The static test is shown in Figure 17 which gave similar results as the prvious test the day before, exept with slightly higher values. The peak was now 31 kPa and residual 26 kPa. Also the cyclic test 3, shown in Figure 18, showed higher values than the day before. Peak friction in first cycle showed 33 kPa which gradually reduced in subsequent cycles down to 27 kPa in cycle 250 with a residual value of 24 kPa. The maximum degradation was then 27 %. The total pressure increased slightly to 225 kPa during the test with the pore pressure constant at 60 kPa.

The pile was now left to reconsolidate (continue to consolidate) for a period of 3 days. The total pressure on the pile wall had now increased to 235 kPa and the pore pressure reduced to 55 kPa. The static test now performed, Figure 19, showed a peak of 30 kPa with a residual of 28 kPa. The subsequent cyclic test 4, Figure 20, gave a peak of 34 kPa in first cycle, which reduced to 29 kPa in cycle 250. Residual value during large slip was 27 kPa, which gives a maximum degradation of 21 %.

These cyclic degradation tests with intermediate time for reconsolidation inbetween tests show that the time left for set-up is sufficient for regain of strength after degradation to residual values, which can be termed as a healing capability. The increase in strength from test to test is considered to be due to set-up effects such as continued consolidation of the clay sample from the constant confining pressures and good drainage conditions provided by the vertical filter strips around the periphery of the sample.

STRENGTH TESTS

After the last parcel in stroke controlled cyclic tests the pile was pulled out of the pile chamber and the sample built out. Pocket penetrometer tests were performed on the side of the sample and in two horizontal layers with results shown in Figure 21.

Three standard triaxial test samples were then prepared from the center of the clay specimen and unconfined compression tests (UCT) were performed with the results shown in Figure 22.

In Figure 23 are shown the water content and interpreted undrained shear strength of

the clay sample versus the distance from the center after completion of the pile test. The water content showed about 30 % with a tendency to decrease towards the center to about 27 %.

TABLE 1.

SAMPLE PROPERTIES TEST 9, STRATUM II

SAMPLE PREPARATION		CONSOLIDATION			END OF PILE TEST
INITIAL WATER CONTENT	INITIAL HEIGHT	AXIAL DEFORMATION	AXIAL STRAIN	WATER CONTENT	WATER CONTENT
w_i (%)	H_o (cm)	ΔH (cm)	ε (%)	w_e (%)	w_{ep} (%)
39.04 39.74	51.13	7.12	13.4	A- 29.52 B- 29.68 C- 29.61	A-29.68 E-28.07 B-30.27 F-29.27 C-30.06 G-29.08 D-27.03

CONFINING PRESSURE		
AXIAL	KPa	300
RADIAL	KPa	210
BACK PRESSURE	KPa	0
SAMPLE CONSOLIDATION		
IN OEDOMETER	Days	26
IN PILE CHAMBER	Days	18
INTERPRETED SHEAR STRENGTH		
END OF CONSOLIDATION	KPa	50
END OF PILE TEST	KPa	60

Fig. 1

CONSOLIDATION DIAGRAM								Test No. 9 Stratum II		Start date	
H_i 53.13 cm		H_e 46.01 cm		$\Delta\varepsilon_v$ 13.4 %						σ_c 300 kPa	
Time h	20	43	67	115	140	166	188	212	283	308	332
Δh cm	1.19	2.59	4.00	5.41	5.80	6.13	6.34	6.52	6.83	6.88	6.94
u kPa	36	84	163	136	115	95	79	68	52	55	55
	356	380	452	472	500	548	620				
	6.98	7.02	7.09	7.1	7.11	7.12	7.12				
	58	61	67	68	69	72	73				

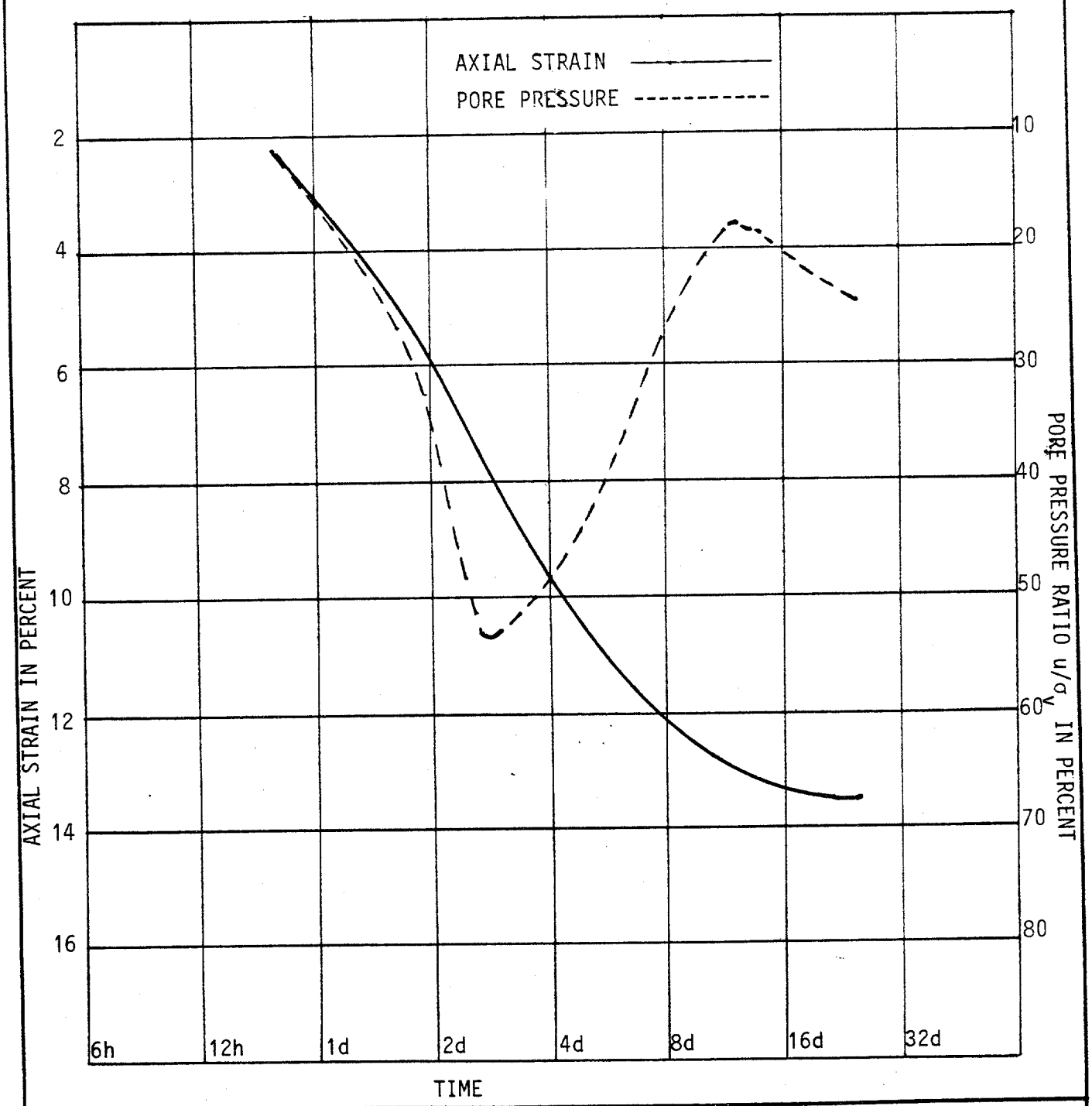

CNRD 13-2 TENSION PILE STUDY LABORATORY MODEL PILE TESTS

TEST 9, STRATUM II, Consolidation diagrams for clay sample

Scale

DET NORSKE VERITAS
Geotechnical Laboratory

Drawn by

Date

Approved

Fig. No. 2

TEST 9, STRATUM II

SHEAR STRENGTH (kPa) FROM POCKET PENETROMETER TESTS AFTER CONSOLIDATION

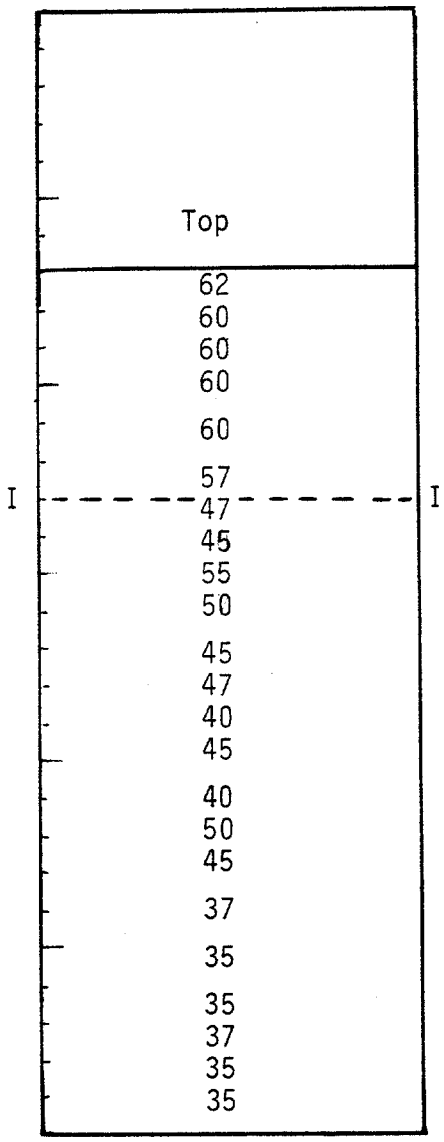

Scale 1:4

Level I-I

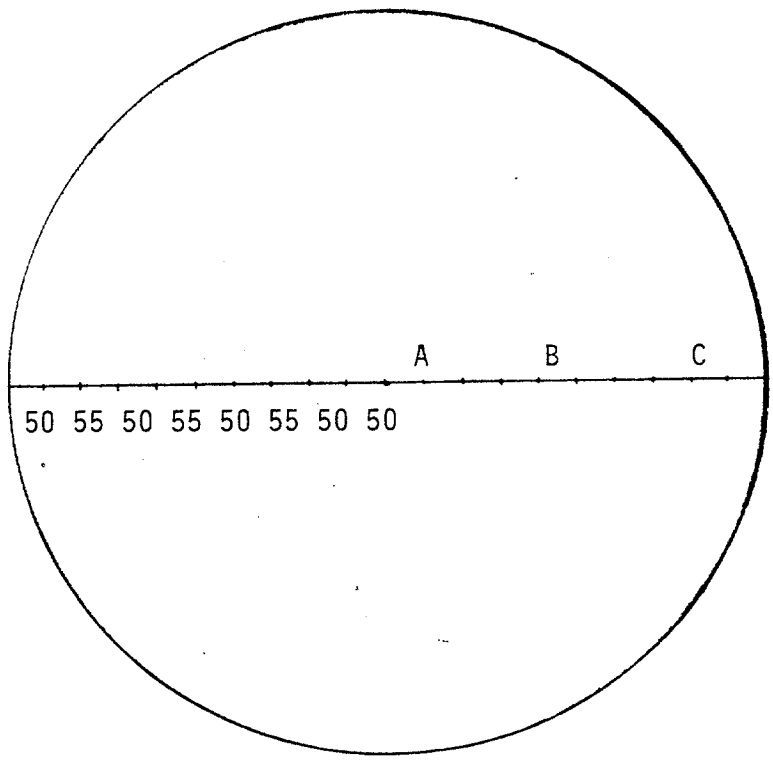

Scale: 1:2

CNRD 13-2 TENSION PILE STUDY LABORATORY MODEL PILE TESTS

TEST 9, STRATUM II, Pocket penetrometer tests		Scale
DET NORSKE VERITAS Geotechnical Laboratory	Drawn by	Date
	Approved	Fig.No. 3

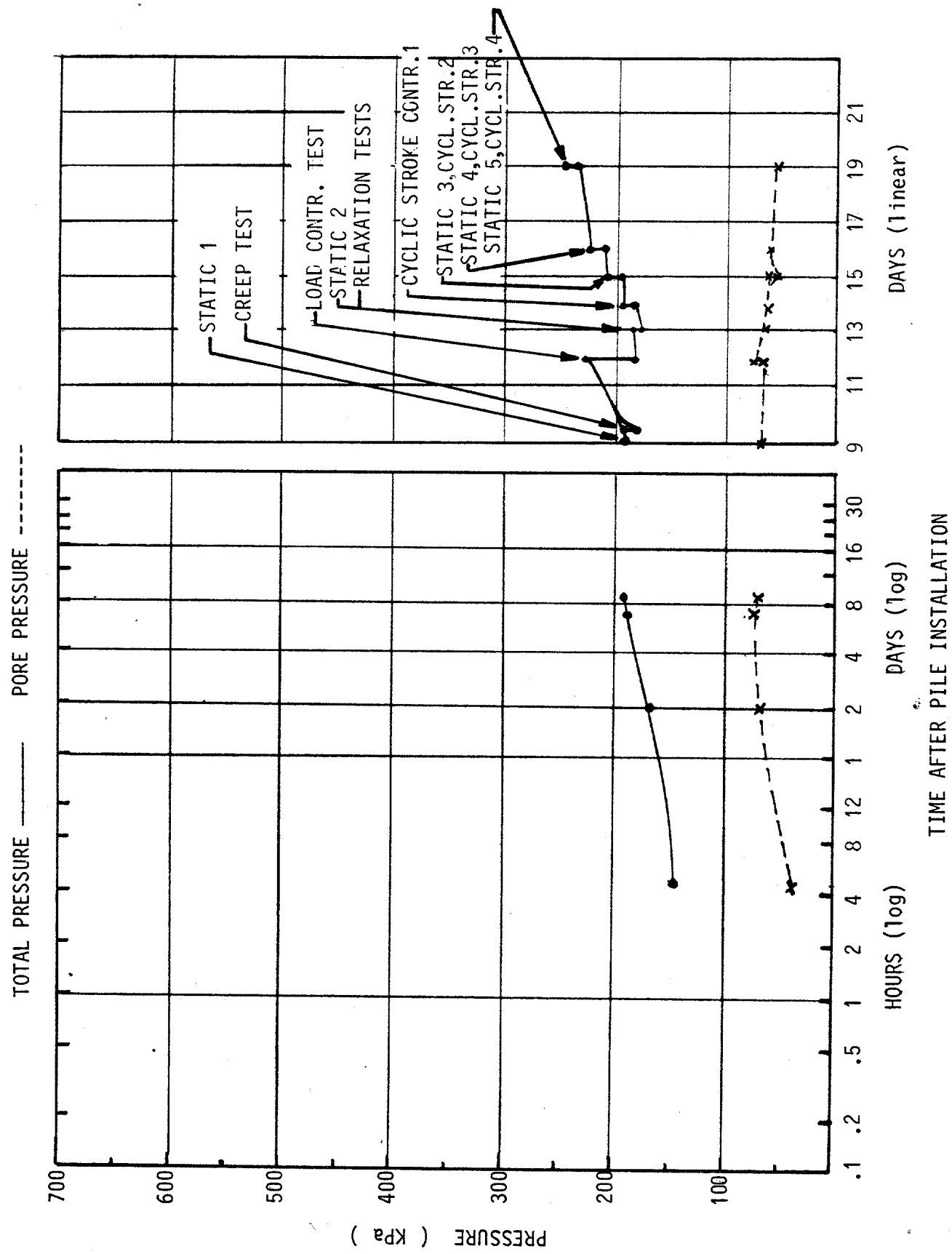

CNRD 13-2 TENSION PILE STUDY LABORATORY MODEL PILE TESTS

TEST 9, STRATUM II, Pressures at pile wall after installation

DET NORSKE VERITAS Geotechnical Laboratory	Drawn by	Scale
	Approved	Date
		Fig. No. 4

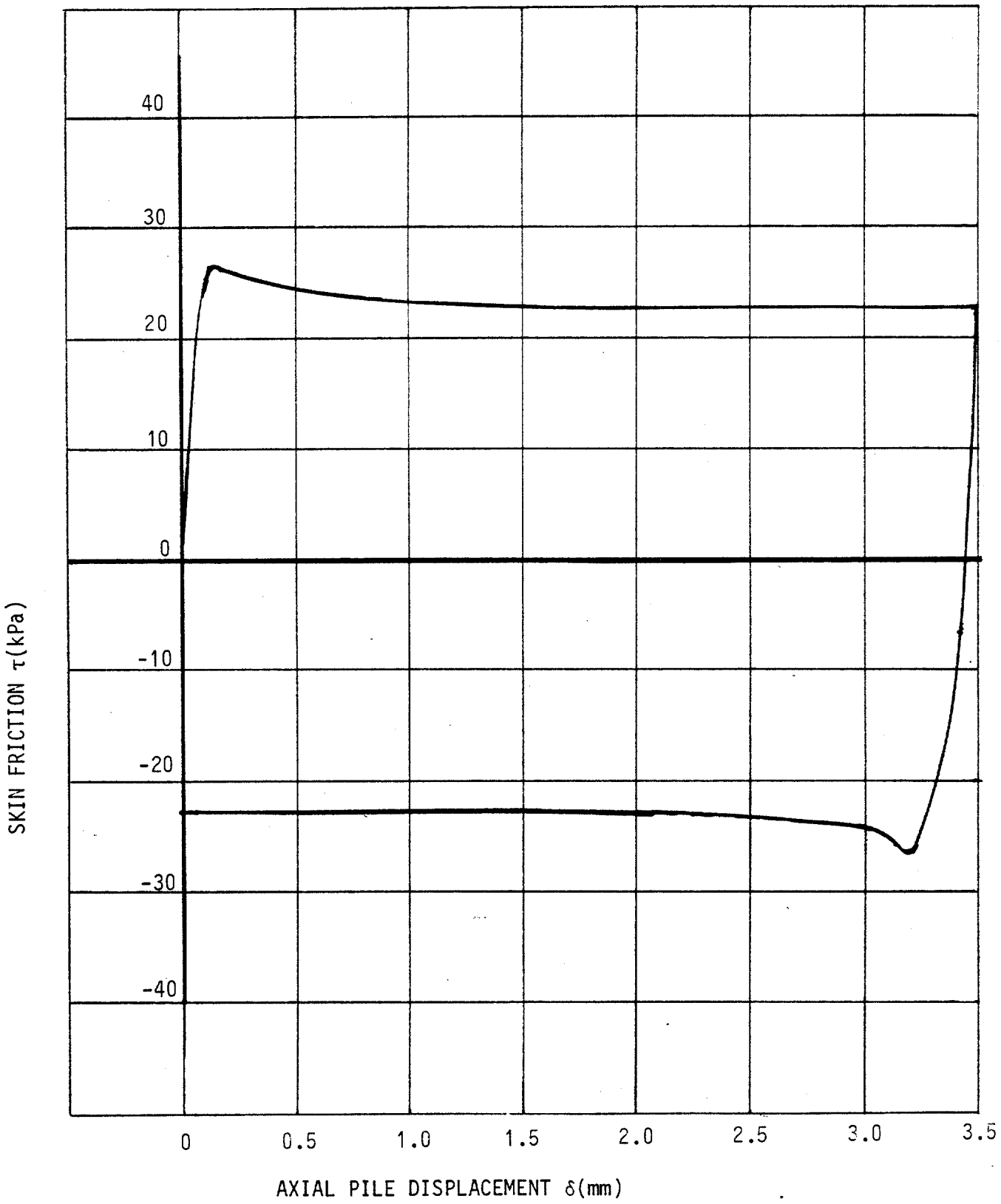

CNRD 13-2 TENSION PILE STUDY LABORATORY MODEL PILE TESTS

TEST 9, STRATUM II, STATIC TEST 1

DET NORSKE VERITAS Geotechnical Laboratory	Drawn by	Scale
	Approved	Date
		Fig. No. 5

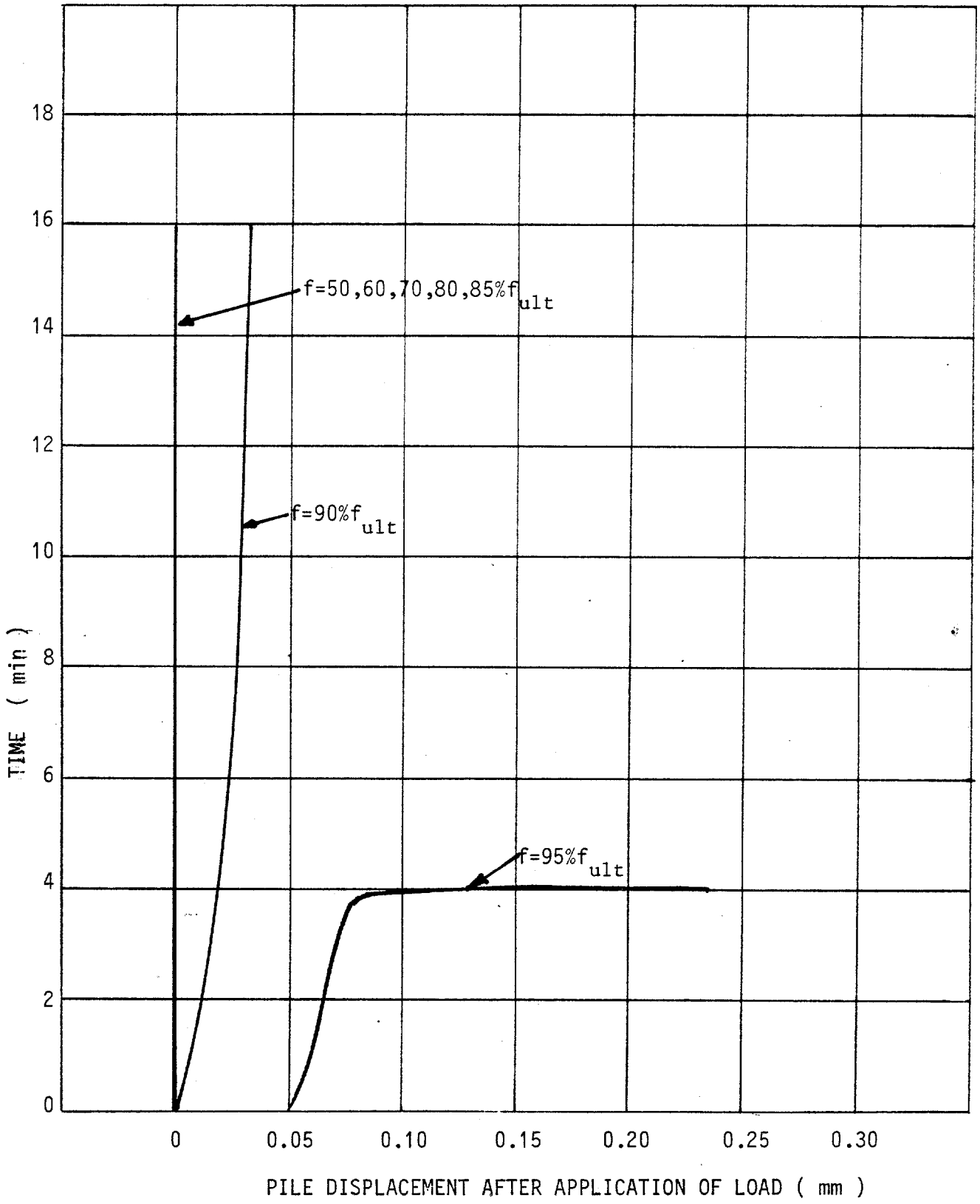

CNRD 13-2 TENSION PILE STUDY LABORATORY MODEL PILE TESTS

TEST 9, STRATUM II, Creep test after static test; f_{ult} = 26.6 kPa

DET NORSKE VERITAS Geotechnical Laboratory	Drawn by	Scale
	Approved	Date
		Fig. No. 6

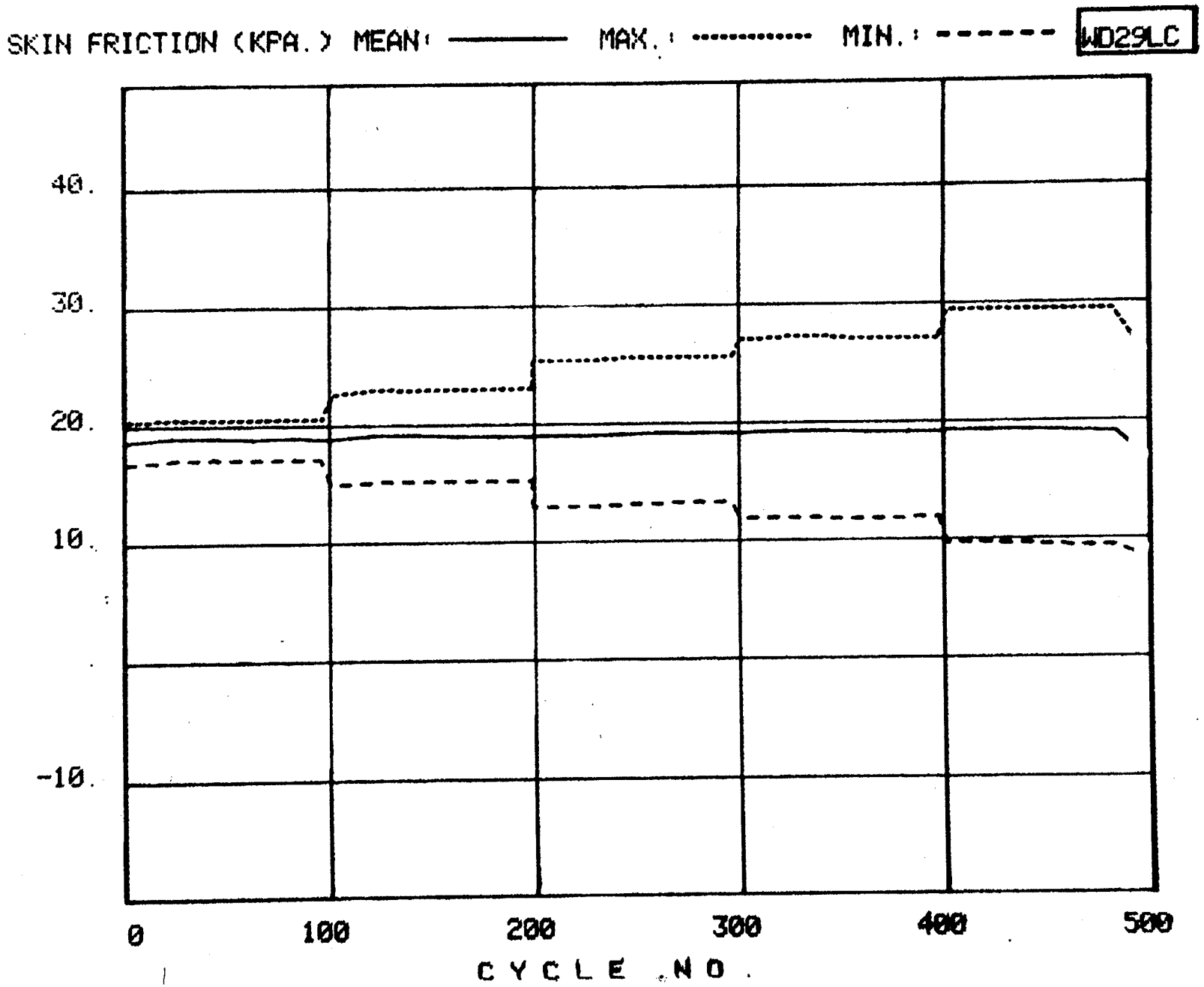
SKIN FRICTION (KPA.) MEAN: MAX.: MIN.:
WD29LC
40.
30.
20.
10.
-10.
0
100
200
300
400
500
CYCLE NO.

Fig.7

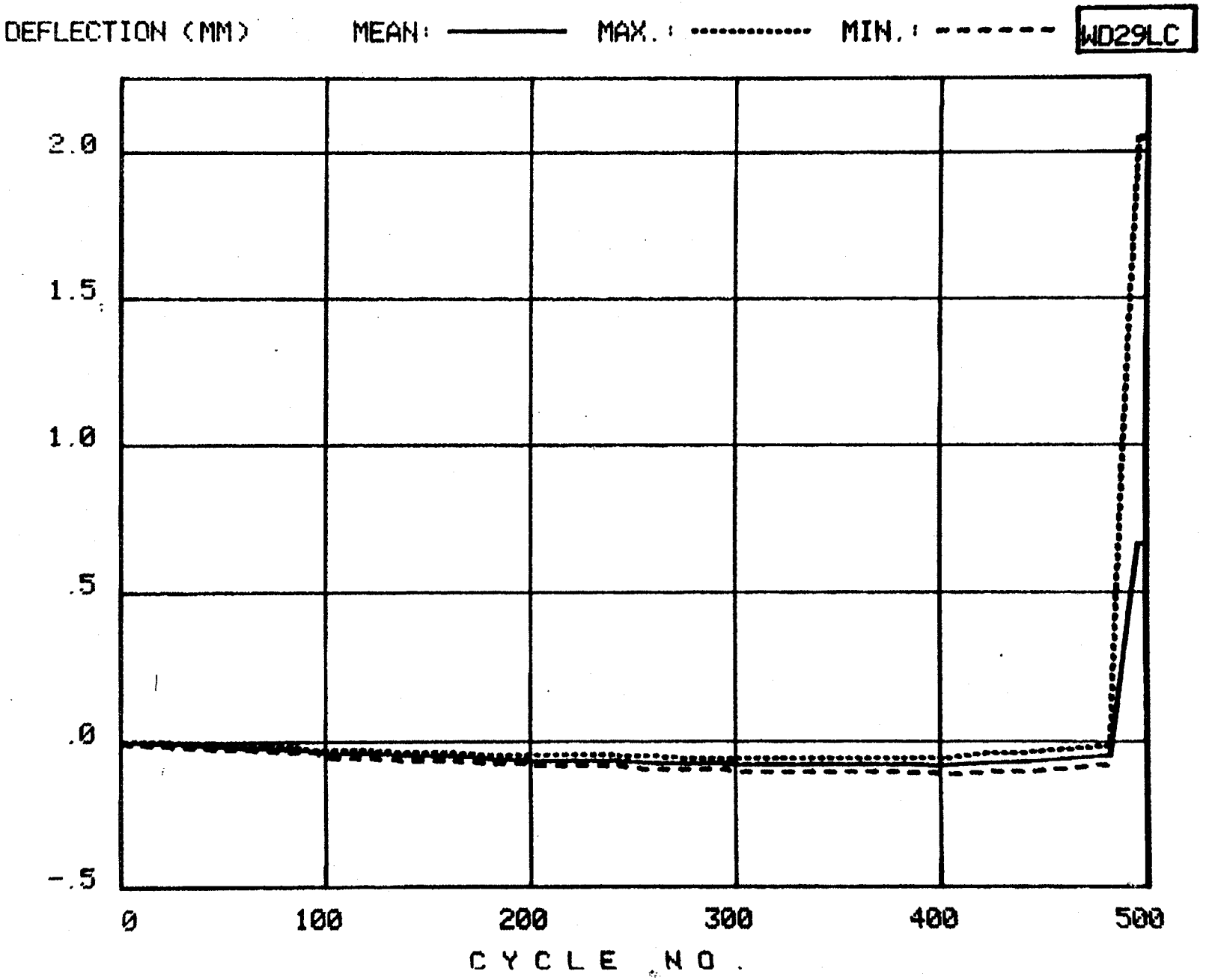
DEFLECTION (MM)
MEAN:
MAX.:
MIN.:
WD29LC
2.0
1.5
1.0
.5
.0
-.5
0
100
200
300
400
500
CYCLE NO.

Fig.8

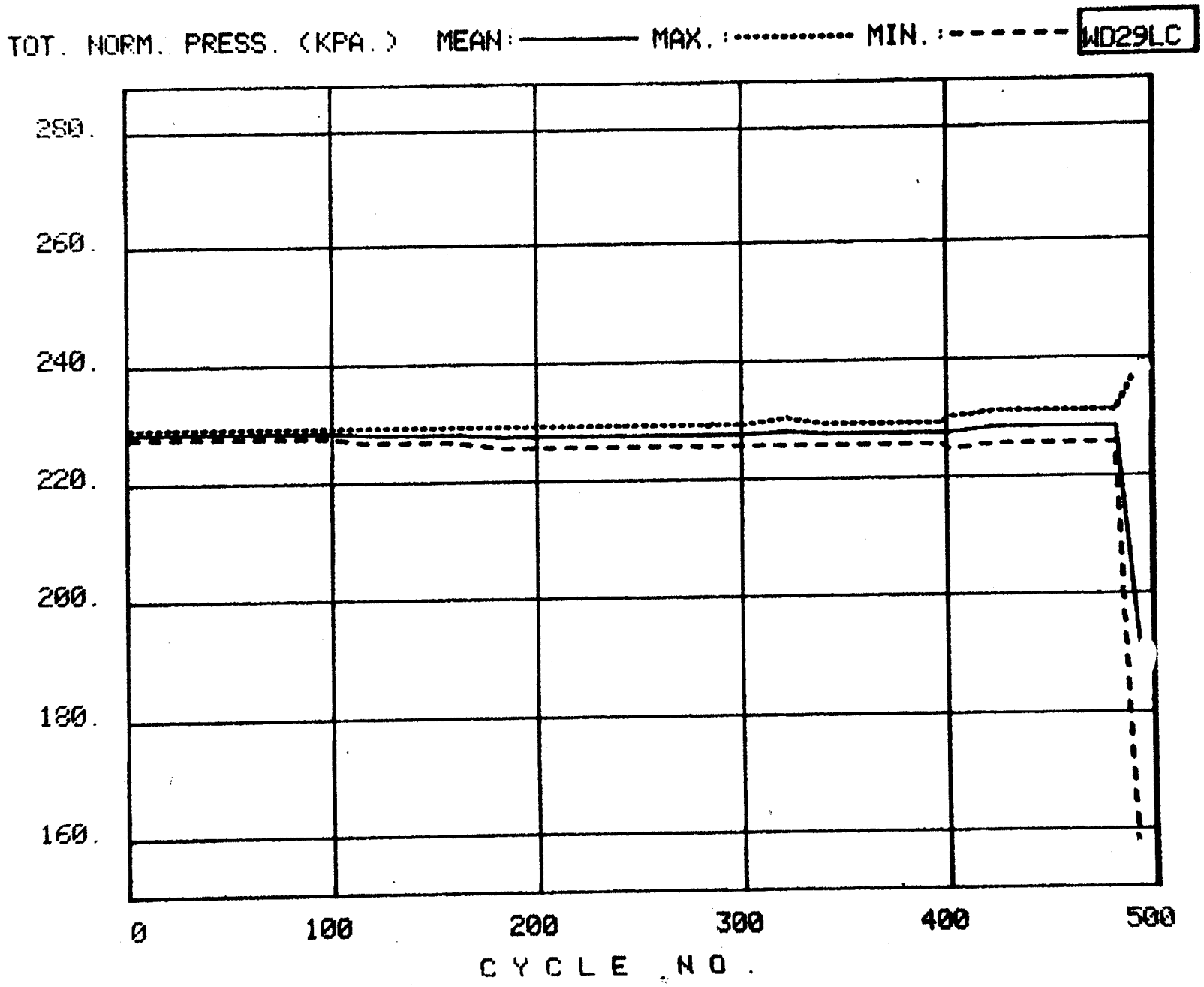
TOT. NORM. PRESS. (KPA.)
MEAN:
MAX.:
MIN.:
WD29LC
280.
260.
240.
220.
200.
180.
160.
0
100
200
300
400
500
CYCLE NO.

Fig.9

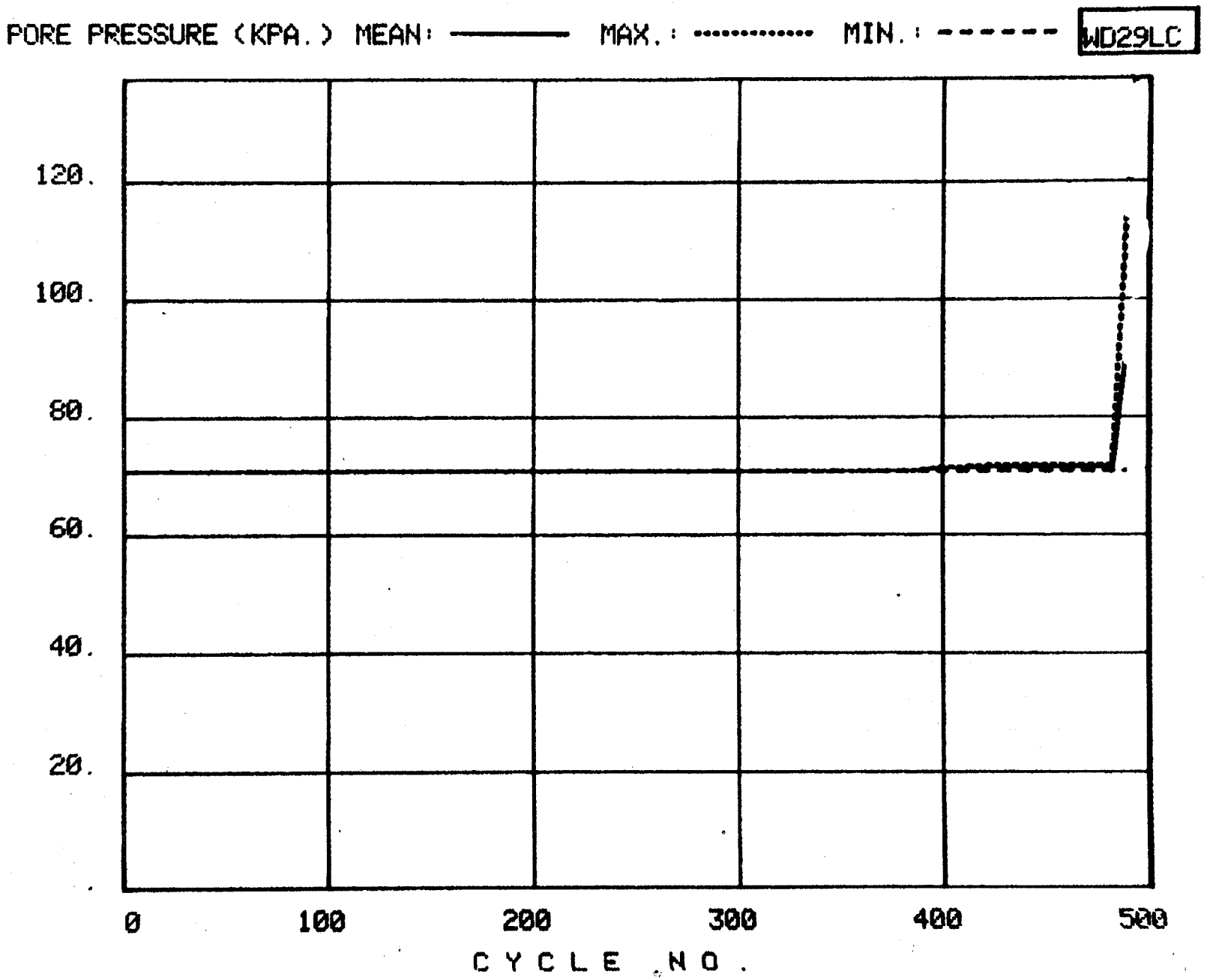
PORE PRESSURE (KPA.) MEAN: MAX.: MIN.:
WD29LC
120.
100.
80.
60.
40.
20.
0
100
200
300
400
500
CYCLE NO.

Fig.10

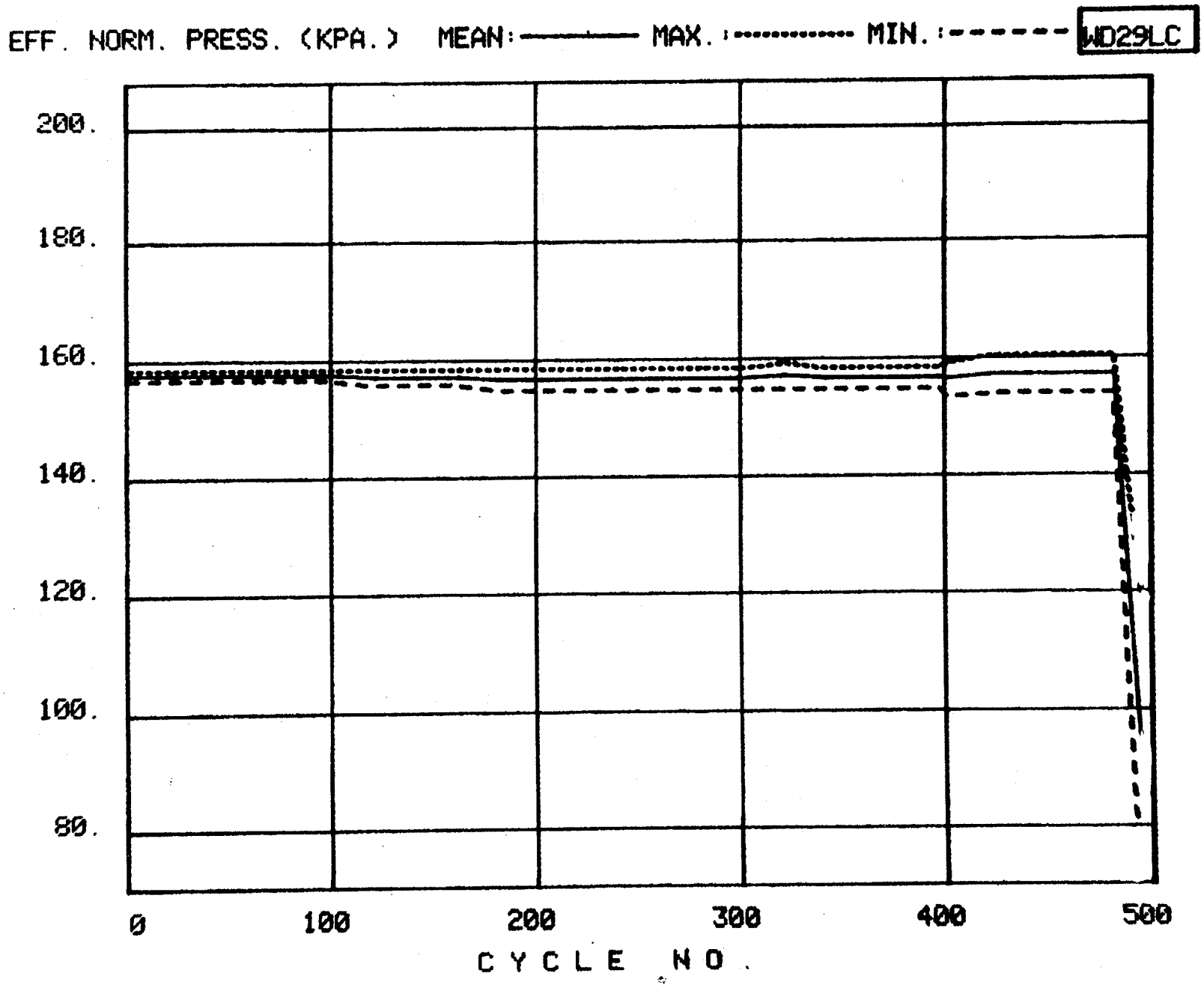
EFF. NORM. PRESS. (KPA.)
MEAN:
MAX.:
MIN.:
WD29LC
200.
180.
160.
140.
120.
100.
80.
0
100
200
300
400
500
CYCLE NO.

Fig.11

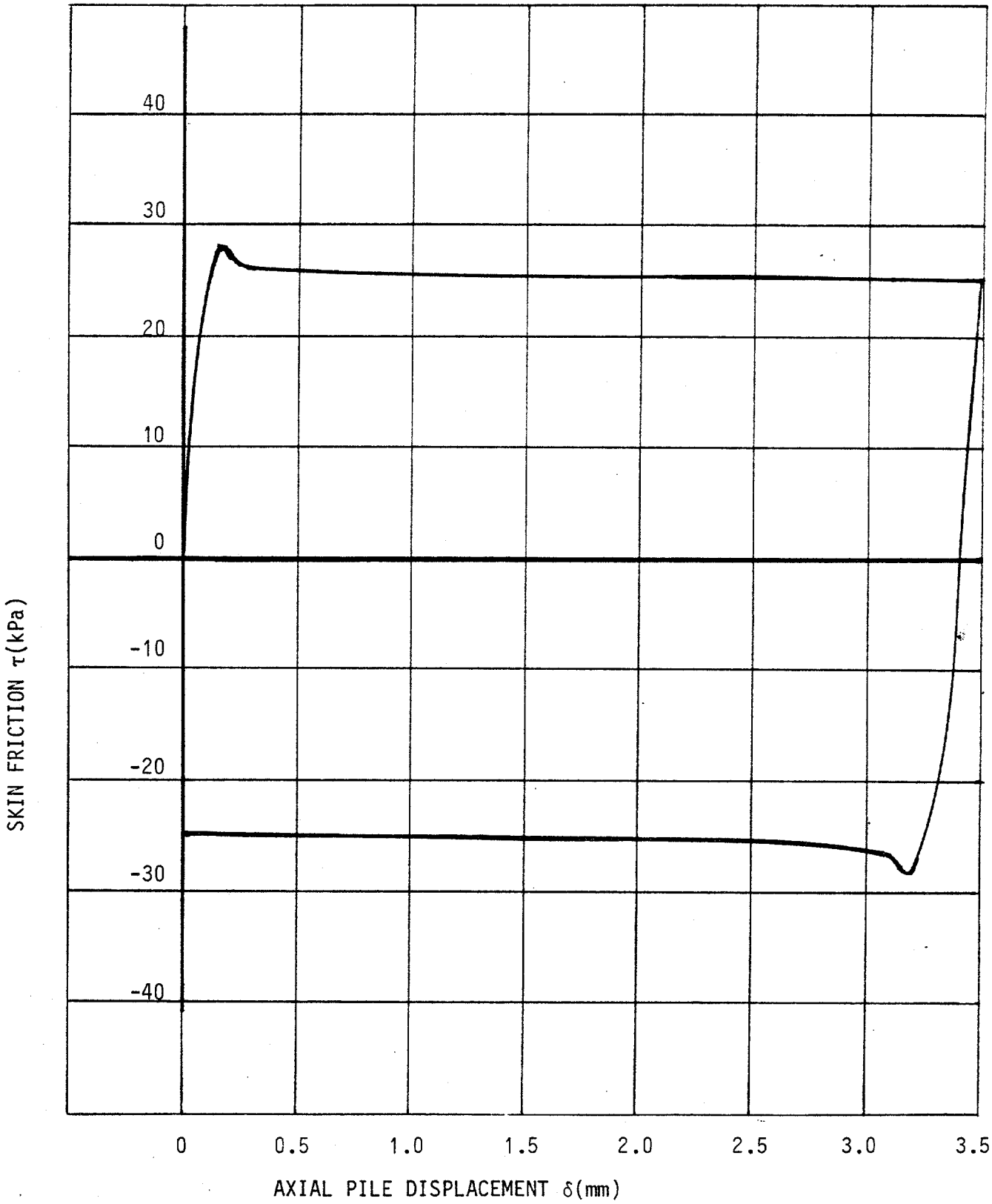

CNRD 13-2 TENSION PILE STUDY LABORATORY MODEL PILE TESTS

TEST 9, STRATUM II, Static test 2

DET NORSKE VERITAS Geotechnical Laboratory	Drawn by	Scale
	Approved	Date
		Fig. No. 12

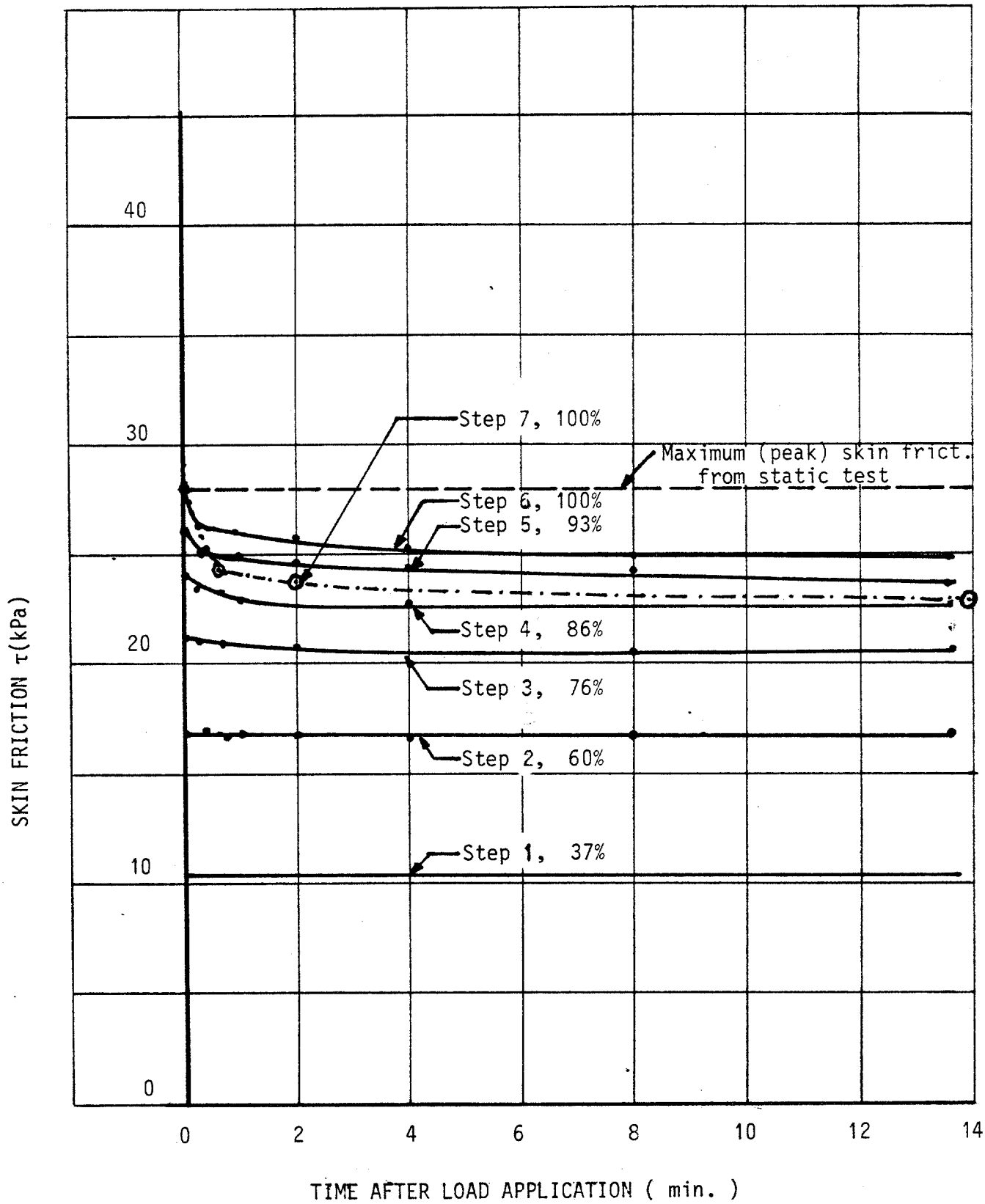

CNRD 13-2 TENSION PILE STUDY LABORATORY MODEL PILE TESTS

TEST 9, STRATUM II, Relaxation tests

DET NORSKE VERITAS Geotechnical Laboratory	Drawn by	Scale
	Approved	Date
		Fig. No. 13

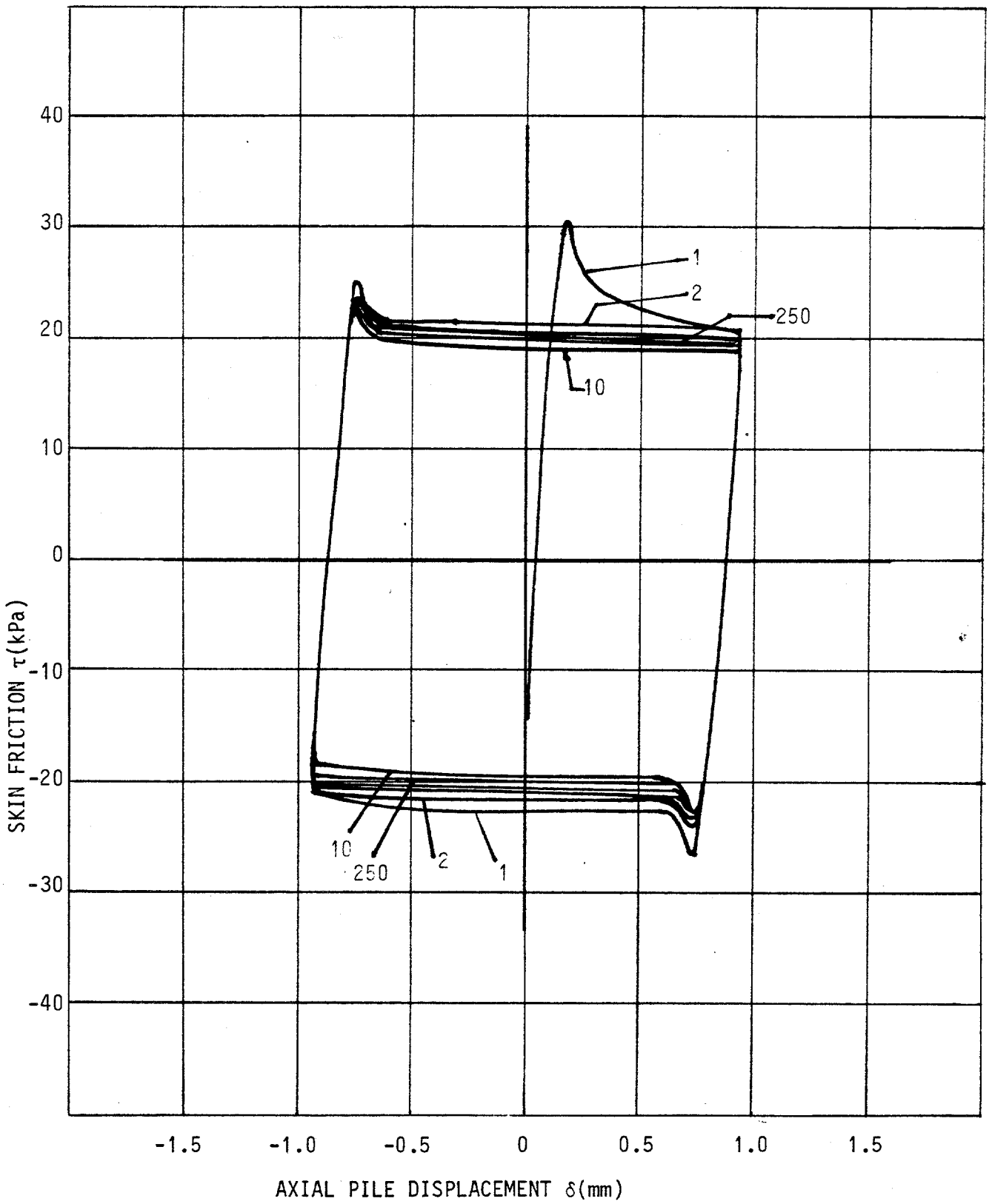

CNRD 13-2 TENSION PILE STUDY LABORATORY MODEL PILE TESTS

TEST 9,STRATUM II, Cyclic stroke controlled test 1, 250 cycles

DET NORSKE VERITAS Geotechnical Laboratory	Drawn by	Scale
	Approved	Date
		Fig. No. 14

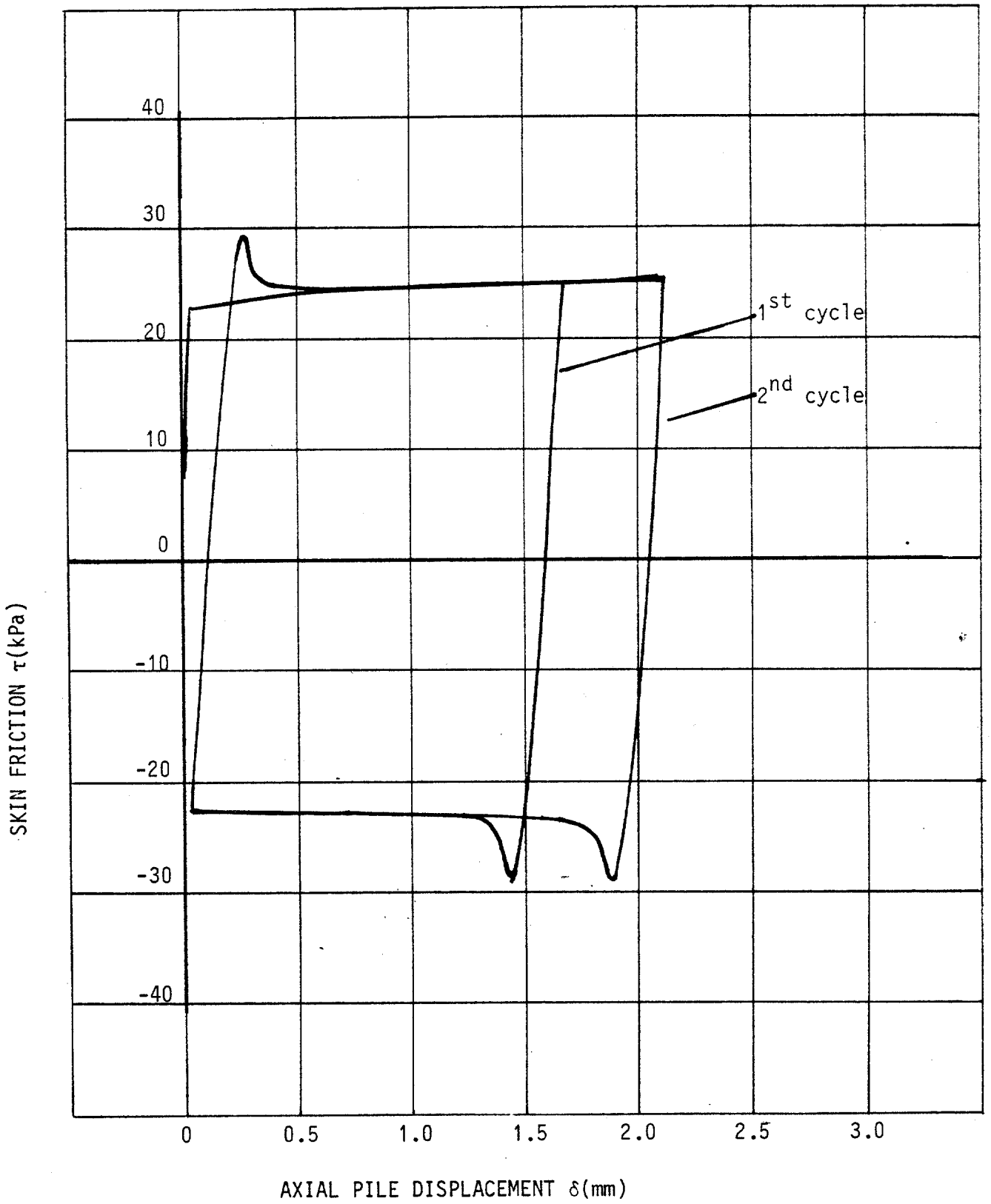

CNRD 13-2 TENSION PILE STUDY LABORATORY MODEL PILE TESTS

TEST 9, STRATUM II, Static test 3, before cycl. stroke test 2

DET NORSKE VERITAS Geotechnical Laboratory	Drawn by	Scale
	Approved	Date
		Fig. No. 15

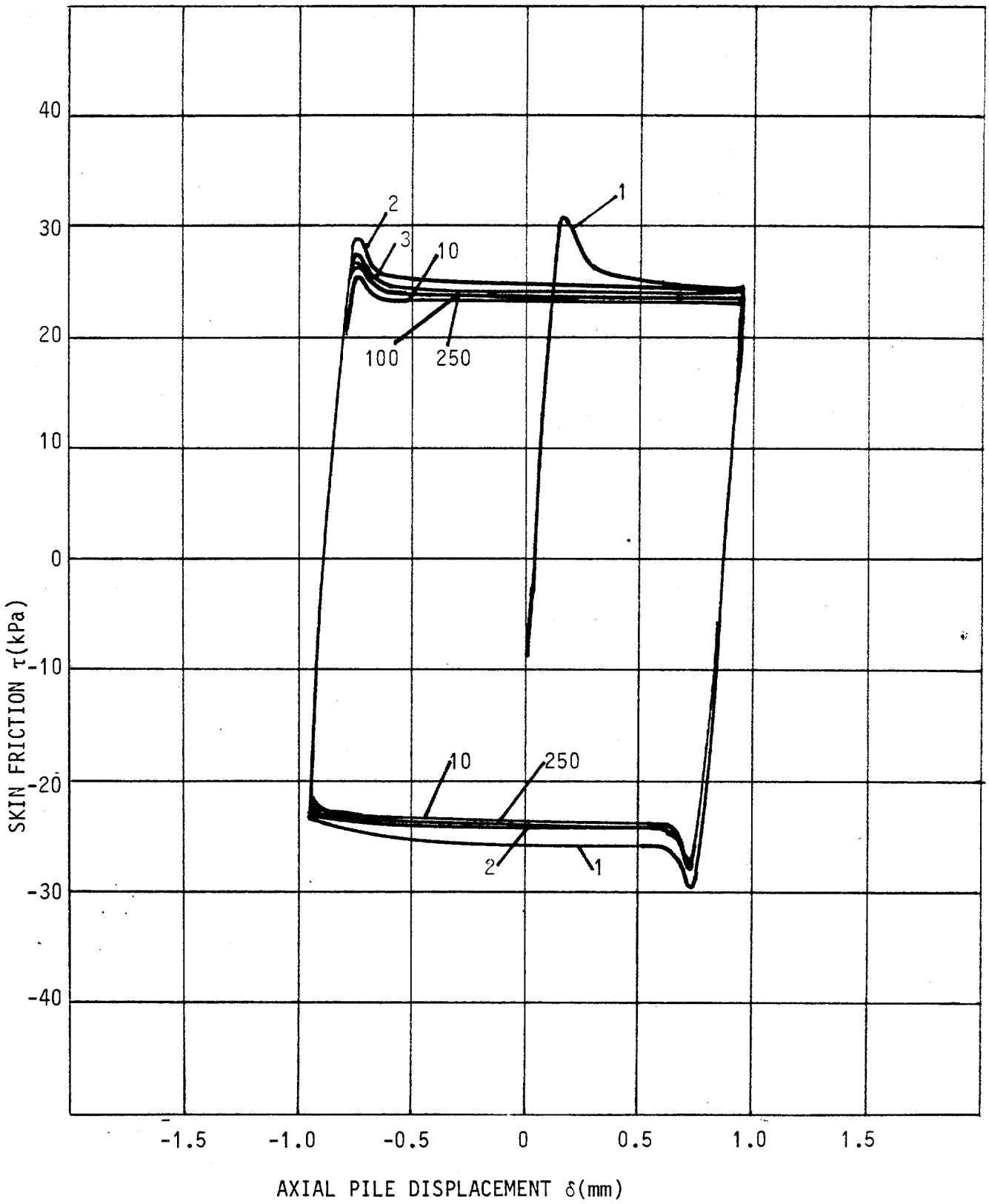

CNRD 13-2 TENSION PILE STUDY LABORATORY MODEL PILE TESTS

TEST 9, STRATUM II , Cyclic stroke controlled test 2, 250 cycles

DET NORSKE VERITAS Geotechnical Laboratory	Drawn by	Scale Date
	Approved	Fig. No. 16

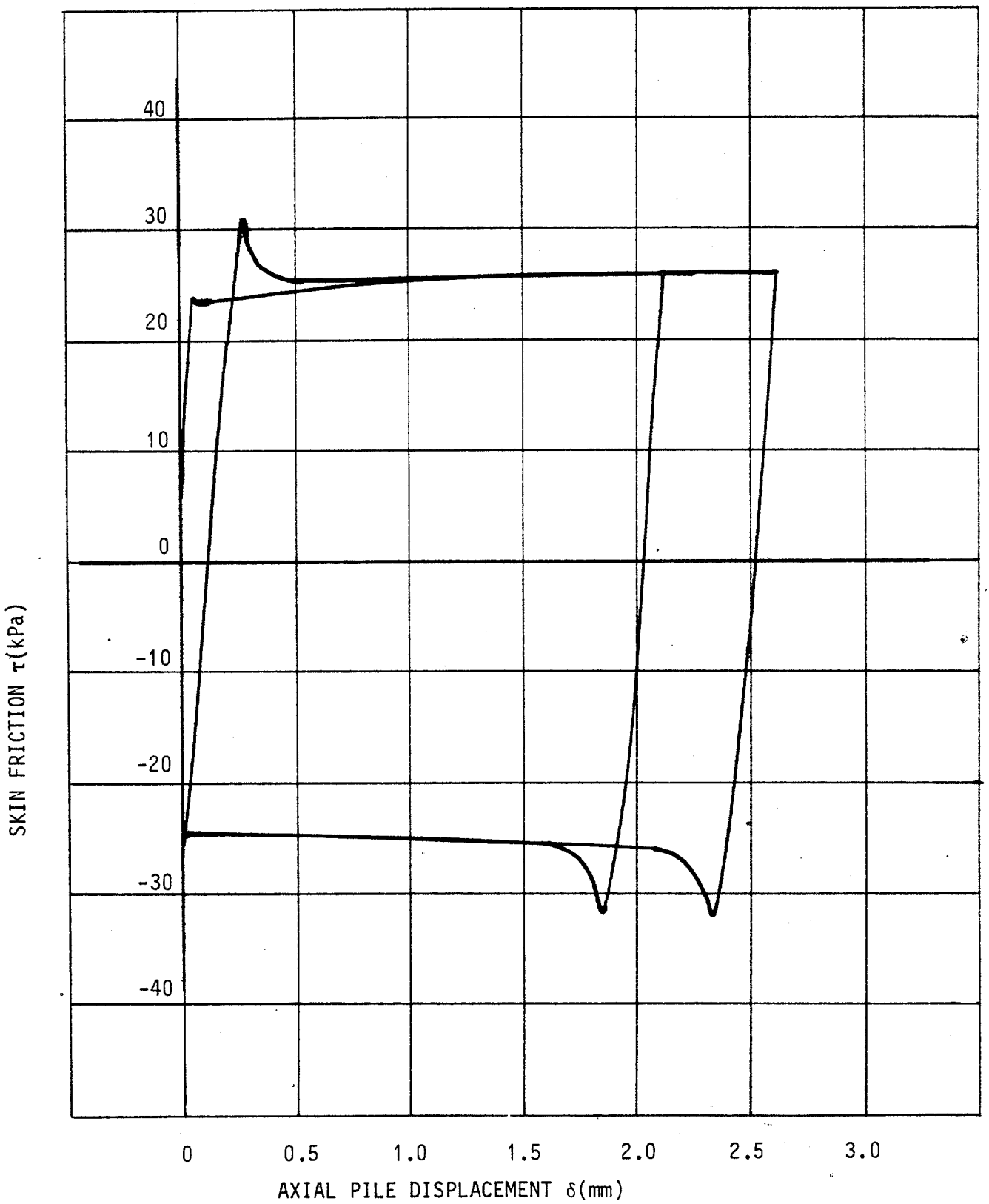

CNRD 13-2 TENSION PILE STUDY LABORATORY MODEL PILE TESTS

TEST 9, STRATUM II, Static test 4, before cycl. stroke test 3

DET NORSKE VERITAS Geotechnical Laboratory	Drawn by	Scale
	Approved	Date
		Fig. No. 17

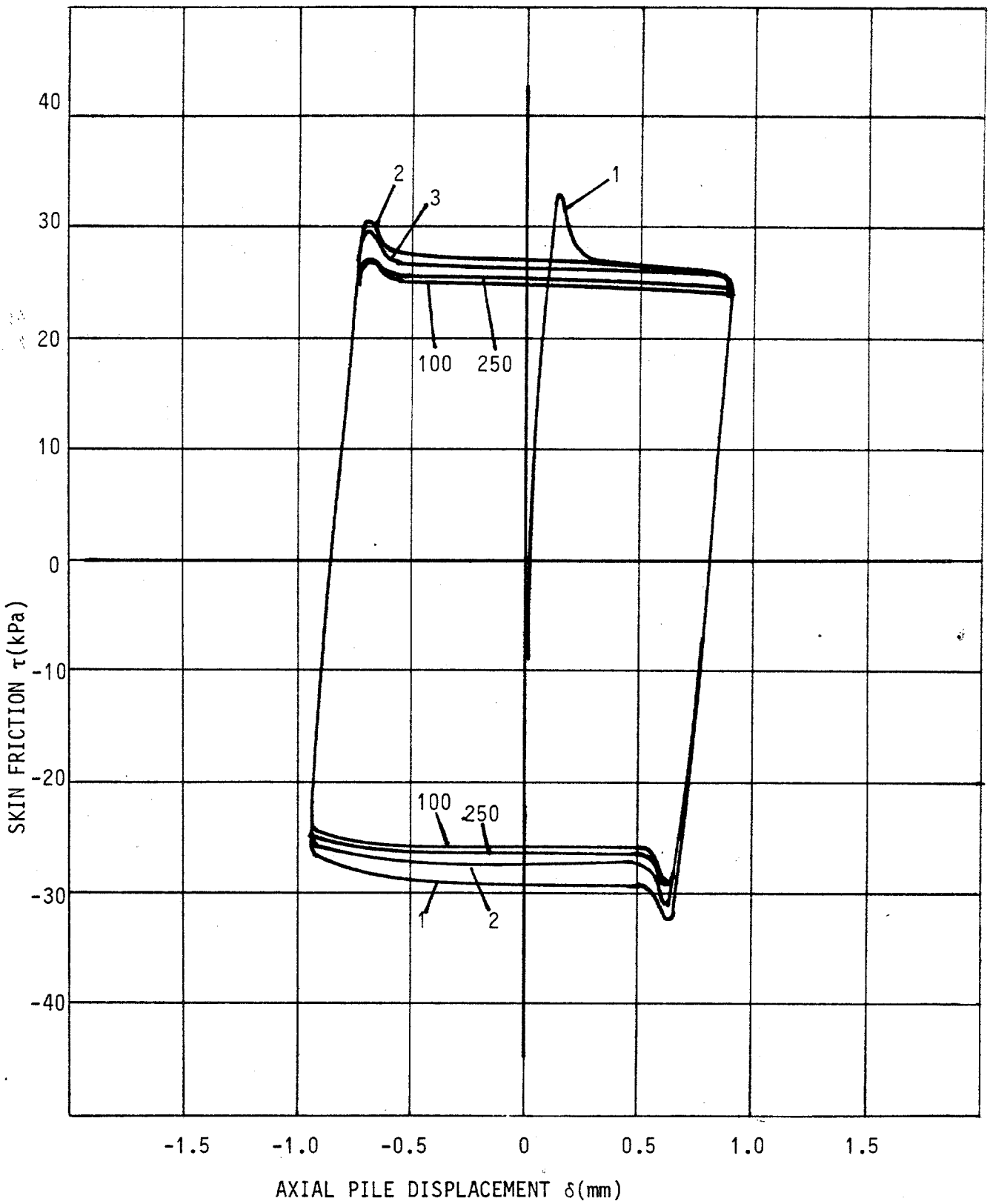

CNRD 13-2 TENSION PILE STUDY LABORATORY MODEL PILE TESTS

TEST 9, STRATUM II, Cyclic stroke controlled test 3, 250 cycles

Scale

DET NORSKE VERITAS
Geotechnical Laboratory

Drawn by

Date

Approved

Fig. No. 18

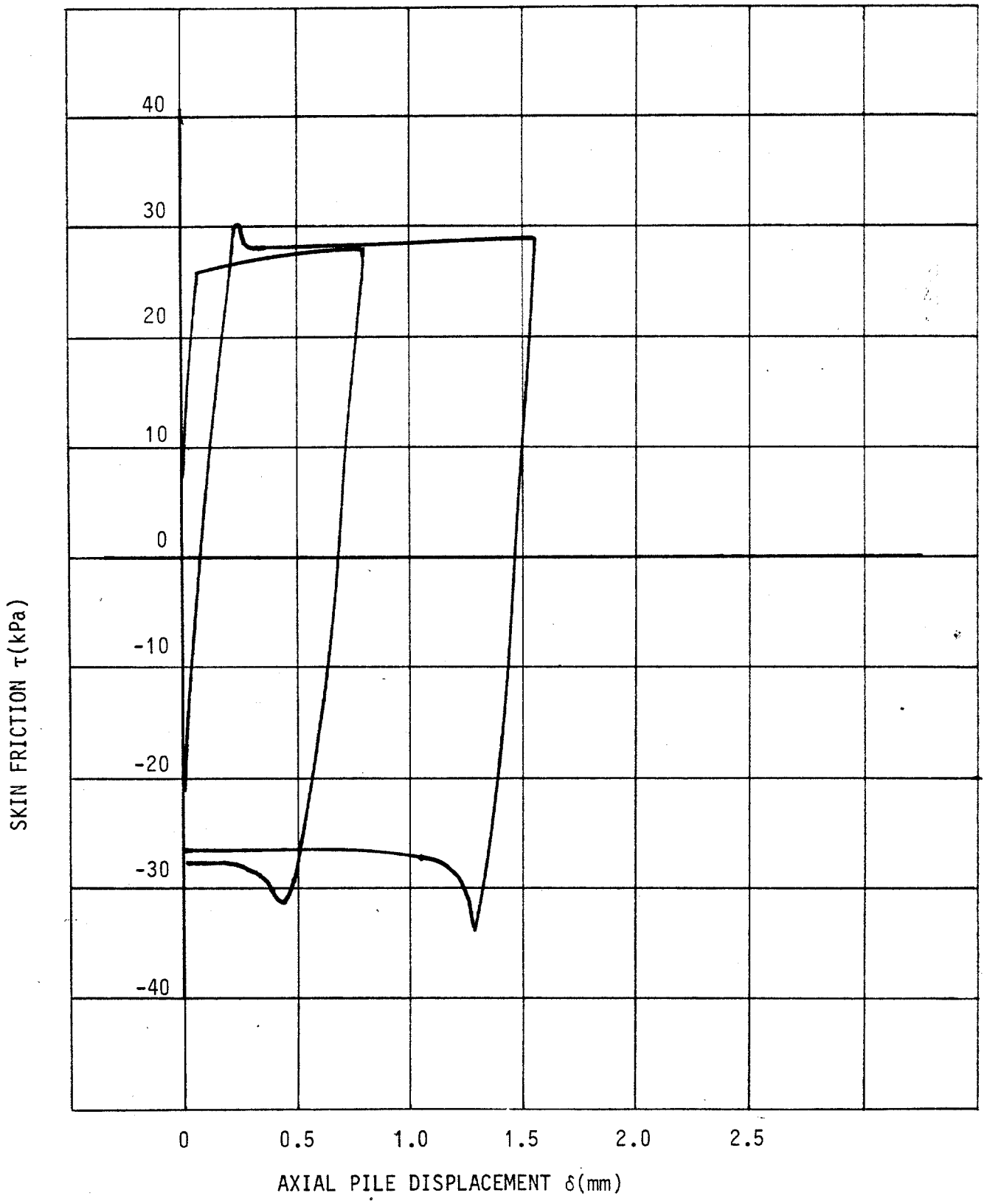

CNRD 13-2 TENSION PILE STUDY LABORATORY MODEL PILE TESTS

TEST 9, STRATUM II, Static test 5, before cycl. stroke test 4

DET NORSKE VERITAS Geotechnical Laboratory	Drawn by	Scale
	Approved	Date
		Fig. No. 19

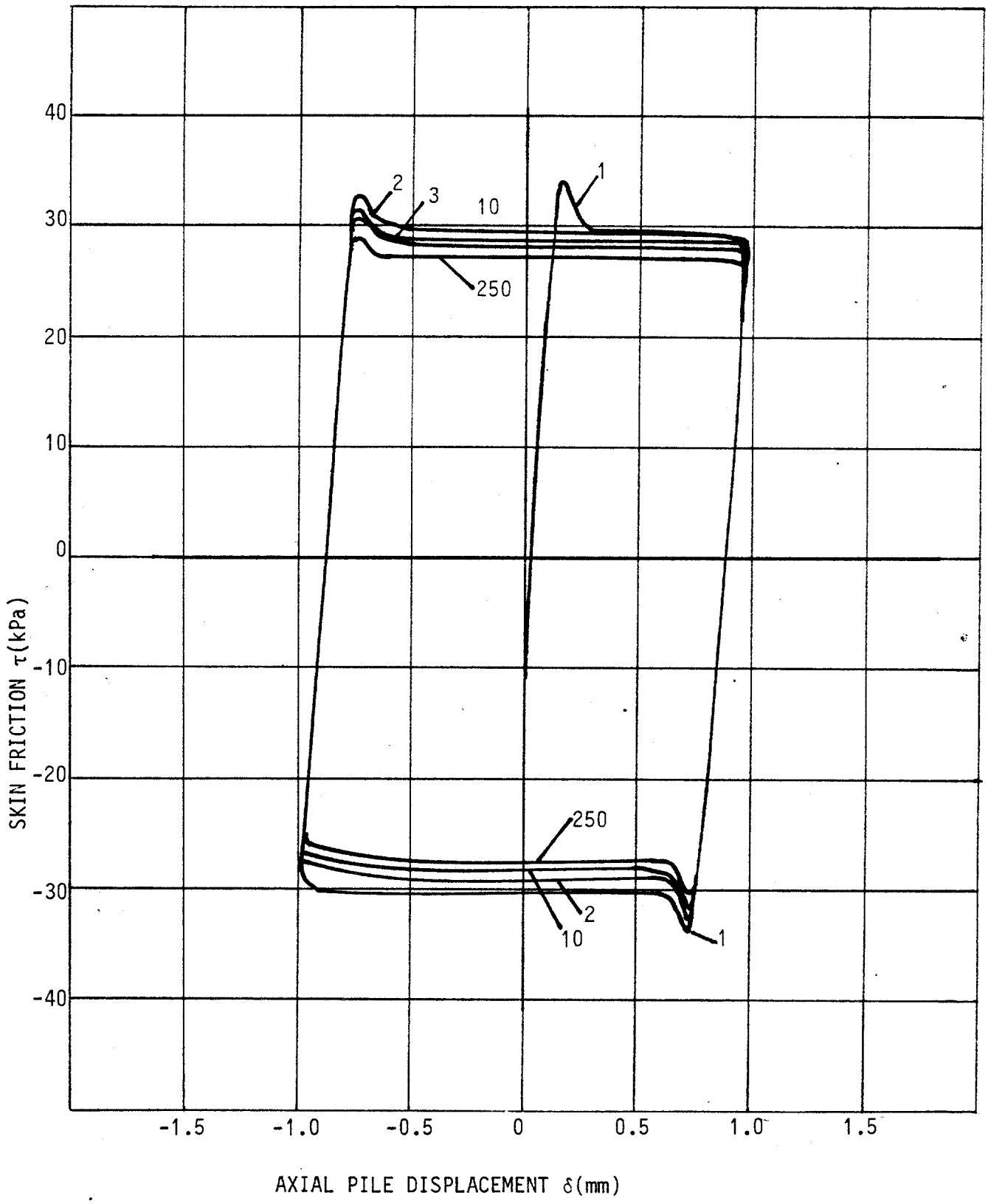

CNRD 13-2 TENSION PILE STUDY LABORATORY MODEL PILE TESTS

TEST 9, STRATUM II, Cyclic stroke controlled test 4, 250 cycles

DET NORSKE VERITAS Geotechnical Laboratory	Drawn by	Scale
	Approved	Date
		Fig. No. 20

TEST 9, STRATUM II

SHEAR STRENGTH FROM POCKET PENETROMETER
AFTER PILE TEST (kPa)

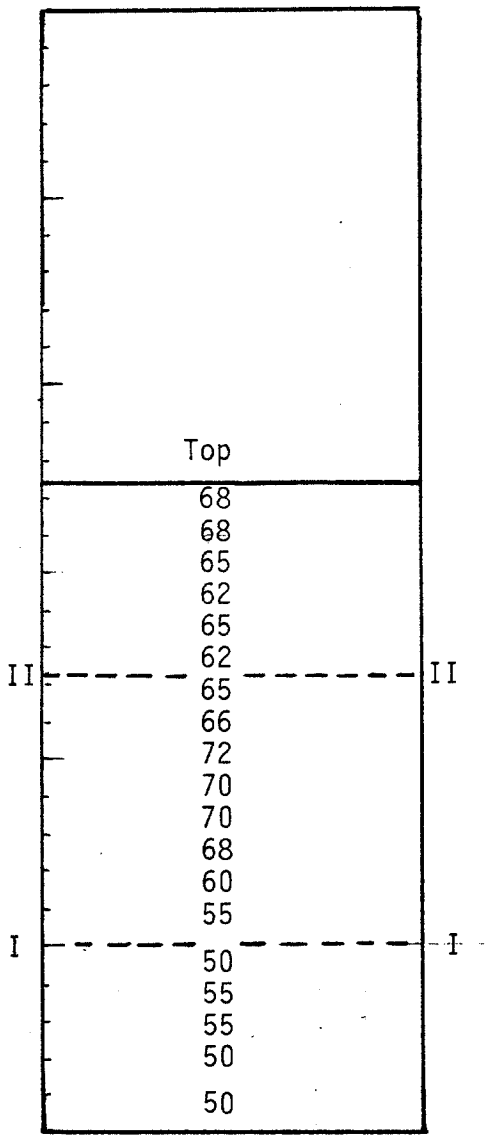

Scale 1:4

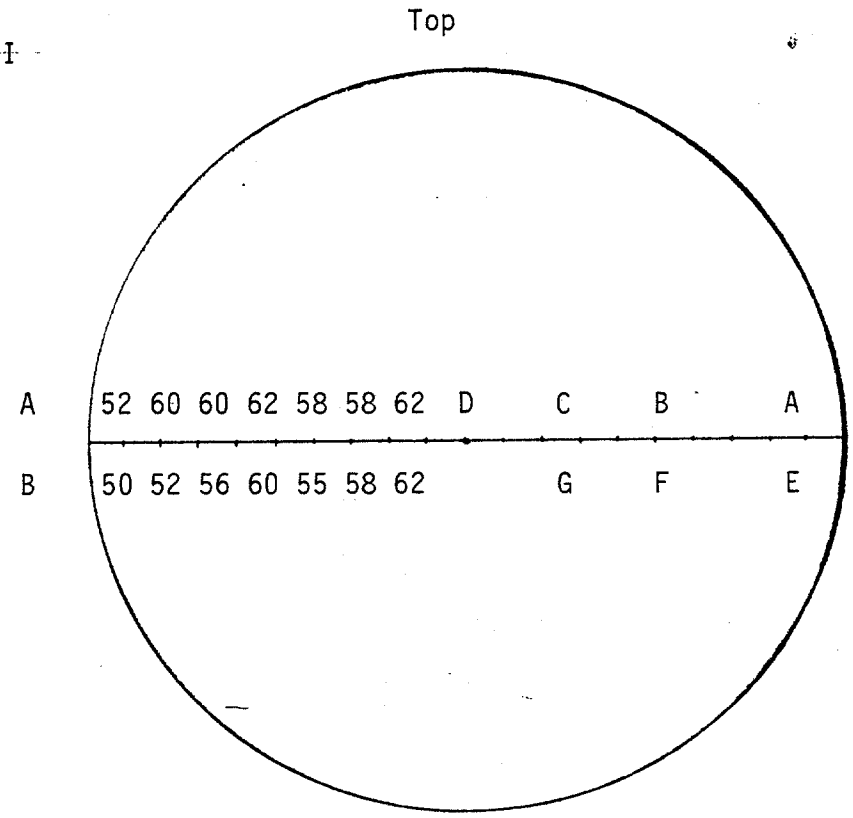

Scale: 1:2

CNRD 13-2 TENSION PILE STUDY LABORATORY MODEL PILE TESTS

TEST 9, STRATUM II, Pocket penetrometer tests after pile test		Scale
DET NORSKE VERITAS Geotechnical Laboratory	Drawn by	Date
	Approved	Fig.No. 21

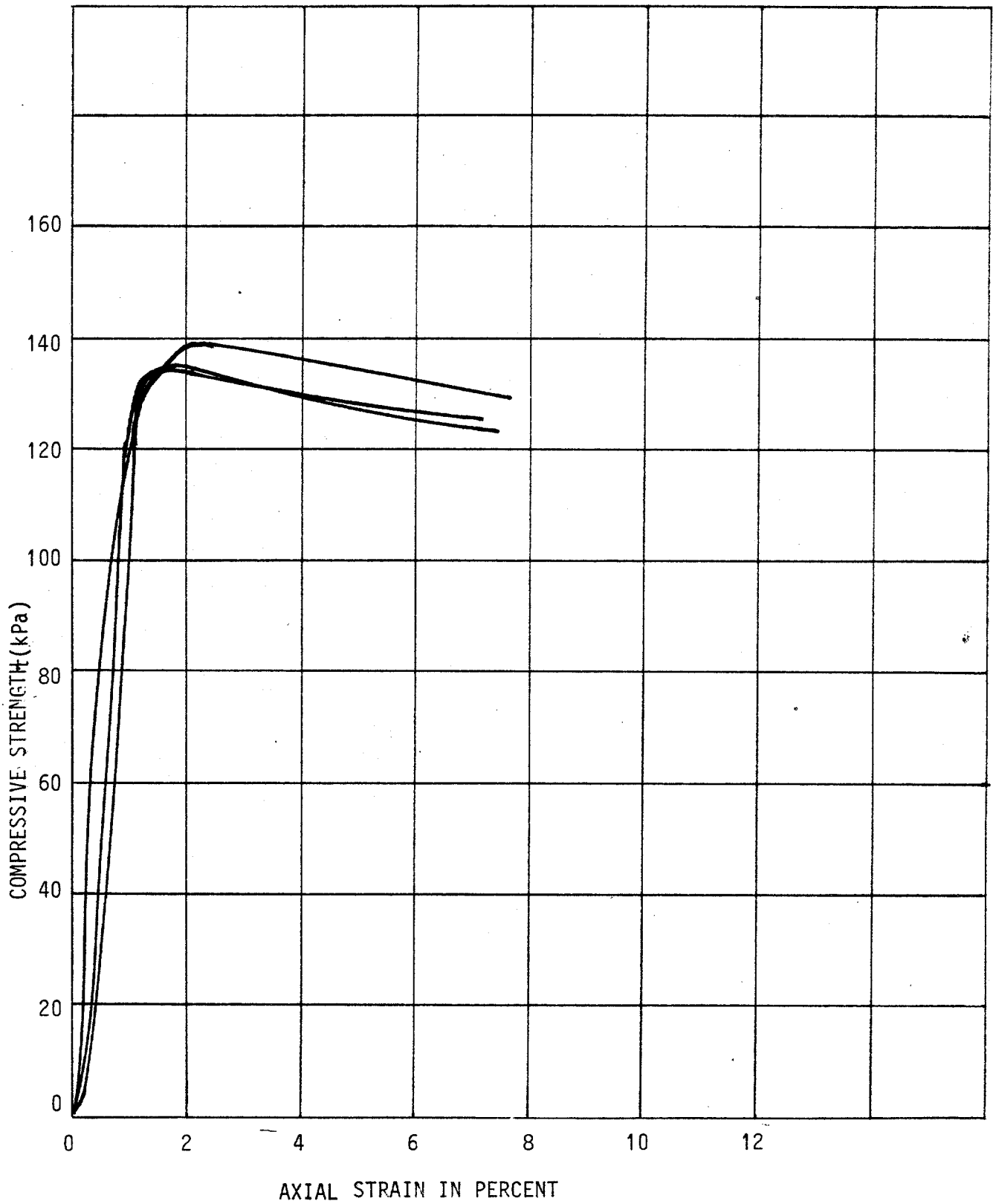

CNRD 13-2 TENSION PILE STUDY LABORATORY MODEL PILE TESTS

TEST 9, STRATUM II, Unconfined compr. tests after pile test

Scale

DET NORSKE VERITAS
Geotechnical Laboratory

Drawn by

Date

Approved

Fig. No. 22

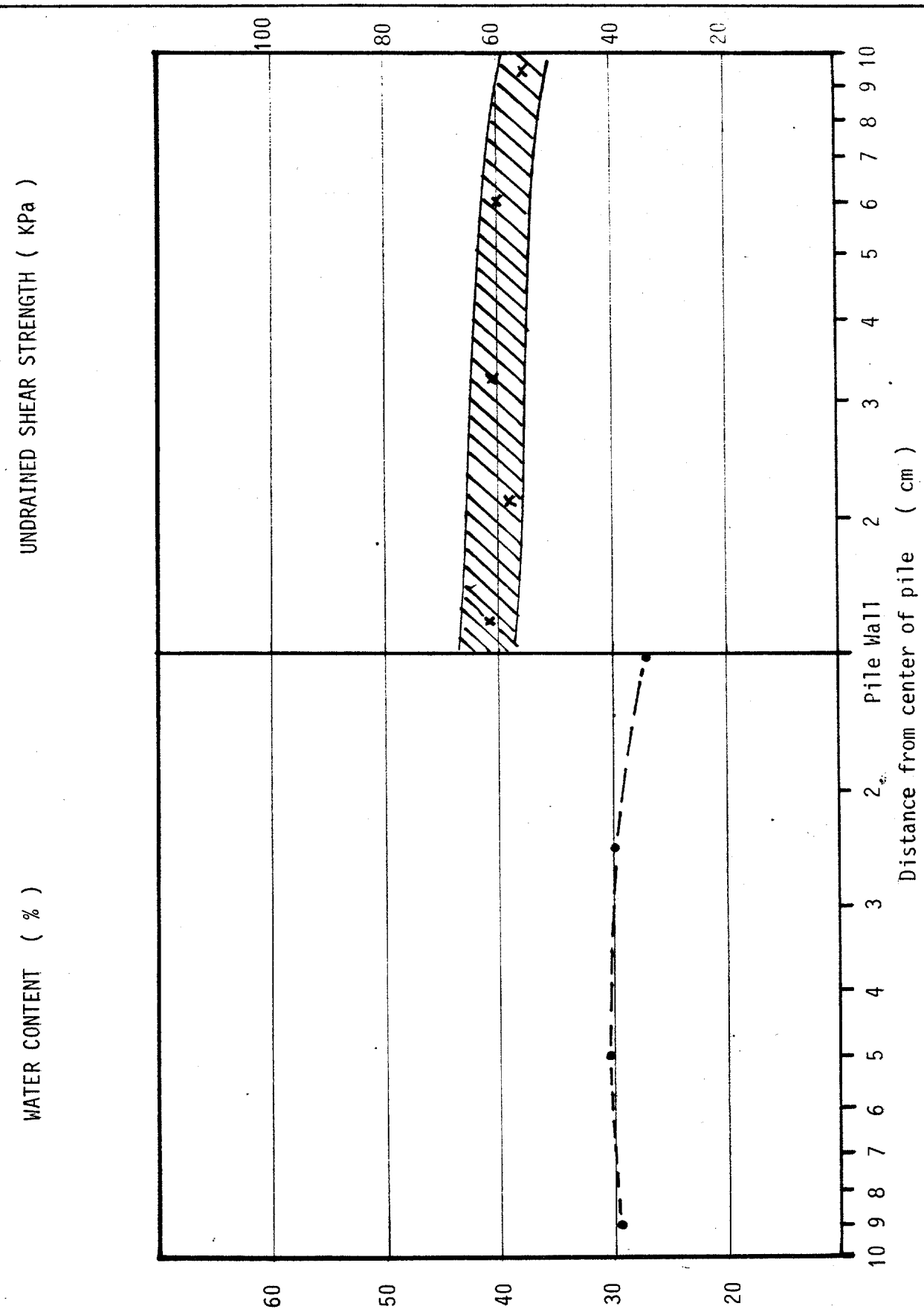

CNRD 13-2 TENSION PILE STUDY LABORATORY MODEL PILE TESTS

TEST 9, STRATUM II, Water content and shear strength after test

DET NORSKE VERITAS Geotechnical Laboratory	Drawn by	Scale
	Approved	Date
		Fig. No. 23

Appendix FA

Plotted Results from WD29LC

Figures FA-1 through FA-5

Skin Friction vs Deflection, Selected Cycles

Figures FA-6 through FA-8

Skin Friction vs Eff. Normal Pressure, Selected Cycl.

Figures FA-9 through FA-18

Skin Friction, Pore and Total Pressure, Selected Cycles

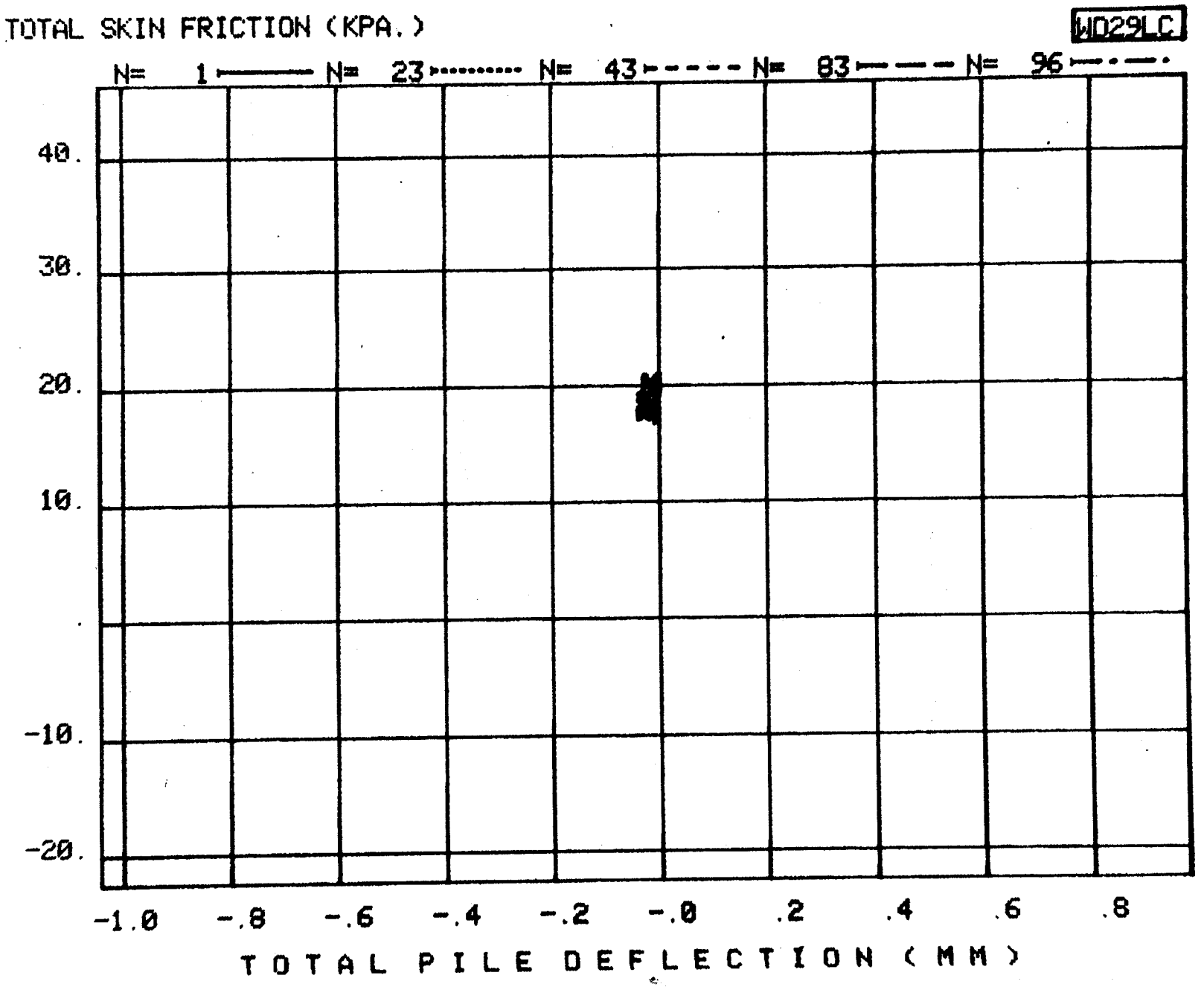
TOTAL SKIN FRICTION (KPA.)
WD29LC
N= 1
N= 23
N= 43
N= 83
N= 96
40.
30.
20.
10.
-10.
-20.
-1.0
-.8
-.6
-.4
-.2
-.0
.2
.4
.6
.8
TOTAL PILE DEFLECTION (MM)

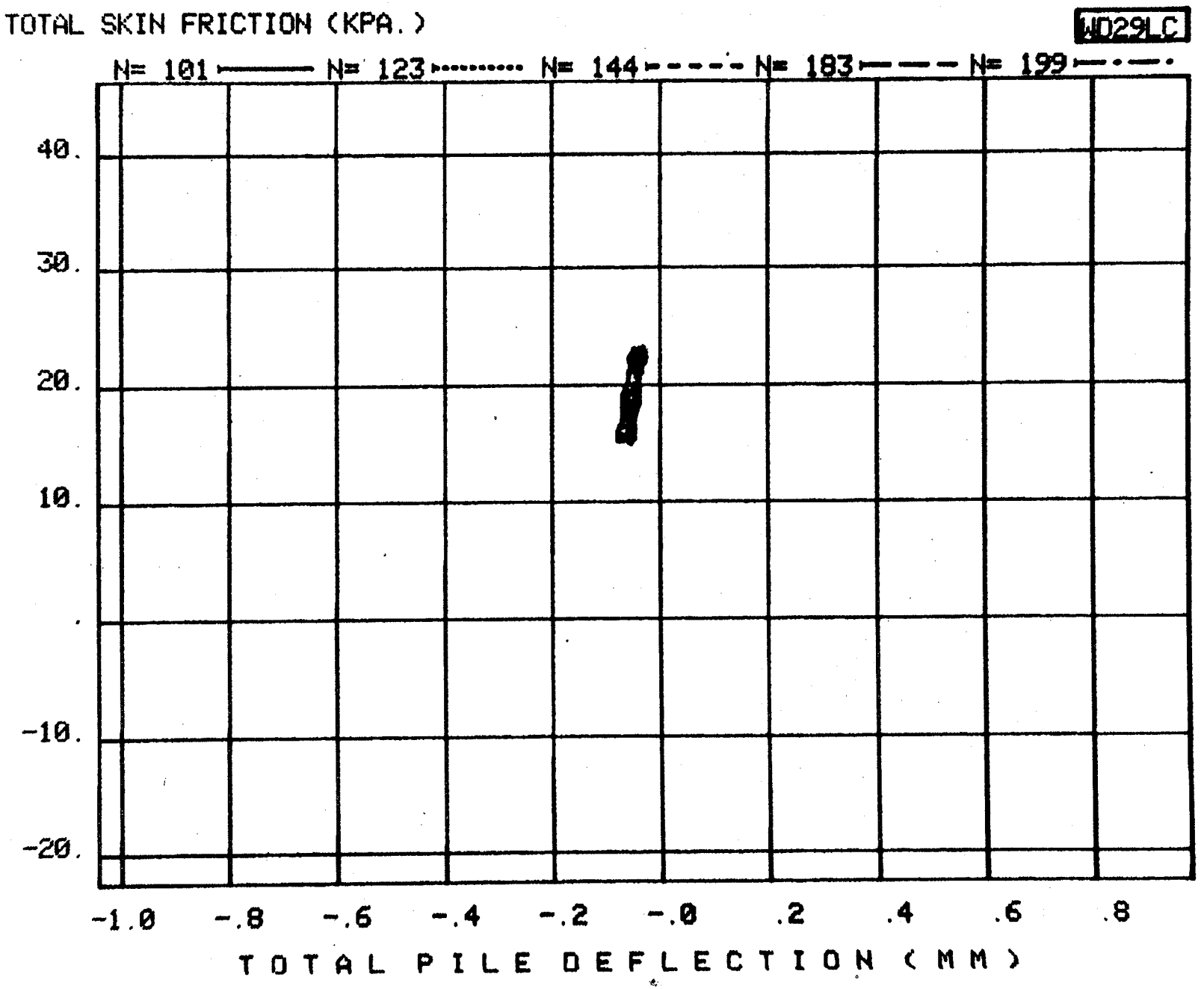
TOTAL SKIN FRICTION (KPA.)
WD29LC
N= 101
N= 123
N= 144
N= 183
N= 199
40.
30.
20.
10.
-10.
-20.
-1.0
-.8
-.6
-.4
-.2
-.0
.2
.4
.6
.8
TOTAL PILE DEFLECTION (MM)

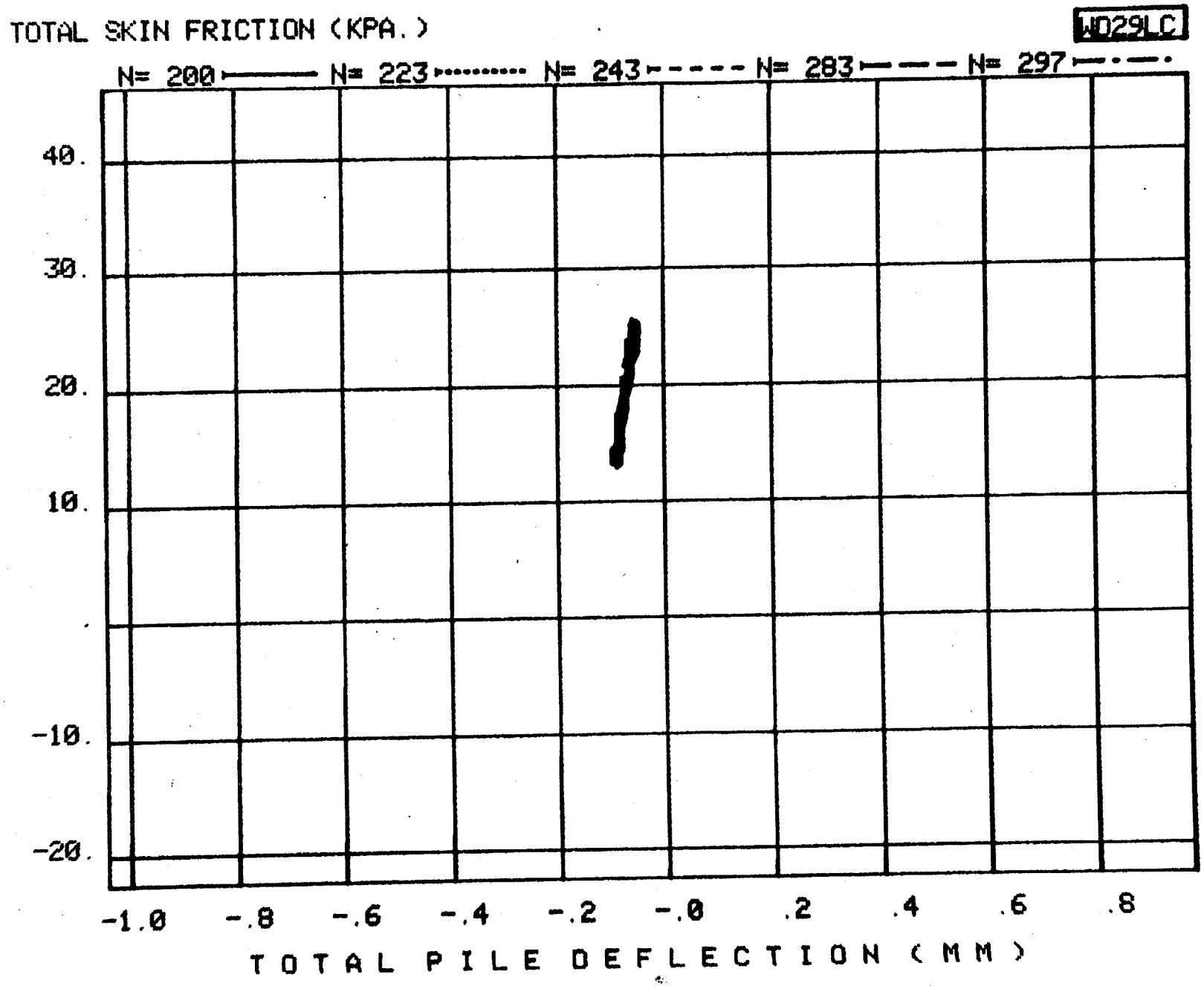
TOTAL SKIN FRICTION (KPA.)
WD29LC
N= 200
N= 223
N= 243
N= 283
N= 297
40.
30.
20.
10.
-10.
-20.
-1.0
-.8
-.6
-.4
-.2
-.0
.2
.4
.6
.8
TOTAL PILE DEFLECTION (MM)

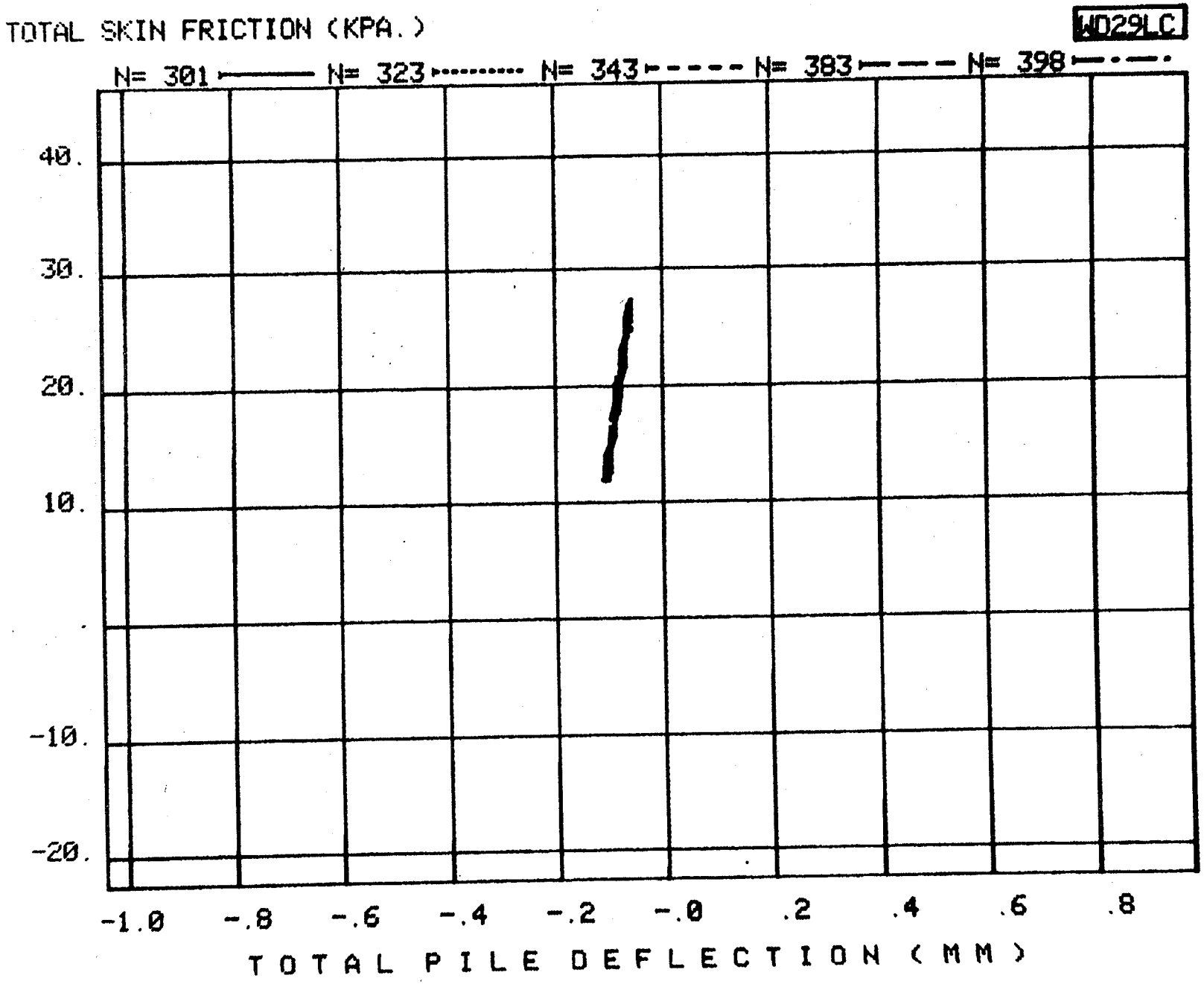
TOTAL SKIN FRICTION (KPA.)
WD29LC
N= 301
N= 323
N= 343
N= 383
N= 398
40.
30.
20.
10.
-10.
-20.
-1.0
-.8
-.6
-.4
-.2
-.0
.2
.4
.6
.8
TOTAL PILE DEFLECTION (MM)

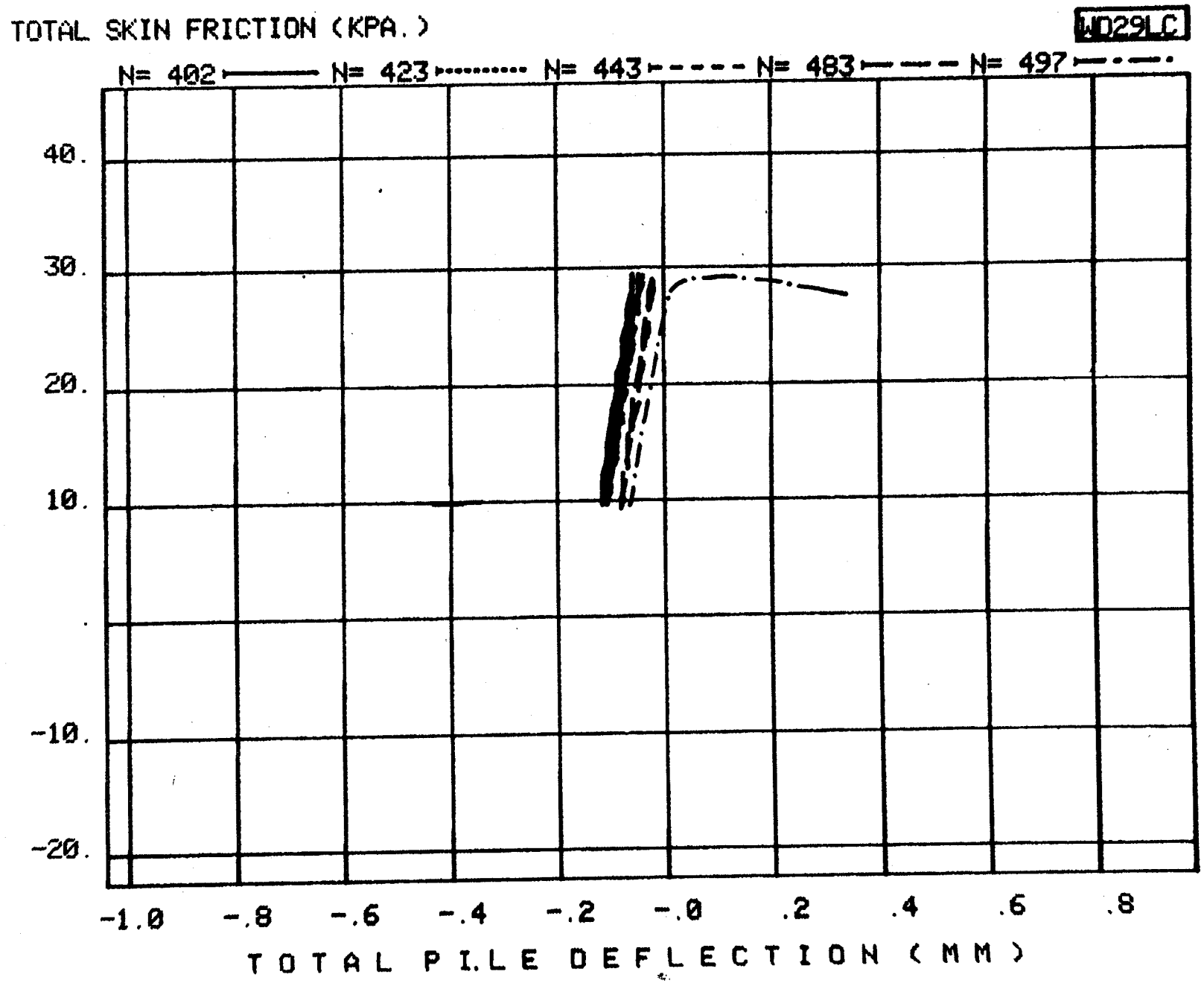
TOTAL SKIN FRICTION (KPA.)
WD29LC
N= 402
N= 423
N= 443
N= 483
N= 497
40.
30.
20.
10.
-10.
-20.
-1.0
-.8
-.6
-.4
-.2
-.0
.2
.4
.6
.8
TOTAL PILE DEFLECTION (MM)

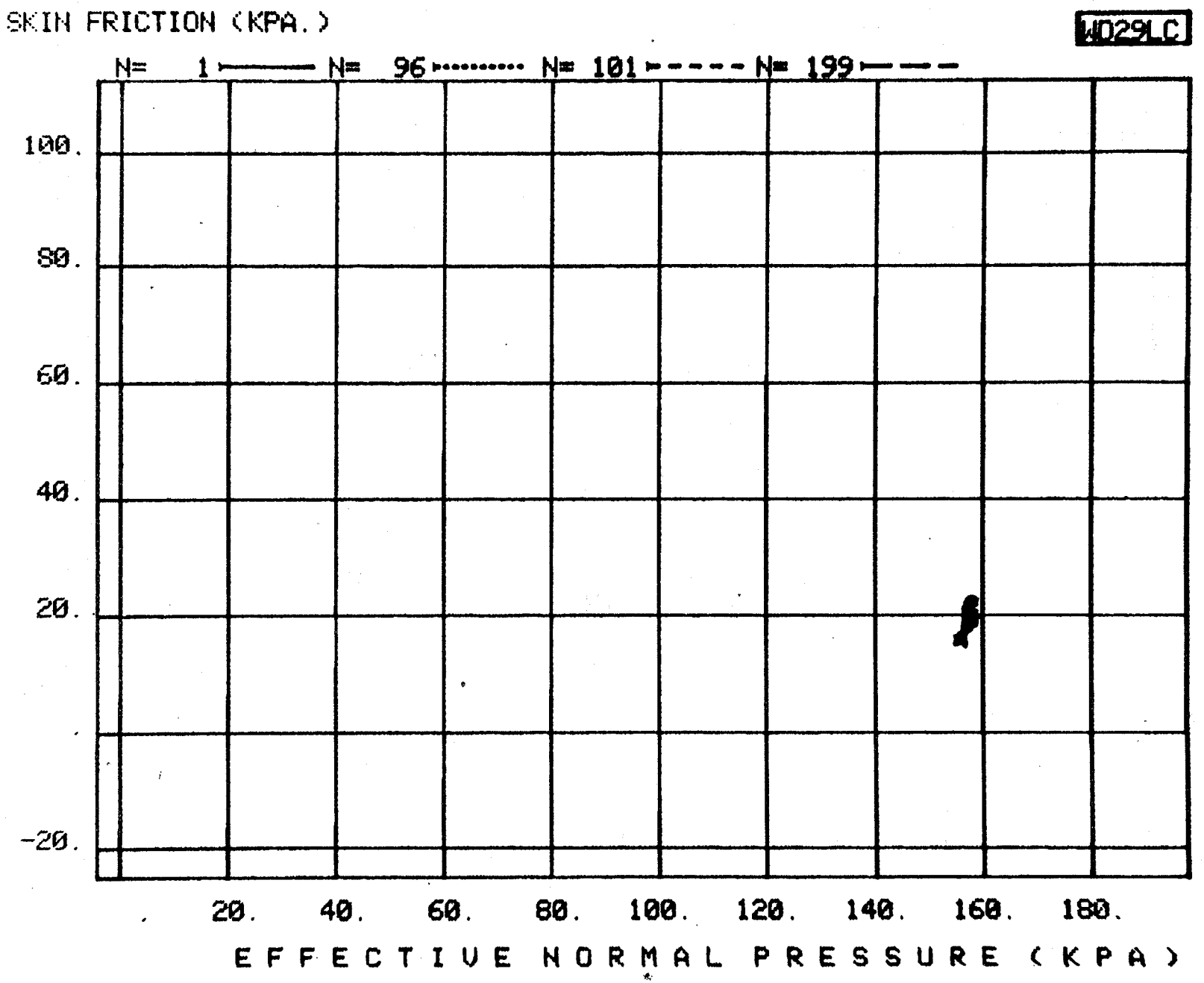
SKIN FRICTION (KPA.)
WD29LC
N= 1
N= 96
N= 101
N= 199
100.
80.
60.
40.
20.
-20.
20.
40.
60.
80.
100.
120.
140.
160.
180.
EFFECTIVE NORMAL PRESSURE (KPA)

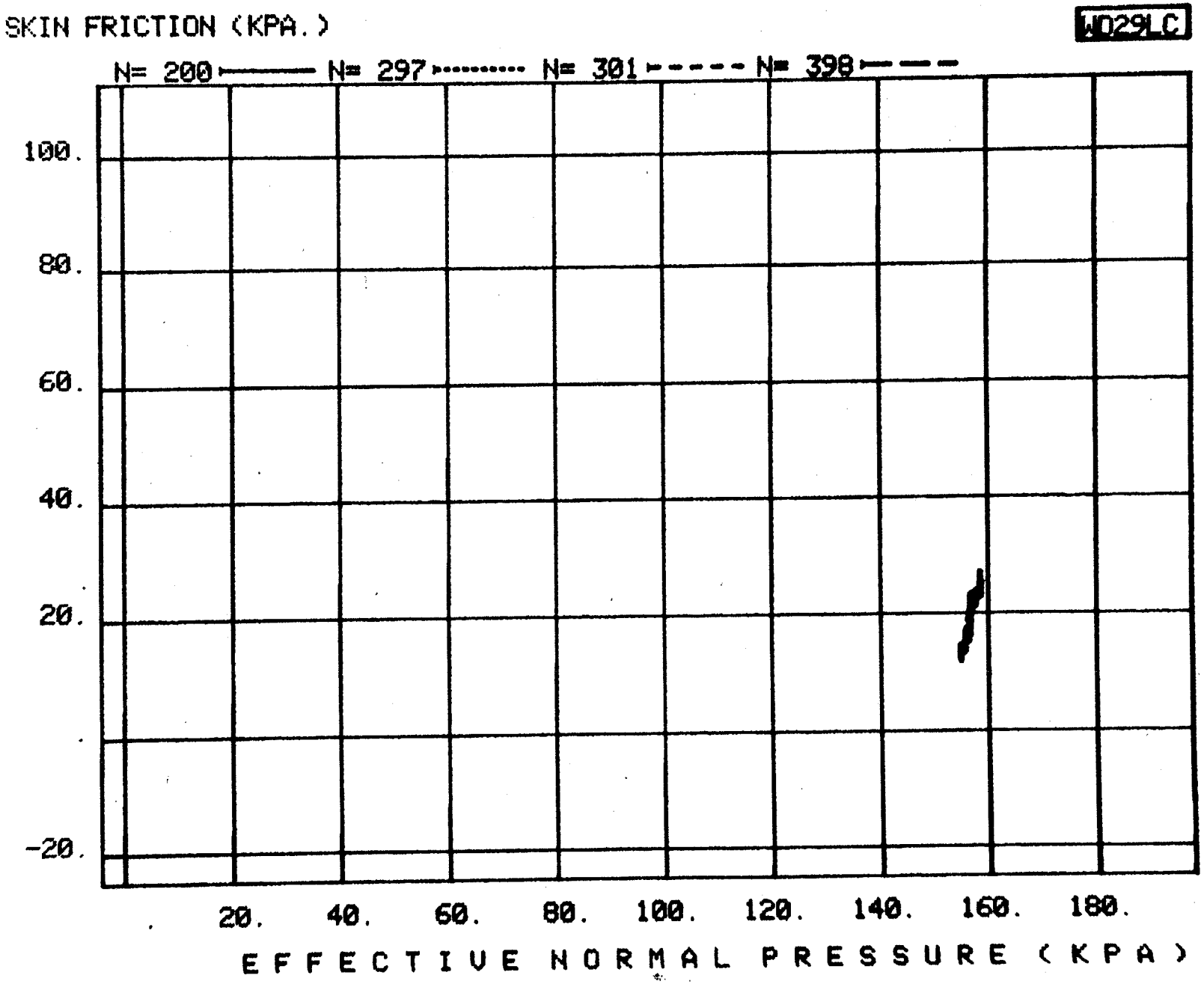
SKIN FRICTION (KPA.)
W029LC
N= 200
N= 297
N= 301
N= 398
100.
80.
60.
40.
20.
-20.
20.
40.
60.
80.
100.
120.
140.
160.
180.
EFFECTIVE NORMAL PRESSURE (KPA)

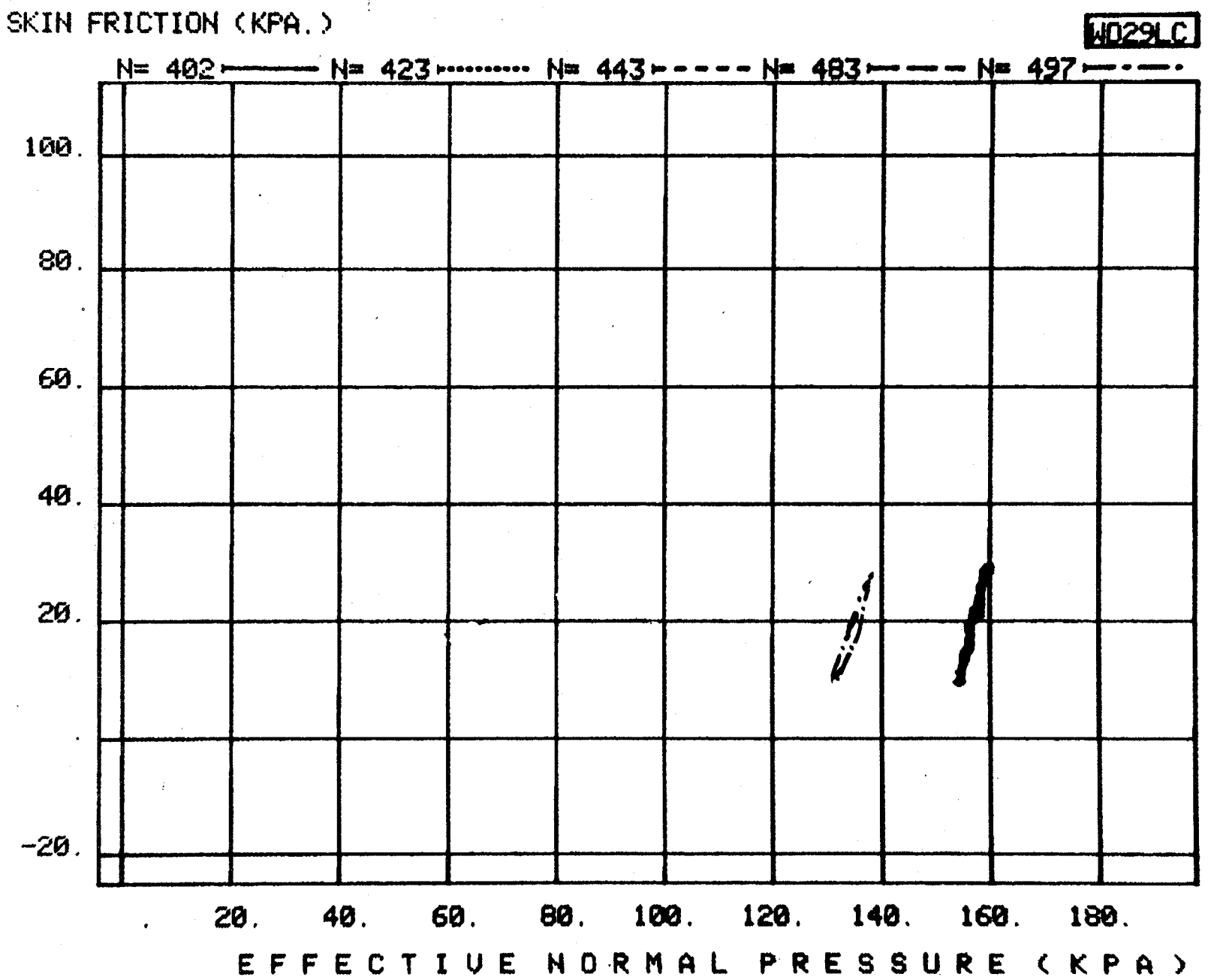
SKIN FRICTION (KPA.)
W029LC
N= 402
N= 423
N= 443
N= 483
N= 497
100.
80.
60.
40.
20.
-20.
20.
40.
60.
80.
100.
120.
140.
160.
180.
EFFECTIVE NORMAL PRESSURE (KPA)

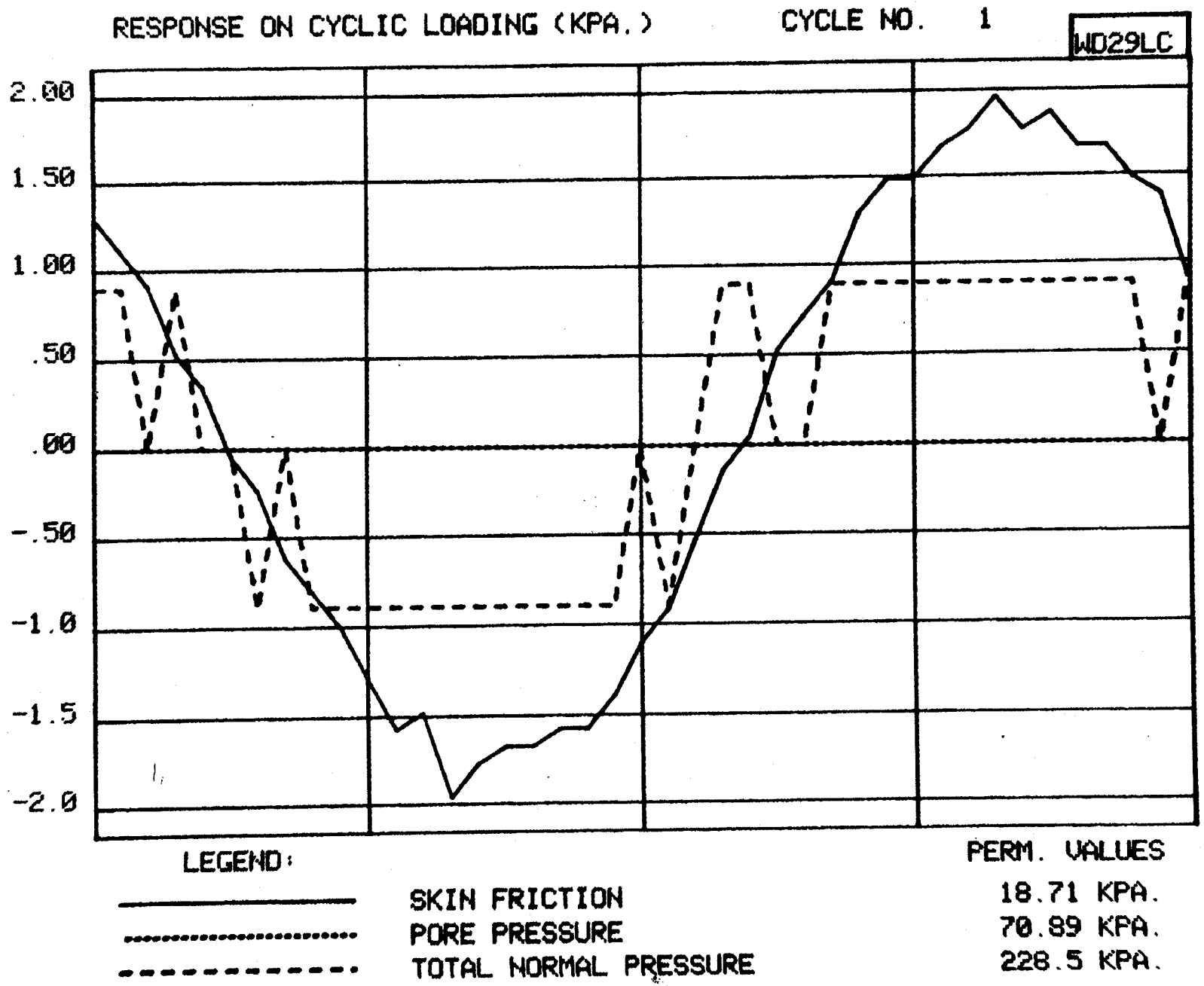
RESPONSE ON CYCLIC LOADING (KPA.)
CYCLE NO. 1
WD29LC
2.00
1.50
1.00
.50
.00
-.50
-1.0
-1.5
-2.0
LEGEND:
SKIN FRICTION
PORE PRESSURE
TOTAL NORMAL PRESSURE
PERM. VALUES
18.71 KPA.
70.89 KPA.
228.5 KPA.

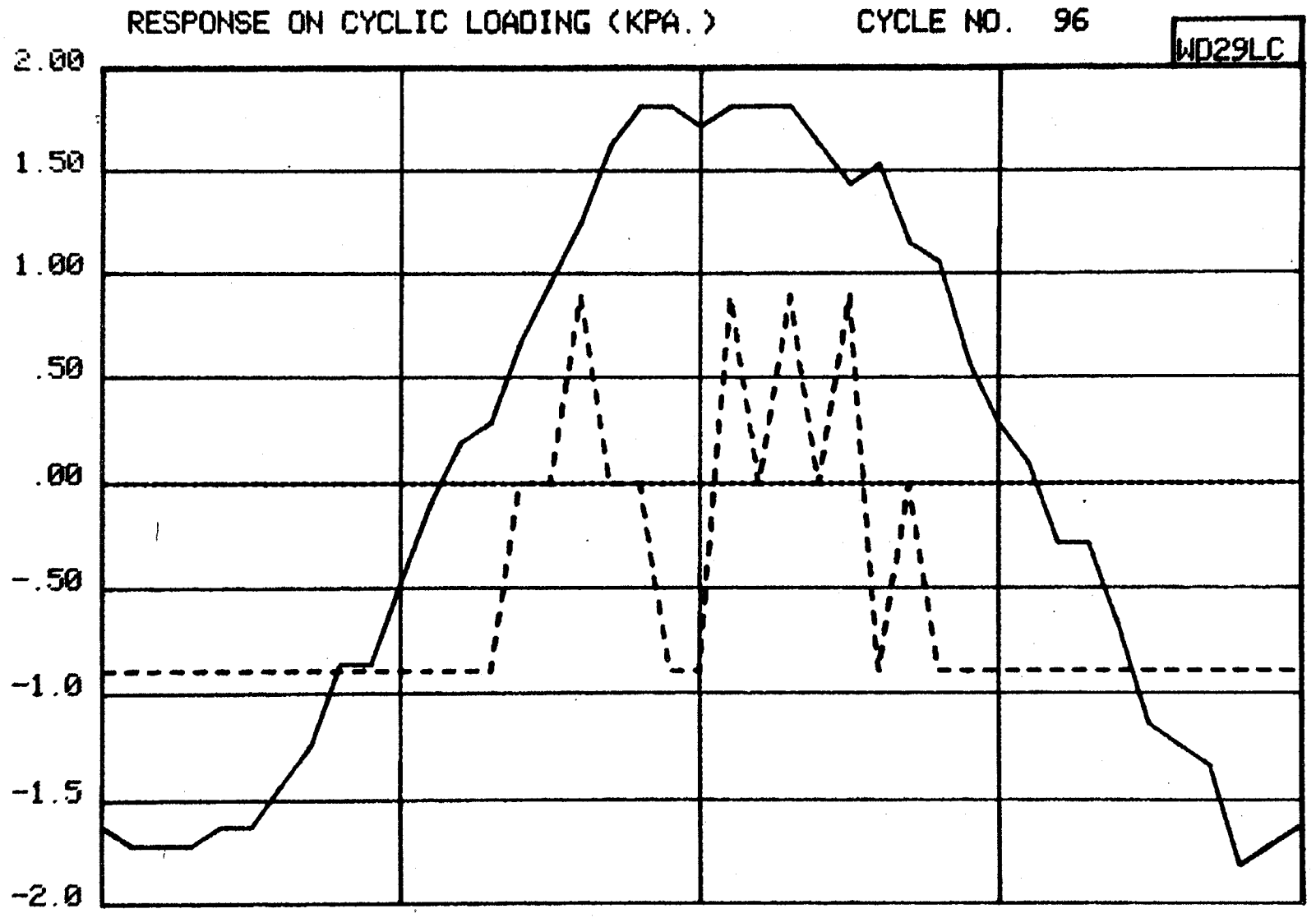

LEGEND:

		PERM. VALUES
———	SKIN FRICTION	18.95 KPA.
·····	PORE PRESSURE	70.89 KPA.
- - - -	TOTAL NORMAL PRESSURE	228.5 KPA.

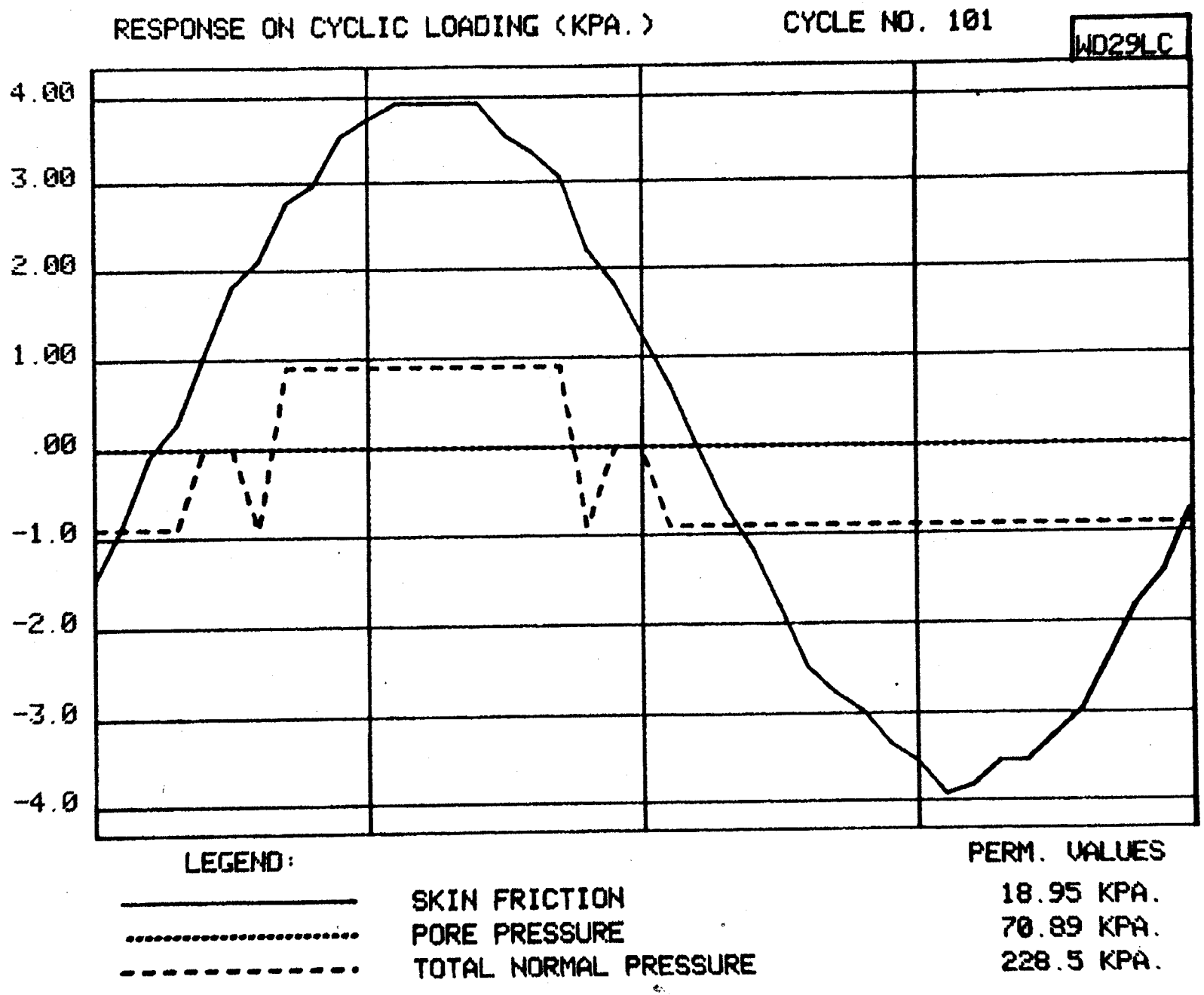
RESPONSE ON CYCLIC LOADING (KPA.)
CYCLE NO. 101
WD29LC
4.00
3.00
2.00
1.00
.00
-1.0
-2.0
-3.0
-4.0
LEGEND:
SKIN FRICTION
PORE PRESSURE
TOTAL NORMAL PRESSURE
PERM. VALUES
18.95 KPA.
70.89 KPA.
228.5 KPA.

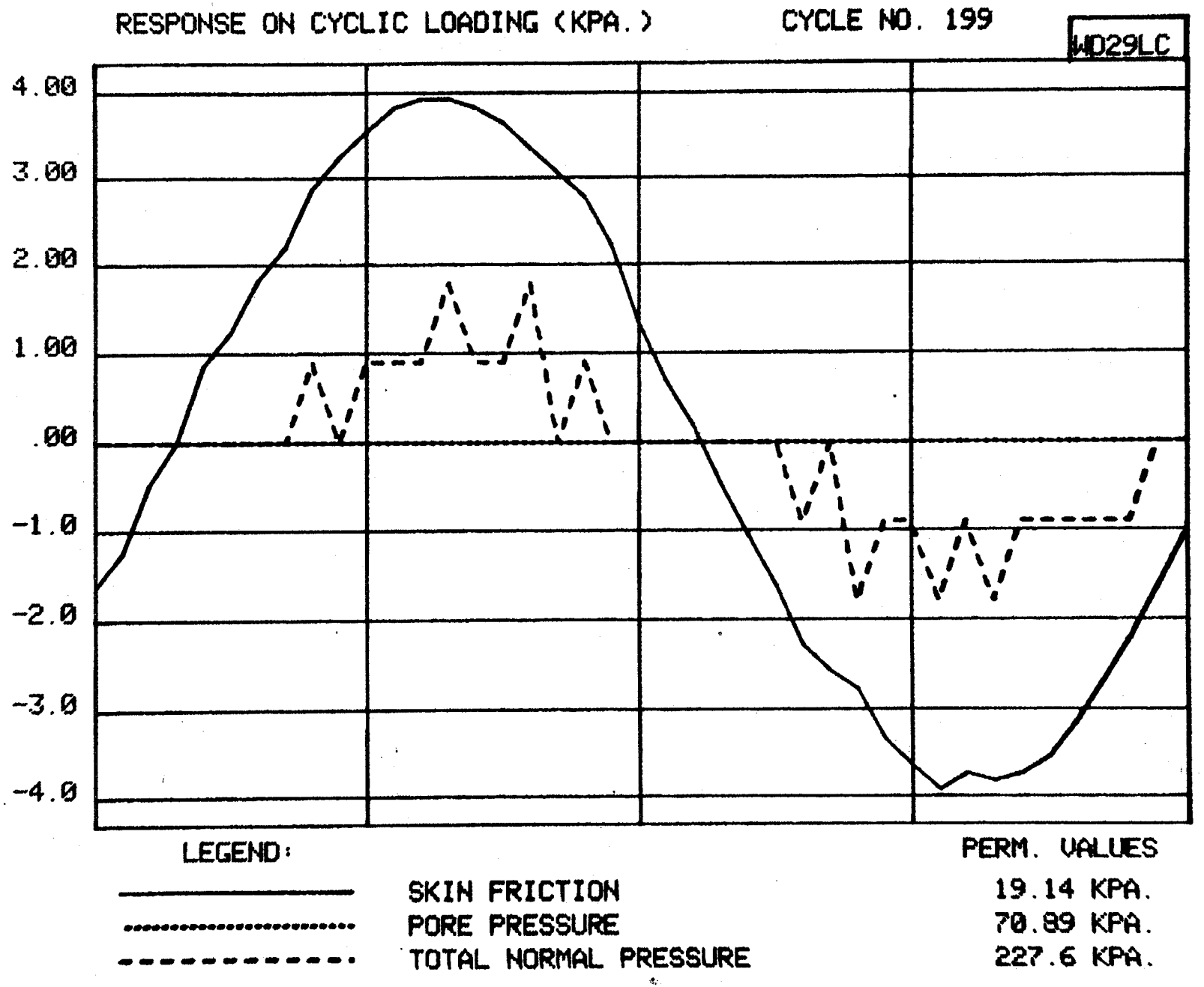
RESPONSE ON CYCLIC LOADING (KPA.)
CYCLE NO. 199
WD29LC
4.00
3.00
2.00
1.00
.00
-1.0
-2.0
-3.0
-4.0
LEGEND:
SKIN FRICTION
PORE PRESSURE
TOTAL NORMAL PRESSURE
PERM. VALUES
19.14 KPA.
70.89 KPA.
227.6 KPA.

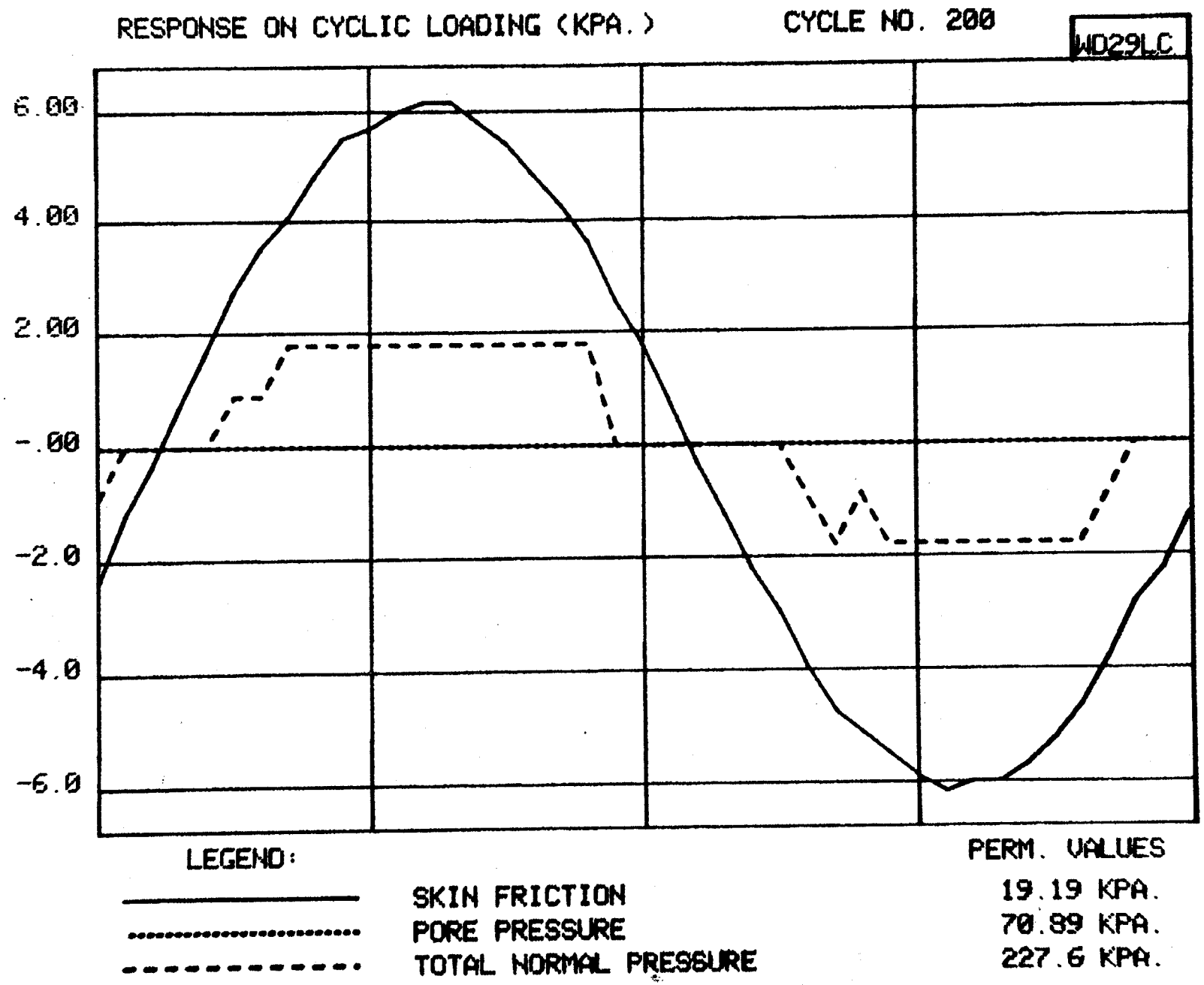
RESPONSE ON CYCLIC LOADING (KPA.)
CYCLE NO. 200
WD29LC
6.00
4.00
2.00
-.00
-2.0
-4.0
-6.0
LEGEND:
SKIN FRICTION
PORE PRESSURE
TOTAL NORMAL PRESSURE
PERM. VALUES
19.19 KPA.
70.89 KPA.
227.6 KPA.

RESPONSE ON CYCLIC LOADING (KPA.) CYCLE NO. 297

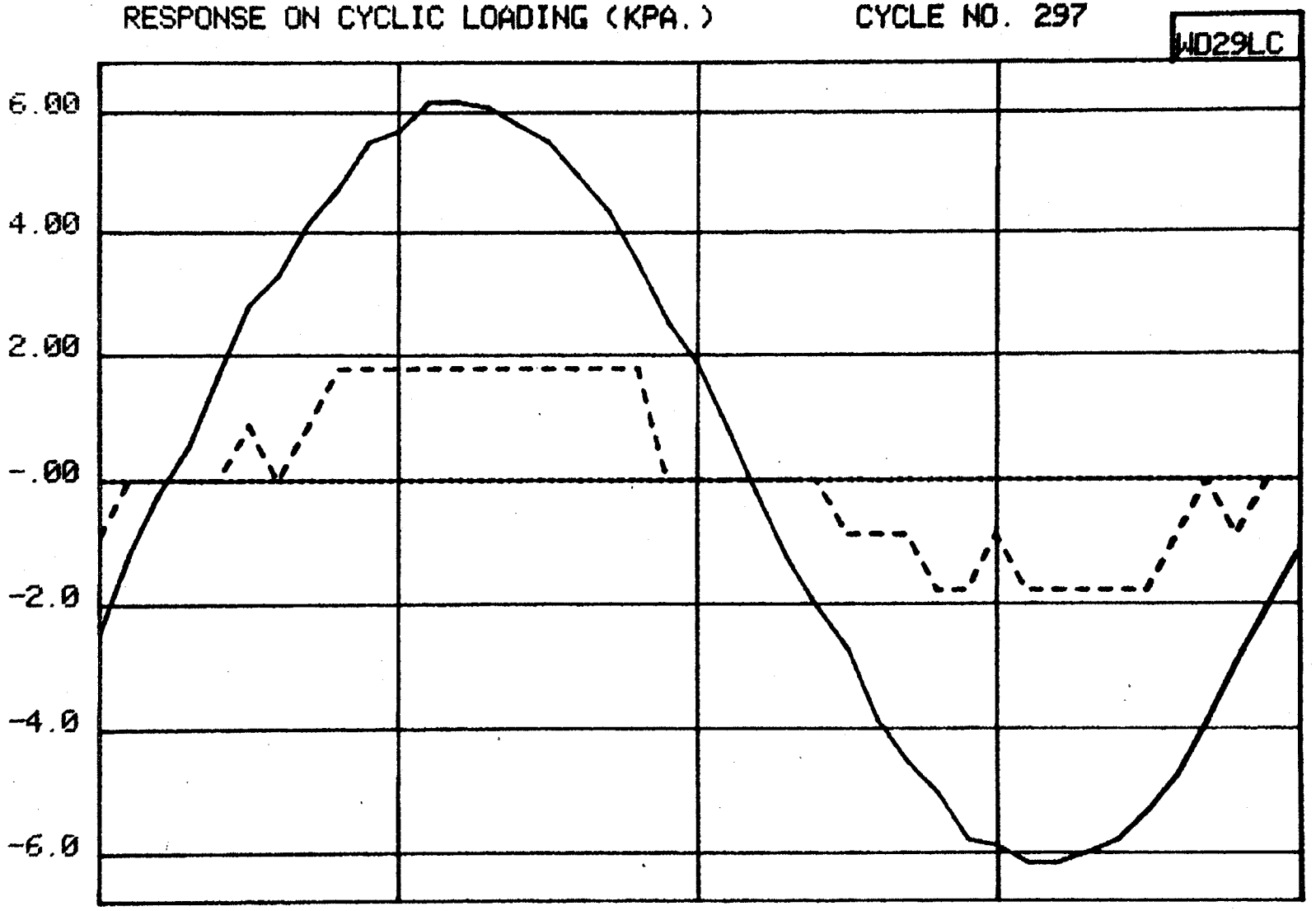

LEGEND:

		PERM. VALUES
———	SKIN FRICTION	19.48 KPA.
·····	PORE PRESSURE	70.89 KPA.
- - - -	TOTAL NORMAL PRESSURE	227.6 KPA.

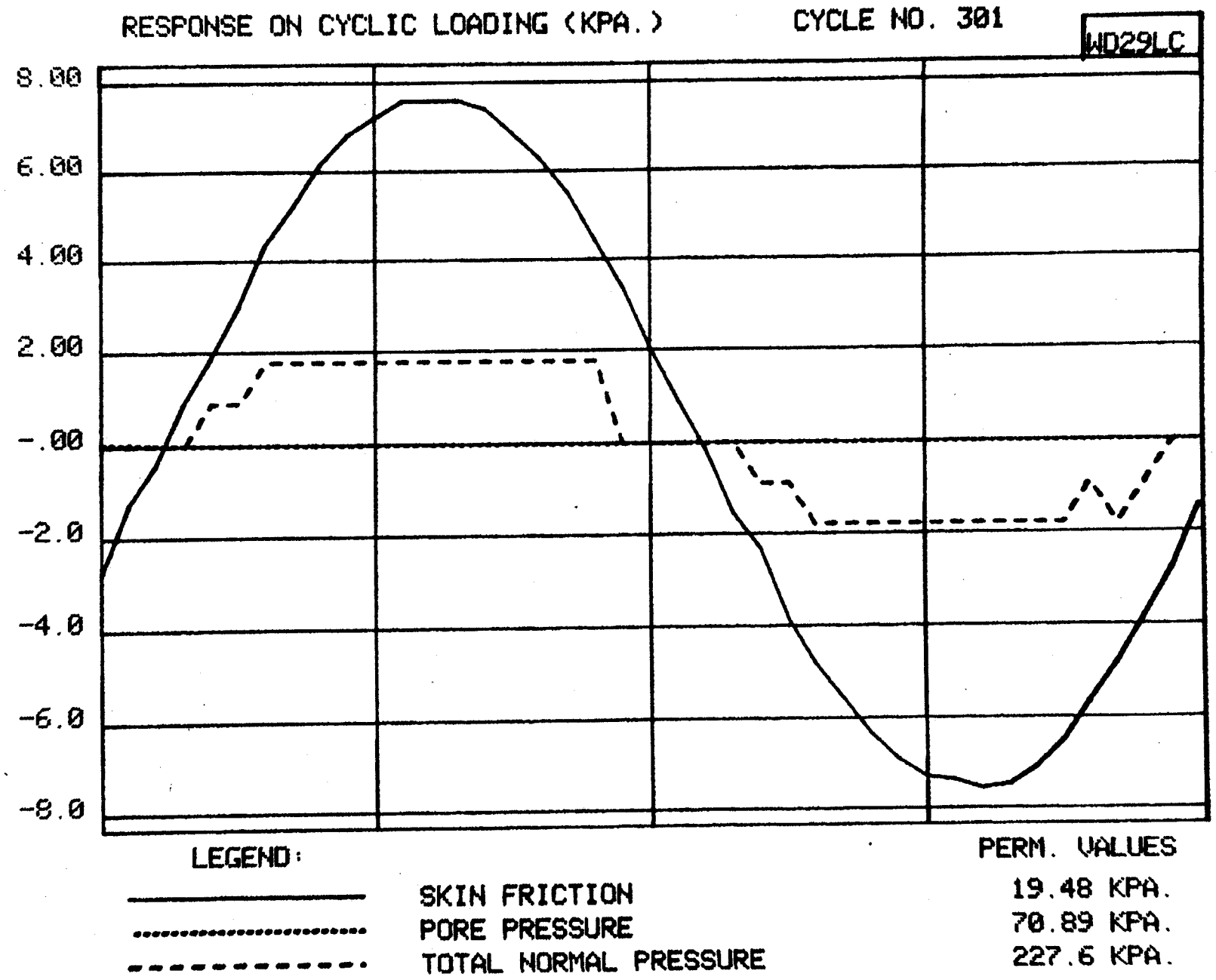
RESPONSE ON CYCLIC LOADING (KPA.)
CYCLE NO. 301
WD29LC
8.00
6.00
4.00
2.00
-.00
-2.0
-4.0
-6.0
-8.0
LEGEND:
SKIN FRICTION
PORE PRESSURE
TOTAL NORMAL PRESSURE
PERM. VALUES
19.48 KPA.
70.89 KPA.
227.6 KPA.

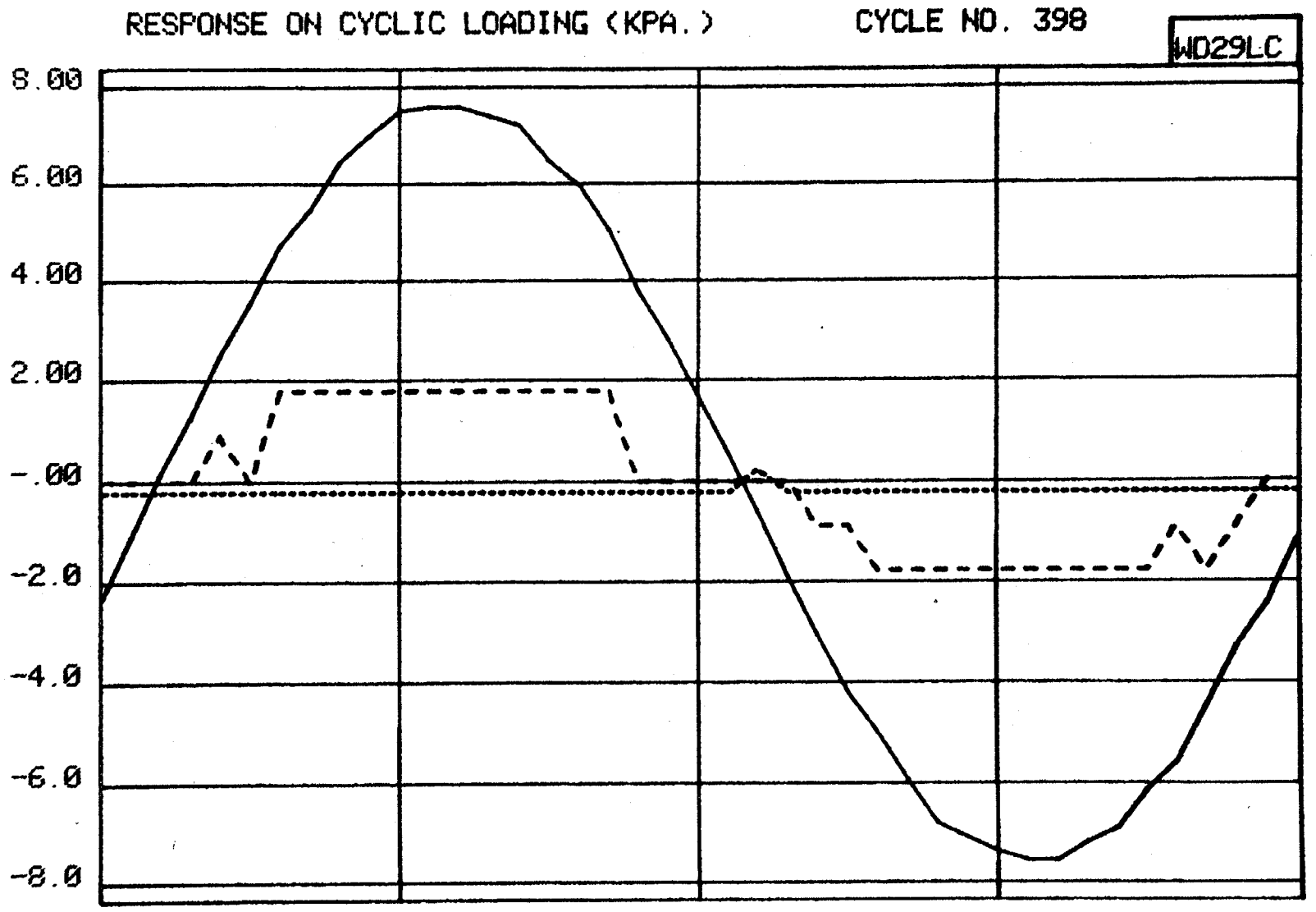

LEGEND:

		PERM. VALUES
———	SKIN FRICTION	19.48 KPA.
·····	PORE PRESSURE	71.13 KPA.
- - - -	TOTAL NORMAL PRESSURE	227.6 KPA.

RESPONSE ON CYCLIC LOADING (KPA.) CYCLE NO. 402 WD29LC

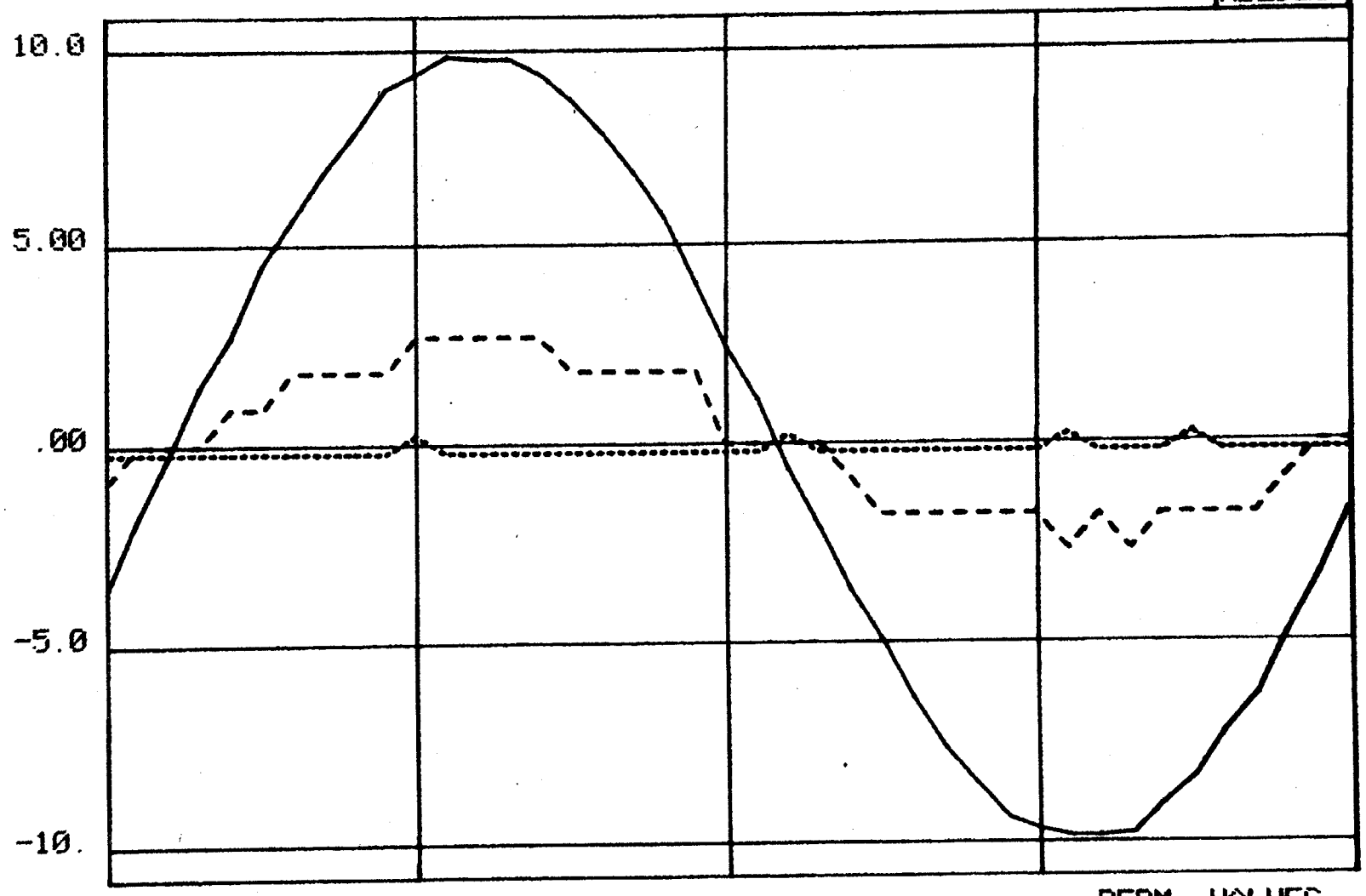

LEGEND:

		PERM. VALUES
———	SKIN FRICTION	19.53 KPA.
·····	PORE PRESSURE	71.13 KPA.
- - - -	TOTAL NORMAL PRESSURE	227.6 KPA.

RESPONSE ON CYCLIC LOADING (KPA.) CYCLE NO. 483

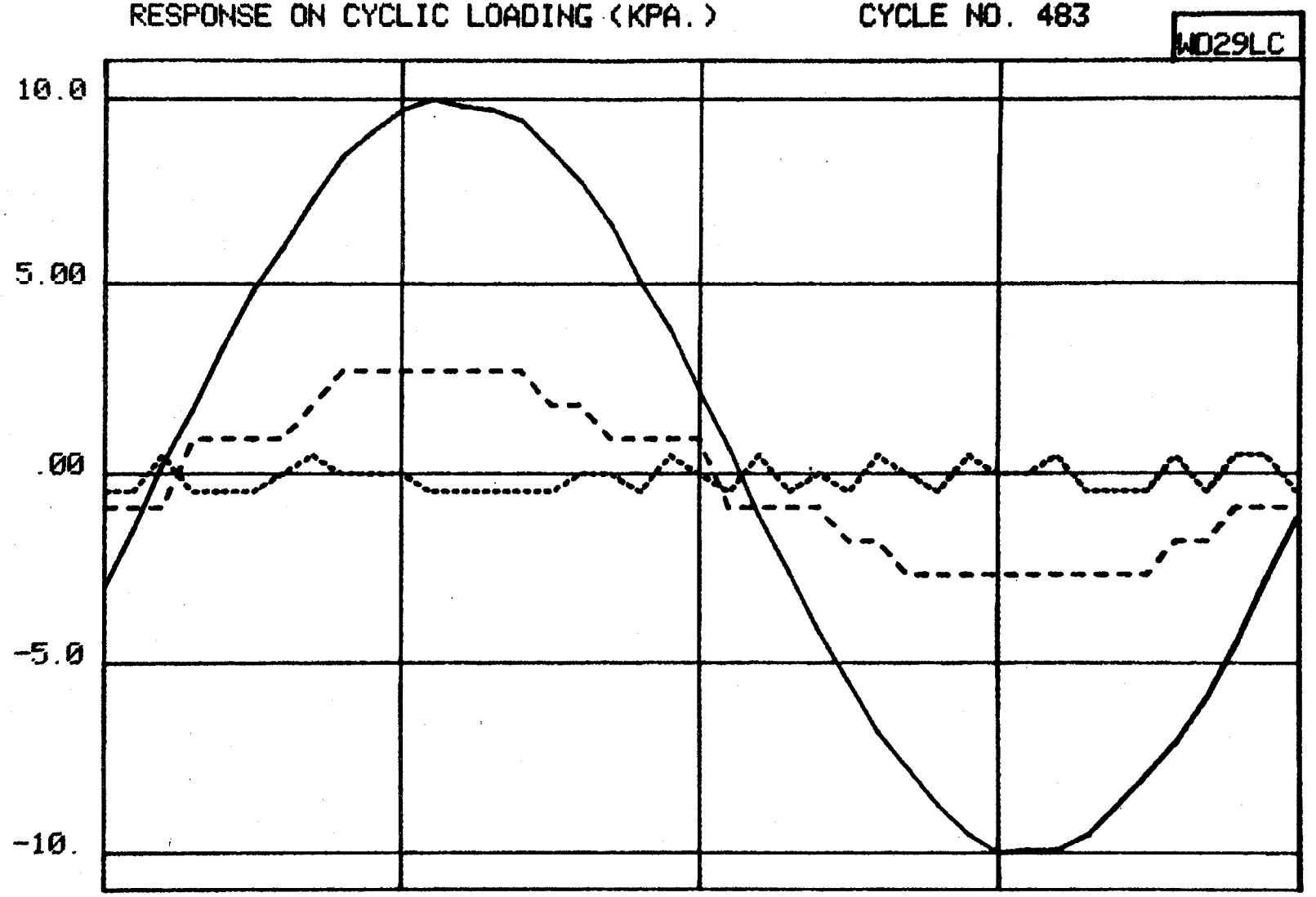

LEGEND:		PERM. VALUES
———	SKIN FRICTION	19.38 KPA.
·····	PORE PRESSURE	71.37 KPA.
- - - -	TOTAL NORMAL PRESSURE	228.5 KPA.

APPENDIX G

DETAILED RESULTS FROM **TEST 10, STRATUM III** MODEL PILE TESTS

CONTENTS

Summary	G3
Test 10, Stratum III	G4
Consolidation	G4
Pile Instatllation and Set-Up	G4
Static Test	G5
Cyclic Tests	G5
Stress Controlled Tests (W310LC)	G6
Stroke Controlled Tests (W310SC)	G7
Creep Test	G8
Relaxation Tests	G9
Strength Tests	G10

LIST OF FIGURES

Figure 1	Sample Properties
Figure 2	Consolidation Diagram
Figure 3	Pocket Penetrometer Tests After Consolidation
Figure 4	Pressures at Pile Wall after Installation
Figure 5	Static Test 1
Figure 6	Skin Friction vs no. of Cycles, W310LC
Figure 7	Deflection vs no. of Cycles, W310LC
Figure 8	Total Normal Pressure vs no. of Cycles, W310LC
Figure 9	Pore Pressure vs no. of Cycles, W310LC
Figure 10	Eff. Normal Pressure vs no. of Cycles, W310LC
Figure 11	Deflection vs no. of Cycles, W310SC

Figure 12 Skin Friction vs no. of Cycles, W310SC
Figure 13 Total Normal Pressure vs no. of Cycles, W310SC
Figure 14 Pore Pressure vs no. of Cycles, W310SC
Figure 15 Eff. Normal Pressure vs no. of Cycles, W310SC
Figure 16 Static Test 2
Figure 17 Creep Tests
Figure 18 Relaxation Tests
Figure 19 Pocket Penetrometer Tests after Pile Test
Figure 20 Unconfined Compression Tests
Figure 21 Water Content and Shear Strength

Appendix GA
Plotted Results from W310LC
Figures GA-1 through GA-7
Skin Friction vs Deflection, Selected Cycles
Figures GA-8 through GA-11
Skin Friction vs Eff. Normal Pressure, Selected Cycl.
Figures GA-12 through GA-18
Skin Friction, Pore and Total Pressure, Selected Cycles

Appendix GB
Plotted Results from W310SC
Figures GB-1 through GB-4
Skin Friction vs Deflection, Selected Cycles
Figures GB-5 through GB-6
Skin Friction vs Eff. Normal Pressure, Selected Cycl.
Figures GB-7 through GB-14
Skin Friction, Pore and Total Pressure, Selected Cycles

SUMMARY

This report contains the results of the laboratory model pile tests designated TEST 10, STRATUM III, in the project CNRD 13-2, TENSION PILE STUDY, for Conoco Norway Inc.

The clay sample was consolidated for 22 days under 500 kPa applied vertical pressure. Pore pressure in the sample was about 9% of the applied pressure. After 53 days of consolidation in the pile chamber a new modified pile was installed with new pore pressure transducer and modified total pressure transducer. The pile had to be reinstalled due to malfunctioning of the pore pressure transducer. After 2 days of set-up the excess pore pressure was about 125 kPa. Testing was then started.

Static test gave peak friction of 46 kPa with residual value of 37 kPa. Undrained shear strength was interpreted to 110 kPa, giving alpha value of 0.42 and 0.34 for peak and residual respectively. Estimating the effective vertical pressure to 423 kPa results in a beta factor of 0.11 .

Cyclic tests which were started one day following the static test started with cyclic stress controlled tests with static tension bias of 30 kPa (65% of previous max. friction) and parcels of 100 cycles with specified cyclic stress amplitude increasing for consecutive parcels resulted in failure (abrupt pull-out of pile) in 23rd cycle of seventh parcel. The maximum friction at failure was measured to 50 kPa. Stroke controlled cyclic tests with two-way loading was then performed. Four parcels of 100 cycles with increasing cyclic displacements were performed. Maximum friction obtained was 45 kPa which reduced to 39 kPa in subsequent parcels. The residual friction during large slip was 32 kPa.

After three days of set-up a new static test with subsequent creep tests were performed. No serious creep occured for stress levels below about 90 % of the static capacity.

Upon 24 hours additional consolidation two relaxation tests were performed. Maximum reduction of mobilized friction was about 38% after 20 hours.

TEST 10, STRATUM III

CONSOLIDATION

The sample was prepared from the same material as used in Test 4. Water was added during the remoulding process to a water content of about 54% . Horizontal filters were placed in the oedometer to provide better vertical drainage.

A vertical pressure of 500 kPa was applied on top. As seen in Figure 2 the pore pressure at middle height had dropped down to about 9% of the consolidation stress after 22 days. At this time the sample was transferred to the pile chamber. Pocket penetrometer tests were performed on the side of the sample and on the top when trimmed in the pile chamber (level I-I) as shown in Figure 3. The shear strength, s_u, showed an average of about 80 kPa.

PILE INSTALLATION AND SET-UP

After pocket penetrometer tests the sample was mounted in the pile chamber and left to reconsolidate for 53 days under a vertical pressure of 300 kPa and radial pressure of 210 kPa (K=0.7). The long time for consolidation in the pile chamber before pile installation was due to machining and adjustments of a new model pile. This new pile was equipped with a commercial miniature pore pressure transducer mounted directly on the inside of the ceramic filter placed on the periphery of the pile wall. The total pressure cell was also modified slightly from the old model pile in an attempt to secure watertightness. The response of the pore and total pressure cells showed improved and satisfactory results during calibration tests.

As in Test 8 no back pressure was applied and vertical filter strips were placed on the outside perimeter of the clay sample with direct drainage on top and bottom of the pile chamber. Again good drainage was proved by formation of salt on the filter strips sticking out, which came from the expelled water from the marine clay.

During insertion of the pile the side friction was measured to about 30 kPa, the total normal pressure showed about 390 kPa and the pore pressure showed about 400 kPa directly after pile installation, and with no tendency to reduce with time. Due to this

unrealistically high pore pressure reading it was decided to pull the pile out and recheck the trancducer. Upon retrieval it was seen that the ceramic filter was cracked and rested directly on the inside membrane. The filter was replaced and the transducer rechecked and calibrated, and the pile then reinstalled. This process took two days with the confining pressures on the clay sample still intact. Directly after reinstallation the total pressure showed 340 kPa and the pore pressure 245 kPa. After two days of set-up the pore pressure had reduced to 125 kPa and the total pressure showed 315 kPa. At this time it was decided to start with the loading program.

STATIC TEST

A displacement controlled static test with deformation rate 1 mm per hour was now conducted, as shown in Figure 5. The pile was pulled in tension through failure and large slip and then pushed down to original position causing failure in compression and large slip (residual friction). A new cycle was then performed with the deformation rate increased to 10 mm per hour.

The displacement to cause failure, as shown in Figure 5, was about 0.3 mm or 1.2% of the pile diameter. A maximum friction of 46 kPa was achieved with a residual friction of 37 kPa. The shear strength of the clay at time of testing was estimated to 110 kPa which results in an alpha (α) value of 0.42 and 0.34 for peak and residual friction respectively.

For the effective stress approach, estimating σ'_{vo} from the relationship

$$s_u = 0.26 \cdot \sigma'_{vo}$$

which gives $\sigma'_{vo} =$ 423 kPa, the beta value (β) becomes 0.11 for maximum friction.

Total pressure on the pile wall at time of failure was about 305 kPa and the pore pressure showed 125 kPa, resulting in a horizontal effective pressure of 180 kPa. The interface friction angle (δ) can then be estimated to 14.3 degrees.

CYCLIC TESTS

After the static test the pile was left to reconsolidate for one day before cyclic testing

was started. During the static test the total pressure reduced to 300 kPa, but was now back at 325 kPa and the pore pressure showed 120 kPa.

Stress Controlled Tests (W310LC)

A stress controlled test comprised of applying a prescribed static tensile (uplift) stress on the pile, superimposed with parcels of 100 cycles with 10 seconds period and prescribed cyclic stress amplitude. The stress amplitude was then increased in the following parcels until failure (excessive uplift) occured in tension.

For this test the static tensile stress (bias) level was about 30 kPa, corresponding to 65% of the previous static capacity. In the first parcel the cyclic level was about 5.0 kPa and for the following parcels the cyclic stress level was incremented by 2.5 kPa as can be seen in Figure 6, showing skin friction (envelope of max. and min.) versus cycle numbers. In Figures 7,8,9 and 10 the resulting deformations and pressures due to the applied skin friction are plotted versus cycle numbers. In Appendix A selected cycle numbers are plotted as friction versus deflection, friction versus effective pressure and friction, pore pressure and total pressure variation during one cycle.

As seen in Figure 6 a total of seven parcels were performed. The first parcel did not produce any significant deformation of the pile as shown in Figure 7 and in Figure A-1, except that a drop in the static level caused by drift in the transducer caused the pile to move down accordingly. In the second parcel the average deformation shows a downward movement which was due to problems keeping the static bias constant. A small drift in the friction control causing a decrease in the static bias will therefore result in a downward movement of the pile from the original start position.

The friction deformation behaviour in parcel two, three, four and five, as shown in Figures A-2,3,4 and A-5 is linear with only minimal signs of hysteresis. Increasing the cyclic level in parcel six results in larger cyclic deformations and some hysteresis, with a small tendency of increasing average deformation. In the seventh parcel with a cyclic level of 20 kPa (maximum friction of 50 kPa) the pile is slowly pulled up for each cycle indicated by the increasing average deformation as seen in Figure 7. This is also depicted in Figure A-7 where the friction- deformation curve is slowly moving to the right. After 23 cycles the pile suddenly fails, by a sudden pull-out.The maximum friction was 50 kPa.

From the pressure diagrams in Figures 8,9 and 10 it is seen that the average pressures during the stress controlled cyclic testing stays fairly constant. The total normal pressure shows only small cyclic variations with an average of about 320 kPa, and the pore pressure shows about 125 kPa untill failure occured. The effective horizontal pressure on the pile wall therefore stays fairly constant at about 195 kPa. This is also depicted in the "effective stress" plots in Figures A-8 through A-11, where the internal friction angle at point of failure can be measured to 14.1 degrees.

Stroke Controlled Tests (W310SC)

After failure in the stress controlled test the pile was brought back to the original position and left to reconsolidate for two hours, at which time a series of stroke controlled tests were performed. A displacement controlled test comprised of applying parcels of 100 cycles with 10 seconds period in two-way cyclic loading from the zero position of the pile. A total of four consecutive parcels were performed with increasing displacement amplitude, starting with 0.25mm in the first parcel and with 0.4, 1.0 and 2.0mm in the following parcels.

The applied displacement versus cycle numbers are shown in Figure 11 with the resulting skin friction, total pressure, pore pressure and effective pressure versus cycle number shown in Figures 12, 13, 14 and 15 respectively. More detailed plots of selected cycles are shown in the Appendix B.

As seen from the resulting skin friction in Figure 12 and in Figure B-1 the two-way cycling of 0.25mm amplitude causes failure and residual value during large slip. The maximum friction in first cycle was 45 kPa which reduced to 37 kPa after 100 cycles. The residual value stabilized at about 32 kPa. In the second parcel the friction in first cycle showed 42 kPa reducing to about 37 kPa after 100 cycles and with residual of about 31 kPa. Similar results appears in parcel three with cyclic stroke amplitude of 1.0mm. In the last parcel with cyclic stroke amplitude of 2.0mm the peak friction shows about 39 kPa in first cycle with residual values during large slip of about 33 kPa. The maximum degradation of strength from maximum friction in first cycle to stable residual value during large slip is therefore 13 kPa or 28 %.

From the pressure diagrams in Figures 13,14 and 15 it is seen that some cyclic variation in both pore and total pressure is taking place in the two-way cycling. The total

pressure tends to increase in the beginning of the first parcel but the average pressure seems to stabilize after about 50 cycles and throughout the test at about 250 kPa. The pore pressure showed a much better response for this pile and indicated cyclic variations. As for the total pressure an increase is seen in the beginning of the first parcel and stabilized at about 165 kPa after about 50 cycles. In the second parcel a distinct decrease down to 140 kPa in the pore pressure results, and in the third parcel with stroke amplitude of 1.0mm the pressure went down to 120 kPa. Finally during the fourth parcel, with stroke amplitude of 2.0mm, the pore pressure decreased to a minimum of 98 kPa before increasing up to about 115 kPa after 80 cycles. The cyclic variation during testing was about 1 to 2 kPa for the pore pressure and about 7 to 10 kPa for the total pressure. The resulting effective pressure on the pile wall, Figure 15, shows a decrease in beginning of first parcel and an increase during subsequent testing, even though the maximum mobilized friction during this part had stabilized at a degraded level of about 40 kPa for the peak and 32 kPa during large slip.

From the "effective stress diagrams" in Figure B-5 the interface friction angle at failure in first cycle was about 19.5 degrees. A typical plot of the pressure variation during one cycle can be seen in Figure B-13 showing second cycle in fourth parcel. Maximum total pressure occurs at maximum cyclic displacement (right before reversal of load on the pile) whereas the pore pressure tends to show an increase when the pile is pulled up and a decrease when pushed down.

CREEP TEST

After the stroke controlled test the pile was left to rest for a period of three days before a static test was performed to make a reference for a series of creep tests. The results of the static test is shown in Figure 16, and gave maximum frction of 53 kPa with a residual during large slip of about 43 kPa.

The creep tests were performed as stress controlled tests where a prescribed tensile stress was applied to the pile and the displacement was then monitored for a period of 60 minutes, keeping the applied stress constant. As can be seen in Figure 17, no creep deformation was seen for the four first stress levels of 60,70,80, and 90% of the peak (ultimate) friction measured in the static test. Increasing the stress level to 95% of the static strength results in a creep deformation of about 0.01 mm after 60 minutes. At 100% of the previous static strength the pile is seen to come up very, very slowly and

has a displacement of about 0.03mm after 60 minutes. Increasing the stress level to 105% of the previous static capacity results in a steadily increasing deformation and sudden pullout after about 12 minutes.

As for Test 9 it must here be noted that some creep might have occured during the first load levels, but the amount of deformation encountered was close to the accuracy of the resolution of the measurement system used. In addition some degree of variation in the stress level applied was seen due to disturbance of the signals from the load sensors in the pile. Also, it might be argued about the length of time, 60 min. (increased from 16 min. in Test 9) for load application in order to give information of the critical load level with respect to creep deformation. However, the tests show that the applied stress on the pile must be very high (here, in the order of 95 %) with respect to the static strength in order to produce any significant creep deformation within the time span tested.

Upon failure of the pile during the creep test the total pressure dropped down to about 260 kPa and the pore pressure down to about 75 kPa. After one day of consolidation the pore pressure was back up at about 100 kPa and the total pressure at 280 kPa.

RELAXATION TESTS

After failure in the creep test the pile was brought back to original position and left to reconsolidate for a period of 24 hours. At this time two relaxation tests were started.

The relaxation tests were performed as stroke controlled tests, where the pile was pulled in tension to a prescribed friction level (a percentage of the peak friction in static test), and the deformation was then held constant while monitoring the friction with time. The results of this are shown in Figure 18. The pile was pulled to a tension of 37 kPa (70% of previous static capacity) and then deformation was held constant for 14 minutes. The loss in mobilized friction was then 7 kPa. The pile was then again pulled to a mobilized friction corresponding to the ultimate capacity and left overnight at this displacement. The friction loss after 20 hours was 20 kPa or about 38% of initial load.

After 20 hours a malfunction in the loading apparatus made the pile to be pushed

down causing failure in compression. The pile was the left at this displacement for eight additional hours and the friction had at this time reduced with about 30 kPa or 56%.

These relaxation tests show that the mobilized friction is dependent on pile displacement and that the mobilized friction will cease or reduce with time if the displacement is held constant. It also shows, however, that the friction loss is limited within the first 12 hours.

STRENGTH TESTS

After the last relaxation test the pile was pulled out of the pile chamber and the sample built out. Pocket penetrometer tests were performed on the side of the sample and in two horizontal layers with results shown in Figure 19.

Three standard triaxial test samples were then prepared from the center of the clay specimen and unconfined compression tests (UCT) were performed with the results shown in Figure 20.

In Figure 21 are shown the water content and interpreted undrained shear strength of the clay sample versus the distance from the center after completion of the pile test. The water content showed about 35 % with a tendency to decrease towards the center.

TABLE 1.

SAMPLE PROPERTIES TEST 10, STRATUM III

SAMPLE PREPARATION		CONSOLIDATION			END OF PILE TEST	
INITIAL WATER CONTENT	INITIAL HEIGHT	AXIAL DEFORMATION	AXIAL STRAIN	WATER CONTENT	WATER CONTENT	
w_i (%)	H_o (cm)	ΔH (cm)	ε (%)	w_e (%)	w_{ep} (%)	
54%	54.24	8.5	15.7	A 38.63 B 39.22 C 39.90	A-33.77 B-34.53 C-35.60	D-36.39 E-36.43 F-36.46

CONFINING PRESSURE		
AXIAL	KPa	500
RADIAL	KPa	350
BACK PRESSURE	KPa	0
SAMPLE CONSOLIDATION		
IN OEDOMETER	Days	22
IN PILE CHAMBER	Days	53
INTERPRETED SHEAR STRENGTH		
END OF CONSOLIDATION	KPa	80
END OF PILE TEST	KPa	110

Fig.1

CONSOLIDATION DIAGRAM								Test No. 10 Stratum III		Start date	
H_i 54.24 cm		H_e 45.74 cm		$\Delta\varepsilon_v$ 15.7 %						σ_c 500 kPa	
Time h	18	26	42	114	138	164	187	210	307	384	525
Δh cm	1.13	1.57	2.56	5.99	6.38	6.76	7.11	7.39	7.95	8.24	8.5
u kPa	53.2	78.3	139.2	298	269	242	227	202	131	97	48.6

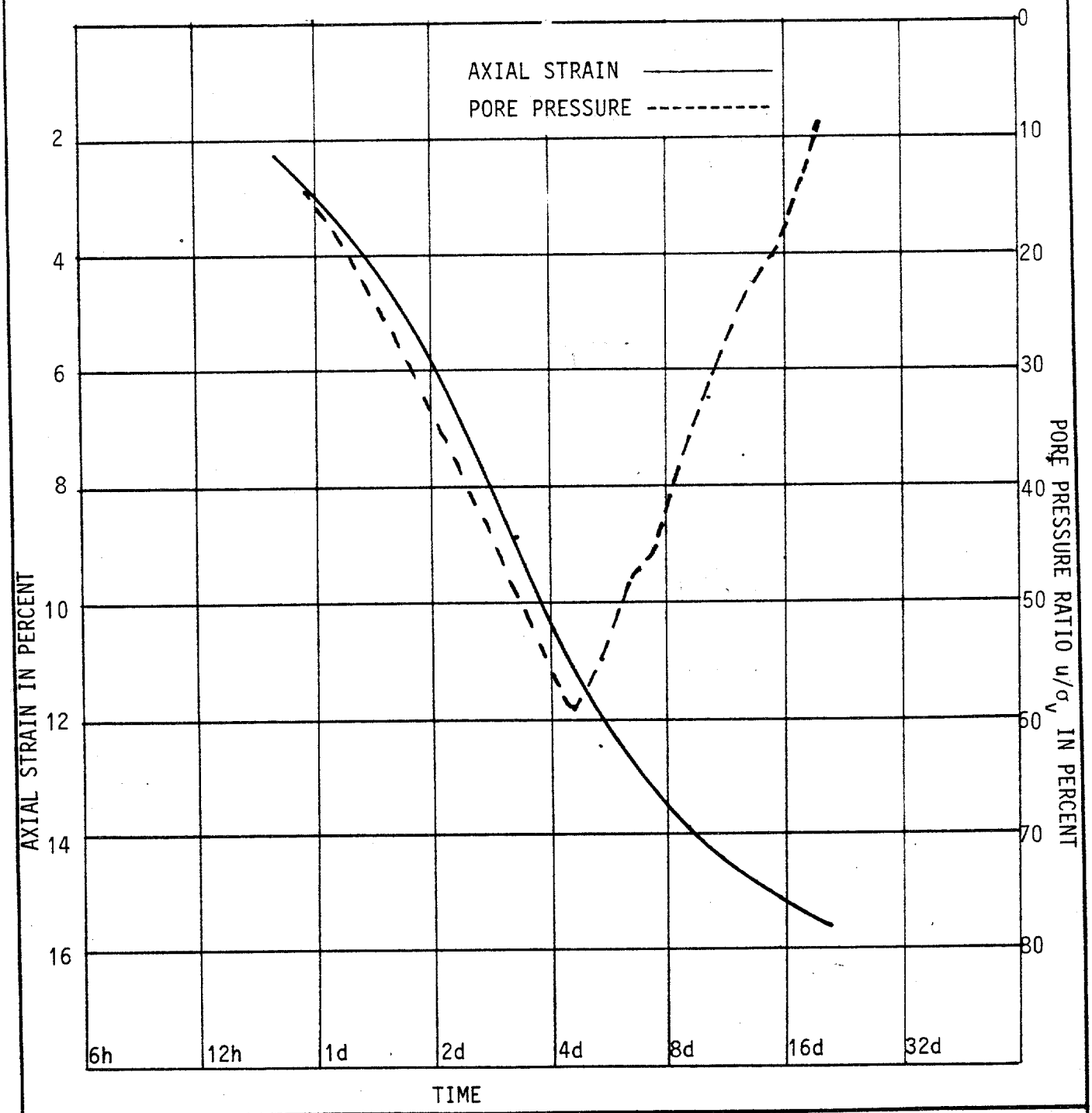

CNRD 13-2 TENSION PILE STUDY LABORATORY MODEL PILE TESTS

TEST 10, STRATUM III, Consolidation diagrams for clay sample

Scale

DET NORSKE VERITAS
Geotechnical Laboratory

Drawn by

Date

Approved

Fig. No. 2

TEST 10, STRATUM III

SHEAR STRENGTH (kPa) FROM POCKET PENETROMETER TESTS AFTER CONSOLIDATION

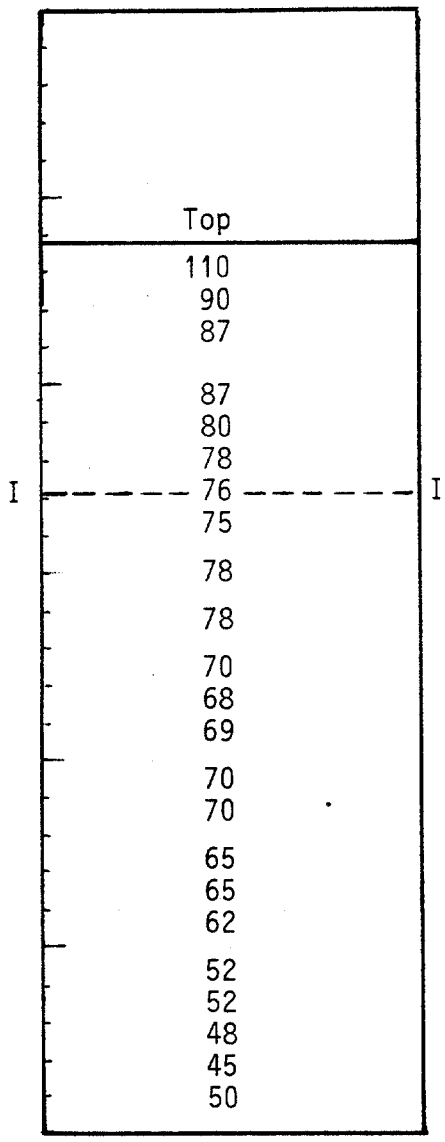

Scale 1:4

Level I-I

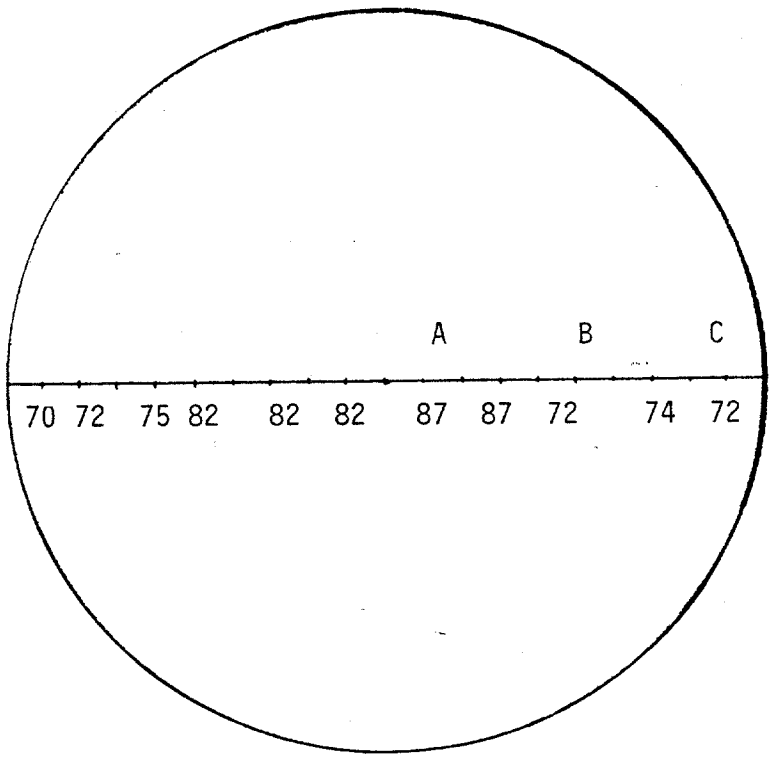

Scale: 1:2

CNRD 13-2 TENSION PILE STUDY LABORATORY MODEL PILE TESTS

TEST 10, STRATUM III, Pocket penetrometer tests after consolid.		Scale
DET NORSKE VERITAS Geotechnical Laboratory	Drawn by	Date
	Approved	Fig.No. 3

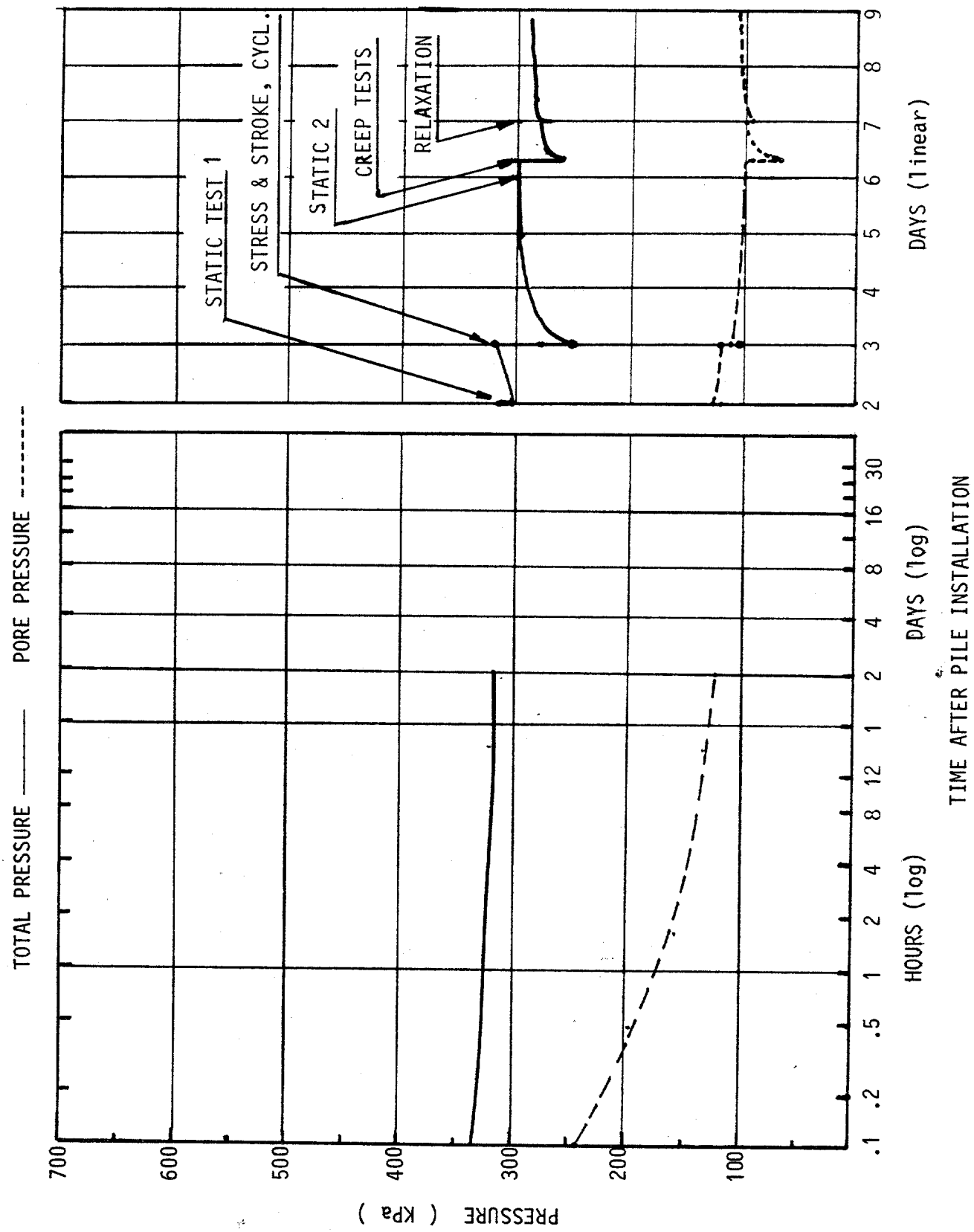

CNRD 13-2 TENSION PILE STUDY LABORATORY MODEL PILE TESTS

TEST 10, STRATUM III, Pressures at pile wall after installation

DET NORSKE VERITAS
Geotechnical Laboratory

Scale	
Drawn by	Date
Approved	Fig. No. 4

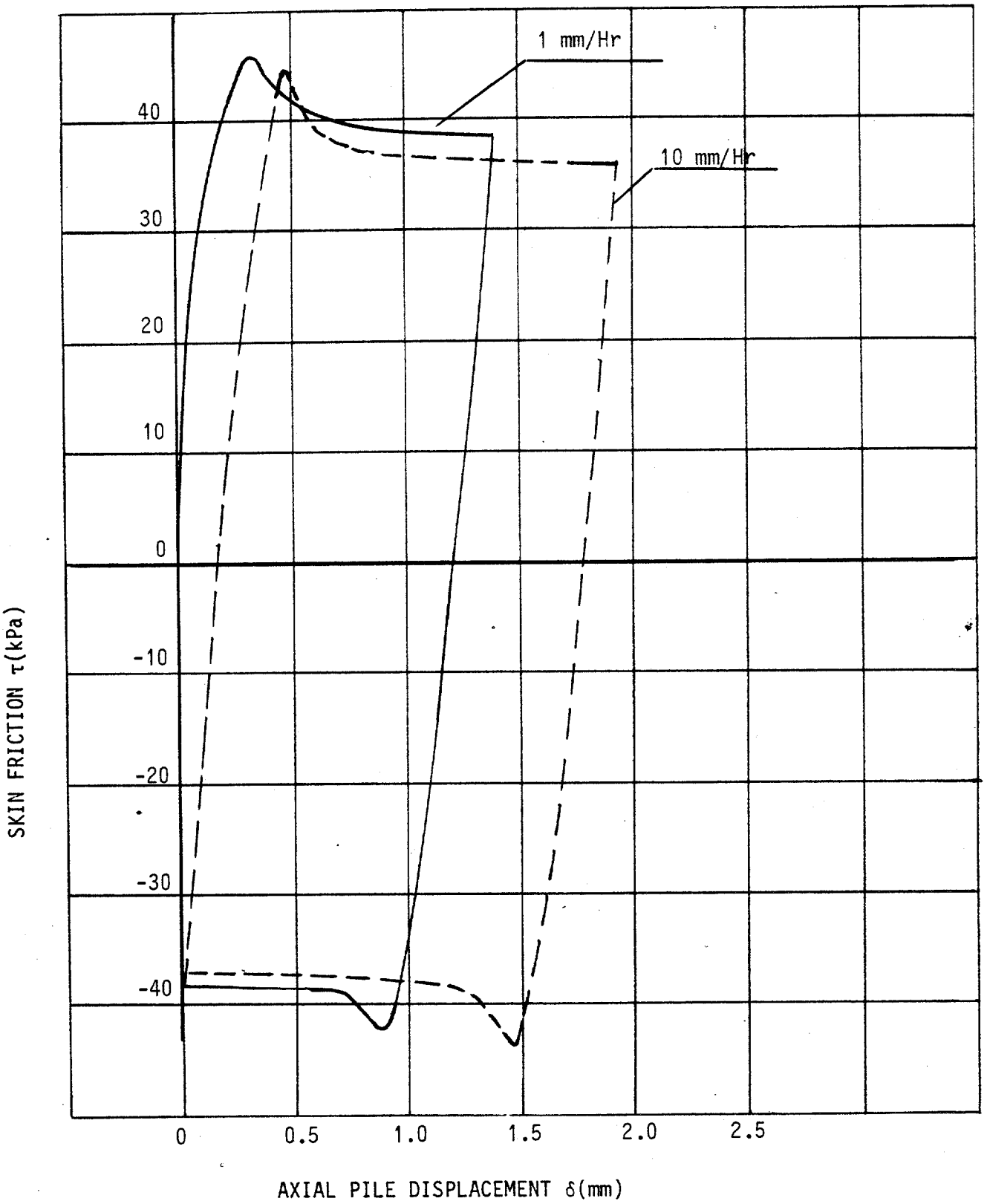

CNRD 13-2 TENSION PILE STUDY LABORATORY MODEL PILE TESTS

TEST 10, STRATUM II, STATIC TEST 1

DET NORSKE VERITAS Geotechnical Laboratory	Drawn by	Scale
	Approved	Date
		Fig. No. 5

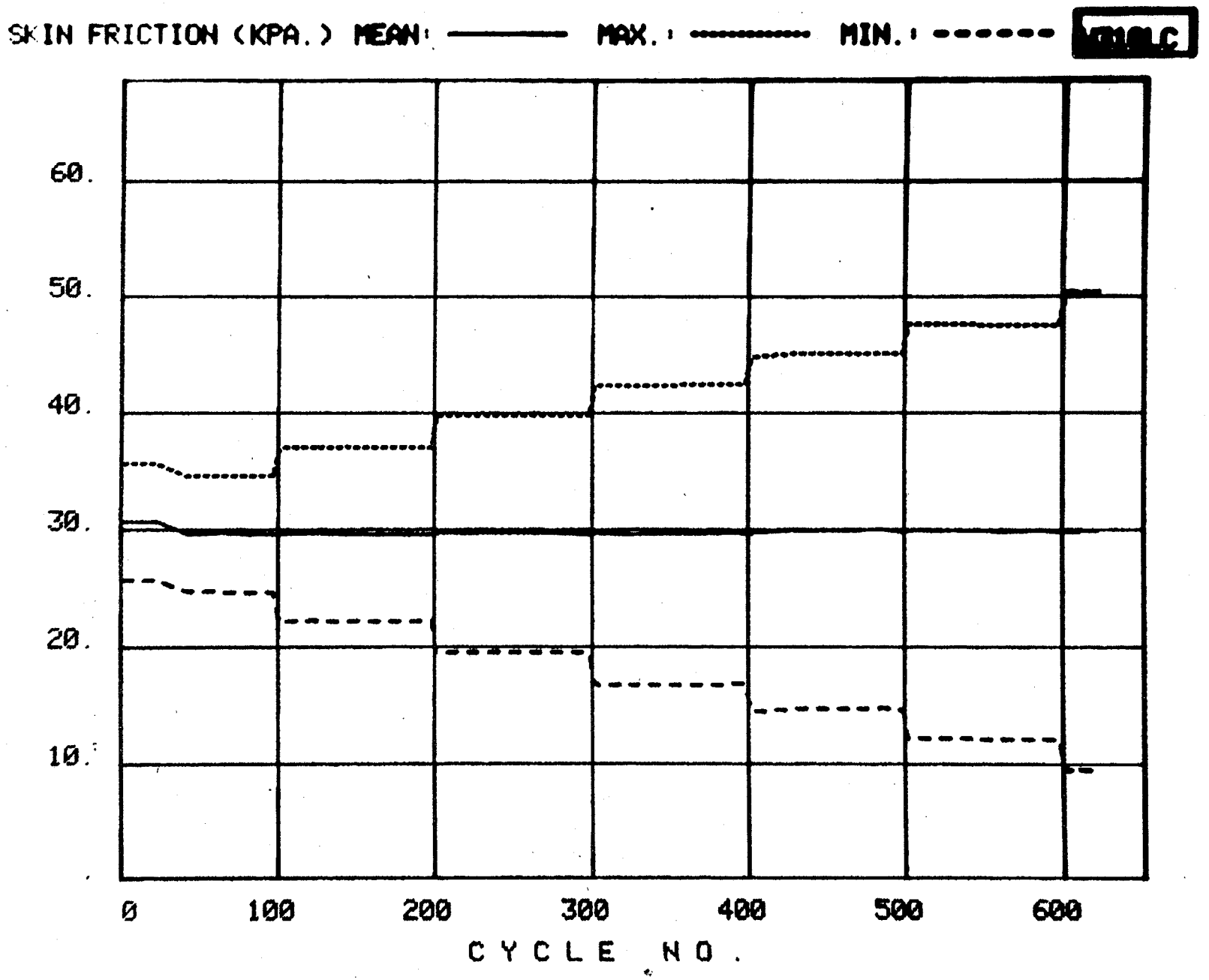
SKIN FRICTION (KPA.) MEAN: MAX.: MIN.:
60.
50.
40.
30.
20.
10.
0
100
200
300
400
500
600
CYCLE NO.

Fig.6

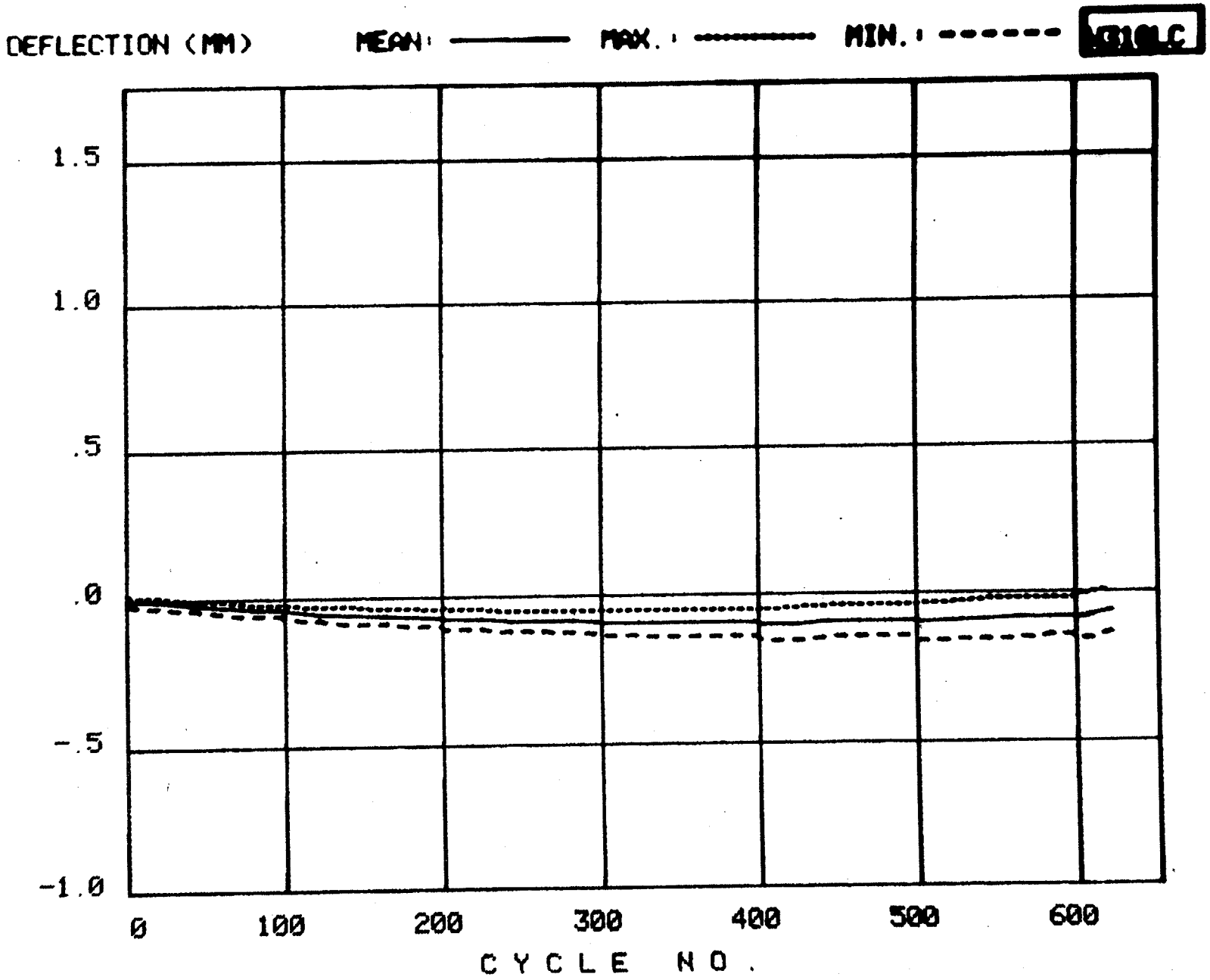
DEFLECTION (MM)
MEAN:
MAX.:
MIN.:
1.5
1.0
.5
.0
-.5
-1.0
0
100
200
300
400
500
600
CYCLE NO.

Fig.7

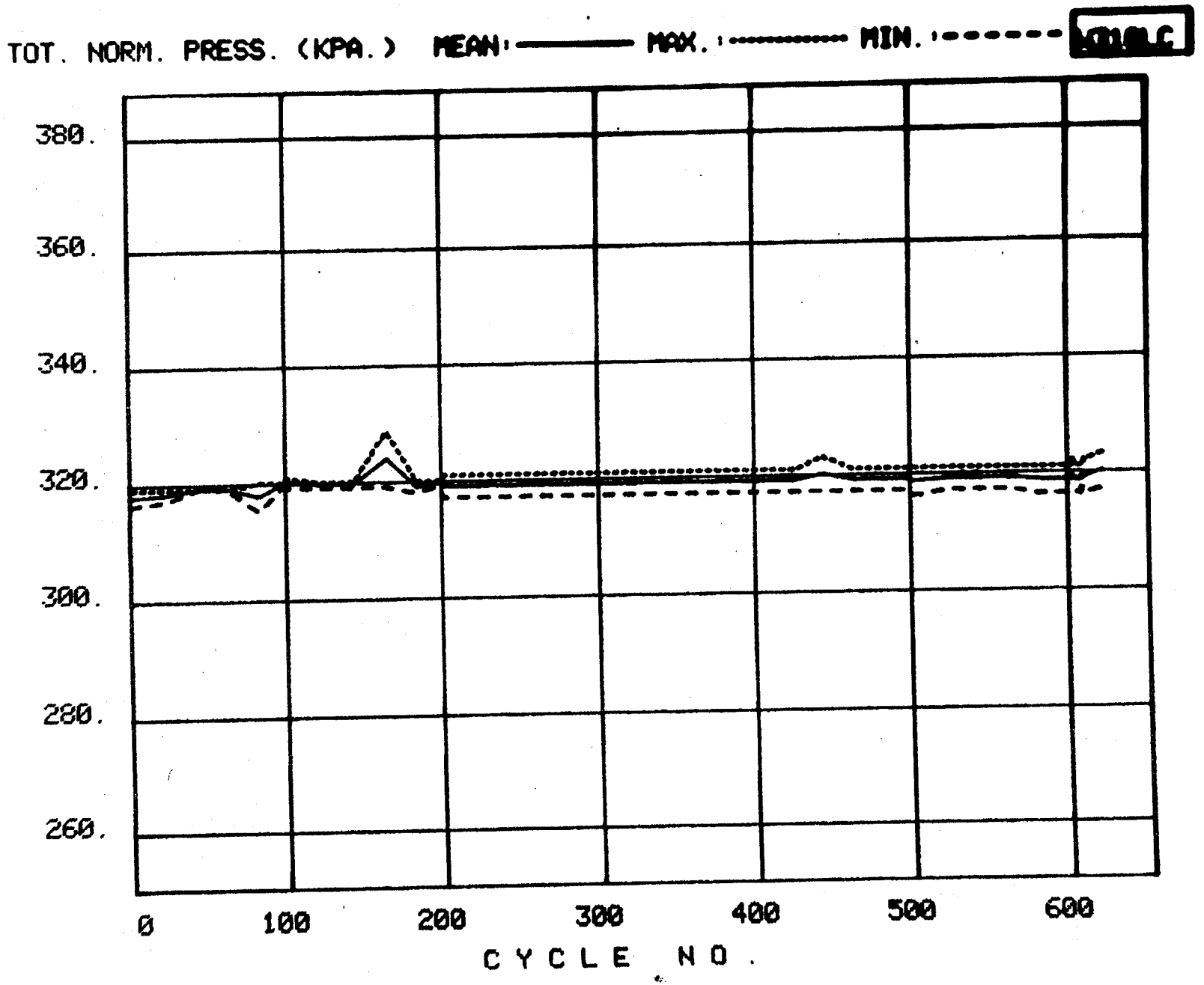
TOT. NORM. PRESS. (KPA.)
MEAN:
MAX.:
MIN.:
380.
360.
340.
320.
300.
280.
260.
0
100
200
300
400
500
600
CYCLE NO.

Fig.3

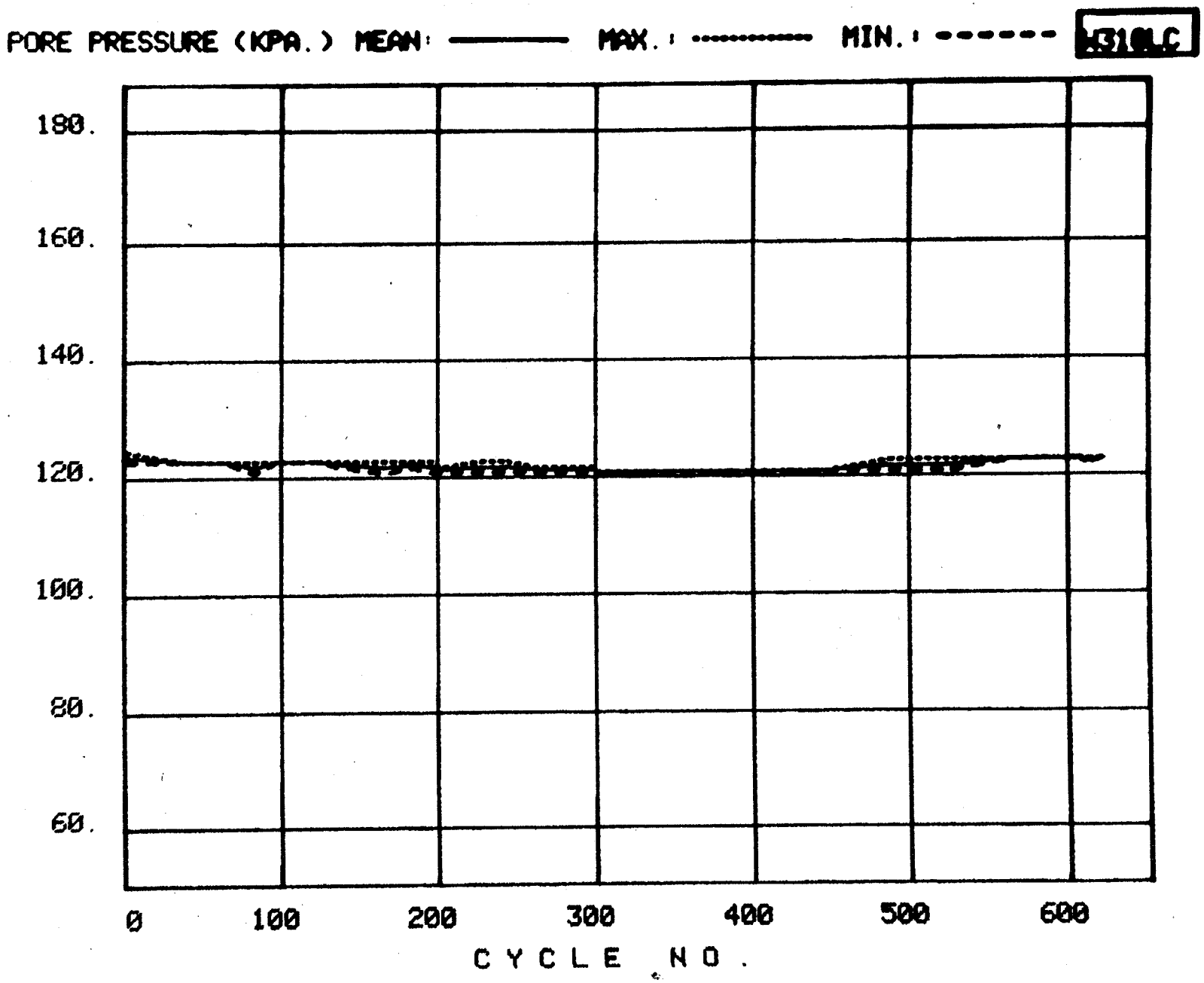
PORE PRESSURE (KPA.) MEAN: MAX.: MIN.:
180.
160.
140.
120.
100.
80.
60.
0
100
200
300
400
500
600
CYCLE NO.

Fig.9

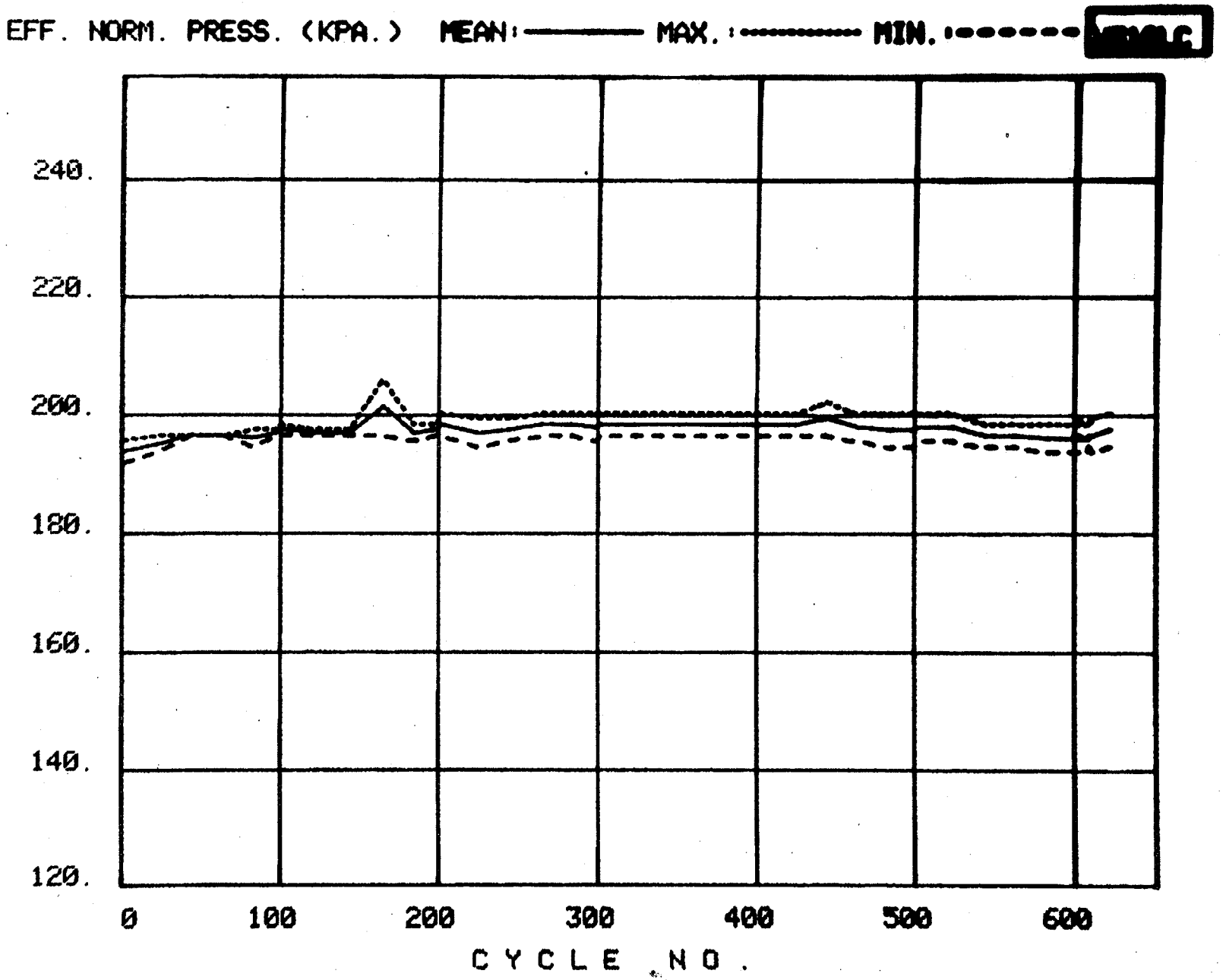
EFF. NORM. PRESS. (KPA.)
MEAN:
MAX.:
MIN.:
240.
220.
200.
180.
160.
140.
120.
0
100
200
300
400
500
600
CYCLE NO.

Fig.10

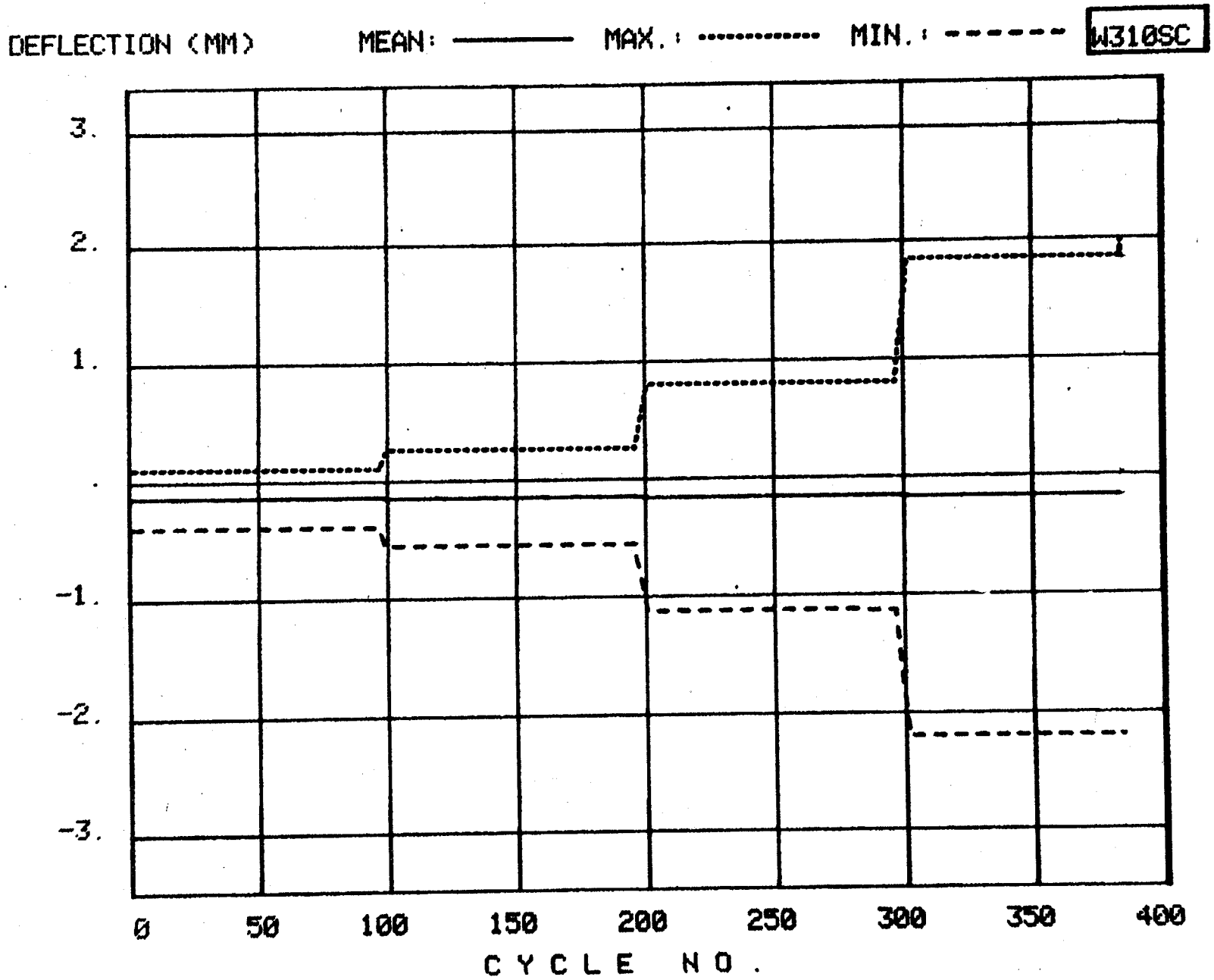
DEFLECTION (MM)
MEAN:
MAX.:
MIN.:
W310SC
3.
2.
1.
-1.
-2.
-3.
0
50
100
150
200
250
300
350
400
CYCLE NO.

Fig.11

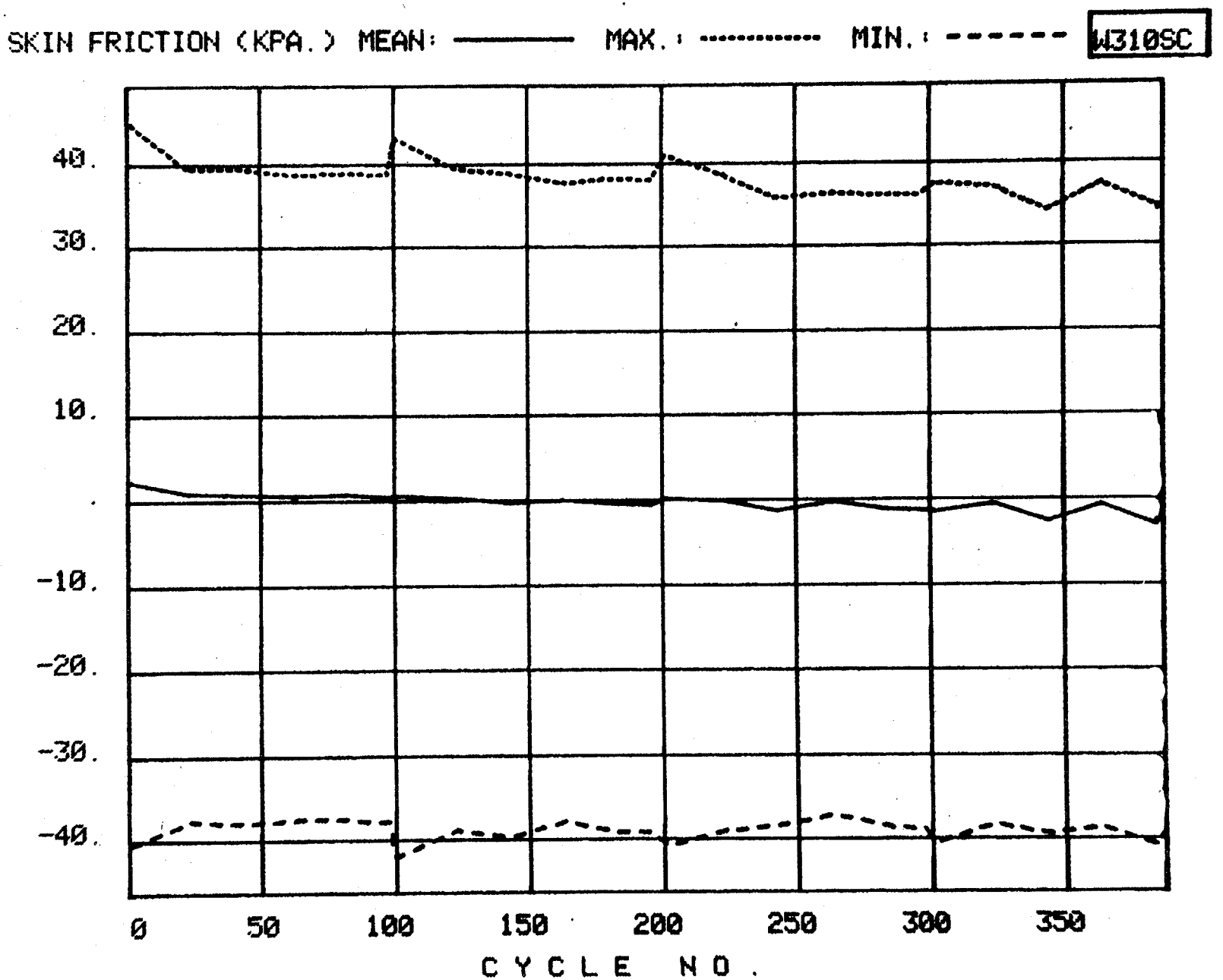
SKIN FRICTION (KPA.) MEAN: MAX.: MIN.:
W310SC
40.
30.
20.
10.
-10.
-20.
-30.
-40.
0
50
100
150
200
250
300
350
CYCLE NO.

Fig.12

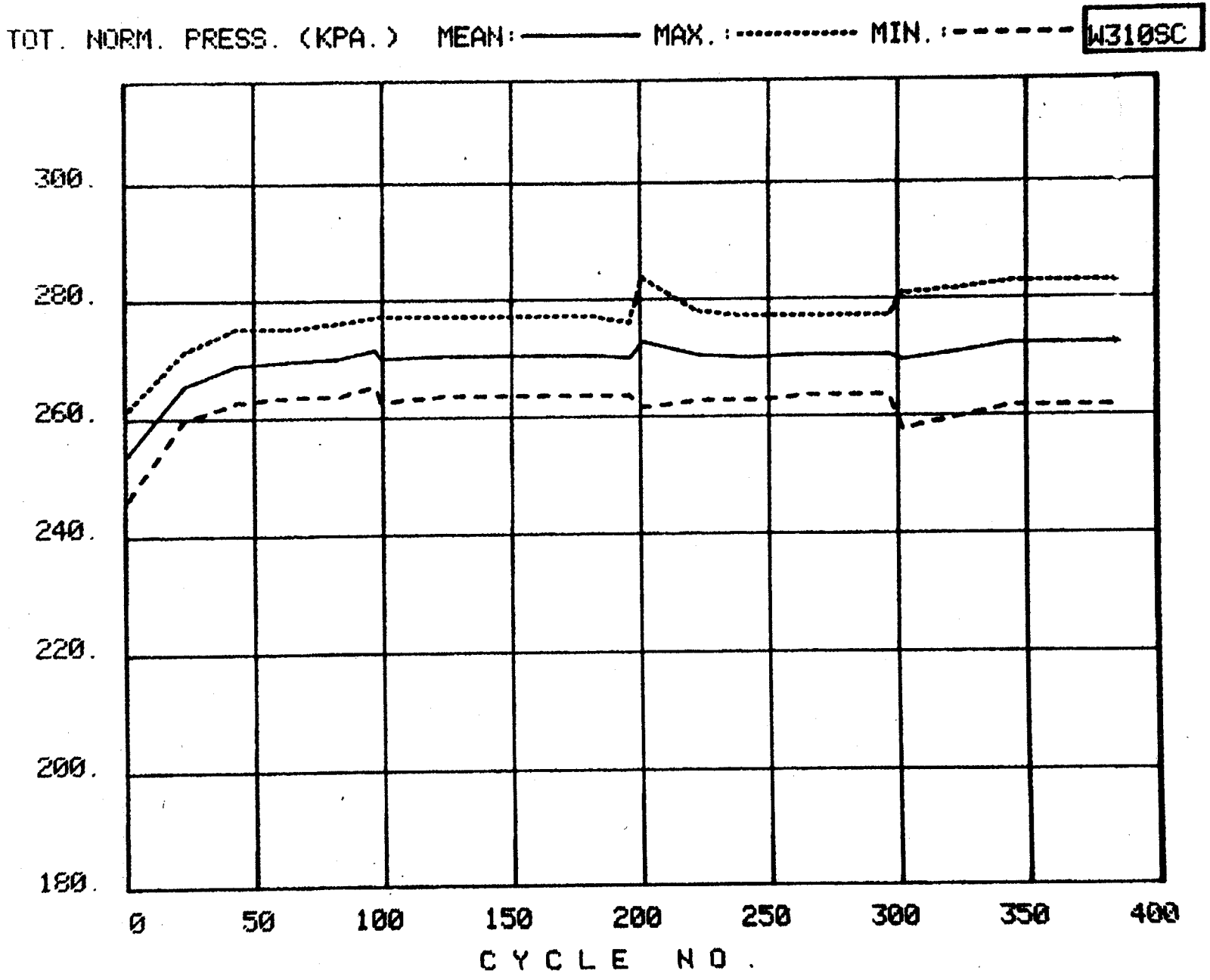
TOT. NORM. PRESS. (KPA.)
MEAN:
MAX.:
MIN.:
W310SC
300.
280.
260.
240.
220.
200.
180.
0
50
100
150
200
250
300
350
400
CYCLE NO.

Fig.13

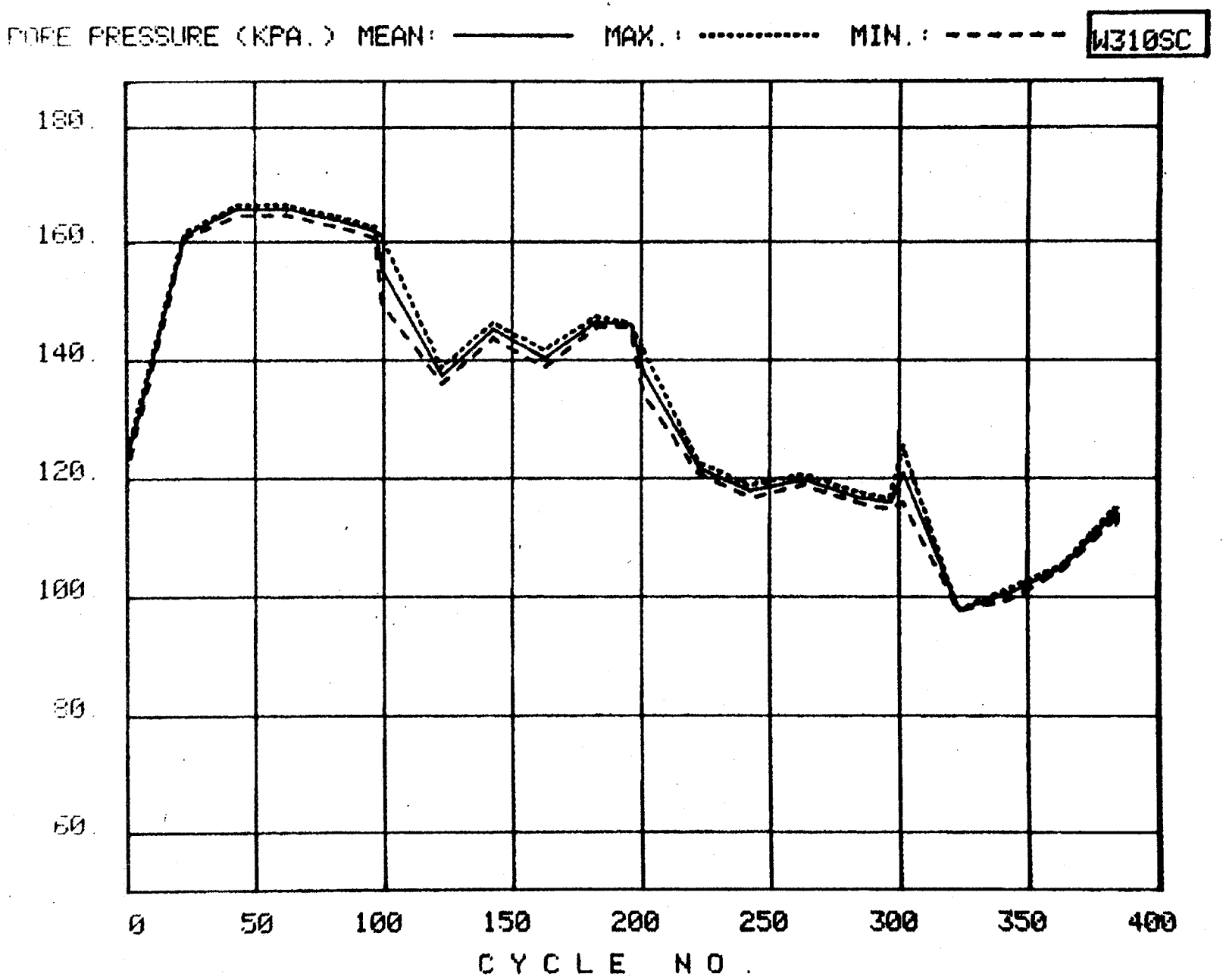
PORE PRESSURE (KPA.) MEAN: MAX.: MIN.:
W310SC
180.
160.
140.
120.
100
80.
60.
0
50
100
150
200
250
300
350
400
CYCLE NO.

Fig.14

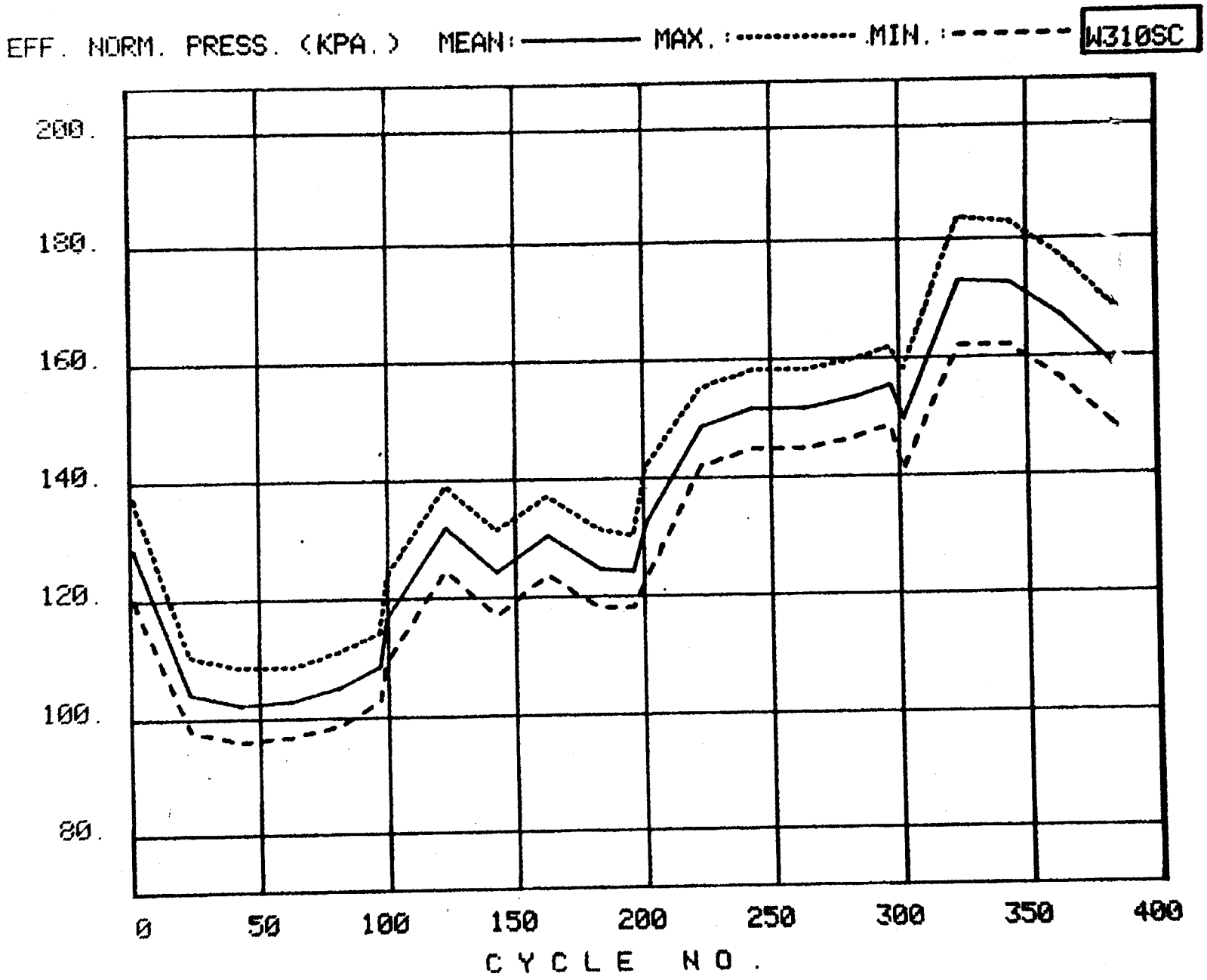
EFF. NORM. PRESS. (KPA.) MEAN: MAX.: MIN.:
W310SC
200.
180.
160.
140.
120.
100.
80.
0
50
100
150
200
250
300
350
400
CYCLE NO.

Fig.15

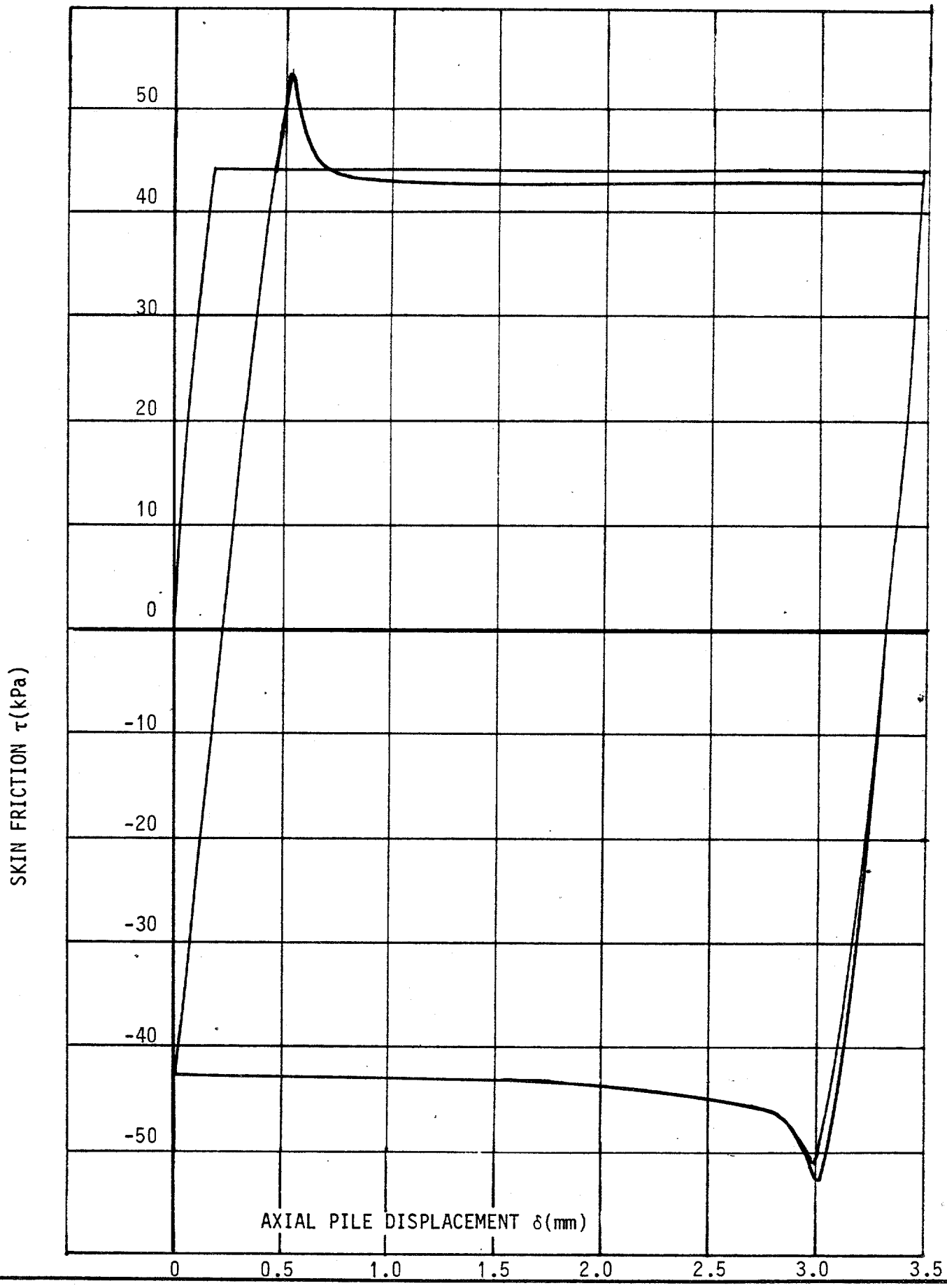

CNRD 13-2 TENSION PILE STUDY LABORATORY MODEL PILE TESTS

TEST 10, STRATUM III, STATIC TEST 2

Scale

DET NORSKE VERITAS
Geotechnical Laboratory

Drawn by

Date

Approved

Fig. No. 16

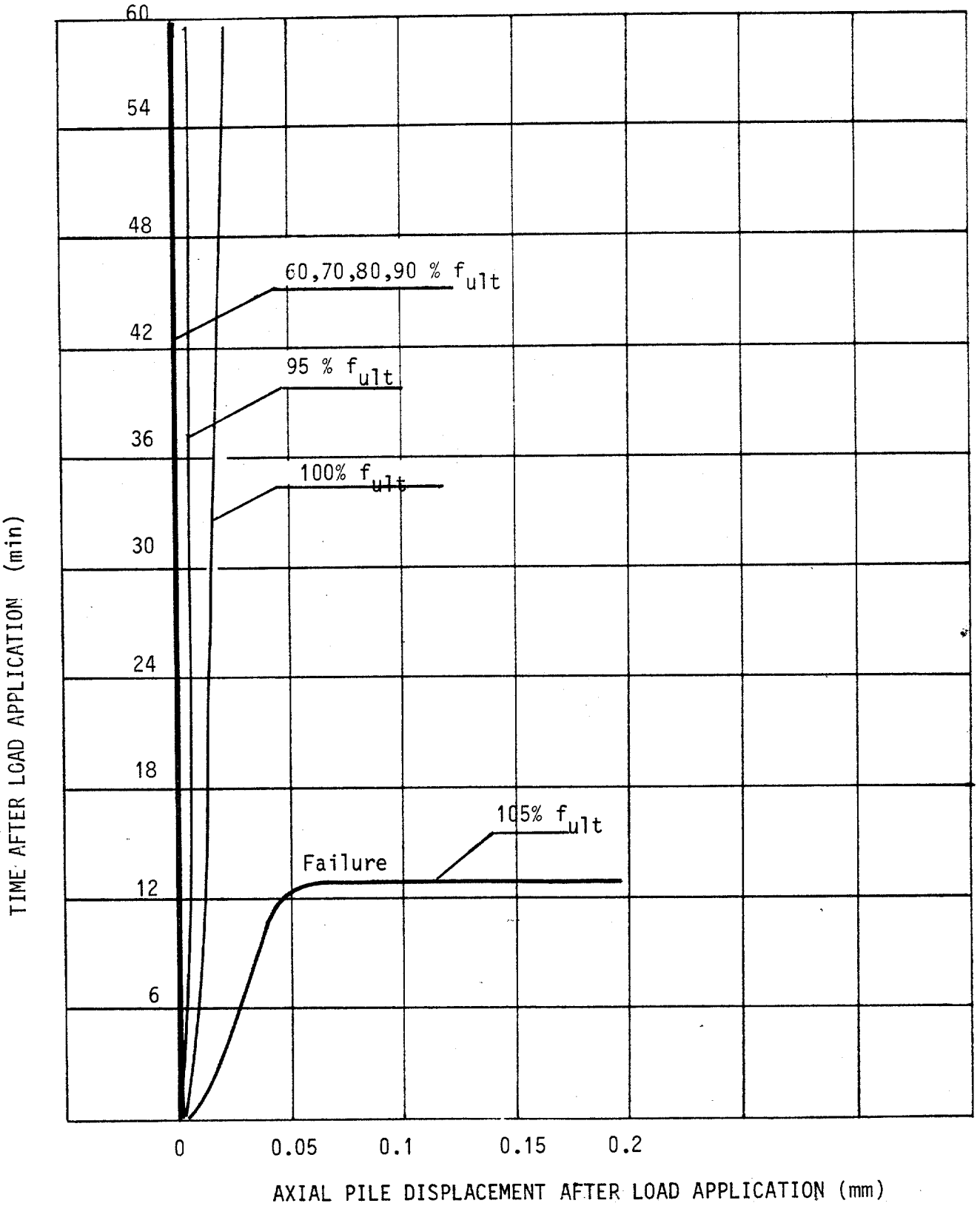

CNRD 13-2 TENSION PILE STUDY LABORATORY MODEL PILE TESTS

TEST 10, STRATUM III, CREEP TESTS

DET NORSKE VERITAS Geotechnical Laboratory	Drawn by	Scale
	Approved	Date
		Fig. No. 17

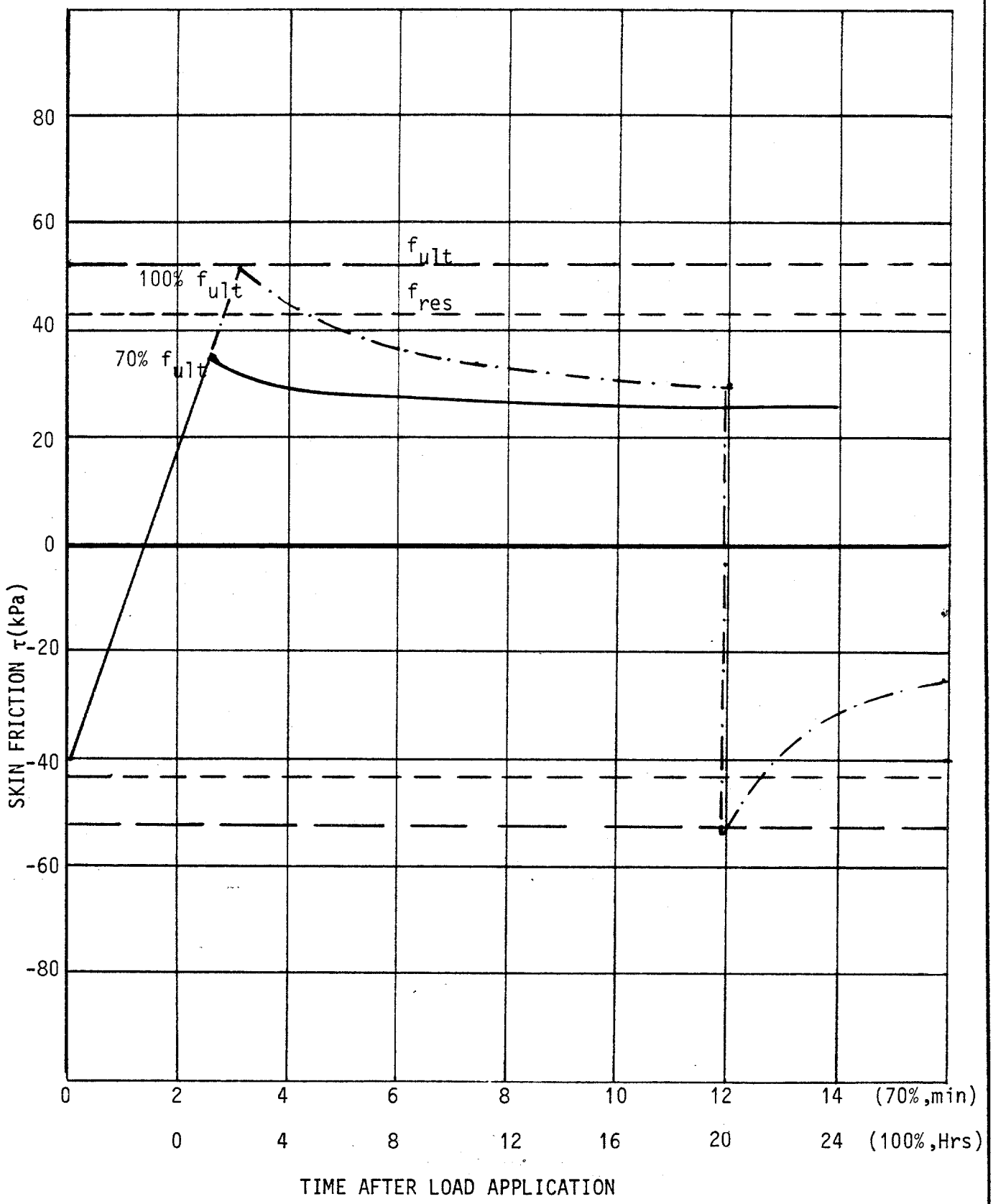

CNRD 13-2 TENSION PILE STUDY LABORATORY MODEL PILE TESTS

TEST 10, STRATUM III, RELAXATION TESTS

DET NORSKE VERITAS Geotechnical Laboratory	Drawn by	Scale
	Approved	Date
		Fig. No. 18

TEST 10, STRATUM III

SHEAR STRENGTH (kPa) FROM POCKET PENETROMETER TESTS AFTER PILE TEST

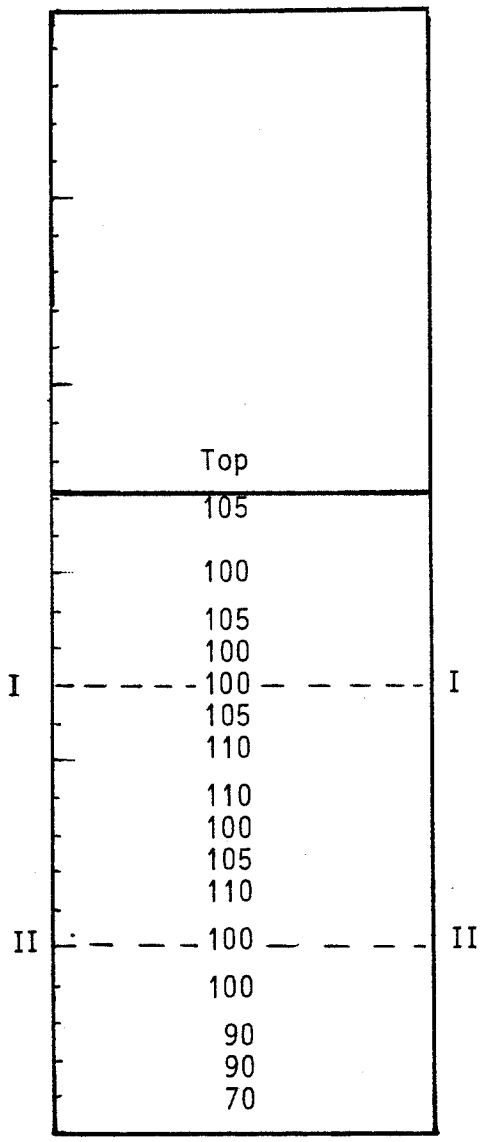

Scale 1:4

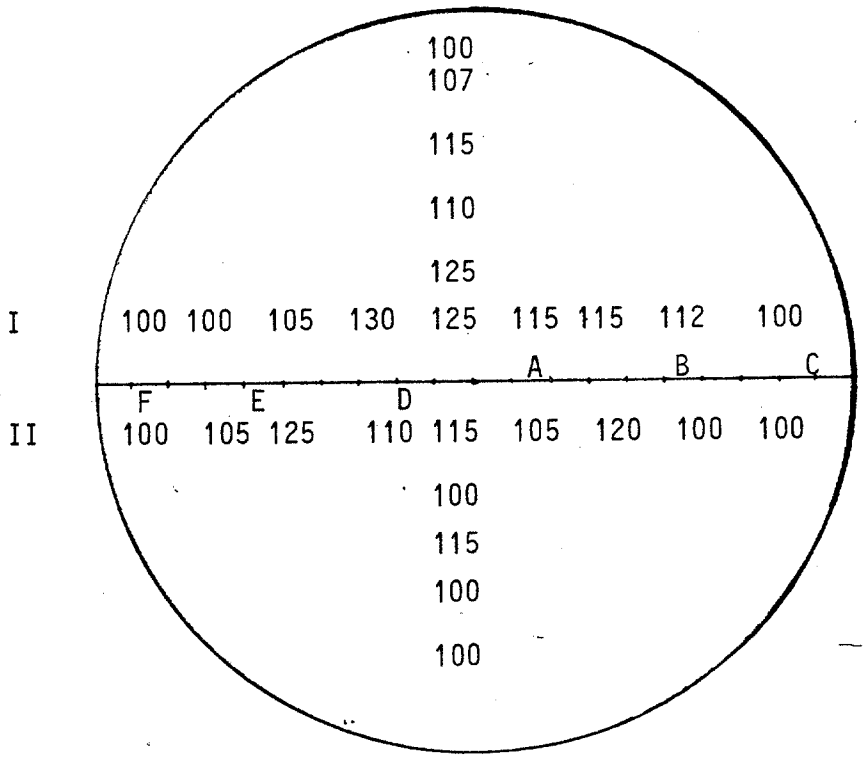

Scale: 1:2

CNRD 13-2 TENSION PILE STUDY LABORATORY MODEL PILE TESTS

TEST 10, STRATUM III, Pocket penetrometer tests after pile test		Scale
DET NORSKE VERITAS Geotechnical Laboratory	Drawn by	Date
	Approved	Fig. No. 19

Unconfined Compression Test
on material after Pile Test
completed

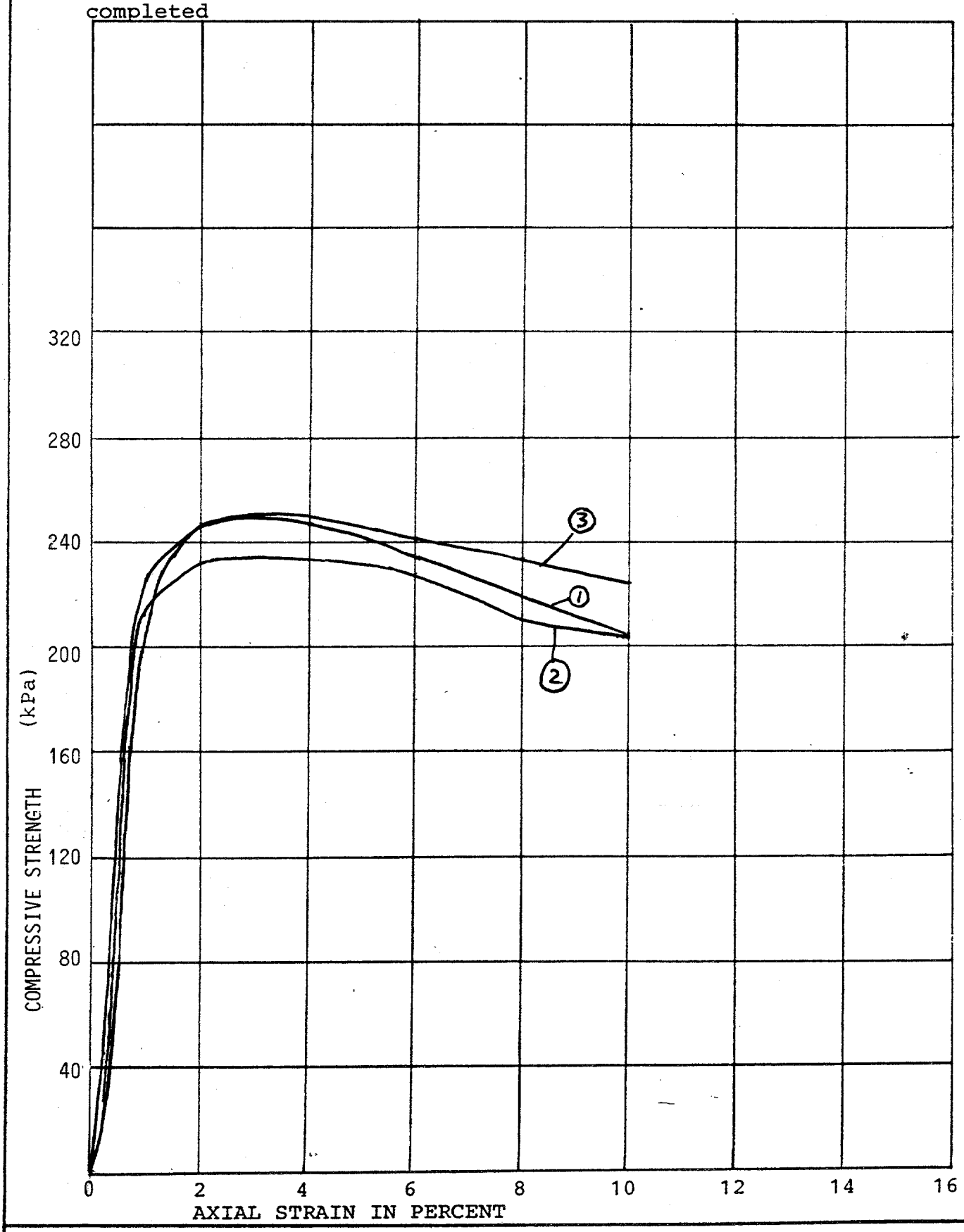

CNRD 13-2 TENSION PILE STUDY LABORATORY MODEL PILE TESTS

TEST 10, STRATUM III, Unconfined compression tests after test

DET NORSKE VERITAS Geotechnical Laboratory	Drawn by	Scale
	Approved	Date
		Fig. No. 20

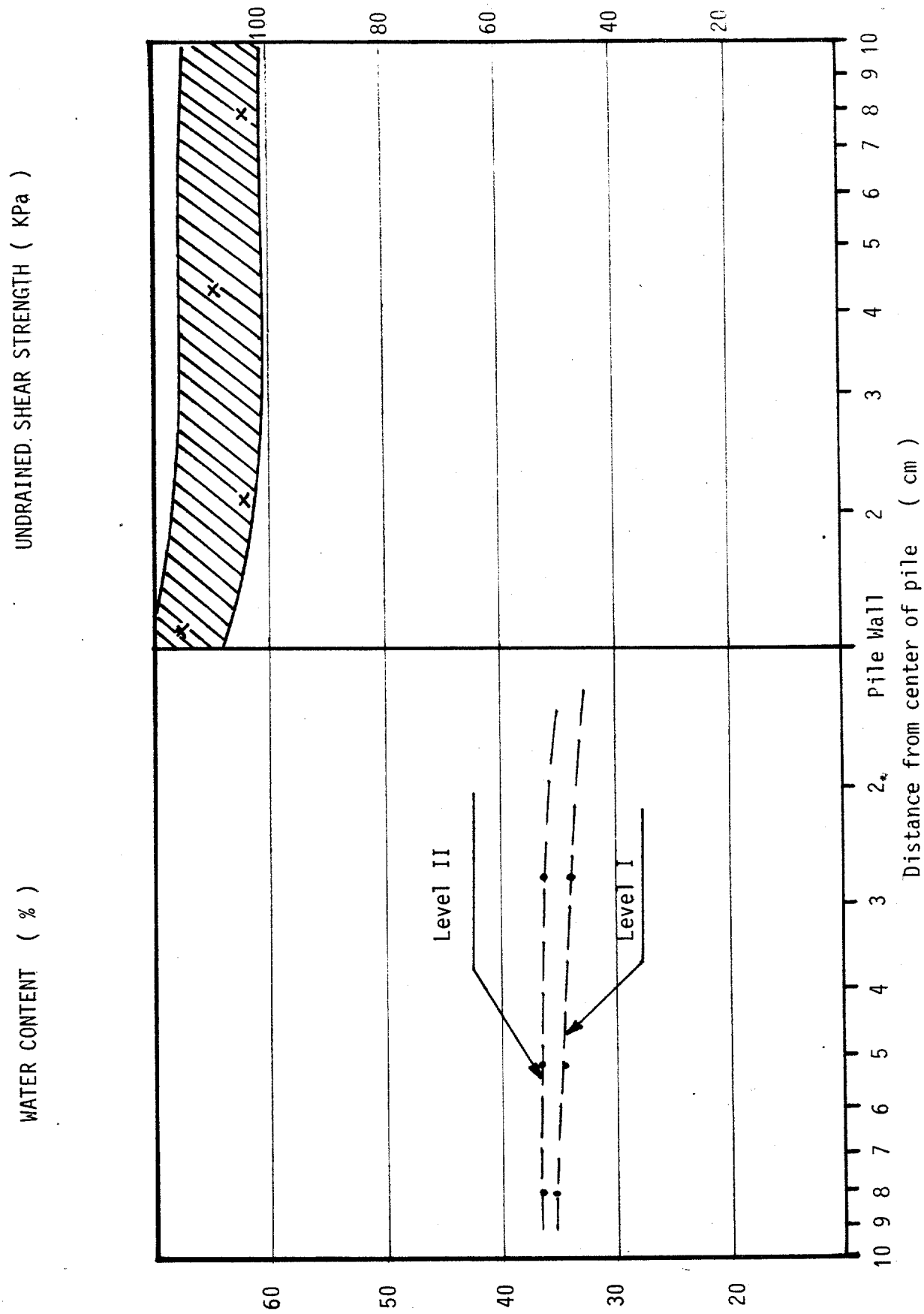

CNRD 13-2 TENSION PILE STUDY LABORATORY MODEL PILE TESTS

TEST 10, STRATUM III, Water content and shear strength after test

DET NORSKE VERITAS Geotechnical Laboratory	Drawn by	Scale
	Approved	Date
		Fig.No. 21

Appendix GA

Plotted Results from W310LC

Figures GA-1 through GA-7

Skin Friction vs Deflection, Selected Cycles

Figures GA-8 through GA-11

Skin Friction vs Eff. Normal Pressure, Selected Cycl.

Figures GA-12 through GA-18

Skin Friction, Pore and Total Pressure, Selected Cycles

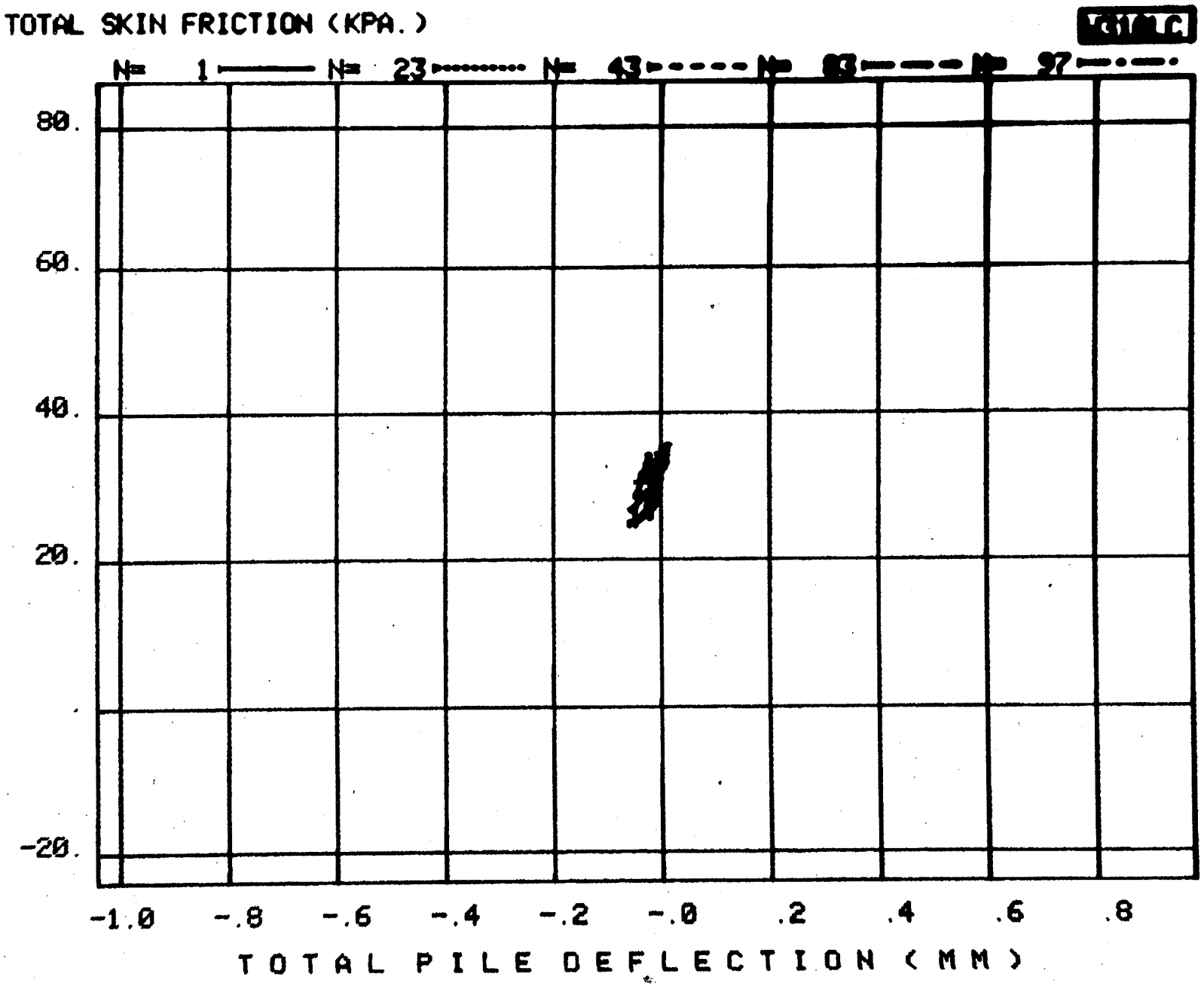
TOTAL SKIN FRICTION (KPA.)
N= 1
N= 23
N= 43
N= 97
80.
60.
40.
20.
-20.
-1.0
-.8
-.6
-.4
-.2
-.0
.2
.4
.6
.8
TOTAL PILE DEFLECTION (MM)

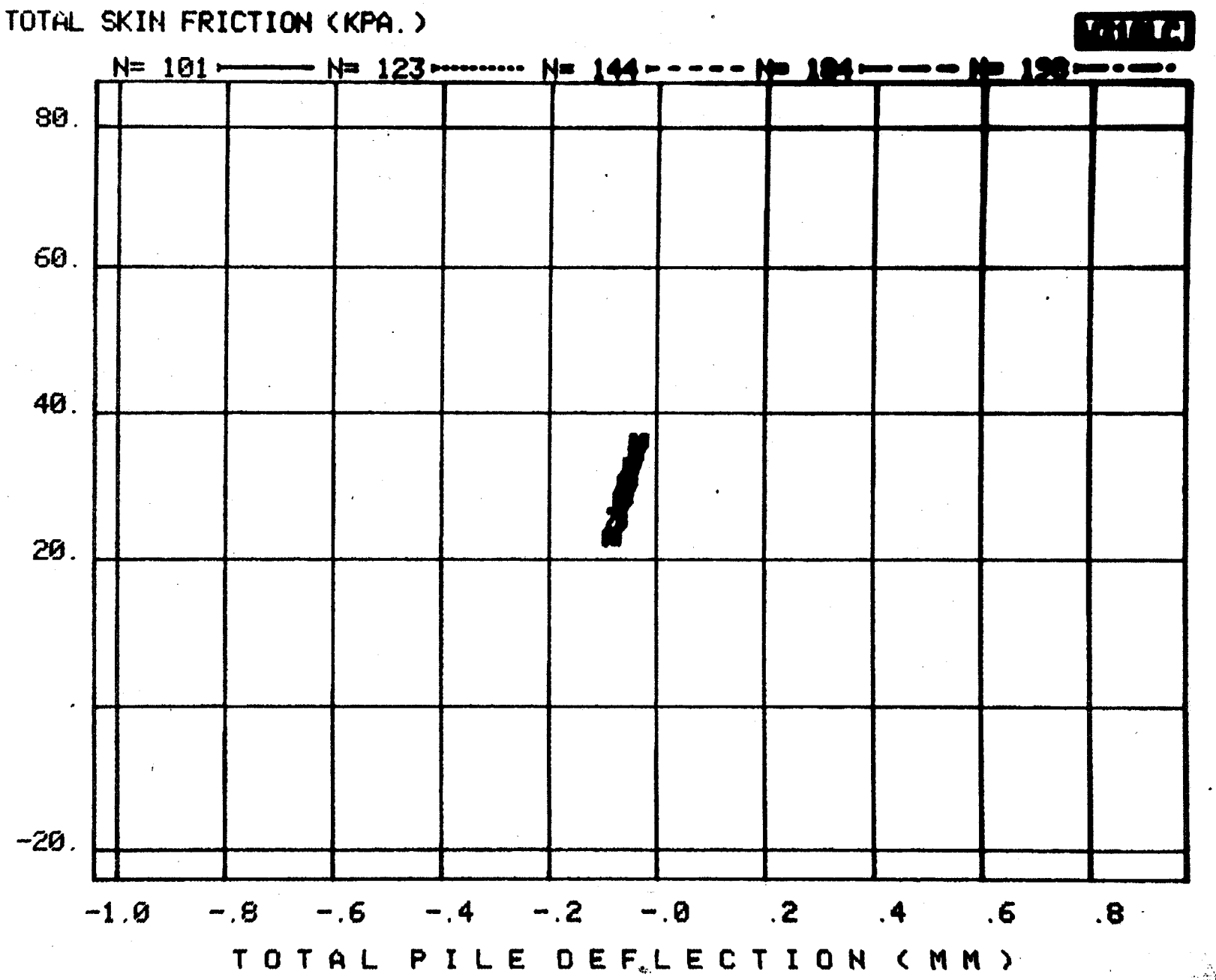
TOTAL SKIN FRICTION (KPA.)
N= 101
N= 123
N= 144
80.
60.
40.
20.
-20.
-1.0
-.8
-.6
-.4
-.2
-.0
.2
.4
.6
.8
TOTAL PILE DEFLECTION (MM)

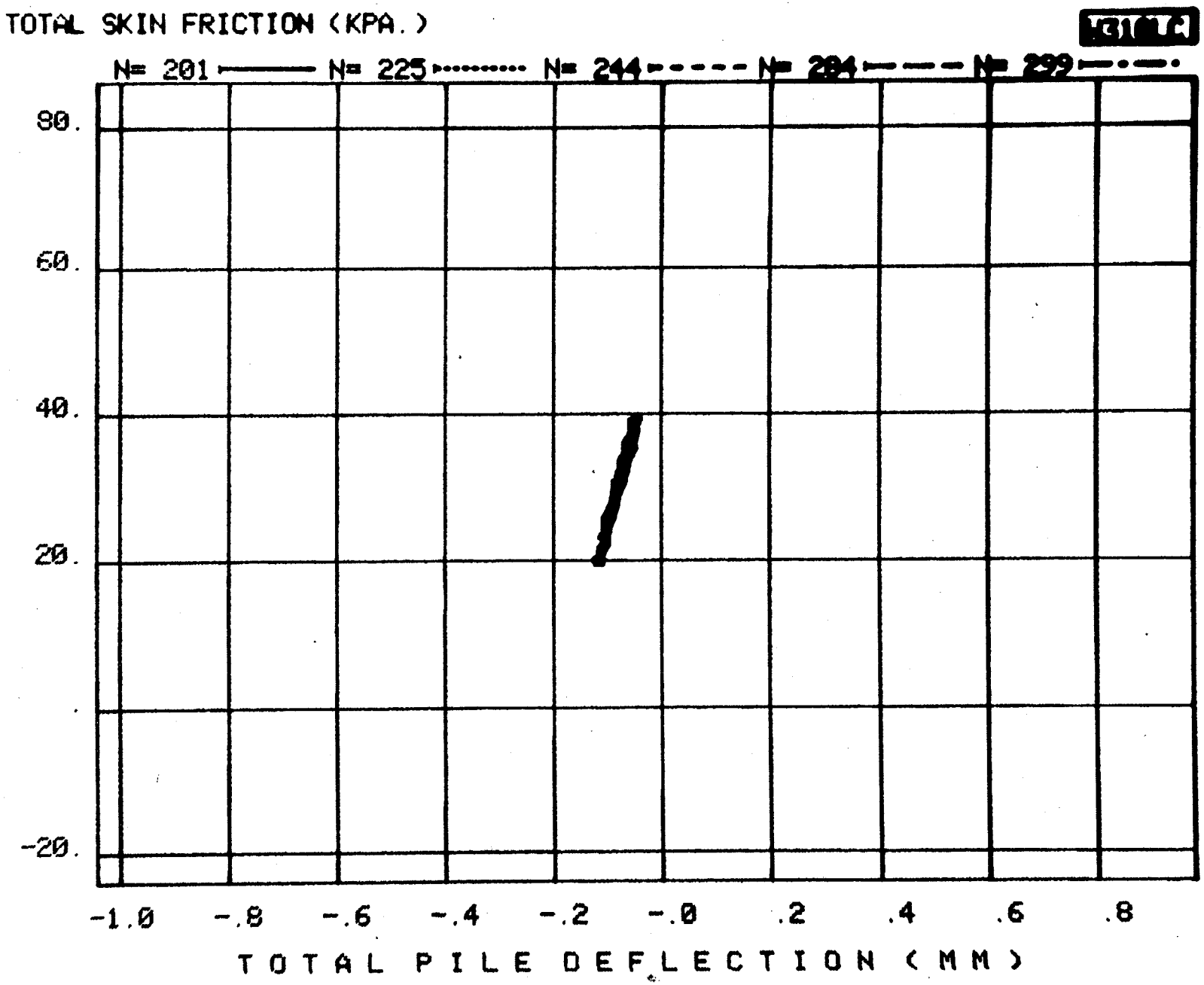
TOTAL SKIN FRICTION (KPA.)
N= 201
N= 225
N= 244
N= 284
N= 299
80.
60.
40.
20.
-20.
-1.0
-.8
-.6
-.4
-.2
-.0
.2
.4
.6
.8
TOTAL PILE DEFLECTION (MM)

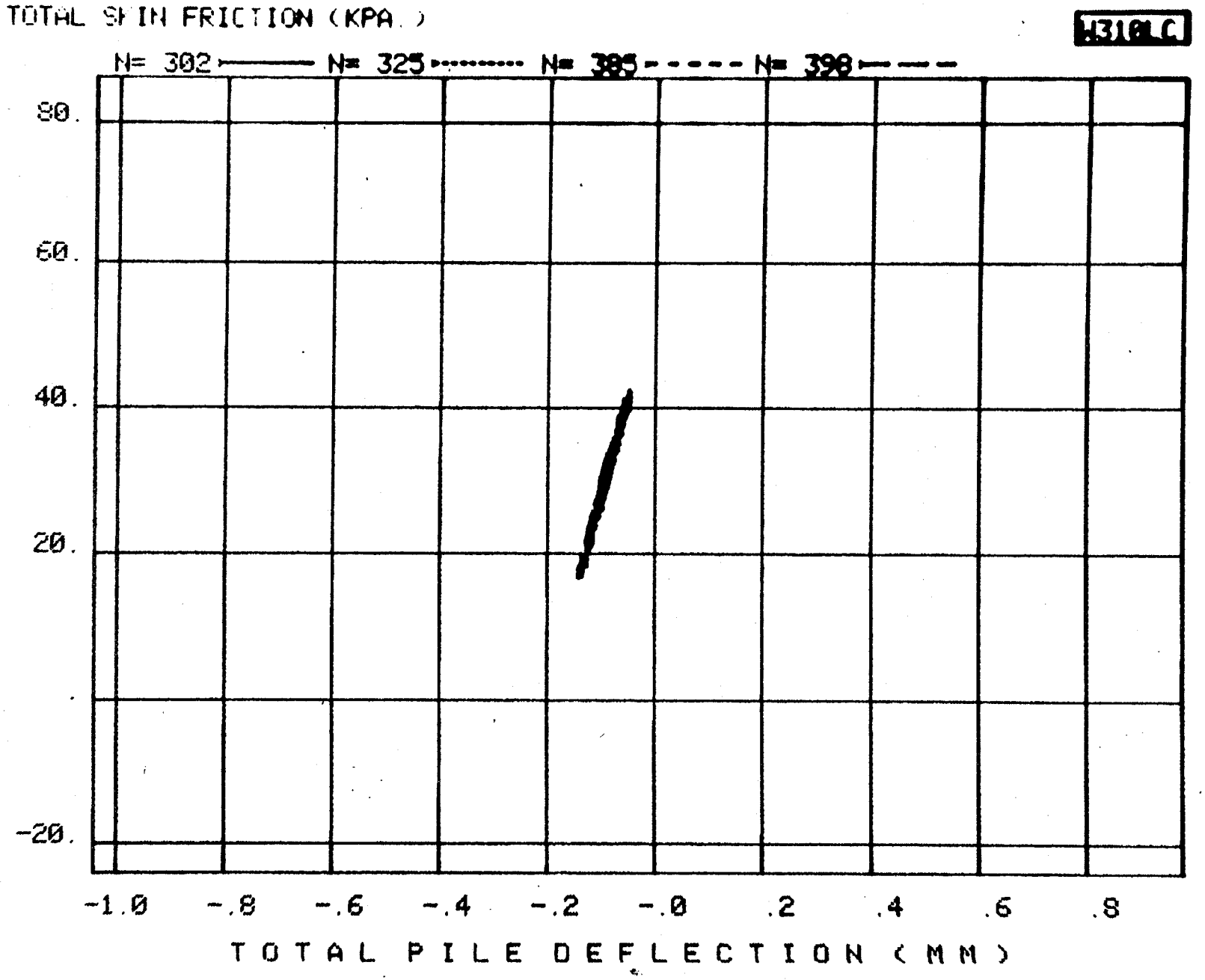
TOTAL SKIN FRICTION (KPA.)
W310LC
N= 302
N= 325
N= 385
N= 398
80.
60.
40.
20.
-20.
-1.0
-.8
-.6
-.4
-.2
-.0
.2
.4
.6
.8
TOTAL PILE DEFLECTION (MM)

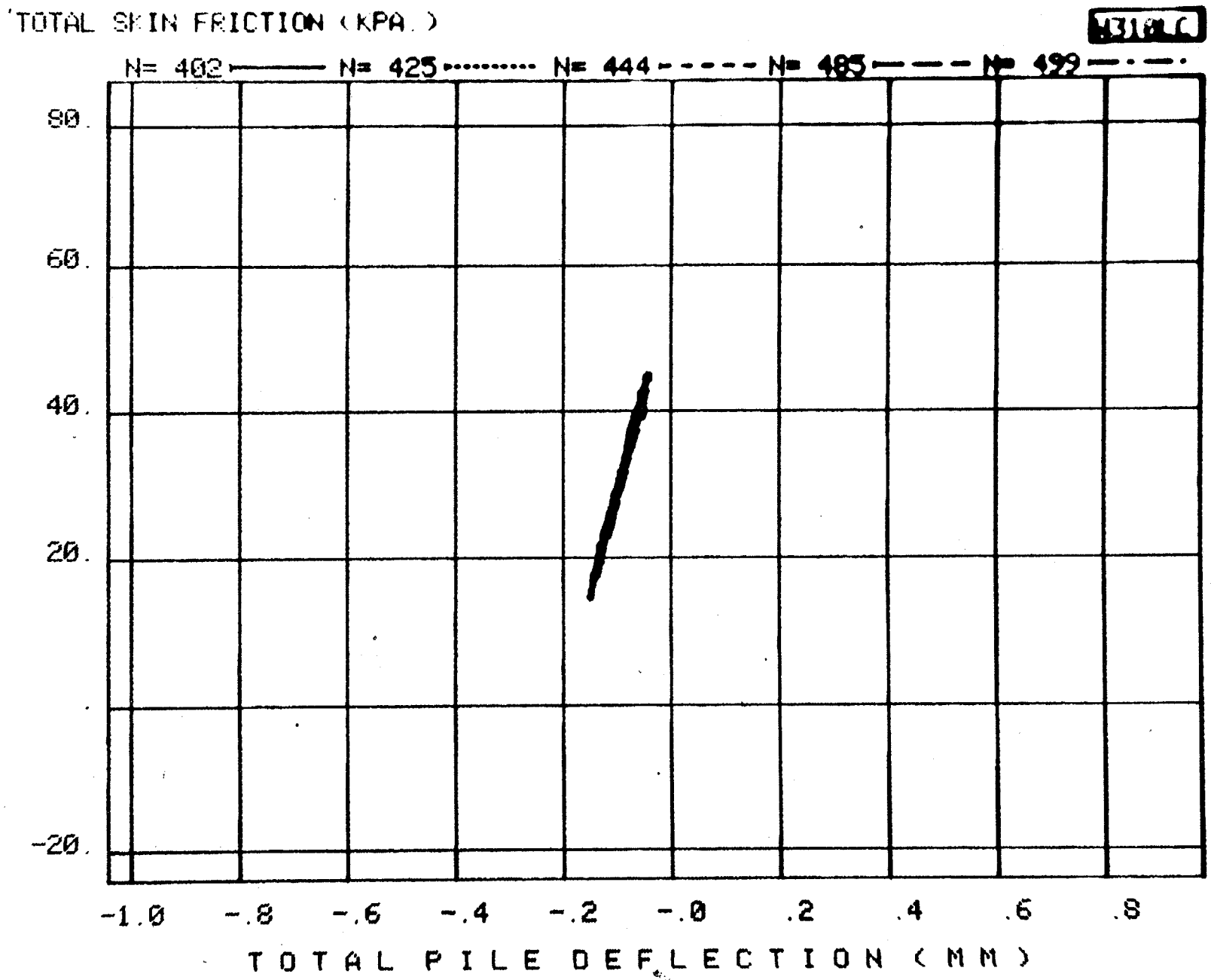
TOTAL SKIN FRICTION (KPA.)
N= 402
N= 425
N= 444
N= 485
N= 499
80.
60.
40.
20.
-20.
-1.0
-.8
-.6
-.4
-.2
-.0
.2
.4
.6
.8
TOTAL PILE DEFLECTION (MM)

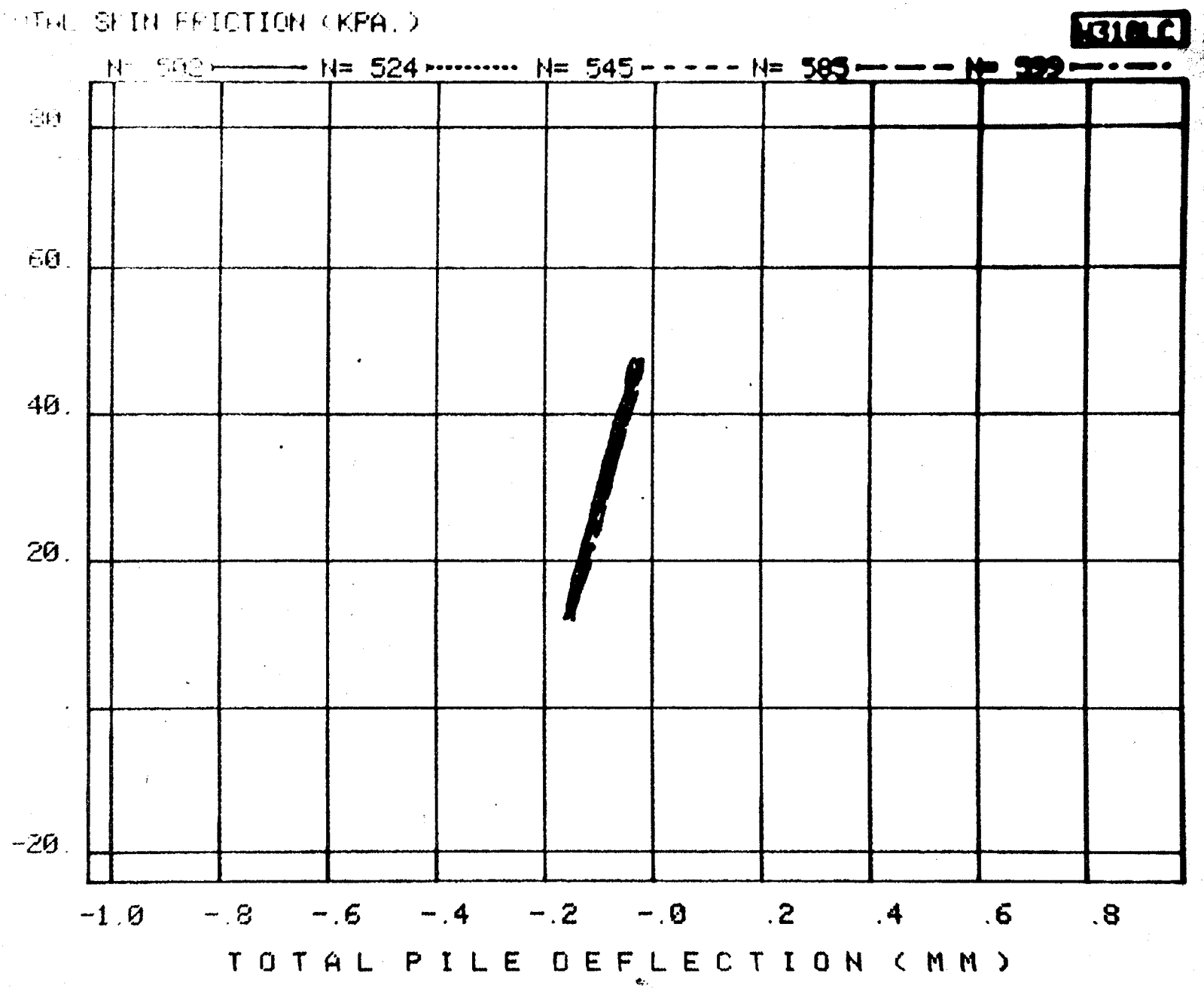
TOTAL SKIN FRICTION (KPA.)
N= 524
N= 545
N= 585
80
60.
40.
20.
-20.
-1.0
-.8
-.6
-.4
-.2
-.0
.2
.4
.6
.8
TOTAL PILE DEFLECTION (MM)

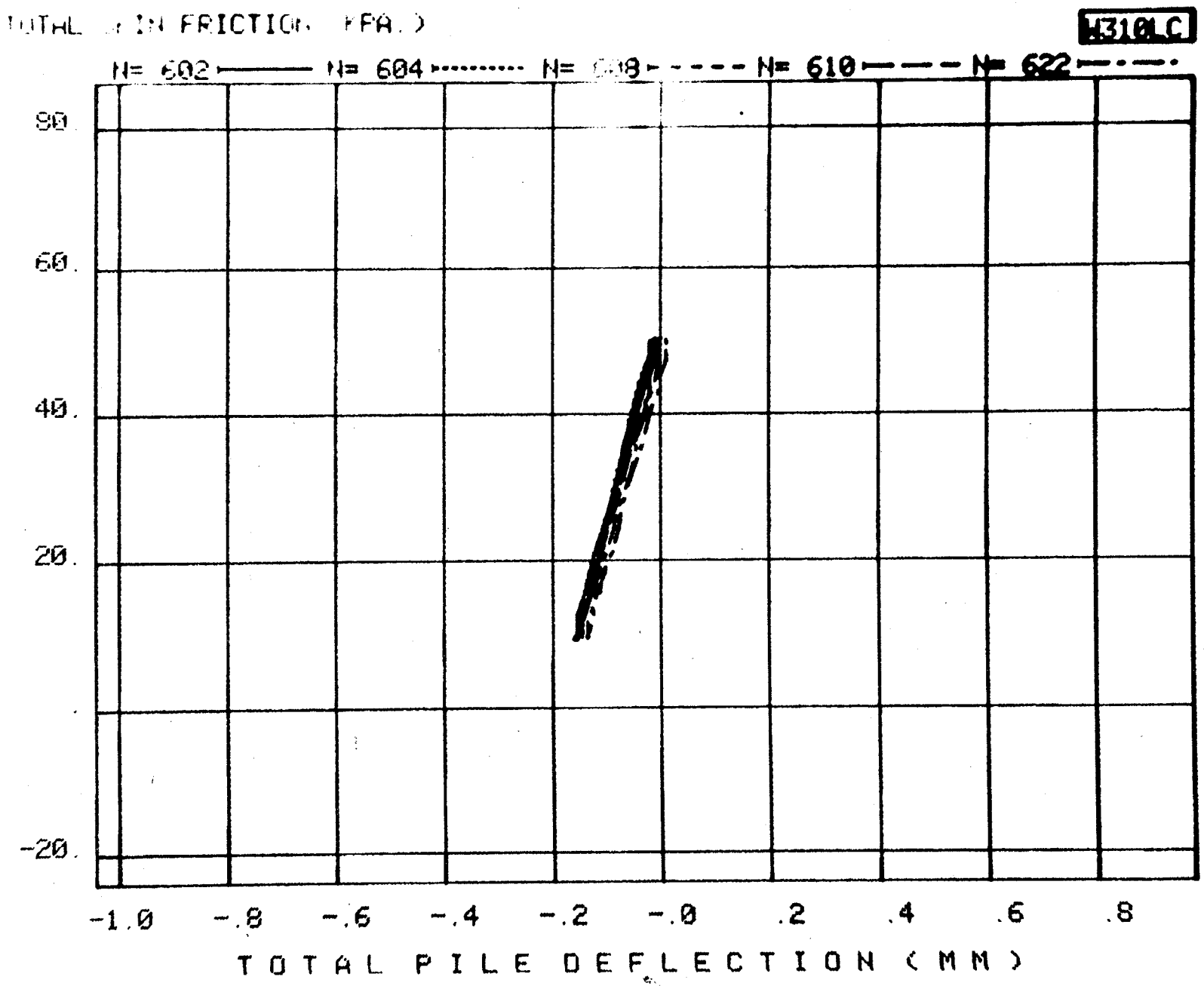
TOTAL (IN FRICTION, KPA.)
M310.C
N= 602
N= 604
N= 608
N= 610
N= 622
80.
60.
40.
20.
-20.
-1.0
-.8
-.6
-.4
-.2
-.0
.2
.4
.6
.8
TOTAL PILE DEFLECTION (MM)

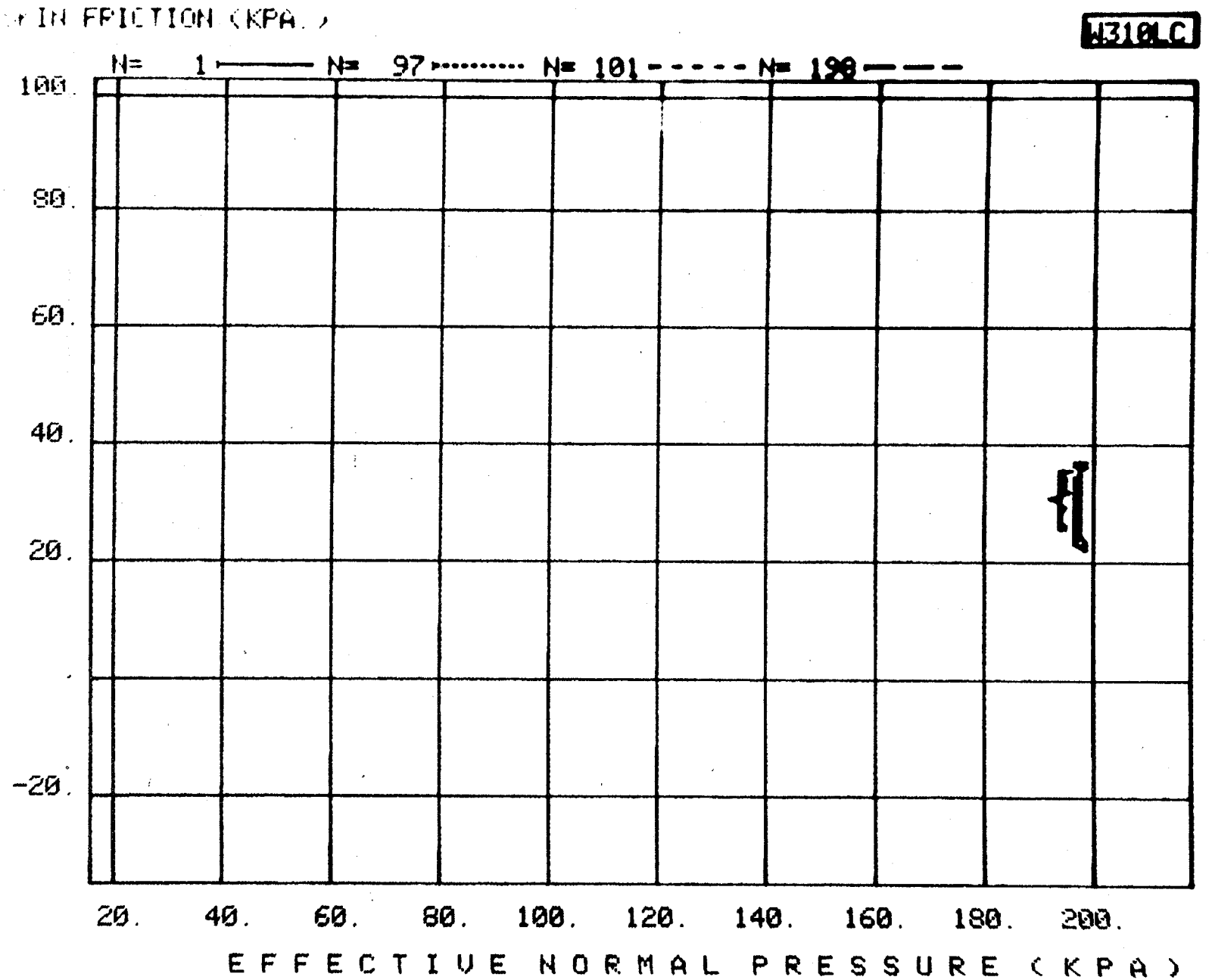
W310LC
IN FRICTION (KPA.)
N= 1
N= 97
N= 101
N= 198
100.
80.
60.
40.
20.
-20.
20.
40.
60.
80.
100.
120.
140.
160.
180.
200.
EFFECTIVE NORMAL PRESSURE (KPA)

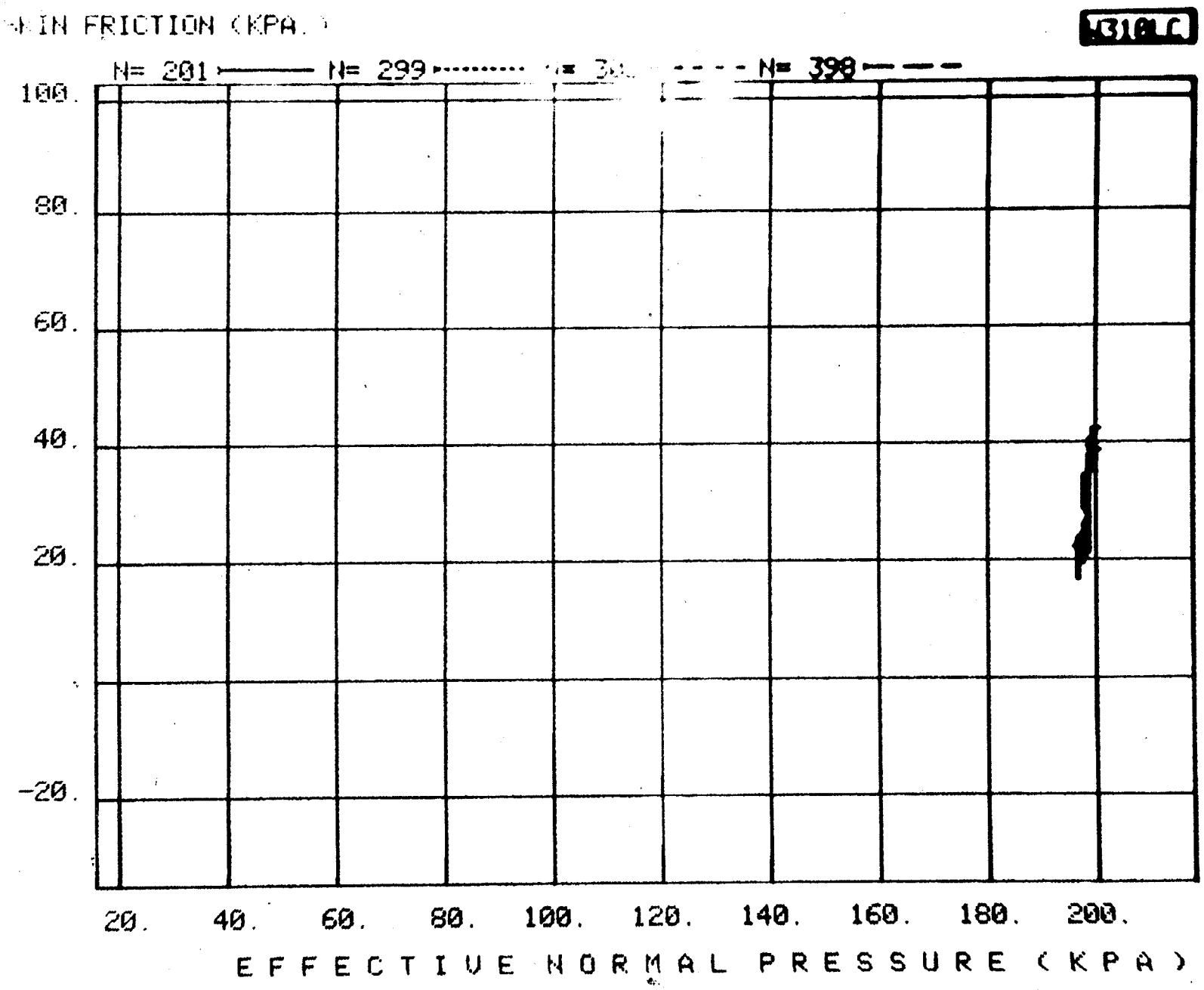
IN FRICTION (KPA.)
N= 201
N= 299
N= 398
100.
80.
60.
40.
20.
-20.
20.
40.
60.
80.
100.
120.
140.
160.
180.
200.
EFFECTIVE NORMAL PRESSURE (KPA)

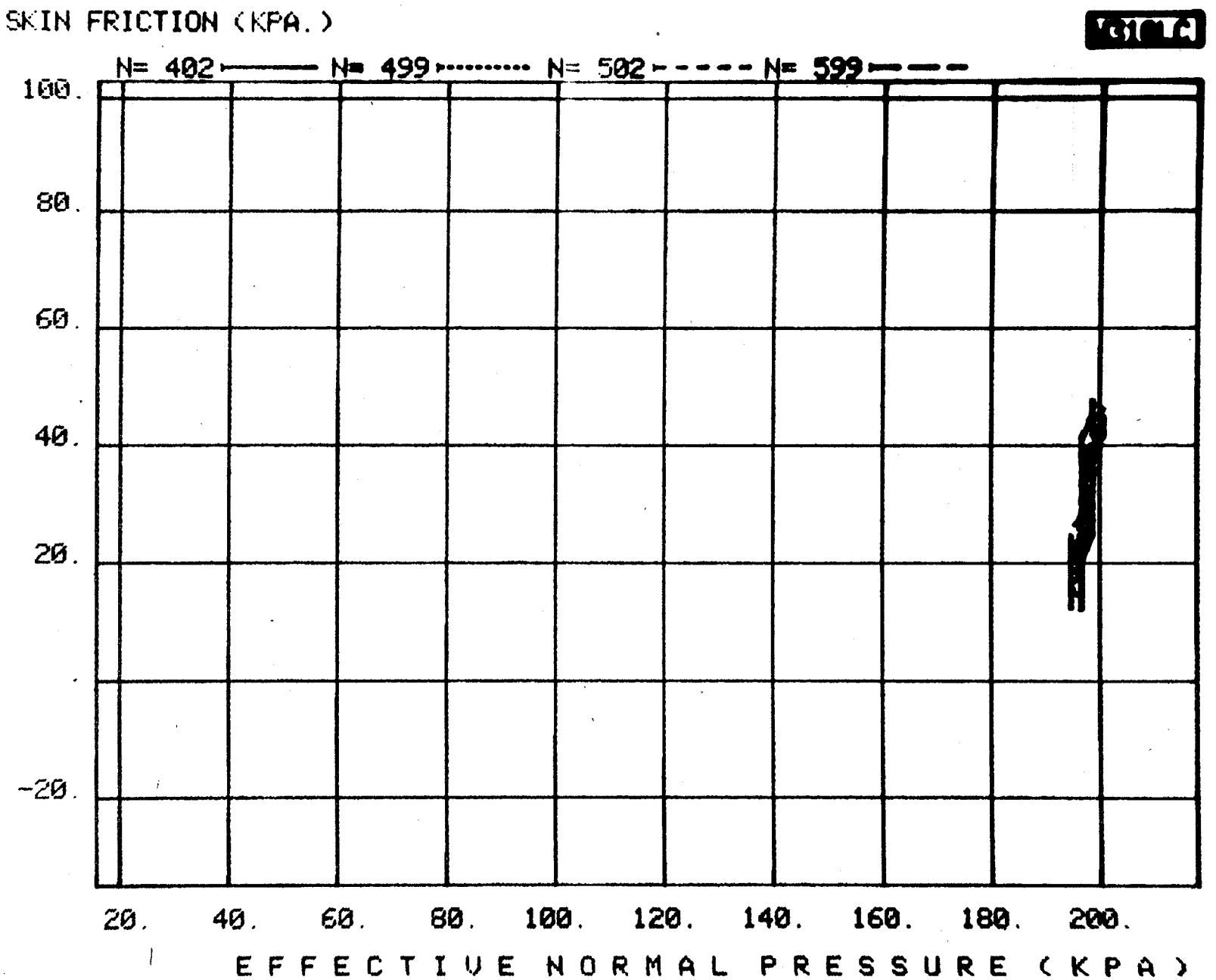
SKIN FRICTION (KPA.)
N= 402
N= 499
N= 502
N= 599
100.
80.
60.
40.
20.
-20.
20.
40.
60.
80.
100.
120.
140.
160.
180.
200.
EFFECTIVE NORMAL PRESSURE (KPA)

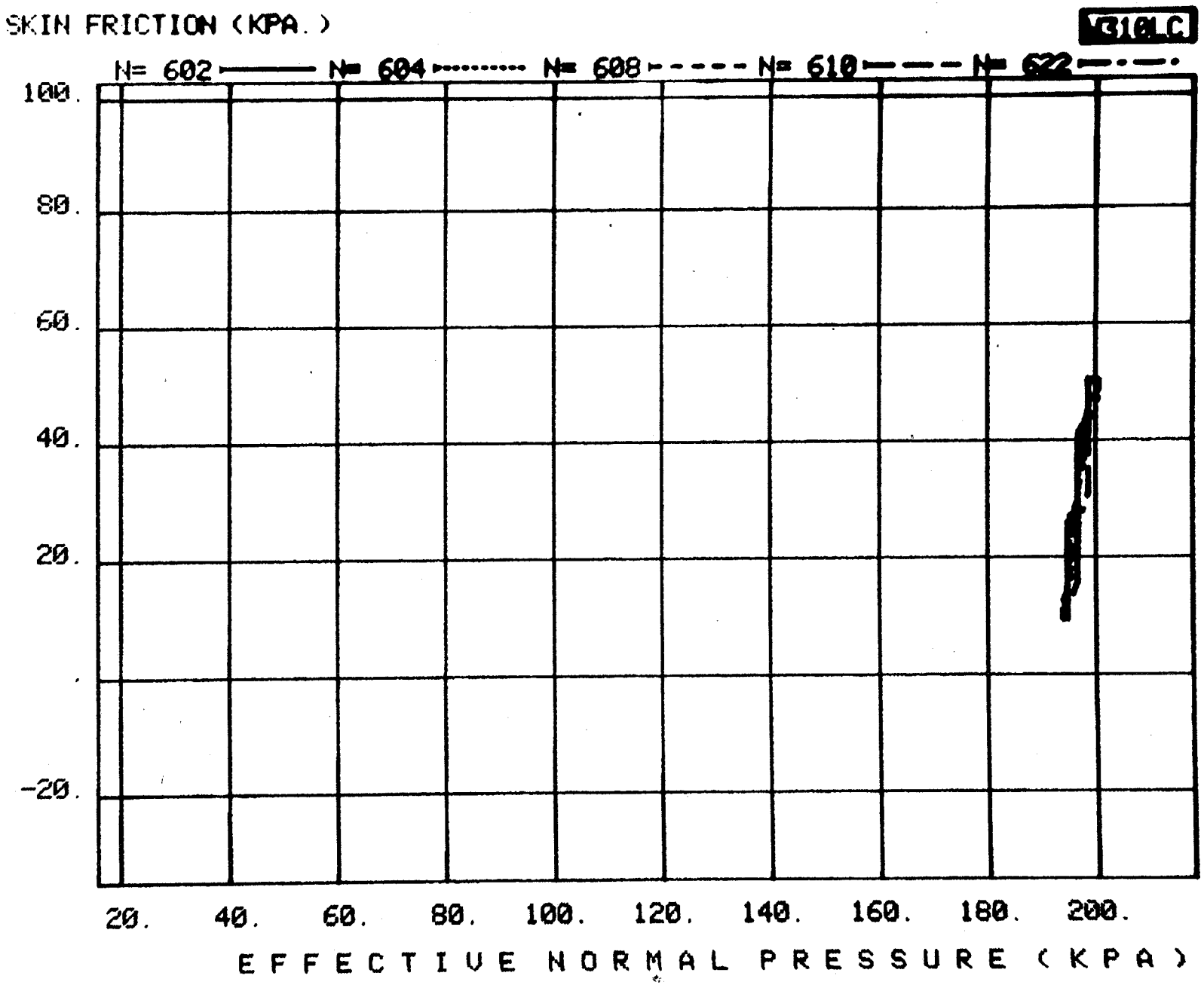
SKIN FRICTION (KPA.)
310LC
N= 602
N= 604
N= 608
N= 610
N= 622
100.
80.
60.
40.
20.
-20.
20.
40.
60.
80.
100.
120.
140.
160.
180.
200.
EFFECTIVE NORMAL PRESSURE (KPA)

RESPONSE ON CYCLIC LOADING (KPA.) CYCLE NO. 1

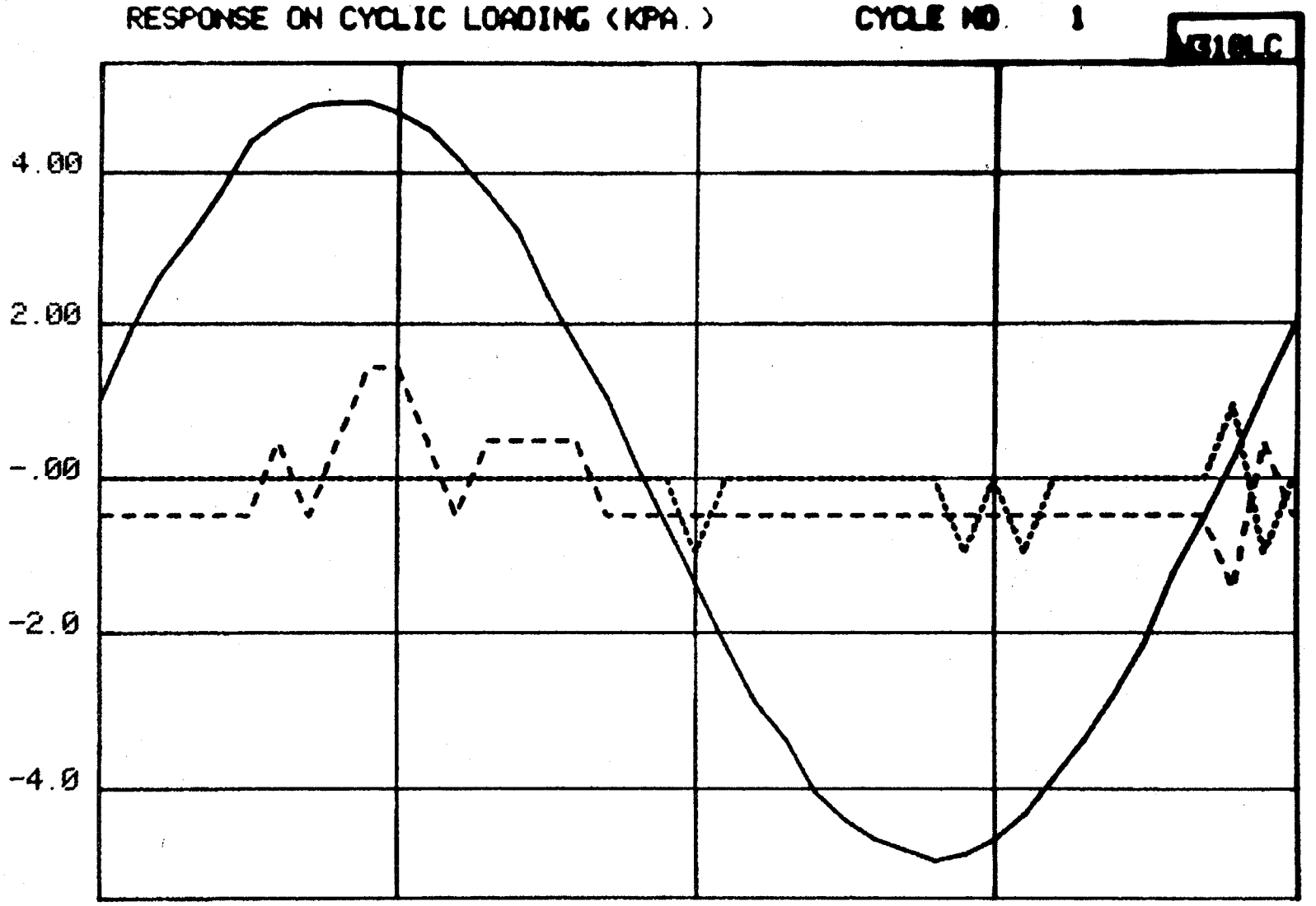

LEGEND:

		PERM. VALUES
———	SKIN FRICTION	30.63 KPA.
·····	PORE PRESSURE	123.6 KPA.
- - - -	TOTAL NORMAL PRESSURE	317.8 KPA.

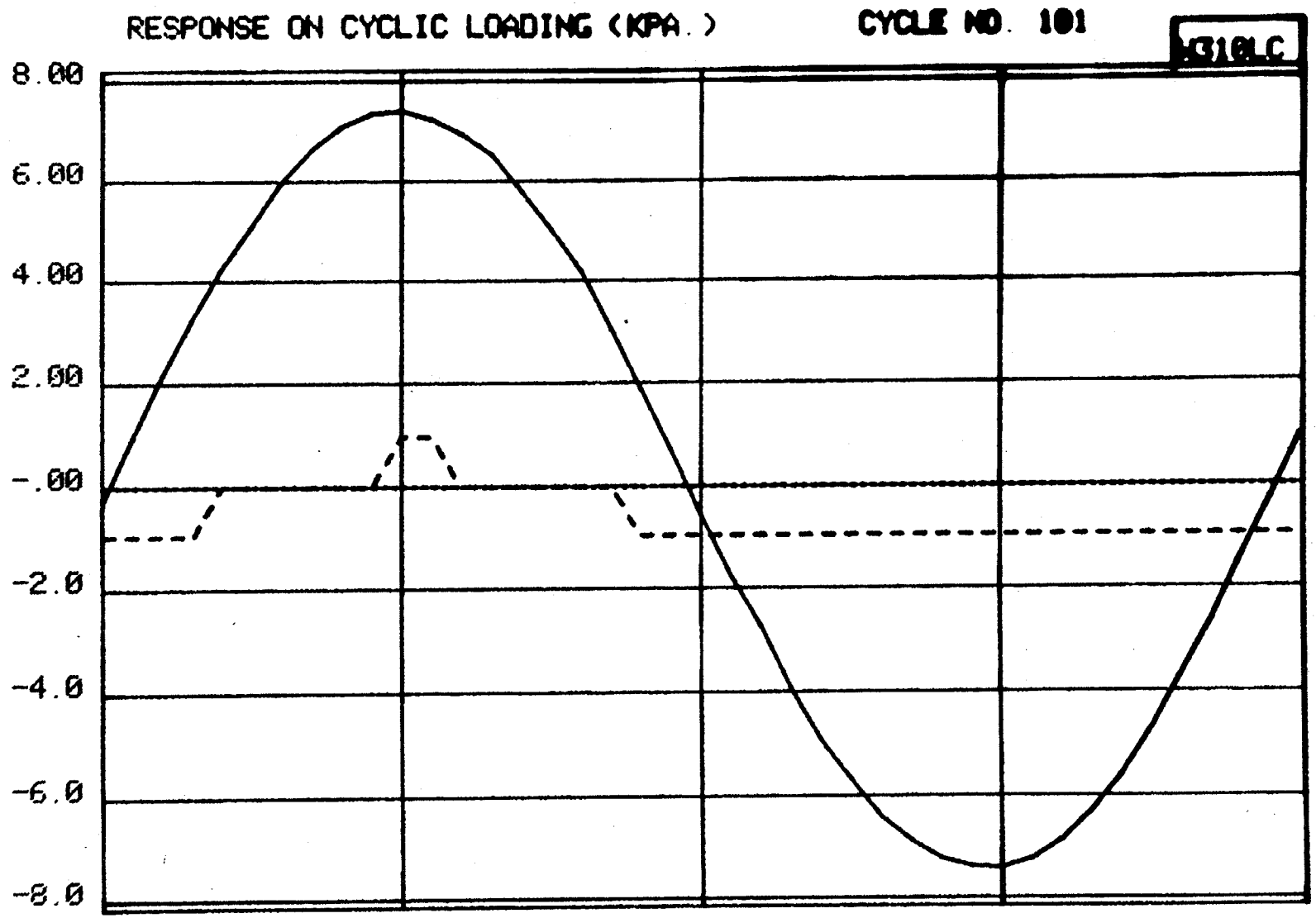

LEGEND:

		PERM. VALUES
———	SKIN FRICTION	29.60 KPA.
·····	PORE PRESSURE	122.6 KPA.
- - - -	TOTAL NORMAL PRESSURE	320.2 KPA.

RESPONSE ON CYCLIC LOADING (KPA.) CYCLE NO. 201

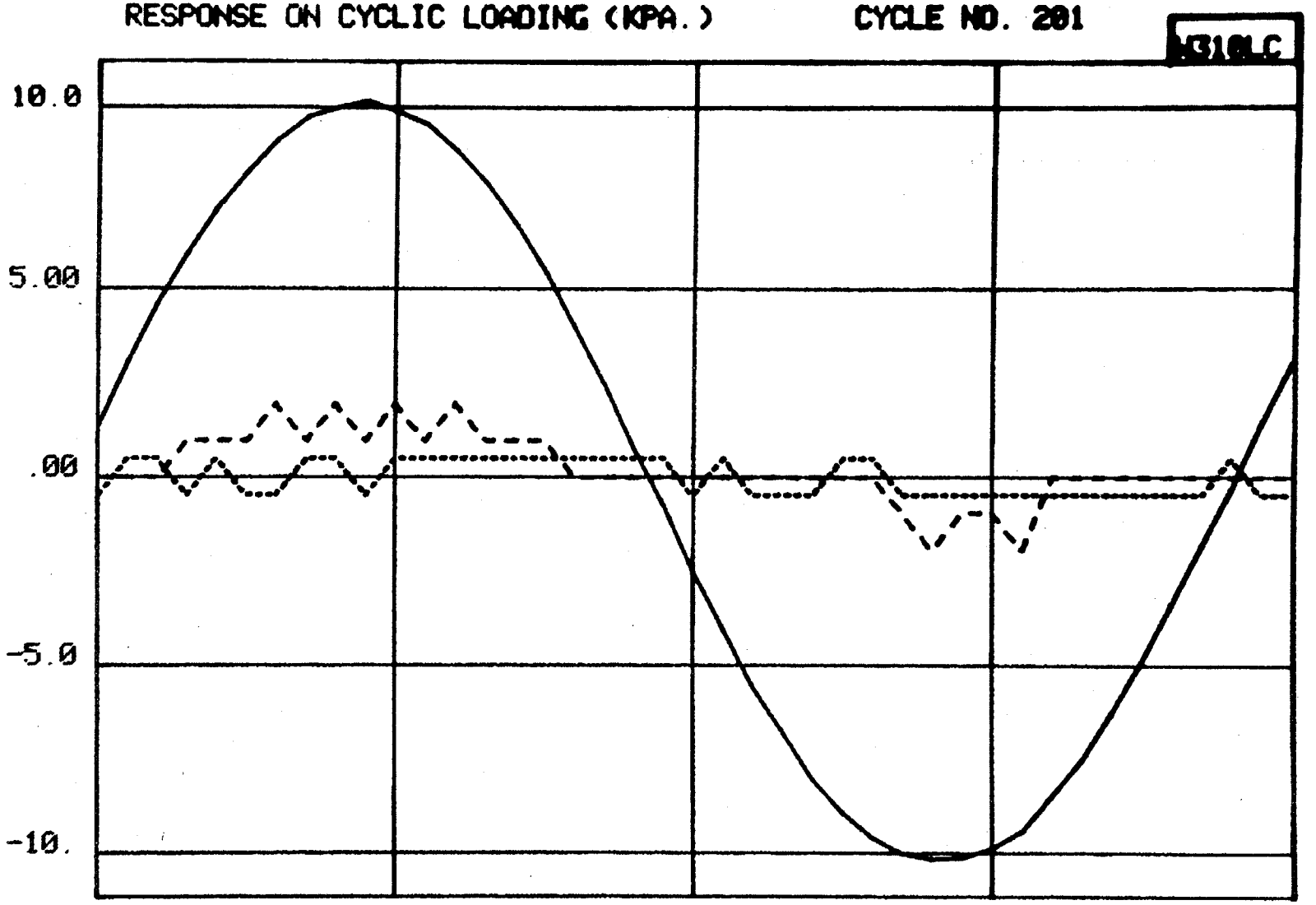

LEGEND:

		PERM. VALUES
———	SKIN FRICTION	29.68 KPA.
·····	PORE PRESSURE	121.2 KPA.
- - - -	TOTAL NORMAL PRESSURE	319.2 KPA.

RESPONSE ON CYCLIC LOADING (KPA.) CYCLE NO. 302

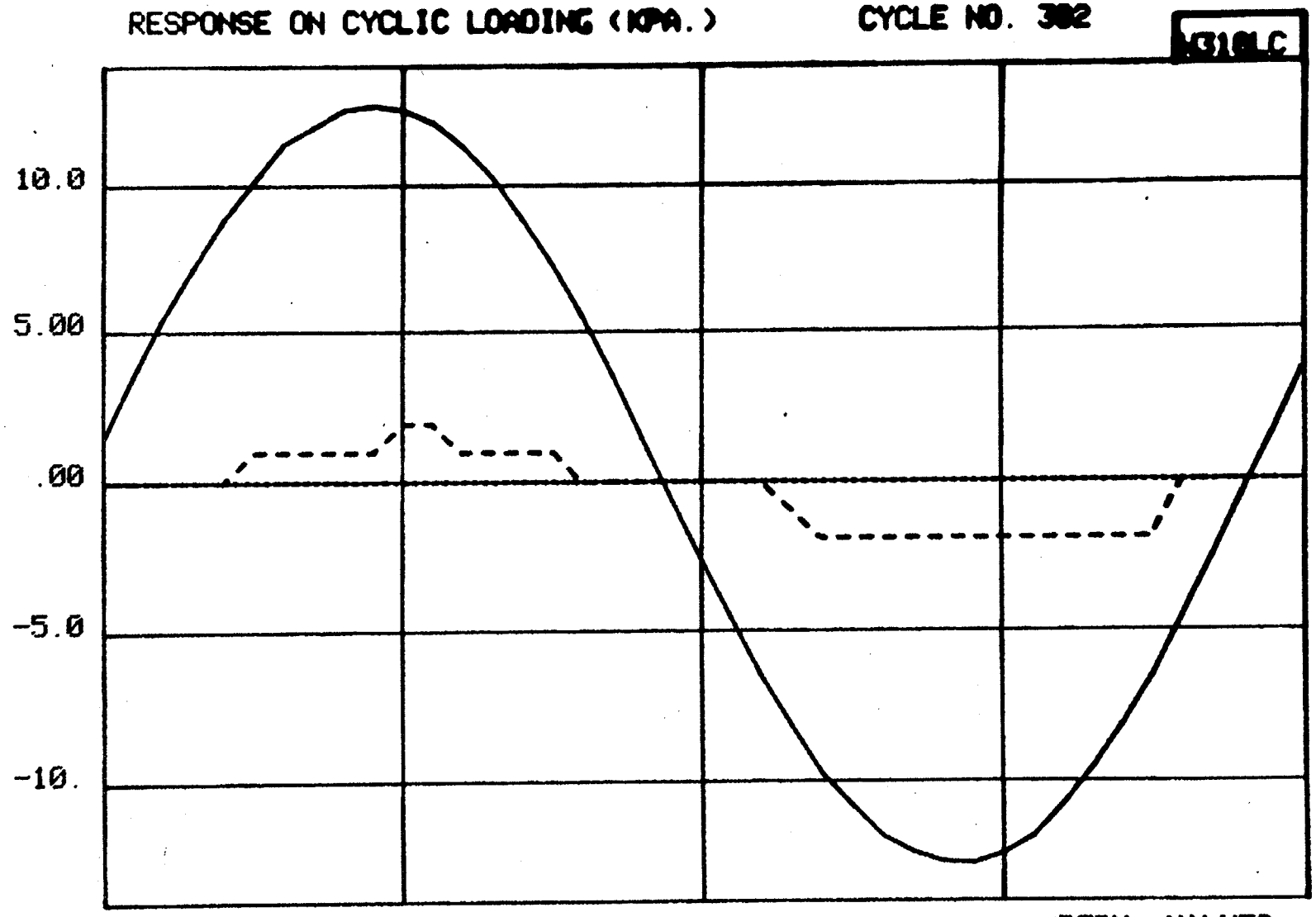

LEGEND:

		PERM. VALUES
————	SKIN FRICTION	29.63 KPA.
·····	PORE PRESSURE	120.7 KPA.
- - - - -	TOTAL NORMAL PRESSURE	319.2 KPA.

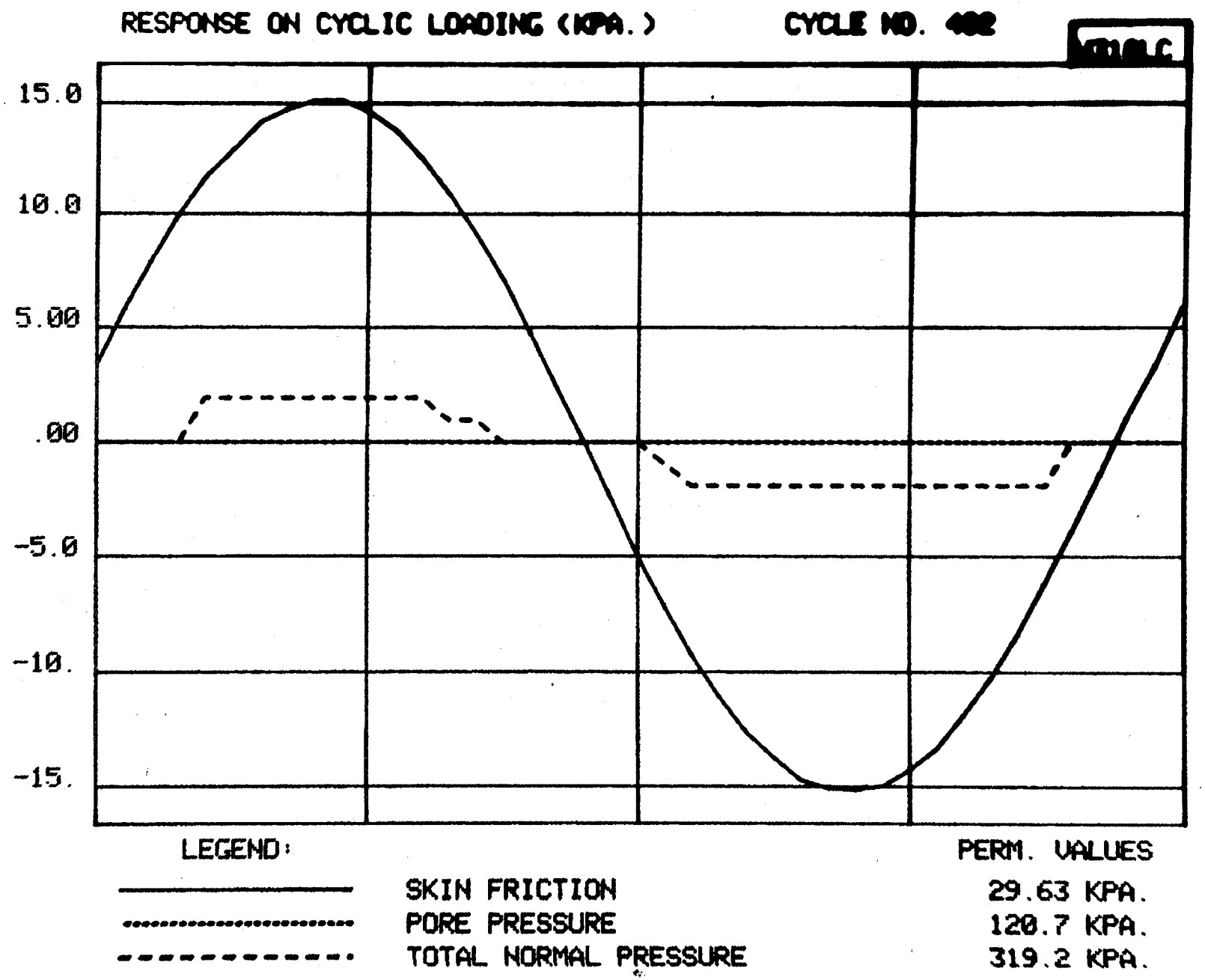
RESPONSE ON CYCLIC LOADING (KPA.)
CYCLE NO. 402
15.0
10.0
5.00
.00
-5.0
-10.
-15.
LEGEND:
PERM. VALUES
SKIN FRICTION
29.63 KPA.
PORE PRESSURE
120.7 KPA.
TOTAL NORMAL PRESSURE
319.2 KPA.

RESPONSE ON CYCLIC LOADING (KPA.) CYCLE NO. 302

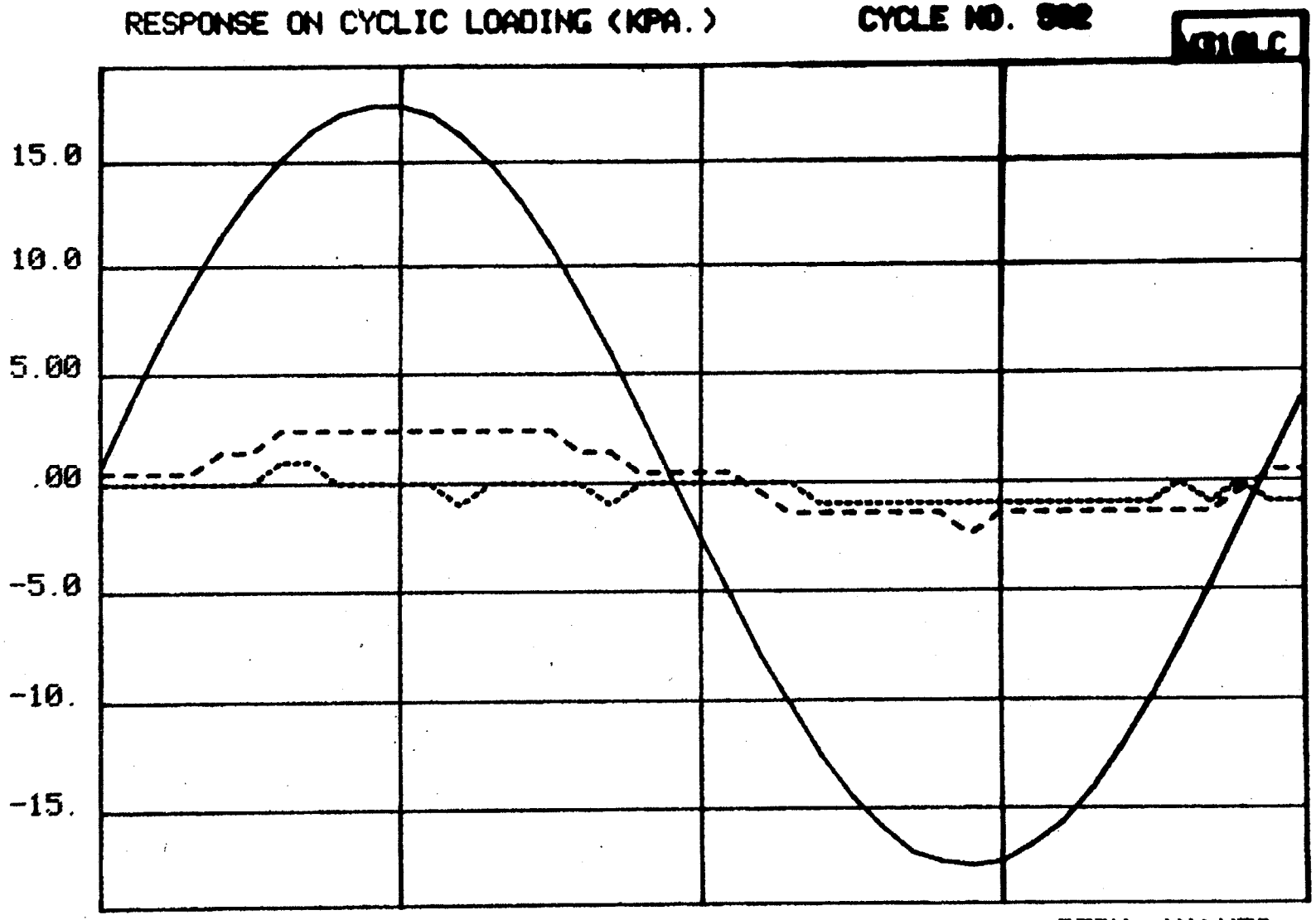

LEGEND:

		PERM. VALUES
———	SKIN FRICTION	29.84 KPA.
·····	PORE PRESSURE	121.7 KPA.
- - - -	TOTAL NORMAL PRESSURE	318.7 KPA.

RESPONSE ON CYCLIC LOADING (KPA.) CYCLE NO. 602

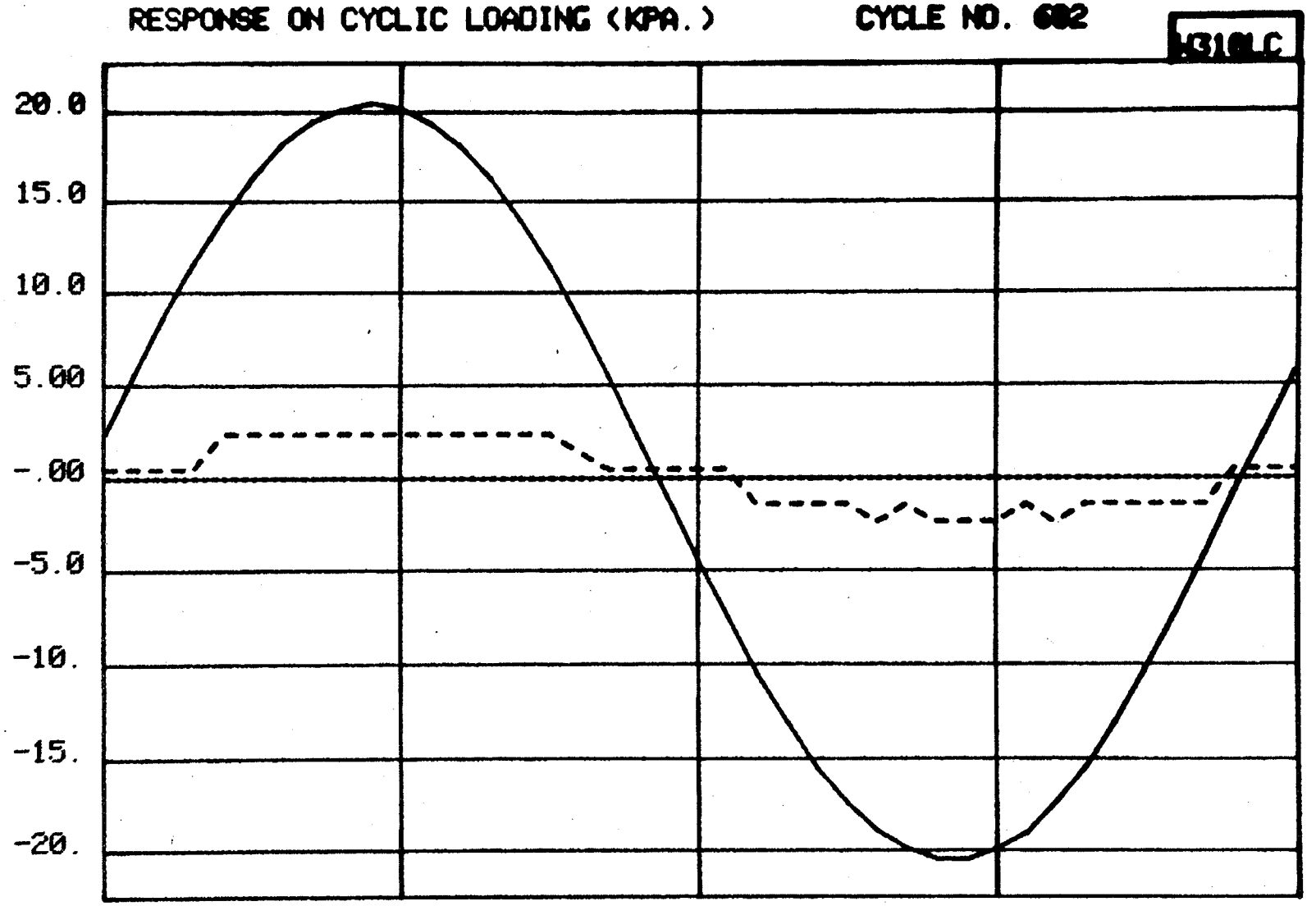

LEGEND:

		PERM. VALUES
———	SKIN FRICTION	29.84 KPA.
·····	PORE PRESSURE	122.6 KPA.
- - - -	TOTAL NORMAL PRESSURE	318.7 KPA.

Appendix GB

Plotted Results from W310SC

Figures GB-1 through GB-4

Skin Friction vs Deflection, Selected Cycles

Figures GB-5 through GB-6

Skin Friction vs Eff. Normal Pressure, Selected Cycl.

Figures GB-7 through GB-14

Skin Friction, Pore and Total Pressure, Selected Cycles

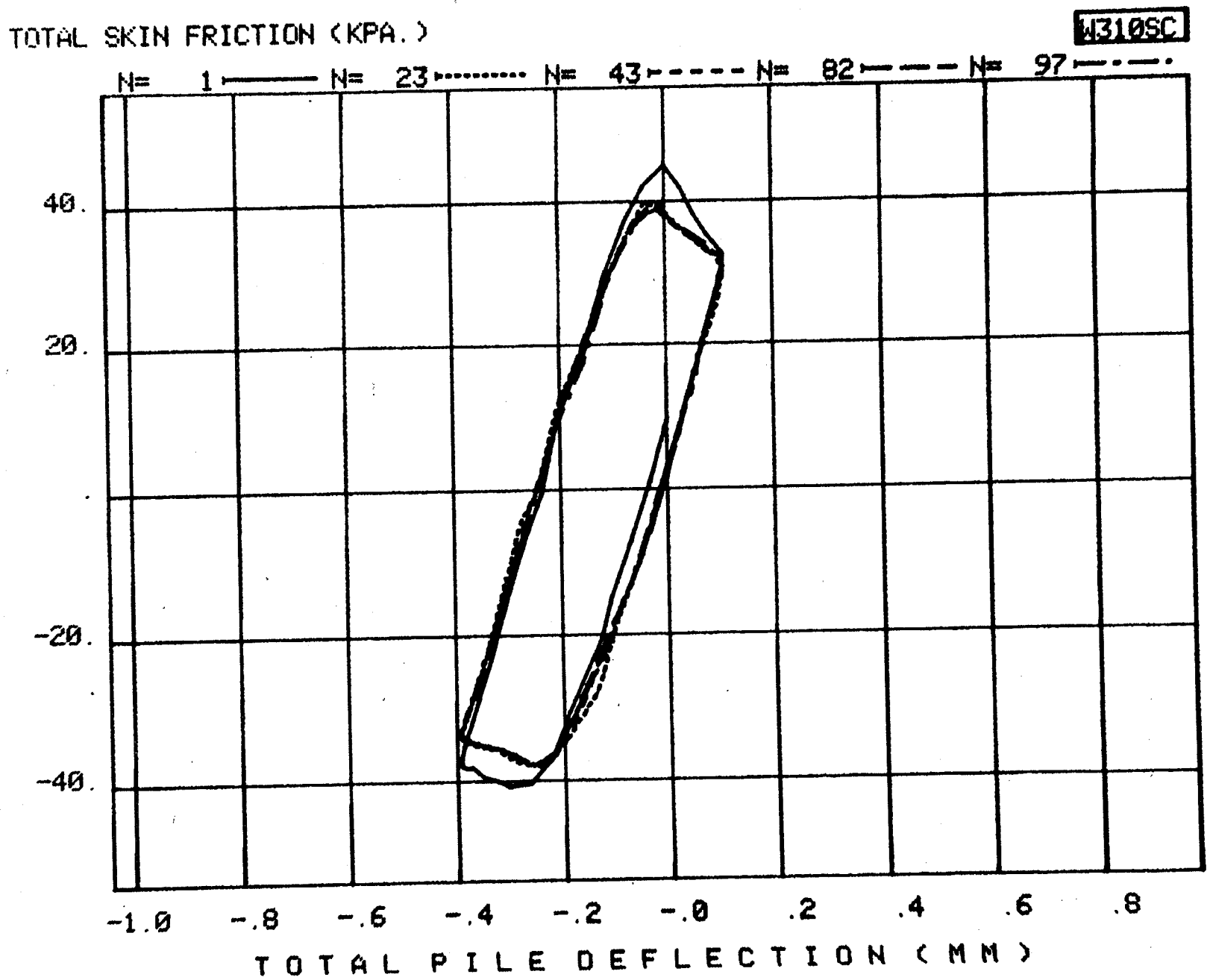
TOTAL SKIN FRICTION (KPA.)
W310SC
N= 1
N= 23
N= 43
N= 82
N= 97
40.
20.
-20.
-40.
-1.0
-.8
-.6
-.4
-.2
-.0
.2
.4
.6
.8
TOTAL PILE DEFLECTION (MM)

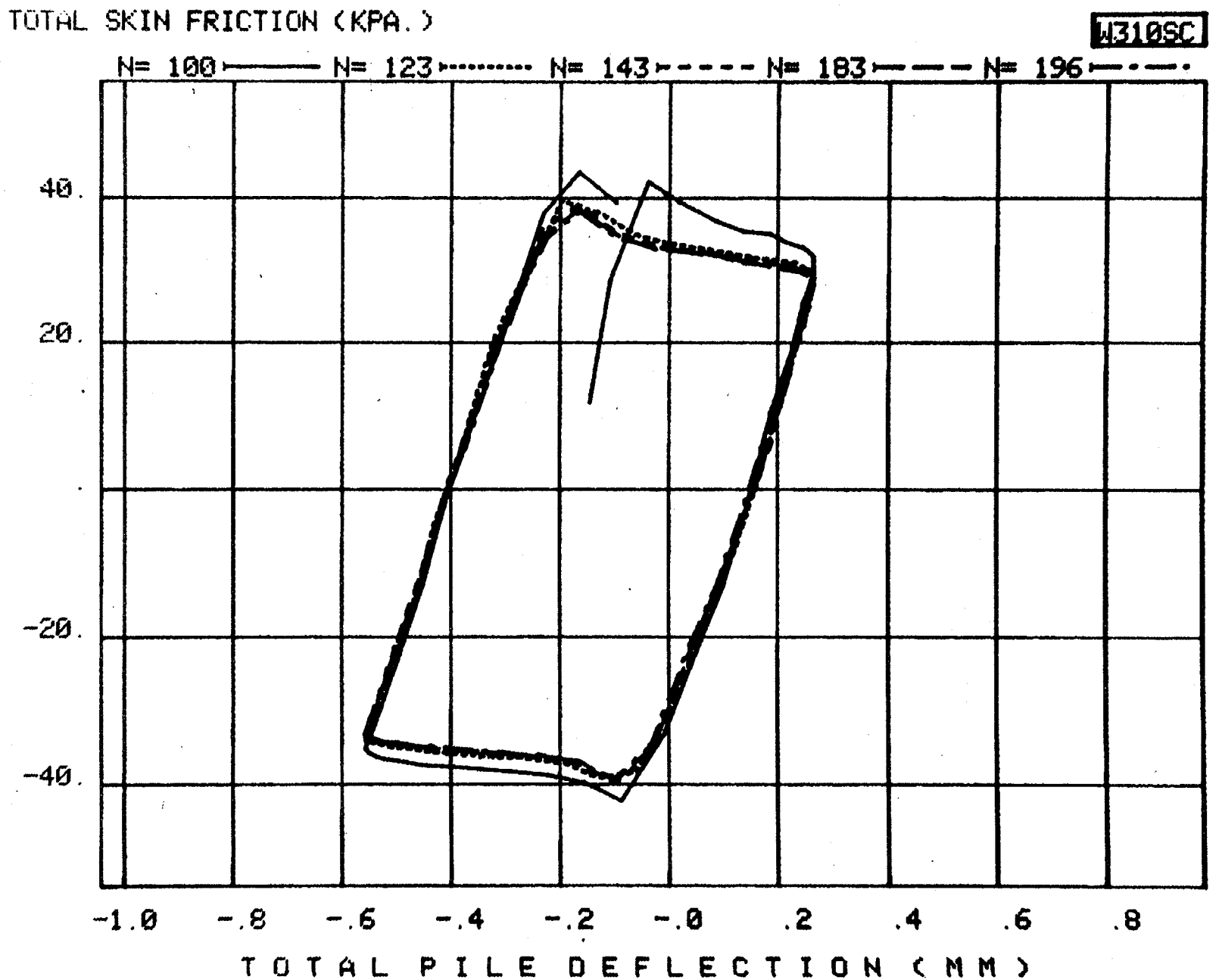
TOTAL SKIN FRICTION (KPA.)
W310SC
N= 100
N= 123
N= 143
N= 183
N= 196
40.
20.
-20.
-40.
-1.0
-.8
-.6
-.4
-.2
-.0
.2
.4
.6
.8
TOTAL PILE DEFLECTION (MM)

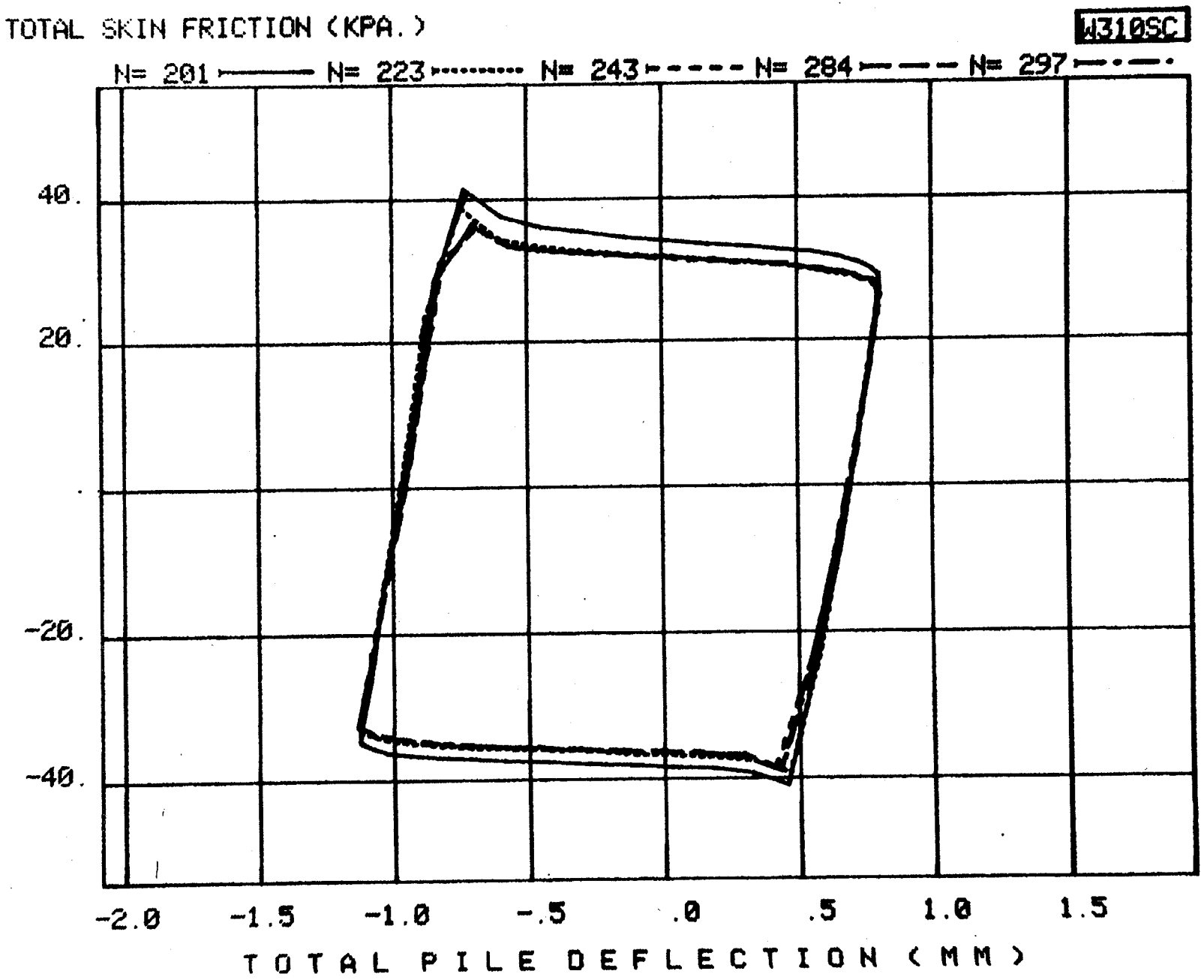
TOTAL SKIN FRICTION (KPA.)
W310SC
N= 201
N= 223
N= 243
N= 284
N= 297
40.
20.
-20.
-40.
-2.0
-1.5
-1.0
-.5
.0
.5
1.0
1.5
TOTAL PILE DEFLECTION (MM)

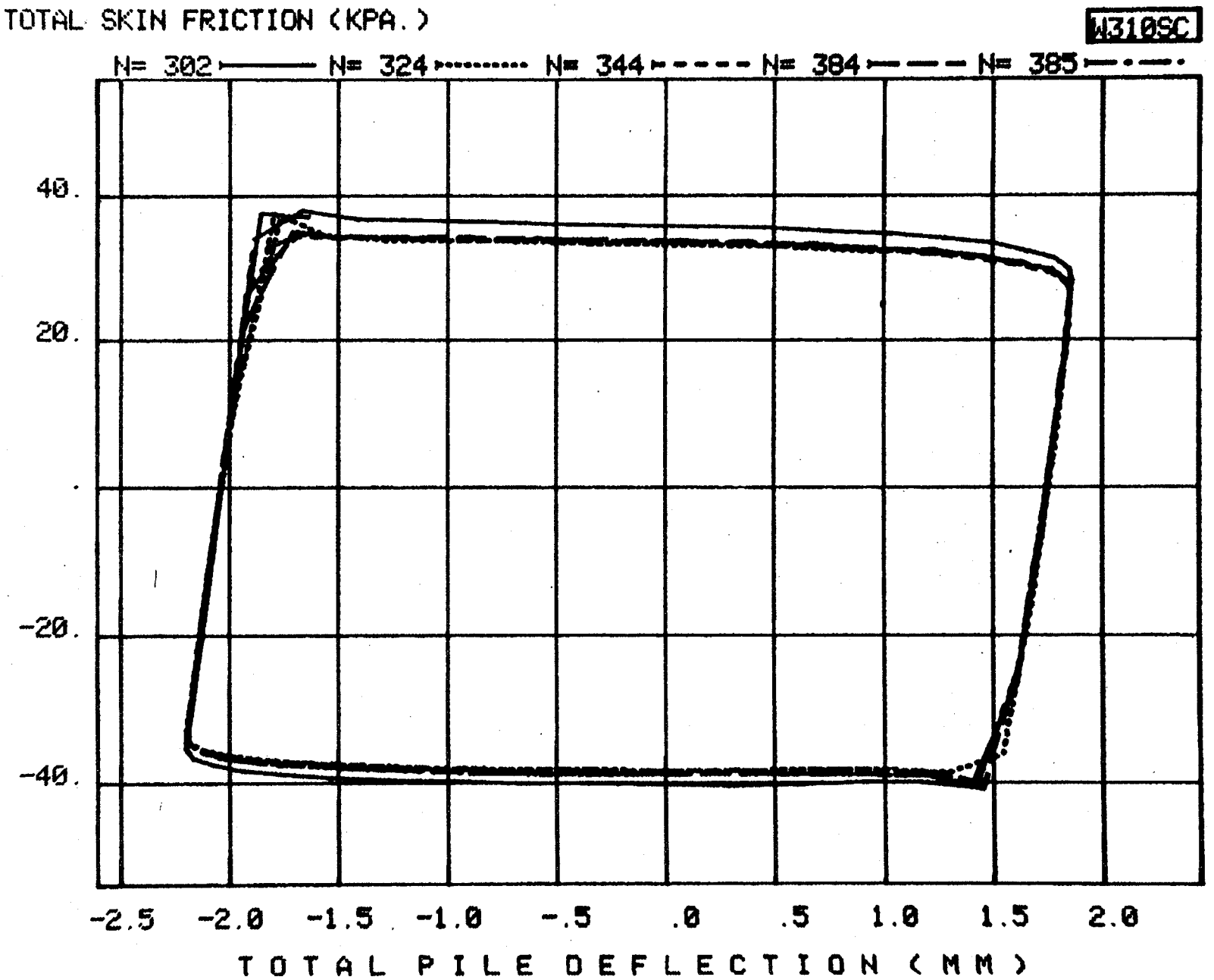
TOTAL SKIN FRICTION (KPA.)
W310SC
N= 302
N= 324
N= 344
N= 384
N= 385
40.
20.
-20.
-40.
-2.5
-2.0
-1.5
-1.0
-.5
.0
.5
1.0
1.5
2.0
TOTAL PILE DEFLECTION (MM)

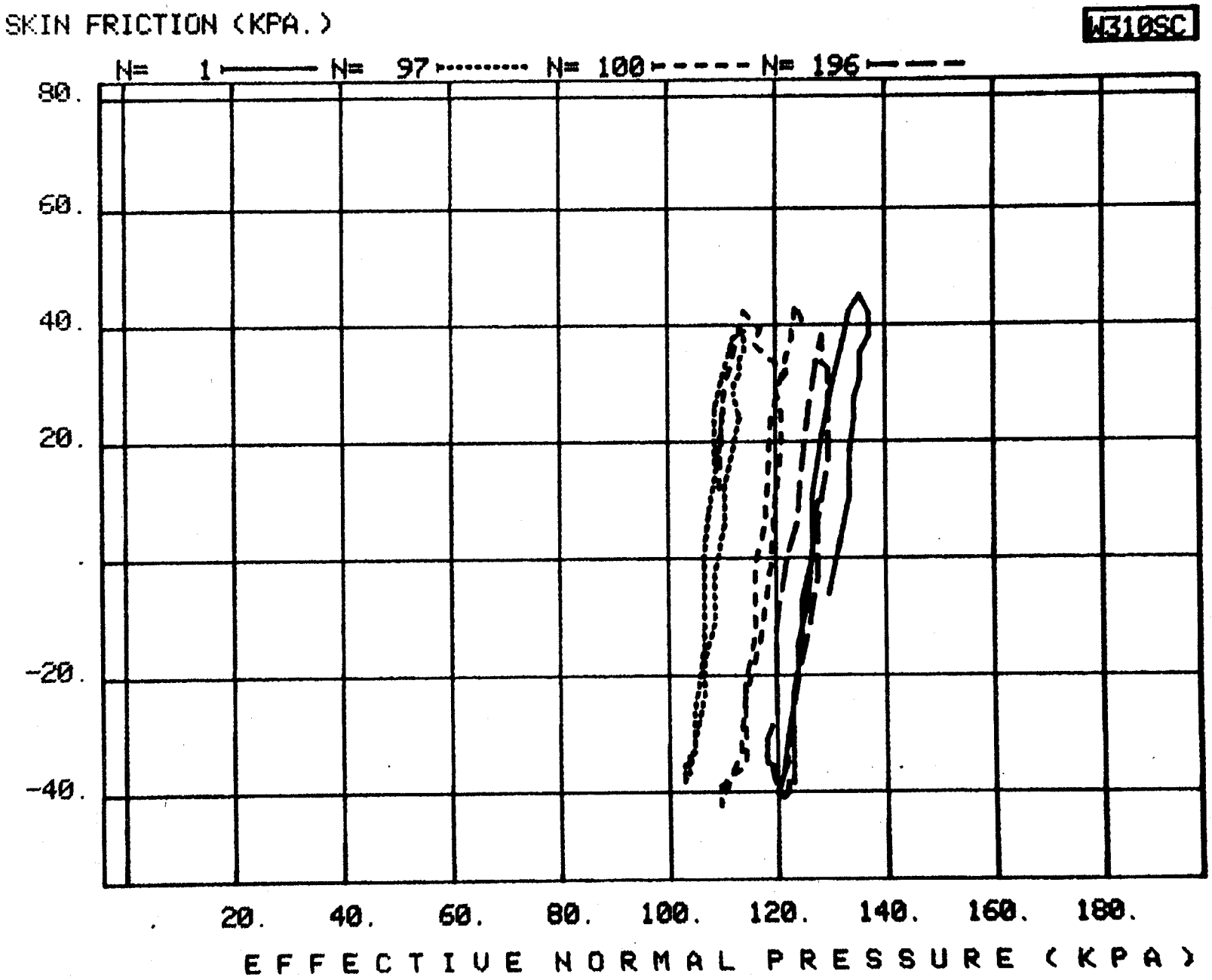
SKIN FRICTION (KPA.)
W310SC
N= 1
N= 97
N= 100
N= 196
80.
60.
40.
20.
-20.
-40.
20.
40.
60.
80.
100.
120.
140.
160.
180.
EFFECTIVE NORMAL PRESSURE (KPA)

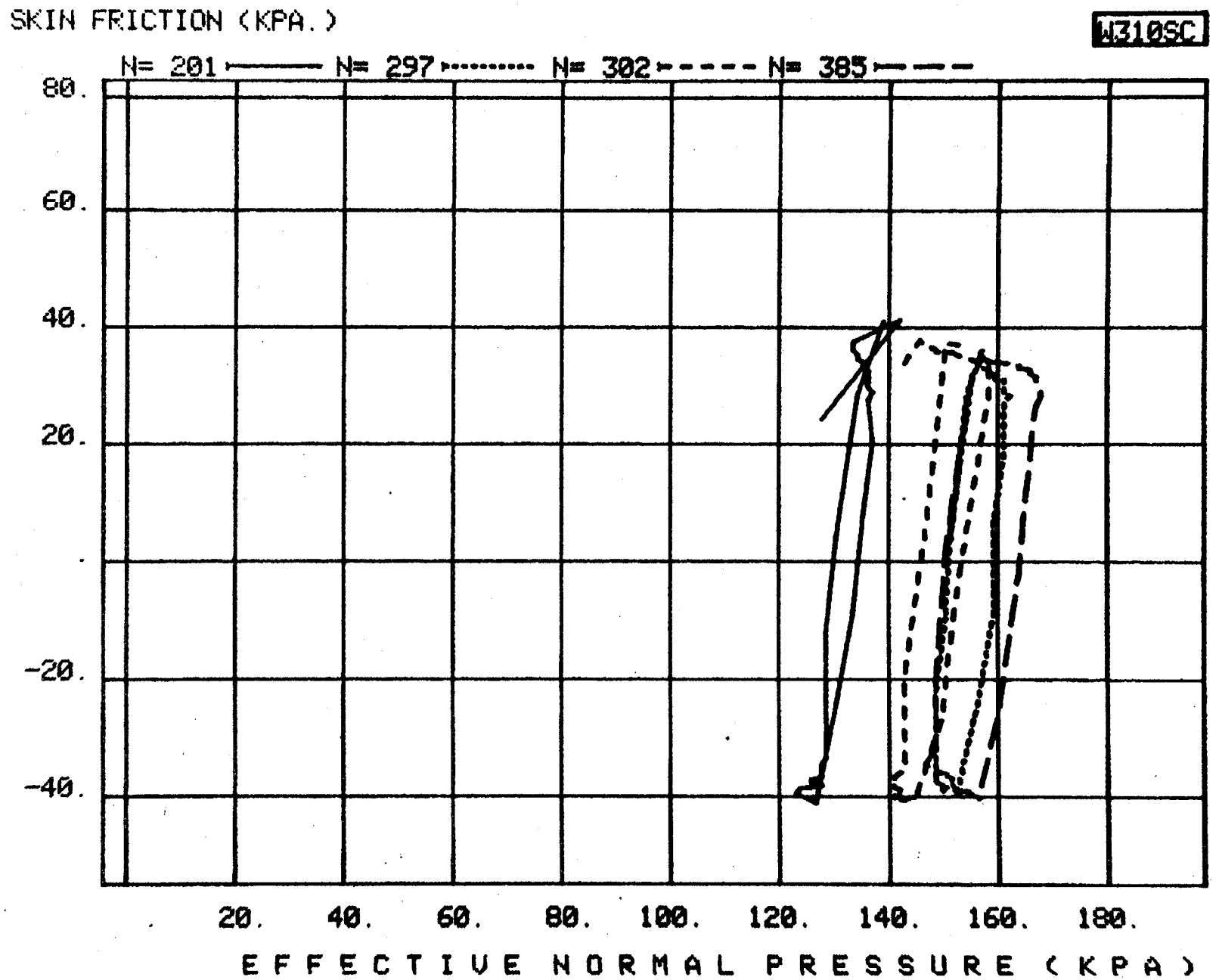
SKIN FRICTION (KPA.)
W310SC
N= 201
N= 297
N= 302
N= 385
80.
60.
40.
20.
-20.
-40.
20.
40.
60.
80.
100.
120.
140.
160.
180.
EFFECTIVE NORMAL PRESSURE (KPA)

RESPONSE ON CYCLIC LOADING (KPA.) CYCLE NO. 1

W310SC

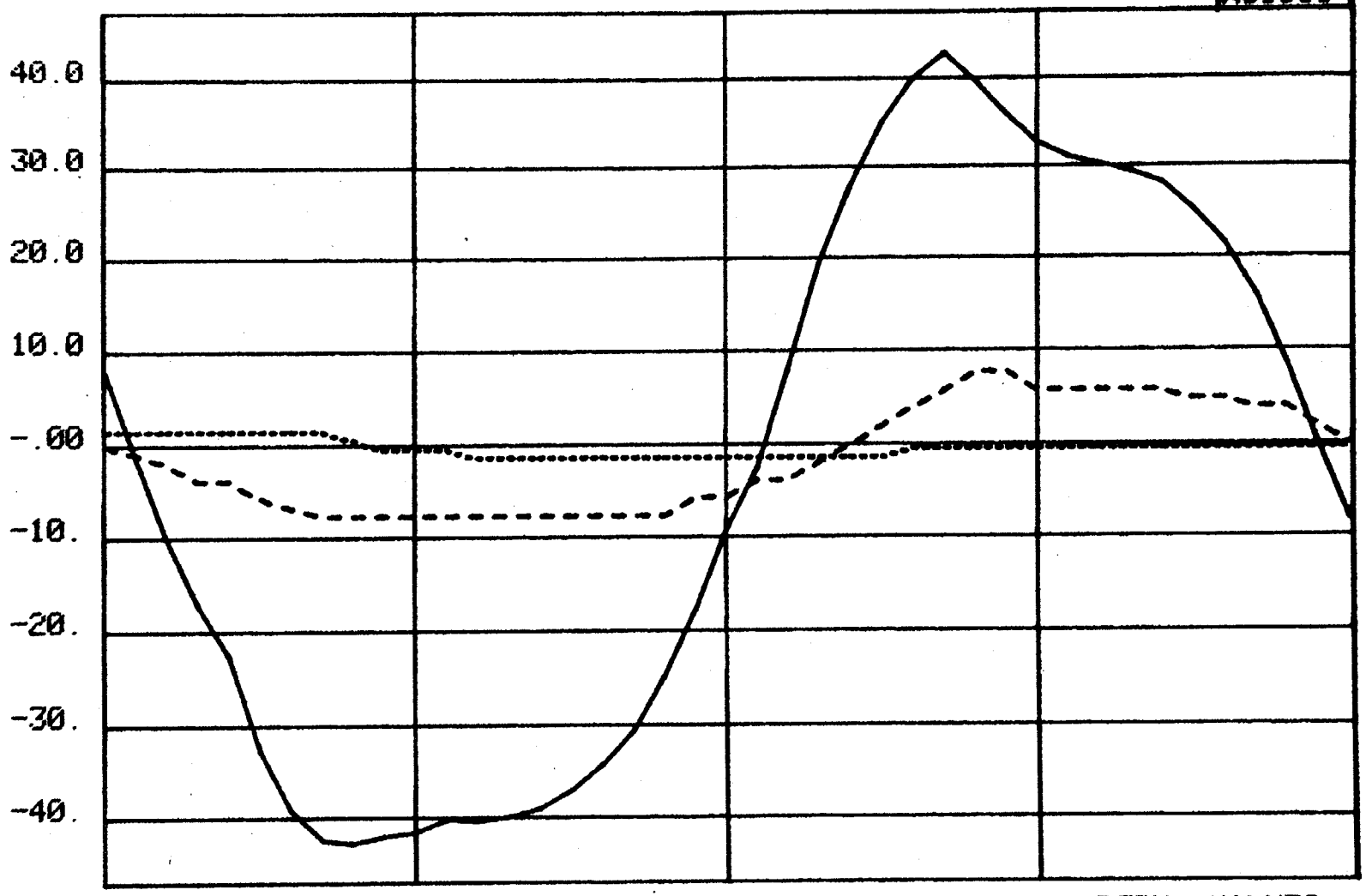

LEGEND:

		PERM. VALUES
———	SKIN FRICTION	2.21 KPA.
·····	PORE PRESSURE	125.0 KPA.
- - - -	TOTAL NORMAL PRESSURE	254.1 KPA.

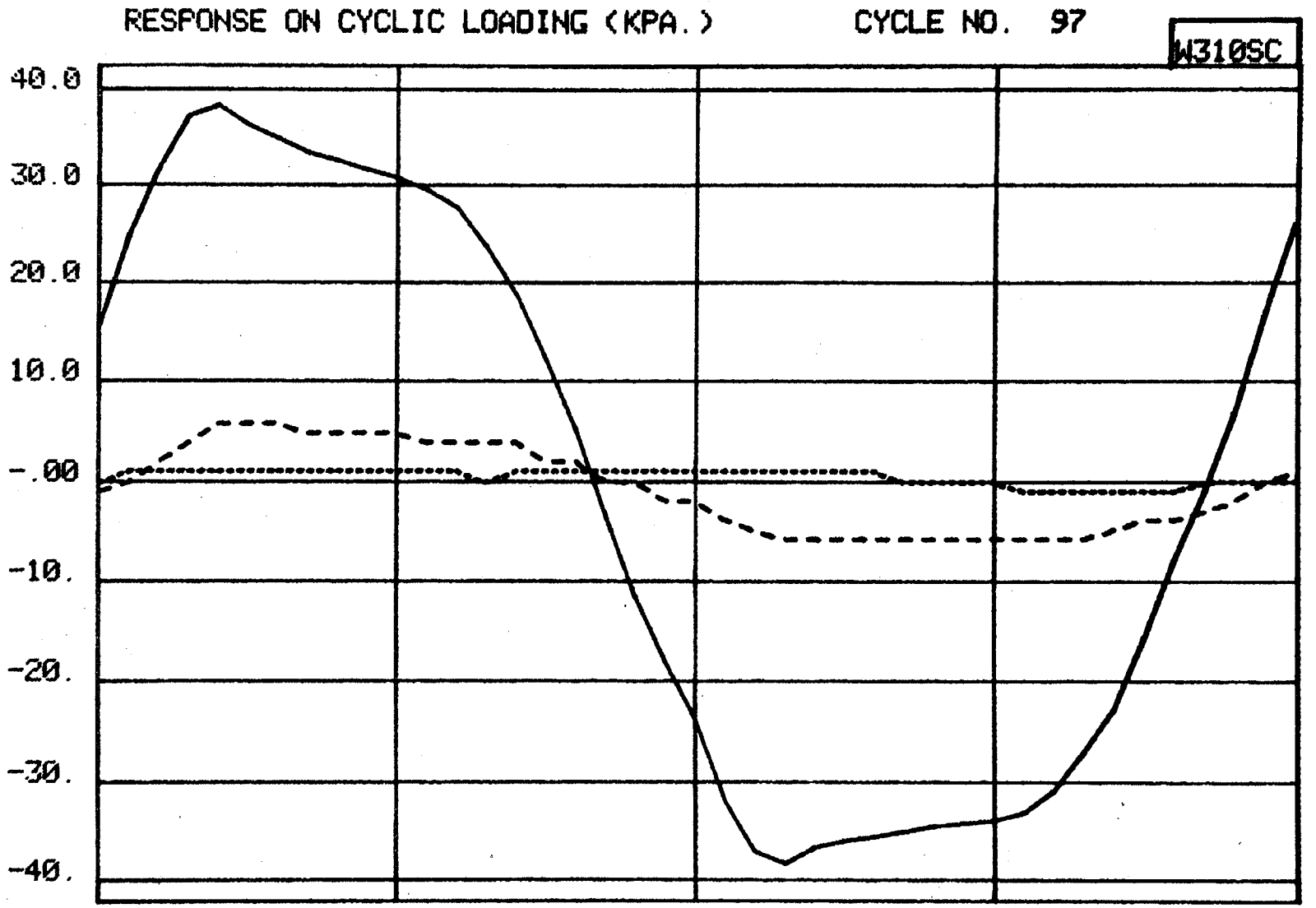

LEGEND:

		PERM. VALUES
———	SKIN FRICTION	.43 KPA.
·····	PORE PRESSURE	161.9 KPA.
- - - -	TOTAL NORMAL PRESSURE	271.3 KPA.

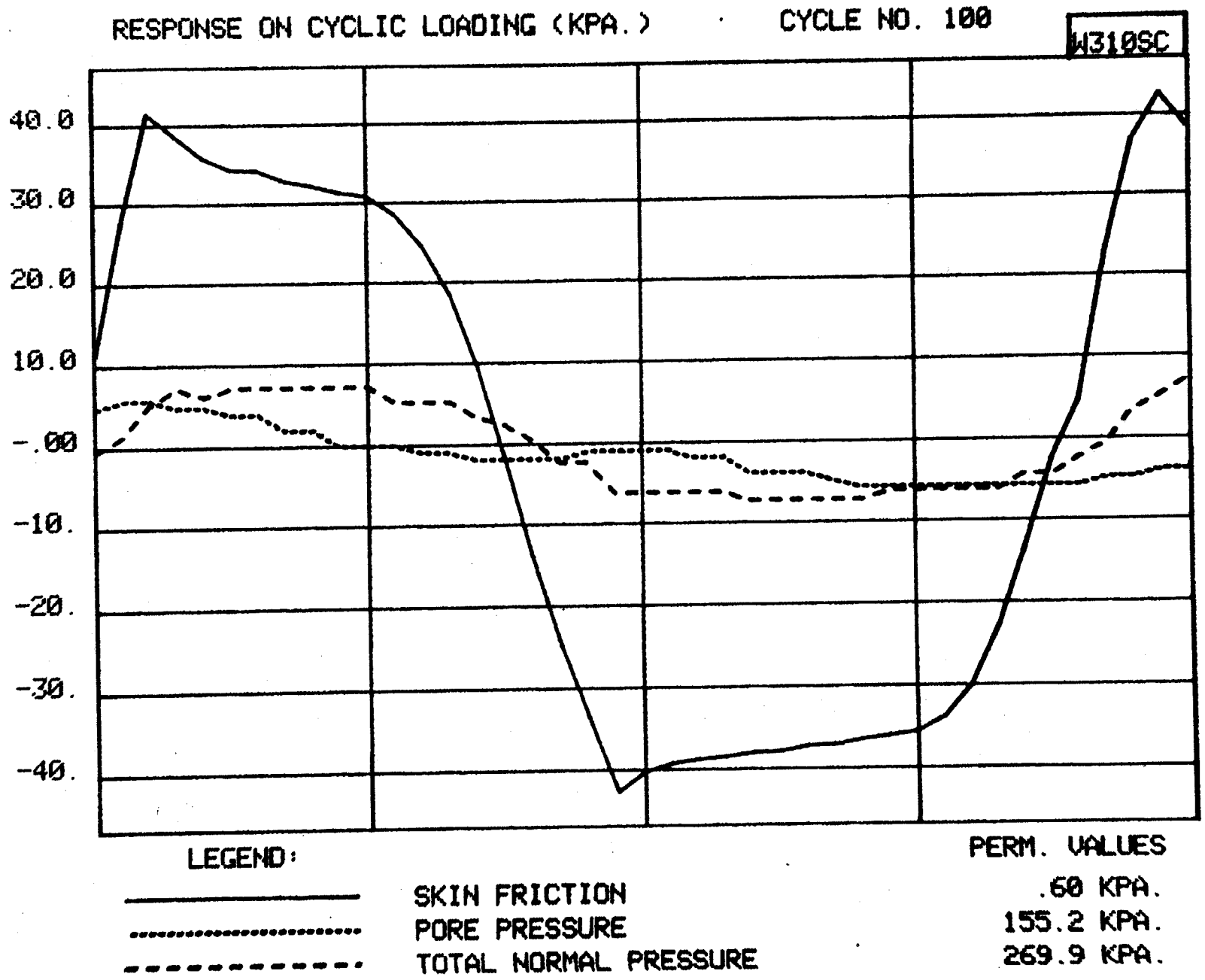
RESPONSE ON CYCLIC LOADING (KPA.)
CYCLE NO. 100
W310SC
40.0
30.0
20.0
10.0
-.00
-10.
-20.
-30.
-40.
LEGEND:
SKIN FRICTION
PORE PRESSURE
TOTAL NORMAL PRESSURE
PERM. VALUES
.60 KPA.
155.2 KPA.
269.9 KPA.

RESPONSE ON CYCLIC LOADING (KPA.) CYCLE NO. 196

W310SC

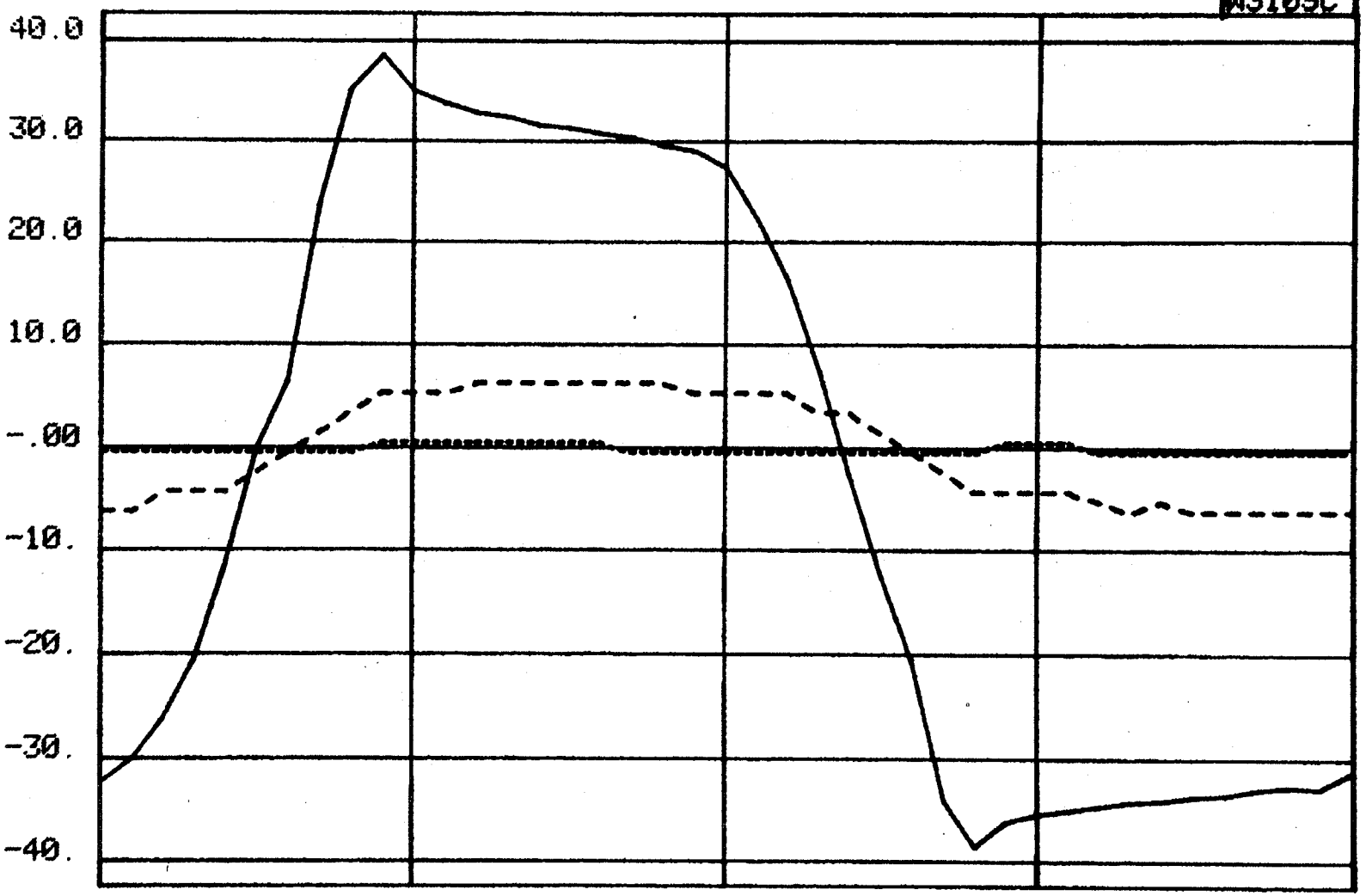

LEGEND:

		PERM. VALUES
———	SKIN FRICTION	-.60 KPA.
·····	PORE PRESSURE	146.1 KPA.
- - - -	TOTAL NORMAL PRESSURE	269.9 KPA.

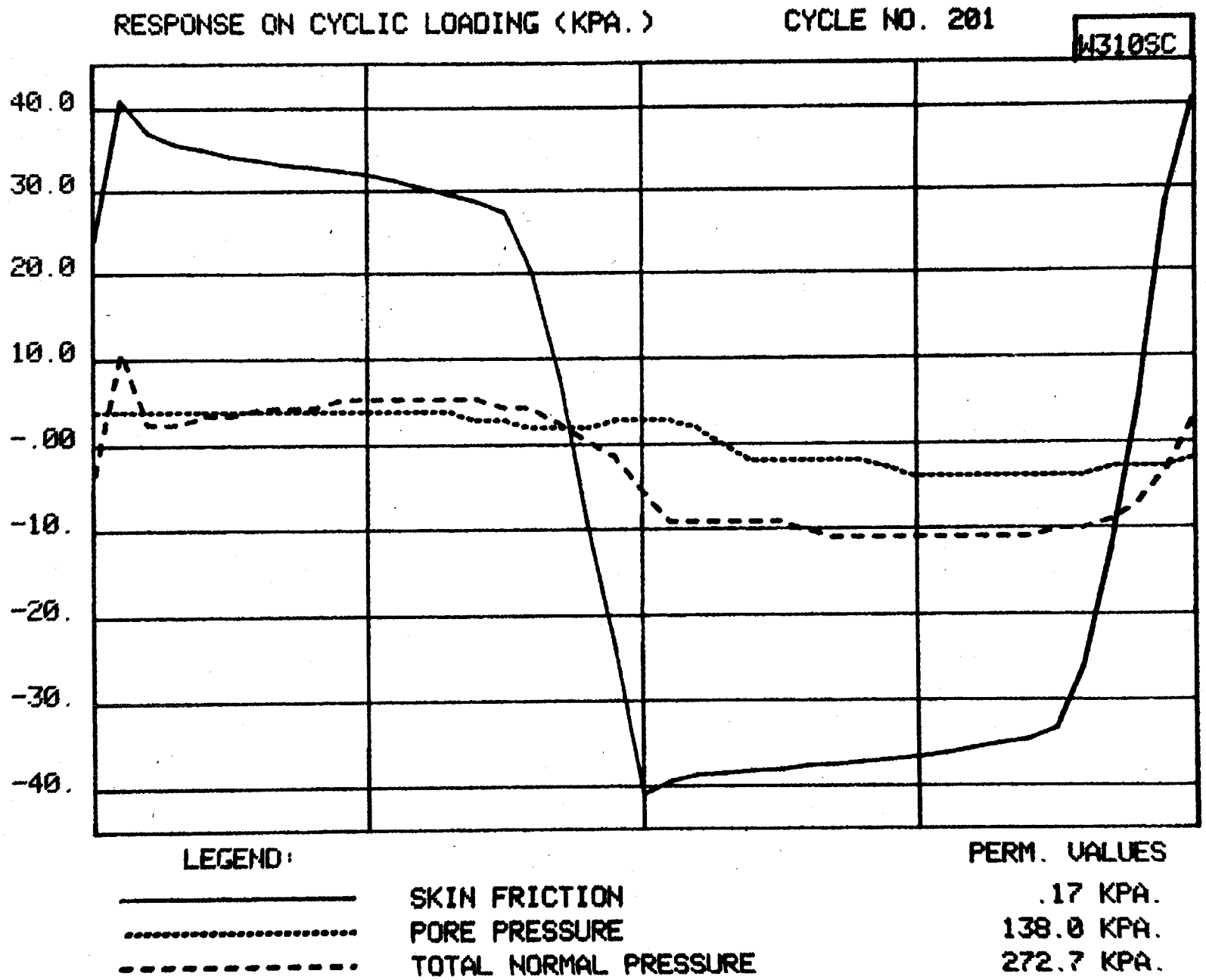
RESPONSE ON CYCLIC LOADING (KPA.)
CYCLE NO. 201
W310SC
40.0
30.0
20.0
10.0
-.00
-10.
-20.
-30.
-40.
LEGEND:
SKIN FRICTION
PORE PRESSURE
TOTAL NORMAL PRESSURE
PERM. VALUES
.17 KPA.
138.0 KPA.
272.7 KPA.

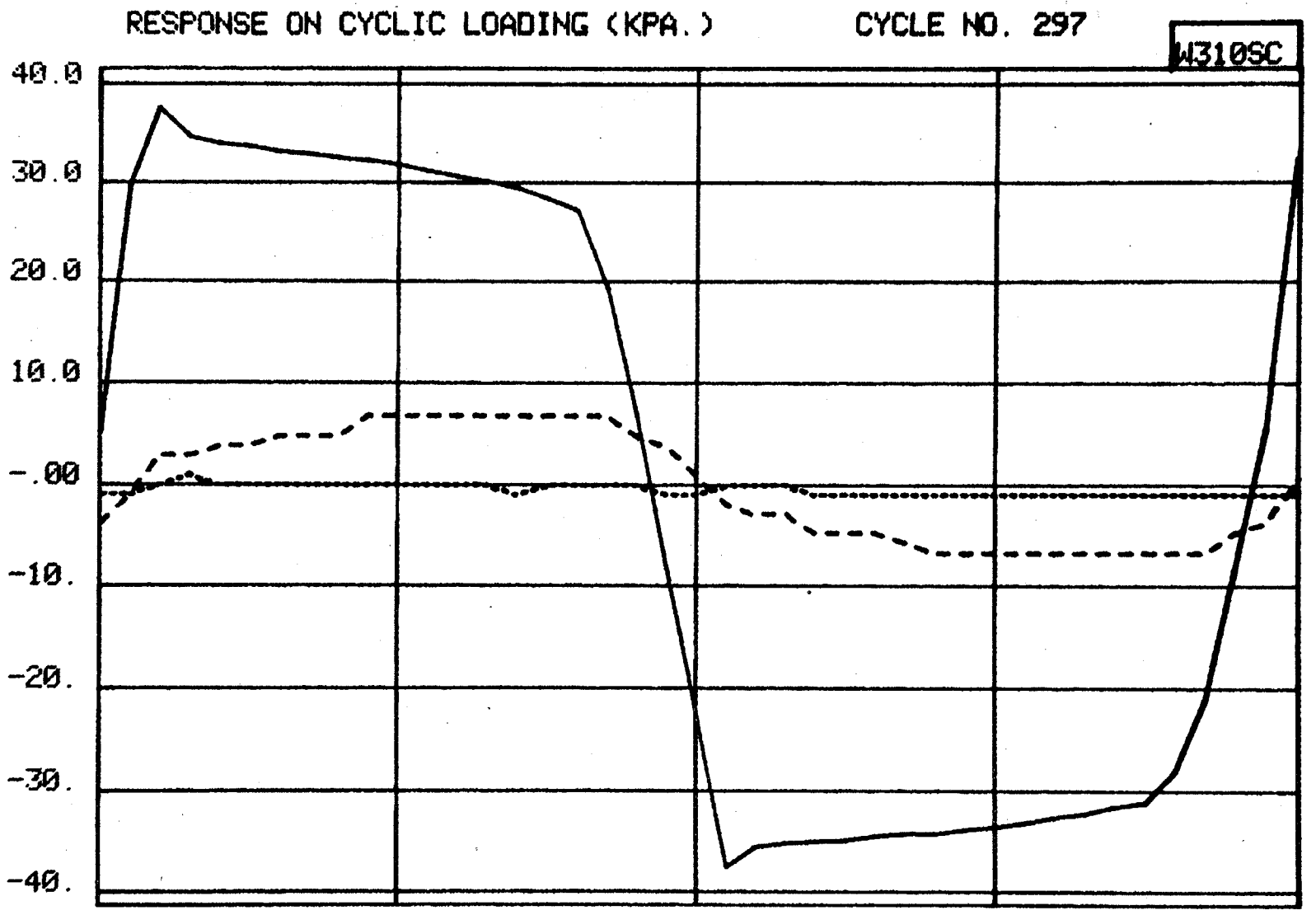

LEGEND:

		PERM. VALUES
———	SKIN FRICTION	-1.32 KPA.
·····	PORE PRESSURE	115.9 KPA.
- - - -	TOTAL NORMAL PRESSURE	270.3 KPA.

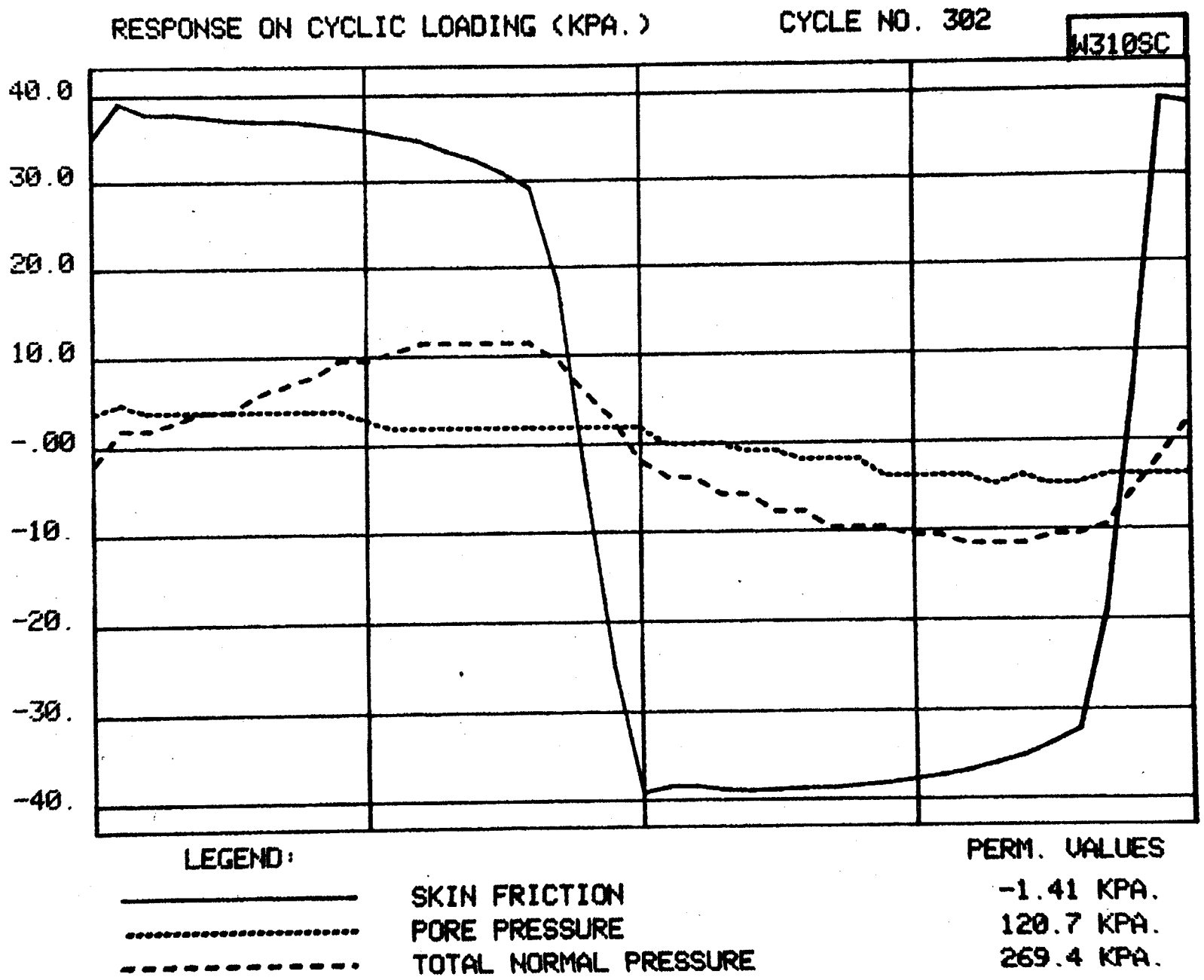
RESPONSE ON CYCLIC LOADING (KPA.)
CYCLE NO. 302
W310SC
40.0
30.0
20.0
10.0
-.00
-10.
-20.
-30.
-40.
LEGEND:
SKIN FRICTION
PORE PRESSURE
TOTAL NORMAL PRESSURE
PERM. VALUES
-1.41 KPA.
120.7 KPA.
269.4 KPA.

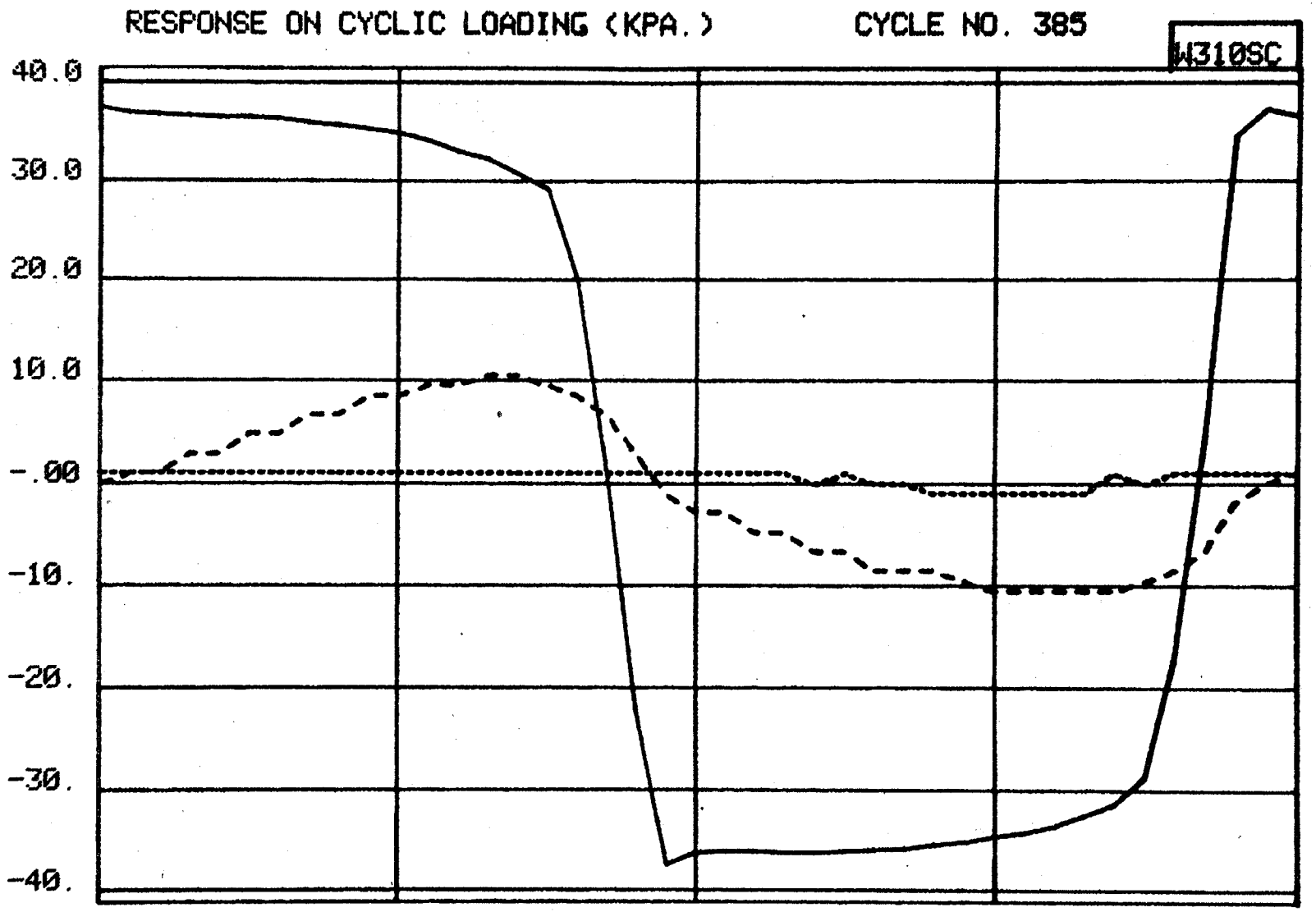

LEGEND:

		PERM. VALUES
———	SKIN FRICTION	-2.70 KPA.
·····	PORE PRESSURE	114.0 KPA.
- - - -	TOTAL NORMAL PRESSURE	272.3 KPA.

APPENDIX H

DETAILED RESULTS FROM **TEST 11, STRATUM II** MODEL PILE TESTS

CONTENTS

Summary	H3
Test 11, Stratum II	H4
Consolidation	H4
Pile Instatllation and Set-Up	H4
Static Test	H5
Cyclic Tests	H5
Stress Controlled Tests (W211LC)	H5
Stroke Controlled Tests (W211SC)	H7
Strength Tests	H8

LIST OF FIGURES

Figure 1	Sample Properties
Figure 2	Consolidation Diagram
Figure 3	Pocket Penetrometer Tests After Consolidation
Figure 4	Pressures at Pile Wall after Installation
Figure 5	Static Test 1
Figure 6	Skin Friction vs no. of Cycles, W211LC
Figure 7	Deflection vs no. of Cycles, W211LC
Figure 8	Total Normal Pressure vs no. of Cycles, W211LC
Figure 9	Pore Pressure vs no. of Cycles, W211LC
Figure 10	Eff. Normal Pressure vs no. of Cycles, W211LC
Figure 11	Skin Friction vs no. of Cycles, W211SC
Figure 12	Deflection vs no. of Cycles, W211SC
Figure 13	Total Normal Pressure vs no. of Cycles, W211SC

Figure 14 Pore Pressure vs no. of Cycles, W211SC
Figure 15 Eff. Normal Pressure vs no. of Cycles, W211SC
Figure 16 Static Test 2
Figure 17 Pocket Penetrometer Tests after Pile Test
Figure 18 Unconfined Compression Tests
Figure 19 Water Content and Shear Strength

Appendix HA
Plotted Results from W211LC
Figures HA-1 through HA-4
Skin Friction vs Deflection, Selected Cycles
Figures HA-5 through HA-6
Skin Friction vs Eff. Normal Pressure, Selected Cycl.
Figures HA-7 through HA-14
Skin Friction, Pore and Total Pressure, Selected Cycles

Appendix HB
Plotted Results from W211SC
Figures HB-1 through HB-3
Skin Friction vs Deflection, Selected Cycles
Figures HB-4 through HB-6
Skin Friction vs Eff. Normal Pressure, Selected Cycl.
Figures HB-7 through HB-16
Skin Friction, Pore and Total Pressure, Selected Cycles

SUMMARY

This report contains the results of the laboratory model pile tests designated TEST 11, STRATUM II, in the project CNRD 13-2, TENSION PILE STUDY, for Conoco Norway Inc.

The clay sample was consolidated for 59 days under 300 kPa applied vertical pressure. Pore pressure in the sample was about 3% of the applied pressure. After 6 days of consolidation in the pile chamber the new modified pile was installed with new pore pressure transducer and modified total pressure transducer. After 15 days of set-up the excess pore pressure was about 175 kPa. Testing was then started.

Static test gave peak friction of 41 kPa with residual value of 32 kPa. Undrained shear strength was interpreted to 60 kPa, giving alpha value of 0.7 and 0.53 for peak and residual respectively. Estimating the effective vertical pressure to 250 kPa results in a beta factor of 0.17 .

Cyclic stress controlled tests which were started two hours following the static test had static tension bias of 14 kPa (40% of previous max. friction in second cycle of static test) and parcels of 100 cycles with specified cyclic stress amplitude increasing for consecutive parcels resulted in failure (abrupt pull-out of pile) in 21st cycle of third parcel. The maximum friction at failure was measured to 33.5 kPa. Stroke controlled cyclic tests with two-way loading was performed after three days of set-up. One parcel of 100 cycles with cyclic displacements of about 1.5 mm was performed. Maximum friction obtained was 40 kPa which reduced to 29 kPa in subsequent cycles. The residual friction during large slip was about 28 kPa.

A static test following the stroke controlled cyclic test gave maximum peak friction of 35 kPa with residual value of 29 kPa.

TEST 11, STRATUM II

CONSOLIDATION

The sample was prepared from the same material as used in Test 5. Water was added during the remoulding process to a water content of about 37% . Horizontal filters were placed in the oedometer to provide better vertical drainage.

A vertical pressure of 300 kPa was applied on top. As seen in Figure 2 the pore pressure at middle height had dropped down to about 3% of the consolidation stress after 59 days. At this time the sample was transferred to the pile chamber. Pocket penetrometer tests were performed on the side of the sample and on the top as shown in Figure 3. The shear strength, s_u, showed an average of about 55 kPa.

PILE INSTALLATION AND SET-UP

After pocket penetrometer tests the sample was mounted in the pile chamber and left to reconsolidate for 6 days under a vertical pressure of 300 kPa and radial pressure of 210 kPa (K=0.7).

As in Test 8 no back pressure was applied and vertical filter strips were placed on the outside perimeter of the clay sample with direct drainage on top and bottom of the pile chamber. Again good drainage was proved by formation of salt on the filter strips sticking out, which came from the expelled water from the marine clay.

During insertion of the pile the side friction was measured to about 20 kPa, the total normal pressure showed about 340 kPa and the pore pressure showed about 260 kPa directly after pile installation. After two days of set-up the pore pressure had reduced to 150 kPa and the total pressure showed 310 kPa. Upon additional consolidation the porepressure started to increase as seen in Figure 4 and reached a peak after seven days of installation at which time it started to decrease again down to about 170 after 15 days upon installation. At this time it was decided to start with the loading program. The total pressure was at this time about 325 kPa. The reason for this increase in pore is not clearly understood.

STATIC TEST

A displacement controlled static test with deformation rate 1 mm per hour was now conducted, as shown in Figure 5. The pile was pulled in tension through failure and large slip and then pushed down to original position causing failure in compression and large slip (residual friction). A new cycle was then performed with the deformation rate increased to 10 mm per hour.

The displacement to cause failure, as shown in Figure 5, was about 0.35 mm or 1.4% of the pile diameter. A maximum friction of 41 kPa was achieved with a residual friction of 32 kPa. These values decreased quite substancially in the second cycle to a peak of about 33 kPa and residual value of 29 kPa. The shear strength of the clay at time of testing was estimated to 60 kPa which results in an alpha (α) value of 0.7 and 0.53 for peak and residual friction respectively.

For the effective stress approach, estimating σ'_{vo} from the relationship

$$s_u = 0.24 \cdot \sigma'_{vo}$$

which gives $\sigma'_{vo} =$ 250 kPa, the beta value (β) becomes 0.17 for maximum friction.

Total pressure on the pile wall at time of failure was about 375 kPa and the pore pressure showed 175 kPa, resulting in a horizontal effective pressure of 200 kPa. The interface friction angle (δ) can then be estimated to 11.6 degrees.

CYCLIC TESTS

After the static test the pile was left to reconsolidate for two hours before cyclic testing was started. The total pressure had now reduced to 352 kPa, and the pore pressure showed 200 kPa.

Stress Controlled Tests (W211LC)

A stress controlled test comprised of applying a prescribed static tensile (uplift) stress on the pile, superimposed with parcels of 100 cycles with 10 seconds period and prescribed cyclic stress amplitude. The stress amplitude was then increased in the

following parcels until failure (excessive uplift) occured in tension.

For this test the static tensile stress (bias) level was about 14 kPa, corresponding to 40% of the previous static capacity (in the second cycle of the static test). In the first parcel the cyclic level was about 7 kPa and in the next parcel the cyclic stress level was incremented by 7 kPa. In the third parcel the stress level was incremented with 6 kPa as can be seen in Figure 6, showing skin friction (envelope of max. and min.) versus cycle numbers. In Figures 7,8,9 and 10 the resulting deformations and pressures due to the applied skin friction are plotted versus cycle numbers. In Appendix A selected cycle numbers are plotted as friction versus deflection, friction versus effective pressure and friction, pore pressure and total pressure variation during one cycle.

As seen in Figure 6 a total of three parcels were performed. The first parcel did not produce any significant deformation of the pile as shown in Figure 7 and in Figure A-1.

The friction deformation behaviour in parcel two as shown in Figure A-2 is linear with only minimal signs of hysteresis. Increasing the cyclic level in parcel three results in larger cyclic deformations and again minimal hysteresis. after 21 cycles the pile suddenly fails as depicted in Figure A-4, and in subsequent cycles the pile cannot produce the prescribed friction. At the same time the pile is pulled up in an attempt to produce this prescribed friction, as can be seen in Figure 7 and in Figure A-4.

From the pressure diagrams in Figures 8,9 and 10 it is seen that the average pressures during the stress controlled cyclic testing stays fairly constant up until time of failure. The total normal pressure shows only small cyclic variations with an average of about 345 kPa, and the pore pressure shows about 200 kPa untill failure occured. At time of failure the total pressure suddenly increased and the pore pressure decreased as seen in Figures 8 and 9. The effective horizontal pressure on the pile therefore stayed fairly constant at 145 kPa up to time of failure at which time it increased. This is also depicted in the "effective stress" plots in Figures A-5 and A-6, where the internal friction angle at point of failure can be measured to 12.6 degrees.

In Figures A-7 through A-14 are shown the cyclic variation of friction, total and pore pressure during one cycle for selected cycle numbers. As seen from these the total pressure shows some cyclic variation whereas the pore pressure does not seem to be affected by this type of loading. Also no sign of build-up of the pore pressure was

seen before failure occured.

Stroke Controlled Tests (W211SC)

After failure in the stress controlled test the pile was brought back to the original position and left to reconsolidate for three days at which time a one parcel of stroke controlled tests were performed. A displacement controlled test comprised of applying 75 cycles with 10 seconds period in two-way cyclic loading from the zero position of the pile. The cyclic displacement amplitude applied was about 1.5 mm.

The applied displacement versus cycle numbers are shown in Figure 12 with the resulting skin friction, total pressure, pore pressure and effective pressure versus cycle number shown in Figures 11, 13, 14 and 15 respectively. More detailed plots of selected cycles are shown in the Appendix B.

As seen from the resulting skin friction in Figure 11 and in Figures B-1 through B-3 the two-way cycling of 1.5mm amplitude causes failure and residual value during large slip. The maximum friction in first cycle was 40 kPa which reduced to 32 kPa after 75 cycles. The residual value stabilized at about 27 kPa. The maximum degradation of strength from maximum friction in first cycle to stable residual value during large slip is therefore 13 kPa or 33 %.

From the pressure diagrams in Figures 13,14 and 15 cyclic variation in both pore and total pressure is seen to take place in the two-way cycling. The total pressure tends to increase in the beginning but the average pressure seems to stabilize after about 10 cycles and throughout the test at about 330 kPa. Again the pore pressure showed good response for this pile and indicated cyclic variations. The cyclic variation during testing was about 10 to 15 kPa for both the pore pressure and total pressure. The resulting effective pressure on the pile wall, Figure 15, shows a small increase in the beginning and steady average values during the rest of the test. The cyclic variation was about 15 to 20 kPa with the average at about 160 kPa.

From the "effective stress diagrams" in Figure B-4 through B-6 the interface friction angle at failure in first cycle was about 14 degrees. Plots of the pressure variation during one cycle can be seen in Figure B-7 through B-16 for selected cycles. Maximum total pressure occurs at maximum cyclic displacement (right before reversal of load on

the pile) whereas the pore pressure tends to show an increase when the pile is pulled up and a decrease when pushed down.

STRENGTH TESTS

After the stroke controlled test a new static test was performed after two hours of set-up, with results shown Figure 16. Maximum friction obtained was 35 kPa with a residual of 29 kPa. The pile was then pulled out of the pile chamber and the sample built out. Pocket penetrometer tests were performed on the side of the sample and in two horizontal layers with results shown in Figure 17.

Three standard triaxial test samples were then prepared from the center of the clay specimen and unconfined compression tests (UCT) were performed with the results shown in Figure 18.

In Figure 19 are shown the water content and interpreted undrained shear strength of the clay sample versus the distance from the center after completion of the pile test. The water content showed about 30 % with a tendency to decrease towards the center.

TABLE 1.

SAMPLE PROPERTIES TEST 11, STRATUM II

SAMPLE PREPARATION		CONSOLIDATION			END OF PILE TEST
INITIAL WATER CONTENT	INITIAL HEIGHT	AXIAL DEFORMATION	AXIAL STRAIN	WATER CONTENT	WATER CONTENT
w_i (%)	H_o (cm)	ΔH (cm)	ε (%)	w_e (%)	w_{ep} (%)
36.27 38.47	49.57	4.22	8.51	-	A-29.01 D-29.34 B-29.29 E-30.21 C-30.39 F-29.72

CONFINING PRESSURE		
AXIAL	KPa	300
RADIAL	KPa	210
BACK PRESSURE	KPa	0
SAMPLE CONSOLIDATION		
IN OEDOMETER	Days	59
IN PILE CHAMBER	Days	6
INTERPRETED SHEAR STRENGTH		
END OF CONSOLIDATION	KPa	55
END OF PILE TEST	KPa	60

Fig.1

CONSOLIDATION DIAGRAM								Test No. 11 Stratum II		Start date	
H_i 49.57 cm		H_e 45.35 cm		$\Delta\varepsilon_v$ 8.51 %						σ_c 300 kPa	
Time h	4	23	47	70	6 d	9 d	10 d	16 d	31 d	48 d	59 d
Δh cm	0.18	1.14	2.04	2.44	3.13	3.53	3.62	3.84	4.17	4.21	4.22
u kPa	3.8	28	157	184	155	132	126	95	54.4	15.8	8.7

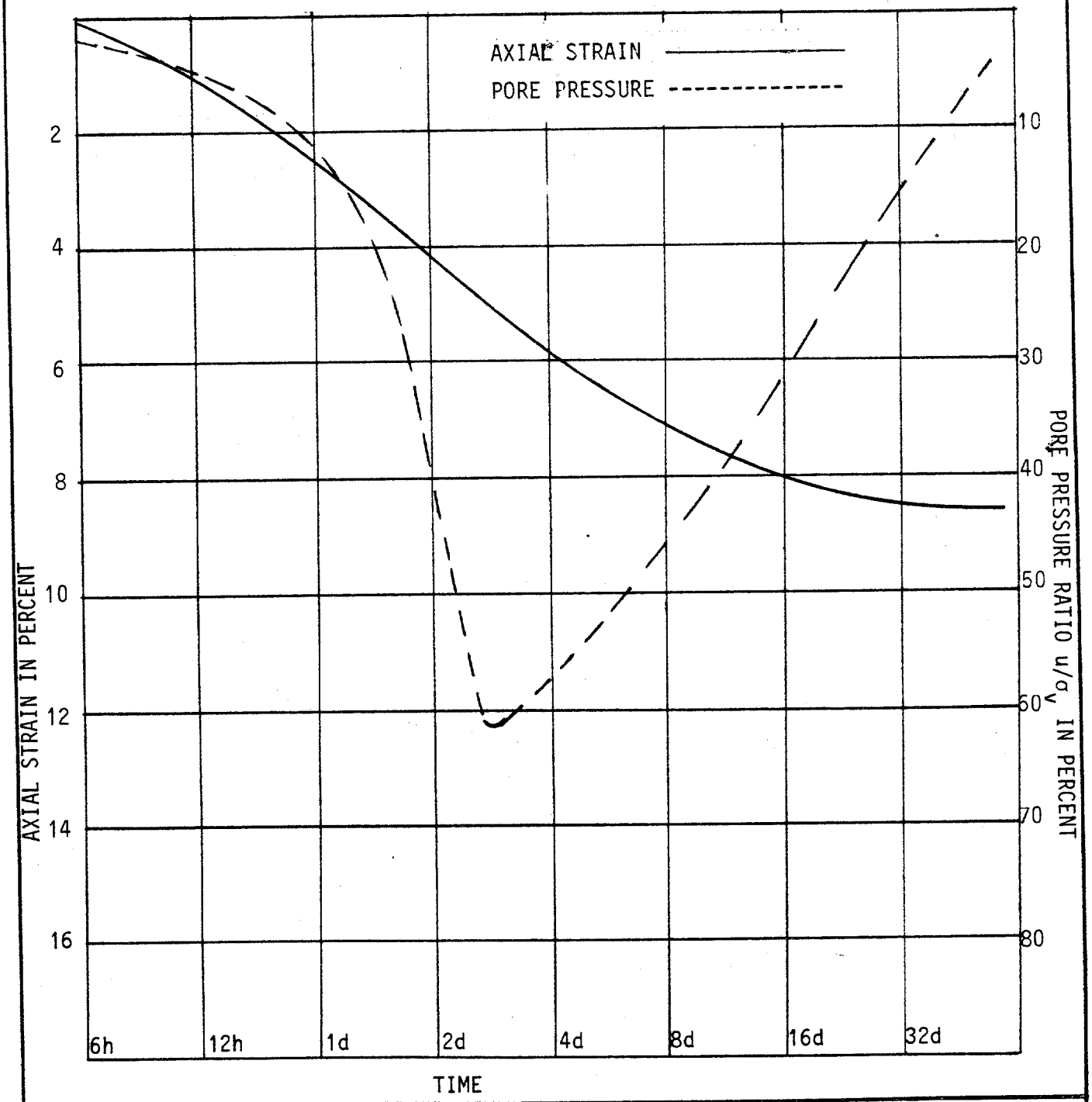

CNRD 13-2 TENSION PILE STUDY LABORATORY MODEL PILE TESTS

TEST 11, STRATUM II, Consolidation diagrams for clay sample

DET NORSKE VERITAS
Geotechnical Laboratory

Scale

Drawn by

Date

Approved

Fig. No. 2

TEST 11, STRATUM II

SHEAR STRENGTH (kPa) FROM POCKET PENETROMETER TESTS AFTER CONSOLIDATION

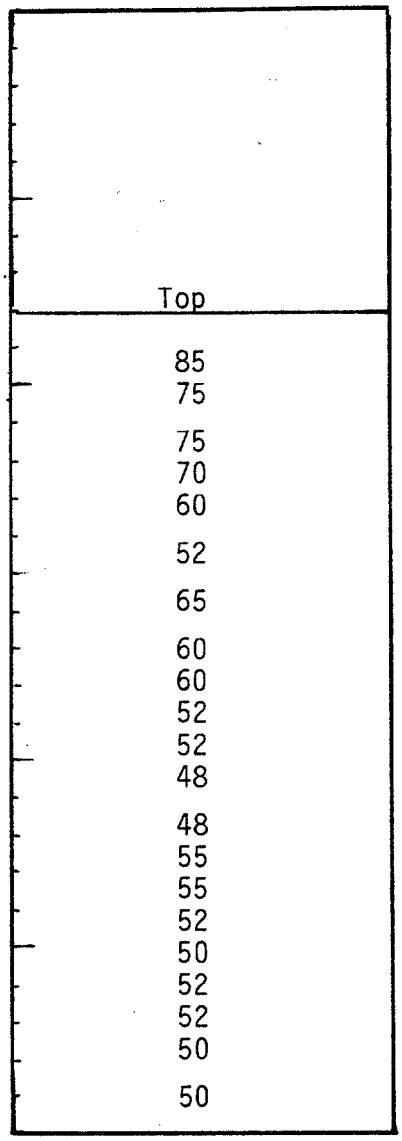

Scale 1:4

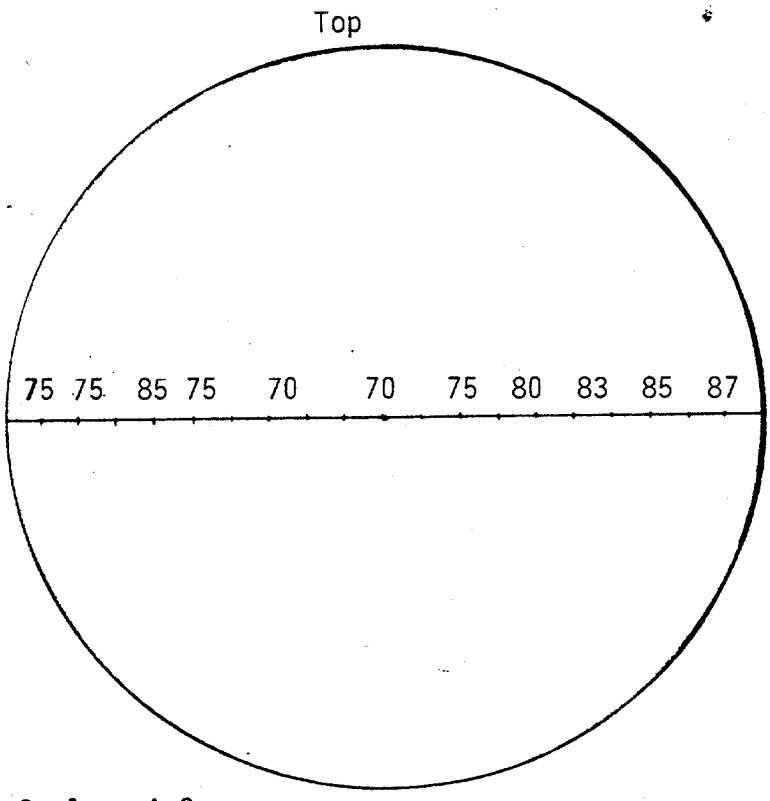

Scale: 1:2

CNRD 13-2 TENSION PILE STUDY LABORATORY MODEL PILE TESTS

TEST 11, STRATUM II, Pocket penetrometer tests after consolidation

DET NORSKE VERITAS Geotechnical Laboratory	Drawn by	Scale
	Approved	Date
		Fig. No. 3

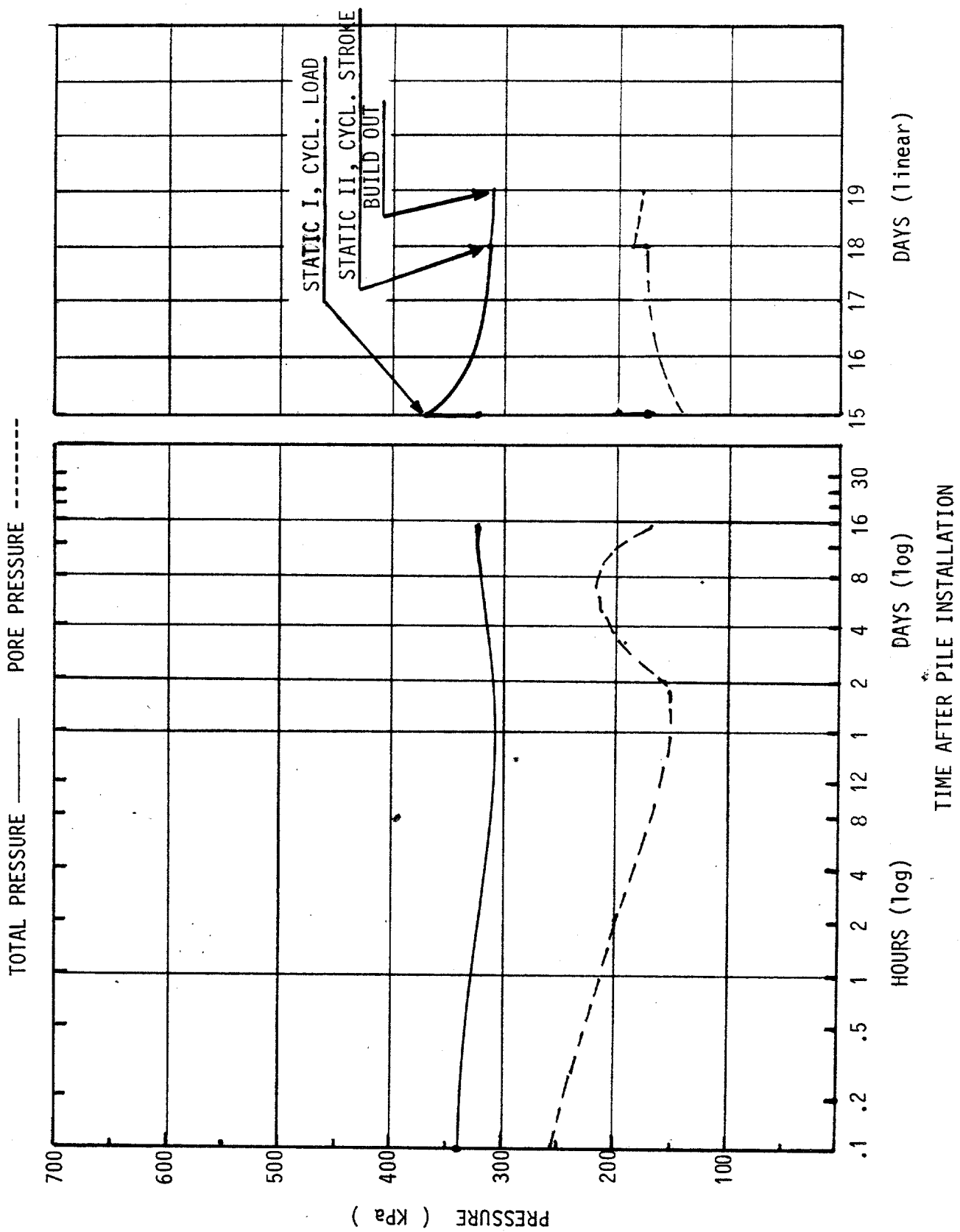

CNRD 13-2 TENSION PILE STUDY LABORATORY MODEL PILE TESTS

TEST 11, STRATUM II, Pressures at pile wall after installation

DET NORSKE VERITAS Geotechnical Laboratory	Drawn by	Scale
	Approved	Date
		Fig. No. 4

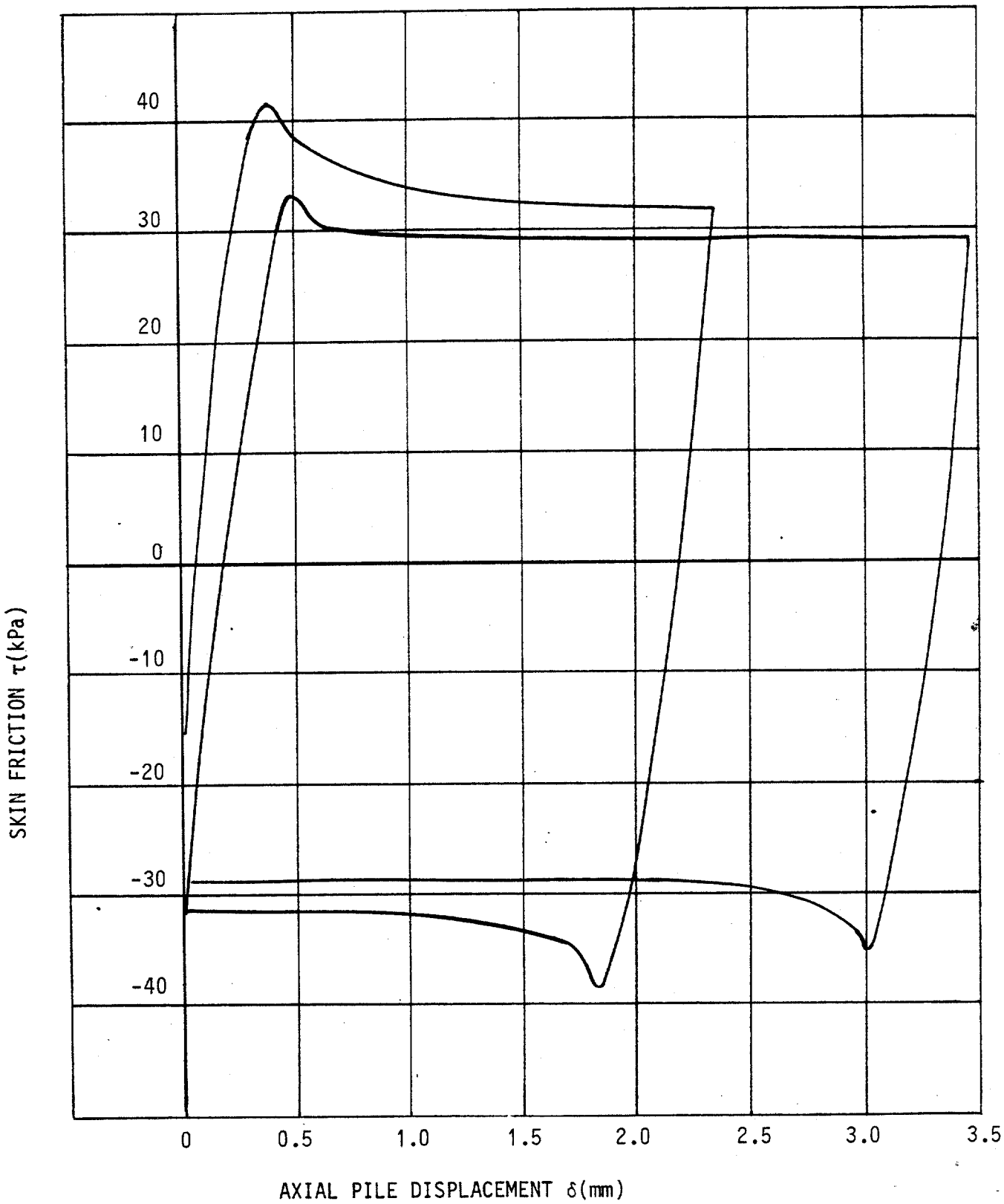

CNRD 13-2 TENSION PILE STUDY LABORATORY MODEL PILE TESTS

TEST 11, STRATUM II STATIC TEST I

DET NORSKE VERITAS Geotechnical Laboratory	Drawn by	Scale
	Approved	Date
		Fig. No. 5

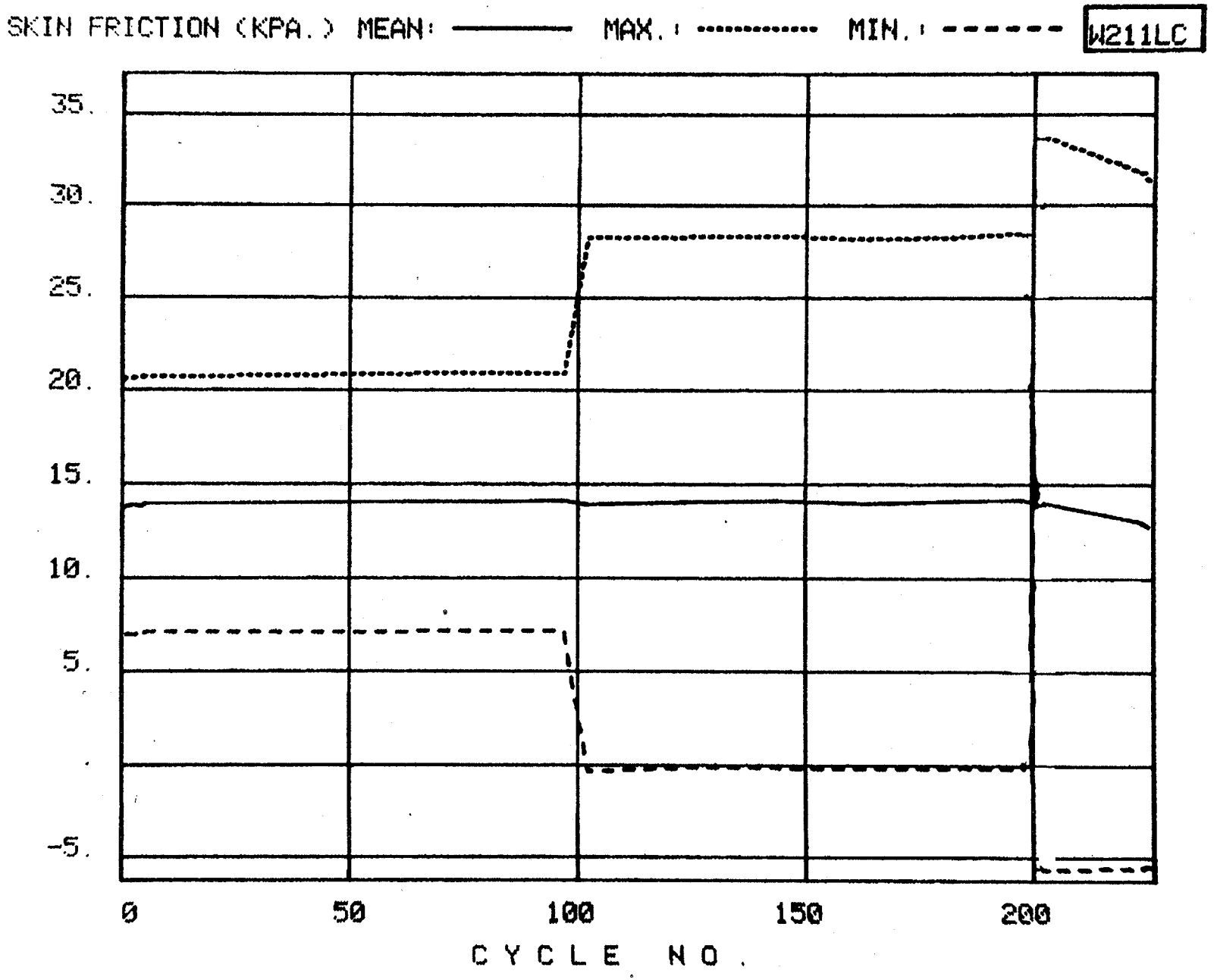
SKIN FRICTION (KPA.) MEAN: MAX.: MIN.:
W211LC
35.
30.
25.
20.
15.
10.
5.
-5.
0
50
100
150
200
CYCLE NO.

Fig.6

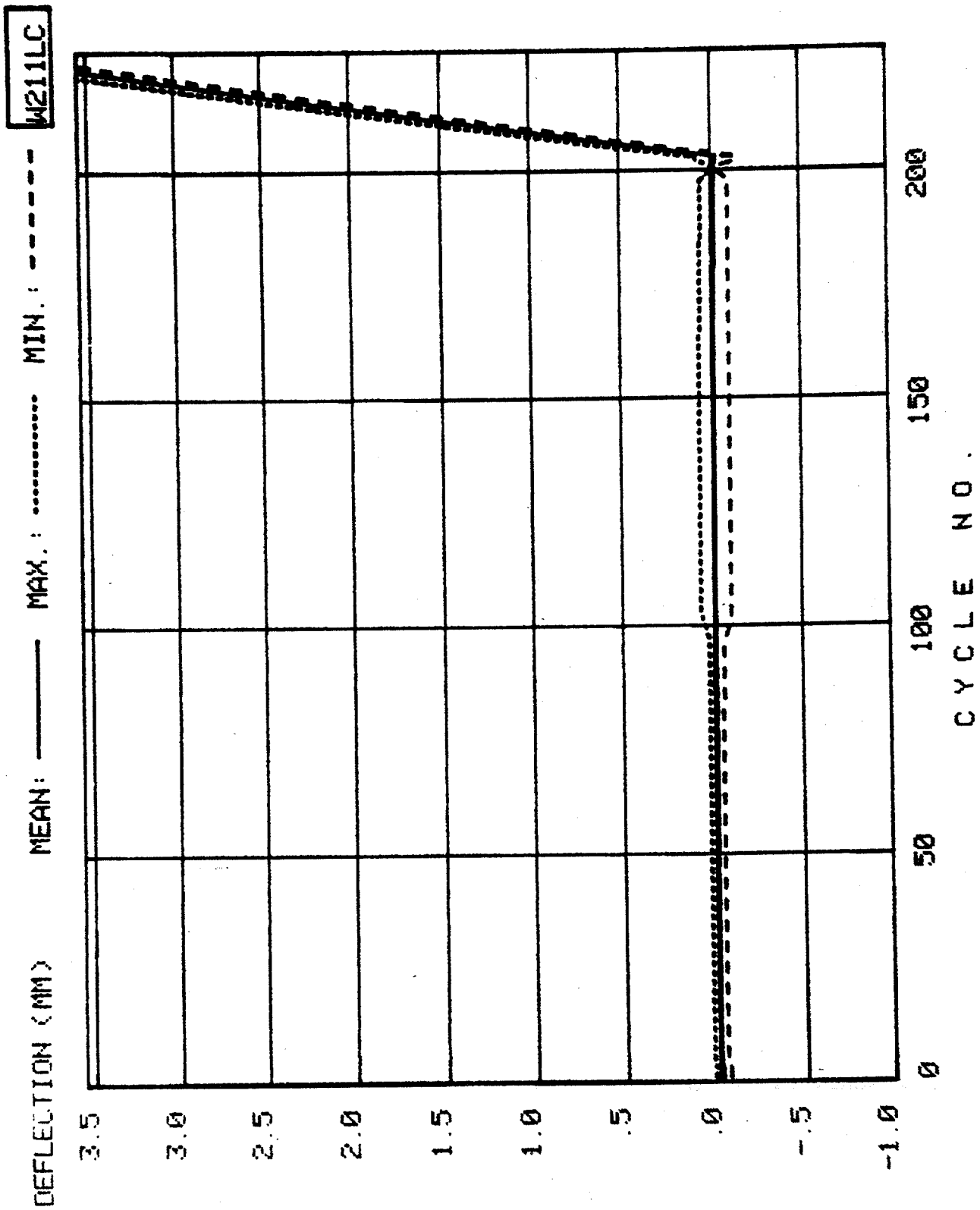
W211LC
MEAN: ——— MAX.: ..... MIN.: - - - - - -
DEFLECTION (MM)
3.5
3.0
2.5
2.0
1.5
1.0
.5
0.0
-.5
-1.0
0
50
100
150
200
CYCLE NO.

Fig.7

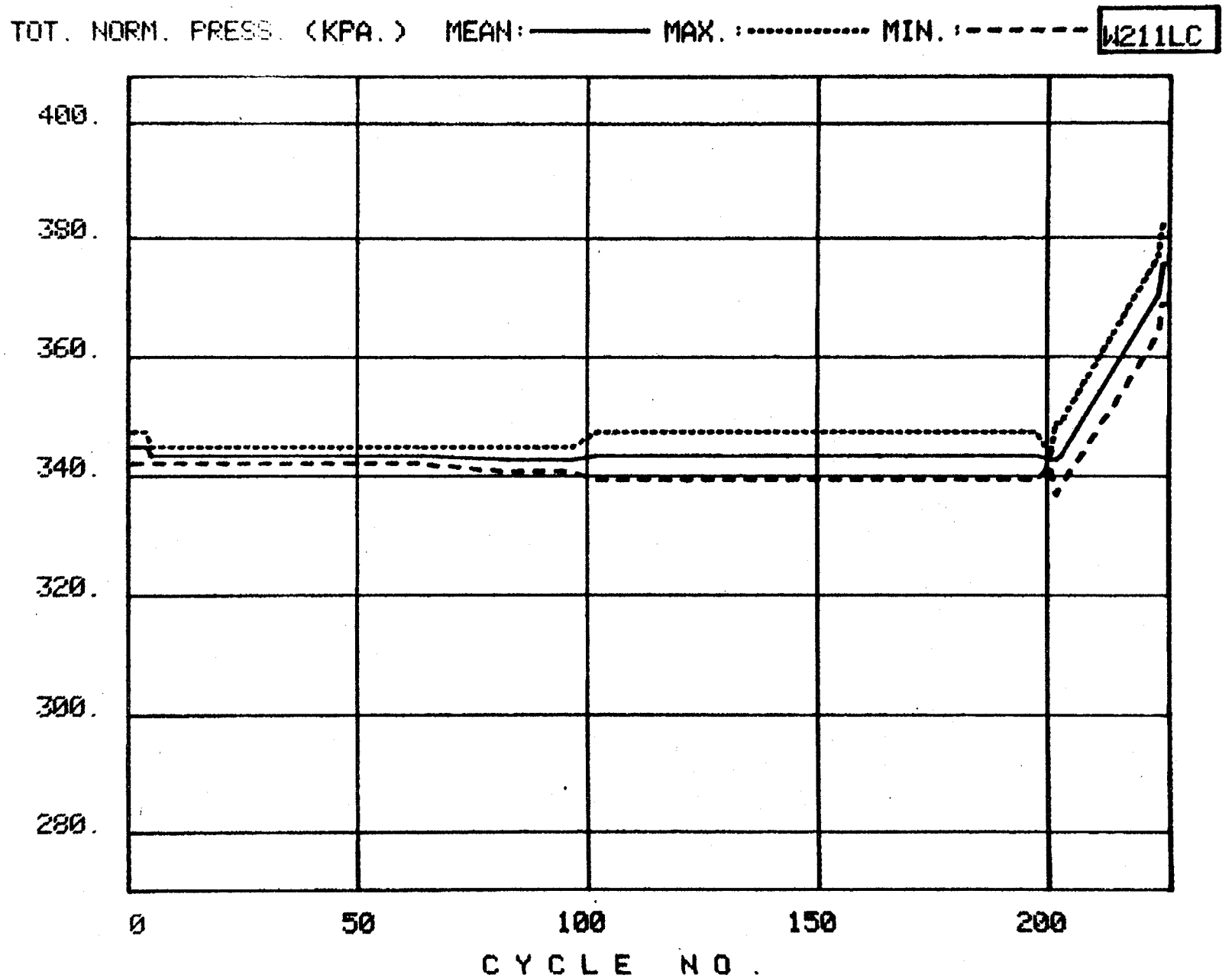
TOT. NORM. PRESS. (KPA.) MEAN: MAX.: MIN.:
W211LC
400.
380.
360.
340.
320.
300.
280.
0
50
100
150
200
CYCLE NO.

Fig.8

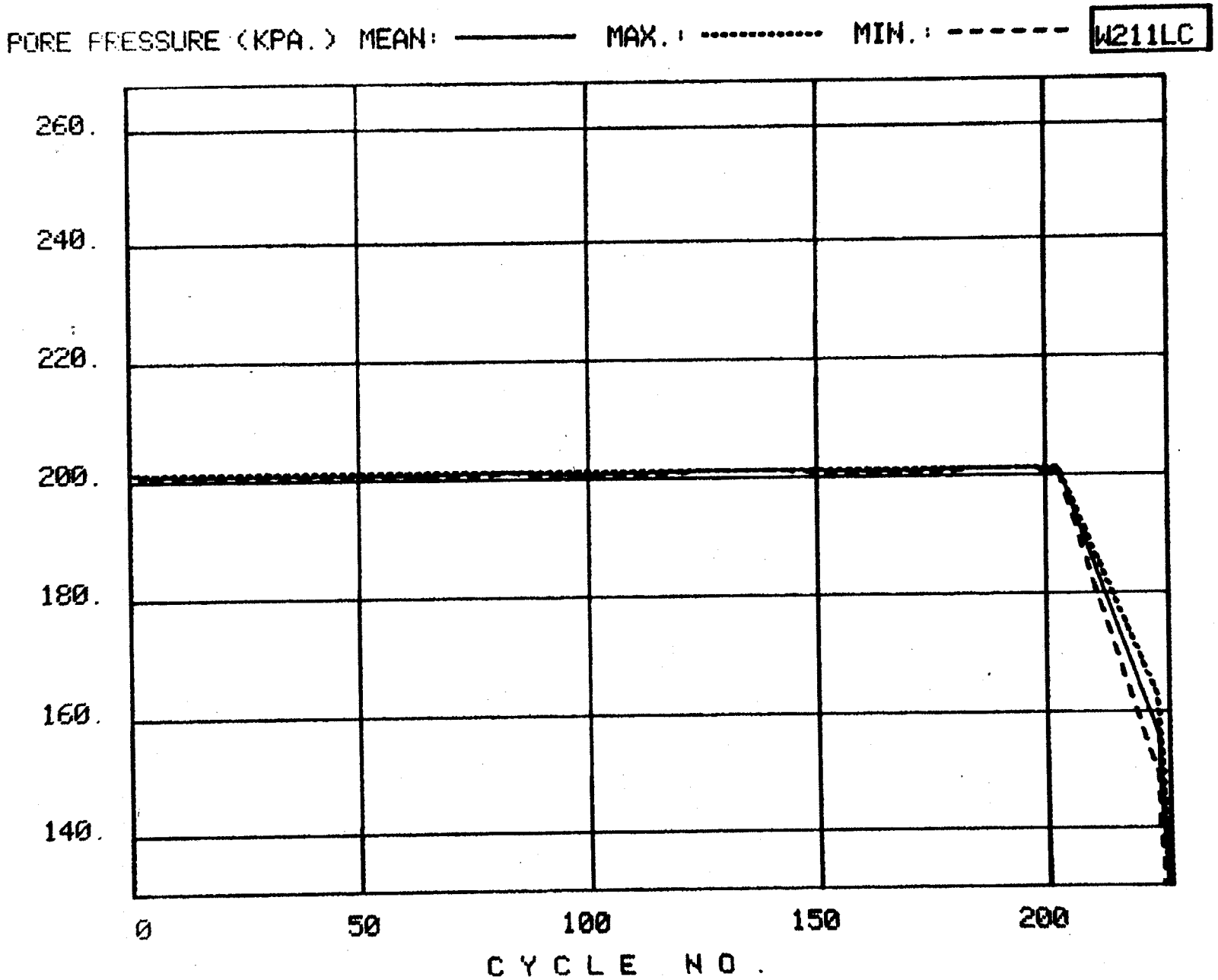
PORE PRESSURE (KPA.) MEAN: MAX.: MIN.:
W211LC
260.
240.
220.
200.
180.
160.
140.
0
50
100
150
200
CYCLE NO.

Fig.9

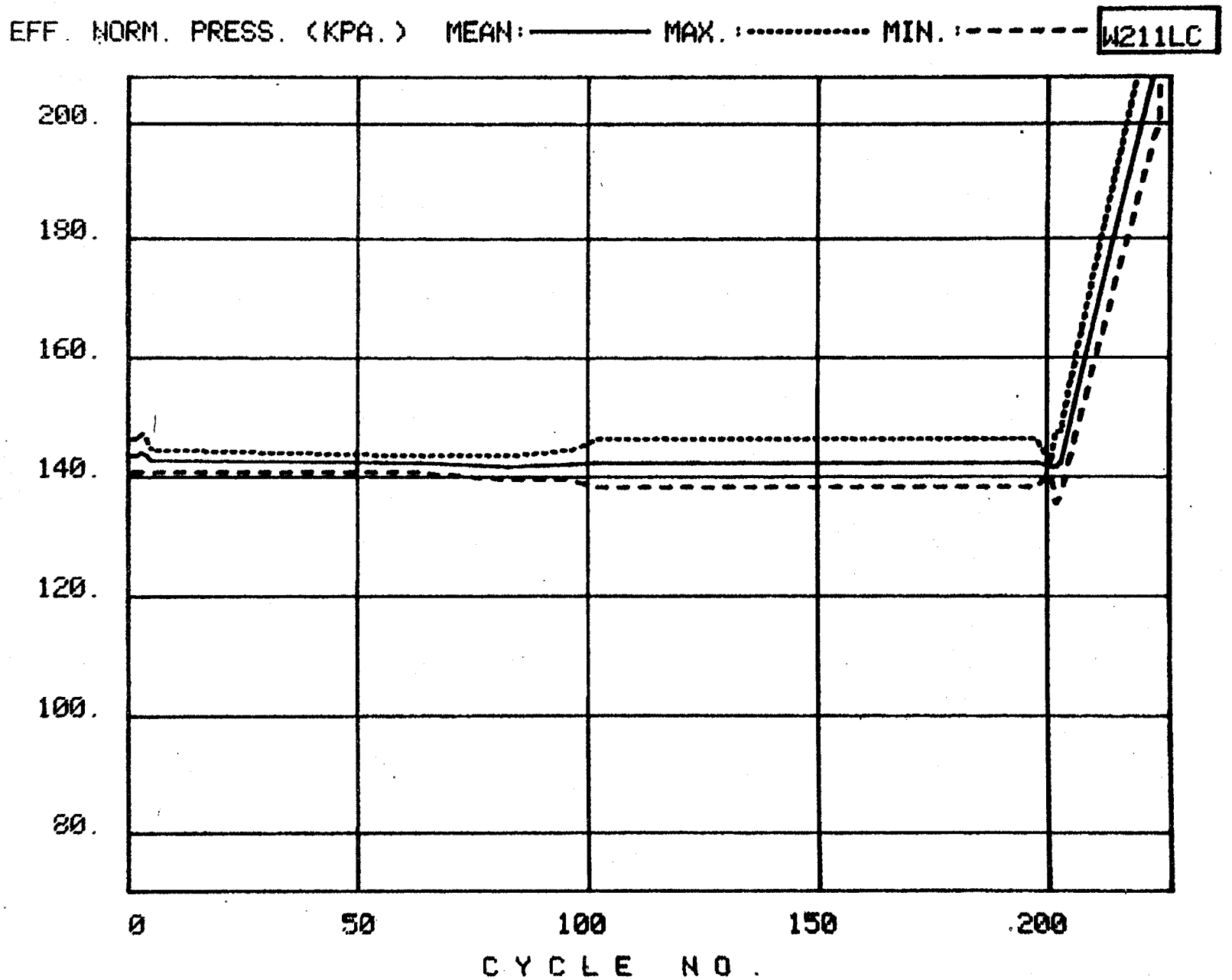
EFF. NORM. PRESS. (KPA.) MEAN: MAX.: MIN.:
W211LC
200.
180.
160.
140.
120.
100.
80.
0
50
100
150
200
CYCLE NO.

Fig.10

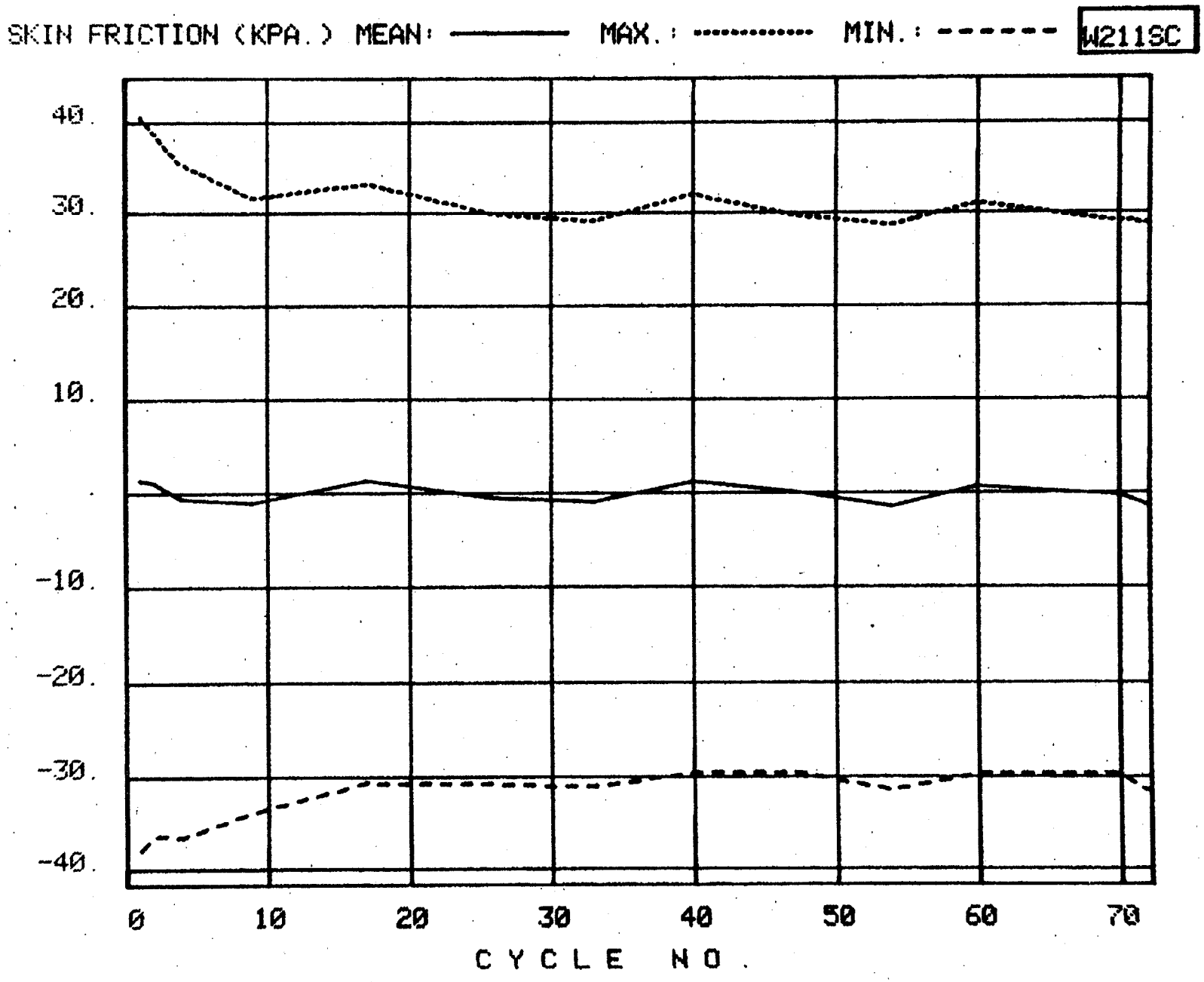
SKIN FRICTION (KPA.) MEAN: MAX.: MIN.:
W211SC
40.
30.
20.
10.
-10.
-20.
-30.
-40.
0
10
20
30
40
50
60
70
CYCLE NO.

Fig.11

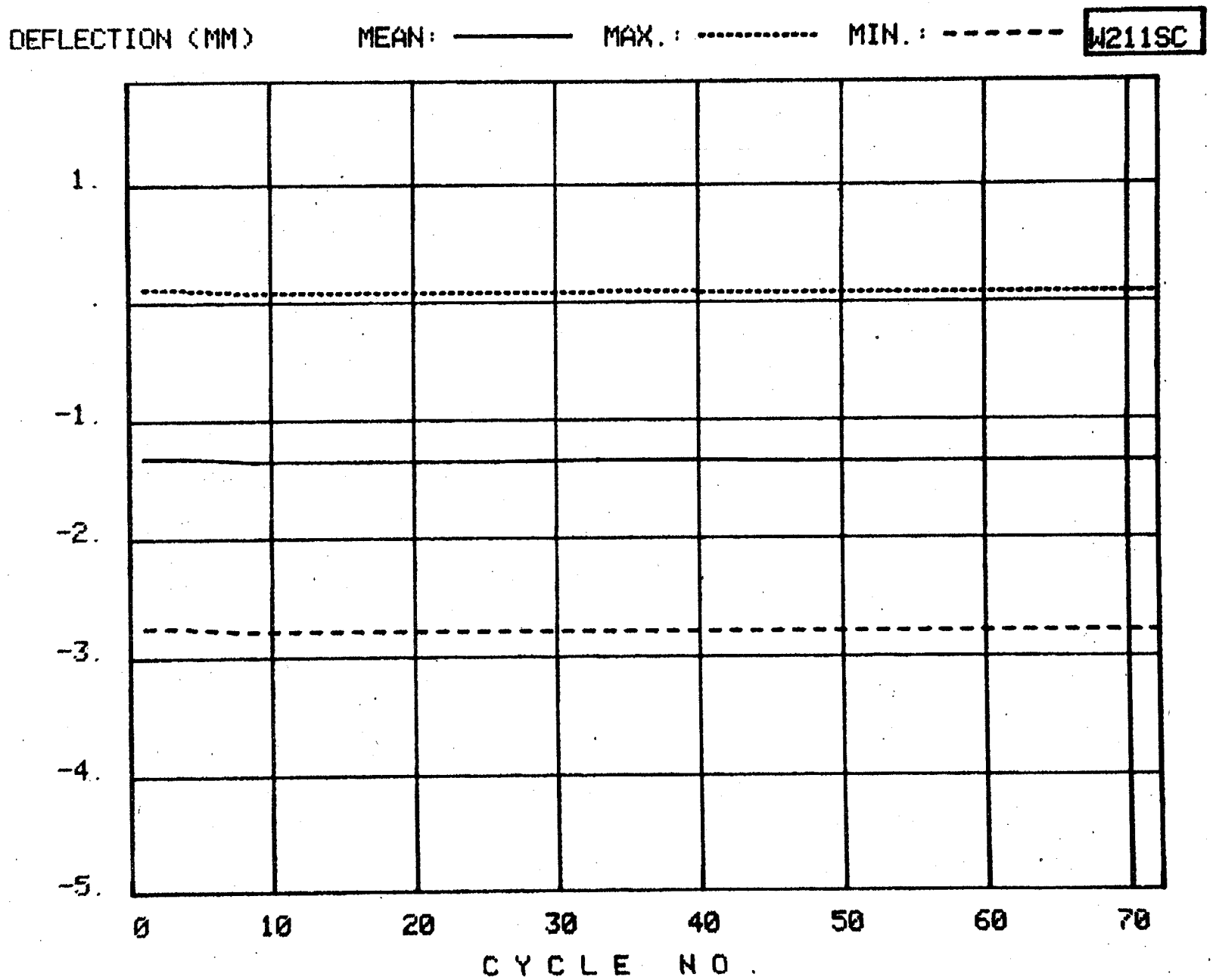
DEFLECTION (MM)
MEAN:
MAX.:
MIN.:
W211SC
1.
-1.
-2.
-3.
-4.
-5.
0
10
20
30
40
50
60
70
CYCLE NO.

Fig.12

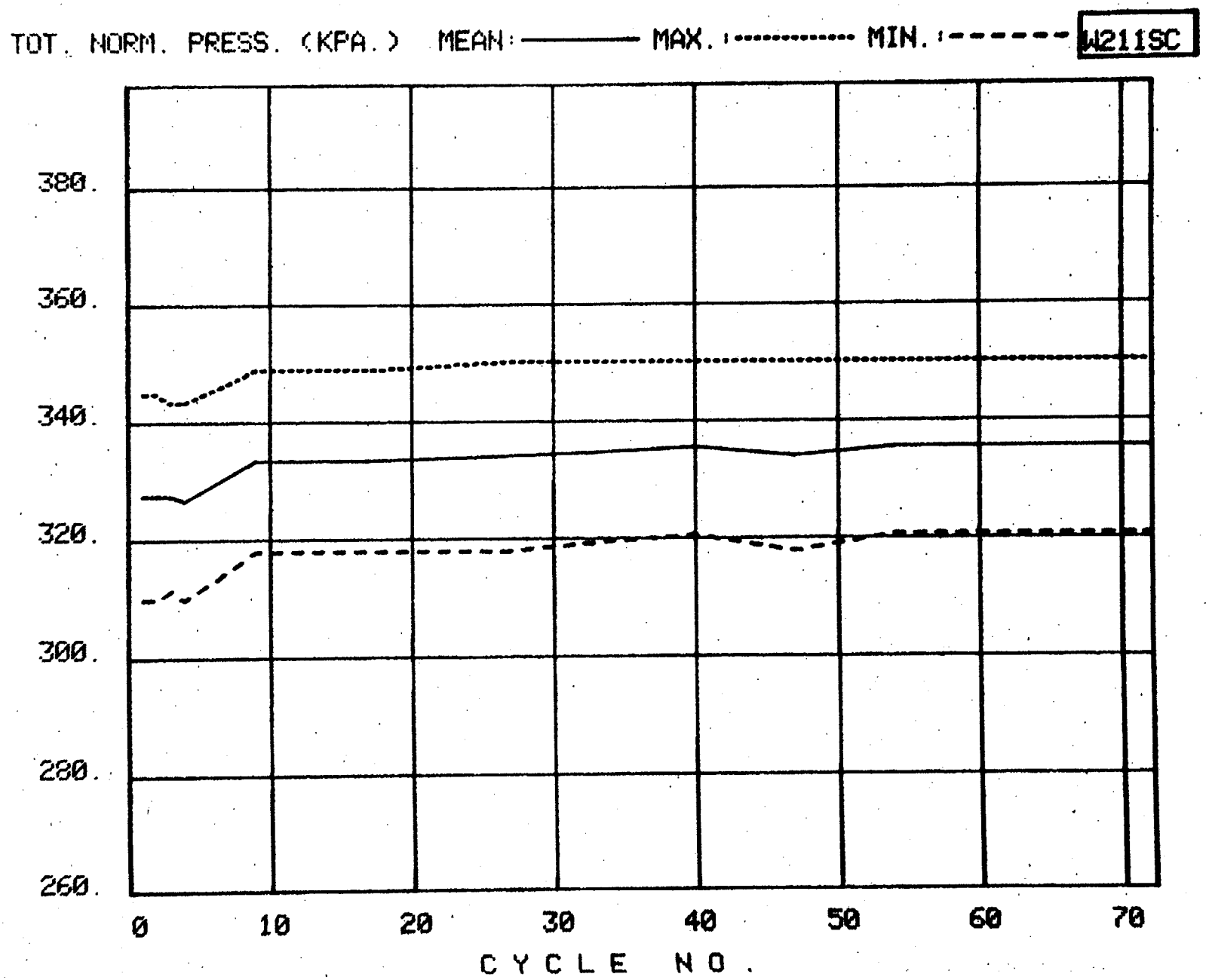
TOT. NORM. PRESS. (KPA.) MEAN: MAX.: MIN.:
W211SC
380.
360.
340.
320.
300.
280.
260.
0
10
20
30
40
50
60
70
CYCLE NO.

Fig.13

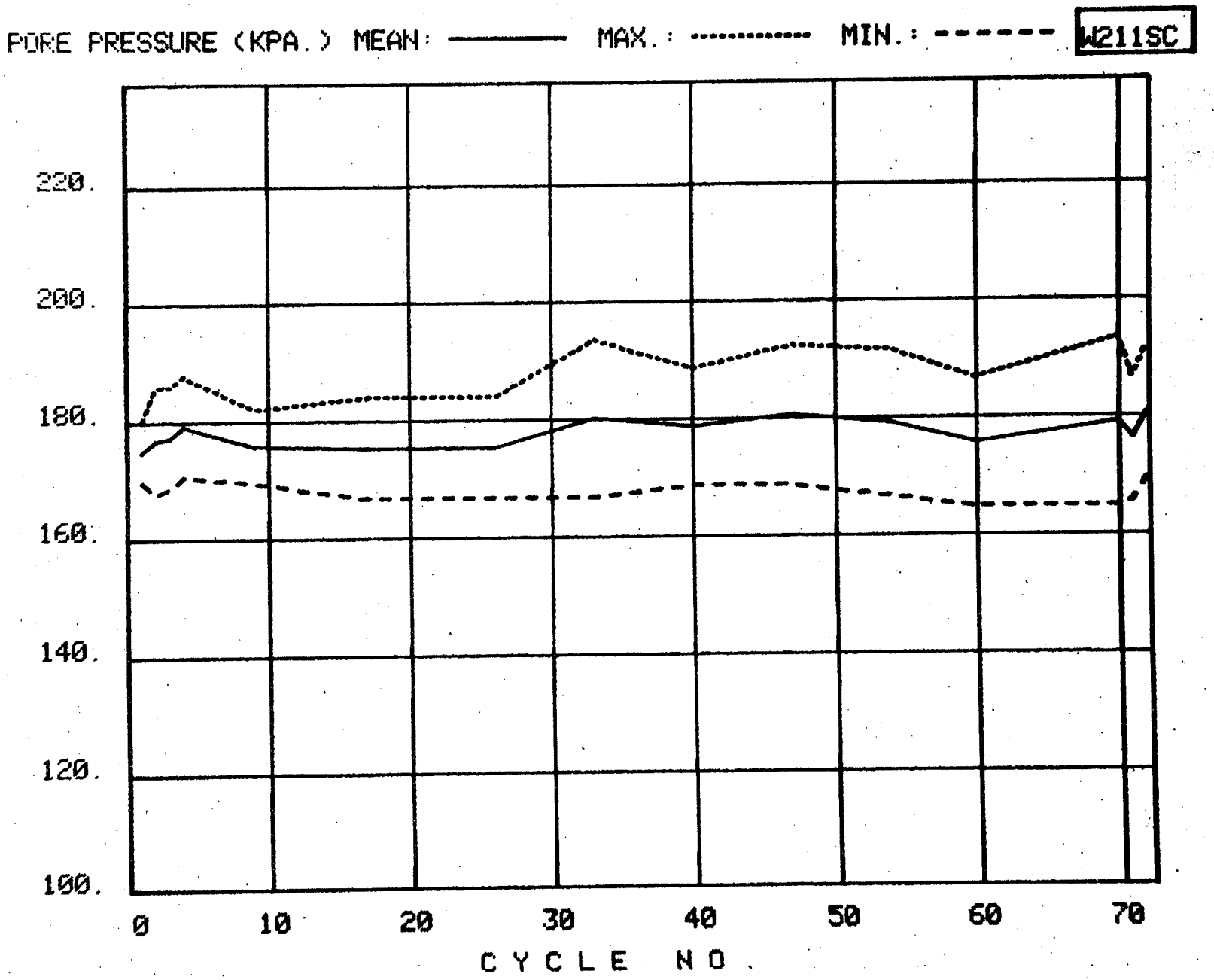
PORE PRESSURE (KPA.) MEAN: ——— MAX.: ····· MIN.: - - - - - -
W211SC
220.
200.
180.
160.
140.
120.
100.
0
10
20
30
40
50
60
70
CYCLE NO.

Fig.14

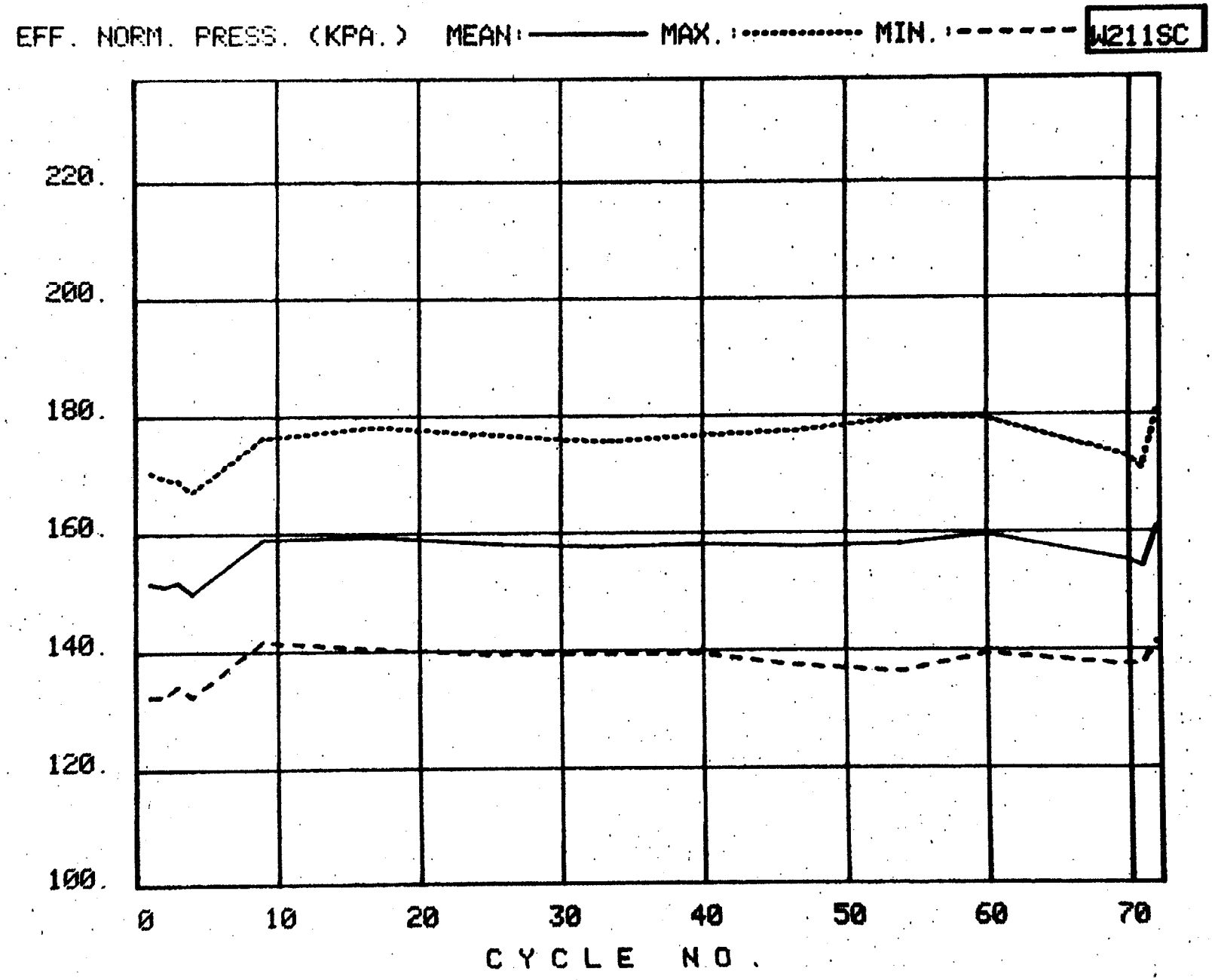
EFF. NORM. PRESS. (KPA.)
MEAN:
MAX.:
MIN.:
W211SC
220.
200.
180.
160.
140.
120.
100.
0
10
20
30
40
50
60
70
CYCLE NO.

Fig.15

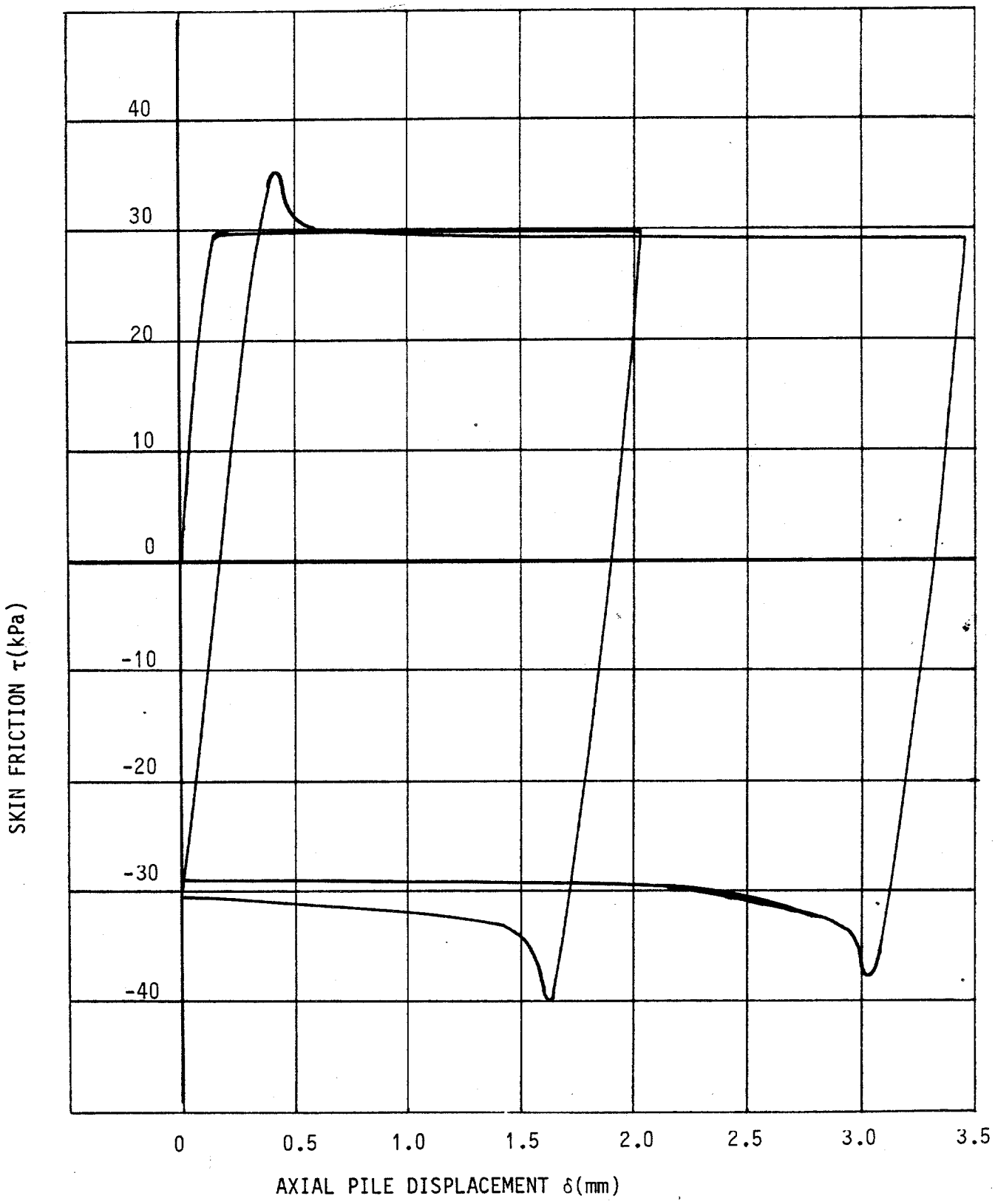

CNRD 13-2 TENSION PILE STUDY LABORATORY MODEL PILE TESTS

TEST 11, STRATUM II, STATIC TEST II

DET NORSKE VERITAS Geotechnical Laboratory	Drawn by	Scale
	Approved	Date
		Fig. No. 16

TEST 11, STRATUM II

SHEAR STRENGTH (kPa) FROM POCKET PENETROMETER TESTS AFTER PILE TEST

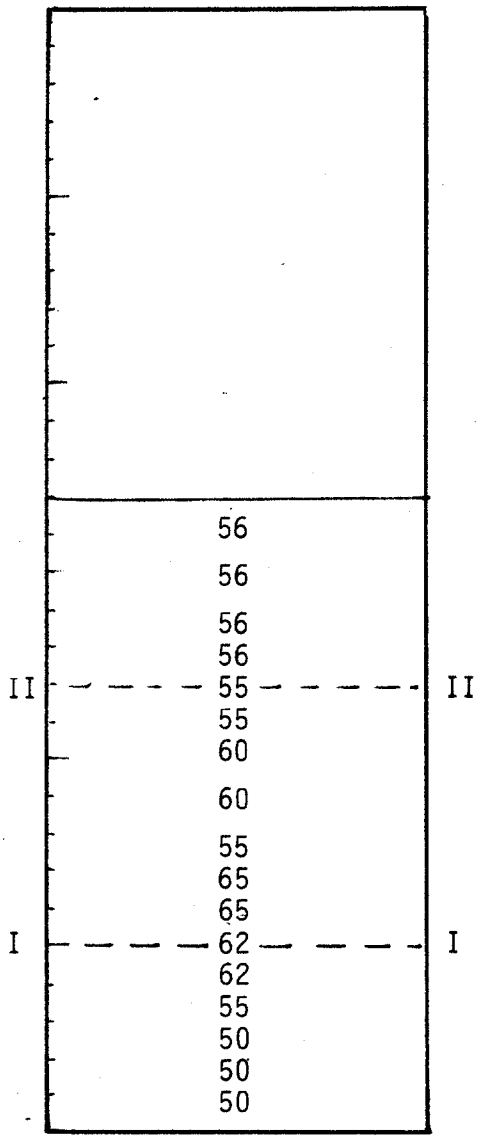

Scale 1:4

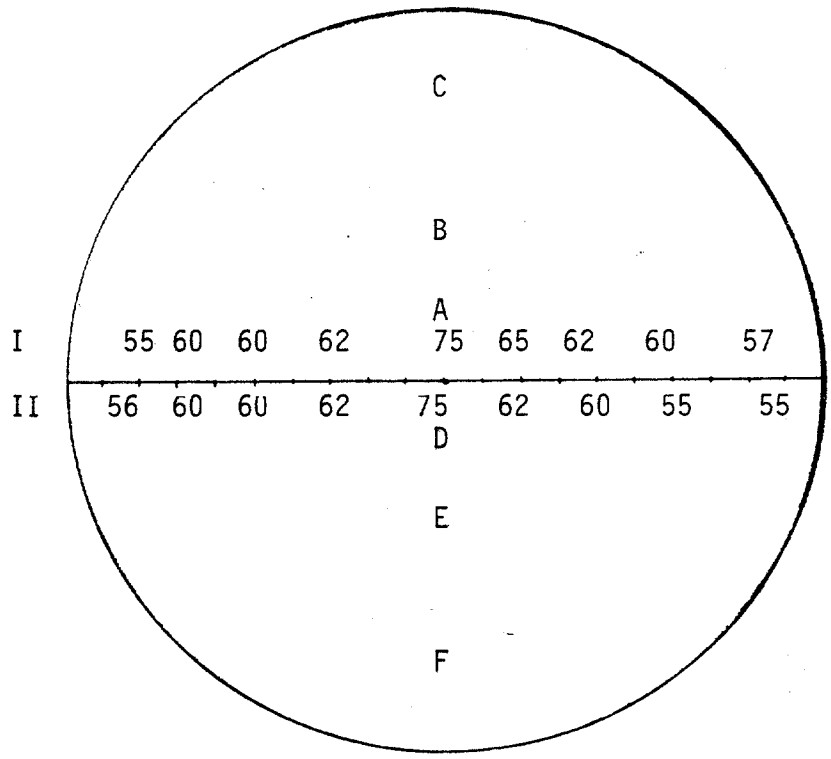

Scale: 1:2

CNRD 13-2 TENSION PILE STUDY LABORATORY MODEL PILE TESTS

TEST 11, STRATUM II, Pocket penetrometer tests after pile test

DET NORSKE VERITAS Geotechnical Laboratory	Drawn by	Scale
	Approved	Date
		Fig.No. 17

Unconfined Compression Test
on material after Pile Test
completed

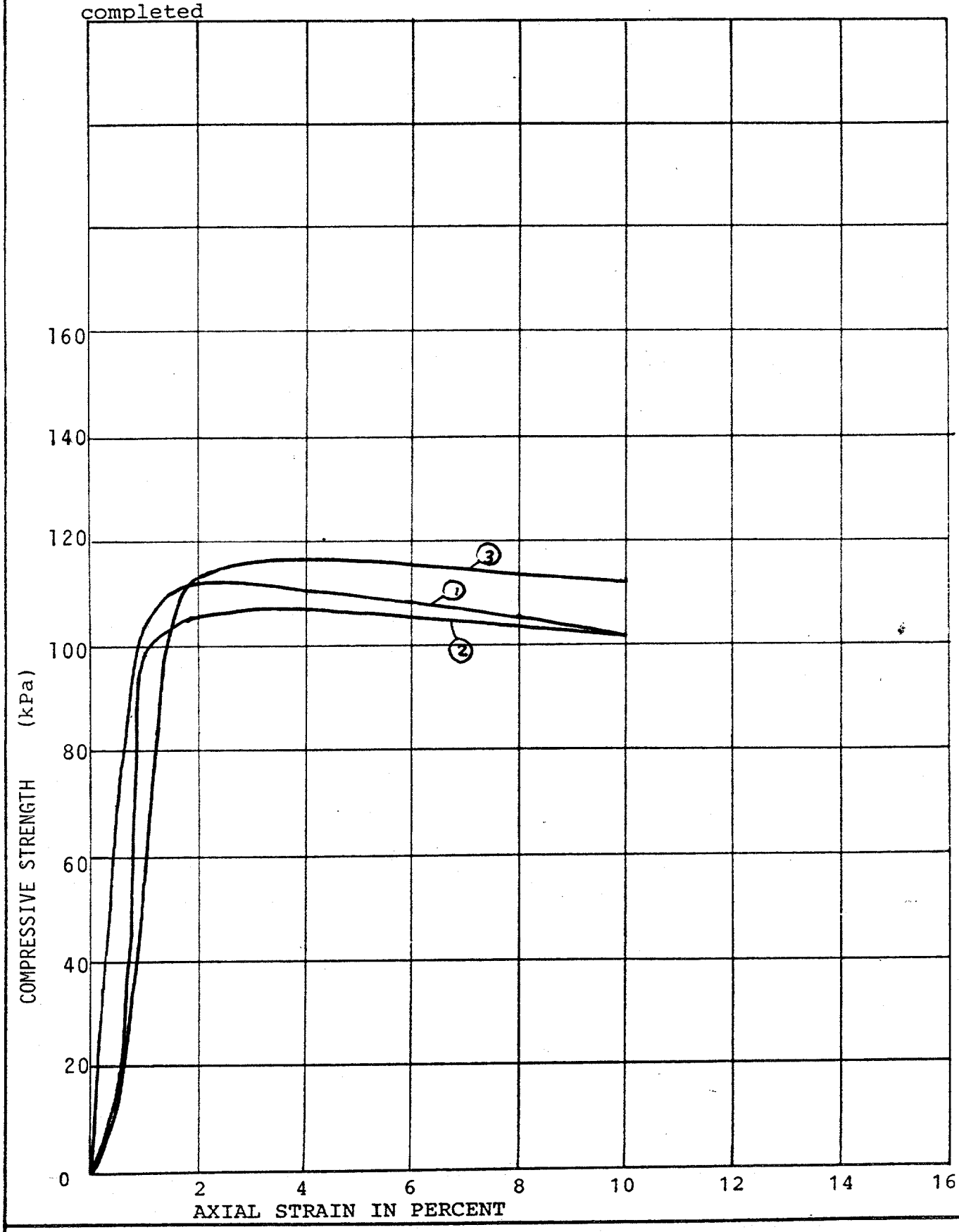

CNRD 13-2 TENSION PILE STUDY LABORATORY MODEL PILE TESTS

TEST 11, STRATUM II, Unconfined compression tests after pile test

DET NORSKE VERITAS Geotechnical Laboratory	Drawn by	Scale
	Approved	Date
		Fig. No. 18

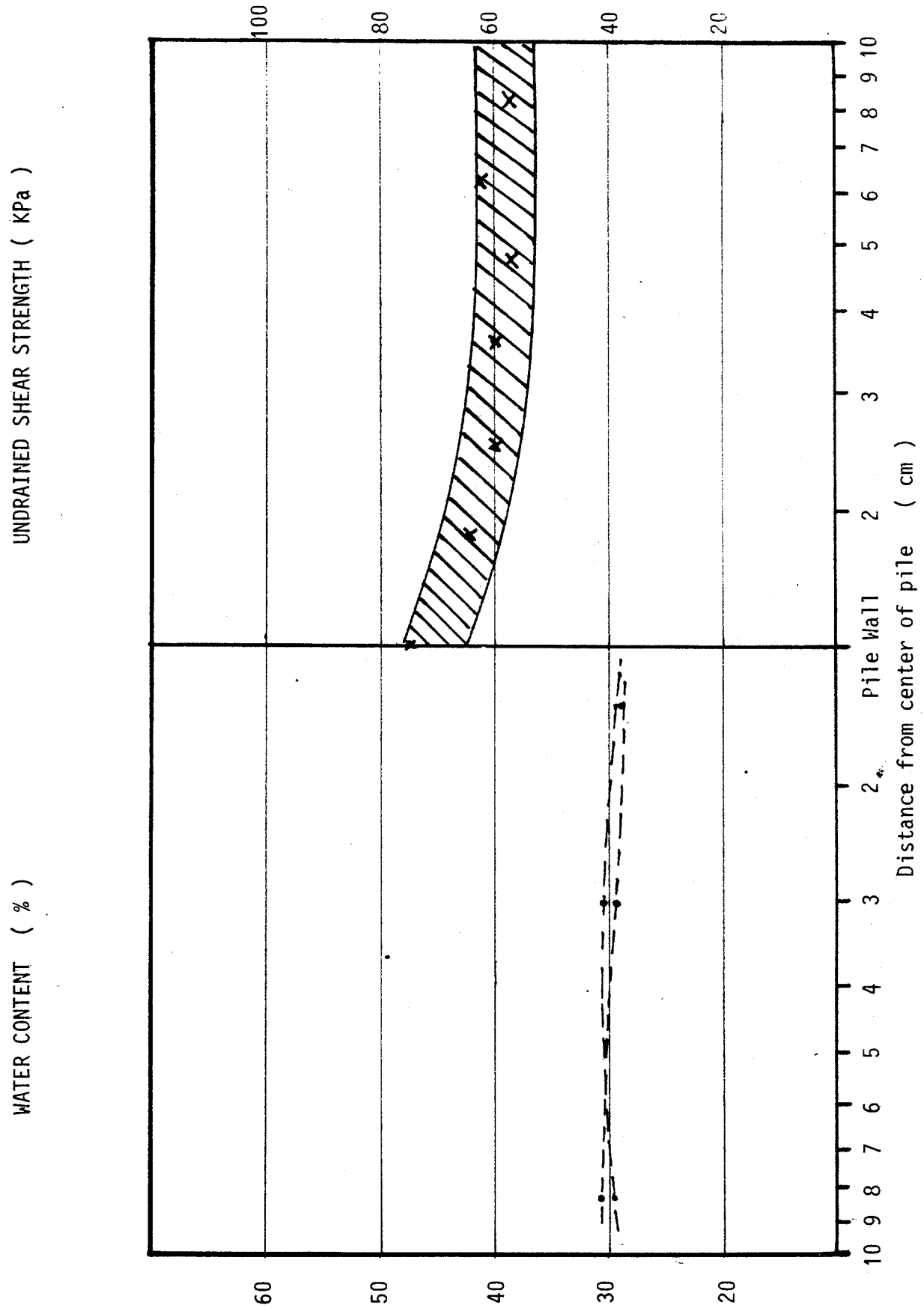

CNRD 13-2 TENSION PILE STUDY LABORATORY MODEL PILE TESTS

TEST 11, STRATUM II, Water content and shear strength after test

DET NORSKE VERITAS Geotechnical Laboratory	Drawn by	Scale
	Approved	Date
		Fig. No. 19

Appendix HA

Plotted Results from W211LC

Figures HA-1 through HA-4

Skin Friction vs Deflection, Selected Cycles

Figures HA-5 through HA-6

Skin Friction vs Eff. Normal Pressure, Selected Cycl.

Figures HA-7 through HA-14

Skin Friction, Pore and Total Pressure, Selected Cycles

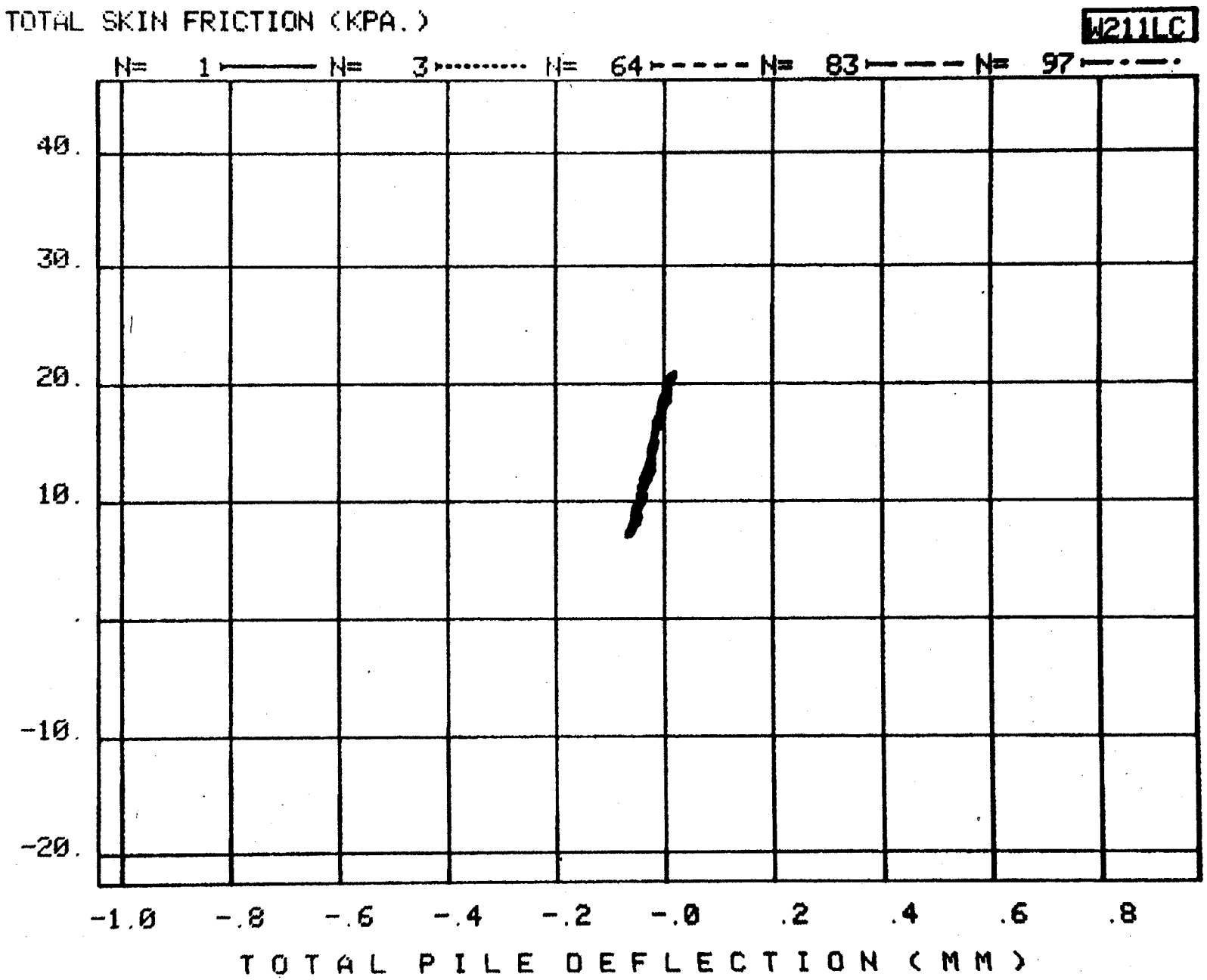
TOTAL SKIN FRICTION (KPA.)
W211LC
N= 1
N= 3
N= 64
N= 83
N= 97
40.
30.
20.
10.
-10.
-20.
-1.0
-.8
-.6
-.4
-.2
-.0
.2
.4
.6
.8
TOTAL PILE DEFLECTION (MM)

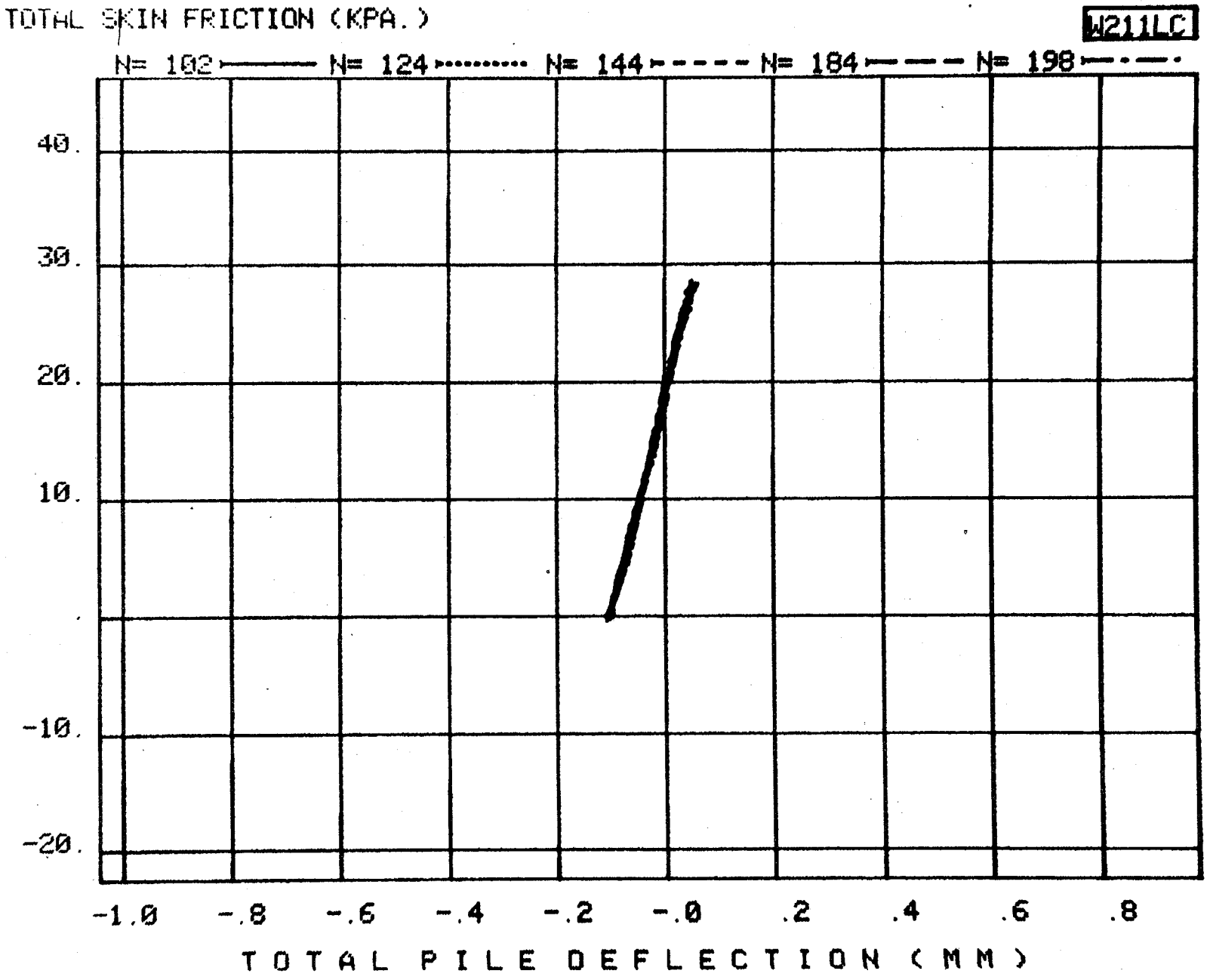
TOTAL SKIN FRICTION (KPA.)
W211LC
N= 102
N= 124
N= 144
N= 184
N= 198
40.
30.
20.
10.
-10.
-20.
-1.0
-.8
-.6
-.4
-.2
-.0
.2
.4
.6
.8
TOTAL PILE DEFLECTION (MM)

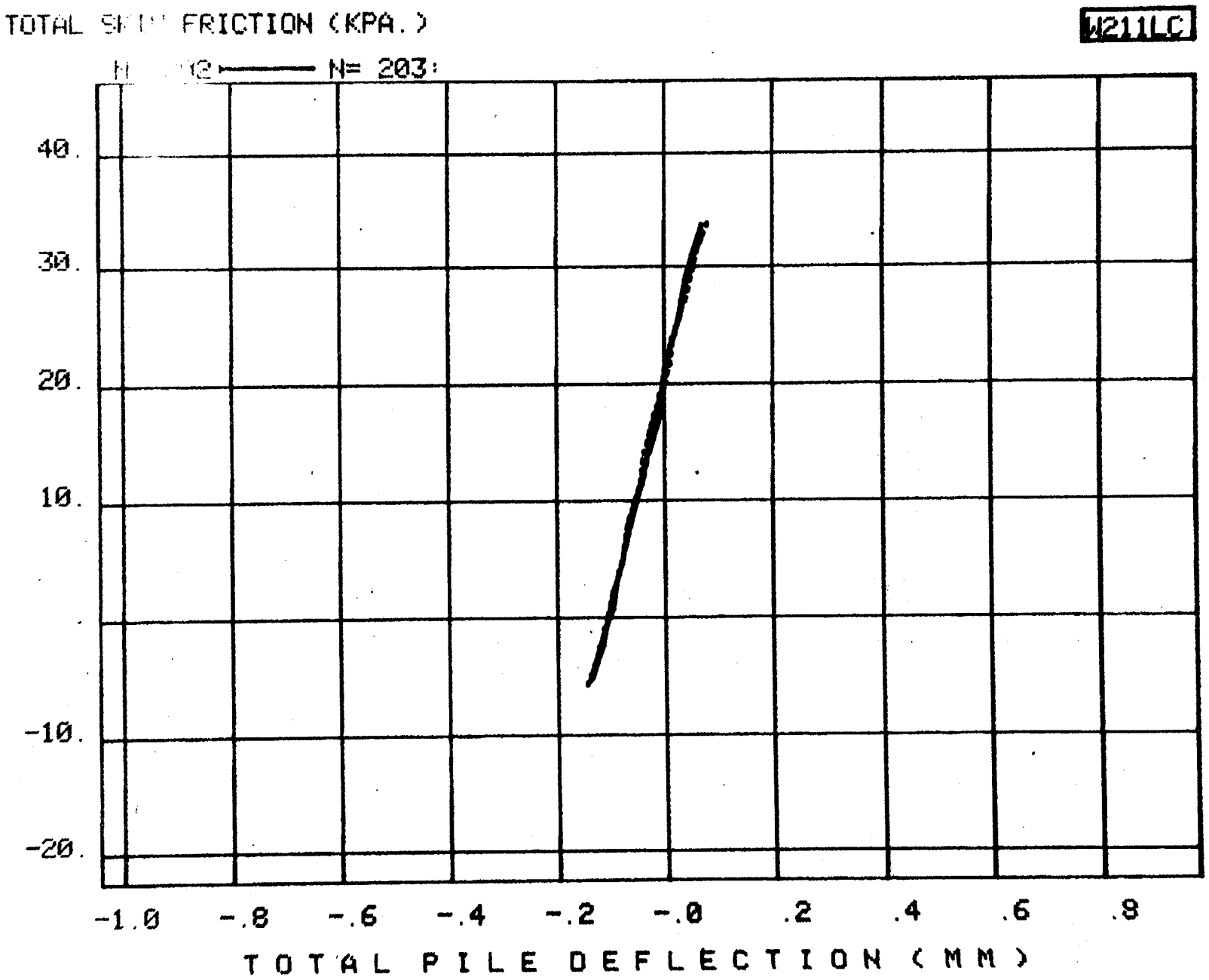
TOTAL SKIN FRICTION (KPA.)
W211LC
N= 203
40.
30.
20.
10.
-10.
-20.
-1.0
-.8
-.6
-.4
-.2
-.0
.2
.4
.6
.8
TOTAL PILE DEFLECTION (MM)

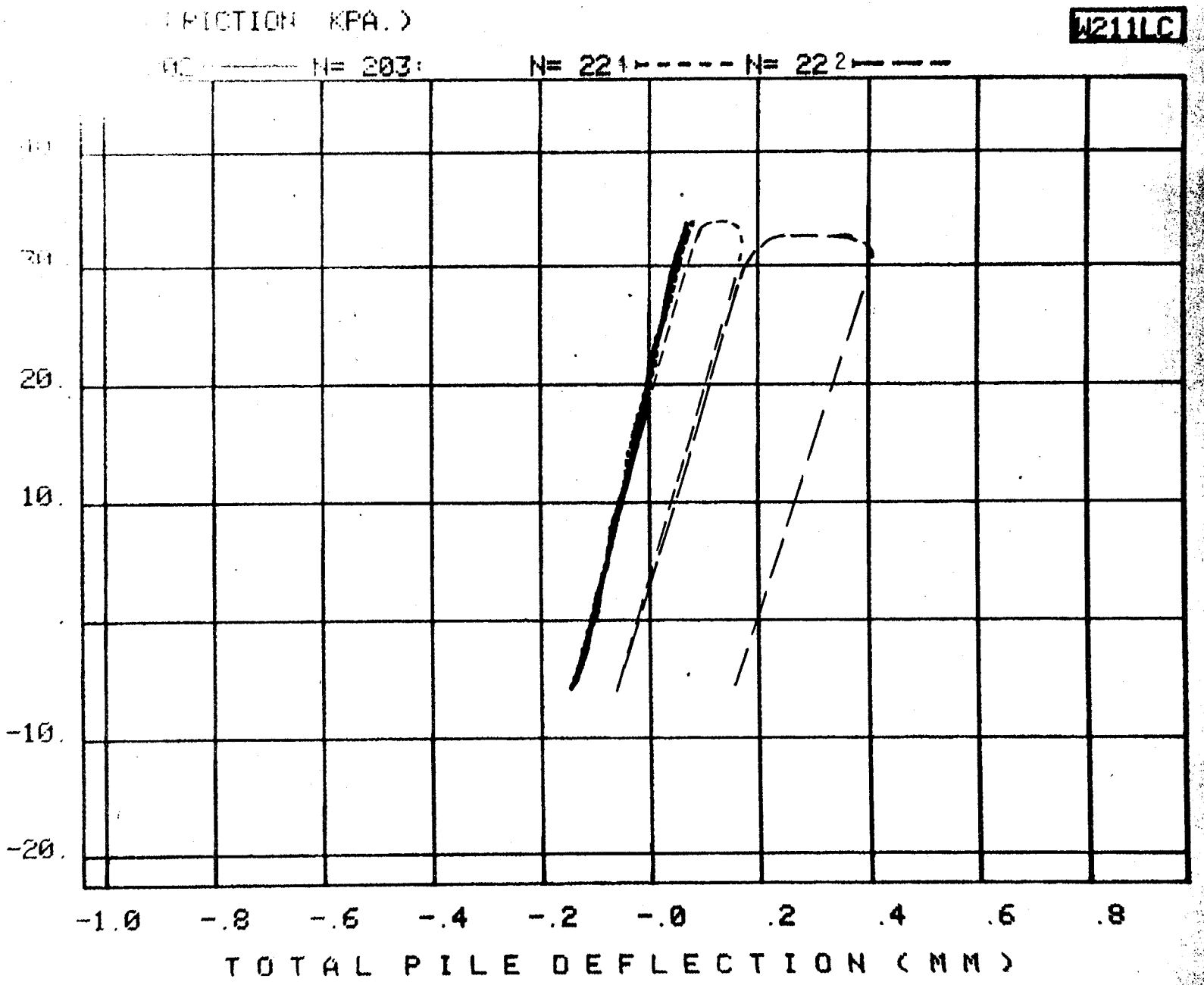
W211LC
FRICTION (KPA.)
N= 203
N= 221
N= 222
30.
20.
10.
-10.
-20.
-1.0
-.8
-.6
-.4
-.2
-.0
.2
.4
.6
.8
TOTAL PILE DEFLECTION (MM)

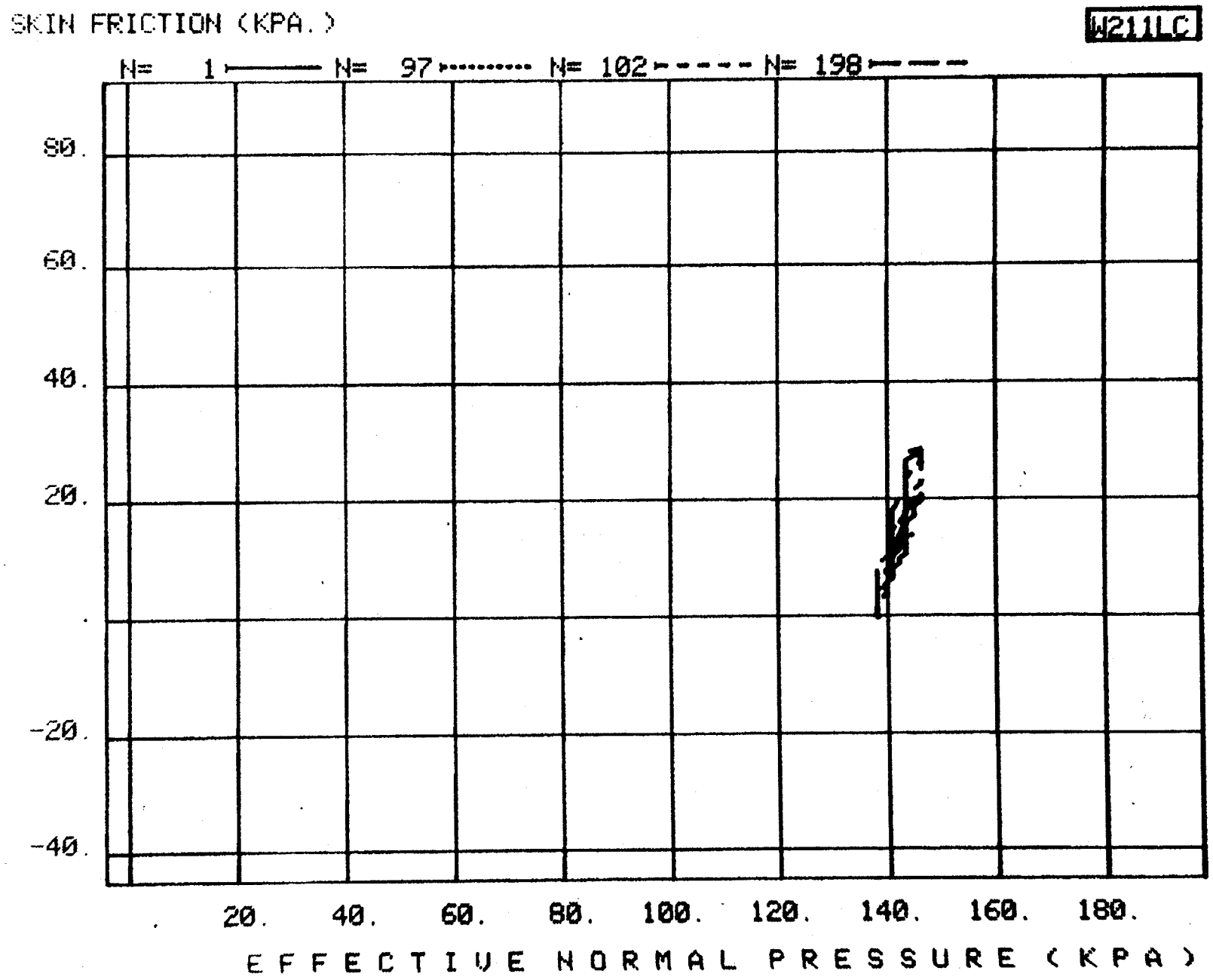
SKIN FRICTION (KPA.)
W211LC
N= 1
N= 97
N= 102
N= 198
80.
60.
40.
20.
-20.
-40.
20.
40.
60.
80.
100.
120.
140.
160.
180.
EFFECTIVE NORMAL PRESSURE (KPA)

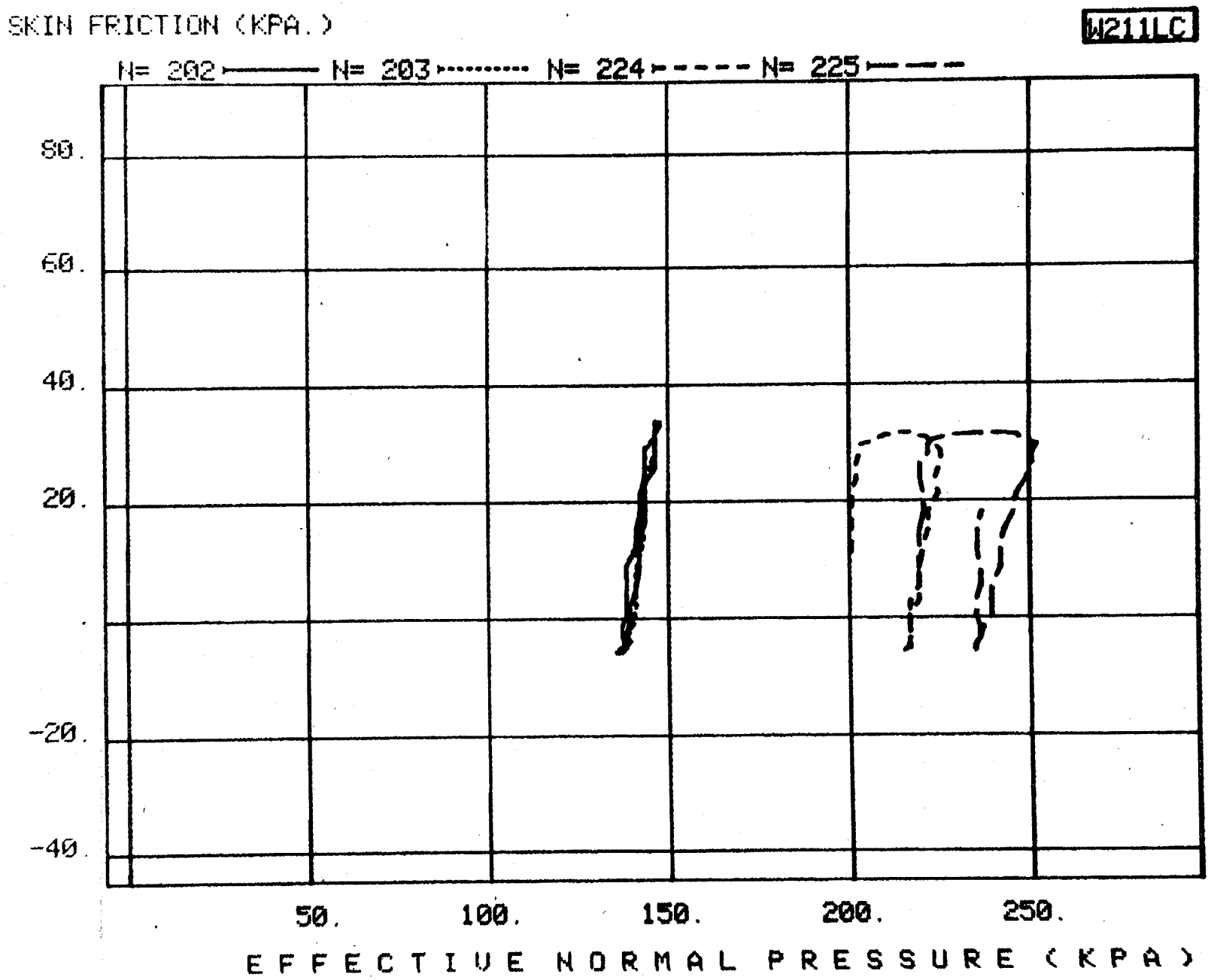
SKIN FRICTION (KPA.)
W211LC
N= 202
N= 203
N= 224
N= 225
80.
60.
40.
20.
-20.
-40.
50.
100.
150.
200.
250.
EFFECTIVE NORMAL PRESSURE (KPA)

RESPONSE ON CYCLIC LOADING (KPA.) CYCLE NO. 1

W211LC

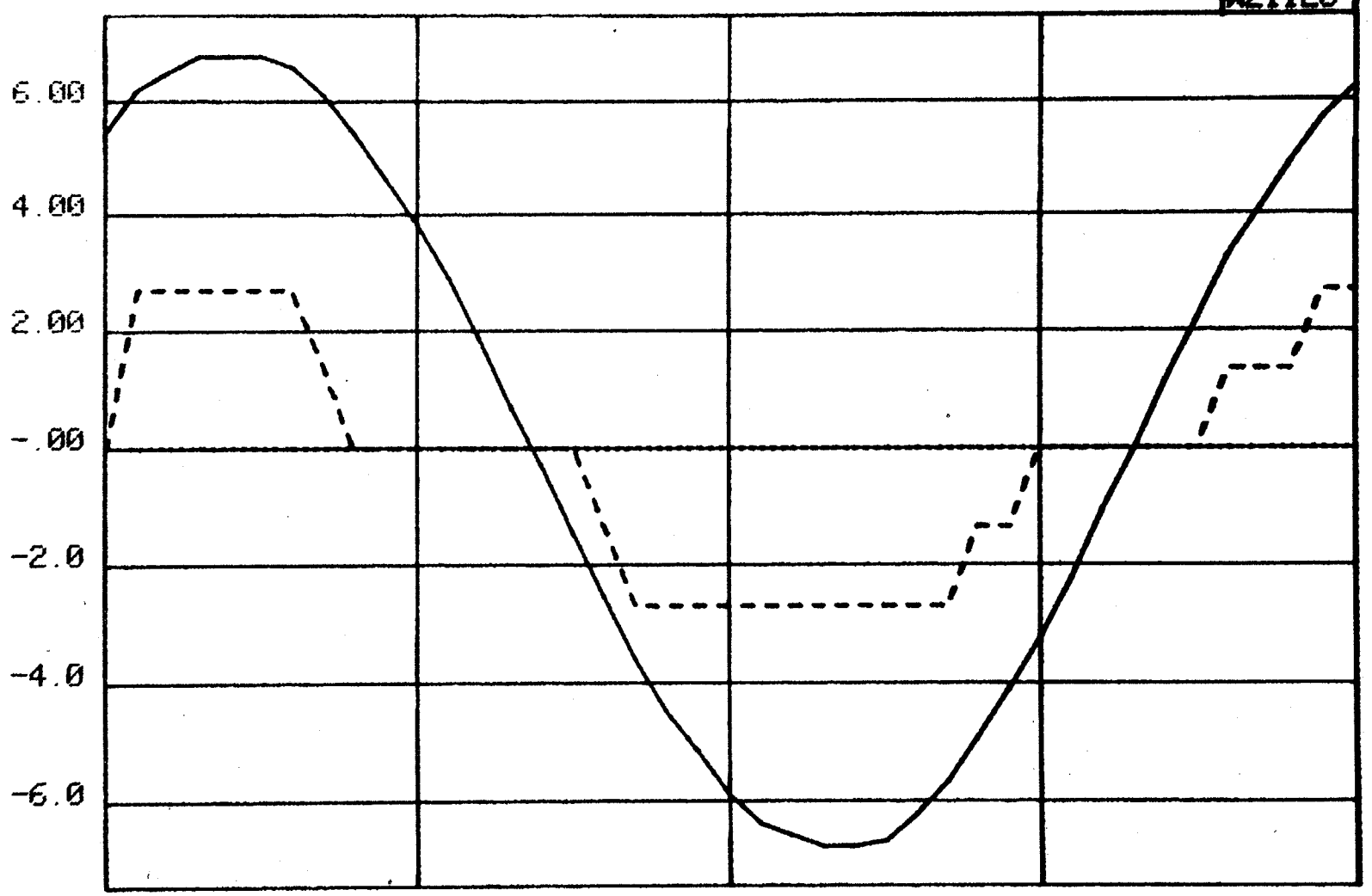

LEGEND:		PERM. VALUES
———	SKIN FRICTION	13.80 KPA.
·····	PORE PRESSURE	201.2 KPA.
- - - -	TOTAL NORMAL PRESSURE	344.8 KPA.

RESPONSE ON CYCLIC LOADING (KPA.) CYCLE NO. 97 W211LC

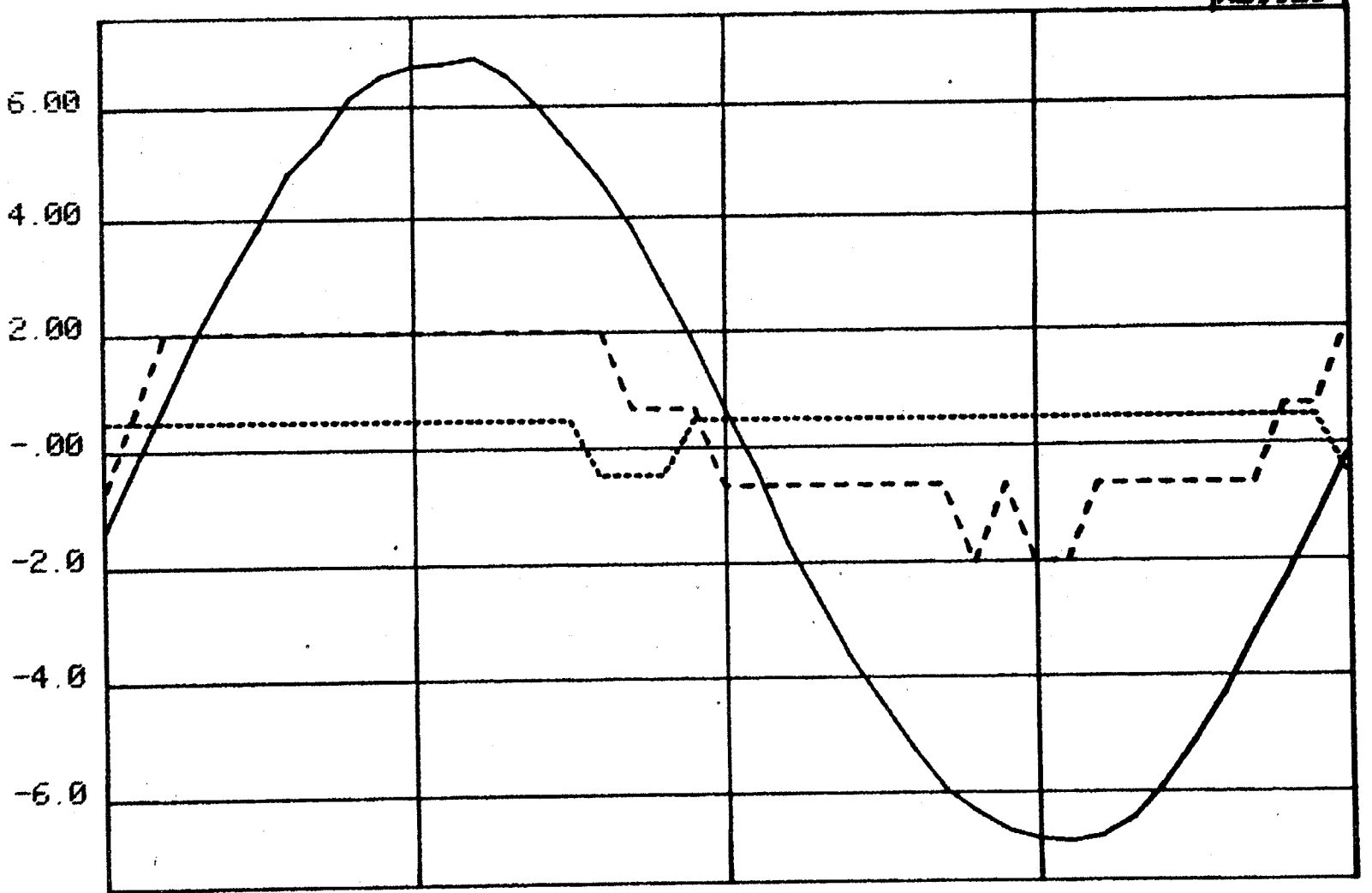

LEGEND:

		PERM. VALUES
———	SKIN FRICTION	14.11 KPA.
·····	PORE PRESSURE	200.7 KPA.
- - - -	TOTAL NORMAL PRESSURE	342.8 KPA.

RESPONSE ON CYCLIC LOADING (KPA.) CYCLE NO. 102 W211LC

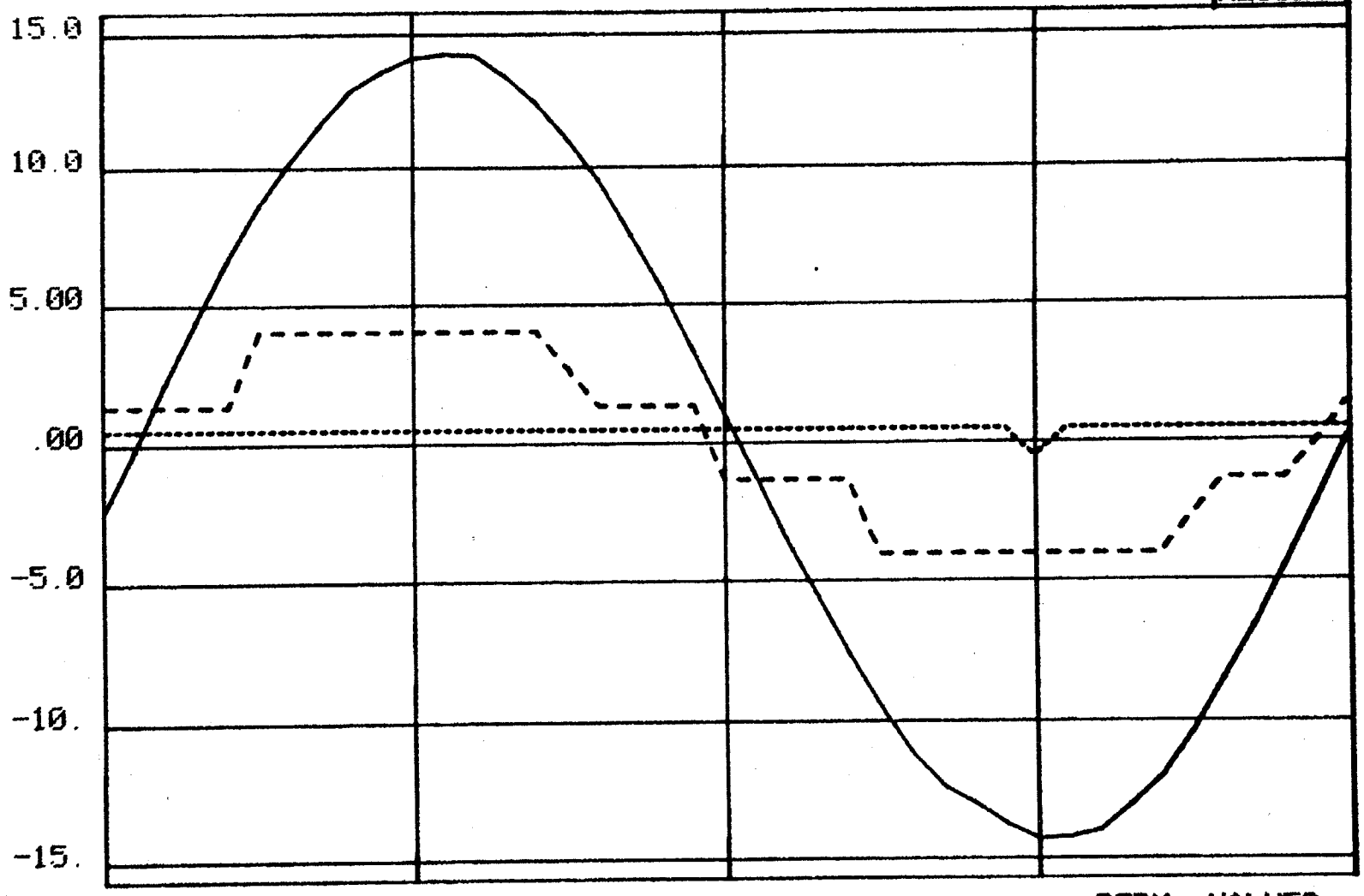

LEGEND:

		PERM. VALUES
———	SKIN FRICTION	13.96 KPA.
·····	PORE PRESSURE	200.7 KPA.
- - - -	TOTAL NORMAL PRESSURE	343.4 KPA.

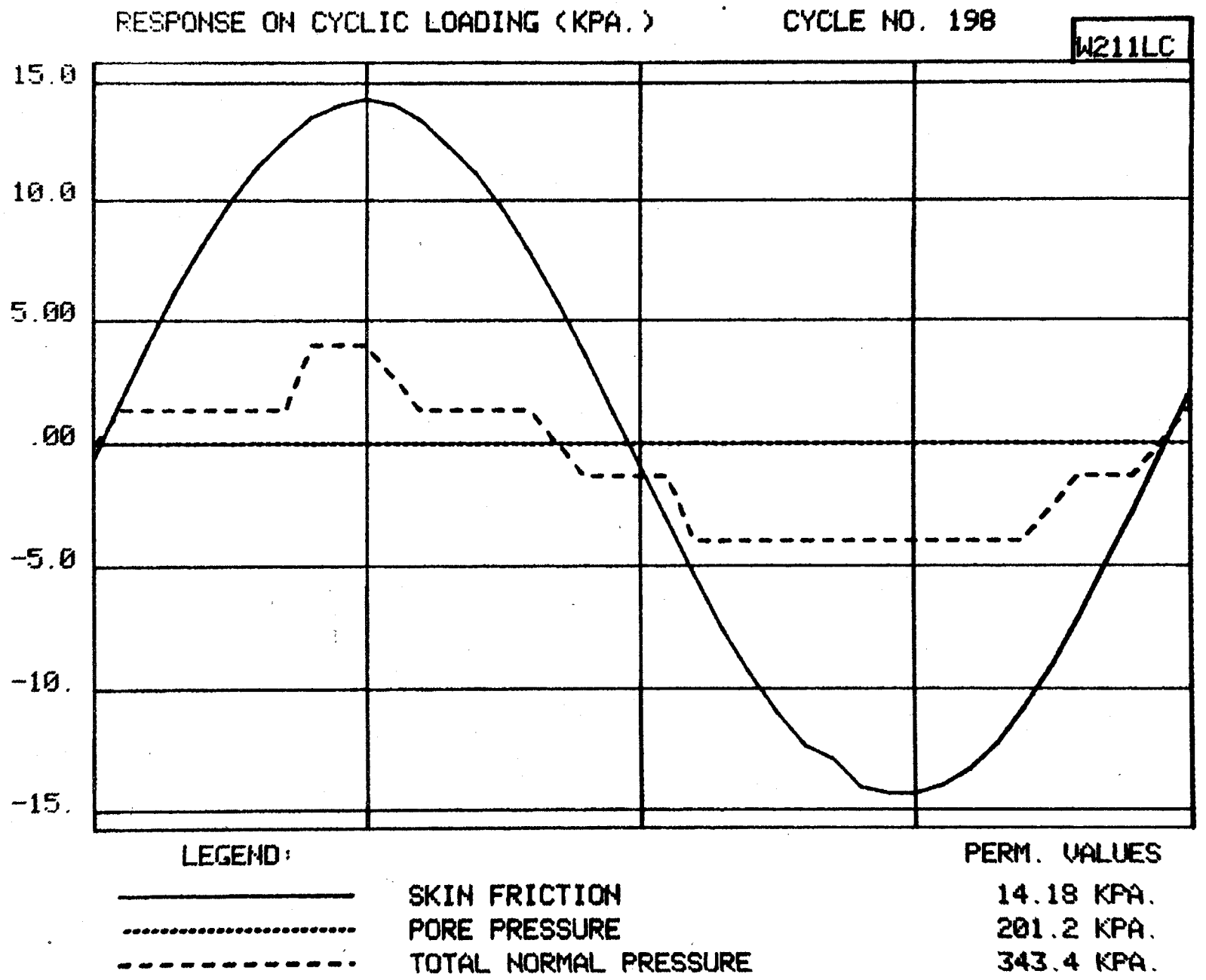
RESPONSE ON CYCLIC LOADING (KPA.)
CYCLE NO. 198
W211LC
15.0
10.0
5.00
.00
-5.0
-10.
-15.
LEGEND:
PERM. VALUES
SKIN FRICTION
14.18 KPA.
PORE PRESSURE
201.2 KPA.
TOTAL NORMAL PRESSURE
343.4 KPA.

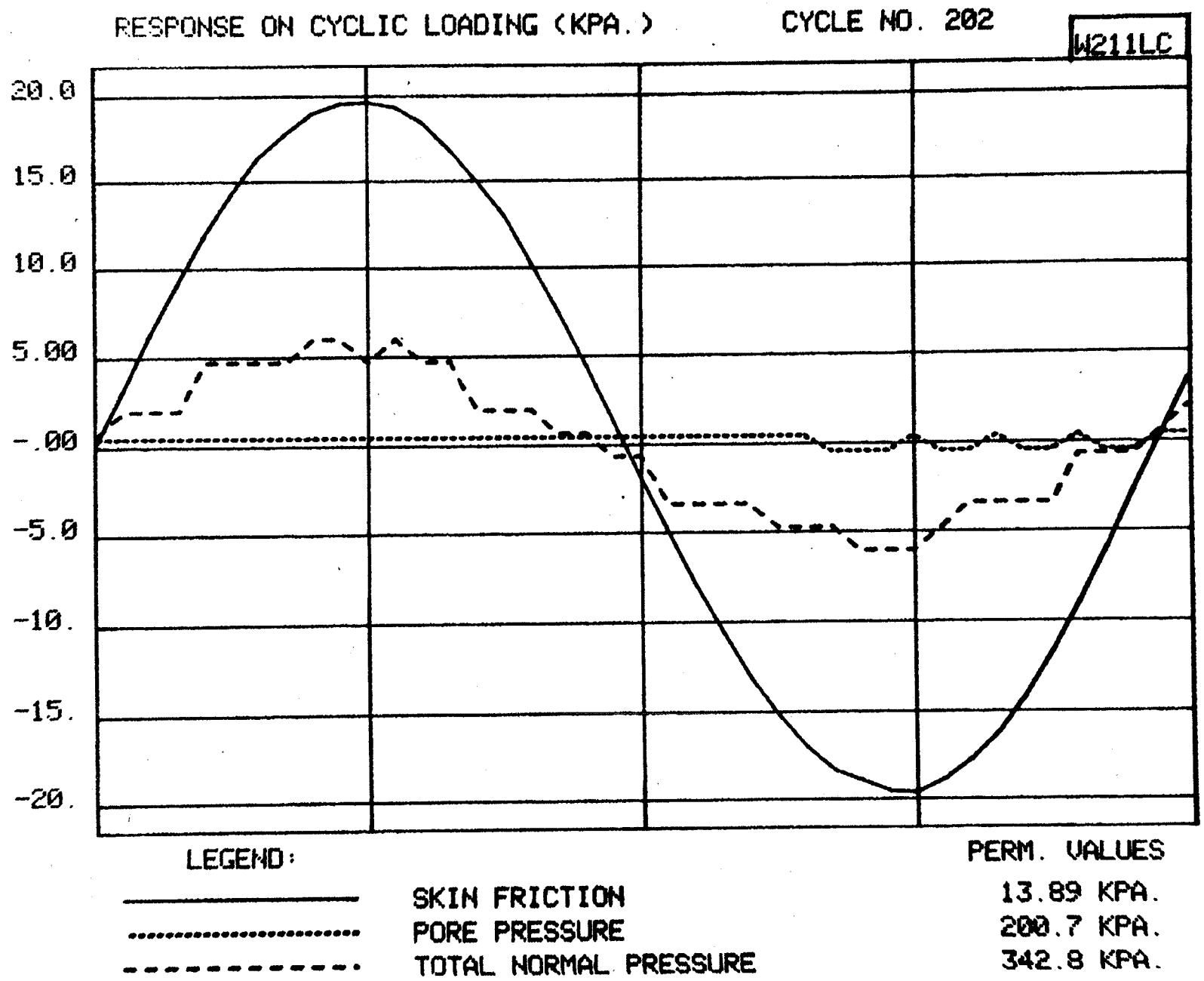
RESPONSE ON CYCLIC LOADING (KPA.)
CYCLE NO. 202
W211LC
20.0
15.0
10.0
5.00
-.00
-5.0
-10.
-15.
-20.
LEGEND:
SKIN FRICTION
PORE PRESSURE
TOTAL NORMAL PRESSURE
PERM. VALUES
13.89 KPA.
200.7 KPA.
342.8 KPA.

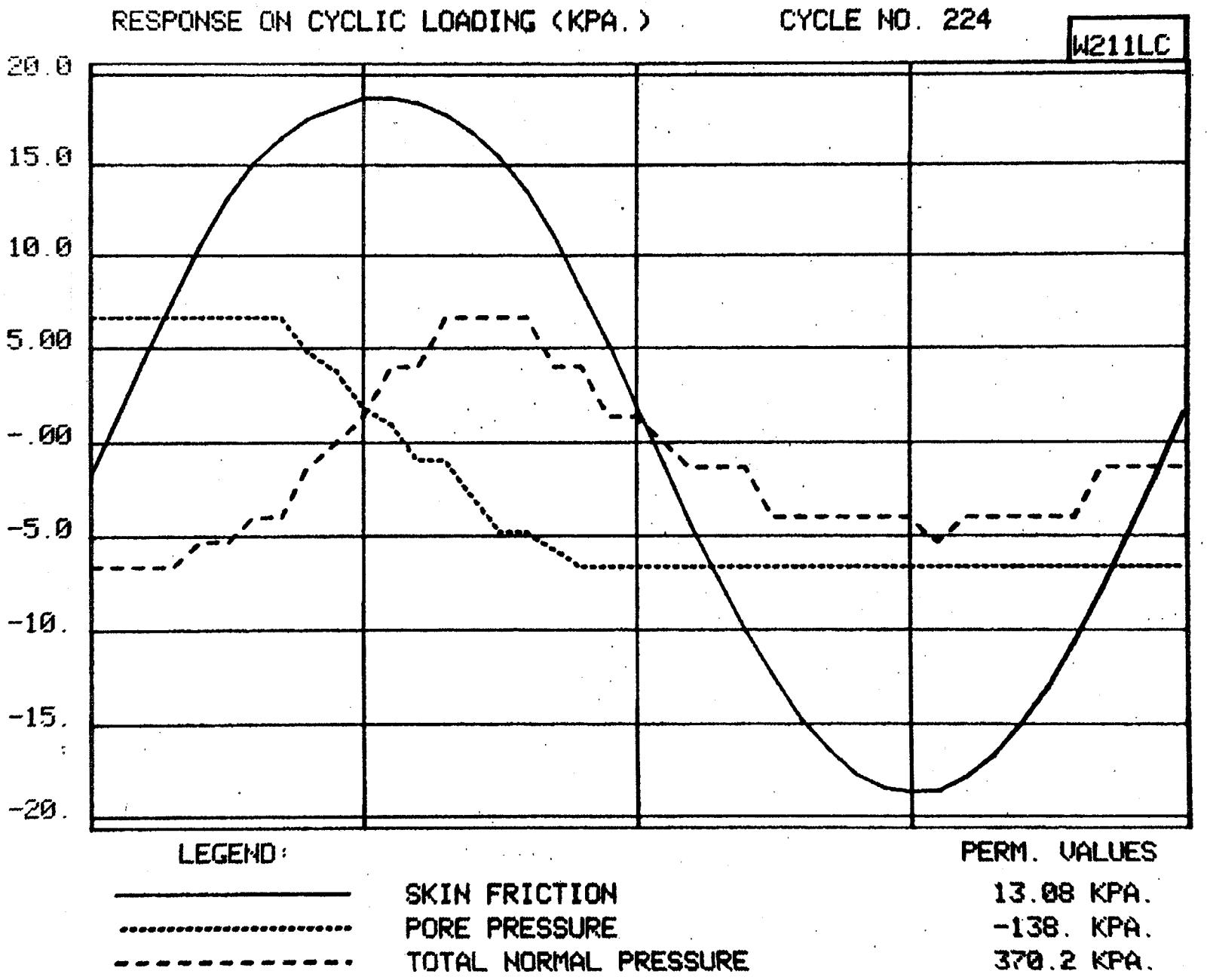
RESPONSE ON CYCLIC LOADING (KPA.)
CYCLE NO. 224
W211LC
20.0
15.0
10.0
5.00
-.00
-5.0
-10.
-15.
-20.
LEGEND:
PERM. VALUES
SKIN FRICTION
13.08 KPA.
PORE PRESSURE
-138. KPA.
TOTAL NORMAL PRESSURE
370.2 KPA.

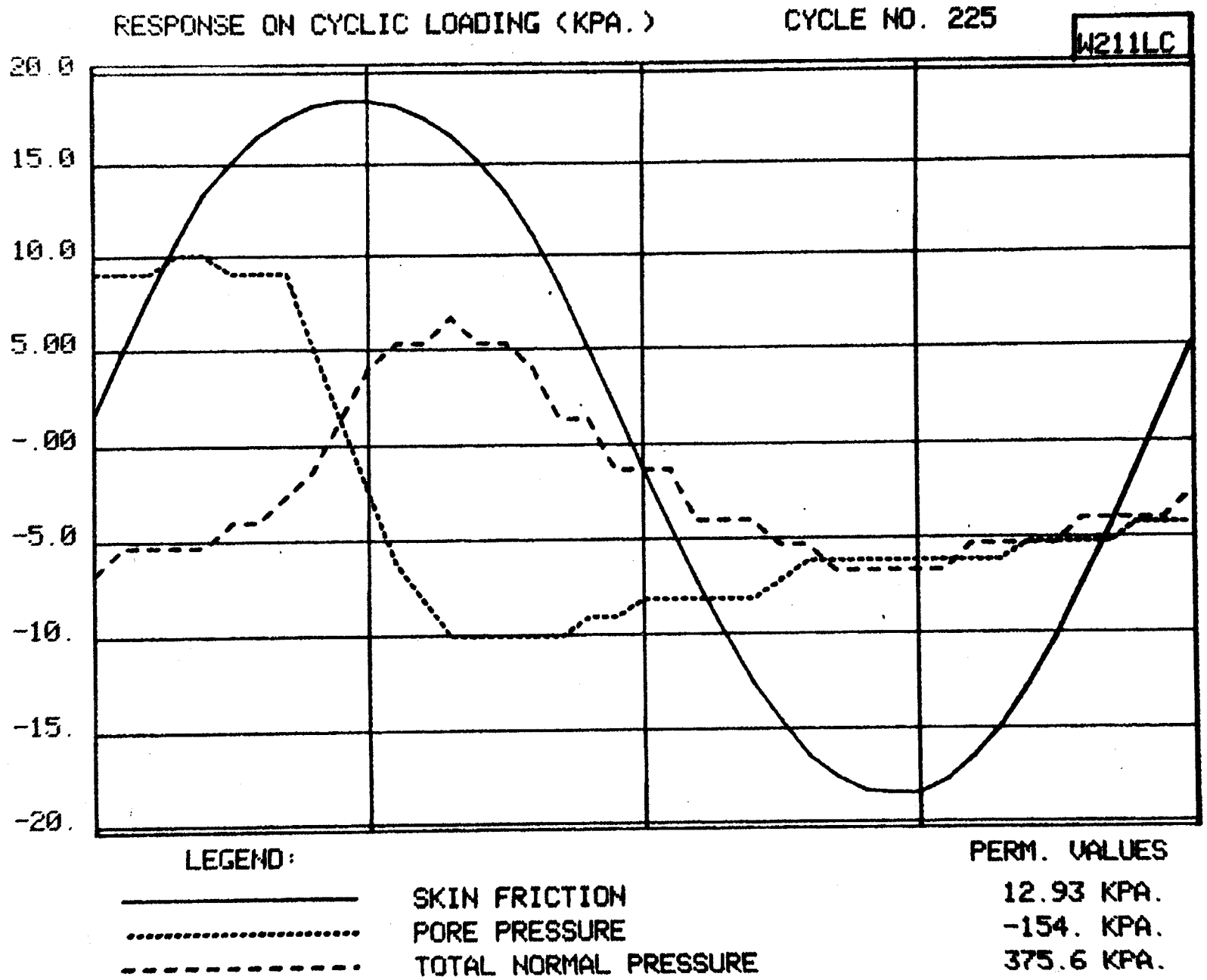
RESPONSE ON CYCLIC LOADING (KPA.)
CYCLE NO. 225
W211LC
20.0
15.0
10.0
5.00
-.00
-5.0
-10.
-15.
-20.
LEGEND:
SKIN FRICTION
PORE PRESSURE
TOTAL NORMAL PRESSURE
PERM. VALUES
12.93 KPA.
-154. KPA.
375.6 KPA.

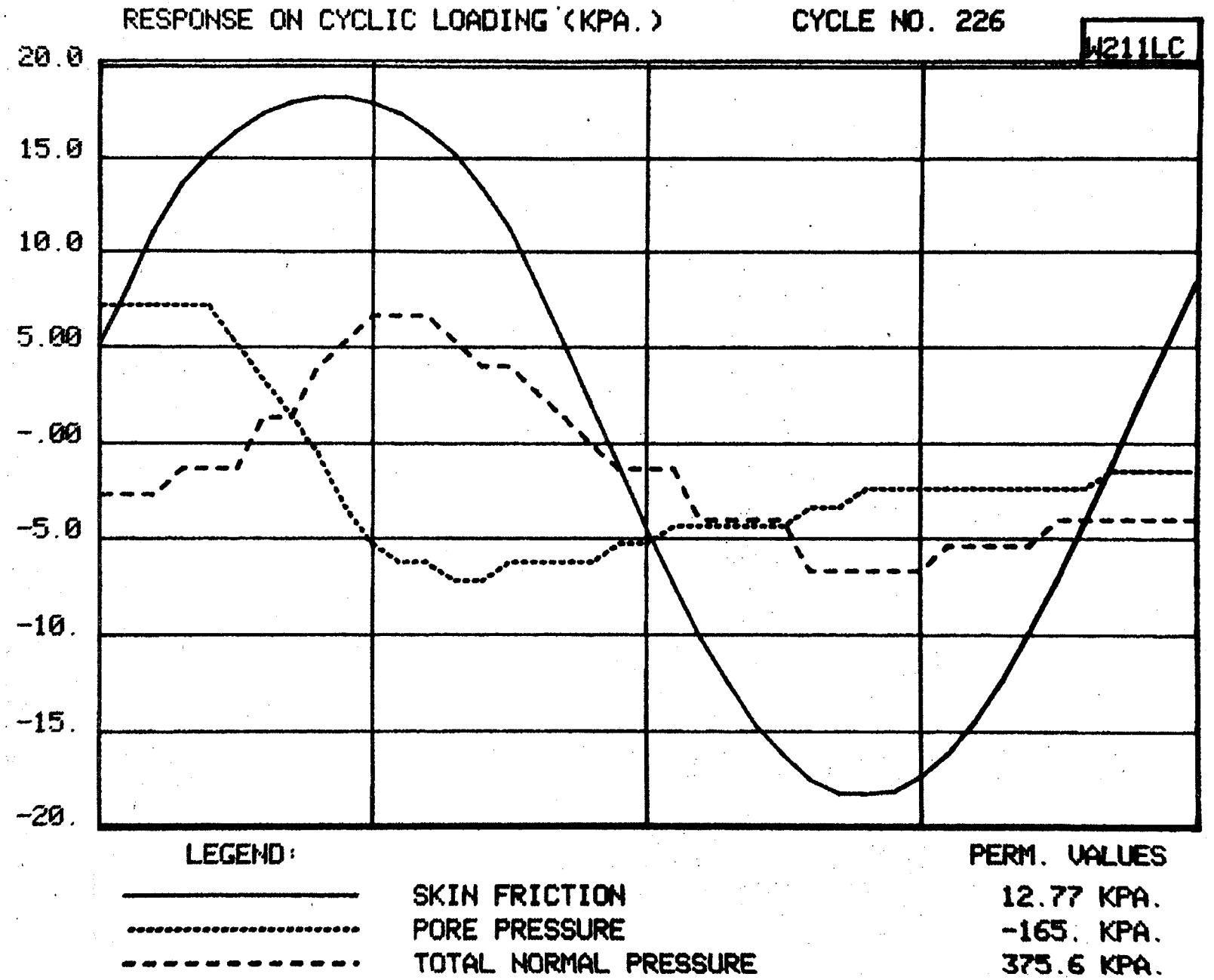
RESPONSE ON CYCLIC LOADING (KPA.)
CYCLE NO. 226
W211LC
20.0
15.0
10.0
5.00
-.00
-5.0
-10.
-15.
-20.
LEGEND:
SKIN FRICTION
PORE PRESSURE
TOTAL NORMAL PRESSURE
PERM. VALUES
12.77 KPA.
-165. KPA.
375.6 KPA.

Appendix HB

Plotted Results from W211SC

Figures HB-1 through HB-3

Skin Friction vs Deflection, Selected Cycles

Figures HB-4 through HB-6

Skin Friction vs Eff. Normal Pressure, Selected Cycl.

Figures HB-7 through HB-16

Skin Friction, Pore and Total Pressure, Selected Cycles

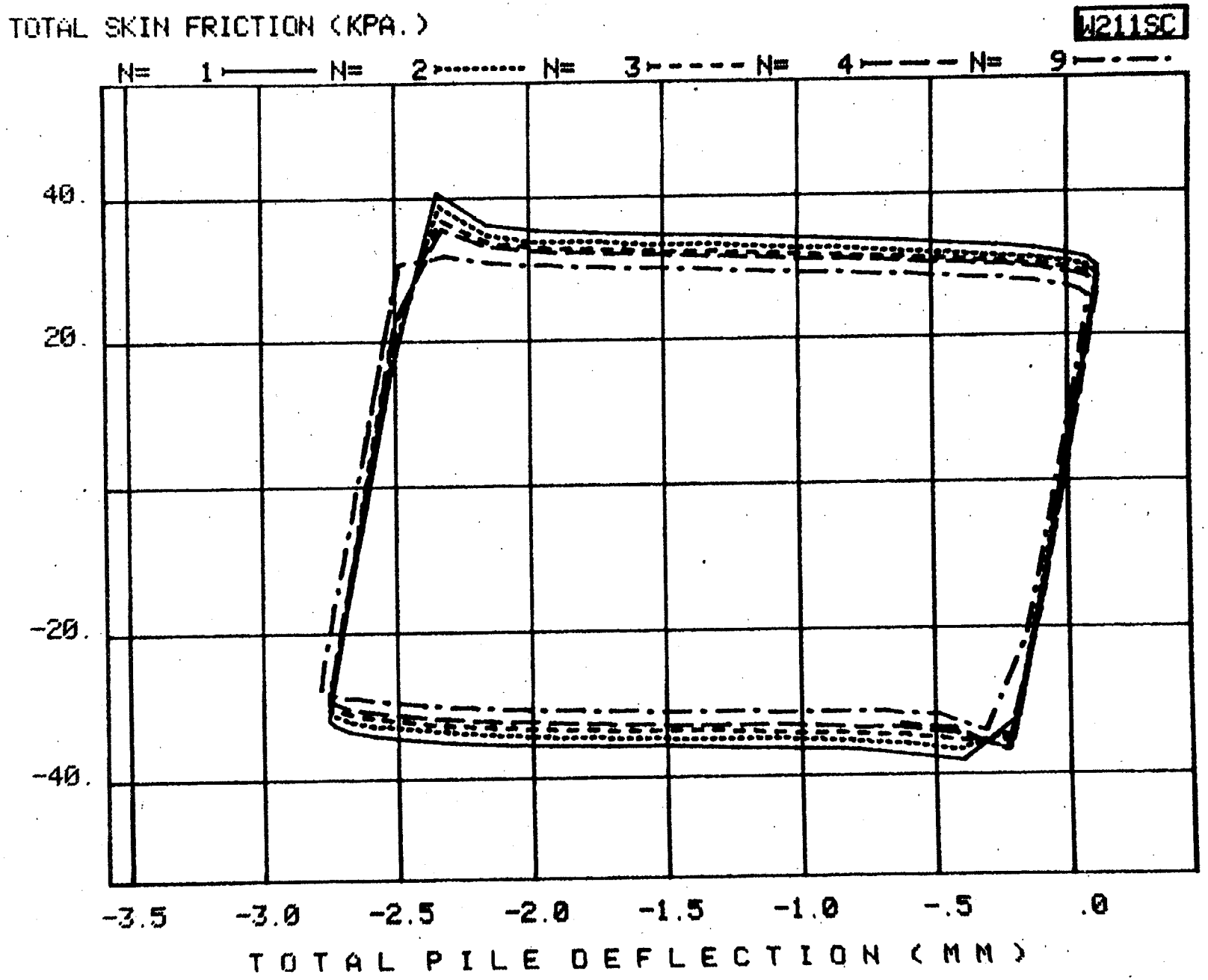
TOTAL SKIN FRICTION (KPA.)
W211SC
N= 1
N= 2
N= 3
N= 4
N= 9
40.
20.
-20.
-40.
-3.5
-3.0
-2.5
-2.0
-1.5
-1.0
-.5
.0
TOTAL PILE DEFLECTION (MM)

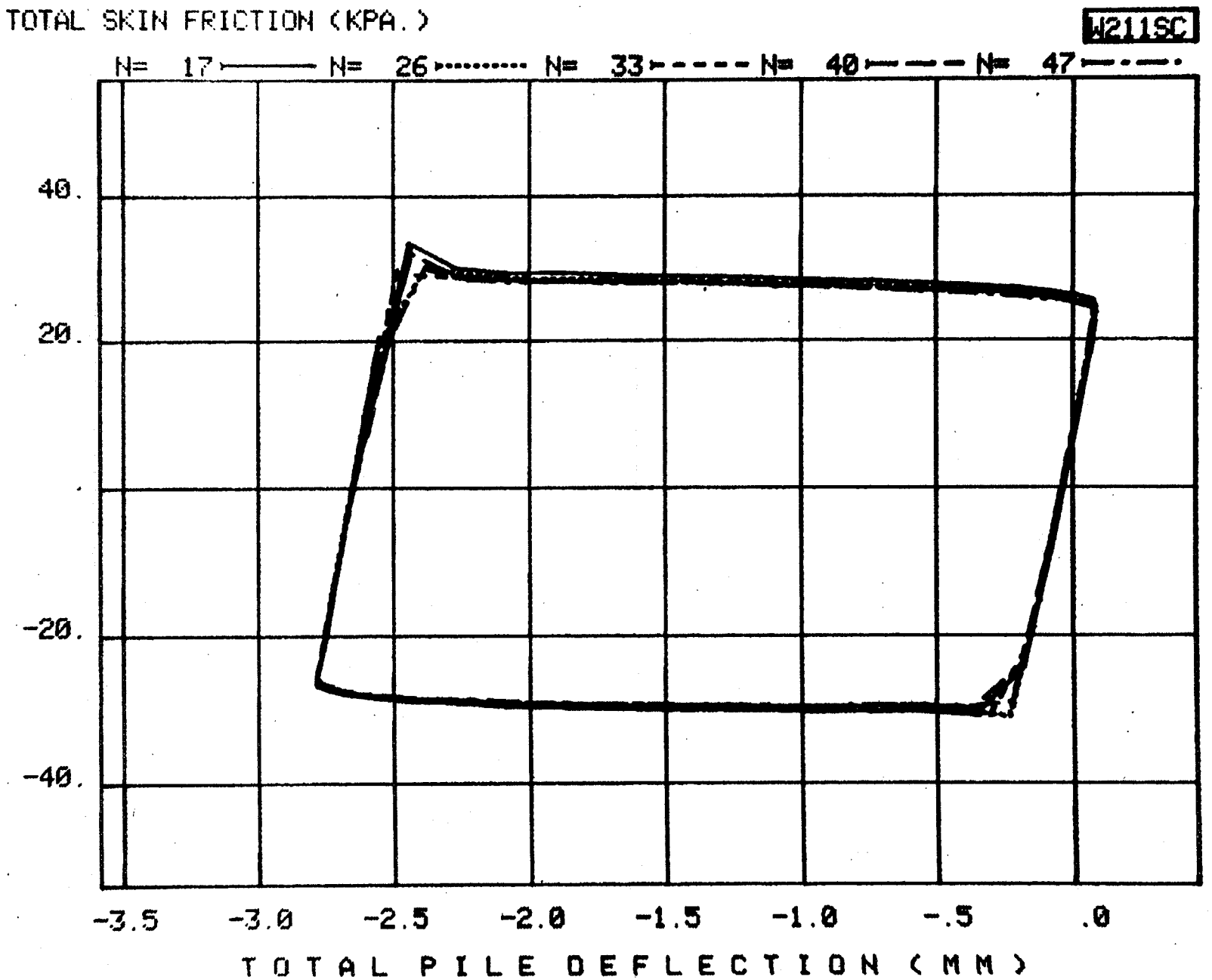
TOTAL SKIN FRICTION (KPA.)
W211SC
N= 17
N= 26
N= 33
N= 40
N= 47
40.
20.
-20.
-40.
-3.5
-3.0
-2.5
-2.0
-1.5
-1.0
-.5
.0
TOTAL PILE DEFLECTION (MM)

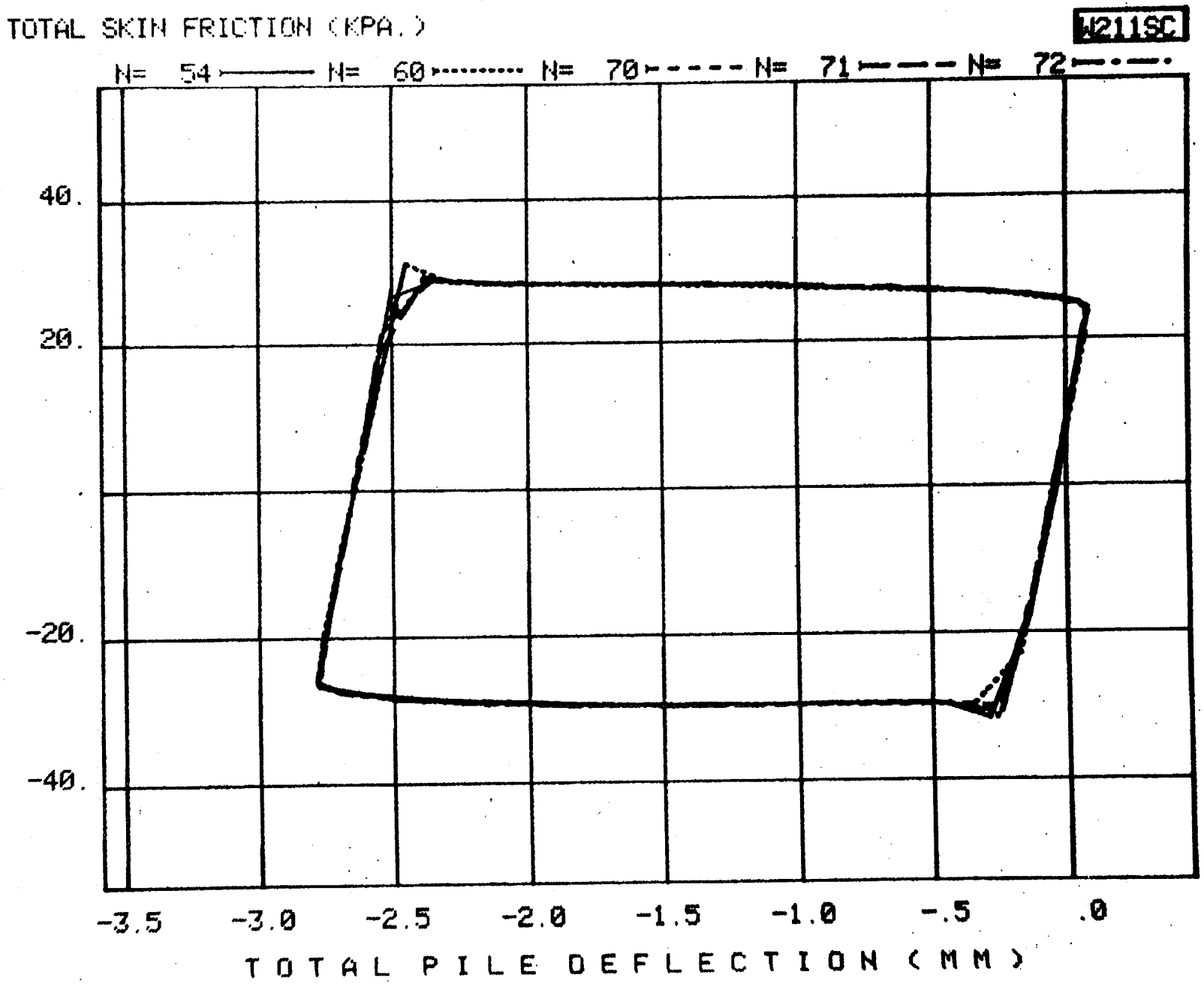
TOTAL SKIN FRICTION (KPA.)
W211SC
N= 54
N= 60
N= 70
N= 71
N= 72
40.
20.
-20.
-40.
-3.5
-3.0
-2.5
-2.0
-1.5
-1.0
-.5
.0
TOTAL PILE DEFLECTION (MM)

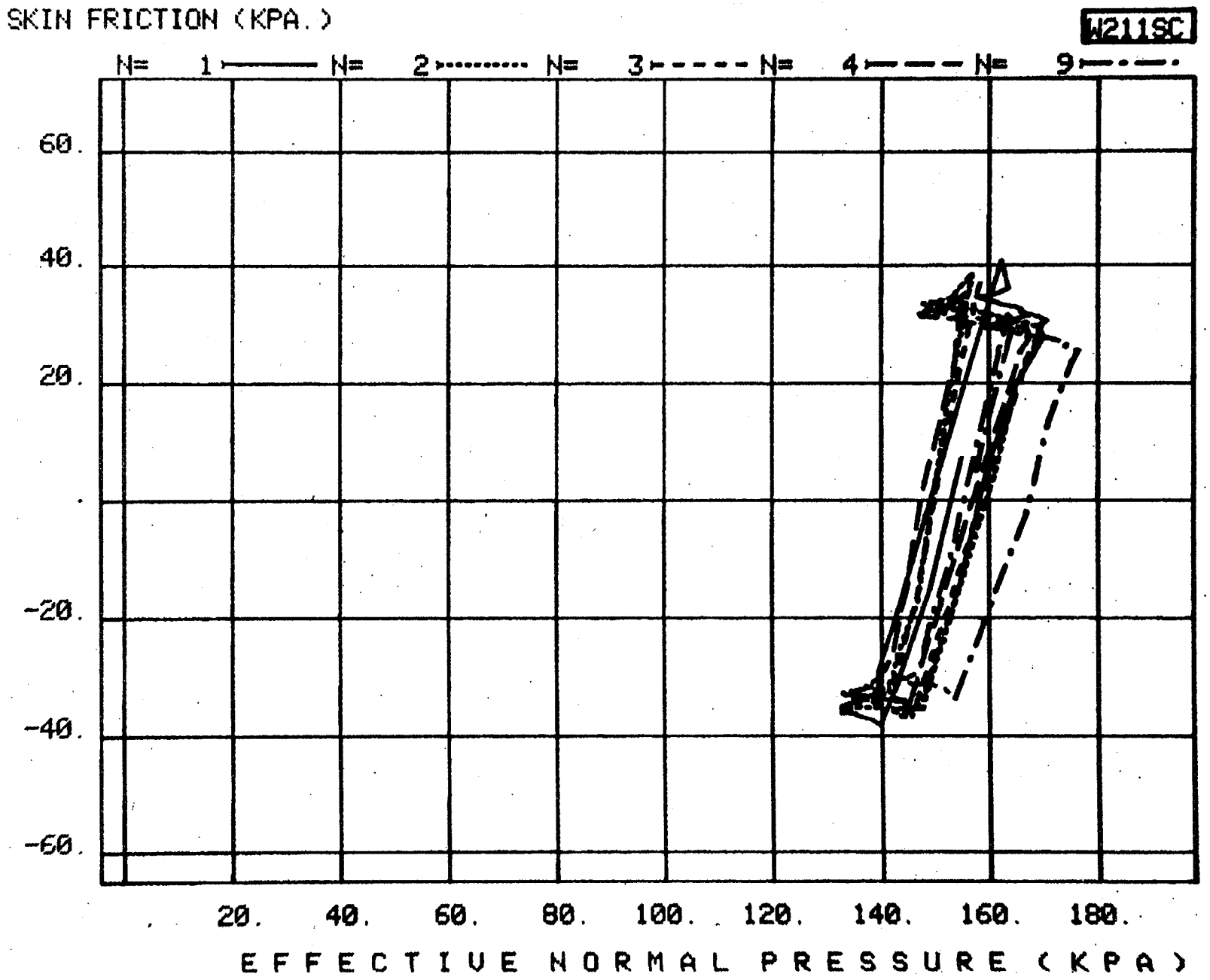
SKIN FRICTION (KPA.)
W211SC
N= 1
N= 2
N= 3
N= 4
N= 9
60.
40.
20.
-20.
-40.
-60.
20.
40.
60.
80.
100.
120.
140.
160.
180.
EFFECTIVE NORMAL PRESSURE (KPA)

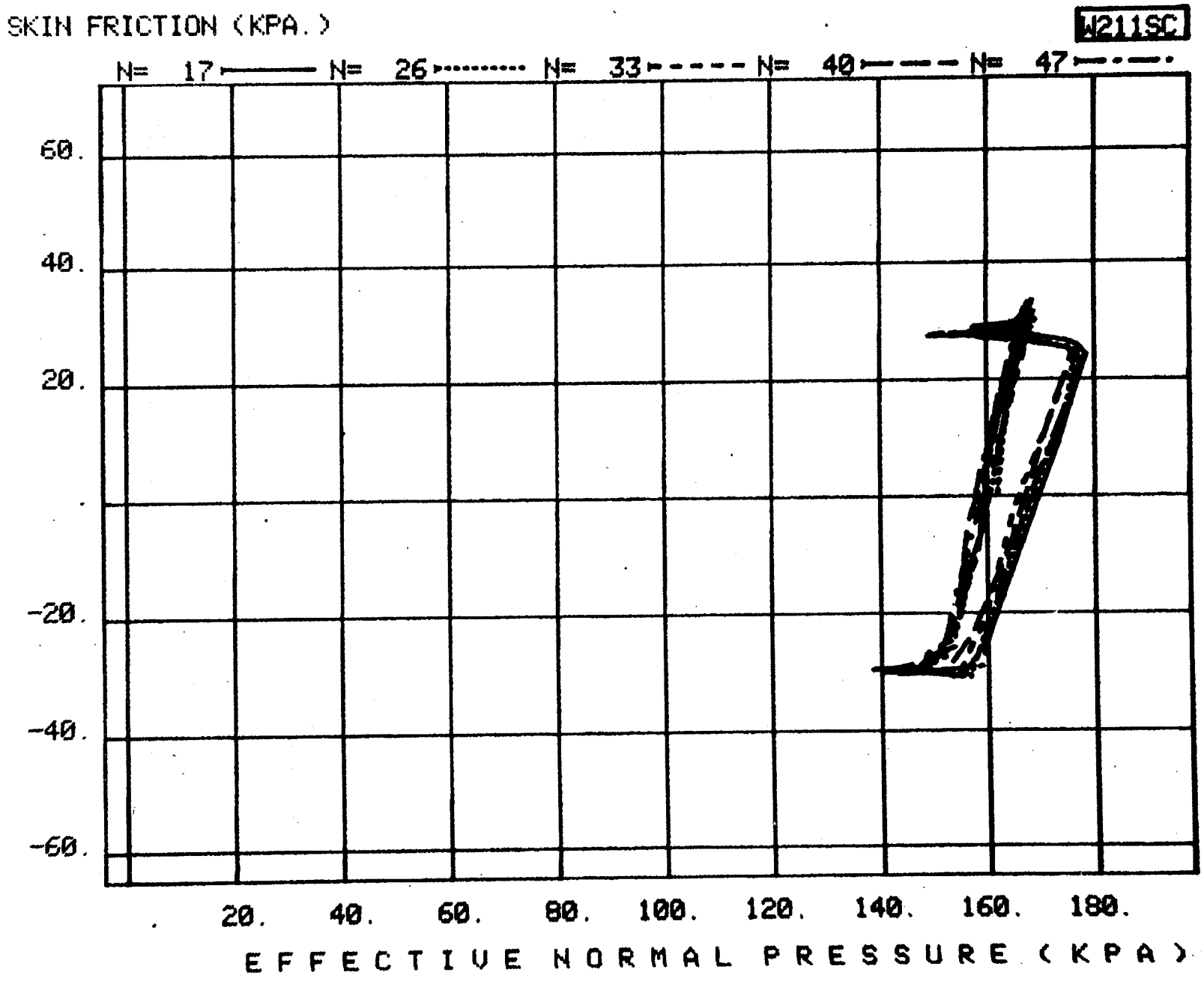
SKIN FRICTION (KPA.)
W211SC
N= 17
N= 26
N= 33
N= 40
N= 47
60.
40.
20.
-20.
-40.
-60.
20.
40.
60.
80.
100.
120.
140.
160.
180.
EFFECTIVE NORMAL PRESSURE (KPA)

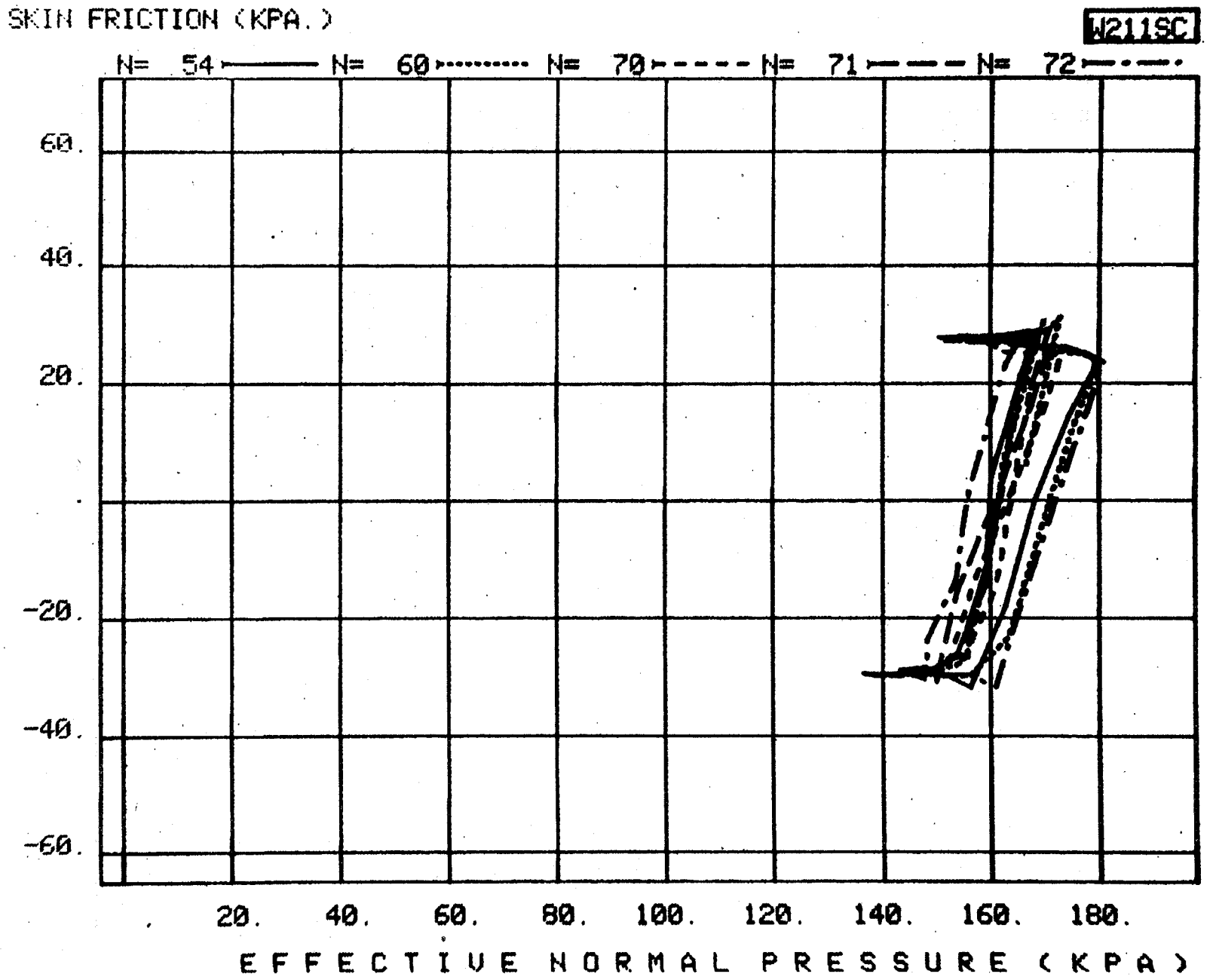
SKIN FRICTION (KPA.)
W211SC
N= 54
N= 60
N= 70
N= 71
N= 72
60.
40.
20.
-20.
-40.
-60.
20.
40.
60.
80.
100.
120.
140.
160.
180.
EFFECTIVE NORMAL PRESSURE (KPA)

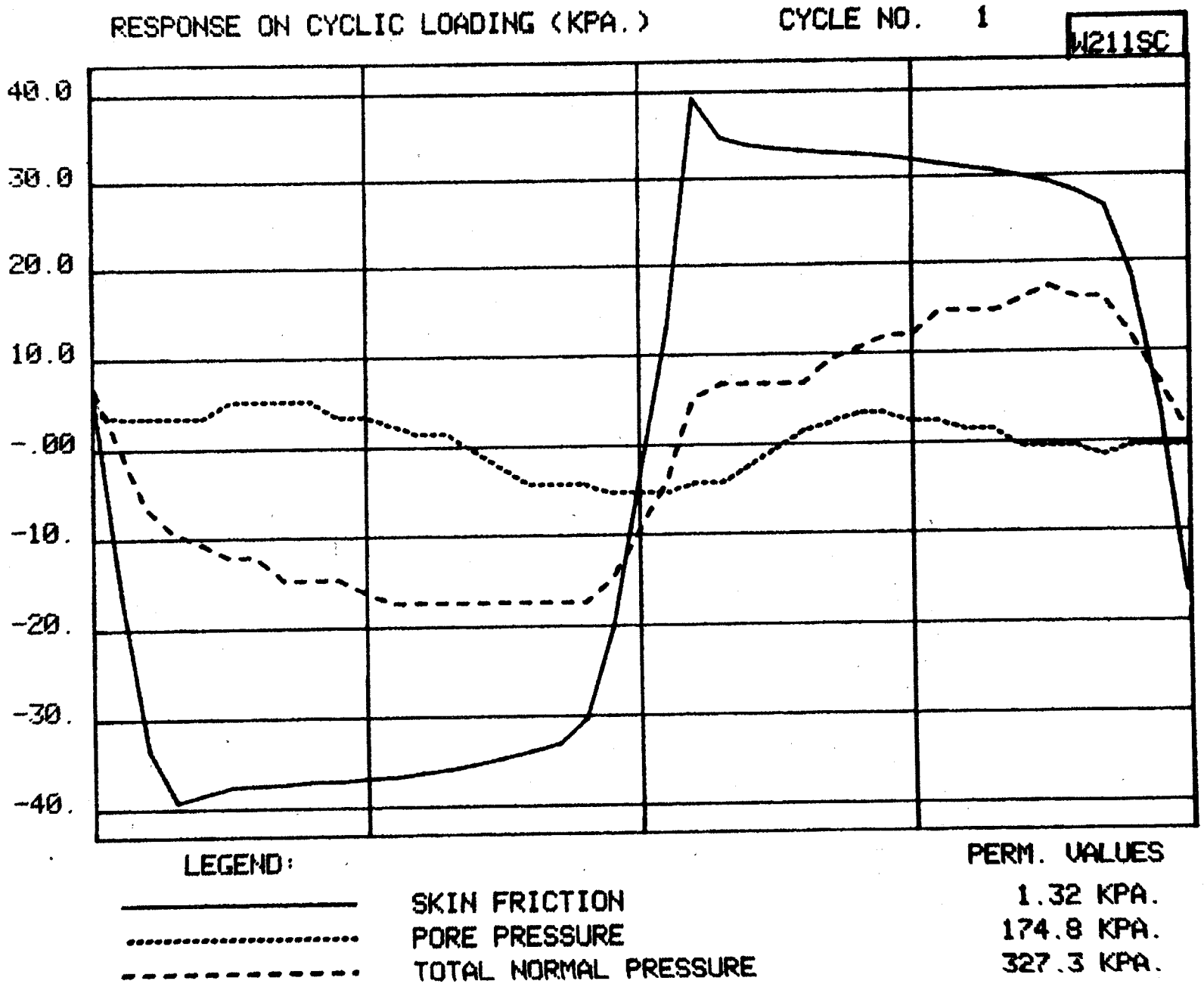
RESPONSE ON CYCLIC LOADING (KPA.)
CYCLE NO. 1
W211SC
40.0
30.0
20.0
10.0
-.00
-10.
-20.
-30.
-40.
LEGEND:
SKIN FRICTION
PORE PRESSURE
TOTAL NORMAL PRESSURE
PERM. VALUES
1.32 KPA.
174.8 KPA.
327.3 KPA.

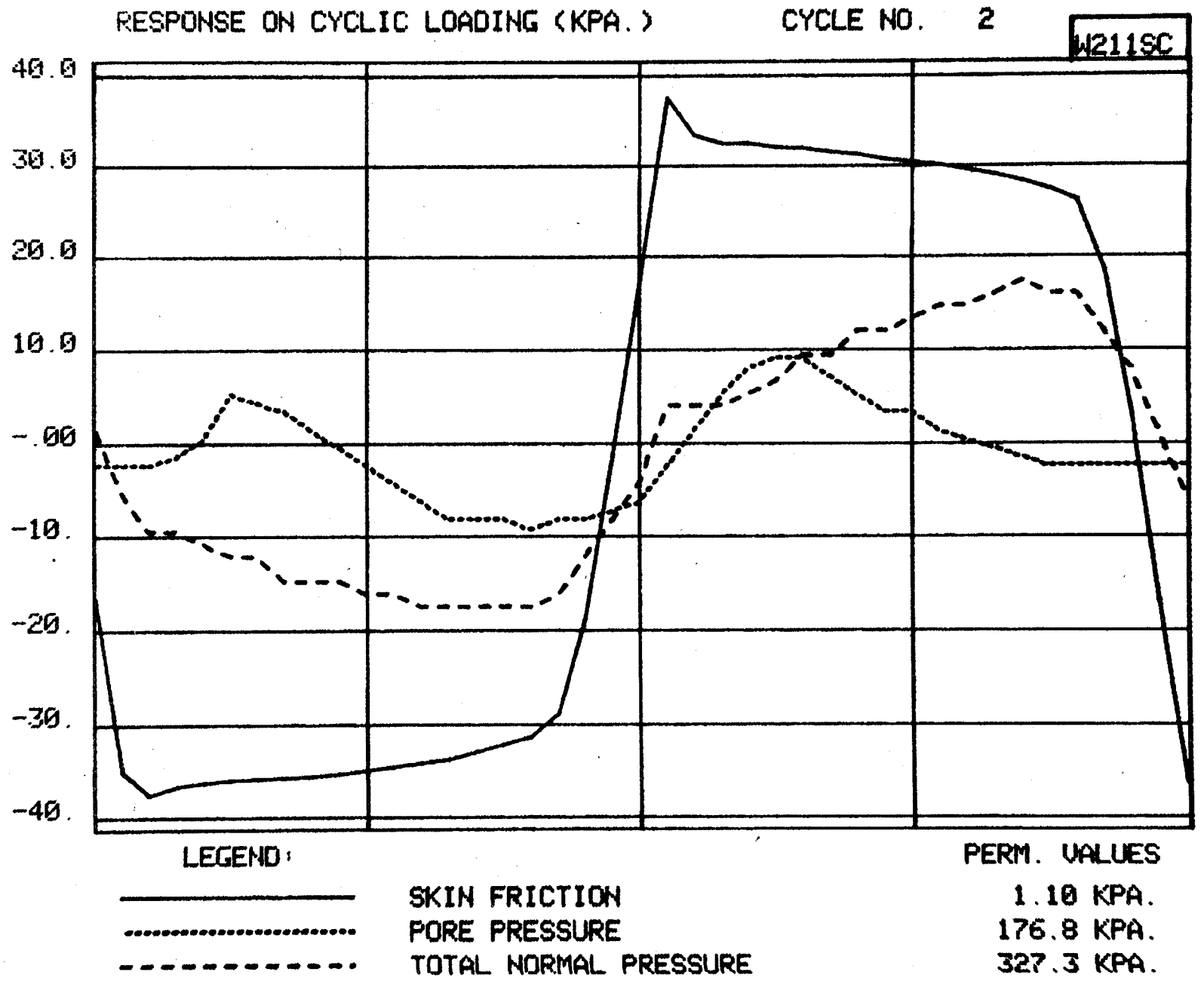
RESPONSE ON CYCLIC LOADING (KPA.)
CYCLE NO. 2
W211SC
40.0
30.0
20.0
10.0
-.00
-10.
-20.
-30.
-40.
LEGEND:
PERM. VALUES
SKIN FRICTION
1.10 KPA.
PORE PRESSURE
176.8 KPA.
TOTAL NORMAL PRESSURE
327.3 KPA.

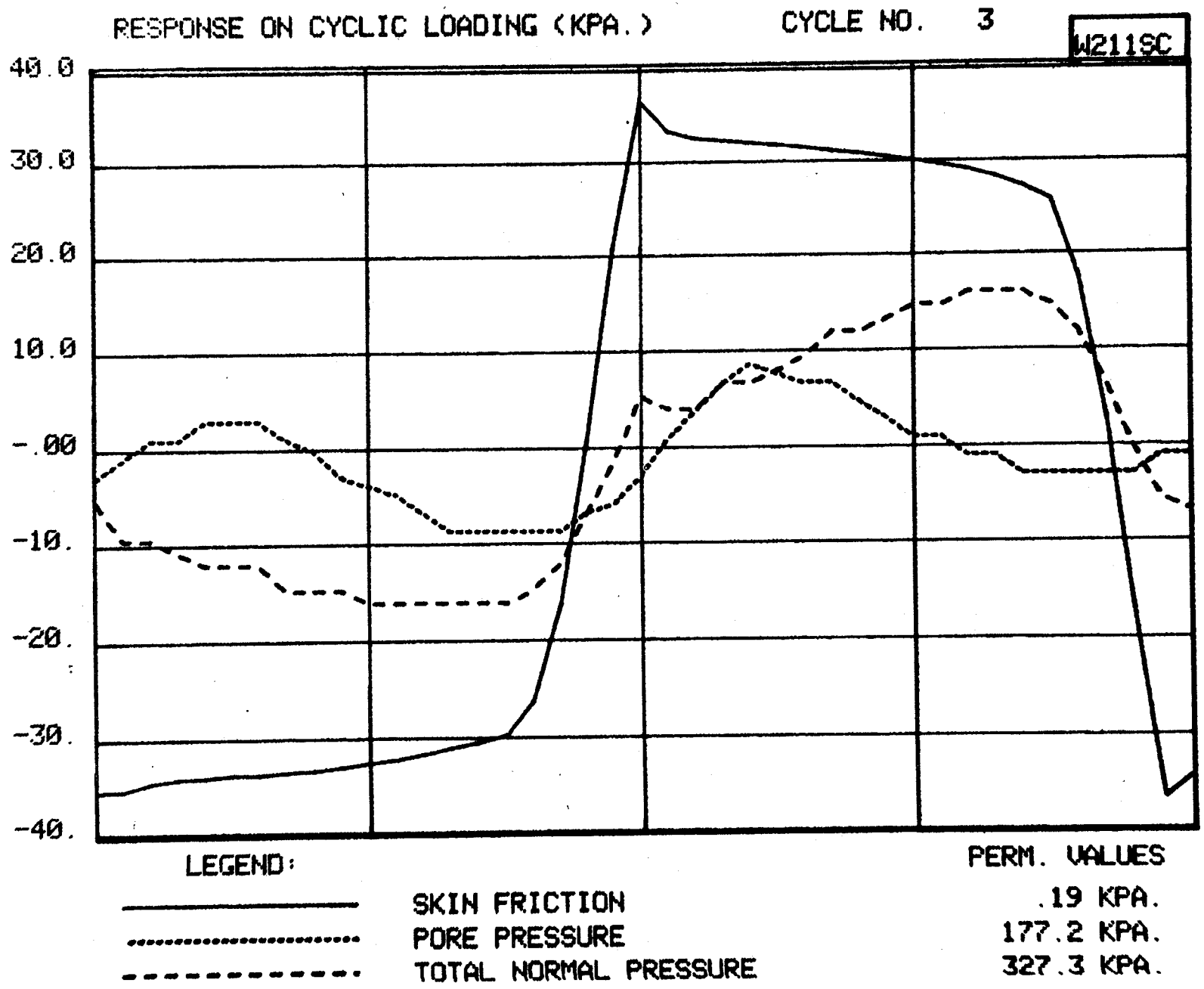
RESPONSE ON CYCLIC LOADING (KPA.)
CYCLE NO. 3
W211SC
40.0
30.0
20.0
10.0
-.00
-10.
-20.
-30.
-40.
LEGEND:
SKIN FRICTION
PORE PRESSURE
TOTAL NORMAL PRESSURE
PERM. VALUES
.19 KPA.
177.2 KPA.
327.3 KPA.

RESPONSE ON CYCLIC LOADING (KPA.) CYCLE NO. 4

W211SC

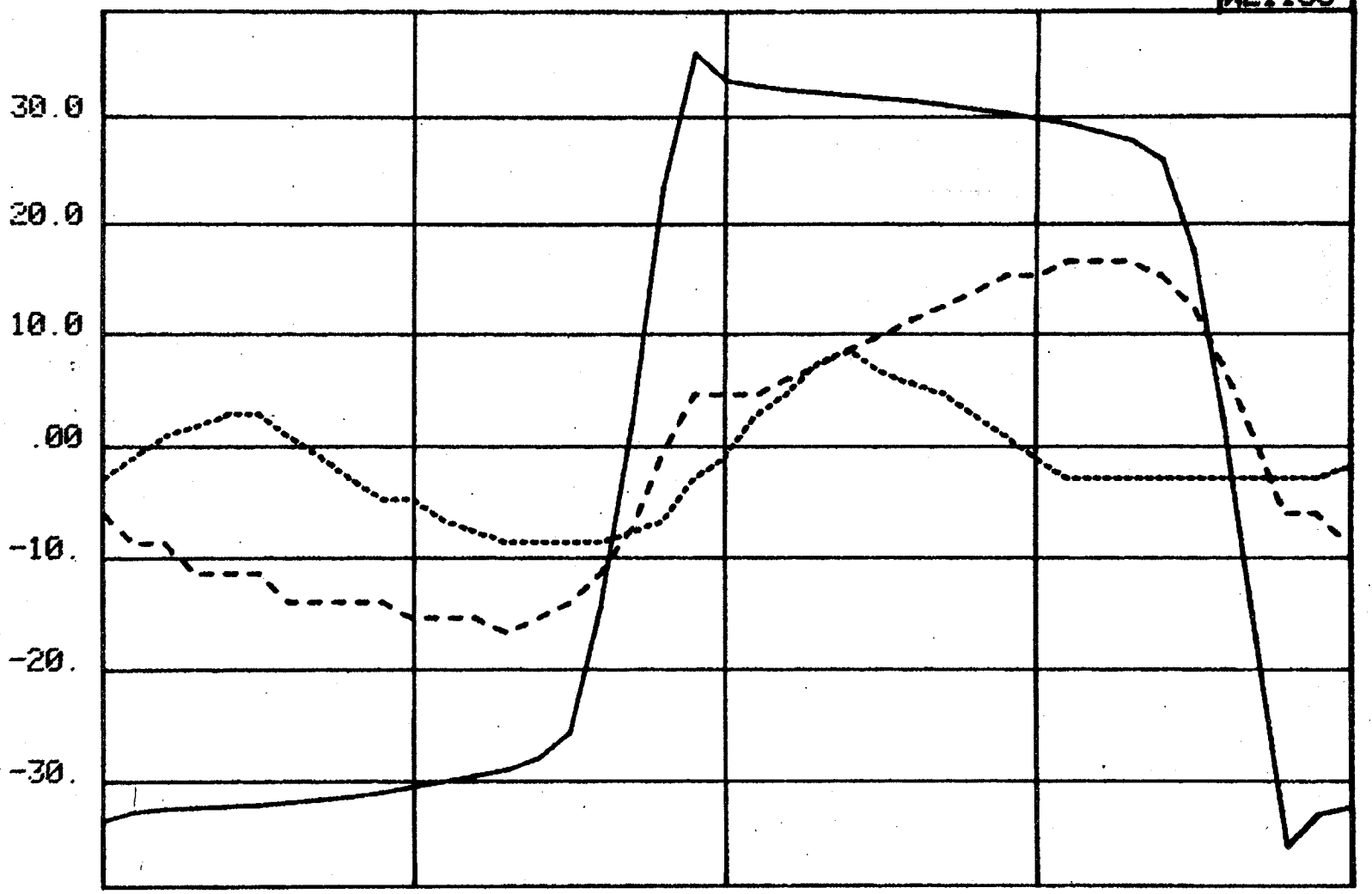

LEGEND:		PERM. VALUES
———	SKIN FRICTION	-.60 KPA.
·····	PORE PRESSURE	179.1 KPA.
- - - -	TOTAL NORMAL PRESSURE	326.7 KPA.

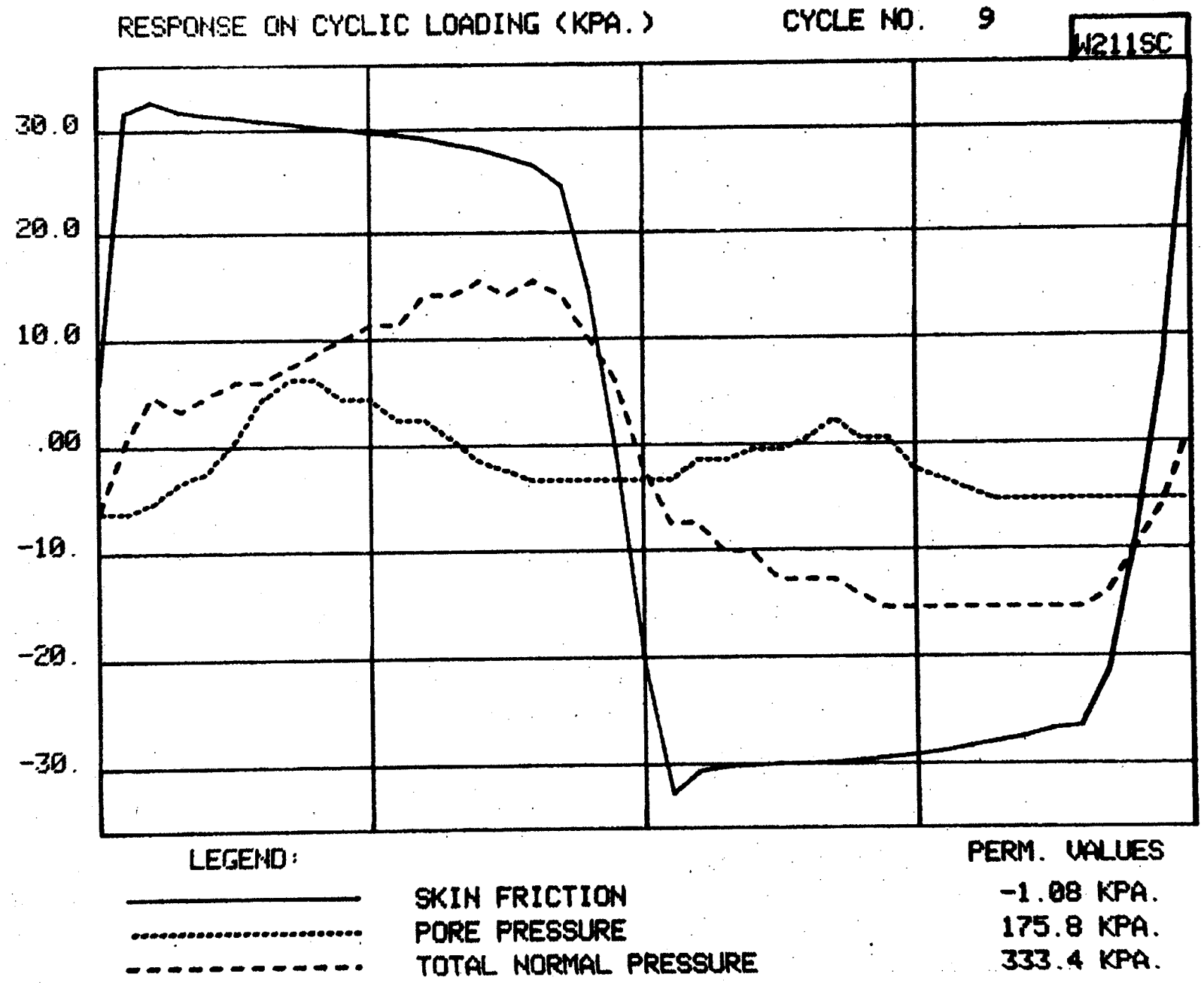
RESPONSE ON CYCLIC LOADING (KPA.)
CYCLE NO. 9
W211SC
30.0
20.0
10.0
.00
-10.
-20.
-30.
LEGEND:
SKIN FRICTION
PORE PRESSURE
TOTAL NORMAL PRESSURE
PERM. VALUES
-1.08 KPA.
175.8 KPA.
333.4 KPA.

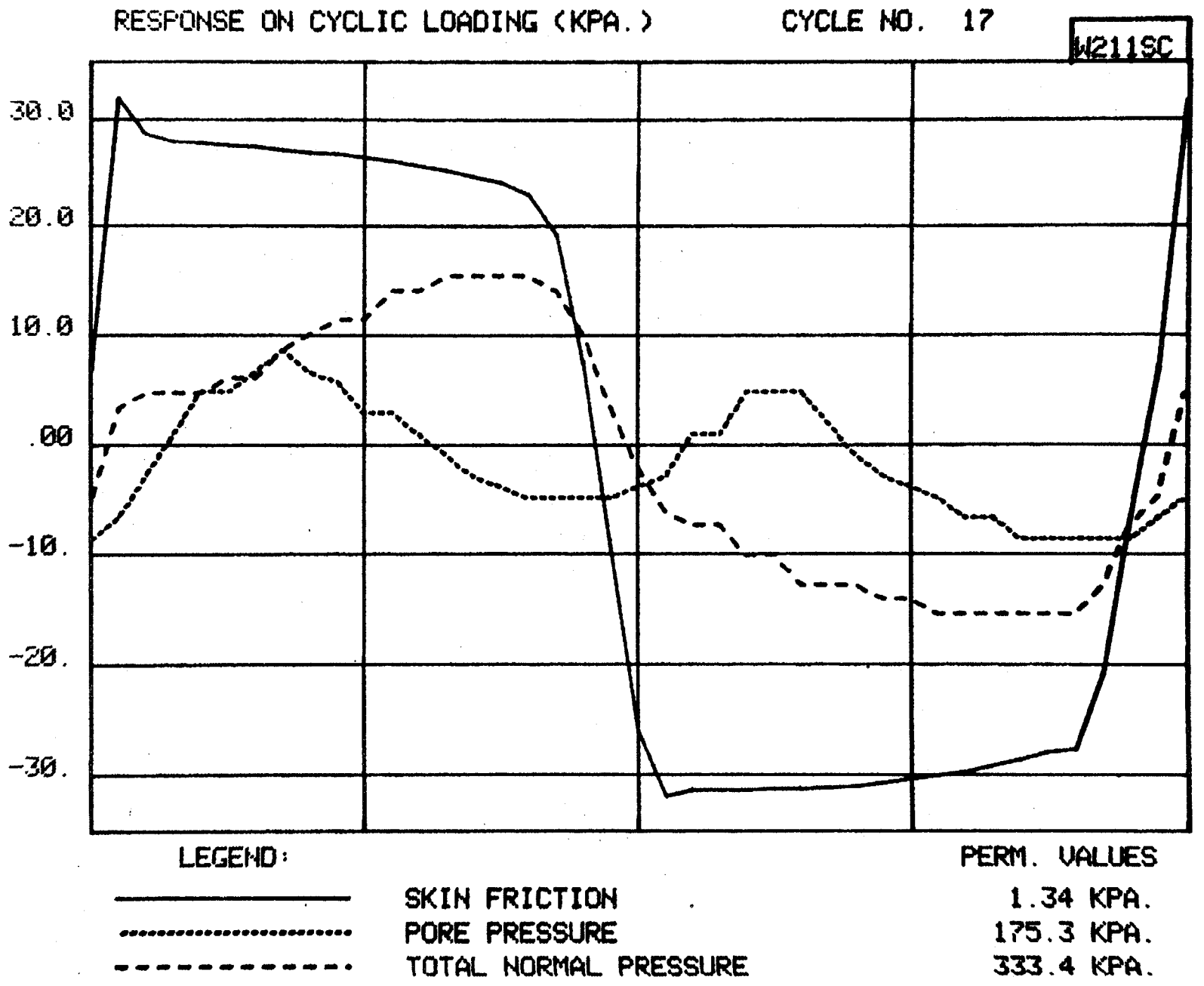
RESPONSE ON CYCLIC LOADING (KPA.)
CYCLE NO. 17
W211SC
30.0
20.0
10.0
.00
-10.
-20.
-30.
LEGEND:
PERM. VALUES
SKIN FRICTION
1.34 KPA.
PORE PRESSURE
175.3 KPA.
TOTAL NORMAL PRESSURE
333.4 KPA.

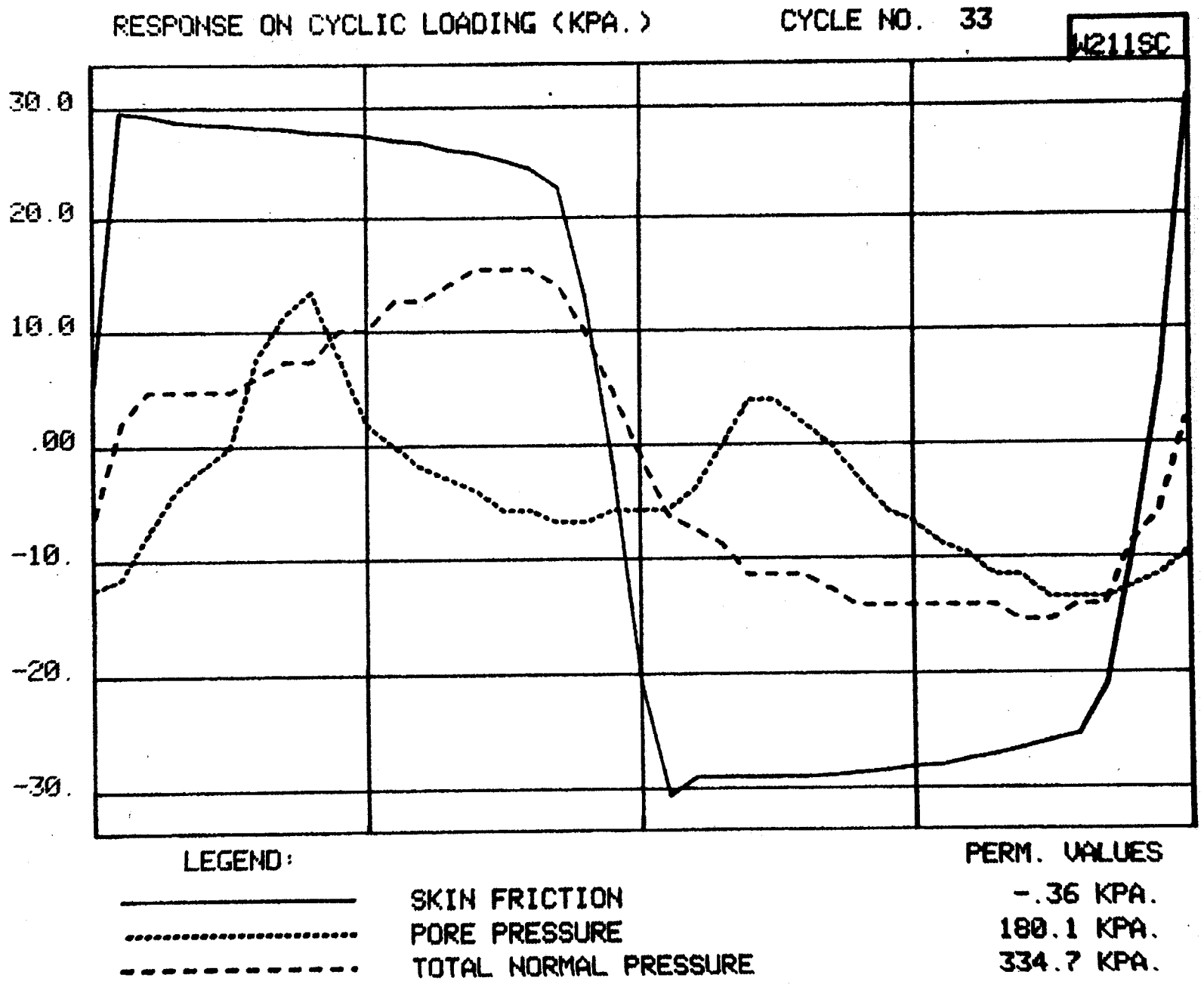
RESPONSE ON CYCLIC LOADING (KPA.)
CYCLE NO. 33
W211SC
30.0
20.0
10.0
.00
-10.
-20.
-30.
LEGEND:
SKIN FRICTION
PORE PRESSURE
TOTAL NORMAL PRESSURE
PERM. VALUES
-.36 KPA.
180.1 KPA.
334.7 KPA.

RESPONSE ON CYCLIC LOADING (KPA.) CYCLE NO. 47

W211SC

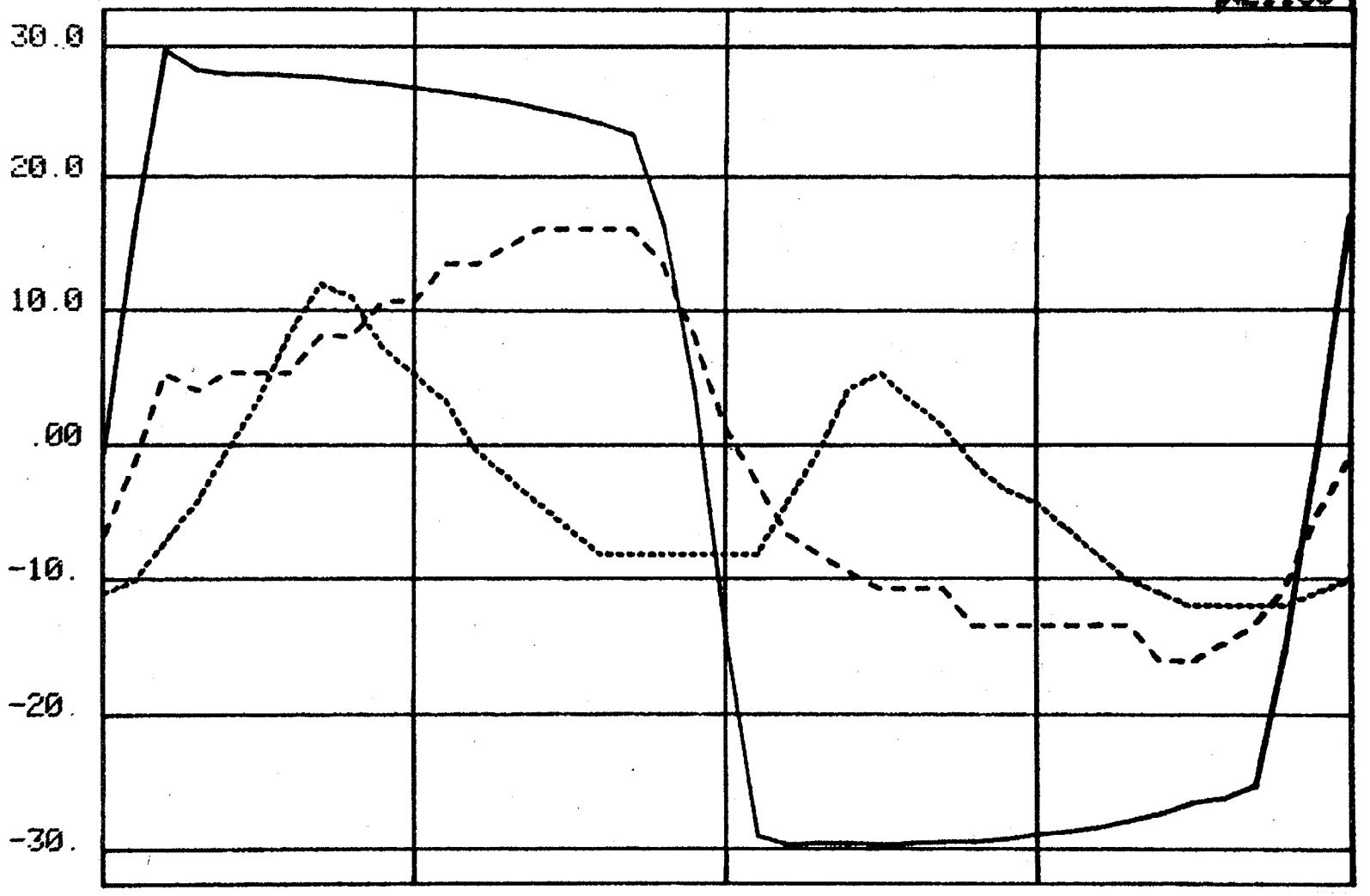

LEGEND:		PERM. VALUES
———	SKIN FRICTION	.21 KPA.
·····	PORE PRESSURE	180.6 KPA.
- - - -	TOTAL NORMAL PRESSURE	334.0 KPA.

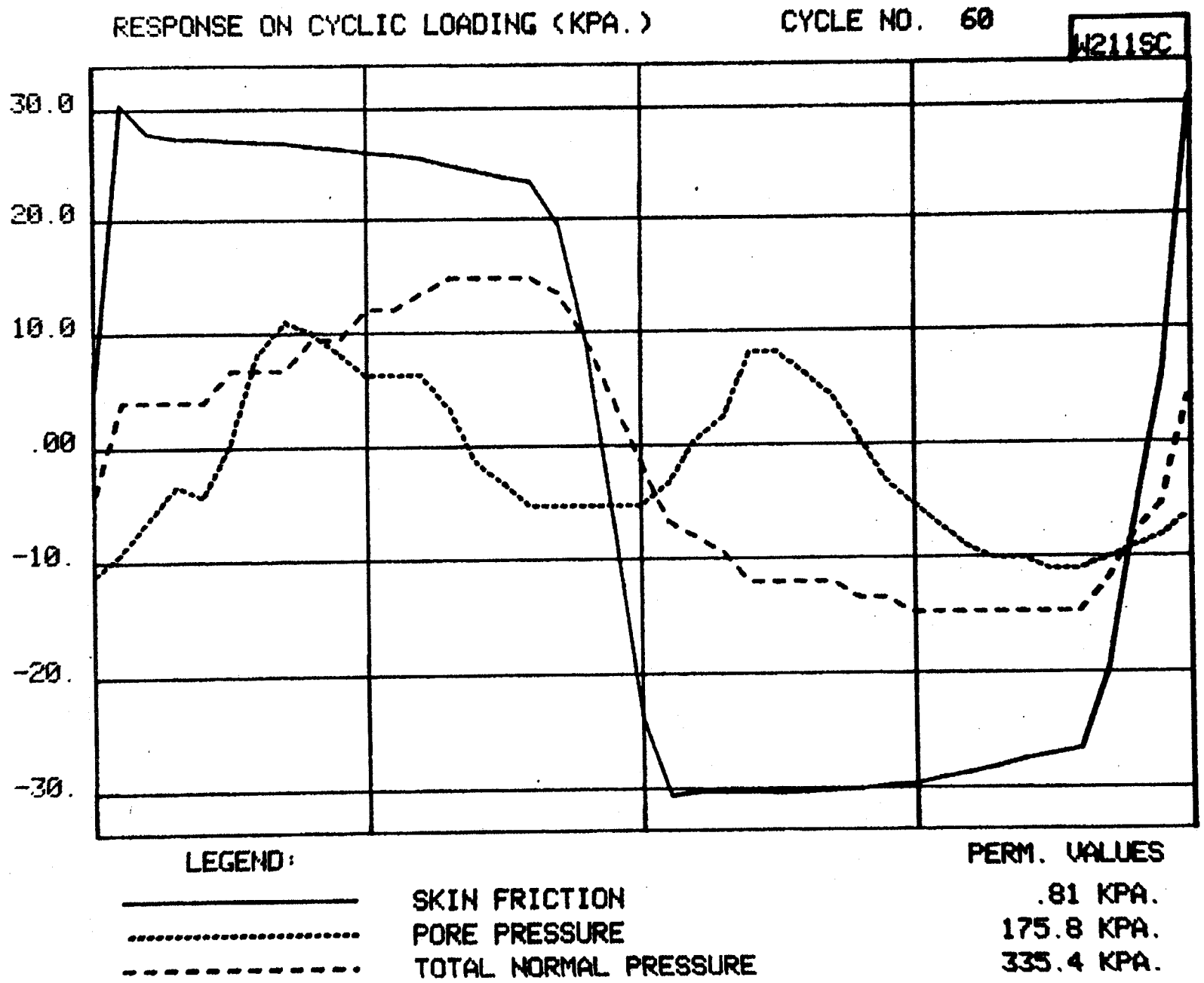
RESPONSE ON CYCLIC LOADING (KPA.)
CYCLE NO. 60
W211SC
30.0
20.0
10.0
.00
-10.
-20.
-30.
LEGEND:
SKIN FRICTION
PORE PRESSURE
TOTAL NORMAL PRESSURE
PERM. VALUES
.81 KPA.
175.8 KPA.
335.4 KPA.

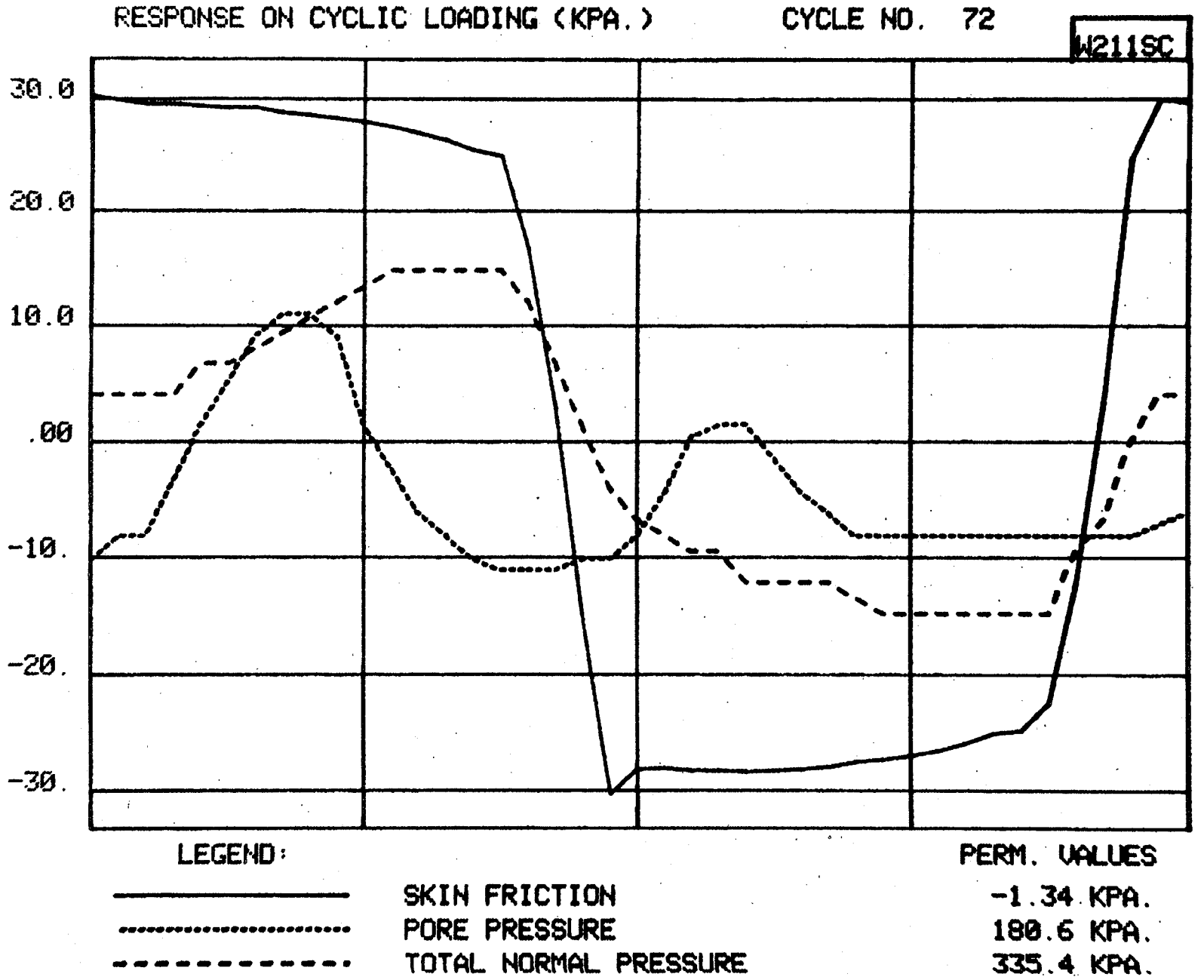
RESPONSE ON CYCLIC LOADING (KPA.)
CYCLE NO. 72
W211SC
30.0
20.0
10.0
.00
-10.
-20.
-30.
LEGEND:
SKIN FRICTION
PORE PRESSURE
TOTAL NORMAL PRESSURE
PERM. VALUES
-1.34 KPA.
180.6 KPA.
335.4 KPA.

APPENDIX I

DETAILED RESULTS FROM **TEST 12, STRATUM III** MODEL PILE TESTS

CONTENTS

Summary	I3
Test 12, Stratum III	I4
Consolidation	I4
Pile Instatllation and Set-Up	I4
Static Test	I5
Random Cyclic Tests	I5
Strength Tests	I7

LIST OF FIGURES

Figure 1	Sample Properties
Figure 2	Consolidation Diagram
Figure 3	Pocket Penetrometer Tests After Consolidation
Figure 4	Pressures at Pile Wall after Installation
Figure 5	Static Test 1
Figure 6	Static Test 2
Figure 7	Random Tests 1-3
Figure 8	Static Test 3
Figure 9	Static Test 4
Figure 10	Random Tests 4-5
Figure 11	Random Test 5
Figure 12	Random Test 5

Figure 13 Pocket Penetrometer Tests after Pile Test
Figure 14 Unconfined Compression Tests
Figure 15 Water Content and Shear Strength

SUMMARY

This report contains the results of the laboratory model pile tests designated TEST 12, STRATUM III, in the project CNRD 13-2, TENSION PILE STUDY, for Conoco Norway Inc.

The clay sample was consolidated for 21 days under 500 kPa applied vertical pressure. Pore pressure in the sample was about 20% of the applied pressure. After 20 days of consolidation in the pile chamber the modified pile was installed with new pore pressure transducer and modified total pressure transducer. After 30 days of set-up the excess pore pressure was about 295 kPa. Testing was then started.

Static test gave peak friction of 35 kPa with residual value of 32 kPa. Undrained shear strength was interpreted to 40 kPa, giving alpha value of 0.87 and 0.8 for peak and residual respectively. Estimating the effective vertical pressure to 167 kPa results in a beta factor of 0.21 .

Random cyclic stress controlled tests were started 24 hours following the static test had static tension bias of 11.5 kPa (35% of previous max. friction in static test) and consisted of about 1200 cycles with the amplitude generated by a random signal generator. The maximum cyclic friction was set to 11.5 kPa (33% of the frictional capacity). The 1200 cycles produced no sign of permanent deflecton and only minimal cyclc deflection. A total of five random tests were performed. In the last test the static level was 26 kPa (70% of the capacity in static test) and the maximum cyclic amplitude was set at 18.5 kPa (50% of the static capacity). An abrupt uplift of the pile occured after about 343 cycles at a friction level lower than previously produced by the soil-pile interface.

A reconsolidation time of 24 hours was generally allowed inbetween the random tests and a random test was followed by a static test to check the capacity with time.

TEST 12, STRATUM III

CONSOLIDATION

The sample was prepared from the same material as used in Test 4. Water was added during the remoulding process to a water content of about 50% . Horizontal filters were placed in the oedometer to provide better vertical drainage.

A vertical pressure of 500 kPa was applied on top. As seen in Figure 2 the pore pressure at middle height had dropped down to about 11% of the consolidation stress after 15 days. At this time the pressure is seen to increase to about 20% of the consolidation stress in the next four days. The axial strain is at the same time seen to increase its rate and it is therefore concluded that the piston in the oedometer was obstructed during the course of the consolidation and then came loose after 15 days, causing an increased settlement rate and therefore also an increase in the pore pressure. The sample was at this time transferred to the pile chamber. Pocket penetrometer tests were performed on the side of the sample and on the top as shown in Figure 3. The shear strength, s_u, showed an average of about 40 kPa.

PILE INSTALLATION AND SET-UP

After pocket penetrometer tests the sample was mounted in the pile chamber and left to reconsolidate for 20 days under a vertical pressure of 500 kPa and radial pressure of 350 kPa (K=0.7).

As in Test 8 no back pressure was applied and vertical filter strips were placed on the outside perimeter of the clay sample with direct drainage on top and bottom of the pile chamber. Again good drainage was proved by formation of salt on the filter strips sticking out, which came from the expelled water from the marine clay.

After insertion of the pile the total normal pressure showed about 625 kPa and the pore pressure showed about 535 kPa. At this time an "immediate" static test was performed to check the friction, as shown in Figure 5. The maximum friction showed 25 kPa with a residual value of about 22 kPa.

After 8 days of set-up the pore pressure had reduced to 275 kPa and the total pressure showed 435 kPa. Upon additional consolidation the porepressure started to increase as seen in Figure 4 and reached a steady state at 295 kPa after 30 days from installation. At this time it was decided to start with the loading program. The total pressure was at this time about 420 kPa.

STATIC TEST

A displacement controlled static test with deformation rate 1 mm per hour was now conducted, as shown in Figure 5. The pile was pulled in tension through failure and large slip and then pushed down to original position causing failure in compression and large slip (residual friction).

The displacement to cause failure, as shown in Figure 6, was about 0.3 mm or 1.2% of the pile diameter. A maximum friction of 35 kPa was achieved with a residual friction of 32 kPa. An increase of about 40% from the static test immediately after installation is the result of the set-up time. The shear strength of the clay at time of testing was estimated to 40 kPa which results in an alpha (α) value of 0.87 and 0.8 for peak and residual friction respectively.

For the effective stress approach, estimating σ'_{vo} from the relationship

$$s_u = 0.26 \cdot \sigma'_{vo}$$

which gives $\sigma'_{vo} =$ 167 kPa, the beta value (β) becomes 0.21 for maximum friction.

Total pressure on the pile wall at time of failure was about 410 kPa and the pore pressure showed 295 kPa, resulting in a horizontal effective pressure of 115 kPa. The interface friction angle (δ) can then be estimated to 16.9 degrees.

RANDOM CYCLIC TESTS

After the static test the pile was left to reconsolidate for 24 hours before cyclic testing was started. Both the total pressure and the pore presure were unchanged and showed 410 and 295 kPa respectively. A random cyclic test comprised of applying a prescribed static tensile (uplift) stress on the pile, superimposed with cycles of

randomly varying amplitude. The cyclic period is held constant at 10 seconds for all cycles and the maximum number of cycles applied was about 1250. The resulting deformations and pressures on the pile wall were monitored during the cycling. The static level and the maximum cyclic level were increased in subsequent random tests until the pile finally fails (abrupt pullout).

For the first random test the static tensile stress (bias) level was 11.5 kPa, corresponding to 33% of the previous static capacity. The maximum cyclic amplitude was set to 11.5 kPa, resulting in only one- way loading (tensile) as shown in Figure 7. The test resulted in no permanent deflection of the pile and the pressures on the pile wall were almost constant throughout the test. The pile was now left to reconsolidate for three days at which time a new static test was performed, with results shown in Figure 8. The static capacity was here evaluated to 37 kPa. A new period of 24 hours was given for reconsolidation before random test number two was started. The total pressure and pore pressure showed 395 kPa and 290 kPa respectively.

In random test two the static level was half the static strength, or 18.5 kPa, with the maximum cyclic amplitude set to 15 kPa, corresponding to 40% of the static capacity. Again, as for the previous test, the 1250 cycles with these load combinations resulted in no measurable permanent displacement and with only minimal cyclic displacements during the applied load cycles. A static test after the random test resulted in the same static capacity as previous tests, as depicted in Figure 9. The pressures on the pile wall also stayed steady during these tests.

Random test number three was started after 24 hours of reconsolidation with the static level still at 50% of the static capacity and now with the maximum cyclic stress amplitude of the same magnitude as the static level as shown in Figure 7. As for the two previous random tests still no sign of permanent deflection of the pile was seen and no substantial change in the pressures at the pile wall resulted from the random loading. Two additional days of reconsolidation was now allowed before a new random test was initiated. The load combinations are shown in Figure 10 where it is seen that random test four had a static load level of 60% of the static capacity and the maximum cyclic stress level was held at 50% of the static capacity. This implies that for the maximum peaks the actual mobilized friction was larger (10%) than the static capacity measured earlier. The test, however, rvealed that even for this load combination no permanent displacement of the pile resulted and the cyclic deformations were also minimal. Again the pressures at the pile wall were fairly constant throughout the test.

It was decided to allow only three hours of set-up before a new random test was started, which had a load combinatoon as shown in Figure 10 and designated Random Test 5. The static level was here increased to 70% (26 kPa) of the previous static strength (37 kPa) with the maximum cyclic stress amplitude held at 50%, or 18.5 kPa. The results of this test is shown in Figures 11 and 12, with the latter showing the mobilized friction versus pile displacement. After about 343 cycles the pile is seen to experience an excessive deformation with a mobilized friction lower than what had previously been produced with no sign of failure. In Figure 11 the pore pressure, total pressure, deflection (stroke) and mobilized skin friction are shown versus time (number of cycles). In this figure signs of permanent deformation can be seen about 30 cycles before the point of failure occurs.

It is interesting to note that large deformation of the pile occured after the initial failure, at stresslevels significantly lower than previously obtained and also lower than the stress level for the initial failure. The measurements of the pressures on the pile wall showed a decrease in the pore pressure and an increase in the total pressure at the time of failure and for subsequent cycles producing excessive deformations.

STRENGTH TESTS

After the random test leading to failure the pile was left to monitore the pressures on the pile wall, which slightly reduced during the next six days. At this time the pile was extruded from the sample and the clay was built out. Pocket penetrometer tests were performed on the side of the sample and in two horizontal layers with results shown in Figure 13.

Three standard triaxial test samples were then prepared from the center of the clay specimen and unconfined compression tests (UCT) were performed with the results shown in Figure 14.

In Figure 15 are shown the water content and interpreted undrained shear strength of the clay sample versus the distance from the center after completion of the pile test. The water content showed about 45 % with a tendency to decrease towards the center. This relatively high water content can explain the fairly low undrained shear strength measured for this test. The reason for this fact is most likely the incomplete consolidation of the clay sample due to the fact that the piston in the oedometer was stuck, as mentioned earlier in the section describing the consolidation.

TABLE 1.

SAMPLE PROPERTIES TEST 12, STRATUM III

SAMPLE PREPARATION		CONSOLIDATION			END OF PILE TEST
INITIAL WATER CONTENT	INITIAL HEIGHT	AXIAL DEFORMATION	AXIAL STRAIN	WATER CONTENT	WATER CONTENT
w_i (%)	H_o (cm)	ΔH (cm)	ε (%)	w_e (%)	w_{ep} (%)
50.15 49.31	51.30	5.07	9.88	A 38.86 B 47.39 C 51.21 D 49.80	A 40.97 D 41.88 B 44.61 E 42.81 C 46.76 F 43.22

CONFINING PRESSURE		
AXIAL	KPa	500
RADIAL	KPa	350
BACK PRESSURE	KPa	0
SAMPLE CONSOLIDATION		
IN OEDOMETER	Days	21
IN PILE CHAMBER	Days	20
INTERPRETED SHEAR STRENGTH		
END OF CONSOLIDATION	KPa	40
END OF PILE TEST	KPa	40

Fig. 1

CONSOLIDATION DIAGRAM								Test No. 12 Stratum III		Start date 1/12 82	
H_i 51.30 cm		H_e 46.23 cm		$\Delta\varepsilon_v$ 9.88 %						σ_c 500 kPa	
Time h	20	44	116	140	188	357	506				
Δh cm	1.7	3.03	4.01	4.08	4.25	4.47	5.07				
u kPa	15	81	117	98	93	56	101				

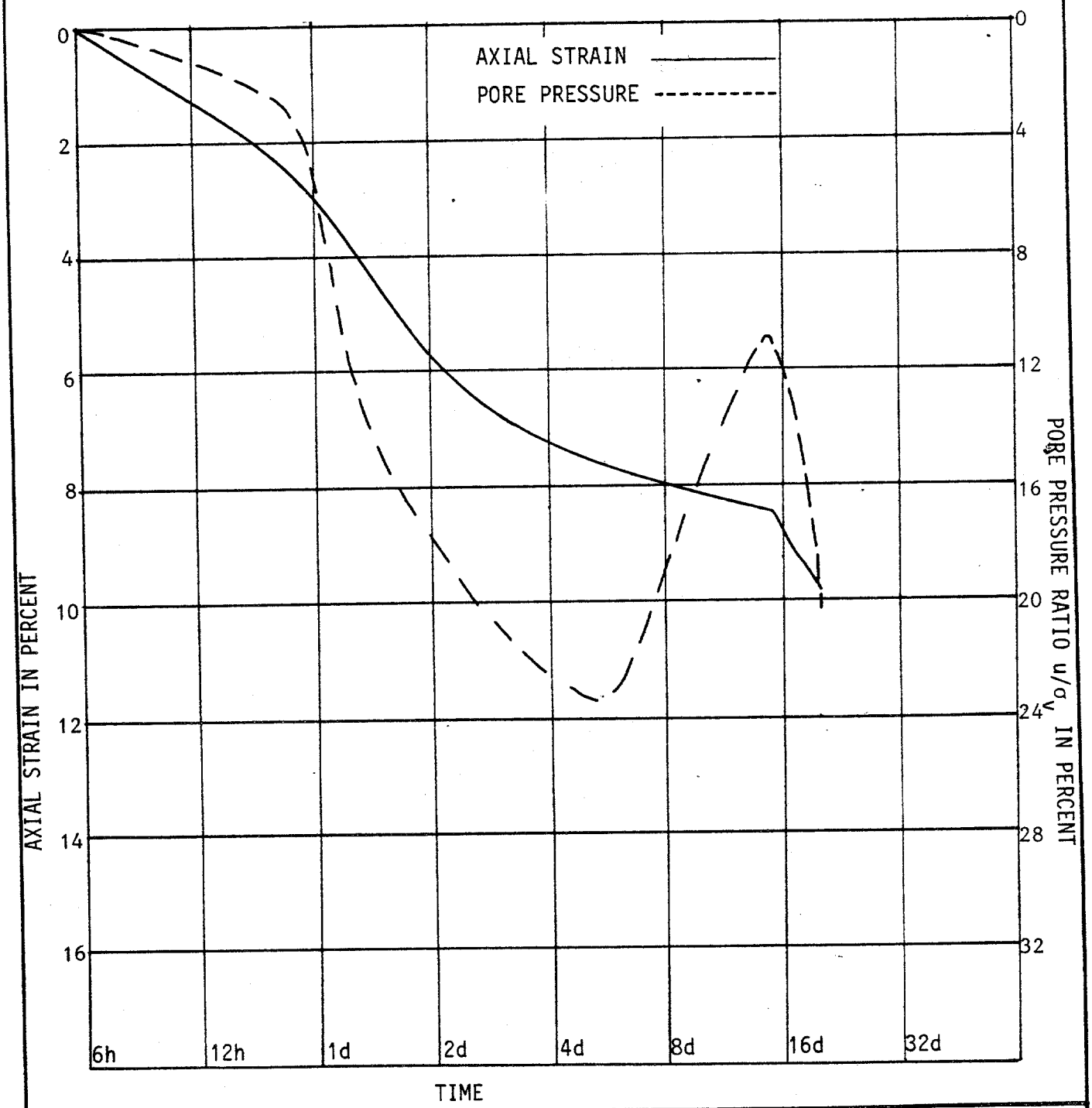

CNRD 13-2 TENSION PILE STUDY LABORATORY MODEL PILE TESTS

TEST 12, STRATUM III, Consolidation diagrams for clay sample

Scale

DET NORSKE VERITAS
Geotechnical Laboratory

Drawn by

Date

Approved

Fig. No. 2

TEST 12, STRATUM III

SHEAR STRENGTH (kPa) FROM POCKET PENETROMETER TESTS AFTER CONSOLIDATION

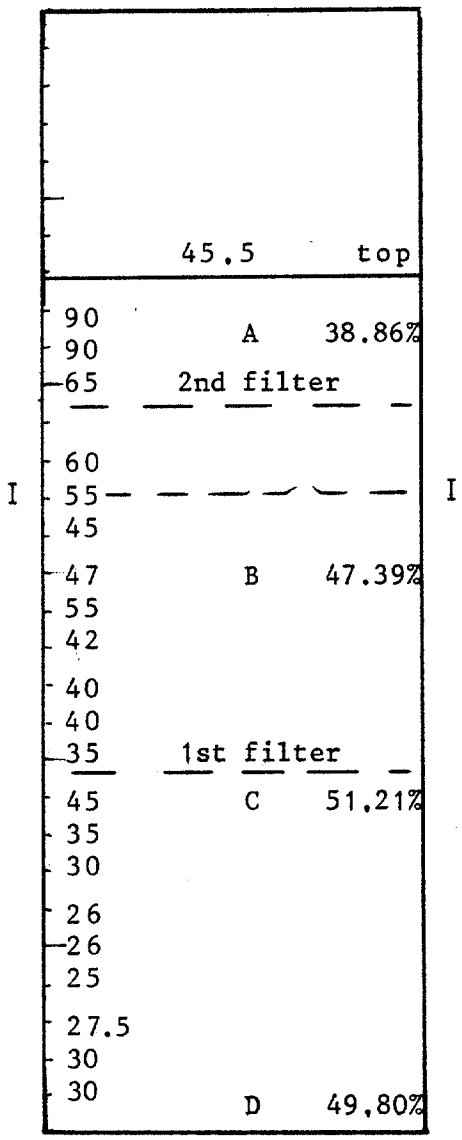

Scale 1:4

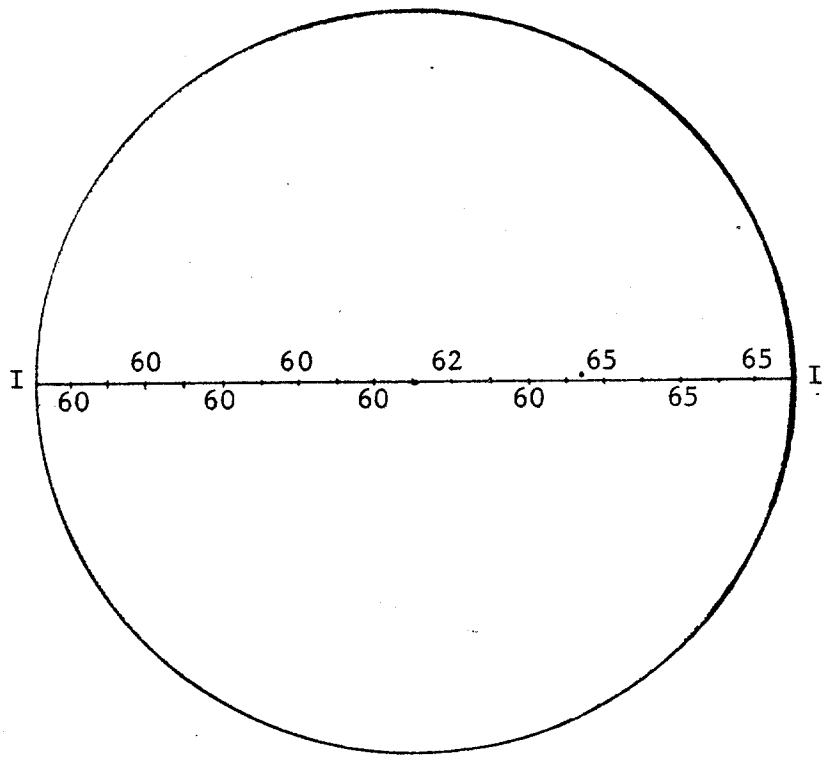

Scale: 1:2

CNRD 13-2 TENSION PILE STUDY LABORATORY MODEL PILE TESTS

TEST 12, STRATUM III, pocket penetrometer tests		Scale
DET NORSKE VERITAS Geotechnical Laboratory	Drawn by	Date
	Approved	Fig.No. 3

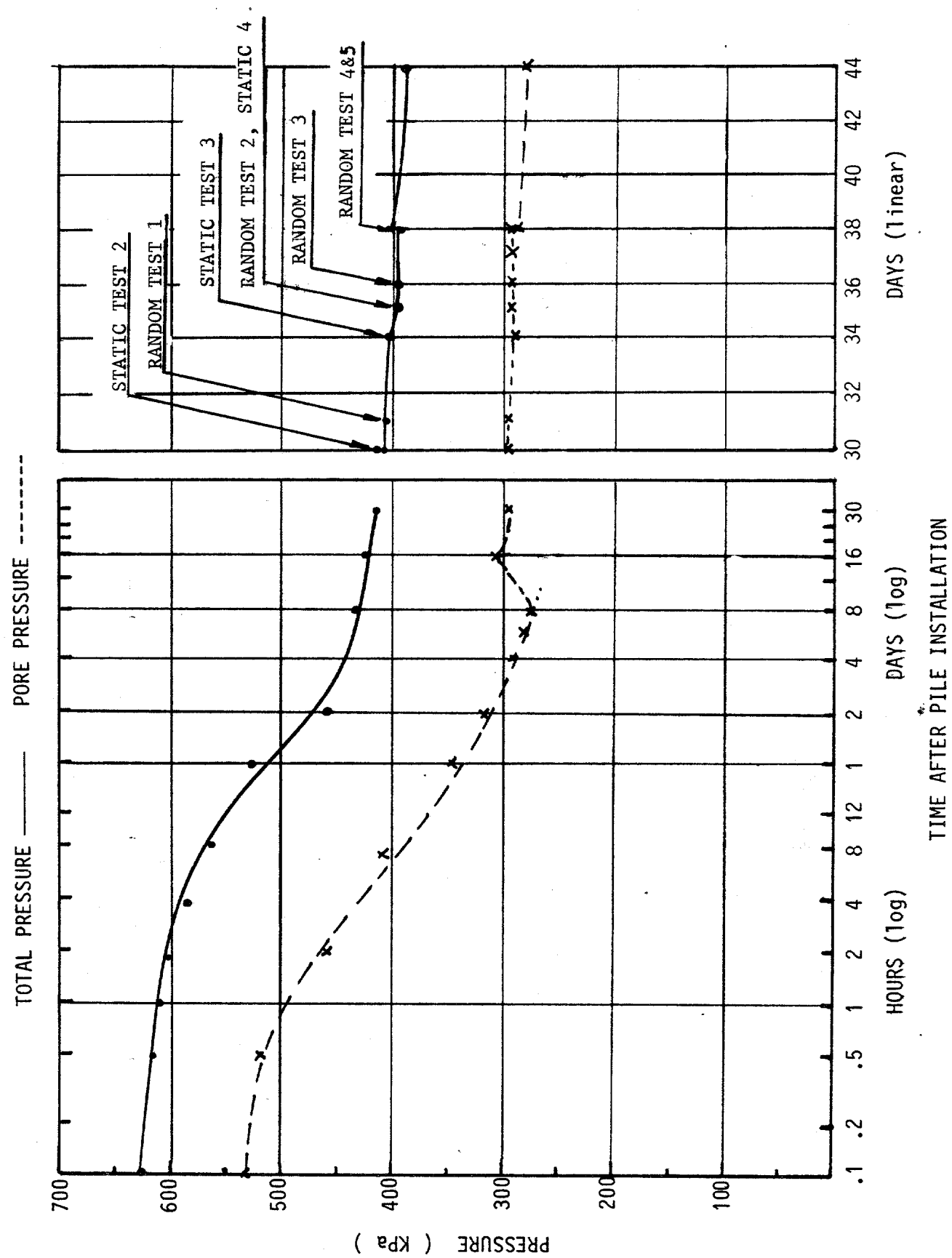

CNRD 13-2 TENSION PILE STUDY LABORATORY MODEL PILE TESTS 231004

TEST 12, STRATUM III, Pressures at pile wall after installation

DET NORSKE VERITAS Geotechnical Laboratory	Drawn by	Scale
	Approved	Date
		Fig. No. 4

STATIC TEST IMMEDIATELY AFTER INSTALLATION

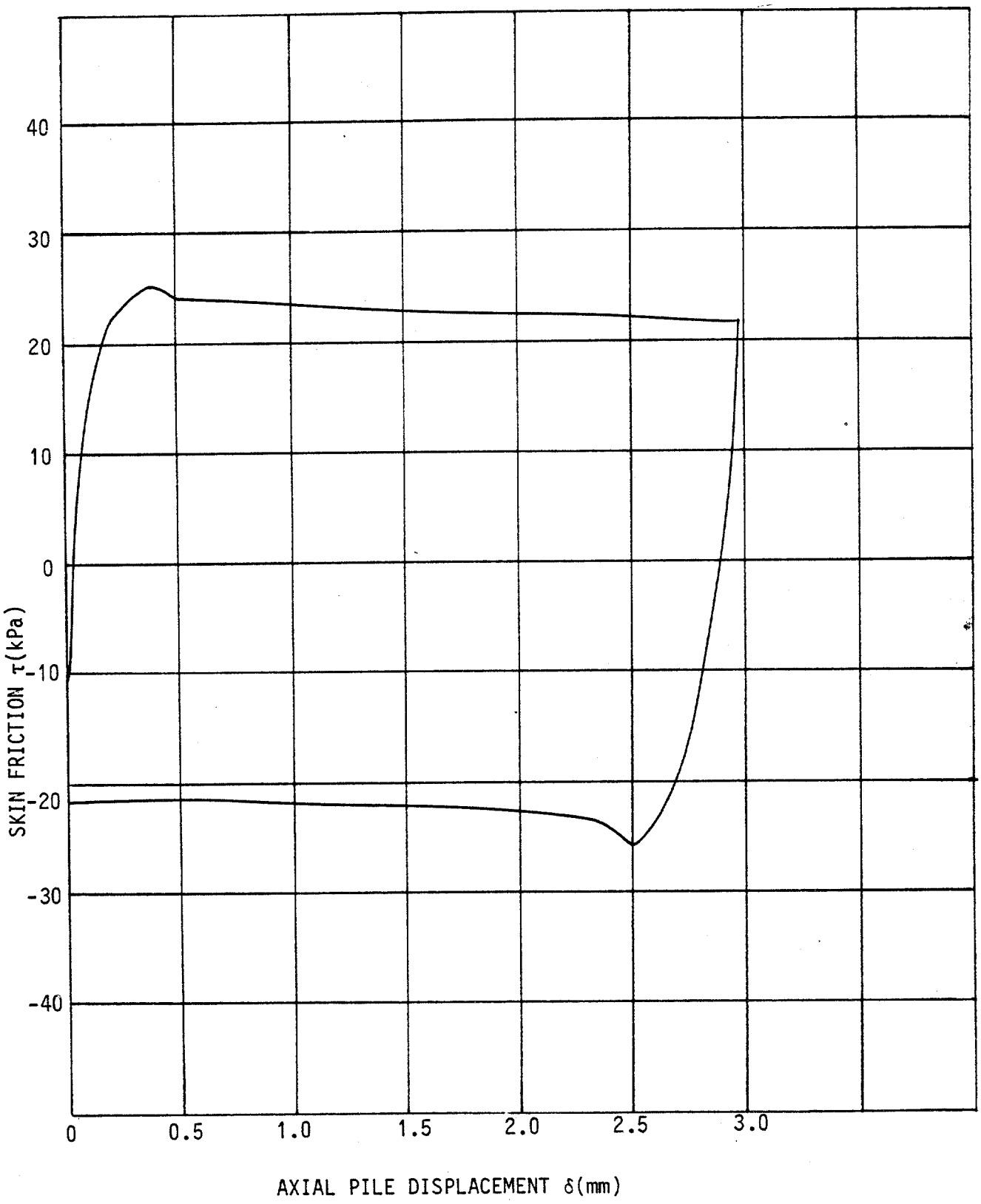

CNRD 13-2 TENSION PILE STUDY LABORATORY MODEL PILE TESTS 231604

TEST 12, STARTUM III, STATIC TEST I

DET NORSKE VERITAS Geotechnical Laboratory	Drawn by	Scale
	Approved	Date
		Fig. No. 5

STATIC TEST BEFORE
RANDOM LOADING NO.1

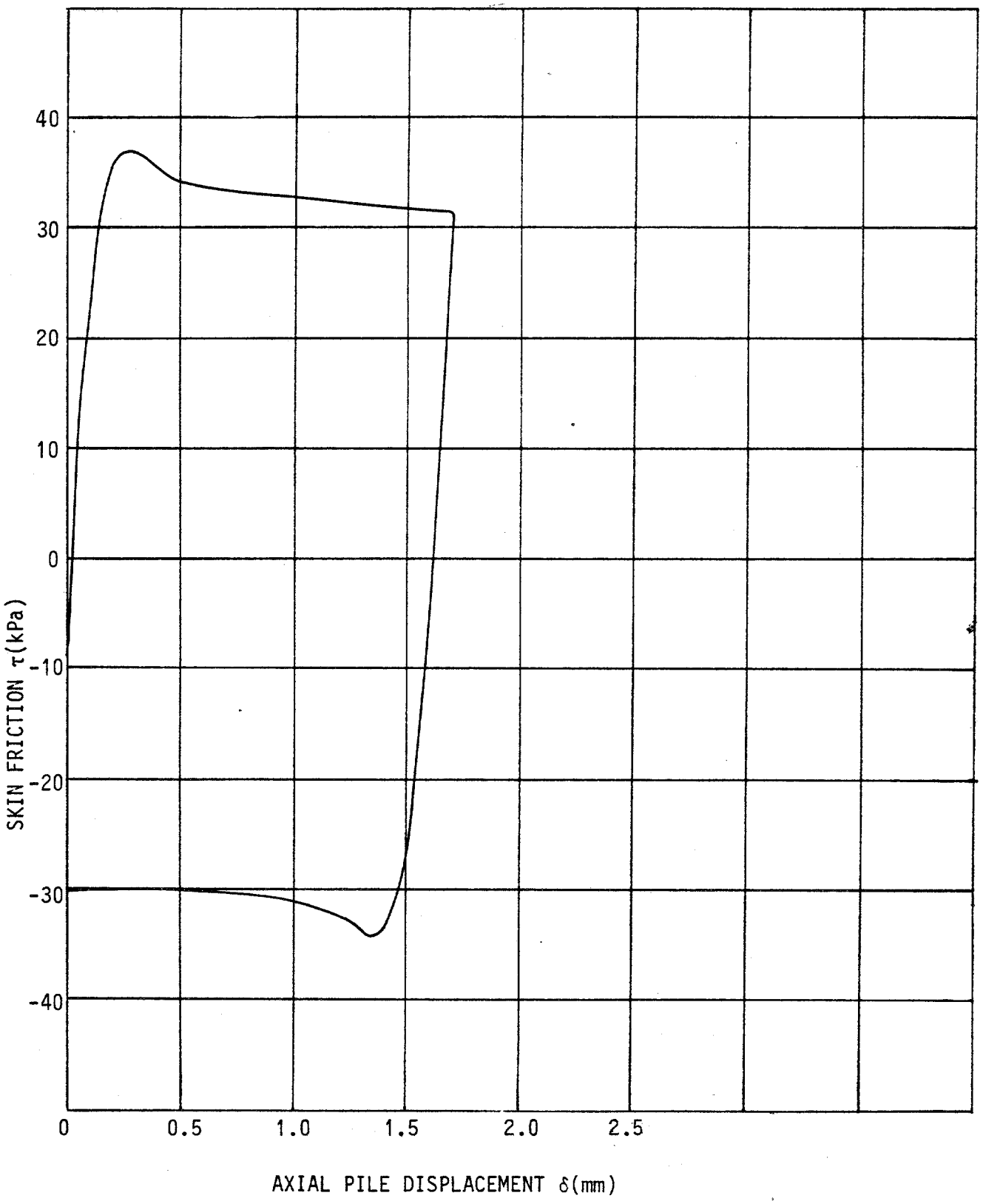

CNRD 13-2 TENSION PILE STUDY LABORATORY MODEL PILE TESTS

TEST 12, STRATUM III, STATIC TEST 2

DET NORSKE VERITAS Geotechnical Laboratory	Drawn by	Scale
	Approved	Date
		Fig. No. 6

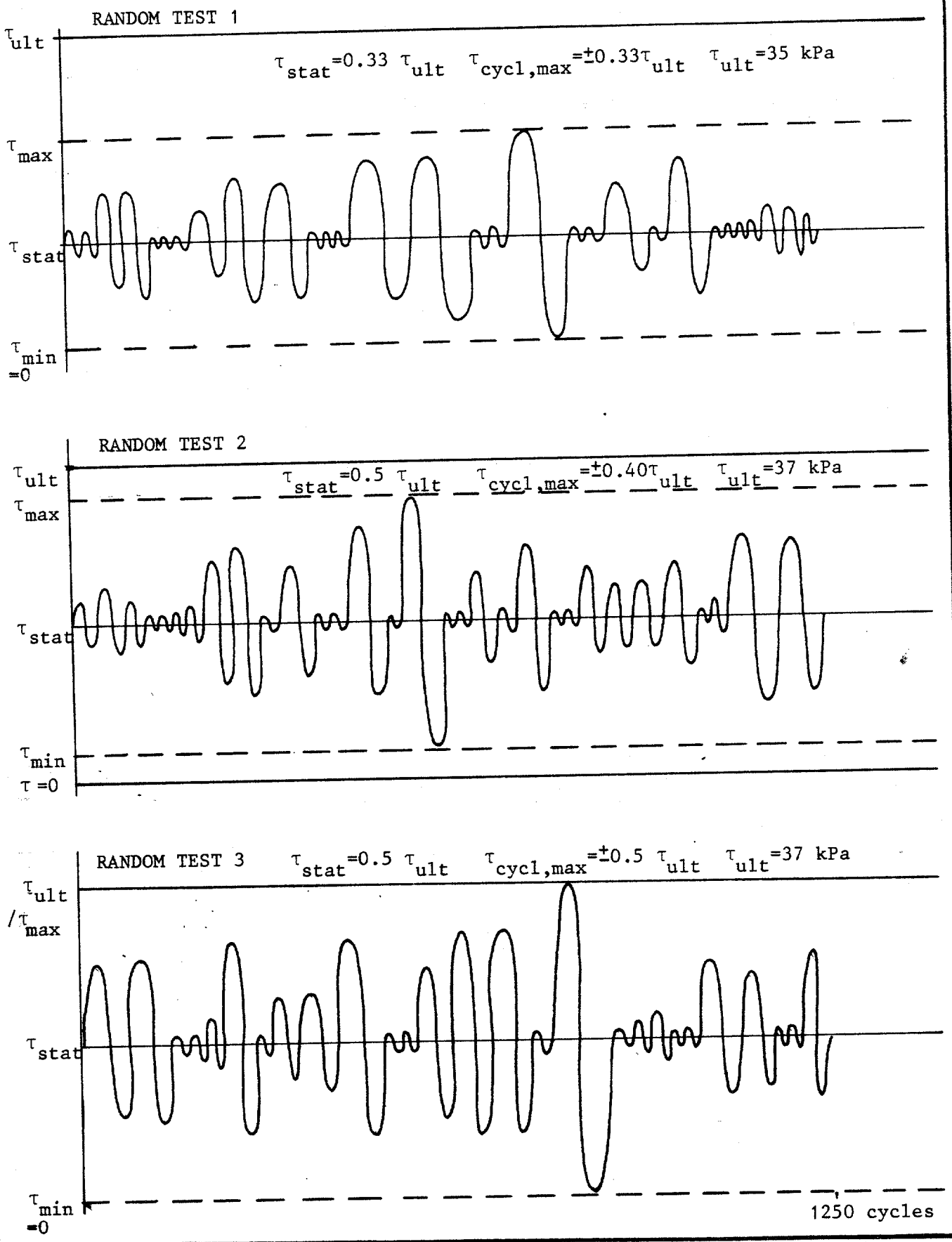

CNRD 13-2 TENSION PILE STUDY LABORATORY MODEL PILE TESTS

TEST 12, STRATUM III, Random tests 1-3

DET NORSKE VERITAS Geotechnical Laboratory	Drawn by	Scale
	Approved	Date
		Fig. No. 7

STATIC TEST AFTER RANDOM TEST 1

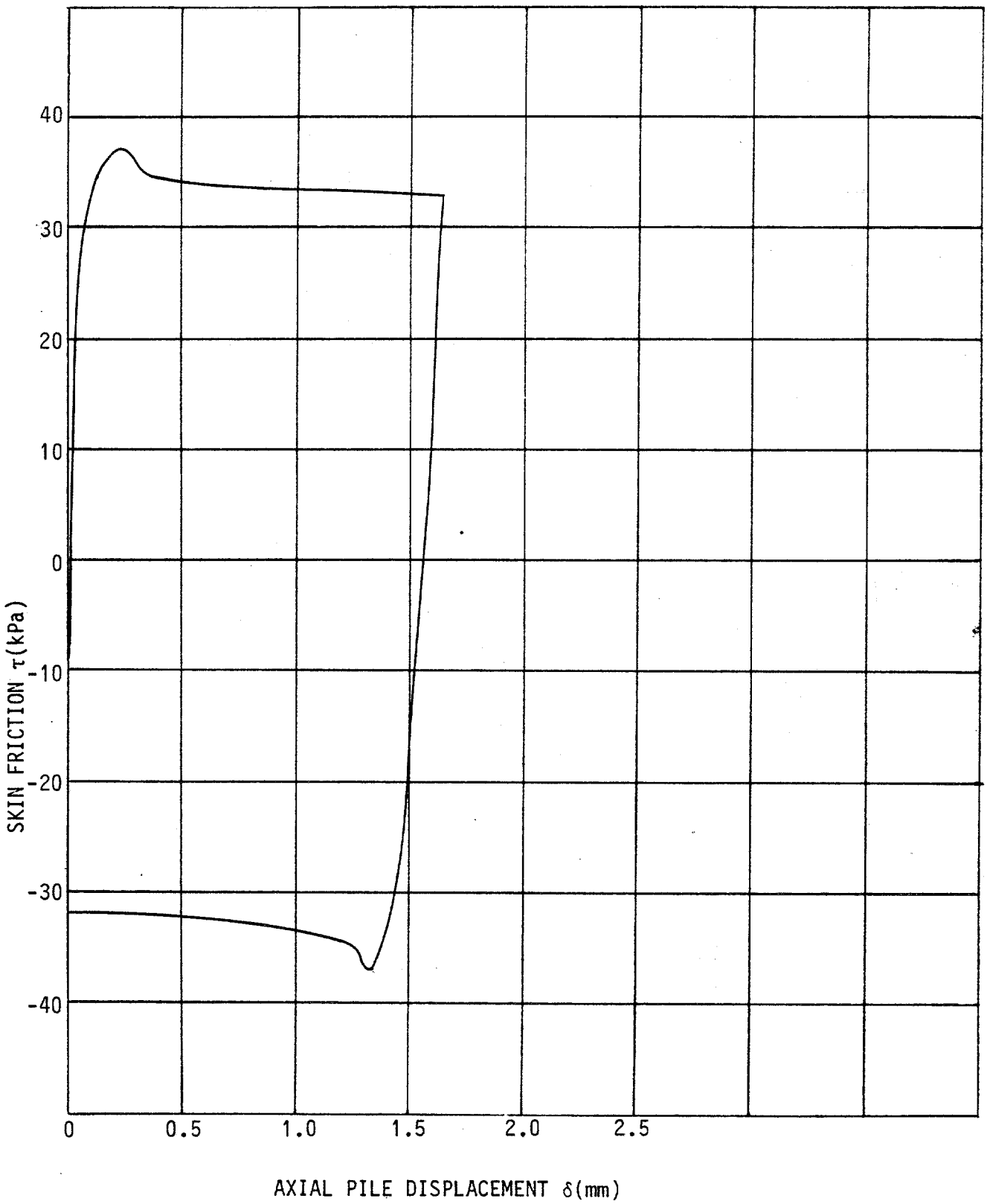

CNRD 13-2 TENSION PILE STUDY LABORATORY MODEL PILE TESTS 231004

TEST 12, STRATUM III, STATIC TEST 3

DET NORSKE VERITAS Geotechnical Laboratory	Drawn by	Scale
	Approved	Date
		Fig. No. 8

STATIC TEST AFTER RANDOM TEST 2

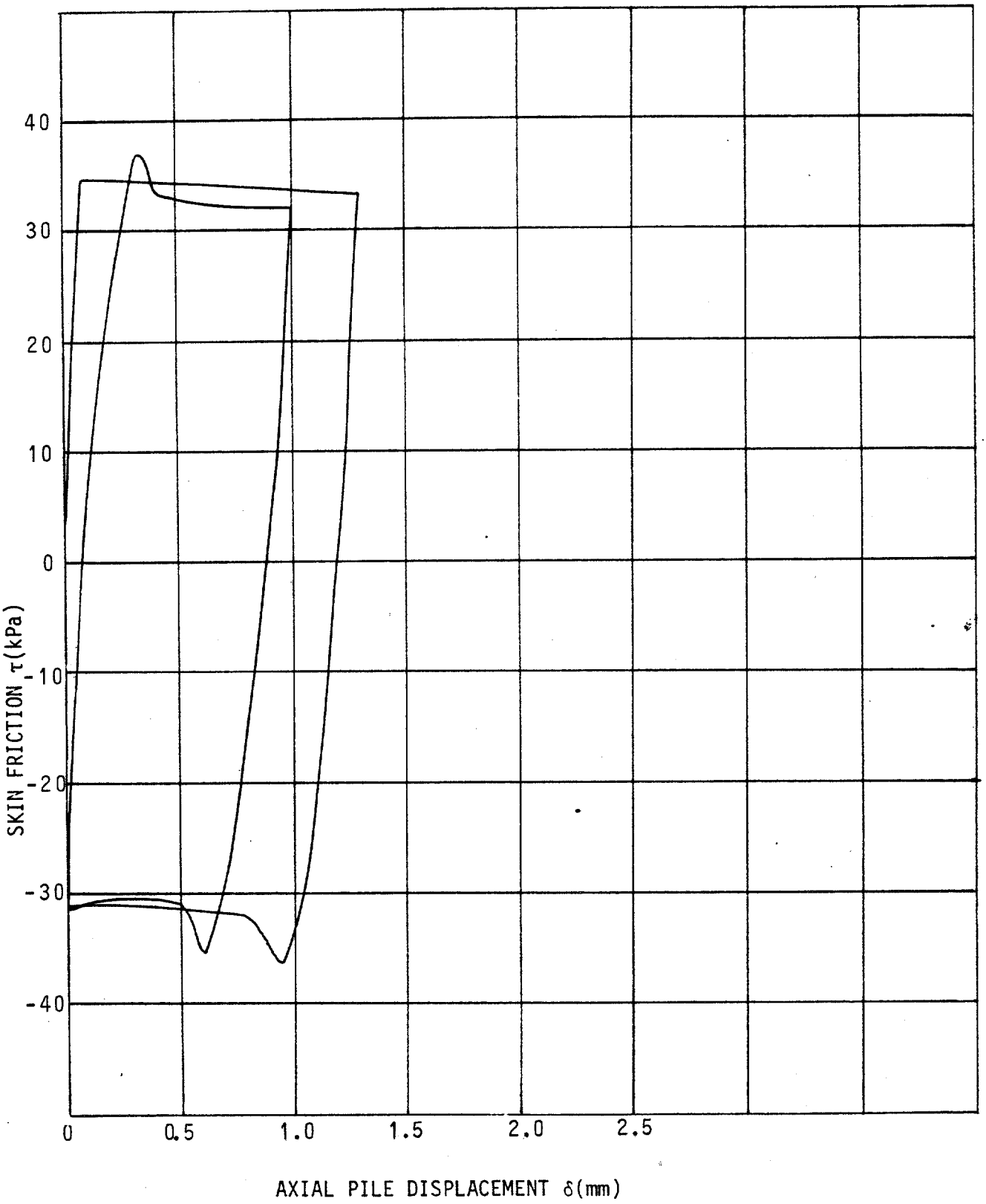

CNRD 13-2 TENSION PILE STUDY LABORATORY MODEL PILE TESTS 231604		
TEST 12,STRATUM III, STATIC TEST 4		Scale
DET NORSKE VERITAS Geotechnical Laboratory	Drawn by	Date
	Approved	Fig.No. 9

RANDOM TEST 4 $\tau_{stat}=0.60\ \tau_{ult}$ $\tau_{cycl,max}=\pm 0.50\ \tau_{ult}$ $\tau_{ult}=37$ kPa

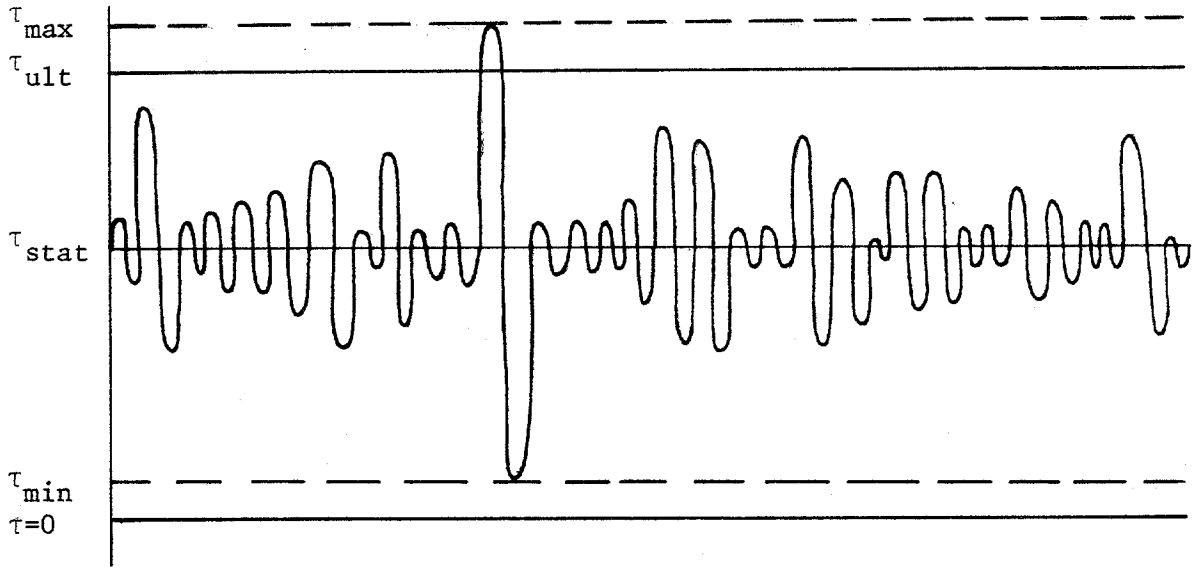

RANDOM TEST 5 $\tau_{stat}=0.70\ \tau_{ult}$ $\tau_{cycl,max}=\pm 0.50\ \tau_{ult}$ $\tau_{ult}=37$ kPa

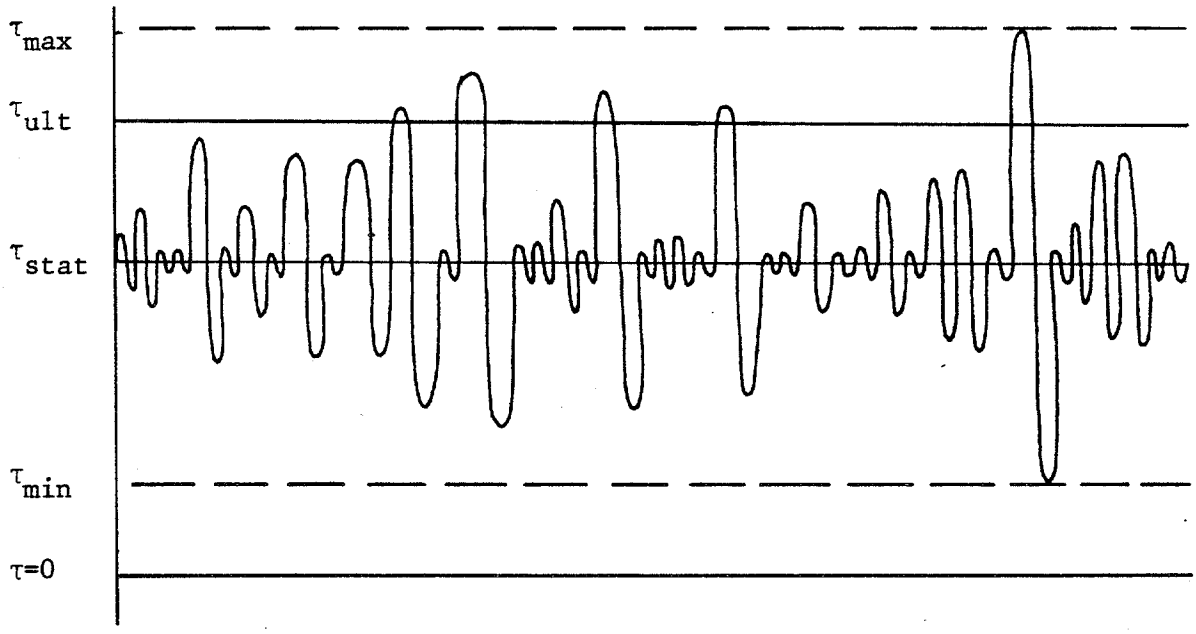

CNRD 13-2 TENSION PILE STUDY LABORATORY MODEL PILE TESTS

TEST 12, STRATUM III, Random tests 4-5

DET NORSKE VERITAS Geotechnical Laboratory	Drawn by	Scale
	Approved	Date
		Fig. No. 10

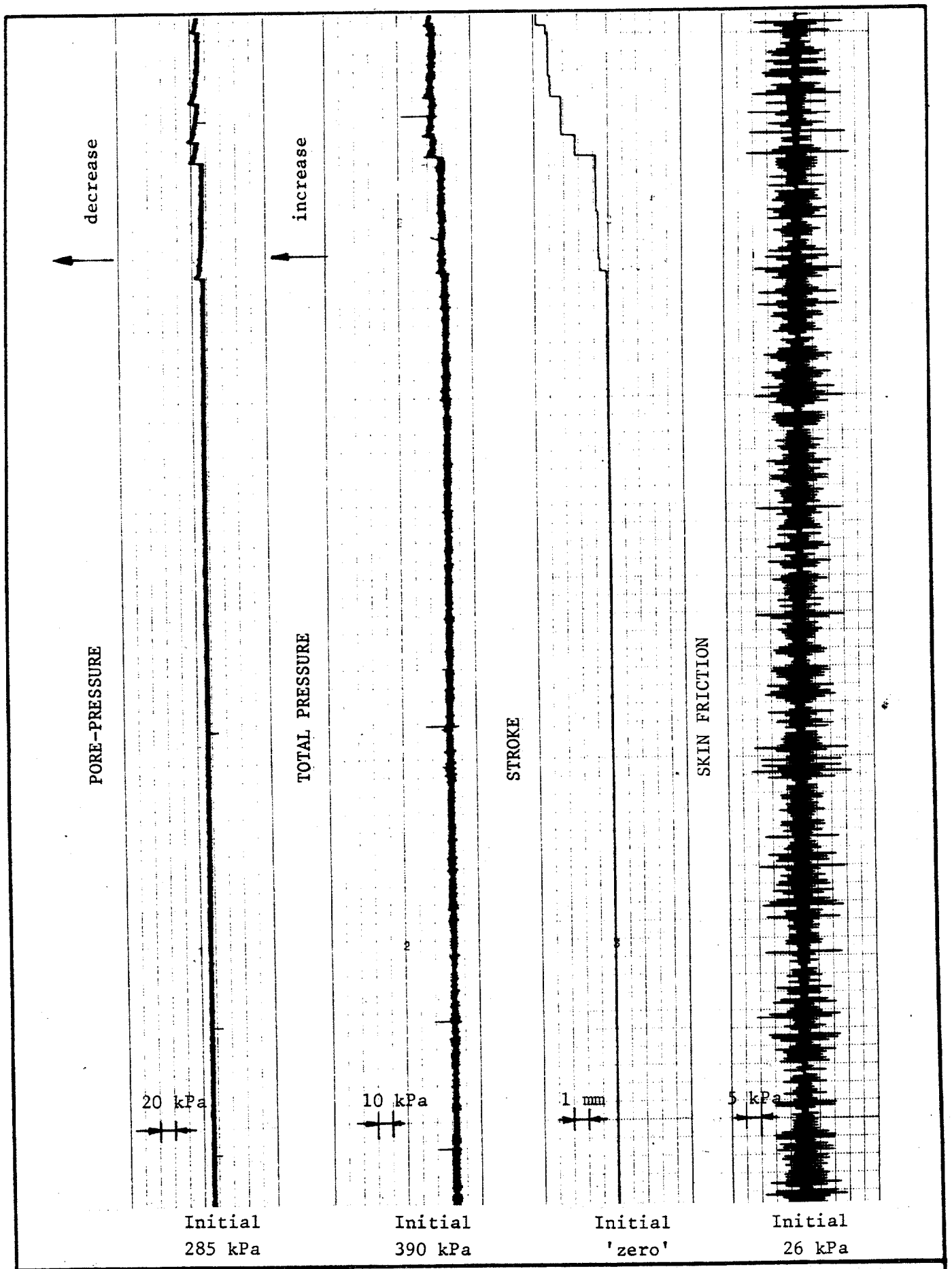

CNRD 13-2 TENSION PILE STUDY LABORATORY MODEL PILE TESTS

TEST 12, STRATUM III, Random test 5

Scale

DET NORSKE VERITAS
Geotechnical Laboratory

Drawn by

Date

Approved

Fig. No. 11

TEST 12, Random no. 5 $\tau_{cycl,max}$=18.5 kPa (50%τ_{ult})

τ_{stat}=26 kPa (70% τ_{ult})

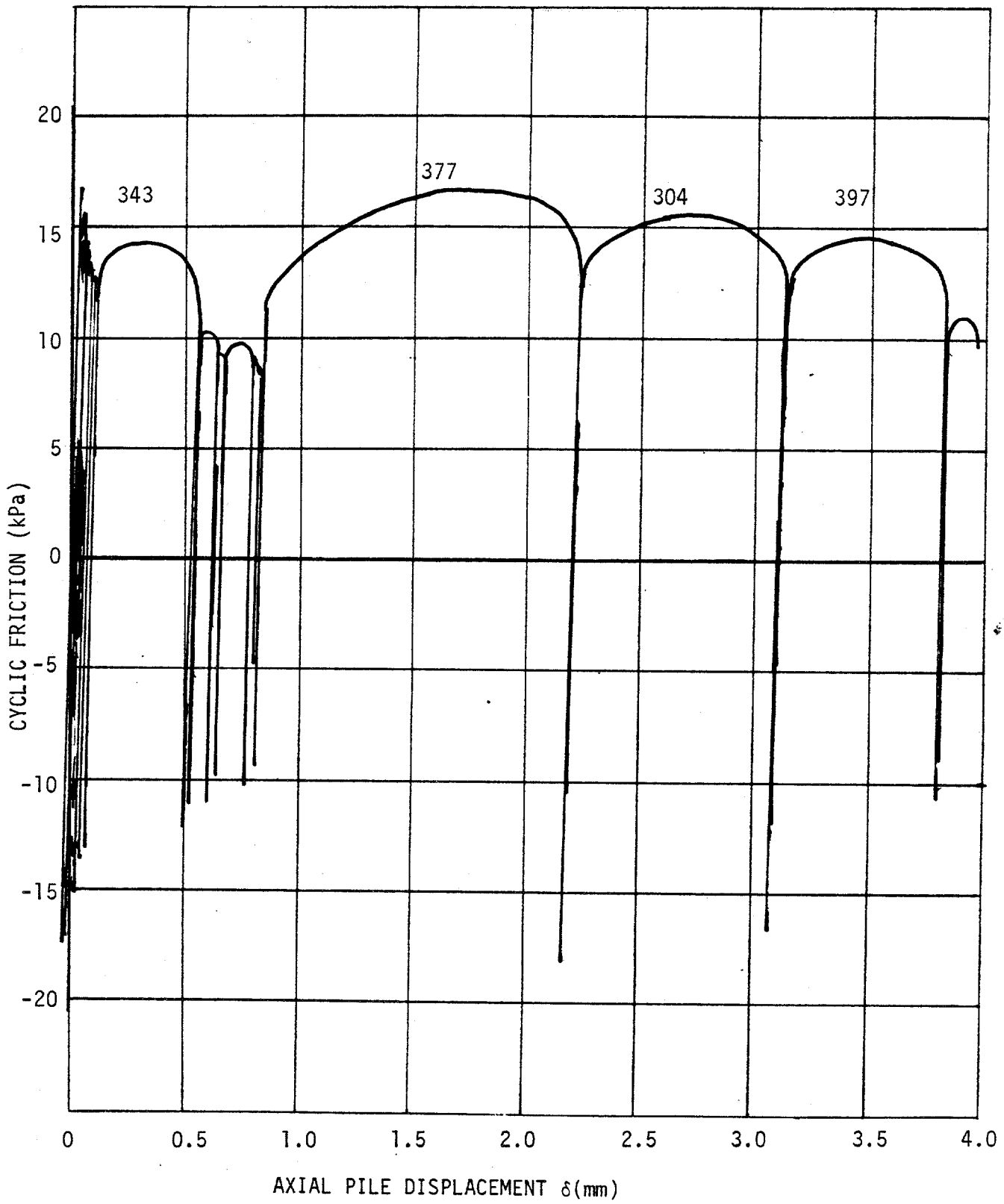

CNRD 13-2 TENSION PILE STUDY LABORATORY MODEL PILE TESTS

TEST 12, STRATUM III, RANDOM TEST NO. 5

DET NORSKE VERITAS Geotechnical Laboratory	Drawn by	Scale
	Approved	Date
		Fig. No. 12

TEST 12, STRATUM III

SHEAR STRENGTH (kPa) FROM POCKET PENETROMETER TESTS AFTER PILE TEST COMPLETED

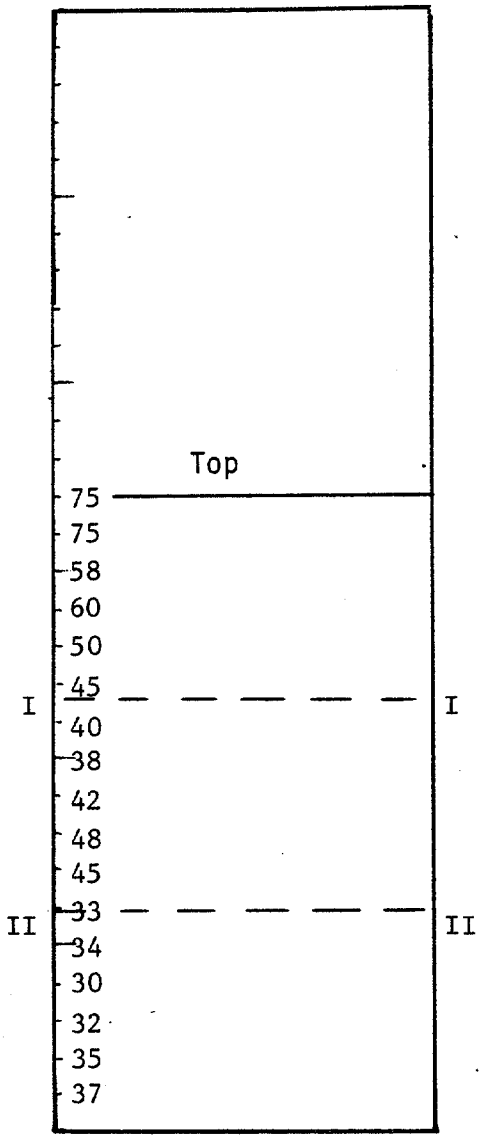

Scale 1:4

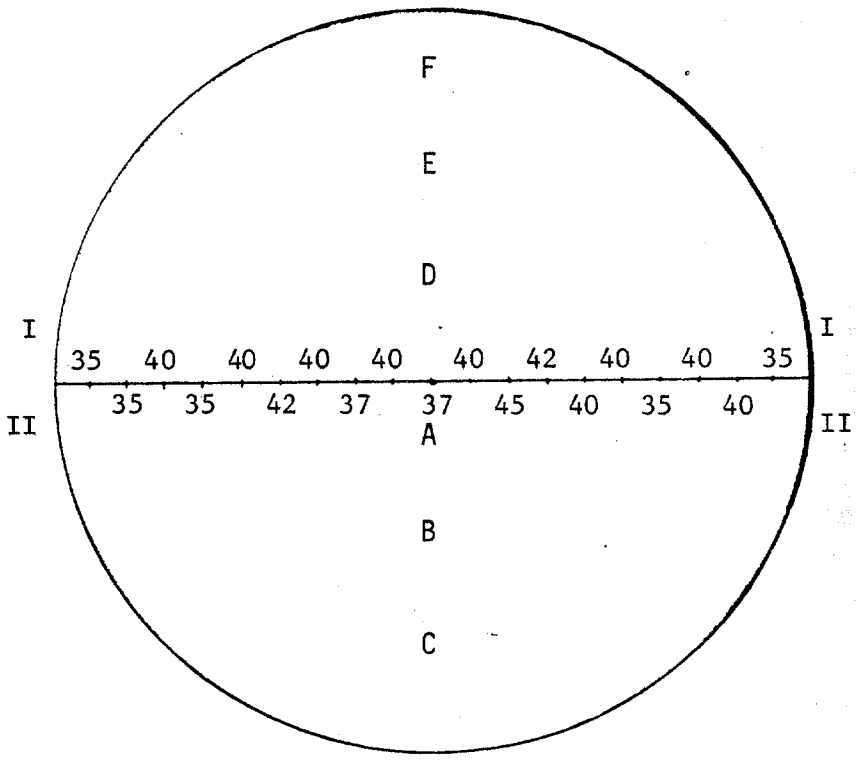

Scale: 1:2

CNRD 13-2 TENSION PILE STUDY LABORATORY MODEL PILE TESTS

TEST 12, STRATUM III, pocket penetrometer tests

DET NORSKE VERITAS
Geotechnical Laboratory

Scale	
Drawn by	Date
Approved	Fig. No. 13

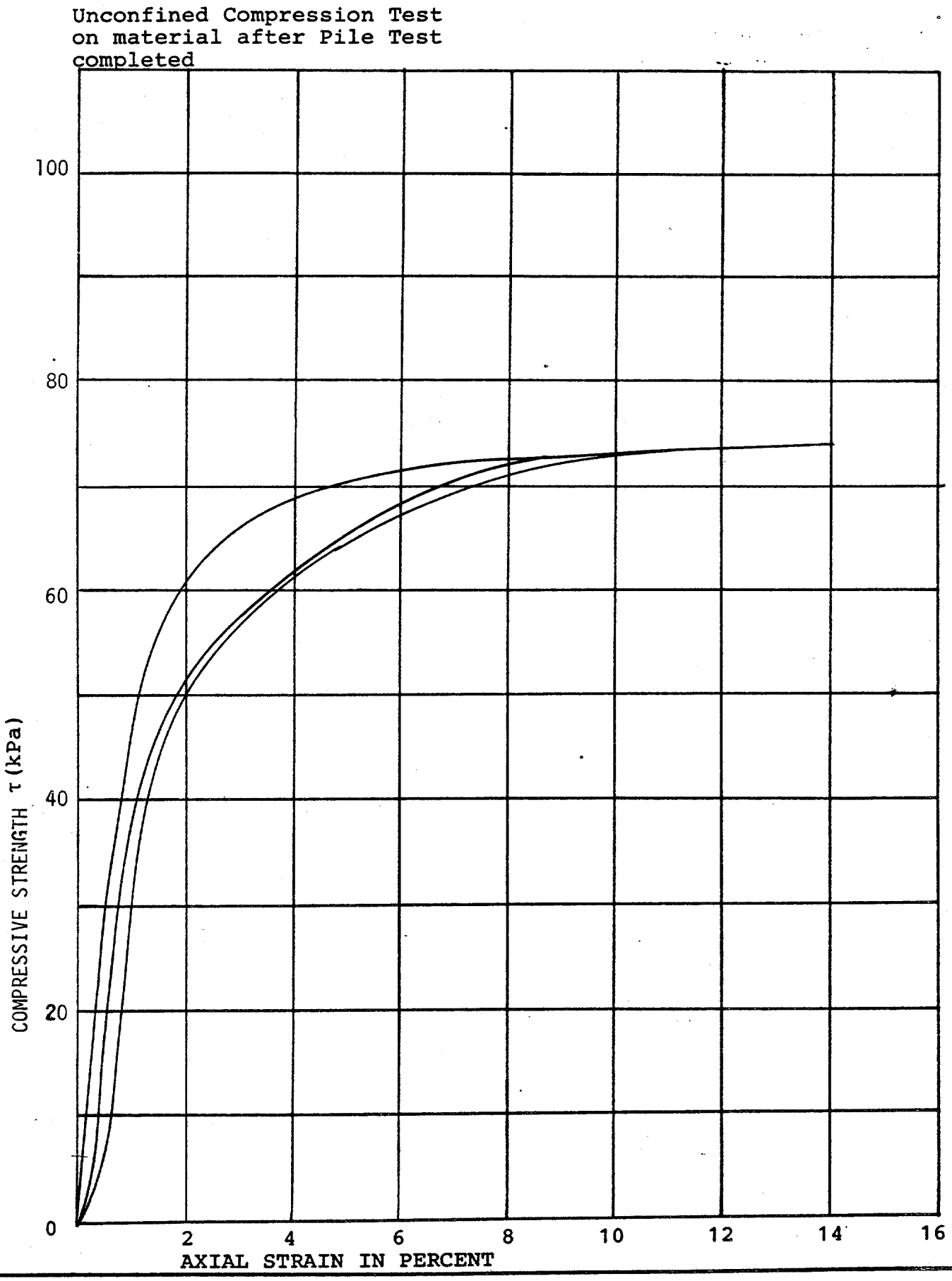

CNRD 13-2 TENSION PILE STUDY LABORATORY MODEL PILE TESTS

TEST 12, STRATUM III, Uncofined compression after pile test

DET NORSKE VERITAS Geotechnical Laboratory	Drawn by	Scale
	Approved	Date
		Fig.No. 14

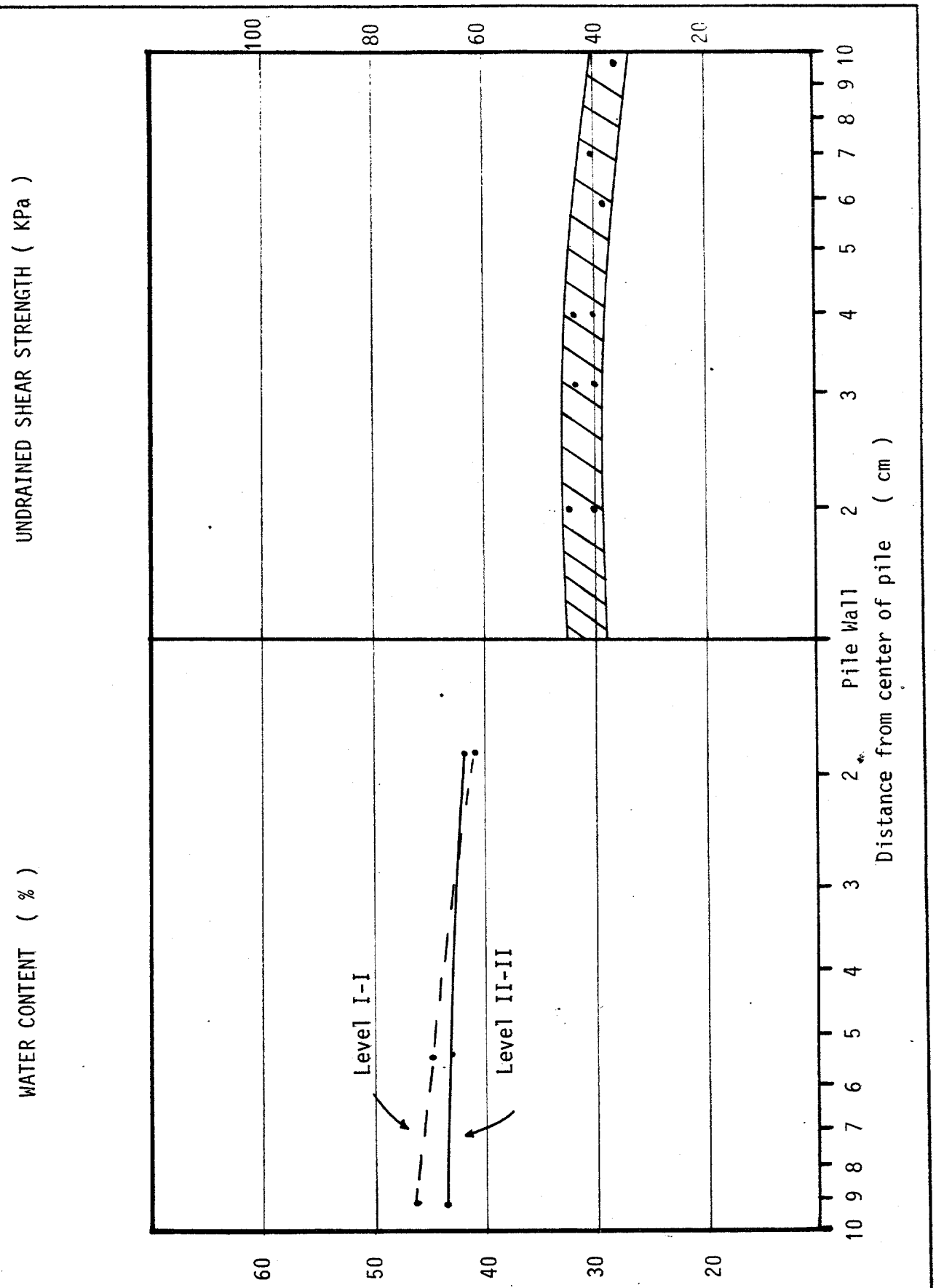

CNRD 13-2 TENSION PILE STUDY LABORATORY MODEL PILE TESTS

TEST 12, STRATUM III, Water content and shear strength after test

DET NORSKE VERITAS Geotechnical Laboratory	Drawn by	Scale
	Approved	Date
		Fig. No. 15

APPENDIX J

DETAILED RESULTS FROM **TEST 13, STRATUM II** MODEL PILE TESTS

CONTENTS

Summary	J3
Test 13, Stratum II	J4
Consolidation	J4
Pile Instatllation and Set-Up	J4
Static Test	J5
Random Cyclic Tests	J5
Confining Pressure Reduction	J7
Strength Tests	J7

LIST OF FIGURES

Figure 1	Sample Properties
Figure 2	Consolidation Diagram
Figure 3	Pocket Penetrometer Tests After Consolidation
Figure 4	Pressures at Pile Wall after Installation
Figure 5	Static Test 1
Figure 6	Random Tests 1&2
Figure 7	Random Tests 3&4
Figure 8	Static Test 2
Figure 9	Random Test 4
Figure 10	Random Test 4
Figure 11	Static Test 3
Figure 12	Static Test 4
Figure 13	Static Test 5
Figure 14	Static Test 6

Figure 15 Static Test 7
Figure 16 Pocket Penetrometer Tests after Pile Test
Figure 17 Unconfined Compression Tests
Figure 18 Water Content and Shear Strength

SUMMARY

This report contains the results of the laboratory model pile tests designated TEST 13, STRATUM II, in the project CNRD 13-2, TENSION PILE STUDY, for Conoco Norway Inc.

The clay sample was consolidated for 61 days under 300 kPa applied vertical pressure. Pore pressure in the sample was about 0% of the applied pressure. After 21 days of consolidation in the pile chamber the modified pile with new pore pressure transducer and modified total pressure transducer was installed. After 28 days of set-up the excess pore pressure was about 175 kPa. Testing was then started.

Static test gave peak friction of 70 kPa with residual value of 55 kPa. Undrained shear strength was interpreted to 85 kPa, giving alpha value of 0.87 and 0.65 for peak and residual respectively. Estimating the effective vertical pressure to 300 kPa results in a beta factor of 0.23 .

Random cyclic stress controlled tests were started 24 hours following the static test had static tension bias of 35 kPa (50% of previous max. friction in static test) and consisted of about 1200 cycles with the amplitude generated by a random signal generator. The maximum cyclic friction was set to 28 kPa (40% of the frictional capacity). The 1200 cycles produced no sign of permanent deflecton and only minimal cyclc deflection. A total of four random tests were performed. In the last test the static level was 49 kPa (70% of the capacity in static test) and the maximum cyclic amplitude was set at 35 kPa (50% of the static capacity). An abrupt uplift of the pile occured after about 221 cycles at a friction level lower than previously produced by the soil-pile interface.

A reconsolidation time of 24 hours was generally allowed inbetween the random tests and a random test was followed by a static test to check the capacity with time.

TEST 13, STRATUM II

CONSOLIDATION

The sample was prepared from the same material as used in Test 5. Water was added during the remoulding process to a water content of about 38.5% . Horizontal filters were placed in the oedometer to provide better vertical drainage.

A vertical pressure of 300 kPa was applied on top. As seen in Figure 2 the pore pressure at middle height had dropped down to zero percent of the consolidation stress at the end of the 61 days consolidation period. The sample was at this time transferred to the pile chamber. Pocket penetrometer tests were performed on the side of the sample and on the top as shown in Figure 3. The shear strength, s_u, showed an average of about 60 kPa.

PILE INSTALLATION AND SET-UP

After pocket penetrometer tests the sample was mounted in the pile chamber and left to reconsolidate for 21 days under a vertical pressure of 300 kPa and radial pressure of 210 kPa (K=0.7).

As in Test 8 no back pressure was applied and vertical filter strips were placed on the outside perimeter of the clay sample with direct drainage on top and bottom of the pile chamber. Again good drainage was proved by formation of salt on the filter strips sticking out, which came from the expelled water from the marine clay.

After insertion of the pile the total normal pressure showed about 280 kPa and the pore pressure showed about 220 kPa.

After one day of set-up the pore pressure had reduced to 120 kPa and the total pressure showed 250 kPa. Upon additional consolidation the pore pressure started to increase as seen in Figure 4 and reached a steady state at 175 kPa after 28 days from installation. At this time it was decided to start with the loading program. The total pressure was at this time about 275 kPa.

STATIC TEST

A displacement controlled static test with deformation rate 10 mm per hour was now conducted, as shown in Figure 5. The pile was pulled in tension through failure and large slip and then pushed down to original position causing failure in compression and large slip (residual friction).

The displacement to cause failure, as shown in Figure 6, was about 0.5 mm or 2% of the pile diameter. A maximum friction of 70 kPa was achieved with a residual friction of 55 kPa. The shear strength of the clay at time of testing was estimated to 85 kPa which results in an alpha (α) value of 0.87 and 0.65 for peak and residual friction respectively.

For the effective stress approach, estimating σ'_{vo} to be 300 kPa, the beta value (β) becomes 0.23 for maximum friction.

Total pressure on the pile wall at time of failure was about 250 kPa and the pore pressure showed 150 kPa, resulting in a horizontal effective pressure of 100 kPa. The interface friction angle (δ) can then be estimated to 35 degrees.

RANDOM CYCLIC TESTS

After the static test the pile was left to reconsolidate for 24 hours before cyclic testing was started. The total pressure was unchanged whereas the pore pressure had increased to about 145 kPa. A random cyclic test comprised of applying a prescribed static tensile (uplift) stress on the pile, superimposed with cycles of randomly varying amplitude. The cyclic period was held constant at 10 seconds for all cycles and the maximum number of cycles applied was about 1250. The resulting deformations and pressures on the pile wall were monitored during the cycling. The static level and the maximum cyclic level were increased in subsequent random tests until the pile finally failed (abrupt pullout).

For the first random test the static tensile stress (bias) level was 35 kPa, corresponding to 50% of the previous static capacity. The maximum cyclic amplitude was set to 28 kPa (40% of static capacity), resulting in only one-way (tensile) loading, as shown in Figure 6. The test resulted in no permanent deflection of the pile and the pressures on

the pile wall were almost constant throughout the test. The pile was now left to reconsolidate for 24 hours before a new random test was performed as shown in Figure 6.The total pressure and pore pressure showed 220 kPa and 145 kPa respectively.

In random test two the static level was held at half the static strength, or 35 kPa, with the maximum cyclic amplitude also set to 35 kPa, corresponding to 50% of the static capacity. Again, as for the previous test, the 1250 cycles with these load combinations resulted in no measurable permanent displacement and with only minimal cyclic displacements during the applied load cycles.

Random test number three was started after 24 hours of reconsolidation with the static level increased to 60% of the static capacity and with the maximum cyclic stress amplitude still at half of the static level, as shown in Figure 7. This meant that the maximum friction applied was larger than the previously measured static capacity. As for the two previous random tests still no sign of permanent deflection of the pile was seen and no substantial change in the pressures at the pile wall resulted from the random loading. A static test was performed after this random test to check the static capacity, with the results shown in Figure 8. The maximum friction in the first "cycle" gave 75 kPa and in the second about 70 kPa, with residual values of about 57 and 53 kPa respectively for the two "cycles". The pressures on the pile wall reduced during the static test down to about 215 and 130 kPa for the total and pore pressure respectively.

A new period of 24 hours was allowed before a new random test was performed. The maximum cyclic level was held unchanged from previous test and the static level was increased to 70% of the static capacity as shown in Figure 7. The results of this test are shown in Figure 9 and 10 with the latter showing skin friction versus pile deflection. After 221 cycles the pile suddenly fails with a mobilized friction lower than previously produced. In Figure 9 the pore pressure, total pressure, pile deflection and skin friction are shown versus time (number of cycles), and it can here be seen that no permanent pile deflection occurs before the failure occurs. Only small cyclic deformations results from the applied load combination.

It is interesting to note that large deformation of the pile occured after the initial failure, at stress-levels significantly lower than previously obtained and also lower than the stress level for the initial failure. The measurements of the pressures on the pile wall showed a decrease in the pore pressure and an increase in the total pressure at

the time of failure and for subsequent cycles producing excessive deformations as can be seen in Figure 9.

A static test was performed immediately after the pile had been brought back to original position. The result is shown in Figure 11, and indicates that the capacity now had reduced from before the failure in the random test.

CONFINING PRESSURE REDUCTION

The pile was now left for reconsolidation for six days, during which time the pressures on the pile wall slightly increased. At this time a new static test was performed with results shown in Figure 12. The maximum friction was about 70 kPa with a residual value of 55 kPa. The confining pressures were then reduced to 250 and 175 for the vertical and radial pressures respectively. A new static test was then made, as shown in Figure 13. The pressures on the pile wall reduced to about 275 and 135 kPa for total and pore pressure respectively.The mobilized friction was only slightly reduced from the test prior to pressure reduction. A new test 24 hours after the pressure reduction indicated still only small reduction in the mobilized friction. A period of three days gave a further reduction in the static capacity, with maximum friction of about 65 kPa and a residual value of 49 kPa.

STRENGTH TESTS

After the last static test the pile was extruded from the sample and the clay was built out. Pocket penetrometer tests were performed on the side of the sample and in two horizontal layers with results shown in Figure 16.

Three standard triaxial test samples were then prepared from the center of the clay specimen and unconfined compression tests (UCT) were performed with the results shown in Figure 17.

In Figure 18 are shown the water content and interpreted undrained shear strength of the clay sample versus the distance from the center after completion of the pile test. The water content showed about 27% with a tendency to decrease towards the center. This relatively low water content can explain the fairly high undrained shear strength

measured for this test. The low water content is a result of good drainage compared to the fact that extensive time for sample consolidation was given.

TABLE 1.

SAMPLE PROPERTIES TEST 13, STRATUM II

SAMPLE PREPARATION		CONSOLIDATION			END OF PILE TEST
INITIAL WATER CONTENT	INITIAL HEIGHT	AXIAL DEFORMATION	AXIAL STRAIN	WATER CONTENT	WATER CONTENT
w_i (%)	H_o (cm)	ΔH (cm)	ε (%)	w_e (%)	w_{ep} (%)
38.94 38.25	47.89	5.21	10.9	Not measured	A 26.02 D 25.83 B 26.96 E 27.21 C 27.06 F 28.57

CONFINING PRESSURE		
AXIAL	KPa	300
RADIAL	KPa	210
BACK PRESSURE	KPa	0
SAMPLE CONSOLIDATION		
IN OEDOMETER	Days	61
IN PILE CHAMBER	Days	21
INTERPRETED SHEAR STRENGTH		
END OF CONSOLIDATION	KPa	60
END OF PILE TEST	KPa	85

Fig. 1

CONSOLIDATION DIAGRAM								Test No. 13 Stratum II		Start date 29/12 .82	
H_i 47.89 cm		H_e 42.68 cm		$\Delta\varepsilon_v$ 10.9 %						σ_c 300 kPa	
Time h	26	115	139	163	211	283	384	480	672	792	960
Δh cm	1.43	3.69	3.90	4.19	4.36	4.64	4.89	4.96	5.11	5.12	5.15
u kPa	31	145	118	110	94	72	53	38	23	14	9
1128	1296	1464									
5.20	5.20	5.21									
-6	-5	-4									

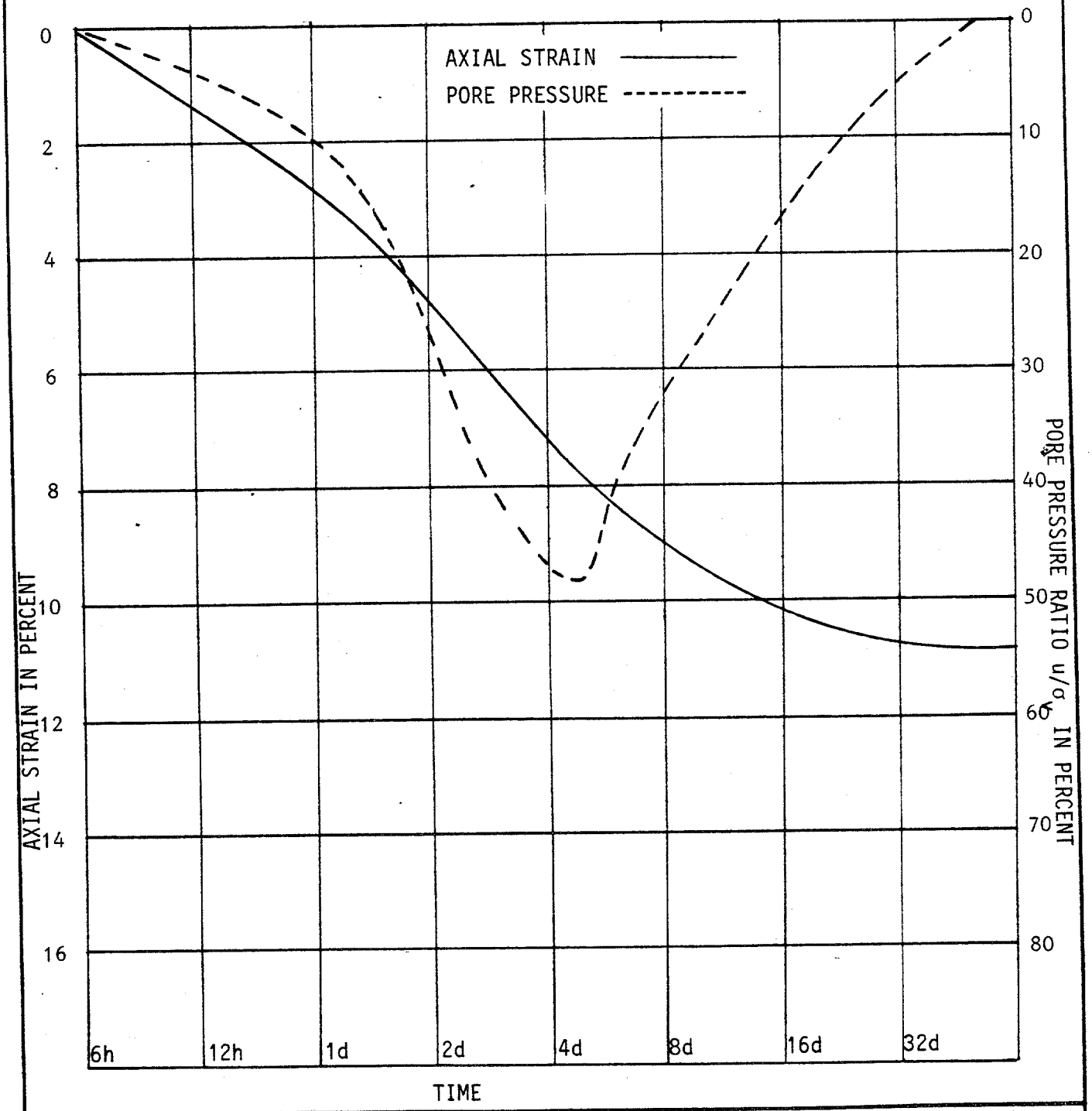

CNRD 13-2 TENSION PILE STUDY LABORATORY MODEL PILE TESTS

TEST 13, STRATUM II, Consolidation diagrams for clay sample

DET NORSKE VERITAS
Geotechnical Laboratory

Scale
Drawn by
Date
Approved
Fig. No. 2

TEST 13, STRATUM II

SHEAR STRENGTH (kPa) FROM POCKET PENETROMETER TESTS AFTER CONSOLIDATION

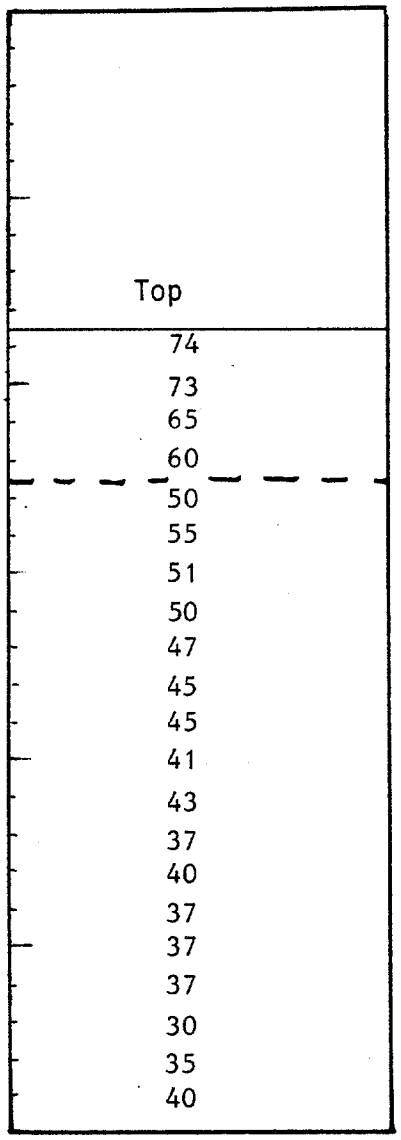

Scale 1:4

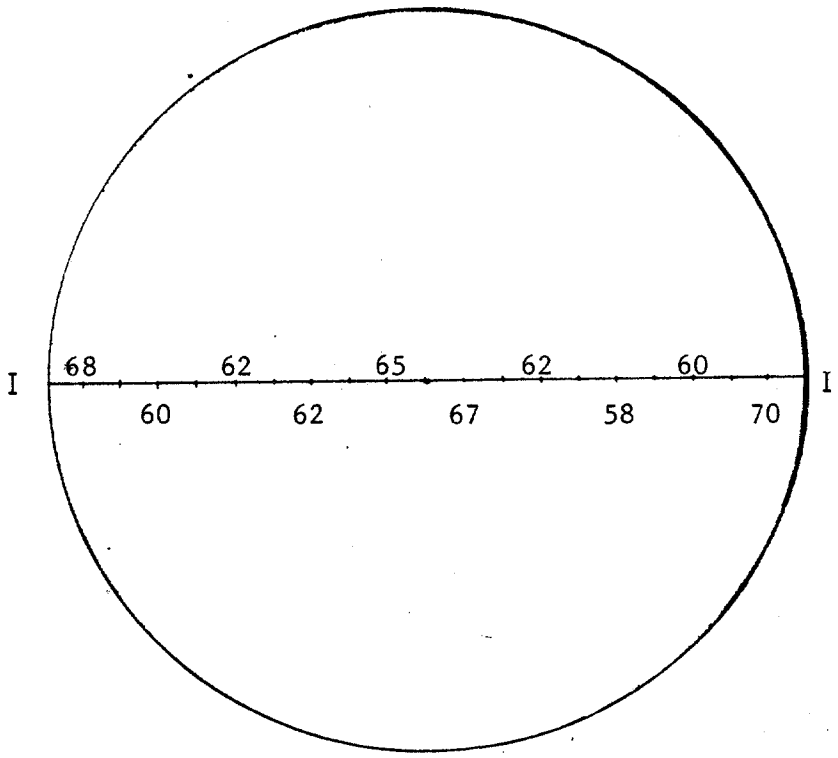

Scale: 1:2

CNRD 13-2 TENSION PILE STUDY LABORATORY MODEL PILE TESTS

TEST 13, STRATUM II, Pocket penetrometer tests		Scale
DET NORSKE VERITAS Geotechnical Laboratory	Drawn by	Date
	Approved	Fig. No. 3

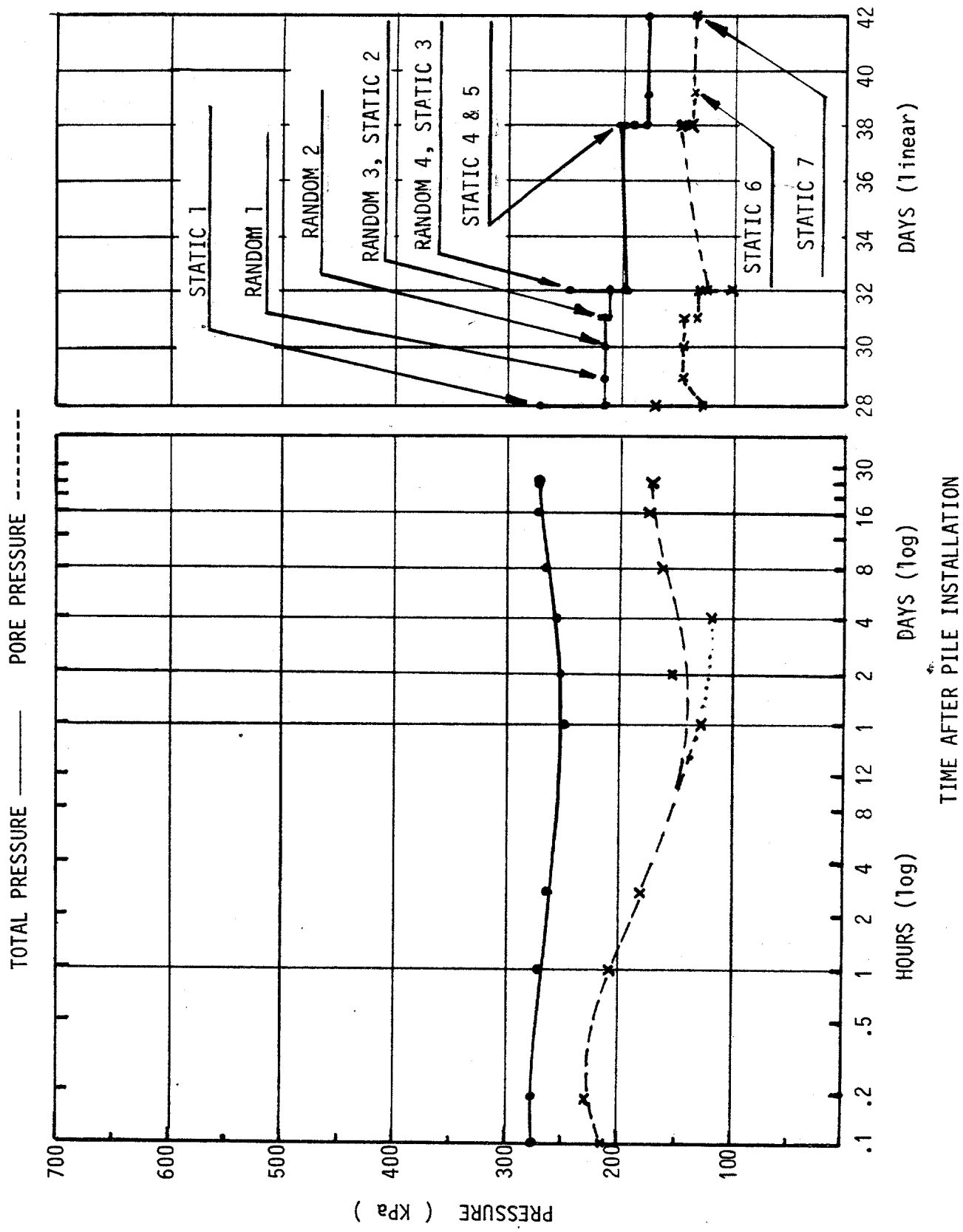

CNRD 13-2 TENSION PILE STUDY LABORATORY MODEL PILE TESTS

TEST 13, STRATUM II, Pressures at pile wall after installation

Scale

DET NORSKE VERITAS
Geotechnical Laboratory

Drawn by

Date

Approved

Fig. No. 4

BEFORE RANDOM 1

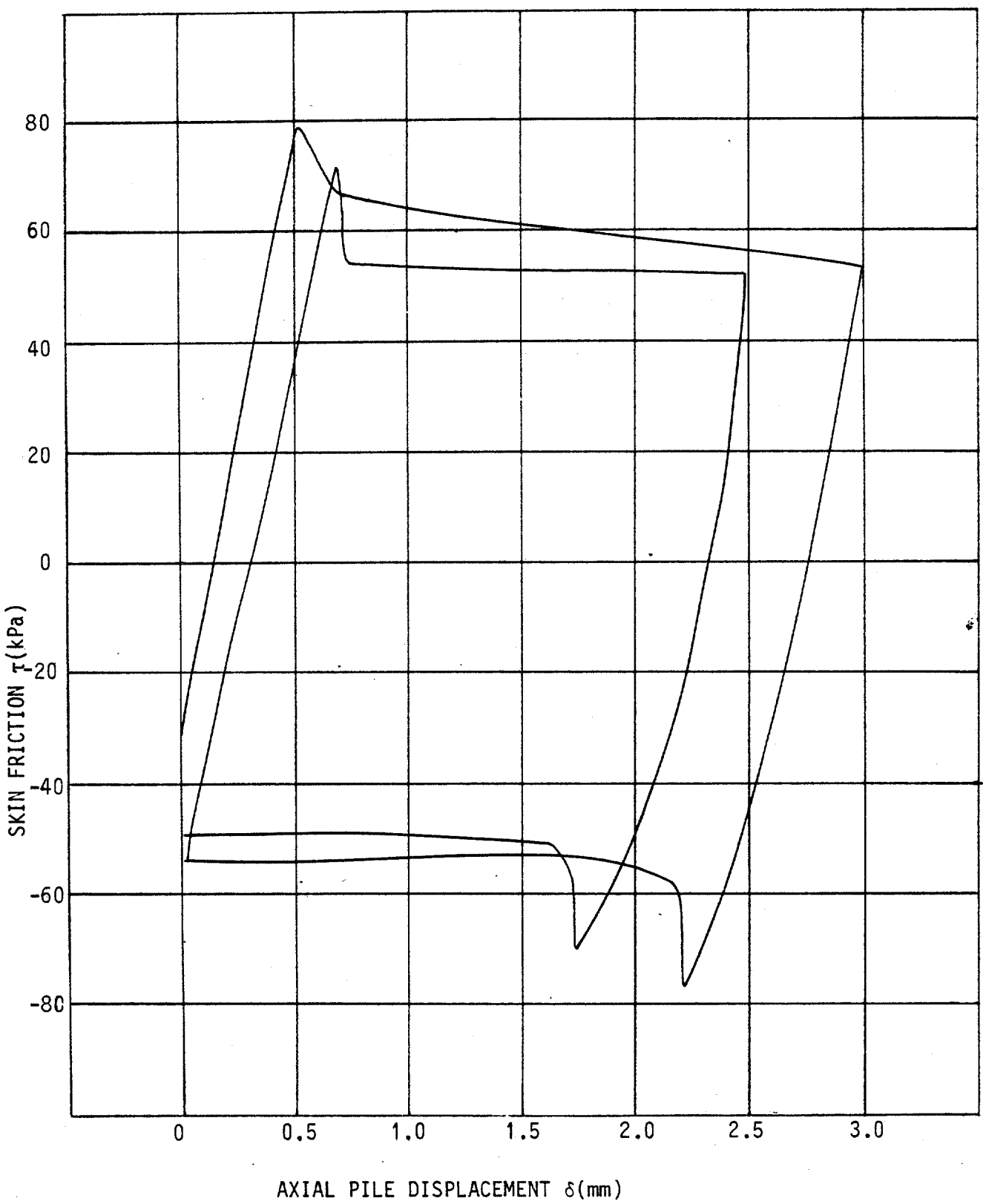

CNRD 13-2 TENSION PILE STUDY LABORATORY MODEL PILE TESTS

TEST 13, STRATUM II, STATIC TEST 1

DET NORSKE VERITAS Geotechnical Laboratory	Drawn by	Scale
	Approved	Date
		Fig. No. 5

RANDOM TEST NO. 1

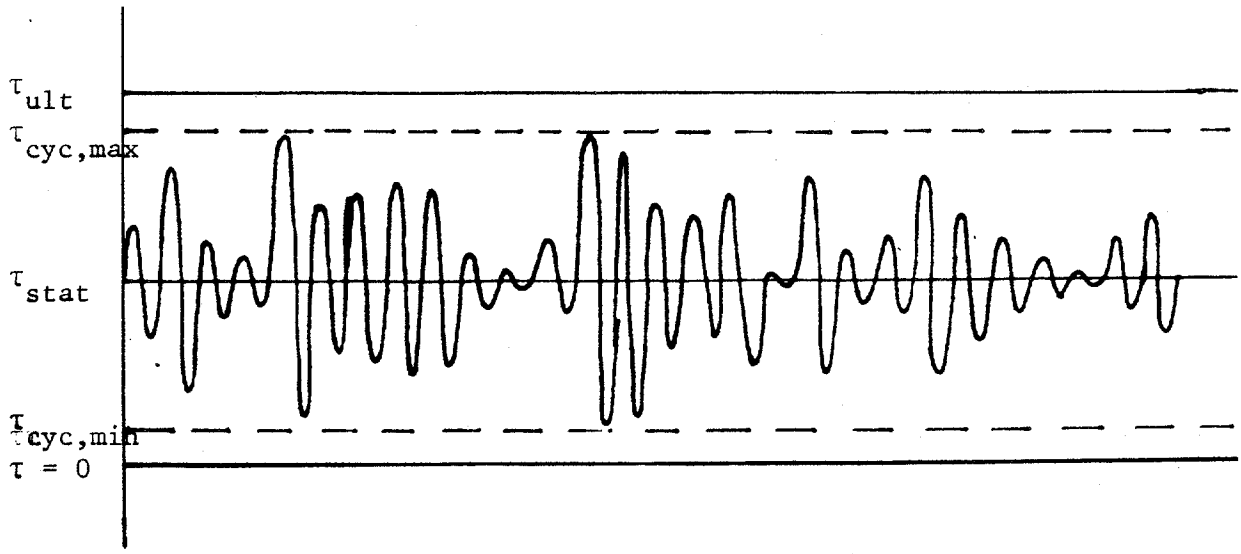

$\tau_{stat} = 50\%\ \tau_{ult}$, $\tau_{cycl,max} = 40\%\ \tau_{ult}$, $\tau_{ult} = 70$ kPa

RANDOM TEST NO. 2

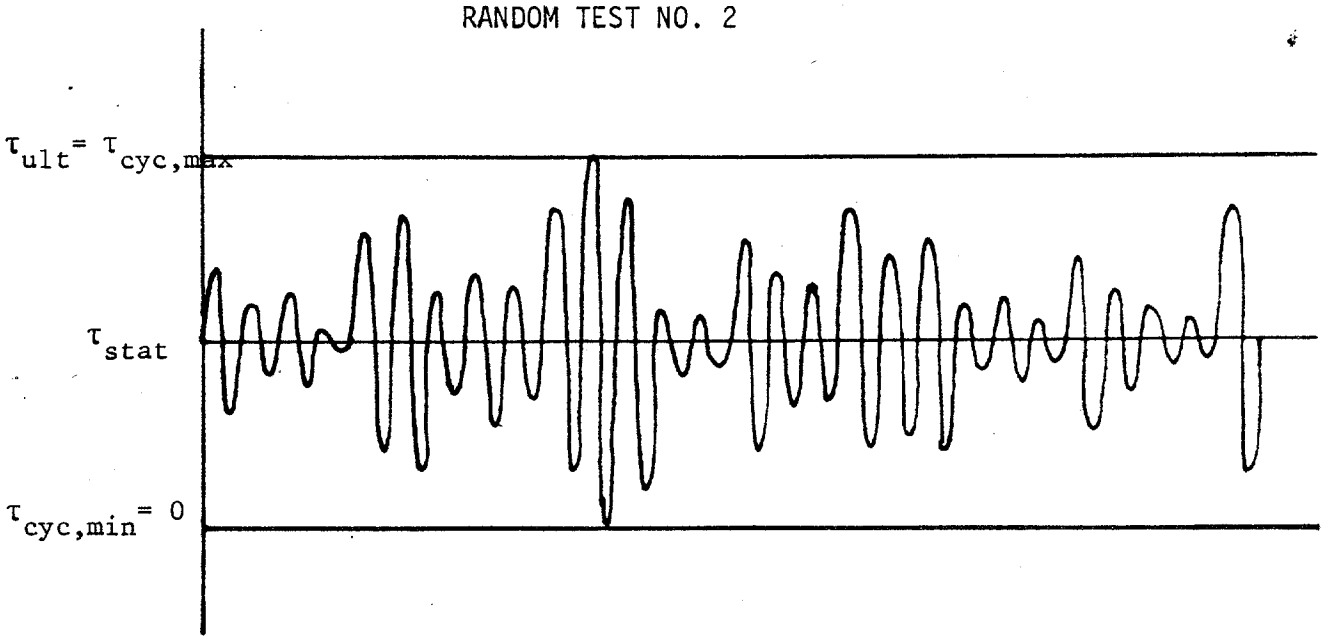

$\tau_{stat} = 50\%\ \tau_{ult}$, $\tau_{cycl,max} = 50\%\ \tau_{ult}$, $\tau_{ult} = 70$ kPa

CNRD 13-2 TENSION PILE STUDY LABORATORY MODEL PILE TESTS

TEST 13, STRATUM II , RANDOM TESTS NO. 1 & 2

DET NORSKE VERITAS
Geotechnical Laboratory

Scale	
Drawn by	Date
Approved	Fig. No. 6

RANDOM TEST NO. 3

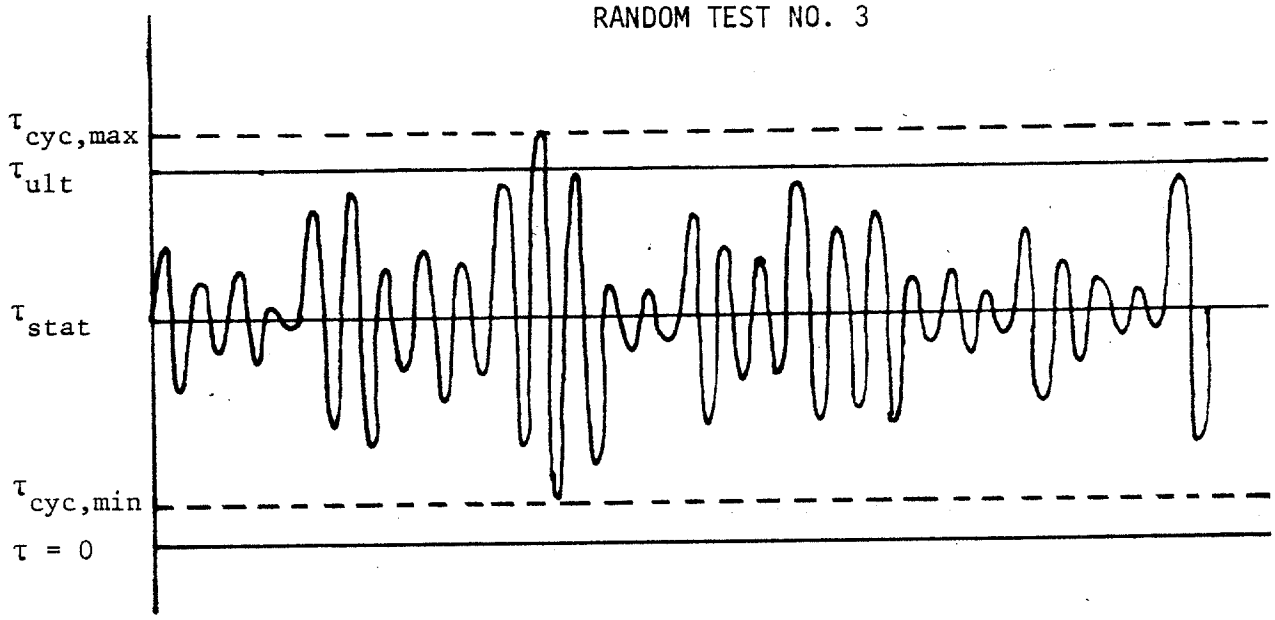

τ_{stat} = 60% τ_{ult}, $\tau_{cycl,max}$ = 50% τ_{ult}, τ_{ult} = 70 kPa

RANDOM TEST NO. 4

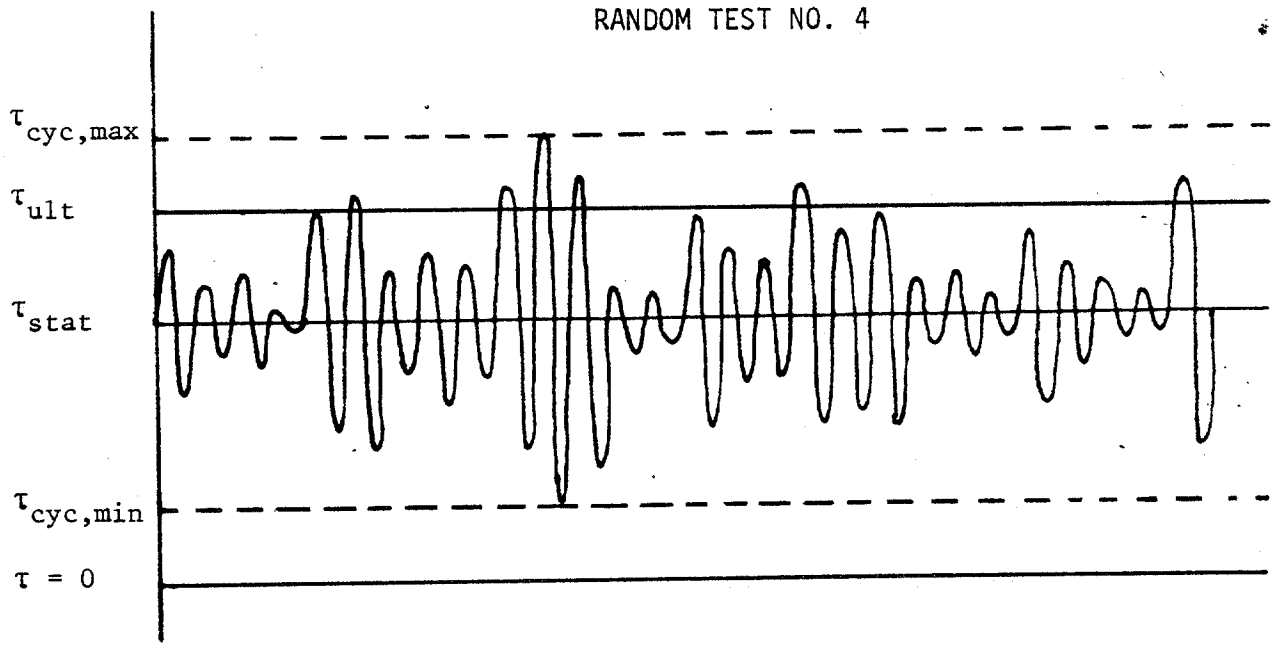

τ_{stat} = 70% τ_{ult}, $\tau_{cycl,max}$ = 50% τ_{ult}, τ_{ult} = 70 kPa

CNRD 13-2 TENSION PILE STUDY LABORATORY MODEL PILE TESTS

TEST 13, STRATUM II, RANDOM TESTS NO. 3 & 4

DET NORSKE VERITAS Geotechnical Laboratory	Drawn by	Scale
	Approved	Date
		Fig. No. 7

AFTER RANDOM TEST 3

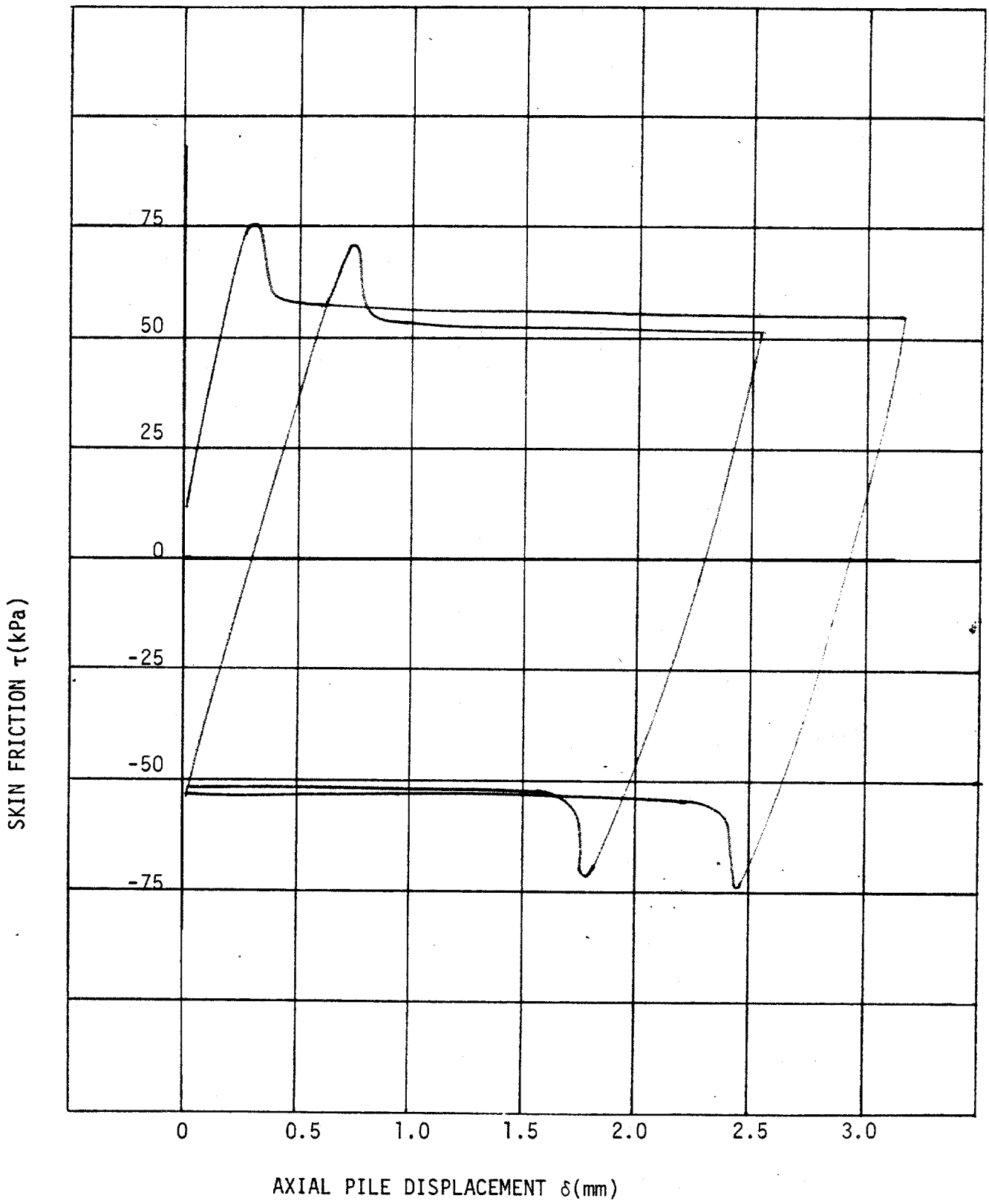

CNRD 13-2 TENSION PILE STUDY LABORATORY MODEL PILE TESTS

TEST 13, STRATUM II, STATIC TEST 2

DET NORSKE VERITAS Geotechnical Laboratory	Drawn by	Scale
	Approved	Date
		Fig. No. 8

RANDOM TEST NO. 4

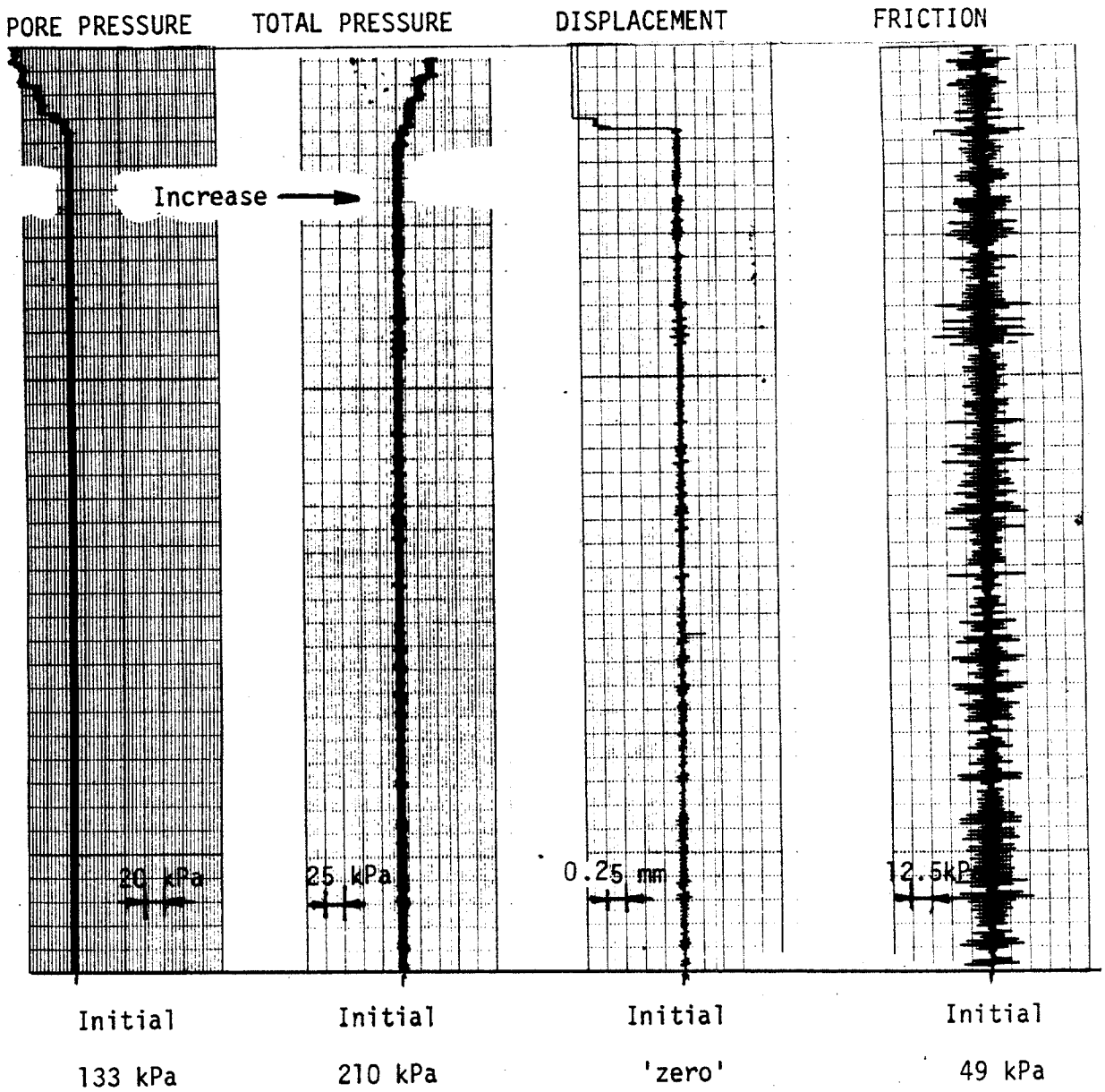

CNRD 13-2 TENSION PILE STUDY LABORATORY MODEL PILE TESTS

TEST 13, STRATUM II, RANDOM TEST NO.4, $\tau_{stat} = 70\%\ \tau_{ult}$, $\tau_{cyc,max} = 50\%\ \tau_{ult}$

DET NORSKE VERITAS Geotechnical Laboratory	Drawn by	Date
	Approved	Fig. No. 9

RANDOM TEST NO. 4

$\tau_{stat} = 70\% \ \tau_{ult}$

$\tau_{cyc,max} = 50\% \ \tau_{ult}$

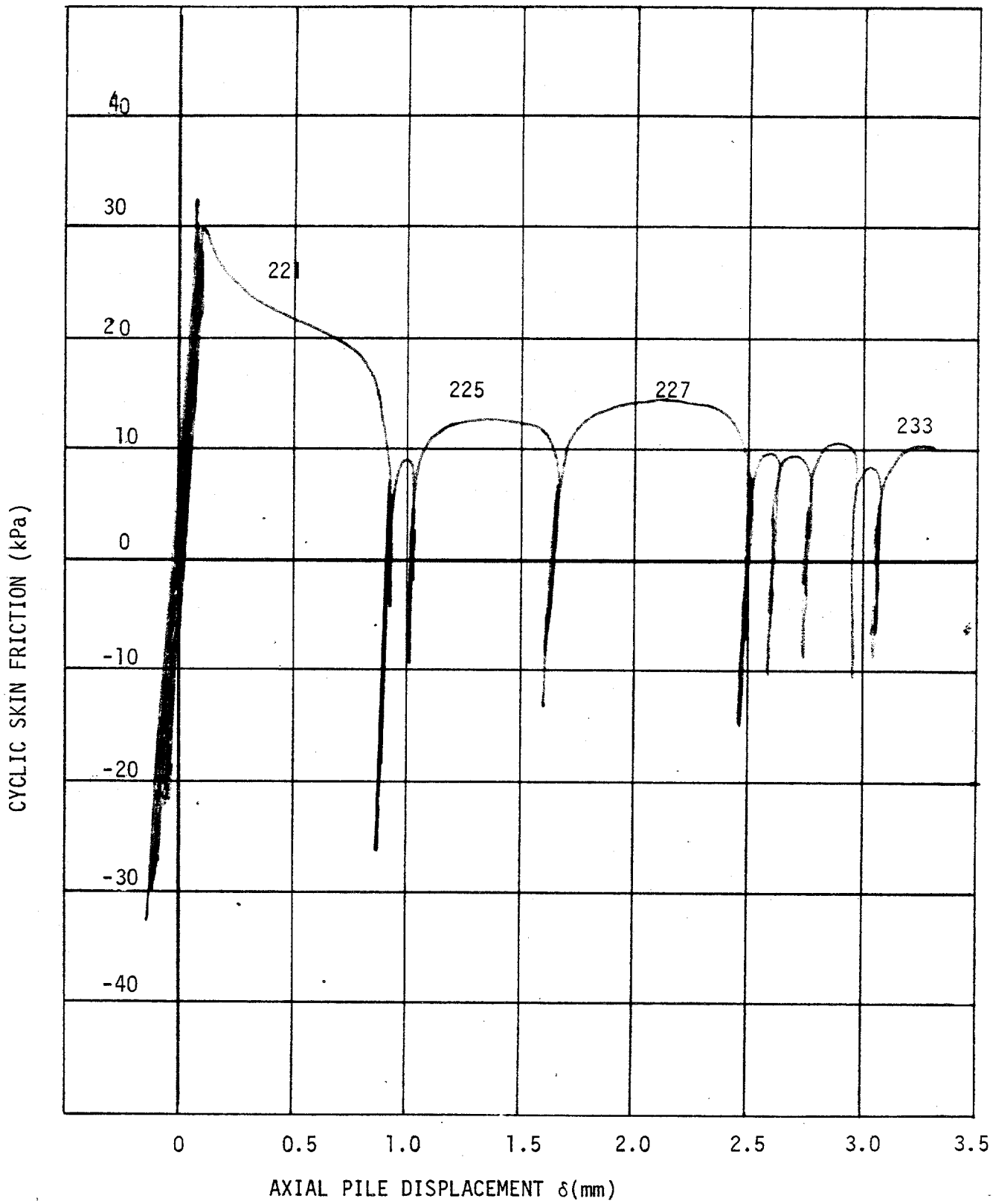

CNRD 13-2 TENSION PILE STUDY LABORATORY MODEL PILE TESTS

TEST 13, STRATUM II, RANDOM TEST NO. 4

DET NORSKE VERITAS
Geotechnical Laboratory

Scale	
Drawn by	Date
Approved	Fig. No. 10

STATIC TEST AFTER RANDOM NO. 4

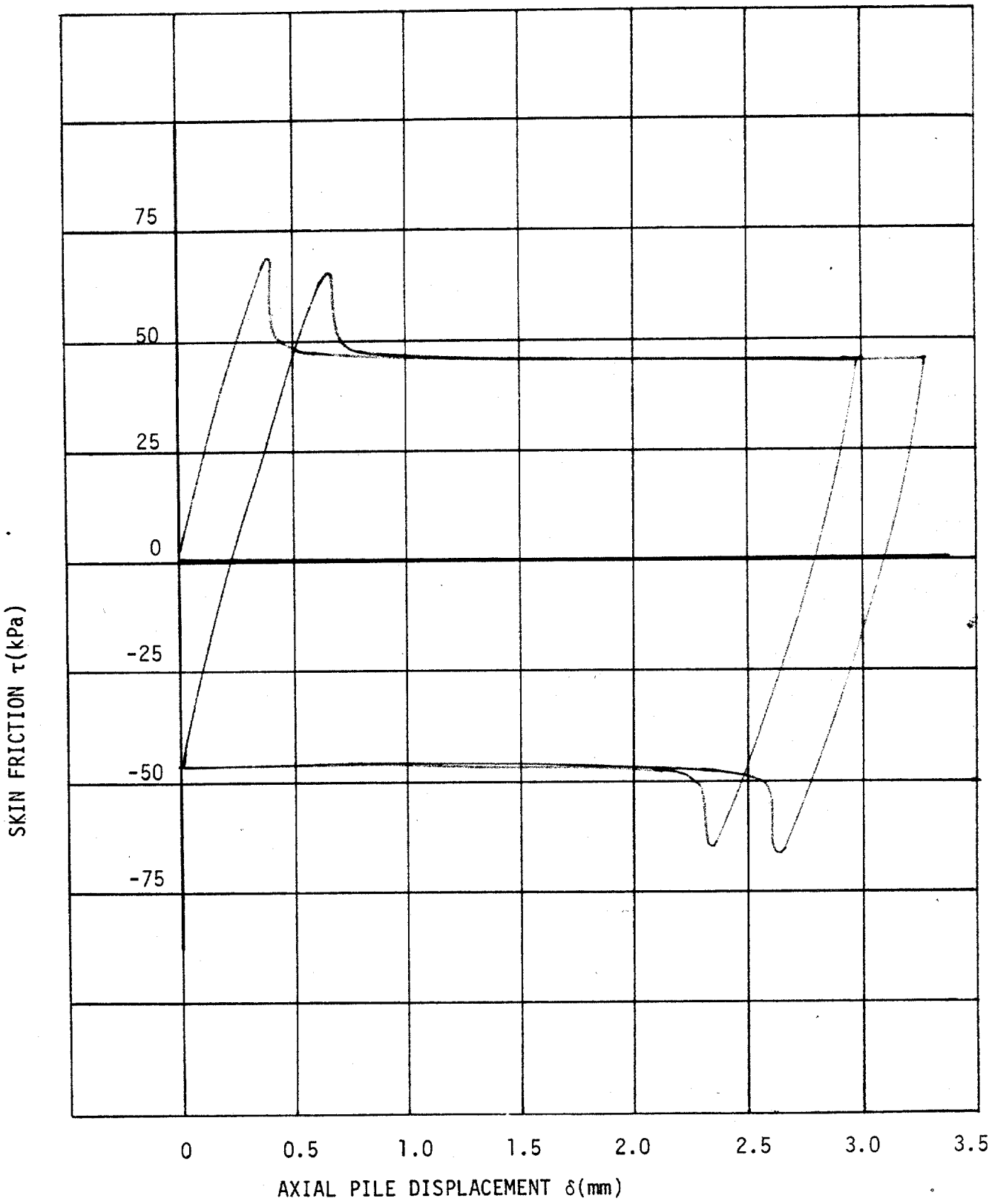

CNRD 13-2 TENSION PILE STUDY LABORATORY MODEL PILE TESTS

TEST 13, STRATUM II, STATIC TEST 3

DET NORSKE VERITAS Geotechnical Laboratory	Drawn by	Scale
	Approved	Date
		Fig. No. 11

STATIC TEST WITH STANDARD CONFINING PRESSURE

σ_v = 300 kPa σ_r = 210 kPa

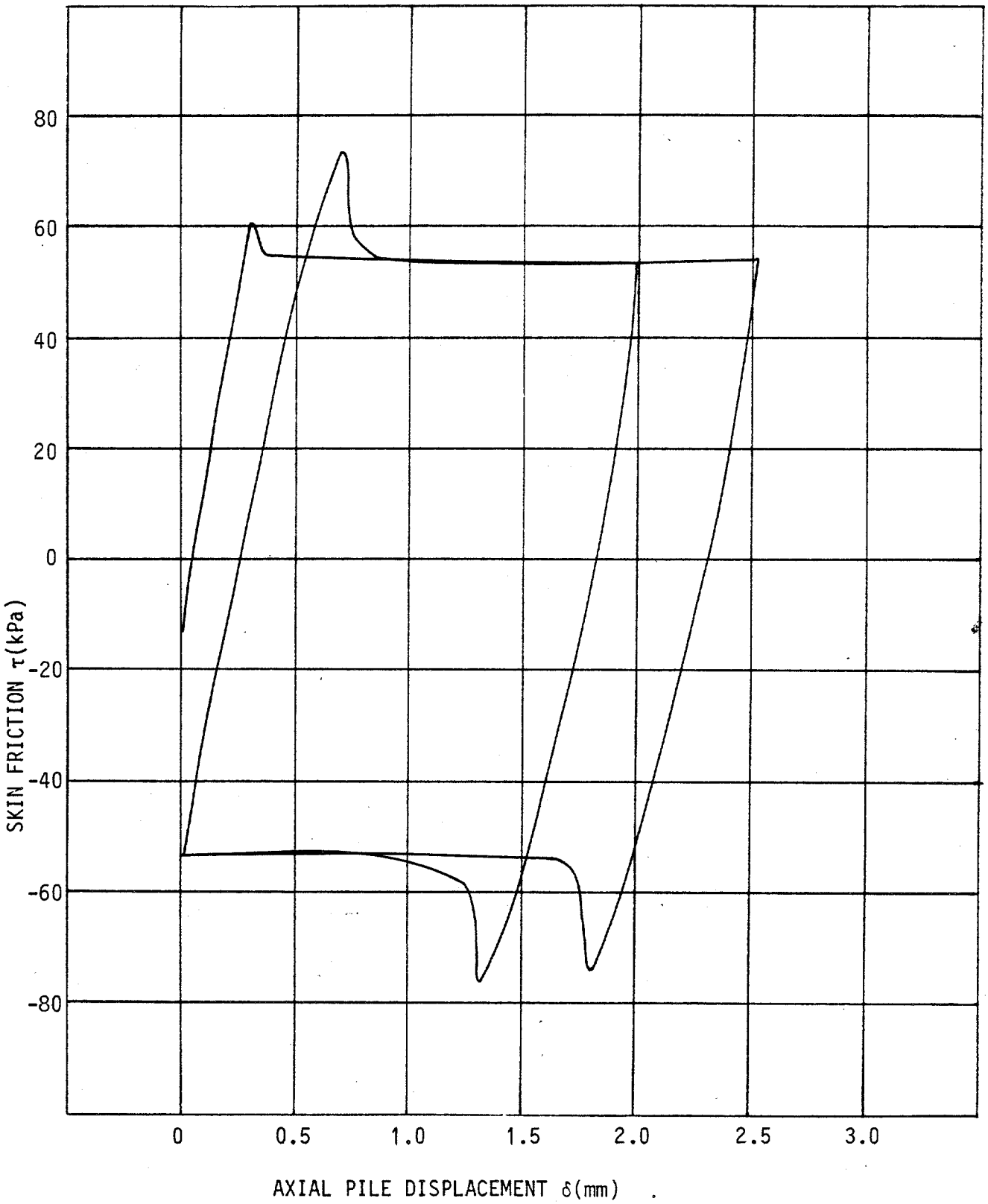

CNRD 13-2 TENSION PILE STUDY LABORATORY MODEL PILE TESTS

TEST 13, STRATUM II, STATIC TEST 4

DET NORSKE VERITAS Geotechnical Laboratory	Drawn by	Scale
	Approved	Date
		Fig. No. 12

STATIC TEST WITH REDUCED CONFINING PRESSURE

IMMEDIATLY AFTER PRESSURE REDUCTION

σ_v = 250 kPa σ_r = 175 kPa

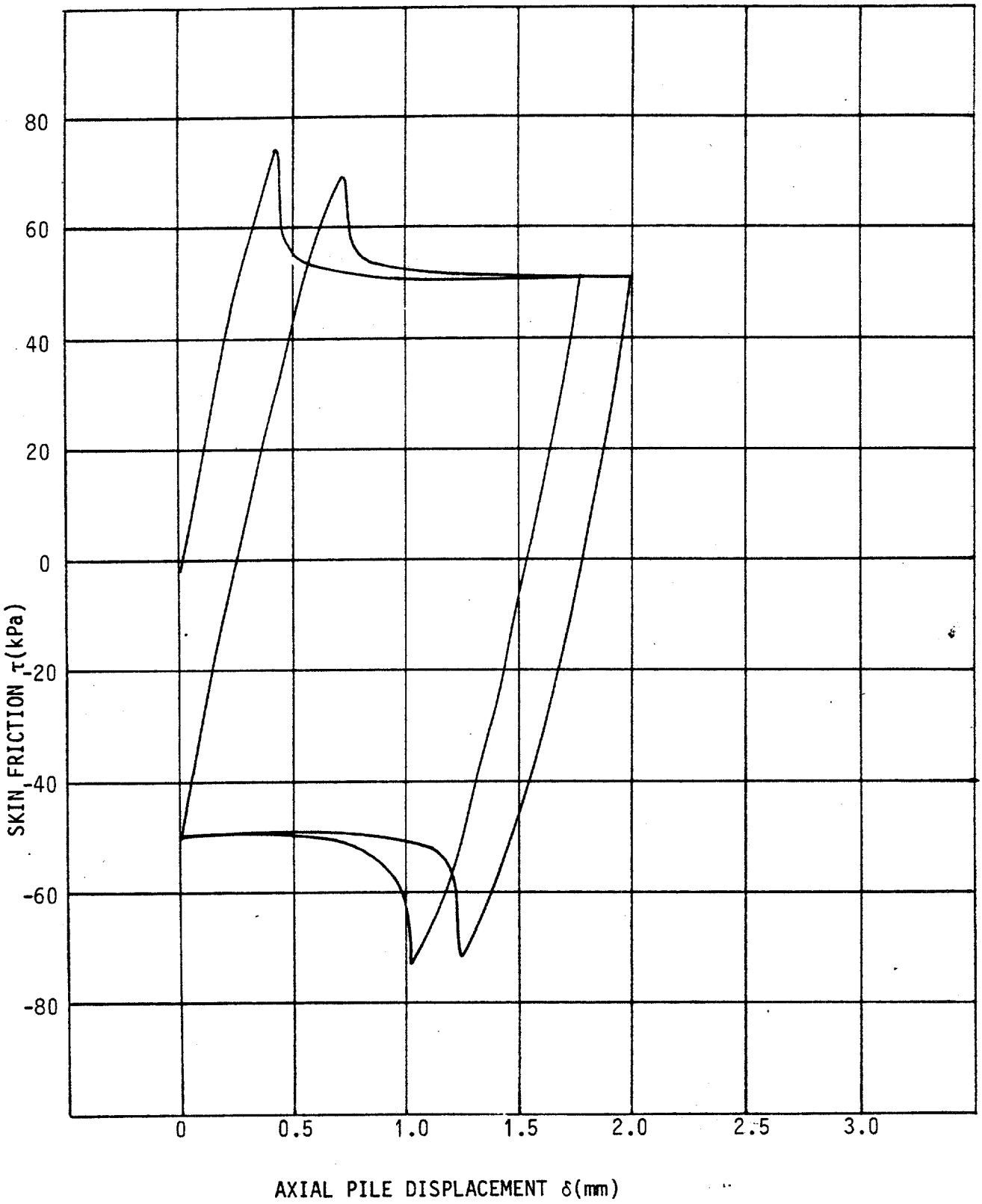

CNRD 13-2 TENSION PILE STUDY LABORATORY MODEL PILE TESTS

TEST 13, STRATUM II, STATIC TEST 5

Scale

DET NORSKE VERITAS
Geotechnical Laboratory

Drawn by

Date

Approved

Fig. No. 13

STATIC TEST WITH REDUCED CONFINING PRESSURE

24 HOURS AFTER PRESSURE REDUCTION σ_v=250 kPa σ_r=175 kPa

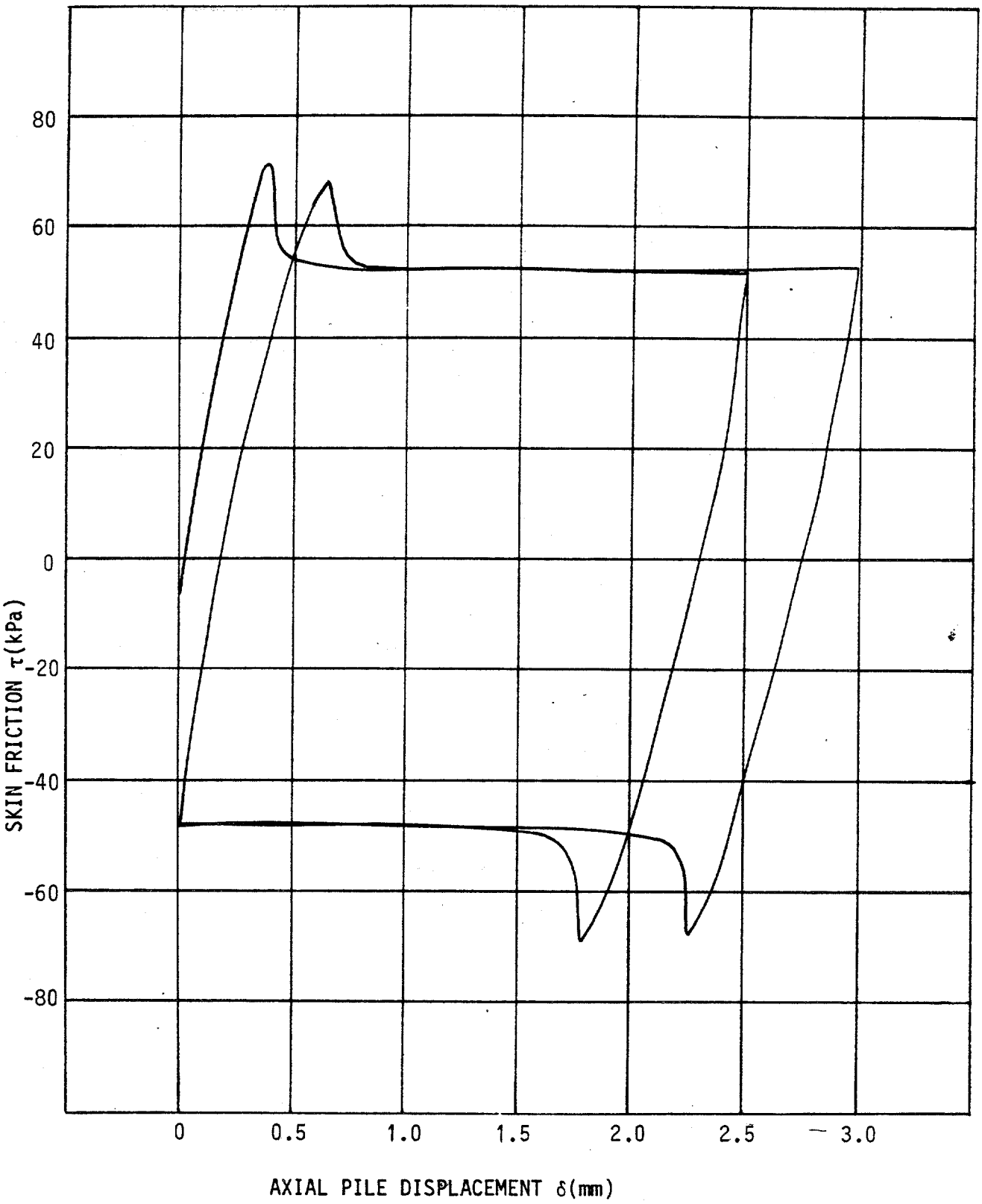

CNRD 13-2 TENSION PILE STUDY LABORATORY MODEL PILE TESTS

TEST 13, STRATUM II, STATIC TEST 6

DET NORSKE VERITAS Geotechnical Laboratory	Drawn by	Scale
	Approved	Date
		Fig. No. 14

STATIC TEST WITH REDUCED CONFINING PRESSURE

FOUR DAYS AFTER PRESSURE REDUCTION σ_v = 250 kPa σ_r = 175 kPa

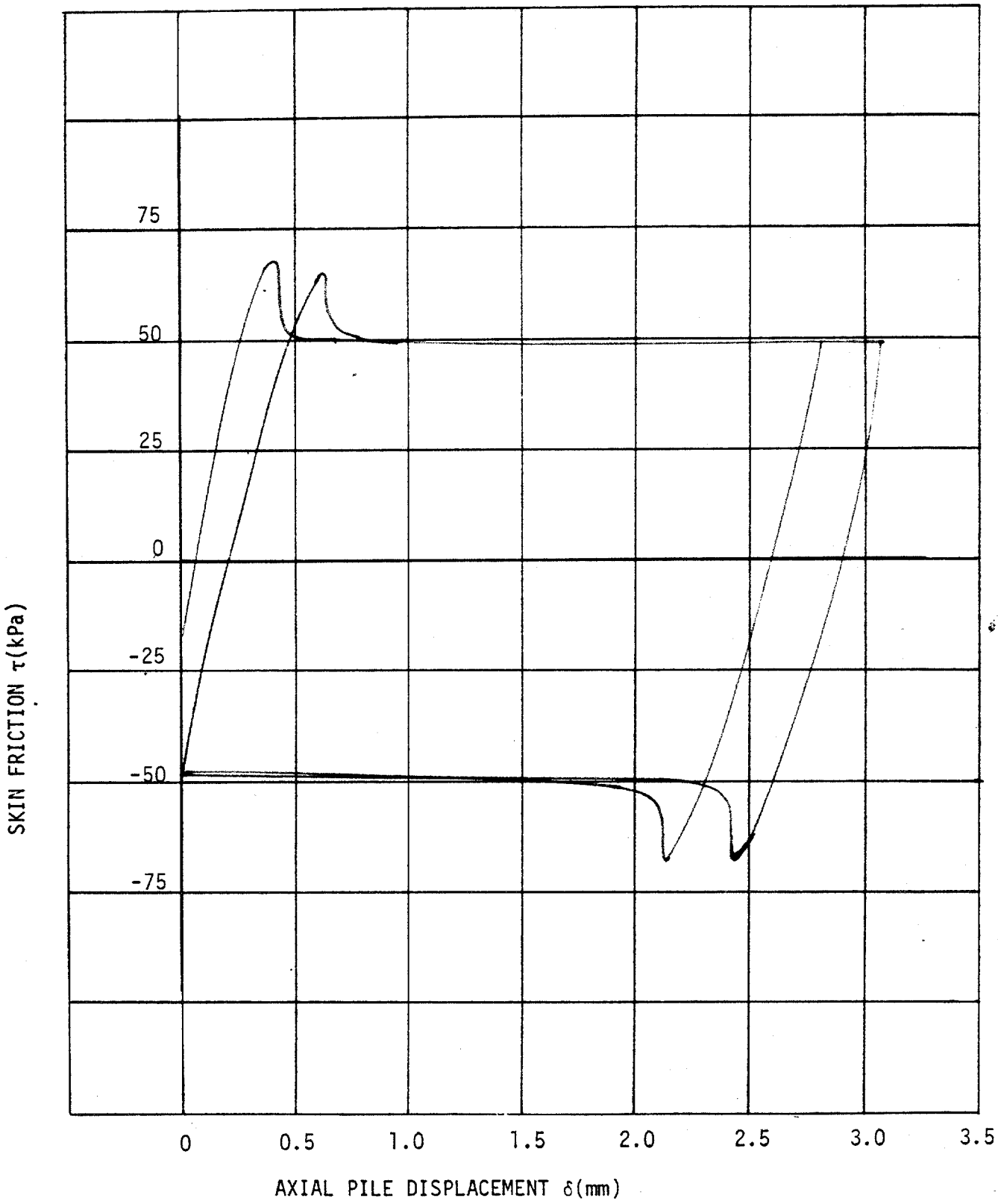

CNRD 13-2 TENSION PILE STUDY LABORATORY MODEL PILE TESTS

TEST 13, STRATUM II, STATIC TEST 7

Scale

DET NORSKE VERITAS
Geotechnical Laboratory

Drawn by

Date

Approved

Fig. No. 15

TEST 13, STRATUM II

SHEAR STRENGTH (kPa) FROM POCKET PENETROMETER TESTS AFTER PILE TEST COMPLETED

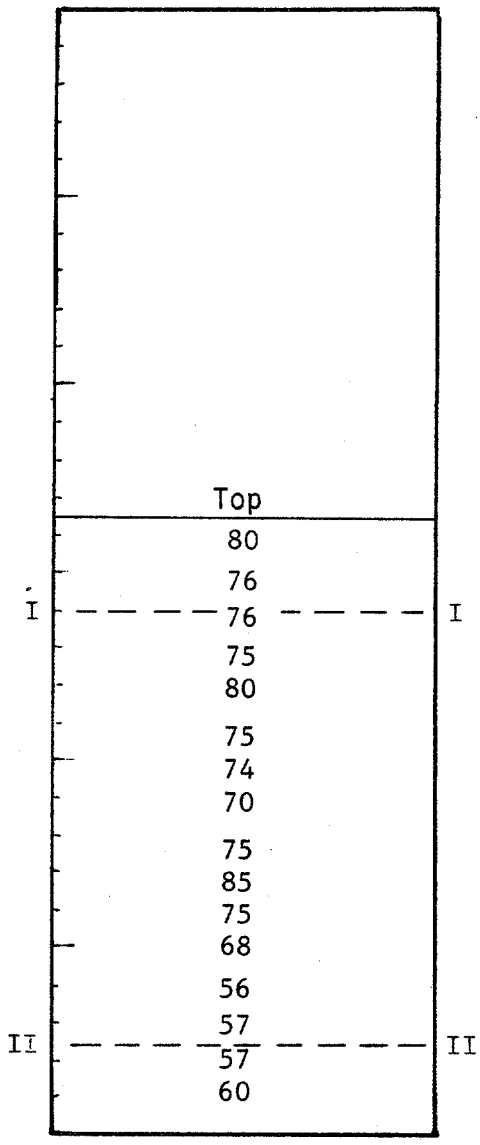

Scale 1:4

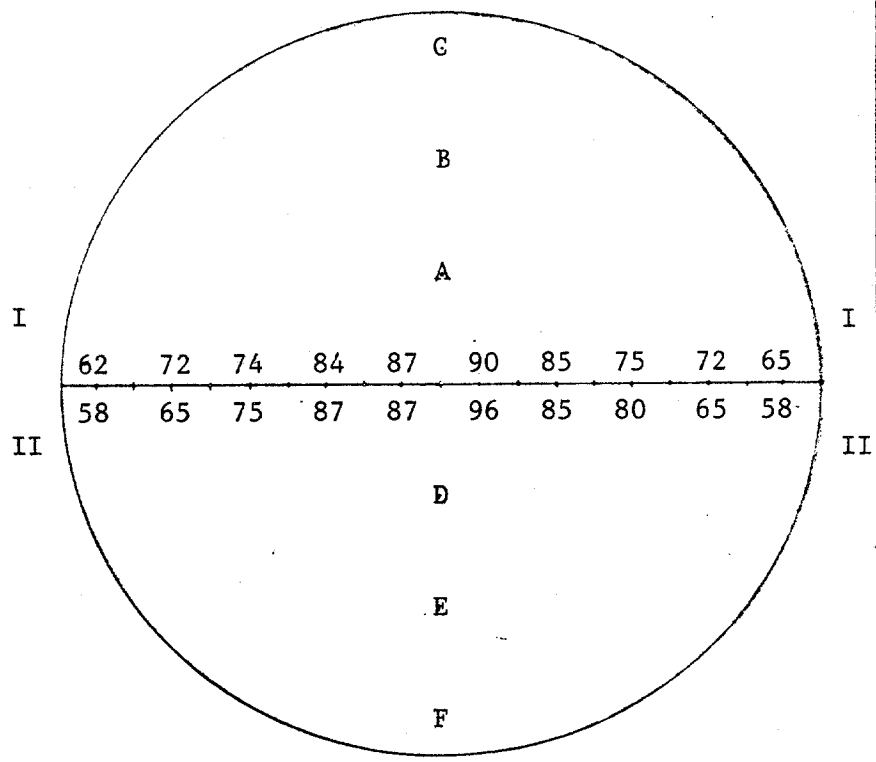

Scale: 1:2

CNRD 13-2 TENSION PILE STUDY LABORATORY MODEL PILE TESTS

TEST 13, STRATUM II, pocket penetrometer tests

Scale

DET NORSKE VERITAS
Geotechnical Laboratory

Drawn by

Date

Approved

Fig. No. 16

Unconfined Compression Test
on material after Pile Test completed

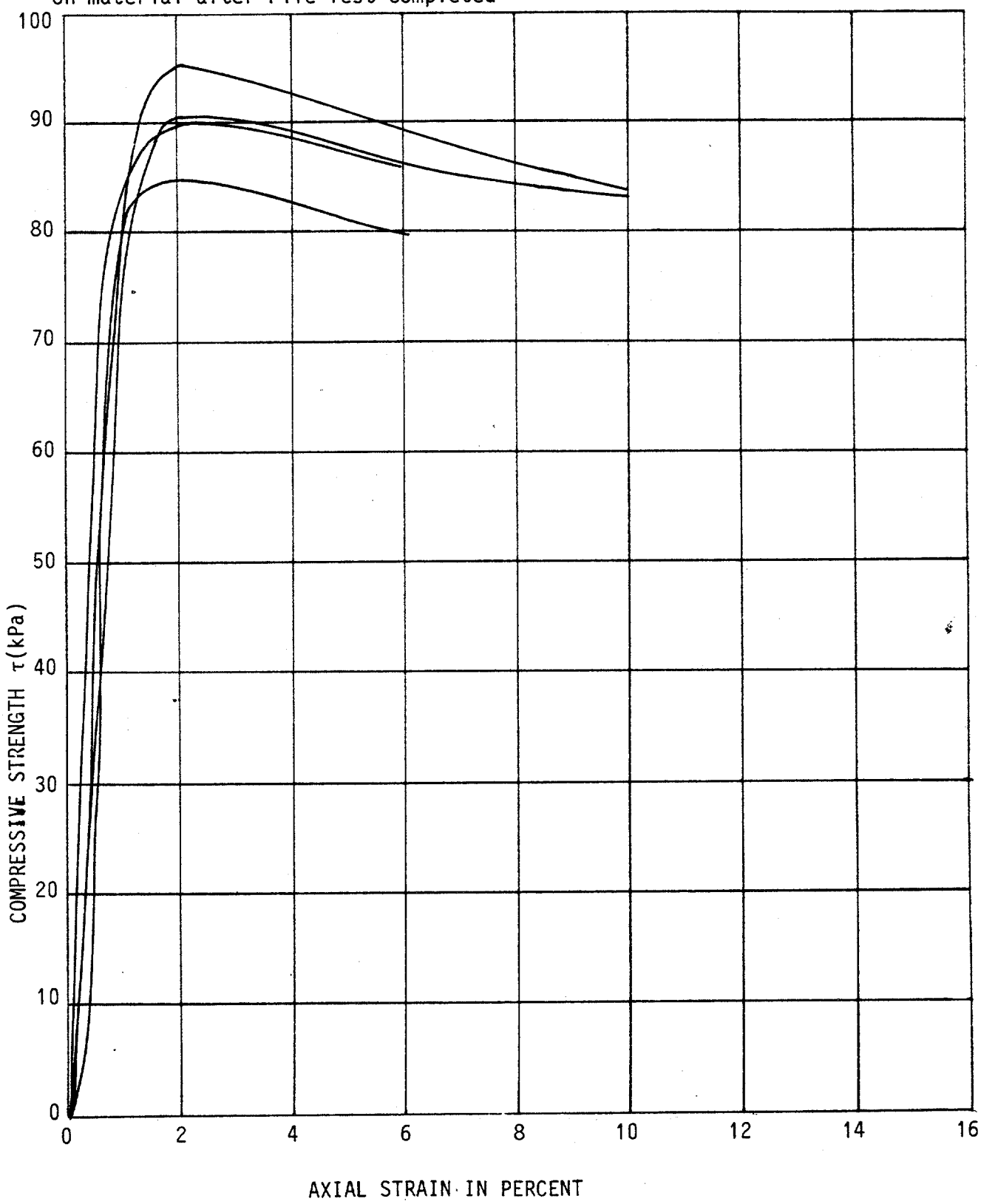

CNRD 13-2 TENSION PILE STUDY LABORATORY MODEL PILE TESTS

TEST 13, STRATUM II, unconfined compression after pile test

DET NORSKE VERITAS Geotechnical Laboratory	Drawn by	Scale
	Approved	Date
		Fig. No. 17

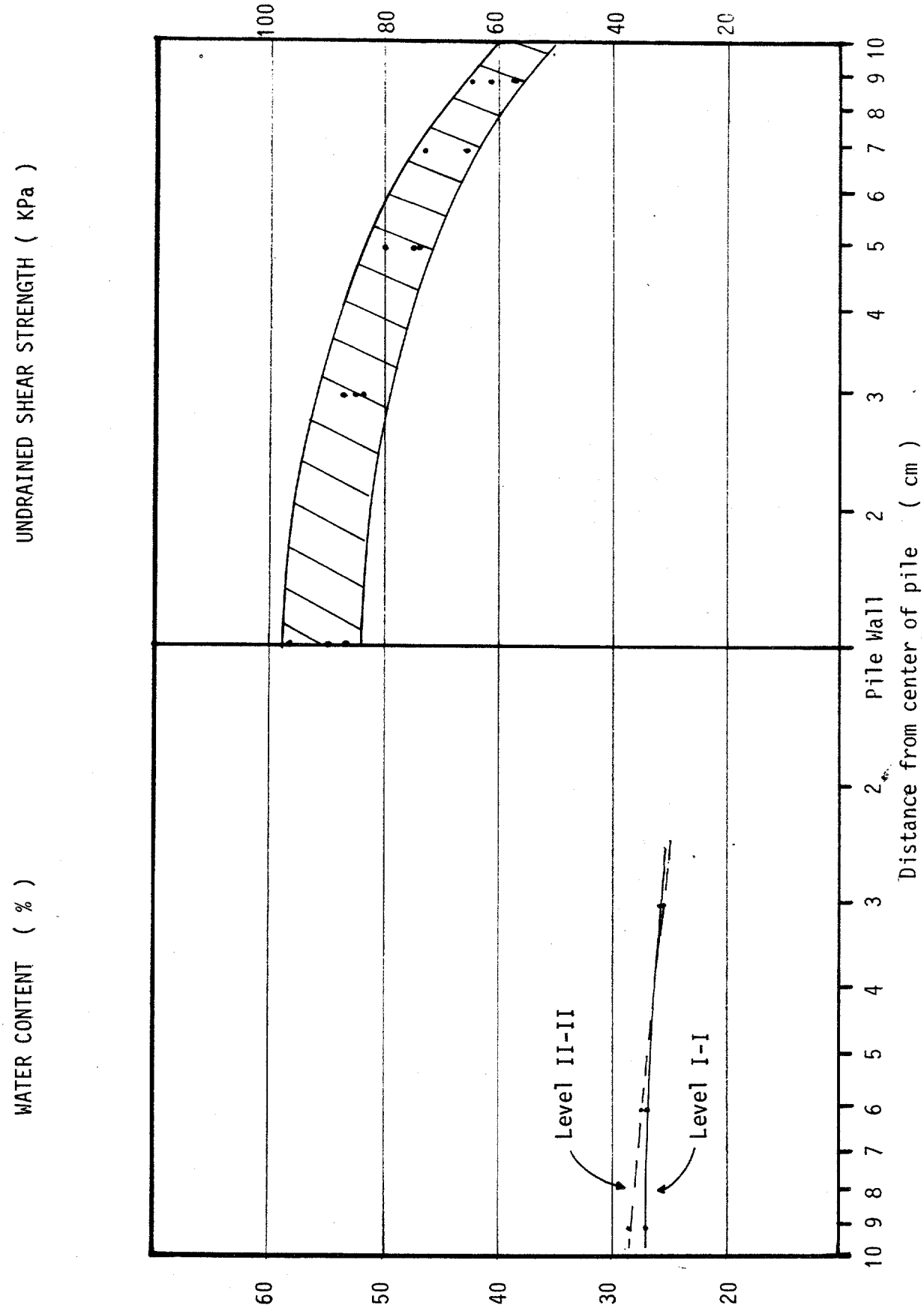

CNRD 13-2 TENSION PILE STUDY LABORATORY MODEL PILE TESTS

TEST 13, STRATUM II, Water content and shear strength after test

DET NORSKE VERITAS Geotechnical Laboratory	Drawn by	Scale
	Approved	Date
		Fig. No. 18

APPENDIX K

RESULTS OF LABORATORY TESTS FOR COMPARISON OF REMOULDED,RECONSOLIDATED MATERIAL AND UNDISTURBED MATERIAL

CONTENT

Introduction		K2
Test Program		K2
Test Procedures		K3
	Triaxial Tests	K3
	One-Dimensional Consolidation Tests	K4
List of Tables		K5
List of Figures		K5

1. INTRODUCTION

This Appendix K of the CNRD 13-2 TENSION PILE STUDY, FINAL REPORT, carried out for CONOCO NORWAY INC. presents the detailed results of the consolidation tests and the triaxial tests carried out by Veritas for comparison of remoulded, reconsolidated material with undisturbed material. General reference is made to Section 2.5 of the main report.

The material used for the laboratory model pile test program was taken at the CAGC-platform location at West Delta Block 58. The material was sorted according to the main stratification in the West Delta area and samples from different depths within each stratum had to be mixed, remoulded and reconsolidated in order to prepare test samples suitable to the model pile tests.

The repeated remoulding and reconsolidation of the soil material was expected to change the soil material properties to some extent compared to the in-situ conditions. The test program described in this Appendix was therefore directed towards the evaluation of the main differences in material behaviour.

The results of simple shear strength determinations, water content and plasticity index determinations during sample opening are presented in Figure 1.

2. TEST PROGRAM

The test program consisted of thirteen triaxial tests; five pure static tests and eight cyclic tests with post cyclic static loading performed partly on remoulded, reconsolidated material and partly on undisturbed material from Stratum II and III. Water content and plasticity properties were determined on a number of samples during the test program.

Further, seven oedometer tests were carried out on remoulded material in order to allow a comparison of compressibility, permeability and coefficient of consolidation with data from undisturbed samples.

3. TEST PROCEDURES

3.1 Triaxial Tests

After trimming the samples to 20 cm^2 circular cross section and 10 *cm* height the samples were built in using saturated filter stones. A consolidation stress of 50 kPa (isotropic) was applied for 1 hour before back-pressure and cell pressure were increased to the chosen level. Then the drainage valves were opened and the sample allowed to consolidate under net cell-pressures of 300 and 500 kPa for Stratum II and III materials respectively.

The samples were drained from both ends and the change in height and the volume of expelled pore water were recorded. The consolidation time required varied from 1 to 2 days for undisturbed material to nearly a week for the remoulded material.

The cyclic load program consisted of uniform load cycles with controlled sinusoidal variation of the axial load. In order to prevent accumulation of large axial strains in extension a permanent axial stress of about 10 kPa was applied to the samples. The tests were continued to failure in all cases except for one where the cyclic loading was stopped after more than 8000 cycles. Pore pressure development and increase in static and cyclic shear strains were recorded.

After failure the samples were tested by monotonic increase in axial deformation to failure in the same way as in standard static triaxial testing at an axial deformation rate of 3% per hour.

The results for the tests are presented as:

- percentage volume change versus log consolidation time
- effective stress paths for static tests
- deviator stress and pore pressure change vs. axial strain for static tests
- development of pore pressure and shear strain vs. number of cycles for cyclic tests
- cyclic stress-strain hysteresis loops

A strain contour diagram for 3% cyclic shear strain, i.e. number of cycles to reach 3% cyclic strain, vs. shear stress level, is presented in Figure 2.

3.2 One-Dimensional Consolidation Tests

Samples with 20 cm^2 cross section and a height of 20 mm were cut and trimmed from the samples prepared for model pile testing. The oedometer apparatus used was designed by the Swedish Geotechnical Institute. The load was applied in increments allowing 24 hrs consolidation for each step.

The results of the tests are shown as:

- Coefficient of consolidation and confined compression modulus vs. the logarithm of vertical stress

Some of the samples were cut horizontally in order to allow evaluation of anisotropic effects in the consolidation properties.

APPENDIX K

LIST OF TABLES

Table 1: Summary of Triaxial Tests, Stratum II
Table 2: Summary of Triaxial Tests, Stratum III

LIST OF FIGURES

Figure 1: Boring log based on samples used in the laboratory model pile tests
Figure 2: Strain contour comparison diagram, i.e. number of cycles to failure vs. cyclic shear stress level
Figure 3: Effective Stress path diagram, Stratum II, Remoulded
Figure 4: Effective Stress path diagram, Stratum II, Undisturbed
Figure 5: Effective Stress path diagram, Stratum III, Undisturbed
Figure 6: Effective Stress path diagram, Stratum III, Remoulded

Figure 7: Triaxial Test T1; Deviator Stress and Pore Pressure vs. Axial Strain
Figure 8: Triaxial Test T1; Consolidation Diagram

Figure 9: Triaxial Test T2; Pore Pressure and Shear Strain vs. Number of Cycles
Figure 10: Triaxial Test T2; Shear Stress vs. Shear Strain, Cyclic Loading
Figure 11: Triaxial Test T2; Deviator Stress and Pore Pressure vs. Axial Strain
Figure 12: Triaxial Test T2; Consolidation Diagram

Figure 13: Triaxial Test T3; Pore Pressure and Shear Strain vs. Number of Cycles

Figure 14: Triaxial Test T3; Shear Stress vs. Shear Strain, Cyclic Loading
Figure 15: Triaxial Test T3; Deviator Stress and Pore Pressure vs. Axial Strain
Figure 16: Triaxial Test T3; Consolidation Diagram

Figure 17: Triaxial Test T4; Pore Pressure and Shear Strain vs. Number of Cycles
Figure 18: Triaxial Test T4; Shear Stress vs. Shear Strain, Cyclic Loading
Figure 19: Triaxial Test T4; Deviator Stress and Pore Pressure vs. Axial Strain
Figure 20: Triaxial Test T4; Consolidation Diagram

Figure 21: Triaxial Test T5; Deviator Stress and Pore Pressure vs. Axial Strain
Figure 22: Triaxial Test T5; Consolidation Diagram

Figure 23: Triaxial Test T6; Pore Pressure and Shear Strain vs. Number of Cycles
Figure 24: Triaxial Test T6; Shear Stress vs. Shear Strain, Cyclic Loading
Figure 25: Triaxial Test T6; Deviator Stress and Pore Pressure vs. Axial Strain
Figure 26: Triaxial Test T6; Consolidation Diagram

Figure 27: Triaxial Test T7; Pore Pressure and Shear Strain vs. Number of Cycles
Figure 28: Triaxial Test T7; Shear Stress vs. Shear Strain, Cyclic Loading
Figure 29: Triaxial Test T7; Deviator Stress and Pore Pressure vs. Axial Strain
Figure 30: Triaxial Test T7; Consolidation Diagram

Figure 31: Triaxial Test T8; Deviator Stress and Pore Pressure vs. Axial Strain
Figure 32: Triaxial Test T8; Consolidation Diagram

Figure 33: Triaxial Test T9; Pore Pressure and Shear Strain vs. Number of Cycles
Figure 34: Triaxial Test T9; Shear Stress vs. Shear Strain, Cyclic Loading
Figure 35: Triaxial Test T9; Deviator Stress and Pore Pressure vs. Axial Strain
Figure 36: Triaxial Test T9; Consolidation Diagram

Figure 37: Triaxial Test T10; Pore Pressure and Shear Strain vs. Number of Cycles
Figure 38: Triaxial Test T10 Shear Stress vs. Shear Strain, Cyclic Loading
Figure 39: Triaxial Test T10; Deviator Stress and Pore Pressure vs. Axial Strain
Figure 40: Triaxial Test T10; Consolidation Diagram

Figure 41: Triaxial Test T11; Deviator Stress and Pore Pressure vs. Axial Strain
Figure 42: Triaxial Test T11; Consolidation Diagram

Figure 43: Triaxial Test T12; Deviator Stress and Pore Pressure vs. Axial Strain
Figure 44: Triaxial Test T12; Consolidation Diagram

Figure 45: Triaxial Test T13; Pore Pressure and Shear Strain vs. Number of Cycles
Figure 46: Triaxial Test T13; Shear Stress vs. Shear Strain, Cyclic Loading

Figure 47: Triaxial Test T13; Shear Stress vs. Shear Strain, Cyclic Loading

Figure 48: Triaxial Test T13; Deviator Stress and Pore Pressure vs. Axial Strain

Figure 49: Triaxial Test T13; Consolidation Diagram

Figure 50: Compression Test on Material from Model Pile Test 5, Stratum II

Figure 51: Compression Test on Material from Model Pile Test 6, Stratum III

Figure 52: Compression Test on Material from Model Pile Test 8, Stratum III

Figure 53: Compression Test on Material from Model Pile Test 9, Stratum II

TEST NO	OCR	BUILDING - IN						END OF TEST			DATA FROM CONSOLIDATION									CYCLIC LOADING							UNDRAINED SHEARING			REMARKS
											AFTER LOADING				AFTER UNLOADING															
		w	w_L	w_P	I_P	s_u 1)	S_t 1)	w	s_u 1)	S_t 1)	ε_v	ε_{vol}	σ'_{vpc}	σ_{hpc}	ε_v	ε_{vol}	σ_{vc}	σ_{hc}	B	τ	$\frac{\tau}{s_u}$	N AT END OF TEST	ε_{vN} %		u_N kPa		s_u	ε_{vf}	u_f	
		%	%	%	%	kPa		%	kPa		%	%	kPa	kPa	%	%	kPa	kPa		kPa			min	max	min	max	kPa	%	kPa	
T1	1	27.96				62		27.71	52		1.1	2.8	350	350													108	10.1	211	Remoulded
T2	1	27.84	62.03	20.20	41.83	62		28.59	52		1.3	2.1	300	300						68	0.72	89	-2.9	+0.2	40	53	88	10.7	196	Remoulded
T3	1	27.42				63		27.47	50		1.2	2.0	300	300						58	0.58	570	-3.8	+1.6	160	196	85	10.1	213	Remoulded
T4	1	27.98				62		27.04	74		1.3	2.6	300	300						45	0.45	8765	-0.38	+0.31	124	148	95	6.1	184	Remoulded
T5	1	50.29				60	2	40.16	60		6.9	10.2	300	300													97	10.8	182	Undisturbed
T6	1	49.18	79.07	24.38	54.69	63	2	38.05	65		5.0	11.8	300	300						77	0.77	70	-3.6	+2.4	137	189	95	8.9	234	Undisturbed
T7	1	49.16				54	2	41.41	54		6.0	14.5	300	300						54	0.54	2200	-0.92	+2.36	161	200	102	10.5	222	Undisturbed

1) by pocket penetrometer

Table 1: Summary of Triaxial Tests, Stratum II

TEST NO	OCR	BUILDING - IN						END OF TEST			DATA FROM CONSOLIDATION									CYCLIC LOADING							UNDRAINED SHEARING			REMARKS
											AFTER LOADING				AFTER UNLOADING															
		w	w_L	w_P	I_P	s_u 1) 2)	S_t 1)	w	s_u 1) 2)	S_t 1)	ε_v	ε_{vol}	σ_{vpc}	σ_{hpc}	ε_v	ε_{vol}	σ_{vc}	σ_{hc}	B	τ	$\frac{\tau}{s_u}$	N AT END OF TEST	ε_{vN} %		u_N kPa		s_u	ε_{vf}	u_f	
		%	%	%	%	kPa		%	kPa		%	%	kPa	kPa	%	%	kPa	kPa		kPa			min	max	min	max	kPa	%	kPa	
T8	1	58.62				63	1	47.62	135/80		5.4	14.6	500	500													143	10.8	307	Undisturbed
T9	1	58.67	98.57	27.86	70.71	63	1	45.67	145/85		6.4	18.1	500	500						84	0.55	3000	-0.71	+2.4	255	293	141	8.7	377	Undisturbed
T10	1	53.70				73	2	44.02	120/80		5.4	16.3	500	500						100	0.74	96	-1.1	+3.6	137	156	144	8.7	372	Undisturbed
T11	1	40.39				100/73		36.49	125/95		1.9	5.8	500	500													107	9.2	269	Remoulded (not compl. consol.)
T12	1	40.63	92.30	26.24	66.06	100/73		34.85	155/105		2.6	7.4	500	500													134	8.4	234	Remoulded
T13	1	40.16				122/78		36.19	140/97		2.9	10.6	500	500						100 70	0.77 0.55	10 120	-1.9	+3.3	32	34	104	8.8	230	Remoulded (not compl. consol.)

1) by fall cone

2) by pocket penetrometer

Table 2: Summary of Triaxial Tests, Stratum III

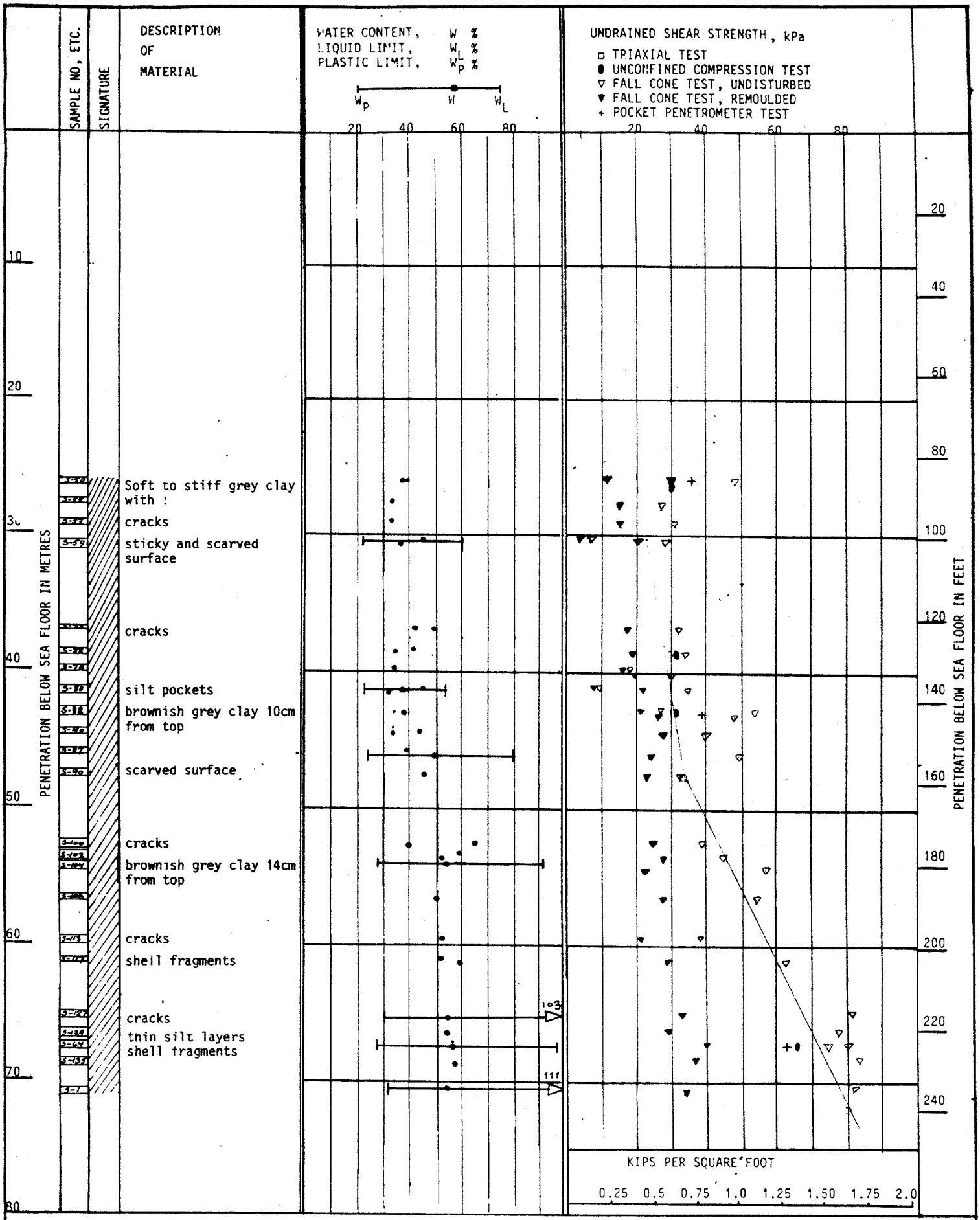

CNRD 13-2 TENSION PILE STUDY

Boring log from clay used in model pile tests

DET NORSKE VERITAS
Geotechnical Laboratory

Drawn by | Scale | Approved | Date | Fig. No. 1

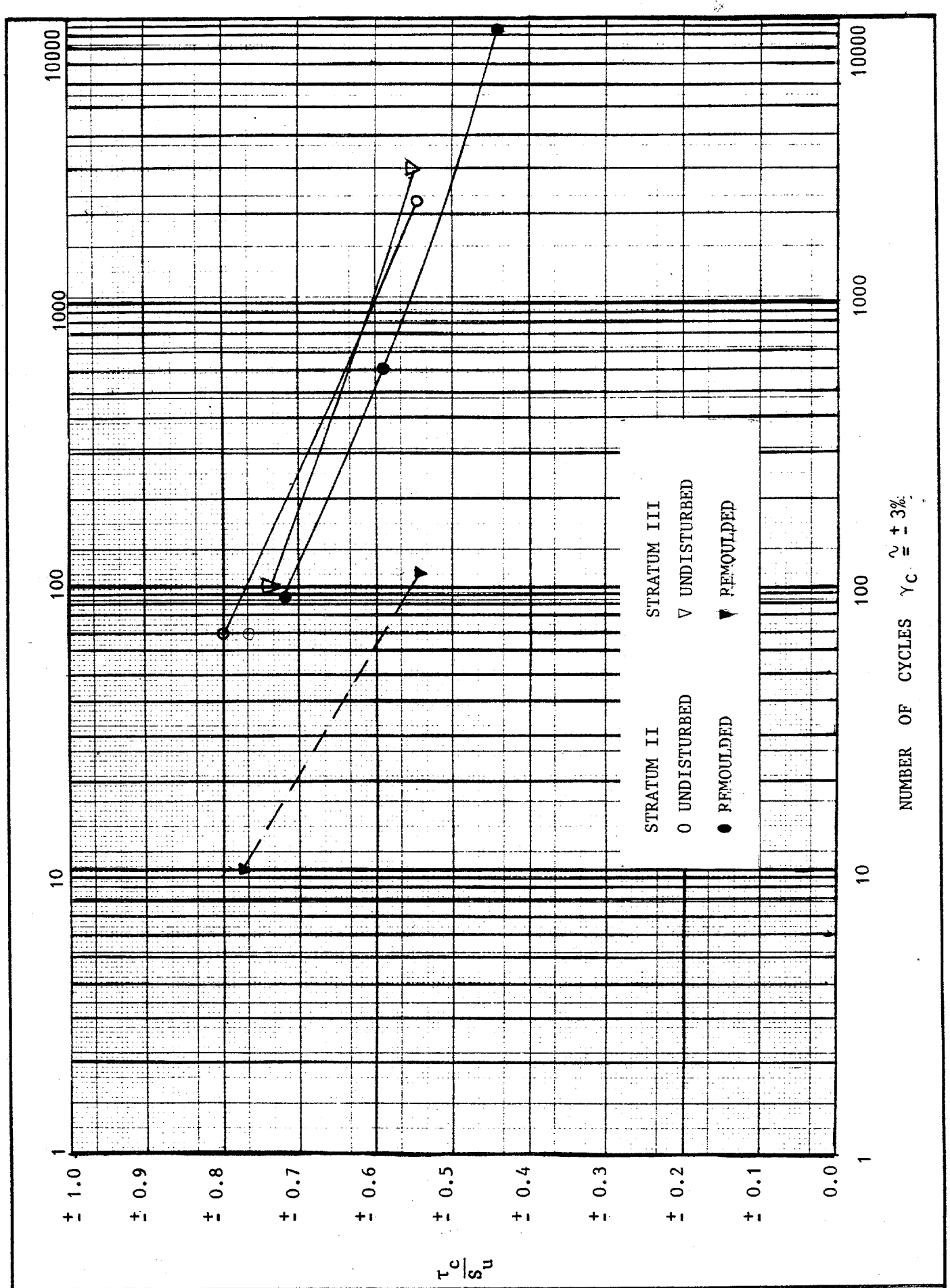

Figure 2: Strain contour comparison diagram, i.e. number of cycles to failure vs. cyclic shear stress level

DET NORSKE VERITAS Geotechnical Laboratory	Drawn by	Proj.No.
	Approved	Scale
		Date
		Fig.No.

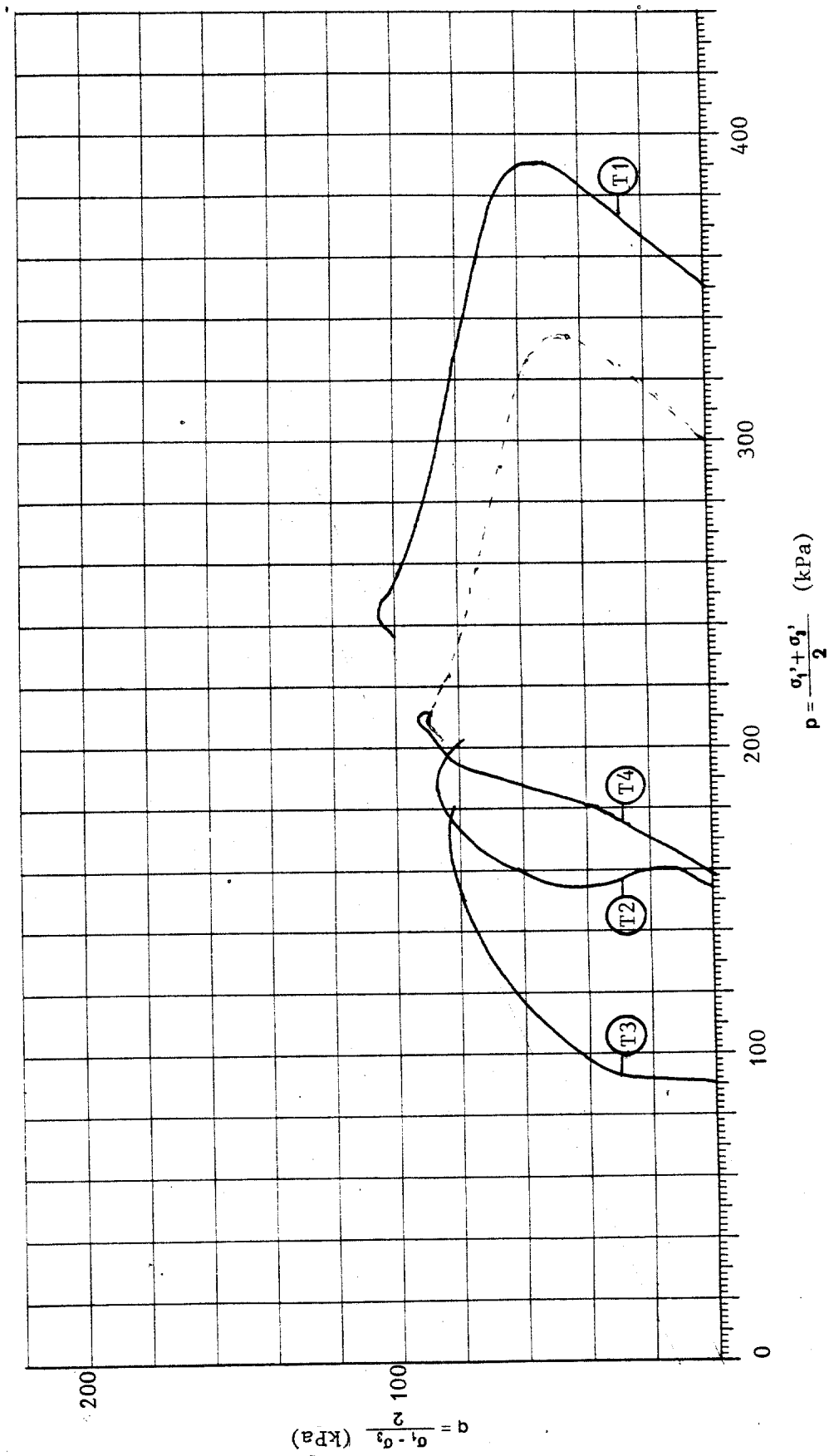

Figure 3: Effective Stress path diagram, Stratum II, Remoulded

		Proj.No.
		Scale
DET NORSKE VERITAS Geotechnical Laboratory	Drawn by	Date
	Approved	Fig.No.

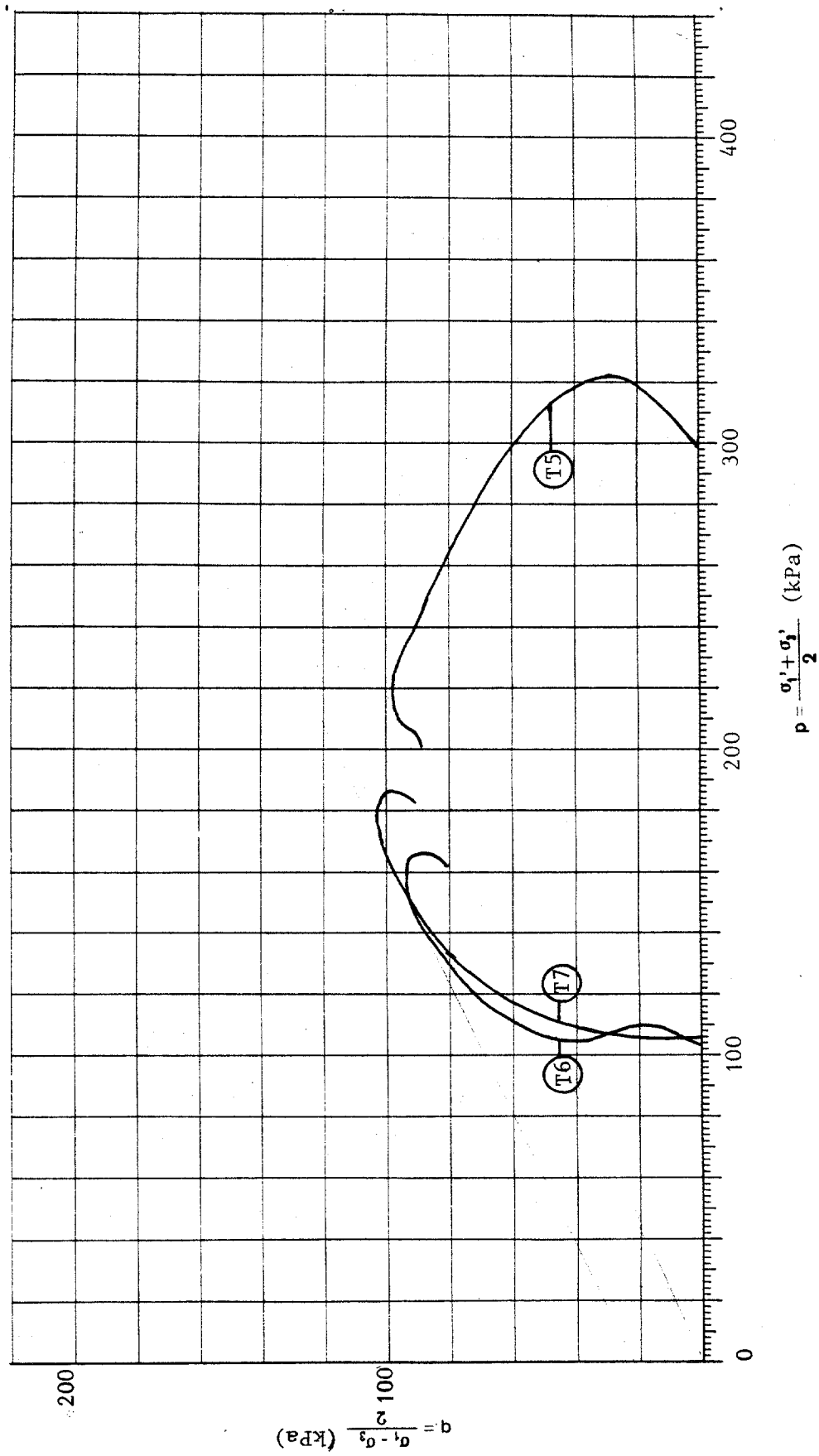

Figure 4: Effective Stress path diagram, Stratum II, Undisturbed

		Proj. No.
		Scale
DET NORSKE VERITAS Geotechnical Laboratory	Drawn by	Date
	Approved	Fig. No.

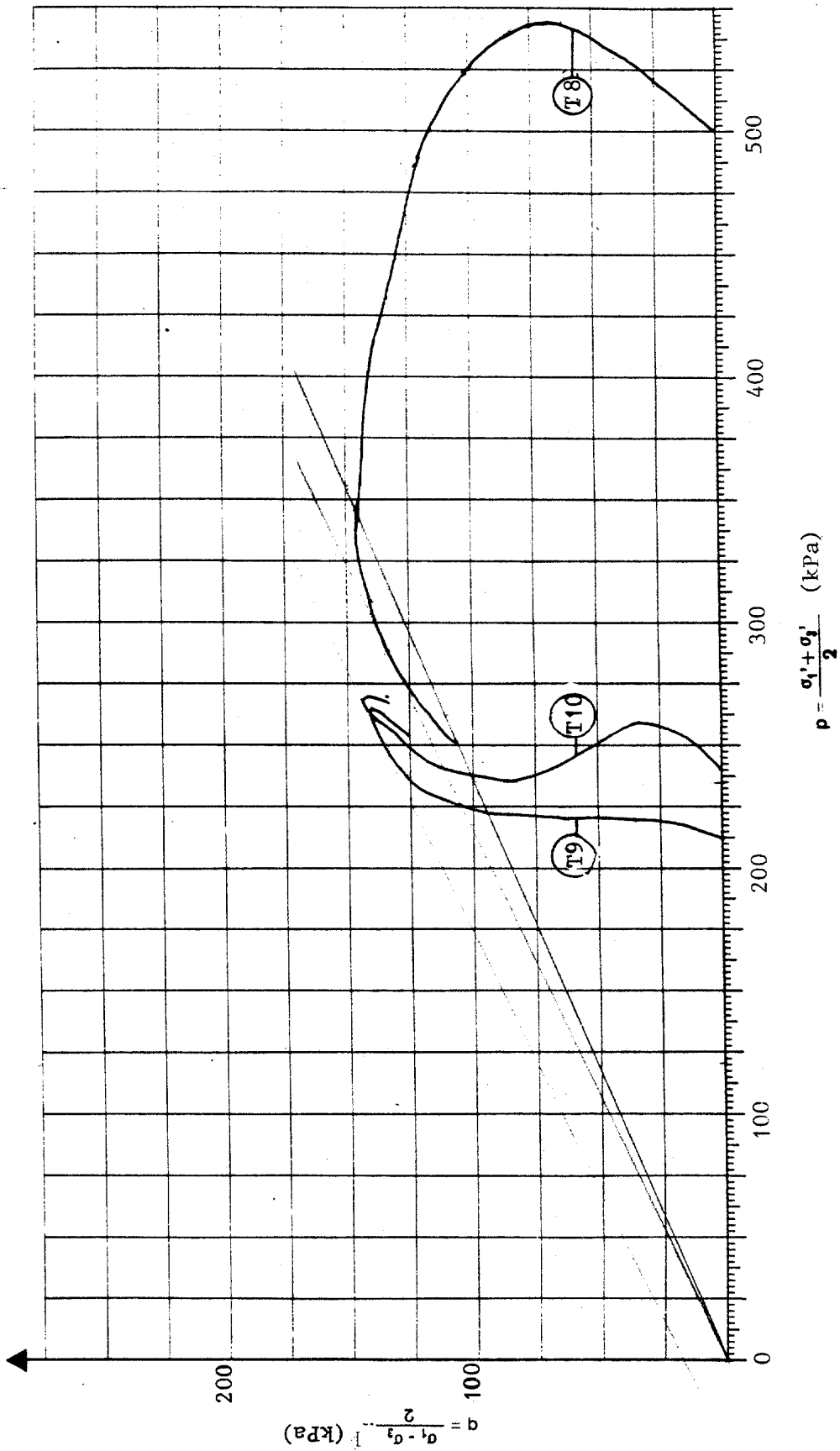

Figure 5: Effective Stress path diagram, Stratum III, Undisturbed

		Proj. No.
		Scale
DET NORSKE VERITAS Geotechnical Laboratory	Drawn by	Date
	Approved	Fig. No.

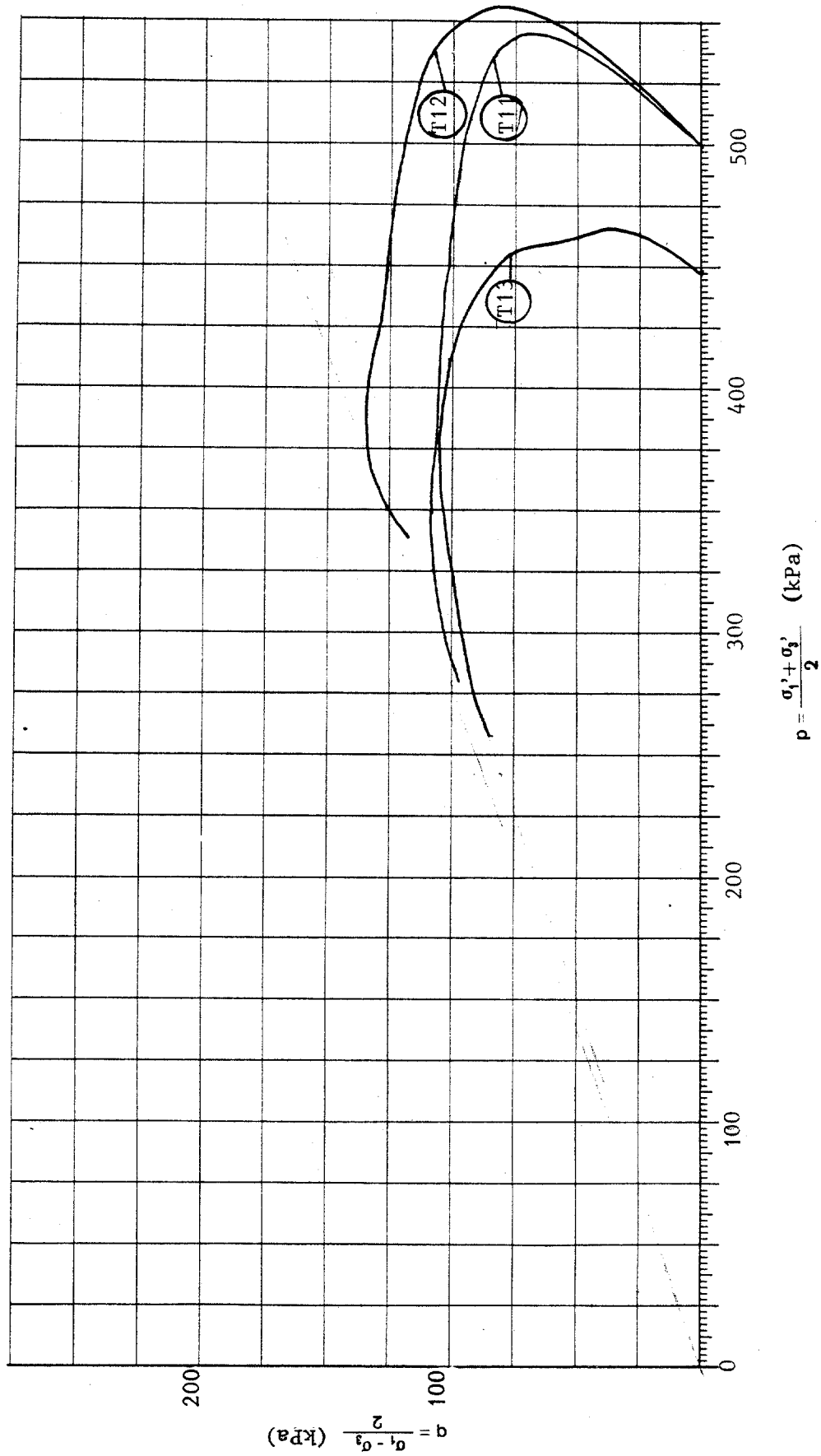

Figure 6: Effective Stress path diagram, Stratum III, Remoulded

		Proj.No.
		Scale
DET NORSKE VERITAS Geotechnical Laboratory	Drawn by	Date
	Approved	Fig.No.

TEST No. : T 1

STRATUM : II

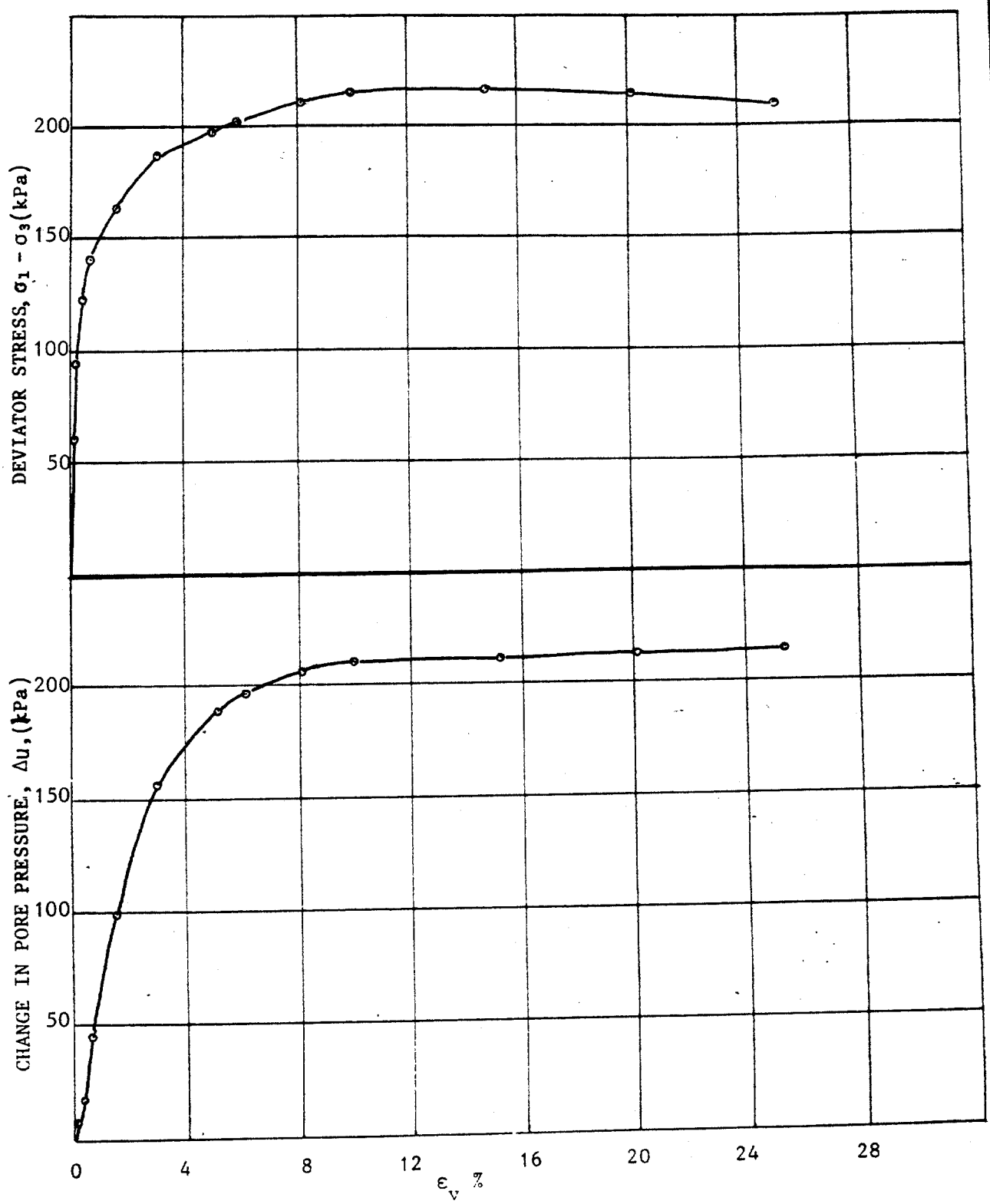

CNRD 13-2 TENSION PILE STUDY

STANDARD TRIAXIAL TEST, CIU

DET NORSKE VERITAS
Geotechnical Laboratory

Scale	
Drawn by	Date
Approved	Fig. No. 7

REMOULDED SAMPLE

FROM PILE TEST 13,

CONSOLIDATION PRESSURE : 350 kPa

TEST No.: T1

STRATUM : II

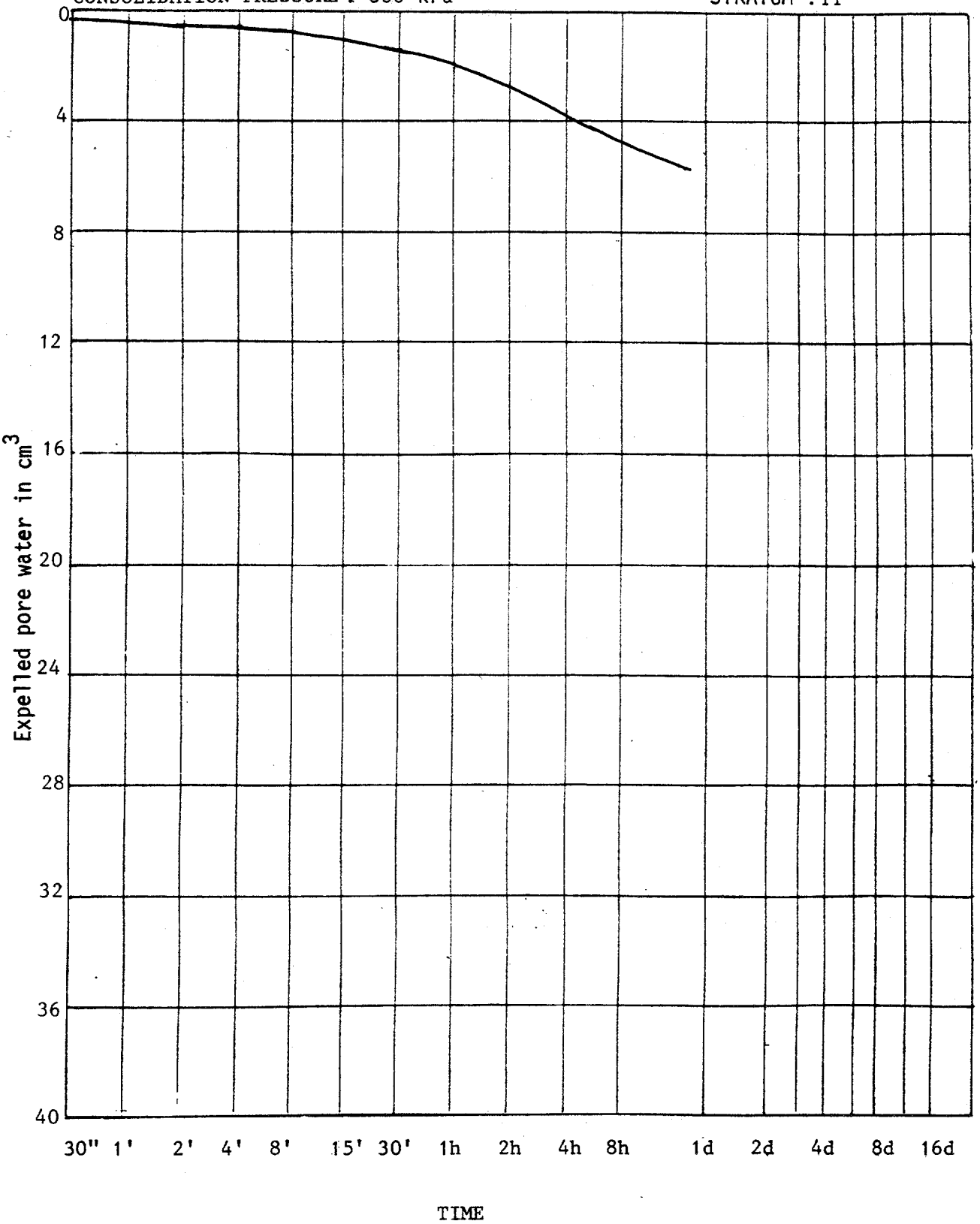

CNRD 13-2 TENSION PILE STUDY

CONSOLIDATION DIAGRAM

DET NORSKE VERITAS
Geotechnical Laboratory

Scale	
Drawn by	Date
Approved	Fig.No. 8

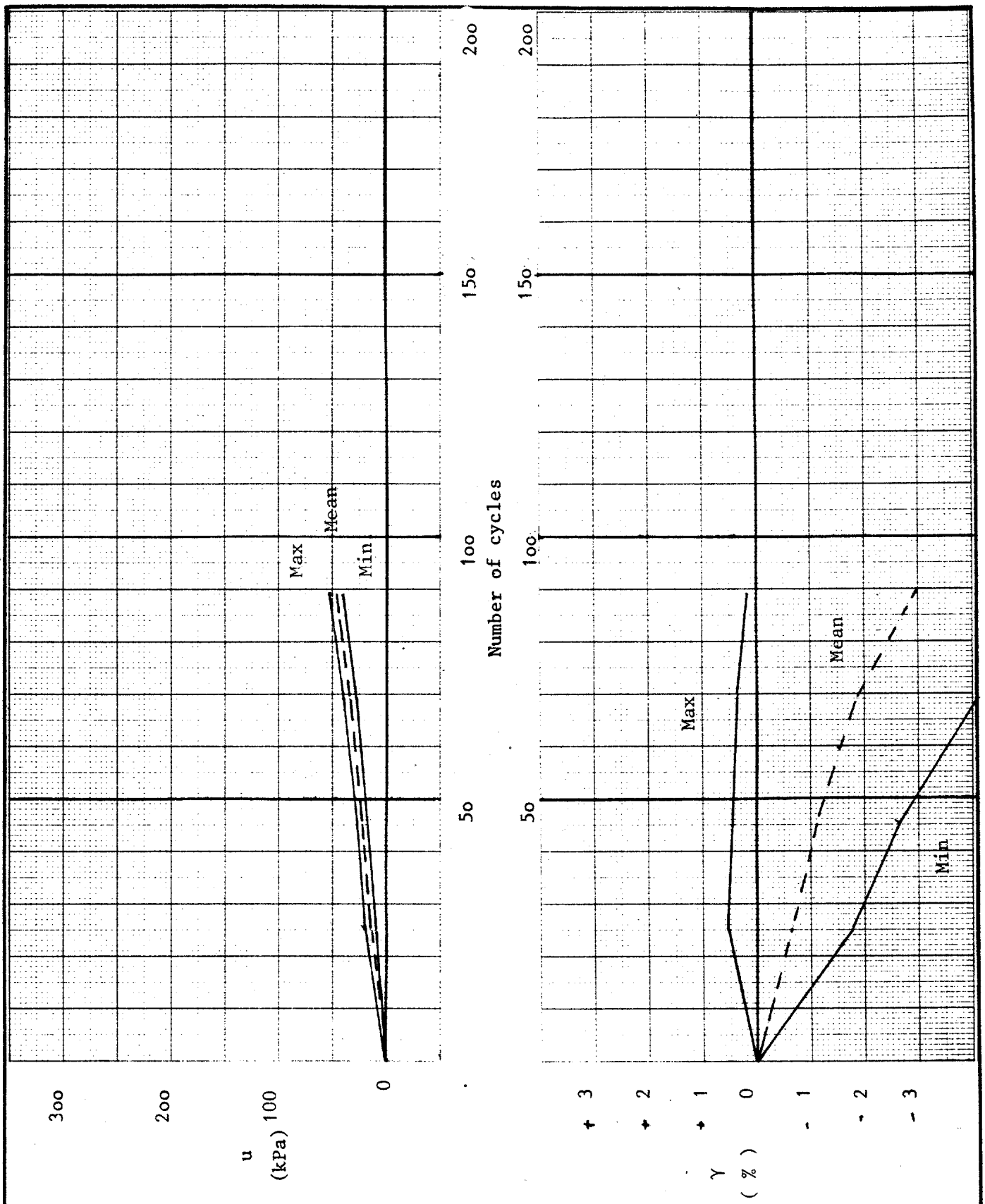

SAMPLE NO: T2 $\tau_e/S_u = \pm 0.72$

CYCLIC TRIAXIAL TEST

DET NORSKE VERITAS
Geotechnical Laboratory

Proj. No.	
Scale	
Drawn by	Date
Approved	Fig. No. 9

SAMPLE NO.: T 2

τ_{stat} : 10 kPa

τ_{cyclic} : ± 68 kPa

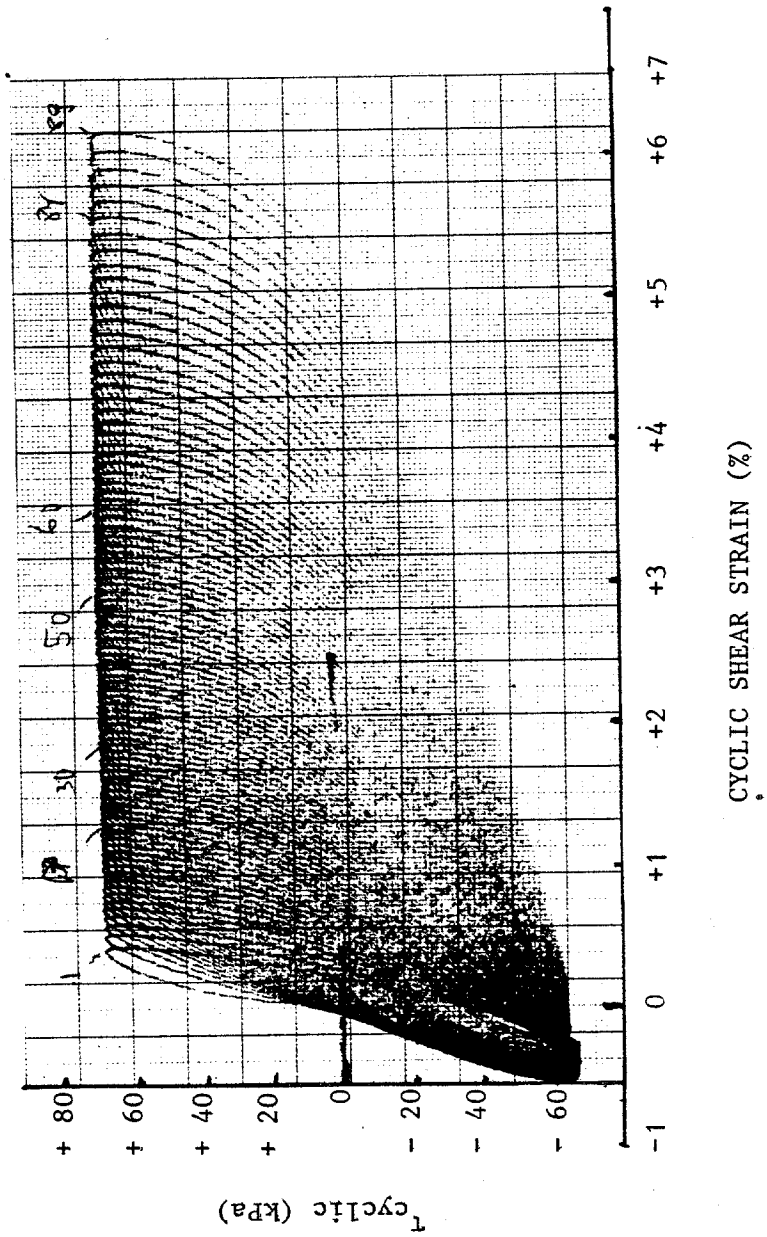

CNRD 13-2 TENSION PILE STUDY

CYCLIC TRIAXIAL TEST, STRESS VS STRAIN, DIRECT PLOT

DET NORSKE VERITAS Geotechnical Laboratory	Drawn by	Scale
	Approved	Date
		Fig. No. 10

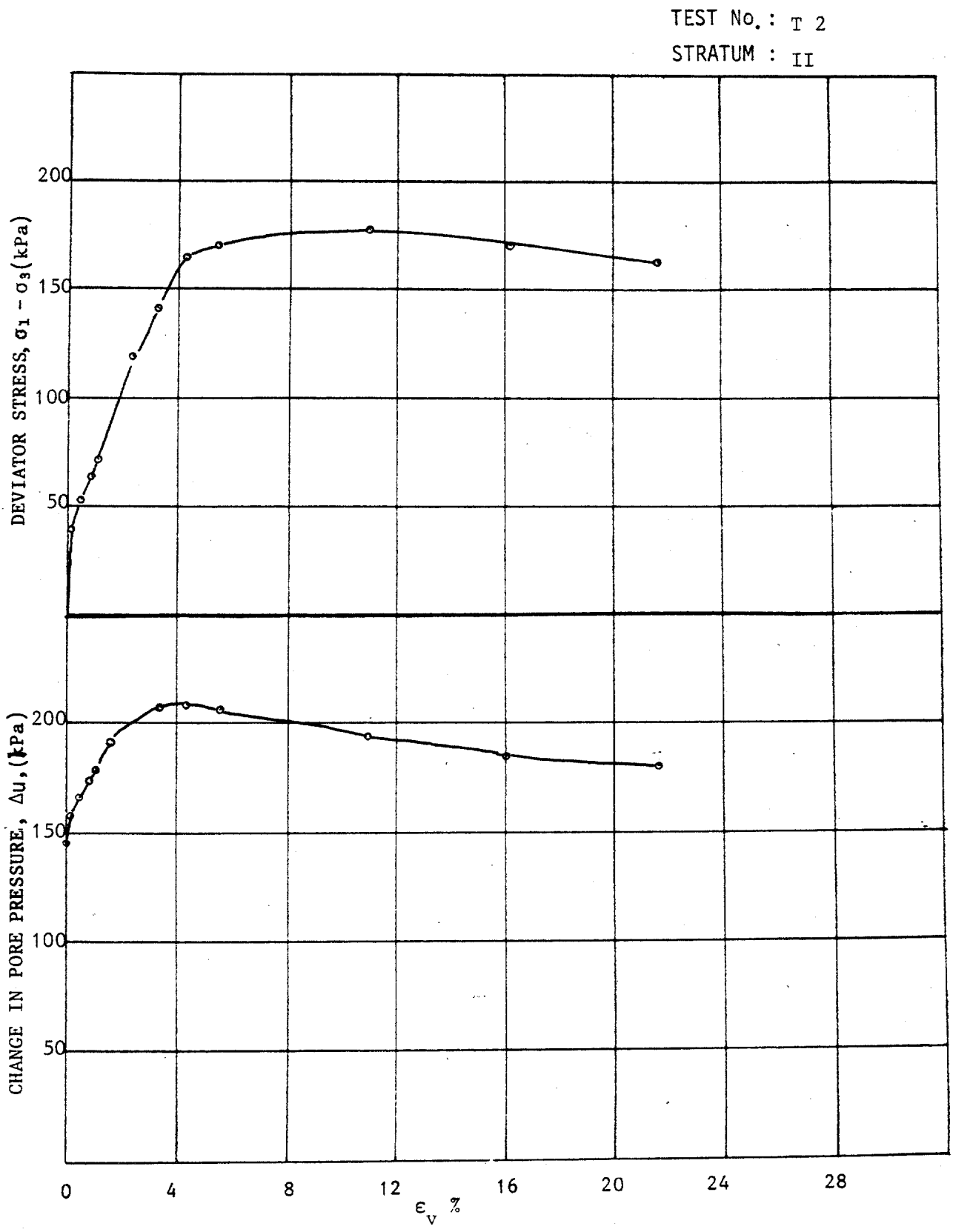

CNRD 13-2 TENSION PILE STUDY

STANDARD TRIAXIAL TEST, CIU, AFTER CYCLIC LOADING

DET NORSKE VERITAS Geotechnical Laboratory	Drawn by	Scale
	Approved	Date
		Fig. No. 11

REMOULDED SAMPLE

FROM PILE TEST 13,

CONSOLIDATION PRESSURE : 300 kPa

TEST No.: T2

STRATUM : II

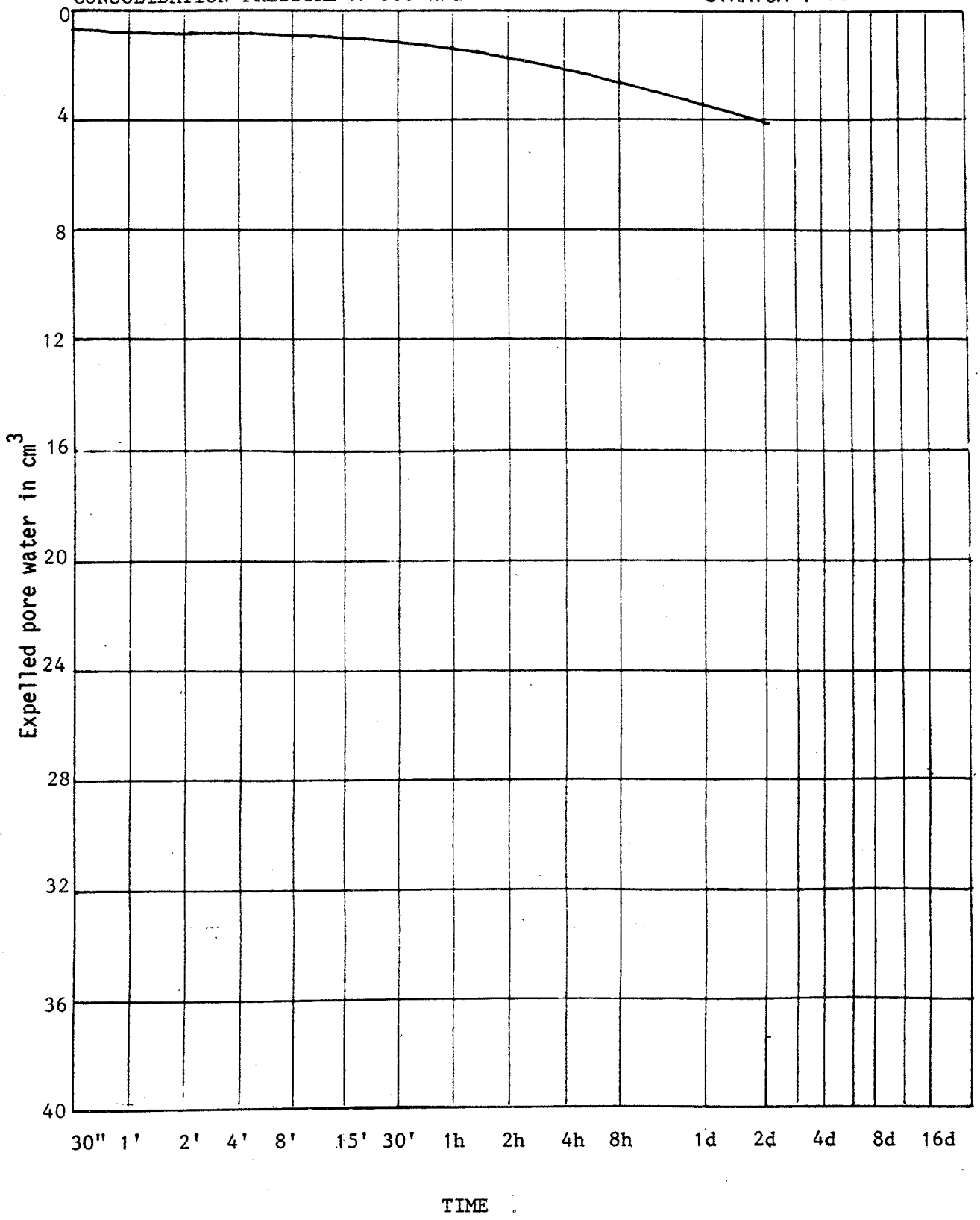

CNRD 13-2 TENSION PILE STUDY

CONSOLIDATION DIAGRAM

DET NORSKE VERITAS Geotechnical Laboratory	Drawn by	Scale
	Approved	Date
		Fig.No. 12

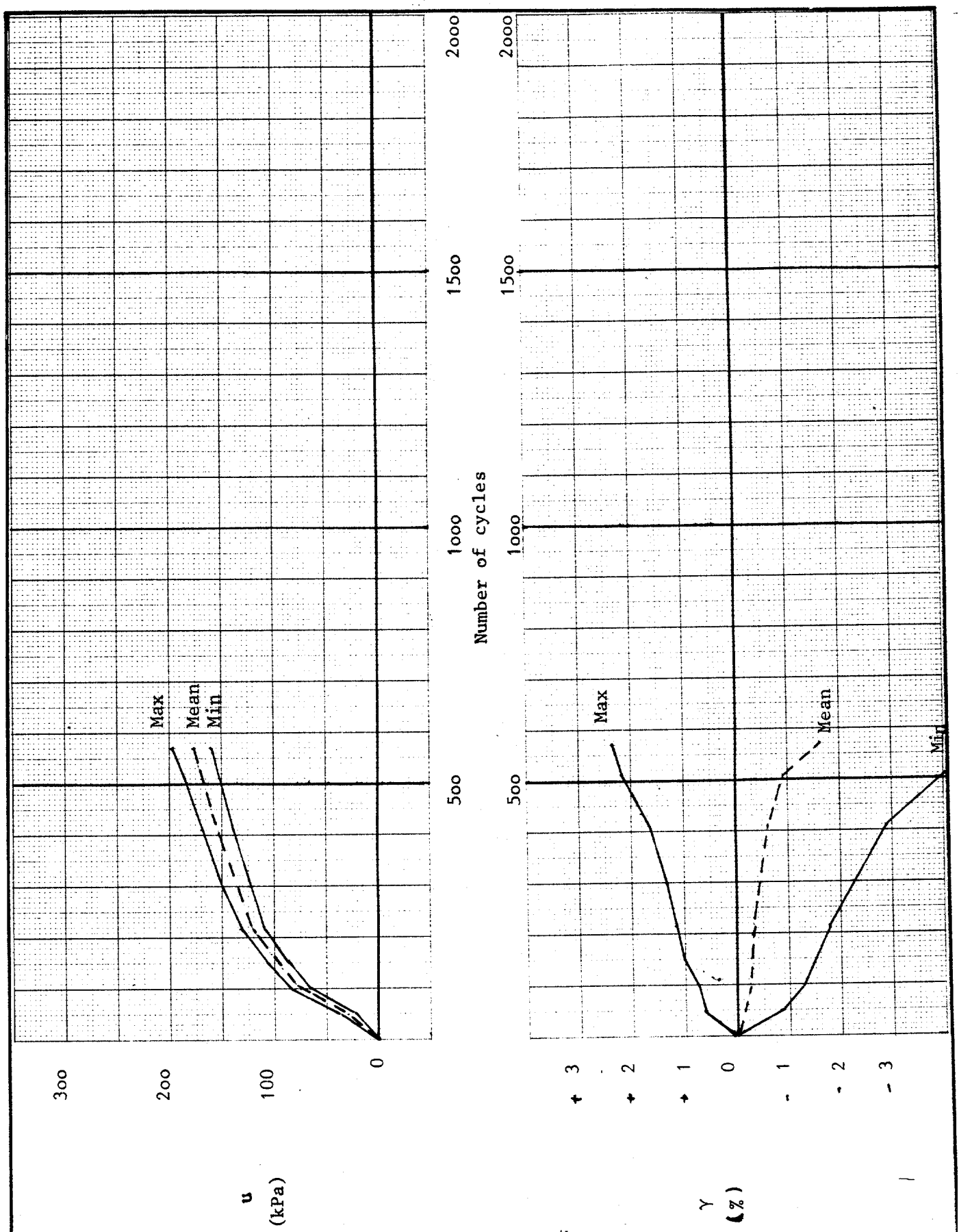

SAMPLE NO: T3 $\tau_c/S_u = \pm 0.58$

CYCLIC TRIAXIAL TEST

DET NORSKE VERITAS
Geotechnical Laboratory

Proj.No.	
Scale	
Drawn by	
Date	
Approved	
Fig.No.	13

SAMPLE NO.: T3

τ_{stat} : 0

τ_{cyclic} : $\pm$ 58 kPa

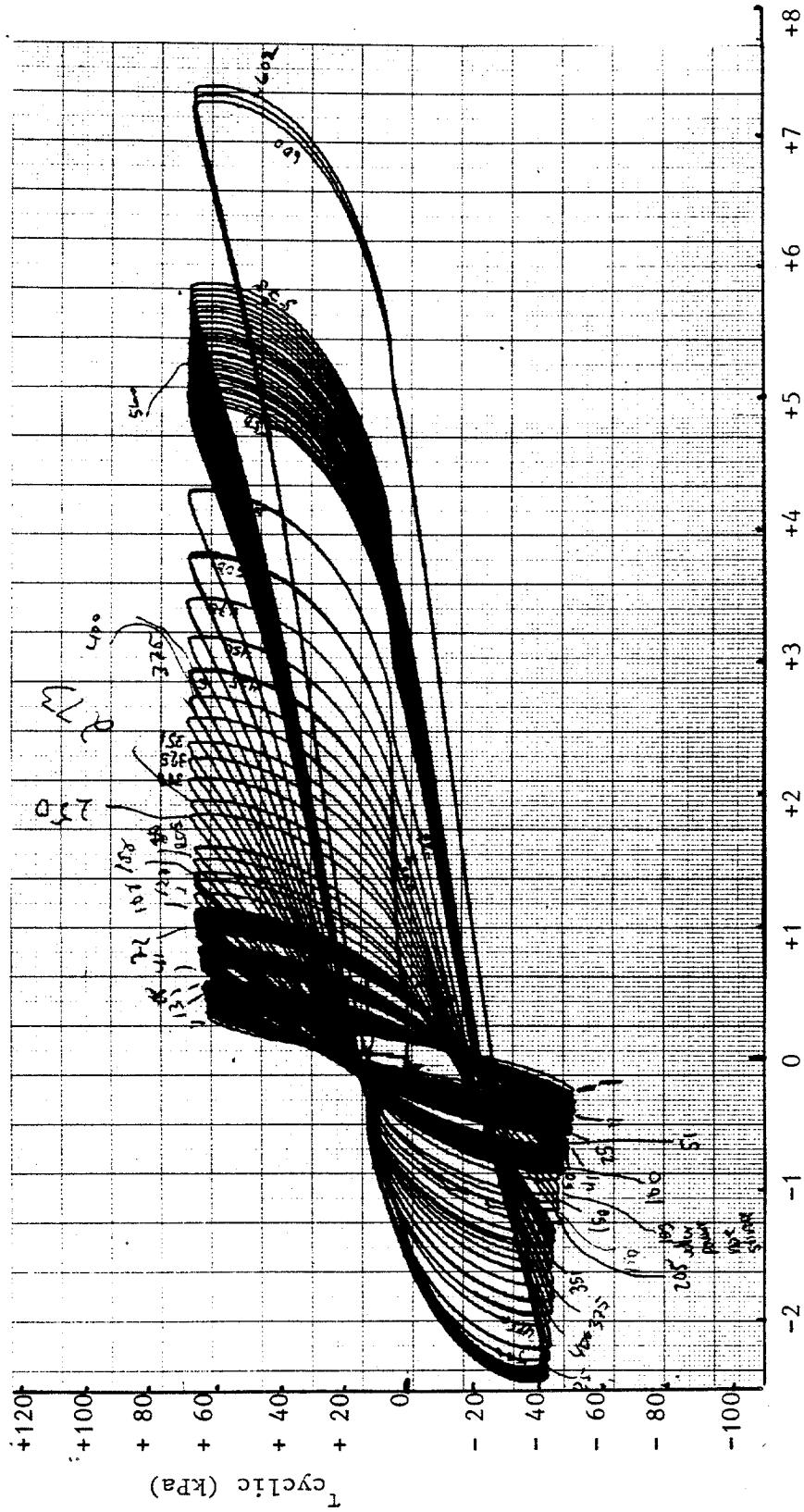

CNRD 13-2 TENSION PILE STUDY

CYCLIC TRIAXIAL TEST, STRESS VS STRAIN, DIRECT PLOT

DET NORSKE VERITAS
Geotechnical Laboratory

Scale	
Drawn by	Date
Approved	Fig. No. 14

TEST No. : T 3

STRATUM : II

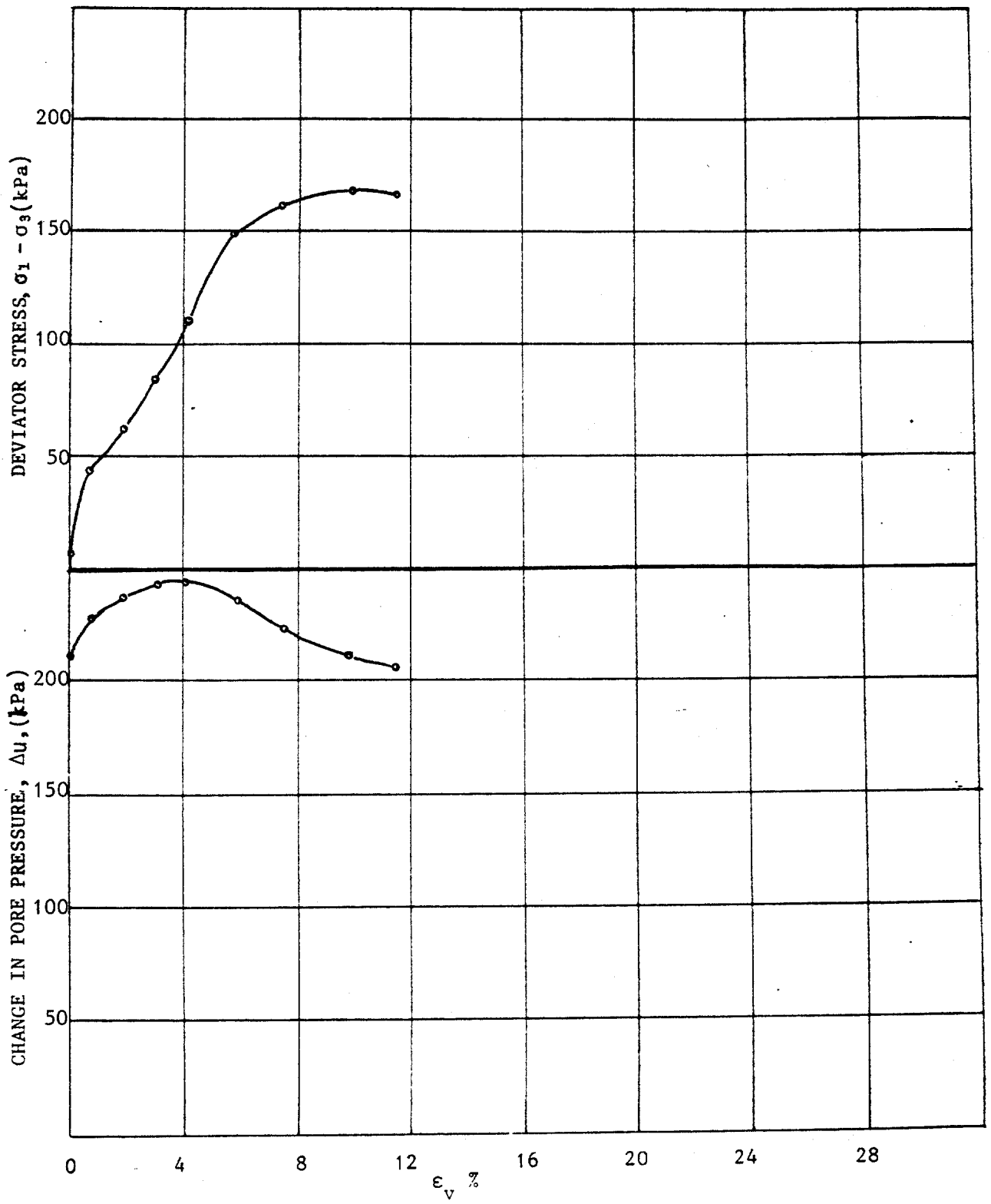

CNRD 13-2 TENSION PILE STUDY

STANDARD TRIAXIAL TEST, CIU, AFTER CYCLIC LOADING

DET NORSKE VERITAS Geotechnical Laboratory	Drawn by	Scale
	Approved	Date
		Fig. No. 15

REMOULDED SAMPLE

FROM PILE TEST 13,

CONSOLIDATION PRESSURE : 300 kPa

TEST No.: T3

STRATUM : II

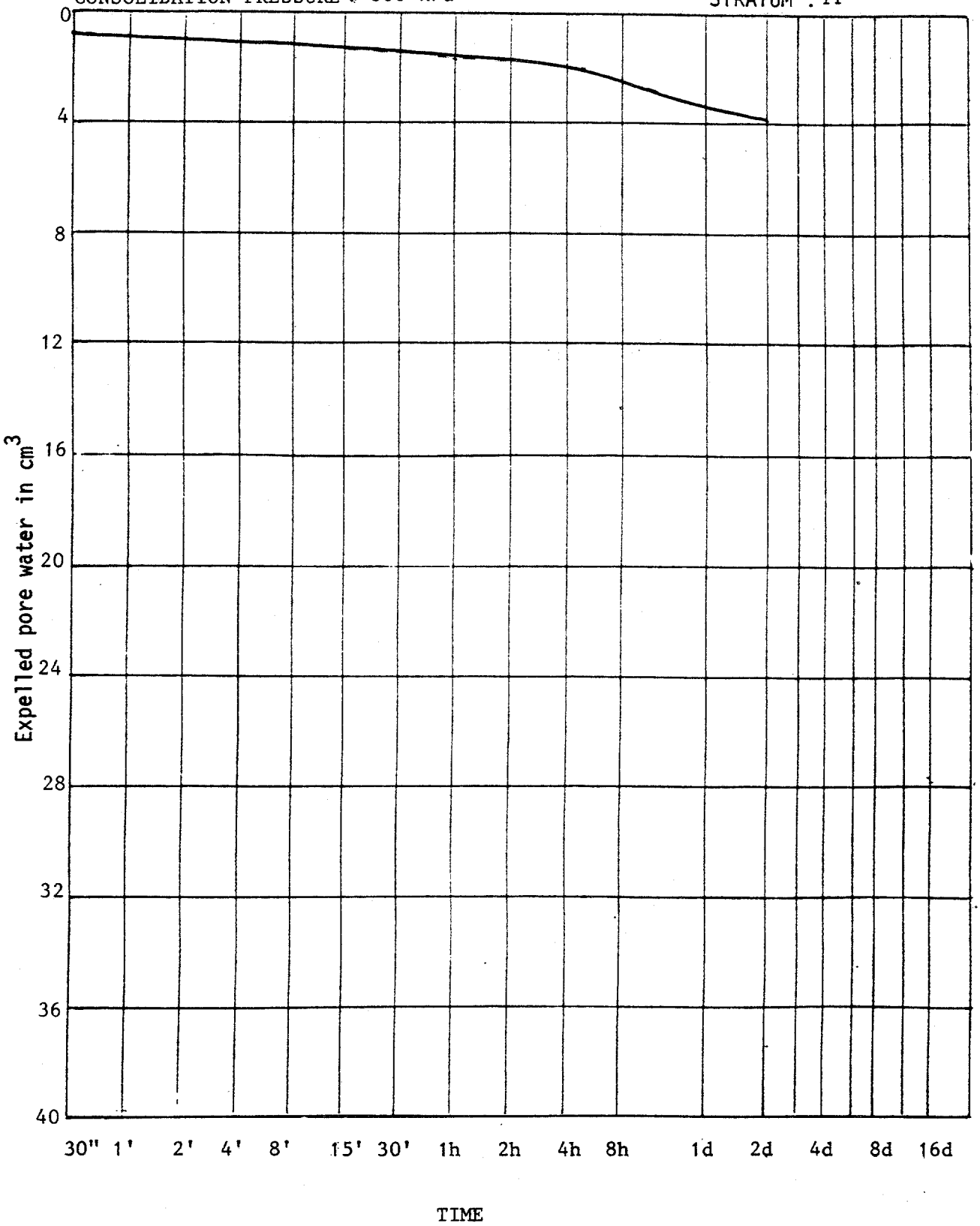

CNRD 13-2 TENSION PILE STUDY

CONSOLIDATION DIAGRAM

DET NORSKE VERITAS
Geotechnical Laboratory

Drawn by	Scale
Approved	Date
	Fig.No. 16

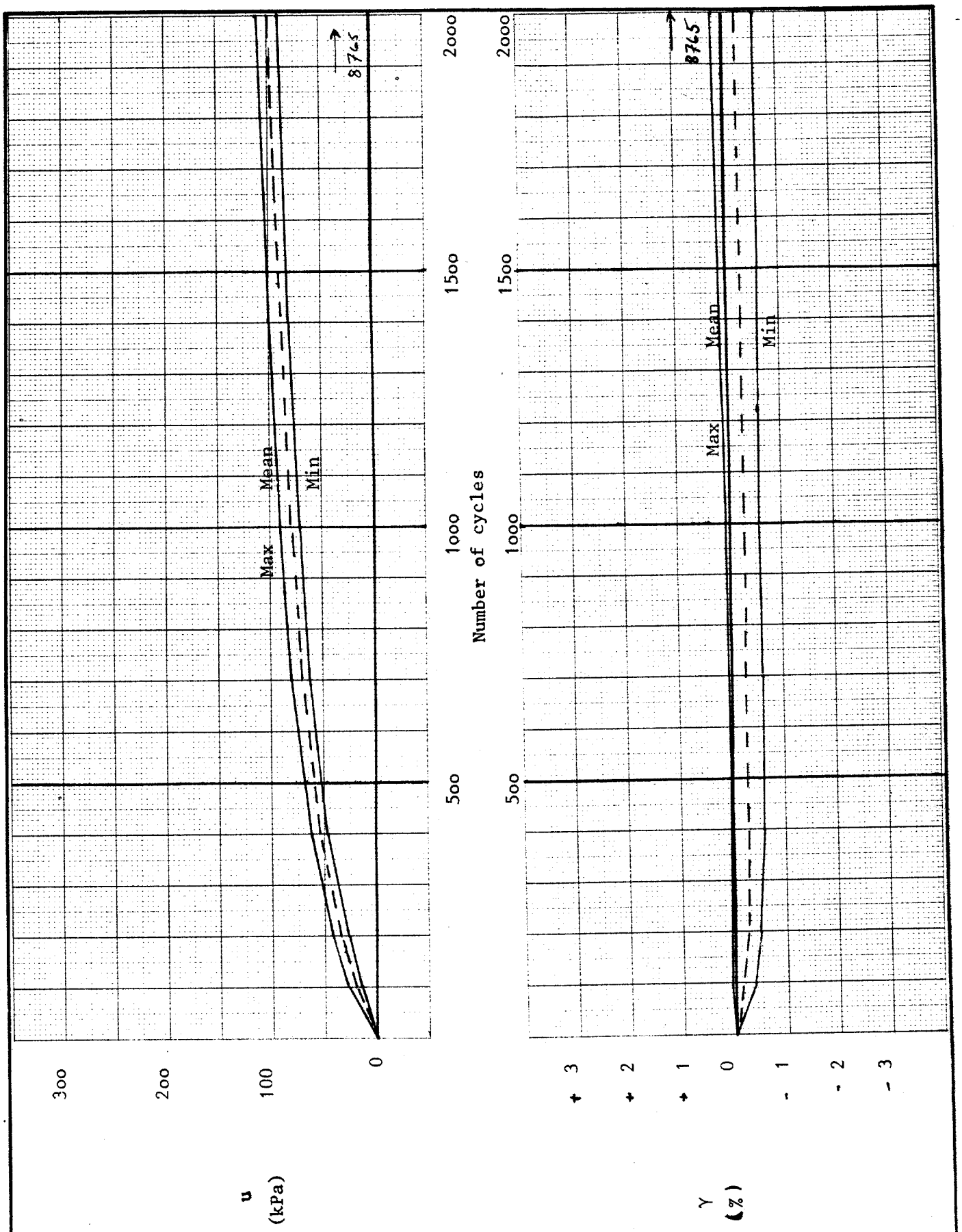

SAMPLE NO: T4 $\tau_c/S_u = \pm 0.45$

CYCLIC TRIAXIAL TEST

DET NORSKE VERITAS
Geotechnical Laboratory

Proj. No.	
Scale	
Drawn by	Date
Approved	Fig. No. 17

SAMPLE NO.: T4
τ_{stat} : 0
τ_{cyclic} : ± 45 kPa

CNRD 13-2 TENSION PILE STUDY

CYCLIC TRIAXIAL TEST, STRESS VS STRAIN, DIRECT PLOT

DET NORSKE VERITAS
Geotechnical Laboratory

Scale	
Drawn by	Date
Approved	Fig. No. 18

TEST No. : T 4

STRATUM : II

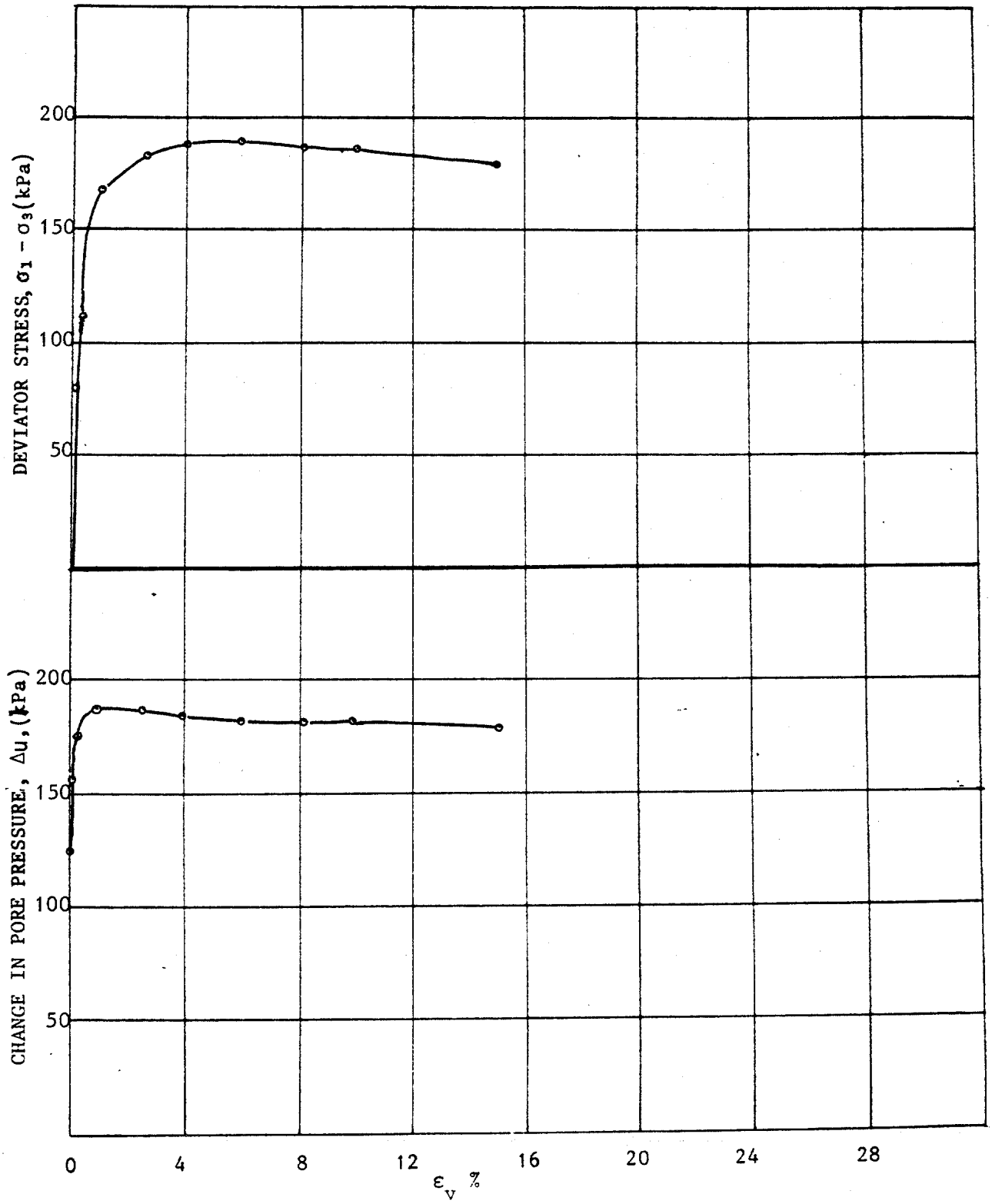

CNRD 13-2 TENSION PILE STUDY

STANDARD TRIAXIAL TEST, CIU, AFTER CYCLIC LOADING

DET NORSKE VERITAS
Geotechnical Laboratory

Scale	
Drawn by	Date
Approved	Fig. No. 19

REMOULDED SAMPLE

FROM PILE TEST 13

CONSOLIDATION PRESSURE : 300 kPa

TEST No.: T4

STRATUM : II

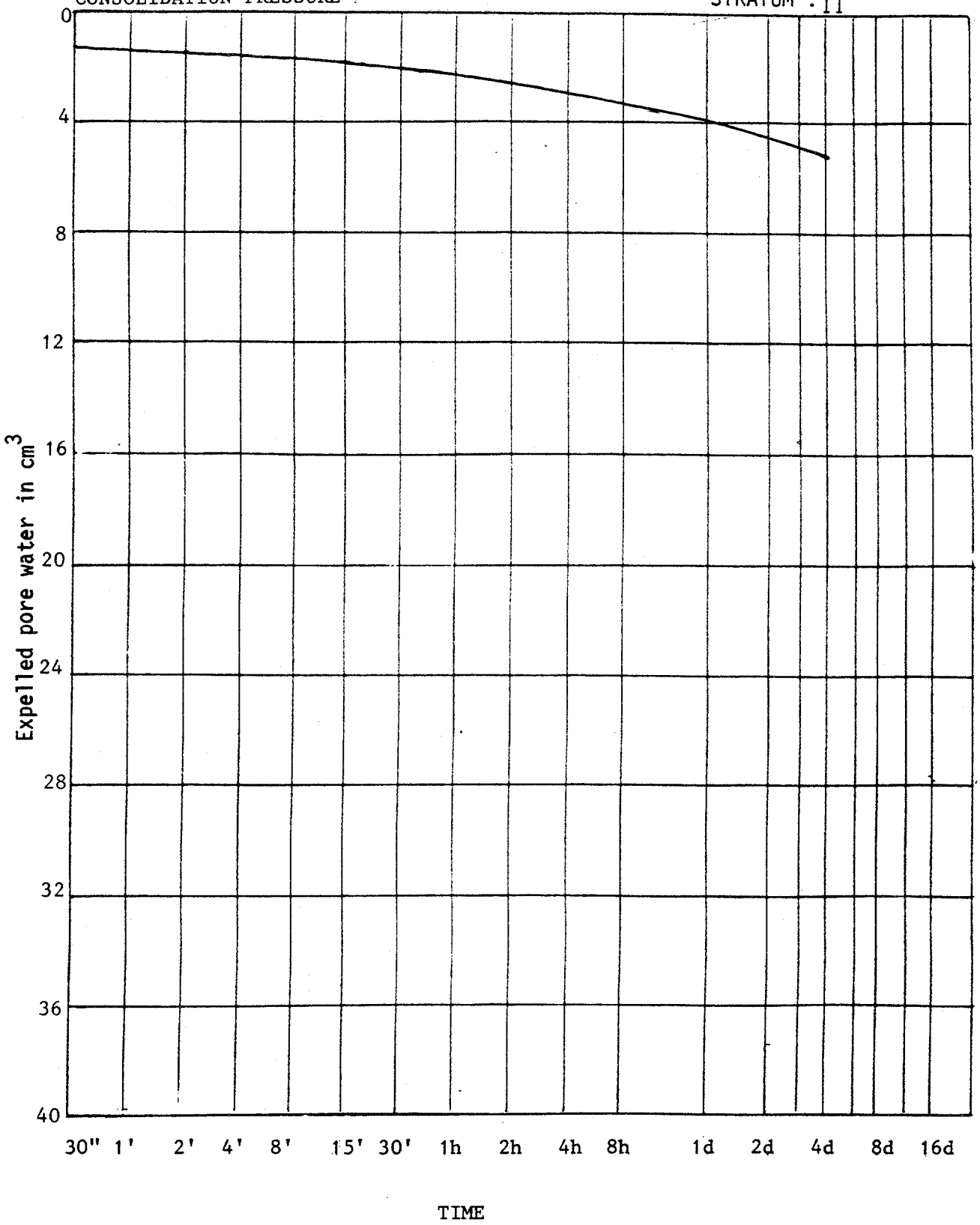

CNRD 13-2 TENSION PILE STUDY

CONSOLIDATION DIAGRAM

DET NORSKE VERITAS Geotechnical Laboratory	Drawn by	Scale
	Approved	Date
		Fig.No. 20

TEST No. : T 5

STRATUM : II

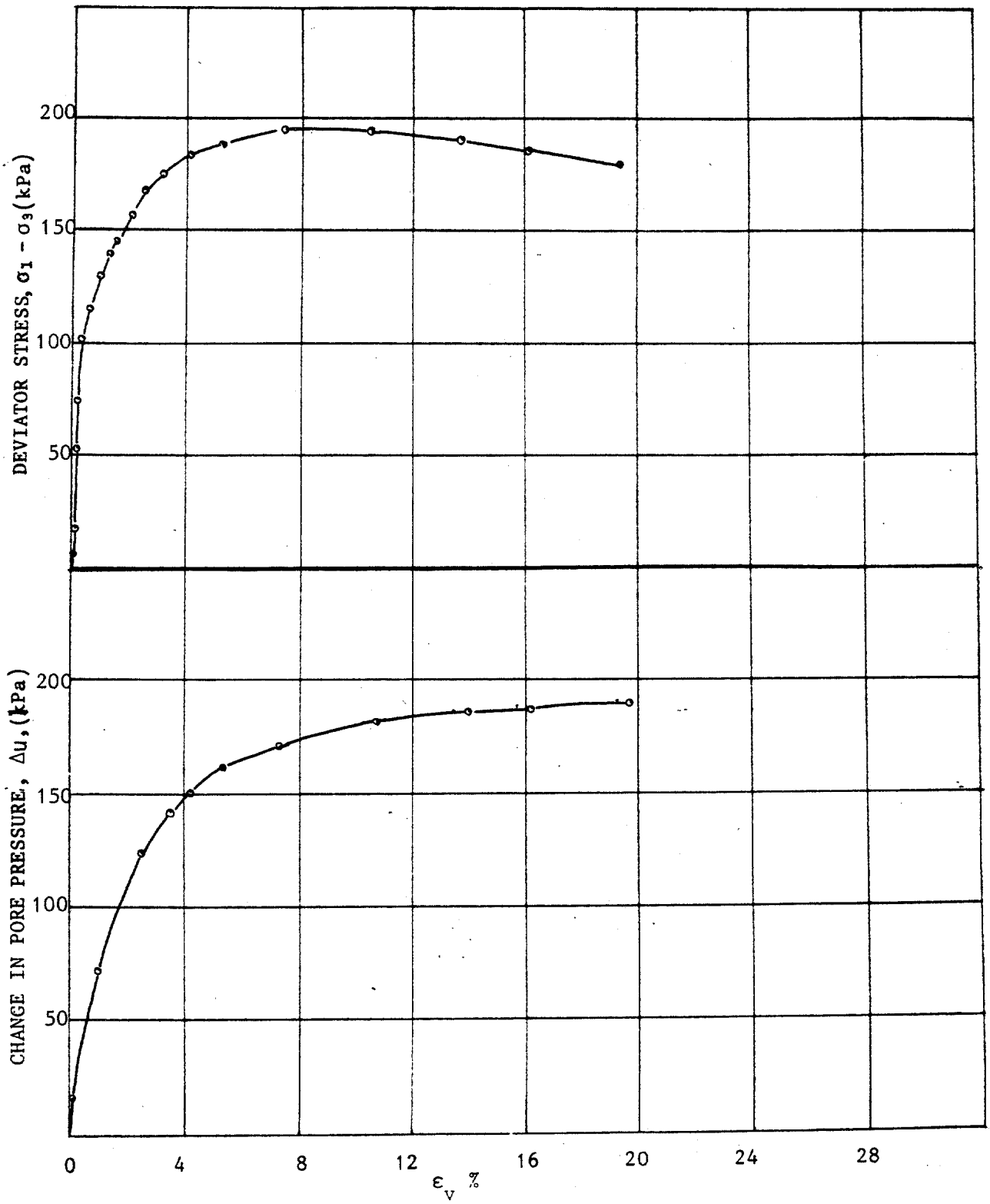

CNRD 13-2 TENSION PILE STUDY

STANDARD TRIAXIAL TEST, CIU

DET NORSKE VERITAS
Geotechnical Laboratory

Scale	
Drawn by	Date
Approved	Fig. No. 21

UNDISTURBED SAMPLE

S - 87, DEPTH 45.9 m

CONSOLIDATION PRESSURE = 300 kPa

TEST No.: T 5

STRATUM : II

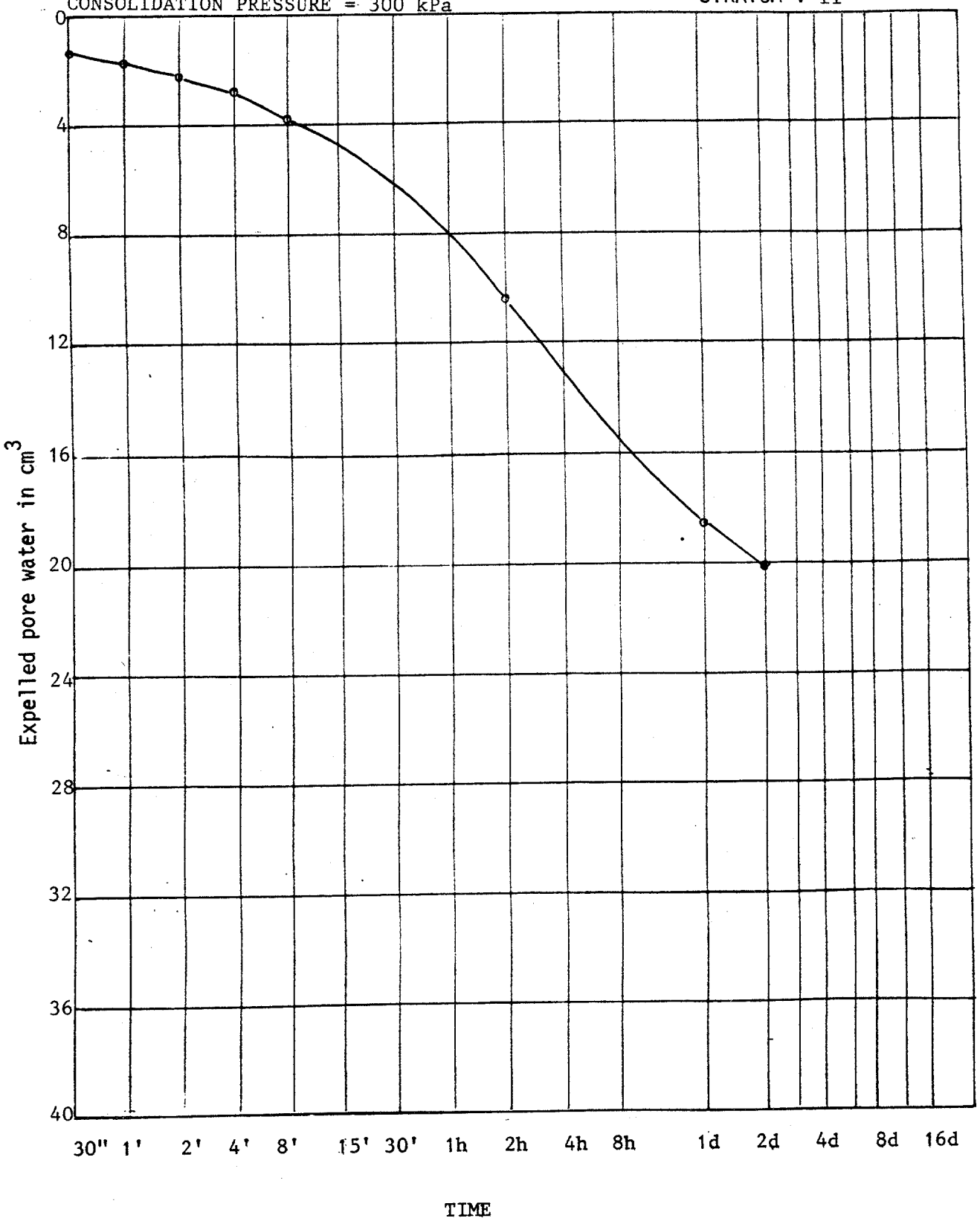

CNRD 13-2 TENSION PILE STUDY

CONSOLIDATION DIAGRAM

DET NORSKE VERITAS
Geotechnical Laboratory

Scale	
Drawn by	Date
Approved	Fig. No. 22

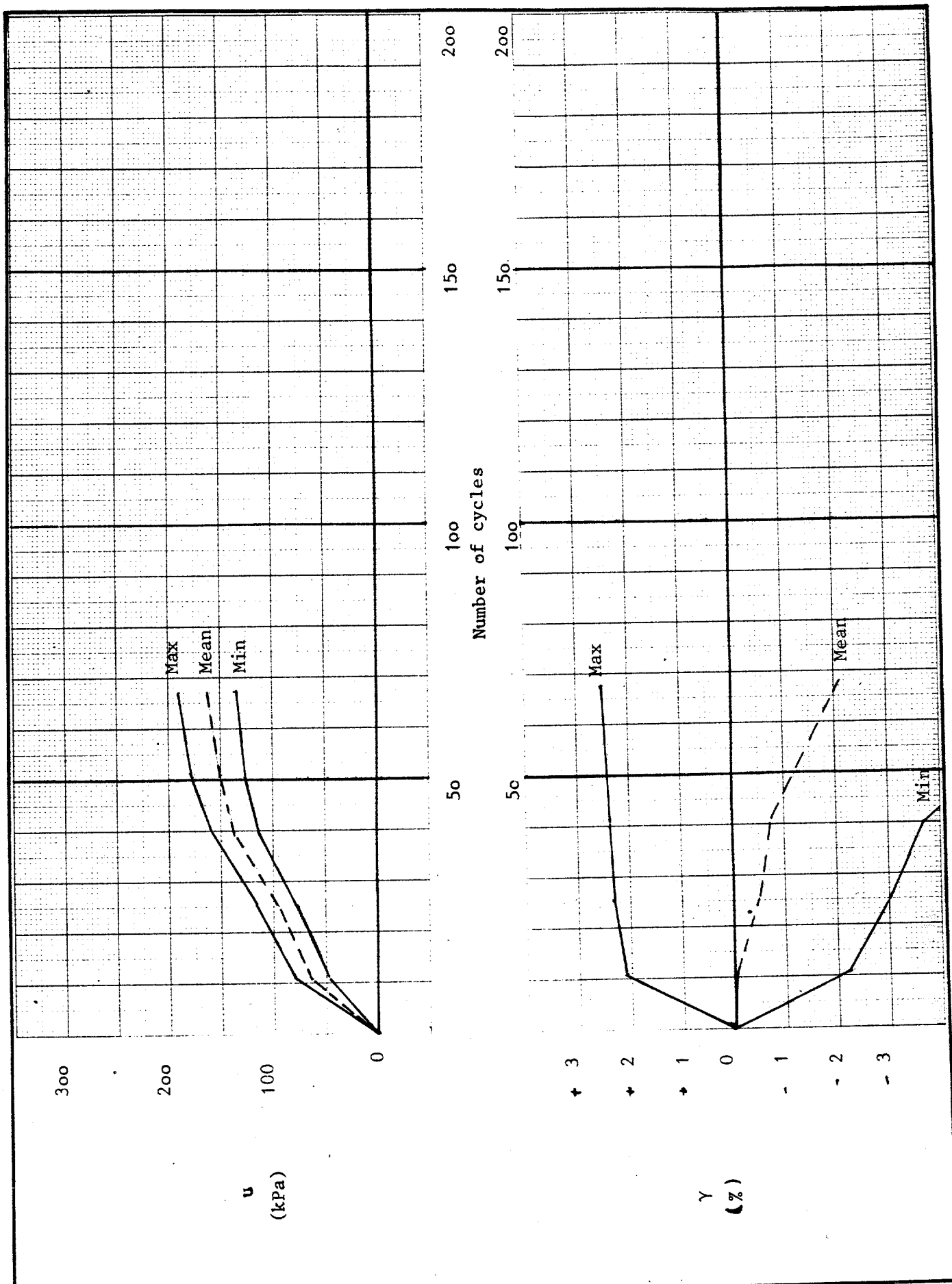

SAMPLE NO: T6 $\tau_c/S_u = \pm 0.77$

CYCLIC TRIAXIAL TEST

DET NORSKE VERITAS
Geotechnical Laboratory

Proj.No.	
Scale	
Drawn by	Date
Approved	Fig.No. 23

SAMPLE NO.: T6
τ_{stat} : 0
τ_{cyclic}: $\pm$ 77kPa

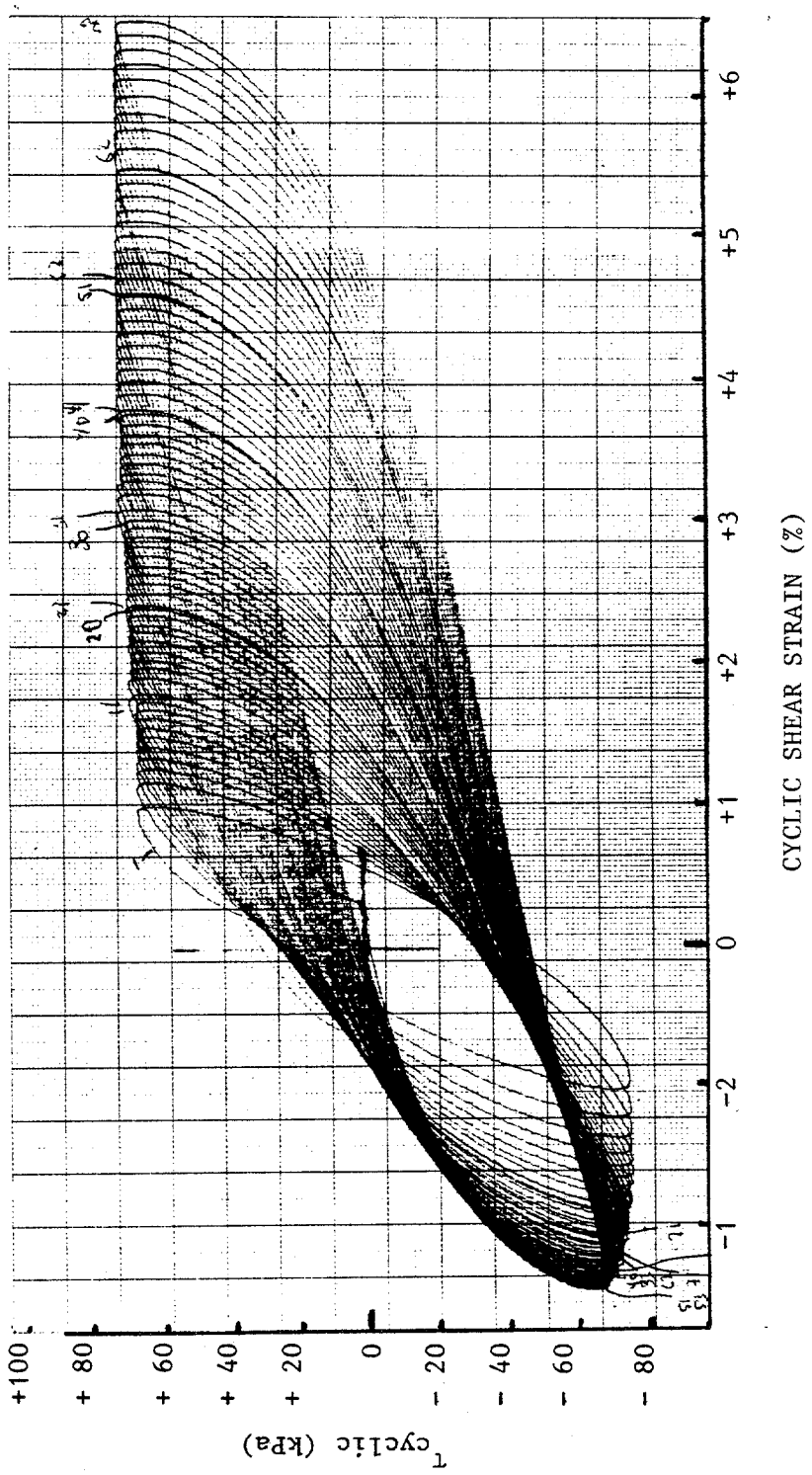

CNRD 13-2 TENSION PILE STUDY

CYCLIC TRIAXIAL TEST, STRESS VS STRAIN, DIRECT PLOT

DET NORSKE VERITAS
Geotechnical Laboratory

Scale	
Drawn by	Date
Approved	Fig. No. 24

TEST No. : T 6

STRATUM : II

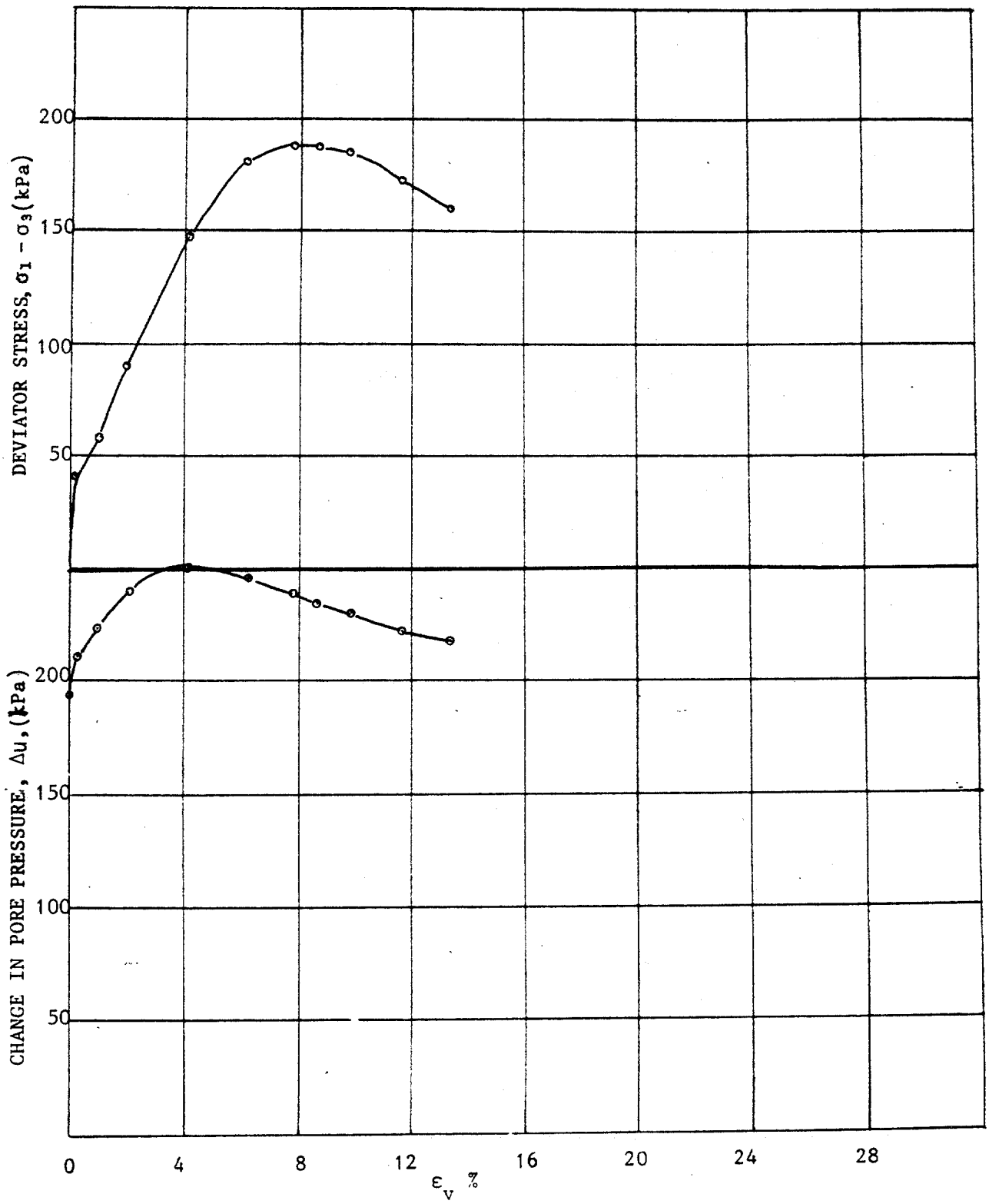

CNRD 13-2 TENSION PILE STUDY

STANDARD TRIAXIAL TEST, CIU, AFTER CYCLIC LOADING

DET NORSKE VERITAS Geotechnical Laboratory	Drawn by	Scale
	Approved	Date
		Fig. No. 25

UNDISTURBED SAMPLE

S -87 , DEPTH 46.1 m

CONSOLIDATION PRESSURE = 300 kPa

TEST No.: T 6

STRATUM : II

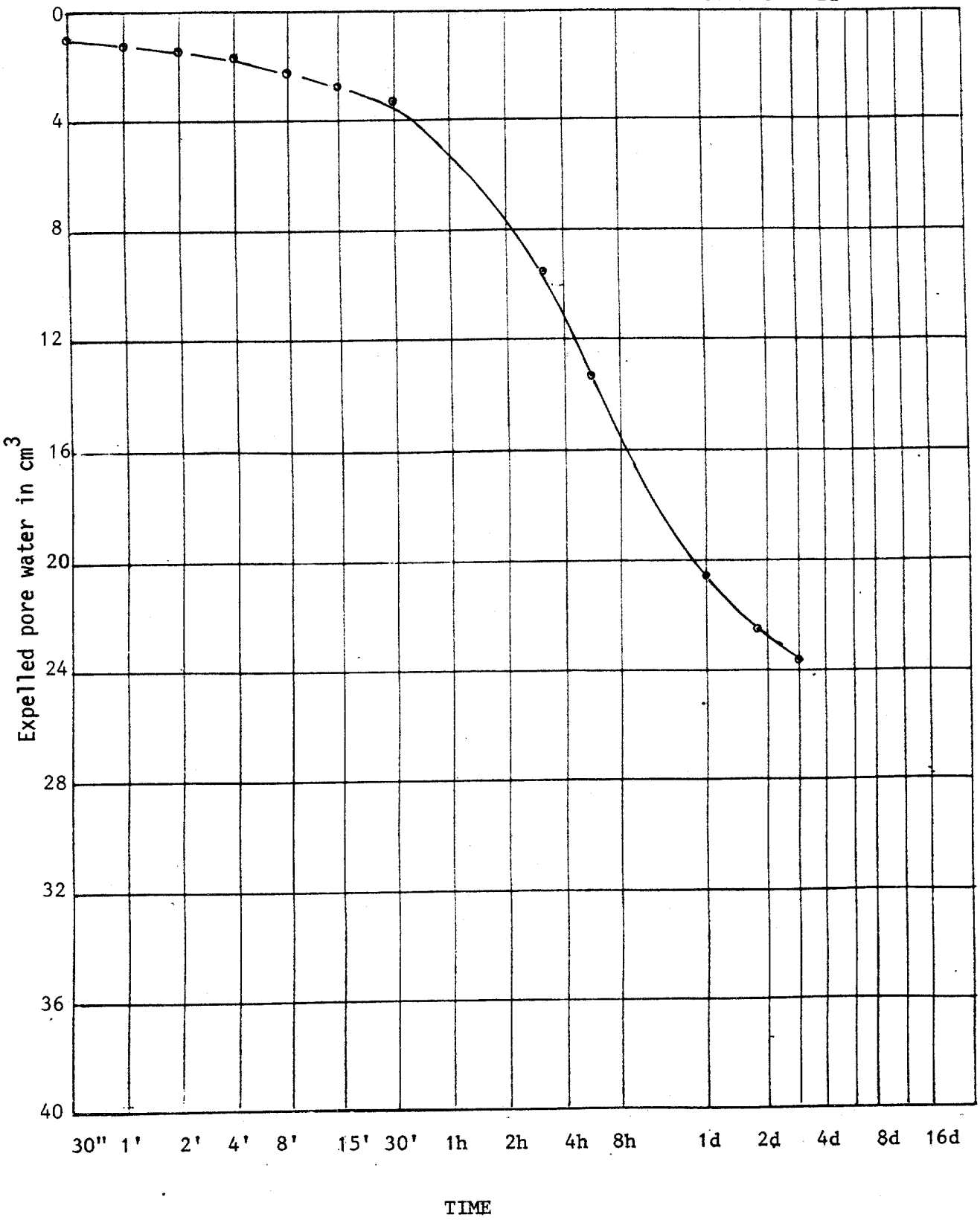

CNRD 13-2 TENSION PILE STUDY

CONSOLIDATION DIAGRAM

DET NORSKE VERITAS
Geotechnical Laboratory

Scale	
Drawn by	Date
Approved	Fig.No. 26

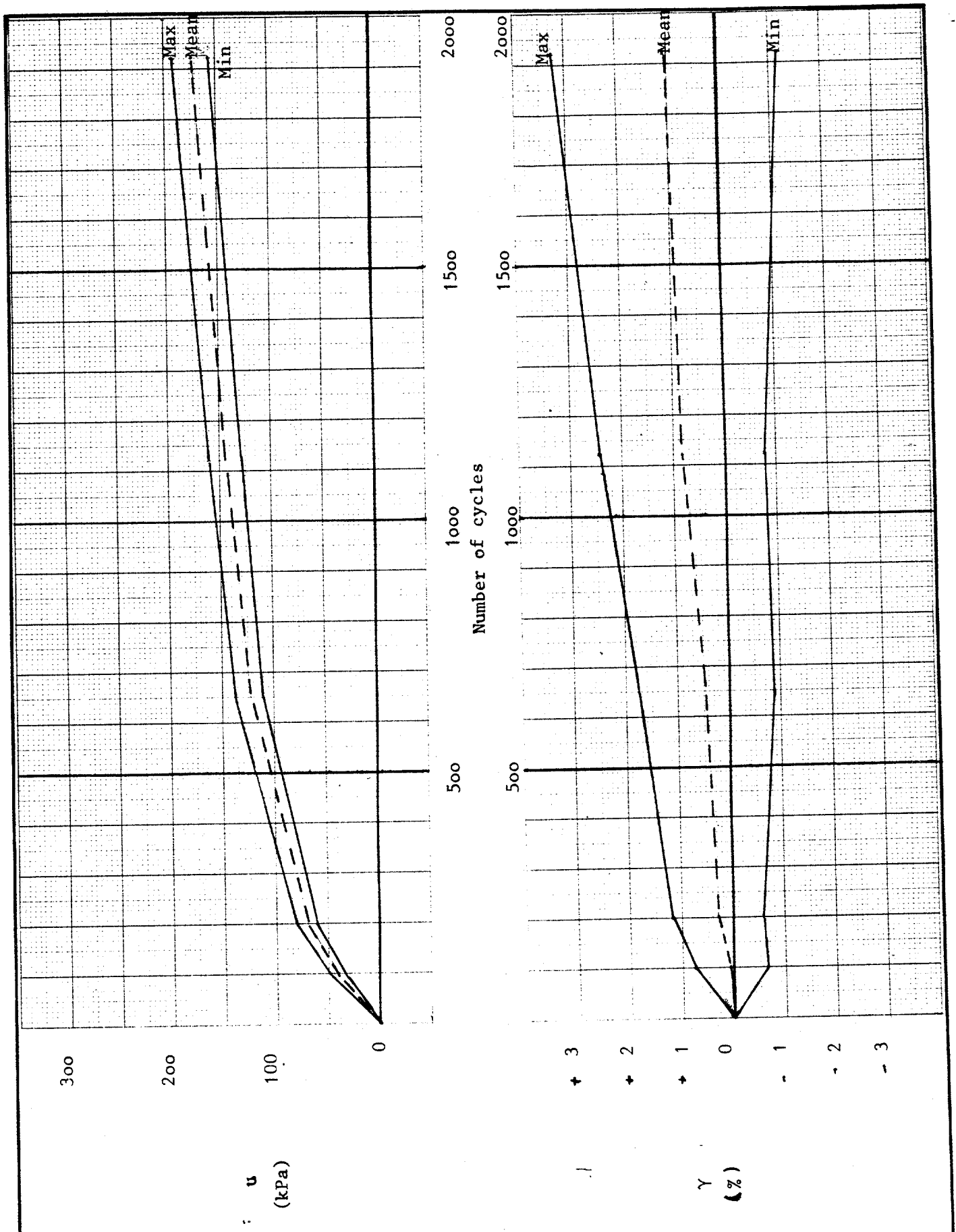

SAMPLE NO: T7 τ_c/S_u = ± 0.54

CYCLIC TRIAXIAL TEST

DET NORSKE VERITAS
Geotechnical Laboratory

Proj.No.	
Scale	
Drawn by	Date
Approved	Fig.No. 27

SAMPLE NO.: T7

τ_{stat} : 0

τ_{cyclic} : ± 54 kPa

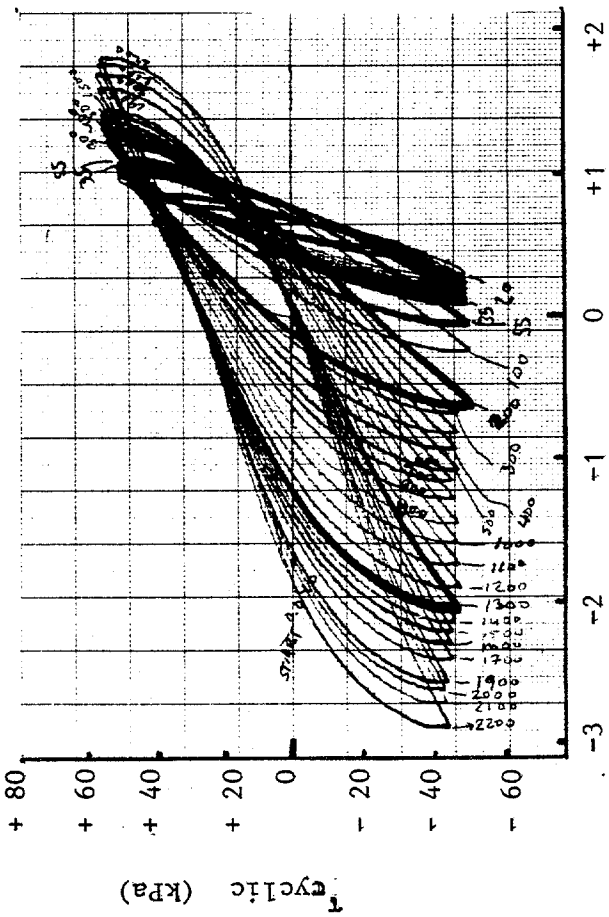

CNRD 13-2 TENSION PILE STUDY

CYCLIC TRIAXIAL TEST, STRESS VS STRAIN, DIRECT PLOT

DET NORSKE VERITAS
Geotechnical Laboratory

Scale	
Drawn by	Date
Approved	Fig. No. 28

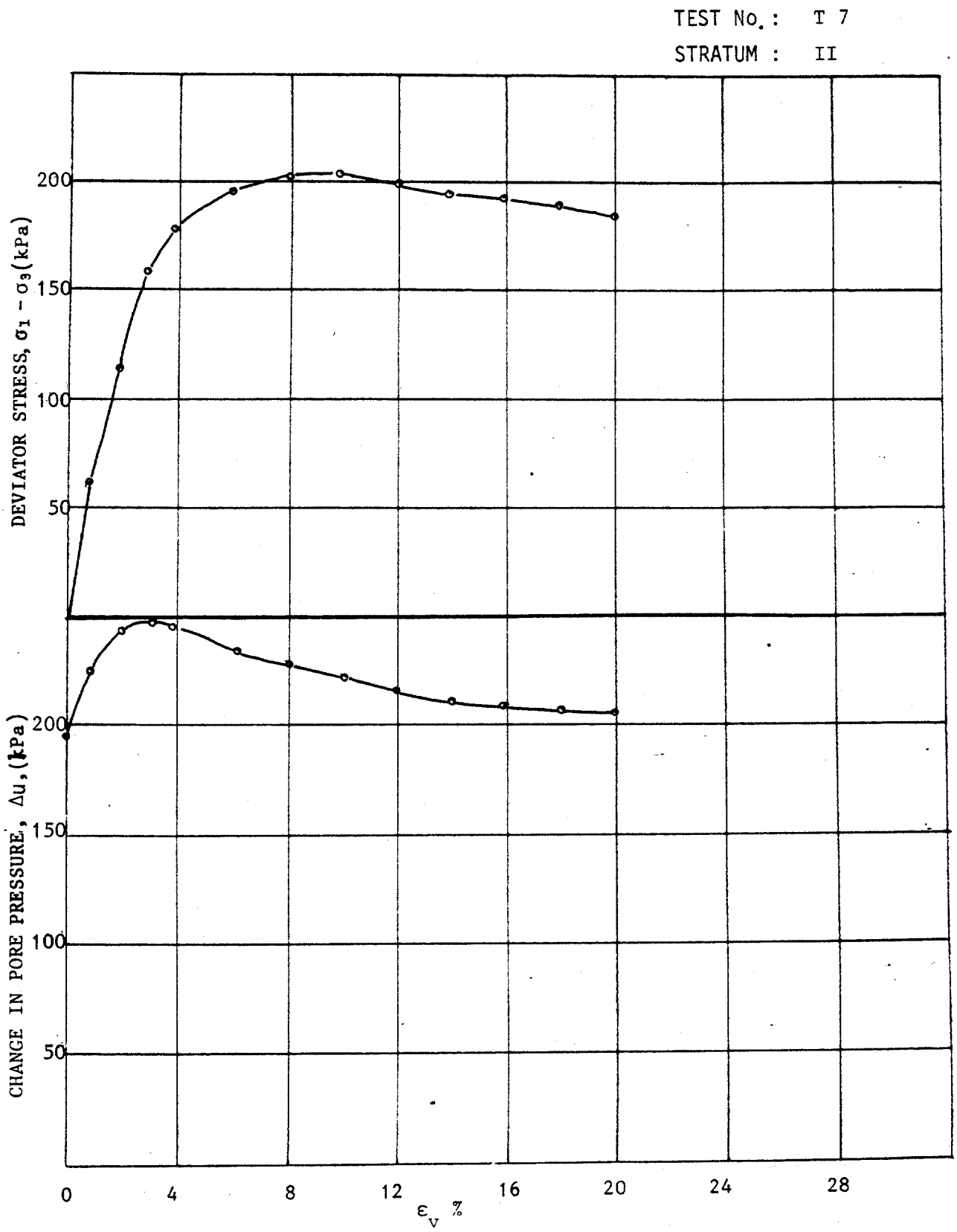

CNRD 13-2 TENSION PILE STUDY

STANDARD TRIAXIAL TEST, CIU, AFTER CYCLIC LOADING

DET NORSKE VERITAS Geotechnical Laboratory	Drawn by	Scale
	Approved	Date
		Fig. No. 29

UNDISTURBED SAMPLE

S - 87, DEPTH 46.2 m

CONSOLIDATION PRESSURE = 300 kPa

TEST No.: T 7

STRATUM : II

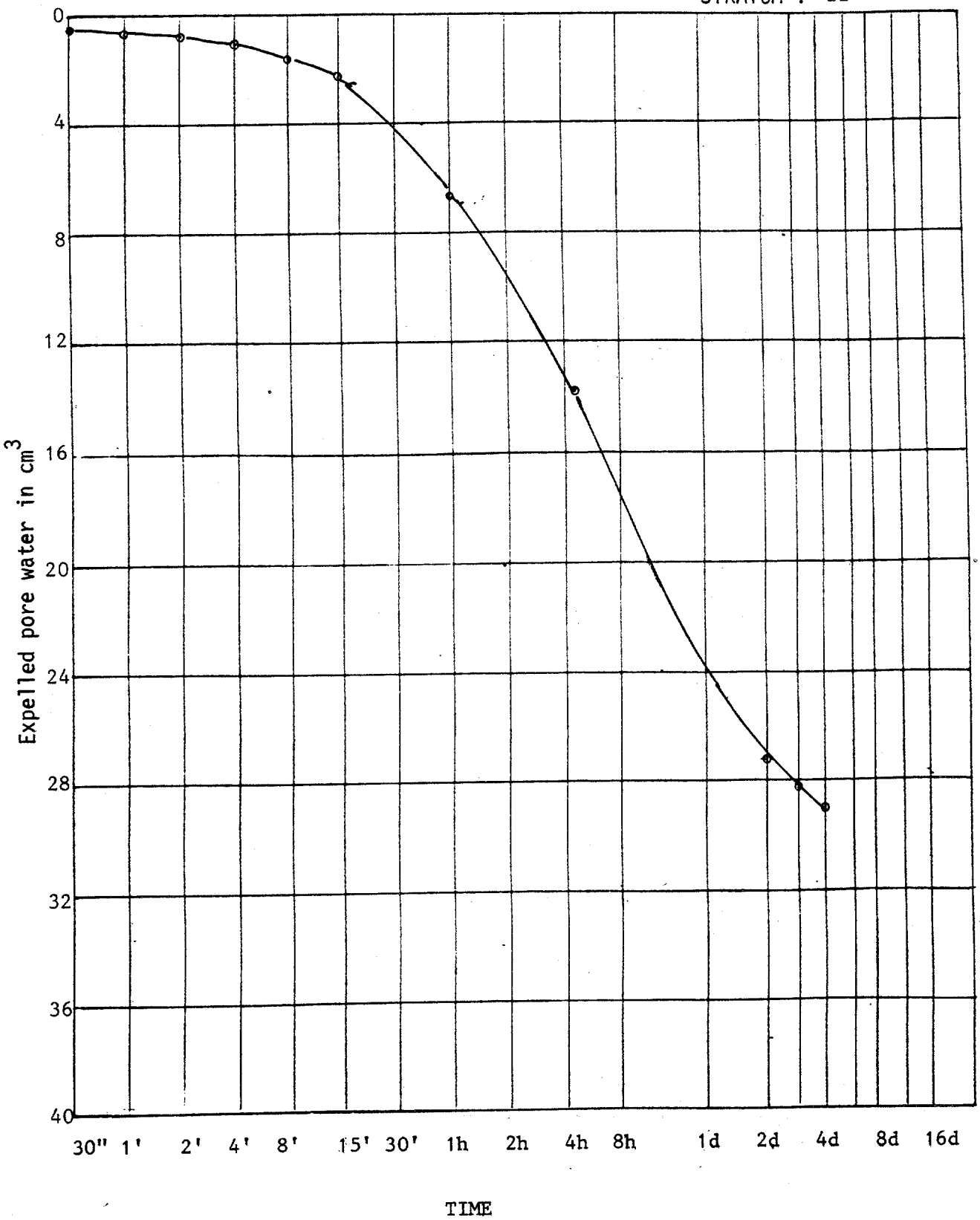

CNRD 13-2 TENSION PILE STUDY

CONSOLIDATION DIAGRAM

DET NORSKE VERITAS
Geotechnical Laboratory

Scale	
Drawn by	Date
Approved	Fig. No. 30

TEST No. : T 8

STRATUM : III

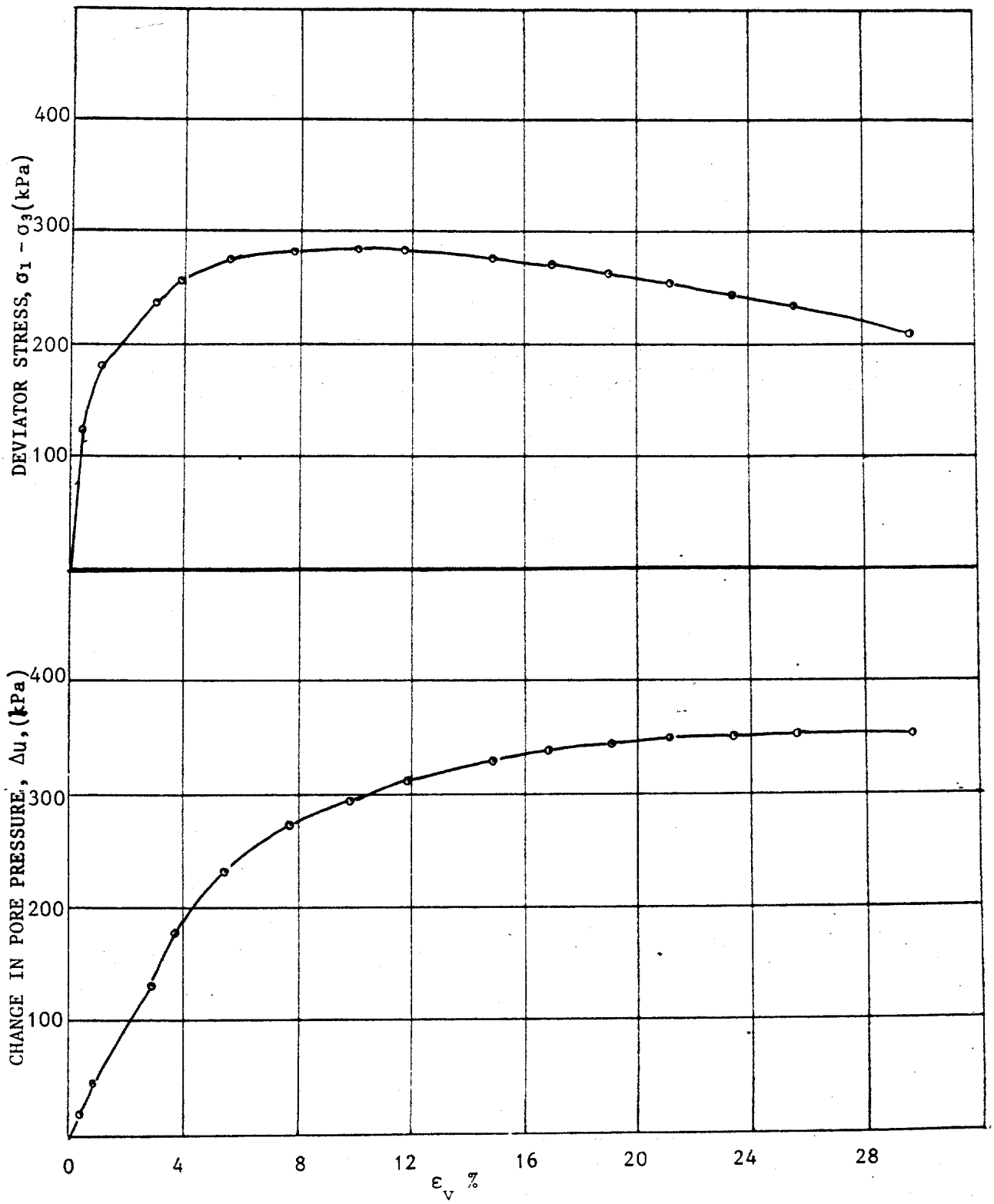

CNRD 13-2 TENSION PILE STUDY

STANDARD TRIAXIAL TEST, CIU

DET NORSKE VERITAS
Geotechnical Laboratory

Scale	
Drawn by	Date
Approved	Fig. No. 31

UNDISTURBED SAMPLE

S -64 , DEPTH 67.3 m

CONSOLIDATION PRESSURE = 500 kPa

TEST No.: T 8

STRATUM : III

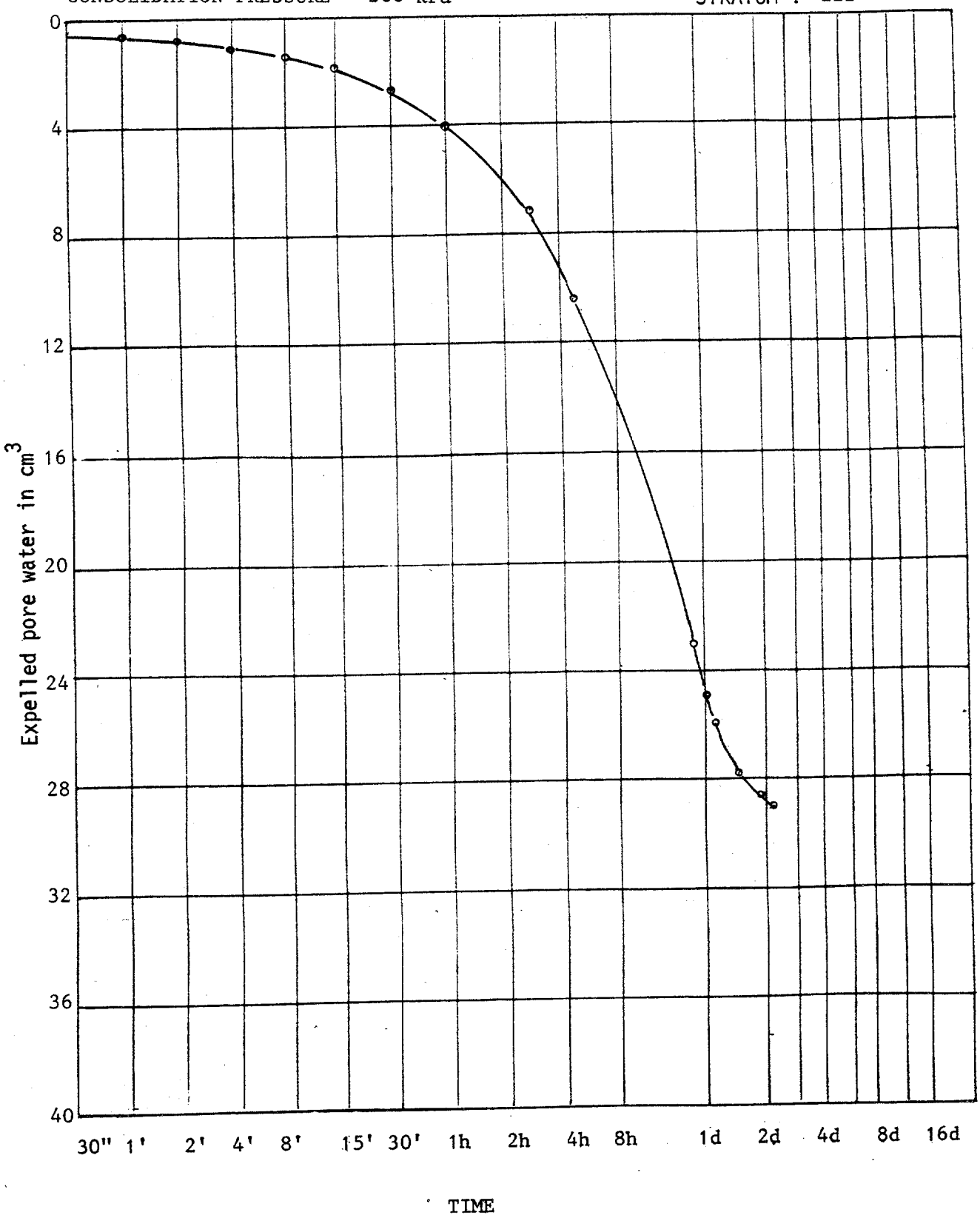

CNRD 13-2 TENSION PILE STUDY

CONSOLIDATION DIAGRAM

DET NORSKE VERITAS
Geotechnical Laboratory

Drawn by	Scale
Approved	Date
	Fig.No. 32

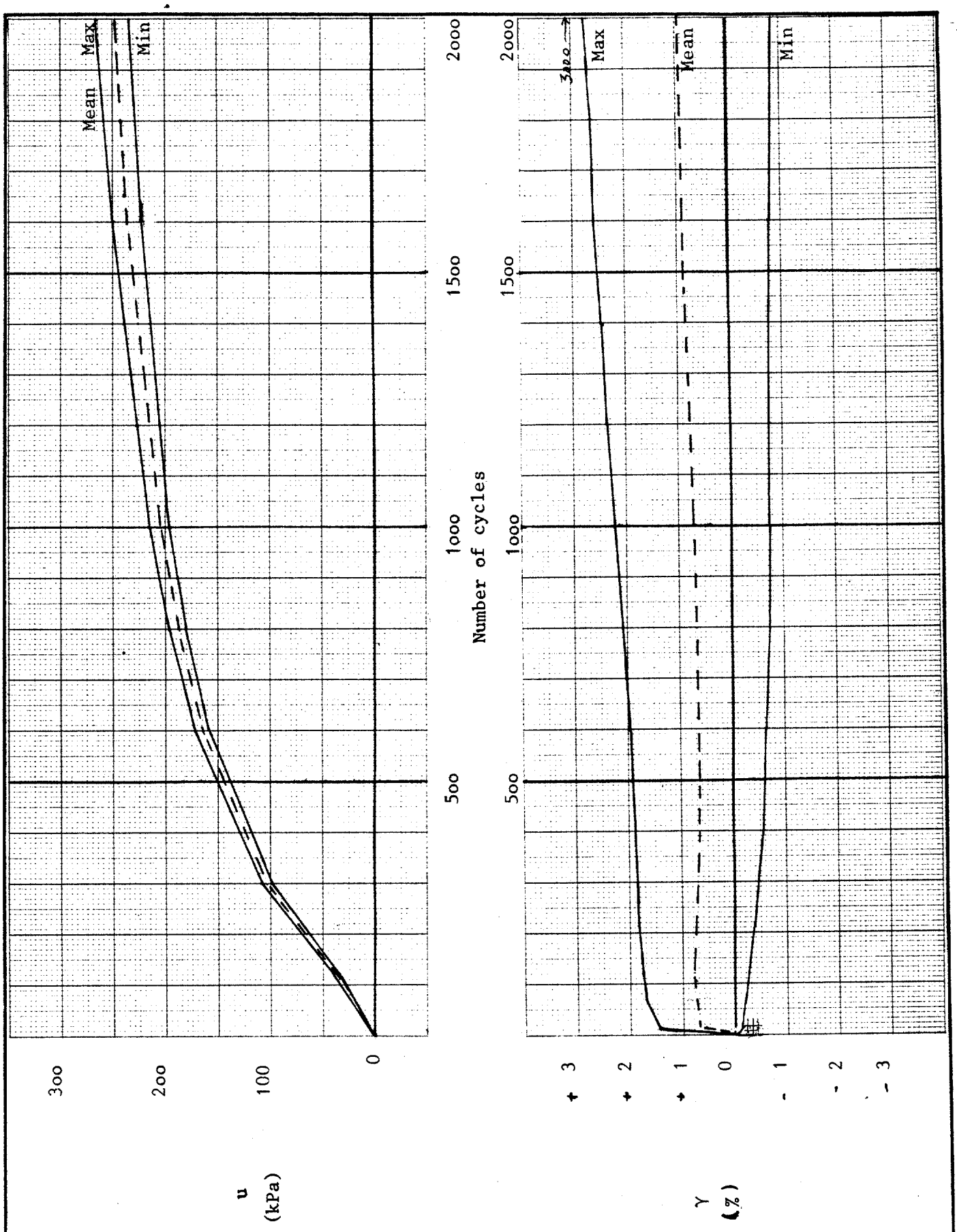

SAMPLE NO: T9 $\tau_c/S_u = \pm 0.55$

CYCLIC TRIAXIAL TEST

DET NORSKE VERITAS
Geotechnical Laboratory

Proj.No.	
Scale	
Drawn by	Date
Approved	Fig.No. 33

SAMPLE NO.: T9
τ_{stat} : 0
τ_{cyclic} : $\pm$ 84 kPa

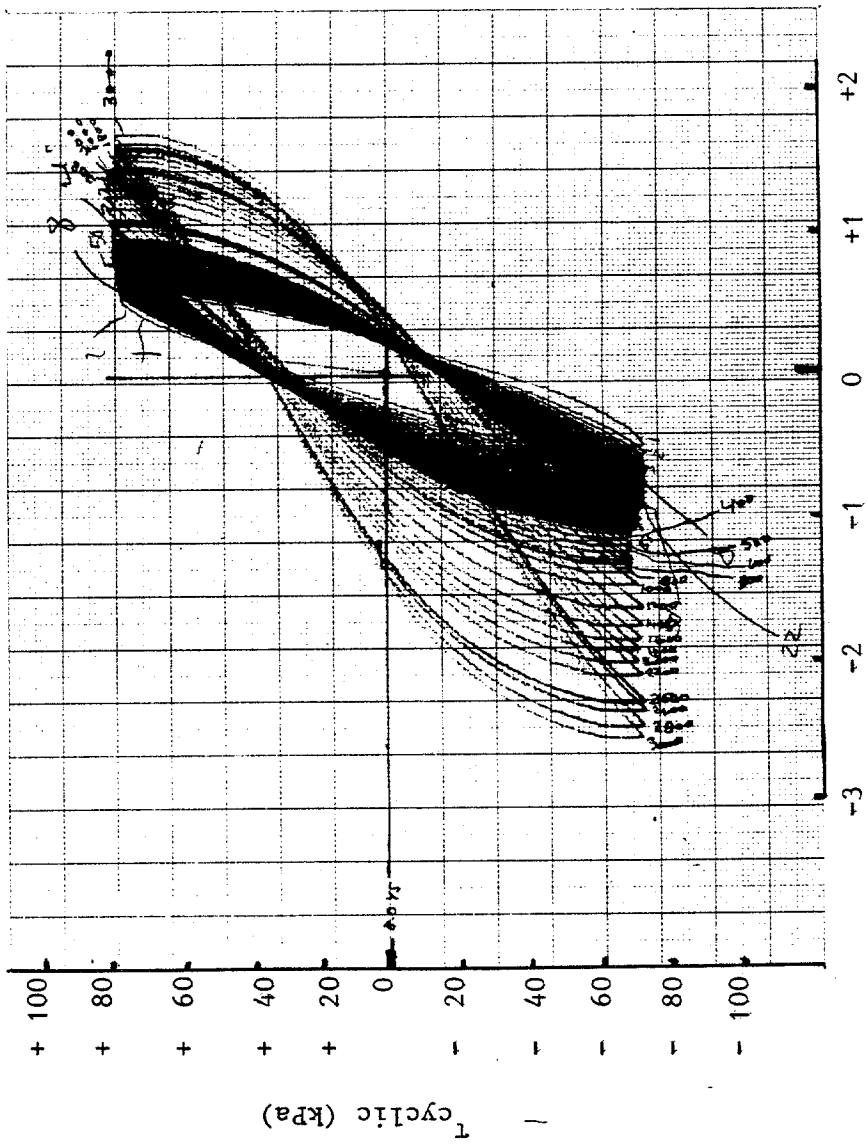

CNRD 13-2 TENSION PILE STUDY

CYCLIC TRIAXIAL TEST, STRESS VS STRAIN, DIRECT PLOT

DET NORSKE VERITAS
Geotechnical Laboratory

Scale	
Drawn by	Date
Approved	Fig. No. 34

TEST No. : T 9

STRATUM : III

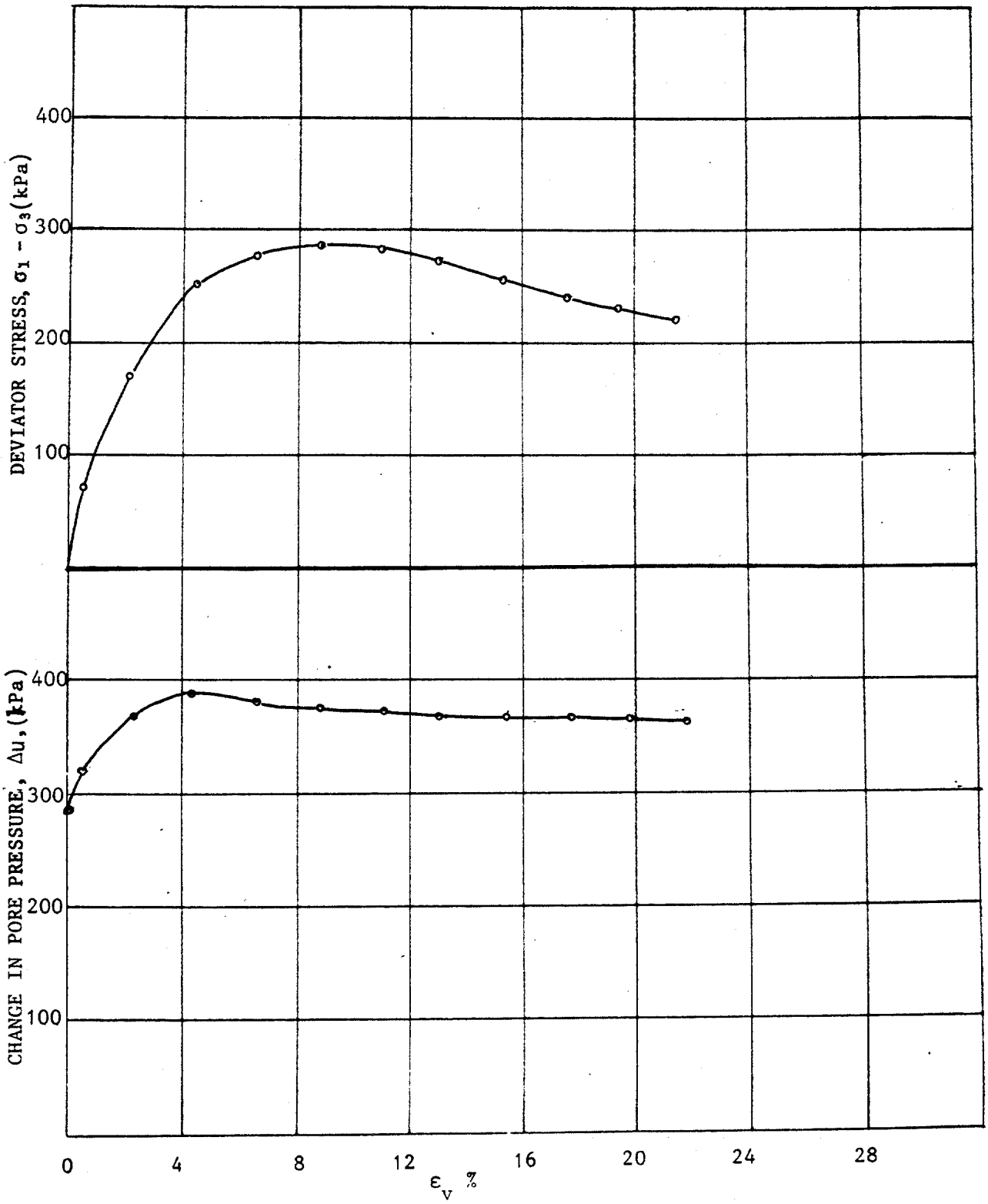

CNRD 13-2 TENSION PILE STUDY

STANDARD TRIAXIAL TEST, CIU, AFTER CYCLIC LOADING

DET NORSKE VERITAS Geotechnical Laboratory	Drawn by	Scale
	Approved	Date
		Fig. No. 35

UNDISTURBED SAMPLE

S - 64 , DEPTH 67.4 m

CONSOLIDATION PRESSURE = 500 kPa

TEST No.: T 9

STRATUM : III

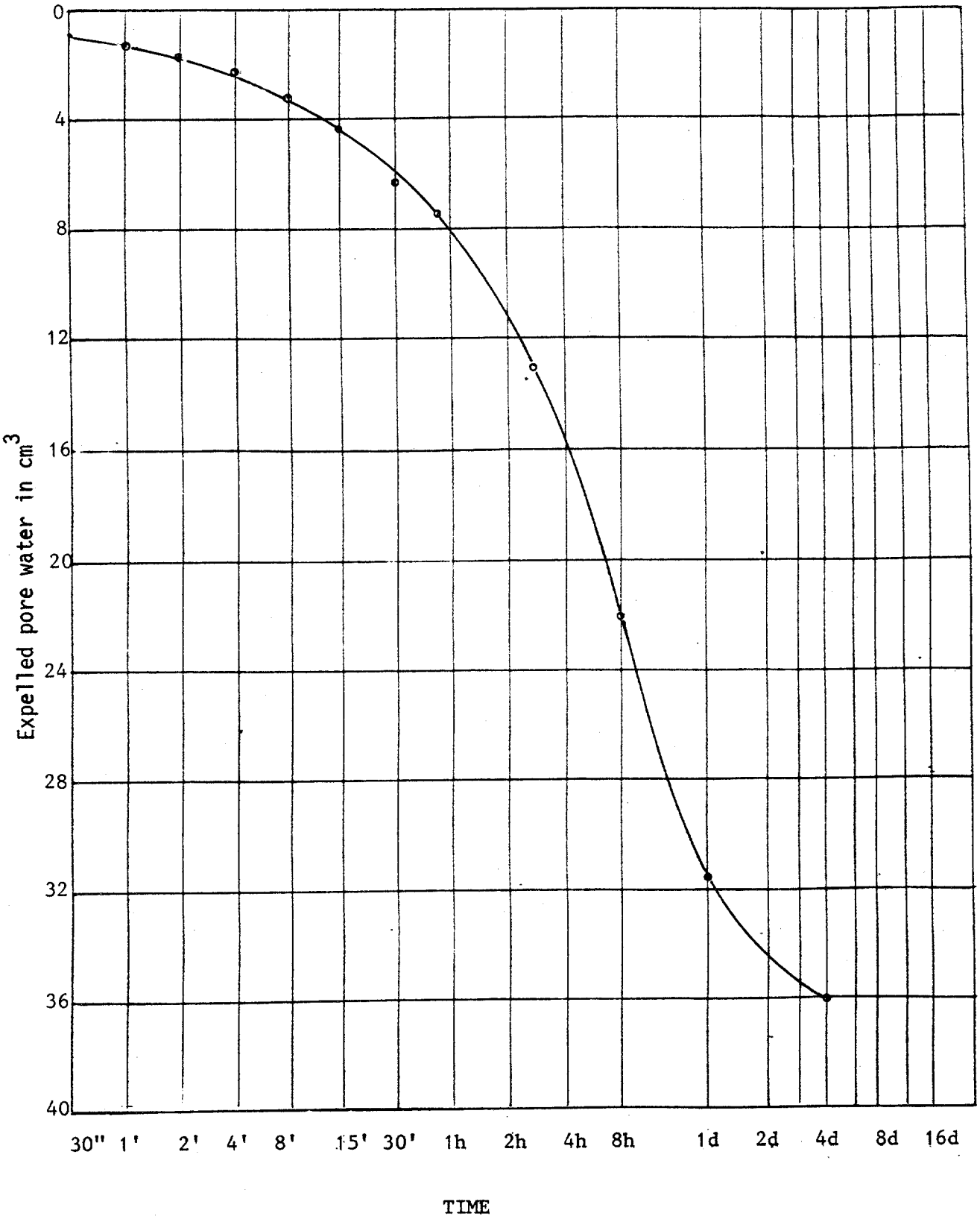

CNRD 13-2 TENSION PILE STUDY

CONSOLIDATION DIAGRAM

DET NORSKE VERITAS
Geotechnical Laboratory

Drawn by	Scale
Approved	Date
	Fig.No. 36

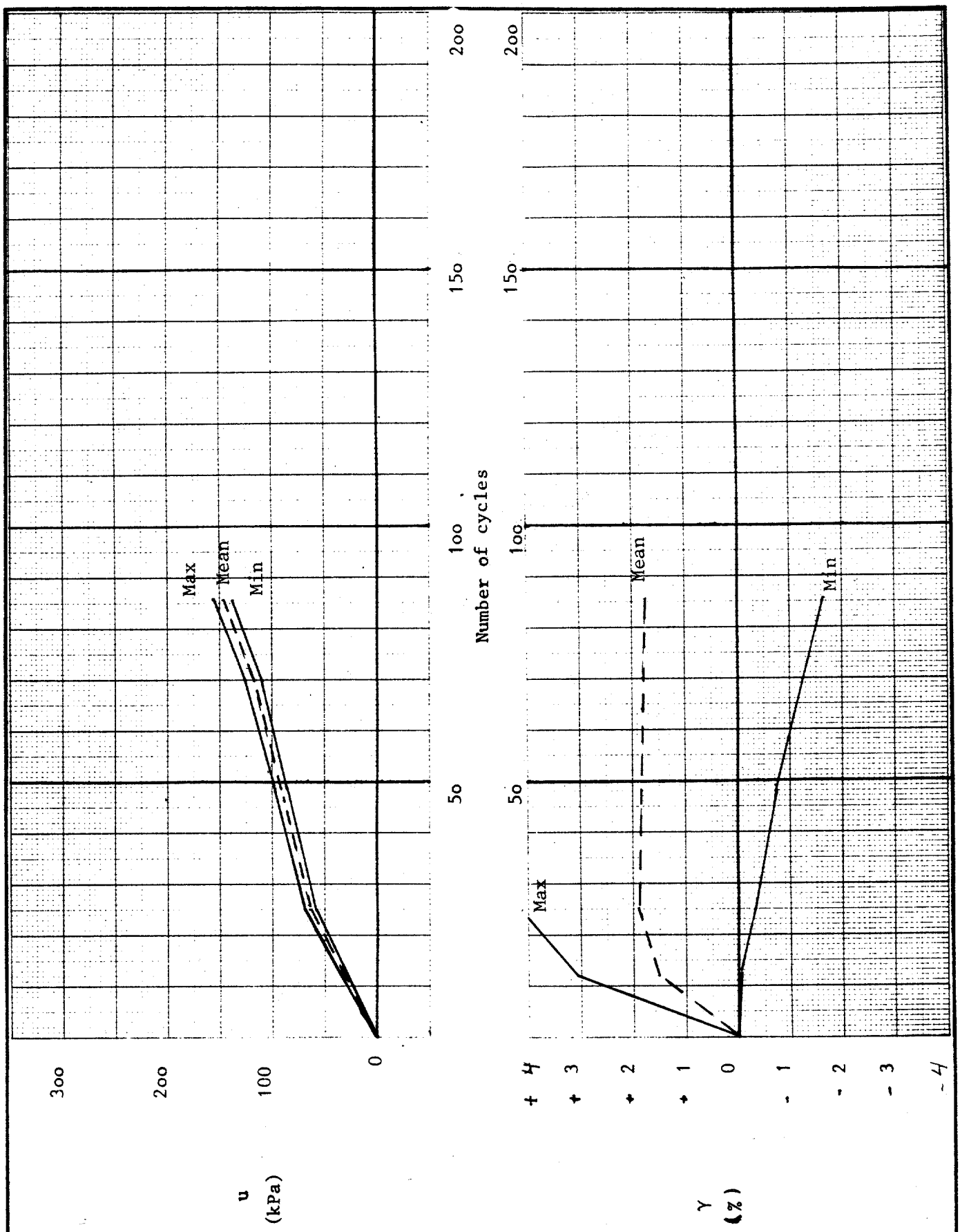

SAMPLE NO: T 10 $\tau_c/s_u = \pm 0.74$

CYCLIC TRIAXIAL TEST

DET NORSKE VERITAS
Geotechnical Laboratory

Proj.No.	
Scale	
Drawn by	Date
Approved	Fig.No. 37

SAMPLE NO.: T10

stat : 0

cyclic : ± 100 kPa

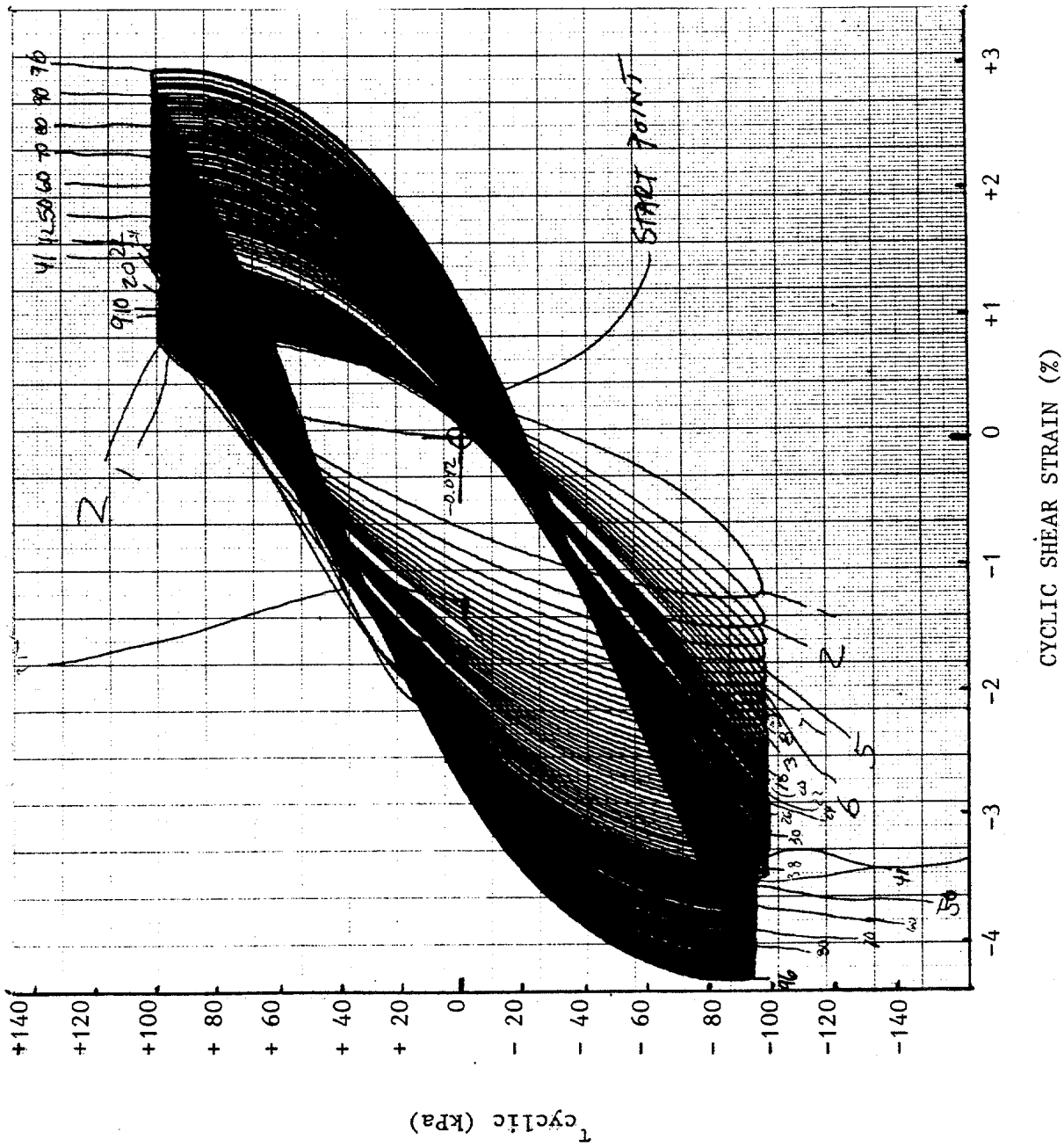

CNRD 13-2 TENSION PILE STUDY

CYCLIC TRIAXIAL TEST, STRESS VS STRAIN, DIRECT PLOT

DET NORSKE VERITAS
Geotechnical Laboratory

Scale	
Drawn by	Date
Approved	Fig. No. 38

TEST No. : T 10

STRATUM : III

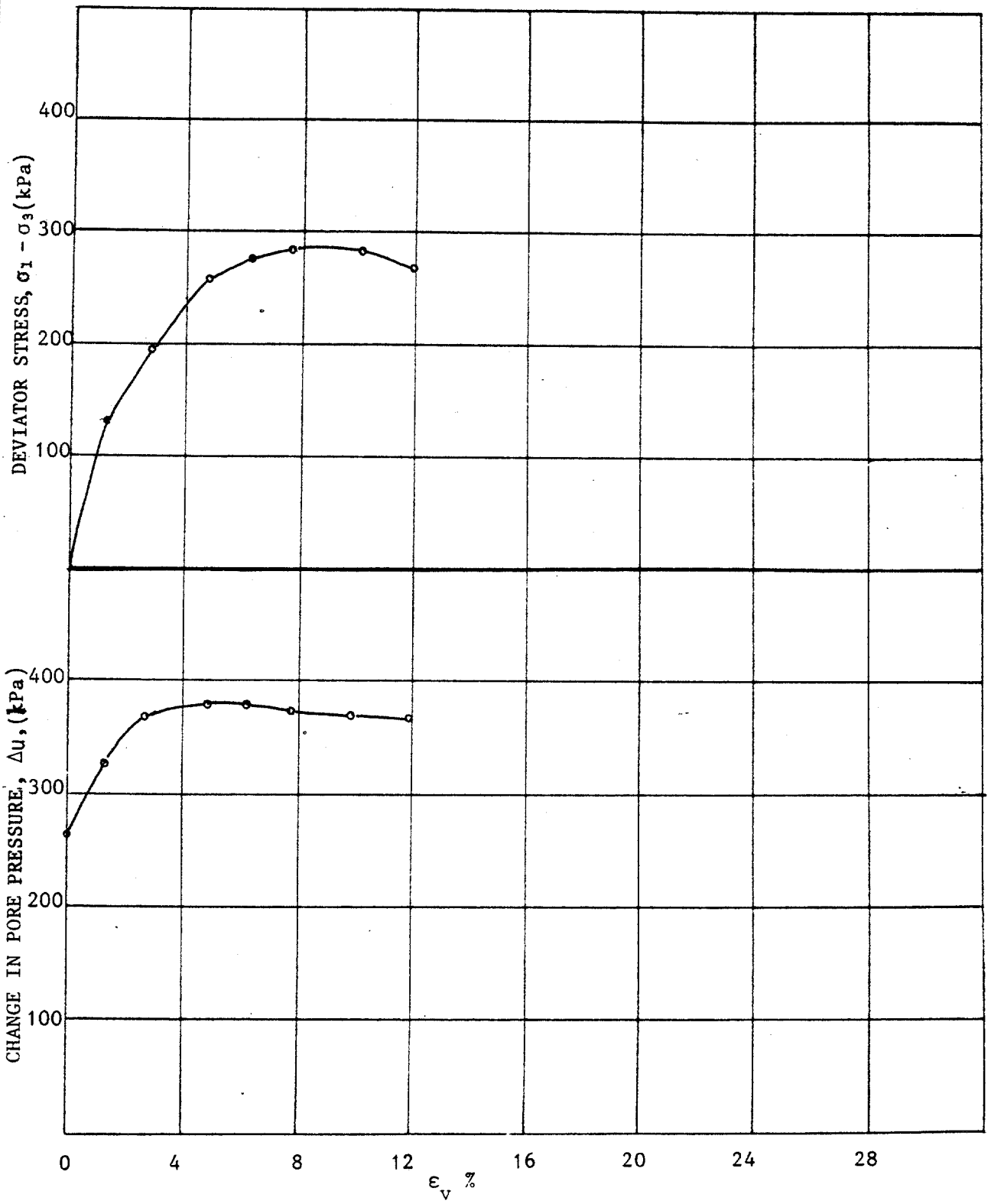

CNRD 13-2 TENSION PILE STUDY

STANDARD TRIAXIAL TEST, CIU, AFTER CYCLIC LOADING

DET NORSKE VERITAS Geotechnical Laboratory	Drawn by	Scale
	Approved	Date
		Fig. No. 39

UNDISTURBED, SAMPLE

S - 64 , DEPTH 67.6 m

CONSOLIDATION PRESSURE = 500 kPa

TEST No.: T 10

STRATUM : III

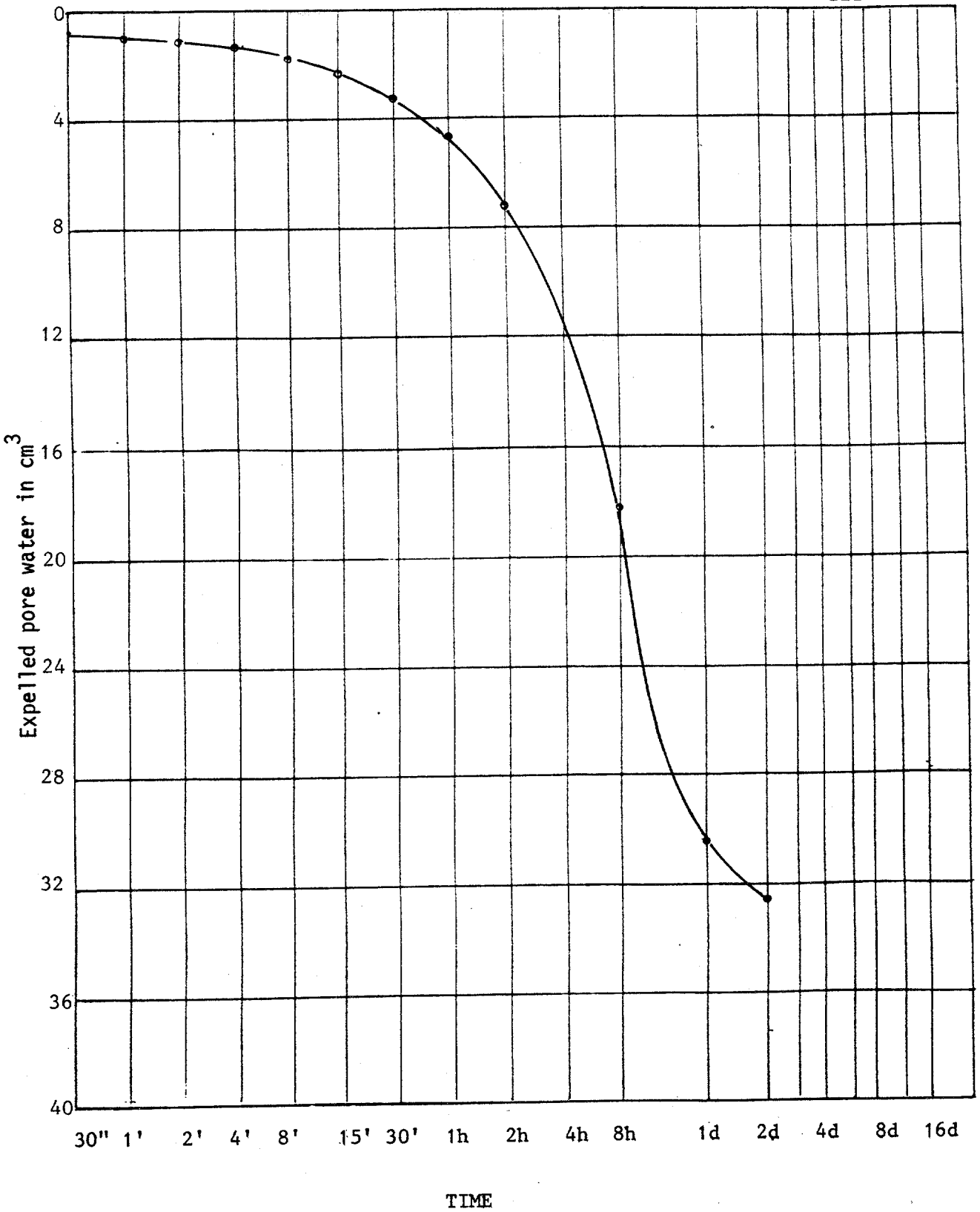

CNRD 13-2 TENSION PILE STUDY

CONSOLIDATION DIAGRAM

DET NORSKE VERITAS
Geotechnical Laboratory

Scale	
Drawn by	Date
Approved	Fig.No. 40

TEST No. : T 11

STRATUM : III

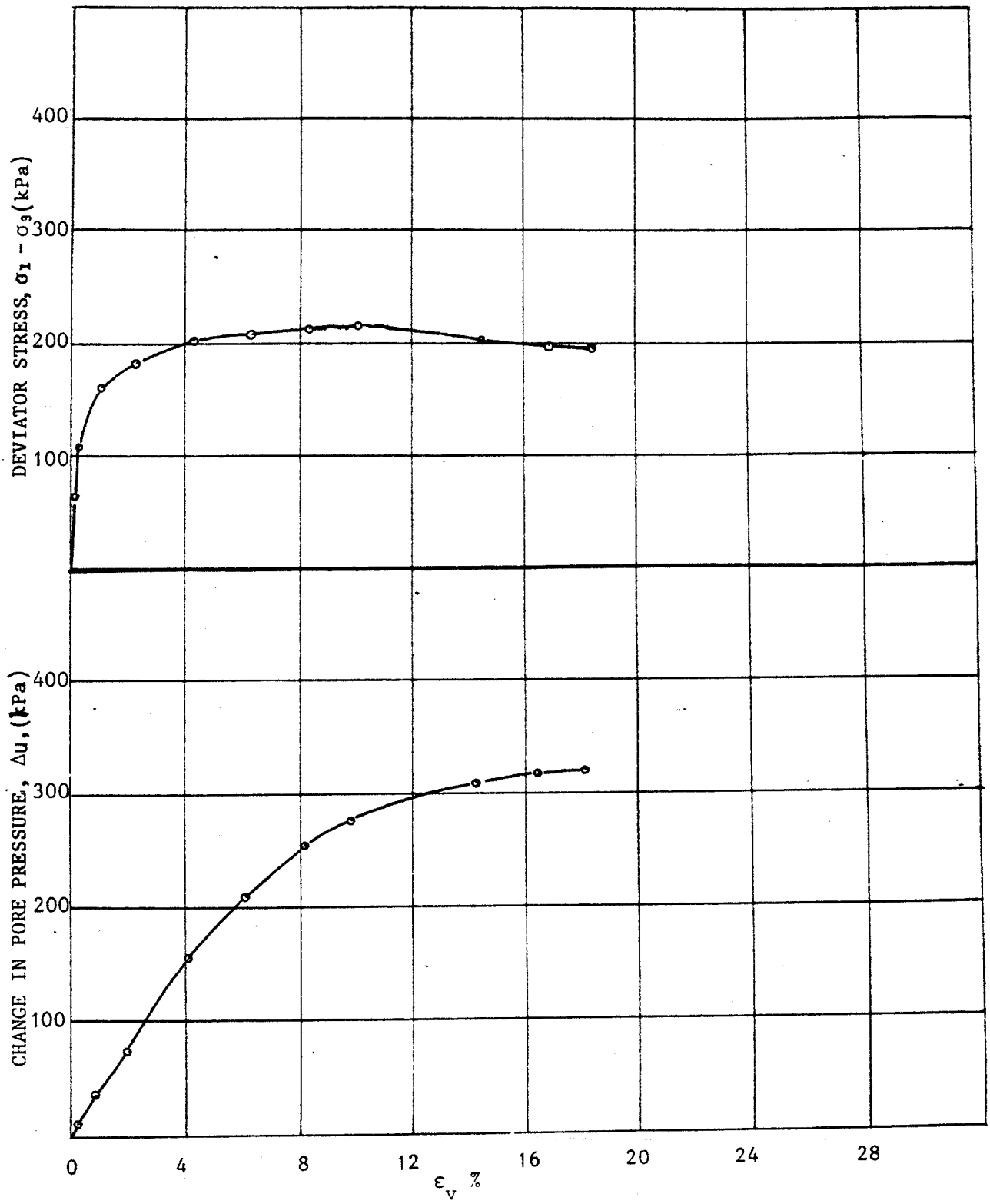

CNRD 13-2 TENSION PILE STUDY

STANDARD TRIAXIAL TEST, CIU

DET NORSKE VERITAS Geotechnical Laboratory	Drawn by	Scale
	Approved	Date
		Fig. No. 41

REMOULDED SAMPLE

FROM PILE TEST 14

CONSOLIDATION PRESSURE = 500 kPa

TEST No.: T 11

STRATUM : III

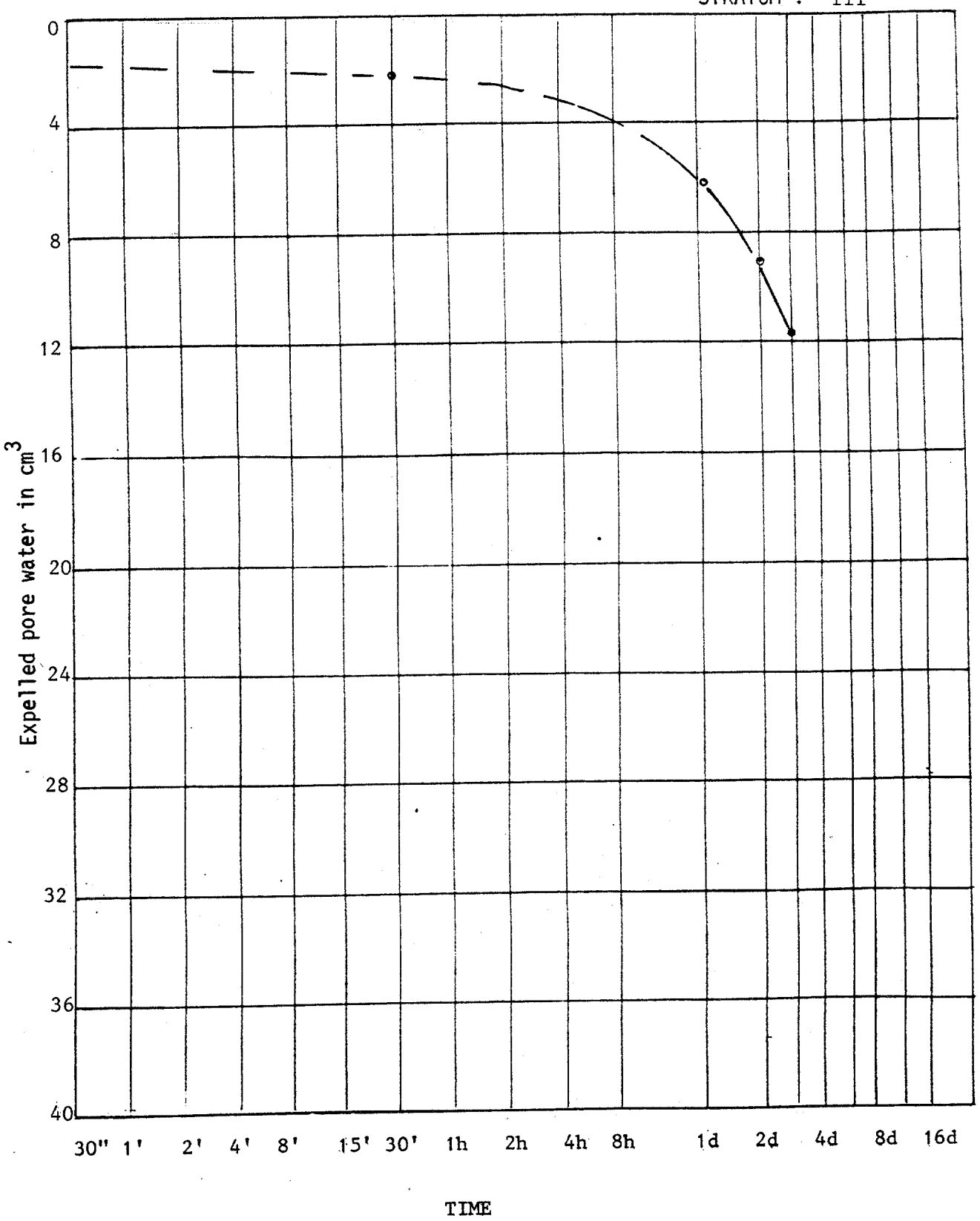

CNRD 13-2 TENSION PILE STUDY

CONSOLIDATION DIAGRAM

DET NORSKE VERITAS
Geotechnical Laboratory

Scale	
Drawn by	Date
Approved	Fig.No. 42

TEST No. : T 12

STRATUM : III

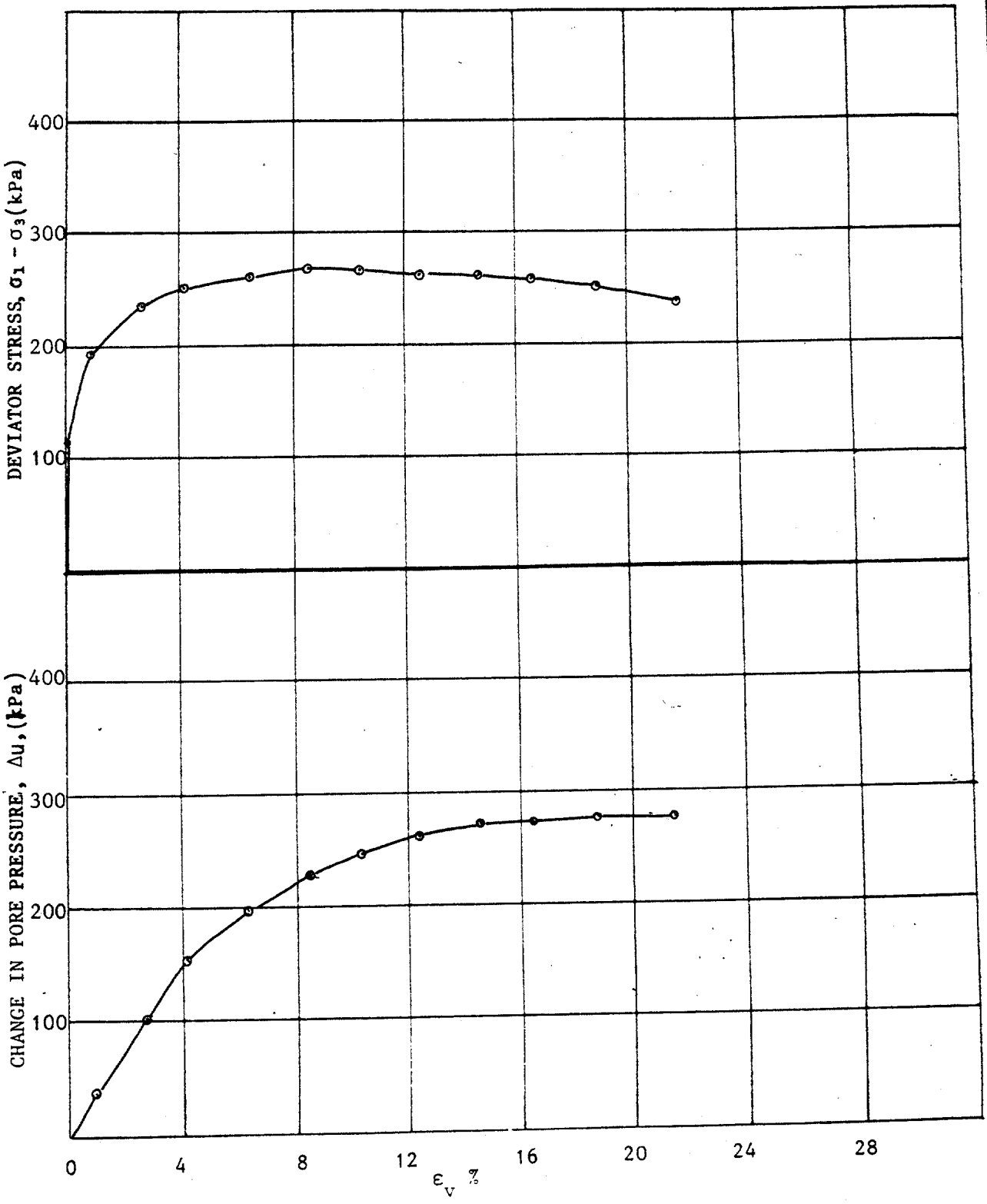

CNRD 13-2 TENSION PILE STUDY

STANDARD TRIAXIAL TEST, CIU

DET NORSKE VERITAS
Geotechnical Laboratory

Scale	
Drawn by	Date
Approved	Fig. No. 43

REMOULDED SAMPLE

FROM PILE TEST 14

CONSOLIDATION PRESSURE = 500 kPa

TEST No.: T 12

STRATUM : III

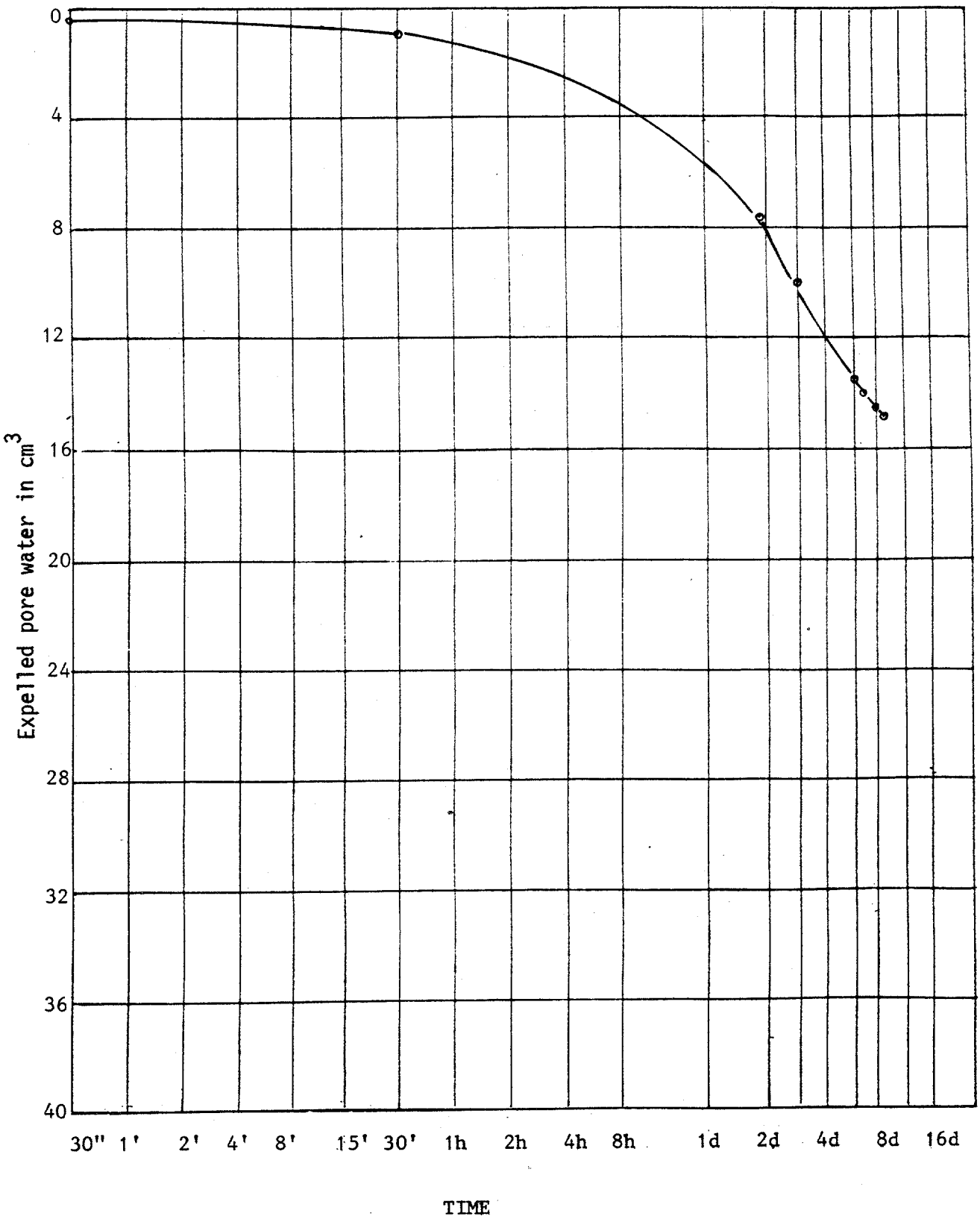

CNRD 13-2 TENSION PILE STUDY

CONSOLIDATION DIAGRAM

DET NORSKE VERITAS
Geotechnical Laboratory

Scale	
Drawn by	Date
Approved	Fig. No. 44

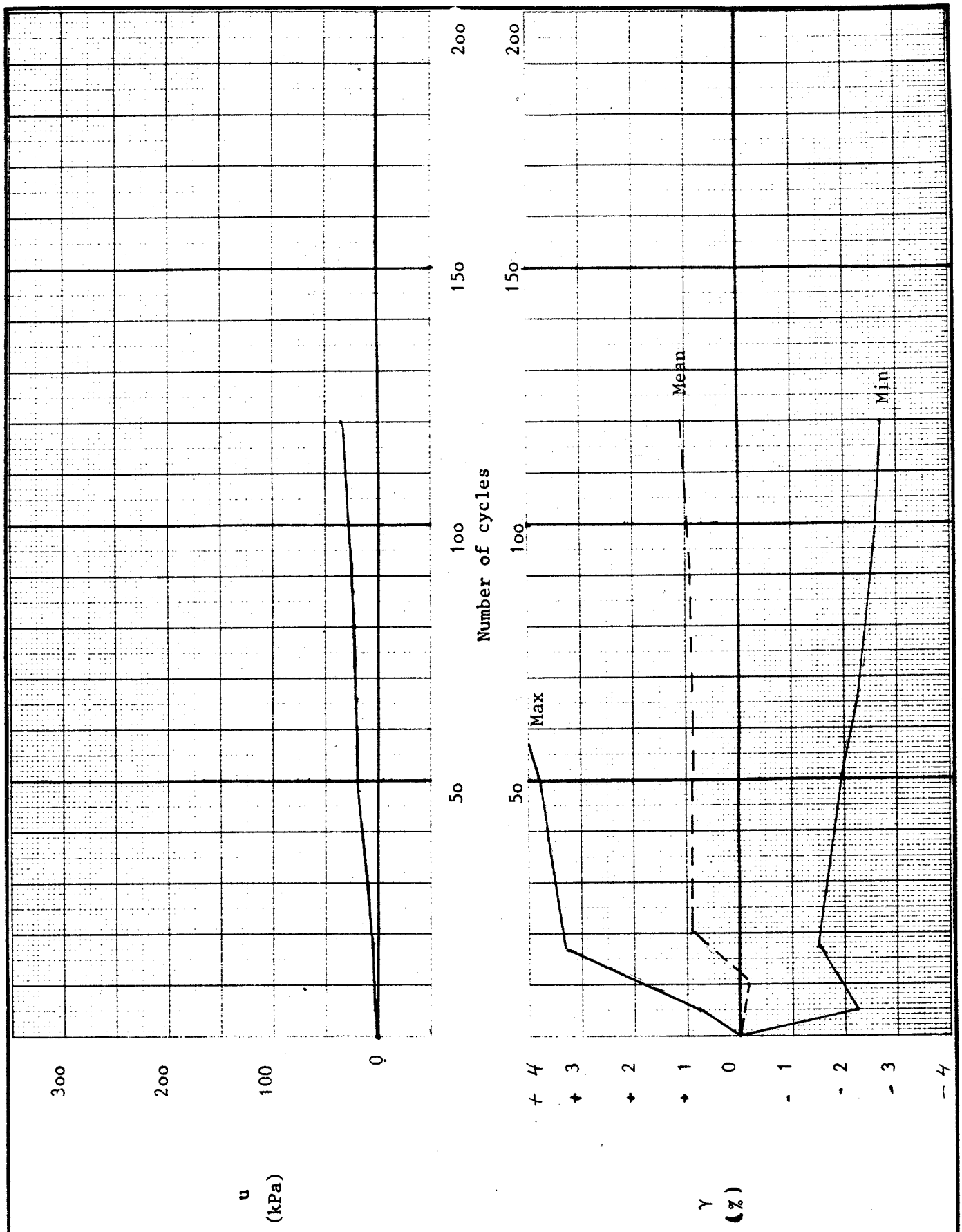

SAMPLE NO: T13 [illegible] τ_c/S_u = ± 0.77 and ± 0.55

CYCLIC TRIAXIAL TEST

DET NORSKE VERITAS
Geotechnical Laboratory

Proj. No.	
Scale	
Drawn by	Date
Approved	Fig. No. 45

SAMPLE NO.: T13

τ_{stat} : 0

τ_{cyclic} : ± 100 kPa

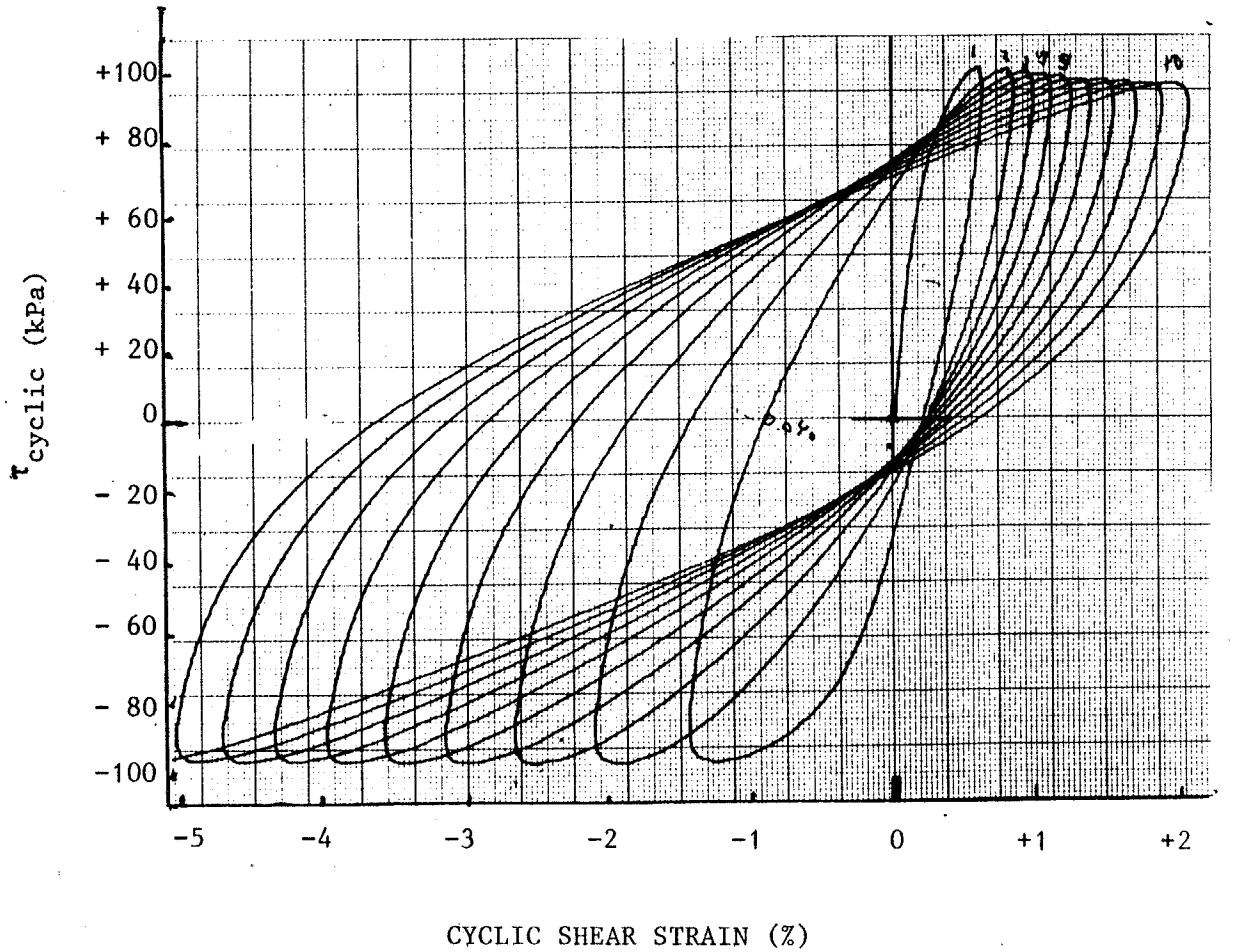

CNRD 13-2 TENSION PILE STUDY

CYCLIC TRIAXIAL TEST, STRESS VS STRAIN, DIRECT PLOT

DET NORSKE VERITAS
Geotechnical Laboratory

Drawn by

Approved

Date

Scale

Fig. No. 46

SAMPLE NO: T 13

τ_{stat} : 0

τ_{cyclic} : ± 70 kPa

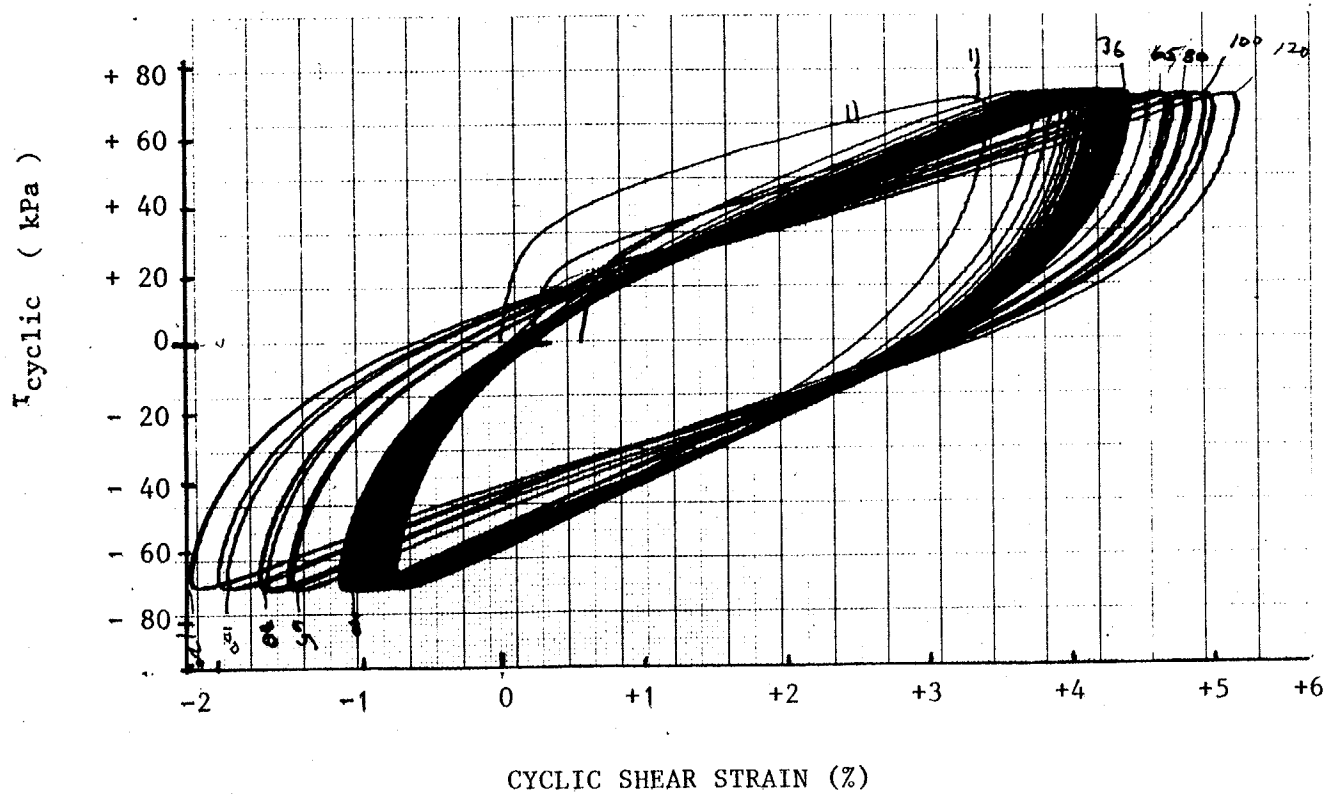

CNRD 13-2 TENSION PILE STUDY

CYCLIC TRIAXIAL TEST, STRESS VS STRAIN, DIRECT PLOT

DET NORSKE VERITAS
Geotechnical Laboratory

Drawn by	Scale
Approved	Date
Fig. No. 47	

TEST No. : T 13

STRATUM : III

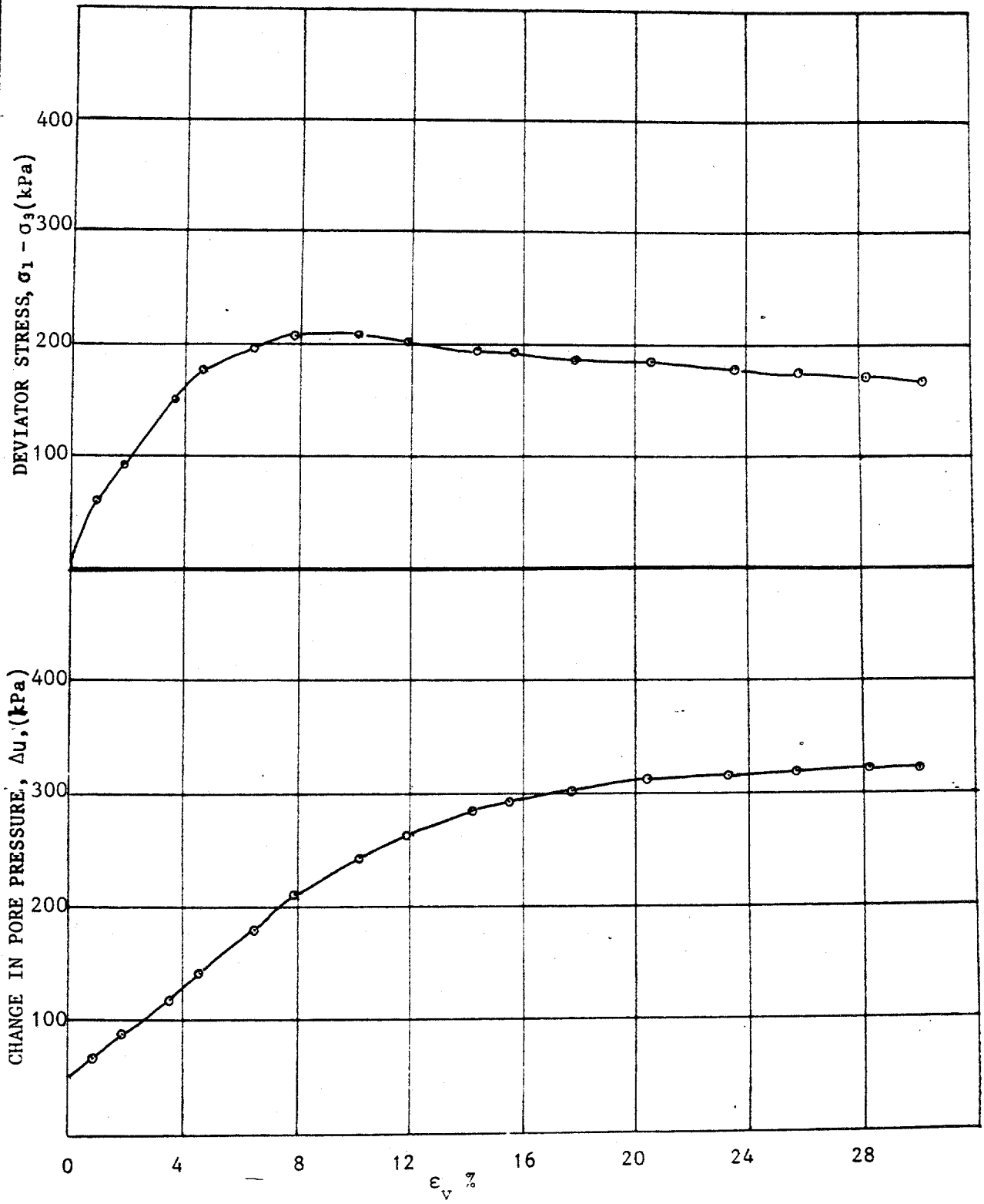

CNRD 13-2 TENSION PILE STUDY

STANDARD TRIAXIAL TEST, CIU, AFTER CYCLIC LOADING

DET NORSKE VERITAS Geotechnical Laboratory	Drawn by	Scale
	Approved	Date
		Fig. No. 48

REMOULDED SAMPLE

FROM PILE TEST 14

CONSOLIDATION PRESSURE = 500 kPa

TEST No.: T 13

STRATUM : III

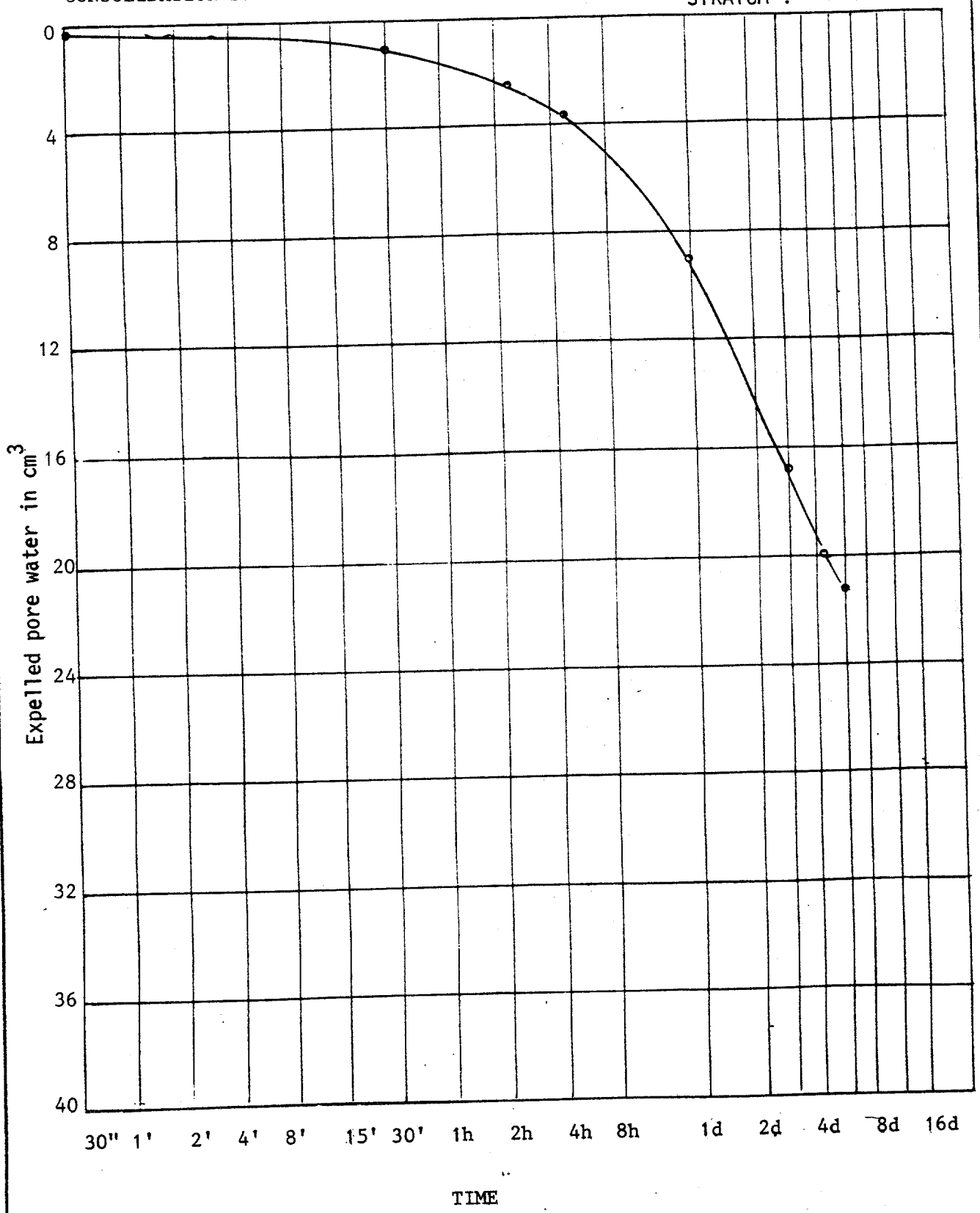

CNRD 13-2 TENSION PILE STUDY

CONSOLIDATION DIAGRAM

DET NORSKE VERITAS
Geotechnical Laboratory

Scale	
Drawn by	Date
Approved	Fig.No. 49

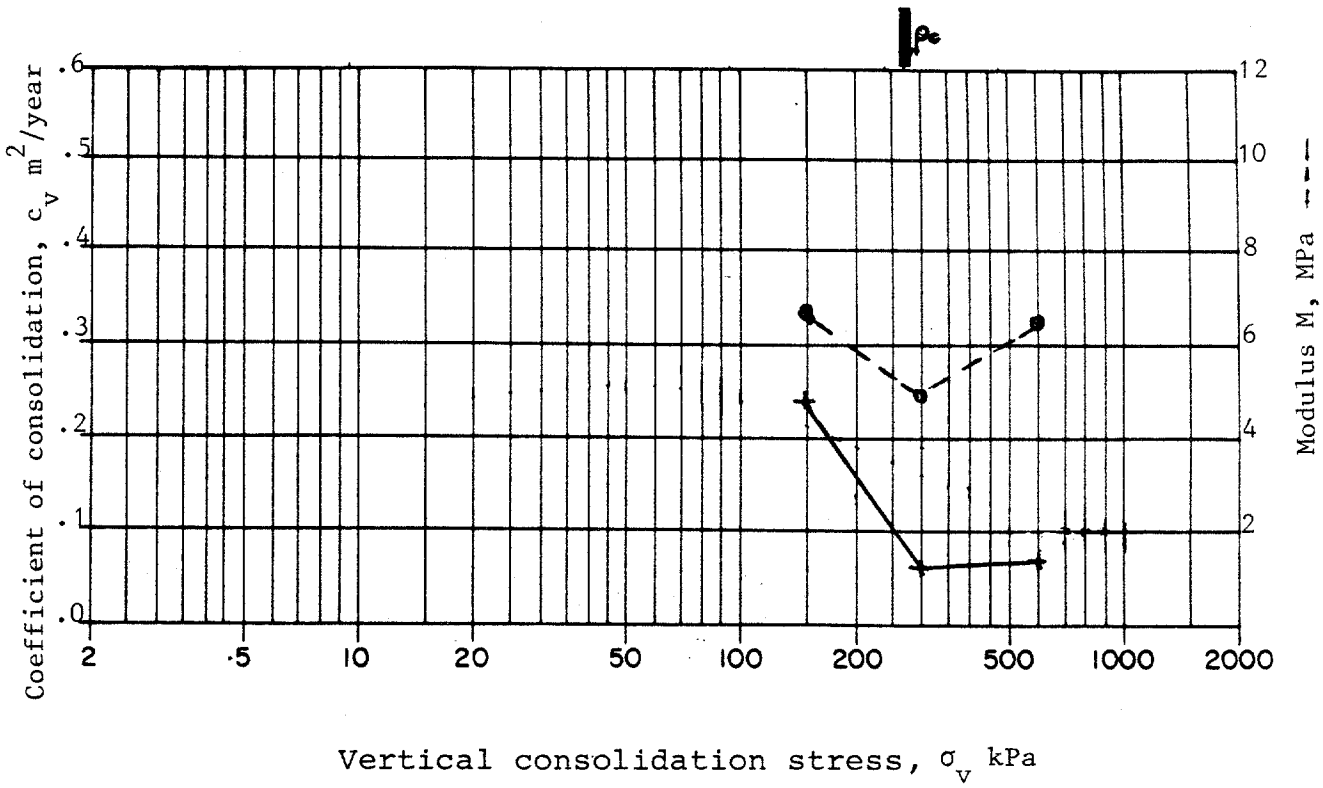

Test 5, Stratum II

Parallel to consolidation direction

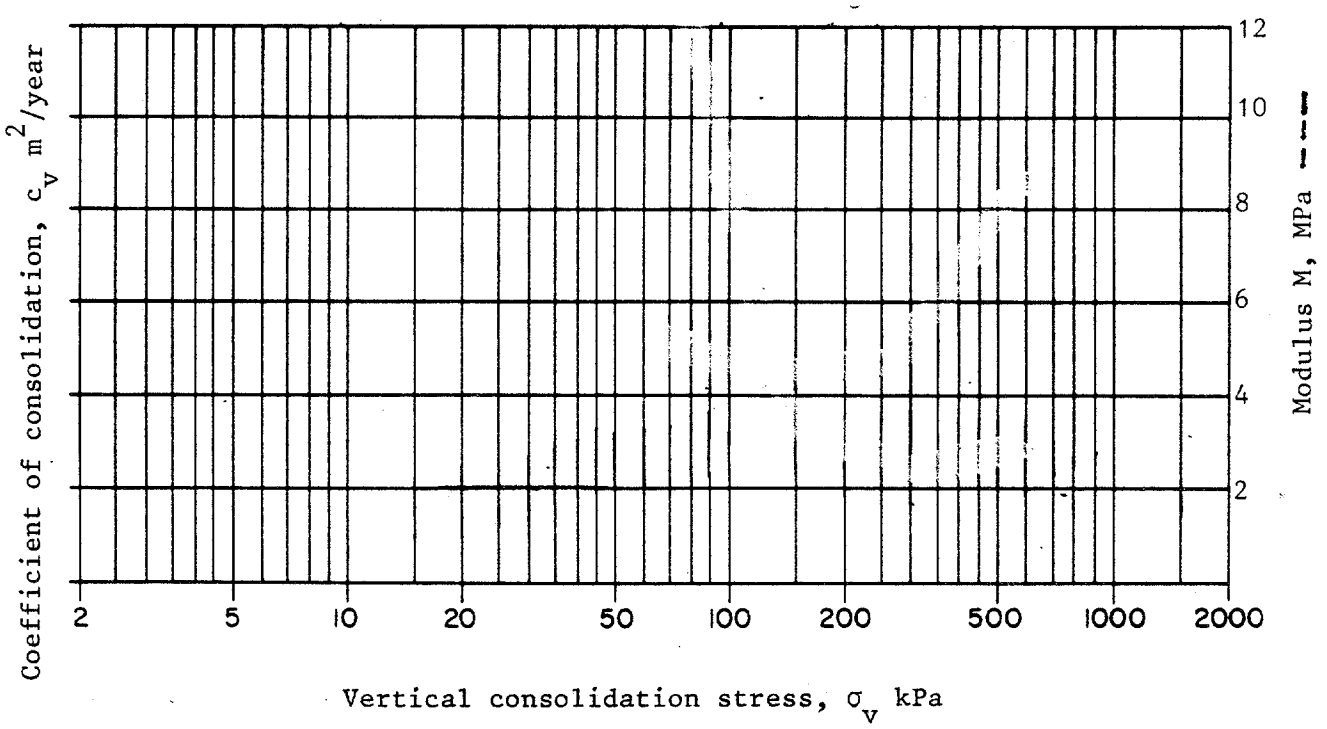

Normal to consolidation direction

CNRD 13-2. TENSION PILE STUDY	Proj.No.
COMPRESSION TESTS ON REMOULDED, RECONSOLIDATED MATERIAL	Scale
DET NORSKE VERITAS Geotechnical Laboratory	Drawn by / Date
	Approved / Fig.No. 50

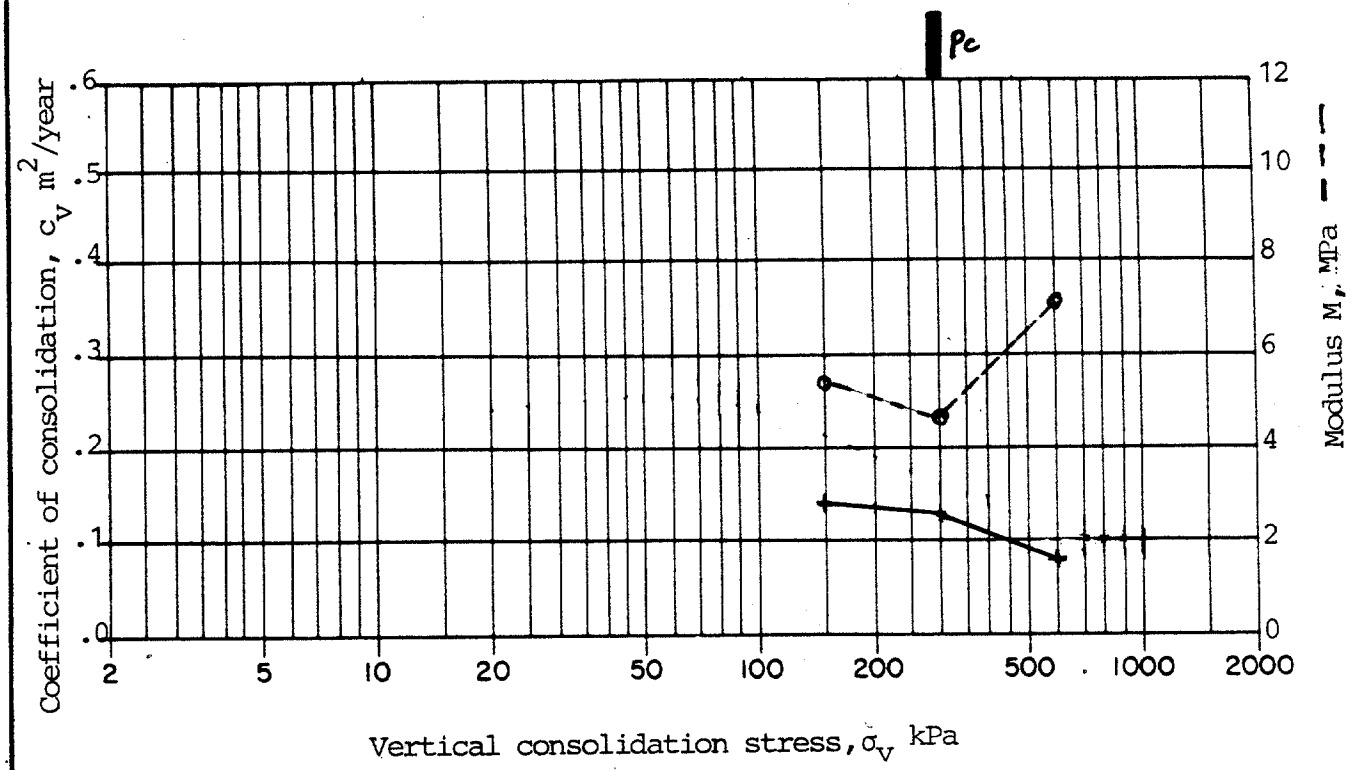

Test 6, Stratum III

Parallel to consolidation direction

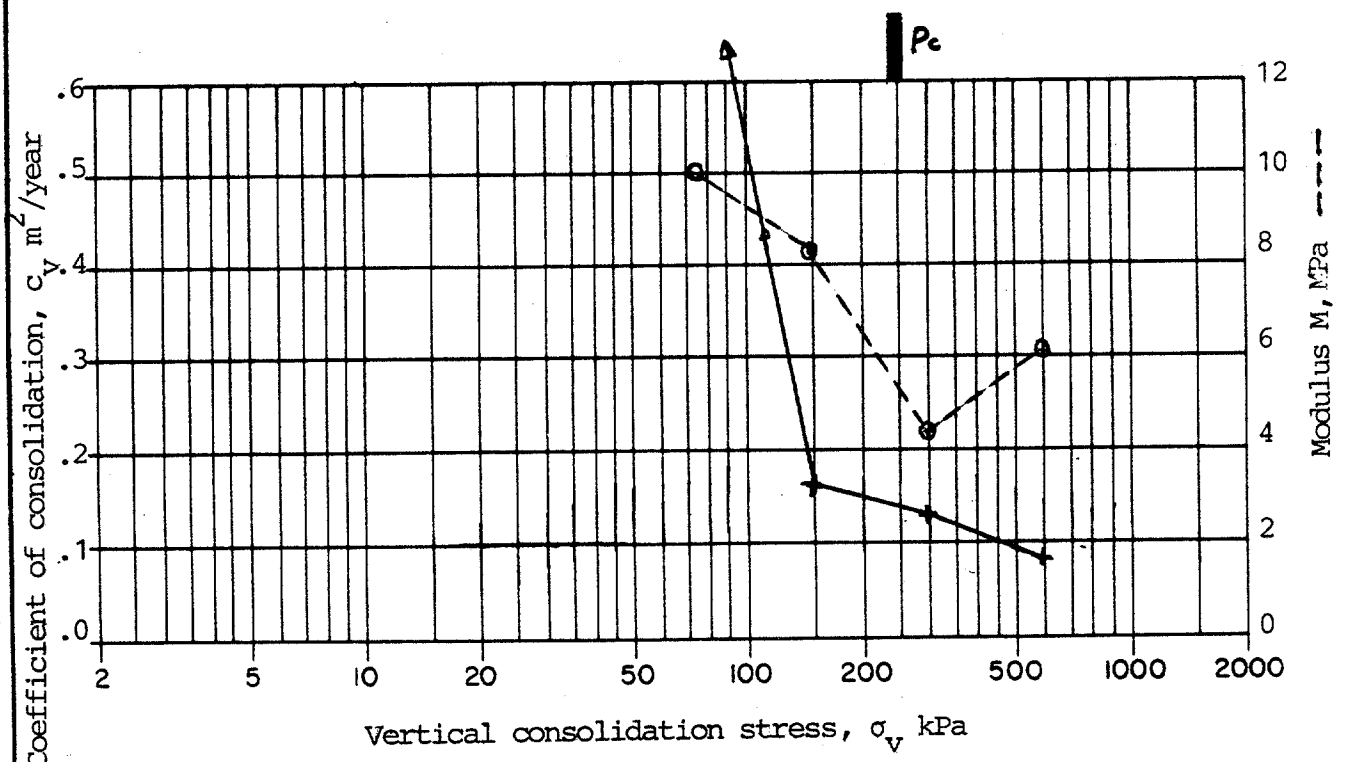

Test 6, Stratum III

Normal to consolidation direction

CNRD 13-2, TENSION PILE STUDY	Proj.No.
COMPRESSION TESTS ON REMOULDED, RECONSOLIDATED MATERIAL	Scale
DET NORSKE VERITAS Geotechnical Laboratory	Drawn by / Date
	Approved / Fig.No. 51

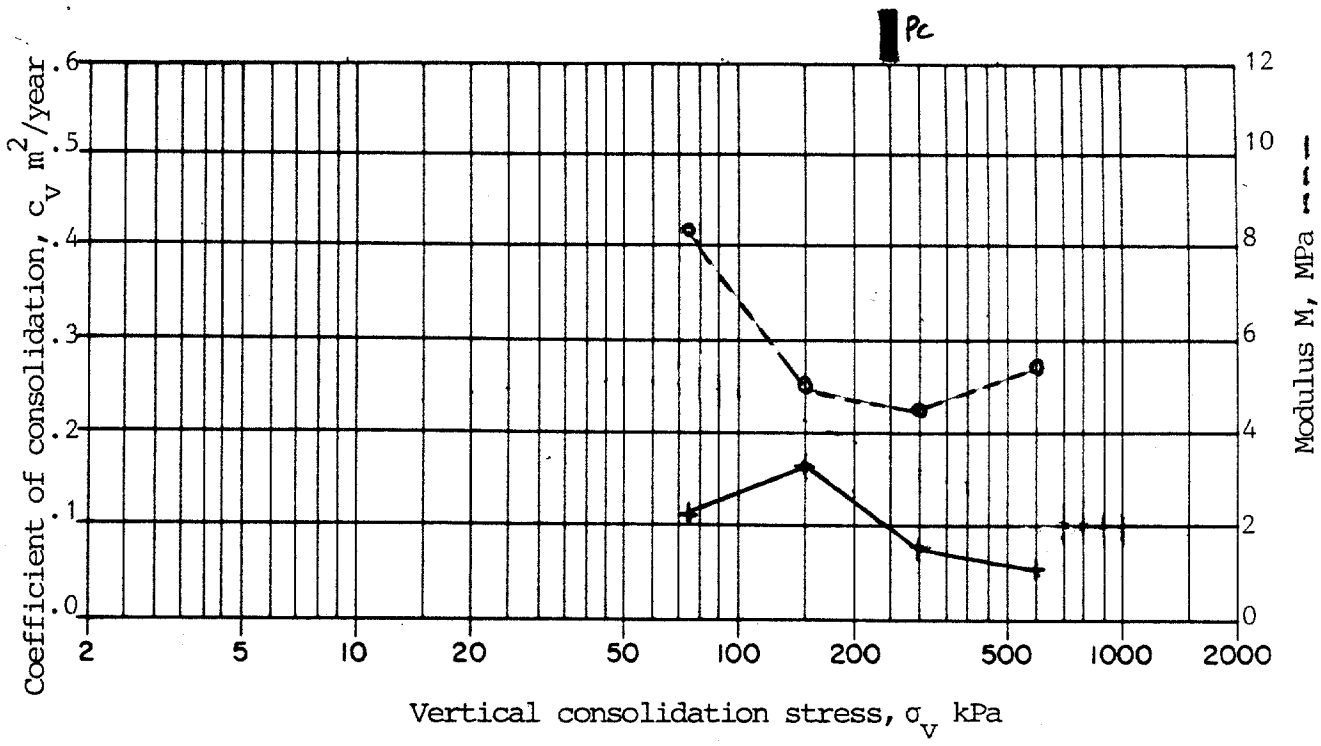

Test 8, Stratum III
Parallel to consolidation direction

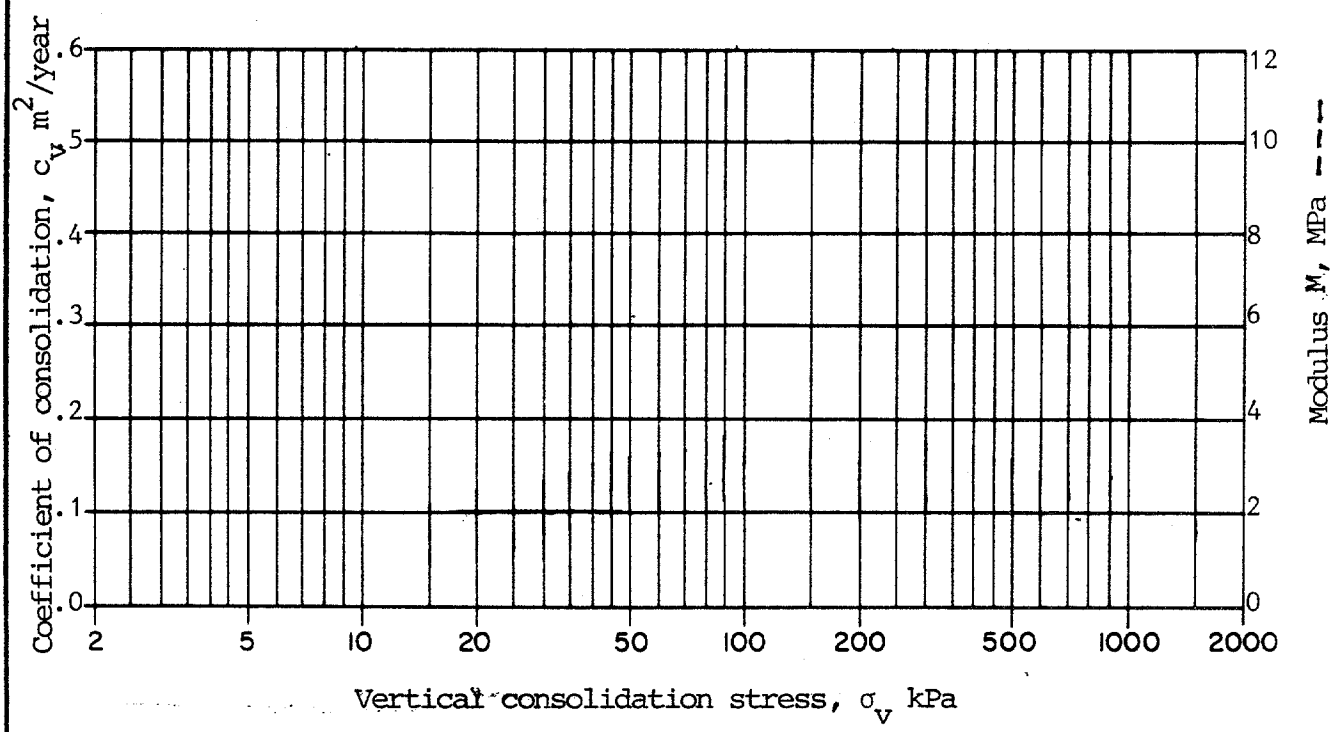

Test 8, Stratum III

Normal to consolidation direction

CNRD 13-2. TENSION PILE STUDY		Proj.No.
COMPRESSION TESTS ON REMOULDED, RECONSOLIDATED MATERIAL		Scale
DET NORSKE VERITAS Geotechnical Laboratory	Drawn by	Date
	Approved	Fig.No. 52

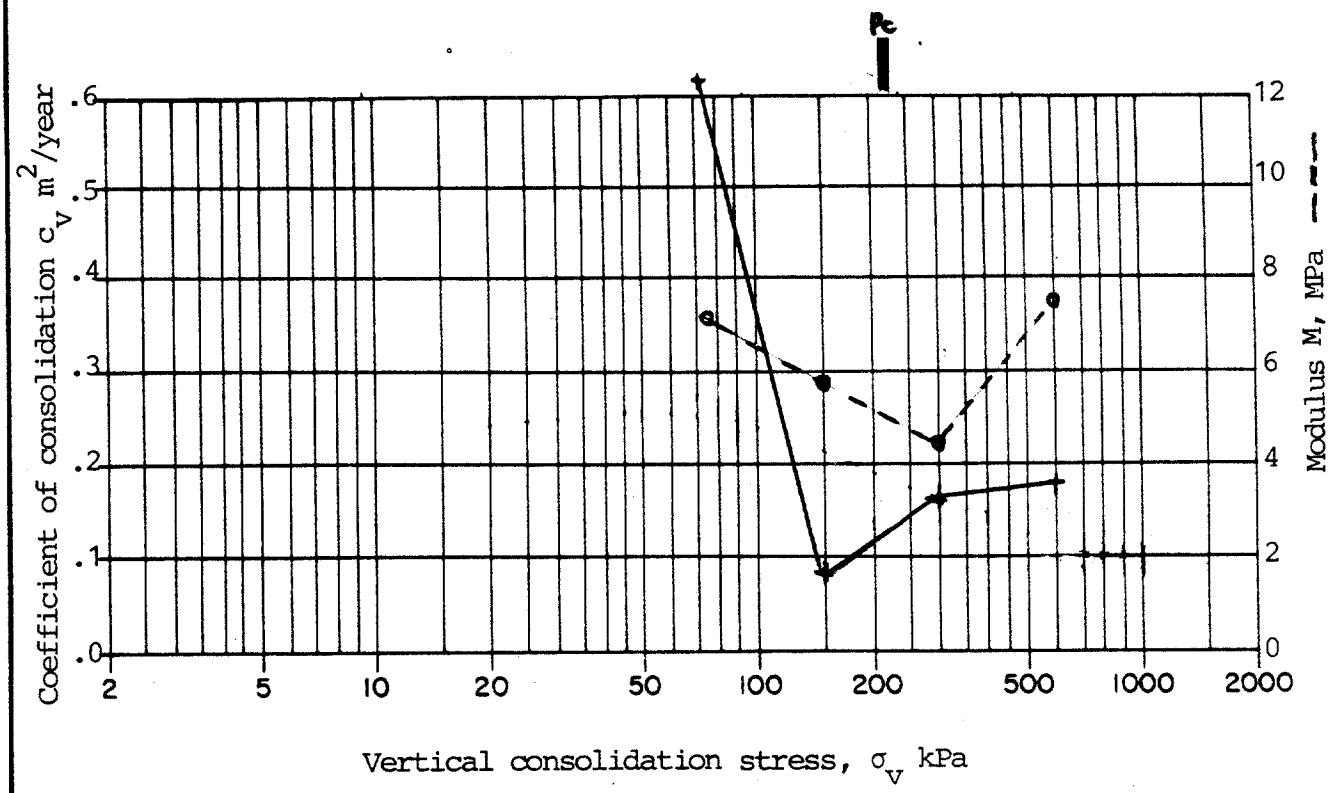

Test 9, Stratum II

Parallel to consolidation direction

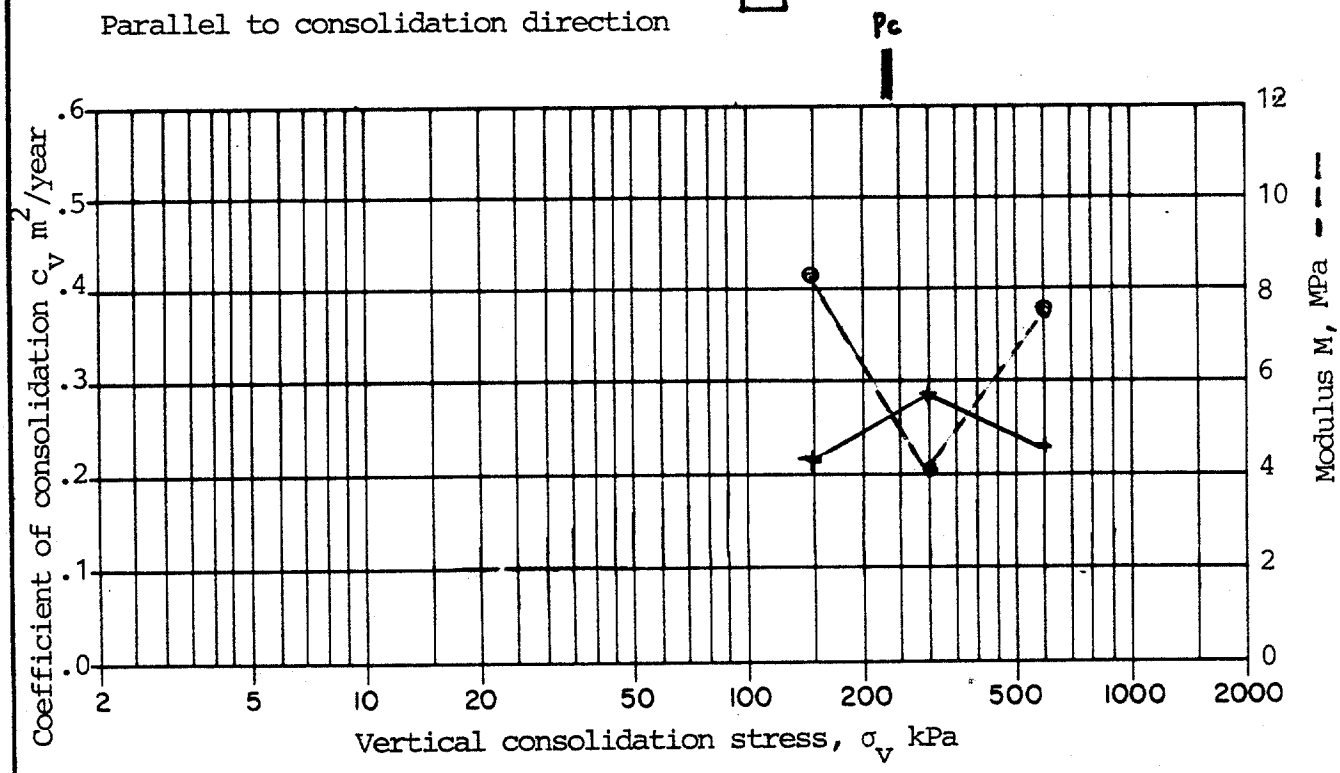

Test 9, Stratum II

Normal to consolidation direction

CNPD 13-2, TENSION PILE STUDY		Proj.No.
COMPRESSION TESTS ON REMOULDED, RECONSOLIDATED MATERIAL		Scale
DET NORSKE VERITAS Geotechnical Laboratory	Drawn by	Date
	Approved	Fig.No. 53

APPENDIX L

PROGRAM CRAPIL

CReep Analysis of **PIL**es

PROGRAM DESCRIPTION AND USERS MANUAL

CONTENT

1. Introduction L2
2. Description of Subroutines L3
3. Input Data Procedure L4
4. Example Input L6
5. Example Output L7
6. Program Listing L14

1. INTRODUCTION

This Appendix L of the CNRD 13-2 TENSION PILE STUDY, FINAL REPORT, carried out for CONOCO NORWAY INC. presents a short description of the computer program CRAPIL (**CR**eep **A**nalysis of **PIL**es) developed for evaluation of the effect of cyclic creep effects on the shear stress distribution and pile head deflection of long piles in clay subjected to axial load variations.

CRAPIL is an extension and modification of a program developed about 1980 within Veritas for evaluation of pipeline creep. The material model and the loading procedure has been changed completely and the stepwise application of a variable number of cycles to allow a rapid analysis of a complete storm was developed within the CNRD 13-2 program.

The theory related to the material model is described in Section 4.8 of the main report. There are additionally extensive comments in the program listing which should be sufficient for the user to allow him to follow the chosen approach. Furthermore, sample runs have been presented and commented on in Section 4.8 of the main report.

In the following we have therefore restricted the program description to a short summary of the subroutines, a description of the input procedure and examples of input and output followed by a program listing.

The program is written in standard Fortran IV and has been run on Veritec's VAX 750 computer.

The program also allows pure static analysis of axially loaded piles and shows excellent agreement with the DRIVE 15 program.

2.DESCRIPTION OF SUBROUTINES

MAIN Program

- Reads and prints the input information.
- Forms elastic pile stiffness matrix.
- Controls the loading procedure and the material modifications due to creep.
- Calls subroutines for inversion of stiffness matrix and calculation of shear stresses and displacements along the pile.

Subroutine ITER

- Performes the calculation of shear stresses and displacements along the pile subjected to a pile head load . The method applied is the method of initial stiffness. The pile is treated elastic and the soil springs follow an ideal elasto-plastic load (shear stress) - displacement relationship.

Subroutine SPBCO

- Triangulizes and estimates the condition of the elastic pile stiffness matrix. This is a library routine.

Subroutine SPBSL

- Invertes the pile stiffness matrix. This is a library routine.

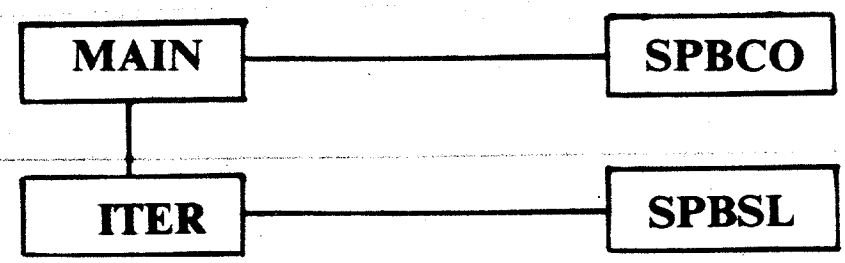

3. INPUT DATA PROCEDURE

1. HEADING CARD — FORMAT (20A4)

Columns	1-80	TEXT(I)	One (1) card for identification of problem to be analysed

2. CONTROL DATA CARD — FORMAT (4I5)

Columns	1-5	NEL	number of pile elements
	6-10	NLC	number of load cards
	11-15	IUNI	unit switch =1 Mn and meter, =0 N and meter
	16-20	IFOC	boundary condition of the pile bottom =1 clamped, =0 free
	21-25	IPRI	printer switch =1 activated, =0 not activated

3. ITERATION SPEED-UP CARD — FORMAT (I5,2F10.3)

Columns	1-5	NIMAX	maximum number of iterations
	6-15	DLI	displacement closure tolerance [m]
	16-25	FID	displacement decreasing factor DMUL can be adjusted with this value (10 is suitable)

4. PILE DATA CARD — FORMAT (3F10.3)

Columns	1-10	DOP	external diameter [m]
	11-20	WT	wall thickness [m]
	21-30	ELP	discrete length of pile element [m]

5. SOIL DATA CARD FORMAT (4F10.3)

this card should be repeated NEL times I=1,NEL

Columns	1-10	TAUULT(I)	ultimate shear capacity of the soil element [N/m^2 or MN/m^2]
	11-20	SLIM(I)	limit shear of the soil's linear behaviour as percent of the ultimate shear capacity
	21-30	ALFAR(I)	elasticity slope of the soil [N/$m \cdot m^2$ or MN/$m \cdot m^2$]
	31-40	C(I)	damping coefficient of the soils elasto-visco plastic model [N·s/m or MN·s/m]

6. LOAD DATA CARD FORMAT (I5,4F10.3)

this card should be repeated NLC times I=1,NLC

Columns	1-5	NCY(I)	number of cycles in each wave-parcel
	6-15	FPRET(I)	pretension or static force [MN or N]
	16-25	FMAX(I)	max. load in wave parcel [MN or N]
	26-35	FMIN(I)	min. load in wave parcel [MN or N]
	36-45	T(I)	wave period [s]

4. EXAMPLE INPUT

The input format is shown below for one of the sample calculations described in Section 4.8.

```
CONCCO-PILE    SAFETY FACTOR 1 2
   20     9     1     0     1
 3000     0.002        10.0
     0.762    0.01905        3.35
  0.006872        0.60      0.9043      1000.
  0.008944        0.60      1.1769      1000.
  0.01102         0.60      1.4497      1000.
  0.013091        0.60      1.7225      1000.
  0.01516         0.60      1.9949      1000.
  0.017243        0.60      2.2688      1000.
  0.01931         0.60      2.5412      1000.
  0.021382        0.60      2.8135      1000.
  0.02345         0.60      3.0858      1000.
  0.025534        0.60      3.3598      1000.
  0.02760         0.60      3.6321      1000.
  0.029673        0.60      3.9044      1000.
  0.03174         0.60      4.1768      1000.
  0.033825        0.60      4.4507      1000.
  0.03589         0.60      4.7230      1000.
  0.042390        0.60      5.5773      1000.
  0.04888         0.60      6.4325      1000.
  0.055394        0.60      7.2888      1000.
  0.06189         0.60      8.1435      1000.
  0.068400        0.60      8.9966      1000.
    0        2.0
 1110        2.0        2.44        1.56        12.0
  500        2.0        2.87        1.13        12.0
  100        2.0        3.17        0.83        12.0
   50        2.0        3.33        0.67        12.0
   20        2.0        3.48        0.52        12.0
   12        2.0        3.60        0.40        12.0
    6        2.0        3.76        0.24        12.0
    2        2.0        3.95        0.05        12.0
```

5. EXAMPLE OUTPUT

The output shown in the following is a part of the output from one of the sample runs described in Section 4.8.

```
*****************************************************
*                                                   *
*      PROGRAM  "  C R A P I L  "                   *
*                                                   *
*       CREEP ANALYSIS OF PILES                     *
*                                                   *
*     VERSION 3, NOVEMBER 22, 1983                  *
*          TORE J. KVALSTAD                         *
*      VERITAS RESEARCH DIVISION                    *
*****************************************************

CONOCO PILE   safety-factor 1.5
*******************************


CONTROL DATA:
*************

   NUMBER OF PILE ELEMENTS          :   20
   NUMBER OF LOAD CARDS             :    7
   UNIT SWITCH                      :    1   IF = 0   N AND M
                                                IF = 1   MN AND M
   PILE BOTTOM SWITCH               :    0   IF = 1   CLAMPED
                                                IF = 0   FREE
   PRINT SWITCH                     :    1   IF = 0   NOT ACTIVATED
                                                IF = 1   ACTIVATED

ITERATION DATA:
***************

   MAX. NUMBER OF ITERATIONS        : 3000
   DISPLACEMENT TOLERANCE           :0.00050000
   DISPLACEMENT DECREASE FACTOR     :   10.0000


PILE DATA:
**********

   OUTER DIAMETER OF PILE           :     0.762
   WALL THICKNESS                   :   0.01905
   PILE ELEMENT LENGTH              :     3.350


SOIL DATA:
**********

   ELEM.     SKIN       CREEP       SOIL        DAMPING
    NO.    FRICTION     RATIO     STIFFNESS     CONSTANT

      1 0.6872E-02 0.7000E+00 0.9043E+00 0.1000E+03
      2 0.8944E-02 0.7000E+00 0.1177E+01 0.1000E+03
      3 0.1102E-01 0.7000E+00 0.1450E+01 0.1000E+03
      4 0.1309E-01 0.7000E+00 0.1722E+01 0.1000E+03
      5 0.1516E-01 0.7000E+00 0.1995E+01 0.1000E+03
      6 0.1724E-01 0.7000E+00 0.2269E+01 0.1000E+03
      7 0.1931E-01 0.7000E+00 0.2541E+01 0.1000E+03
      8 0.2138E-01 0.7000E+00 0.2813E+01 0.1000E+03
      9 0.2345E-01 0.7000E+00 0.3086E+01 0.1000E+03
     10 0.2553E-01 0.7000E+00 0.3360E+01 0.1000E+03
     11 0.2760E-01 0.7000E+00 0.3632E+01 0.1000E+03
     12 0.2967E-01 0.7000E+00 0.3904E+01 0.1000E+03
     13 0.3174E-01 0.7000E+00 0.4177E+01 0.1000E+03
     14 0.3382E-01 0.7000E+00 0.4451E+01 0.1000E+03
     15 0.3589E-01 0.7000E+00 0.4723E+01 0.1000E+03
     16 0.4239E-01 0.7000E+00 0.5578E+01 0.1000E+03
     17 0.4888E-01 0.7000E+00 0.6432E+01 0.1000E+03
     18 0.5539E-01 0.7000E+00 0.7289E+01 0.1000E+03
     19 0.6189E-01 0.7000E+00 0.8144E+01 0.1000E+03
     20 0.6840E-01 0.7000E+00 0.8997E+01 0.1000E+03
```

LOAD DATA:
****

LOAD CARD NO.	NO. OF CYCLES IN PARCEL	PRETENSION OR STATIC FORCE	MAX. LOAD IN WAVE PARCEL	MIN. LOAD IN WAVE PARCEL	WAVE PERIOD
1	0	0.2000E+01	0.0000E+00	0.0000E+00	0.00
2	1110	0.2000E+01	0.2440E+01	0.1560E+01	12.00
3	500	0.2000E+01	0.2870E+01	0.1150E+01	12.00
4	100	0.2000E+01	0.3170E+01	0.8300E+00	12.00
5	50	0.2000E+01	0.3030E+01	0.6700E+00	12.00
6	20	0.2000E+01	0.3430E+01	0.2200E+00	12.00
7	12	0.2000E+01	0.3600E+01	0.4000E+00	12.00
8	6	0.2000E+01	0.3760E+01	0.2400E+00	12.00
9	2	0.2000E+01	0.3960E+01	0.5000E+01	12.00

STEEL CROSS SECTION OF PILE : 0.044
PILE ELEMENT STIFFNESS, EI : 0.279E+04
SURFACE AREA OF PILE ELEMENT : 8.021
STATIC AXIAL CAPACITY OF PILE : 4.794
ULTIMATE CREEP CAPACITY : 3.356

CONOCO-PILE safety factor 1.2

LOAD CASE NO.: 1 STATIC ANALYSIS WITHOUT CYCLIC CREEP
STATIC LOAD = 0.2000E+01

RESULTS FROM LOAD CASE NO : 1
NUMBER OF ITERATIONS PERFORMED: 91
NUMBER OF ELEMENTS ACCEPTED : 20

ELEM. NO.	INCREMENTAL VALUES DDISPL	DTAU	ACCUMULATED VALUES DISPL	TAU	FORCE PER ELEMENT	ULTIMATE CAPACITY	STRESS PATH NO.
1	0.0090	0.0069	0.0090	0.0069	0.0851	0.0851	2
2	0.0083	0.0089	0.0083	0.0089	0.0717	0.0717	2
3	0.0077	0.0110	0.0077	0.0110	0.0884	0.0884	2
4	0.0070	0.0121	0.0070	0.0121	0.0970	0.1050	2
5	0.0064	0.0128	0.0064	0.0128	0.1086	0.1216	2
6	0.0058	0.0133	0.0058	0.0133	0.1163	0.1383	2
7	0.0053	0.0135	0.0053	0.0135	0.1082	0.1549	2
8	0.0048	0.0135	0.0048	0.0135	0.1086	0.1715	2
9	0.0044	0.0134	0.0044	0.0134	0.1079	0.1881	2
10	0.0039	0.0132	0.0039	0.0132	0.1062	0.2048	2
11	0.0036	0.0129	0.0036	0.0129	0.1037	0.2214	2
12	0.0032	0.0126	0.0032	0.0126	0.1008	0.2380	2
13	0.0029	0.0122	0.0029	0.0122	0.0976	0.2546	2
14	0.0026	0.0118	0.0026	0.0118	0.0943	0.2713	2
15	0.0024	0.0114	0.0024	0.0114	0.0918	0.2879	2
16	0.0022	0.0123	0.0022	0.0123	0.0985	0.3400	2
17	0.0020	0.0131	0.0020	0.0131	0.1050	0.3920	2
18	0.0019	0.0139	0.0019	0.0139	0.1114	0.4443	2
19	0.0018	0.0148	0.0018	0.0148	0.1184	0.4964	2
20	0.0018	0.0158	0.0018	0.0158	0.1269	0.5486	2

SUM QGU(I), I =1,N : 1.9998

CONOCO-PILE safety factor 1.2

LOAD CASE NO.: 2 WAVE PARCEL CREEP ANALYSIS
MAX. LOAD = 0.2440E+01

RESULTS FROM LOAD CASE NO : 2
NUMBER OF ITERATIONS PERFORMED: 89
NUMBER OF ELEMENTS ACCEPTED : 20

ELEM. NO.	INCREMENTAL VALUES DDISPL	DTAU	ACCUMULATED VALUES DISPL	TAU	FORCE PER ELEMENT	ULTIMATE CAPACITY	STRESS PATH NO.
1	0.0023	0.0000	0.0113	0.0069	0.0551	0.055.	2
2	0.0021	0.0000	0.0105	0.0089	0.0717	0.0717	2
3	0.0020	0.0000	0.0096	0.0110	0.0884	0.0884	2
4	0.0018	0.0010	0.0086	0.0131	0.1050	0.1050	2
5	0.0016	0.0024	0.0081	0.0152	0.1216	0.1216	2
6	0.0015	0.0034	0.0073	0.0167	0.1336	0.1383	2
7	0.0014	0.0035	0.0067	0.0170	0.1360	0.1549	2
8	0.0012	0.0035	0.0061	0.0170	0.1366	0.1715	2
9	0.0011	0.0035	0.0055	0.0169	0.1356	0.1881	2
10	0.0010	0.0034	0.0050	0.0167	0.1336	0.2048	2
11	0.0009	0.0033	0.0045	0.0163	0.1305	0.2214	2
12	0.0008	0.0033	0.0041	0.0158	0.1269	0.2380	2
13	0.0008	0.0032	0.0037	0.0153	0.1229	0.2546	2
14	0.0007	0.0031	0.0033	0.0148	0.1189	0.2713	2
15	0.0006	0.0030	0.0030	0.0143	0.1149	0.2879	2
16	0.0006	0.0032	0.0028	0.0155	0.1243	0.3400	2
17	0.0005	0.0034	0.0026	0.0165	0.1325	0.3920	2
18	0.0005	0.0036	0.0024	0.0175	0.1406	0.4443	2
19	0.0005	0.0039	0.0023	0.0187	0.1497	0.4964	2
20	0.0005	0.0043	0.0022	0.0201	0.1610	0.5486	2

SUM QGU(I), I =1,N : 2.4396

CONOCO-PILE safety factor 1.2

LOAD CASE NO.: 3 WAVE PARCEL CREEP ANALYSIS
MIN. LOAD = 0.1560E+01

RESULTS FROM LOAD CASE NO : 3
NUMBER OF ITERATIONS PERFORMED: 53
NUMBER OF ELEMENTS ACCEPTED : 20

ELEM. NO.	INCREMENTAL VALUES DDISPL	DTAU	ACCUMULATED VALUES DISPL	TAU	FORCE PER ELEMENT	ULTIMATE CAPACITY	STRESS PATH NO.
1	-0.0039	-0.0035	0.0074	0.0034	0.0270	0.0551	3
2	-0.0036	-0.0042	0.0067	0.0047	0.0380	0.0717	3
3	-0.0033	-0.0047	0.0063	0.0063	0.0503	0.0884	3
4	-0.0030	-0.0052	0.0058	0.0079	0.0636	0.1050	3
5	-0.0027	-0.0055	0.0053	0.0097	0.0778	0.1216	3
6	-0.0025	-0.0057	0.0049	0.0110	0.0883	0.1383	3
7	-0.0023	-0.0058	0.0044	0.0112	0.0899	0.1549	3
8	-0.0021	-0.0058	0.0040	0.0113	0.0902	0.1715	3
9	-0.0019	-0.0057	0.0036	0.0112	0.0896	0.1881	3
10	-0.0017	-0.0057	0.0033	0.0110	0.0881	0.2048	3
11	-0.0015	-0.0056	0.0030	0.0107	0.0860	0.2214	3
12	-0.0014	-0.0054	0.0027	0.0104	0.0834	0.2380	3
13	-0.0013	-0.0053	0.0024	0.0100	0.0805	0.2546	3
14	-0.0012	-0.0052	0.0022	0.0097	0.0776	0.2713	3
15	-0.0011	-0.0050	0.0020	0.0093	0.0746	0.2879	3
16	-0.0010	-0.0055	0.0018	0.0100	0.0800	0.3400	3
17	-0.0009	-0.0059	0.0016	0.0106	0.0849	0.3920	3
18	-0.0009	-0.0063	0.0015	0.0112	0.0899	0.4443	3
19	-0.0008	-0.0067	0.0015	0.0120	0.0960	0.4964	3
20	-0.0008	-0.0071	0.0014	0.0130	0.1040	0.5486	3

SUM QGU(I), I =1,N : 1.5598

CONOCO-PILE safety factor 1.2

LOAD CASE NO.: 2 WAVE PARCEL CREEP ANALYSIS
PRETENSION = 0.2000E+01 RESULTS BEFORE CREEP

RESULTS FROM LOAD CASE NO : 2
NUMBER OF ITERATIONS PERFORMED: 52
NUMBER OF ELEMENTS ACCEPTED : 20

ELEM. NO.	INCREMENTAL VALUES DDISPL	DTAU	ACCUMULATED VALUES DISPL	TAU	FORCE PER ELEMENT	ULTIMATE CAPACITY	STRESS PATH NO.
1	0.0019	0.0017	0.0090	0.0081	0.0406	0.0851	2
2	0.0017	0.0020	0.0086	0.0088	0.0542	0.0717	2
3	0.0016	0.0025	0.0079	0.0085	0.0685	0.0884	2
4	0.0014	0.0025	0.0073	0.0104	0.0833	0.1050	2
5	0.0013	0.0026	0.0066	0.0183	0.0987	0.1216	2
6	0.0012	0.0027	0.0060	0.0137	0.1098	0.1383	2
7	0.0011	0.0027	0.0055	0.0139	0.1118	0.1549	2
8	0.0010	0.0027	0.0050	0.0140	0.1123	0.1715	2
9	0.0009	0.0027	0.0045	0.0139	0.1116	0.1881	2
10	0.0008	0.0027	0.0041	0.0137	0.1099	0.2048	2
11	0.0007	0.0027	0.0037	0.0134	0.1075	0.2214	2
12	0.0007	0.0026	0.0033	0.0130	0.1047	0.2380	2
13	0.0006	0.0026	0.0030	0.0127	0.1015	0.2546	2
14	0.0006	0.0026	0.0028	0.0123	0.0984	0.2713	2
15	0.0006	0.0026	0.0025	0.0119	0.0954	0.2879	2
16	0.0005	0.0029	0.0023	0.0129	0.1036	0.3400	2
17	0.0005	0.0032	0.0021	0.0138	0.1106	0.3920	2
18	0.0005	0.0034	0.0020	0.0147	0.1176	0.4443	2
19	0.0004	0.0036	0.0019	0.0156	0.1252	0.4964	2
20	0.0004	0.0038	0.0019	0.0168	0.1347	0.5486	2

SUM QGU(I), I =1,N : 1.9999

EL.NO	TMAX	TMIN	TAV	TCY	TCRP	DCRP	FCRP(I	RCR
1	0.687E-02	0.337E-02	0.518E-02	0.175E-02	0.481E-02	0.862E-04	0.779E-04	0.113E-01
2	0.894E-02	0.474E-02	0.684E-02	0.210E-02	0.686E-02	0.119E-03	0.140E-03	0.156E-01
3	0.110E-01	0.627E-02	0.865E-02	0.237E-02	0.771E-02	0.154E-03	0.223E-03	0.202E-01
4	0.131E-01	0.793E-02	0.105E-01	0.258E-02	0.916E-02	0.193E-03	0.333E-03	0.254E-01
5	0.152E-01	0.970E-02	0.124E-01	0.273E-02	0.106E-01	0.237E-03	0.474E-03	0.313E-01
6	0.167E-01	0.110E-01	0.138E-01	0.283E-02	0.121E-01	0.286E-03	0.535E-03	0.310E-01
7	0.170E-01	0.112E-01	0.141E-01	0.288E-02	0.135E-01	0.146E-03	0.370E-03	0.198E-01
8	0.170E-01	0.113E-01	0.141E-01	0.289E-02	0.150E-01	0.657E-04	0.185E-03	0.864E-02
9	0.169E-01	0.112E-01	0.140E-01	0.287E-02	0.164E-01	0.778E-05	0.238E-04	0.102E-02
10	0.167E-01	0.110E-01	0.138E-01	0.283E-02	0.179E-01	0.000E+00	0.000E+00	0.000E+00
11	0.163E-01	0.107E-01	0.135E-01	0.278E-02	0.193E-01	0.000E+00	0.000E+00	0.000E+00
12	0.158E-01	0.104E-01	0.131E-01	0.271E-02	0.208E-01	0.000E+00	0.000E+00	0.000E+00
13	0.153E-01	0.100E-01	0.127E-01	0.264E-02	0.222E-01	0.000E+00	0.000E+00	0.000E+00
14	0.148E-01	0.967E-02	0.122E-01	0.258E-02	0.237E-01	0.000E+00	0.000E+00	0.000E+00
15	0.143E-01	0.930E-02	0.118E-01	0.252E-02	0.251E-01	0.000E+00	0.000E+00	0.000E+00
16	0.155E-01	0.998E-02	0.127E-01	0.276E-02	0.297E-01	0.000E+00	0.000E+00	0.000E+00
17	0.165E-01	0.106E-01	0.136E-01	0.297E-02	0.342E-01	0.000E+00	0.000E+00	0.000E+00
18	0.175E-01	0.112E-01	0.144E-01	0.316E-02	0.388E-01	0.000E+00	0.000E+00	0.000E+00
19	0.187E-01	0.120E-01	0.153E-01	0.335E-02	0.433E-01	0.000E+00	0.000E+00	0.000E+00
20	0.201E-01	0.130E-01	0.165E-01	0.356E-02	0.479E-01	0.000E+00	0.000E+00	0.000E+00

START OF CREEP REDISTRIBUTION
****
ALLOWABLE NUMBER OF CYCLES : 3
NO. OF CYCLES PERFORMED : 3
NO. OF CYCLES LEFT IN PARCEL : 1107
MAX. CREEP RATIO :0.031
ALLOWABLE CREEP RATIO :0.100

TAU	DCRP	ALF2	ALFAR	TAUULT
0.0051	0.0001	0.8643	0.9043	0.0069
0.0068	0.0001	1.1083	1.1769	0.0089
0.0085	0.0002	1.3445	1.4497	0.0110
0.0104	0.0002	1.5715	1.7225	0.0131
0.0123	0.0002	1.7883	1.9949	0.0152
0.0137	0.0002	2.0307	2.2888	0.0172
0.0139	0.0001	2.3537	2.5412	0.0193
0.0140	0.0001	2.7064	2.8135	0.0214
0.0139	0.0000	3.0700	3.0858	0.0235
0.0137	0.0000	3.3598	3.3598	0.0255
0.0134	0.0000	3.6321	3.6321	0.0276
0.0130	0.0000	3.9044	3.9044	0.0297
0.0127	0.0000	4.1768	4.1768	0.0317
0.0123	0.0000	4.4507	4.4507	0.0338
0.0119	0.0000	4.7230	4.7230	0.0359
0.0129	0.0000	5.5778	5.5778	0.0424
0.0138	0.0000	6.4325	6.4325	0.0489
0.0147	0.0000	7.2888	7.2888	0.0554
0.0156	0.0000	8.1435	8.1435	0.0619
0.0168	0.0000	8.9966	8.9966	0.0684

CONOCO PILE safety-factor 1.2

LOAD CASE NO.: 2 WAVE PARCEL CREEP ANALYSIS
MAX. LOAD = 0.2440E+01

RESULTS FROM LOAD CASE NO : 2
NUMBER OF ITERATIONS PERFORMED: 89
NUMBER OF ELEMENTS ACCEPTED : 20

ELEM. NO.	INCREMENTAL VALUES DDISPL	DTAU	ACCUMULATED VALUES DISPL	TAU	FORCE PER ELEMENT	ULTIMATE CAPACITY	STRESS PATH NO.
1	0.0019	0.0018	0.0115	0.0068	0.0545	0.0551	2
2	0.0018	0.0021	0.0106	0.0087	0.0700	0.0717	2
3	0.0016	0.0024	0.0098	0.0106	0.0851	0.0884	2
4	0.0015	0.0026	0.0090	0.0124	0.0997	0.1050	2
5	0.0014	0.0027	0.0082	0.0142	0.1136	0.1216	2
6	0.0013	0.0029	0.0075	0.0155	0.1245	0.1363	2
7	0.0011	0.0029	0.0068	0.0163	0.1304	0.1549	2
8	0.0010	0.0029	0.0062	0.0168	0.1351	0.1715	2
9	0.0009	0.0029	0.0056	0.0172	0.1380	0.1881	2
10	0.0009	0.0029	0.0051	0.0170	0.1365	0.2048	2
11	0.0008	0.0028	0.0046	0.0166	0.1334	0.2214	2
12	0.0007	0.0027	0.0041	0.0162	0.1297	0.2380	2
13	0.0006	0.0026	0.0037	0.0157	0.1256	0.2546	2
14	0.0006	0.0026	0.0034	0.0151	0.1215	0.2713	2
15	0.0005	0.0025	0.0031	0.0146	0.1175	0.2879	2
16	0.0005	0.0027	0.0028	0.0158	0.1271	0.3400	2
17	0.0004	0.0029	0.0026	0.0169	0.1355	0.3920	2
18	0.0004	0.0031	0.0025	0.0179	0.1438	0.4443	2
19	0.0004	0.0033	0.0023	0.0191	0.1532	0.4964	2
20	0.0004	0.0036	0.0023	0.0205	0.1648	0.5486	2

SUM QGU(I), I =1,N : 2.4395

CONOCO-PILE safety-factor 1.2

LOAD CASE NO.: 2 WAVE PARCEL CREEP ANALYSIS
MIN. LOAD = 0.1560E+01

RESULTS FROM LOAD CASE NO : 2
NUMBER OF ITERATIONS PERFORMED: 53
NUMBER OF ELEMENTS ACCEPTED : 20

ELEM. NO.	INCREMENTAL VALUES DDISPL	DTAU	ACCUMULATED VALUES DISPL	TAU	FORCE PER ELEMENT	ULTIMATE CAPACITY	STRESS PATH NO.
1	-0.0039	-0.0035	0.0076	0.0033	0.0264	0.0551	3
2	-0.0036	-0.0042	0.0071	0.0045	0.0364	0.0717	3
3	-0.0033	-0.0047	0.0065	0.0059	0.0471	0.0884	3
4	-0.0030	-0.0052	0.0060	0.0073	0.0583	0.1050	3
5	-0.0027	-0.0055	0.0055	0.0087	0.0699	0.1216	3
6	-0.0025	-0.0056	0.0050	0.0099	0.0792	0.1383	3
7	-0.0023	-0.0057	0.0046	0.0105	0.0843	0.1549	3
8	-0.0021	-0.0058	0.0041	0.0111	0.0889	0.1715	3
9	-0.0019	-0.0057	0.0037	0.0115	0.0920	0.1881	3
10	-0.0017	-0.0057	0.0034	0.0114	0.0911	0.2048	3
11	-0.0015	-0.0055	0.0031	0.0111	0.0889	0.2214	3
12	-0.0014	-0.0054	0.0028	0.0108	0.0862	0.2380	3
13	-0.0013	-0.0053	0.0025	0.0104	0.0833	0.2546	3
14	-0.0012	-0.0051	0.0022	0.0100	0.0802	0.2713	3
15	-0.0011	-0.0050	0.0020	0.0096	0.0771	0.2879	3
16	-0.0010	-0.0055	0.0019	0.0103	0.0828	0.3400	3
17	-0.0009	-0.0059	0.0017	0.0110	0.0879	0.3920	3
18	-0.0009	-0.0063	0.0016	0.0116	0.0931	0.4443	3
19	-0.0008	-0.0067	0.0015	0.0124	0.0993	0.4964	3
20	-0.0008	-0.0071	0.0015	0.0134	0.1076	0.5486	3

SUM QGU(I), I =1,N : 1.5599

CONOCO-PILE safety-factor 1.2

LOAD CASE NO.: 2 WAVE PARCEL CREEP ANALYSIS
PRETENSION = 0.2000E+01 RESULTS BEFORE CREEP

RESULTS FROM LOAD CASE NO : 2
NUMBER OF ITERATIONS PERFORMED: 52
NUMBER OF ELEMENTS ACCEPTED : 20

ELEM. NO.	INCREMENTAL VALUES DDISPL	DTAU	ACCUMULATED VALUES DISPL	TAU	FORCE PER ELEMENT	ULTIMATE CAPACITY	STRESS PATH NO.
1	0.0019	0.0017	0.0095	0.0050	0.0379	0.0551	2
2	0.0017	0.0020	0.0088	0.0066	0.0525	0.0717	2
3	0.0016	0.0023	0.0081	0.0081	0.0653	0.0884	2
4	0.0014	0.0025	0.0074	0.0097	0.0781	0.1050	2
5	0.0013	0.0026	0.0068	0.0113	0.0907	0.1216	2
6	0.0012	0.0027	0.0062	0.0126	0.1008	0.1383	2
7	0.0011	0.0027	0.0056	0.0132	0.1063	0.1549	2
8	0.0010	0.0027	0.0051	0.0138	0.1109	0.1715	2
9	0.0009	0.0027	0.0046	0.0142	0.1140	0.1881	2
10	0.0008	0.0027	0.0042	0.0141	0.1129	0.2048	2
11	0.0007	0.0027	0.0038	0.0138	0.1104	0.2214	2
12	0.0007	0.0026	0.0034	0.0134	0.1075	0.2380	2
13	0.0006	0.0026	0.0031	0.0130	0.1043	0.2546	2
14	0.0006	0.0026	0.0028	0.0126	0.1011	0.2713	2
15	0.0006	0.0026	0.0026	0.0122	0.0980	0.2879	2
16	0.0005	0.0029	0.0024	0.0133	0.1063	0.3400	2
17	0.0005	0.0032	0.0022	0.0142	0.1136	0.3920	2
18	0.0005	0.0034	0.0021	0.0150	0.1207	0.4443	2
19	0.0004	0.0036	0.0020	0.0160	0.1286	0.4964	2
20	0.0004	0.0038	0.0019	0.0172	0.1383	0.5486	2

SUM QGU(I), I =1,N : 1.9999

EL.NO	TMAX	TMIN	TAV	TCY	TCRP	DCRP	FCRP(I)	RCR
1	0.679E-02	0.329E-02	0.504E-02	0.175E-02	0.481E-02	0.809E-04	0.751E-04	0.108E-01
2	0.873E-02	0.453E-02	0.663E-02	0.210E-02	0.626E-02	0.103E-03	0.121E-03	0.136E-01
3	0.106E-01	0.587E-02	0.824E-02	0.237E-02	0.771E-02	0.125E-03	0.181E-03	0.164E-01
4	0.124E-01	0.727E-02	0.985E-02	0.258E-02	0.916E-02	0.143E-03	0.247E-03	0.189E-01
5	0.142E-01	0.871E-02	0.114E-01	0.273E-02	0.106E-01	0.159E-03	0.317E-03	0.209E-01
6	0.155E-01	0.988E-02	0.127E-01	0.282E-02	0.121E-01	0.148E-03	0.337E-03	0.195E-01
7	0.163E-01	0.105E-01	0.134E-01	0.287E-02	0.135E-01	0.102E-03	0.260E-03	0.135E-01
8	0.168E-01	0.111E-01	0.140E-01	0.289E-02	0.150E-01	0.571E-04	0.161E-03	0.751E-02
9	0.172E-01	0.115E-01	0.143E-01	0.287E-02	0.164E-01	0.149E-04	0.458E-04	0.195E-02
10	0.170E-01	0.114E-01	0.142E-01	0.283E-02	0.179E-01	0.000E+00	0.000E+00	0.000E+00
11	0.166E-01	0.111E-01	0.139E-01	0.277E-02	0.193E-01	0.000E+00	0.000E+00	0.000E+00
12	0.162E-01	0.108E-01	0.135E-01	0.271E-02	0.208E-01	0.000E+00	0.000E+00	0.000E+00
13	0.157E-01	0.104E-01	0.130E-01	0.264E-02	0.222E-01	0.000E+00	0.000E+00	0.000E+00
14	0.151E-01	0.100E-01	0.126E-01	0.257E-02	0.237E-01	0.000E+00	0.000E+00	0.000E+00
15	0.146E-01	0.961E-02	0.121E-01	0.252E-02	0.251E-01	0.000E+00	0.000E+00	0.000E+00
16	0.158E-01	0.103E-01	0.131E-01	0.276E-02	0.297E-01	0.000E+00	0.000E+00	0.000E+00
17	0.169E-01	0.110E-01	0.139E-01	0.297E-02	0.342E-01	0.000E+00	0.000E+00	0.000E+00
18	0.179E-01	0.116E-01	0.148E-01	0.316E-02	0.388E-01	0.000E+00	0.000E+00	0.000E+00
19	0.191E-01	0.124E-01	0.157E-01	0.336E-02	0.433E-01	0.000E+00	0.000E+00	0.000E+00
20	0.205E-01	0.134E-01	0.170E-01	[illegible]	0.479E-01	0.000E+00	0.000E+00	0.000E+00

START OF CREEP REDISTRIBUTION
****
ALLOWABLE NUMBER OF CYCLES : 5
NO. OF CYCLES PERFORMED : 3
NO. OF CYCLES LEFT IN PARCEL : 1102
MAX. CREEP RATIO :0.021
ALLOWABLE CREEP RATIO :0.100

TAU	DCRP	ALF2	ALFAR	TAUULT
0.0050	0.0001	0.8424	0.9043	0.0069
0.0066	0.0001	1.0770	1.1769	0.0089
0.0081	0.0001	1.3049	1.4497	0.0110
0.0097	0.0001	1.5285	1.7225	0.0131
0.0113	0.0002	1.7499	1.9949	0.0152
0.0126	0.0001	2.0008	2.2688	0.0172
0.0132	0.0001	2.3139	2.5412	0.0193
0.0138	0.0001	2.6591	2.8135	0.0214
0.0142	0.0000	3.0368	3.0858	0.0235
0.0141	0.0000	3.3598	3.3598	0.0255
0.0138	0.0000	3.6321	3.6321	0.0276
0.0134	0.0000	3.9044	3.9044	0.0297
0.0130	0.0000	4.1768	4.1768	0.0317
0.0126	0.0000	4.4507	4.4507	0.0338
0.0122	0.0000	4.7230	4.7230	0.0359
0.0133	0.0000	5.5778	5.5778	0.0424
0.0142	0.0000	6.4325	6.4325	0.0489
0.0150	0.0000	7.2888	7.2888	0.0554
0.0160	0.0000	8.1435	8.1435	0.0619
[illegible]	0.0000	8.9966	8.9966	0.0684

```
C     ***********************************************************
C     *                                                         *
C     *            PROGRAM ' C R A P I L '                      *
C     *                                                         *
C     *   C R E E P   A N A L Y S I S   O F   P I L E S         *
C     *                                                         *
C     *                                                         *
C     *   VERSION 3, NOVEMBER 22, 1983                          *
C     *   T.J. KVALSTAD, VERITAS RESEARCH DIVISION              *
C     ***********************************************************
C
C     THIS PROGRAM IS A MODIFIED VERSION OF THE VERITAS PROGRAM
C     ' SOPCORE '  DEVELOPED FOR AXIAL CREEP OF PIPELINES
C
C     THE PURPOSE OF THE PROGRAM IS TO ALLOW EVALUATION OF
C     HOW CYCLIC CREEP OF A TENSION PILE SUBJECTED TO COMBINED
C     STATIC AND CYCLIC LOADING INFLUENCE THE PILE HEAD
C     DISPLACEMENT AND SHEAR STRESS DISTRIBUTION. THE
C     PROGRAM ALLOWS SIMULATION OF A STORM WITH WAVE LOADS
C     SORTED IN GROUPS OF EQUAL AMPLITUDE (WAVE PARCELS)
C     COMBINED WITH STATIC PRETENSION (WHICH MAY BE CHANGED
C     FROM PARCEL TO PARCEL.
C
C     IF THE MAXIMUM SHEAR STRESS EXCEEDS A CREEP LEVEL TAUCR(I)
C     GIVEN AS A PERCENTAGE SLIM(I) OF THE STATIC ULTIMATE SKIN
C     FRICTION TAUULT(I), THE CREEP PROCESS IS STARTED. THE SOIL IS
C     MODELLED AS A SPRING K AND A FRICTION ELEMENT R1 COUPLED IN
C     SERIES TO SIMULATE IDEAL ELASTO-PLASTIC BEHAVIOUR.
C     THIS ELEMENT IS FURTHER COUPLED IN SERIES WITH A
C     CREEP ELEMENT CONSISTING OF A FRICTION ELEMENT R2  AND
C     A DASHPOT C COUPLED IN SERIES.
C
C
      COMMON/CONTRL/NEL,NLC,IUNI,IFOC,NC
      COMMON/HEADNG/TEXT(20)
      COMMON/ITER/NIMAX,DLI,FID,DMUL
      COMMON/PILE/DOP,WT,ELP,ACP,EP,SM(2,60),SI,AS
      COMMON/SOIL/ALFAR(60),SLIM(60),C(60),QULT(60),ALF2(60)
      COMMON/DELTA/DELN(60),DELGU(60),DELO(60),DEL(60),DELNU
C
      DIMENSION QGU(60),TAUGU(60),TAU(60),TAUULT(60),TAUCR(60)
      DIMENSION NCY(30),FPRET(30),FMAX(30),FMIN(30),T(30),
     1FCRP(60),TAUUCR(60),TU(60,3),F(4),JC(60),DCRP(60)
C
C     START READING INPUT DATA
C
C     READ HEADING
C
      READ(5,8000) (TEXT(I),I=1,20)
      WRITE(6,9000) (TEXT(I),I=1,20)
C
C     READ CONTROL DATA
C
      READ(5,8010) NEL,NLC,IUNI,IFOC,IPRI
      WRITE(6,9010) NEL,NLC,IUNI,IFOC,IPRI
C
C     READ ITERATION SPEED-UP DATA
```

```
C
      READ(5,8020) NIMAX,DLI,FID
      WRITE (6,9020) NIMAX,DLI,FID
C
C     READ PILE DATA
C
      READ(5,8030) DOP,WT,ELP
      WRITE(6,9030) DOP,WT,ELP
C
C     READ SOIL DATA
C
      WRITE(6,9035)
      READ(5,8040) (TAUULT(I),SLIM(I),ALFAR(I),C(I),I=1,NEL)
      WRITE(6,9040) (I,TAUULT(I),SLIM(I),ALFAR(I),C(I),I=1,NEL)
C
C     READ LOAD CARDS
C     IF NCY=0 STATIC CASE WITH NO CREEP,
C     IF NCY>0 CYCLIC CREEP CASE
C
      WRITE(6,9045)
      READ(5,8050) (NCY(I),FPRET(I),FMAX(I),FMIN(I),T(I),I=1,NLC)
      WRITE(6,9050) (I,NCY(I),FPRET(I),FMAX(I),FMIN(I),T(I),I=1,NLC)
C
C
C     CALCULATE STEEL AREA OF PILE
      ACP=3.142*(DOP**2.-(DOP-2.*WT)**2.)/4.
C
C     DATA FOR PILE (STEEL)
C
C     YOUNG MODULUS FOR STEEL (MN/M**2 OR N/M**2)
C
      IF(IUNI.EQ.1)GO TO 100
      EP=21.*10.**(10)
C
      GO TO 120
  100 EP=21.*10.**(4)
C
      SI=EP*ACP/ELP
C
C     CALCULATE SURFACE AREA OF A PILE ELEMENT
C
  120 AS=3.142*DOP*ELP
C
C
C     ULTIMATE SOIL RESISTANCE OF ELEMENT, QULT(I):
C
      CAPST=0.
      CAPCR=0.
      DO 130 I=1,NEL
      QULT(I)=AS*TAUULT(I)
      TAUCR(I)=SLIM(I)*TAUULT(I)
      CAPST=CAPST+QULT(I)
      CAPCR=CAPCR+AS*TAUCR(I)
  130 CONTINUE
C
C
      WRITE(6,9060) ACP,SI,AS,CAPST,CAPCR
```

```
C
C     PILE STIFFNESS-MATRIX CONSTRUCTION
C     **********************************
C
      DO 140 I=1,NEL
      SM(2,I)=2*SI
      IF(I.EQ.NEL)GO TO 140
      SM(1,I+1)=-SI
  140 CONTINUE
      SM(1,1)=0.00
      SM(2,1)=SI
C
C     SUBROUTINE SPBCO SPLITS THE THREE DIAGONAL STIFFNESS MATRIX
C     INTO TWO ONE-SIDE BANDED MATRIXES ONE BEING THE TRANSPONSE
C     OF THE OTHER.
C
      CALL SPBCO(SM,2,NEL,1,RCOND,JC,INFO)
C
      IF(INFO.NE.0)GO TO 150
C
      GO TO 160
  150 CONTINUE
      WRITE(6,9500)
      STOP
  160 CONTINUE
C
C     FACTOR TO DECREASE THE DEVIATION FACTOR EADF
C
      DMUL=ELP/100.
C
      FT=0.
C
C     SET THE SOIL SPRING STIFFNESS ALF2(I)=ALFAR(I)
C     ALF2(I) DIFFERS FROM ALFAR(I) ONLY IN THE CREEP
C     REDISTRIBUTION ANALYSIS (I.E FOR NCASE=4 AND THERE
C     ONLY FOR ELEMENTS WITH MAXIMUM SHEAR STRESS EXCEEDING
C     THE CREEP LIMIT
C
C
      DO 170 I=1,NEL
      ALF2(I)=ALFAR(I)
  170 CONTINUE
C
C
C     START LOOPING ON ALL LOADCASES
C     ******************************
C
      DO 5000 NC=1,NLC
      NI=0
      IF(NCY(NC).NE.0) GO TO 1000
C
C     STATIC CASE
C
      FTN=FPRET(NC)
      WRITE(6,9100) (TEXT(I),I=1,20),NC,FTN
      NCASE=0
C
```

```
      CALL ITER(FT,FTN,TAUULT,TAU,NCASE)
C
      GO TO 5000
C
C
 1000 CONTINUE
C
C     THE FOLLOWING PART OF THE PROGRAM CALCULATES CYCLIC CREEP
C     DURING A WAVE PARCEL WITH NCY(NC) LOAD CYCLES WITH PERIOD T(NC)
C     VARYING BETWEEN A MAX LOAD OF FMAX(NC) AND A MIN LOAD OF FMIN(NC)
C     WITH A PRETENSION LOAD OF FPRET(NC)
C
C     CREEP DISPLACEMENTS IN THE SOIL DASHPOTS ARE EVALUATED PER CYCLE
C     FOR EACH SOIL ELEMENT AND AN 'ALLOWABLE' NUMBER OF CYCLES IS
C     COMBINED IN ONE ITERATION STEP. THE ALLOWABLE NUMBER IS IN THIS
C     VERSION OF THE PROGRAM CHOSEN SO THAT THE DASHPOT CREEP RESULTS
C     IN A MAXIMUM RELAXATION OF THE SPRING FORCE LESS OR EQUAL TO
C     10 PERCENT OF THE ULTIMATE CAPACITY OF THE FRICTION ELEMENT,
C     I.E 10 PERCENT OF TAUULT.
C
C     THE STEPS ARE PERFORMED UNTIL ALL CYCLES IN A WAVE
C     PARCEL HAVE BEEN RUN THROUGH BEFORE THE NEXT WAVE PARCEL
C     IS STARTED ON.
C
      NREST=NCY(NC)
      F(1)=FMAX(NC)
      F(2)=FMIN(NC)
      F(3)=FPRET(NC)
      F(4)=FPRET(NC)
C
C
 1040 CONTINUE
C
C     CALCULATE MAX., MIN. AND PRETENSION SHEAR STRESS DISTRIBUTION
C     AND CORRESPONDING DISPLACEMENTS ASSUMING NO CREEP
C
      DO 1050 LC=1,3
      NCASE=LC
      FTN=F(LC)
      IF(LC.EQ.1) WRITE(6,9150) (TEXT(I),I=1,20),NC,FTN
      IF(LC.EQ.2) WRITE(6,9200) (TEXT(I),I=1,20),NC,FTN
      IF(LC.EQ.3) WRITE(6,9250) (TEXT(I),I=1,20),NC,FTN
C
      CALL ITER(FT,FTN,TAUULT,TAU,NCASE)
C
      DO 1045 I=1,NEL
      TU(I,LC)=TAU(I)
 1045 CONTINUE
 1050 CONTINUE
C
C     CALCULATE AVERAGE SHEAR STRESS IN ALL ELEMENTS
C
      RCRMAX=0.
      WRITE(6,9260)
      DO 1100 I=1,NEL
      FCRP(I)=0.
      TMAX=TU(I,1)
```

```
      TMIN=TU(I,2)
      TAV=0.5*(TMAX+TMIN)
      TCY=ABS(TMAX-TAV)
      TCRP=TAUCR(I)
C
C     THE SHEAR STRESS IS ASSUMED TO BE A SINE FUNCTION OF TIME
C     VARYING BETWEEN TMAX AND TMIN AROUND THE AVERAGE SHEAR
C     STRESS TAV WITH AN AMPLITUDE TCY.
C
C     THIS IS A SIMPLIFYING ASSUMPTION WHICH IS NOT 100 PERCENT
C     CORRECT FOR ELEMENTS WHERE THE ULTIMATE CAPACITY IS
C     REACHED. THE ASSUMPTION WILL LEAD TO A SLIGHT UNDERESTIMATION
C     OF CREEP DISPLACEMENT PER CYCLE
C
C     CALCULATE AREA OF ASSUMED SINE LOAD ABOVE +TAUCR AND
C     BELOW -TAUCR BY NUMERICAL INTEGRATION AND DIVIDE BY THE
C     DAMPING CONSTANT C OF THE DASHPOT TO CALCULATE THE
C     CREEP DISPLACEMENT DCRP(I) PER CYCLE FOR A FREESTANDING ELEMENT
C     I.E. IF THE ELEMENT WAS NOT CONNECTED TO THE REST OF THE PILE.
C
C     PERIOD T(NC) IS SPLIT IN 20 INCREMENTS AND THE SHEAR STRESS TAUTTI IN THE
C     MIDDLE OF EACH INCREMENT IS CALCULATED BASED ON THE ABOVE DESCRIBED
C     SINE VARIATION.
C
      DCRP(I)=0.
      TTI=0.
      DT=T(NC)/20.
      DO 1060 K=1,20
      TTI=DT/2.+(K-1)*DT
      TAUTTI=TAV+TCY*SIN(6.283185*TTI/T(NC))
      IF(ABS(TAUTTI).LT.TCRP) GO TO 1060
      FAC=1.0
      IF(TAUTTI.LT.0.) FAC=-1.
      DCRP(I)=DCRP(I)+(TAUTTI-FAC*TCRP)*DT/C(I)
 1060 CONTINUE
C
C     CALCULATE RELAXATION FORCE FCRP(I) CAUSED BY THE CREEP
C     DISPLACEMENT OF ONE CYCLE DCRP(I). CALCULATE THE RATIO
C     BETWEEN THE RELAXATION FORCE AND THE ULTIMATE CAPACITY
C     OF THE SOIL ELEMENT RCR AND DEFINE THE MAXIMUM VALUE
C     AMONG ALL PILE ELEMENTS
C
      FCRP(I)=ALFAR(I)*DCRP(I)
      RCR=FCRP(I)/TAUULT(I)
      IF(RCR.GT.RCRMAX) RCRMAX=RCR
      WRITE(6,9265) I,TMAX,TMIN,TAV,TCY,TCRP,DCRP(I),FCRP(I),RCR
 1100 CONTINUE
      IF(RCRMAX.GT.0.) GO TO 1110
      WRITE(6,9270)
      GO TO 5000
C
C     CHECK IF SOIL SPRING RELAXATION DUE TO CREEP OF DCRP IN ONE
C     CYCLE EXCEEDS 10 PERCENT (0.1) OF THE CAPACITY IN ANY SOIL ELEMENT
C     IF YES: PERFORM ONLY 1 CYCLE PER STEP
C     IF NO:  CALCULATE ALLOWABLE NUMBER OF CYCLES FOR MOST CREEPING
C             ELEMENT TO AVOID MORE THAN 10 PERCENT RELAXATION
C
```

```
 1110 RCRALW=0.1
      KCY=1
      IF(RCRMAX.GE.RCRALW) GO TO 1120
      RKCY=RCRALW/RCRMAX
      KCY=ANINT(RKCY)
 1120 IF(KCY.GE.NREST) KCY=NREST
C
C     CALCULATE THE NUMBER OF CYCLES EVALUATED WITHIN THIS WAVE PARCEL
C     NPERF INCLUDING THE KCY CYCLES OF THIS STEP AND CALCULATE THE
C     NUMBER OF CYCLES LEFT IN THE PARCEL, NREST.
      NREST=NREST-KCY
      NPERF=NCY(NC)-NREST
C
C     CALCULATE REDUCED SOIL STIFFNESS ALF2(I) ACCORDING TO CALCULATED
C     CREEP DISPLACEMENTS CAUSED BY KCY CYCLES FOR EACH ELEMENT
C
      WRITE(6,9274) KCY,NPERF,NREST,RCRMAX,RCRALW
      WRITE(6,9280)
      DO 1150 I=1,NEL
      ALF2(I)=TAU(I)/(DEL(I)-DELO(I)+DCRP(I)*KCY)
      WRITE(6,9275) TAU(I),DCRP(I),ALF2(I),ALFAR(I),TAUULT(I)
 1150 CONTINUE
C
C
C
C     CALCULATE NEW SHEAR STRESS AND DISPLACEMENT DISTRIBUTION
C     BY ITERATING WITH PRETENSION FORCE AND REDUCED SOIL STIFFNESS
C     CORRESPONDING TO CREEP DISPLACEMENT IN CREEPING ELEMENTS
C
      NCASE=4
      FTN=F(4)
      WRITE(6,9300) (TEXT(I),I=1,20),NC,FTN,NPERF
C
      CALL ITER(FT,FTN,TAUULT,TAU,NCASE)
C
C     RESET SOIL STIFFNESS FROM ALF2 TO ALFAR FOR EVALUATION OF
C     NEXT PART OF WAVE PARCEL OR FOR START ON NEW WAVE PARCEL
C
      DO 1160 I=1,NEL
      ALF2(I)=ALFAR(I)
 1160 CONTINUE
C
      IF(NREST.LE.0) GO TO 5000
      GO TO 1040
C
 5000 CONTINUE
C
C
 8000 FORMAT(20A4)
 8010 FORMAT(10I5)
 8020 FORMAT(I5,5F10.3)
 8030 FORMAT(8F10.4)
 8040 FORMAT(4F10.3)
 8050 FORMAT(I5,4F10.3)
C
 9000 FORMAT(1H1//
     15X,'*************************************************',/
```

```
      25X,'*                                                  *',/
      35X,'*      PROGRAM  '  C R A P I L  '                  *',/
      35X,'*                                                  *',/
      45X,'*       CREEP ANALYSIS OF PILES                    *',/
      55X,'*                                                  *',/
      55X,'*     VERSION 3, NOVEMBER 22, 1983                 *',/
      55X,'*          TORE J. KVALSTAD                        *',/
      55X,'*      VERITAS RESEARCH DIVISION                   *',/
      65X,'*****************************************************',///
      71X,20A4/
      81X,'*******************************************************'///)
 9010 FORMAT(' CONTROL DATA:'/' *************'//
     1'     NUMBER OF PILE ELEMENTS        :',I5/
     2'     NUMBER OF LOAD CARDS           :',I5/
     3'     UNIT SWITCH                    :',I5,'  IF = 0   N AND M'/
     4'                                           IF = 1  MN AND M'/
     5'     PILE BOTTOM SWITCH             :',I5,'  IF = 1  CLAMPED'/
     6'                                           IF = 0  FREE'/
     7'     PRINT SWITCH                   :',I5,'  IF = 0  NOT ACTIVATED'/
     8'                                           IF = 1  ACTIVATED'//)
 9020 FORMAT(' ITERATION DATA:'/' ***************'//
     1'     MAX. NUMBER OF ITERATIONS      :',I5,/
     2'     DISPLACEMENT TOLERANCE         :',F10.8/
     3'     DISPLACEMENT DECREASE FACTOR   :',F10.4//)
 9030 FORMAT(' PILE DATA:'/' **********'//
     1'     OUTER DIAMETER OF PILE         :',F10.3/
     2'     WALL THICKNESS                 :',F10.5/
     3'     PILE ELEMENT LENGTH            :',F10.3//)
 9035 FORMAT(1H1,' SOIL DATA:'/' **********'//
     1'     ELEM.    SKIN       CREEP       SOIL        DAMPING'/
     2'      NO.   FRICTION    RATIO     STIFFNESS     CONSTANT'//)
 9040 FORMAT(5X,I3,4E11.4)
 9045 FORMAT(1H1,' LOAD DATA:'/' **********'//
     1'      LOAD  NO. OF  PRETENSION  MAX. LOAD  MIN. LOAD   WAVE'/
     2'      CARD  CYCLES  OR STATIC    IN WAVE    IN WAVE   PERIOD'/
     3'       NO. IN PARCEL  FORCE      PARCEL     PARCEL'//)
 9050 FORMAT(3X,I5,I7,3E11.4,F10.2)
 9060 FORMAT(///
     1'     STEEL CROSS SECTION OF PILE    :',F10.3/
     2'     PILE ELEMENT STIFFNESS, SI     :',E11.3/
     3'     SURFACE AREA OF PILE ELEMENT   :',F10.3/
     4'     STATIC AXIAL CAPACITY OF PILE  :',F10.3/
     5'     ULTIMATE CREEP CAPACITY        :',F10.3/)
 9100 FORMAT(1H1//1X,20A4//
     1' LOAD CASE NO.: ',I5,'  STATIC ANALYSIS WITHOUT CYCLIC CREEP'/
     2' STATIC LOAD =',E11.4//)
 9150 FORMAT(1H1//1X,20A4//
     1' LOAD CASE NO.: ',I5,'  WAVE PARCEL CREEP ANALYSIS'/
     2' MAX. LOAD   =',E11.4//)
 9200 FORMAT(1H1//1X,20A4//
     1' LOAD CASE NO.: ',I5,'  WAVE PARCEL CREEP ANALYSIS'/
     2' MIN. LOAD   =',E11.4//)
 9250 FORMAT(1H1//1X,20A4//
     1' LOAD CASE NO.: ',I5,'  WAVE PARCEL CREEP ANALYSIS'/
     2' PRETENSION  =',E11.4,' RESULTS BEFORE CREEP'//)
 9260 FORMAT(1H1
     1'     EL.NO      TMAX        TMIN        TAV         TCY
```

```
      2        TCRP       DCRP        FCRP(I)        RCR'//)
 9265 FORMAT(I5,6X,8E11.3)
 9270 FORMAT(//
     1' ****************************************'/
     2' * NO ELEMENTS CREEPING IN THIS STEP   *'/
     3' * CONTNUE WITH NEXT WAVE PARCEL       *'/
     3' ****************************************'//)
 9274 FORMAT(///
     1' START OF CREEP REDISTRIBUTION'/
     1' ******************************'/
     1' ALLOWABLE NUMBER OF CYCLES    :',I5/
     2' NO. OF CYCLES PERFORMED       :',I5/
     3' NO. OF CYCLES LEFT IN PARCEL  :',I5/
     4' MAX. CREEP RATIO              :',F5.3/
     5' ALLOWABLE CREEP RATIO         :',F5.3//)
 9275 FORMAT(5F12.4)
 9280 FORMAT(
     1'    TAU        DCRP        ALF2       ALFAR        TAUULT'/)
 9300 FORMAT(1H1//1X,20A4//
     1' LOAD CASE NO.: ',I5,'  WAVE PARCEL CREEP ANALYSIS'/
     2' PRETENSION  =',E11.4,' RESULTS AFTER ',I5,' CYCLES'//)
 9500 FORMAT(//' ******ERROR IN SUBROUTINE SPBCO'//)
C
      END
```

PROGRAM SECTIONS

	Name	Bytes	Attributes
0	$CODE	2700	PIC CON REL LCL SHR EXE RD NOWRT LONG
1	$PDATA	3175	PIC CON REL LCL SHR NOEXE RD NOWRT LONG
2	$LOCAL	3684	PIC CON REL LCL NOSHR NOEXE RD WRT LONG
3	CONTRL	20	PIC OVR REL GBL SHR NOEXE RD WRT LONG
4	HEADNG	80	PIC OVR REL GBL SHR NOEXE RD WRT LONG
5	ITER	16	PIC OVR REL GBL SHR NOEXE RD WRT LONG
6	PILE	508	PIC OVR REL GBL SHR NOEXE RD WRT LONG
7	SOIL	1200	PIC OVR REL GBL SHR NOEXE RD WRT LONG
8	DELTA	964	PIC OVR REL GBL SHR NOEXE RD WRT LONG
	Total Space Allocated	12347	

ENTRY POINTS

Address	Type	Name
0-00000000		CRAPIL$MAIN

VARIABLES

Address	Type	Name	Address	Type	Name
6-0000000C	R*4	ACP	6-000001F8	R*4	AS
8-000003C0	R*4	DELNU	5-00000004	R*4	DLI
2-00000DF8	R*4	DT	6-00000008	R*4	ELP
5-00000008	R*4	FID	2-00000DC4	R*4	FT
3-0000000C	I*4	IFOC	2-00000DBC	I*4	INFO
3-00000008	I*4	IUNI	2-00000DFC	I*4	K
3-00000010	I*4	NC	2-00000DD0	I*4	NCASE
5-00000000	I*4	NIMAX	3-00000004	I*4	NLC
2-00000DB8	R*4	RCOND	2-00000E08	R*4	RCR
2-00000E14	R*4	RKCY	6-000001F4	R*4	SI
2-00000DF0	R*4	TCRP	2-00000DEC	R*4	TCY
2-00000DF4	R*4	TTI	6-00000004	R*4	WT

Address	Type	Name	Address	Type	Name
2-00000DB4	R*4	CAPCR	2-00000DB0	R*4	CAPST
5-0000000C	R*4	DMUL	6-00000000	R*4	DOP
6-00000010	R*4	EP	2-00000E04	R*4	FAC
2-00000DCC	R*4	FTN	2-00000DA8	I*4	I
2-00000DC0	I*4	INFO	2-00000DAC	I*4	IPRI
2-00000E10	I*4	KCY	2-00000DD8	I*4	LC
3-00000000	I*4	NEL	2-00000DCB	I*4	NI
2-00000E18	I*4	NPERF	2-00000DD4	I*4	NREST
2-00000E0C	R*4	RCRALW	2-00000DDC	R*4	RCRMAX
2-00000E00	R*4	TAUTTI	2-00000DE8	R*4	TAV
2-00000DE0	R*4	TMAX	2-00000DE4	R*4	TMIN

ARRAYS

Address	Type	Name	Bytes	Dimensions
7-000003C0	R*4	ALF2	240	(60)
7-00000000	R*4	ALFAR	240	(60)
7-000001E0	R*4	C	240	(60)
2-00000CB8	R*4	DCRP	240	(60)
8-000002D0	R*4	DEL	240	(60)
8-000000F0	R*4	DELGU	240	(60)
8-00000000	R*4	DELN	240	(60)
8-000001E0	R*4	DELO	240	(60)
2-00000BB8	R*4	F	16	(4)
2-00000708	R*4	FCRP	240	(60)
2-000005A0	R*4	FMAX	120	(30)
2-00000618	R*4	FMIN	120	(30)
2-00000528	R*4	FPRET	120	(30)
2-00000BC8	I*4	JC	240	(60)
2-000004B0	I*4	NCY	120	(30)
2-00000000	R*4	QGU	240	(60)
7-000002D0	R*4	QULT	240	(60)
7-000000F0	R*4	SLIM	240	(60)
6-00000014	R*4	SM	480	(2, 60)
2-00000690	R*4	T	120	(30)
2-000001E0	R*4	TAU	240	(60)
2-000003C0	R*4	TAUCR	240	(60)
2-000000F0	R*4	TAUGU	240	(60)
2-000007F8	R*4	TAUUCR	240	(60)
2-000002D0	R*4	TAUULT	240	(60)
4-00000000	R*4	TEXT	80	(20)
2-000008E8	R*4	TU	720	(60, 3)

LABELS

Address	Label	Address	Label	Address	Label
0-000003E4	100	0-000003F9	120	**	130
**	170	0-000005A3	1000	0-000005CE	1040
**	1100	0-00000BAC	1110	0-000008D1	1120
1-00000008	8000'	1-0000000D	8010'	1-00000012	8020'
1-0000002E	9000'	1-0000028D	9010'	1-0000046C	9020'
1-00000644	9045'	1-00000718	9050'	1-00000727	9060'
1-00000904	9250'	1-00000971	9260'	1-000009DC	9265'
1-00000B95	9280'	1-00000BCE	9300'	1-00000C40	9500'

Address	Label	Address	Label	Address	Label
0-000004BB	140	0-000004D7	150	0-000004F4	160
**	1045	**	1050	0-000007CE	1060
**	1150	**	1160	0-00000A7C	5000
1-0000001A	8030'	1-00000020	8040'	1-00000026	8050'
1-0000050F	9030'	1-000005A9	9035'	1-0000063A	9040'
1-000007F8	9100'	1-00000858	9150'	1-000008AE	9200'
1-000009E6	9270'	1-00000A92	9274'	1-00000B8F	9275'

FUNCTIONS AND SUBROUTINES REFERENCED

Type	Name	Type	Name	Type	Name	Type	Name
	ITER	R*4	MTH$ANINT	R*4	MTH$SIN		SP8CO

COMMAND QUALIFIERS

```
FORTRAN /STANDARD=ALL/LIS/NOST CRAPIL,ITER

/CHECK=(NOBOUNDS,OVERFLOW,NOUNDERFLOW)
/DEBUG=(NOSYMBOLS,TRACEBACK)
/STANDARD=(NOSYNTAX,NOSOURCE_FORM)
/SHOW=(NOPREPROCESSOR,NOINCLUDE,MAP)
/F77  /NOG_FLOATING  /I4  /OPTIMIZE  /WARNINGS  /NOD_LINES

/NOCROSS_REFERENCE  /NOMACHINE_CODE  /CONTINUATIONS=19
```

COMPILATION STATISTICS

```
Run Time:            7.21 seconds
Elapsed Time:        10.06 seconds
Page Faults:         543
Dynamic Memory:      198 pages
```

```
      SUBROUTINE ITER(FT,FTN,TAUULT,TAU,NCASE)
C
C
C     THIS SUBROUTINE PERFORMS THE CALCULATION OF SHEAR STRESS
C     DISTRIBUTION AND DISPLACEMENTS ALONG A PILE SUBJECTED TO
C     AN AXIAL PILE HEAD LOAD FTN AND BEING SUPPORTED BY SOIL
C     SPRINGS HAVING A ULTIMATE CAPACITY EQUAL QULT CORRESPONDING
C     TO AN ULTIMATE SKIN FRICTION EQUAL TAUULT.
C
C     PLEASE NOTE THAT MOST OF THE ITERATION SCHEME,
C     APPROXIMATELY DOWN TO LABEL 350, WAS TAKEN
C     DIRECTLY FROM THE VERITAS PROGRAM SOPCORE USED FOR
C     ANALYSIS OF PIPELINE CREEP AND HAS NOT BEEN REVISED
C     OR OPTIMIZED TO FIT THE SPECIAL PURPOSE OF PILE
C     CREEP ANALYSIS.
C
C     THE METHOD APPLIED IS THE METHOD OF INITIAL STIFFNESS.
C     THE PILE IS TREATED ELASTIC AND THE SOIL FOLLOWS A
C     IDEAL ELASTO-PLASTIC LOAD (SHEAR STRESS) - DISPLACEMENT
C     RELATIONSHIP.
C
C     THE PILE STIFFNESS MATRIX HAS BEEN SET UP AND INVERTED
C     IN THE MAIN PROGRAM. A PILE DISPLACEMENT VECTOR DELGU(I) IS
C     GUESSED. THE CORRESPONDING SOIL REACTION FORCES FF(I) ARE
C     CALCULATED AND THE LOAD VECTOR FP(I) TO BE APPLIED ALONG THE
C     PILE IS THUS SET UP BEING COMPOSED OF THE PILE HEAD LOAD
C     AND THE NEGATIVE SOIL REACTION FORCES.
C
C     THE NEW PILE DISPLACEMENTS DELN(I) CAN NOW BE CALCULATED
C     BY BACKSUBSTITUTION IN THE INVERTED STIFFNESS MATRIX.
C     THE NEW DISPLACEMENTS ARE COMPARED WITH THE GUESSED
C     DISPLACEMENTS. IF ALL PILE DISPLACEMENTS ARE WITHIN THE
C     TOLERANCE LIMIT CALLED DLI THE OVERALL EQUILIBRIUM
C     BETWEEN SOIL REACTION FORCES AND PILE HEAD LOAD IS
C     CHECKED. IF THIS DIFFERENCE IS ALSO WITHIN THE TOLERANCE
C     LIMIT THE SOLUTION IS ACCEPTED. IF ONE OF THESE
C     ACCEPTENCE CRITERIA IS NOT FULFILLED, THE ITERATIVE
C     PROCESS IS CONTINUED. BASED ON THE DIFFERENCE BETWEEN
C     GUESSED AND CALCULATED DISPLACEMENTS OR THE DIFFERENCE .
C     BETWEEN SUM OF SOIL REACTION FORCES AND PILE HEAD LOAD
C     EITHER THE GUESSED DISPLACEMENTS ARE ADJUSTED OR THE
C     LOAD VECTOR IS ADJUSTED TO IMPROVE THE ACCURACY.
C
C     A PRINT OF THE CHANGES IN DISPLACEMENT AND SHEAR STRESS
C     DISTRIBUTION COMPARED WITH THE LAST LOAD STEP, THE NEW
C     SHEAR STRES AND DISPLACEMENT DISTRIBUTIONS, THE SOIL
C     REACTION FORCE ON EACH PILE ELEMENT AND THE CORRESPONDING
C     CAPACITY IS PRINTED AND FINALLY THE TOTAL SOIL REACTION
C     FORCE IS PRINTED  TO ALLOW A COMPARISON WITH THE
C     SPECIFIED PILE HEAD LOAD BEFORE THE RETURN TO THE
C     MAIN PROGRAM IS MADE
C
      COMMON/HEADNG/TEXT(20)
      COMMON/CONTRL/N,NLC,IUNI,IFOC,NC
      COMMON/ITER/NIMAX,DLI,FID,DMUL
      COMMON/PILE/DOP,WT,ELP,ACP,EP,SM(2,60),SI,AS
      COMMON/SOIL/ALFAR(60),SLIM(60),C(60),QULT(60),ALF2(60)
```

```
      COMMON/DELTA/DELN(60),DELGU(60),DELO(60),DEL(60),DELNU
C
C
      DIMENSION QGU(60),TAUULT(60),IGRAPH(60),FF(60),FP(60)
      DIMENSION TAU(60),TAUGU(60),DDEL(60),DTAU(60)
C
C     START OF ITERATION LOOP, MAXIMUM NUMBER OF ITERATIONS
C     IS NIMAX
C
      NI=0
C
  200 CONTINUE
      DO 268 I=1,N
C
C        THE FOLLOWING CORRECTION FACTORS ARE APPLIED TO ESTIMATE
C        DELGU(I)):
C
C        EADF  = DEVIATION FACTOR
C
C        DMUL  = FACTOR DEPENDENT ON THE PILE ELEMENT LENGTH
C                CALCULATED IN THE MAIN PROGRAM AS ELP/100.
C
C        FID   = ITERATION SPEED-UP FACTOR SPECIFIED BY THE USER
C
C        ERSPR = ELASTICITY RATIO BETWEEN SOIL AND PILE
C
C     THE TOTAL CORRECTION FACTOR APPLIED TO THE DISPLACEMENT
C     DIFFERENCE DELN(I)-DELGU(I) IS EQUAL TO ERSPR*DMUL*FID
C     THIS SEEMS TO BE DEPENDENT ON THE UNITS USED. A SIMPLER
C     APPROACH SHOULD BE SOUGHT, POSSIBLY A SPECIFIED FRACTION
C     OF THE DISPLACEMENT DIFFERENCE COULD BE USED AS A
C     CORRECTION FACTOR, I.E A STATEMENT AS BELOW WOULD
C     PROBABLY BE EQUALLY EFFICIENT:
C
C     DELGU(I)=DELGU(I)+(DELN(I)-DELGU(I))*FACTOR
C
C
      EADF=(DELN(I)-DELGU(I))*DMUL*FID
      ERSPR=SI/(400.*AS*ALFAR(I))
C
  201 IF(FTN-FT)208,216,216
C
  208 CONTINUE
      IF(DELGU(I)-DELO(I))210,210,212
C
C
  210 SO=-1.0
      DELGU(I)=DELGU(I)+ERSPR*EADF
      IF(DELGU(I)-DELO(I))260,260,250
C
C
  212 SO=1.0
      DELGU(I)=DELGU(I)+ERSPR*EADF
      IF(DELGU(I)-DELO(I))260,260,250
C
C
  216 CONTINUE
```

```
      IF(DELGU(I)-DELO(I))218,220,220
C
C
  218 SO=-1.0
      DELGU(I)=DELGU(I)+ERSPR*EADF
      IF(DELGU(I)-DELO(I))240,230,230
C
C
  220 SO=1.0
      DELGU(I)=DELGU(I)+ERSPR*EADF
      IF(DELGU(I)-DELO(I))240,230,230
C
C
  230 IGRAPH(I)=2
      IF(TAU(I))234,232,232
  232 DELO(I)=DEL(I)-TAU(I)/ALFAR(I)
  234 TAUGU(I)=(DELGU(I)-DELO(I))*ALF2(I)
      GO TO 266
C
C
  240 IGRAPH(I)=5
      DELO(I)=DEL(I)-TAU(I)/ALFAR(I)
      TAUGU(I)=(DELGU(I)-DELO(I))*ALF2(I)
      IF(TAUGU(I)-TAU(I))246,246,248
  246 TAUGU(I)=TAU(I)
  248 GO TO 266
C
C
  250 IGRAPH(I)=3
      DELO(I)=DEL(I)-TAU(I)/ALFAR(I)
      TAUGU(I)=(DELGU(I)-DELO(I))*ALF2(I)
      IF(TAUGU(I)-TAU(I))256,256,254
  254 TAUGU(I)=TAU(I)
  256 GO TO 266
C
C
  260 IGRAPH(I)=4
      IF(TAU(I))262,262,264
  262 DELO(I)=DEL(I)-TAU(I)/ALFAR(I)
  264 TAUGU(I)=(DELGU(I)-DELO(I))*ALF2(I)
      GO TO 266
C
C
  266 CONTINUE
  268 CONTINUE
  269 CONTINUE
C
C     TAUGU CAN NOT EXCEED TAUULT
C
  270 DO 274 I=1,N
      IF(ABS(TAUGU(I)).LE.TAUULT(I))GO TO 271
      TAUGU(I)=(ABS(TAUGU(I))/TAUGU(I))*TAUULT(I)
C
C     SOIL'S REACTION FORCE
C
  271 FF(I)=AS*TAUGU(I)
      FP(I)=-FF(I)
```

```
  274 CONTINUE
      FP(1)=FTN-FF(1)
      IF(IFOC.EQ.1)GO TO 280
C
C     CALCULATING THE EQUIVALENT FORCE TAKEN BY THE LAST ELEMENT
C     IN THE PILE WHEN THE PILE'S TIP IS FREE
C
      FP(N)=FP(N)+SI*DELNU+FALF
  280 CONTINUE
C
C     SUBROUTINE SPBSL - BACKWARDS SUBSTITUTION TO FIND THE DISPLA-
C     CEMENTS DUE TO THE LOAD VECTOR FP
C     SM = INVERTED PILE STIFFNESS MATRIX
C     FP = LOAD VECTOR AS INPUT TO SPBSL
C     FP = DISPLACEMENT VECTOR WHEN RETURNED TO THIS SUBROUTINE
C
  300 CALL SPBSL(SM,2,N,1,FP)
C
      DO 301 I=1,N
      DELN(I)=FP(I)
  301 CONTINUE
C
      DELNU=DELN(N)
C
C
  310 NACCEP=0
      NI=NI+1
C
C     CHECK DISPLACEMENT CONVERGENCE
C
      DO 340 I=1,N
      IF(ABS(DELN(I)-DELGU(I))-DLI)320,338,338
  320 NACCEP=NACCEP+1
  338 CONTINUE
  340 CONTINUE
C
C     CHECK NUMBER OF ITERATIONS PERFORMED
C
      IF(NI.GT.NIMAX) GO TO 375
      IF(NACCEP-N)350,370,370
C
  350 GO TO 200
C
C     SUM UP SOIL REACTION FORCES ALONG PILE
C
  370 TQGU=0.0
      DO 601 I=1,N
      QGU(I)=AS*TAUGU(I)
      TQGU=TQGU+QGU(I)
  601 CONTINUE
C
C     CHECK EQUILIBRIUM, SUM OF SOIL REACTION FORCES = PILE TOP LOAD
C
      IF(ABS(TQGU-FTN)-DLI)372,372,373
C
C
  373 IF(IFOC.EQ.1)GO TO 372
```

```
  371 IF(FTN.NE.0.)GO TO 602
      FALF=TQGU*DLI
      GO TO 200
  602 FALF=(FTN-TQGU)*DLI
      GO TO 200
C
C     END OF ITERATION LOOP
C
  375 WRITE(6,9000)
  372 WRITE(6,9010) NC,NI,NACCEP
      WRITE(6,9100)
C
C
      DO 380 I=1,N
      DDEL(I)=DELGU(I)-DEL(I)
      DTAU(I)=TAUGU(I)-TAU(I)
      DEL(I)=DELGU(I)
      DELN(I)=DEL(I)
      TAU(I)=TAUGU(I)
      WRITE(6,9120) I,DDEL(I),DTAU(I),DEL(I),TAU(I),QGU(I),QULT(I),
     1IGRAPH(I)
  380 CONTINUE
      FT=FTN
      FALF=0.0
      WRITE(6,9130)TQGU
      RETURN
 9000 FORMAT(/////,5X,'MAXIMUM NUMBER OF ITERATIONS EXCEEDED')
 9010 FORMAT(/
     1' RESULTS FROM LOAD CASE NO     :',I5/
     2' NUMBER OF ITERATIONS PERFORMED:',I5/
     3' NUMBER OF ELEMENTS ACCEPTED   :',I5//)
 9100 FORMAT(/
     1' ELEM.  INCREMENTAL VALUES      ACCUMULATED VALUES    FORCE PER
     2 ULTIMATE   STRESS'/
     3'  NO.    DDISPL      DTAU        DISPL        TAU      ELEMENT
     4 CAPACITY  PATH NO.'/
     5' ****************************************************************
     6*******************'//)
 9120 FORMAT(I4,6F12.4,I3)
 9130 FORMAT(/,1X,'SUM QGU(I), I =1,N :',F12.4)
      END
```

PROGRAM SECTIONS

	Name	Bytes	Attributes								
0	$CODE	1602	PIC	CON	REL	LCL	SHR	EXE	RD	NOWRT	LONG
1	$PDATA	470	PIC	CON	REL	LCL	SHR	NOEXE	RD	NOWRT	LONG
2	$LOCAL	1800	PIC	CON	REL	LCL	NOSHR	NOEXE	RD	WRT	LONG
3	HEADNG	80	PIC	OVR	REL	GBL	SHR	NOEXE	RD	WRT	LONG
4	CONTRL	20	PIC	OVR	REL	GBL	SHR	NOEXE	RD	WRT	LONG
5	ITER	16	PIC	OVR	REL	GBL	SHR	NOEXE	RD	WRT	LONG
6	PILE	508	PIC	OVR	REL	GBL	SHR	NOEXE	RD	WRT	LONG
7	SOIL	1200	PIC	OVR	REL	GBL	SHR	NOEXE	RD	WRT	LONG
8	DELTA	964	PIC	OVR	REL	GBL	SHR	NOEXE	RD	WRT	LONG
	Total Space Allocated	6660									

ENTRY POINTS

Address	Type	Name
0-00000000		ITER

VARIABLES

Address	Type	Name	Address	Type	Name
6-0000000C	R*4	ACP	6-000001F8	R*4	AS
5-0000000C	R*4	DMUL	6-00000000	R*4	DOP
6-00000010	R*4	EP	2-0000069C	R*4	ERSPR
AP-00000004@	R*4	FT	AP-00000008@	R*4	FTN
4-00000008	I*4	IUNI	4-00000000	I*4	N
AP-00000014@	I*4	NCASE	2-00000690	I*4	NI
6-000001F4	R*4	SI	2-000006A0	R*4	SO

Address	Type	Name	Address	Type	Name
8-000003C0	R*4	DELNU	5-00000004	R*4	DLI
2-00000698	R*4	EADF	6-00000008	R*4	ELP
2-000006A4	R*4	FALF	5-00000008	R*4	FID
2-00000694	I*4	I	4-0000000C	I*4	IFOC
2-000006A8	I*4	NACCEP	4-00000010	I*4	NC
5-00000000	I*4	NIMAX	4-00000004	I*4	NLC
2-000006AC	R*4	TQGU	6-00000004	R*4	WT

ARRAYS

Address	Type	Name	Bytes	Dimensions
7-000003C0	R*4	ALF2	240	(60)
7-00000000	R*4	ALFAR	240	(60)
7-000001E0	R*4	C	240	(60)
2-000004B0	R*4	DDEL	240	(60)
8-000002D0	R*4	DEL	240	(60)
8-000000F0	R*4	DELGU	240	(60)
8-00000000	R*4	DELN	240	(60)
8-000001E0	R*4	DELO	240	(60)
2-000005A0	R*4	DTAU	240	(60)
2-000001E0	R*4	FF	240	(60)
2-000002D0	R*4	FP	240	(60)
2-000000F0	I*4	IGRAPH	240	(60)
2-00000000	R*4	QGU	240	(60)
7-000002D0	R*4	QULT	240	(60)
7-000000F0	R*4	SLIM	240	(60)
6-00000014	R*4	SM	480	(2, 60)
AP-00000010@	R*4	TAU	240	(60)
2-000003C0	R*4	TAUGU	240	(60)
AP-0000000C@	R*4	TAUULT	240	(60)
3-00000000	R*4	TEXT	80	(20)

LABELS

Address	Label	Address	Label	Address	Label
0-00000021	200	0-0000007A	201	0-00000081	208
0-00000105	218	0-00000133	220	0-0000015C	230
0-00000211	246	0-0000021D	248	0-00000220	250
0-0000029D	262	0-000002BE	264	0-000002E2	266
0-0000033D	271	0-0000035C	274	0-0000039C	280
0-00000417	320	0-0000041A	338	0-0000041A	340
0-000004C9	372	0-00000486	373	0-000004B3	375
1-00000008	9000'	1-00000037	9010'	1-000000A9	9100'

Address	Label	Address	Label	Address	Label
0-00000094	210	0-000000C3	212	0-000000F2	216
0-00000170	232	0-00000191	234	0-000001B6	240
0-0000027B	254	0-00000287	256	0-00000289	260
0-000002E2	268	0-000002EA	269	0-000002EA	270
0-0000039C	300	0-000003C6	301	0-000003DF	310
0-00000436	350	0-00000439	370	0-0000048F	371
0-00000611	380	0-0000046C	601	0-000004A1	602
1-000001AF	9120'	1-000001B9	9130'		

FUNCTIONS AND SUBROUTINES REFERENCED

Type	Name
	SPBSL

COMMAND QUALIFIERS

```
FORTRAN /STANDARD=ALL/LIS/NOOP Æ23OCEAN.CREEPAITER

/CHECK=(NOBOUNDS,OVERFLOW,NOUNDERFLOW)
/DEBUG=(NOSYMBOLS,TRACEBACK)
/STANDARD=(SYNTAX,SOURCE_FORM)
/SHOW=(NOPREPROCESSOR,NOINCLUDE,MAP)
/F77  /NOG_FLOATING  /I4  /NOOPTIMIZE  /WARNINGS  /NOD_LINES

/NOCROSS_REFERENCE  /NOMACHINE_CODE  /CONTINUATIONS=19
```

COMPILATION STATISTICS

Run Time:	4.97 seconds
Elapsed Time:	28.04 seconds
Page Faults:	180
Dynamic Memory:	167 pages

```
      SUBROUTINE DPBSL(ABD,LDA,N,M,B)
      INTEGER LDA,N,M
      DOUBLE PRECISION ABD(LDA,1),B(1)
C
C     DPBSL SOLVES THE DOUBLE PRECISION SYMMETRIC POSITIVE DEFINITE
C     BAND SYSTEM  A*X = B
C     USING THE FACTORS COMPUTED BY DPBCO OR DPBFA.
C
C     ON ENTRY
C
C        ABD      DOUBLE PRECISION(LDA, N)
C                 THE OUTPUT FROM DPBCO OR DPBFA.
C
C        LDA      INTEGER
C                 THE LEADING DIMENSION OF THE ARRAY  ABD .
C
C        N        INTEGER
C                 THE ORDER OF THE MATRIX  A .
C
C        M        INTEGER
C                 THE NUMBER OF DIAGONALS ABOVE THE MAIN DIAGONAL.
C
C        B        DOUBLE PRECISION(N)
C                 THE RIGHT HAND SIDE VECTOR.
C
C     ON RETURN
C
C        B        THE SOLUTION VECTOR  X .
C
C     ERROR CONDITION
C
C        A DIVISION BY ZERO WILL OCCUR IF THE INPUT FACTOR CONTAINS
C        A ZERO ON THE DIAGONAL.  TECHNICALLY THIS INDICATES
C        SINGULARITY BUT IT IS USUALLY CAUSED BY IMPROPER SUBROUTINE
C        ARGUMENTS.  IT WILL NOT OCCUR IF THE SUBROUTINES ARE CALLED
C        CORRECTLY AND  INFO .EQ. 0 .
C
C     TO COMPUTE  INVERSE(A) * C  WHERE  C  IS A MATRIX
C     WITH  P  COLUMNS
C           CALL DPBCO(ABD,LDA,N,RCOND,Z,INFO)
C           IF (RCOND IS TOO SMALL .OR. INFO .NE. 0) GO TO ...
C           DO 10 J = 1, P
C              CALL DPBSL(ABD,LDA,N,C(1,J))
C        10 CONTINUE
C
C     LINPACK.  THIS VERSION DATED 08/14/78 .
C     CLEVE MOLER, UNIVERSITY OF NEW MEXICO, ARGONNE NATIONAL LAB.
C
C     SUBROUTINES AND FUNCTIONS
C
C     BLAS DAXPY,DDOT
C     FORTRAN MIN0
C
```

```
      SUBROUTINE DPBCO(ABD,LDA,N,M,RCOND,Z,INFO)
      INTEGER LDA,N,M,INFO
      DOUBLE PRECISION ABD(LDA,1),Z(1)
      DOUBLE PRECISION RCOND
C
C     DPBCO FACTORS A DOUBLE PRECISION SYMMETRIC POSITIVE DEFINITE
C     MATRIX STORED IN BAND FORM AND ESTIMATES THE CONDITION OF THE
C     MATRIX.
C
C     IF  RCOND  IS NOT NEEDED, DPBFA IS SLIGHTLY FASTER.
C     TO SOLVE  A*X = B , FOLLOW DPBCO BY DPBSL.
C     TO COMPUTE  INVERSE(A)*C , FOLLOW DPBCO BY DPBSL.
C     TO COMPUTE  DETERMINANT(A) , FOLLOW DPBCO BY DPBDI.
C
C     ON ENTRY
C
C        ABD     DOUBLE PRECISION(LDA, N)
C                THE MATRIX TO BE FACTORED.  THE COLUMNS OF THE UPPER
C                TRIANGLE ARE STORED IN THE COLUMNS OF ABD AND THE
C                DIAGONALS OF THE UPPER TRIANGLE ARE STORED IN THE
C                ROWS OF ABD .  SEE THE COMMENTS BELOW FOR DETAILS.
C
C        LDA     INTEGER
C                THE LEADING DIMENSION OF THE ARRAY  ABD .
C                LDA MUST BE .GE. M + 1 .
C
C        N       INTEGER
C                THE ORDER OF THE MATRIX  A .
C
C        M       INTEGER
C                THE NUMBER OF DIAGONALS ABOVE THE MAIN DIAGONAL.
C                0 .LE. M .LT. N .
C
C     ON RETURN
C
C        ABD     AN UPPER TRIANGULAR MATRIX  R , STORED IN BAND
C                FORM, SO THAT  A = TRANS(R)*R .
C                IF  INFO .NE. 0 , THE FACTORIZATION IS NOT COMPLETE.
C
C        RCOND   DOUBLE PRECISION
C                AN ESTIMATE OF THE RECIPROCAL CONDITION OF  A .
C                FOR THE SYSTEM  A*X = B , RELATIVE PERTURBATIONS
C                IN  A  AND  B  OF SIZE  EPSILON  MAY CAUSE
C                RELATIVE PERTURBATIONS IN  X  OF SIZE  EPSILON/RCOND .
C                IF  RCOND  IS SO SMALL THAT THE LOGICAL EXPRESSION
C                           1.0 + RCOND .EQ. 1.0
C                IS TRUE, THEN  A  MAY BE SINGULAR TO WORKING
C                PRECISION.  IN PARTICULAR,  RCOND  IS ZERO  IF
C                EXACT SINGULARITY IS DETECTED OR THE ESTIMATE
C                UNDERFLOWS.  IF INFO .NE. 0 , RCOND IS UNCHANGED.
C
C        Z       DOUBLE PRECISION(N)
C                A WORK VECTOR WHOSE CONTENTS ARE USUALLY UNIMPORTANT.
C                IF  A  IS SINGULAR TO WORKING PRECISION, THEN  Z  IS
C                AN APPROXIMATE NULL VECTOR IN THE SENSE THAT
C                NORM(A*Z) = RCOND*NORM(A)*NORM(Z) .
C                IF  INFO .NE. 0 , Z  IS UNCHANGED.
C
C        INFO    INTEGER
C                = 0  FOR NORMAL RETURN.
C                = K  SIGNALS AN ERROR CONDITION.  THE LEADING MINOR
C                     OF ORDER  K  IS NOT POSITIVE DEFINITE.
```

```
C     BAND STORAGE
C
C           IF  A  IS A SYMMETRIC POSITIVE DEFINITE BAND MATRIX,
C           THE FOLLOWING PROGRAM SEGMENT WILL SET UP THE INPUT.
C
C                   M = (BAND WIDTH ABOVE DIAGONAL)
C                   DO 20 J = 1, N
C                      I1 = MAX0(1, J-M)
C                      DO 10 I = I1, J
C                         K = I-J+M+1
C                         ABD(K,J) = A(I,J)
C                10    CONTINUE
C                20 CONTINUE
C
C           THIS USES  M + 1  ROWS OF  A , EXCEPT FOR THE  M BY M
C           UPPER LEFT TRIANGLE, WHICH IS IGNORED.
C
C     EXAMPLE..  IF THE ORIGINAL MATRIX IS
C
C           11 12 13  0  0  0
C           12 22 23 24  0  0
C           13 23 33 34 35  0
C            0 24 34 44 45 46
C            0  0 35 45 55 56
C            0  0  0 46 56 66
C
C     THEN  N = 6 , M = 2  AND  ABD  SHOULD CONTAIN
C
C            *  * 13 24 35 46
C            * 12 23 34 45 56
C           11 22 33 44 55 66
C
C     LINPACK.  THIS VERSION DATED 08/14/78 .
C     CLEVE MOLER, UNIVERSITY OF NEW MEXICO, ARGONNE NATIONAL LAB.
C
C     SUBROUTINES AND FUNCTIONS
C
C     LINPACK DPBFA
C     BLAS DAXPY,DDOT,DSCAL,DASUM
C     FORTRAN DABS,DMAX1,MAX0,MIN0,DREAL,DSIGN
C
```